HANDBOOK OF PHYSIOLOGY

SECTION 2: Circulation, VOLUME I

HANDBOOK EDITORIAL COMMITTEE

HANDBOOK OF PHYSIOLOGY

A critical, comprehensive presentation

of physiological knowledge and concepts

SECTION 2: **Circulation**

VOLUME I

Section Editor: W. F. HAMILTON

Executive Editor: PHILIP DOW

American Physiological Society, WASHINGTON, D. C., 1962

Library of Congress Catalog Card No. 60-4587

Printed in the United States of America by Waverly Press, Inc., Baltimore 2, Maryland

Distributed by The Williams & Wilkins Company, Baltimore 2, Maryland

Preface

The section on the circulation of the *Handbook of Physiology* is offered in three volumes. The first of these was planned to cover the physiology of the heart and its controls, along with certain material about the volume of the blood and the biophysical background of the organs of the circulation. The second volume was planned to include the functional morphology of the vessels and their coordination in regulating the distribution of blood flow to the several organs. The third volume was planned to deal with the circulation as the functions of an organ system whose normally coordinated or abnormal action plays upon the organism as a whole.

This original plan has been modified somewhat in the interests of prompt authors and at the expense of tardy ones. Some have advanced into Volume I; we hope that some chapters originally scheduled for Volume I may be fitted into the later ones.

The circulation is a subject whose ramifications are protean. Not only does it have an intrinsic regulation feeding back from the circulatory organs themselves, but changes in the circulation alter the functions of other organs which in turn work new changes in the circulation. Another complication in dealing with the physiology and biophysics of the circulation is the fact that certain fields are in vigorous controversy.

It is to be expected, therefore, that some topics will be covered more than once by different authors. We have tried to provide that the two coverages are not mere repetitions and a great deal of material has been discarded for this reason. On the other hand if the overlap is not really an overlap, but shows the material or argument in different context, from different viewpoints, and with different interpretation, the outcome seems to us to be good.

Each chapter is written in the hope that it will be an authoritative systematic account of the present status of the field and a contribution to Physiology as a science in its own right. The chapters are as detailed as over-all space will permit. Coverage of all the literature is not attempted. Citations are restricted, for the most part, to the factual evidence and theoretical interpretations that bear upon concepts that are seriously advocated at the present time. Recent contributions are not allotted space because of their recency, but only as they are constructive of current ideas.

Each chapter is written to fit the needs of three groups of readers: *1*) the graduate student who wants to go more deeply and broadly into the meanings of current physiological concepts and their background than he can in standard text books; *2*) the teacher who is dissatisfied with the comprehensiveness of his understanding outside his own specialty; and *3*) the investigator who will use it as a springboard for references and current concepts in a field which he is beginning to explore. The contributions are written by qualified experts, modern in viewpoint, and emphatically are not esoteric polemics between specialists.

In selecting these specialists, advice was sought on an international basis. One of us met in Ghent with a committee of representative European physiologists selected and chaired by Prof. C. Heymans. This group gave valuable advice concerning our tentative chapter list and nominated authors for each of the chapters. This editor also met with a similar group in London, selected by O. G. Edholm and Prof. J. McMichael. In the hands of these men the plan was further revised and additional authors were nominated. The final selection of authors and alternates and the final revision of the plan were made by an *ad hoc* committee accepted by the Board of Publication Trustees and composed of knowledgeable members of our own Society. The

list of chapters and authors will, in the minds of these advisors, give the *Handbook* a comprehensive definitive coverage with an international viewpoint.

The editors want to express their gratitude to these advisors, to the authors who have so conscientiously and constructively done their arduous tasks at great personal sacrifice, to our colleagues here in Georgia, R. P. Ahlquist and Carleton Baker, who have helped willingly and well. Especially valuable has been the knowledgeable and cooperative assistance of John W. Remington who has turned to, well beyond the call of duty. We are most indebted to the energy and accuracy of the departmental secretary, Mrs. Juanita Coufal. Our greatest debt of all is to Mrs. Walter J. Brown Jr., whose clairvoyant insight into the meaning of strange sentences from abroad, whose feeling for the right word in their "translation," and whose understanding of physiological principles have borne worthy fruit.

W. F. HAMILTON, *Section Editor*

PHILIP DOW, *Executive Editor*

Contents

The circulation and circulation research in perspective

CARL J. WIGGERS | *Frank E. Bunts Educational Foundation, affiliated with Cleveland Clinic, Cleveland, Ohio*

CHAPTER CONTENTS

THIS CHAPTER is divided into two sections: the first represents a perspective of the general features of the circulatory system and considers some of the vascular mechanisms concerned with the redistribution of blood flow in accordance with regional metabolic requirements. The second deals with changes of opinion that have taken place within the memory of the present author with regard to the mechanisms by which cardiac output is nicely adjusted to the vicissitudes of everyday life. The role that improvements in methodologies have played are briefly discussed. Since the perspective presented is essentially a review of reviews, references are largely restricted to surveys made at various periods of the present century that the reader may care to consult as extensions to this brief discussion.

In perusing this exposition, the reader is warned that it represents the considered interpretations of an oldster who has not been privileged to participate actively in circulation research for a number of years. There are both advantages and disadvantages in watching the research game from the sidelines; one is not so close to trivial incidents that perspective is lost, yet one is unaware of how important they may be in determining the final result. Consequently, the present author's considered judgment as to the status of current opinion on many problems may not accord with that expressed in subsequent chapters by those still active in circulation research.

THE TECHNIQUE OF EVALUATING SCIENTIFIC DATA

It has been a part of the present author's philosophy that assessment of current opinion of course requires recognition of new data procured through constant improvement in methodologies. However, it is likewise important to acknowledge valid discoveries and deductions of the past and to integrate new ones with them. In assessing older data, and doctrines derived from them, an author must constantly remain aware that results once considered crucial have, in many instances, become less certain when viewed in the light of new advances. Further, the interpretation of experimental results, both old and new, depends on the sagacity of the investigator and on the scientific atmosphere at the time. That is to say, investigators acquire diverse senses of values as a result of their scientific training; few are completely free from bias, and many are afflicted with a natural disposition

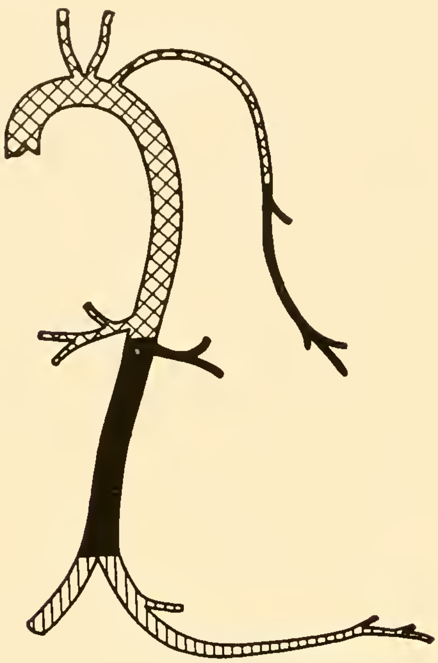

FIG. 1. Diagram illustrating the translocation of successive stroke volumes through the aorta and its branches. [After Lequime (43).]

either to maintain allegiance to or to revolt against traditional viewpoints.

THE ARCHITECTURE AND FUNCTION OF THE CIRCULATORY SYSTEM

From a functional standpoint, the systemic circuit may be divided into *a*) a distributing system (left ventricle, aorta and its branches, and their final subdivisions into arterioles); *b*) a division for the interchange of substances (capillaries and venules); and *c*) a collecting system (small and large veins, venae cavae, and right atrium). The pulmonary circuit similarly begins with the right ventricle and drains into the left atrium.

The entire cardiovascular system is lined with a continuous smooth layer of endothelium which minimizes friction between the flowing blood and vascular walls, and thus limits resistance to flow to shearing forces in layers of blood near the vascular walls.

The Distributing System

The architecture of the arterial tree is adapted in many ways to the proper distribution of blood but also introduces a number of complexities in its propulsion. The main branches of the aorta divide dichotomously, each time widening the stream bed and broadening the areas of distribution. The longitudinal divisions of the abdominal aorta into iliac and femoral arteries and the extension of axillary arteries into the brachial and radial arteries (fig. 1) create physical resonating systems of low natural frequencies that modify the fluctuating aortic pressures and flow in their transmission to the periphery.

The greatest proportion of blood injected into the aorta by the left ventricle leaves it by numerous lateral branches which form parallel circuits (fig. 2). This physical arrangement serves two important dynamic purposes: *1*) it permits redistribution of blood from one territory to another through regional changes in resistance without necessarily altering mean aortic pressure, and *2*) it reduces the total resistance to efflux from the arterial system The latter is occasioned by the fact that, as in parallel electric circuits, total peripheral resistance (TPR) depends on reciprocal relations, for example,

$$1/TPR = 1/r_1 + 1/r_2 + 1/r_3 \cdots 1/r_n,$$

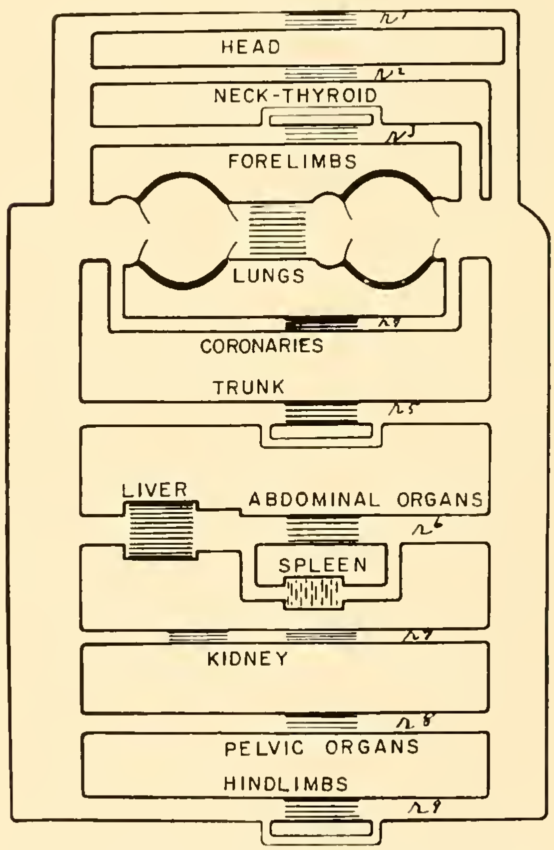

FIG. 2. Diagram illustrating the principle of parallel circuits and resistances. [Modified from Wezler & Böger (67).]

in which r_1, r_2, r_3, etc. represent regional or territorial resistance in the different parallel circuits shown in figure 2 (Wezler & Böger, 67). As an example of the relation of parallel circuits to TPR, it has been estimated that whereas the regional resistance of the cerebral or coronary circuits of dogs have magnitudes of 18,000 dyne-sec per cm^5, the TPR is very much less in proportion, as the regional flow is less than the total cardiac output.

Dynamics of the Arterial System

Since the distributing system accomplishes its biological functions in a mechanical way, numerous attempts have been made to express its dynamics by mathematical formulations. A detailed exposition and an evaluation of their present status is of course excluded in an introductory chapter. The historical fact may however be noted that mathematical treatment of pressure waves in elastic tubes dates from the early work of Euler (1775), Young (1808), W. E. Weber (1866), Resal (1876), Moens (1878), and v. Kries (1892). The interested reader may consult the reviews by A. Müller (45), H. Straub (58), A. Aperia (1, 2), Wezler & Böger (67), Gómez (23), Wezler & Sinn (69), Womersley (74), and W. Sinn (54). A survey of such reviews reveals that, whereas there is at present no consensus as to particulars, there is agreement on general mathematical formulations which, for our purpose, can be translated into simple language [see also (27, 59, 66)].

Pressure and flow in the arterial tree are maintained by the rhythmic action of the cardiac pump. During each systole, the left ventricle ejects a definite volume of blood into the aorta—about 60 to 100 ml in man—variously called the stroke volume, systolic discharge, and pulse volume. The period of ejection is very short; about 0.25 sec at normal heart rate and less during cardiac acceleration. Moreover, fully two-thirds of the stroke volume is displaced into the aorta within about 0.1 sec, and very little during the final 0.05 sec of systole. Since the aorta, at the onset of ejection, is already distended under a pressure of about 75 mm Hg, aortic uptake is accomplished partly by accelerating the stationary blood column and moving it ahead—kinetic energy—and partly by distending the elastic walls. The potential energy thus stored in the elastic walls presses back on the blood in accordance with Newton's third law of motion and causes the rise of systolic pressure. In short, the elasticity coefficient, which can be expressed in dynes per cm^5, is the basic determinant of pulse pressure (67).

The systolic elevation of pressure thus created in the aorta is transmitted as a pressure wave through the arterial tree at rates varying from 3 to 14 meters per sec. However, as already intimated, the form of the pulse pressure is altered in transmission by damping and by summation with reflected or standing waves, and possibly by the unequal rates at which harmonics of the pressure pulse are transmitted [Peterson (48)].

In contrast to the high speed with which pressure waves are propagated, the velocity with which blood flows through the arterial tree ranges from 14 to 18 cm per sec. The reason for these differences may be visualized by reference to figure 1. As indicated by the cross-hatched area, blood ejected during any given systole is accommodated in the aorta and its immediate branches. Blood already within this space is displaced under pressure to a more distal segment of the arterial tree as indicated by the black area. This translocates blood to a third segment under pressure, as indicated by the lined area. Thus whereas the pressure wave may reach vessels in the feet within 0.2 to 0.3 sec, corpuscles ejected during any heart beat do not arrive there until several more heart beats have occurred.

At the onset of diastole, the blood column reverses momentarily during closure of the semilunar valves; then it moves forward again as the elastic aortic walls recoil slowly and reconvert the stored potential energy into energy of flow. This buffering function that maintains a constant flow through capillaries was recognized by Borelli (1680) and by Hales (1733), and was baptized as the *Windkessel* by E. H. Weber (1834). Although, in a sense, the entire distributing system aids in smoothing blood flow through the capillaries, the aorta and its immediate branches probably constitute the effective compression chamber; the volume uptake of more peripheral branches per mm Hg per unit length decreases rapidly, owing to increasing stiffness of their walls [Remington (50)].

The elastic properties of the aortic walls are largely due to the elastic fibers dispersed throughout the intima, media, and adventitia. Their conformance to Hooke's law probably explains the almost proportional relationship between pulse pressure and aortic uptake at ranges of end-diastolic pressure between 40 and 100 mm Hg. Within these pressure ranges the corrugated collagenous fibers merely unfold and only act to stiffen the walls at end-diastolic pressures above 100 mm Hg. The aortic walls also

contain some obliquely oriented smooth muscle cells which are apparently inserted on elastic fibers (4). Their action and function are difficult to assess. It is the current opinion that they exert tension on the elastic fibers and thus affect both the caliber and distensibility of the aorta *in situ* (4, 6, 68).

In the so-called muscular arteries, such as the carotids, brachials, radials, iliacs, femorals, mesenterics, etc., elastic and collagenous fibers are found chiefly in the intima and adventitia; the media, which comprises two-thirds of the wall's thickness, is composed almost entirely of smooth muscle fibers arranged concentrically or, as some histologists say, spirally (68). The muscle fibers are under a plastic as well as contractile tonus. The former determines the viscous characteristics of the wall; the latter resists the tendency of internal pressures to distend the arteries. Physically, the muscle elements are arranged in parallel with the elastic and collagenous fibers; they participate in resisting distention by internal pressures and replace the action of collagenous elements in stiffening the walls under high internal pressures (4, 68). The autonomous state of contractile tonus is increased by mechanical and chemical agents, as well as through excitation by vasoconstrictor nerves. Hilton (34) has recently presented evidence that muscular arteries, such as the femoral, may dilate secondarily to a primary dilatation of arterioles, as a result of the centripetal spread of a wave of inhibition within the arterial walls.

It was formerly believed that the contractile tonus of the smooth muscle fibers alters the distensibility of the muscular arteries and perhaps also adapts their capacity to the volume of circulating blood, but exerts no significant effect on resistance to flow. During the past two decades evidence has accrued that changes in the diameter of long arteries may affect regional resistance materially. The claim that vascular contraction acts as an accessory mechanism in the propulsion of blood is based on tenuous evidence only; smooth muscles contract much too slowly to follow the pace set by the heart.

Arterioles

The arterioles constitute the terminal branches of the distributing system and are the primary stopcocks that regulate capillary flow. Their walls are relatively thick compared to their lumens. The abundant circularly arranged muscular elements are under an autonomous state of contraction (tonus) which can be augmented or inhibited by chemical agents or by the action of vasomotor nerves. Vasoconstrictor fibers are generally routed over sympathetic pathways. It is in fact probable that so-called sympathetic dilators to the coronary arteries are misnamed; they seem to cause dilatation through release of metabolites [Gregg (24)]. Vasoconstrictor nerves have been demonstrated for vessels of all organs, but the intensity of vasomotion induced is less marked in vessels of the lungs, brain, and heart. Because of these differences in vasomotor reactivity, increased discharges from the medullary vasomotor center can induce large changes in splanchnic and renal resistances, thereby mechanically diverting more blood to vital organs, such as the brain and heart. This hemodynamic concept is not new. For example, L. Hill (33) stated in 1900, "It is by means of the great splanchnic area that the blood supply of the brain is controlled. . . We have in the vasomotor center a protective mechanism by which blood can be drawn at need from the abdomen and supplied to the brain." [See also Folkow (16–18).]

Neurogenic vasodilatation is generally induced through inhibition of vasoconstrictor activity which, however, still leaves arterioles under a state of autonomous contraction. In the heart, abdominal organs, and skeletal muscles, this residual tonus can also be inhibited by action of sympathetic vasodilator nerves, thus causing additional dilatation. In vessels of the head, pelvic organs, and genitals, excitation of parasympathetic nerves induces extreme dilatation. The interpretation of Gesell (21) that such vasodilatation is not due to direct nervous action but through release of vasodilator metabolites has recently received considerable support (18, 65). In the skin, vasodilatation may occur through operation of axon reflexes, and in mucous membranes by action of posterior root dilators (18, 65).

Through reflex control of vasomotion, shifts of blood from viscera to the skin and vice versa may take place, as for example during exercise and digestion as well as in hemorrhage and shock (32, 49, 72).

Control of Capillary Blood Flow

The capillary walls consist of a single layer of endothelial cells mounted on a basement membrane. The thin walls adapt the capillaries admirably for interchange of substances between the blood and tissue spaces. According to older views (8), a "cement substance" between cells is produced by them and can be modified by such agents as the Ca:K ratio and hormones. Advances in methodologies, including

electron microscopy, reveal no evidence of any substances between the endothelial cells [Kisch (38)]. At present opinions are divided as to whether the exchange of substances occurs through submicroscopic intercellular fenestrations or through ultramicroscopic perforations in the endothelial cells [Bennett *et al.* (3), Kisch (38), Pappenheimer (47)].

The passage of solutes and solvents through the endothelial walls is largely regulated by capillary pressure and flow [Landis (40)]. During the early part of the present century, capillaries were believed to be straight subdivisions of arterioles. Capillary pressure and flow were considered to be regulated solely by the intensity of arteriolar and venular constriction. The concept that capillaries could change their caliber actively began with observations of Dale & Richards (13) that histamine apparently constricts arterioles and dilates capillaries. It received major support from the microcirculatory studies of Krogh and his colleagues (39) and from the human studies of Lewis (42). Krogh's observations, made chiefly on amphibia, were not generally confirmed by microcirculatory studies of mammalian blood vessels [Clark & Clark (10)], and his inference that active changes in capillaries are caused by a squeezing action of pericytes (Rouget cells) attached to their walls, is currently out of favor [Burton (6)]. A new concept of the finer regulation of capillary flow than is provided by arteriolar vasomotion was introduced by Chambers & Zweifach (7). Their microcirculatory studies of the tongue and mesentery revealed that arterioles give rise first to thin-walled, contractile metarterioles or precapillaries which lead into arteriovenous channels 12 to 16 μ in diameter. As schematically shown in figure 3, these thoroughfare channels give off side branches that form an anastomotic network of true capillaries. The metarterioles and precapillary sphincters undergo periodic contractions at intervals of 15 sec to 3 min. It is therefore the present consensus that whereas the arterioles dominate resistance to flow from arteries to capillaries and hence the pressure gradient, the metarterioles and their sphincters control capillary filling and patency to a finer degree.

The smallest postcapillary venules (prevenules) should probably be included in the category of "minute vessels" as defined by Lewis (42) and are likewise concerned in the interchange of solvents and solutes. According to Hooker (35), small venules are distinguishable by their somewhat larger size

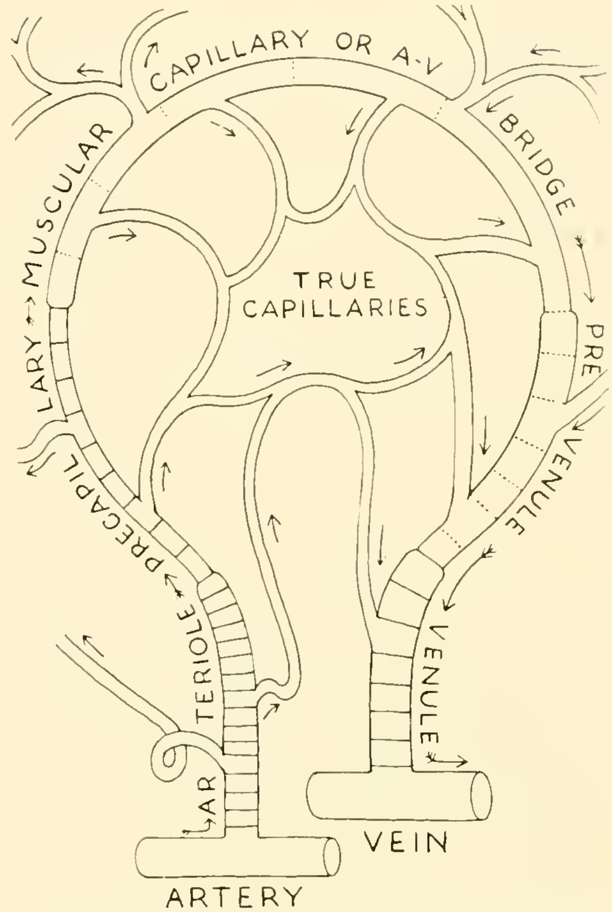

FIG. 3. Diagram of true capillary network and A-V capillary bridges. [After Chambers & Zweifach (7).]

than capillaries and by the presence of a slight investment of connective tissue. In some regions smooth muscle cells are seen in venules 20 to 30 μ in diameter; in other regions they are absent in small veins visible to the eye [Franklin (20)].

Collecting Veins and Venous Return

Blood from the venules is collected by merging veins of increasing size. Their thin walls are composed of many collagenous and scanty elastic fibers in which muscle cells are dispersed in circular, spiral, or longitudinal directions [Franklin (20)]. Veins collapse when incompletely filled and, when distended to a cylindrical shape, display only limited distensibility [Clark (11)]. Up to internal pressures of 5 to 10 cm of water, the increment of pressure per increment of volume is quite small, but above such pressures dP/dV rapidly increases until the veins become relatively indistensible.

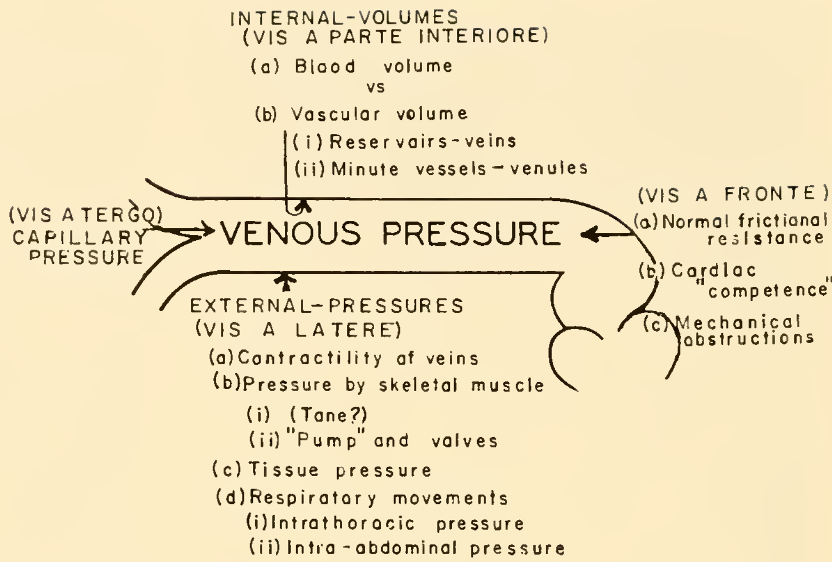

FIG. 4. Factors affecting venous pressure. [After Landis & Hortenstine (41).]

Normally, blood is propelled through the collecting system by a pressure gradient of about 6 to 8 cm of water between the peripheral veins and the right atrium [Brecher (5)]. The various coefficients that determine the gradient are nicely summed up in the diagram of Landis (41), reproduced as figure 4.

Only a few points deserve editorial comment: the author has been impressed with the major extent to which the venous pressure gradient is controlled by cardiac activity. For instance, when the cardiac output increases, more blood is drained from the atrium per unit time, central venous pressure decreases, and the pressure gradient augments through reduction of the *vis a fronte*. Evidence clearly indicates that the small and large veins contract as a result of venomotor activity [Franklin (20), Gollwitzer-Meier (22), McDowall (44)]. Further, veins participate in vascular contractions reflexly induced from the carotid sinus [Heymans & Neil (32)]. Despite contrary opinions, the present author believes that the extent to which such reduction in venous capacity augments venous return has not been established experimentally.

ADJUSTMENT OF CARDIAC OUTPUT TO METABOLIC REQUIREMENTS

It has long been recognized that enhanced metabolism is associated with increase in heart rate and presumably with a greater cardiac output. The question whether stroke volume also increases has been debated for the past 60 years. At the beginning of the present century, technical procedures were essentially limited *a*) to metering aortic flow in rabbits, calculating volume flow per unit body weight, then extrapolating results to man; and *b*) to estimation of cardiac output in dogs and horses by use of the Fick principle (1870, 1886). Nevertheless, Tigerstedt (62) in his *Lehrbuch* (1897) ventured the guess that the stroke volume in man ranged from 50 to 100 ml, values that have subsequently proven correct (14). But data acquired by such imperfect methods showed such inconstant ratios between heart rate and cardiac output that the two were considered independent variables. This interpretation fitted in with Engelmann's concept that cardiac rhythmicity, excitability, conductivity, and contractility could be altered independently by humoral and nervous agencies. On the other hand, experiments of Howell and Donaldson (1884) on N. Martin's limited circulation preparation had indicated that cardiac output varies consistently with venous supply and right atrial pressures [for details, see Tigerstedt (63, 64)].

During the first decade of the present century physiologists began to question the accuracy of data obtained by available methods and the applicability to intact animals and man of values obtained from use of partially or totally isolated hearts. Progress during the next 30 years was beset with many frustrations in attempting to develop better procedures (46). The efforts made to understand the laws of cardiac performance and to estimate changes in cardiac output in man under different conditions illustrate admirably that a goal in research is reached only through development of a great number of methodologies which, though inadequate, do offer

clues for their betterment. Hence a brief historical recall does not seem out of place in an introductory chapter.

Methods for Studying the Determinants of Cardiac Performance

The reactions of isolated ventricles of frogs, contracting isotonically and isometrically under various degrees of filling, had been studied by Frank (19) in 1895. He found that within limits stepwise inincreases in end-diastolic filling and pressure determine the magnitude of the all-or-none response. He concluded that the magnitude of end-diastolic pressure was the basic determinant.

In 1905, it was my privilege to witness Y. Henderson's demonstration of a method for recording the volume curves of the ventricles in dogs. This technique appeared to be a definite advance, because it permitted registration of the details of ventricular filling and ejection as well as the magnitude of successive stroke volumes. It therefore constituted a better way for determining the principles underlying ventricular performance. As reviewed by Henderson (29), he and various associates concluded *a*) that atrial contraction contributes so little to ventricular filling that it could be ignored and *b*) that the ventricles contract in so uniform a manner that curves taken at different heart rates can be superimposed like triangles in geometry. Further analysis indicated *c*) that stroke volume is not affected by increases in venous pressures above the normal, and *d*) that stroke volumes change very little at ranges of heart rate from 20 to 100 per min, but, *e*) that at higher heart rates they decrease progressively, because contractions encroach more and more on the rapid inflow during early diastole. The corollary followed that the only way that cardiac output can be altered is through changes in heart rate. Henderson's conclusions were contested partly on the grounds of unreliability of the procedure and failure to recognize the importance of atrial systole, but chiefly because all his reports were linked with the hypothesis that acapnia is the cause of shock (30). In short, Henderson violated a well-known principle in advertising, namely, that favorable features of a product must not be associated with unpopular notions. Physiologists have been slow to learn that new viewpoints are more often accepted on the basis of their psychological appeal than on the validity of data and the conservatism with which conclusions are drawn.

During my visit to Starling's laboratory in 1923, he told me that his decision to develop a heart-lung preparation was motivated by his impression that opening of the chest of an anesthetized dog did something that weakened cardiac contractions. The preparation developed with Jerusalem and Patterson allowed heart rate, venous inflow, and arterial resistance to be altered one at a time. It immediately came into general favor for studying the principles of ventricular behavior. On the basis of observations made with various associates (56, 57), Starling concluded, contrary to Henderson, that cardiac output is not altered by changes in heart rate between 60 and 160 per min, and can be changed only by alteration of filling and stroke volume. Starling (56) held that changes in end-diastolic volume or stretch, rather than pressure, were the basic determinants (Starling's law of the heart).

It is not uncommon in research that adversaries are right in general but wrong in particulars. This was the conclusion to which Katz and I came in 1922; we found elements of truth in both Henderson's and Starling's interpretations. Since knowledge is slow afoot, but wisdom limps far behind, it was not until later that the present author (70, 71, 73) realized that the concepts could be harmonized with each other and also with the postulates of Englemann [see also Katz (36, 37)]. It remained a question, however, whether changes in end-diastolic pressure and volume or alterations in contractility, produced by humoral or nervous influences, constituted the prepotent factor in stresses to which the body is submitted under normal conditions. For instance, when it seemed demonstrated that venous pressure rises during moderate exercise [Eyster (15)], it seemed a reasonable assumption that stroke volume increases during exertion in accordance with Starling's law despite cardiac acceleration. Katz, Opdyke, and Bulkley and their respective co-workers have studied the importance of varying impedance to ventricular filling in heart preparations in which one ventricle only performs work.

It is not surprising that all the dynamic factors capable of affecting ventricular performance were not thought of by experimenters of past generations and remained fertile fields for study in the present era. Better apparatus was designed and new types of special circulatory preparations were developed. While the results of numerous studies still seem contradictory in many respects, they will undoubtedly be integrated in subsequent chapters. Here, it is only possible to refer very briefly to a few of the many notable contributions of recent years: Katz and his

co-workers (36, 37) have related ventricular pressure/volume curves to work diagrams, and focused attention on factors affecting stroke work. Sarnoff and collaborators (53) have related stroke work of the right and left ventricles to pressures in corresponding atria as ventricular function curves. More recently, they restressed the importance of ventricular tension-time in cardiodynamics, and revived the old idea that the force of atrial contractions is of controlling importance. Nylin, Bing, Holt, and their respective collaborators have measured the residual ventricular volumes more accurately, and others have emphasized the emergency value of the "cardiopulmonary reserve" in increasing cardiac output. Holt and Duomarco, independently, have shown the importance of end-systolic pressure as an additional regulatory coefficient of cardiac output and work. Guyton and his group (26) have studied the intrinsic response of the ventricles to changes in venous return in dogs whose reflexes were all abolished. Rushmer and his school (51) developed many ingenious appliances that permitted continuous quantitative recordings of multiple cardiac activities in unanesthetized dogs. They concluded that changes in cardiac output during exercise are caused entirely by chronotropic and inotropic effects mediated by the diencephalon and modulated by reflexes of vascular origin. Thus the wheel of circulation research has revolved back to concepts prevalent at the beginning of the present century.

Methods for Determining Cardiac Output in Man

Pari passu with the growth of laboratory techniques for elucidating mechanisms of cardiac adaptation, continued efforts were made during the present century to establish more reliable methods for measuring cardiac output in man. While many technologies, such as roentgenkymography, cineroentgenography, electrokymography, ballistocardiography and the integration of pressure pulses achieved some measure of usefulness, the greatest advances have come from improvements in the application of the Fick principle and the blood-dilution technique of Stewart-Hamilton [Hamilton (28)]. Early attempts to obtain probable values for blood gases indirectly or to use foreign gases led to many confusing results (9, 25, 28, 63). Two technical developments—Stadie's method of obtaining arterial blood samples by arterial puncture (55) and Cournand & Ranges' method for obtaining mixed venous blood by cardiac catheterization (12)—were largely responsible for the great impetus to recent studies of cardiac output in man under normal and pathological conditions. For instance, it was definitely established (14, 28, 43) that cardiac output may increase from about 4 liters per minute at rest to 20 or more liters per minute during strenuous exercise. Simple calculations indicate that the heart cannot deliver such large quantities of blood by an increase in heart rate, say from 70 to 180 per min, without considerable increase in stroke volume. Nevertheless, the net information gained by other avenues of approach led to the conclusion of a conference in 1955 (59) that the Frank-Starling postulate is operative only to a minor degree (52): For example, the views were well documented that demonstrable changes in end-diastolic tension and ventricular size were not necessarily associated with more forceful ventricular beats and that both systolic and diastolic sizes decreased as the heart accelerated during exercise. It was not generally recognized that these conclusions corresponded in great detail with those of Henderson (29) in his 1923 review. However, it must be noted that at that time Henderson slyly amended his concept of the uniformity of cardiac behavior by adding an intrinsic ability of the ventricles to alter their process of filling and ejection.

There is no doubt that the current emphasis on the central nervous system control of cardiac output (60, 61) was strongly influenced by advances in the field of neurophysiology, chiefly in unraveling the structure and functions of the reticular formation and diencephalon. This is a good illustration of how advances in one field of physiology accrue through those made in cognate ones. In our zeal to accept such a concept we must not lose sight of the fact that physical and chemical changes in the environment of cardiac tissue also affect its reactivity. Indeed, with the rapid development of endocrinology and knowledge that hormones, such as epinephrine, pitressin, thyroxin, and aldosterone, cause changes in cardiac reactivity, one senses already an inclination in some laboratories to postulate a dominant endocrinological control of cardiac output.

Venous Return, the Fulcrum of the Circulation

Regardless of the direction that future thinking with regard to the mechanisms of cardiac adaptation to stresses may take, it must conform to the obvious fact that the heart cannot pump more blood than is returned. As phrased by Henderson, "venous return is the fulcrum of the circulation." The present author finds it difficult to understand why so much current

emphasis is given to mechanisms of blood supply that can be only temporary emergency mechanisms. Accepting current estimates that the ventricles contain residual volumes that may exceed those ejected, and that the pulmonary venous system also constitutes a reservoir of blood, my calculations indicate that the total cardiopulmonary reserve can be pumped out within 5 or 6 sec after the onset of strenuous exercise. Thereafter, augmented cardiac output can be maintained only by a corresponding increase in venous return.

Despite many earnest efforts to elucidate the sources of additional venous blood and the mechanisms by which venous return is augmented (5, 22, 26, 31, 41), most of the conclusions are based on inferences and extrapolations rather than on direct experimental evidence. Hence the study of venopressor mechanisms remains a promising field for future investigations.

A few words in conclusion: the reader may infer that the author of this chapter has reached an age when the tendency to recall significant advances of the past exceeds his capacity to appreciate the full value of contemporaneous ones. They may be reassured however that he had no intention of downgrading the highly significant contributions of the present generation of active workers. Since these new advances will be stressed predominantly in subsequent chapters, it seemed appropriate to recall that the scholarly assessment of current work also requires recognition of accomplishments of the past and some knowledge of the underlying reasons for frequently changing points of view. Research, as the word implies, consists in searching again and again to make quite certain that propositions regarded as established are indeed true. A historical perspective teaches us not to repeat investigations made by simpler means too often, just because more complicated methods have become available.

REFERENCES

1. Aperia, A. *Hemodynamical Studies.* Berlin: de Gruyter, 1940.
2. Aperia, A. Peripheral circulation. *Texas Rept. Biol. and Med.* 3: 3–29, 1945.
3. Bennett, H. S., J. H. Luft, and J. C. Hampton. Morphological classification of vertebrate blood capillaries. *Am. J. Physiol.* 196: 381–390, 1959.
4. Benninghoff, A. Blutgefässe und Herz. In: *Möllindorff's Handbuch der Microscop. Anatomie.* Berlin: Springer, VI/1: 1, 1930.
5. Brecher, G. *Venous Return.* New York: Grune & Stratton, 1956.
6. Burton, A. C. Relation of structure to function of the tissues of the wall of blood vessels. *Physiol. Rev.* 34: 619–642, 1954.
7. Chambers, R., and B. W. Zweifach. Topography and function of mesenteric capillary circulation. *Am. J. Anat.* 75: 173–205, 1944.
8. Chambers, R., and B. W. Zweifach. Intercellular cement and capillary permeability. *Physiol. Rev.* 27: 436–463, 1947.
9. Christensen, E. H. Das Herzminutenvolumen. *Ergebn. Physiol.* 39: 348–407, 1937.
10. Clark, E. R., and E. L. Clark. Caliber changes in minute blood vessels observed in living mammal. *Am. J. Anat.* 73: 215–250, 1943.
11. Clark, J. H. The elasticity of veins. *Am. J. Physiol.* 105: 418–427, 1933.
12. Cournand, A., and H. A. Ranges. Catheterization of right auricle in man. *Proc. Soc. Exper. Biol. & Med.* 46: 462–466, 1941.
13. Dale, H. H., and A. N. Richards. The vasodilator action of histamine and of some other substances. *J. Physiol.* 52: 110–165, 1918.
14. Dittmer, D. S., and R. M. Grebe (editors). *Handbook of Circulation.* Philadelphia: Saunders, 1959, pp. 77–79.
15. Eyster, J. A. E. Venous pressure and its clinical applications. *Physiol. Rev.* 6: 281–315, 1926.
16. Folkow, B. Nervous control of the blood vessels. *Physiol. Rev.* 35: 629–663, 1955.
17. Folkow, B. Peripheral circulation. *Ann. Rev. Physiol.* 18: 159–194, 1956.
18. Folkow, B. Role of the nervous system in the control of vascular tone. *Circulation* 21: 760–768, 1960.
19. Frank, O. Zur Dynamik der Herzmuskels. *Ztschr. f. Biol.* 32: 370–447, 1895. On the dynamics of cardiac muscle. Translated by C. B. Chapman and E. Wasserman. *Am. Heart J.* 58: 282–317, 467–478, 1959.
20. Franklin, K. J. *A Monograph on Veins.* Springfield, Ill.: Thomas, 1937.
21. Gesell, R. Studies on the submaxillary gland. III. Some factors controlling the volume flow of blood. *Am. J. Physiol.* 47: 438–467, 1919.
22. Gollwitzer-Meier, K. Venensystem und Kreislaufregulierung. *Ergebn. Physiol.* 34: 1145–1255, 1932.
23. Gómez, D. M. *Hémodynamique et Angiocinétique.* Paris: Hermann, 1941.
24. Gregg, D. E. *Coronary Circulation in Health and Disease.* Philadelphia: Lea & Febiger, 1950.
25. Grollman, A. *The Cardiac Output of Man in Health and Disease.* Springfield, Ill.: Thomas, 1932.
26. Guyton, A. C. Determination of cardiac output by equating venous return curves with cardiac response curves. *Physiol. Rev.* 35: 123–136, 1955.
27. Hamilton, W. F. Notes on the development of the physiology of the cardiac output. *Fed. Proc.* 4: 183–195, 1945.
28. Hamilton, W. F. The physiology of the cardiac output. *Circulation* 8: 527–543, 1953.
29. Henderson, Y. Volume changes of the heart. *Physiol. Rev.* 3: 165–208, 1923.

30. HENDERSON, Y. *Adventures in Respiration.* Baltimore: Williams & Wilkins, 1938.
31. HENDERSON, Y. Tonus and venopressor mechanism; clinical physiology of major mode of death. *Medicine* 22: 223–249, 1943.
32. HEYMANS, C., AND E. NEIL. *Reflexogenic Areas of the Cardiovascular System.* Boston: Little, Brown, 1958.
33. HILL, L. In: *Schäfer's Textbook of Physiology.* London: Macmillan, 1900.
34. HILTON, S. M. A peripheral arterial conducting mechanism underlying dilatation of the femoral artery and concerned in functional vasodilatation in skeletal muscle. *J. Physiol.* 149: 93–111, 1959.
35. HOOKER, D. R. Evidence of functional activity on the part of capillaries and venules. *Physiol. Rev.* 1: 112, 1921.
36. KATZ, L. N., H. FEINBERG, AND A. B. SHAFFER. Hemodynamic aspects of congestive heart failure. *Circulation* 21: 95, 1960.
37. KATZ, L. N. The performance of the heart. *Circulation* 21: 483–498, 1960.
38. KISCH, B. *Electron Microscopy of the Cardiovascular System.* (Translated by Arnold I. Kisch.) Springfield, Ill.: Thomas, 1960.
39. KROGH, A. *The Anatomy and Physiology of Capillaries*, rev. ed. New Haven: Yale Univ. Press, 1929.
40. LANDIS, E. M. Capillary pressure and capillary permeability. *Physiol. Rev.* 14: 404–481, 1934.
41. LANDIS, E. M., AND J. C. HORTENSTINE. Functional significance of venous blood pressure. *Physiol. Rev.* 30: 1–32, 1950.
42. LEWIS, T. *The Blood Vessels of the Human Skin and Their Responses.* London: Shaw, 1927.
43. LEQUIME, J. *Le Débit Cardiaque.* Paris: Masson, 1940.
44. McDOWALL, R. J. S., G. E. MALCOMSON, AND I. McWHAN. *The Control of the Cirulation of the Blood.* New York: Longmans, Green, 1938.
45. MÜLLER, A. Einführung in die Mechanik des Kreislaufes. In: *Abderhalden's Handbuch der biologischen Arbeitsmethoden.* Abtlg. V. Teil 8: 142, 1928.
46. MÜLLER, E. A. Die Beziehungen zwischen Volumen, Leistung, Tonus und Kontraktionsfähigheit am isolierten Säugetierherzen. *Ergebn. Physiol.* 43: 89–132, 1940.
47. PAPPENHEIMER, J. R. Passage of molecules through capillary walls. *Physiol. Rev.* 33: 387–423, 1953.
48. PETERSON, L. H. Peripheral circulation. *Ann. Rev. Physiol.* 19: 255–298, 1957.
49. REIN, H. Ueber Durchblutungsmessungen an Organen in Situ, insbesondere mit der Thermostromuhr. *Ergebn. Physiol.* 45: 514, 1944.
50. REMINGTON, J. W. Volume quantitation of the aortic pressure pulse. *Fed. Proc.* 11: 750–761, 1952.
51. RUSHMER, R. F. Anatomy and physiology of ventricular function. *Physiol. Rev.* 36: 400–425, 1956.
52. SCHAEFER, H. Heart. *Ann. Rev. Physiol.* 18: 195–224, 1956.
53. SARNOFF, S. J. Myocardial contractility as described by ventricular function curves; observations on Starling's law of the heart. *Physiol. Rev.* 35: 107–120, 1955.
54. SINN, W. Die Elastizität der Arterien und ihre Bedeutung für die Dynamik des arteriellen Systems. Akad. d. Wissensch. u. Literatur in Mainz, Wiesbaden: Steiner, 1957.
55. STADIE, W. C. Oxygen of arterial and venous blood in pneumonia and its relation to cyanosis. *J. Exper. Med.* 30: 215, 1919.
56. STARLING, E. H. *The Linacre Lecture on the Law of the Heart.* London: Longmans, Green, 1918.
57. STRAUB, H. The diastolic filling of the mammalian heart. *J. Physiol.* 40: 378–388, 1910.
58. STRAUB, H. In: *Bethe's Handbuch d. norm. u. pathol. Physiol.* 7: 247, 1926.
59. Symposium on the regulation of the performance of the heart. *Physiol. Rev.* 35: 90–168, 1955.
60. Symposium. Central nervous system control of the circulation, edited by L. W. Eichna and D. G. McQuarrie. *Physiol. Rev.* 40: Suppl. 4, 1960
61. Symposium on regulation of the cardiovascular system in health and disease. *Circulation* 21: 739–778, 1176–1192, 1960.
62. TIGERSTEDT, R. *Lehrbuch der Physiologie des Menschens.* Leipzig: Hirzel, 1897. *A Text-Book of Human Physiology*, translated by J. R. Murlin. New York: Appleton, 1906.
63. TIGERSTEDT, R. Die Geschwindigkeit des Blutes in den Arterien. *Ergebn. Physiol.* 4: 481–516, 1905.
64. TIGERSTEDT, R. *Physiologie des Kreislaufes.* (2nd ed.). Berlin: de Gruyter, 1921.
65. UVNÄS, B. Sympathetic vasodilator outflow. *Physiol. Rev.* 34: 608, 1954.
66. WETTERER, E. Die Wirkung der Herztätigkeit auf die Dynamik des Arteriensystems. *Verhandl. deutsch. Gesellsch. f. Kreislauffsch.* 22: 26–60, 1956.
67. WEZLER, K., AND A. BÖGER. Die Dynamik des arteriellen Systems. Der arterielle Blutdruck und seine Komponenten. *Ergebn. Physiol.* 41: 292–606, 1939.
68. WEZLER, K., AND F. SCHLUTER. Die Querdehnbarkeit isolierter kleiner arterien vom muskulären Typ. Akad. d. Wissensch. u. Literatur in Mainz, Wiesbaden: Steiner, 1953.
69. WEZLER, K., AND W. SINN. *Das Strömungsgesetz des Blutkreislaufes.* Aulendorf i. Wurtt.: Cantor KG., 1953.
70. WIGGERS, C. J. *The Pressure Pulses in the Cardiovascular System.* New York: Longmans, Green, 1928.
71. WIGGERS, C. J. *Physiology in Health and Disease* (5th ed.). Philadelphia: Lea & Febiger, 1949.
72. WIGGERS, C. J. *The Physiology of Shock.* New York: Commonwealth Fund, 1950.
73. WIGGERS, C. J. *Circulatory Dynamics.* New York: Grune & Stratton, 1952.
74. WOMERSLEY, J. R. *An Elastic Tube Theory of Pulse Transmission and Oscillatory Flow in Mammalian Arteries.* Wright Air Development Center, Tech. Rept. No. 56–614, 1958.

The historical development of cardiovascular physiology

CHAUNCEY D. LEAKE | *The Ohio State University, Columbus, Ohio*

CHAPTER CONTENTS

FROM THE TIME that humans started to think and to observe themselves and their surroundings, they have been interested in the way in which living things work. Of course we are mostly interested in ourselves: what makes us tick has been the subject of long centuries of search and research. Cross analogies between muscles and bones on the one hand, and levers and tackle on the other, must have early developed. Certainly analogies from levers and tackle were early applied to ideas on muscular motion, and it may very well have been that notions about muscle action suggested the development of various kinds of levers and pulleys. Certainly people must have thought hard how to devise ways whereby muscular work could be made easier. Analogies from human feelings were applied to the way in which forces in nature may work. Animistic ideas still color our language about the movement of the winds and waters. It took many long centuries before functional or physiological generalities could be tentatively expressed.

Cardiovascular function is central to an understanding of mammalian and human physiology. The history of this phase of intellectual advance is long and full of intense human interest. It also has had great practical significance in stimulating ways by which knowledge of the operation of the heart and blood vessels could be applied to practical medical affairs in the diagnosis, prognosis, prevention, and treatment of disease. It is also stimulating in a practical way to consider how our knowledge of the operation of the heart and blood vessels was obtained.

The first consistent comprehensive scheme to explain the manner in which animals work was developed by Galen, the great Greek physician to the Roman emperor Marcus Aurelius. His explanation, applicable to those living things we call "mammals," persisted for 1500 years. While it may have been the practical success of cinchona bark in "curing" fevers, which really overthrew Galenical scholasticism in the seventeenth century, it was the theoretical consequences of the demonstration of the circulation of the blood in animals, by William Harvey, that eventually removed the arbitrary Galenical system, and established modern experimental methods to make possible the science of physiology.

HARVEY'S PREDECESSORS

Through injury and warfare, with resulting wounds and bleeding, people even in primitive societies universally developed ideas at a very early time about the heart beat, and how warm blood is necessary for life. The relation of the pulse to the heart beat was vaguely appreciated in antiquity, and became formalized in such great static ancient cultures as the Chinese, the Hindu, and the Egyptian. These early notions on the

heart and blood were conventionalized, and remained unquestioned for millenniums.

Stone and Bronze Age cultures all over the earth were fully appreciative of the importance of blood. It was recognized as being the essential life factor in humans. Not only did injury and warfare contribute to vague notions about the primacy of the blood and heart, but also the deeply emotional factors associated with widespread human sacrifice must have profoundly influenced thought on the functions of the heart and the great vessels carrying blood from it. The awe-inspiring Aztec divination, based on whether or not the heart would continue to beat after being torn from the body by the powerful priests, certainly reveals to our sophisticated insight that the heart has automaticity. To the Aztecs, however, it was merely a magical indication that events might continue to go well: if it came from the body without beating, the future might be disastrous. Thus was the individual merely a part of the social milieu.

The change in heart action, under the influence of the emotions, which may be consciously felt, was probably the background for the ancient idea that the heart is the location of thought. The editorial writer of Genesis referred to "The thoughts of my heart." Even Aristotle (384–322 B.C.), the great Greek philosophizing founder of modern science, made this same mistake.

The old Chinese ideas regarding heart and blood vessels are expressed in Nei Ching, *The Yellow Emperor's Classic of Internal Medicine*. Here it is said "the heart influences the face and fills the pulse with blood. . . the heart is in accord with the pulse . . . the heart rules over the kidneys . . . the pulse is the storehouse of the blood . . . the viscera are in communication and bound to the heart, and the blood that is stored by the heart fills the pulse with the forces of life." There is much subsequent discussion of pulse lore. Some of this indicates the direct application of observations on the pulse to disease, "when the pulse is quick, and contains 6 beats to one cycle of respiration, then it indicates heart trouble; and when the pulse is large the disease becomes grave."

Among the Indus, Charaka and the surgeon, Susruta, both of whom flourished in the sixth century B.C., are reported as using the pulse at the wrist to give an indication of heart action.

The old Egyptian notions about the heart and blood vessels were the most sophisticated of those of ancient people, as far as we know, and were included in one of the great teaching texts, which has survived from around 1700 B.C. In the Ebers Papyrus, which recently has become so well studied, there is a section, on sheets 99 to 103, entitled "The beginning of the secrets of the physician: knowledge about the movements of the heart."

This starts with noting the relation of the heart to the pulse, indicating that in examining the patient, a physician applying his fingers to the arms or legs, actually examines the heart, for "all the limbs possess its vessels, so that the heart speaks from the vessels of every limb." There follows much detail on 2, 4, and 6 vessels which were thought to go from the heart to each part of the body. Much of this seems to be annotations and glosses, made by the scribe in reference to some lost writing which apparently was being copied. The material in general suggests etiological ideas based on Whdw, the principle of putrefaction and excrements, accumulation of which was thought to cause disease. This etiological notion has been well analyzed by Robert Steuer.

There is nothing to suggest that the old Egyptians had any notion of heart action in relation to blood movement. There is, however, the explicit statement that the breath which enters the nose goes into the heart from the lung. This may have influenced later Greek and Alexandrian writers to give background for the Galenical scheme, part of which was based on the observation that the arteries when opened after death are empty, and thus were thought to contain air.

Egyptian culture passed gradually into the Mediterranean area, and profoundly affected the later development of Greek culture. Greek medicine seems in large part to have developed from old Egyptian medicine, not only with regard to the great health temples, but also with respect to technical ideas and procedures. At the large health temple school at Kos, Hippocrates (460–375 B.C.) developed the concept that health depends upon a balance of four humors: blood (hot and moist, most alive), phlegm (cold and moist), yellow bile (hot and dry), and black bile (cold and dry, least alive). Excesses were thought to determine temperaments, which still come to us under the terms sanguine, phlegmatic, choleric, and melancholic. The primacy of blood in the humoral pathology was unquestioned.

Systematic work in biology was first undertaken by Aristotle (384–322 B.C.), the great pupil of Plato, and the tutor of Alexander the Great. Realizing that effective study could be aided by orderly arrangement of material, he made the first organized classification for animals, recognizing the relation of form and

function, thus beginning comparative anatomy and physiology. He also started studies on embryology, noting the developing chick, and observing that the first thing to show life in the developing organism is the beating heart. Centuries later his work on generation and on the heart influenced William Harvey.

The study of human anatomy and physiology seemingly began with Erasistratus, in Alexandria, in the third century B.C. He first observed that arteries are empty after death, and concluded that they must carry air. He indicated that it is brought in the form of "vital spirits" from the heart to all parts of the body.

The work of Erasistratus was systematically developed by Galen (131–201 A.D.), a brilliant Greek physician from Pergamon, who founded experimental physiology, and was a resounding success as a practicing physician in Rome. Actually Galen showed that arteries contain blood, but he was so impressed by the general theory which he had in mind, that he did not grasp the significance of his observation.

According to the Galenical tradition, elaborated over many centuries, body function proceeds from *a*) "coction" of food in the stomach, where it is prepared for absorption by ducts from the intestines for transfer to the liver; *b*) here it is made into blood containing "nutritive spirits" necessary for nourishing all parts of the body, and distributed thereto by veins; *c*) some of these nutritive spirits, passing through pores in the septum of the heart, are combined in the left chamber of the heart with air coming from the lungs, to form the "vital spirits," necessary for life and heat in all parts of the body, to which they are distributed, through boiling over of the heart, by arteries; and *d*) some of these vital spirits, permeating the cribriform plate, are converted in the brain into "animal spirits" necessary for motion in every part of the body, to which they are distributed by nerves.

This logical scheme, so easily correlated with the Greek humoral pathology, became traditional dogma during the Middle Ages, and various details were elaborated by Arabic and medieval commentators. Galenical generalities on the cardiovascular system were important factors in justification of scholastic dogma in medical practice. The Greek humoral pathology, probably elaborated from earlier Egyptian concepts, gave the rationale for diagnosis, prognosis, and treatment. Health consisted in the balance of the humors; disease resulted from an excess or deficiency of any one. Sensible treatment consisted in removing the excess, or in making up the deficiency. In a plethora of blood, a vein should be opened and the excess removed. In a deficiency, the patient should receive drugs which have the qualities of blood; that is, heat and moistness,—like warm rusty water, or warm red wine. It was the abuse of blood-letting, with the obvious debilitating effect of blood loss even in "sanguine" men, which gradually raised doubts about the validity of Galenical cardiovascular detail.

Jean Fernel (1497–1558), the keen Parisian physician, began the questioning of scholastic tradition by opposing routine blood-letting. Ambroise Paré (1510–1590), the great humanistic surgeon to the French kings, must have realized some of the fallacies of Galenical cardiovascular theory as he pondered the character of war wounds and reintroduced ligatures for controlling blood loss from ruptured vessels.

Meanwhile, there gradually accumulated knowedge of the cardiovascular system as based on the occasional and hurried dissection of human cadavers, made legally available for teaching as part of the formality of execution of criminals. Jacopo Berengario da Carpi (1470–1550), professor of anatomy at Bologna, described heart valves in his *Isagogae*, which appeared in 1522. He followed the course of arteries by injecting them with warm water, and he noted cardiac dilatation. Guido Guidi (1500?–1569), who taught at Pisa, was skeptical of the scholastic teaching of pores in the septum of the heart. Valves in the veins were noted by Carolus Stephanus (Estienne) of Paris (1500–1564), and even by that staunch supporter of Galen, Jacques Dubois, or Sylvius (1478–1555), the great Parisian teacher. Neither had much of an idea of the possible function of these tiny structures.

That observant dissector, Leonardo da Vinci (1452–1519), distorted his beautiful anatomical drawings to fit the scholastic tradition. However, he did not show the pores in the septum of the heart as going directly through from one ventricle to another. Leonardo's drawings and notes indicate his interest in the function of the cardiac valves. They also show his appreciation of eddy formation in blood flow.

It was essentially the dogmatic character of this doctrine which Harvey attacked so successfully in the seventeenth century. Meanwhile, however, certain changes and corrections in it had been recorded, but not for general and public use. There was such a weight of opinion for the conventional Galenical tradition, and it was so logical and in accord with churchly doctrine, that any modification of it was simply neither noticed nor comprehended.

While Galen in his great physiological schema had

clearly indicated the way in which the heart valves work, he had not carried out the implications of his observations. The authority of Aristotle was unquestioned as to the function of the heart in supplying vital spirits to the body, by the boiling of nutritive spirits with air, and the lungs were considered to be chiefly for the purpose of cooling the blood. This notion seems to have been explored more fully by the Arab physician, Ibn-al-Nafis (d. 1289), who described the pulmonary circulation anatomically, and indicated its function in cooling the blood, putting air into it, and removing "fuliginous vapors." But this work seems to have been little appreciated until it was resurrected by Mohyi el Dinel Tatawi for his Breisgau thesis in 1924, and analyzed by Max Meyerhof in 1933.[1]

It also is strange that the remarkable drawings and notations of Leonardo da Vinci on the heart and vessels seem to have had so little influence in their time. These not only indicate the direction of blood flow through the heart valves, but also show the eddies and movement of blood in the large arteries. Leonardo himself was so bound by tradition that he could not see the truth under his own eyes, skilled hydraulic engineer though he was. It may be, however, that his anatomical drawings had more influence than we realize.

In his great description of the structure of the human body in 1543, Andreas Vesalius (1514–1564) raised doubt about the idea that there are tiny pores in the septum of the heart. Leonardo had shown the pores in the septum, but not as though they go right through the septum. This was the question raised by Vesalius. Now Vesalius was teaching at Padua, not far from where Melzi, the devoted pupil of Leonardo, was keeping the master's drawings, and showing them on occasion to friends or visitors who might be interested. Certainly the existence and value of these manuscript drawings must have been well known around the area. Indeed it is not impossible that Vesalius was stimulated to illustrate his description of the structure of the human body in the grand manner suggested by the Leonardine anatomical drawings. Later, around 1600, when the cultured Fabricius (1537–1619) had built the anatomical theater at Padua that Vesalius dreamed about, he had as his pupil working with him on the development of the chick, the young Englishman, William Harvey. Could it be that one holiday they went over to the old Melzi villa to look at Leonardo's anatomical sketches?

It is intriguing to speculate on how Leonardo's great treasure of anatomical notes came to England. Perhaps Harvey, when traveling with Lord Arundel to Vienna in 1636, learned that the Melzi heirs were dispersing the Leonardo drawings. Harvey came over to Italy, and was quarantined in Venice for a couple of weeks, when he had to rush back to Vienna. For what had he made this sudden trip? Later when Lord Arundel was in Spain, he acquired the Leonardo anatomical sketches, and had them sent hurriedly to Windsor Castle, where they stayed. How was it that he realized their value, and secured them for England? Could it have been that Harvey had seen them while studying at Padua, and that they had given him a hunch or two about the heart valves?

It is as difficult to assess the influence of Miguel Serveto (Servetus) (1511–1553) in regard to the pulmonary circulation as it is to appraise the effect of Leonardo's anatomy on his contemporaries. Servetus was a stormy figure; a fellow student at Paris with Vesalius, he had written on medicinal preparations, and then become involved in churchly arguments. He incurred the suspicion of the authorities when he wrote on the errors of the Trinity. Driven by some inner conviction he pursued the matter in a volume, *Christianismi restitutio*, which he realized was too much for the Roman Church. He took the page sheets to Geneva, hoping to find protection with another fellow student from Paris, the reformer John Calvin. Calvin, however, tried and condemned him for heresy, and he was burned in 1553, supposedly with all copies of the work. Three escaped the flames. Amazingly the book contains a concise description of the lesser circulation. It is doubtful that his notions could have been appreciated.

In the anatomy of Realdus Colombo (1516–1559) published the year of his death, there is again a con-

[1] E. D. Coppola (*Bull. Hist. Med.* 31: 44–77, 1957) suggests that Andrea Alpago (died 1521 after studying 30 years in the Near East) had translated Ibn-al-Nafis, and that R. Columbo (1516–1559) and his pupil, Juan Valverde (fl. mid-16th century), may have known of the translation through Andrea's nephew, Paolo (died 1553?), who had studied at Padua. Actually Valverde's volume (*Historia de la composición del cuerpo humano*, Rome, 1556) contains a description of the pulmonary circulation probably derived from Columbo, although published before Columbo's *De re anatomica* appeared in 1559. An excellent study of Ibn-al-Nafis has been made by E. E. Bittar (*Bull. Hist. Med.* 29: 352–368, 429–447, 1955). Both Coppola and Bittar were Yale pupils of John F. Fulton (1899–1960), who stimulated so many to do so much in the history of physiology and medicine. In his characteristically keen manner, C. D. O'Malley (*J. Hist. Med.* 12: 248–253, 1957) analyzes the evidence regarding the anti-Galenical ideas of Ibn-al-Nafis as appearing in Andrea Alpago's *Avicenna philosophi*, as published by Paolo in Venice in 1546.

cise description of the pulmonary circulation and also of the simultaneous beat of the two ventricles of the heart. Harvey quotes Colombo, and also credits him with claiming that blood mixes with air in the lungs instead of in the heart as the Galenical doctrine postulates. However, Colombo did question the dogma about pores in the cardiac septum. This was beginning to be a crucial problem for the validity of scholastic cardiovascular theory. Actually Galen may have seen the Thebesian vessels, named for Adam Christian Thebesius (1686–1732), which however drain venous sinuses from the coronary vessels. The error in the interpretation of these endocardial openings was paramount in scholastic dogma, and, when fully exposed, led to its repudiation.

Andrea Cesalpino (1519–1603) raised the question of blood circulation academically, but decided against it on the basis of Galenical theory. Yet he showed the centripetal flow of blood in veins, without however impressing his contemporaries or his followers. He noted the differences in structure between the pulmonary arteries and the pulmonary veins with reflections on their function, in comparison with systemic arteries and veins. He showed connections between portal veins and the vena cava, and described the reciprocal relations between cardiac contraction and arterial dilatation. Further, he raised the question of possible communications between arteries and veins.[2]

Meanwhile, critical study was gaining a following in anatomy. Gabriele Falloppio (1523–1562), a pupil and successor of Vesalius at Padua, corrected his teacher's account of the course of cerebral arteries, and described a nerve plexus in the heart. Giulio Cesare Aranzio (1530–1589), another of the great Bolognese anatomists, noted the fetal ductus arteriosus and ductus venosus. He also observed the *corpora arantii* in heart valves. The fetal heart was further described by Arcangelo Piccolomini (1525–1586), with an account of the foramen ovale. Piccolomini correctly ascribed the arrangement of valves in the jugular veins, and in veins in the limbs, to the function of preventing reflux of blood on change of position. Thus there was much in the state of knowledge at the time to prepare the way for such a conceptual synthesis as Harvey achieved.

[2] In discussing Cesalpino's studies, S. Peller emphasizes how Harvey's quantitative reasoning led him flashingly to go beyond Cesalpino's cautious approach to the irrefutable demonstration of blood circulation (*Bull. Hist. Med.* 23: 213–235, 1949). However, W. Pagel shows clearly how the ancient Aristotelean doctrine of circular motion was part of the philosophical climate of the late Renaissance and greatly influenced both Cesalpino and Harvey. The symbol of a circle was applied to blood movement by Plato (427–347 B.C.), and elaborated by Giordano Bruno (1548–1600); it was applied scholastically to a cyclical movement of the heart by Thomas Aquinas (1225?–1274). Indeed, as F. Boenheim suggests (*J. Hist. Med.* 12: 181–188, 1957), the circular philosophy was implied in very ancient Chinese ideas on the similarities between motions in the macrocosm (the universe) and the microcosm (man).

HARVEY'S ACHIEVEMENT

A great medical teacher was Girolamo Fabrizzi (1537–1619), who attracted students from all Europe to his anatomical demonstrations in Padua. Some, like the keen young Englishman, William Harvey (1578–1657), helped him with experiments on the developing chick and with his dissections of the valves of the veins. Long he puzzled over the possible function of these structures. Perhaps he passed his curiosity to his famed pupil. Harvey had returned to London when his master's book, *De venarum ostiolis*, appeared in 1603. Long afterward Harvey acknowledged the inspiration received from Fabrizzi. He must have been considering the complicated matter of blood flow by the time he was appointed Lumleian Lecturer to the Royal College of Physicians in 1615, for his manuscript notes for the first "visceral" lecture in 1616, given the very month Shakespeare died, raised the question of the systemic circulation, with preliminary observations to justify it.

It was not until twelve years later that Harvey published his famed *De motu cordis* from an obscure Frankfurt printer, William Fitzer. It is a remarkable item of only 70 pages comprising a preface, introduction and 17 chapters. It not only established the central principle of modern physiology and indeed of medicine, but it also demonstrated the most effective method of procedure in the natural sciences: *a)* careful and accurate observation and description of a phenomenon; *b)* a tentative explanation of how the phenomenon occurs; *c)* a controlled testing of the hypothesis, and *d)* conclusions based on the results of the experiments. In addition, he introduced the method of quantitative reasoning which forced validity of the conclusions.

For all the greatness of the achievement, the effort may be severely criticized in the light of our present practices, as Wiggers has done. However, Harvey was a pioneer and had no example to follow. In spite of his occasional fumbling logic, in spite of his failure to deal effectively with the pulmonary circulation, and

in spite of long delays in accepting his conclusions or in making practical applications of them in medical practice, Harvey's 1628 publication really began modern physiology and medicine.

As pointed out in the preface to my tercentennial translation, the differences in Harvey's style in the book suggest that it was written at different times. The introduction, in critique of the Galenical dogma, is vigorous and youthful. The first chapter, however, apologizing for the effort, has the meditative calm of middle age. The last three chapters seem like afterthoughts: they are appendages trying to reconcile opposing viewpoints without adequate data. In chapters two to five there is the careful analysis of observed phenomena; in chapters ten, eleven, and thirteen there are offered experimental results to test the proposed hypothesis, while chapters nine, ten, and thirteen give quantitative reasoning to prove the brief conclusion offered in chapter fourteen. Chapter eight offers the hypothesis, while the last three chapters are largely speculative. The sixth and seventh chapters, on the pulmonary circulation, are puzzling. Harvey seems to have taken it for granted, as Donald Fleming so well argues (*Isis* 46: 319–327, 1955). There is discussion of the comparative and embryological aspects of the matter, and then an interesting return to the authority of Galen as evidence. Harvey really was interested in demonstrating the circulation of the blood in general in all animals, and the pulmonary circulation may have seemed unessential to him in this regard.[3]

Apart from measuring blood volume by drainage in sheep and probably some other mammals, Harvey made no actual measurements in regard to circulation. Yet he used quantitative reasoning in a most effective way to prove his point. First, he considered the amount of blood put out by the heart in a single beat, and then showed that the amount which would be forced out of the heart in a relatively short while, say an hour, would be much more than could be in the body at any one time, as he knew from having measured blood volume. His figure here, of about one-tenth body weight, is fair. In the interesting illustrations to the book, which are styled like those illustrating Fabrizzi's work on the venous valves, the function of the valves is made clear, and again there is demonstration of the fact that by milking an arm vein rapidly, one can have pass under one's finger in not too many minutes more blood than there is in the whole body. Obviously it must be the same blood going around in a circulation.

Lack of satisfactory application of Harvey's demonstration to practical medicine made it relatively unappreciated for more than a century, except as a matter of scientific interest. Indeed, William Welch, wise Nestor of American medicine, once surmised that the practical demonstration of Thomas Sydenham (1624–1689) of the curative effect of cinchona bark in fever, regardless of any connection with accepted dogma, had a greater influence in overthrowing Galenical tradition than did Harvey's demonstration of the circulation.[4]

HARVEY'S FOLLOWERS

Actually Harvey's demonstration of the circulation was not complete: he had to postulate capillary anastomoses between arteries and veins; he could not find them since he had no microscope. They were found by Marcello Malpighi (1628–1694) in 1661 while studying the lungs of frogs, and Antonj van Leeuwenhoek (1632–1723), who first described workable microscopes, also observed the capillaries. These observations may have revived interest in Harvey's demonstration from the standpoint of practical application.

Transfusions were attempted, but failed tragically, probably because of what we now recognize as in-

[3] According to F. J. Cole (*J. Hist. Med.* 12: 106–113, 1957), Harvey indicates that he studied 128 types of animals, from zoophytes, through worms, crustacea, insects, and various kinds of vertebrates, to many species of mammals.

[4] Nevertheless, Harvey's demonstration was promptly accepted during the 17th century as a significant scientific contribution for teaching. This is shown by the "first physiological textbook," *De homine figuris*, Leyden, 1662, of René Descartes (1596–1650), and by the reception of Harvey's work in Italy, as described by W. Pagel & F. N. L. Poynter (*Bull. Hist. Med.* 34: 419–429, 1960), and even in America, as pointed out so well by F. Guerra (*Bull. Hist. Med.* 33: 212–229, 1959). An early experimental confirmation of Harvey's findings was written in 1652 by Henry Power (1623–1688), but has only recently been published from manuscript (F J. Cole, *J. Hist. Med.* 12: 291–324, 1957). By an interesting coincidence, a contemporary poem published in 1656 by John Collop (1625–post 1676) in praise of Harvey and the circulation, was simultaneously rediscovered by F. N. L. Poynter & C. Hilberry (*J. Hist. Med.* 11: 374–411, 1956). E. Weil (*J. Hist. Med.* 12: 167–174, 1957) lists 69 publications referring to Harvey's work, from its initial appearance, by Robert Fludd (1574–1637), in 1629, to 1656, the year before Harvey died, when Collop's poem appeared. As L. R. O. Agnew indicates, Harvey's report was so intellectually stimulating to his contemporaries that it could result in another rhapsodic poem from the Bishop of Chichester, Robert Grove (1634–1696), published in 1685 (*Bull. Hist. Med.* 34: 318–330, 1960).

compatible bloods. Successful transfusion, now so standard a procedure in surgery, had to wait until Karl Landsteiner (1868–1943) showed iso-agglutinins in human blood in 1900, an observation which gradually led to practical blood grouping and blood banks. The seventeenth century efforts at transfusion, however, had one practical result which Harvey foresaw: Sigmund Elsholtz (1623–1688) showed that drugs could be directly injected into the blood stream to produce the effects desired. This observation also waited nearly two centuries before being used in medical practice.

One of the staunch scientific supporters of Harvey's work was Jean Pecquet (1622–1674). In his anatomical studies at Paris he described the thoracic duct, the *receptaculum chyli*, and the connections to the venous system. This observation began the clarification of the relation of the lymphatic system to the general circulatory system. Appearing in 1651, this report must have been singularly gratifying to Harvey as an example of the scientific stimulus afforded by his efforts.

Although Harvey's conclusions implied the muscular activity of the heart in its contractions, the anatomical recognition of the muscular character of the heart was detailed by the Danish priest-scientist, Niels Stensen (1638–1686). Leeuwenhoeck correctly pictured the peculiarities of cardiac muscle, but without appreciating their significance. Giorgio Baglivi (1668–1706) of Rome differentiated smooth from striated muscle, but the correct interpretation of the branched muscle layers of the heart, with their striations, had to wait for the keen mind of Albert von Kölliker (1817–1905) of Zurich and Würzburg. This was further well elucidated by Franklin P. Mall (1862–1917), of the Johns Hopkins Medical School, Baltimore, who demonstrated the scroll-like arrangement of the ventricular musculature. He showed the presence of two spiral bands, one going from the tricuspid or sinus part of the heart to the apex of the right ventricle, and the other going from the aortic and mitral region to the apex of the left ventricle. These spiral bands, in contracting, produce the characteristic motion of the heart, which Harvey had so well described.

Two scientifically oriented Cornishmen, Richard Lower (1631–1691) and John Mayow (1643–1679), began the train of studies which led to our understanding of the respiratory function of the blood and circulation. Lower found in animals that dark venous blood injected into an insufflated lung becomes bright red, and concluded the blood absorbs something from the air in the change. Mayow noted that this occurs when venous blood is shaken with a gas obtained from niter. This gas we now call oxygen. Lower also studied cardiac mechanics and realized the muscular character of cardiac contraction. He found anastomoses between coronary arteries by injection, and he illustrated his famed *Tractatus de corde* (London, 1669) with superimposable flaps to show the arrangement of heart valves. Mayow recognized heat production in muscle contraction. He also noted dilatation of the right ventricle in mitral stenosis. This was a start in the understanding of the consequences of cardiac malfunction.

The great Dutch biologist, Jan Swammerdam (1637–1680), clinched the Harveian problem of anastomoses between arteries and veins by hot wax injections. He also tried to measure the movements of muscles and the heart by simple plethysmographic methods. He found that muscles do not increase their volume in contraction, and thus refuted the belief of Giovanni Borelli (1608–1679) of Pisa that a supposed nerve fluid enters a muscle to swell it in contraction. Swammerdam noted (confirming Harvey) that the heart is smaller in systole than in diastole, in proportion to the blood ejected.

At the beginning of the eighteenth century, Raymond Vieussens (1641–1715) of Montpellier correctly described the course of the coronary vessels in relation to the structure of the heart, and noted the valve in the large coronary vein as well as coronary sinus. This is basic to an appreciation of coronary factors in cardiac malfunction. Vieussens also discussed the back-pressure symptoms in mitral stenosis. In his comments on cyanosis, he observed that it might occur when there is no mixture of arterial and venous blood, and thus suggested our concept of anoxia.

The first really significant advance in our knowledge of the circulation occurred more than a century after Harvey's demonstration. In 1733, the Reverend Stephen Hales (1677–1761), conventional vicar of Teddington, reported on his amazing direct measurement of blood pressures in a variety of animals including horses. How he managed to handle the animals is a mystery, but he succeeded admirably, and established the significance of the pressure relations in arteries and veins. However, it was almost another century before Jean L. M. Poiseuille (1799–1869) made an effective follow-up in 1828 with his hemodynamometer showing blood pressure changes in relation to respiration and the extent of arterial dilation with each heart beat.

The real scientific significance of Hales's work is in

its quantitation. He measured blood pressure for the first time and showed its variation with heart beat and respiration in the arteries, and its relatively low level in veins. He estimated the rate of circulation, and the slow velocity of venous blood. Further, by using wax injections, he estimated the volume of cardiac chambers and of the aorta. By his direct method of measurement, he estimated systolic blood pressure in humans to be around 7½ feet of blood, which is a reasonable approximation as balanced against atmospheric pressure only. Practical application of these observations had to wait a century until Scipione Riva-Rocci (1863–1937) developed the mercury sphygmomanometer (1896) which is the principle for our current clinical instruments. It is interesting that Hales's "haemastaticks" probably developed from his earlier studies on "vegetable staticks" in which he ingeniously measured sap pressure in plants. To minds that are intelligent and imaginatively curious, all living things can be found to yield associative concepts.

Steadily accelerating progress now came in our knowledge of the functional activity of the cardiovascular system. Much was sparked by the realization of the work of Antoine Lavoisier (1743–1794) who before his death as a martyr of the French Revolution had founded modern chemistry by his quantitative studies on the significance of oxygen, and who showed the real relation between respiration, the oxygen transport of the blood, and bodily heat formation. This came more than a century after Robert Boyle (1627–1691) studied the function of air in respiration and combustion, and after Lower and Mayow showed that the change from venous to arterial blood in the lung is due to something absorbed from air.

The great and handsome teacher François Magendie (1783–1855) showed the importance of the blood in transport of nutriments, and his pupil James Blake (1815–1893), the brilliant Englishman who migrated in the gold rush to California, measured circulation time. Magendie's greatest pupil was Claude Bernard (1813–1878) who discovered vascular nerves and the functions of vasoconstriction and vasodilation in regulating blood supply to the various parts of the body.

German precision studies on the cardiovascular system began with Ernst Weber (1795–1878) and his brother Eduard (1806–1871) who measured the pulse wave in 1825. Carl Ludwig (1816–1895), the superb self-effacing teacher, promoted rapid progress by his invention of the kymograph for recording blood pressure changes under varying conditions. Karl Vierordt (1818–1884) introduced sphygmographic methods for indirectly measuring blood pressure, thus laying the basis for practical clinical applications. He showed the influence of blood volume, pulse rate, and respiration on the rate of blood flow, while Ludwig followed up an observation of Harvey's in devising methods for perfusing organs, including the heart.

The practical applications of Harvey's work to medicine began with the recognition of pathological details involving the cardiovascular system. Giovanni Lancisi (1654–1720) laid the basis for cardiac pathology with his observation of valvular lesions and of cardiac dilatation in correlation with symptoms of disease. This was extended by Giovanni Morgagni (1682–1771) in describing mitral stenosis and heart block. In France, Raymond Vieussens (1641–1715) had already noted the circulatory effects of aneurisms and the symptoms of aortic regurgitation.

When William Withering (1741–1799) introduced digitalis for cardiac dropsy in 1785, he greatly advanced the practical applications of Harvey's work on the heart and circulation by showing that something could be done when the cardiovascular system is not functioning properly. But he did not differentiate between cardiac and renal dropsy. This was done by Richard Bright (1789–1858) in 1827, and further ramifications of the applications of Harvey's work began. These led to the realization of the effects of "hardening of the arteries," and later to various aspects of hypertension which we are still vigorously exploring.

The clinical significance of blood pressure, as a ready guide to diagnosing disturbances of the cardiovascular system, led to systematic efforts to analyze the factors involved. This was best done by J. R. McLeod (1876–1935) in the first edition of his famed text on physiology, which appeared in 1920. Here he well surveyed the five factors which control blood pressure: *1*) the pumping action of the heart, as dependent on its rate and output per beat; *2*) the peripheral resistance offered to blood by the various parts of the circulation, with its balanced nervous and chemical control; *3*) blood volume, and its variations under varying conditions; *4*) blood viscosity and its variations, and *5*) the elasticity of blood vessel walls, with their variations especially with age. Harvey had vaguely anticipated many of these factors, and it is remarkable how slowly they were studied in relation to the practical significance they have in clinical

conditions. We still have great difficulty estimating the volume output of the heart.

Toward the middle of the nineteenth century the acceleration of scientific knowledge about the heart and circulation increased markedly. The Webers discovered the cardio-inhibitory function of the vagus, and Étienne Marey (1830–1904) showed a relationship between blood pressure and cardiac action. Albert Bezold (1836–1868) discovered the accelerator nerves to the heart, and Johann Czermak (1828–1873) slowed the heart by pressure near the carotid sinus. Here then was the background for much recent and current study on the balanced functions of the autonomic nervous system and of the significance of the carotid sinus in regulating the circulation. Chemical factors involved were not appreciated until the twentieth century studies of Walter Cannon (1871–1945) which opened the way for the concept of adrenergic factors, and of Otto Loewi (b. 1873) which prepared the way for the idea of cholinergic influences.

When the neck of a mammal is compressed around the carotid arteries, the animal becomes drowsy. This was known to the ancients. Indeed this procedure was sometimes used in antiquity to produce a kind of anesthesia, and the carotid arteries were known as the "arteries of sleep" (the word "carotid" is derived from a Greek word meaning "deep sleep"). It is amazing that this important phenomenon was not systematically studied until recently. Rufus of Ephesus, a Greek physician at the beginning of our era, believed the phenomenon was due to pressure on nerves near the carotid arteries. No one commented further until Heinrich Irenaeus Quincke (1842–1922) showed that pressure on the carotids produces slowing of the heart. He thought this was caused by stimulation of the vagi. The baro-receptor reflex function of the carotid sinus was described by H. E. Hering in 1924. Then the phenomenon was vigorously studied by the great Nobel laureate Belgian physiologist, Corneille Heymans, and his pupils. They described full details of chemo- and baro-receptor reflexes of the cardiovascular system, and have beautifully summarized their investigations.[5] Many of these were based on skillful cross-circulation experiments which had been devised by Professor Heymans' father, Jean-François Heymans, who founded the renowned pharmacological institute in Ghent, and the *Archives Internationales de Pharmacodynamie et de Therapie*.

[5] C. Heymans & E. Neil, *Reflexogenic Areas of the Cardiovascular System*. London: Churchill, 1958, 279 pp.

Meanwhile Adolph Fick (1829–1901) had described the basic principle for estimating cardiac output, and John Scott Burdon-Sanderson had observed electrical action currents in heart contractions and had recorded them. This was developed by Augustus Waller (1856–1922) and brought to the high pitch of current electrocardiography by the string galvanometer of Willem Einthoven (1860–1927). The clinical applications of these great advances were promptly made by James Mackenzie (1853–1925) and Thomas Lewis (1881–1945). The functional importance of the capillaries was explored by August Krogh (1874–1949) with prompt clinical application again by Thomas Lewis.

While quantitative analysis of blood gases had been made in 1837 by Heinrich Magnus (1802–1870), it was Eduard Pflüger (1829–1910) who showed the respiratory changes which occur between blood and tissues as the blood circulates. The respiratory function of the blood in circulation was fully explored by Joseph Barcroft (1872–1947), with momentous consequences for current studies on aviation and space physiology. This field had been opened by the pioneering work of Paul Bert (1833–1886), although it took a couple of generations to catch up with the importance of what he showed.

Both as a skilled comparative physiologist and as a pioneering embryologist, Harvey had been fascinated by the problem of the origin and conduction of the heart beat. He had observed the beginning of the beat in the embryonic chick, and he had carefully analyzed, as well as he could with his naked eyes, the spread of the contraction over the adult heart. It was not until two centuries had passed, however, that Hermann Stannius (1808–1883) analyzed by means of his famed ligatures the automaticity and rhythmicity of the various parts of the heart, with the beat apparently originating at the sinus node. Walter Gaskell (1847–1914) investigated the nerve supply to the heart, while Wilhelm His, Jr. (1863–1934) and Albert Kent (1863–1945) showed the function of the auriculo-ventricular bundle in bridging contractions from the auricle to the ventricle. The problem of the origin and conduction of the heart beat was analyzed in a classic paper in the first issue of *Physiological Reviews* (1921), by my revered teachers, Walter J. Meek and J. A. E. Eyster of Wisconsin. Certain aspects of this matter led to a realization of the importance of venous pressure in regard to filling the heart. Harvey had indicated the existence of venous pressure factors in cardiac filling.

The state of knowledge on cardiovascular physiology at the beginning of the twentieth century was admirably summarized with full documentation by Leonard Hill (The Mechanism of the Circulation of the Blood, in *Text-Book of Physiology*, edited by E. A. Schäfer, Edinburgh: Y. J. Pentland, 1900, vol. II, pp. 1–168). In the same classic compendium, W. H. Gaskell summarized his own studies, in relation to other pertinent contributions, on *The Contraction of Cardiac Muscle* (ibid. pp. 169–227), which finally established the validity of the myogenic theory of cardiac contractility. The way had been paved in part in Ludwig's laboratory, where Henry P. Bowditch (1840–1911) of Boston had demonstrated the all-or-none principle, and had shown that the frog-heart's apex, devoid of ganglion cells, can beat rhythmically. Another of Ludwig's famed pupils, Robert Tigerstedt (1853–1923) of Helsinki, extended Gaskell's work, and closed his own career with a monumental review of cardiovascular physiology (*Physiologie des Kreislaufes*. Berlin: de Gruyter, 1921).

PROSPECT

It is clear that Harvey started something. However, the time was ripe for him. His demonstration about blood circulation was clearly in the air. The surprising thing is that it took so long to realize the practical consequences of his little 1628 publication. This historical survey has merely touched some of the high points in the gradual accumulation of our verifiable knowledge about the mammalian cardiovascular system, before Harvey's time, and after him, until the history merges into our current studies. The remainder of this *Handbook* will indicate not only the amazing extent of our present-day investigations in cardiovascular physiology, but also how each advance has been made possible by a long succession of what has gone before. Always both the stimulus and the goal of this effort have been the same: to find what verifiable and agreed-upon factors determine the normal activity or malfunction of the system, so that human cardiovascular disease can be understood and handled, and perhaps prevented. In this respect cardiovascular pathology is to be considered as abnormal cardiovascular physiology, and historically the two disciplines have gone together admirably. That this joint venture will continue is now well assured.

Currently we are making amazing advances in the understanding of cardiovascular physiology: the brilliant but slowly acknowledged accomplishment of Werner Forssmann (b. 1904) in catheterizing his own heart and opening the way for the accurate diagnosis of cardiac anomalies; the amazing development of successful cardiac and vascular surgery, after the development of effective anesthesia, asepsis, and blood transfusion; the detailed analysis of the cardiac cycle, with the pressure and electrical changes that accompany each step, all giving direct improvement in diagnosis and management of cardiovascular disease, all of this topped by the magnificent appreciation by the American public of the importance of supporting scientific study further. Here is a continuing climax of progress stemming directly from the irascible seventeenth century Englishman, William Harvey.

How far in the future did he project his thoughts when he was writing, or traveling, or studying with his secret feminine companion in his hidden retreat, or dissecting and experimenting whenever he could? How far ahead can we project our thoughts, visioning what the future may hold in our knowledge and control of our hearts and blood vessels? It is a long way from the emotional reactions of the writer of Genesis, who believed, as did Aristotle, the wisest of the ancient Greeks, that the heart was the seat of thought, to our modern sophistication in being increasingly able to manage the most difficult and obscure of cardiovascular disorders; but the path goes to Harvey, and from him it has become a great highway of knowledge and communication. Harvey painted his picture of the heart and circulation in bold, simple, and very broad strokes: since his time we have merely been filling in the more obvious details with more precise and delicate lines. The masterpiece, however, is still Harvey's.

BIBLIOGRAPHIC NOTE

The foregoing account of the development of knowledge about the vertebrate cardiovascular system deals mainly with physiological aspects. Yet pathological factors have often entered into the studies concerned. This is nicely illustrated in the well-devised volume prepared by F. A. Willius and T. J. Dry (*A History of the Heart and Circulation*, Philadelphia: Saunders, 1948, 473 pp.). Useful chronological appendices consider anatomy, aneurysm, cardiac arrhythmia, cardiovascular diagnostic signs, congenital malformations, coronary vessels and their diseases, electrophysiology and electrocardiography, endocardium and its diseases, heart block, paroxysmal tachycardia, pathology of the heart and circulation (in general), pericardium and its diseases, physiology of the heart and circulation, pulse, surgery of the heart and vessels, symptoms of diseases of the heart and circulation, and therapy of cardio-

vascular conditions. All can be shown to be interrelated. Yet always the successful practical clinical advance comes as a result of the wise application of demonstrable scientific fact and principle. Reciprocal feed-back keeps the two parts of the system in acceleration.

Specific bibliographic reference to the major contributions to knowledge of the cardiovascular system can readily be obtained from L. T. Morton's *Medical Bibliography* (London: Grafton & Co., 1954, 2nd ed., 668 pp.). This lists 106 "classic" contributions to knowledge of the anatomy and physiology of the cardiovascular system and of the heart. Many other pertinent references occur under various other categories, chiefly in reference to diseases.

A special comprehensive analysis has been made by K. D. Keele on the studies of *Leonardo da Vinci on Movement of the Heart and Blood* (Philadelphia: Lippincott, 1952, xviii + 142 pp., 68 pl.). It is pointed out that Leonardo's work on the mechanism of the heart was shaped by criticism of Galen, a mechanistic theory of life, and an analogy between the macrocosm and microcosm. These philosophical ideas also shaped Harvey's work, but they were implemented powerfully by comparative observation and quantitative reasoning.

There is much bio-bibliographical material on Servetus. The classic is by Sir William Osler (*Johns Hopkins Hosp. Bull.* 21: 1–11, 1910). H. Tollin pioneered in studying Servetus (*Jena:* H. Dufft, 1876), and was followed by R. Willis (*Servetus and Calvin.* London: H. S. King, 1877).

For Harvey and his great study, special bibliographies have been prepared. The most important of these is by Sir Geoffrey Keynes (*A Bibliography of the Writings of William Harvey.* Cambridge: University Press, 1953). A selected bibliography about Harvey was issued by The Wellcome Historical Medical Library of London, in January 1956 (*Current Work in the History of Medicine*, No. 9, pp. 57–62). This lists 76 items. Outstanding are Robert Willis, *William Harvey: A History of the Circulation of the Blood.* London: Kegan Paul, 1878; J. M. Da Costa, *Harvey and His Discovery.* Philadelphia: Lippincott, 1879; Sir D'Arcy Power, *William Harvey.* London: Fisher Unwin, 1897; J. G. Curtis, *Harvey's Views on the Use of the Circulation of the Blood.* New York: Columbia Univ. Press, 1915; C. Singer, *The Discovery of the Circulation of the Blood.* London: G. Bell, 1922; J. J. Izquierdo, *Harvey.* Mexico: Ciencia, 1936, and P. Lain-Entralgo, *Harvey*, 2 vols. Madrid: Centauro, 1948. A special Harvey number of *The Journal of the History of Medicine* was issued in April 1957, with 21 contributions. Two important notes have been made by H. P. Bayon and W. Pagel (*Isis* 33: 443–453, 1942; 42: 22–38, 1951). E. B. Krumbhaar well discussed bibliographical matters relating to the discovery of blood circulation (*Ann. Med. Hist.* n.s. 1: 57–86, 1929).

At the request of the Royal Society, Stephen Hales published his experiments on sap pressure in plants (*Vegetable Staticks.* London: W. Innys, 1727), and followed it later with his studies on blood pressure (*Statical Essays: Containing Haemastaticks.* London: W. Innys, 1733). These two reports went into subsequent editions and translations as *Statical Essays*, vols. I and II. The classic account of Hales is by P. M. Dawson (*Johns Hopkins Hosp. Bull.* 15: 185–191, 232–237, 1904).

The distinguished Chicago cardiologist, James Bryan Herrick (1861–1954), who gave the classic account of coronary thrombosis, wrote *A Short History of Cardiology.* This deals more with clinical cardiology than with cardiovascular physiology. This is also the case, as the title would indicate, in the admirable collection of extracts (all offered in English) from *Classics in Arterial Hypertension*, so well arranged by Arthur Ruskin (Springfield, Ill.: Thomas, 1956, 383 pp.). However, both these volumes contain much fundamental physiological material regarding the cardiovascular system. This same comment applies to another broader selection of *Cardiac Classics*, compiled by F. A. Willius and T. E. Keys, and including comprehensive biographical accounts of authors (St. Louis: Mosby, 1941). Further extracts dealing chiefly with scientific physiological contributions to our knowledge of the cardiovascular system may be found in the excellent *Selected Readings in the History of Physiology*, arranged by the late John Farquhar Fulton (1899–1960) of Yale (Springfield: Thomas, 1930, 337 pp.).

For primary sources on the history of cardiovascular physiology, there are many excellent English translations available. Outstanding are those of Kenneth J. Franklin of London: *De Venarum Osteolis (1603) of Hieronymous Fabricius of Aquapendente* (Springfield: Thomas, 1933); *Movement of the Heart and Blood in Animals, an Anatomical Essay by William Harvey* (Oxford: Blackwell, 1957); and *The Circulation of the Blood, Two Anatomical Essays by William Harvey* (Oxford: Blackwell, 1958). My own translation of Harvey's *De Motu Cordis* has many notes and references and is now on its 4th edition (Springfield: Thomas, 4th ed., 1958). The Leonardine cardiovascular studies are translated and discussed by C. D. O'Malley and J. B. deC. M. Saunders (*Leonardo on the Human Body*, New York: H. Schuman, 1952). Charles Singer, the late great English historian of science, has given an excellent translation of some of Galen's demonstrations on the cardiovascular system (*Galen on Anatomical Procedures*, London: Oxford Univ. Press, 1956, pp. 180–200).

References to the works of contributors mentioned in the main discussion are appended.

An excellent review of significant advances in cardiac physiology during the nineteenth century was made by C. J. Wiggers of Cleveland, the great American cardiologist (*Bull Hist. Med.* 34: 1–15, 1960). This emphasizes the increasing importance of technical instrumentation in getting precise information on cardiovascular physiology. Satisfactory interpretation, however, still depends on brains. H. Feil has prepared a history of the treatment of heart disease in the nineteenth century (*Bull. Hist. Med.* 34: 19–28, 1960), and G. A. H. Clowes, Jr. has given an account of the important development of surgical treatment of heart disease, based on physiological principles (*Bull. Hist. Med.* 34: 29–51, 1960). An interesting exhibit was arranged by V. A. McKusick, W. D. Sharpe, and A. O. Warner, on the history of knowledge about cardiovascular sounds and stethoscopes (*Bull. Hist. Med.* 31: 463–487, 1957).

REFERENCES

ARISTOTLE (384–322 B.C.). *De motu animalium; De incessu animalium*, In: *Works*, edited by J. A. Smith and W. D. Ross, Oxford: Univ. Press, vol. 5, 1912.

CESALPINO, A. (1519–1603). *Peripateticarum questionum libri quinque.* Venice: Junta, 1571.

EBELL, B. *The Papyrus Ebers: The Greatest Egyptian Medical Document.* Copenhagen: Levin & Munksgaard, 1937.

FABRIZZI, G. (1537–1619). *De venarum ostiolis.* Patavii: L. Pasquati. 1603; English translation by K. J. Franklin.

GALEN (130–200 A.D.). *On the Natural Faculties.* English transla-

tion by A. J. Brock. London: Putnam, 1916. For evaluation see C. Singer, *History of Biology*. New York: Harper, 1950.

HIPPOCRATES (460–375 B.C.). *Works*, with English translation, edited by W. H. S. Jones and E. T. Withington. London: Loeb Classical Library, Heinemann, 1923–1931, 4 vols.

IBN-AL-NAFIS (d. 1289). Ibn-al-Nafis und seine Theorie des Lungenkreislaufs. English translation by M. Meyerhof *Quell. Stud. Gesch. Med.* 4: 37–88, 1933.

LEONARDO DA VINCI (1452–1519). *Leonardo da Vinci on the Human Body*. English translation by C. D. O'Malley and J. B. deC. M. Saunders. New York: H. Schuman, 1952.

NEI CHING. *The Yellow Emperor's Classic of Internal Medicine*. English translation by Ilza Veith, Baltimore: Williams & Wilkins, 1949.

M. SERVETUS (1511–1553). *Christianismi restitutio*. Vienne. Arnollet, 1553. Passages on pulmonary circulation translated by J. F. Fulton. *Selected Readings in Physiology*. Springfield, Ill.: Thomas, 1930, with commentary by C. D. O'Malley. In: *Michael Servetus*. Philadelphia: American Philosophical Society, 1953.

R. O. STEUER, Whdw, Aetiological Principle of Pyaemia in Ancient Egyptian Medicine. *Suppl. Bull. Hist. Med.*, No. 10, Baltimore: Johns Hopkins Press, 1948.

A. VESSALIUS (1514–1564) *De humani corporis fabrica*. Basel: J. Opernius, 1543.

The volume of blood—a critical examination of methods for its measurement

HAMPDEN C. LAWSON[1,2] | *Department of Physiology, University of Louisville School of Medicine, Louisville, Kentucky*

CHAPTER CONTENTS

THE CONCEPTUAL DEFINITION of blood volume as the volume of contents of the circulatory system (95) provides no clue to methods of quantitation. Herbst, in 1882, measured in animals the volume drained from opened arteries under circulatory pressure, and found it much less than the capacity of the system as estimated by anatomical methods (see 149). The volume obtained by bleeding to circulatory standstill, commonly called the bleeding volume, is now known to represent something like one-half the blood volume (138, 139, 235). In the hope of simply displacing the residual blood to the exterior where it could be measured, Lehman and Weber in 1853, in their study of two criminals sentenced to decapitation, washed out the vessels with water after blood had ceased to flow, and converted the total solids to a volume of blood. There seems little doubt that solutes were added to the washings by extraction of extravascular tissues, since the blood volume estimated for one of the subjects was 124 ml per kg (see 149).

A washout of hemoglobin, as a specific blood constituent, was introduced by Welcker in 1854 (see 64). Although it is usually called the "direct method," it is actually indirect for all other constituents than hemoglobin. Calculation of plasma volume or of total blood volume requires the assumption of a uniform hemoglobin concentration throughout the vascular system, an assumption which is shown later to be unwarranted. Interchange with extravascular tissues precludes the use of a washout procedure to obtain a direct measurement of plasma volume, using any normal plasma constituent.

The idea of an indirect approach to the measurement of blood volume is usually credited to Valentin, who in 1838 suggested that a known volume of distilled water be infused in living animals, the circulating blood volume to be estimated from the resulting dilution of total blood solids (see 64). The dilution

[1] Dr. Lawson died on June 23, 1961.

[2] The author's studies since 1957 have been aided by grant No. H-3228 from the United States Public Health Service.

principle is used by all current methods, though not in the form proposed by Valentin. The basic proposition is that in any solution in which a quantity of solute Q is dissolved in a volume V, the concentration

$$c = \frac{Q}{V} \tag{1}$$

so that if both Q and c are known, the equation may be solved for V. In Valentin's proposal, Q represents the total normal blood solids, whose value need not be known if they remain unchanged by the infusion of water, since

$Vc_1 = Q$, before the infusion, and

$(V + v)c_2 = Q$, after a volume v of water has been infused, so that

$Vc_1 = Vc_2 + vc_2$

and

$$V = \frac{vc_2}{c_1 - c_2} \tag{2}$$

Even if more physiological diluents than water are employed, the use of equation 2 demands the addition of relatively large volumes to the circulation, with the possibility that V, v, or Q may change as a consequence. It is accordingly of limited usefulness in blood volume studies. This equation, however, makes it possible to obtain the space occupied by normal cells or plasma if a foreign substance, attached to cell or plasma constituents, has previously been injected and allowed to achieve a stable distribution. If a volume v of normal cells or plasma is then infused, and the resulting dilution of the circulating foreign substance is measured as $c_1 - c_2$, solution of equation 2 for V gives the distribution space of the infused normal cells or plasma (142).

Equation 1 is used by all current methods. In these methods Q is a recognizable foreign material called label or tag, and c is its measured concentration in the circulation after mixing is complete. The volume of label is usually kept so small that it may be ignored. It is apparent that two basic requirements must be met, if solution of the equation for V is to represent the actual volume of the blood vascular system. The first is that the value taken for c must be equal to the mean concentration for the entire system. The second is that the value Q must be known at the time c is measured.

Of primary concern is the selection of a suitable label. No substance which meets the technical requirements is partitioned equally between the cells and the plasma. No single foreign substance, accordingly, is a label for blood as such. The commonly employed cell labels, carbon monoxide, Fe^{59}, Cr^{51}, and P^{32}, and the plasma labels, which include protein-bound dyes such as Evans blue, and radioactive tracers such as I^{131}, are discussed individually in the last sections of this chapter. The volume V which is obtained in equation 1 is defined by the dimensions of Q and c. If Q is a red cell label, and its concentration or activity is measured in packed red cells, V is the apparent volume of red cells in the circulatory system. If plasma label is injected, and its concentration in circulating plasma is measured, V is the apparent volume of circulating plasma.

Little attention has been given to the volume of white cells and platelets. In centrifuged samples of blood they rarely contribute more than 2 per cent to the total volume of the sample. Whether they are included in the estimate of plasma volume or of red cell volume depends upon the procedure chosen for reading the hematocrit of blood samples. They are included in the estimate of the plasma compartment if the hematocrit reading is taken at the top of the packed red cell column; in the estimate of the cell compartment, if the reading is taken at the top of the buffy coat.

Agreement between the conceptual definition of blood volume and its operational quantitation cannot be taken for granted. It is the purpose of this chapter to examine the extent of agreement. Since blood volume as such cannot be defined operationally, the chapter considers cell and plasma labels and their distribution, separately. Little attention is given to technical details, which are exhaustively described elsewhere (see refs. 29, 95, 189), or to the values obtained by different methods, except as these are essential to the stated purpose. (Reference 53 may be consulted for tables of values in various species.)

CIRCULATORY MIXING

The first requirement, that the value c used in the calculation of distribution space be equal to the mean for the entire system, is not easily met when impermanent labels are employed. If a liberal period is allowed for mixing within the circulation, unknown amounts of label may be lost, so that the second requirement, for a known value of Q, may be contravened. Correction for such loss is discussed subsequently. It requires that the exact time of injection be known and, for this reason, labels are usually injected rapidly, with little chance of mixing with blood at the injection site. The concentrated slug of

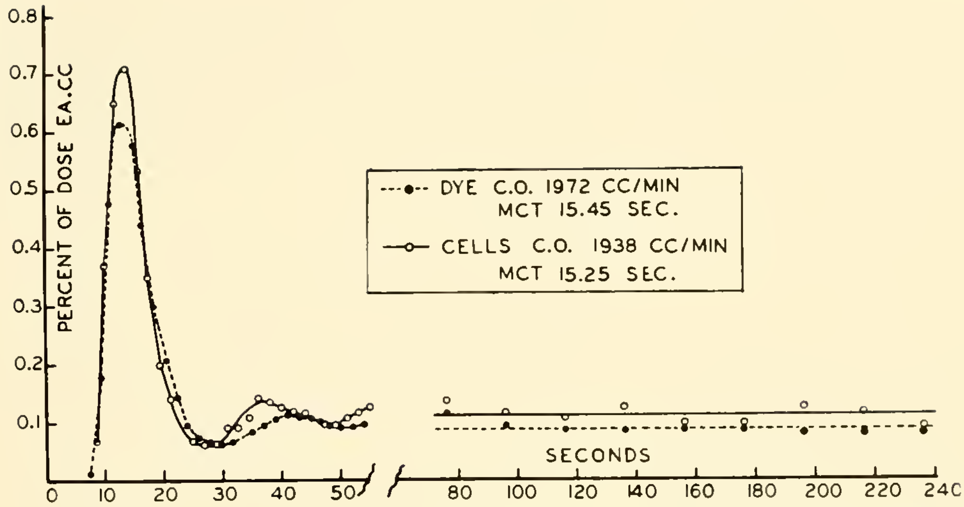

FIG. 1. Flow-dilution curves for P^{32} cells and T-1824 injected simultaneously into right ventricle, samples drawn from aorta at origin of brachiocephalic artery. Barbitalized dog. Periodic mixing phase ends at about 60 sec (note change in time scale). Ordinates show percentage of injected label present in 1 ml of whole blood at sampling site. A primary pulmonary transit curve and one recirculation curve are discernible for both labels. Although the mean circulation time (MCT) for dye is 0.2 sec longer than for cells, the area of the primary curves for the two labels is nearly identical, since they yield essentially the same value for cardiac output (C.O.). No attempt has been made to estimate disappearance slopes beyond the first minute, the horizontal lines being drawn through the arithmetic means for the two labels in the aperiodic phase of mixing.

label becomes gradually mixed in the circulation by processes of flow fractionation into circuits with different transit times, and recombination with blood having different activity at circuit confluences. If samples are drawn at suitably short intervals, label concentration may be seen to rise to a peak as the primary wave of label passes the sampling site, and then to decline more slowly. Attenuated waves may usually be observed on first recirculation, and sometimes on third or even fourth passage (fig. 1). Complete disappearance of such waves in the central circulation means only that there is no longer a front of rising label concentration in the system consisting of the heart and the most rapid circuits, and offers no assurance that mixing is complete elsewhere. Mixing is obviously incomplete even in the central circulation during the periodic phase. It is not complete in the peripheral circuits until they as a group are returning label to the central circulation at the same rate as it enters them. Until this happens, there is a net loss of label from the central to the peripheral circulation. Unfortunately, there is no simple way of distinguishing such loss from loss to extravascular regions.

Since samples drawn from the central circulation show a declining label concentration for several minutes after permanently tagged cells are injected (106), there is no question that mixing contributes to the fall observed when other labels are used. Mixing is usually considered complete, for impermanent labels, when the initial phase of rapidly falling concentration is terminated, and a slower rate of disappearance is begun (fig. 2).

Correction for Loss of Label During Mixing Period

All plasma labels continue to leave the central circulation after circulatory mixing is complete, until they finally disappear completely. Erlanger (64) was the first to suggest, in 1921, that in the case of those which disappear at a nearly constant rate, it might be possible to extrapolate through the mixing period to an intercept at the zero time ordinate. If the rate of loss during mixing is the same as that observed later, this intercept represents the concentration which would be produced by instantaneous mixing, with Q at its injected value. Most plasma labels disappear at a nearly exponential rate after circulatory mixing. It is accordingly customary to follow the procedure introduced by Gibson & Evans (77), in which the logarithm of label concentration is plotted against time, for purposes of extrapolating. This method of correcting for the unobserved loss during the mixing period can obviously be only an approximation. If, as

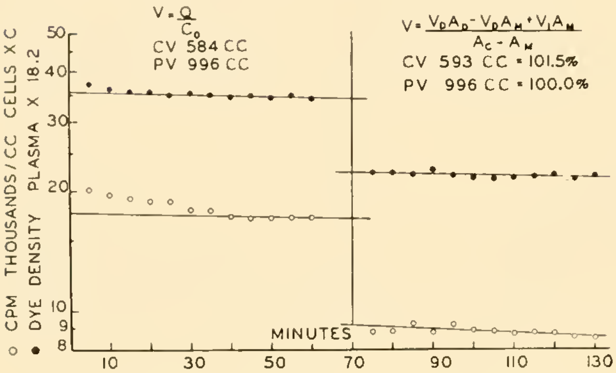

FIG. 2. Distribution volumes of P^{32} cells and T-1824 in a barbitalized dog. Labels injected simultaneously at time 0 in a femoral vein, samples from a femoral artery. Values for *CV* and *PV* by equation 1, using time 0 intercepts shown, are given above on left. A simultaneous infusion-withdrawal procedure was begun at 62 min and completed at 70 min. During this period 700 ml of previously prepared autologous whole blood containing neither cell nor plasma label was infused, while at the same time 700 ml of blood was withdrawn from the circulation. The distribution spaces of the infused unlabeled cells and plasma were calculated by equation 2, modified as shown above on the right. All volumes V and activities A refer either to cells or to plasma, and have the following definitions: V_d is the volume drawn, V_i the volume infused. A_d is the label activity in the pooled drawn blood; A_m is the activity circulating at the completion of the exchange, obtained by backward extrapolation of the second-hour curve to an intercept at 70 min; and A_c is the activity circulating before the exchange, read at the 70-min intercept of the first-hour curve, extrapolated forward. The distribution spaces of the unlabeled cells and plasma, corrected for sampling, are shown below the working equation, and are also given as percentages of the previously measured label distribution volumes.

an exponential disappearance rate suggests, the amount cleared from plasma is dependent upon the plasma concentration, loss during the mixing period must be excessive, since plasma concentration is excessive at this time. It is difficult to see how the loss during the periodic phase of the mixing period, in particular, could be predictably related to the rate at any subsequent time. Unless special clearing mechanisms operate during the mixing period alone, which seems unlikely, the uncorrected loss of plasma label during this period should be greater for labels which have a high postmixing disappearance rate, than for those with lower rates. Uncorrected loss during the mixing period probably accounts for the overestimation of plasma volume which is obtained with rapidly disappearing plasma labels (94).

Criteria of Uniform Mixing

From the point of view of semantics, mixing is not complete until the concentration of label is the same throughout the circulatory system. Sampling the venous effluent from individual circuits is a direct approach from this point of view, but yields data which are difficult to interpret because of the time lapse in transit of the local circuits. If the time-concentration curve for venous blood is periodic, the intersection of its rising limb with the arterial time-concentration curve is not predictably related to label concentration within the local circuit. If, on the other hand, the local venous curve is aperiodic because of nonuniformity of individual transit times, and the mean transit time is long, equalization of arterial and venous label concentrations may be indefinitely delayed (182, 237).

Study of tissues for their label content has shown that in some tissues label concentrations do not stabilize until long after stable concentrations have been achieved in blood. In mice, the Fe^{59} activity of circulating cells does not change after 15 min. But the activity of spleen and kidney continues to rise for an hour, whereas that of the liver rises excessively during the first few minutes and then declines (74).

From the operational point of view, it is immaterial whether a uniform concentration of label has actually been achieved throughout the cardiovascular system. The only requirement is that label activity in the sampled blood represent the mean for the system. If permanent labels are injected, the finding of constant activity in the central circulation over a reasonably long period is the most reliable indication that this requirement has been met. When temporary labels are used, the best indication is the achievement of a constant rate of disappearance.

The Predicted Time Requirement for Mixing

Equations for mixing have been formulated in terms of the concentration of injected label, the fractional concentration returning to the sampling site after one circulation, and the transit time for the latter (214). These are of limited applicability to the cardiovascular system because of the impossibility of defining transit time in a quantitatively useful way. The minimal mixing time may be defined with confidence, albeit with some naïveté, as the time required for a volume equivalent to the blood volume to pass once through the heart. Using approximate values for cardiac output and blood volume, the minimal time in man is about 1 min, in medium-sized dogs about 20 sec, and in rats about 10 sec (53). In these and other species for which data are available, the actual mixing requirement appears to be many times the minimal

predicted values. Reliable data are scattered because of the need for multiple sampling at short intervals over a considerable period. Most investigators have been concerned only with obtaining evidence that mixing is complete after a liberal time has been allowed.

The Observed Mixing Time for Labeled Cells

In the earliest studies with Fe^{59}-tagged cells in dogs, the conclusion was reached that cell mixing is complete in 4 to 5 min, since no decline in sample activity was observed thereafter (106). The conclusion appears to have been based on inadequate data, however, as it was subsequently found that injections of epinephrine even later than this produced a drop in circulating iron activity (101). In barbitalized dogs, whose splenomegaly and muscular inactivity would be expected to prolong mixing, most investigators allow 10 min. But if the spleen is removed 30 min after injection of Cr^{51}-labeled cells, it is found to contain cells, unmixed with label, equivalent to 4 to 5 per cent of the total cell volume (131). By using equation 2 to distinguish mixing from tag elution, it has been possible to show that P^{32}-labeled cells may require as much as 40 min for mixing in intact barbitalized dogs (143).

In human studies, samples are usually not taken at sufficiently short intervals to determine when cell mixing is actually complete. Early data with carbon monoxide suggested a 20-min mixing requirement (54), but much of this is now attributed to an expanding extravascular distribution. When cells labeled with K^{42} and with P^{32} are injected in normal men, the initial fast disappearance phase is terminated for both labels in 7.5 to 10 min (23). The mixing period for P^{32} cells in man appears to be less than 20 min, since their distribution space is the same at 20 and at 30 min (194). Another study in man suggests that the period is less than 15 min, since vigorous exercise at that time caused no change in circulating P^{32} activity (172). It may be prolonged somewhat, however, by dependent pooling of blood in the erect posture (173), and in cases of splenomegaly, where cell-mixing may require as much as 30 min (204), a mixing time approaching that in the dog with spleen enlarged by barbiturates. Very long mixing times, up to 1 hour, have been reported for Cr^{51} cells in battlefield casualties with lacerating wounds (184). This greatly exceeds the prolongation of mixing for plasma labels which has been reported for men in states of shock (170).

In small animals, such as rats and mice, groups are usually sampled at different times to avoid volume depletion. In studies of this kind on normal unanesthetized rats, Cr^{51} cells have been found with essentially the same distribution space at 15, 30, and 60 min (180). Similar data have been obtained in mice with Fe^{59} cells (74). Cell-mixing times were not reported in recent studies on horses (126) and swine (30). It is unfortunate that more precise data are not available for animals of extreme size.

The Observed Mixing Time for Labeled Plasma

The predicted minimal mixing time would under most conditions be somewhat greater for labeled plasma than for labeled cells. As is shown in a later section, the ratio cells:plasma in the blood pumped by the heart (central circulation) is usually higher than the mean ratio for the whole circulatory system. As a consequence, a larger fraction of the total cell volume than of the total plasma volume passes through the heart in any interval of time. It is apparent, however, that mixing time cannot be predicted from these simplest parameters, since most of the available data fail to reveal a significant difference in the mixing time for cell and for plasma labels. In man, the initial steep disappearance slope is terminated at the same time for radio-iodinated serum albumin and for the two cell labels K^{42} and P^{32} (23). In normal subjects with arterial blood continuously monitored for 2 hours, the flattening of the disappearance slope for I^{131} albumin occurs at 4 to 15 min, with an average of 9 min (185). Even in congestive heart failure, with mixing time for both cell and plasma labels prolonged to 10 to 15 min, no consistent difference between the two has been observed (110, 159, 207). No difference has been observed in the mixing time of the two plasma labels T-1824 and I^{131} albumin (170, 185).

Barbitalized dogs in our laboratory often have an appreciably longer mixing time for P^{32} cells than for the plasma label T-1824. In a series of 24 dogs sampled at 5-min intervals for 1 hour, the average cell mixing time was 20.5 min, while simultaneously injected T-1824 had an average time of 14 min (fig. 2). In eight acutely splenectomized dogs, removal of the spleen appeared to have abolished the difference, cells mixing in 14.4 min, and plasma in 13.8 min (Lawson, unpublished data).

Only limited data are available for other species. In the cow, serial samples have been drawn for 1 hour after injection of T-1824, and the initial rapid disappearance phase found to terminate at 5 to 10 min (195). That plasma mixing in an animal of this large

size takes no longer than in man (170) and in the dog (78) is most unexpected. It is unfortunate that data on mixing are not given in other studies on the cow (57). The mixing time for radio-iodinated albumin in the rat averages about 3 min (196). An arbitrary 6-min mixing time for all species was used by Courtice (45) in his studies of T-1824 plasma volume in rabbits, goats, dogs, and horses.

If plasma labels such as T-1824 and I^{131} albumin are observed over a period of several hours or days, it becomes clear that they do not begin to disappear at a truly exponential rate immediately at the termination of the initial period of rapid disappearance (75, 151, 176). The disappearance rate of all the common plasma labels decreases progressively with time for a fairly long period, to become exponential at a time which differs for the different labels. In man, for example, T-1824 does not begin to disappear exponentially until about the 7th day, whereas only 3 days are required for I^{131} albumin (75). The disappearance rate of T-1824 in man, which is 4 to 10 per cent for the first hour, has decreased to about 2 per cent at the 16th hour (77).

It is not, obviously, a simple matter to determine just when plasma labels are completely mixed within their circulatory distribution. Both during and after the circulatory mixing period they are progressively expanding their distribution to include ultimately the entire extracellular, exchangeable protein pool. Probably something like 60 per cent of this is extravascular (24, 40). The ideal operational criterion for mixing, the achievement of a constant rate of disappearance, indicates that mixing is complete in the total pool rather than in the circulatory system alone. In using this criterion for circulatory mixing, accordingly, it is necessary to assume that mixing in the circulation is complete when the initial period of rapid disappearance is terminated.

Sequestration of Cells and Plasma

If significant volumes of red cells were permanently immobilized anywhere in the circulatory system, they would, of course, fail to mix with injected tagged cells, and would accordingly escape measurement by present methods. Temporary sequestration, on the other hand, which should be demonstrable, has not been observed in normal animals or men, since the distribution volume of Fe^{59} cells remains constant for days following their injection, after completion of the initial mixing phase (104). Gibson and his collaborators (82) used cells tagged with two radioisotopes of iron to show the completeness of cell mixing in normal dogs. Three to five hours after an initial injection of Fe^{55} cells, cells tagged with Fe^{59} were injected, and 1 hour later the animals were killed and the ratio $Fe^{59}:Fe^{55}$ was determined in samples of a variety of tissues. Since the ratio of the two isotopes was the same as in blood drawn from the central circulation, it was concluded that the more recently injected cells had mixed thoroughly with those injected earlier.

When arterial pressure has been lowered by hemorrhage or by certain other types of shock-producing procedures, microscopic examination of the living circulation in accessible vascular areas reveals marked slowing and complete stoppage of flow in many small vessels (130, 145, 245, 246). Attempts to measure the volume of sequestered cells by distribution space techniques, however, have given conflicting results. That many cells injected into dogs in shock fail to enter small vessels has been shown by the use of the two iron isotopes. If Fe^{55} cells are injected during the normal state, and the animal is in shock when Fe^{59} cells are given, the ratio $Fe^{59}:Fe^{55}$ in tissue samples is considerably less than in blood and nearly half the cells remaining in the circulatory system appear to have stopped circulating (83). This estimate of cell sequestration is considerably larger than the values found by most other investigators (193). Some of the differences may be attributed to differences in type or severity of shock. Some may be due simply to differences in methods of reporting. Huggins and his collaborators (119), for example, in studies on acute hemorrhage, reported that after approximately one-half the total cells had been withdrawn, only 4 to 6 per cent of the total were unaccounted for by a second tagged cell injection. This is some 8 to 12 per cent of the cells remaining in the circulatory system. In nembutalized dogs subjected to acute blood loss, cell sequestration is demonstrable only when arterial pressure has been lowered to 50 mg Hg or less. At a pressure of 35 mm Hg, about 16 per cent of the cells remaining in the circulatory system appear to have stopped circulating (52, 119).

A report that no cell sequestration is demonstrable in rats subjected to tourniquet shock or to acute blood loss is difficult to evaluate, as no data were reported on arterial pressure (180). For the same reason, it is not possible to judge whether conditions conducive to cell sequestration were present in studies on man in which large quantities of blood were impounded in the extremities. The estimate of cell volume with carbon monoxide was unchanged, although a longer mixing

time had to be allowed for both it and the plasma label T-1824 (28).

It may be assumed that plasma is sequestered along with cells whenever blood stops circulating in these abnormal states, but the estimation of its volume by present methods is of uncertain reliability. Both the T-1824 space and the thiocyanate space have been reported to be reduced by about 30 per cent in rabbits and chickens in deep hypothermia, without demonstrable extravasations of fluid (197). In most studies of other types of shock, however, it has not been possible to demonstrate the sequestration of plasma, presumably because its loss from the circulation is masked by plasma volume replenishment in remaining vascular circuits (3, 119, 141).

DISTRIBUTION OF CELLS AND PLASMA IN THE CIRCULATORY SYSTEM

The first requirement stated in the introduction is that the value c used in equation 1 must be equal to the mean concentration of label for the circulatory system as a whole. Even after labels have achieved their final circulatory distribution, they may not have the same concentration throughout the system as in samples of drawn blood. It has long been known that the ratio cells:plasma is not the same in all parts of the circulatory system, the spleen being demonstrably cell-rich, and many small vessels in other tissues being visibly cell-poor. Since all labels attach themselves either to cell constituents or to plasma constituents, an unequal distribution of cells and plasma in the circulatory system will produce a correspondingly uneven distribution of label.

Despite such inequalities of distribution, if the hematocrit of centrally circulating blood represents the mean hematocrit for the entire circulatory system, a single label, for either cells or plasma, may be used. As long ago as 1874 Malassez (152) recognized that this relationship between the central and the systemic hematocrit would exist only by chance, in the statement "La richesse globulaire du sang variant selon les régions de l'arbre circulatoire, rien ne dit que le nombre des globules trouvé représente la richesse globulaire moyenne de tout le sang de l'économie" (152). Although it is now generally recognized that the central hematocrit does not represent the mean in most species, and under most conditions, it has been proposed that a constant relationship exists, so that the mean hematocrit may be derived from the observed hematocrit of drawn blood (38, 80, 191, 192). It is one of the purposes of this section to examine the validity of this proposal.

Cell:Plasma Ratio of Drawn Blood

All procedures, whether they measure label activity in whole blood or after blood has been centrifugally separated into cell and plasma compartments, use the hematocrit directly or indirectly. The hematocrit is usually stated as the percentage volume of packed cells in a sample of blood, but in the present discussion it will be given in its simpler form, as the decimal ratio of cells to total volume. Blood drawn from any definable vascular site with the exception of the splenic pulp and the erythropoietic bone marrow has essentially the same hematocrit as blood drawn from any other site, including the heart and great vessels. Whenever hematocrits are obtained on drawn blood, accordingly, they represent the hematocrit of the central circulation.

Although centrifugation readily produces plasma which is free of red cells, it is impossible to drive the plasma completely out of the packed cell column in this way (156). The percentage of occluded plasma which remains varies with the centrifugal force applied and with the duration of its application (183), and may vary with different kinds of blood. Gregersen & Schiro (96) in 1937 found that about 4 per cent of the dye T-1824 which had been added to samples of whole blood was missing from the plasma column separated by centrifuging at 1500 g for 30 min. Centrifugal hematocrits were not reported. If it is assumed that these were about 0.40, approximately 6 per cent of the packed cell column must have consisted of plasma. Somewhat similar data were obtained by Chapin & Ross (35), who used smaller centrifuge tubes (Wintrobe) subjected to a centrifugal force of 1800 g for 1 hour, and found 8.5 per cent occluded plasma, a value which was checked by observing the dilution of plasma proteins when saline was added.

It is now apparent that a constant correction cannot be applied to the centrifugal hematocrit, since the percentage of occluded plasma increases with increasing hematocrit or with the height to which the centrifuge tubes are filled (37, 61, 114). This is due to a shortening of the effective radius of gyration as the length of the cell column is increased. Relative centrifugal force may be precisely formulated as

$$RCF = \frac{(2\pi n)^2 r}{980} g$$

where n is the number of revolutions per second, and

r is the radius of rotation in centimeters. But it is obvious that r cannot be precisely defined for the cells throughout their descent from the top to the bottom of the centrifuge tubes. A close approximation is the distance measured from the center of rotation to the middle of the final packed cell column. Precision could undoubtedly be improved by determining the relationship between r as measured in this way and the percentage of occluded plasma, applying to each sample the correction derived from this relationship. Most investigators prefer to use a centrifugal force and duration sufficient to keep the average percentage small, and to accept the modest error due to variations (177).

All the earlier studies, using hematocrits uncorrected for occluded plasma, overestimate cell volume regardless of method employed. Since the error appears equally in all the measurements reported, however, the conclusions drawn from a comparison of methods are perfectly valid.

Although some increase in the mean corpuscular volume may be expected with an increase in the CO_2 content of blood, the difference between arterial and venous red cells from this cause is hardly measurable. An increase in P_{CO_2} from 5 to 700 mm Hg produces only a 13 per cent increase in the volume of rabbit cells, 9 per cent in the volume of human cells, and 7 per cent in that of ox and sheep cells (124). None of these change measurably in size within the physiological range of 40 to 60 ml of CO_2 per 100 ml of blood (124). It is thus immaterial whether the central circulation is sampled from an artery or a vein. If changes in the mean corpuscular volume are suspected, they may be demonstrated by measuring the hemoglobin content of packed cells, a procedure which is more reliable than cell counting (191).

The Error in Computing Cell Volume from Plasma Volume and the Central Hematocrit

Whipple and his colleagues (240) found in 1920 that when cell volume was calculated from a dye-distribution value for plasma volume and the venous hematocrit, dogs subjected to measured blood loss appeared to have a reduction in circulating cells considerably greater than the volume drawn. This calculation is obtained as

$$CV_h = PV \times \frac{H_c}{1 - H_c} \tag{3}$$

where PV is the distribution volume of plasma label, and H_c is the central hematocrit. Subsequent studies by the same group of investigators revealed that CV_h was approximately 20 per cent greater than the volume of cells measured by hemoglobin washout, and the suggestion was made that the discrepancy might be due to the existence of cell-free plasma in the small vessels (222). The over-reduction in CV_h by bleeding is readily demonstrated in splenectomized dogs (223). When bleeding is done in intact dogs, however, restoration of the central hematocrit by cells from splenic stores often masks the error (175). That the overreduction is due to a systematic error in CV_h is shown by adding cells to the circulation. There is an excess increase in CV_h comparable to the excess decrease when cells are withdrawn (141). It is apparent that a volume of cells, which is known to have a certain value outside the circulation, is overestimated as CV_h when it becomes a circulating volume. The discordant finding that cell volume as measured by carbon monoxide agrees well with CV_h in normal, splenectomized, and hemorrhaged dogs (201) is no longer pertinent. It is now known that the carbon monoxide method also overestimates cell volume (200), agreement between the two invalid methods being fortuitous.

Definitive proof of the error in CV_h was afforded by the first measurement of cell volume as the distribution volume of injected Fe^{59}-tagged cells, in 1941. In the dogs studied, the tagged cell distribution volume averaged about 75 per cent of CV_h (104). Similar comparative studies have since been done for other species including man, using a variety of tagged-cell methods (38, 80, 86, 153, 188, 194, 242).

The Mean Circulatory Hematocrit

When cell and plasma labels are injected simultaneously, and the virtual distribution volume is calculated for each, the ratio cells:plasma may be computed for the circulatory system as a whole. If this is expressed as an hematocrit, which is customary, it becomes the mean circulatory hematocrit, H_m, and is calculated as

$$H_m = \frac{CV}{CV + PV} \tag{4}$$

where CV is the distribution volume of cell label, and PV that of plasma label. A large number of studies have been reported on the relationship between H_m and the central hematocrit H_c. If assurance could be had that the relationship H_m/H_c is constant, it would be possible to use a single label, for either cells or plasma, and to estimate the unlabeled compartment

by using this relationship. If, for example, a plasma label were used, and PV measured, then

$$CV_h' = PV \times \frac{H_c'}{1 - H_c'} \qquad (5)$$

where CV_h' is CV_h corrected for differences between the mean and the central hematocrit, and H_c' is H_m estimated from the observed value for H_c, using the predicted relationship between H_m and H_c. The ratio H_m/H_c is termed F_{cells} by Reeve, Gregersen, and their collaborators (191).

Since the ratio of H_c to its complement appears in equation 3, the error in estimating the unlabeled compartment from a single label injection, using this equation, is considerably greater than would be suggested by the ratio H_m/H_c. When H_c is 0.50, the percentage error in equation 3 is $2 \times 100(1 - H_m/H_c)$, and the error increases with increasing values of H_c. For the same reason, when equation 5 is used, the percentage error due to individual variations in the relationship between H_m and H_c is greater than the coefficient of variation for H_m/H_c. These relationships become apparent if calculations are made from a hypothetical example. Suppose that in a dog both the cell label volume CV and the plasma label volume PV are found to be 500 ml; the mean circulatory hematocrit is obviously $H_m = 500/(500 + 500) = 0.50$. If blood drawn from the central circulation has the hematocrit $H_c = 0.55$, the ratio $H_m/H_c = 0.50/0.55 = 0.91$. Since the mean and the central hematocrits differ by only 9 per cent, it might be supposed that CV_h would be fairly close to CV. That this is not the case is shown by the calculation of $CV_h = PV \times H_c/(1 - H_c) = 500 \times 0.55/0.45 = 610$ ml, a value which is 22 per cent too large. Table 1 gives data reported by Chaplin *et al.* (38) for a group of human subjects with widely varying central hematocrits, showing a relatively constant ratio H_m/H_c at 0.910. Yet if values for CV_h are calculated, as has been done for the table, the average overestimate of cell volume is 20.5 per cent. If a constant ratio H_m/H_c is assumed, and CV_h' calculated using H_c', as is done in the table, although the average value of CV_h' is of necessity the same as the average value of CV, the coefficient of variation is 5.36 per cent. This is nearly double the coefficient of variation for the ratio H_m/H_c.

The average ratio H_m/H_c in normal adult humans is reported to be between 0.89 and 0.94 by a large number of investigators (23, 27, 38, 80, 86, 110, 154, 194, 204, 207, 233). It is reduced to 0.87 in the newborn (161), and to a still lower value of 0.81 in early pregnancy (33).

TABLE 1

Subject	PV	CV	H_c	H_m/H_c	CV_h	$CV_h/CV \times 100$	CV_h'	$CV_h'/CV \times 100$
1	4880	426	.087	.926	466	109.2	419	98.1
2	2920	359	.119	.924	395	110.0	353	98.3
3	3213	602	.174	.909	676	111.2	569	94.5
4	2933	728	.221	.900	835	111.5	739	101.2
5	3949	1519	.281	.989	1546	102.0	1360	89.5
6	2931	1073	.298	.900	1243	116.0	1090	101.7
7	2760	1056	.300	.923	1182	112.1	1030	97.8
8	2862	1105	.308	.906	1277	115.5	1110	100.5
9	2494	1173	.355	.901	1372	117.1	1183	101.0
10	2450	1296	.384	.901	1525	117.9	1330	101.6
11	2397	1366	.398	.912	1584	116.0	1332	97.8
12	2403	1691	.433	.954	1850	109.0	1561	92.4
13	3590	2300	.445	.878	2880	125.1	2447	106.2
14	3467	2293	.451	.883	2850	124.2	2408	105.0
15	3205	2289	.456	.915	2690	117.5	2280	99.4
16	2392	1740	.463	.909	2065	118.7	1738	99.8
17	3060	2140	.464	.888	2642	123.5	2235	104.4
18	2900	2243	.480	.909	2675	119.2	2250	100.3
19	3238	2813	.516	.901	3452	122.7	2870	102.0
20	4300	4283	.535	.933	4950	115.3	4090	95.3
21	4920	4432	.544	.871	5870	132.2	4790	108.0
22	3635	3758	.590	.862	5240	139.3	4200	111.9
23	2950	3724	.611	.914	4640	124.5	3680	98.8
24	3508	3972	.615	.863	5605	141.1	4440	111.8
25	1903	3197	.678	.924	4020	125.6	3060	96.0
26	2048	3713	.696	.926	4700	126.2	3540	95.4
27	2037	4325	.731	.930	5530	128.0	4030	93.3
28	2355	5890	.776	.920	8160	138.5	5660	96.3
Mean				.910		120.5		100.0
S.D.				.026				5.36
Coef. var.				2.86				5.36

The first 4 columns are data reported by Chaplin *et al.* (38). PV is the T-1824 distribution volume, CV is the P^{32} cell volume, H_c the venous (central) hematocrit. The ratio H_m/H_c was obtained by equation 4 (their calculation). I have calculated the remaining values from their data. CV_h was obtained from equation 3 and is defined in the text. CV_h' was obtained from equation 5 of the text, taking $H_c' = 0.91 \times H_c$.

There are large and unexplained differences in the ratio H_m/H_c reported by different investigators for the dog. In intact dogs under barbiturate anesthesia its average value is variously reported as 0.90 (118), 1.02 (59), and 1.10 (191). In normal dogs without anesthesia one group finds an average ratio of 1.0 with large variations (191), while another finds an

TABLE 2

Monkey Number	PV ml/kg	CV ml/kg	H_c	H_m/H_c	CV_h' ml/kg	$CV_h'/CV \times 100$	XPV, % of BV*
1	30.8	15.0	.399	0.82	15.5	103.3	17.9
2	33.9	19.1	.422	0.85	18.3	95.9	14.5
3	39.0	18.5	.396	0.81	19.0	102.7	18.8
4	36.9	20.0	.418	0.84	19.1	95.5	16.0
5	36.4	18.7	.411	0.82	18.8	100.5	17.6
6	35.7	17.7	.376	0.88	16.2	91.5	11.8
8	33.8	15.9	.421	0.76	18.2	114.3	24.2
9	38.6	16.4	.361	0.82	16.5	100.5	17.4
10	34.8	16.3	.407	0.79	17.7	108.6	21.7
11	36.3	18.2	.416	0.80	19.2	105.5	19.8
12	30.0	14.3	.398	0.81	14.8	103.5	18.7
13	32.8	17.6	.428	0.82	18.1	102.9	18.4
14	33.9	18.4	.393	0.91	16.4	89.2	10.3
15	48.4	18.2	.356	0.77	20.2	111.0	23.2
16	41.3	18.9	.372	0.85	18.4	97.4	15.6
17	38.0	16.8	.383	0.80	17.7	105.3	19.9
18	33.6	18.4	.406	0.87	17.1	93.0	12.9
19	40.6	19.6	.371	0.88	18.0	92.0	12.3
Mean (n = 18)				0.83		100.0	17.3
SD				0.039		7.06	

* $BV = PV + CV$.

Data on rhesus monkeys from Gregersen *et al.* (97). The first 4 columns are from their report, to which I have added a calculation of the standard deviation for H_m/H_c, termed "F_{cells}" in their report. CV_h' has been calculated as in table 1. The values given under the heading XPV are for excess plasma, and are discussed in the next section of this chapter.

average of 0.917 with less variation (63). Since the spleen in the dog contains an appreciable volume of cells which are included in the calculation of H_m, but which do not influence H_c, its removal would be predicted to reduce the ratio H_m/H_c. Reported values for the ratio in unanesthetized splenectomized dogs average 0.899 (191).

Scattered data are available for other species. The ratio H_m/H_c in unanesthetized normal rats is given in one report as 0.739, standard deviation 0.053 (236); while other investigators find the average ratio to be 0.986, standard deviation 0.067 (117). If T-1824 is used for PV in mice, the average ratio is 0.73, whereas if the smaller value for I^{131}-albumin PV is used it is 0.88 (242). Table 2 shows data obtained by Gregersen and his colleagues (97) on the rhesus monkey, to which I have added additional calculations as in table 1, and a final column of values for "excess plasma" which are discussed in a later section.

Local Circulatory Hematocrits

A variety of methods has been used to show that the ratio cell label: plasma label in individual vascular areas is different from the ratio in the central circulation. They agree in showing that within a short time after injection plasma label has expanded its virtual distribution space in most tissues out of proportion to the expansion of cell label space. Unfortunately, none of the methods defines the extra plasma space either anatomically or quantitatively, since none of them distinguishes intravascular from extravascular plasma label. It may be assumed with some confidence that firmly bound cell label remains intravascular, but this assumption cannot be made with equal confidence for plasma label.

Gibson and his colleagues (82) made the first study of local differences by examining specimens of tissues without grossly recognizable large vessels, 15 min or so after cell and plasma labels had been injected. Assuming that the ratio of the two labels represents the ratio of cells to plasma in the small vessels of the tissues, they obtained mean hematocrits for the contents of these vessels by reference to the label ratio and hematocrit of blood drawn from the central circulation. Table 3 shows representative data from their study. Similar data have been obtained by other investigators, using other cell and plasma labels (51, 58, 65).

Special attention has been given to the kidney, which has been shown to be relatively cell-poor by several independent methods. Pappenheimer & Kinter (179) adjusted the arterial hematocrit by injecting cells or plasma, and measured the change in total renal hemoglobin in excised kidneys. When the

TABLE 3

Tissue	H_t	H_t/H_c
Arterial blood (H_c)	.40	
Spleen	.82	2.05
Liver	.41	1.02
Lungs	.33	0.83
Kidneys	.15	0.37
Heart	.22	0.55
Bowel	.17	0.42
Muscle	.21	0.53
Brain	.18	0.45

From Gibson *et al.* (82). Average values for 7 normal dogs under morphine narcosis. H_t is the tissue hematocrit with large vessels excluded (see text for method). H_t/H_c is the ratio of the tissue hematocrit to the hematocrit of the central circulation (arterial blood drawn from a large artery).

hemoglobin content was plotted against the arterial hematocrit, it was possible to extrapolate to an arterial hematocrit of 100 per cent cells, thus obtaining a value for the total renal vascular volume. From this and the actual renal hemoglobin content at various arterial hematocrit levels, renal blood was estimated to have a mean hematocrit about one-half that of the central circulation. This is of the same order of magnitude as the values shown in table 3. A confirmatory observation, which cannot be correlated quantitatively, is that the last blood to drain from the renal vein after the vessels are clamped is very poor in cells (230). The origin of the extra fluid is obscure, however, since its composition differs from that of centrally circulating plasma.

A totally different procedure consists of injecting cell and plasma labels simultaneously into the blood flowing into a vascular region, and measuring the transit time for each label as the two pass a sampling site in effluent vessels (140). The space traversed by each label is the product of its mean transit time by its volume flow (109, 225, 226). If plasma label traverses the total plasma space, and cell label the total cell space, it should be possible to calculate the two latter volumes by this method. When the procedure is applied to the kidney, however, the plasma space appears much smaller than it does by either of the foregoing methods, the renal hematocrit being only about 10 per cent less than that of the central circulation (147, 174). The difference seems too great to be attributed to the inclusion of large vessel volume in the spaces estimated by the transit-time method. It seems likely that in a single transit of the renal circuits plasma label does not have time to traverse the total space accessible to it. The reported data fail to show whether plasma label was completely recovered in the effluent blood. When Cr^{51} cells and I^{131} albumin are continuously infused into the renal artery, it has been reported that the albumin transit times can be resolved into two major categories, the shorter one resembling that of the cells, the longer one being about ten times as long (43).

Data from flow-dilution studies of cell and plasma label are also available for the pulmonary circulation. They agree in showing that tagged cells traverse this system somewhat more rapidly than labeled plasma (fig. 1) and that an equal percentage of the two labels ultimately passes the sampling site (55, 140, 146, 186). Table 4 shows data reported by Rapaport *et al.* (186) for the pulmonary circulation of the dog, which I have attempted to convert into values for the complete lesser circulation by excluding the portion of the systemic circulation traversed by the labels, but including the one-half heart volume. The labels in this study were injected into the pulmonary artery, and samples were drawn from a femoral artery. The transit times and calculated spaces thus include values for the aorta and its primary branches. For the table I have estimated this portion of the greater circulation to have a volume of 60 ml, which has been converted into volumes of cells and plasma, by using the observed arterial hematocrits. It is apparent from the table that the space traversed by plasma label is larger, in relation to the flow of plasma, than is the space traversed by cells in relation to their flow. The excess plasma space is shown in the column headed *XPV*-ml, and is given in the last column of the table as a percentage of the total pulmonary blood volume. The next section of this chapter considers the excess plasma space at greater length. The hematocrit of the pulmonary circulation, including one-half the heart, appears by the transit-time method from the data of the table to be about 94 per cent of the arterial hematocrit. This is somewhat larger than the hematocrit found for the small vessels of the lungs by tissue analysis, after the injected labels have had time to achieve their complete circulatory distribution (see table 3).

It has not been possible to make comparable transit-time calculations for the greater circulation alone. If label is injected into the aorta and its return to the

TABLE 4

CV	PV	BV	H_a	H_m	PV_c	XPV ml	$XPV\%$
103	168	271	.396	.380	158	10	3.7
96	195	291	.320	.330	204	−9	−3.1
114	189	303	.400	.376	171	18	5.9
73	223	296	.288	.246	180	43	14.5
205	286	491	.432	.417	270	16	3.3
141	269	410	.368	.344	242	27	6.6
107	169	276	.422	.388	147	22	8.0
92	215	307	.309	.300	206	9	2.9
58	109	167	.405	.347	85	24	14.4
156	181	337	.529	.463	139	42	12.4
123	177	300	.418	.410	171	6	2.0
78	110	188	.441	.415	99	11	5.9
195	277	472	.437	.414	252	25	5.3
Avg.	(n = 13)		.397	.372			6.3

From data reported by Rapaport *et al.* (186). See text for explanation. The column headings are: CV = cell volume in ml, PV = plasma volume in ml, BV = sum of cell and plasma volumes in ml, H_a = observed arterial hematocrit, H_m = mean hematocrit calculated as CV/BV, PV_c = plasma volume in ml, calculated as $CV \times (1 - H_a)/H_a$, XPV = excess plasma volume in ml calculated as $PV - PV_c$, $XPV\%$ = excess plasma volume as percentage of BV.

right atrium monitored, the time-concentration curve for returning label is so complex that mean transit time for the system as a whole cannot be estimated (Lawson, unpublished data). It may be significant, however, that in the dog, within 20 to 40 sec after intravenous injection of labeled cells and plasma, samples drawn from the aorta show plasma label to have decreased its concentration in blood by about 20 per cent more than cell label (234). Figure 1 shows a confirmation of this observation by our laboratory, and demonstrates, in addition, that the excessive distribution space for plasma label persists for at least 4 min.

The method devised by Bradley and his colleagues (26) for estimating regional vascular volumes computes the quantity of label distributed within a region from the volume of flow and the accumulated difference in label activity of inflowing and outflowing blood until the two activities have become equal. If label activity throughout the region at the instant of equilibration is assumed to be the same as that of the blood flowing in and out at that instant, volume may be calculated from equation 1. By using cell and plasma labels simultaneously, and making separate calculations for each, this procedure has been used in man to estimate the hematocrit of the splanchnic vascular bed as about 91 per cent of the central hematocrit (136). The mean transit times, calculated in these studies as volume/flow, were 36 sec for tagged cells, and 42 sec for tagged plasma. Since the spleen was included in the circuits studied, the data are difficult to reconcile with data on the splenic circuits alone in barbitalized dogs, which show mean splenic transit times of 19 min for cells, and of 3.75 min for plasma (218). The discrepancy seems too great to be attributed to differences, however large, in the cell-storage function of the spleen in man and in the barbitalized dog. The ratio between the mean circulatory hematocrit and that of drawn blood is reported to be unchanged in splenectomized dogs by complete evisceration (91). After the spleen has been removed from the splanchnic area, accordingly, the hematocrit of the region appears to be typical of the circulatory system as a whole.

Attempts to withdraw or express blood from the minute vessels for direct determination of its hematocrit have given equivocal results. Ebert & Stead (62) reported that blood stripped from the upper extremity in man by means of an elastic bandage had a lower hemoglobin content than blood drawn from the other arm. Since the procedure produces circulatory stasis and local asphyxia, however, it is not at all certain that the expressed fluid represents the normal contents of the small vessels. It also seems unlikely that a representative sample could be obtained through a catheter wedged distally in an artery, since any significant volume drawn through such a catheter must have come from collaterals. This probably explains a recent finding that blood drawn through 0.5 mm tubes wedged distally in the dog's foreleg arteries has the same hematocrit as blood drawn from large vessels (99). A report that external compression of the kidney expels blood through the renal vein with the same hematocrit as large vessel blood is more difficult to evaluate (163). It appears to be in conflict with the finding that cell-poor blood drains spontaneously from the kidney after the renal artery has been clamped (230). If a peripheral layer of adherent, stagnant plasma is maintained in vessels despite the viscous drag of blood flow through them, it seems improbable that it could be displaced by any of these procedures.

Excess Plasma

In the original study of Smith *et al.* (222), which first demonstrated the error in CV_h, it was estimated that a volume of cell-free plasma equivalent to 9 per cent of the total intravascular space could explain the error. Although this amount of cell-free plasma does not seem preposterous, it is obviously an underestimate if there are also cell-rich areas, such as the spleen. Since equal volumes of cell-poor and comparably cell-rich blood would cancel out in the calculation, any estimate of cell-free plasma represents not its total volume, but only its excess over comparably cell-rich blood.

When plasma volume and cell volume are measured independently and at the same time, the virtual volume of cell-free plasma can readily be calculated. This is the difference in the plasma volume measured from the distribution of plasma label, and the volume which would be required to suspend the total cell volume in plasma at the hematocrit found for the central circulation. For example, Huggins and his colleagues (personal communication) have found average values for 100 morphinized-nembutalized dogs as follows: Cell volume (by Fe^{59}, Cr^{51}, or P^{32}) = 33.5 ml per kg; plasma volume (by T-1824 or iodinated albumin) 50.2 ml per kg; venous hematocrit 0.452. If cells were associated with plasma throughout their distribution space in the same ratio as in venous blood, there would be a plasma volume equal to $33.5 \times .548/.452 = 40.6$ ml per kg. The excess plasma is

thus 50.2 − 40.6 = 9.6 ml per kg, or 11.5 per cent of the virtual vascular space. The percentage in splenectomized dogs under barbital anesthesia is considerably larger, as might be expected since the excess cells of the spleen cancel out an equivalent volume of excess plasma. In a series of 12 barbitalized dogs, splenectomized for at least 2 weeks in our laboratory, the average volume of excess plasma was equivalent to 19 per cent of the virtual vascular space (Lawson, unpublished data). The values given in table 2 for excess plasma in the intact rhesus monkey are of the same order of magnitude. When excess plasma is calculated from transit-time data, as was done in table 4 for the dog's pulmonary circulation, it is considerably less.

The percentage excess plasma in the total vascular space may be calculated directly from H_m/H_c, since it is equal to $(1 - H_m/H_c) \times 100$. The tissues studied by Gibson and his colleagues (82) and shown in table 3 of this chapter were allowed to bleed when they were excised, and contained no grossly large vessels. It is therefore not possible to estimate with any reliability the fractions of the original vascular spaces which are represented by the data. If the excess plasma is calculated, however, as a fraction of the residual vascular volume, substituting H_t for H_m in the calculation, the excess plasma in the kidney samples represents 63 per cent, in the bowel samples 58 per cent, and in cardiac and skeletal muscle tissues 45 to 47 per cent of the volume.

Anatomical Limits of the Plasma Compartment

The mechanisms known or postulated for rendering peripheral segments of the circulatory system poorer in cells than the central circulation are limited in operation to minute vessels. These are the phenomena of plasma skimming as described by Krogh (134), and axial cell streaming as demonstrated by Fåhraeus (66, 67). Cohnstein & Zuntz (42) in 1888 were the first to comment on the paucity of cells in the smallest vessels, and the cell enrichment which visibly occurs as they dilate. Since their data were obtained by microscopic inspection, they cannot be quantitated. It may be significant for the present purposes, however, that the largest vessels which became recognizably cell-poor on constriction, in their observations, had diameters of 30 to 40 μ. It is neither feasible nor profitable to estimate the total volume, in cardiovascular segments of all diameters, of the layer of stagnant, cell-free plasma. In all segments of large diameter it is an insignificant fraction of the total

TABLE 5

Segment	Volume, ml	% of total	
Heart	140	14.0	
Systemic arteries greater than 0.3	109	10.9	
Pulmonary arteries greater than 0.3	40	4.0	
Systemic veins greater than 0.3	345	34.5	
Pulmonary veins greater than 0.3	114	11.4	
Systemic arteries 0.1–0.3	10	1.0	12.9
Pulmonary arteries 0.1–0.3	28	2.8	
Systemic veins 0.1–0.3	64	6.4	
Pulmonary veins 0.1–0.3	27	2.7	
Systemic vessels less than 0.1	112	11.2	12.3
Pulmonary vessels less than 0.1	11	1.1	
Totals	1000	100	25.2

The probable volume distribution in segments of the cardiovascular system. Computed for a 12 kg dog with blood volume of 1000 ml, from data of Green (89) and Schleier (206). The numbers designating segments refer to diameters in mm.

contents. In Fåhraeus' studies, a reduction in hematocrit and in relative viscosity were just measurable in tubes of 0.3 mm diameter, and became marked only in tubes smaller than 0.1 mm diameter (66, 67). Plasma skimming, as a general phenomenon, appears to be related to axial streaming, and is accordingly limited to vessels of similar small size. Table 5 is an attempt, on the basis of admittedly inadequate data, to formulate for the entire circulatory system the percentage of blood in vessels less than 0.3 mm and 0.1 mm diameter. In constructing the table I have used Green's expansion of Mall's measurements of the mesenteric vessels (89) and Schleier's presentation of Miller's measurements on the pulmonary vessels (206). I have included an estimate of mean heart volume based on an assumed stroke volume of 25 ml, 50 per cent ventricular emptying, and a mean atrial volume equal to 75 per cent of the ventricular volume. All values have been adjusted for a 12-kg dog, with blood volume equal to 1000 ml. It appears unlikely from the table that more than 12 per cent of the total circulatory volume is composed of vessels smaller than 0.1 mm diameter, or 25 per cent of vessels smaller than 0.3 mm diameter. These are somewhat larger estimates than those of Landis & Hortenstine (135), who, using Lewis' definition of minute vessels, estimated them to comprise 19 per cent of the systemic and 21 per cent of the pulmonary circuits. If their estimates are corrected to include the 14 per cent of

the total blood volume which occupies the heart, the minute vessel segments of the entire circulatory system would contain 17.4 per cent of the total blood volume. Taking the 0.3 mm upper limit of table 5 as the most liberal estimate, and assuming that the mean hematocrit in all vessels smaller than 0.3 mm diameter is one-half that of blood in the central circulation, room can be found within the anatomical confines of the circulatory system for excess plasma equal to no more than 13 per cent of the total volume. Our concepts of the quantitative anatomy of the cardiovascular system need revision if 25 per cent of it is to be filled with cell-free plasma in the rat (236), 19 per cent in the splenectomized dog (Lawson, unpublished data), and 17 per cent in the monkey (97).

Recent studies raise serious doubts about the ability of blood capillaries to keep even the largest macromolecular plasma labels within the confines of the vascular system. The isolated perfused hind limb of the dog under certain experimental conditions behaves as though the capillaries have pores of fairly uniform radius in the range of 35 to 45 Å (178). Electron microscopy of a variety of capillaries, however, reveals no such uniformity. Capillaries in muscle, lung, and the central nervous system have no visible pores, whereas those in the kidneys, intestinal villi, and some endocrine glands do. At the other extreme, there are sizeable gaps between endothelial cells in the liver and spleen (21). The appearance of dextrans of graded molecular size in leg, cervical, and hepatic lymph in the dog following their intravenous injection suggests that, in addition to pores of rather uniform radius, there are an even larger number of leaks permitting bulk flow of particles up to 350 Å radius (98). Furthermore, the permeability to large molecules seems to be increased in the dog by expansion of the plasma volume. The concentration in lymph of previously injected radioiodinated albumin or dextran is increased when plasma volume is increased by infusing large volumes of albumin solution, at the same time that the concentration in plasma is lowered by dilution. The increase in lymph concentration occurs for all dextrans up to mol wt 255,000, but seems to be more marked in the case of the larger molecules (215).

In the rabbit there appears to be a rapid flux of large molecules such as antipneumococcus globulin between plasma and extravascular regions. The plasma titre falls to about one-half within 24 hours after these globulins are injected, and rises, presumably by exchange with extravascular pools, for about the same length of time after normal plasma has been infused (85). There is good reason to believe that in the cat I^{131} albumin spreads to a considerable extravascular distribution in the kidney within 5 min of its injection. Lowering arterial pressure in the cat causes an increase in both the hemoglobin content and the I^{131} content of the kidney, such that if both labels remained intravascular, and their increase represented an increase in cell and plasma volume, kidney weight must increase by about 6.5 per cent. Since the weight of the kidney not only failed to increase, but actually decreased significantly, it was concluded that the increase in I^{131} content did not represent an increase in plasma volume, but an increase in the distribution space of this label beyond the vascular system (179). This may be comparable to the extravascular spread of I^{131} albumin which has been reported for the small intestine of the rabbit, where I^{131} appears in intestinal juice in presumably undamaged loops within a few minutes of label injection (14).

It is obviously not possible, on the basis of present knowledge, to reconcile the operational definition of plasma volume with its conceptual definition. Whether the conceptual definition needs revision to permit bulk flow of plasma beyond the confines of the vascular system remains to be seen. Differences in the distribution of individual plasma labels are discussed in the next section.

PLASMA LABELS

Barratt & Yorke (20) in 1909 injected a solution of hemoglobin into rabbits, and calculated plasma volume from its concentration in plasma samples. This appears to have been the first use of a plasma label whose concentration, of necessity, was measured in plasma rather than in whole blood. The following year Abderhalden & Schmid (1) injected dextrin into dogs and calculated plasma volume from plasma concentrations. Regarding this simply as a technically necessary step toward the calculation of blood volume, only the latter values were reported. From the data given in their protocols, however, it is apparent that the plasma volumes found in the three dogs of their study were 66.6, 64.5, and 57.7 ml per kg, respectively. The average plasma volume found for dogs with T-1824 by modern techniques is about 48 ml per kg (25). It seems probable, therefore, that fairly large losses of dextrin occurred during the 5-minute period which Abderhalden and Schmid allowed for mixing.

Schürer's foreign protein precipitation procedure, introduced in 1911, was also carried out on plasma, but his concern for measuring blood volume as an entity was such that he neglected to report data from which plasma volume may be computed (209). This is true of most of the earlier work, which introduced a variety of plasma labels, including those mentioned above, and others such as antitoxins and gum acacia. Erlanger (64) has written a critical review of the earlier methods, and Gregersen & Rawson (95) have published a synopsis of events in the history of methodology.

The introduction of a dye label for plasma by Keith *et al.* (127) in 1915 made it technically imperative to measure concentrations in plasma. Since plasma volume was calculated as a first step toward the calculation of blood volume, it was usually reported separately, along with the final value for blood volume. The dye chosen for the original studies, known as vital red, was nontoxic in doses adequate for visual colorimetry, and disappeared from circulating plasma, after the mixing period, at rates less than 20 per cent per hour. In order to avoid an overestimation of plasma volume due to dye loss (methods for correction had not yet been proposed), plasma samples were taken at the earliest moment after mixing was thought to be complete. Usually the average concentration for two samples, drawn at 3 and 6 min, was used in the calculation. The mean plasma volume found in a group of 42 normal human males was 48.1 ml per kg (127), which is in fairly good agreement with the value of 46.5 ml per kg obtained by current methods with T-1824 (93).

Since both the supply and the characteristics of the original dye were unreliable, Dawson *et al.* (50) in 1920 examined a large number of additional dyes for their potentialities as plasma labels. Twenty-nine were found with slow disappearance rates comparable to that of vital red. All of them gave about the same value for plasma volume in a group of dogs, when calculations were made from the 4-minute plasma dye concentration. A blue azo dye, known as Evans blue, was selected as somewhat superior to the rest because of its slow disappearance rate, and because it could readily be distinguished from hemoglobin in the event of hemolysis. The synthetic structure of this dye is indicated by the designation T-1824, which means that it is synthesized by combining orthotolidine with 2 moles of 1,8-amidonaphthol 2,4-disulphonic acid (6).

Evans Blue Dye, T-1824

Systematic studies of this dye were started in 1935 by Gibson & Evans (77) and Gregersen and collaborators (92). They have resulted in a more complete investigation of this material as a plasma label than of any other, and many of the techniques which have become standard practice for T-1824 have been carried over for other labels.

The dye, with a molecular weight of 960, is readily diffusible in aqueous solution, but is made nondiffusible through collodion by the addition of plasma. When it has been added to plasma, and its electrophoretic and ultracentrifugal behavior are observed, it becomes apparent that it is bound to plasma albumin (187). The exact nature of its attachment to protein is poorly understood, as is true of biological stains in general (18). Since it is an anionic or acid dye, it is thought to combine with available basic groups in the albumin molecule, such as lysine, arginine, and histidine (129). The absorption spectrum of the dye, however, differs in the plasma of different species, suggesting that there are several different types of binding (5). Crystalline bovine albumin has 11 demonstrable binding sites, with dissociation constants for the reaction at the first site which indicate firm binding (6). Its binding is not so firm, however, as to resist removal of considerable amounts of dye by ion-exchange resins (144).

The kinetics of the dye-albumin interaction has been studied by measuring the time required for optical density to stabilize after the two are mixed. At 37°C this requires 40 to 50 sec (19). Although the possibility exists that unbound, and hence diffusible, dye may reach capillary beds under some conditions, there is no published evidence for dye loss before binding has occurred. If plasma is predyed before injection, its distribution volume within the circulation is the same as that of injected unbound dye (142). Furthermore, plasma volume in the dog is the same when it is measured by intra-arterial and by intravenous injections of T-1824 (Lawson, unpublished data). Although the percentage of uncombined dye increases as the molar ratio dye:albumin increases, a one-hundredfold increase in the dye dosage does not change the value obtained for plasma volume in the dog (4).

In the postmixing period, plasma dye concentration usually declines at the rate of 4 to 15 per cent for the first 2 hours in man (77) and in the dog (7, 191,

200). The apparent disappearance rate may be exaggerated by dilution with recruited plasma if frequent large samples are drawn (3, 9). The mechanisms which clear the plasma of dye are not fully known, and appear to be of several different kinds. Some appear to be specific for dyes as a group. Others are operative for all plasma labels, and involve processes which mix labeled plasma proteins with the total extracellular protein pool, from which they are removed metabolically.

Azo dyes as a group have long been known to be phagocytized by reticuloendothelial cells (220, 221). In rat and rabbit granules of T-1824 can be seen within liver cells 1 min after intravenous dye injection (121). In the rabbit, 24 hours after injection, dye granules are visible in macrophages in the kidney, liver, spleen, and lymph nodes (137). The rate of dye disappearance in the rabbit is unusually high, averaging about 18 per cent per hour. It is doubled by administration of histamine, and is reduced by antihistaminics or by Thorotrast, the latter presumably producing endothelial blockade (122). It may be significant that the distribution space of T-1824 in the rabbit is about 8 per cent larger than that of radioiodinated serum albumin (244). Cruickshank & Whitfield (49) reported in 1945 that if cats were previously injected with India ink or with a priming dose of T-1824, the fall in dye concentration during the mixing period when T-1824 was subsequently injected was reduced and abbreviated, and the value calculated for plasma volume was considerably smaller. It was suggested that excessive amounts of dye are phagocytically removed during the mixing period unless the phagocytic cells are already saturated. This observation has not been confirmed in the unanesthetized cat, second dye injections shortly following the first giving approximately the same value for plasma volume (Gregersen, personal communication). Studies on other species have also failed to demonstrate that tissues which might be capable of such excessive unobserved dye removal can be saturated. A constant value for plasma volume is obtained by repeated dye injections in man (27, 31, 190), in the dog (176, 228), and in the rabbit (46).

Dye appears in bile within 1 half-hour of its injection in the dog, but the amount excreted in this way during the first few hours accounts for only 2 to 7 per cent of that lost from blood (157). Insignificant amounts are excreted through any channel in the first 6 to 8 hours in the rat, carcass extraction at this time yielding nearly the entire injected dose. Since plasma concentration has fallen to about one-third, the remainder of the dye has obviously moved into an extravascular distribution (39). Extravascular accumulations have been demonstrated in cells of the proximal convoluted tubules of the rat's (212) and the dog's (47) kidney. Radioiodine also appears in the dog's tubular cells after radioiodinated serum albumin has been injected, but its accumulation follows quite a different course from that of the dye. Whereas I^{131} rapidly reaches a plateau of activity in the tubular cells, the dye progressively increases in concentration for a period of 24 hours (47).

Other known mechanisms for clearing plasma of dye seem to be nonspecific, and to remove other plasma labels as well. Within a few minutes after intravenous injection of dye and radioiodinated albumin, both labels appear in thoracic duct lymph (32, 69, 132, 220, 237). The concentration in lymph remains below that in plasma for several hours (69, 237), and since the flow of lymph is small, it seems unlikely that the return of label to blood by way of the lymphatic system could influence the plasma disappearance curve. Of much greater significance is the obvious fact that label must have traversed extravascular spaces before it can appear in lymph. The amount of label lost to these spaces, and the volume of the latter, cannot be computed from any available data (32). Newly formed capillaries appear to be more permeable to dye than older vessels, since dye can be seen outside the youngest capillaries in the rabbit's ear chamber preparation, as soon as 30 min after injection (2). Extravascular dye has been demonstrated in the pinna of the human ear within 2 hours, by applying sufficient external pressure to render the ear temporarily bloodless for spectrophotometry (44).

Since excessive removal of dye during the mixing period cannot be dismissed on a priori grounds, proof of the validity of dye measurements of plasma volume has had to rest upon a comparison of dye distribution volume with that of other labels. Gregersen and his colleagues have found the same distribution volume in the dog for T-1824, for three antigens of different molecular size, bovine albumin, bovine globulin, and pneumococcus polysaccharide (90), and for hemoglobin (7). The distribution space of T-1824 in the turtle is the same as that of dextran with molecular weight 66,000 (213). The dye and radioiodinated albumin are found by the majority of investigators to have nearly identical distribution volumes in man (48, 73, 123, 208) and in the dog (73, 210). Technical errors, or an interaction between the two labels

when they are injected as a mixture (73), may account for the differences which have occasionally been reported for these two species (16, 17, 133, 227). In some other species, however, there seems little doubt that T-1824 has a consistently larger distribution volume than radioiodinated albumin. This has been reported for the rabbit (242, 244) and for the mouse (242). Comparative values are not available for the rat. They might throw light on the widely varying T-1824 distribution volumes reported by different investigators for this species. These vary from a low of 27.3 ml per kg (148) to a high of about 40 ml per kg (155, 236).

Comparative studies with a variety of plasma labels are needed in other species, in view of demonstrated species differences. They are also needed in man and in the dog under abnormal conditions. The dye T-1824, along with others such as Congo red, disappears at very fast rates in human subjects with amyloidosis, with improbably large initial distribution spaces in the neighborhood of 100 ml per kg (232). In congestive heart failure it is still not clear whether the enlargement of plasma volume is as great as it is made to appear by T-1824, or whether this is in part due to abnormal dye distribution. Blood volume appears to be increased in this condition when it is estimated with T-1824 as the only label, but not when it is estimated with P^{32} (202, 203). The error in such estimates has already been discussed. The magnitude of the error, especially when attempts are made to correct H_c to H_m, is likely to be greater in those abnormal states in which precise knowledge of blood volume would be of the greatest value. When both cells and plasma are labeled, the distribution volumes of both are found to be increased in congestive failure, and the ratio mean circulatory hematocrit:central hematocrit reduced (207). Although it is clear that other plasma labels such as radioiodinated albumin have an expanded distribution in this condition, it is not clear, in the absence of comparative data, whether the expansion is the same as it is for dye (207).

An attempt was made in our laboratory a number of years ago to compare, in acutely splenectomized dogs, the distribution space of T-1824 with that of undyed albumin, by using equation 2 as explained in the introduction to this chapter (142). When these studies were repeated recently on intact dogs, using a continuous exchange to replace dyed circulating plasma with undyed plasma without disturbing arterial pressure, the dye and the undyed plasma which replaced it seemed to have the same distribution volume (fig. 2). Although such studies throw no light on the anatomical distribution of the dye, it is clear that any dye which may have escaped from circulating plasma in normal dogs is freely exchangeable with it.

Other Dyes

A red dye resembling the original Rowntree dye but with better controlled composition, and known as brilliant vital red, was introduced in 1920 (115). In its early circulatory behavior it is indistinguishable from T-1824 (56, 182). A number of other blue dyes have been used by European workers (see ref. 95). The composition of T-1824 from readily available sources is more carefully standardized than that of most dyes, and more is known about its physiological behavior, spectral characteristics in plasma, and protein binding. There is little reason to believe that search for a superior dye label for plasma would be worthwhile.

Dyes which are rapidly cleared from plasma by hepatic, renal or other special excretory mechanisms were discarded by Dawson *et al.* (50) as being unsuited for plasma volume measurement. If unobserved disappearance rates during the mixing period are proportional to the observed rates for the post-mixing period, present methods of correcting for loss during the mixing period should be inadequate for reasons that were stated earlier. It is difficult to reconcile with these considerations a report that rose Bengal, which has a disappearance rate of 50 per cent in 8 min in the dog, has the same distribution volume as T-1824 (216).

Plasma Proteins Labeled with Radioactive Tracers

These were introduced by Seligman & Fine (70, 71, 211) in 1943. It is now possible to label albumins or globulins in vitro with I^{131} or Cr^{51}; or in vivo by administering tracer-labeled amino acids to donors. The tracers most commonly employed in vivo are C^{14} and S^{35}, and since they become metabolically incorporated in plasma proteins, there is every reason to believe that the labeled proteins follow completely normal metabolic pathways. There is, on the other hand, no reason to believe that artificially labeled proteins, whether the label is a dye, I^{131}, or Cr^{51}, will have a normal metabolic history. For metabolic studies, the disappearance of protein label from plasma is followed for a period of days or weeks, and the biological half-life is usually computed

from such data, as the time when the circulating label has declined to one-half its initial value, corrections being made for radioactive decay. Such studies show that the half-life of proteins artificially labeled with I^{131} is considerably shorter than that of proteins naturally labeled with C^{14} or S^{35}, and becomes progressively less as the iodination is increased (11–13, 151). The half-life of T-1824 dyed albumin is less even than that of I^{131} albumin (210). The interpretation of such data is complicated, however, by label reutilization after metabolic breakdown of the labeled protein. There is no evidence for transfer of dye to other circulating protein, and there seems to be little retention of I^{131} released by metabolic degradation of iodinated protein (24). Even the naturally incorporated labels C^{14} and S^{35} have different half-lives, due to differences in the rates of metabolic degradation of the protein moieties containing them (241).

The requirements for metabolic studies, of course, are much more rigorous than those for measurements of plasma volume. A labeled protein is adequate for the latter purpose if its initial distribution space after circulatory mixing is the same as that of normal plasma proteins. It is unfortunate for the present purposes that most studies comparing naturally and artificially labeled proteins have been done with a primary interest in metabolic history. Samples are usually taken at such long intervals that it is impossible to extrapolate the disappearance slope for the first hour or two to an exact intercept in order to compare initial distribution volumes. The reported data permit a comparison of the total exchangeable protein pools accessible to various labels, rather than of the initial circulatory distributions (151). In the few studies, however, in which attention has been given to the initial distribution, no difference has been found for proteins artificially labeled with I^{131} and those naturally labeled with C^{14} or S^{35} (40, 65).

Because of its commercial availability as prepared radioiodinated human serum albumin, its convenient radioactive half-life, and its ease of measurement, I^{131} has been the most widely used radioactive plasma label. Relatively few studies have been done on species other than man with homologous iodinated albumin (179, 242, 244). Still fewer have compared heterologous and homologous albumins, and these have failed to reveal a difference, so far as behavior related to plasma volume measurement is concerned (14, 237). Since dyed canine albumin and iodinated human albumin have the same initial distribution volume in the dog, heterology seems to be of no consequence in this species (210).

The preparation of Cr^{51} proteins as suggested by Gray & Sterling (88) in 1950 is technically much simpler than the preparation of I^{131} proteins (120, 150, 165), and should facilitate studies with radioactively labeled autologous proteins. The only reported studies with Cr^{51} as a plasma label, however, have been done by injecting unbound $Cr^{51}Cl_3$ on the assumption that protein binding would occur within the circulation before appreciable loss had occurred (72, 219). Insufficient data have been reported with this technique to permit evaluation.

Only scattered data on other radioactive plasma labels are available. The report in abstract that radioiodinated globulin has a smaller distribution volume in man than T-1824 is puzzling (198). It is in conflict with the documented report of identical initial spaces for the dye and globulins in the dog (90) and with data on the time required for albumins and globulins to mix in the total exchangeable protein pool (40, 151, 158).

CELL LABELS

The first practical approach, in 1882, to measurement of blood volume as a distribution space, made use of carbon monoxide. Although it is a cell label, and was selected by Gréhant and Quinquaud because of its affinity for hemoglobin, cell volume was not calculated separately (see reference 64). Carbon monoxide remained the only systematically employed cell label throughout the period when dye methods were being developed for plasma volume. When the concentration of carbon monoxide was measured in whole blood, and a value for total blood volume was calculated, this usually agreed fairly well with the value obtained by adding the dye distribution space and CV_h. Since a cell label and a plasma label thus seemed to have the same distribution volume in circulating whole blood, no need was apparent for labeling both compartments and calculating them separately (116, 201).

It was not until other cell labels were introduced, during the decade beginning in 1940, that the inadequacy of carbon monoxide as a cell tag began to become apparent. Improved methods have been developed for administering the gas and for measuring its concentration (199). For clinical use, procedures have been devised which obviate the need for drawing blood samples, blood concentrations being calculated

from the gas tensions in alveolar air (8, 217). These do not eliminate the basic defect which makes this an unsuitable label for measuring the red cell volume. It seems possible that the procedures may be modified, with a longer mixing period, so as to obtain values for the total body content of hemoglobin-like pigments.

It has long been known that blood carbon monoxide concentration continues to fall for a considerable period after its administration has been discontinued (54). Only 60 to 70 per cent of the gas which disappears from blood during the first hour is found in expired air, although ultimately all of it is excreted in this way (205). Whipple (239), suspecting an exchange between circulating carbon monoxide hemoglobin and the hemoglobin of muscle, extracted muscle in dogs, and estimated that muscle hemoglobin combined with 10 to 80 per cent as much of the gas as did the hemoglobin of blood. This was a far greater extravascular distribution of the gas, and a larger and less constant error, than the 5 per cent estimate of early investigators (107). The extravascular accumulation of carbon monoxide in muscle has been demonstrated in dogs by injecting Cr^{51}-tagged cells at the time the gas is administered, and measuring the activity of both labels in muscle tissue. The ratio $CO:Cr^{51}$ is consistently higher in muscle than in blood (238). As would be expected, cell volume, measured as the distribution volume of carbon monoxide, is consistently larger than that measured with more specific and firmly fixed cell labels (168, 171, 200).

Cells may be labeled with methemoglobin by treating drawn blood with nitrites (162), or with Heinz granules by treating with phenylhydrazine (169). Serologically identifiable untreated cells are probably preferable (15, 19). Labeling with radioactive tracers permits the choice of a fairly large number of materials, some of which remain attached to the cell for its life, and some of which are less permanent. Some tracers may be introduced metabolically in donors, others are incorporated in cells in vitro, and thus permit the labeling of autologous cells. Radioactive cell labels have superseded all others for blood volume studies.

Radioiron

Hahn *et al.* (102) observed in 1939 that when salts of Fe^{59} were fed to anemic dogs, the isotope became concentrated in newly formed red cells. Cells labeled in this manner in donor dogs were first used for cell volume studies in 1941 (104, 106). The use of donors is imperative, as there is no Fe^{59} uptake by cells or by hemoglobin solution in vitro (103). When the procedure is employed in man, satisfactory labeling of donor cells is achieved within about 3 weeks following a single radioiron injection, even though the donor is not anemic (84). The other radioisotope of iron, Fe^{55}, with a much longer half-life, has also been used (84). The two isotopes are readily distinguished by differences in type of radiation (181).

The labeling of erythrocyte hemoglobin is permanent, and persists for the life of the cell (76, 79). Since the labeled cells are all freshly released young cells, and since, if they are prepared in anemic donors, they are also microcytic and hypochromic, their distribution may not be typical of the whole population of circulating cells (100). If blood incompatibilities are avoided, however, their distribution space is the same as that of injected autologous cells labeled with P^{32} (167). Anomalous data may be obtained if incompatibilities exist between recipient and donor. This seems to be a greater hazard in the dog (100, 166) than in man (84), probably because blood typing in man has been more thoroughly studied and is technically simpler than in the dog (108, 231). Even less is known for other species.

Radiophosphorus P^{32}

Hahn & Hevesy (105) introduced P^{32} as a cell label in 1940. They first attempted to achieve firm labeling of cells by tagging the phosphatids in maturing erythrocytes in donor animals which received $NaHP^{32}O_4$, but found most of the P^{32} in freely exchangeable acid-soluble forms. Although they consequently abandoned this procedure in favor of in vitro labeling of mature autologous cells (113), phosphatid tagging of donor cells is sometimes done when there is need for a more permanent label (34, 179). Despite the rapid uptake of inorganic P^{32} by the cells of drawn blood, it is released relatively slowly when the cells are placed in inactive plasma (10, 113, 128, 189). The difference in rate of P^{32} ingress and egress is undoubtedly due to the fact that its specific activity in plasma is high and in cells low at the time when equilibrium is reached (113).

If, after incubation with P^{32}, the cells are properly washed before they are injected (36), the label disappears from circulating blood at the average rate of about 6 per cent per hour in man (194) and in the unanesthetized dog (191). Neither barbital anesthesia

nor acute splenectomy in the dog seems to influence the disappearance rate. In our laboratory, 41 intact barbitalized dogs had an average P^{32} disappearance of 5.25 per cent per hour, while 31 acutely splenectomized dogs under the same anesthetic had an average rate of 5.88 per cent (Lawson, unpublished data). The near identity of disappearance rates in different species and under different experimental conditions is reassuring, in view of the fact that the turnover of inorganic phosphorus is probably influenced by metabolic processes (68).

There appears to be no excessive loss of this label during the mixing period, since its distribution volume is the same as that of cells firmly tagged with Fe^{55} or Fe^{59} (22, 167), or with Cr^{51} (160). That its distribution space is the same as that of transfused unlabeled cells has been shown by using the procedure described in the introduction for equation 2 (see fig. 2).

Radiochromium

Cr^{51} was found by Sterling & Gray (87, 88) in 1950 to be rapidly attached to red cells in drawn blood if it was added to blood in the form of the hexavalent anion. As much as 90 per cent of added chromium may become bound by erythrocytes in a half-hour at room temperature (224). Most of the Cr^{51} is bound to the globin moiety of hemoglobin (88), and the binding appears to be quite stable in vitro. If unlabeled red cells are incubated with hemolyzed Cr^{51}-labeled cells, they take up none of the label (60). When Cr^{51} is added to blood in the form of the trivalent cation, very little enters the cells but it combines with the plasma proteins. These chromium-protein complexes also appear to be quite stable in vitro, no transchromation being demonstrable when labeled and unlabeled proteins are allowed to stand together for periods of several days (88).

There is less certainty about the persistence of Cr^{51}-labeled cells in the circulation. The labeling slightly increases their mechanical fragility (164). This may be partially responsible for the reduced life span of Cr^{51}-labeled cells as shown by serological techniques (60, 81, 164). Damage to the cells, as suggested by such studies, is due to chromation per se, and not to mishandling while the cells are being treated, since identical decay curves for Cr^{51} are obtained for cells prepared in vitro and injected into the circulation, and for cells chromated in vivo by injecting $Na_2Cr^{51}O_4$ into the subject (229). Slow elution of Cr^{51} at the rate of about 1 per cent per day can be demonstrated by suspending chromated cells in saline, and dialyzing (164).

Despite uncertainty about the life span of chromated cells, there is no evidence of excessive destruction during the mixing period. The distribution space calculated for them is the same as that of P^{32} labeled cells (160). Except for the initial mixing period, the rate of Cr^{51} disappearance from blood is exponential throughout, including the first day, unless very high concentrations of chromium are employed (125).

Other Radioactive Labels

Insufficient data have been presented on other radioactive labels to permit their evaluation. Cells labeled in vitro with K^{42} have been reported to have the same virtual distribution space as those labeled with P^{32} (243). Thorium B has been proposed as a suitable cell label for blood volume studies (111, 112), and it has been suggested that firm P^{32} labeling be accomplished by administering to donors the drug diisopropylfluorophosphonate with the phosphonate group containing the radioisotope (41).

REFERENCES

1. ABDERHALDEN, E., AND J. SCHMID. Bestimmung der Blutmenge mit Hilfe der "Optischen Methode." *Ztschr. Physiol. Chem.* 66: 120, 1910.
2. ABELL, R. G. The permeability of blood capillary sprouts and newly formed blood capillaries as compared to that of older blood capillaries. *Am. J. Physiol.* 147: 237, 1946.
3. ADOLPH, E. F., M. J. GERBASI, AND M. J. LEPORE. The rate of entrance of fluid into the blood in hemorrhage. *Am. J. Physiol.* 104: 199, 1945.
4. ALLEN, T. H., AND M. I. GREGERSEN. Measurement of plasma volume in the dog with high concentrations of T-1844. *Am. J. Physiol.* 172: 377, 1953.
5. ALLEN, T. H., M. OCHOA, R. F. ROTH, AND M. I. GREGERSEN. Spectral absorption of T-1844 in plasma of various species and recovery of the dye by extraction. *Am. J. Physiol.* 175: 243, 1953.
6. ALLEN, T. H., AND P. D. OROHOVATS. Combination of toluidine dye isomers with plasma albumin. *Am. J. Physiol.* 161: 473, 1950.
7. ALLEN, T. H., C. PALLAVICINI, AND M. I. GREGERSEN. Simultaneous measurement of plasma volume with hemoglobin and with T-1824. *Am. J. Physiol.* 175: 236, 1953.
8. ALLEN, T. A., AND W. S. ROOT. Partition of carbon

monoxide and oxygen between air and whole blood of rats, dogs, and men as affected by plasma pH. *J. Appl. Physiol.* 10: 186, 1957.

9. ALLEN, T. H., AND R. E. SEMPLE. Effects of repeated sampling on plasma and cell volumes in dogs as estimated with small and large amounts of T-1824. *Am. J. Physiol.* 165: 205, 1951.
10. ANDERSON, R. S. The use of radioactive phosphorus for determining circulating erythrocyte volumes. *Am. J. Physiol.* 137: 539, 1942.
11. ARMSTRONG, S. H., J. KUKRAL, J. HERSHMAN, K. MCLEOD, J. WOLTER, AND D. BRONDEY. Persistence in the blood of radioactive label. *J. Lab. & Clin. Med.* 45: 51, 1955.
12. ARMSTRONG, S. H., J. KUKRAL, J. HERSHMAN, K. MCLEOD, AND J. WOLTER. Comparison of the persistence in blood of gamma globulins labeled with S^{35} and I^{131} in the same subjects. *J. Lab. & Clin. Med.* 44: 762, 1954.
13. ARMSTRONG, S. H., K. MCLEOD, J. WOLTER, AND J. KUKRAL. Persistence in the blood of radioactive label (of proteins). *J. Lab. & Clin. Med.* 43: 918, 1954.
14. ARMSTRONG, F. B., S. MARGEN, AND H. TARVER. Site of degradation of serum albumin. *Proc. Soc. Exper. Biol. & Med.* 103: 592, 1960.
15. ASHBY, W. The determination of the length of life of transfused blood corpuscles in man. *J. Exper. Med.* 29: 267, 1919.
16. AUST, J. B., S. N. CHOU, J. F. MARVIN, E. L. BRAGKNEY, AND G. E. MOORE. A rapid method for clinical total blood volume determination using RIHSA. *Proc. Soc. Exper. Biol & Med.* 77: 514, 1951.
17. AUST, J. B., S. N. CHOU, J. F. MARVIN, E. L. BRACKNEY, AND G. E. MOORE. The use of radioactive iodinated human serum albumin for clinical total blood volume studies. *Surg. Forum* 1951, p. 601.
18. BAKER, J. R. *Principles of Biological Microtechnique.* London: Methuen, 1958.
19. BARNES, D. W. H., J. F. LOUTIT, AND E. B. REEVE. Observations on the estimate of the circulating red blood cell volume in man by T-1824 and the hematocrit, with special reference to uncorrected dye loss from the circulation. *Clin. Sc.* 7: 155, 1948.
20. BARRATT, J. O. W., AND W. YORKE. A method of estimating the total volume of blood contained in the living body. *Proc. Roy. Soc., London, ser. B* 81: 381, 1909.
21. BENNETT, H. S., J. H. LUFT, AND J. C. HAMPTON. Morphological classifications of vertebrate blood capillaries. *Am. J. Physiol.* 196: 381, 1959.
22. BERLIN, N. I., R. L. HUFF, D. C. VAN DYKE, AND T. G. HENNESSY. The blood volume of the adult rat as determined by Fe^{59} and P^{32} labeled red cells. *Proc. Soc. Exper. Biol. & Med.* 71: 176, 1949.
23. BERSON, S. A., AND R. S. YALOW. The use of K^{42} or P^{32} labeled erythrocytes and I^{131} tagged human serum albumin in simultaneous blood volume determinations. *J. Clin. Invest.* 31: 572, 1952.
24. BERSON, S. A., R. S. YALOW, S. S. SCHREIBER, AND J. POST. Tracer studies with I^{131} labeled human serum albumin: Distribution and degradation studies. *J. Clin. Invest.* 32: 746, 1953.
25. BONNYCASTLE, D. D., AND R. A. CLEGHORN. A study of the blood volume of a group of untrained normal dogs. *Am. J. Physiol.* 137: 380, 1942.
26. BRADLEY, S. E., P. A. MARKS, P. C. REYNELL, AND J MELTZER. The circulating splanchnic blood volume in dog and man. *Tr. A. Am. Physicians* 66: 294, 1953.
27. BRADY, L. W., D. Y. COOPER, M. COLODZIN, J. E. MCCLENATHAN, E. R. KING, AND R. WILLIAMS. Blood volume studies in normal humans. *Surg. Gynec. & Obst.* 97: 25, 1953.
28. BROWN, E., J. HOPPER, J. J. SAMPSON, AND C. MUDRICK Venous congestion of the extremities in relation to blood volume determinations and to mixing curves of carbon monoxide and T-1824 in normal human beings. *J. Clin. Invest.* 30: 1441, 1951.
29. BRUNER, H. D., (editor). *Methods in Medical Research*, vol. 8. Chicago: Yr. Bk. Pub. 1960.
30. BUSH, J. A., W. N. JENSEN, G. E. CARTWRIGHT, AND M. M. WINTROBE. Blood volume studies in normal and anemic swine. *Am. J. Physiol.* 181: 9, 1955.
31. CAMPBELL, W. N., A. SOKALCHUK, AND R. PENMAN. Validity of T-1824 in plasma volume determinations in the human. *Am. J. Physiol.* 152: 563, 1948.
32. CARDOZO, E. L. The disappearance of the blue dye T-1824 from the bloodstream into the thoracic duct lymph. *Arch. Néerl. Physiol.* 25: 410, 1940.
33. CATON, W. L., C. C. ROBY, D. E. REID, R. CASWELL, C. J. MALETSKOS, R. G. FLUHARTY, AND J. G. GIBSON. The circulating red cell volume and body hematocrit in normal pregnancy and the puerperium. *Am. J. Obst. & Gynec.* 61: 1207, 1951.
34. CHAIKOFF, I. L., AND D. B. ZILVERSCHMIT. *Advances in Biological and Radioactive Phosphorus: Its Application to the Study of Phospholipid Metabolism. Medical Physics.* New York: Acad. Press, p. 321, 1948.
35. CHAPIN, M. A., AND J. F. ROSS. The determination of the true cell volume of dye dilution, by protein dilution, and with radioactive iron. The error of the centrifuge hematocrit. *Am. J. Physiol.* 137: 447, 1942.
36. CHAPLIN, H. Precision of red cell volume measurement using P^{32} labeled cells. *J. Physiol.* 123: 22, 1954.
37. CHAPLIN, H., AND P. L. MOLLISON. Correction for plasma trapped in the red cell column of the hematocrit. *Blood* 7: 1227, 1952.
38. CHAPLIN, H., P. L. MOLLISON, AND H. VETTER. The body/venous hematocrit ratio: Its constancy over a wide hematocrit range. *J. Clin. Invest.* 32: 1309, 1953.
39. CLAUSEN, D. F., AND N. LIFSON. Determination of Evans blue dye in blood and tissues. *Proc. Soc. Exper. Biol. & Med.* 91: 11, 1956.
40. COHEN, S., R. C. HALLOWAY, C. MATTHEWS, AND A. S. MCFARLANE. Distribution and elimination of I^{131} and C^{14} labeled plasma proteins in the rabbit. *Biochem. J.* 62: 143, 1956.
41. COHEN, J. A., AND M. G. P. J. WARRINGA. The fate of P^{32} labeled diisopropylfluorophosphonate in the human body and its use as a labeling agent in the study of the turnover of blood plasma and red cells. *J. Clin. Invest.* 33: 459, 1954.
42. COHNSTEIN, J., AND N. ZUNTZ. Untersuchungen uber den Flussigkeits-Austausch swischen Blut und Geweben unter verschiedenen physiologischen und pathologischen Bedingungen. *Pflüger's Arch. ges. Physiol.* 44: 303, 1888.
43. COLLINGS, W. D., AND H. G. SWANN. Blood and interstitial spaces of the functional kidney. *Fed. Proc.* 17: 28, 1958.

44. CONNOLLY, D. C., AND E. H. WOOD. Simultaneous measurement of the appearance and disappearance of T-1824 (Evans blue) in blood and tissue after intravenous injection in man. *J. Appl. Physiol.* 7: 73, 1954.
45. COURTICE, F. C. The blood volume of normal animals. *J. Physiol.* 102: 290, 1943.
46. COURTICE, F. C., AND R. W. GUNTON. The determination of blood volume by the carbon monoxide and dye (T-1824) methods in rabbits. *J. Physiol.* 108: 405, 1949.
47. COYE, R. D., D. BLINK, AND E. KLOPPEDAL. Comparison of T-1824 and I^{131} as protein labels in study of extravascular serum protein space in dogs. *Fed. Proc.* 19: 81, 1960.
48. CRISPELL, K. R., B. PORTER, AND R. T. NIESET. Studies of plasma volume using human serum albumin tagged with radioactive iodine. *J. Clin. Invest.* 29: 513, 1950.
49. CRUICKSHANK, E. W. H., AND I. C. WHITFIELD. The behavior of T-1824 in circulating blood and a modified method for the estimation of plasma volume. *J. Physiol.* 104: 52, 1945.
50. DAWSON, A. B., H. M. EVANS, AND G. H. WHIPPLE. Behavior of a large series of dyes introduced into the circulating blood. *Am. J. Physiol.* 51: 232, 1920.
51. DEAVERS, S., R. A. HUGGINS, AND E. L. SMITH. Changes in cell and plasma volumes of various organs produced by a massive transfusion in dogs. *Am. J. Physiol.* 191: 159, 1957.
52. DEAVERS, S., E. L. SMITH, AND R. A. HUGGINS. Critical role of arterial pressure during hemorrhage in the dog on release of fluid into the circulation and trapping of red cells. *Am. J. Physiol.* 195: 73, 1958.
53. DITTMER, D. S. (editor) *Handbook of Circulation*, Natl. Acad. Sci. Natl. Res. Council. Philadelphia: Saunders 1959.
54. DOUGLAS, C. G. The determination of the total oxygen capacity and blood volume at different altitudes by the carbon monoxide method. *J. Physiol.* 40: 472, 1910.
55. DOW, P., P. F. HAHN, AND W. F. HAMILTON. Simultaneous transport of T-1824 and radioactive red cells through the heart and lungs. *Am. J. Physiol.* 147: 493, 1946.
56. DOW, P., AND R. W. PICKERING. Behavior of dog serum dyed with brilliant vital red or Evans blue toward precipitation with ethanol. *Am. J. Physiol.* 161: 212, 1950.
57. DOYLE, J. T., J. L. PATERSON, J. V. WARREN, AND D. K. DETWEILER. Observations on the circulation of domestic cattle. *Circulation Res.* 8: 4, 1960.
58. DUNN, J. R., S. DEAVERS, R. A. HUGGINS, AND E. L. SMITH. Effect of hemorrhage on the red cell and plasma volume of various organs in the dog. *Am. J. Physiol.* 195: 69, 1958.
59. DUPONT, J. R., R. A. HUGGINS, S. DEAVERS, AND E. L. SMITH. Effects of certain anesthetics on distribution of red cells in the dog. *Am. J. Physiol.* 197: 978, 1959.
60. EBAUGH, F. G., C. P. EMERSON, AND J. F. ROSS. The use of radioactive chromium 51 as an erythrocyte tagging agent for the determination of red cell survival in vivo. *J. Clin. Invest.* 32: 1260, 1953.
61. EBAUGH, F. G., P. LEVINE, AND C. P. EMERSON. The amount of trapped plasma in the red cell mass of the hematocrit tube. *J. Lab. & Clin. Med.* 46: 409, 1955.
62. EBERT, R. V., AND E. A. STEAD. Demonstration that the cell: plasma ratio of blood contained in minute vessels is lower than that of venous blood. *J. Clin. Invest.* 20: 317, 1941.
63. EPSTEIN, F. H., AND T. B. FERGUSON. The effect of the formation of an arteriovenous fistula upon blood volume. *J. Clin. Invest.* 34: 434, 1955.
64. ERLANGER, J. Blood volume and its regulation. *Physiol. Rev.* 1: 177, 1941.
65. EVERETT, N. B., B. SIMMONS, AND E. P. LASHER. Distribution of blood (Fe^{59}) and plasma (I^{131}) volumes of rats determined by liquid nitrogen freezing. *Circulation Res.* 4: 419, 1956.
66. FÅHRAEUS, R. The suspension stability of the blood. *Physiol. Rev.* 9: 241, 1929.
67. FÅHRAEUS, R., AND T. LINDQUIST. The viscosity of the blood in narrow capillary tubes. *Am. J. Physiol.* 96: 562, 1931.
68. FARRAN, H. E., P. MILUTINOVIC, AND A. S. MASON. The *in vitro* uptake of P^{32} by red blood cells in thyroid disease. *Lancet* 2: 537, 1959.
69. FERREBEE, J. W., O. C. LEIGH, AND R. W. BERLINER. Passage of the blue dye T-1824 from blood stream into lymph. *Proc. Soc. Exper. Biol. & Med.* 46: 549, 1941.
70. FINE, J., AND A. M. SELIGMAN. Traumatic shock IV. A study of the problem of the "lost plasma" in hemorrhagic shock by the use of radioactive plasma protein. *J. Clin. Invest.* 22: 285, 1943.
71. FINE, J., AND A. M. SELIGMAN. A study of the problem of lost plasma in hemorrhagic, tourniquet, and burn shock by the use of radioactive iodoplasma protein. *J. Clin. Invest.* 23: 720, 1944.
72. FRANK, H., AND S. J. GRAY. The determination of plasma volume in man with radioactive chromic chloride. *J. Clin. Invest.* 32: 991, 1953.
73. FREINKEL, N., G. E. SCHREINER, J. W. ATHENS, C. W. HIATT, AND S. BREESE. Artifactual difference in the distribution of T-1824 and I^{131} labeled albumin resulting from mixing prior to administration. *J. Lab. & Clin. Med.* 43: 215, 1954.
74. FRIEDMAN, J. J. Distribution of red blood cells between tissues of mouse. *Proc. Soc. Exper. Biol. & Med.* 103: 80, 1960.
75. GARROW, J. S., AND J. C. WATERLOW. Observations on Evans blue dye as a tracer for human plasma albumin. *Clin. Sc.* 18: 35, 1959.
76. GIBSON, J. G., J. C. AUB, R. D. EVANS, W. C. PEACOCK, J. W. IRVINE, AND T. SACK. The measurement of post-transfusion survival of preserve stored human erythrocytes by means of two isotopes of radioactive iron. *J. Clin. Invest.* 26: 704, 1947.
77. GIBSON, J. G., AND W. A. EVANS. Clinical studies of the blood volume: Application of a method employing the azo dye Evans blue and the spectrophotometer. *J. Clin. Invest.* 16: 301, 1937.
78. GIBSON, J. G., J. L. KEELEY, AND M. PIJOAN. Blood volume of normal dogs. *Am. J. Physiol.* 121: 800, 1938.
79. GIBSON, J. G., W. C. PEACOCK, R. D. EVANS, T. SACK, AND J. C. AUB. The rate of post-transfusion loss of non-viable stored human erythrocytes and the re-utilization of hemoglobin-derived radioactive iron. *J. Clin. Invest.* 26: 739, 1947.
80. GIBSON, J. G., W. C. PEACOCK, A. M. SELIGMAN, AND T. SACK. Circulating red cell volume measured simultaneously by the radioactive iron and dye methods. *J. Clin. Invest.* 25: 838, 1946.
81. GIBSON, J. G., AND W. A. SCHEITLIN. A method employing

radioactive chromium for assaying the viability of human erythrocytes returned to the circulation after refrigerated storage. *J. Lab. & Clin. Med.* 46: 679, 1955.

82. Gibson, J. G., A. M. Seligman, W. C. Peacock, J. C. Aub, J. Fine, and R. D. Evans. The distribution of red cells and plasma in large and minute vessels of the normal dog, determined by radioactive isotopes of iron and iodine. *J. Clin. Invest.* 25: 848, 1946.
83. Gibson, J. G., A. M. Selighan, W. C. Peacock, J. Fine, J. C. Aub, and R. D. Evans. The circulating red cell and plasma volume and the distribution of blood in large and small vessels in experimental shock in dogs, measured by radioactive isotopes of iron and iodine. *J. Clin. Invest.* 26: 126, 1947.
84. Gibson, J. G., S. Weiss, R. D. Evans, W. C. Peacock, J. W. Irvine, W. M. Good, and A. F. Kip. The measurement of the circulating red cell volume by means of two radioactive isotopes of iron. *J. Clin. Invest.* 25: 616, 1946.
85. Gitlin, D., and C. A. Janeway. The dynamic equilibrium between circulating and extravascular plasma proteins. *Science* 118: 301, 1953.
86. Gray, S. J., and H. Frank. Simultaneous determination of red cell mass and plasma volume in man with radioactive sodium chromate and chromic chloride. *J. Clin. Invest.* 32: 1000, 1953.
87. Gray, S. J., and K. Sterling. Determination of circulating red cell volume by radioactive chromium. *Science* 112: 179, 1950.
88. Gray, S. J., and K. Sterling. The tagging of red cells and plasma proteins with radioactive chromium. *J. Clin. Invest.* 29: 1604, 1950.
89. Green, H. D. *Medical Physics*, edited by Glasser, 1944, p. 210.
90. Gregersen, M. I., A. A. Boyden, and J. B. Allison. Direct comparison in dogs of plasma volume measured with T-1824 and with antigens. *Am. J. Physiol.* 163: 517, 1950.
91. Gregersen, M. I., L. J. Cizek, and T. H. Allen. Proportion of "extra plasma" in the eviscerate dog. *Am. J. Physiol.* 175: 224, 1953.
92. Gregersen, M. I., J. G. Gibson, and E. A. Stead. Plasma volume determination with dyes; errors in colorimetry; use of the blue dye T-1824. *Am. J. Physiol.* 113: 54, 1935.
93. Gregersen, M. I., and J. L. Nickerson. Relation of blood volume and cardiac output to body type. *J. Appl. Physiol.* 3: 329, 1950.
94. Gregersen, M. I., and R. A. Rawson. The disappearance of T-1824 and structurally related dyes from the blood stream. *Am. J. Physiol.* 138: 698, 1943.
95. Gregersen, M. I., and R. A. Rawson. Blood volume. *Physiol. Rev.* 39: 307, 1959.
96. Gregersen, M. I., and H. Schiro. The behavior of the dye T-1824 with respect to its absorption by red blood cells and its fate in blood undergoing coagulation. *Am. J. Physiol.* 121: 284, 1937.
97. Gregersen, M. I., H. Sear, R. A. Rawson, S. Chien, and G. L. Saiger. Cell volume, plasma volume, total blood volume and F_{cells} in the rhesus monkey. *Am. J. Physiol.* 196: 184, 1959.
98. Grotte, G. Passage of dextran molecules across the blood-lymph barrier. *Acta Chir. Scandinav.* Suppl. 211, 1956.
99. Haddy, F. Comparison of small and large vessel hematocrits at two flow rates. *Physiologist* 2 (No. 3): 51, 1959.
100. Hahn, P. F., and W. F. Bale. Linear relationship between the circulating red cell mass and the venous hematocrit as determined with radioactive iron. *Am. J. Physiol.* 136: 314, 1942.
101. Hahn, P. F., W. F. Bale, and J. F. Bonner. Mechanism of the effect of epinephrine on the venous hematocrit value of the normal unanesthetized dog. *Am. J. Physiol.* 137: 717, 1942.
102. Hahn, P. F., W. F. Bale, E. O. Lawrence, and G. H. Whipple. Radioactive iron and its metabolism in anemia. *J. Exper. Med.* 69: 739, 1939.
103. Hahn, P. F., W. F. Bale, J. F. Ross, R. A. Hettig, and G. H. Whipple. Radioiron in plasma does not exchange with hemoglobin iron in red cells. *Science* 92: 131, 1940.
104. Hahn, P. F., W. M. Balfour, J. F. Ross, W. F. Bale, and G. H. Whipple. Red cell volume circulating and total as determined by radio-iron. *Science* 93: 87, 1941.
105. Hahn, P. F., and G. Hevesy. A method for blood volume determination. *Acta physiol. scandinav.* 1: 3, 1940.
106. Hahn, P. F., J. F. Ross, W. F. Bale, W. M. Balfour, and G. H. Whipple. Red cell and plasma volumes (circulating and total) as determined by radio-iron and by dye. *J. Exper. Med.* 75: 221, 1942.
107. Haldane, J., and J. L. Smith. The mass and oxygen capacity of the blood in man. *J. Physiol.* 25: 331, 1899.
108. Hamilton, A. S. Study of in vitro methods for the demonstration of isoagglutination with the bloods of normal and of ill dogs. *Am. J. Physiol.* 154: 525, 1948.
109. Hamilton, W. F., J. W. Moore, J. M. Kinsman, and R. G. Spurling. Studies on the circulation IV: Further analysis of the injection method, and of changes in hemodynamics under physiological and pathological conditions. *Am. J. Physiol.* 99: 534, 1931.
110. Hedlung, S. Studies on erythropoiesis and red cell volume in congestive heart failure. *Acta med. scandinav.* Suppl. 284, 1953.
111. Hevesy G., and G. Nylin. Application of K^{42} labeled red corpuscles in blood volume measurements. *Acta physiol. scandinav.* 24: 285, 1951.
112. Hevesy, G., and G. Nylin. Application of Thorium B labeled red corpuscles in blood volume studies. *Circulation Res.* 1: 102, 1953.
113. Hevesy, G., and K. Zerahn. Determination of the red corpuscle content. *Acta physiol. scandinav.* 4: 376, 1942.
114. Hlad, C. J., and J. H. Holmes. Factors affecting hematocrit determinations: Trapped plasma, its amount and distribution. *J. Appl. Physiol.* 5: 457, 1953.
115. Hooper, C. W., H. P. Smith, A. E. Belt, and G. H. Whipple. Experimental control of a dye blood volume method. *Am. J. Physiol.* 51: 205, 1920.
116. Hopper, J., H. Tabor, and A. W. Winkler. Simultaneous measurements of the blood volume by means of Evans blue dye and by means of carbon monoxide. *J. Clin. Invest.* 23: 628, 1944.
117. Huang, K. C., and J. H. Bondurant. Simultaneous estimation of plasma volume, red cell volume, and thiocyanate space in unanesthetized normal and splenectomized rats. *Am. J. Physiol.* 185: 441, 1956.
118. Huggins, R. A., E. L. Smith, and S. Deavers. Distribution of red cells and plasma in the dog. *Am. J. Physiol.* 191: 163, 1957.

119. HUGGINS, R. A., E. L. SMITH, S. DEAVERS, AND R. C. OVERTON. Changes in cell and plasma volume in the dog produced by hemorrhage and reinfusion. *Am. J. Physiol.* 189: 249, 1957.
120. HUGHES, W. L., AND R. STRAESSLE. Iodination of human serum albumin. *J. Am. Chem. Soc.* 72: 452, 1950.
121. HYMAN, C., S. BERNICK, AND R. L. PALDINO. Histological studies on the influence of thorotrast on the intra-hepatic distribution of T-1824. *Fed. Proc.* 14: 78, 1955.
122. HYMAN, C., AND R. L. PALDINO. Influence of reticulo-endothelial blockade and stimulation on the rate of disappearance of Evans blue from the circulation. *Am. J. Physiol.* 179: 594, 1954.
123. INKLEY, S. R., L. BROOKS, AND H. KRIEGER. A study of methods for the prediction of plasma volume. *J. Lab. & Clin. Med.* 45: 841, 1955.
124. JACKSON, D. M., AND M. E. NUTT. The effect of carbon dioxide on relative red cell volume. *J. Physiol.* 123: 367, 1954.
125. JONES, N. C. H., AND P. L. MOLLISON. The interpretation of measurements with Cr^{51} labeled red cells. *Clin. Sc.* 15: 207, 1956.
126. JULIAN, L. M., J. H. LAWRENCE, N. I. BERLIN, AND G. M. HYDE. Blood volume, body water, and body fat of the horse. *J. Appl. Physiol.* 8: 651, 1956.
127. KEITH, N. M., L. G. ROWNTREE, AND J. T. GERAGHTY. A method for the determination of plasma and blood volume. *A.M.A. Arch. Int. Med.* 16: 547, 1915.
128. KELLY, F. J., D. H. SIMONSEN, AND R. ELMAN. Blood volume determination in the human with red cells containing radioactive phosphorus and with pure human albumin. *J. Clin. Invest.* 27: 795, 1948.
129. KLOTZ, I. M., AND F. M. WALKER. The binding of organic ions by proteins. *J. Am. Chem. Soc.* 69: 1609, 1947.
130. KNISELY, M. H., T. S. ELIOT, AND E. H. BLOCH. Sludged blood in traumatic shock. *A.M.A. Arch. Surg.* 51: 220, 1945.
131. KRAINTZ, L., J. DE BOER, E. L. SMITH, AND R. A. HUGGINS. Mixing of labeled erythrocytes in the dog's spleen. *Am. J. Physiol.* 195: 628, 1958.
132. KRIEGER, H., W. D. HOLDEN, C. A. HUBAY, M. W. SCOTT, J. P. STORAASLI, AND H. L. FRIEDELL. Appearance of protein tagged with radioactive iodine in thoracic duct lymph. *Proc. Soc. Exper. Biol. & Med.* 73: 124, 1950.
133. KRIEGER, H., J. P. STORAASLI, H. L. FRIEDELL, AND W. D. HOLDEN. A comparative study of blood volume in dogs. *Proc. Soc. Exper. Biol. & Med.*, 68: 511, 1948.
134. KROGH, A. *The Anatomy and Physiology of Capillaries.* New Haven: Yale Univ. Press, 1922.
135. LANDIS, E. M., AND J. C. HORTENSTINE. Functional significance of venous blood pressure. *Physiol. Rev.* 30: 1, 1950.
136. LATHEM, W., AND M. E. GORDON. The circulating splanchnic red blood cell and plasma volumes and the splanchnic hematocrit in man. *Clin. Res. Proc.* 3: 37, 1955.
137. LATTA, H., D. GITLIN, AND C. A. JANEWAY. Experimental hypersensitivity in the rabbit—the cellular localization of soluble azo-proteins. *A.M.A. Arch. Path.* 51: 260, 1951.
138. LAWSON, H. C. The measurement of bleeding volume in the dog for studies on blood substitutes. *Am. J. Physiol.* 140: 420, 1943.
139. LAWSON, H C. The effect of blood withdrawal and replacement on the bleeding volume of normal dogs under barbital anesthesia. *Am. J. Physiol.* 141: 677, 1944.
140. LAWSON, H. C., W. F. CANTRELL, J. E. SHAW, D. L. BLACKBURN, AND S. ADAMS. Measurement of cardiac output in the dog by the simultaneous injection of dye and radioactive red cells. *Am. J. Physiol.* 170: 277, 1952.
141. LAWSON, H. C., AND W. S. REHM. The effect of hemorrhage and replacement on the apparent volume of plasma and cells. *Am. J. Physiol.* 144: 199, 1945.
142. LAWSON, H. C., O. W. SHADLE, J. C. MOORE, AND D. T. OVERBEY. Measurement of plasma volume as the distribution volume of injected autogenous plasma. *Am. J. Physiol.* 151: 297, 1947.
143. LAWSON, H. C., J. D. SHANKLIN, AND J. KABAL. The circulatory mixing time for erythrocytes in intact barbitalized dogs. *Fed. Proc.* 18: 88, 1959.
144. LEVEEN, H., AND W. H. FISHMAN. Combination of Evans blue with plasma protein: Its significance in capillary permeability studies, blood dye disappearance curves, and its use as a protein tag. *Am. J. Physiol.* 151: 26, 1947.
145. LEVINSON, J. P., AND H. E. ESSEX. Effect of shock on the small blood vessels of the ear of the rabbit. *Proc. Soc. Exper. Biol. & Med.* 52: 361, 1943.
146. LILIENFIELD, L. S., R. D. KOVACH, P. A. MARKS, L. M. HERSHENSEN, G. P. RODNAN, F. G. EBAUGH, AND E. D. FREIS. The hematocrit of the lesser circulation in man. *J. Clin. Invest.* 35: 3385, 1956.
147. LILIENFIELD, L. S., J. C. ROSE, AND F. A. PORFIDO. Evidence for a red cell shunting mechanism in the kidney. *Circulation Res.* 5: 64, 1957.
148. LORING, W. E. A rapid, simplified method for serial blood volume determinations in the rat. *Proc. Soc. Exper. Biol. & Med.* 85: 350, 1954.
149. *Human Physiology I:* Cited by L. Luciani, London: Macmillan 1911, p. 98.
150. LUTWAK, L. Preparation of radioactive iodinated serum albumin. *Proc. Soc. Exper. Biol. & Med.* 80: 741, 1952.
151. MCFARLANE, A. S. Labeling of plasma proteins with radioactive iodine. *Biochem. J.* 62: 135, 1956.
152. MALASSEZ, L. Nouveaux procédés pour apprécier la masse totale du sang. *Arch. Physiol. Norm. Path.* 2nd Ser. 1: 797, 1874.
153. MAYERSON, H. S., C. LYONS, W. PARSONS, R. T. NIESET, AND W. V. TROUTMAN. Comparison of results of measurement of red blood cell volume by direct and indirect techniques. *Am. J. Physiol.* 155: 232, 1948.
154. MENEELY, G. R., E. B. WELLS, AND P. F. HAHN. Application of the radioactive red cell method for determination of blood volume in humans. *Am. J. Physiol.* 148: 531 1947.
155. METCOFF, J., AND C. B. FAVOUR. Total circulating protein and hemoglobin in the growing rat. *Am. J. Physiol.* 141: 695, 1944.
156. MILLAR, W. G. Observations on the hematocrit method of measuring the volume of the erythrocytes. *Quart. J. Exper. Physiol.* 15: 187, 1925.
157. MILLER, A. T., JR. Excretion of the blue dye T-1824 in the bile. *Am. J. Physiol.* 151: 229, 1947.
158. MILLER, L. L., W. F. BALE, C. L. YUILE, R. E. MASTERS, G. H. TISHKOFF, AND G. H. WHIPPLE. Use of radioactive lysine in studies of protein metabolism. *J. Exper. Med.* 90: 297, 1949.

159. Moir, T. W., W. H. Pritchard, and A. B. Ford. The early disappearance of I^{131} serum albumin from the circulation of edematous subjects and its implications in the clinical determination of blood volume. *J. Lab. & Clin. Med.* 47: 503, 1956.

160. Mollison, P. L., and N. Veall. The use of the isotope Cr^{51} as a label for red cells. *Brit. J. Haemat.* 1: 62, 1955.

161. Mollison, P. L., N. Veall, and M. Cutbush. Red cell and plasma volume in newborn infants. *Arch. Dis. Childhood* 25: 242, 1950.

162. Moore, J. C., O. W. Shadle, and H. C. Lawson. Measurement of the circulating red cell volume with methemoglobin-tagged cells. *Am. J. Physiol.* 153: 322, 1948.

163. Morgan, D. P. Hematocrit of blood expressed from the perfused dog kidney. *Physiologist* 2 (No. 3): 84, 1959.

164. Necheles, T. F., I. M. Weinstein, and G. V. LeRoy. Radioactive sodium chromate for the study of survival of red blood cells. *J. Lab. & Clin. Med.* 42: 358, 1953.

165. Newerly, K., and S. A. Berson. Lack of specificity of insulin-I^{131} binding by isolated rat diaphragm. *Proc. Soc. Exper. Biol. & Med.* 94: 751, 1957.

166. Nickerson, J. L., M. I. Gregersen, W. S. Root, and L. M. Sharpe. Influence of blood incompatibilities on measurement of blood volume by cell-tagging methods. *Proc. Soc. Exper. Biol. & Med.* 75: 61, 1950.

167. Nickerson, J. L., H. Sear, and E. B. Reeve. Simultaneous measurements of cell volume with Fe^{55} and P^{32} in splenectomized dogs. *Am. J. Physiol.* 175: 230, 1953.

168. Nickerson, J. L., L. M. Sharpe, W. S. Root, T. C. Fleming, and M. I. Gregersen. Simultaneous blood volume determinations in dogs with dye (T-1824), carbon monoxide, and radioactive iron Fe^{55}. *Fed. Proc.* 9: 94, 1950.

169. Nizet, A. Determination of blood volume in dog by means of visually labeled erythrocytes. *Quart. J. Exper. Physiol.* 34: 123, 1948.

170. Noble, R. P., and M. I. Gregersen. Mixing time and disappearance rate of T-1824 in normal subjects and in patients in shock. *J. Clin. Invest.* 25: 158, 1946.

171. Nomof, N., J. Hopper, E. Brown, K. Scott, and R Wennesland. Simultaneous determinations of the total volume of red blood cells by use of carbon monoxide and chromium[51] in healthy and diseased human subjects. *J. Clin. Invest.* 33: 1382, 1954.

172. Nylin, G. The effect of heavy muscular work on the volume of circulating red corpuscles in man. *Am. J. Physiol.* 149: 180, 1947.

173. Nylin, G., and R. Pannier. L'influence de l'orthostatisme et du shock sur la vitesse circulatoire determinée à l'aide du phosphore radioactif. *Arch. internat. pharmacodyn.* 73: 401, 1947.

174. Ochwadt, O. Durchflusszeiten von Plasma und Erythrocyten, intrarenaler Hämatokrit und Widerstandsregulation der isolierten Niere. *Arch. ges. Physiol.* 256: 112, 1957.

175. Overbey, D. T. The recruitment of blood from the spleen during hemorrhage. *Fed. Proc.* 5: 78, 1946.

176. Overbey, D. T., J. C. Moore, O. W. Shadle, and H. C. Lawson. Rate of disappearance of dye T-1824 from arterial blood. *Am. J. Physiol.* 151: 290, 1947.

177. Owen, C. A., and M. H. Power. Intercellular plasma of centrifuged human erythrocytes as measured by means of iodo (I^{131}) albumin. *J. Appl. Physiol.* 5: 323, 1952.

178. Pappenheimer, J. R. Passage of molecules through capillary walls. *Physiol. Rev.* 33: 387, 1953.

179. Pappenheimer, J. R., and W. B. Kinter. Hematocrit ratio of blood within mammalian kidney and its significance for renal hemodynamics. *Am. J. Physiol.* 185: 377, 1956.

180. Pareira, M. D., K. D. Serkes, and S. Lang. Early response of plasma volume, red cell mass and plasma proteins to massive hemorrhage. *Proc. Soc. Exper. Biol. & Med.* 103: 9, 1960.

181. Peacock, W. C., R. D. Evans, J. W. Irvine, W. M. Good, A. F. Kip, S. Weiss, and J. G. Gibson. The use of two radioactive isotopes of iron in tracer studies of erythrocytes. *J. Clin. Invest.* 25: 605, 1946.

182. Pickering, R., and P. Dow. Arterio-venous distribution of brilliant vital red and T-1824 injected into dogs. *Am. J. Physiol.* 161: 221, 1950.

183. Ponder, E. *Medical Physics*, edited by Glasser. Chicago: Yr. Bk. Pub. 1944, p. 597.

184. Prentice, T. C., J. M. Olney, C. P. Artz, and J. M. Howard. Studies of blood volume and transfusion therapy in the Korean battle casualty. *Surg. Gynec. & Obst.* 99: 542, 1954.

185. Pritchard, W. H., T. W. Moir, and W. J. MacIntyre. Measurement of the early disappearance of iodinated (I^{131}) serum albumin from circulating blood by a continuous recording method. *Circulation Res.* 3: 19, 1955.

186. Rapaport, E., H. Kuida, F. W. Haynes, and L. Dexter. Pulmonary red cell and plasma volumes and pulmonary hematocrit in the normal dog. *Am. J. Physiol.* 185: 127, 1956.

187. Rawson, R. A. The binding of T-1824 and structurally related diazo dyes by the plasma proteins. *Am. J. Physiol.* 138: 708, 1942.

188. Read, R. C. Studies of red cell volume and turnover using radiochromium. *New England J. Med.* 250: 1021, 1954.

189. Reeve, E. B. Methods of estimating plasma and total red cell volume. *Nutrition Abstr. & Rev.* 17: 811, 1948.

190. Reeve, E. B., and J. Armin. Observations on plasma volume estimations with the dye T-1824. *J. Physiol.* 105: 72, 1946.

191. Reeve, E. B., M. I. Gregersen, T. H. Allen, and H. Sear. Distribution of cells and plasma in the normal and splenectomized dog and its influence on blood volume estimates with P^{32} and T-1824. *Am. J. Physiol.* 175: 195, 1953.

192. Reeve, E. B., M. I. Gregersen, T. H. Allen, H. Sear, and W. W. Walcott. Effects of alteration in blood volume and venous hematocrit in splenectomized dogs on estimates of total blood volume with P^{32} and T-1824. *Am. J. Physiol.* 175: 204, 1953.

193. Reeve, E. B., M. I. Gregersen, T. H. Allen, H. Sear, and W. W. Walcott. Validity of cell and blood volume measurements in the bled splenectomized dog. *Am. J. Physiol.* 175: 211, 1953.

194. Reeve, E. B., and N. Veall. A simplified method for the determination of circulating red cell volume with radioactive phosphorus. *J. Physiol.* 108: 12, 1949.

195. Reynolds, M. Plasma and blood volume in the cow using the T-1824 method. *Am. J. Physiol.* 173: 421, 1953.

196. RIEKE, W. O., AND N. B. EVERETT. Effect of pentobarbital anesthesia on the blood values of rat organs and tissues. *Am. J. Physiol.* 188: 403, 1957.

197. RODBARD, S., H. SAIKI, A. MALIN, AND C. YOUNG. Significance of changes in plasma and extracellular volumes in induced hyperthermia and hypothermia. *Am. J. Physiol.* 167: 485, 1951.

198. RODNAN, G. P. Simultaneous estimation of plasma volume with Evans blue dye and I^{131} globulin. *Clin. Res. Proc.* 4: 90, 1956.

199. ROOT, W. S., AND T. H. ALLEN. Determination of red cell volume with carbon monoxide. *Methods in Medical Research* 8: 80, 1960. Chicago: Yr. Bk. Pub.

200. ROOT, W. S., T. H. ALLEN, AND M. I. GREGERSEN. Simultaneous determinations in splenectomized dogs of cell volume with CO and P^{32}, and plasma volume with T-1824. *Am. J. Physiol.* 175: 233, 1953.

201. ROOT, W. S., F. J. W. ROUGHTON, AND M. I. GREGERSEN. Simultaneous measurement of blood volume with dye T-1824 and with carbon monoxide (improved method). *Fed. Proc.* 4: 60, 1945.

202. ROSS, J. F., A. C. BARGER, S. C. FINCH, R. S. ROSS, H. L. PRICE, AND E. J. FREIREICH. The blood volume before and following experimentally produced congestive heart failure in dogs. *Tr. A. Am. Physicians* 66: 278, 1953.

203. ROSS, J. F., R. B. CHODOS, W. H. BAKER, AND E. D. FREIS. The blood volume in congestive heart failure. *Tr. A. Am. Physicians* 65: 75, 1952.

204. ROTHSCHILD, M. A., A. BAUMAN, R. S. YALOW, AND S. A. BERSON. Effect of splenomegaly on blood volume. *J. Appl. Physiol.* 6: 701, 1954.

205. ROUGHTON, F. J. W., AND W. S. ROOT. The fate of CO in the body during recovery from mild carbon monoxide poisoning in man. *Am. J. Physiol.* 145: 239, 1945.

206. SCHLEIER, J. Der Energieverbrauch in der Blutbahn. *Pflüger's Arch. ges. Physiol.* 173: 172, 1919.

207. SCHREIBER, S. S., A. BAUMAN, R. S. YALOW, AND S. A. BERSON. Blood volume alterations in congestive heart failure. *J. Clin. Invest.* 33: 578, 1954.

208. SCHULTZ, A. L., J. F. HAMMARSTEN, B. I. HELLER, AND R. V. EBERT. A critical comparison of the T-1824 dye and iodinated albumin methods for plasma volume measurement. *J. Clin. Invest.* 32: 107, 1953.

209. SCHÜRER, J. Versuche zur Bestimmung der Blutmenge durch Injektion von artfremdem Serum. *Arch. exper. Path. u. Pharmakol.* 66: 171, 1911.

210. SEAR, H., T. H. ALLEN, AND M. I. GREGERSEN. Simultaneous measurement in dogs of plasma volume with I^{131} human albumin and T-1824 with comparisons of their long term disappearance from the plasma. *Am. J. Physiol.* 175: 240, 1953.

211. SELIGMAN, A. M., AND J. FINE. Traumatic shock I. The production of radioactive plasma protein from amino acids containing radioactive sulfur. *J. Clin. Invest.* 22: 265, 1943.

212. SELLERS, A. L., N. GRIGGS, J. MARMORSTON, AND H. C. GOODMAN. Filtration and reabsorption of protein by the kidney. *J. Exper. Med.* 100: 1, 1954.

213. SEMPLE, R. E. The measurement of plasma volume and of capillary permeability in the turtle using T-1824 and various dextran fractions. *Fed. Proc.* 19: 79, 1960.

214. SHEPPARD C. W., R. R. OVERMAN, W. S. WILDE, AND W. C. SANGREN. The disappearance of K^{42} from the nonuniformly mixed circulation pool in dogs. *Circulation Res.* 1: 284, 1953.

215. SHIRLEY, H. H., C. G. WOLFRAM, K. WASSERMAN, AND H. S. MAYERSON. Capillary permeability to macromolecules: Stretched pore phenomenon. *Am. J. Physiol.* 190: 189, 1957.

216. SIMPSON, A. M., L. EZROW, AND L. A. SAPIRSTEIN. Measurement of plasma volume with rose Bengal. *Am. J. Physiol.* 177: 319, 1954.

217. SJÖSTRAND, T. Volume and distribution of blood cells and their significance in regulating the circulation. *Physiol. Rev.* 33: 202, 1953.

218. SLIWINSKI, A. J., AND L. S. LILIENFIELD. Red cell and plasma transit through spleen: The splenic hematocrit. *Proc. Soc. Exper. Biol. & Med.* 99: 648, 1958.

219. SMALL, W. J., AND M. C. VERLOOP. Determination of the blood volume using radioactive Cr^{51}; modifications of the original technique. *J. Lab. & Clin. Med.* 47: 255, 1956.

220. SMITH, H. P. The fate of an intravenously injected dye (brilliant vital red) with special reference to its use in blood volume determinations. *Bull. Johns Hopkins Hosp.* 36: 325, 1925.

221. SMITH, H. P. The removal of brilliant vital red from the blood stream. Distribution of dye between blood stream and body tissues. *J. Exper. Med.* 51: 379, 1930.

222. SMITH, H. P., H. R. ARNOLD, AND G. H. WHIPPLE. Comparative values of Welcker, carbon monoxide, and dye methods for blood volume determinations. Accurate estimation of absolute blood volume. *Am. J. Physiol.* 56: 336, 1921.

223. STEAD, E. A., AND R. V. EBERT. Relationship of the plasma volume and the cell:plasma ratio to the total red cell volume. *Am. J. Physiol.* 132: 411, 1941.

224. STERLING, K. Radioactive chromium technic for circulating red cell volume (CRCV). *Methods in Medical Research* 8: 69, 1960. Chicago. Yr. Bk. Pub.

225. STEWART, G. N. The output of the heart. *J. Physiol.* 22: 159, 1897.

226. STEWART, G. N. The output of the heart in dogs. *Am. J. Physiol.* 57: 27, 1921.

227. STORAASLI, J. P., H. KRIEGER, H. L. FRIEDELL, AND W. D. HOLDEN. Use of radioactive iodinated plasma protein in the study of blood volume. *Surg. Gynec. & Obst.* 91: 458, 1950.

228. SURTSHIN, A., AND D. ROLF. Plasma dye concentration curves following two successive injections. *Am. J. Physiol.* 161: 483, 1950.

229. SUTHERLAND, D. A., AND M. S. MCCALL. The measurement of the survival of human erythrocytes by in vivo tagging with Cr^{51}. *Blood* 10: 646, 1955.

230. SWANN, H. G., A. A. ORMSBY, J. B. DELASHAW, AND W. W. THARP. Relation of lymph to distending fluids of kidney. *Proc. Soc. Exper. Biol. & Med.* 97: 517, 1958.

231. SWISHER, S. N., M. J. IZZO, AND L. E. YOUNG. A method of quantitative differential agglutination of dog erythrocytes. *J. Lab. & Clin. Med.* 41: 936, 1953.

232. UNGER, P. N., M. ZUCKERBROD, G. J. BECK, AND J. M. STEELE. Study of the disappearance of Congo red from the blood of non-amyloid subjects and patients with amyloidosis. *J. Clin. Invest.* 27: 111, 1948.

233. Verel, D. Observations on the distribution of plasma and red cells in disease. *Clin. Sc.* 13: 51, 1954.

234. Vidt, D. G., and L. A. Sapirstein. Distribution volumes of T-1824 and chromium[51] labeled red cells immediately following intravenous injection. *Circulation Res.* 5: 129, 1957.

235. Walcott, W. W. Blood volume in experimental hemorrhagic shock. *Am. J. Physiol.* 143: 247, 1945.

236. Wang, L. Plasma volume, cell volume, total blood volume, and F_{cells} factor in the normal and splenectomized Sherman rat. *Am. J. Physiol.* 196: 188, 1959.

237. Wasserman, K., and H. S. Mayerson. Exchange of albumin between plasma and lymph. *Am. J. Physiol.* 165: 15, 1951.

238. Wennesland, R., N. Nomof, E. Brown, J. Hopper, and B. Bradley. Distribution of CO and Cr^{51} in blood and tissues of rabbit and dog. *Proc. Soc. Exper. Biol. & Med.* 96: 655, 1957.

239. Whipple, G. H. The hemoglobin of striated muscle. *Am. J. Physiol.* 76: 693, 1926.

240. Whipple, G. H., C. W. Hooper, and F. S. Robscheit. Blood regeneration following simple anemia. *Am. J. Physiol.* 53: 151, 1920.

241. Wiggans, D. S., W. W. Burr. and H. W. Rumsfeld. Metabolism of serum proteins. *Arch. Biochem. Biophys.* 72: 169, 1957.

242. Wish, L., J. Furth, and R. H. Storey. Direct determinations of plasma, cell, and organ blood volumes in normal and hypervolemic mice. *Proc. Soc. Exper. Biol. & Med.* 74: 644, 1950.

243. Yalow, R. S., and S. A. Berson. The use of K^{42} tagged erythrocytes in blood volume determinations. *Science* 114: 14, 1951.

244. Zizza, F., and E. B. Reeve. Erroneous measurement of plasma volume in the rabbit by T-1824. *Am. J. Physiol.* 194: 522, 1958.

245. Zweifach, B. W., S. G. Hershey, E. A. Rovenstein, and R. Chambers. Influence of anesthesia on circulatory changes in dogs subjected to graded hemorrhage. *Proc. Soc. Exper. Biol. & Med.* 56: 73, 1944.

246. Zweifach, B. W., B. E. Lowenstein, and R. Chambers. Responses of blood capillaries to acute hemorrhage in the rat. *Am. J. Physiol.* 142: 80, 1944.

Blood volume

TORGNY SJÖSTRAND | *Laboratory of Clinical Physiology, Karolinska sjukhuset, Stockholm, Sweden*

CHAPTER CONTENTS

THE BLOOD may be regarded as a tissue consisting of cells and intercellular substance which fills the vascular system. Thus, the blood volume varies with the vascular system and its adjustment to the size and metabolism of the tissues which it supplies.

The blood volume may also be regarded as the volume of fluid in a closed pumping system with elastic "pipes," in which the maximal rate of flow is determined (among other things) by the fluid volume and the filling pressure of the pump. It is therefore to be expected that the total blood volume is adjusted to meet the maximum circulatory requirements that arise under different conditions. These requirements vary with external circumstances, which primarily influence the development and functional capacity of the locomotive organs.

The variations of blood volume between individuals and in an individual should be analyzed from these two viewpoints in order to determine whether such variations are bound by any laws. This also applies to the regulation of the total volume of blood and its composition of cellular elements and plasma. Accordingly, the blood volume, regarded as a tissue, can be expected to have a certain optimum in relation to the supplied tissues, as well as a certain optimal ratio between cells and plasma. In the hemodynamic adjustment, other additional factors can be expected to influence these relationships.

NORMAL VALUES IN ANIMALS AND IN MAN

Evaluation of Results Obtained by Different Methods

Up to the present numerous values for blood volumes, plasma volumes, and red cell volumes in different animals have been published. In many cases, however, the determinations are not directly comparable, because different methods have been used. Earlier direct determinations of blood volume with bleeding-out and infusion of the vessels are, on the whole, mutually comparable but not directly by indirect dilution methods. Values obtained by indirect methods based on determination of the plasma volume differ significantly from values obtained by the methods by which the blood cell volume is directly

determined. The former give about 10 per cent higher blood volume values than do the latter (34). Correction for this deviation should therefore be made in a comparison between the values. Generally, the carbon monoxide methods also give higher values than do the blood cell methods using other labels. Most CO determinations, however, are not sufficiently accurate as to the volume of administered carbon monoxide, and only with the alveolar CO method is the carbon monoxide concentration in blood before administration of CO taken into consideration (54). Especially in determinations in man, this inaccuracy may be the cause of considerable errors. On the other hand, the amount of CO taken up by the myoglobin is probably not of such great significance as had earlier been presumed. Values obtained with the alveolar CO method in man fall, on the whole, between those found with other blood cell and plasma methods (68, and our own observations), and can, therefore, be directly compared with these after correction for the deviation of the body hematocrit from the hematocrit in the analyzed blood. With due attention to these corrections the abundant material published on blood volume determinations under different conditions has been used for an analysis of the variations and regulation of the blood volume.

Variation in Blood Volume with Body Size

In mammals—from the mouse to the horse—the blood volume (BV/g) varies, on the whole, directly with the body weight (b. wt. kg) according to the regression equation 1.

$$BV = 0.055 \text{ b wt. } 0.99$$

However, different animal species deviate more or less from the blood volume values calculated from the regression equation (see table 1). Only to some extent can these deviations be attributed to the use of different methods of determination. Another reason for the deviations could be that the blood volume varies only indirectly with the total body weight but directly with the metabolically active body mass, and that the latter varies in different animal species in relation to body weight.

The blood vessel volume per volume of tissue varies markedly from organ to organ. It is large for instance, in the liver, kidneys, and spleen; small in adipose and connective tissue. And so it is to be expected that the blood volume per kg body weight should vary according to the body's composition of different tissues and, particularly, inversely with that of adipose tissue. The relationship of blood volume to the so-called lean body mass was found to be essentially closer than between blood volume and body weight only (48). The adipose tissue too has some blood supply and cannot therefore be ignored in this connection (42). However, the blood volume in adipose tissue calculated by these authors seems too high. Blood volume was also found to be constant in adults (49) in spite of gain or loss of body weight.

A closer analysis of the variation between different species of mammals with respect to the relationship of blood volume and blood cell volume, respectively, to body weight shows that animals known for great physical activity, as hares, dogs, and horses, have both large blood volumes and large blood cell volumes per kg body weight; and that physically inactive animals, e.g., rats and rabbits, have small volumes. The larger blood volume per kg body weight in the physically active animals is not accompanied by a higher basal metabolic rate. This is, therefore, probably explained by an adjustment of the vascular system to the demand for a higher cardiac output, that is, adjustment to temporary requirements of the circulation rather than to changes in the basal circulatory demand.

Observations in man also point in this same direction. If a comparison is made of the blood volume per body weight ratios between different subjects with different physical activity (individuals, for instance, who are forced into extreme inactivity because of a physical handicap—ordinarily active women and men, and especially well-trained female

TABLE 1. *Blood Volume in Different Mammalian Species*

Species	Blood Vol., ml	Blood Vol., ml/kg/b. wt.	Blood Vol., ml/cal/day (basal)
Rat	12.3	54.3	0.25
Guinea pig	31.0	72.0	0.79
Rabbit	124	56.4	0.93
Dog	2,840	92.5	3.5
Sheep	2,480	58.0	2.2
Man, female	3,960	66.1	2.9
Man, male	5,420	77.7	3.2
Cow	24,100	57.4	4.1
Horse, warm-blood*	42,750	109.6	6.2
Horse, cold-blood†	48,400	71.7	5.0

Comparable values have been selected from the literature as far as possible. Except for horses, all values have been obtained by plasma volume determinations. [For original data and references see (11) and (20).]

* Racing breeds. †Working breeds.

TABLE 2. *Blood Volume in Groups of Subjects Differing in Physical Activity*

Group	Number	Age, Mean	Blood Vol., ml	Blood Vol., ml/kg b. wt	Blood Vol., l/m B.H.
Blind women	13	27	3,780	67	2.36
Children	16	10	2,520	73	1.75
Women, average	15	28	4,160	73	2.53
Men, average	17	28	5,180	74	2.92
Athletes: wrestlers and weight-lifters	48	26	5,380	73	3.10
Athletes, cyclists	10	21	5,580	79	3.18
Athletes, runners	28	26	5,850	88	3.28

Blood volume values have been obtained by the alveolar CO method under the same experimental conditions for the different groups. The directly obtained values have been corrected for the overestimation inherent in the CO method and in the hemoglobin standard used.

and male athletes) great differences will be found (see table 2). For groups of people who are not selected especially on the basis of body build, the height of the body can be used as a reference value for the lean body mass. It is therefore of interest that about the same differences as those between the blood volume per body weight ratios are noted if the blood volume is compared to the body height.

In view of this variability of the blood volume with external circumstances, it is incorrect to give fixed normal values and to compare these in different subjects. The less physically active an individual is, the more the blood volume approaches the minimum necessary for maintenance of adequate circulation (and, hence, adequate oxygen supply to the tissues under conditions determined solely by endogenous factors). Determinations in blind women, whose handicap forced them into physical inactivity, indicate that this level in humans would be a blood volume somewhat below 60 ml per kg body weight. This corresponds also to the lowest values in mammals, that have been determined by means of comparable techniques and calculations (45). Assuming that in the blind the lean weight is 75 per cent of the body weight, the "basal" blood volume per kg lean weight would be about 70 ml.

Variation with Body Type

The blood volume in man has been related to body type, differentiated according to Sheldon's system, and certain variations have been observed (33). Since the adipose tissue also varies with body type, a closer evaluation of these observations is difficult. It is, however, extremely probable that the size of the vascular system in relation to the tissue supplied by it is larger, the greater the body height, in other words, the total volume of the vascular system varies with the longitudinal dimension of the body. This concept has also been supported by statistical analysis (3).

Variation with Sex

As regards the variation of the blood volume with sex, the published data differ. According to most reports on such comparisons, men have a larger blood volume per kg body weight than women; according to others there is no significant sex difference. Any differences can be explained by different external conditions, particularly as regards physical activity. In dogs (10) and rats (29) there seems to be no significant sex difference with respect to the blood volume. The total blood cell volume, on the other hand, is smaller in women as well as in the females of other mammalian species generally. The difference corresponds to the 10 per cent difference in hematocrit and the hemoglobin concentrations observed between the sexes (23). This difference seems to be associated with the influence of the sex hormones. Thus, after castration, the difference disappears completely or almost completely (29).

Variation with Age

The blood volume varies during body growth, largely directly with age and commensurate to body weight (44). After cessation of growth the blood volume remains unchanged in the average human subject (55). The same seems to be true for the rat (60). Since body weight in adults tends to increase with age because of excessive development of fat, the blood volume per kg of body weight decreases on the whole linearly with age (55). In a subject that does not show an increase of body weight with age this change, as expected, is not observed (15).

INTERNAL FACTORS THAT AFFECT BLOOD VOLUME

Plasma Volume/Blood Cell Volume Ratio

Within certain limits the total blood volume remains rather constant in spite of variations in the plasma volume/cell volume ratio. With a marked disturbance of this ratio the blood volume may

decrease, as in extreme anemia (31, 36), or may increase as in extreme polycythemia (7, 63). In anemia it is to be expected that the blood volume will tend to increase when the effect of anemia must be offset by an increase of the cardiac output. In polycythemia the blood volume increase can be assumed to occur when the increased viscosity of the blood leads to a redistribution of the blood between the central and peripheral sections of the vascular system. In polycythemia, conditioned by hypoxia, it may be that the hypoxia also causes a demand for increased cardiac output, so that the blood volume is adjusted accordingly (see below).

Arterial Oxygen Content

As will be further discussed the blood volume increases in prolonged hypoxia in decompression-chamber experiments which lead to maximal polycythemia, and in which the arterial oxygen content is reduced (58, 61). The same is the case in anemia. On the other hand, in hypoxia of more acute onset, in which the hematopoiesis has not made up for the reduction of arterial oxygen content, the blood volume seems to decrease (12, 62), perhaps because of changes of the circulation (see below).

Basal Metabolic Rate

As regards the relationship of blood volume to basal metabolic rate, no studies dealing directly with this question seem to have been published. Indirectly, investigations into the variations of the blood volume in hypothyroidism and hyperthyroidism in man (32) and in animal experiments (47) favor the idea that the blood volume can vary with the basal metabolic rate. This view is also indirectly supported by observations on ground squirrels during dormancy, which showed that the blood volume decreased to less than half, mainly by a decrease of plasma volume (59).

The total red cell volume is more markedly affected by thyroid activity. In hypothyroidism the cell volume is smaller than normal. This may, however, be explained by the effect of thyroxin on the formation of red cells as well as on cell formation generally, and cannot be taken as evidence of a direct influence of changes in the metabolic rate on hematopoiesis.

Hormone Levels

The total blood volume seems to vary rather slightly with the variation of endocrine activity. Hypophysectomy seems to produce a small reduction of the total blood volume (28), whereas adrenalectomy increases it (30). If ACTH is given to hypophysectomized rats and hydrocortisone to adrenalectomized rats, the blood volume tends to increase in relation to body weight. The growth hormone does not seem to alter the blood volume in relation to body weight (28). After thyroidectomy (47), as in hypothyroidism in man (32), the blood volume tends to decrease; whereas hyperthyroidism and the administration of thyroid hormone cause an increase of the blood volume. Because these different hormones greatly influence the deposition of fat and cell metabolism generally, it is difficult to draw any definite conclusion about their effect on the vascular system. Administration of these hormones to animals has not been shown to have any significant effect on their blood volume. On the other hand, the blood volume can be indirectly influenced by aldosterone via the renal function. Increased aldosterone production apparently leads to an increase of blood volume.

Castration of male and female rats does not seem to have any constant and definite effect on blood volume in relation to body weight. By giving testosterone to normal rats, on the other hand, it seems possible to provoke a small increase of the blood volume absolutely and in relation to body weight (29).

The endocrine organs influence hematopoiesis, and hence the red cell volume, more markedly than the total blood volume (23). Hypophysectomy, adrenalectomy, and thyroidectomy lead to a decrease of the red cell volume. This is explained by the influence of these organs on cellular proliferation and protein metabolism generally. But administration of ACTH, growth hormone, hydrocortisone, and thyroxin to normal animals does not produce an increase of red cell volume. Testosterone, on the other hand, seems to have a stimulating effect on the bone marrow, whereas estrone inhibits hematopoiesis (29).

Intravascular Pressure

As a result of intravascular pressure variations, the volume may change greatly on the venous side of the vascular system. This leads to a disturbance in the distribution of blood with altered pressure/volume ratios in other parts of the vascular system. If it persists, the change seems to be offset by an increase in total blood volume. Under normal conditions, only changes in body position produce marked changes in the pressure-volume relationship. At the

same time, however, the hydrostatic pressure in most of the peripheral vessels changes. This may directly influence the exchange of water between the blood and the extracellular fluid space and cause temporary changes counteracting any compensatory increase of blood volume, and restoring the normal volume-pressure relationships. The suggestion that such a compensatory mechanism plays some role under normal conditions is supported by the fact that the blood volume tends to decrease in the first weeks of confinement to bed (19). Here the reduced physical activity may, however, be a contributory factor.

Under pathological conditions, on the other hand, particularly cardiac decompensation, considerable pressure elevations occur on the venous side that may lead to an increase of the blood volume. During treatment of cardiac insufficiency the blood volume decreases, seemingly in proportion to clinical improvement [for references, see (12)].

In patients with heart disease without decompensation, the blood volume is not increased as compared with that of healthy persons. On the other hand, in patients with signs of raised pressure in the pulmonary circulation without decompensation, there seems to be an increase of blood volume in comparison with patients who have cardiac symptoms and enlargement of the heart without a rise in pressure in the pulmonary circulation (56). The blood volume variations in cardiac decompensation and during treatment thereof result mainly from variations of plasma volume, although hematopoietic activity also seems to be influenced. The latter may be explained by the fact that the relative anemia caused by the increase of plasma volume stimulates hematopoiesis. It has often been suggested that this is due to a "hypoxic effect" on the bone marrow. But this interpretation has gained no direct support and the hypothesis may be said to be superfluous, since the effect on hematopoietic activity can be explained by well-known factors.

Increased Cardiac Output

An increased load on the circulation without a simultaneous change in metabolic rate occurs in a case of arteriovenous fistula. The blood volume tends to increase, judging from observations in clinical cases, before and after operation on the fistula (53) as well as from experimentally provoked fistulas in dogs (24), the variations being noted particularly in the plasma volume.

Pregnancy

A great number of studies have shown that the blood volume increases during pregnancy [for references, see (27)]. The increase occurs fairly continuously up to the 35th week, and thereafter the blood volume remains constant or decreases slightly. Primarily, the plasma volume seems to increase and, if hematopoiesis is inhibited by iron deficiency, a relative anemia develops despite the fact that the total hemoglobin concentration and red cell volume may be increased (52). After delivery the blood volume is quickly restored to normal both as a result of the bleeding at delivery and also of a plasma volume decrease.

EXTERNAL FACTORS THAT AFFECT BLOOD VOLUME

Season

Minor seasonal variations of blood volume were observed in a series of five women in the author's laboratory (56). The observations covered several consecutive years and the average difference between the yearly maximum (spring-early summer) and yearly minimum (autumn-winter) was statistically significant. These variations seemed to show a positive correlation with the length of daylight and to be associated with the frequent observation that the concentration of reticulocytes increases in early spring. Observations in studies on seasonal variations in the hemoglobin concentration might also be interpreted in accordance with the above observations on blood volume. These show, in fact, a peak value in the winter (usually in February) and a minimum value in the autumn (usually September or October) with the onset of the decrease between January and April (16). Assuming that the volume of the vascular system increases with the increase in the length of daylight, we may expect primarily an increase of plasma volume and, thus, a decrease of the hemoglobin concentration which stimulates hematopoiesis. And, conversely, with the diminishing length of daylight in late summer and in the autumn the volume of the vascular system, and thus the plasma volume, should decrease with a tendency to an increase in hemoglobin concentration. Observations on changes in the tone of the skin vessels seem to point in the same direction (5). Whether such seasonal variations occur more generally is not known, but, if so, they should be slight in view of the fact that the blood volume

shows great constancy in determinations made at intervals of a few months.

Climate

Several, partly contradictory, investigations have been published relative to variations of blood volume in connection with climatic changes (12, 34). An analysis of these data seems to show that the blood volume tends to increase slightly in a warm climate and to decrease in a cold climate. This is also consistent with the changes observed in experimental studies (6). The variations represent only a small percentage, however. Since other external factors, such as physical activity, influence the blood volume, the effect of temperature may be masked by the effect of reduced physical activity, for instance in the inhabitants of tropical or subtropical regions. The reverse may be expected in people living in colder regions. Among the Eskimos, it has been found that those working outdoors have larger blood volumes than those living indoors during the coldest part of the year (13).

Barometric Pressure

The effect of prolonged hypoxia, as at low barometric pressure, has been dealt with in the section on "Arterial Oxygen Content." Several studies have been made on the blood volume of people and animals living at high altitudes (12, 43, 58). At low barometric pressure the anoxemia is offset first by an increase of the hemoglobin concentration, and not until marked polycythemia develops is there an additional compensatory increase of the total blood volume. It has been observed both in man and in animal experiments that in a change from sea level to high altitudes or from high to low atmospheric pressure there occurs first a hemoconcentration, thus a decrease of blood volume.

CIRCUMSTANTIAL FACTORS THAT AFFECT BLOOD VOLUME

Nutrition

In excessive nutritional disturbances with changes in the electrolyte-water balance, resulting directly and indirectly from protein deficiency, the body's power for regulation may be affected with consequent changes of blood volume. In cases of malnutrition the blood volume seems to decrease at the same rate as the serum-proteins (64). Hematopoiesis in some deficient states is influenced more than is the blood volume, and in such cases the proportion of blood cells to plasma volume is altered.

Physical Activity

Many data support the view that the blood volume varies with physical activity, and this question has been partly dealt with in the foregoing paragraphs. The supporting evidence for such variation can be summarized as follows:

a) Animal species which show high physical activity and performance have essentially larger blood volumes per kg body weight or per calorie of basal metabolic rate than have less physically active animals.

b) Individuals who are physically active (e.g., athletes) have a larger blood volume than those who are inactive but comparable in other respects.

c) Blood volume increases during periods of physical training.

In earlier studies, in which Welcker's technique was used, considerable differences were noted in blood volume per kg body weight among different animal species (21, 22). More recent investigations with the dilution technique have, to some extent, confirmed these observations (see table 1). In more physically active animals, such as dogs and horses, the blood volume per kg body weight is up to twice that of less physically active animals, such as tame rabbits, rats, sheep, and cows. The most striking difference is found when rabbits are compared with hares. The hare has been reported to have more than twice the blood volume and about three times the amount of hemoglobin as the tame rabbit (22).

As the blood volume varies directly with the body weight and the basal metabolic rate with the two-thirds to three-fourths power of the body weight, the blood volume calculated per unit of basal energy metabolism of small and large animals cannot be directly compared. However, as can be seen from table 1, there are great differences in blood volume per unit of basal metabolic rate among animals that cannot be explained by the differences in basal energy metabolism per unit of tissue mass. Thus, the dog has greater blood volume per calorie per day than larger animals, like sheep, cows, and ordinarily physically trained men and women. The "warm-blooded" horses (thoroughbred and other racing breeds) also have larger blood volumes per

calorie per day than the "cold-blooded" typed (working breeds).

Men who participate in sports that require vigorous effort, like running, skiing, and cycling, have been found generally to have larger blood volumes per kg body weight than those ordinarily physically active; more also than those athletes who take part in more static muscular training, like wrestling and weight-lifting (see table 2). Women trained in sports involving great physical effort, like skiing, also have been found to have essentially larger blood volumes than ordinarily found (46). Determinations of the blood volume of blind women whose handicap has forced them to lead physically inactive lives showed lower values than those in the average woman. This is also the case when the blood volume is calculated on the basis of body height, as mentioned above.

In experiments on dogs it has been found that physical exercise increases the blood volume (18). The same has been observed in man, in a series of neurotic patients, and in a series of healthy subjects who were put through systematic exercises (40, 41). Even a short period of intensive exercise with daily skiing has been found to cause a significant increase of blood volume.

The larger blood volume per kg body weight in more physically active animal species and humans, and the increase of blood volume during physical training could be attributable, as has been pointed out above, to an increase of the metabolically more active body mass at the expense of metabolically inactive tissue. However, the blood volume/basal metabolic ratio is larger in physically active animals than in the inactive but otherwise comparable animals. A study of the proportion of blood volume to body height shows the same difference among groups of people with varying physical activity, as the blind, ordinarily active individuals, and athletes. It seems probable therefore that larger blood volumes in physically active individuals are associated with an adjustment of the vascular system to meet the circulatory requirements determined by external conditions.

Stress

The blood volume under conditions of work and hypoxia is dealt with elsewhere in this chapter. Studies of the blood volume under other stress conditions seem to have given ambiguous results. During an acute stress reaction with raised arterial pressure and increased adrenaline secretion some reduction of the blood volume should be expected. But such a reduction has not been unequivocally demonstrated in animal experiments (34). Chronic stress conditions can be expected to be attended by minor changes in blood volume in association with disturbances in the function of the thyroid and the adrenals (see above).

EXPERIMENTAL SITUATIONS THAT AFFECT BLOOD VOLUME

Body Position

In short-term experiments it has been shown that the blood volume decreases in the erect position and increases with a change to the recumbent position (8, 66). The observation is explained by the changes in the hydrostatic capillary pressure resulting from changes of posture (see below). After prolonged positional changes a compensation seems to occur (67). Besides the hydrostatic pressure changes, the reduced recumbent physical activity may be a contributory factor here.

Physical Work

During muscular work the blood volume decreases by a reduction of the plasma volume [for references, see (39)]. The decrease occurs principally in the first 10 to 15 min after onset of work and seems to be related to the intensity of work. The effect is attributable to an increase of pressure in the capillaries on exertion. This acute response is not to be confused with the opposite long-term effect of habituation to muscular work.

Bleeding

Normally, the decrease of blood volume after a hemorrhage is compensated for by an increase in plasma volume. This occurs by a shift of fluid from the extracellular space (14, 17). The degree and rate of compensation depend on the fluid balance and on the extent to which the lost interstitial fluid is replaced by intake of water. A 10 per cent blood loss in human experiments was not fully compensated even a week or more after the venesection (35, 50). After profuse bleeding the compensation seems to be incomplete and the blood volume remains smaller than normal for some time (55).

Blood Transfusion

When blood is administered, the blood volume seems to be reduced by a compensatory decrease of plasma volume. The blood volume can thus remain constant within certain limits after repeated transfusions. The hemoglobin concentration increases along with the increase of blood cell volume. However, more systematic investigations into this question have been made only on patients who received preoperative blood transfusions, since they were anemic or suspected of having a small blood volume (25).

Plasma Expander Infusions

Administration of high molecular substances, as plasma volume expanders, may cause an increase of the total blood volume (12). Infused dextran (Macrodex) has been found to increase the blood volume by as much as 40 per cent in humans (9). With such infusions the plasma volume seems to increase with the increase of the colloid-osmotic pressure and, thus, the concentration of dextran in the blood. The molecular size plays an important role here. Infusion of high molecular dextran solutions does not cause a compensatory diuresis, as infusion of low molecular dextran does in animals which have not been bled (56). The blood volume decreases to the ordinary level at the same rate as the elimination of dextran from the blood.

REGULATION OF BLOOD VOLUME

Regulation of the Body's Water Balance

Plasma is a part of the extracellular fluid, the volume of which is related to the intracellular fluid volume and, hence, to the body's total water content. The blood volume is therefore dependent upon the water balance of the body, on the one hand, and upon the distribution of water between the blood vessels and the extracellular fluid space, on the other. A discussion of regulatory mechanisms influencing the blood volume must therefore be based on the regulation of the water balance (34, 51).

A detailed description of the normal regulation of the body water content falls outside the scope of this section. It will only be pointed out here that the normal water balance depends primarily upon two factors: *1*) steady supply of water, and *2*) the ability of the kidneys to remove adequate amounts of water in the control of the constancy of the salt content of the blood. Any alteration of water intake or of renal output can upset the water balance in a negative or a positive direction and thus lead to a change in blood volume as well. Here the central and humoral regulation of water intake and diuresis, respectively, may play a part, as has been shown experimentally. Under exceptional circumstances a negative water balance may be present, for instance during hard work in the heat, when the blood volume may be greatly reduced. Under pathological conditions the water balance is often disturbed, as in excessive vomiting, diarrhea, circulatory insufficiency, and renal failure. In the former two conditions the blood volume may, as expected, be reduced; and in the latter two it may be increased. Normally, however, the water content of the body varies only slightly and the blood volume changes that thus occur seem to be very small. Moderate variations of the body's total water content, as by the intake of 1 to 2 liters of water or experimentally induced diuresis, need not cause any measurable changes of blood volume (34). This suggests the presence of an active regulation of water distribution in the extracellular space in such a way that, within certain limits, the blood volume is kept constant.

Factors Influencing Distribution of Water Between Blood Vessels and Extracellular Space

The continuous exchange of water between the blood and the extracellular space means that a certain balance of distribution is brought about, conditioned primarily by hydrostatic and colloid-osmotic pressures on each side of the capillary wall. Of these forces, the intravascular hydrostatic pressure may undergo quick changes and may be thought to influence the blood volume via nervous and hormonal factors. The reflexes thought to be involved here are primarily concerned with the regulation of the blood circulation; thus regulation of blood volume may be expected to be intimately related to vasomotor regulation.

An increase of the blood flow through the body is as a rule dependent upon an increase of the hydrostatic pressure in the peripheral vessels, resulting in a decrease of blood volume, as during muscular work. A decrease of the cardiac output, as during sleep, may be expected to have the opposite effect. During increased arterial pressure as a result of constriction of arterioles, with cardiac output and other

conditions being unchanged, the peripheral intravascular pressure may remain unaltered, and the blood volume will not necessarily be altered. On the other hand, any increase of venous pressure will increase the peripheral hydrostatic pressure and cause loss of water from the blood. The magnitude of these blood volume changes is determined not only by hydrostatic pressure changes but also by simultaneous colloid-osmotic pressure changes. A primary change of the colloid-osmotic pressure of the blood is not known to occur under normal physiological conditions. However, in certain pathological conditions a decrease of the plasma protein concentration occurs which may influence the blood volume.

Upon a primary change in blood volume, the same regulatory mechanisms may be expected to be called into action, as in a change of the circulatory rate. A sudden decrease of blood volume leads first to a reduction of the amount of blood in the central veins, decreasing the filling pressure of the right and left heart. This may be expected to lead to a decrease of stroke volume and cardiac output, and to falling arterial pressure. However, these effects are largely offset by an increase of the pulse rate and constriction of the arterioles. This effect is not observed immediately after a small bleeding in recumbent humans. However, a cardioacceleration could be demonstrated in upright subjects shortly after deprivation of 10 per cent of their blood volume. In the recumbent position the acceleration may occur 1 to 3 days after bleeding (35). The pressure in the aorta is restored by changes in vasomotor tone on the arterial side and, as a consequence, the hydrostatic pressure in the peripheral part of the vascular system falls. Water is then drawn into the blood vessels from the extracellular space, tending to restore the blood volume. This compensation for blood loss occurs slowly, however. Studies on man suggest that after withdrawal of 10 per cent of the blood volume full compensation for the loss requires 1 to 2 weeks.

Factors Influencing the Capacity of the Vascular System

The blood volume varies secondarily with changes in the capacity of the vascular system, for instance during pregnancy and resulting from pressure changes on the venous side (57). Thus, the volume-pressure relationships in the rest of the vascular system seem to be restored to normal by a compensatory increase of the total blood volume.

Primary changes of vascular tone may also be expected to occur and be compensated for by the mechanisms which influence blood volume. Such general variations of vascular tone may occur in disturbances of adrenal function. Blood volume variations related to changes in the ambient temperature should also be included here. Such volume changes of the vascular system may be expected to influence the blood volume through the same reflex mechanisms as respond to primary variations of blood volume. The change in blood distribution brought about thereby influences the circulatory equilibrium, and hence the cardiac and vasomotor reflex mechanisms are called into action. Some observations also suggest the presence of an active regulation of the capacity of the vascular system—probably mainly by a change in venous tone—which to some extent may compensate for primary changes of the blood volume. Accordingly, bleeding experiments in man seem to show that the effects on the circulation from changes of body position and from work recede greatly the day after the venesection and before the hemoglobin concentration indicates that the plasma volume increase has made up for the blood loss (35). The total blood volume seems also to remain smaller than normal for a long time after a large blood loss (55). Here variations in the quantities of active vasoconstrictor substances in the blood may be the mediator mechanism (4). The change of vascular tone seems to occur gradually, however; in bleeding experiments in man it is not noticed during the first hour after the withdrawal of blood. A seemingly reflex venous tone change has also been observed in experiments with venous congestion in dogs (2).

Regulatory Mechanisms

The intimate relationship between blood volume and blood circulation discussed above suggests that the blood volume may be largely controlled indirectly by hemodynamic factors, and by the regulation of the water balance. Here the different blood pressure-regulating reflex mechanisms play a role, such as the aortic and carotid sinus reflexes, the peripheral and central vasomotor regulation of a nervous, hormonal, and metabolic nature, and the hormonal regulation of renal function.

It has also been assumed that there would be special blood volume-regulating reflex mechanisms. From the central veins and the left (probably also the right) auricle of the heart, impulses would be discharged

centrally, depending on the distention of these parts of the vascular system (37). Since the blood volume variations will first influence the filling of this low pressure part of the vascular system, it can be expected that the impulses of these vessel-wall receptors will signal variations of blood volume under certain conditions, and that the average frequency of impulses discharged during a prolonged period of time will reflect the degree of filling of the vascular system (26, 38). The effector link in the reflex mechanism would be the pituitary production of hormones for regulation of diuresis.

The evidence presented in support of this regulatory principle is indirect, and in the author's opinion it tends to show that the body's water balance can be influenced in this way and, hence, indirectly the blood volume, too. In combination with vasomotor reflexes it is very probable, however, that diuresis-regulating reflexes could influence the blood volume and aid its adjustment to the circulation.

The factors and mechanisms discussed above, which might influence the blood volume, and under various conditions have, in fact, been shown to do so, can be expected to be involved in the regulation of the blood volume, although none can be said to be the one regulatory mechanism. A number of observations also show that this matter of regulation is actually much more complicated than can be intimated by a schematic account (34, 51). Nor has it been possible to demonstrate the existence of a simple central regulatory mechanism, the disturbance of which would provoke extreme changes in blood volume leading to plethora or circulatory failure.

In the introduction it was pointed out that the blood may be regarded as a tissue filling the vascular system, and that the total blood volume is a factor of paramount importance in the circulatory adjustment to meet varying endogenous and exogenous demands. Looking upon the blood as a tissue we can expect the blood volume to be adjusted to the elementary functions of the body, similarly to other organs and tissues, such as the liver, kidneys, connective tissue, and mucous membranes. There are no evidences for an adjustment of these organs and tissues homeostatically by special central regulatory mechanisms. There is no more reason to assume that the capacity of the vascular system, and hence the blood volume, should be under any such influence. The innumerable factors that constantly influence the various organs and tissues in different ways determine the quantitative relationships between them. In this way the blood volume can also be expected to be adapted to the growth of the organism before more differentiated mechanisms exist.

As a factor in the adjustment of the cardiac output to varying external circumstances the blood volume can, to some extent, be compared with the skeletal muscles. These are adjusted to the demands of the external circumstances apparently without specific regulatory mechanisms. External conditions are the stimuli that bring on adjustment of the size of skeletal muscle and thus its functional ability, according to the requirements. In the same way, the functional demands upon the circulatory system may be supposed to act as stimuli causing the size of the heart and the vascular system to become adjusted to these requirements. Between the size and function of different organs and tissues there are, presumably, optimal relationships which determine the structure of the organism under the influence of internal and external circumstances. In the adjustment of the functions of different organs, nervous reflexes play a regulatory role in restoring optimal relationships after a temporary disturbance. On the other hand, they do not determine these optimal relations. These are determined by the plan of the organism and the properties of the different tissue structures, which, in turn, determine the particular characteristics of each animal genus. Accordingly, the different reflex mechanisms which influence the body's water balance and which seem to be called into action at a change of pressure in certain parts of the vascular system, as well as some vasomotor reflexes influencing the hydrostatic pressure in the peripheral vessels, may be regarded as mechanisms which act in an adaptive manner to more sudden changes of the blood volume, but which do not themselves determine its size and its adjustment to internal and external circumstances.

Regulation of Hematopoietic Activity

The assumption that the blood volume is regulated primarily by hematopoiesis has not been supported by any evidence. An increase in hematopoiesis under physiological and pathological conditions does not as a rule lead to an increase in total blood volume but merely in blood cell volume. Only in severe polycythemia and in hypoplastic anemia is there a change in the total blood volume: in both conditions an increase. Hematopoietic activity thus regulates the composition of the blood as regards blood cells and plasma, but not the total blood volume.

REFERENCES

1. Adolf, E. F. Quantitative relations in the physiological constitutions of mammals. *Science*, 109: 579, 1949.
2. Alexander, R. S. Reflex alterations in venomotor tone produced by venous congestion. *Circulation Res.* 4: 49, 1956.
3. Allen, T. H., M. T. Peng, K. P. Cheng, T. F. Huang, C. Chang, and H. S. Fang. Prediction of blood volume and adiposity in man from body weight and cube of height. *Metabolism* 5: 328, 1956.
4. Arnim, J., and R. T. Grant. Vasoconstrictor activity in the rabbit's blood and plasma. *J. Physiol.* 128: 511, 1955.
5. Bárány, F. R. Abnormal vascular reactions in diabetes mellitus. *Acta med. scandinav.* 152, Suppl. 304, 1955.
6. Bass, D. E., and A. Henschel. Responses of body fluid compartments to heat and cold. *Physiol. Rev.* 36: 128, 1956.
7. Berlin, N. J., J. H. Lawrence, and J. Gartland. Blood volume in polycythemia as determined by P^{32} labelled red blood cells. *Am. J. Med.* 9: 747, 1950.
8. Berson, S. A., R. S. Yalow, A. Azulay, S. Schreiber, and B. Roswitt. The biological decay curve of P^{32} tagged erythrocytes. Application to study of acute changes in blood volume. *J. Clin. Invest.* 31: 581, 1952.
9. Birke, G., S.-O. Liljedahl, and L. Troell. Dextran concentration, electrolytes, blood volume and total hemoglobin. *Acta chir. scandinav.* Suppl. 228, 19, 1957.
10. Bonnycastle, D., and R. A. Cleghorn. A study on the blood volume of a group of untrained normal dogs. *Am. J. Physiol.* 137: 380, 1942.
11. Brody, S. *Bioenergetics and Growth.* New York: Reinhold, 1945.
12. Brown, E., J. Hopper, and R. Wennesland. Blood volume and its regulation. *Ann. Rev. Physiol.* 19: 231, 1957.
13. Brown, G. M., G. S. Bird, L. M. Boag, D. J. Delahaye, J. E. Green, J. D. Hatcher, and J. Page. Blood volume and basal metabolic rate in Eskimos. *Metabolism* 3: 247, 1954.
14. Calvin, D. B. Plasma volume and plasma protein concentration after severe hemorrhage. *J. Lab. & Clin. Med.* 26: 1144, 1941.
15. Cohn, J., and N. W. Shock. Blood volume studies on middle aged and elderly males. *Am. J. M. Sc.* 217: 388, 1949.
16. Coulthard, A. J. The annual cycle of blood hemaoglobin values. *Clin. Chim. Acta* 3: 226, 1958.
17. Danowski, T. S., J. R. Elkinton, and A. W. Winkler. Movements of body water in response to acute blood loss. *Am. J. Physiol.* 147: 306, 1946.
18. Davis, Y. E., and N. Brewer. Effect of physical training on blood volume, hemoglobin, alkali reserve and osmotic resistance of erythrocytes. *Am. J. Physiol.* 113: 586, 1935.
19. Deitrick, J. E., G. D. Whedon, and E. Shon. Effects of immobilization upon various metabolic and physiologic functions of normal men. *Am. J. Med.* 4: 3, 1948.
20. Dittmer, D. C., and R. M. Grebe. *Handbook of Circulation.* Philadelphia: Saunders, 1959, p. 65.
21. Dreyer, G., and W. Ray. The blood volume of mammals as determined by experiments upon rabbits, guinea pigs and mice. *Phil. Trans. Roy. Soc. London*, 201:B, 133, 1910–11.
22. Dreyer, G., and W. Ray. Further experiments upon the blood volume of mammals and its relation to the surface area of the body. *Phil. Trans. Roy. Soc. London*, 202:B, 191, 1911–12.
23. van Dyke, D. C., A. N. Contopoulos, B. S. Williams, U. E. Simpson, J. H. Lawrence, and H. M. Evans. Hormonal factors influencing erythropoiesis. *Acta haemat.* 11: 203, 1954.
24. Epstein, F. H., and T. B. Ferguson. The effect of the formation of an arteriovenous fistula upon blood volume. *J. Clin. Invest.* 34: 434, 1955.
25. Fretheim, B. The total circulating serum protein in patients with gastric carcinoma. *Acta chir. scandinav.* 108: 125, 1954.
26. Gauer, O. H., J. P. Henry, and H. O. Sieker. Changes in central venous pressure after moderate hemorrhage and transfusion in man. *Circulation Res.* 4: 79, 1956.
27. Gemzell, C. A., H. Robbe, and G. Ström. Total amount of hemoglobin and physical working capacity in normal pregnancy and puerperium (with iron medication). *Acta obst. et gynec. scandinav.* 36: 93, 1957.
28. Gemzell, C. A., and T. Sjöstrand. Effect of hypophysectomy, ACTH and growth hormone on total amount of haemoglobin and blood volume in male rats. *Acta Endocrinol.* 16: 6, 1954.
29. Gemzell, C. A., and T. Sjöstrand. The effect of the gonads on the total amount of haemoglobin and blood volume in rats. *Acta Endocrinol.* 21: 86, 1956.
30. Gemzell, C. A., and T. Sjöstrand. Effect of adrenalectomy and of hydrocortisone on the total amount of haemoglobin and blood volume in male rats. *Acta Endocrinol.* 27: 446, 1958.
31. Gibson, J. G. Clinical studies of the blood volume. VI. Changes in blood volume in pernicious anemia in relation to the hematopoietic response to intramuscular liver extract therapy. *J. Clin. Invest.* 18: 401, 1939.
32. Gibson, J. G., and A. W. Harris. Clinical studies of the blood volume. V. Hyperthyroidism and myxoedema. *J. Clin. Invest.* 18: 59, 1939.
33. Gregersen, M. I., and J. L. Nickerson. Relation of blood volume and cardiac output to body type. *J. Appl. Physiol.* 3: 329, 1950.
34. Gregersen, M. I., and R. A. Rawson. Blood volume. *Physiol. Rev.* 39: 307, 1959.
35. Gullbring, B., A. Holmgren, T. Sjöstrand, and T. Strandell. The effect of blood volume variations on the pulse rate in supine and upright positions and during exercise. *Acta physiol. scandinav.* 50: 62, 1960.
36. Hallberg, L. Blood volume and regeneration of blood in pernicious anemia. *Scandinav. J. Clin. & Lab. Invest.* 7, Suppl. 16, 1955.
37. Henry, J. P., O. H. Gauer, and J. L. Reeves. Evidence of the atrial location of receptors influencing urine flow. *Circulation Res.* 4: 85, 1956.
38. Henry, J. P., and J. W. Pearce. The possible role of cardiac atrial stretch receptors in the induction of changes in urine flow. *J. Physiol.* 131: 572, 1956.
39. Holmgren, A. Circulatory changes during muscular work in man. *Scandinav. J. Clin. & Lab. Invest.* 8: Suppl. 24, 1956.
40. Holmgren, A., B. Jonsson, M. Levander, H. Linderholm, F. Mossfeldt, T. Sjöstrand, and G. Ström. Effect of physical training in vasoregulatory asthenia, in Da Costas' syndrome, and in neurosis without heart symptoms. *Acta med. scandinav.* 165: 89, 1959.

41. Holmgren, A., F. Mossfeldt, T. Sjöstrand, and G. Ström. Effect of training on work capacity, total haemoglobin, blood volume, heart volume and pulse rate in recumbent and upright positions. *Acta physiol. scandinav.* 50: 72, 1960.
42. Huff, R. Z., and D. D. Feller. Relation of circulatory red cell volume to body density and obesity. *J. Clin. Invest.* 35: 1, 1956.
43. Hurtado, A., C. Merino, and E. Delgado. Influence of anoxemia on the hemopoietic activity. *A. M. A. Arch. Int. Med.* 75: 284, 1945.
44. Karlberg, P., and J. Lind. Studies of the total amount of hemoglobin and the blood volume in children. *Acta paediat.* 44: 17, 1955.
45. Kee-Chang Huang, and J. H. Bondurant. Simultaneous estimation of plasma volume, red cell volume and thiocyanate space in unanesthetized normal and splenectomized rats. *Am. J. Physiol.* 185: 441, 1956.
46. Kjellberg, S. R., U. Rudhe, and T. Sjöstrand. The amount of hemoglobin and the blood volume in relation to the pulse rate and cardiac volume during rest. *Acta physiol. scandinav.* 19: 136, 1949.
47. Lippman, R. W., and E. C. Persike. Effect of thyro-parathyroidectomy upon the blood and plasma volumes of the rat. *Proc. Soc. Exper. Biol. & Med.* 67: 383, 1948.
48. Muldowney, F. P. The relationship of total red cell mass to lean body mass in man. *Clin. Sc.* 16: 163, 1957.
49. Perera, G. A. Effect of significant weight change on the predicted plasma volume. *J. Clin. Invest.* 25: 401, 1946.
50. Post, R. L., and C. R. Spealman. Variation of total circulating hemoglobin and reticulocyte count of man with season and following hemorrhage. *J. Appl. Physiol.* 1: 227, 1948.
51. Reeve, E. B., T. H. Allen, and J. E. Roberts. Blood volume regulation. *Ann. Rev. Physiol.* 22: 349, 1960.
52. Robbe, H. Total amount of haemoglobin and physical working capacity in anaemia of pregnancy. *Acta obst. et gynec. scandinav.* 37: 312, 1958.
53. Schreiner, G. E., N. Freinkel, J. W. Athens, and W. Stone. Dynamics of T-1824 distribution in patients with traumatic arteriovenous fistulas. *Circulation Res.* 1: 548, 1953.
54. Sjöstrand, T. A Method for the determination of the total haemoglobin content of the body. *Acta physiol. scandinav.* 16: 211, 1948.
55. Sjöstrand, T. The total quantity of hemoglobin in man and its relation to age, sex, body weight and height. *Acta physiol. scandinav.* 18: 324, 1949.
56. Sjöstrand, T. Volume and distribution of blood and their significance in regulating the circulation. *Physiol. Rev.* 33: 202, 1953.
57. Sjöstrand, T. Blutverteilung und Regulation des Blutvolumens. *Klin. Wchnschr.* 34: 561, 1956.
58. Stickney, J. C., and E. J. van Liere. Acclimatization to low oxygen tension. *Physiol. Rev.* 33: 13, 1953.
59. Svikla, A., and H. C. Bowman. Oxygen carrying capacity of the blood of dormant ground squirrels. *Am. J. Physiol.* 171: 479, 1952.
60. Tribukait, B. Hämoglobinmenge und Blutvolumen der Ratte und ihre Beziehung zum Körpergewicht. *Acta physiol. scandinav.* 49: 35, 1960.
61. Tribukait, B. Hämoglobinmenge und Blutvolumen der Ratte während chronischer Hypoxie entsprechend einem Unterdruck von 1000–8000 m. Höhe. *Acta physiol. scandinav.* In press.
62. Tribukait, B. Hämoglobinmenge und Blutvolumen der Ratte während der Initialphase von Hypoxie. *Acta physiol. scandinav.* In press.
63. Wahlund, H. The total amount of haemoglobin in polycythaemia vera treated with radiophosphorus. *Acta med. scandinav.* 150: 199, 1954.
64. Walters, J. H., H. Lehmann, and R. J. Rossiter. Blood volume changes in protein deficiency. *Lancet* (253) 1: 244, 1947.
65. Wasserman, K., and H. S. Mayerson. Plasma, lymph and urine studies after dextran infusions. *Am. J. Physiol.* 171: 218, 1952.
66. Waterfield, R. L. The effect of posture on the circulating blood volume. *J. Physiol.* 72: 110, 1931.
67. Widdowson, E. M., and R. A. McCance. The effect of rest in bed on plasma volume as indicated by haemoglobin and haematocrit levels. *Lancet* 1 (258): 539, 1950.
68. Wiklander, O. Blood volume determinations in surgical practice. *Acta chir. scandinav.* Suppl. 208, 1956.

Plasma substitutes

NOBLE O. FOWLER | *Cardiac Laboratory, University of Cincinnati and Cincinnati General Hospital, Cincinnati, Ohio*

CHAPTER CONTENTS

HISTORY

ONE OF THE EARLIER experimental studies of the intravenous injection of colloids in experimental animals was performed by Czerny (24) in 1894. Czerny injected gum arabic or gelatin intravenously into cats, rabbits, and dogs. He observed increased blood viscosity following intravenous injections of gum arabic and a decrease in red blood cell count in his experimental animals after the injection of intravenous colloids. In 1915, Hogan (50) first used colloidal gelatin intravenously in humans suffering from shock. He noted an improvement in the blood pressure in these patients. In 1918, Bayliss (8) first used 3 or 6% gum arabic (acacia) in saline in treating wound shock. He observed that many patients in shock responded; those who failed also did not respond to blood. He observed no immediate unfavorable reaction to the intravenous infusion of gum arabic in saline. Early studies of dextran were made by Gronwall & Ingelman (43) in 1945. These authors suggested that dextran be employed in the treatment of shock for the following reasons: its colloidal osmotic pressure is equal to that of the plasma proteins; it is nontoxic and devoid of antigenic properties; its viscosity is of the same order as that of blood; it is eliminated and not stored in the organs of the body.

REQUIREMENTS OF AN ACCEPTABLE PLASMA SUBSTITUTE

There are a number of requirements which must be met before a plasma substitute may be considered acceptable. Some of these requirements were listed by Gropper and co-workers (44). The plasma expander or substitute *a*) must be able to maintain a satisfactory colloid osmotic pressure; *b*) must be capable of being manufactured at a constant composition and at reasonable cost; *c*) must have a viscosity suitable for intravenous injection; *d*) should be stable on storage and on exposure to wide temperature variation; *e*) must be easily sterilized; *f*) must be pyrogen free; *g*) must be ultimately excreted or

metabolized, not causing either immediate or delayed tissue damage; *h*) must not be antigenic. Squire and associates (94) have also indicated that the plasma substitute must remain in the blood stream for an appreciable time, preferably that not more than 25% be excreted in the urine in the first 24 hours, or that at least 50% of the amount infused be present in the blood stream for at least 12 hours and preferably for 24 hours following infusion. The solution should be fluid at temperatures above zero degrees centigrade. It should withstand sterilizing by autoclaving. It should not be locally or generally toxic. It should not act as a diuretic and should cause no increase, or only slight increase, in the erythrocyte sedimentation rate. The agent should not produce hemolysis or red cell agglutination. Additional requirements have been listed by Hartman (47). The normal number and function of the formed elements of the blood should be maintained. Rapid accumulation of the plasma expander in organs and tissues, thus possibly interfering with their function, should not occur. Prolonged retention of the plasma substitute in organs or tissues contraindicates its use. The material should be at least partially metabolized in the body. Recent studies have indicated that an additional requirement should be made to the above: namely, that the infusion of reasonable amounts of the plasma volume expander, approaching perhaps one-third of normal blood volume, should not be associated with significant impairment of hemostasis.

ADVANTAGES OF COLLOIDAL INFUSIONS AS PLASMA SUBSTITUTES

If ample blood and plasma are available there would seem to be limited use, if any, for plasma substitutes; however, in dealing with emergency situations or casualties involving a large population, or in working in remote areas where blood or plasma is not available, plasma expanders may become of extreme importance. Plasma expanders have the advantage that they may be manufactured in unlimited quantities, whereas the supply of blood plasma is always limited. Plasma expanders can be stored for many months, whereas whole blood can be stored for only 3 weeks, and cannot be procured in unlimited quantities. In most instances of shock there is a considerable reserve of oxygen carrying capacity, and the primary objective is restoring the circulatory blood volume (45). This, the plasma expanders are able to do. In addition, a suitable plasma expander, which can be autoclaved, is free of the risk of transmission of bacterial infection and of viral hepatitis, problems which still exist with regard to blood and plasma. The problems of transfusion reaction and Rh sensitization, which are present with the use of blood, are also avoided. Plasma substitutes may be of value in the treatment of shock due to blood loss when blood is not available and when the blood loss is not excessive They are of value in the treatment of shock due to plasma depletion and in the treatment of hypoproteinemia with edema, and they provide useful physiologic tools for studies of experimental hypervolemia and experimental anemia.

PROPERTIES OF PLASMA SUBSTITUTES

Plasma expanders may be classified as follows: *a*) blood derivatives: albumin, plasma, globin; *b*) modified proteins: gelatin, oxypolygelatin; *c*) polymerized carbohydrates: dextran, levan; and *d*) plastics: polyvinylpyrrolidone (PVP).

Since most of the plasma substitutes are available in varying molecular weights and in several different concentrations, only general statements about their properties can be made. According to Hueper (53) acacia is a polysaccharide composed of arabinose and galactose molecules with various hexoses, pentoses, and uronic acids. Polyvinyl alcohol is a polymerized form of unsaturated vinyl alcohol $(CH_2{=}CHOH)_n$. The molecular size depends on the degree of polymerization. Pectins are long-chained compounds of galacturonic acid molecules with various additional groups—e.g., galactose, araban, acetic acid, and methyl alcohol. Polyvinylpyrrolidone (97) has the following formula:

PVP 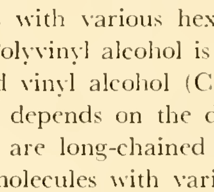

Dextran, according to Squire and associates (94), is a collective name for a series of polyglucoses, having a high dextrorotation of the order of plus 200°. There are various species of cocci belonging to the genus *Leuconostoc*; two of these, *Leuconostoc mesenteroides* and *Leuconostoc dextranicum*, under suitable conditions may produce dextran by the fermentation of sucrose. Dextran is a polyglucose in which the majority of bonds linking the glucose units are of the alpha 1:6 type. Dextrans may have a wide variety

of molecular weight. According to Squire, average molecular weights of various dextrans may range from 11,000 to 1,700,000 as determined by the ultracentrifuge. According to Marshall and associates (69) the Swedish dextran Macrodex used in their studies as 6% dextran in 0.9% sodium chloride was slightly greater than three times water viscosity. Plasma was one and one-half times water viscosity. In our studies (31) a comparison was made between the viscosity of 6% dextran in saline (Abbott Laboratories) and that of dog blood at various hematocrits. The blood-to-dextran viscosity ratio was 1.12 when the hematocrit was 36. When the hematocrit was 40.5 the ratio was 1.23, and when the hematocrit was 50 it was 1.31.

Roome and associates (90) studied properties of various polyvinyl alcohols using grade Rh 623. They found that this substance was sterilizable by autoclaving, that it did not gel at ordinary temperatures. Its viscosity was five times that of water. Solutions of 2.8 and 3.8% gave osmotic pressures of 30 and 40 mm Hg, respectively.

Taylor & Waters (102) studied the properties of 7% isinglass or fish swim bladder gelatin in 0.9% saline. Its osmotic pressure was higher than that of plasma (38 mm Hg). Its viscosity was twice that of plasma and three times that of water, but less than that of whole blood. The solution was readily sterilized at 100° C for 5 min.

FATE OF PLASMA SUBSTITUTES ON INTRAVENOUS INJECTION

In considering the use of plasma substitutes it is desirable to know how long they remain in the plasma, to what extent they are excreted in the urine, whether or not they are metabolized, whether or not they are stored for extended periods in the reticuloendothelial system or in other organs, and whether or not they produce damage to the organs in which they are stored either temporarily or permanently. In addition it is desirable to know whether there are other pathways than the urine for elimination, e.g., into the bile and by secretion into the gastrointestinal tract.

Dick and associates (26) treated four children with nephrosis by means of intravenous acacia. In one patient who had received a total of 129 g of acacia, acacia was found at necropsy in the liver, spleen, kidney, lungs, lymph nodes, and bone marrow. Analysis of the liver revealed 3.9% acacia. The plasma level was 2.1% at this time; the pericardial fluid 0.6%, the peritoneal fluid 1.1%, and bile 2%. Bollman (15) stated that he gave dogs acacia intravenously at approximately weekly intervals for 6 months. Ten years later liver biopsy in these animals showed acacia still to be present in the liver, although liver function tests were normal. Andersch & Gibson (4) gave rabbits intracardiac injections of 30% acacia at 2- to 4-day intervals. At necropsy 35% to 60% of the injected amount was found in the liver, with lesser amounts in the spleen, kidney, and skeletal muscles. The liver cells were enlarged and vacuolated. The Kupffer cells appeared to be normal. In a patient who was treated for nephrosis with acacia, 43% of the injected acacia was found to be in the liver. Injections of acacia had been given up to the time of death. Dogs given acacia were found to have hepatic retention, output of acacia into the bile, and decreased excretion of bilirubin and bile acids.

Polyvinyl Alcohol

Roome and associates (90) gave five dogs 14.1 to 70 g of polyvinyl alcohol, grade Rh 623. Autopsy showed no evidence of storage or visceral damage in these animals. Hueper (54), using a different fraction of polyvinyl alcohol, gave to three rabbits daily injections of 5% polyvinyl alcohol in 0.85% sodium chloride. One rabbit received 10 injections of 10 ml each, one received 15 injections, one received 25 injections, the last 5 being 20 ml. At necropsy the lungs showed perivascular and peribronchial eosinophils and lymphocytes with occlusion of smaller blood vessels by leucocytic thrombi. The spleen showed foam cells, and there were foam cells in the bone marrow of the rabbit receiving the largest dose. Spermatogenesis was arrested, and in the blood vessels of the brain a blue material filling or coating the inner walls of the blood vessels was seen. Scattered pulmonary obliterative arteriosclerosis was observed. Tubular degeneration was seen in the kidneys, perhaps due to coating of the walls of the renal blood vessels and interfering with the exchange of nutritive substances and metabolites. Hueper concluded that polyvinyl alcohol was removed and stored principally by the reticuloendothelial cells of the spleen, adrenals, and liver; and, to a lesser degree, by those of the lymph nodes. The only parenchymal cells containing polyvinyl alcohol were the renal tubules, adrenal cortex, and some brain ganglion cells.

Pectin

Hartman (47) depolymerized pectin by heat at 212° F for 24 hours. The molecular weight of the compound used was 40,000 to 70,000. Seven intravenous injections of 0.3 g/kg into mice resulted in retention of pectin in the reticuloendothelial cells and in the parenchyma of the liver, and renal tubules. Popper *et al.* (85) gave to patients pectin in saline, molecular weight 45,000 to 60,000, in amounts of 1 to 9 liters. Pectin appeared to be stained as a structureless material in the splenic pulp with resultant splenomegaly. It was found in the Kupffer cells and portal triads, in glomerular loops and in renal tubules. The pectin was stained in this study by ruthenium red, supposedly specific for pectin. The histologic picture resembled that of amyloidosis but the material was not believed to be amyloid on staining. The tissue changes with pectin were more extensive than those seen with comparable amounts of gelatin which was administered as a 5% solution with an average molecular weight of 35,000 in saline and dextrose in amounts of 1 to 10 liters. Handford and associates (45) used 4% glycerol pectate of 4.4 viscosity. The pectin was obtained from lemon rind. They gave approximately 5% body weight equivalent to normal dogs. No gross or microscopic evidence of pathologic changes in the tissues or organs of animals were seen following large single or multiple infusions of glycerol pectate. These authors believed that autoclaving the pectin prevented histologic changes described after unautoclaved pectin. The plasma concentration was negligible at 12 hours; at 48 hours 45% of the pectin was recovered in the urine. The fate of the glycerol pectate not recovered in the urine was unknown. Bryant *et al.* (19) used pectin (mol wt 150,000 to 300,000) in 0.85% saline. This was given intravenously to rabbits, on alternate days for 2 months, with a total of 15 g of pectin per 4 kg rabbit. At necropsy, no abnormalities were seen in the liver, spleen, kidney, heart, lungs, or digestive tract. There was no evidence of storage of pectin in the liver or kidney. There was no pectin in the blood 7 days after the last injection.

Gelatin

Waters (109) infused bled dogs with isinglass or gelatin. There was no isinglass nitrogen in the blood at 9.5 to 18 hours, whereas gelatin was still present in appreciable amounts at 24 hours, leading the author to believe the gelatin was superior as a plasma expander. Hartman (47) injected mice with seven intravenous injections each of 1.8 ml/kg of 6% osseous gelatin which produced gelatin nephrosis of brief duration. Frawley and associates (34) infused ten wounded soldiers with Knox gelatin (average mol wt 34,000). The total amount infused was 1 to 3 liters at an average rate of 300 ml of gelatin in 2.5 hours. Six hours after the infusion 23% of the gelatin remained in the circulation. At this time 60% of the gelatin had appeared in the urine; at 72 hours, 75% of the gelatin had appeared in the urine. Gray and Pulaski (40) gave 200 ml of 5% oxypolygelatin in saline to phlorhizinized starved dogs with a constant D/N ratio. The D/N ratio in the urine increased after infusion, suggesting metabolism of oxypolygelatin to glucose. Gordon and associates (37) used 8% or 10% bone gelatin in 0.9% saline. Dogs were infused with 40 ml/kg body weight after bleeding, and were infused again 9 to 11 weeks later. At postmortem they showed no evidence of thrombosis, embolism, hemolysis, or capillary damage, and there were no other pathologic changes seen. Jacobson & Smyth (60) used 5% osseous gelatin in isotonic sodium chloride (Upjohn). They gave 56 injections of 450 to 1000 ml each to 45 human subjects. At 24 hours 87% of the injected amount had disappeared from the blood. The average urine recovery was 76% in 24 hours and 81.3% in 48 hours. In 3 autopsied patients no tissue changes were seen. The blood amino acids did not change and the authors thought gelatin was probably not metabolized. Hoffman & Kozoll (49) gave 1000 ml of 5% osseous gelatin to each of 42 hospital subjects. There were appreciable plasma levels at 48 and 72 hours. By 72 hours 80% of the gelatin was excreted in the urine.

Polyvinylpyrrolidone (PVP)

Hartman (47) injected 3.5% PVP in saline into mice. At autopsy he found foam cells in the lymph nodes, granules and vacuoles in the liver, kidney, adrenals, bone marrow, lung, and blood vessels. He concluded that PVP was stored more rapidly and in larger quantities than either dextran, gelatin, or pectin. Steel and associates (97) gave 1 ml of 3.5% PVP solution intravenously to mice. The PVP was tagged with carbon-14. These authors recovered 76 to 77% of the PVP in 58 days, mostly in the urine but some in the feces. Virtually none was found in the expired air; however, at 58 days only 15 to 16% of the PVP was found still in the carcass. The authors estimate that this would have been excreted in 217 to 232 days. They concluded that PVP which was not

excreted was stored in unaltered form by the fixed body phagocytes. Thrower & Campbell (104) gave 10 to 40 ml/kg of 3.5% PVP to rabbits. The rabbits were killed in 14 to 28 days. No gross or significant microscopic changes were seen. There was no evidence of storage in the liver. Four patients given 500 to 1500 ml of PVP showed at autopsy no changes ascribable to PVP. About 75% of the injected amount could be recovered in the urine. If 500 ml of PVP was infused intravenously, plasma levels were 3.5 g % initially and 0.2 g % at the end of 50 hours. Gall and associates (36) studied 22 patients who had received a single infusion of 1000 ml of 3.5% or 4.5% PVP. Liver biopsy specimens were obtained as controls and after intervals of 1.5 to 13 months. Histologic studies of the liver showed basophilic globular deposits up to 50 micra in diameter. These were in the Kupffer cells or free in the sinusoids. There was occasionally a mild inflammatory reaction in relation to these. Deposits were seldom seen before 3 months from the time of infusion, but almost uniformly after 6 months. The histochemical studies were consistent with the hypothesis that the material was PVP. Loeffler & Scudder (68) gave carbon-14 tagged PVP to four patients who died (from other causes) in 2 to 8 days. One-third of this material was excreted in the urine in 24 hours, and two-thirds in 48 hours. Small amounts were excreted in the feces. The greatest amount of the unexcreted portion was found in the kidneys, liver, spleen, and lymph nodes. There was no histologic evidence of damage caused by it. These patients each received 540 ml of PVP (Macrose). Hueper (55) gave rats and mice subcutaneous, intraperitoneal, and intravenous PVP of molecular weight 20,000 to 300,000. In survival periods up to 24 months, tumors of the lymphoid and reticuloendothelial tissues developed; also carcinomas of the uterus, skin, ovary, and breast were found. The doses used were large and would rarely be employed in man, except possibly in the treatment of burns or nephrosis. The tumor incidence, both malign and malignant, was 20 to 25% in rats. Frommer (35) gave low, medium, and high molecular weight fractions of PVP to mice in doses of 0.5 ml in a series of 20 injections totaling 10 ml. Changes occurred in the Kupffer cells and histiocytes of the periportal tissue. Some macrophages were distended with vacuoles, giving them the appearance of foam cells. Foam cell production seemed to be a function of molecular size; the larger molecular weights gave rise to many more foam cells than did the lower weight in equivalent amount. A single injection, equivalent to 20 to 25% of blood volume, did not produce hepatic changes. Stern (98) injected 3.5% PVP into mice. Storage of it or a derivative was seen in the reticuloendothelial cells of the mouse. Simultaneous administration of PVP and sulfonated azo dyes led to renal excretion of dye and decrease of dye storage in the reticuloendothelial system. Polyvinylpyrrolidone given after the dye eluted it from the reticuloendothelial cells. Polyvinylpyrrolidone given before dye prevented its storage in the reticuloendothelial cells.

Altemeier and associates (3) studied the hepatic storage of PVP in 25 patients receiving 1000 ml of 3.5% PVP (Macrose). The results were described earlier in this chapter (36). Ravin and associates (87) used PVP fractions tagged with I^{131} and carbon-14 and showed that PVP is not metabolized to any significant degree by rat, dog, or man. It does not penetrate to the brain or fetus. The reticuloendothelial system retains PVP with a molecular weight greater than 110,000 for a long time, probably for years. Polyvinylpyrrolidone with a molecular weight below 25,000 leaves promptly by way of the glomerulus and is of little value as a plasma expander; that below 40,000 can be excreted through the glomerulus in a few days. The authors recommended PVP of 25,000 to 40,000 molecular weight with extremes of 20,000 to 70,000 molecular weight as plasma volume expanders. These would expand plasma to 80 to 90% of infused volume at once and maintain 30% expansion at 12 hours. Sixty per cent of this molecular weight PVP would be excreted in the urine in a few days. The remainder would probably be totally excreted in a year or more.

Dextran

Nelson & Lusky (81) gave rabbits 10 ml/kg of 6% dextran (Macrodex) or 3.5% Periston (PVP) intravenously on 16 occasions over a 2-month period. No systemic effects were seen. At autopsy the outstanding observation was that of foam cells in the PVP group; in the spleen these were 1/3 to 1/2 the entire organ. They were also seen in moderate degree in lymph nodes, bone marrow, and adrenal medulla; and to a lesser extent in the lungs, liver, and thymus. In the dextran animals changes were minor. Gray and associates (41) studied the effect of dextran in starved phlorhizinized dogs. After infusing 200 ml of 6% dextran the 24- to 48-hour post-infusion urine showed an increased D/N ratio, suggesting metabolism of dextran to glucose. These authors failed to find significant excretion of dextran into the gastrointestinal tract in

three dogs. Gray (39) showed that carbon-14 dextran was metabolized. It was broken down by the animal, incorporated into the carbon pool, and distributed throughout the body in the form of normal biochemical constituents. It appeared in lipids and amino acids as early as the first day after administration. Its metabolic half-life was 61 days in mice. This author concluded that the possibility of dextran retention in the body with adverse effects is unlikely. Mowry & Millican (79) gave mice 6% dextran intravenously. The mice were sacrificed at intervals. Histochemical tissue studies showed dextran widely distributed in the blood, renal tubules, liver cells, and reticuloendothelial system. In the hepatic cell cytoplasm the dextran appeared in 2 hours and was maximal at 12 to 24 hours. None was seen in the hepatic cells after 1 month. In the Kupffer cells, dextran lasted longer and some was still present after 2 months. It also persisted in the phagocytes of lymph nodes, spleen, pancreas, myocardium, fat, lung, kidney, and skin. Hartman (47) gave 6% dextran (CSC) to mice in seven intravenous injections of 1.8 g/kg body weight each. This was shown to produce retention in the lymph nodes, liver, kidneys, and blood vessels. The liver cells showed granular and vascular change, and the kidneys showed nephrosis. There were foam cells in the lung blood vessels and in the lymph nodes. Most of these changes were found to be reversible. Frawley and associates (34) gave dextran (average mol wt 42,000) to 16 wounded soldiers. The soldiers received 1 to 3 liters with an average infusion rate of 500 ml in 2.7 hours. Six hours after infusion 21% of the dextran was still in the circulation and 45% of it had appeared in the urine. At 72 hours 58% of the dextran had appeared in the urine. There was no significant difference in the plasma disappearance curves of gelatin and dextran in this study. Hehre & Sery (48) demonstrated that an enzyme elaborated by certain gram negative intestinal bacteria in man (Bacteroides group) is able to cause breakdown of native and clinical dextrans, releasing some as reducing sugar. The importance of this mechanism in the metabolism of dextran given to patients is unknown. Mowry and associates (80), using a histochemical method, showed a material believed to be dextran in the hepatic cells and renal tubules of mice given CSC dextran 6% in saline intravenously and sacrificed at 5 hours. Wolman (117) compared the livers of mice injected with clinical levan and clinical dextran. With dextran there was found to be no increased liver glycogen and most Kupffer cells were normal. Para-aminosalicylic acid (PAS) positive granules were in the Kupffer cells or in renal tubules, but most were free in the blood vessels and between the cells. After clinical levan there were found liver cell vacuoles which stained like glycogen with aqueous PAS and which were digested with saliva. Otherwise, the organ changes were similar. The liver cell material was not conclusively proved to be glycogen chemically, but this was strongly suggested. If so, this may mean that levan is metabolized more quickly than dextran and thus a more desirable plasma expander. Terry and associates (103) gave C^{14}-labeled dextran to dogs. The average molecular weight was 30,000. With an intravenous dose of 1 g/kg, plasma levels approached zero at 70 hours. In 24 hours, 40 to 50% of the dextran appeared in the urine by chemical tests, and 70% by carbon-14 tests (the radioactive dextran had a smaller molecular size). The amounts in the plasma were negligible at 72 hours. The tissues contained 5 to 10.7% of the dose at this time, mostly in the liver, lymph nodes, adrenals, and spleen. In 72 hours the equivalent of 4.6 to 7.8% of the dextran had appeared in expired air. The authors postulated that, since C^{14} carbon dioxide continues to appear in expired air, all the dextran may be metabolized in about 5 weeks. The liver was the only organ with PAS positive diastase-resistant material in its parenchyma; there was none in the kidneys. Bloom (11) gave patients 30 g of dextran intravenously. The majority of the excretable material was found in the urine within 24 hours with a total of 42% over a 5-day period. After a 30-gram infusion the plasma dextran had disappeared by 5 days. No metabolic products were identified in the blood and urine, although the dextran remaining in the body was believed to be metabolized slowly. Turner & Maycock (105) studied the distribution of injected dextran in mice given 360 mg of dextran per 100 g of mouse. About half of this had left the body by 24 hours, 70% by 7 days, and 80% by 3 weeks. Lorenz, cited by Turner (105), observed that mice given 60 mg of dextran intravenously excreted 15 to 20% in the urine in 24 to 36 hours; 93 to 95% had left the body in 8 weeks. Dextran was serologically but not chemically detectable in saline extracts of whole mouse after 32 weeks, but not after 1 year. Bloom (12) treated 52 patients in shock with dextran. When a hepatic vein was catheterized, there was no evidence of dextran removal by the liver. After 500 ml of 6% dextran, mean plasma levels were 726 mg/100 ml, falling slowly to a mean of 88 mg at 96 hours. Most of the urinary excretion occurred in the first 48 hours and

this accounted for 42% of the amount administered. Howard and associates (52) showed that the amount of dextran remaining in the plasma was related to molecular size. These authors used Commercial Solvents Corporation dextran. Of that having an average molecular weight of 34,000, very little remained in the plasma 24 hours after 1000 ml had been given intravenously over a period of 1 hour. Of molecular weight 51,000 dextran, little remained in the plasma after 72 hours. Other fractions of higher molecular weight remained in the plasma in appreciable amounts at 72 hours. Engstrand & Aberg (27) gave 40 ml of dextran intravenously to cats weighing 2.5 kg and found excretion into the gastric juice, the pancreaticoduodenal juice, but none in the bile. The total amount excreted in 9 hours was 28% of that injected. In three humans, excretion into the gastric juice was found. Bloom & Wilhelmi (13) showed that oral feeding of dextran in rat and man led to an increase of blood reducing substance, most of which was fermentable. There was also an increase of liver glycogen in rats. Dextran was capable of being broken down in the intestine to products which yield glucose and glycogen.

In summary, it may be said that acacia may persist in the hepatic cells for years after intravenous injection. Certain fractions of polyvinyl alcohol are stored in the reticuloendothelial system, and may produce vascular damage. Certain pectin preparations may be stored in the Kupffer cells and splenic pulp; others are not. Gelatin does not appear to produce significant tissue changes, and may be metabolized in part. Polyvinylpyrrolidone which is not excreted in the urine is stored in fixed body phagocytes; it does not appear to be metabolized. The infusion of dextran is associated with minor tissue changes. There is good evidence that dextran is metabolized, and that 93 to 95% will leave the body within 8 weeks after infusion.

ANTIGENIC PROPERTIES OF PLASMA SUBSTITUTES

Pectin

McClure and associates (73) used 1% pectin with a relative viscosity of 2 at 38° C, which was given to 275 patients in amounts of 200 to 1600 ml. No toxicity or antigenicity was seen except for a purpuric rash in 2 patients who received over 5000 ml. These patients received daily injections of 1000 ml.

Bovine Plasma and Albumin

Wangensteen and associates (106) gave citrated bovine plasma to 66 patients who received 2 to 10 ml intravenously. Fifteen per cent of these subjects had reactions; these were mild to moderate in 9 instances, but in one patient with asthma, severe dyspnea occurred. State and associates (96) used purified bovine serum albumin, made by precipitation with ethanol at 5° C. In 469 injections to 410 patients, 12 (2.9%) had immediate reactions and 38 (9.2%) had delayed reactions. The immediate reactions were of two types—anaphylactoid with dyspnea, cyanosis, and fall in blood pressure; or pyrogenic, with chills and fever. The delayed reactions took the form of urticaria, erythema, myalgia, and fever, and occurred at 12 to 24 hours. Twenty-five per cent bovine albumin was effective in treating shock, but was not recommended by the authors because of the persistence of reactions and the incapacity caused by the delayed reactions.

Globin

Strumia and associates (99) used modified globin (mol wt 34,000) which was stable in 0.85% saline. Two hundred and ten injections were given intravenously to 108 humans. The largest single dose was 57 g; the largest amount in 24 hours was 60 g. One patient received a total of 192 g. The concentration of the infused globin was 1.8 to 6.8%. There were a few pyrogenic reactions; these were eliminated by biological control. No antigenicity was seen following a second injection.

Gelatin

Taylor & Waters (102) gave 7% isinglass (fish swim bladder gelatin) in 0.9% saline as a plasma expander. These authors noted a mild sensitization on repeated injections within 2 weeks in some dogs, but not afterwards. This was assumed to be due to contaminating fish protein. Gordon and associates (37), using 8 or 10% bone gelatin in 0.9% saline, infused dogs with 20 ml per kg body weight at 3 ml per kg per min; no untoward effects were seen upon blood pressure or respiration. Dogs given 40 ml per kg body weight after bleeding did not show antigenic effects on reinjection of 40 ml per kg body weight after 9 weeks. Jacobson & Smyth (60) used 5% osseous gelatin in isotonic sodium chloride (Upjohn). These authors gave 56 injections of 450 to 1000 ml each to 45

subjects. Fifty others received gelatin for shock. No reactions were seen and there was no sensitivity when injections were repeated. Artz and associates (6) gave combat casualties 200 units of modified fluid gelatin; the injection units were 500 ml each. The average molecular weight of the gelatin was 34,000. As much as 3000 ml was given to some subjects. The circulation was supported for the period of evacuation —3.5 hours. There was no toxicity. These injections were made in human combat casualties. Maurer & Lebovitz (72) studied the antigenicity of modified fluid gelatin. This was used in human volunteers in four groups of five each. Each group received five daily injections of 2, 5, 15, or 30 mg of modified fluid gelatin per ml at each injection. Three weeks after the last injection, 50 ml of blood was taken and intracutaneous tests were performed. No skin reactions or precipitating antibodies were produced. Modified fluid gelatin was antigenic in rabbits only when injected in water-in-oil emulsion, but not in saline or as an alum precipitate.

Polyvinylpyrrolidone

Arden and associates (5) gave 3.8% PVP to 37 patients. Blood pressure effects were favorable and there were no untoward reactions. Maurer (70) studied PVP K 30, average molecular weight 40,000, which when used as a plasma volume expander showed no evidence of antigenicity in man or rabbit. Rabbit sera showed no antigenicity to this PVP preparation. PVP K 87, average molecular weight 1,000,000, showed evidence of antigenicity in man via antibody production in the serum. Also two subjects developed itching, and one a rash after PVP K 87. This fraction, however, is not used as a clinical plasma volume expander.

Ohlke & Scales (82) used dextran in 56 surgical cases, none of whom had a reaction. Wilkinson & Storey (114) gave 5 normal subjects 6% dextran in 0.9% saline. They were given 500 ml or 1000 ml in 47 to 110 minutes. These subjects developed vasomotor instability which lasted up to 1 week. The dextran which was used had a molecular weight of 130,000 to 250,000 in 65% of the fraction. The name of the manufacturer was not given. In contrast only 2 of 40 infusions made in patients in shock were associated with mild and transient reactions. Allen & Kabat (2) showed that levan was capable of producing skin sensitivity and precipitins in man. Kabat & Berg (65) showed production of cutaneous sensitivity and precipitins in man after two subcutaneous dextran injections of 0.5 ml each. The tests were made 21 days after the second injection. The materials were native dextran or Swedish clinical dextran of high molecular weight. The authors thought there was insufficient nitrogen impurity in dextran to account for the reaction. Bryan & Scudder (18) showed a cross activity between tissue antibodies to native dextran and pneumococcus polysaccharides, Types II, XII, and XX. Bowman (17) in over 500 infusions of 6% dextran in isotonic saline observed only two reactions, which took the form of itching, urticaria, chills, and a rise in body temperature to as much as 103° F. The material used was Plavolex. Jaenike & Waterhouse (61) gave daily infusions of 6% dextran in physiological saline to five patients, in amounts of 1000 to 2000 ml per day for 2 to 10 days, and 12% dextran in 0.5% sodium chloride to two patients, 1000 ml daily for 6 days. There were no vasomotor or pyrogenic reactions. One 58-year-old patient with hypertension developed pulmonary congestion after 2 days and the study was discontinued. One patient with neurodermatitis developed an exudative hemorrhagic quality to the skin lesions on the third day. Stucki & Thompson (100) showed that intraperitoneal dextran produced edema of the paws, snout, ears, and external genitalia of the rat. Anesthetic doses of phenobarbital, chlorpromazine, antihistaminics, or epinephrine were effective in inhibiting this edema. The amount of dextran used was 300 mg or 600 mg of 6% dextran in saline. Bennett (10) studied the production of fever and the Schwartzman phenomenon by native dextran. In rabbits, the skin was prepared with a polysaccharide from *Serratia marcescens*. Twenty-four hours later 50 mg of native dextran given intravenously produced local hemorrhage in 50%. Two hundred milligrams of dextran caused hemorrhage in 95%. Native dextran with a molecular weight of several million produced fever and leukopenia. It is important to know that this dextran is not used clinically. Clinical dextran did not produce fever, leukopenia, or the Schwartzman reaction. Maurer (71) showed that the intracutaneous injection of dextran was followed in 3 weeks by dextran precipitins and cutaneous sensitivity in the form of wheal and erythema production. Both native and clinical dextrans were used. Antibodies to dextran were shown to persist in human sera for over 1 year. Tarrow & Pulaski (101) infused 109 volunteers with Macrodex (Swedish dextran) and 97 with Commercial Solvents Corporation United States dextran. The amounts infused were from 500 to 1000 ml in 10 to 65 minutes. These authors observed headache, chills, flushing, urticaria, angioneurotic edema,

wheezing, abdominal pain, cramps, vasomotor rhinitis, and swelling of the joints or extremities, or orthostatic hypotension. Reactions were seen in 51.5% of the group receiving Swedish dextran and in 8.2% of those receiving American dextran. The reactions were less frequent in patients who were given spinal anesthesia.

PHYSIOLOGICAL EFFECTS OF COLLOIDAL INFUSIONS IN NORMAL MAN AND IN ANIMALS

Plasma Volume

If plasma substitutes are to be effective they must function as effective expanders of plasma volume. Jenkins and associates (63) gave 38 convalescent patients 1000 ml of PVP (3.5% PVP Macrose, Schenley) intravenously over a 2-hour period. The average fall of hematocrit was 5.5 volume %. After 24 hours the hematocrit was within normal range except in 7 patients in whom hemodilution lasted 24 hours or longer. Plasma volumes, measured by T-1824 dye, showed in 2 hours expansion of plasma volume averaging 50% of the infused volume. Using thiocyanate to measure total available fluid (extracellular fluid) 1 liter of PVP was followed by an average increase in extracellular fluid of 2350 ml exclusive of the plasma volume change. Jackson & Frayser (58) gave dogs 1 g of acacia per kg intravenously daily for 20 days. A sharp increase in plasma volume occurred. The hematocrit and hemoglobin fell strikingly. Handford and associates (45), using 4% glycerol pectate, gave an amount equivalent to 5% of body weight to normal dogs and produced effective plasma volume expansion that persisted for 12 hours. Barker and associates (7) bled nine normal humans 1000 ml of blood and gave 1000 ml of a plasma expander over a 30-min period. Four received oxypolygelatin, three isotonic saline, and two plasma. The oxypolygelatin was 5% in isotonic saline (Baxter). The plasma volume was well maintained by plasma or oxypolygelatin, but not by saline. The blood volume after saline decreased to 88% of the post-infusion volume in 15 min.

Wasserman & Mayerson (107) studied Expandex 6% dextran, average molecular weight 60,000 with a range of 25,000 to 200,000. Also these workers used two other dextrans, one small enough to get into the urine (mol wt range 5,900 to 10,400) and the other too large to appear (90,000 to 155,000 mol wt). The plasma volume was expanded to a greater degree by the suprarenal fraction in both bled and unbled dogs. The percentage remaining in the circulation was greatest with the suprarenal threshold fraction. Only 2% of the dose of the large molecular dextran was in the urine in 4 hours, but with clinical dextran, average 60,000 molecular weight, 35% was in the urine in 4 hours in bled dogs and 50% in unbled dogs. Forty ml per kg body weight infusions of dextran increased lymph flow. Wasserman & Mayerson (108) gave 6% clinical dextran infusions into dogs. Dextran was found to be a more effective plasma expander than plasma itself when plasma volumes were measured by I^{131} human serum albumin. Dogs bled to a blood pressure of 40 mm Hg showed an expansion of plasma volume equivalent to 80% of the infusion volume 4 hours after the end of the infusion. In unbled dogs, the plasma volume was expanded only 25% of infusion volume at this time. Dextran levels in thoracic duct lymph remained below plasma dextran levels. The dextran plasma-lymph concentration gradient remained for at least 24 hours and was higher than that for albumin and globulin. It is suggested that dextran leaks into interstitial fluid more slowly than plasma protein and is therefore a good plasma expander.

Metcalf & Rousselot (74) gave 500 ml of 6% dextran in saline to 12 convalescents. The plasma volume increment after 6 hours was from 238 to 610 ml. Meyer and associates (75) gave six normal humans 500 ml of 6% dextran in normal saline. Using P^{32} tagged red cells, they found the increase of blood volume to be between 960 to 2850 ml. The maximum increase was between 15 min and 6 hours and 15 min after the completion of the infusion. Bowman (17), using Plavolex 6% dextran in isotonic sodium chloride, found 20-hour increases of blood volume to be greater with dextran than with gelatin, serum albumin, or plasma.

Bloom & Wilcox (14) described a method for measuring dextran in the blood and the urine. The method is not specific in that it will measure any polysaccharide resistant to digestion with hot alkali, precipitable by ethanol, and yielding a color similar to that of glucose with the anthrone reagent. However, substances meeting these requirements are not ordinarily found in blood and urine.

Hemostasis

One of the more important side effects of the infusion of plasma volume expanders, particularly dextran, is their impairment of hemostasis. Davidsohn & Stern (25) gave to rabbits weighing 2500 to 3500 g intravenous or subcutaneous injections of 3.5% PVP.

A single injection of 0.35 g/kg was given. Two molecular sizes were used; 35,000 to 40,000 and about 150,000. Twelve to 19 g of the small size PVP gave slight prolongation of bleeding time in only one of four rabbits. Eight to 10.5 g of the large size PVP produced prolonged bleeding time in each of four rabbits. Some animals showed thrombocytopenia with poor clot retraction which was not prevented by splenectomy. These authors proposed four factors in the hemostatic disturbance: *1*) damage to the endothelial lining of the blood vessels; *2*) degeneration of marrow megakaryocytes which was demonstrated in the autopsied rabbits; *3*) hypersensitivity; *4*) platelet agglutination.

The authors caution that results similar to this are not reported in man after PVP. Also they indicated that the effects may be less drastic in oligemic animals. Behrmann & Hartman (9) injected dogs daily with 20 ml/kg body weight of PVP, dextran, or methyl cellulose. These animals showed a decline in fibrinogen to one-half or less of the initial level, but not after gelatin. After PVP, dextran, or methyl cellulose there was initial fall in platelets. If the reticuloendothelial system was blocked by India ink, then platelet recovery occurred in splenectomized dogs. After PVP, dextran, and methyl cellulose there was swelling, granulation, and absence of platelet formation by megakaryocytes. These changes were not seen after gelatin. Thrower & Campbell (104) gave to four patients 500 to 1500 ml of 3.5% PVP. The clotting and bleeding times of these patients were unaffected.

Adelson and associates (1) studied the bleeding time after dextran in dogs before and after irradiation. After irradiation, the tendency to increased bleeding time was increased. This was not always correlated with X-ray induced decrease of platelet count. The prolonged bleeding time after dextran was thought to be due to an effect upon the platelets, but not due to simple dilution. Two dogs receiving intravenous gelatin had platelet counts of 140,000 and 110,000 after radiation and 82,000 and 48,000 after intravenous gelatin; yet, no hemostatic defect developed. Howard and associates (52) studied the effect of various molecular weight fractions of dextran upon bleeding time in human subjects. They infused 1000 ml of dextran in saline intravenously in a 1-hour period. With fractions of 34,000 molecular weight there was no bleeding time prolongation beyond the normal 3 to 4 min. With the 51,000 molecular weight fractions the bleeding time was 7 min, 1 hour after infusion in one of three subjects. With infusion of the 90,000 molecular weight fraction, the bleeding time was 18 min after 12 hours in one of three subjects. With infusion of a dextran average molecular weight fraction of 135,900, the bleeding time was 8.5 min in one of three subjects. With infusion of a molecular weight fraction of 194,900, the bleeding time was prolonged for 48 hours in all three subjects, two of whom bled seriously. With Commercial Cutter dextran the bleeding time was not prolonged in any of five subjects. The average molecular weight of this dextran was 80,000. Bleeding time prolongation was not associated with thrombocytopenia. It would appear from these studies that bleeding time prolongation is much more likely to occur with large molecular weight fractions of dextran.

Carbone and associates (20) gave 1000 to 1500 ml of dextran daily intravenously to each of 11 patients until their bleeding times exceeded 11 min. The amount required was from 1500 to 6500 ml. The bleeding time exceeded 30 min in 7 subjects. The bleeding time was maximal 9 to 12 hours after infusion and returned to normal in 24 hours with one exception. The prothrombin activity declined to 50 to 75% of normal. The clotting times were not abnormal. The platelet counts were not below 150,000 per mm^3, the normal being 200,000 to 300,000 per mm^3. Prothrombin consumption was normal and no antithrombin was demonstrated. Clot retraction was normal. The plasma fibrinogen decreased from 400 to 500 mg/100 ml to 200 to 300 mg/100 ml and returned to normal in 24 hours. Plasma fibrinogen was not significantly depressed when the bleeding time was maximal. Fifteen subjects received 500 ml of dextran and showed an increase of bleeding time in two from the normal of 3 to 4 min to 8 and 9 min. Fifty subjects received a single infusion of 1000 ml of dextran. Fourteen of the 50 developed a bleeding time greater than 10 min within 9 hours. This study suggested that the prolongation was not due to lowering of prothrombin which should be below 10% in order to affect the bleeding time. The changes were thought to be unrelated to increase of blood volume since the changes were minimal when the blood volume was maximal. The authors comment that hemostatic problems were not reported in 2000 battle casualties receiving 4000 units of dextran. Horvath and associates (51) gave to rabbits and dogs 40 ml/kg body weight of Plavolex (6% dextran) or Expandex (6% dextran) or 6% gelatin or 2.5% gelatin, or 5% human serum albumin. The bleeding time was not prolonged with human albumin or modified fluid gelatin (Knox). The other substances prolonged

bleeding times in varying degrees without consistency as to duration or onset of the hemostatic defect. The data suggest that macromolecules, per se, are not the basic factor involved. Seegers and associates (92) show that dextran in vivo, in concentrations likely to be produced by infusion, interfered with the conversion of prothrombin to a derivative by inhibition of threone. They showed significant inhibition at concentrations of 1.68 mg of dextran ml. Inhibition was pronounced at 5 mg/ml and maximum at 10 mg/ml. In the study made by these authors small molecular weight dextran, 91,700, inhibited thrombin production more than equal concentrations of a large fraction average molecular weight, 194,900. Thrombin reverses the dextran inhibition of threone.

Weil & Webster (111) found that dextran of unstated type produced fibrinogen precipitation in fresh plasma when the dextran to plasma ratio was 2:1 or more. Platelets were also decreased in blood when the ratio of dextran to blood was 2:1 or more. The clotting time was prolonged when the dextran to blood ratio was 2:1 or more. In their study of patients receiving 500 to 1000 ml of dextran for operating room blood loss, none were found to have prolonged bleeding time. They concluded that dextran was safe if the volume infused was limited to 1000 ml.

Jacobaeus (59) made an extensive study and review of the effects of dextran on hemostasis. He used Swedish Macrodex for his own studies. Decreases in prothrombin, proaccelerin, and proconvertin were proportional to hemodilution. No decrease in platelets was found at 24 and 96 hours after infusions of 500 to 2000 ml of dextran. Prothrombin consumption was reduced and delayed. There was a tendency to delayed clot retraction. Dextran had no influence on the activation of proconvertin or the interaction between proconvertin and thromboplastin. Dextran inhibited platelet activity, possibly due to an inactivation of platelet factor 3. The authors thought the delay and reduction of prothrombin consumption with dextran was an important factor in the bleeding tendency. They suggested that a molecular weight of dextran between 60,000 to 80,000 might be least likely to cause trouble. The prothrombin consumption was actually increased in the presence of low molecular weight dextran (27,000). With 41,000 molecular weight dextran the prothrombin consumption was the same as with a saline diluent. With 83,000 molecular weight dextran, prothrombin consumption was reduced. Langdell and associates (66) studied the effects of dextran infusions upon the bleeding time in 22 women and 235 men. The dextrans used were 6% solutions; some were of British and some were of American manufacture. In 42% of the subjects the infusion of 1 liter of 6% dextran measurably prolonged the bleeding time. In 8% of the subjects, the bleeding time after infusion exceeded 30 min. The effect was maximum at 3 to 9 hours after the infusion. It was not accounted for by any demonstrable dilution or reduction of fibrinogen or thrombocytes. Comparison of the dextran preparations showed that those with the highest molecular weight had the most marked effects in prolonging the bleeding time. Of 38 subjects receiving dextran in the molecular weight range of around 50,000 only 13% had bleeding times greater than 15 min. Of 52 subjects receiving dextran of molecular weight greater than 100,000, 22% had bleeding times greater than 15 min. Albumin solution was infused into 40 subjects. Of these, one had a bleeding time of 11 min. All others had a bleeding time of less than 10 min. The albumin used was 1000 ml of 5% solution in sodium chloride. One liter of 3.5% PVP was infused into 51 subjects. Of these, 7 developed a bleeding time of greater than 10 min and 2 a bleeding time greater than 15 min. The authors attempted to correlate the bleeding prolongation with the plasma volume expansion using chromium-51 tagged red cells. The initial increase in blood volume was approximately 1000 ml after dextran. By 9 hours the blood volume had returned to about the control level. There seemed to be no correlation between the prolongation of the bleeding time and the increase of blood volume. Forty per cent of the bleeding times greater than 10 min occurred at 3, 6, or 9 hours when the blood volume was increased by only 500 ml or less. Two dogs bled 350 ml and immediately infused with equal volume of dextran solution showed a prolongation of bleeding time from an original of 1 min to 9 min after dextran. Reinfusion of the dog's own blood into him several days later did not produce any change in bleeding time although the animal was temporarily hypervolemic. The authors concluded that moderate hypervolemia, per se, does not alter the bleeding time. Platelet counts were done simultaneously with bleeding time determinations in 12 subjects who received 1000 ml of dextran. Platelet counts done prior to the infusion were in the range of 160,000 to 280,000 mm^3. In all subjects the platelet count was decreased after the infusion, but the decline was predictable on the basis of dilution by the amount of fluid given. There was no direct correlation between bleeding time and platelet counts. The mechanism of the dextran inhibition of hemostasis was not clear, but was believed to be due to an inhibition of

platelet function. The authors considered that dextran infusions were contraindicated in patients with known bleeding tendency or to whom large transfusions of whole blood had been given, or those in whom surgery was contemplated. In summary, it appears that dextran is most likely of the plasma expanders studied to cause prolongation of the bleeding time following intravenous infusion. Polyvinylpyrrolidone is the next most likely agent to cause this hemostatic defect. Gelatin and albumin are relatively innocuous in this regard.

Blood Constituents

A number of authors have studied the effect of the plasma volume expanders upon the constituents of the blood. Handford and associates (45) infused 4% glycerol pectate in amounts equivalent to 5% of body weight in normal dogs. These workers found changes in plasma protein levels which were entirely due to dilution. Increase of the erythrocyte sedimentation rate was seen in human subjects infused with pectin. Carbone and associates (21) gave patients infusions of 1000 ml 6% dextran in saline daily for 4 to 15 days. A fall in serum protein, hematocrit, zinc turbidity, and in serum cholinesterase occurred. Serum globulin decreased more than the serum albumin in all subjects, including those with liver disease. The authors thought that not all of the fall in the protein was due to hemodilution. They believed that the decrease in serum cholinesterase suggested decreased albumin synthesis. Jaenike & Waterhouse (61) gave daily infusions of 6% dextran in physiological saline to five patients at the rate of 1000 to 2000 ml/day for 2 to 10 days. The hematocrits fell in all subjects and were still decreased in four subjects observed 40 days later. The serum protein fell in all subjects during the period of dextran administration, and in four it rose above control level 13 to 23 days after dextran. Jackson & Frayser (58) gave dogs 1 g of acacia per kg body weight intravenously daily for 20 days. The total plasma proteins decreased more than would be expected from a dilution effect alone. The plasma volume returned to normal in 7 days, but the serum proteins were low for many weeks. Immediately after acacia the plasma albumins were often below 2 g/100 ml. The plasma cholesterol also decreased and then increased as the proteins increased. The platelets fell in some instances. Hematocrits and hemoglobins fell strikingly and then rose *pari passu* with the serum proteins. They concluded that the body compensates for acacia infusion by storing or destroying plasma proteins which are then slowly regenerated. Globulin and fibrinogen were decreased as well as albumin. The total osmotic pressure was actually lowered during the period when plasma acacia and proteins were both decreased. Metcalf & Rousselot (74) gave 500 ml of 6% dextran in saline to 12 convalescent patients. There was no essential change in serum proteins or chloride, sodium, or potassium levels in the serum. Fowler and associates (31) studied the serum electrolytes in dogs bled 80 ml/kg with simultaneous partial blood volume replacement by 60 ml/kg body weight of 6% dextran in 5% dextrose. These animals showed a decrease of serum sodium from a control level of approximately 150 meq/liter to approximately 115 meq/liter at 5 min. The serum sodium slowly returned toward normal over a period of 24 hours. Serum potassium levels were only slightly decreased, but serum calcium levels were decreased from an average of 10 mg/100 ml blood to an average of 5.7 mg/100 ml and were still below normal at 48 hours. Serum chloride decreased from 114 meq/liter to 87 meq/liter at 5 min, with a return toward normal in about 2 hours. Hardwicke and associates (46) showed that infusions of 700,000, 220,000, and 124,000 molecular weight dextran increased the erythrocyte sedimentation rate in proportion to their concentration. The increase in sedimentation rate was greater for a given concentration with higher molecular weight dextran. Roche and co-workers (89) showed that 500 ml of 6% dextran intravenously did not interfere with typing, crossmatching, or Rh determination of blood. Five hundred to 1500 ml of dextran given to patients in shock also did not interfere with these determinations. Thrower & Campbell (104) showed that the erythrocyte sedimentation rate increased with infusions of 500 to 1500 ml of 3.5% PVP given to four subjects. There was no evidence of hemolysis and the blood grouping reactions were not disturbed. Christie and associates (22) gave dogs 4.5 g/kg body weight of 15% acacia in distilled water, showing that there was a decrease in hemoglobin and hematocrit with an increase in sedimentation rate. The oxygen content of the arterial blood fell out of proportion to the fall in hemoglobin. Jacobson & Smyth (60) used 5% osseous gelatin in isotonic saline (Upjohn). They gave 56 injections of 450 to 1000 ml to 45 subjects. Fifty others received gelatin for shock. The erythrocyte sedimentation rate increased in 12 subjects studied. Greenman and associates (42) gave 8 patients 375 to 1000 ml of 12% sodium-free dextran in 88 to 350 min. Five of these subjects were edematous,

4 having the nephrotic stage of chronic glomerulonephritis. Serum albumin and globulin fell in proportion to increased plasma volume. There were no changes in absolute amounts of chloride, sodium, potassium, or nitrogen excretion. There were no essential changes of serum bicarbonate, chloride, sodium, or potassium.

Hueper and associates (56) gave intravenous or intraperitoneal polyvinyl alcohol to dogs or rabbits. This produced prolonged clotting time and increased the erythrocyte sedimentation rate; there was also anemia lasting up to 77 days. The anemia occurred immediately and was attributed to the retention of red cells in lung capillaries, spleen, and lymph node sinusoids with later destruction plus hydremia. Prolonged clotting time was attributed to mechanical interference with the fibrin network. Platelets fell and fibrinogen decreased in some instances.

Semple (93) bled each of 10 dogs 45% of its blood volume and replaced the blood removed with 5.7% dextran in 0.9% saline (Connaught Laboratories). The changes in the albumin and globulin were due to dilution only, but fibrinogen fell more than simple dilution would explain. No evidence was found that dextran retarded protein restoration. Leusen & Essex (67) gave to rabbits 1 ml/kg of 6% dextran. There was clumping of leukocytes in the vessels seen by ear chamber, with an initial decrease in white count. The white count then exceeded the control at 105 min. By 175 min leukocytosis occurred with a predominance of polymorphonuclear leukocytes. During the original leukopenia the polymorphonuclear leukocytes decreased strikingly with a relative increase in mononuclear cells. The same effects were seen during leukocytosis of infection. One ml/kg body weight of 6% acacia had much less leukopenic effect in rabbits. A second injection of dextran 24 hours later had little effect on white blood cell count or on clumping.

Hepatic Function

The effect of plasma expanders upon hepatic function has been studied by several authors. Reinhold and associates (88) studied patients who received 1 liter of 6% Commercial Solvents Corporation dextran or 1 liter of 3.5% PVP intravenously. Some received a second infusion the following day. The following liver function tests were performed: serum bilirubin, thymol turbidity, zinc turbidity, phenol turbidity and Bromsulphalein retention, and cephalin flocculation test. These tests showed little change after either dextran or PVP. Scott & Howard (91) studied the hepatic function of wounded patients following resuscitation with plasma expanders. Hepatic function was studied by means of plasma bilirubin, Bromsulphalein retention, urine urobilinogen, cephalin flocculation, and thymol turbidity in nine patients resuscitated with dextran and modified 3% gelatin. As compared to casualties receiving bank blood, no evidence of hepatic functional impairment was found. Reinhold and associates (88) studied 23 patients who received 1, 2, or 6 liter infusions of dextran; 15 additional patients received 1 or 2 liters of polyvinylpyrrolidone intravenously. There were no significant changes in serum bilirubin, cephalin flocculation, zinc sulphate turbidity or Bromsulphalein retention, thymol turbidity or flocculation, urine urobilinogen, urine coproporphyrin, or serum globulin.

Renal Function

Also of interest has been the effect of plasma substitutes upon renal function. Raisz (86) gave dogs 20 ml/kg body weight of either Expandex (Commercial Solvents Corporation dextran, mol wt average 40,000) or of 5% oxypolygelatin (Don Baxter, Inc., average mol wt 20,000). There was an increase of glomerular filtration rate, effective renal plasma flow, and in excretion of sodium, potassium, and water. The effects were similar with dextran, oxypolygelatin, saline, and albumin, except that albumin increased renal plasma flow the most and saline the least. Greenman and associates (42) studied the effect of the infusion of 375 to 1000 ml of 12% sodium-free dextran in eight patients, five of whom were edematous, four having the nephrotic state of chronic glomerulonephritis. Seven of the eight subjects developed increased urinary flow. There were no changes in the absolute amounts of chloride, sodium, potassium, or nitrogen excreted. In edematous patients there was usually a negative water balance by the end of diuresis. The infusions were well tolerated, except in one patient with congestive heart failure who became dyspneic, and the infusion was therefore discontinued. The authors concluded that dextran was useful in the edema associated with hypoproteinemia. Stamler and co-workers (95) injected 200 ml of 6% dextran in water in 1 to 2 min in dogs infused with Ringer's solution. In some experiments there was a sustained increase of water, sodium, and total solute diuresis. The glomerular filtration rate was unchanged. Renal plasma flow was increased; venous pressure rose and hematocrits fell.

Plasma sodium and total solute concentration tended to decline slightly. James and associates (62) gave 12% dextran (Commercial Solvents Corporation) to 16 children with the nephrotic syndrome. The patients received 300 to 400 ml/m² of body surface area daily or on alternate days. All save one lost weight. A decrease of serum sodium and potassium was seen. There was a decrease of total serum osmolarity. Water, sodium and chloride diuresis were produced. Glomerular filtration rate increased significantly in two of four instances. Renal plasma flow (CPAH) increased markedly in all seven instances where determined. Michie and associates (77) gave six patients 1000 ml of 3% modified fluid gelatin (Knox) daily intravenously for 6 days. There were no important variations in glomerular filtration rate or renal plasma flow. The Tm PAH was increased in two and unchanged in four. Michie & Ragni (76) gave human subjects 1000 ml of 6% dextran intravenously daily for 6 days. Renal function studies were made before and 4 days after the last infusion. The maximal tubular excretion of para-aminohippurate was significantly depressed in 2 of 5 patients with normal kidneys and in 3 of 4 patients with pre-existing renal disease. Fleming and associates (29) studied 13 patients who received from 500 to 1500 ml of 6 per cent dextran intravenously. There were no marked changes in glomerular filtration rate, tubular excretory mass, or in para-aminohippurate clearance. Gowdey & Young (38) infused 6% dextran in normal saline intravenously at a rate of 1 ml per kg per min into dogs. Progressive decreases of glomerular filtration rate and renal blood flow were produced by the infusion. The ratio of renal blood flow to cardiac output fell consistently and was as low as 50% of control. The dextran infusion invariably caused a diuresis, but when cardiac failure occurred there was a marked decrease in urine flow and occasionally anuria. The authors believed that hypoxia produced by dextran-induced anemia caused renal vasoconstriction, thus producing a redistribution of blood to other vascular beds.

Hemodynamic Effects

The hemodynamic effects produced by dextran infusions in normovolemic and oligemic man and animals have been of great interest. Witham and associates (116) gave 500 ml of 6% dextran intravenously to five human subjects at a rate of 25 ml/min. Ten minutes after the infusion the subjects were found to have an average increase in cardiac output of 38% and comparable increase of stroke volume, but little change in heart rate. The mean pulmonary arterial pressure rose an average of 6 mm Hg. Pulmonary wedge pressure rose in two subjects in whom it was measured. Systemic venous pressure rose in two subjects where it was measured. Hematocrits fell in each instance. Two subjects studied showed no change in vital capacity. The venous pressure rose less than the pulmonary arterial pressure. Fleming & Bloom (30) made further studies of the hemodynamic effects of dextran infusion in normal human subjects. Sixteen patients received 1000 to 1500 ml of 6% or 12% dextran intravenously at a rate of 25 ml/min. The cardiac output increased in 13 of the 16; in 10 subjects the increase averaged 44%; in the other 3 the increases were small. There was no correlation between right atrial or pulmonary arterial pressure rise and the increase of cardiac output. The highest peripheral venous pressure increase was associated with no change in cardiac output. The pulmonary arterial pressure increased in all 8 subjects where measured, the mean increase being 11.5 mm Hg. The right atrial pressure increased in all 10 subjects studied and remained elevated in 8 of the 10 during the study period of 22 to 120 min. The pulmonary wedge pressure increased between 7 and 15 mm Hg in 5 patients studied. Pulmonary vascular resistance did not change. The hematocrits fell, showing that plasma volume expansion occurred. Systemic blood pressure rose an average of 17 mm Hg. The pressures were still elevated at 1 hour. Systemic arterial pulse pressure increased an average of 8.3 mm Hg.

Werkö (113) infused dextran into 20 normal subjects and 25 patients with heart disease, 15 of whom had mitral stenosis. Dextran was given as a 6% solution at a rate of 25 ml/min; normal subjects received the infusion for 60 min; the subjects with heart disease were infused for 30 to 50 min. The infusion was interrupted if the pulmonary arterial pressure rose rapidly. Normal subjects showed at first progressive increase in blood volume with increases of right atrial mean pressure and pulmonary arterial mean pressure, but with constant cardiac output. With greater expansion of blood volume, average cardiac outputs and stroke outputs were increased 31% and 20% respectively. In 7 subjects, however, increases of right heart filling pressure of 4 to 12 mm Hg were associated with cardiac output changes of less than 15%. There was no consistent relationship between right heart filling pressure and stroke volume, cardiac output, or right ventricular stroke work. Similar changes were seen in the patients with heart disease, except that in

the patients with mitral valvular disease, the pressure in the pulmonary arteries increased more rapidly and more markedly than in the normal subjects for the same increase of plasma volume and right atrial pressure. As in normal subjects, a variable relation was found between right heart filling pressure and cardiac output, stroke volume, or right ventricular stroke work. With the expansion of the plasma volume cardiac output increased at times, but not always. Hemoglobin concentration in these studies was never below 10 g/100 ml of blood and thus anemia could not be expected to have affected the cardiac output.

Studies of hemodynamic effects of dextran infusion have also been made in animals. Gowdey & Young (38) infused 6% dextran at a rate of 1 ml per kg per min into dogs. In these animals increases of right atrial pressure and of cardiac output were observed; however, there was no consistent relationship between rise in right atrial pressure and increase of cardiac output. Usually the cardiac output continued to rise as the infusion progressed until a volume of dextran equivalent to about 10% of body weight had been given. With further infusion high output heart failure suddenly developed and the animal died within a few minutes. Heart failure was defined here as a state in which the increased cardiac output had begun to fall and continued to fall while right atrial pressure rose abruptly. During the early stages of infusion arterial oxygen transport was maintained, the increasing cardiac output compensating for the decreasing arterial oxygen content; however, when the hematocrit level had fallen below 20% the arterial oxygen transport was reduced; when cardiac failure occurred, oxygen transport was markedly reduced. Arteriovenous oxygen differences grew progressively smaller throughout the infusion. Systemic arterial blood pressure either did not change appreciably or rose with the infusion. The total peripheral resistance invariably decreased, often to 50% of control values, until the cardiac output ceased to rise and then the total peripheral resistance began to increase. The pulse rate showed no consistent response to infusion, but usually decreased with cardiac failure. Fowler and associates (32) studied the hemodynamic effects of dextran infusion in hypervolemic and normovolemic dogs. Eleven dogs were given three separate infusions of 6% dextran, totaling 8% of the body weight. Ten other dogs were bled 6% of body weight and the blood removed was replaced with 6% iso-oncotic dextran. Cardiac output increased significantly after infusions in both the bled (normovolemic) and unbled (hypervolemic) animals. Significant increase in cardiac output was seen when the hemoglobin was lowered to between 7.7 and 10 g%. Significant decrease in hematocrits was observed in both groups of dogs. Right atrial mean pressure showed no increase in bled dogs, but did show an increase in unbled dogs. Both groups of dogs showed significant increases in pulmonary arterial pressure. There was no positive association between right atrial mean pressure increase and increase of cardiac output. Cardiac output increased comparably with similar degrees of anemia in hypervolemic and normovolemic animals. In a further study, Fowler and associates (33) rendered 21 dogs hypervolemic without anemia either by the infusion of red cells suspended in dextran or by the infusion of fresh whole blood, each animal receiving a total infusion equivalent to 8% of body weight. The hypervolemic animals showed no increase in cardiac output and no striking changes in mean arterial blood pressure 20 min after the infusion, although outputs did increase during the infusion. Pulmonary arterial pressure rose moderately in both groups of dogs and right atrial pressure rose slightly. Ten animals which had received fresh whole blood equivalent to 8% of body weight were then bled 700 to 1000 ml with simultaneous replacement of the blood removed with an equal volume of 6% dextran. After bleeding and dextran infusion there was a slight rise in both pulmonary arterial and right atrial pressure, and striking increase in cardiac output. These studies suggested that the increase in cardiac output following dextran infusion was related to the anemia produced thereby and not to the expansion of whole blood volume or to the increase of cardiac filling pressure. No relationship between changes in stroke volume and right heart filling pressure was shown in these studies. In later studies Fowler and associates (31) studied the effect of dextran-induced anemia in hypovolemic dogs. Dogs were rendered hypovolemic by bleeding 20 ml/kg. Hypovolemic anemia then was produced by further bleeding of 60 ml/kg with simultaneous dextran volume replacement, the dextran used being 6% iso-oncotic dextran in normal saline. The mean blood volumes were decreased 15.5% during hypovolemic anemia. The mean of hematocrits was 48.4% in the control period and 16.2% in the anemic period. During hypovolemic anemia there was an increase of cardiac output, stroke volume and right ventricular stroke work, but no increase of right atrial transmural pressure. The rise in cardiac output during hypovolemic anemia above that of the hypovolemic period was due to increase in both stroke volume and in heart rate. The increase of cardiac output over control,

however, was due to an increase of heart rate, the stroke volume decreasing significantly. For this reason right ventricular stroke work during hypovolemic anemia was not significantly increased over the control period. The results suggested that the increase of right atrial transmural pressure was not an important mechanism for increasing cardiac output, stroke volume, or cardiac stroke work in these experiments.

The mechanism by which the cardiac output is increased with acute anemia produced by dextran infusion is still uncertain. Justus and co-workers (64) made dogs anemic by bleeding and dextran infusion. Transfusion of blood from these anemic dogs into other dogs without producing anemia in the recipient animals was associated with increased cardiac output in the recipient dogs. These observations suggested that a humoral substance may be important in mediating the increase of cardiac output associated with acute anemia.

PHYSIOLOGIC EFFECTS OF COLLOIDAL INFUSION IN OLIGEMIC ANIMALS

We should now like to consider the effect of plasma substitutes in animals made hypovolemic by bleeding. Wasserman & Mayerson (108) lowered the blood pressure of dogs to 40 mm Hg by bleeding. Four hours after the infusion of 6% clinical dextran, there was an expansion of plasma volume, as measured by I^{131} human serum albumin, equivalent to 80% of the infused volume. In unbled dogs the plasma volume was expanded only 25% of the infused volume at this time. Dextran levels in thoracic duct lymph remained below plasma dextran levels. The dextran plasma-lymph concentration gradient remained for at least 24 hours and was higher than that for albumin and globulin. It was suggested that dextran leaked into interstitial fluid more slowly than plasma protein and was therefore a good plasma expander. Parkins and associates (84) bled dogs and then reinfused them with dextran, oxypolygelatin, modified fluid gelatin, or saline. In one test procedure where reinfusion was immediate there was no significant difference in the three colloids. All were slightly less effective than heparinized blood and more effective than saline. When hypotension was prolonged for 1 hour, modified fluid gelatin was almost as effective as blood. Dextran and oxypolygelatin were less effective, but were still considerably more so than saline. Padhi and co-workers (83) bled dogs up to 35% of their total blood volume and replaced the blood which had been removed with dextran in equal volume. Blood pressure and pulse rate responded equally well to blood or dextran; however, all the animals replaced with dextran showed a tendency to bleed, and three of six died the following day. Waud (110) bled dogs to a blood pressure level of 50 mm Hg and then transfused them with an equal volume of 6% dextran (Intradex) (average mol wt 75,000). Blood pyruvate and lactate rose after bleeding and then fell with dextran. Blood sugar remained unchanged. The blood pressure returned to near normal with dextran. Heart and respiratory rates, which rose following bleeding, fell with dextran. Following dextran, there was a fall in hematocrit, in the red blood cell count and white blood cell count, and in rectal temperature, with a rise in the sedimentation rate of erythrocytes. Twenty dogs given dextran all lived; 8 not infused with dextran died. Morrison and associates (78) compared the effects of various replacement agents in bled rats, guinea pigs, and dogs. After bleeding rats 3.5 ml/100 g body weight, none survived without infusion; with isotonic saline replacement, 10% survived; with dextran, 70% survived; with 3.5% PVP, 80% survived; with 5% bovine osseous gelatin, 80% survived; with serum albumin, 90% survived; with heparinized rat blood, 100% survived. In guinea pigs that were bled followed by blood volume replacement with plasma expanders, none survived with saline infusion; 50% survived with dextran; with 3.5% PVP, 60% survived; with 5% bovine osseous gelatin, 80% survived; with serum albumin or heparinized guinea pig blood, all survived. In dogs, dextran was more efficient than other substitutes and approximately as effective as human plasma. Bollman and associates (16) studied the effects of various plasma substitutes as plasma volume expanders in rabbits who were bled 20 ml/kg of body weight, reducing the blood volume to 60% of control. Dextran of 24,000 molecular weight did not maintain blood volume better than saline; however, dextran of molecular weight 120,000 maintained blood volume with but slight fall during a 24-hour period. Without bleeding 20 ml/kg body weight of dextran increased the blood volume to 120% in 30 min and at 6 hours; the blood volume returned to control levels at 24 hours. Five per cent PVP in volume equal to the blood removed in bled rabbits maintained the blood volume at 95% of the original for 24 hours. Two and a half per cent and 3.5% PVP maintained the blood volume at about 85% of control. Three to 8% gelatin in saline maintained the blood volume at 85 to 90% for 6 hours with a decline to 70 to 75% at 24 hours. Nine per cent acacia in saline

maintained the blood volume at 90% at 24 hours. Six per cent acacia produced the same effect. Three per cent acacia maintained the blood volume at 85% of control at 24 hours. Handford and associates (45) bled dogs a volume of blood equivalent to 5% of body weight and then infused an equal volume of pectin as 4% glycerol pectate. The blood pressure returned to control levels and was maintained, but fell slowly over a 24-hour period. The plasma volume was expanded and remained expanded for 12 hours. Taylor & Waters (102) showed that 7% isinglass in 0.9% saline was capable of restoring blood pressure in bled animals and permitted an increased percentage of recovery from otherwise fatal bleeding in dogs. Ivy and associates (57) found only a slight improvement in death rate of bled dogs when the volume of blood removed was replaced with 5% gelatin instead of normal saline.

CLINICAL USES AND EFFECTS OF PLASMA SUBSTITUTES

We should now like to consider the effects of plasma substitutes in human subjects suffering from various types of shock. Bayliss (8) used 3% or 6% gum arabic in saline in wound shock. His patients appeared to respond well to this. Those who did not respond also failed to respond to subsequent blood infusions. Bayliss stated that one must use a colloid to maintain blood volume. Gelatin was said to be objectionable because it may contain tetanus spores and may cause intravascular clotting. He found no evidence of hemolysis, red cell agglutination, or increased blood viscosity with gum arabic. Gum arabic in amounts equal to half the whole blood volume was stated to be innocuous. Figueroa & Lavieri (28) used 1% grapefruit pectin in dogs shocked by intestinal massage and found that the onset of shock was delayed as compared to saline-treated controls. Five patients received 350 to 1000 ml of 0.75% pectin. The blood pressure rose if low, but there was no immediate or delayed reaction. The blood volume at 4 hours was increased to a degree comparable to the amount infused. After 20 hours the blood volume was still slightly increased. Jacobson & Smyth (60) used 5% osseous gelatin in isotonic sodium chloride (Upjohn). Fifty injections were given to patients in shock. The response in shock was satisfactory and no sensitivity was seen when the injections were repeated. In three patients, in whom postmortems were performed, no tissue changes were seen. No reactions or urinary changes were seen. Blood amino acids did not change and the authors thought that gelatin was probably not metabolized. Popper and associates (85) used 5% gelatin, average molecular weight 35,000, in saline and dextrose, and used pectin in saline with a molecular weight of 45,000 to 60,000 in their studies. Both substances produced hemodilution, which was more pronounced in shock patients. One liter of gelatin lowered the hematocrit an average of 11.6% in controls and 19.5% in shock patients. Pectin lowered the hematocrit an average of 10.3% in controls and 18.8% in shock patients. Both increased the sedimentation rate of erythrocytes. The authors concluded that the hemodynamic effects of the two substances were similar, but tissue changes after pectin caused them to prefer gelatin. Strumia and associates (99) treated 15 patients with shock with modified globin, average molecular weight 34,000, in 0.85% saline. All patients treated responded satisfactorily. Artz and associates (6) gave 4000 units of dextran to 2000 battle casualties. No urticaria, bronchospasm, vasomotor instability, or untoward bleeding was observed. The dextran employed was made by Commercial Solvents Corporation, and was of average molecular weight 43,000 to 48,000. Early effective resuscitation was accomplished when blood loss was 20 to 30% of estimated blood volume. Blood was usually required in addition if the loss was equal to 35% of blood volume. These authors stated that 25% depression of hematocrit by dextran seemed to be the lower limit of safety. Freezing did not impair the effectiveness of dextran. Also, modified fluid gelatin was used in 200 units of 500 ml each. The gelatin had an average molecular weight of 34,000. As much as 3000 ml of gelatin were received by some wounded soldiers. The circulation was supported for the period of evacuation, which was 3.5 hours, and no toxicity was observed. In some patients 2000 ml of dextran was given before and during wound debridement. The authors felt that blood should be added if over 1500 ml of plasma expander was required. Ohlke & Scales (82) used dextran in 56 surgical cases, and PVP (3.5% Subtosan) in 60 surgical cases. None of these had reactions, and the majority had a good blood pressure response. These writers found that the blood pressure rose to expected levels if low, or did not fall when the expanders were given prophylactically. Weil & Webster (112) used dextran and Subtosan PVP in patients with blood loss. These agents were able to maintain or restore blood pressure in instances where blood loss did not exceed 1000 ml. No allergic or pyrogenic or other reactions were seen. No remote complications were seen, and there was no

interference with blood typing or crossmatching. The authors stated that the advantages of these plasma substitutes were that there was no Rh factor sensitization, no hepatitis, and no reaction due to hemolysis or contaminated blood. Bloom (12) (115) treated with dextran 52 patients in shock. There was no difficulty in blood typing, crossmatching, or Rh determinations in 27 patients with dextran blood levels ranging from 421 to 3000 mg/100 ml. Sedimentation rates were increased in relation to dextran blood level, returning to normal when blood dextran level fell. There was no proteinuria, or abnormal urinary sediment, and the blood NPN did not change. After 500 ml of 6% dextran, the mean plasma level was 726 mg/100 ml, falling slowly to a mean of 88 mg at 96 hours. Jenkins and associates (63) used PVP for hypotension in 24 patients. The amount used was 500 to 1000 ml which was usually given in 20 to 120 min. Twenty of 24 patients showed a satisfactory response—a sustained rise in blood pressure if no longer bleeding, or a steady blood pressure if still bleeding. Twelve of the 24 patients did not require blood after PVP. One patient who received 500 ml PVP in 15 min developed pulmonary edema. Arden and associates (5) gave 3.8% PVP to 37 patients in shock. The blood pressure effects were favorable and there were no untoward reactions. Cordice and associates (23) used PVP Macrose (3.5% PVP in Ringer's solution) as an emergency treatment of 38 cases of traumatic and hemorrhagic shock due to head injury, fractures, and penetrating wounds of the chest and abdomen. Some of these patients required blood and plasma later. In all instances there was good clinical response with rise of blood pressure, slowing of pulse, rise of pulse pressure, improvement of vital signs, decrease of hematocrit, and plasma proteins. No sensitivity or toxicity was seen. No interference with blood typing or coagulability occurred. The volumes used were 500 to 2500 ml.

Plasma substitutes have also been employed in the treatment of edema associated with nephrosis. Dick and associates (26) treated four children with nephrosis by means of intravenous acacia. One patient showed at first some loss of edema but later failed to respond. In a second case at first marked edema reduction occurred. Two other cases showed similar temporary improvement, with fall in serum proteins and hepatic enlargement accompanying the acacia infusion. Autopsy findings in one patient showed acacia in the liver, spleen, kidneys, lungs, lymph nodes, and bone marrow; the liver containing 3.9% acacia, the plasma 2.1%, pericardial fluid 0.6%, peritoneal fluid 1.1%, and bile 2%. The authors concluded that acacia in the treatment of nephrosis was not of value and was associated with undesirable results. Greenman and associates (42) treated eight patients with 375 to 1000 ml of 12% sodium-free dextran given over a period of 88 to 350 min. Five of these patients were edematous, four with the nephrotic stage of chronic glomerulonephritis. After the dextran infusion, the plasma volume increased 34 to 67% and was still elevated at 20 to 24 hours, although it began to fall at 3 hours. The serum albumin and globulin fell in proportion to the increased plasma volume. Seven of the eight patients had increased urinary flow, but no change in the absolute amounts of chloride, sodium, potassium, or nitrogen excreted. In edematous patients there was usually a negative water balance by the end of the diuresis. The infusions were well tolerated except in one patient with congestive heart failure who became dyspneic, and the infusion was discontinued. The authors concluded that dextran is useful in the edema associated with hypoproteinemia. James and co-workers (62) gave 12% dextran (Commercial Solvents Corporation) in water to 16 children with the nephrotic syndrome. The children received 300 to 400 ml per m^2 daily or on alternate days. All save one lost weight. Three or more daily infusions in 13 children produced significant loss of edema in 9 and virtually complete diuresis in 6. The edema recurred rapidly in all subjects; the maximum period of remission was 1 month. The infusions increased plasma volume 25 to 50%. There was a decrease of serum sodium and potassium, and a decrease of total serum osmolarity. Water, sodium, and chloride diuresis was produced.

SUMMARY

Plasma substitutes are of potential importance in the treatment of shock under circumstances where adequate supplies of blood or plasma are not available, such as in remote areas or in casualties involving a large segment of the population. The plasma expanders are also useful tools for the study of the physiologic effect of anemia and of hypervolemia. The substances discussed in this chapter: gum arabic (acacia), gelatin, pectin, polyvinyl alcohol, polyvinylpyrrolidone, and dextran are each capable of producing expansion of plasma volume with attendant decline in hematocrit and plasma proteins, and increase of the red cell sedimentation rate, and of increasing the blood pressure in animals or patients

in shock. The fall in hematocrit and plasma proteins appears to be due principally to hemodilution and not to destruction or impairment of synthesis. However, the prolonged tissue and organ retention of such substances as acacia and PVP militate against their use in human subjects. Dextran, although fairly rapidly excreted and metabolized, suffers from one serious handicap, namely, its tendency to impair hemostasis. This is manifested by a prolongation of the bleeding time, which appears to be related more to an impairment of platelet function than to hemodilution or hypervolemia. Thus one hesitates to use dextran in large amounts or in patients suffering from a hemorrhagic defect. Gelatin appears to produce less prolongation of the bleeding time than dextran, and may, upon further study, prove superior in this respect. Dextran, PVP, and gelatin did not alter hepatic function in acute studies. In clinical usage, dextran and gelatin were found to have no deleterious effects upon renal function or urine composition. Although the plasma expanders are potentially antigenic, this does not seem to be a serious contraindication to their clinical or experimental use.

Hemodynamic studies of dextran-infused human subjects and animals have demonstrated that in some instances right atrial pressure and blood volume may be increased without increase of cardiac stroke output. When anemia is produced by dextran infusion in bled dogs, cardiac stroke work may be increased without elevation of right atrial transmural pressure.

REFERENCES

1. Adelson, E., W. H. Crosby, and W. H. Roeder. Further studies of a hemostatic defect caused by intravenous dextran. *J. Lab. & Clin. Med.* 45: 441–448, 1955.
2. Allen, R. Z., and E. A. Kabat. Studies on the capacity of some polysaccharides to elicit antibody formation in man. *J. Exper. Med.* 105: 383–393, 1957.
3. Altemeier, W. A., L. Schiff, E. A. Gall, J. Guiseffi, D. Hamilton, D. Freiman, and H. Braunstein. Long-term studies on the effect of polyvinylpyrollidone retention in human patients. *Surg. Forum.* 4: 724–730, 1953.
4. Anoersch, M., and R. B. Gibson. Studies on the effects of intravenous injections of colloids. I. Deposition of acacia in the liver and other organs and its excretion in urine and bile. *J. Pharmacol. & Exper. Therap.* 52: 390–407, 1934.
5. Arden, G. P., G. A. Mandow, and F. J. R. Stoneham. Plasmosan in the prevention and treatment of shock. *Lancet* 1: 1099–1100, 1951.
6. Artz, C. P., J. M. Howard, and J. P. Frawley. Clinical observations on the use of dextran and modified fluid gelatin in combat casualties. *Surgery* 37: 612–621, 1955.
7. Barker, H. G., J. D. Elder, J. M. Walker, and H. M. Vars. The retention of certain plasma volume expanders within the circulation of human subjects following a 1000 cubic centimeter hemorrhage. A preliminary report. *Surgery* 32: 299–304, 1952.
8. Bayliss, W. M. Intravenous injection in wound shock. *Brit. M. J.* 1, 553, 1918.
9. Behrmann, V. G., and F. W. Hartman. Factors altering capillary resistance after macromolecular infusions. *Fed. Proc.* 15: 14, 1956.
10. Bennett, I. L. Production of fever and the Schwartzman phenomenon by native dextran. *Proc. Soc. Exper. Biol. & Med.* 81: 248–250, 1952.
11. Bloom, W. L. Disposition of dextran following intravenous injection. *J. Lab. & Clin. Med.* 47: 938–949, 1956.
12. Bloom, W. L. Present status of plasma volume expanders in the treatment of shock. *A.M.A. Arch. Surg.* 63: 739, 1951.
13. Bloom, W. L., and A. E. Wilhelmi. Dextran as a source of liver glycogen and blood reducing substance. *Proc. Soc. Exper. Biol. & Med.* 81: 501–503, 1952.
14. Bloom, W. L., and M. L. Willcox. Determination of dextran in blood and urine. *Proc. Soc. Exper. Biol. & Med.* 76: 3, 1951.
15. Bollman, J. L. Discussion. Symposium on plasma volume expanders in the treatment of shock. *A.M.A, Arch. Surg.* 63: 749, 1951.
16. Bollman, J. L., R. C. Knutson, and J. S. Luncy. Volemic substances for replacement of blood. *A.M.A. Arch. Surg.* 63: 718–727, 1951.
17. Bowman, H. W. Clinical evaluation of dextran as a plasma volume expander. *J.A.M.A.* 153: 24–26, 1953.
18. Bryan, G. C., and J. Scudder. Dextran and pneumococcus polysaccharide cross-reactivity in skin tests and serum precipitin tests. *Ann. New York Acad. Sc.* 55: 477–478, 1952.
19. Bryant, E. F., G. H. Palmer, and G. H. Joseph. Nonaccumulation of pectin intravenously injected into rabbits. *Proc. Soc. Exper. Biol. & Med.* 49: 279–282, 1942.
20. Carbone, J. V., F. W. Furth, R. Scott, and W. H. Crosby. An hemostatic defect associated with dextran infusion. *Proc. Soc. Exper. Biol. & Med.* 85: 101, 1954.
21. Carbone, J. V., L. L., Uzman, and I. C. Plough. Changes in serum proteins produced by infusions of dextran. *Proc. Soc. Exper. Biol. & Med.* 90: 68–70, 1955.
22. Christie, A., N. M. Phatak, and M. B. Olney. Effect of intravenous acacia on physio-chemical properties of the blood. *Proc. Soc. Exper. Biol. & Med.* 32: 670–672, 1934–35.
23. Cordice, J. W. V., J. E. Suess, and J. Scudder. Polyvinylpyrrolidone in acute traumatic and hemorrhagic shock. *Surg. Gynec. & Obst.* 97: 361, 1953.

24. Czerny, A. Versuche uber bluteindickung und ihre folgen. *Arch. exp. Pathol. u Pharmakol.* 34: 268–280, 1894.
25. Davidsohn, I., and K. Stern. Disturbance of hemostasis in rabbits treated with polyvinylpyrrolidone (PVP). *J. Mt. Sinai Hospital New York* 24: 777–792, 1957.
26. Dick, M. W., E. Warweg, and M. Andersch. Acacia in the treatment of nephrosis. *J.A.M.A.* 105: 654–657, 1935.
27. Engstrand, L., and B. Aberg. Excretion of intravenously administered dextran. *Lancet* 1: 1071–1073, 1950.
28. Figueroa, L., and F. J. Lavieri. The use of pectin and other agents to prevent shock. *Surg. Gynec. & Obst.* 78: 600–605, 1944.
29. Fleming, J. W., W. H. Cargill, and W. L. Bloom. Effects of intravenous administration of dextran on renal function. *Proc. Soc. Exper. Biol. & Med.* 79: 604–606, 1952.
30. Fleming, J. W., and W. L. Bloom. Further observations on the hemodynamic effect of plasma volume expansion by dextran. *J. Clin. Invest.* 36: 1233, 1957.
31. Fowler, N. O., R. Shabetai, D. Anderson, and J. R. Braunstein. Some circulatory effects of experimental hypovolemic anemia. *Am. Heart J.* 60:551–561, 1960.
32. Fowler, N. O., R. H. Franch, and W. L. Bloom. Hemodynamic effects of anemia with and without plasma volume expansion. *Circulation Res.* 4: 319, 1956.
33. Fowler, N. O., W. L. Bloom, and J. A. Ward. Hemodynamic effects of hypervolemia with and without anemia. *Circulation Res.* 6: 163, 1958.
34. Frawley, J. P., C. P. Artz, and J. M. Howard. Plasma retention and urinary excretion of dextran and modified fluid gelatin in combat casualties. *Surgery* 37: 384–391, 1955.
35. Frommer, J. The pathogenesis of reticulo-endothelial foam cells. Effect of polyvinylpyrrolidone on liver of the mouse. *Am. J. Path.* 32: 433, 1956.
36. Gall, E. A., W. A. Altemeier, L. Schiff, D. L. Hamilton, H. Braunstein, J. Guiseffi, and D. G. Freeman. Liver lesions following intravenous administration of polyvinylpyrrolidone (PVP). *Am. J. Clin. Path.* 23: 1187–1198, 1953.
37. Gordon, H., L. J. Hoge, and H. Lawson. Gelatin as a substitute for blood after experimental hemorrhage. *Am. J. M. Sc.* 204: 4–11, 1942.
38. Gowdey, C. W., and I. E. Young. Cardiorenal effects of large infusions of dextran in dogs. *Canad. J. Biochem. & Physiol.* 32: 559, 1954.
39. Gray, I. Metabolism of plasma expanders studied with carbon-14-labeled dextran. *Am. J. Physiol.* 174: 462–466, 1953.
40. Gray, I., and E. J. Pulaski. Metabolism of plasma substitutes II. Oxypolygelatin. *Proc. Soc. Exper. Biol. & Med.* 78: 421, 1951.
41. Gray, I., P. K. Siiteri, and E. J. Pulaski. Metabolism of plasma substitute I, Dextran (Macrodex). *Proc. Soc. Exper. Biol. & Med.* 77: 626–627, 1951.
42. Greenman, L., E. B. Fergus, F. M. Mateer, F. A. Weigand, and T. S. Danowski. Blood, plasma, serum and urine changes following hyperoncotic and iso-oncotic dextran. *J. Appl. Physiol.* 6: 79, 1953.
43. Gronwall, A., and B. Ingelman. Dextran as a substitute for plasma. *Nature* 155: 45, 1945.
44. Gropper, A. L., L. G. Raisz, and W. H. Amspacher. Plasma expanders. *Surg. Gynec. & Obst.* 95: 521–542, 1952.
45. Handford, S. W., C. McC. Smythe, J. P. Gilmore, R. S. Leopold, R. H. Kathan, and H. G. Arm. Glycerol pectate for plasma volume replacement and expansion: an experimental study. *J. Appl. Physiol.* 7: 553–576, 1954–55.
46. Hardwicke, J., C. R. Ricketts, and J. R. Squire. Effect of dextran of various molecular sizes on erythrocyte sedimentation rate. *Nature* 166: 988, 1950.
47. Hartman, F. W. Tissue changes following the use of plasma substitutes. *A.M.A. Arch. Surg.* 63: 728–738, 1951.
48. Hehre, E. J., and T. W. Sery. Dextran-splitting anaerobic bacteria from the human intestine. *J. Bact.* 63: 424–426, 1952.
49. Hoffman, W. S., and D. D. Kozoll. The fate of intravenously injected gelatin in human subjects. *J. Clin. Invest.* 25: 575–585, 1946.
50. Hogan, J. J. The intravenous use of colloidal (gelatin) solutions in shock. *J.A.M.A.* 64: 721, 1915.
51. Horvath, S. M., L. H. Hamilton, G. B. Spurr, E. B. Allbaugh, and B. K. Hutt. Plasma expanders and bleeding times. *J. Appl. Physiol.* 7: 614–616, 1954–55.
52. Howard, J. M., C. T. Teng, and R. K. Loeffler. Studies of dextrans of various molecular sizes. *Ann. Surgery* 143: 369, 1956.
53. Hueper, W. C. Macromolecular substances as pathogenic agents. *A.M.A. Arch. Path.* 33: 267–290, 1942.
54. Hueper, W. C. Organic lesions produced by polyvinyl alcohol in rats and rabbits. *A.M.A. Arch. Path.* 28: 510–531, 1939.
55. Hueper, W. C. Experimental carcinogenic studies in macromolecular chemicals. I. Neoplastic reactions in rats and mice after parenteral introduction of polyvinylpyrrolidones. *Cancer* 10: 8, 1957.
56. Hueper, W. C., J. W. Landsberg, and L. C. Eskridge. The effects of intravenous and intraperitoneal introduction of polyvinyl alcohol solutions upon the blood. *J. Pharmacol. & Exper. Therap.* 70: 201, 1940.
57. Ivy, A. C., H. Greengard, I. F. Stein, F. S. Grodins, and D. F. Dutton. The effect of various blood substitutes in resuscitation after an otherwise fatal hemorrhage. *Surg. Gynec. & Obst.* 76: 85–90, 1943.
58. Jackson, R. L., and L. Frayser. The effect of acacia on the blood. *J. Pharmacol. & Exper. Therap.* 65: 440–452, 1939.
59. Jacobaeus, U. Studies on the effect of dextran on the coagulation of blood. *Acta med. Scandinav.* suppl. 322 p. 3–103, 1957.
60. Jacobson, S. D., and C. J. Smyth. Gelatin as a substitute for plasma. *A.M.A. Arch. Int. Med.* 74: 254–257, 1944.
61. Jaenike, J. R., and C. Waterhouse. Metabolic and hemodynamic changes induced by the prolonged administration of dextran. *Circulation* 11: 1–13, 1955.
62. James, J., G. Gordillo, and J. Metcoff. Effects of infusion of hyperoncotic dextran in children with the nephrotic syndrome. *J. Clin. Invest.* 33: 1346–1357, 1954.
63. Jenkins, L. B., F. E. Kredel, and W. M. McCord. Evaluation of polyvinylpyrrolidone as a plasma expander. *A.M.A. Arch. Surg.* 72: 612, 1956.
64. Justus, D. W., R. W. Cornett, and J. D. Hatcher. A humoral influence on cardiovascular adjustments to acute and chronic post-hemorrhagic anemia in dogs. *Circulation Res.* 5: 207, 1957.

65. KABAT, E. A., AND D. BERG. Production of precipitins and cutaneous sensitivity in man by injection of small amounts of dextran. *Ann. New York Acad. Sc.* 55: 471–477, 1952.
66. LANGDELL, R. D., E. ADELSON, F. W. FURTH, AND W. H. CROSBY. Dextran and prolonged bleeding time. Results of a sixty-gram one-liter infusion given to one hundred sixty-three normal human subjects. *J.A.M.A.* 166: 346, 1958.
67. LEUSEN, I. R., AND H. E. ESSEX. Leukopenia and changes in differential leucocyte counts produced in rabbits by dextran and acacia. *Am. J. Physiol.* 172: 231–236, 1953.
68. LOEFFLER, R. K., AND J. SCUDDER. Excretion and distribution of polyvinylpyrrolidone in man as determined by use of radiocarbon as a tracer. *Am. J. Clin. Path.* 23: 311–321, 1953.
69. MARSHALL, L. H., C. H. HANNA, H. SPECHT, AND P. A. NEAL. Blood changes of normal dogs during chronic blood volume expansion with dextran. *Proc. Soc. Exper. Biol. & Med.* 79: 363–366, 1952.
70. MAURER, P. H. The antigenicity of polyvinylpyrrolidone. *J. Immunol.* 77: 105, 1956.
71. MAURER, P. H. Dextran, an antigen in man. *Proc. Soc. Exper. Biol. & Med.* 83: 879–884, 1953.
72. MAURER, P. H., AND H. LEBOVITZ. Studies on the antigenicity of modified fluid gelatin. *J. Immunol.* 76: 335–341, 1956.
73. MCCLURE, R. D., K. W. WARREN, AND L. S. FALLIS. Intravenous pectin solution in the prophylaxis and treatment of shock. *Canad. M.A.J.* 51: 206, 1944.
74. METCALF, W., AND L. M. ROUSSELOT. Some physiologic effects following dextran infusion in normal subjects. *Surg. Forum* 1952, 5:428–433.
75. MEYER, L. M., N. I. BERLIN, G. M. HYDE, R. J. PARSONS, AND B. WHITTINGTON. Changes in blood volume following administration of dextran—determined by P^{32} labeled red cells. *Surg. Gynec. & Obst.* 94: 712–714, 1952.
76. MICHIE, A. J., AND M. C. RAGNI. Effect of repeated infusions of dextran on renal function. *J. Appl. Physiol.* 5: 625–627, 1952–53.
77. MICHIE, A. J., C. E. KOOP, W. S. BLAKEMORE, AND M. C. RAGNI. Effect of modified fluid gelatin on renal function. *J. Appl. Physiol.* 5: 621–624, 1952–53.
78. MORRISON, A. E., J. S. LUNDY, AND H. E. ESSEX. An evaluation of replacement fluids in laboratory animals following control hemorrhage. *Circulation* 5: 208–214, 1952.
79. MOWRY, R. W., AND R. C. MILLICAN. A histochemical study of the distribution and fate of dextran in tissues of the mouse. *Am. J. Path.* 29: 523–545, 1953.
80. MOWRY, R. W., J. B. LONGLEY, AND R. C. MILLICAN. Histochemical demonstration of intravenously injected dextran in kidney and liver of the mouse. *J. Lab. & Clin. Med.* 39: 211–217, 1952.
81. NELSON, A. A., AND L. M. LUSKY. Pathological changes in rabbits from repeated intravenous injections of Periston (polyvinylpyrrolidone) or dextran. *Proc. Soc. Exper. Biol. & Med.* 76: 765, 1951.
82. OHLKE, R. F., AND J. J. SCALES. Plasma augmenters in clinical surgery. *Canad. M.A.J.* 68: 260–261, 1953.
83. PADHI, R. K., E. M. NANSON, AND R. B. LYNN. Hemodynamic changes in graded hemorrhage with special reference to the peripheral circulation. *Ann. Surg.* 148: 827–834, 1958.
84. PARKINS, W. M., J. H. PERLMUTT, AND H. M. VARS. Dextran, oxypolygelatin, and modified fluid gelatin as replacement fluids in experimental hemorrhage. *Am. J. Physiol.* 173: 403, 1953.
85. POPPER, H., B. W., VOLK, K. A. MEYER, D. D. KOZOLL, AND F. STEIGMANN. Evaluation of gelatin in pectin solutions as substitutes for plasma in the treatment of shock. *A.M.A. Arch. Surg.* 50: 34, 1945.
86. RAISZ, L. G. Dextran and oxypolygelatin as plasma volume expanders: renal excretion and effects on renal function. *J. Lab. & Clin. Med.* 40: 880, 1952.
87. RAVIN, H. A., A. M. SELIGMAN. AND J. FINE. Polyvinylpyrrolidone as a plasma expander. *New England J. Med.* 247: 921–929, 1952.
88. REINHOLD, J. G., C. A. J. VON FRIJTAG DRABBE, M NEWTON, AND J. THOMAS. Effects of dextran and of polyvinylpyrrolidone administration on liver function in man. *A.M.A. Arch. Surg.* 65: 706–713, 1952.
89. ROCHE, P., R. A. DODELIN, AND W. L. BLOOM. Effect of dextran on blood typing and crossmatching. *Blood* 7: 373–375, 1952.
90. ROOME, N. W., L. RUTTLE, L. WILLIAMS, AND W. SMITH. The polyvinyl alcohols as blood substitutes. *Canad. M.A.J.* 51: 293–299, 1944.
91. SCOTT, R., AND J. M. HOWARD. Hepatic function following wounding and resuscitation with plasma expanders. *Ann. Surg.* 141: 357–365, 1955.
92. SEEGERS, W. H., W. G. LEVINE, AND S. A. JOHNSON. Inhibition of prothrombin activation with dextran. *J. Appl. Physiol.* 7: 617–620, 1954–55.
93. SEMPLE, R. E. Changes in protein fractions of dog plasma after bleeding and dextran infusion. *J. Lab. & Clin. Med.* 45: 61–65, 1955.
94. SQUIRE, J. R., J. P. BALL, W. D'A. MAYCOCK, AND C. R. RICKETTS. *Dextran. Its Properties and Uses in Medicine.* Springfield, Ill.: Thomas, 1955, 91 pp.
95. STAMLER, J., L. DREIFUS, L. N. KATZ, AND I. J. LICHTON. Response to rapid water, sodium, and dextran loads of intact Ringer's-infused unanesthetized dogs. *Am. J. Physiol.* 195: 362–367, 1958.
96. STATE, D., F. T. ROMERO, M. CASTELLANOS, AND O. H. WANGENSTEEN. Clinical evaluation of bovine serum albumin as a blood substitute. *Surgery* 22: 424–441, 1947.
97. STEEL, R., D. D. VAN SLYKE, AND J. PLAZIN. The fate of intravenously administered polyvinylpyrrolidone. *Ann. New York Acad. Sc.* 55: 479–484, 1952.
98. STERN, K. Effect of polyvinylpyrrolidone on reticuloendothelial storage. *Proc. Soc. Exper. Biol. & Med.* 79: 618–623, 1952.
99. STRUMIA, M. M., F. W. CHORNOCK, A. D. BLAKE, AND W. G. KARR. The use of a "modified globin" from human erythrocytes as a plasma substitute. Preliminary Report. *Am. J. M. Sc.* 209: 436–442, 1945.
100. STUCKI, J. C., AND C. R. THOMPSON. A screening procedure for substances which inhibit dextran edema in the rat. *Am. J. Physiol.* 193: 275, 1958.
101. TARROW, A. B., AND E. J. PULASKI. Reactions in man from infusion with dextran. *Anesthesiology* 14: 359–366, 1953.
102. TAYLOR, N. B., AND E. T. WATERS. Isinglass as a transfusion fluid in hemorrhage. *Canad. M.A.J.* 44: 547, 1941.
103. TERRY, R., C. L. YUILE, A. GOLODETZ, C. E. PHILLIPS, AND R. R. WHITE. Metabolism of dextran—a plasma

volume expander. Studies of radioactive carbon-labeled dextran in dogs. *J. Lab. & Clin. Med.* 42: 6, 1953.

104. Thrower, W. R., and H. Campbell. Plasmosan. A synthetic substitute for plasma. *Lancet* 1: 1096–1099, 1951.

105. Turner, P. A., and W. d'A. Maycock, Distribution of injected dextran in the mouse. *J. Path. & Bact.* 75: 145–150, 1958.

106. Wangensteen, O. H., H. Hall, A. Kremen, and B. Stevens. Intravenous administration of bovine and human plasma to man: Proof of utilization. *Proc. Soc. Exper. Biol. & Med.* 43: 616–621, 1940.

107. Wasserman, K., and H. S. Mayerson. Relative importance of dextran molecular size in plasma volume expansion. *Am. J. Physiol.* 176: 104–112, 1954.

108. Wasserman, K., and H. S. Mayerson. Plasma, lymph, and urine studies after dextran infusion. *Am. J. Physiol.* 171: 218–232, 1952.

109. Waters, E. T. A comparison of isinglass and gelatin as blood substitutes. *Canad. M.A.J.* 45: 395–398, 1941.

110. Waud, R. A. Blood and hemodynamic changes in dogs following hemorrhagic hypotension and its treatment with dextran. *J. Pharmacol. & Exper. Therap.* 119: 85–92, 1957.

111. Weil, P. G., and D. R. Webster. Studies on the bleeding tendency following dextran infusion. *Surg. Forum* 6: 88–90, 1955.

112. Weil, P. G., and D. R. Webster. Clinical experience with plasma augmenters, dextran and PVP. *Surg. Forum* 4: 712–714. 1953.

113. Werkö, L. The effect of experimentally induced hypervolemia on the cardiac function in normal individuals and patients with acquired heart disease. In: *Pulmonary Circulation*, edited by W. Adams and I. Veith. New York: Grune & Stratton, 1959, pp. 263–272.

114. Wilkinson, A. W., and I. D. E. Storey. "Reactions" to dextran. *Lancet* 2: 956–958, 1953.

115. Wilson, J. S., E. H. Estes, J. T. Doyle, W. L. Bloom, and J. V. Warren. The use of dextran in the treatment of blood loss and shock. *Am. J. Med. Sci.* 223: 364, 1952.

116. Witham, A. C., J. W. Fleming, and W. L. Bloom. The effect of the intravenous administration of dextran on cardiac output and other circulatory dynamics. *J. Clin. Invest.* 30: 897, 1951.

117. Wolman, M. Histological changes produced by injections of polysaccharides. *A.M.A. Arch. Path.* 62: 149–154, 1956.

Physical principles of circulatory phenomena: the physical equilibria of the heart and blood vessels

ALAN C. BURTON *Department of Biophysics, University of Western Ontario, London, Ontario, Canada*

CHAPTER CONTENTS

I. IMPORTANCE OF THE SIZE OF THE VESSELS

THE BLOOD VESSELS of the vascular bed include a very wide range of size, thickness of wall, and number of vessels that are "in parallel" as well as "in series" with each other. The mean pressure of the blood within these various vessels also ranges from over 100 mm Hg in the aorta to values near zero in the large veins. Figure 1 schematically illustrates this wide variety in dimensions of the blood vessels (6), and in the composition of their walls as to the four main tissues, endothelium, elastin, collagenous and smooth muscle fibers. Since these different tissue elements have very different physical properties, we have a right to expect that this great variety of composition and size has a physiological importance.

The system of blood vessels has, of course, the function of distribution of blood to the different parts of the body, in amounts related to the needs of the various tissues and organs. The distribution will be determined by the relative "resistance to flow" of the various routes through which the driving pressure difference, between aorta and vena cava, may propel the blood. The law of Poiseuille relates to flow of simple fluids through rigid pipes. The modifications of the law when it is applied to the flow of blood

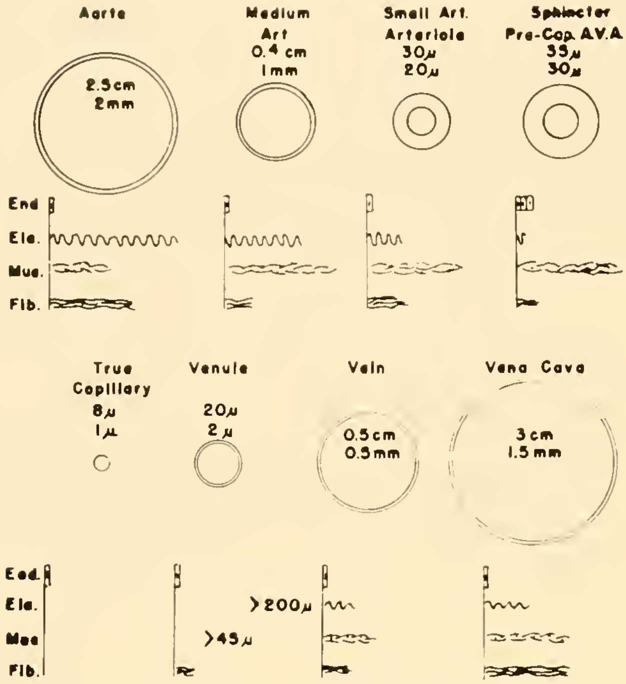

FIG. 1. The variety of sizes and composition of the wall of the different blood vessels. [From Burton (6).]

through nonrigid, distensible blood vessels are discussed elsewhere in this volume and in the literature (15). Poiseuille's law is that the flow F is given by:

$$F = \Delta P \times \left(\frac{\pi}{8}\right) \times \left(\frac{1}{\eta}\right) \times \left(\frac{r^4}{l}\right) \tag{1}$$

where ΔP is the pressure difference (i.e., the driving force), $(\pi/8)$ is the "numerical factor" arising from the integration over a cross section of a cylindrical tube in the development by Hagen, $(1/\eta)$ is the "viscosity factor," and (r^4/l) is the "geometrical factor" involving the values r and the length l of the vessel concerned. By definition, the resistance to flow is the ratio of the driving force, i.e., the pressure difference, to the flow that results.

$$R = \frac{\Delta P}{F} = \left(\frac{8}{\pi}\right) \times \eta \times \frac{l}{r^4} \tag{2}$$

The resistance then depends on the two factors, the viscosity factor η, and the geometrical factor (l/r^4).

The "fourth power law," by which the resistance to flow is inversely proportional to the fourth power of the radius, gives a very sensitive control of the distribution of blood flow by the caliber of the resistance vessels, i.e., the arterioles. A reduction in radius of only 16 per cent will double the resistance, and of 50 per cent will increase the resistance by 2^4, i.e., 16 times.

For a fluid, e.g., water, which obeys Newton's law of viscosity, and thus is a "Newtonian fluid," the coefficient of viscosity η is independent of the rate of flow or of the size of the vessel. Blood, however, is a complicated fluid containing large particles (e.g., the erythrocytes), is not Newtonian in its viscosity, and η varies with the rate of flow (axial accumulation) and with the size of vessels (Fåhraeus-Lindqvist effect) (16). For explanation of these see the following chapter. It has been shown that in spite of this, in the physiological range of blood flow, blood behaves very accurately as if it were Newtonian (15).

2. IMPORTANCE OF THE DISTENSIBILITY OF BLOOD VESSELS: TRANSMURAL PRESSURES

The factor of more importance, in the Poiseuille equation, which can alter the resistance and the distribution of blood in the body is thus the "geometrical factor" (l/r^4). In rigid tubes, as used by Poiseuille, this factor is a constant. Blood vessels are distensible, so that their geometry depends upon the pressure within them. The particular pressure concerned is, for each vessel, its "transmural pressure," P_{TM}, i.e., the difference of pressure from inside, where the pressure is the "intravascular pressure," P_{iv}, to the outside, where the pressure is the "tissue pressure," P_T, i.e.,

$$P_{iv} - P_T = P_{TM} \tag{3}$$

While in equation 2 the resistance R does not depend explicitly upon the pressure difference ΔP, nevertheless where the vessels are distensible the resistance will depend upon ΔP. This is because any change in ΔP will usually involve a change in the transmural pressure, P_{TM}, of the "resistance vessels." For example, the usual way to produce a flow-pressure curve would be to keep the venous pressure constant, and change the arterial pressure to different values. This will inevitably change the transmural pressures in all the vessels between artery and vein, so their geometrical factors (l/r^4) will be changed.

In another, quite different, experiment, to verify equation 1 we might increase the driving pressure ΔP by keeping the arterial pressure constant, but reducing the venous pressure. In this case the transmural pressure of all the vessels would decrease as ΔP was increased (whereas in the first case it would increase) and the effect on the geometry of the vessels

would be the opposite. It becomes clear that with distensible tubes there is no one relation between flow and pressure difference, but a whole family of such relations, depending upon the transmural pressure of the resistance vessels. This has been demonstrated in vascular beds (7). Equation 1 therefore becomes insufficient to define the flow-pressure relations and does not contain all the necessary data to determine the flow. We must add an equation which recognizes the dependence of the geometry of vessels on their transmural pressure, i.e.,

$$\frac{l}{r^4} = f(P_{TM}) \tag{4}$$

where f represents some function, which we might call the "distensibility function." It becomes of great importance to determine this function f, i.e., to study how the size of distensible vessels depends upon their transmural pressures.

3. FORCES CONCERNED WITH THE EQUILIBRIUM OF THE BLOOD VESSEL WALL (5)

A. *The Distending Force*

Consider a unit length of a cylindrical blood vessel, where first we consider the wall as very thin compared to the radius r of the cylinder (fig. 2*A*): the intravascular pressure P_{iv} dynes per cm² is everywhere at right angles to the wall, and gives a force, per unit length of the cylindrical vessel, equal to $2\pi r P_{iv}$ dynes, tending to increase the radius. On the outside of the vessel, the tissue pressure opposes this, with a total force of $2\pi r P_T$. The total "expanding" force is then, in dynes per centimeter:

$$F = 2\pi r(P_{iv} - P_T) = 2\pi r P_{TM} \tag{5}$$

B. *The Constricting Force*

The force holding this expanding force in equilibrium is that due to a "circumferential tension" T_c, in dynes per unit length of the cylindrical vessel (fig. 2*B* and 2*C*).

4. EQUILIBRIUM BETWEEN THESE FORCES: THE LAW OF LAPLACE

There are two ways of equating these forces, to be found in any college physics text. Forces may be resolved from figure 2*B*, or, in a better method, use

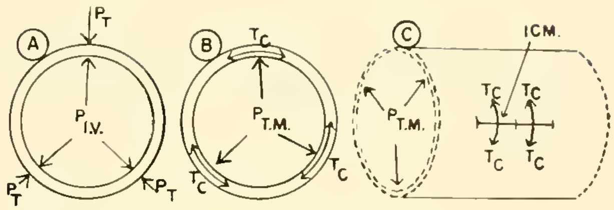

FIG. 2. The forces that are in equilibrium at the blood vessel wall. P_{iv}—intravascular pressure, P_T—tissue pressure, P_{TM}—transmural pressure, T_c—circumferential tension in dynes/cm length of the cylindrical vessel.

is made of the "principle of virtual work." The tension in the wall, T_c, may be expressed either as dynes per centimeter length of the cylinder, or as ergs per square centimeter of surface of the wall (just as surface tension is expressed as dyne/cm or as ergs/cm²). The "principle of virtual work" states that if a small displacement is made from the equilibrium, as increasing the radius r to $r + dr$, the work done must equal the change in energy that would result. This is simply a special case of the general principle of conservation of energy. In this particular case, for an increase of radius to $(r + dr)$, the pressure, which is everywhere at right angles to the wall, will do work equal to $2\pi r P_{TM}\, dr$. The total energy of the wall will have increased, because the surface of a unit length of the cylinder has increased from a value $2\pi r$ to $2\pi(r + dr)$. The increase in surface area is then $2\pi \cdot dr$ square centimeters, and in the surface energy is $2\pi T_c \cdot dr$.

Equating, we have

$$2\pi r P_{TM}\, dr = 2\pi T_c \cdot dr$$
$$\therefore P_{TM} = \frac{T_c}{r} \tag{6}$$

For equilibrium, then, the transmural pressure must always equal the circumferential tension divided by the radius. This means that the circumferential tension in the wall has a sort of mechanical advantage in opposing the transmural pressure. The smaller the radius of the cylinder, the greater the pressure that can be held in equilibrium by a given tension in the wall. This principle is well known to engineers who have to design piping for transport of fluids under high pressures, e.g., O_2, against bursting under high pressure. A pipe of small radius will be safe, where a larger pipe, with the same thickness of metal in the wall, would easily burst.

The same application of the principle of virtual

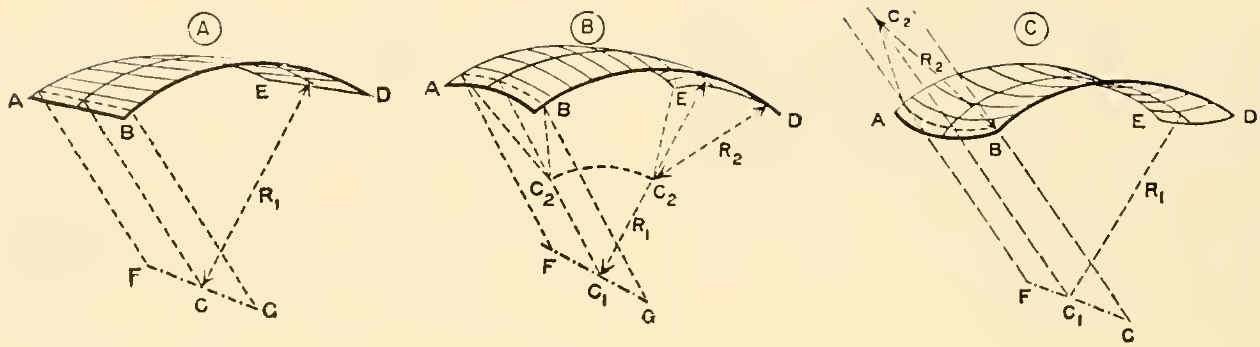

FIG. 3. Illustration of how a surface has, at any point in it, two principal radii of curvature. *A:* a cylindrical surface, where one radius of curvature is infinite: *B:* a synclastic surface, where the two centers of curvature lie on the same side of the surface; *C:* an anticlastic surface, with centers of curvature on opposite sides of it. [From *General Physics for Students.* Edwin Edser. London: Macmillan, 1911.]

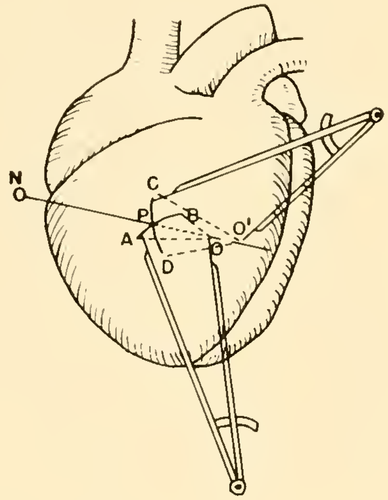

FIG. 4. The two principal radii of curvature at a point on the surface of a cardiac ventricle. NP—normal at this point. APB, CPD, circular arcs, touching the surface, O and O' centers of curvature. [From Burton (8).]

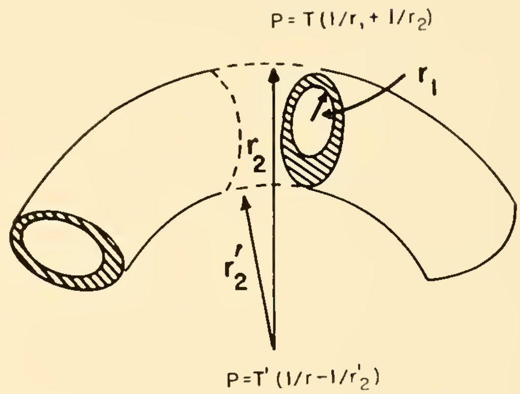

FIG. 5. Illustration of how the wall at the top of the aortic arch is synclastic, at the bottom anticlastic. The wall thickness has to alter accordingly.

work to a sphere rather than a cylinder gives the result

$$P_{TM} = \frac{2T}{r} \tag{7}$$

This is familiar as the formula for liquid drops, where T is the surface tension. (For soap bubbles, $P = 4T/R$, as there are two air-liquid interfaces of the soap film.) The two special cases, the cylinder and the sphere, are part of the general law of Laplace (c. 1821) for a surface "membrane" that divides two spaces, which we can call "inside" and "outside." The membrane may be of any shape at all, but, for equilibrium, we must have:

$$P_{TM} = T\left(\frac{1}{r_1} + \frac{1}{r_2}\right) \tag{8}$$

where r_1 and r_2 are the "principal radii of curvature" of the membrane at any given point (fig. 3). The definition of these "principal radii" is as follows. At any point on the surface (as of the heart, fig. 4) we may draw the normal (NP) at that point, at right angles to a "tangent plane" (like a sheet of paper touching the surface at that point). With their centers at two different points (O and O') somewhere on this normal, we may describe two arcs which touch the surface in two different planes, at right angles to each other. The two arcs will have two different radii of curvature r_1 and r_2, and we could find an infinite number of such pairs of arcs (at right angles to each other, but oriented differently in the surface). The "principal radii of curvature" are

the maximum and minimum values of all the radii so found (8, 28).

For a sphere, equation 8 becomes equation 7, where $r_1 = r_2 = r$, and becomes equation 6 for a cylinder, where $r_2 = \infty$. For surfaces where the two principal curvatures are in the same "sense," i.e., the centers of curvature are on the same side of the surface, the terms $1/r_1 + 1/r_2$ add together. These are called "synclastic surfaces" (fig. 3). The walls of ventricles of the heart are "synclastic." Other surfaces may have the principal radii of curvature in opposite sense, and are called "anticlastic" surfaces. The wall of the inside of the arch of the aorta is an example. Here the two terms subtract from each other. In contrast, the wall on the outer curvature of the arch is synclastic (fig. 5). As a consequence of equation 8 and the above, the tension required in the wall on the inside of the arch, to hold the aortic pressure in equilibrium, is much greater than that required on the outside of the arch, and it is no surprise to find that the wall is correspondingly thicker at the bottom of the arch than at the top.[1]

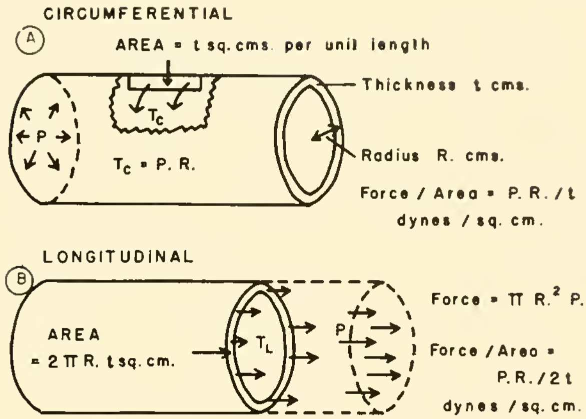

FIG. 6. Comparison between the calculations for the circumferential tension and the longitudinal tensions in the wall. [From Roach & Burton (23).]

5. EQUILIBRIUM FOR THE LONGITUDINAL TENSION

In addition to the circumferential tension, there must be a longitudinal tension in the wall of a cylindrical vessel, if it is to be in equilibrium with the transmural pressure. No matter what the shape of the rest of the vascular bed, to which the particular cylindrical segment considered is connected, it can be shown that the result of all the pressure forces acting on the walls of the rest of the bed is equivalent to the force that would be exerted on a plane partition at right angles to the axis, closing off the end of our segment. This force would be $\pi r^2 \times P_{TM}$. If T_L is the longitudinal tension in the wall, reckoned per unit length of the circumference, the total force over the cross section of the wall is $2\pi r \times T_L$ (fig. 6). Equating: $\pi r^2 \times P_{TM} = 2\pi r \times T_L$, i.e.,

$$T_L = \frac{P_{TM}}{2r} \qquad (9)$$

Thus the longitudinal tension T_L is half the circumferential tension, T_c (though it must not be forgotten that the longitudinal tension is reckoned per unit length of the circumference of circular cross section of the wall, while the circumferential tension is reckoned per unit length of wall, parallel to the cylindrical axis).

[1] For those who love mathematical formulas, the ratio of thickness at the bottom to thickness at the top of the arch is given by $(n - 1)(n + 2)/(n + 1)(n - 2)$ where n is the ratio of the radius of the arch (to the axis of the aorta) to the radius of the aorta. For $n = 3$, the ratio of thickness is 2.5, for $n = 4$; 1.8, and for $n = 5$; 1.2.

6. MODIFICATION OF THE LAW OF LAPLACE FOR THICK-WALLED VESSELS

Some doubts have been expressed in the physiological literature that the law of Laplace can be applied to any vessel where the thickness of the wall is not small compared to the radius of the lumen. This ratio in blood vessels runs from less than 3 per cent for veins, 20 per cent only for the aorta, and up to unity or even more for the thick-walled arterioles. In the heart also, particularly at the apex, the thickness of the ventricular wall may be considerable, compared to the radii of curvature. There is no basis whatever for these doubts, though the law must be applied, where the ratio of thickness to radius is considerable, with the aid of the calculus, to successive concentric layers of the wall. This results in an interesting insight into the way in which the tissue pressure within the wall itself must vary from the inner to the outer wall. Even without this type of analysis we may use the device of using an "average tension" in the wall, to allow the simpler form of the law to be used. Take the case of a thick-walled cylindrical vessel of inside radius r_i and outside radius r_o. Instead of using P_{iv}, the intravascular pressure, and P_T, the tissue pressure outside, we may substitute P_{TM} for the inside pressure and zero for the outside tissue pressure.

Consider an annular cylindrical ring of the wall, of unit length of vessel, between radii r and $r + dr$. Let the tension at this radius be T'_r per unit (radial) thickness, i.e., in this annular ring it will be $T'_r\, dr$. (The T' must be used instead of the former T, since this was the total tension, whereas T' is, of course, proportional to the thickness of the ring of wall being considered.) Then the law of Laplace applies, at every point within the wall, and there must be a drop of pressure in the wall between inside this ring and outside it, given by

$$dP = \frac{T_r' \cdot dr}{r} \tag{10}$$

Integrating

$$P_{TM} = \int_{r_i}^{r_o} \frac{T_r'\, dr}{r} \tag{11}$$

where r_i and r_o are the inside and outside radii, respectively.

If we do not wish to introduce a knowledge of the particular way in which T'_r varies through the wall (since this will be determined by the elastic constants and the degree of stretch of each layer, and in contractile tissue, by the "active tension" of the muscle of each layer), we may conveniently work with an "average tension of the wall," $\bar{T}_c$, defined by:

$$\bar{T}_c = \bar{r} \int_{r_i}^{r_o} \frac{T_r'\, dr}{r} \tag{12}$$

where $\bar{r}$ is an average radius, i.e., $(r_i + r_o)/2$. This brings us back to the simple equation for the law of Laplace, i.e.

$$P_{TM} = \frac{\bar{T}_c}{\bar{r}} \tag{13}$$

None of the conclusions reached later, e.g., as to instability of blood vessel equilibrium, is altered by this consideration.

Once the value of the circumferential tension at different places in the wall is known, the value of the integral of equation 11 can be found, and the gradient of pressure through the wall evaluated. However, up to this point, we have given only the equations that determine what the total tension must be, in a vessel of a certain radius, to be in equilibrium with the pressure. When the wall is distensible, however, this "certain radius" is not fixed but determined by another relation, i.e., that between the tension in the wall and the stretch of the wall, which is determined by what is called the "elastic diagram" for the vessel. If the transmural pressure is altered, the equilibrium will be destroyed, and the radius will change until the tension, under the new degree of stretch, once more obeys the equation of Laplace. The solution of the problem then depends upon an analysis of the elastic behavior of the vessel wall. When this has been discussed, it is possible to return to the solution of equation 10 for some simple idealized cases, and to investigate the distribution of tension through the thickness of the wall, e.g., which layers will play the major role of holding the pressure in check; and we can also determine the drop of pressure through the thickness of the wall. These solutions are important for an understanding of the particular architecture of the walls of blood vessels. The pressure gradient in the wall obviously also has a bearing on the possibility of "vasa vasorum," the blood vessels within the arterial wall, remaining open against the pressure in the tissues where they lie. The solution of equation 11 will be given for special cases in the Appendix.

7. NATURE OF THE TENSION IN THE WALL, ELASTIC AND ACTIVE TENSIONS

The law of Laplace tells us the magnitude of the circumferential tension, and the second calculation the longitudinal tension, that must exist in the wall to hold the transmural pressure in equilibrium. These calculations can tell us nothing of the origin of these tensions. The reason for the tension in the wall of living blood vessels is twofold. First, it may be due to the stretch of the wall, with the property of "elasticity" of the tissue. This elasticity would be present also in the "dead" vessels, or indeed in a tube of any "elastic" material. In the second place, it may be due to contraction of living smooth muscle in the wall. The latter may be called the "active tension," T_A. The total tension in the wall:

$$T = T_A + T_E \tag{14}$$

It is important to define these two types of tension in terms of their dependence on stretch, not with respect to any particular tissue. Elastic tension is defined as tension which depends on the degree of stretch of the wall, i.e.

$$T_E = f(r) \tag{15}$$

while active tension is, by definition, independent of stretch, and dependent on the physiological activity of the tissue (vasomotor activity A), i.e.,

$$T_A = f(A) \tag{16}$$

This arbitrary division, by these definitions, does not imply that vascular smooth muscle does not possess elasticity, nor that the force of contraction of smooth muscle may not alter with the degree of stretch of the muscle. There is no doubt that such a dependence on stretch does exist, though the elastic force due to stretch is, from the scanty evidence available, much less than that found in the other elastic elements of the wall, namely, the elastin and the collagen fibers. However, any part of the smooth muscle tension that depends on stretch may, for convenience, be included in the elastic tension, T_E, leaving the rest, T_A, completely independent of stretch. This arbitrary definition of the symbols used effects a great simplification, without loss of validity.

TABLE 1

Type of Vessel	Mean (mm Hg)	Internal Press. (dynes/cm²)	Radius (R)	Tension (T) in Wall (dynes/cm)	Amount of Elastic Tissue
Aorta and large arteries	100	1.3×10^5	1.3 cm or less	170,000	Very elastic, two coats
Small distributing arteries	90	1.2×10^5	0.5 cm	60,000	Much elastic tissue, but more muscular
Arterioles	60	8×10^4	0.15 mm–62 μ	1200 500	Thin elastic intima only
Capillaries	30	4×10^4	4 μ	16	None
Venules	20	2.6×10^4	10 μ	26	None except in largest
Veins	15	2×10^4	200 μ	400	Elastic fibers reappear
Vena cava	10	1.3×10^4	1.6 cm	21,000	Very elastic, fibers increasing in size

8. TOTAL TENSION IN THE WALL OF DIFFERENT VESSELS

Without separating the total tension into the two components, elastic tension (dependent on stretch) and active tension (dependent on vasomotor tone, not dependent on stretch), we may study the value of the total tension in vessels of different categories by applying the law of Laplace (5). In table 1 the approximate radii of the categories of vessel, from aorta to vena cava, are those given in any textbook of anatomy or histology; whereas the values of pressure are those accepted for the mean pressure through the vascular system, after the graphs given in any elementary textbook of circulatory physiology. These are converted from mm Hg to the fundamental units of dynes per square centimeter, and merely multiplied by the appropriate radius to give the total tension in dynes per centimeter (1 mg = 0.98 dynes).

The table shows the enormous range of tension in the wall required for equilibrium with the blood pressure, from 170,000 dynes per cm in the aorta to 16 dynes per cm in the capillary. The dominant factor in determining this is the size of the vessels, so that although the pressure decreases from capillaries to vena cava, the tension very greatly increases. Two rather puzzling problems are elucidated.

First, it has been difficult to see how such a fragile, thin-walled, relatively unsupported structure as the capillary could withstand the pressure within it. Normal capillaries do not burst even under transmural pressures of several hundred millimeters of mercury, though impaired capillaries in hemorrhagic diseases may "burst" at relatively low pressures. The law of Laplace shows that because of the very small radius of the capillary, very little tension is required. A simple test shows that a single layer of the thinnest tissue paper (Kleenex) in a strip 1 cm wide will support 50 g (about 50,000 dynes/cm) before breaking. This is 3000 times as much as a capillary wall needs to withstand, at normal capillary pressure.

The second problem is why elastic tissue, i.e., elastin and collagen fibers, which are so prominent a feature of the larger arteries, is almost absent in the capillaries and venules but reappears in the veins (elastic tissue reappears in vessels more than 200 microns in diameter) in spite of the fact that the blood pressure is less. Again the size factor explains this. There is a very good correlation of the amount of elastic tissue with the tension in the wall given in table 1.

The tension required to withstand the prevailing blood pressure might be called the "maintenance tension." If this is produced by the elasticity of the wall, rather than by vasomotor tone, it will be much more efficient, in that the maintenance of elastic tension, due to stretch, does not involve any continuous expenditure of energy.

Whereas the energy expenditure of smooth muscles, particularly of vascular smooth muscle, has not yet been adequately measured, it seems probable on general physiological principles that the maintenance of active tension by vasomotor tone requires continuous energy expenditure. The provision of maintenance tension by elasticity, reserving the activity of smooth muscle in the wall for accomplishing changes in the total tension, and thus of the size of the vessels, would appear teleologically to offer optimal efficiency.

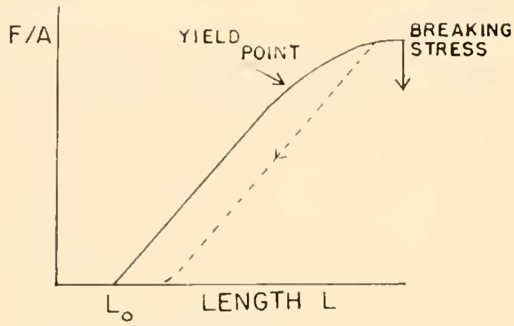

FIG. 7. Illustration of Hooke's law. F/A—Elastic force per unit area of cross section; L_0—unstretched length. Homogeneous materials eventually reach a "yield point" and give completely when a "breaking stress" is reached.

9. ELASTIC TENSION IN THE WALL

Elasticity is the property of matter by which it develops a force resisting deformation. For simple homogeneous substances the relation between the force and the amount of deformation is linear, obeying Hooke's law. This law is that the force F per unit cross section area (as of a steel wire) is proportional to the elongation (*ut tenso, sic vis*), i.e., the difference between the stretched length, l, and the "unstretched length," l_0. The relation is, in modern terms:

$$F/A = Y\left(\frac{l - l_0}{l_0}\right) \tag{17}$$

Y is the Young's modulus of elasticity. The linear law of Hooke is only approximate, even for such materials as steel or rubber, since as the material is stretched in one direction the cross-sectional area is necessarily reduced (fig. 7). Its application is also limited, for if the stretched length exceeds a certain point, called the "yield point," the material "yields" or "flows" and will not return to its original unstretched length when the elongating force is removed. For details any physics text on elasticity may be consulted, as also for the connection between Young's modulus and the two fundamental moduli, namely the "bulk modulus," resisting change of volume of the material, and the "shear modulus," resisting change of shape.

As early as 1880, Roy (22) investigated the elastic behavior of the wall of arteries, and there have been many measurements of this since. Roy used the direct method of cutting a strip from the wall and measuring its length under different loads. Better methods are to use circular rings of arteries or to deduce the tension vs radius from the volume-pressure relations of a segment of artery or vein, by the use of

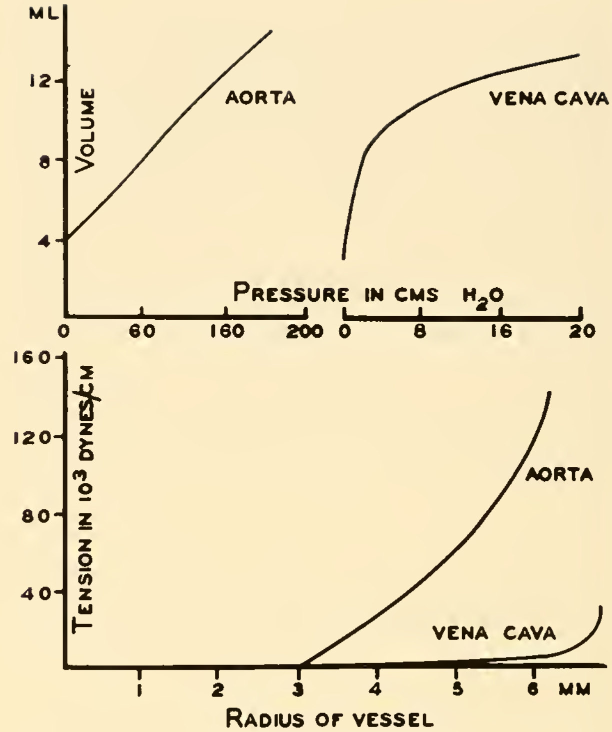

FIG. 8. *A:* volume-pressure curves of aorta and vena cava (after Green). *B:* the same data transformed to give the elastic diagrams. [From Burton (5).]

the law of Laplace (equation 6). Details have been discussed elsewhere (21), but the principle is simply that from the volume, V, in a given length of tissue, the mean radius can be calculated ($V = \pi r^2 l$). The total tension in the wall can then be calculated as equal to the product of the pressure, P, and the radius, r, i.e., $T = P \times r$. Figure 8 is an example of such a transformation from volume-pressure curves to tension-length diagrams, for the aorta and the vena cava from classical data of Hallock and Benson. Though the volume-pressure curves may have very different shapes, as for aortas of different ages (fig. 9), the tension-length diagrams are all of the same character, agreeing with what Roy found. There are also more indirect methods, such as that of measurement of pulse-wave velocity in long arteries, which can estimate the elastic constants of arterial walls, using the relation between pulse-wave velocity and distensibility developed by Bramwell *et al.* (3).

All these methods thus give the same result, that the resistance to stretch of the vessel wall (Young's modulus) increases markedly the more the wall is stretched. The elastic diagram (e.g., fig. 8) shows a curve that turns upward instead of obeying Hooke's law which, as explained already, is a straight line,

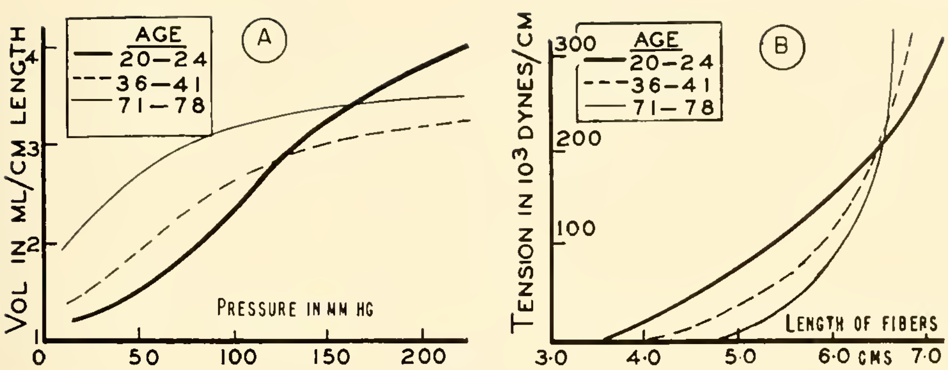

FIG. 9. *A:* volume-pressure curves for human aortas of different age groups (after Hallock and Benson). *B:* same data transformed to give elastic diagrams. [From Burton (5).]

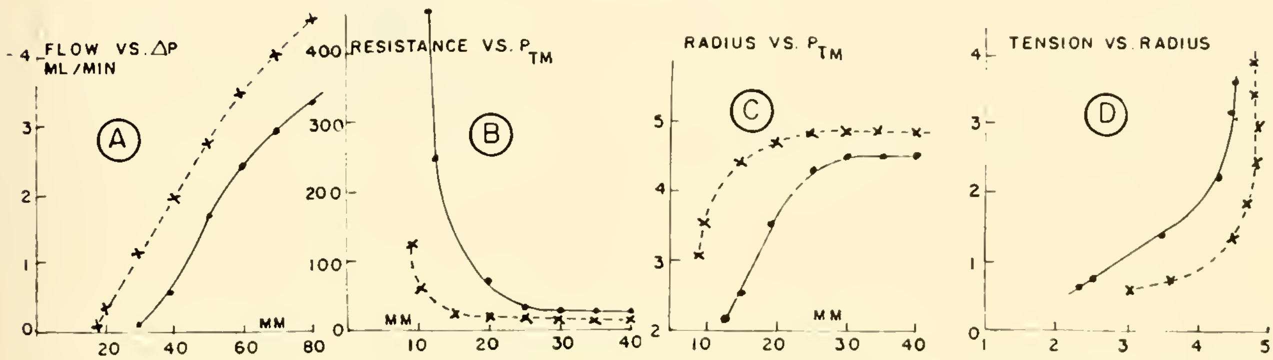

FIG. 10. *A:* typical flow-pressure curves of a vascular bed (rabbit leg). Broken curve—without vasomotor tone: solid curve—with tone produced by sympathetic stimulation. *B:* resistance calculated from same data. *C:* radius, in arbitrary units of a single equivalent vessel giving the resistance. *D:* tension-length diagram, in arbitrary units, for the wall of that single equivalent vessel.

or eventually turns downward at the yield point (fig. 7).

There is evidence that the same generalization applies to the elastic behavior of the smaller vessels such as the arterioles, which offer the important resistance to flow in the circulation. From the flow-pressure relations of a vascular bed (fig. 10*A*) a calculation of the resistance to flow, as pressure-to-flow, can be made for different transmural pressures of these vessels, since the pressure in the resistance vessels will be approximately the mean of arterial and venous pressures, if most of the resistance is in these vessels.[2] Thus the resistance may be plotted vs. the transmural pressure (fig. 10*B*). If now the Poiseuille formula for the resistance is used and changes in length of the vessels are ignored (the resulting conclusion would not be invalidated if the changes in length were significant), the relative changes in radius can be deduced (i.e., $r \propto 1/R^{1/4}$) as in figure 10*C*. The tension in the wall of the resistance vessels must be, by Laplace's law, equal to the pressure times this radius ($T_c = P_{TM} \times r$). Thus from the original flow-pressure curve we can deduce the shape of the tension-length diagram for the wall of a "single equivalent vessel" representing the arterioles (fig. 10*D*). A curve results which turns upwards, i.e., the resistance to stretch increases, as the wall is more stretched. All flow-pressure curves of vascular beds (with the exception of that of the kidney where there is "autoregulation," probably due to some reflex effect) that have been analyzed by us from data in the literature show the same shape of resistance vs. pressure curves, so the generalization about the elasticity of arteries and veins seems to apply also to the small vessels that offer the major part of the resistance to flow.

[2] If this "lumped parameter" theory is permissible, the transmural pressure of this single equivalent vessel will be $\Delta P/2$, for venous pressure near zero.

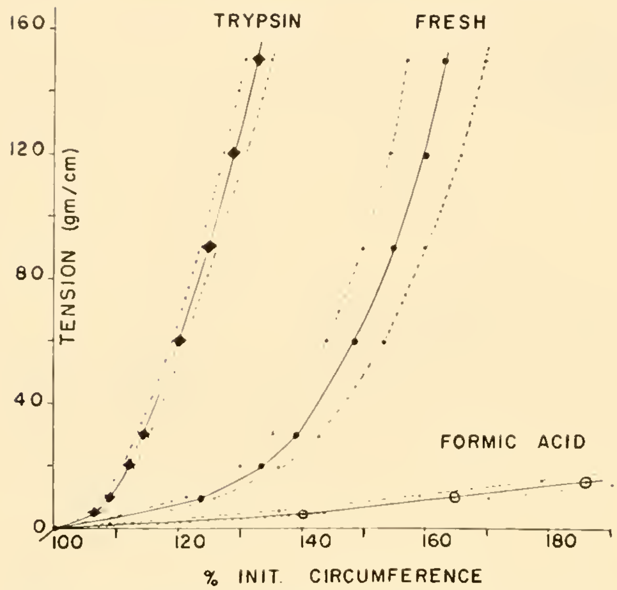

FIG. 11. Tension-length diagrams for the wall of human iliac arteries, after selective digestion of elastin fibers (trypsin), of collagen fibers (acid). [From Roach & Burton (23).]

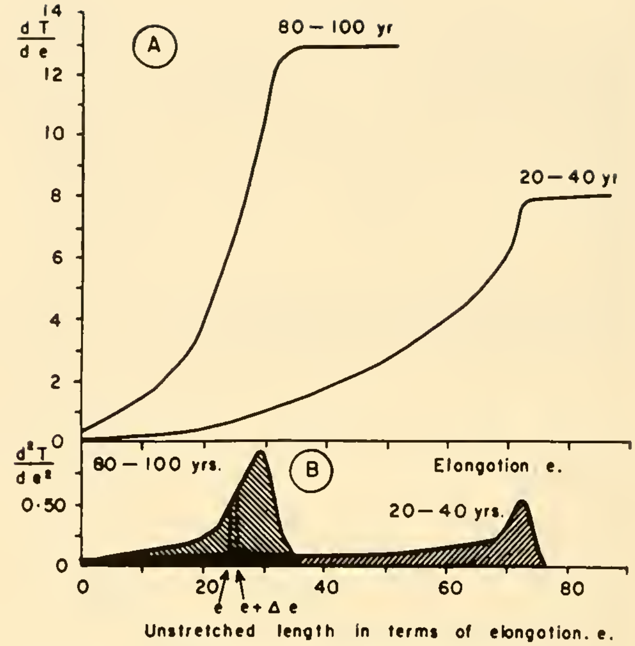

FIG. 12. *A:* the first differential of the elastic diagram, giving the "elastance" at each degree of stretch. *B:* the second differential of the elastic diagram (first differential of *A*) giving the histogram of number of collagen fibers vs. degree of stretch. [From Roach & Burton (23).]

10. THE REASON FOR THE SHAPE OF ELASTIC DIAGRAMS OF BLOOD VESSELS

Why does the vessel wall resist stretch more strongly the greater its stretch? In the case of human iliac arteries (from autopsy), the reason for this behavior has been proved to be a result of the heterogeneity of the wall, and is evidence of the separate roles of elastin and collagenous fibers (23). When the collagenous fibers are removed by digestion with crude formic acid (fig. 11) the remaining elastin fibers obey Hooke's law over a wide range. When, in contrast, the elastin fibers are selectively digested (by crude trypsin) the remaining collagenous fibers also obey Hooke's law over a wide range except for the start of the curve. The much steeper slope is equal to the final slope of the original graph. The final slope of the elastic diagram of the artery denotes that all of the collagenous fibers have reached their unstretched length, whereas the low initial slope, for very small stretch, represents the elasticity of the elastin fibers plus a few of the collagenous fibers that are "tightly strung" in the wall. The upturning of the curve thus is an indication of successive "recruitment" of strong collagen fibers, as they successively reach their respective unstretched length. Indeed, by plotting the second differential of the elastic diagram (i.e., d^2T/dl^2) vs. degree of elongation e (fig. 12) we can derive a histogram of the number of collagenous fibers, vs. the degree of elongation in the wall before their unstretched length is reached (24). The changes in this diagram with age of the arteries are most illuminating, showing that the process of aging is accompanied, not only by an increase in the total number of collagen fibers in the wall, but even more importantly by a tightening up of these fibers so that they are brought into action by a much smaller degree of stretch of the wall. Full explanation of the analysis is given in the papers cited.

11. GRAPHICAL METHOD FOR THE EQUILIBRIUM UNDER ELASTIC TENSION ALONE

Since we can confidently assume the shape of the tension-length diagram of the blood vessel wall, i.e., that the slope increases as the stretch is increased, we can examine the stability of the equilibrium of the vessel under the transmural pressure (fig. 13). The curved line represents the relation between elastic tension and stretch (i.e., the elastic diagram). For equilibrium we must have the law of Laplace (equation 6, $T = P_{TM} \times r$), which is represented by a straight line through the origin, the slope of which

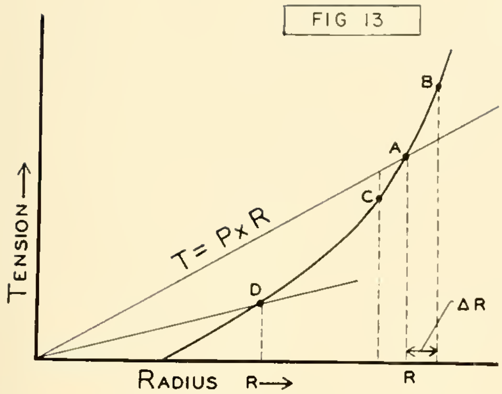

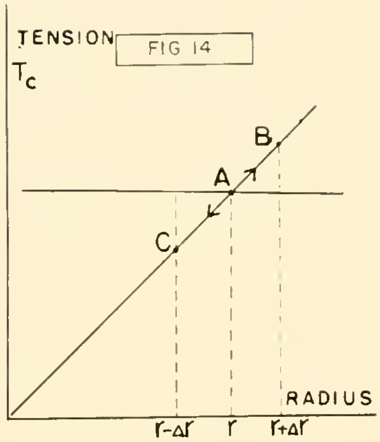

FIG. 13. Equilibrium diagram for a blood vessel wall under elastic tension alone.

FIG. 14. Equilibrium under active tension alone (soap film). [From Burton (5).]

(tangent of the angle) is equal to the transmural pressure, P_{TM}. The point A, where the "Laplacian line" and the curve intersect, represents the point of equilibrium. Its coordinates give the elastic tension in the wall and the radius of the vessel, that will pertain to the particular transmural pressure. If the pressure were reduced, a Laplacian line of reduced slope would result, intersecting the curve at D, indicating the reduced radius that would result at the reduced transmural pressure.

The equilibrium under transmural pressure and elastic tension alone is completely stable, if this is the shape of the tension-length diagram. Suppose that the radius were somehow to be increased from r, corresponding to point A, to $(r + dr)$, corresponding to point B. The tension in the wall, i.e., the ordinate of point B, would now be greater than the value required for equilibrium (point B'), so the net force would tend to reduce the radius back to the original value. Similarly, if the radius were supposed to diminish to point C, a radius $(r - dr)$, the tension would now be less than that required for equilibrium, and the net force would tend to increase the radius back to the original value. The intersection at A represents therefore "stable equilibrium."

12. THE PHENOMENON OF "BLOWOUT"

However, it must be recognized that if the transmural pressure is great enough, equilibrium may not be possible. The curve of tension vs. stretch for arteries does not continue to increase in slope, but becomes a straight line when the stretch is enough to have reached the unstretched length of all the collagenous fibers in the wall. If the Laplacian line has a slope great enough to be parallel to this final slope of the elastic line, no intersection is possible. The vessel radius will increase until the vessel bursts. This is the phenomenon of "blowout," familiar with the rubber inner tube of tires. The transmural pressure required for blowout can be calculated by equating the slope of the Laplace line to the final slope, i.e.,

$$P_{max} = \frac{dTc}{dr}_{max} \qquad (18)$$

The increase in the circumferential tension in the wall, per unit length of the vessel, is given, in terms of Young's Modulus:

$$dT_c = Y.\,t.\,\frac{dr}{r_0} \qquad (19)$$

where t is the thickness of the wall, dr is the increase in radius, and r_0 is the unstretched length of the fibers. When all the fibers are stretched, Y will reach its maximum value, Y_{max}. The product of Y and thickness may be called the "elastance" of the wall E, in dynes per unit elongation, i.e.,

$$\frac{dTc}{dr} = \frac{E}{r_0} \qquad (20)$$

Then the blowout pressure,

$$P_{max} = \frac{E_{max}}{r_0} \text{ dynes/cm}^2 \qquad (21)$$

i.e., to the ratio of the maximum elastance of the wall to the radius. This is, of course, provided the yield point or elastic limit were not reached, as the stretch increased, before the lines of figure 13 became parallel.

Roach & Burton (24) on autopsy specimens of

human iliac arteries found a value for the maximum Young's Modulus (from the final slope of elastic diagrams) of 7×10^6 dynes per cm² per 100 per cent stretch, for vessels of age 30, and 1.8×10^7 for age 80. The thickness of the wall was 0.7 mm, the radius 3.5 mm. Taking the smaller value for the modulus, blowout would occur at a pressure given by:

$$P = \frac{7 \times 10^6 \times 0.07}{0.35} = 1.4 \times 10^6 \text{ dynes/cm}^2$$

Since 1.3×10^3 dynes per cm² equals a pressure of 1 mm Hg, this is equivalent to over 1000 mm Hg. It must be concluded that blowout in normal arteries would never occur except at blood pressures at least 10 times the normal values (it was actually found that pressures of 900 mm Hg did not burst these iliac arteries). However, when disease has weakened the wall, blowout may occur at lower pressures.

13. EQUILIBRIUM UNDER ACTIVE TENSION ALONE

This is a hypothetical situation, where a vessel wall possessed negligible elasticity, but due to active contraction of smooth muscle had an active tension that was independent of the degree of stretch. The sphincters of the gut, and probably the "glomus-bodies" controlling flow through the arterial-venous anastomoses of the stomach vessels, and of the skin of the fingers and toes, possess very little elastic tissue but much smooth muscle. They would approach this case, but of course have some elasticity. (The surface tension in a soap film is the extreme situation of a tension that is independent of stretch of the surface.) Figure 14 shows this situation graphically. The Laplacian line intersects the horizontal line, representing the constant "active tension" at point A, which represents a possible equilibrium at radius r for the vessel. However, it is easily seen that this is a completely unstable equilibrium. If the radius were to increase to $r + \Delta r$, the tension required for equilibrium would be the ordinate of point B, i.e., greater than the tension existing in the wall. The pressure would then continue to increase the radius indefinitely. Similarly, a decrease in radius would result in the active tension exceeding the tension required for equilibrium (point C) and the radius would further decrease. Such complete instability is easily shown in soap bubbles if the pressure within them is kept constant. (A closed, isolated soap bubble is rendered stable because the pressure within automatically falls as its radius increases, by Boyle's law.) If the bubble is connected to a large reservoir of air under pressure, so that the pressure remains practically constant, or if the pressure is otherwise kept constant, a soap bubble is unstable.

14. EQUILIBRIUM UNDER ELASTIC TENSION PLUS ACTIVE TENSION

When, as in the real situation of a blood vessel wall, both elastic tension, a function of stretch, and an active tension independent of stretch are present, the situation is shown by figures 15 and 16. These are alternative ways of showing the conditions for equilibrium graphically, of which figure 15 is perhaps more enlightening. As in figure 13, the curve for the elastic tension only is shown, with the Laplacian line drawn for the particular transmural pressure of the vessels. The intersection, at point A, represents the equilibrium under elastic tension alone, with

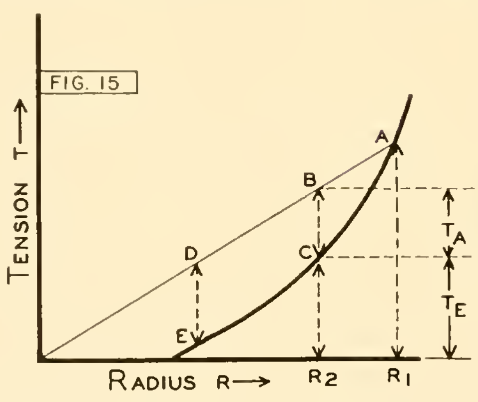

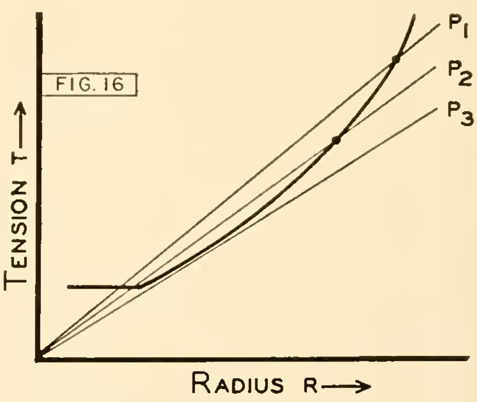

FIG. 15. Equilibrium under both active and elastic tensions. First method. [From Burton (5).]
FIG. 16. Equilibrium under both active and elastic tensions. Second method. [From Burton (5).]

the equilibrium radius R_1 and the elastic tension represented by AR_1. Suppose that due to the development of an active tension the vessel constricts to radius R_2. The total tension, elastic plus active, must be represented by the ordinate BR_2. Yet, since the stretch has decreased, the elastic tension has diminished from AR_1 to CR_2. Therefore the intercept BC, between the Laplacian line at B and the elastic line at C, must represent the amount of the active tension required to produce this diminution of the radius from R_1 to R_2, i.e., the two tensions T_A and T_C are represented by the two parts BC and CR_2 of the ordinate erected at R_2. In this way we can predict how much decrease in radius of the vessel will result from increasing the active tension by a given amount, e.g., a tension of a magnitude represented by DE will reduce the radius almost to the unstretched value. Thus a very small increase over that required to constrict from R_1 to R_2 will reduce the radius a great deal more. Since DE is the maximum intercept, once the radius has approached the unstretched radius R_0, no more active tension will be required to reduce the vessel to zero radius, i.e., to close it altogether (unless some new force, not represented in this diagram, intervenes).

15. THE CRITICAL CLOSING ACTIVE TENSION

We therefore conclude that if the transmural pressure is kept constant, and the active tension (vasomotor tone) is progressively increased, a critical value of this tension (represented by DE) could result in complete closure of the vessel. For a higher transmural pressure the straight line (Laplacian line) would have a steeper slope. The same conclusion would be reached, but the "critical closing active tension" would be greater. The term "critical" is used because an instability appears at this critical point. If, then, the transmural pressure remained constant, and the active tension (vasomotor tone) progressively increased, we would predict that "spasm," or "critical closure" of the vessel would result at a certain level of that vasomotor tone.

16. THE CRITICAL CLOSING PRESSURE

The same conclusion is reached, though more directly in terms of the existence of a "critical closing pressure" rather than a "critical closing active tension," by using the diagram of figure 16. Here the sum of the active and elastic tensions is plotted in the curve, rather than the elastic tension alone, as it was in figure 15. A constant amount of active tension (corresponding to a constant degree of vasomotor tone) has been added to raise the "elastic line" of figure 13 by the same amount for all radii. The Laplacian line for transmural pressure P_1 intersects the curve at two points. Of these, the upper point of intersection represents a stable equilibrium, the lower a completely unstable equilibrium of no real significance. Now imagine a progressive decrease in the transmural pressure P to P_2, P_3, etc. The slope of the Laplacian line will have to be progressively reduced. When a critical pressure (P_3) is reached, the line will touch (be tangent to) the curve. The point of contact of this tangent will represent a real equilibrium, which will be stable for increases in radius, but unstable for decreases in radius. (This is the sort of unilateral stability of a particle on the very edge of a table.) The Laplace line for any pressure less than this critical pressure will have no intersection with the curve at any point. This means that no equilibrium is possible with transmural pressures less than this critical value. The prediction can therefore be made that if vascular beds are in a state of constrictor tone, i.e., the walls of the arterioles have an active tension, independent of stretch, there would be a tendency to complete closure if the transmural pressure dropped below a "critical closing pressure."

17. THE CRITICAL CLOSING PRESSURE AS AN INDEX OF VASOMOTOR TONE

This critical closing pressure would increase, the greater the degree of vasomotor tone, i.e., the greater the active tension. This is because, on figure 16, the curve will be raised if the active tension is increased, so the slope of the tangent will be also increased. It is obvious from the diagram that the tangent will touch the curve at a point very close to the unstretched radius r_0, of the vessel, since this is where the curve begins to increase in slope. Thus, to a close approximation, the critical closing pressure (CCP)

$$\mathrm{CCP} = \frac{T_A}{r_0} \tag{22}$$

This is the basis for the use of the CCP of a vascular bed as an index of vasomotor tone, in terms of T_A. It has the advantage over the use of the resistance to

flow as an index of vasomotor tone in that there is no involvement of the viscosity of the blood (i.e., the CCP will be the same whether blood or Ringer's solution is used, a fact that has been checked experimentally). It has the disadvantage that to measure CCP we need to reduce the perfusion pressure, and thus the transmural pressure, until the flow is zero, which may lead to physiological changes in the tone of the smooth muscle, which we are attempting to measure (e.g., reactive hyperemia). The act of measurement may seriously disturb the quantity that is to be measured. If the pressure is reduced fast enough to the critical level, this may presumably be avoided. This is discussed further under the section dealing with the experimental verification of the theory of critical closure.

18. THE FUNDAMENTAL INSTABILITY OF VESSELS UNDER CONSTRICTOR TONE: THE STABILIZING ROLE OF ELASTIC TISSUE AND SENSITIVITY OF CONTROL

There are several ways of considering the origin of this property of instability in cylindrical blood vessels. Without any elastic tension, i.e., if there were no "automatic" adjustment of the tension in the wall with the degree of stretch, it has been seen (section 13) that there is complete instability of a cylindrical vessel. There can be only a precarious equilibrium between the dilating force of the transmural pressure and the constricting force of the tension in the wall. Departure from the equilibrium point of the slightest degree in either direction will be perpetuated. It is interesting to note that in the case of the glomus bodies of the A-V anastomoses of the stomach vascular beds (2), it has been shown (26) by the study of the passage of glass beads that these "shunts" are either "open" or "closed," and cannot hold intermediate positions. This is what the theory would predict for structures richly endowed with contractile muscle bands, but without obvious elastic fibers.

The presence of elastic tissue, which provides an elastic tension automatically increasing the total tension in the wall as the radius increases, removes this complete instability, but over a limited range only. If the transmural pressure exceeds the critical value given by equation 21, related to the maximum elastance of the wall, the instability reappears and blowout occurs. If the transmural pressure is less than that required to stretch the elastic fibers beyond their unstretched length (equation 22), once more the instability, under active tension, will be present.

In section 8 of this chapter a major role of elastic tissue on the walls of blood vessels was suggested; that of providing the "maintenance tension" to be in equilibrium with the blood pressure, without any expenditure of energy. We now see a second important role of elastic tissue, concerned not with steady conditions in the circulation, but with control of the distribution of blood Elastic tissue is necessary to make such control possible in a graded, stable manner.

Cybernetically considered, the arrangement of function between elastic tissue and smooth muscle is ideal for providing the greatest sensitivity of control. We start with a completely unstable situation, where sensitivity to the changes in vasomotor tone would be infinite, but without any possibility of proper control. By adding just enough of the automatic adjustment of tension of elastic tissue, stability is added, but very great sensitivity is still possible. This is reminiscent of the analogous device in electronics, in the early days of radio-receivers, having a positive feedback "plate-coil" which could be brought closer and closer (coupled to) a "grid-coil." To receive a faint signal one increased the coupling until about at the point of self-oscillation (instability), which would result in "howling," and interference with the reception by one's neighbors. By just falling short of the oscillating point, one could achieve a very great sensitivity indeed. The disadvantage is that the stability is limited, with "howling" in the radio-receiver, and critical closure in the control of the circulation (if indeed, this is a disadvantage in the disturbed physiological cases where it occurs). Certainly in the case of the arterial-venous anastomoses of vascular beds, the instability that leads to "open or closed" character of the operation of shunts may be advantageous.

19. EXPERIMENTAL VERIFICATION OF THE THEORY OF CRITICAL CLOSING PRESSURES AND CRITICAL CLOSING ACTIVE TENSIONS

Detailed discussion of this is not the function of this part of the *Handbook*. The physical theory seems incontrovertible, in indicating this type of fundamental instability in small blood vessels under vasomotor tone. Its prediction of CCP seems unequivocal, as being based essentially on the shape of the elastic diagram of the arterioles. The manifestation of CCP in vascular beds, however, might well be impossible, and the phenomenon predicted

by the theory of slight physiological importance. The following considerations apply.

a) The CCP might exist in vascular beds, but be of so small a magnitude, say 1 or 2 mm Hg, as to be of negligible importance in the circulation, where driving pressures (and thus transmural pressures) of 100 mm Hg or more are available to prevent the closure of vessels. The closure of some of the blood vessels of a vascular bed can be detected, in perfusing a vascular bed with a driving pressure which is steadily reduced. If closure takes place at a critically low value of the "arterial" pressure (which corresponds to a certain value of transmural pressure of the vessels which close), that flow will become zero even though the driving pressure has some significant positive value. If flow does so cease, the pressure drop up to the point of closure will disappear (no flow equals no gradient), so the arterial pressure will equal the transmural pressure of the closing vessels, i.e., is equal to the CCP.

b) In view of the fact that vascular beds have an enormous number of channels in parallel through which blood can flow from artery to vein, only if all such parallel channels suffer critical closure will the flow actually reach zero. It is therefore remarkable to find that in several different vascular beds, e.g., the frog's leg (20), the rabbit's ear (14, 20), the rabbit's hind limb (14, 20), the splanchnic vascular bed of dogs (1), the human forearm (4), finger (29), and the hind quarters of rats (11), such "zero-flow" pressures exist, or to find other evidences that arterial and venous systems are not connected (1, 10, 19).

c) Evidently in these beds no parallel channels lacking vasomotor tone, which would fail to close, exist. In other vascular beds there may be critical closure of certain vessels, but since other channels remain open (having very low or no CCP), flow will not fall to zero. However, a careful study of the flow-pressure curves in such cases should reveal an abrupt decrease of flow, though not to zero, at a critical level of perfusion pressure. Indeed, this has been observed in the case of the perfused mesenteric bed in the frog (Burton, unpublished data).

d) In the determination of CCP the perfusion of a vascular bed has to be reduced, and this may, in those cases where "reactive hyperemia" is a prominent feature as in the vessels of skeletal muscle, lead to a disappearance of the original tone, so no CCP will be found. The same may apply to the perfusion with a vasoactive agent, e.g., adrenaline, where there are enzymes, e.g., amineoxidase and O-methyl transferase, which rapidly destroy the agent. As the flow decreases, the enzymic destruction may catch up with the supply, so closure never occurs. In certain circumstances this may be illustrated, in a rabbit ear, by a periodic closure and opening up of the vessels when perfused by adrenaline solutions (19).

e) In many cases in the literature where the existence of closure (or zero-flow pressure) has been denied, the vascular beds under study were probably completely dilated and the pressure was not lowered enough to find the very low CCP that would be expected (5 to 10 mm Hg) in this case.

The proponents of the theory of critical closure are thus in the fortunate position of being able to explain the failure of many experimenters to find evidence of closure when the pressure is lowered, while citing many experimental positive evidences of its occurrence.

The possibility that the cessation of flow is due, not to an active closure of vessels under tone, but perhaps to obstruction of the lumen of vessels, was early excluded (fig. 17). In the experiments the flow-pressure curve was obtained by the "vertical tube method." The constant pressure head perfusing a rabbit's ear was cut off, so the ear was perfused from the column of solution in a vertical tube at the arterial cannula. As the flow proceeded at a steadily diminishing rate, the curve of fall of level in the tube allowed the rate of flow (from knowledge of the cross-sectional area of the tube) at each of the driving pressures to be calculated. With a pressor drug added to the perfusate, the fall of level, and the flow ceased altogether at the critical closing pressure. If at this point (fig. 17) some fluid was removed from the system, lowering the pressure below the critical point, it subsequently rose as shown. The only explanation seems to be that with the lowering of pressure more vessels under tone reach the critical state and close, forcing fluid retrogradely out of the artery as well as out of the venous side.

As for the existence of a critical closing active tension, this is generally accepted, for "spasm" of vessels endowed with smooth muscle has often been observed. In the view of the theory, "spasm" is simply evidence that the critical closing pressure has risen above the available blood pressure. The "critical" nature of such spasm is illustrated by figure 18, where a small rise of perfusion pressure above the critical value resulted in an abrupt opening to allow quite a considerable flow.

The theory of critical closure, and the experimental evidence for its occurrence, have been unacceptable

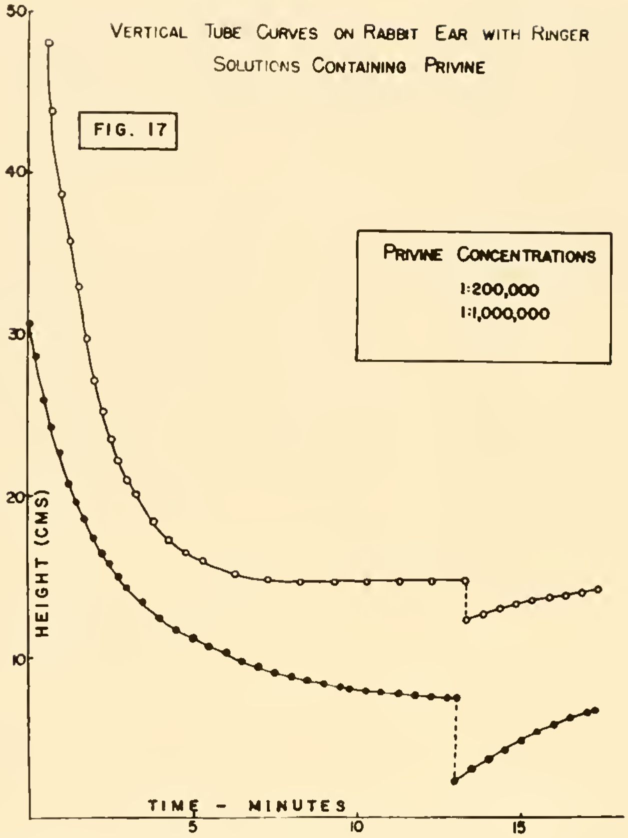

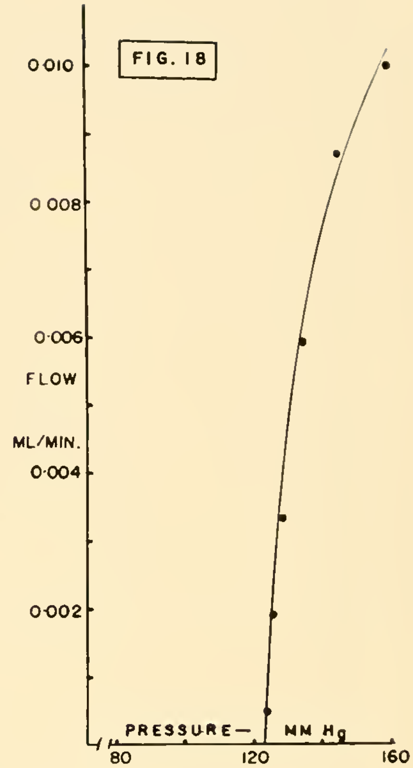

FIG. 17. Proof that the closure of the vessels in the rabbit ear at the CCP is active and not due to obstruction. For explanation see text. [From the work of Nichol (19).]

FIG. 18. The remarkably abrupt opening of a vascular bed of rabbit's leg in spasm, when the pressure was raised above a critical value. [From the work of Girling (14).]

to several physiologists. The objections and misunderstandings of the theory have been summarized in a paper by Folkow & Löfving (13) that should be studied by those wishing to consider both sides of the question.

20. WHICH VESSELS CLOSE AT THE CRITICAL PRESSURE?

The theory shows that the CCP will be given approximately by equation 22. We would therefore expect that the highest CCP, and the greatest tendency to close, would be in those vessels where the possibility of active tension, T_A, was greatest, and where at the same time the radius was least. The arterioles obviously are the most likely candidates for the "critical vessels." Although the capillaries are of smaller radius, their walls are not capable of any active tension, since they lack any smooth muscle.

There is definite experimental evidence that associates "critical closure" with the "resistance vessels" in a vascular circuit, indicating that the vessels that close are those which offer the greatest resistance to flow (at high perfusion pressures). If a number of results for CCP of a perfused vascular bed, produced by various vasoactive drugs and by stimulation, is plotted vs. the resistance to flow of these beds at a high transmural pressure, there is a very high degree of correlation (correlation coefficient > 0.9). If the vessels which were "critical," i.e., the ones that closed, were not those that offered the chief item of the total resistance to flow, we would not expect such a good correlation.

21. MINIMUM VALUES OF CRITICAL CLOSING PRESSURE: RESIDUAL CRITICAL CLOSING PRESSURE

The minimum value for CCP, even in vascular beds without any vasomotor tone, as produced by perfusion with cyanide to paralyze smooth muscle,

seems to be 5 to 10 mm Hg (20). The active tension causing this residual CCP is evidently physicochemical in nature, an "interfacial tension" between blood or perfusion solutions and the blood vessel wall. The evidence for this view is that only by the use of surface-tension lowering agents, e.g., bile salts, Tween 80, can this residual CCP be removed. An interesting confirmation of this physicochemical factor in the cerebrospinal fluid-vascular system has been found by Welch & Friedman (27), who studied the flow-pressure relations through the "valves" between the cerebrospinal fluid (CSF) and blood systems. There was no flow if the driving pressure went below 5 cm H_2O (4 mm Hg), unless Tween 80 was added, after which there was flow down to zero pressure. Yamada (30) found the CCP in the hind limbs of rats reached a minimum value of 10 to 15 mm Hg, but this was reduced by adding bile salts to the perfusate. The force causing closure in these cases would be like that (surface tension) which pulls together two cover slips with water between them, or that which holds a cylinder of water, flowing from a tap, from scattering. There is a good deal of suggestive evidence from other sources that an interfacial tension exists between blood and the endothelium of normal blood vessels. For example, the angle of contact of the meniscus of a bubble of air in a living vein is quite high, and decreases as the vessel wall deteriorates. Also there is a correlation between clotting time of blood and degree of wettability of surfaces with which it is in contact (17), yet clotting in the live vessel does not take place for many hours, even with stasis. Many other references to the role of interfacial tension are given by Nichol (18). A very small degree of "unwettability," a very low interfacial tension, would explain the residual CCP. When the arterioles lack vasomotor tone, the critical vessels are most likely to be the capillaries, because they have the smallest radius. Using equation 22 with a radius $r_0 = 5 \times 10^{-4}$ cm (5 microns), a residual CCP of 10 mm Hg would correspond to an interfacial tension of 5 or 6 dynes per cm. The surface tension of plasma vs. air is about 70 dynes per cm.

22. PHYSIOLOGICAL RANGE OF CRITICAL CLOSING PRESSURES

While the minimum CCP is the above residual CCP of 5 to 10 mm Hg, the values found for the various vascular beds studied under electrical stimulation of the sympathetic vasoconstrictor nerves range from a minimum of about 10 mm Hg to a maximum value, at a frequency of stimuli of 20 per sec, of about 60 mm Hg. In the human forearm (4) the values range from 15 mm Hg, when the subject is warm, and has a vasodilation, to 60 mm Hg when cold and in intense vasoconstriction. The values for the finger have a very similar range (29). In patients with essential hypertension (30) the values are much higher, up to 95 mm Hg. Similarly, the values in the hind limbs of normotensive rats ranged from 10 to 40 mm Hg, but in rats made hypertensive by Compound F the range was from 25 to 55 mm Hg (30). In the case of the rats and the hypertensive patients there was a very good correlation (coefficient greater than 0.9) between the CCP in standard conditions, and the level of sustained hypertension.

In conditions of disturbed physiology, as with secretion of adrenaline into the blood stream, or very violent sympathetic discharge, there is no doubt that CCP can reach very high values, leading to complete shutting off of vascular beds from the circulation.

23. APPLICATION OF THE LAW OF LAPLACE TO THE HEART

The application of the law of Laplace to the heart was made by Woods (28) before the turn of the century. He studied the radii of curvature and the thickness of the ventricular wall in autopsy hearts, fixed in alcohol. The measurement of curvature was made at a number of different points on the surface of the heart, by sticking in a pin normal to the surface and fitting arcs of circles to the surface at that point (fig. 4). The results are shown in table 2.

Woods argued that the tension in the wall was likely to be proportional to the thickness, t. If, then,

$$P = T\left(\frac{1}{R_1} + \frac{1}{R_2}\right)$$

and $$T = kt, \quad \text{then} \quad P = kt\left(\frac{1}{R_1} + \frac{1}{R_2}\right) \qquad (23)$$

and $t(1/R_1 + 1/R_2)$ should be a constant, for the left ventricle where P, in life, was about 120 mm Hg, and a different constant, about one-fifth of the value, for the right ventricle where P was about 25 mm. The table shows that his assumption was correct, for the figures in the last column are remarkably constant, in view of the wide range of values of the radii of curvature.

TABLE 2. *Adult Heart (Normal)*

Label of Point Chosen	r mm	r_1 mm	t mm	$t\left(\frac{1}{r}+\frac{1}{r_1}\right)$
		Under pressure 12 in right ventricle		
z_1	60	60	1.5	.050
c_2	65	80	2.0	.055
d_2	32	75	1.25	.055
a_2	75	90	2.2	.054
e_2	30	45	1.0	.055
f_2	55	90	2.0	.058
				Avg. .0545
		Left ventricle		
p_1	36	60	8.0	.35
z	32	80	8.5	.37
x_1	70	36	9.5	.39
r_1	30	80	8.5	.38
o_1	28	60	7.0	.36
s_1	70	40	8.5	.33
m_1	80	40	10.0	.37
w_1	32	80	8.5	.34
f_1	55	16	5.0	.40
t_1	70	24	6.0	.33
v_1	24	70	6.5	.36
n_1	60	24	6.0	.35
				Avg. .36

The thickness of the ventricular wall, which is much greater in the "flatter" portions of the wall than at the highly curved apices, then is in accordance with the law of Laplace. Woods drew an important conclusion as to the dilated heart. If the heart were to dilate to twice its original linear dimensions (remaining geometrically similar), the radii of curvature would be doubled. The value of $(1/R_1 + 1/R_2)$ would be halved, at every point on the ventricular wall. Thus, to produce the same systolic pressure, the tension T, per unit length of a hypothetical slit in the ventricle, would have to be doubled. Since the total length of such a cut (fig. 19) would also be doubled, the conclusion is inescapable that in a heart dilated to twice its normal size the force of contraction per ventricular muscle fiber would be four times as great (8).

This factor of geometry of the heart, and mechanical advantage, or "disadvantage," of the ventricular muscle in producing pressure within the cavity cannot be ignored in the explanation of the decompensation of congestive heart failure. While an "overstretching" of the fibers, which has been usually cited as explanation, may be a real factor, the consequences of the law of Laplace are equally, perhaps more, important. The influence of this upon the "load" of the heart, related to the O_2 consumption and total energy turnover of the heart muscle, has

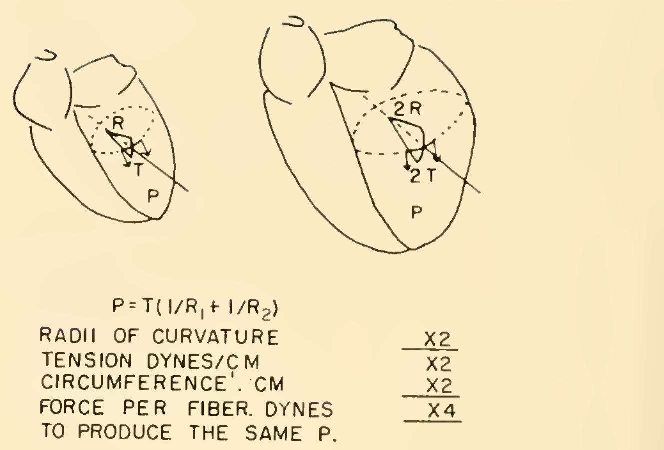

FIG. 19. Effect of doubling the size of the heart on the tension required in ventricular muscle to produce a given systolic pressure. [From Burton (8).]

been pointed out (9). The major factor in this load is not the mechanical work of pumping, but the steady energy consumption to maintain tension in the muscle for a given length of time, i.e., the "tension-time integral" of the ventricular muscle. The practical implication is that increasing the mechanical work of the heart, as in exercise, is not per se as important in increasing the load of the heart as are increases in sytolic pressure, in heart rate, and in the size of the heart.

24. MEASUREMENT OF ACTIVE TENSION IN VASCULAR SMOOTH MUSCLE

The final development of the body of theory concerned with the physical equilibrium has been the attempt to devise methods for measuring the actual tension of vascular smooth muscle under vasomotor tone or vasoactive drugs. The basic difficulty is that when a blood vessel constricts, the total tension in the wall, if the transmural pressure is unchanged, has decreased, according to the law of Laplace. However, as has been shown, this is because though the active tension, T_A, has increased, the elastic tension, T_E, has more than nullified this, in the total tension, by its automatic decrease (fig. 15) because of less stretch. Thus the relation between the radius of the vessel, of which the resistance to flow can serve as an index, and the magnitude of T_A is a very complicated and nonlinear one. Only if the details of the elastic behavior of the vessel were known could the changes in active tension be deduced.

An attempt has been made to devise a "null

method" to overcome this difficulty (9). It suffers from the usual limitations of any method which depends upon a "lumped parameter" theory. In this instance the assumption is made that the actual resistance to flow of a vascular bed can be considered as if it were the resistance of a "single equivalent vessel" representing the actual distributed resistance and distributed distensibility of the whole bed. With respect to the resistance, this assumption is not too far from validity, since so much of the total resistance, particularly with vasomotor tone, resides in the arterioles.

The principle of the method is that if, after the active tension has increased producing a decrease in radius (and increase in resistance), the resistance vessels were brought back to their original size, then the elastic tension would be the original elastic tension. The increase in total tension would then be entirely due to this increase in active tension,

$$T = T_A + T_E = T_A + f(r) \qquad (24)$$

and if r is unchanged,

$$\Delta T = \Delta T_A = \frac{\Delta P_{TM}}{r} \qquad (25)$$

The method of constant flow perfusion was used for an isolated rabbit's ear. When pressor agents, e.g., adrenaline, were added to the perfusate, the vasoconstriction showed itself by increase in driving pressure (measured by the pressure at the arterial cannula).

An increase in transmural pressure of the vessel was then produced by lowering the tissue pressure. The ear was in a box, in which pressures less than atmospheric could be produced. With sufficient negative pressure, the driving pressure could be reduced to the original value that had been recorded before the vasoconstriction had occurred. At this "null point," both flow and driving pressure were at their original values, so the resistance and the radius of an "equivalent single vessel" would also be at their original values. In this circumstance, the change in active tension that had occurred would be proportional to the change in P_{TM}, i.e., to the negative tissue pressure that had been required to reach the null point, i.e.,

$$T_A = -r \times \Delta P_T \quad (r \text{ constant}) \qquad (26)$$

It would be quite impractical to use such a null method routinely to measure active tension, for the large negative tissue pressure very soon causes edema of the tissues of the ear, and leakage from distended venous vessels. However, the method could be used to find whether any of the more commonly used methods of measuring the effect of pressor drugs on vascular beds might give a linear relation to the active tension. There are three ways one can make resistance measurements on vascular beds.

a) At constant pressure of perfusion, measuring the reduction in flow when vasoconstriction occurs. The results can be expressed as an increase in vascular resistance.

b) At constant flow, as provided by a positive perfusion pump, measuring the rise of driving pressure that occurs when vasoconstriction occurs. Again the results can be expressed as an increase of resistance.

c) As in the intact animal, where neither driving pressure nor flow is kept constant, though often the pressure is not altered so much as the flow. Here changes in both pressure and flow must be measured, and the change in resistance calculated.

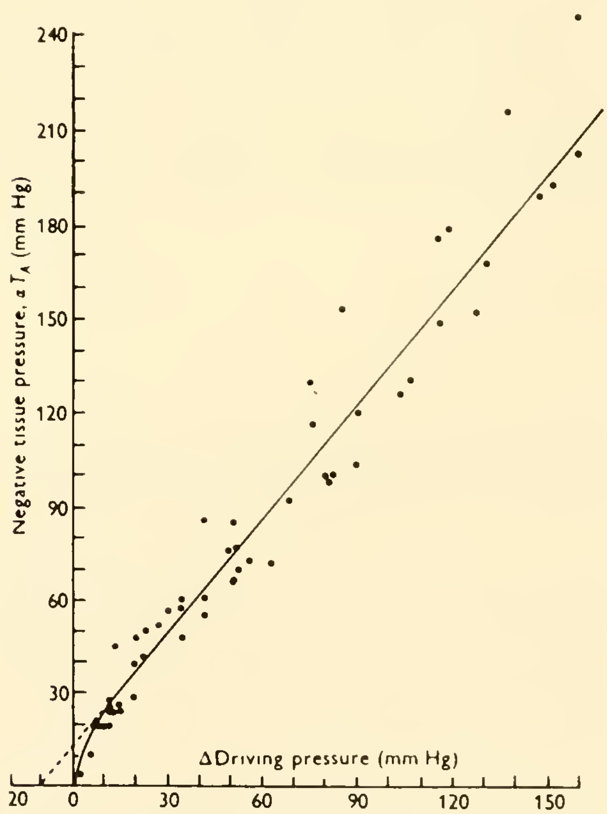

FIG. 20. Linear relation between the active tension in vascular smooth muscle, as estimated by the null method, and the rise in arterial pressure at constant flow. Data for 10 different rabbit ears are included; for individual ears the correlation was much higher. [From Burton & Stinson (28).]

It is obvious that results from these three methods cannot all be linearly related to active tension, for a plot of change of resistance vs. concentration of drug is of very different shape according to whether constant pressure or constant flow is used. It was shown by the experiments that the method of constant flow gave results that were remarkably linear, except near the origin (fig. 20), with the active tension measurements (by the null method). In contrast, measurements of changes of resistance with constant pressure perfusion were completely nonlinear (indeed, when the active tension reaches the critical value, the increase of resistance becomes infinite). Theoretical justification for this astonishing and convenient result is given in the original publication (9), which should be consulted for details.

It seems therefore (though other vascular beds might be different from the rabbit ear) that to obtain a practical measure of the degree of active tension in vascular smooth muscle, the method of constant flow perfusion should be used, where this is possible. On the other hand, where the greatest sensitivity for qualitative assay of vasoactive drugs is desired, the method of constant pressure perfusion is much to be preferred, particularly if the conditions can be such that the vessels are close to their critical closing state, when the sensitivity to vasoactive agents is very high indeed.

APPENDIX

PRESSURE GRADIENT THROUGH THE VESSEL WALL

As explained in section 6, the law of Laplace applies across each successive coaxial shell of the wall, and integration of the equation:

$$dP/dr = -T_r'/r \qquad (1)$$

will give the way in which the pressure falls through the thickness of the wall. The integration is easily made for idealized cases, but the actual case has so many complications that only understanding of the general trends in the solution is worth while. Details of the mathematical solutions are given elsewhere. Only the general result is important.

Case 1: Active Tension Only in the Wall

This is a purely hypothetical case, since, as has been shown, without automatic adjustment of tension to stretch, a cylindrical vessel is completely unstable. However, a very muscular small artery maintained in strong contraction of the smooth muscle might approach this case, though the elasticity of the smooth muscle itself could not be ignored. The ventricular wall of the heart, during systolic contraction, might also approach this case, though, as Rushmer *et al.* (25) have shown, the considerable elasticity of the fibers between the layers of muscle is of great importance in the heart's action.

Considering the tension T'_r to be constant through the wall equal to T', we have:

$$P = -T' \int \frac{dr}{r} = -T' \ln r + c \qquad (2)$$

where C is the constant of integration. Inserting into this equation the boundary conditions, i.e., that for $r = r_i$, $P = P_{iv}$, and for $r = r_o$, $P = P_t$, yields the relation for the pressure P_r at radius r.

$$P_r = P_{IV} - \frac{P_{TM}}{\log r_o/r_i} \log r/r_i. \qquad (3)$$

The pressure through the wall thus falls off in a logarithmic curve. Actually the gradient will not be very far from linear, even where the artery is very thick-walled, as in arterioles (thickness of wall equal to half the radius of lumen). Here we have:

$$\log r/r_i = 0.1761 \times \frac{P_{IV} - P_r}{P_{TM}} \qquad (4)$$

This shows that for the pressure to have fallen to three-fourths of the intravascular pressure $(P_{iv} - P_r)/P_{TM} = 0.25$, r/r_i will be 1.11, i.e., the pressure falls by 25 per cent of its value in the innermost 22 per cent of the wall. Similarly it falls to 50 per cent in the inner 45 per cent, and by 75 per cent in the inner 71 per cent of the thickness of the wall (fig. 21). If the

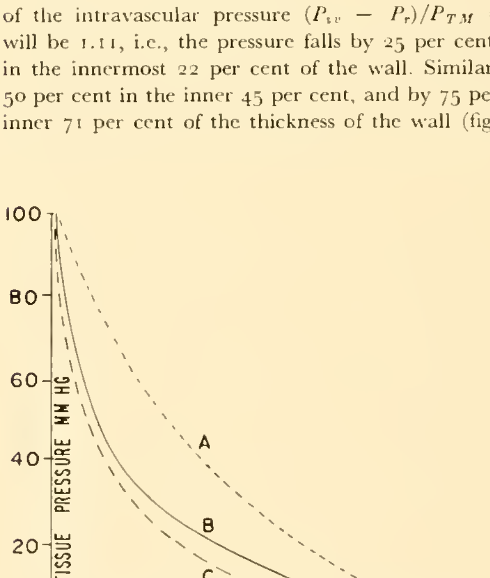

FIG. 21. Calculated fall of pressure in the wall of an artery, with a transmural pressure of 100 mm Hg. For all curves it is assumed that the elasticity is uniformly distributed through the wall. *A:* on the basis of Hooke's law. *B:* on the basis of the experimentally determined nonlinear elasticity of young arteries (20–40 years). *C:* for old arteries (60–80 years).

TABLE 3. *Ratio, as a Percentage, of the Elongation of the Fibers in the Vessel Wall as Radius r to that of the Innermost Fibers, at Radius r_i, for Various Values of the Percentage Elongation (α) of the Innermost Fibers*

α	$r/r_i =$ 1.1	1.2	1.5	1.7	2.0
%					
10	84	70	47	36	26
20	85	72	47	37	28
50	85	74	49	40	29
70	85	75	51	43	31
100	85	75	53	43	32
Average, %	85	73	49	40	29
Approximate formula (6), %	83	69	44	35	25

thickness of the wall compared to the radius of lumen is less, the gradient is even more linear.

Case 2: Purely Elastic Artery

Here we assume that the tension is purely due to stretch, and the variation of tension with radius will depend, in addition, on how the degree of stretch varies through the thickness of the wall. It has perhaps not been generally realized that this degree of stretch must be very different for different layers in a thick-walled elastic tube, where, as with the tissues of the wall of blood vessels, the material is practically incompressible. Let us assume, for simplicity, that when the transmural pressure increases the artery increases in diameter, but not in length. Fenn (12) has shown that this is very closely the case for arteries, though it is very far from true for some other vessels (such as the abdominal vena cava). In this case the cross-sectional area of the wall from inside to a given radius, r, must remain constant. Suppose that when the inner radius r_i increases to αr_i (the innermost circumferential fibers will be stretched in the ratio of α:1), r becomes βr. Then, because of the incompressibility, we must have:

$$\pi(r^2 - r_i^2) = \pi(\beta^2 r^2 - \alpha^2 r_i^2)$$
$$\therefore \beta^2 = 1 + (\alpha^2 - 1)(r_i/r)^2 \qquad (5)$$

The degree of stretch β of the fibers in the wall will be progressively less as we proceed through the thickness of the wall. From equation 5 we can construct a table showing the percentage of stretch of fibers at radius r over the percentage of stretch of the innermost fibers, of radius r_i, for various ratios of r/r_i, and degrees of stretch α of the innermost fibers.

The table shows that the ratio of elongation is only slightly altered by the degree of stretch, and is given quite well by the approximation to equation 5 obtained for small degrees of stretch, i.e.

$$\alpha = 1 + \delta \quad \text{where} \quad \delta \ll 1$$

$$\alpha^2 \simeq 1 + 2\delta, \qquad \beta^2 \simeq 1 + 2\delta(r_i/r)^2, \qquad (6)$$

$$\beta = 1 + \delta(r_i/r)^2(\beta - 1) \simeq (\alpha - 1)(r_i/r)^2.$$

Equation 6 gives a very simple rule. In a thick-walled vessel the degree of elongation ($\beta - 1$) of the outer layers is very much less than that of the inner layers. Correspondingly, the elastic tension in the inner layers will be much higher than that of the outer layers, and the tissue pressure will fall off much more rapidly in the inner layers than in the rest of the wall.

The next step is to translate the degree of stretch in the different layers of the wall into the elastic tension it will produce. The simplest case is to assume that the elastic diagram follows Hooke's law, though this is very far from applying to the arterial wall.

$$T'_r = k(\beta - 1) = k\left[\left(\frac{(\alpha^2 - 1)r_i^2}{r^2} + 1\right)^{1/2} - 1\right]$$
$$= k\left[\left(\frac{A^2 + r^2}{r^2}\right)^{1/2} - 1\right] \qquad (7)$$

where $A \equiv (\alpha^2 - 1)r_i^2$

Inserting this value into equation 1 gives

$$P = -k\int\left(\frac{(A^2 + r^2)^{1/2}}{r^2} - \frac{1}{r}\right)dr \qquad (8)$$

Fortunately, this integral has a standard from which can easily be evaluated

$$P = k[ln(1 + a) - a] + \text{Constant}. \qquad (9)$$

where $a \equiv \dfrac{(A^2 + r^2)^{1/2}}{r}$

By inserting boundary conditions for any given case, the curve of fall of pressure through the wall can be determined (fig. 21). It is much more marked in the innermost layers, so that the pressure has fallen to half in the first 28 per cent of the wall thickness.

A simpler solution is to use the approximate solution, equation 6, which gives

$$P = -kr_i^2\int\frac{dr}{r^3} = \frac{kr_i^2}{2} \times \frac{r_i^2}{r^2} + \text{Constant}.$$

and a parabolic type of curve of fall of pressure.

These solutions, however, do not approach reality for arteries where the tension-length diagram is very far from linear. Resort may be had to graphical integration, using an actual tension-length diagram of an artery (cf fig. 11). The result is an even steeper fall of pressure in the inner layers of the wall (fig. 21) for the young vessels, and yet steeper for the old vessels. It is clear that the tissue pressure in the wall of arteries falls to half the intravascular pressure in a small inner proportion of the thickness of wall, possibly in the first 10 per cent. The exact curve depends on the degree of stretch. The more the vessel is stretched, the more the steep gradient is shifted to the inner layers.

The above calculations, even the final more sophisticated one, assume uniform distribution of elasticity through the wall, which can hardly be the case. The usefulness of the theory lies in the possible insight it may give as to why the various elements of different elasticity, elastin and collagen, are arranged as they are in different arteries.

REFERENCES

1. ALEXANDER, R. S. The influence of constrictor drugs on the distensibility of the splanchnic venous system analyzed on the basis of an aortic model. *Circulation Res.* 2: 140–147, 1954.
2. BARLOW, T. E. Vascular pattern in the alimentary canal. Visceral Circulation. *Ciba Foundation Symposium.* London: Churchill, 1952, p. 21–36.
3. BRAMWELL, J. C., A. V. HILL, AND B. A. MCSWINEY. Velocity of the pulse in man as related to age as measured by the hot-wire sphygmograph. *Heart* 10: 233–255, 1923.
4. BURTON, A. C., AND S. YAMADA. Relation between blood pressure and flow in the human forearm. *J. Appl. Physiol.* 4: 329–339, 1951.
5. BURTON, A. C. Physical equilibrium of the small blood vessels. *Am. J. Physiol.* 164: 319–329, 1951.
6. BURTON, A. C. Relation of structure to function of the tissue of the wall of blood vessels. *Physiol. Rev.* 34: 619–642, 1954.
7. BURTON, A. C., AND E. ROSENBERG. Effects of raised venous pressure in the circulation of the isolated perfused rabbit ear. *Am. J. Physiol.* 185: 465–470, 1956.
8. BURTON, A. C. The importance of the size and shape of the heart. *Am. Heart J.* 54: 801–810, 1957.
9. BURTON, A. C., AND R. H. STINSON. The measurement of tension in vascular smooth muscle. *J. Physiol.* 153: 290–305, 1960.
10. DAVIS, D. L., AND W. F. HAMILTON. Cross circulation at the small blood vessel level in the dog paw. *Am. J. Phsyiol.* 199: 1169–1176, 1960.
11. DOYLE, A. E. The estimation of peripheral vascular resistance to varying rates of flow in the isolated rat hindquarters. *Circulation Res.* 1: 375–379, 1953.
12. FENN, W. O. Changes in length of blood vessels on inflation. In: *Tissue Elasticity*, edited by J. W. Remington. Washington, D. C.: Am. Physiological Soc. 1957.
13. FOLKOW, B., AND B. LÖFVING. The distensibility of the systemic resistance blood vessels. *Acta Phsyiol. Scand.* 38: 37–52, 1957.
14. GIRLING, F. Vasomotor effects of electrical stimulation. *Am. J. Physiol.* 170: 131–135, 1952.
15. HAYNES, R. H., AND A. C. BURTON. Role of non-Newtonian behaviour of blood in hemodynamics. *Am. J. Physiol.* 197: 943–950, 1959.
16. HAYNES, R. H. Physical basis of the dependence of blood viscosity on tube radius. *Am. J. Physiol.* 198: 1193–1200, 1960.
17. MOOLTON, S. E., L. VROMAN, G. M. S. VROMAN, AND B. GOODMAN. Role of blood platelets in thrombo-embolism. *A.M.A. Arch. Internal Med.* 84: 677–710, 1949.
18. NICHOL, J. T. The hemodynamics and reactivity of the rabbit ear. (Ph.D. Thesis) London, Ont.: Univ. of Western Ontario, 1950.
19. NICHOL, J. T., AND A. C. BURTON. Effects of adrenaline on flow in isolated perfused rabbit's ear. *Am. J. Physiol.* 162: 280–288, 1950.
20. NICHOL, J. T., F. GIRLING, W. JERRARD, E. G. CLAXTON, AND A. C. BURTON. Fundamental instability of small blood vessels and critical closing pressures in vascular beds. *Am. J. Physiol.* 164: 330–344, 1951.
21. NICHOL, J. T. The effect of cholesterol feeding on the distensibility of the isolated thoracic aorta of the rabbit. *Can. J. Biochem. & Physiol.* 33: 507–516, 1955.
22. ROY, C. S. Elastic properties of the arterial wall. *J. Physiol.* 3: 125–159, 1880–82.
23. ROACH, M. R., AND A. C. BURTON. The reason for the shape of the distensibility curves of arteries. *Can. J. Biochem. & Physiol.* 35: 681–690, 1957.
24. ROACH, M. R., AND A. C. BURTON. The effect of age on the elasticity of human arteries. *Can. J. Biochem. & Physiol.* 37: 557–569, 1959.
25. RUSHMER, R. F., D. K. CRYSTAL, AND C. WAGNER. The functional anatomy of ventricular contraction. *Circulation Res.* 1: 162–170, 1953.
26. WALDER, D. N. Arterial anastomoses of the human stomach. *Clin. Sc.* 11: 59–71, 1952.
27. WELCH, K., AND V. FRIEDMAN. The cerebrospinal fluid valves. *Brain* 83: 454–469, 1960.
28. WOODS, R. H. A few applications of a physical theorem to membranes in the human body in a state of tension. *J. Anat. and Physiol.* 26: 362, 1892.
29. YAMADA, S. Effects of positive tissue pressure on blood flow in the finger. *J. Appl. Physiol.* 6: 495–500, 1954.
30. YAMADA, S. *Increased vascular resistance in hypertension.* (Ph.D. Thesis) London, Ont.: Univ. of Western Ontario, 1955.

Propagation of pulse waves in visco-elastic tubings

VICTOR HARDUNG *Physiologisches Institut der Universität Freiburg, Freiburg, Switzerland*

CHAPTER CONTENTS

EXACT UNDERSTANDING of the physical phenomena which come into play in the arterial system as a consequence of heart action has been developing rather slowly. This is due in part to the very complicated geometric and physical structure of that system. Also, it may be due in part to the tendency of many investigators to look upon these phenomena as a single entity, without having a clear picture of the different individual physical elements which are the basis of the response as a whole.

The author's personal research published in this chapter has been supported by grants from the Swiss National Foundation for Scientific Research and the Office for Creation of Employment Possibilities.

Such an individual element is the propagation of a pressure wave or pulse wave in a tube with visco-elastic walls filled with viscous fluid. This present chapter deals mainly with this phenomenon. It does in no way claim completeness. Indeed, at this time completeness would not be possible, because even in this narrow field many questions still remain unanswered.

The purpose of the present article is merely to give to the investigator in hemodynamics a clear and, insofar as possible, a simple and illustrative description of all the physical phenomena which may be of importance for pulse-wave propagation in the arterial system.

In order to see how these physical principles can be applied to actual hemodynamics, the reader should consult the very clear monograph, *Blood Flow in Arteries* by D. A. McDonald (10), which appeared recently.

We will not overburden our treatise with a detailed description of the historical development. The interested reader will find a good account in a paper by P. Lambossy (7).

The mathematical development in this chapter does not claim to compete with the more detailed, and in many ways more accurate, hydrodynamic theories of Korteweg (6), Frank (3), Morgan & Kiely (11), Lambossy (8), and Womersley (24). We have merely tried to give a semi-empirical and phenomenological treatment of the kind most used in engineering. Where needed, the treatment includes results of experiments and the afore-mentioned hydrodynamic theories.

1. FUNDAMENTAL NOTIONS AND EQUATIONS FOR THE PULSE WAVE

In order to obtain a clear and illustrative picture of the pulse-wave phenomenon, we will start with a simplified and approximate mathematical description, which we shall improve and complete stepwise as we penetrate deeper into the matter.

For this purpose let us first consider wave propagation in an infinitely long tube, the walls of which are completely elastic; that is to say, the wall material does not show any elastic hysteresis or internal friction, and its stress-strain relationship obeys the law of Hooke. In addition, let us consider the whole problem as essentially a linear one, and suppose the pressure and velocity of the liquid to be constant over the entire cross section of the tube.

If we produce, in a straight elastic tube of infinite length, a sinusoidal pressure variation at a given point $z = 0$, a pressure wave will start from this point in both directions. Let the pressure at this point be

$$p(z = 0, t) = P_0 \sin \omega t \tag{1.1}$$

where ω denotes the angular frequency $2\pi\nu$, ν being the frequency in cycles per second. At any other point z on the tube we observe then, assuming damping to be negligible, a pressure variation of the form

$$p(z, t) = P_0 \sin \omega \left(t - \frac{z}{v} \right) \tag{1.2}$$

In order to understand the physical meaning of that equation, let us assume some arbitrary value for p and then follow that value of p as it progresses along the tube; that is to say, we shall look for the mathematical expression indicating that p is constant. Obviously p remains constant if $t - z/v$ remains constant. If t increases, as from t to t', we must proceed along the tube for a distance $z' = vt'$ in order to find the same pressure again; v signifying the speed of propagation.

As a consequence of pressure variations along the tube, the particles of the liquid will likewise undergo some displacements from their equilibrium positions, which will also vary according to a sinusoidal function

$$\zeta(z, t) = \zeta_0 \sin \left[\omega \left(t - \frac{z}{v} \right) + \psi \right] \tag{1.3}$$

where ψ accounts for a phase shift which might occur between pressure and displacement. The particle velocity $u = d\zeta/dt$ is therefore described by the formula

$$u = \zeta_0 \omega \cos \left[\omega \left(t - \frac{z}{v} \right) + \psi \right] = u_0 \cos \left[\omega \left(t - \frac{z}{v} \right) + \psi \right] \tag{1.4}$$

As a consequence of friction, due to the viscosity of the liquid, the amplitude will generally decrease with increasing distance from the source. To account for this damping of the wave, let us first consider the simplest case, assuming an exponential decrease of the amplitude

$$p(z, t) = P_0 e^{-\beta z} \sin \omega \left(t - \frac{z}{v} \right) \tag{1.5}$$

where β denotes the damping constant. Similar formulas can be used for ζ and u as well.

It is the purpose of the pulse-wave theory to determine the quantities v, β, and ψ from the geometric and physical properties of the tube and its filling.

In order to derive the fundamental equations, let us consider a tube of radius r and cross-sectional area $Q = \pi r^2$. When the wave travels along the tube, the cross-sectional radius r varies with the coordinate z

---

SYMBOLS USED IN THE TEXT

a = wall thickness
i = flow (or current in electrical analog)
$j = \sqrt{-1}$
$k = a/r$ ratio of wall thickness to tube radius
l = length
m, n = integral numbers
p = pressure
r = tube radius
t = time
u = particle velocity (alternating electrical tension in electrical analog)
v = phase velocity
v = group velocity
x, y, z = coordinates
$C = \eta a/(2 r\rho)$
$\mathbf{C}$ = capacity
E = Young's modulus of elasticity
$\mathbf{G}$ = conductivity
$\mathbf{L}$ = self-induction
I = complex amplitude of flow with respective indices
P = complex amplitude of pressure with respective indices
Q = cross section of tube
R, R_1, R_2 = resistance constants
$\bar{R}$ = reflection coefficient
$\mathbf{R}$ = ohmic resistance
T = time of period
V = volume
Z = surge impedance
$\alpha = \omega/v$ or $\alpha = r\frac{\sqrt{\omega\varphi}}{\eta}$
β = damping constant
$\gamma = \beta + j\alpha$ complex propagation constant
$\varphi\psi$ = phase angles
η = viscosity of tube wall
η_1 = viscosity of liquid
ν = frequency
ζ = displacement in Z-direction
ρ = density of fluid
σ = Poisson's ratio
ω = angular frequency $= 2\cdot\pi\cdot\gamma$

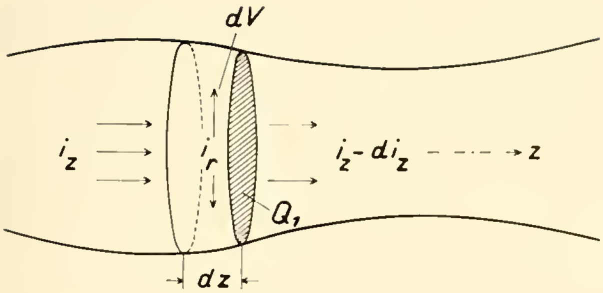

FIG. 1

and the time t; that is to say, $r = r(z, t)$ and $Q = Q(z, t)$. Let us consider as an element of volume a small disc of thickness dz and radius r (see fig. 1). The driving force acting on it in the z-direction is then given by

$$dF_z = -(Q\cdot p)_{z+dz} + (Q\cdot p)_z = -\frac{\partial(Q\cdot p)}{\partial z}\,dz \qquad (1.6)$$

or

$$-dF_z = -Q\cdot\frac{\partial p}{\partial z}\cdot dz - p\cdot\frac{\partial Q}{\partial z}\cdot dz \qquad (1.7)$$

If the relative change dQ/Q is sufficiently small, dQ/dz will also be small and we may drop the second term in equation 1.7. Thus we will have

$$dF_z = Q\cdot\frac{\partial p}{\partial z}\cdot dz \qquad (1.8)$$

The small disc contains the mass $dm = \rho Q\,dz$. Application of Newton's law (force = mass times acceleration) gives the equation the following form

$$\rho\cdot\frac{\partial^2\zeta}{\partial t^2} = -\frac{\partial p}{\partial z} \qquad (1.9)$$

Now, instead of displacement ζ let us use flow volume, which is often used in theoretical acoustics. It is defined as the product of the cross section and the mean particle velocity $d\zeta/dt$. As we have assumed the velocity to be constant over the entire cross section of the tube and the variations in the cross section to be small, we now obtain for the flow volume in z-direction

$$i_z = Q\cdot\frac{d\zeta}{dt} \qquad (1.10)$$

and Newton's equation takes the form

$$\frac{\partial i_z}{\partial t} = -\frac{Q}{\rho}\cdot\frac{\partial p}{\partial z} \qquad (1.11)$$

A further important relationship is furnished by the so-called equation of continuity. For our case, this is identical with the statement that the intake of volume on the front side is equal to the sum of the outflow from the back and the increase in volume of the disc being considered. In mathematical language this is stated as:

$$di_z(z\ t) = \frac{\partial i_z}{\partial z}\,dz = -\,di_r \qquad (1.12)$$

where i_r denotes a radial current. We need still another relationship between the increase of pressure and the corresponding increase in radius. If the pressure on the outside of the tube is taken to be zero, the pressure p in the tube will create a tangential wall tension pr (force per unit length). According to Hooke's law, a strip of wall material of thickness a, width dz, and length $2\pi r$ will be stretched under the influence of a pressure increase dp to the amount

$$2\pi dr = \frac{1}{E}\cdot\frac{\pi 2r}{a\cdot dz}\,d(p\cdot r)\cdot dz \qquad (1.13)$$

where E is Young's modulus of elasticity. Considering as negligible $p\ dr$ as against $r\ dp$,[1] we obtain finally

$$dp = (Ea/r^2)\cdot dr \qquad (1.14)$$

Introducing the radial current $di_r = dr/dt\ 2\pi r\ dz = -di_z$ we obtain

$$-\frac{\partial p}{\partial t} = \frac{1}{2\pi}\frac{\partial i_z}{dz}\,(E\cdot a/r^3) \qquad (1.15)$$

Differentiation with respect to z gives

$$-\frac{\partial}{\partial z}\left(\frac{\partial p}{\partial t}\right) = \frac{E\cdot a}{2\pi r^3}\frac{\partial^2 i_z}{\partial t^2} - \frac{3\cdot E\cdot a}{2\pi r^4}\cdot\frac{\partial i_z}{\partial z}\cdot\frac{\partial r}{\partial z} \qquad (1.16)$$

For small relative changes in r the second term on the right side can again be dropped, and we obtain finally the equation

$$-\frac{\partial^2 p}{\partial t\partial z} = \frac{E\cdot a}{2\pi r^3}\frac{\partial^2 i}{\partial z^2} \qquad (1.17)^2$$

We can eliminate the current from equations 1.11 and 1.17 if we differentiate the former twice with respect to z and the latter once with respect to t. This leads to

$$\frac{Q}{\rho}\frac{\partial^2 p}{\partial z^2} = \frac{2\pi r^3}{E\cdot a}\frac{\partial^2 p}{\partial t^2}$$

[1] We always postulate the relative variation in radius dr/r to be sufficiently small.

[2] The index Z is omitted in this and the following equations.

or with $Q = \pi r^2$ to

$$\frac{\partial^2 p}{\partial t^2} = \frac{E \cdot a}{2r\rho} \frac{\partial^2 p}{\partial z^2} \tag{1.18}$$

This equation is known in physics as the wave equation. It describes the propagation of any periodic or nonperiodic disturbance in the z-direction. Solution of the equation in an analogous way for current rather than pressure leads to the same equation

$$\frac{\partial^2 i}{\partial t^2} = \frac{E \cdot a}{2r\rho} \frac{\partial^2 i}{\partial z^2} \tag{1.19}$$

for the current. If we take for p or i any arbitrarily chosen function $f(t - z/v)$ of the expression $(t - z/v)$, we see at once, by carrying out the differentiations, that it represents a solution of 1.18 or 1.19 if

$$v = \left(\frac{E \cdot a}{2r\rho}\right)^{1/2} \tag{1.20}$$

which is the well-known "Moens-Korteweg equation." A special solution of 1.18 is, of course,

$$p(z) = P_0 \sin \omega(t \mp z/v)$$

where the minus sign corresponds to a wave running in the positive, the plus sign to a wave running in the negative z-direction.

In regard to the derivation of the wave equation, some remarks must be made concerning equation 1.15. This equation holds strictly only for static conditions. Under dynamic conditions the variable part of internal pressure must not only balance the increasing elastic-restoring force but also the inertial resistance of the mass of a part of the liquid and of the wall, due to the acceleration of that mass M. If this modification of equation 1.15 is made, one obtains instead of equation 1.20 the following:

$$v = \left\{\frac{E \cdot a}{2r\rho} - \omega^2 \frac{M}{4\pi\rho}\right\}^{1/2} \tag{1.21}$$

The effective mass M cannot be calculated from the present theory. Frank (3) found for the additional term under the root $\omega^2 v^2/8$. The introduction of that term means that the speed of propagation would drop to zero when a certain frequency limit is reached. It can easily be calculated that this limiting frequency is so high, and that the correction factor so small for the cases to be considered, that it need not be accounted for.

For some purposes, the use of the modulus of volume elasticity may be indicated. To obtain a relationship between p and V, we consider a section of tube of length l. This has the volume $V = \pi r^2 l$ and the differential dV becomes $dV = 2 \cdot \pi \cdot r \cdot l \cdot dr$ for a variation of radius dr. For the modulus $\kappa = (dp/dV) \cdot V$ we obtain therefore

$$\kappa = (dp/dV) \cdot V = {}^1\!/_2 r(dp/dr) \tag{1.22}$$

Using equation 1.14 we get

$$\kappa = {}^1\!/_2 r \cdot dp/dr = E \cdot a/(2r) \tag{1.23}$$

The Moens-Korteweg equation can then be written in the form

$$V = (\kappa/\rho)^{1/2} \tag{1.24}$$

which is used by Frank (3). Like the Moens-Korteweg equation, it only holds for thin-walled tubes.

Equation 1.24 is well known in physics as the equation for propagation of a sound wave in a liquid with the compressibility $1/\kappa$. In liquids, $1/\kappa$ is very small and the velocity of propagation rather high (on the order of 10^5 cm/sec). On the other hand, in a liquid-filled rubber tube, or a blood vessel, $1/\kappa$ depends for the most part, not upon the characteristics of the liquid, but upon the distensibility of the tube wall, which is rather great, the pulse-wave velocities being therefore comparatively small (a few hundred cm/sec).

In the preceding description of the pulse-wave phenomenon we have considered only the geometric features of the conduit, the density of the liquid, and the static modulus of elasticity for the tube walls. Experiments with pulse waves in rubber tubes and researches in hemodynamics show that the amplitudes of such waves diminish with increasing distance from the source (pump or heart), at least if no reflections occur. This damping of the wave is more pronounced for high frequencies than for low ones. Wave propagation is therefore connected with a loss of energy. Such a loss of energy can only be due to friction, either in the liquid or in the tube wall, at least when the tube is freely suspended in air (see equation 1.5).

However, before we try to complete our theoretical picture of wave propagation by taking into account the observed damping, we must learn something about the elastic behavior of the tube walls. We shall see in the following section how these elastic properties depend upon the manner in which the load is applied to the material; that is to say, on the way the stretch occurs in time. We shall see then that internal friction is closely connected with elasticity.

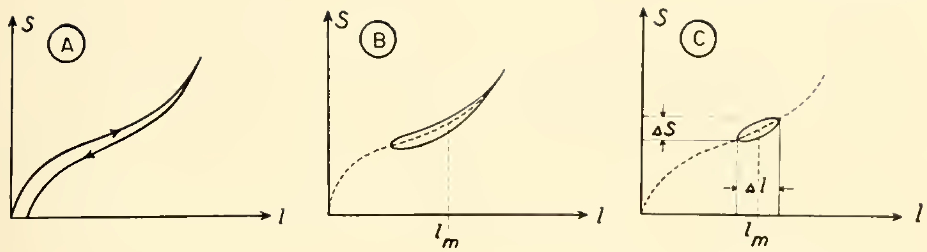

FIG. 2. Types of stress-strain relations for rubberlike materials.

2. DYNAMIC ELASTICITY AND VISCOSITY

If we stretch a strip of rubber, a piece of an artery, or any one of the materials termed today as "elastomers," either in a continuous manner or in graduated steps by hanging on weights, we can graphically present the results of such an experiment in the form of a stress-strain curve. As a rule, such curves will be more or less S-shaped (see fig. 2*A*). If we remove the strain in the same continuous or stepwise fashion, we obtain a characteristic descending curve of similar shape, which does not coincide with the ascending curve and does not return to the zero point of origin of the coordinate system. In other words, when the force applied to the sample is released, a certain amount of stretch remains (at least for some time). Recognizing its analogy to a similar effect well known in magnetism, we term this behavior "hysteresis."

This means that Hooke's law does not apply to such materials because it is valid only when the stress-strain relationship is reversible and can be represented as a straight line passing through the origin.

In order to avoid these difficulties, we shall use a rhythmic stretch of a sinusoidal type, so that the length of the sample (i.e. the rubber strip) under consideration will be given by

$$l(t) = l_m + \Delta l \cdot \sin \omega t \qquad (2.1)$$

where l_m corresponds to the mean prestretch length. If we record the corresponding stress simultaneously with the length $l(t)$, we obtain a closed curve which approaches, more or less, a stretched-out ellipse when the amplitude of stretch ($\frac{1}{2}\Delta l$) is made sufficiently small (fig. 2*C*). The long axis of that ellipse almost coincides with the tangent drawn to the static stress-strain curve at the point (l_m , S_m), S_m representing the strain for the prestretched length l_m .

The appearance of an ellipse means that a phase shift occurs between stretch and strain, and that some of the work done on the sample is transformed into heat. By this ellipsoidal characteristic which can be recorded experimentally, the visco-elastic behavior of the considered material in the state ($l_m S_m$) will be sufficiently well characterized, at least for our purposes.

For the purpose of interpretation, we shall make use of the simplest mechanical model that will describe the above-mentioned characteristic. It is made of a spring, with the spring-constant f, and a dashpot for damping connected in parallel with it (see fig. 3). One end of the spring is considered to be fixed in space, whereas the free end moves in a sinusoidal manner, like the rubber strip mentioned above. If we take as the origin of x-coordinates the free end of the spring at rest, we might describe the movement of that end by the formula

$$x = x_0 \sin \omega t \qquad (2.2)$$

(For the actual sample, the coordinate x corresponds to the displacement $l - l_m$.) The resulting strain S for the model in the x-direction will then be given as the sum of the restoring force $f \cdot x$ and the force $R\, dx/dt$ needed to overcome friction

$$S = f \cdot x + R \frac{dx}{dt} \qquad (2.3)$$

It follows from equation 2.3 that the strain S is also a sinusoidal function of time. This can easily be seen by inserting equation 2.2 into 2.3. We obtain in this way

$$S = f \cdot x_0 \sin \omega t + R\omega x_0 \cos \omega t \qquad (2.4)$$

The sum of a pure sin-function and a pure cos-function can always be put in the form of a pure sin-function with an appropriate phase φ

$$S = S_0 \sin (\omega t + \varphi) \qquad (2.5)$$

For S_0 and φ we obtain in the usual manner

$$S_0 = x_0 \cdot f(1 + \omega^2 R^2/f^2)^{1/2} \quad \tan \varphi = \omega R/f \qquad (2.6)$$

As with the experiment on rubber, the points (S, x)

FIG. 3

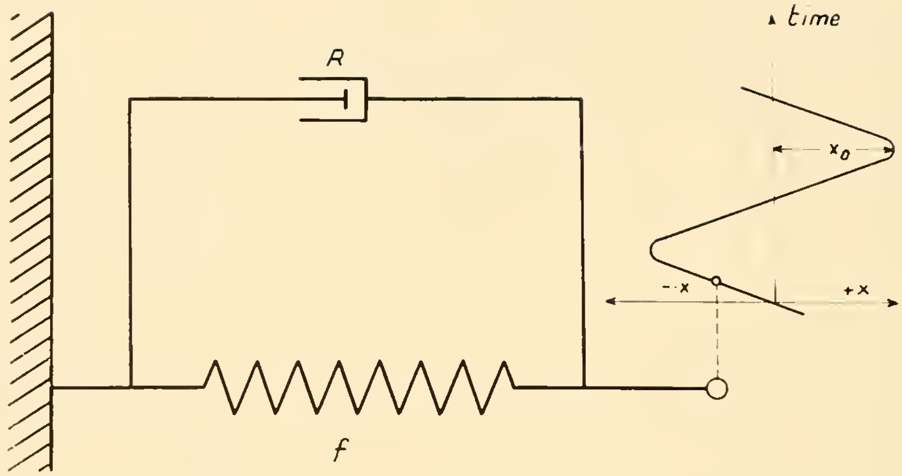

lie on an ellipse (see fig. 4) and the values of S_0 and φ can also be found from this ellipse. For the points of maximal and minimal strain S_1 and S_2 the expression $\omega t + \varphi$ will take on the values $(1/2)\cdot\pi$, $(3/2)\pi\cdots$ and we obtain from equations 2.5 and 2.6

$$S_2 - S_1 = 2x_0 f(1 + \tan^2 \varphi)^{1/2} = 2x_0 f/\cos \varphi \qquad (2.7)$$

or

$$f = \frac{S_2 - S_1}{2x_0} \cdot \cos \varphi \qquad (2.8)$$

The quantity $2x_0$ of our model corresponds to Δl of the actually measured characteristics (fig. 2C) and the difference $S_2 - S_1$, to ΔS. For the restoring force of the measured sample we obtain therefore

$$f = (\Delta l/\Delta S)\cdot\cos \varphi \qquad (2.9)$$

In analogy to Hooke's law we define the dynamic modulus of elasticity by equation

$$E_{\text{dyn}} = \frac{\Delta S}{\Delta l} \cdot \frac{l_m}{q_m} \cos \varphi \quad \text{dyn/cm}^2 \qquad (2.10)$$

where q_m stands for the cross-sectional area which corresponds to the prestretched state of length l_m. The phase angle φ can be read from the ellipse by drawing a vertical line through its center. This line cuts the ellipse at points 3 and 4 (see fig. 4). At these points ωt takes the values 0 and π and we obtain from equation 2.5

$$S_4 - S_3 = 2\cdot S_0\cdot\sin \varphi \qquad (2.11)$$

Since the amplitude S_0 is identical with $(1/2)(S_2 - S_1)$, we obtain

$$\sin \varphi = (S_4 - S_3)/(S_2 - S_1) \qquad (2.12)$$

Because $S_4 - S_3$ and $S_2 - S_1$ are well-defined lengths, $\sin \varphi$ or φ can easily be found from the experiments.

In order to determine the second essential quantity R or, better, the product ωR, we substitute for f in equation 2.6 the value found from 2.9 and obtain

$$\omega R = \frac{\Delta S}{\Delta l} \cdot \sin \varphi \qquad (2.13)$$

Just as we did with the elastic modulus, we define in this case a specific constant η making $R = \eta q_m/l_m$ and obtain instead of 2.13

$$\omega\eta = \frac{\Delta S}{\Delta l}\frac{l_m}{q_m} \cdot \sin \varphi \qquad (2.14)$$

The quantity η has the dimensions of a viscosity constant ($g\ \text{cm}^{-1}\text{sec}^{-1}$) and can therefore be looked upon as the viscosity of the examined material. The symmetrical equations 2.10 and 2.14 determine its visco-elastic behavior.

It is now necessary to comment on experiments and their results: the above-mentioned elliptical characteristic can be produced on the screen of a

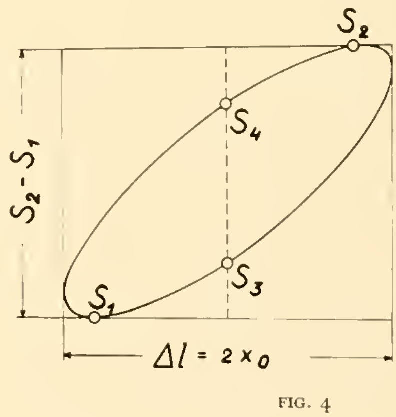

FIG. 4

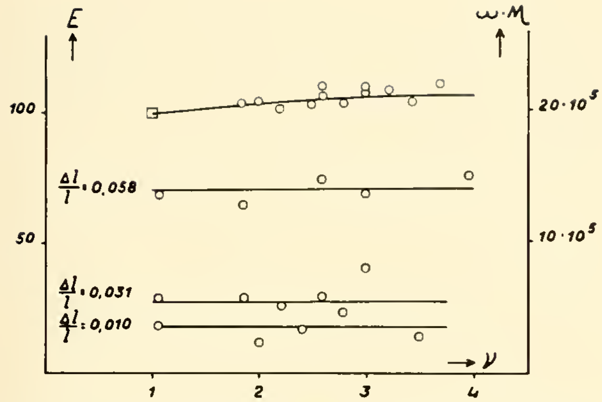

FIG. 5. Stretching rubber. Effect of frequency on dynamic modulus (Edyn, top curve, and ordinate at left) and on the $\eta\omega$ product (lower 3 curves and ordinate at right).

cathode-ray tube when the stresses and strains are transformed into electrical voltages connected to the horizontal and vertical deviating plates of the oscillograph. A method based on this principle has previously been described by the author and his co-workers (1) and has since been considerably improved. Experiments carried out with rubber and pieces of arteries showed that E_{dyn} as well as η showed a dispersion, that is to say a dependence on frequency. A common feature of all elastomers is the fact that (except for a few extreme cases) E_{dyn} increases from $\omega = 0$ (corresponding to the static case) at first moderately, and then more slowly with increasing frequency. For higher frequencies it remains practically constant. Figure 5 shows results for E_{dyn} and $\omega\eta$ obtained simultaneously on a piece of India rubber. The measurements were carried out with three different amplitudes on the same sample. The points for E_{dyn} for the different amplitudes fall, within the limits of experimental error, on the same curve. A dependence of E_{dyn} on the amplitude therefore need not be considered. On the other hand, the product $\omega\eta$ is greatly dependent on amplitude, as can be seen from figure 5. The increase in $\omega\eta$ is more than it would be if it were proportional to $\Delta l/l$. We shall see later that this fact explains in quite a natural way some observations on the damping of pulse waves, which otherwise could hardly be understood.

There are some marked differences between the behavior of arterial wall material and that of India rubber. For arteries, E_{dyn} depends greatly upon the initial state of stretch upon which the periodic stretch is superimposed, whereas for rubber E_{dyn} is practically independent of it. Figure 6 shows a typical example

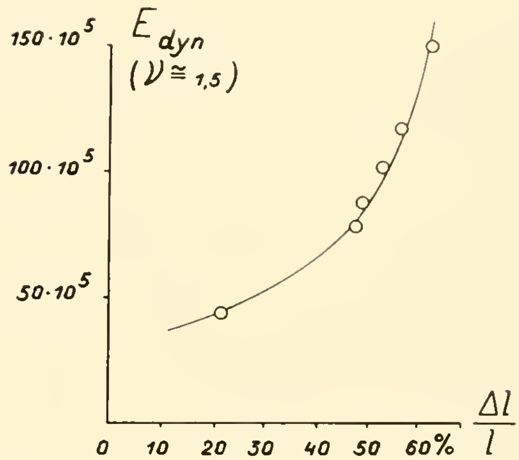

FIG. 6. Dynamic modulus of elasticity of a dog's aorta as a function of initial extension.

of a set of measurements, obtained from a ring-shaped piece of a dog's aorta in oxygenated blood at body temperature. (Not much emphasis shall be placed on the absolute values of E_{dyn} for this experiment.) Also for arterial walls, $\omega\eta$ depends greatly on the amplitude of stretch. Some experiments on a piece of a cow's carotid artery, stretched with a frequency of 1.04 ($\omega = 6.5$), yielded the values $4.4 \cdot 10^6$ dyn/cm² for $\Delta l/l = 0.042$; — $3.9 \cdot 10^6$ for $\Delta l/l = 0.018$; and $2.8\ 10^6$ for $\Delta l/l = 0.007$.

The treatment of dynamic elasticity given above is, of course, highly simplified, and we have retained only the features essential to our problem. The reader interested in more detail and an explanation of the facts on the basis of molecular physics might consult the monograph *The Physics of Rubber Elasticity* by Treloar (22).

3. INFLUENCE OF INTERNAL WALL FRICTION ON DAMPING AND SPEED OF PROPAGATION

O. F. Ranke (16) was the first to introduce wall friction into the theory of pulse waves. In order to describe the visco-elastic behavior of the wall material, he used a model of two springs, one of which was damped by means of a dashpot (see fig. 7). In the meantime, our knowledge about elastomers

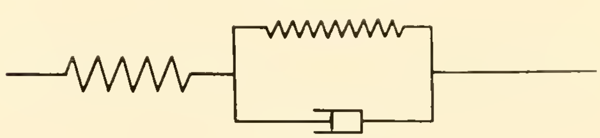

FIG. 7

has been considerably enlarged, and it has been found that no one of the simple mechanical models made up of springs and dashpots can account for all the properties of elastomers in a satisfactory manner. This is especially the case for the dependence on frequency. The best way to overcome this difficulty, therefore, is to use the simplest model of a spring damped by a dashpot connected in parallel to it, and to introduce an eventual frequency dependence of the restoring force (spring constant) and the friction at any suitable step from experimental data. In this way we do not obtain a theory in the strict sense of the word, but merely a set of semi-empirical formulas of the kind used in engineering.

To obtain these formulas, we have to complete the equilibrium condition in the radial direction

$$p - p_0 = E \cdot a\left(\frac{1}{r_0} - \frac{1}{r}\right) \tag{3.1}$$

which is the integral form of equation 1.14, with a frictional term $R_1\ dr/dt$, as we did for the spring model in section 2; and we obtain

$$p - p_0 = E \cdot a\left(\frac{1}{r_0} - \frac{1}{r}\right) + R_1 \frac{\partial r}{\partial t} \tag{3.2}$$ [3]

where p_0 and r_0 denote the equilibrium values of p and r for the tube at rest. Differentiation with respect to t leads to

$$\frac{dp}{dt} = \frac{E \cdot a}{r^2} \cdot \frac{\partial r}{\partial t} + R_1 \frac{\partial^2 r}{\partial t^2} \tag{3.3}$$

Introducing the radial current $di_r = 2\pi r\ (dr/dt) \cdot dz$ we obtain

$$\frac{\partial p}{\partial t} = \frac{E \cdot a}{2\pi r^3} \frac{\partial i_r}{\partial z} + \frac{R_1}{2\pi r} \frac{d^2 i_r}{\partial z \partial t} \tag{3.4}$$

or with the relation $di_r = -di_z$

$$-\frac{\partial p}{\partial t} = \frac{E \cdot a}{2\pi r^3} \cdot \frac{\partial i_z}{\partial z} + \frac{R_1}{2\pi r} \frac{\partial^2 i_z}{\partial z \partial t} \tag{3.5}$$

Differentiating again Newton's equation 1.11 with respect to t and equation 3.5 with respect to z, we can eliminate the pressure and obtain with $Q = r^2\pi$

$$\frac{\partial^2 i}{\partial t^2} = \frac{Ea}{2r\rho} \frac{\partial^2 i}{\partial z^2} + \frac{R_1 r}{2\rho} \frac{\partial^3 i}{\partial z^2 \partial t} \tag{3.6}$$

[3] To avoid confusion, we mention that R_1 in equation 3.2 has a somewhat different meaning from R in equation 2.3 because $R_1\ dr/dt$ has the dimension of a pressure, whereas $R\ dx/dt$ in equation 2.3 has the dimension of a force.

We again dropped the index z for the current in the z-direction. For $R_1 = 0$, that is to say in the absence of damping, equation 3.6 is, of course, identical with equation 1.19. Equation 3.6 may be more concisely written in the form

$$\frac{\partial^2 i}{\partial t^2} = v_0^2 \frac{\partial^2 i}{\partial z^2} + C \cdot \frac{\partial^3 i}{\partial z^2 \partial t} \tag{3.7}$$

where v_0 is the speed of propagation for the undamped case and C stands for $R_1 r/(2\rho)$. For the pressure we obtain the analogous equation

$$\frac{\partial^2 p}{\partial t^2} = v_0^2 \cdot \frac{\partial^2 p}{\partial z^2} + C \cdot \frac{\partial^3 p}{\partial z^2 \partial t} \tag{3.8}$$

For this equation it will be natural to try the solution

$$p = P_0 e^{-\beta z} \cdot \sin \omega\left(t - \frac{z}{v}\right) \tag{3.9}$$

Much more convenient, however, in this case is the use of complex numbers. Instead of equation 3.9 we write, then,

$$p = P_0 \exp\left[j\omega\left(t - \frac{z}{v}\right) - \beta z\right] = P_0 e^{-\gamma z} \cdot e^{j\omega t} \tag{3.10}$$

With this we obtain from equation 3.8

$$-\omega^2 = (\beta^2 - \alpha^2 + 2j\alpha\beta)(v_0^2 + j\omega C) \tag{3.11}$$

This complex equation may be split into two real equations:

$$\begin{aligned} \omega^2 + v_0^2(\beta^2 - \alpha^2) - 2\alpha\beta\omega C &= 0 \\ \omega C(\beta^2 - \alpha^2) - 2\alpha\beta v_0^2 &= 0 \end{aligned} \tag{3.12}$$

and we obtain finally

$$\begin{aligned} \beta^2 - \alpha^2 &= -\omega^2 v_0^2/(v_0^4 + \omega^2 C^2) \\ 2\alpha\beta &= \omega^3 \cdot C/(v_0^4 + \omega^2 C^2) \end{aligned} \tag{3.13}$$

Elimination of α leads to

$$\begin{aligned} 2\beta^2 = &-\omega^2 v_0^2/(v_0^4 + \omega^2 C^2) \\ &\pm \omega^2 (v_0^4 + \omega^2 C^2)^{1/2}/(v_0^4 + \omega^2 C^2) \end{aligned} \tag{3.14}$$

The choice of the right sign can be made using the following reasoning: for vanishing resistance, that is to say, for $R = 0$ and therefore also for $C = 0$, the damping and therefore β must also vanish. This means that we have to use the plus sign and we obtain finally

$$\frac{\omega^2}{v^2} = \alpha^2 = \tfrac{1}{2}\omega^2(v_0^4 + \omega^2C^2)^{-1/2}\cdot[1 + v_0^2(v_0^4 + \omega^2C^2)^{-1/2}] \quad (3.15)^4$$

$$\beta^2 = \tfrac{1}{2}\alpha^2(v_0^4 + \omega^2C^2)^{-1/2} \cdot [1 - v_0^2(v_0^4 + \omega^2C^2)^{-1/2}] \quad (3.16)$$

These two equations tell us how the speed of propagation and the damping constant β depend on the frequency. Nevertheless, it must be kept in mind that the "constants" v_0 and C are not true constants and that these may also be functions of frequency, which must be determined experimentally.

It remains for us now to express the frictional constant R_1 contained in the constant C in terms of the viscosity of the wall and the geometrical data of the conduit. For this purpose we reason as follows: according to equation 3.2 an excess pressure $p - p_0$ in the tube brings about the hoop tension $Ear[(1/r_0) - (1/r)]$ due to the elastic restoring force plus a tension $R_1 \cdot r \cdot dr/dt$ (force per unit length). This additional wall tension is, by definition, equal to the tension on a strip of wall material of length $l = 2\pi r$, thickness a, and breadth b, stretched at the speed $dl/dt = 2\pi dr/dt$. According to section 2, the force $R\ dl/dt$ needed to overcome the friction encountered in stretching a band of length $l = 2\pi r$, breadth b, and thickness $a(q = ab)$ is

$$\frac{dl}{dt} \cdot \eta \cdot \frac{q}{l} = \eta \cdot \frac{a \cdot b}{2\pi r} \cdot 2\pi \frac{dr}{dt} = \eta \cdot \frac{a \cdot b}{r} \frac{dr}{dt} \quad (3.17)$$

The corresponding hoop tension per unit length will therefore be

$$R_1 \cdot r \cdot \frac{dr}{dt} = \frac{\eta \cdot a}{r} \cdot \frac{dr}{dt} \quad (3.18)$$

and we obtain thus

$$R_1 = \frac{\eta \cdot a}{r^2} \quad \text{and} \quad C = \frac{\eta_1 \cdot a}{2r\rho}$$

We shall now compare these theoretical considerations and results with experimental findings. Measurements of the speed of propagation of sinusoidal pulse waves in tubes of soft India rubber show, as a rule, a slight rise with increasing frequencies (12). According to equation 3.15 a dependence on frequency can occur only if either $v_0^2 = Ea/(2r\rho)$ or the product ωC and therefore $\omega\eta$ or both quantities, change with frequency. The determination of $\omega\eta$ is rather difficult when we use a method which permits continuous variation of the frequency. As indicated by figure 5 the product $\omega\eta$ was, at least from frequency 1 on up, practically constant for the kind of rubber used. Similar results have been obtained by other investigators (10). The frequency dependence of v in such cases is therefore determined by the frequency dependence of the dynamic modulus of elasticity. A typical frequency curve for E_{dyn} of India rubber is plotted in figure 8, where the extrapolation to the lower frequencies is, of course, somewhat arbitrary. The increase of E_{dyn} up to frequency 3 amounts to about 35 per cent for the given example. The velocity of propagation must therefore rise at the rate of $1 : 1.35^{1/2}$; that is $1 : 1.16$. In the same figure, values of v obtained on a tube of the same material at about the same time are also plotted. From $\nu = 0$ up to $\nu = 3$ v increases by about 15 per cent, which agrees well with expectation.

If we calculate the quantity $[Ea/(2r\rho)]^{1/2}$ from the measured values E_{dyn}, ν, a, r, and ρ we find that it fits, as a rule, quite well with the obtained values of v extrapolated for zero frequency, if we use instead of E the quantity suggested by Korteweg (6),

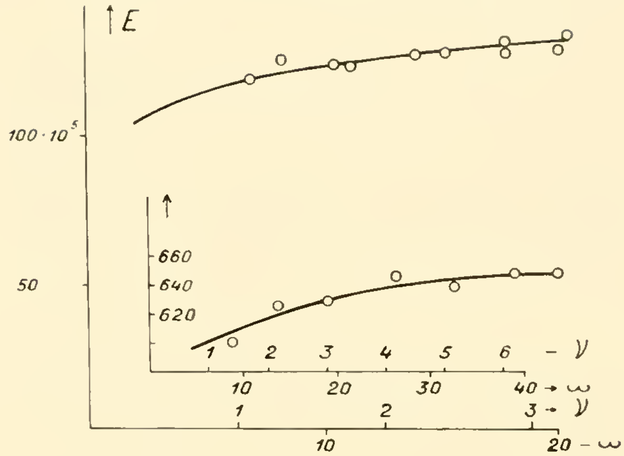

FIG. 8. Dynamic modulus of elasticity versus frequency. Inside picture: velocity of propagation in cm/sec versus frequency.

[4] These equations can also be derived from Ranke's theory (16) if we replace the undamped spring of his model by a rigid bar; that is to say, if we write according to Ranke's notation $E_2 = \infty$, $\kappa_2 = \infty$ $e = \infty$, then Ranke's formula for propagation and damping (16, page 192) are identical with equations 3.15 and 3.16 in this text for $V = a\eta/(2r)$. Ranke's equation 1a (16, page 191) leads likewise to this value for V if we transform it in our notation by replacing volume elasticity by Young's modulus, but is inconsistent with the preceding equation for σ where V stands for η in our notation. That the second term ω^2C^2 under the root sign should only depend on the specific constant and not on the dimensions of the tube can indeed not be understood.

$$E' = E\left(2 + \frac{a}{r}\right) \Big/ \left[2 - \sigma + 2(1 + \sigma)\frac{a}{r} + (1 + \sigma)\left(\frac{a}{r}\right)^2\right] \qquad (3.19)$$

where σ denotes Poisson's ratio. For rubber, as well as for arterial walls, this ratio is almost exactly 1/2. Equation 3.19 can therefore be written as

$$E' = E\left(2 + \frac{a}{r}\right) \Big/ \left[1,5 + 3\frac{a}{r} + 1,5\left(\frac{a}{r}\right)^2\right] \qquad (3.20)$$

From the theoretical point of view, v can only become equal to v_0 according to equation 3.15 if ωC and therefore $\omega\eta$ vanishes for $\nu = 0$. Whether or not this is the case cannot be deduced from our experiments. Nevertheless, it can be shown that in any case the influence of $\omega\eta$ on the speed of propagation is very small. For a maximal value of $14 \cdot 10^5$ dyn/cm² for $\omega\eta$, according to the results of figure 5, we obtain for $\omega C = \omega\eta a/(2r\rho)$, with the data given above, the value $0.48 \cdot 10^5$ and for $\omega^2 C^2$ the value $0.23 \cdot 10^{10}$. On the other hand $v_0^4 = 14.7 \cdot 10^{10}$. The quantity ω^2C^2 is therefore quite small compared with v_0^4, and we obtain for the roots $(v_0^4 + \omega^2C^2)^{1/2}$ in the equations 3.15 and 3.16 the value $1.008\, v_0$. The difference between v and v_0 is therefore too small to be measured. Thus, a wall viscosity of the assumed value has no measurable influence on the speed of propagation which conclusion is in fair agreement with the measurements of A. Müller (12).

The damping constant 6, on the other hand, behaves quite differently. In this case, also, the factor before the bracket in equation 3.16 depends very little upon $\omega\eta$. But the bracket contains a difference between unity and a quantity which is but little less than one. Because $\omega^2C^2 \ll v_0^4$ the bracket can be expanded to read

$$1 - v_0^2/(v_0^4 + \omega^2C^2)^{1/2} \cong 1 - \left(1 + \frac{\omega^2C^2}{2v_0^4}\right)^{-1} \cong 1 - \left(1 - \frac{\omega^2C^2}{2v_0^4}\right) = \frac{\omega^2C^2}{2v_0^4}$$

and we obtain for β the simple approximate formula

$$\beta = \frac{\omega}{2v_0^3}\,\omega C = \omega\,\frac{a \cdot \omega\eta}{4r\rho v_0^3} = K \cdot \omega \qquad (3.21)^5$$

[5] Morgan & Kiely (11, equation 56) find for low viscosity of the liquid in our present notation.

$$\beta = \frac{\omega}{v_0}\left[\frac{1}{r}\left(\frac{\eta_1}{2\omega\rho}\right)^{1/2}\left(1 - \sigma + \frac{\sigma^2}{4}\right) + \frac{\omega\eta}{2E}\right]$$

Neglecting viscosity of the liquid altogether, we obtain $\beta = \omega\ (\omega\eta/2\ v_0\ E)$. It can be seen at once that this is identical with our equation 3.21 if we replace $a/(2\ r\ \rho)$ in the latter by v_0^2/E.

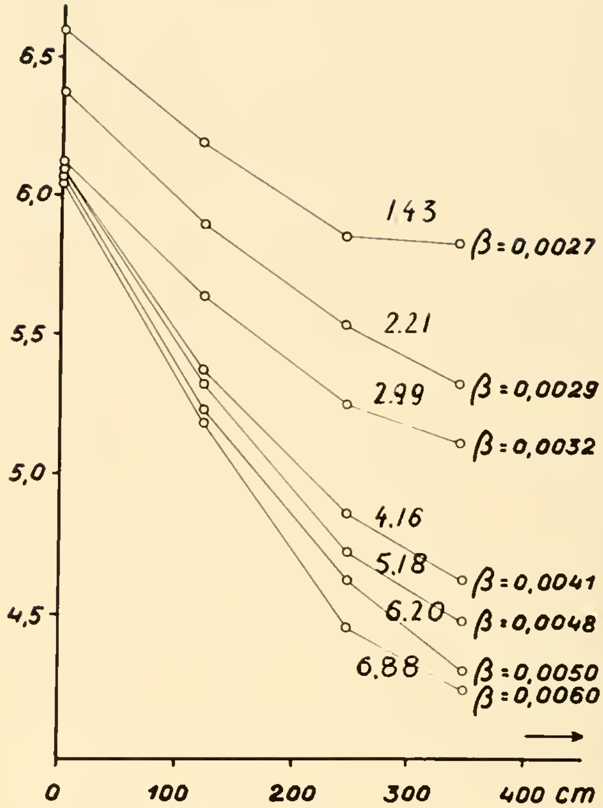

FIG. 9. Decrease of pressure amplitude in pulse-waves of different frequencies.

With $\omega C = 0.48 \cdot 10^5$ and $v_0 = 608$ cm/sec, K becomes $1.08 \cdot 10^{-4}$ or $\beta = 6.75 \cdot 10^{-4}$. The damping constant is therefore roughly proportional to the frequency, if $\omega\eta$ is constant.

The damping constant β can be found when we measure the pressure amplitudes in a tube at different distances from the source of the wave. Care must be taken that at the recording site the waves are truly sinusoidal in shape. Such determinations were carried out first by A. Müller (12) and have been repeated several times by the author. Figure 9 gives an example of such a determination, where the natural logarithm of the pressure amplitude is plotted against the distance from the origin of the line for a number of frequencies. Whereas the data from Müller's paper give a nearly exponential decrease with z, this is not the case for the present example where the distances z are considerably greater. Damping decreases markedly for larger

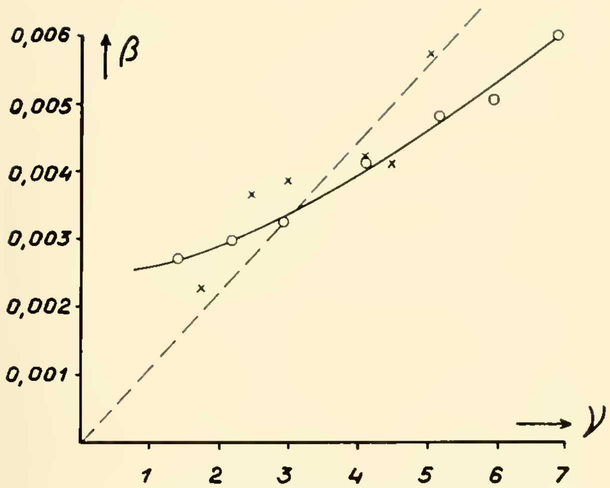

FIG. 10. Damping constants β for pulse-waves versus frequency. ○—○—○—○ = Values obtained from the decrease of pressure-amplitude taken from fig. 11. ×—×—×—× = Values calculated from the impedance of the closed tube.

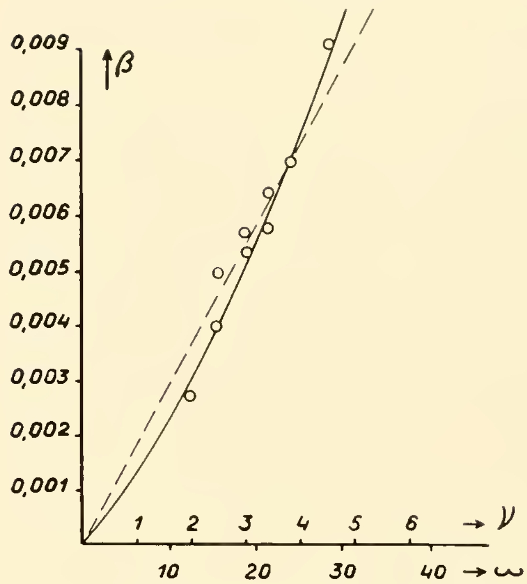

FIG. 11. β-Values of another tube with smaller diameter and thicker walls (see table 4).

distances from the source. This can be easily understood if we consider that the amplitudes become smaller with increasing distance. As we have shown in section 2, $\omega\eta$ diminishes with decreasing amplitude and consequently β must diminish also. Because the waves used for this experiment were very nearly sinusoidal, the observed fact cannot be explained by the presence of more highly damped harmonics. If we compute the β-values for the section of the curves between $z = 125$ and $z = 250$ cm, we obtain the values indicated on the curves together with the frequency used.

A method which we shall explain later permits calculation of an "effective" β from the input impedance of a closed tube (see section 6). We have used this method for the same tube with which the above-mentioned determinations were carried out and which was clamped at $z = 135$ cm. The results are plotted in figure 10 as a function of frequency together with the values obtained with the previously mentioned direct method. The values obtained with the second method, indicated by crosses on the graph, lie approximately on a straight line running through the origin, if we allow for the lack of precision of such measurements. The indicated straight line (dotted line) would correspond to the formula

$$\beta = 1.1 \cdot 10^{-3} \cdot \nu = \omega\eta \cdot \frac{a \cdot \pi \cdot \nu}{2 \cdot r\rho v_0^3}$$

$$\text{or } \omega\eta \cdot \frac{0.107}{2 \cdot 1.37 \cdot 1.14 \cdot 608^3} = \omega\eta \cdot 0.64 \cdot 10^{-9}$$

From this we find for $\omega\eta$ the value $1.1 \cdot 10^{-3}/(0.64 \cdot 10^{-9}) = 17.2 \cdot 10^5$ dyn/cm². This fits quite well with the maximal value of 14.10^5 in figure 5.

Similar measurements have been carried out on a thick-walled tube in which $r = 1.02$ cm, $a = 0.18$ cm, and $v_0 = 880$ cm/sec. The results are plotted in figure 11. The dotted straight line corresponds to the formula

$$\beta = 1.82 \cdot 10^{-3} \cdot \nu$$

Thus we obtain in the same way as above

$$1.82 \cdot 10^{-3} \cdot = \pi \cdot \omega\eta \cdot 0.18/(2 \cdot 1.02 \cdot 1.14 \cdot 6.75 \cdot 10^5)$$

which leads to a value of $50 \cdot 10^5$ dyn/cm² for $\omega\eta$, which has at least the order of magnitude expected. Exact quantitative agreement cannot be expected from such experiments, firstly, because the amplitudes of relative stretch are different from point to point on the tube during the experiment and have not been measured, and secondly, because the physical properties of India rubber changes with time. In addition to this, we have not accounted for the viscosity of the liquids, which is another source of damping. We should therefore not be surprised that our theoretical calculations, especially for the thick-walled tube of small diameter, furnish a higher value for $\omega\eta$ than we obtain from direct measurements (fig. 5). In the next paragraph we shall therefore discuss the influence of the viscosity of the filling liquid.

4. VISCOSITY OF FILLING LIQUID AND ITS INFLUENCE ON DAMPING AND SPEED OF PROPAGATION

In the previous section we have introduced into the theoretical treatment the visco-elastic behavior of the tube walls and ignored the energy loss in the viscous filling fluid. The fact that the theory fits in general, even at this stage of development, with our experience and with the earlier findings of A. Müller [(12) who made determinations in 1951 on propagation and damping of pressure waves in rubber tubes of similar dimensions with fluids of different viscosities], indicates that liquid viscosity cannot have very much influence, at least on the speed of propagation. Nevertheless, we shall complete the theory in this direction and compare the results with experience.

For this purpose, we complete equation 1.9 with a term which accounts for a resistance to flow in the z-direction and obtain

$$-\frac{dp}{dz} = \rho\frac{\partial^2 z}{\partial t^2} + R_2\frac{d\zeta}{\partial t} \tag{4.1}$$

The procedure of calculation is much the same as in the previous section, and we shall give merely the result of it. For the quantities β and α we have the following equations

$$\begin{aligned}\beta^2 - \alpha^2 &= \left(-\omega^2 v_0^2 + \omega^2 C\frac{R_2}{\rho}\right)\Big/(v_0^4 + \omega^2C^2)\\ 2\alpha\beta &= \left(\omega^3 C + \frac{\omega R_2 v_0^2}{\rho}\right)\Big/(v_0^4 + \omega^2C^2)\end{aligned} \tag{4.2}$$

where C stands for $\eta a/(2r\rho)$. Solving for α and β we obtain

$$\begin{aligned}\alpha^2 = \frac{\omega^2}{v^2} &= \omega^2(v_0^4 + \omega^2C^2)^{-1}\left\{\left[\left(v_0^2 - \frac{C\cdot R_2}{\rho}\right)^2 + \left(\omega C + \frac{R_2\, v_0^2}{\rho\cdot\omega}\right)^2\right]^{1/2} + \left(v_0^2 - \frac{CR_2}{\rho}\right)\right\}\\ \beta^2 &= \omega^2(v_0^4 + \omega^2C^2)^{-1}\left\{\left[\left(v_0^2 - \frac{C\cdot R_2}{\rho}\right)^2 + \left(\omega C + \frac{R_2\cdot v_0^2}{\rho\cdot\omega}\right)^2\right]^{1/2} - \left(v_0^2 - \frac{CR_2}{\rho}\right)\right\}\end{aligned} \tag{4.3}$$

In order to discuss the influence of the newly arising terms $R_2v_0^2/(\rho\omega)$ and CR_2/ρ we must first determine the frictional constant R_2. According to equation 4.1 the quantity $R_2\,d\zeta/dt = iR_2/Q$ is equal to a certain gradient of pressure $-dp'/dz$. If we suppose that Poiseuille's law holds, even for pulsating current, we have $i = -(dp'/dz)\pi r^4/(8\eta_1)$, where η_1 stands for the viscosity of the liquid. It follows from this with $Q = r^2\pi$

$$R_2 = \frac{8\eta_1}{r^2} \tag{4.4}$$

However, as we shall see later, Poiseuille's law does not hold for pulsating flow, and formula 4.4 can only be used for very low frequencies. Let us take as an example the thick-walled tube with $r = 1.02$ cm, $a = 0.193$ cm, and $v_0 = 880$ cm sec. For η_1, we take the value 0.078 poises, which we obtain for a glycerine-water mixture of density 1.14. With this we obtain the limiting value $R_2 = 0.6$. From experiments and calculations, which we shall describe later on, we obtain instead of 4.4 the semi-empirical formula

$$R_2 = 0.6 + \omega\cdot 0.06 = 0.6 + \nu\cdot 0.377 \tag{4.5}$$

For a frequency of 10 cps, which corresponds to the highest harmonic which might be safely evaluated by harmonic analysis of pulse curves, R_2 would be 4.37. The term $R_2v_0^2/(\omega\rho)$ would then be $4.37\cdot 880^2/(62.8\cdot 1.14) = 4.27\cdot 10^4$. The quantity $C = \omega\eta a/2r\rho$ becomes then $14.0\cdot 10^5\cdot 0.193/(20.4\cdot 1.14) = 11.6\cdot 10^4$ if we take for $\omega\eta$ the value $14\cdot 10^5$ previously used. The additional term $R_2v_0^2/(\omega\rho)$ is therefore about half as great as ωC. With the small frequency of 2 cps (pulse frequency of a normal dog) $R_2 = 0.6 + 4\pi\cdot 0.06 = 0.6 + 0.725 = 1.352$, and $R_2v_0^2/(\omega\rho)$ becomes $1.35\cdot 880^2/(12.56\cdot 1.14) = 7.32\cdot 10^4$, whereas ωC becomes $2.32\cdot 10^4$. The additional term is therefore about three times larger than ωC. It remains for us to consider the term $C\cdot R_2/\rho$. Because $\omega\eta$ is approximately constant, we write it in the form $\omega CR_2/(\omega\rho)$ and obtain for it: $11.6\cdot 10^4\cdot 1.352/(12.56\cdot 1.14) = 1.09\cdot 10^4$ for the small frequency of 2 cps. It is, therefore, small even for this frequency, and certainly for higher frequencies it is small compared to $v_0^2 = 77.5\cdot 10^4$. We do not know much about the behavior of ωC at very small frequencies below 1 cps. We might assume that it approaches 0 because otherwise $\alpha = \omega/v$ would approach infinity and v would approach zero, which is certainly not the case. Furthermore, we might be justified in supposing that damping also vanishes when the frequency approaches zero. Table 1 shows the values for v and β calculated from equations 4.3. It can be seen from the table that liquid damping at a frequency of 2 cps has only a slight influence, and at a frequency of 10 cps practically no influence, on the velocity of propagation. This is in agreement with the results obtained by A. Müller (12) using a glycerine-water mixture with a density of 1.188 and a viscosity of 0.256 poises and a

TABLE 1

	2 cps Frequency	10 cps Frequency
With liquid damping	v = 754 cm/sec β = 0.0017	v = 888 cm/sec β = 0.0076
Without liquid damping	v = 887 cm/sec β = 0.001	v = 887 cm/sec β = 0.0054
	0 cps Frequency	3.19 cps Frequency (ω = 200)
With liquid damping	$v = v_0$ = 880 cm/sec β = 0 for $\omega = 0$	v = 890 cm/sec β = 0.0229
Without liquid damping	$v = v_0$ = 880 cm/sec β = 0° for $\omega = 0$	v = 887 cm/sec β = 0.0171

TABLE 2

Frequency	2 cps	10 cps	31.9 cps (ω = 200)
β_L/β_0	1.58	1.41	1.31

less viscous mixture for which ρ = 1.087 and η_1 = 0.033 poises.

On the other hand, damping is appreciably influenced by friction within the liquid. If we consider the rate β_L/β_0 of the damping constants with and without friction in the liquid, we obtain, for the frequencies used above, the values in table 2. It is seen from table 2 that the rate β_L/β_0 decreases with increasing frequencies. Müller's attenuation curves for fluids with different viscosities show this effect clearly. Also, Morgan & Kiely (11) obtain a reduction of the propagation velocity as a consequence of liquid friction. With the symbols used by us, their equation 38 takes the form

$$v = v_0\left[1 - 0.562\,\frac{1}{r}\left(\frac{\eta_1}{2\omega\rho}\right)^{1/2}\right] \quad \text{with} \quad \sigma = 0.5$$

where the small influence of wall friction has not been considered. For the damping constant they obtain

$$\beta = \frac{\omega}{v_0}\left[\frac{1}{r}\left(\frac{\eta_1}{2\omega\rho}\right)^{1/2}\cdot 0.562 + \frac{\omega\eta}{2E}\right]$$

where both wall and liquid friction have been accounted for. With v_0 = 880, $\omega\eta = 14\cdot 10^5$, $E = 100\cdot 10^5$, and η_1 = 0.078, we obtain for the frequencies 2, 10, and 31.9 cps the β-values 0.0013, 0.0057, and 0.0188, which are smaller by a factor 0.78 than the corresponding values 0.0017, 0.0076, and 0.0299 of table 2.

To terminate these first sections, we are justified in saying that the simplified treatment which we have given furnishes a fairly complete picture of all the phenomena occurring with purely harmonic wave propagation in conduits free from reflection, even though it is not quantitatively exact in every detail.

A supplementary remark must be made. We have so far considered the tube wall to be infinitely thin. In reality, we always have to deal with walls of measurable thickness. When a rubber tube is expanded, the volume of the tube walls remains constant, as we have already mentioned. As a result, the tube shortens at the places where it is radially expanded. If the tube is freely suspended, longitudinal oscillations can be observed when a wave runs through it. If, on the other hand, the tube is submitted to a longitudinal constraint, which is the case with blood vessels, conditions are somewhat different and the velocity of propagation is no longer the same. As we have already pointed out in section 3, E_{dyn} must be multiplied by a factor given by equation 3.19 in order to obtain a good agreement between the measured velocity for low frequencies and the Moens-Korteweg equation. Equation 3.19 holds for the freely moving tube. For a tube with complete longitudinal constraint, equation 3.19 has to be replaced by the similar equation

$$E' = E_{\text{dyn}}\cdot\left(2 + \frac{a}{r}\right)\Big/\left[2 + 2(1+\sigma)\cdot\frac{a}{r} + (1+\sigma)\left(\frac{a}{r}\right)^2\right] \tag{4.6}$$

or with σ = 0.5

$$E' = E_{\text{dyn}}\cdot\left(2 + \frac{a}{r}\right)\Big/\left[2 + 3\cdot\frac{a}{r} + 1.5\cdot\left(\frac{a}{r}\right)^2\right]$$

For the example used in section 3 with a = 0.107, r = 1.365; $E_{\text{dyn}} = 90\cdot 10^5$, and ρ = 1.14, we obtain $E' = E_{\text{dyn}}\,0.93$ instead of $E' = E_{\text{dyn}}\,1.195$ for the freely suspended tube. In the case of longitudinal constraint, v turns out to be somewhat smaller than indicated by the Moens-Korteweg formula. Moens accounted for this by the semi-empirical formula $v = 0.9[E\cdot a/(2r\rho)]^{1/2}$.

With this we close the discussion of pure harmonic waves in conduits free from reflection. In the following sections we shall deal with more complex phenomena of nonharmonic waves in tubes which are not considered to be free from reflections.

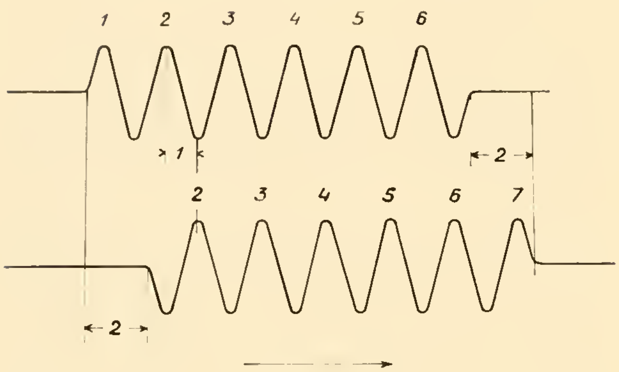

FIG. 12

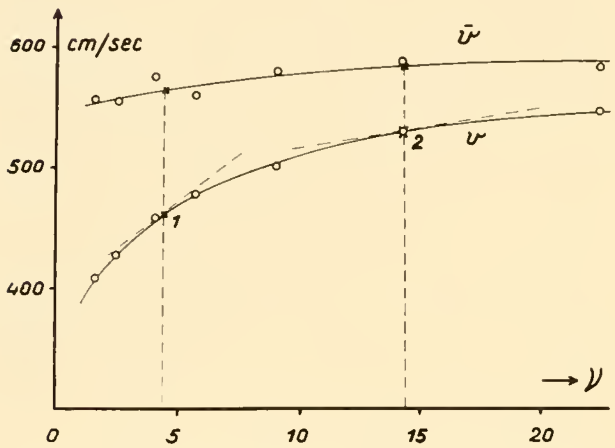

FIG. 13. Measured phase and group velocity as functions of frequency. At point (1) $\nu\, dv/d\nu = 4.4 \cdot 14 = 62$. $\bar{v} = v + \nu\, dv/d\nu = 460 + 62 = 522$ against a measured value of $\bar{v} = 564$. At point (2) $\nu\, dv/d\nu = 14.4 \cdot 31 = 45$. $\bar{v} = 530 + 45 = 575$ against a measured value of 586 cm/sec.

5. DISPERSION, PHASE, AND GROUP VELOCITY, AND THE IMPORTANCE OF HARMONIC ANALYSIS

We speak of dispersion when the velocity of propagation depends on frequency. This dispersion produces some phenomena which we shall now discuss. If we produce a wave train of finite length or finite duration, as sketched in figure 12, the speed of propagation of the head or tail of the wave train will differ from that of the hills and troughs of the wave. The former is called group velocity and the latter phase velocity. The picture is somewhat like that of a caterpillar crawling on a leaf. The two velocities are connected by the equation

$$\bar{v} = v + \nu \cdot \frac{dv}{d\nu} \quad \text{or} \quad \bar{v} = v - \lambda \frac{dv}{d\lambda} \tag{5.1}$$

well known in physics, where $\bar{v}$ denotes the group velocity and λ the wavelength. The graphs of figure 13 show how these two velocities depend on the frequency. The data have been taken from Müller's paper (12, table 3). If we calculate $\nu\, dv/d\nu$ from the slope of the v-curve, we obtain a difference $\bar{v} - v$ which is smaller than the difference measured directly, but at least demonstrates the sense of the deviation. For the derivation of equation 5.1 the reader is referred to any physics textbook.

We now turn to waves which are still assumed to be periodic but no longer sinusoidal in shape. We think, for example, of a pulse-pressure curve recorded with a suitable manometer. It is always possible to represent such a periodic function by an infinite series of sin-functions and cos-function.

$$f(t) = a_0 + \sum_1^\infty a_n \cdot \cos(2\pi nt/T) + \sum_1^\infty b_n \sin(2\pi nt/T) \tag{5.2}$$

or

$$y(x) = a_0 + \sum_1^\infty a_n \cos(n \cdot x) + \sum_1^\infty b_n \cdot \sin(nx)$$

The coefficients a_0, a_n and b_n are called the Fourier coefficients of the given function $f(t)$ or $y(x)$. The integer numbers n may take all the values from 1 to infinity. The coefficient a_0 is simply the mean value of the function to be considered, T being the fundamental period. Instead of using sin-functions and cos-functions, we can also represent $f(t)$ or $y(x)$ by means of sin-functions alone. Instead of equation 5.2 we have, then,

$$f(t) = a_0 + \sum c_n \cdot \sin[(2\pi nt/T) + \psi_n] \tag{5.3}$$

where

$$c_n = (a_n^2 + b_n^2)^{1/2} \quad \text{and} \quad \tan\psi_n = a_n/b_n$$

Because $\tan\psi = \tan(\psi \pm m\pi)$, we use the additional relationship $\sin\psi_n = a_n/c_n$ to determine in which quadrant the angle ψ is to be found. The determination of the coefficients a_n and b_n can be made mathematically, with numerical approximation methods or, best of all, with a harmonic analyzer).[6]

We shall illustrate this with an example. Figure 14

[6] A very practical type of analyzer, which can be made in every laboratory with cheap radio parts, has been described by Rymer & Butler (17) and in an enlarged and improved form by Taylor (20). The author has used such an instrument with success, and it furnishes the larger coefficients of the first three harmonics with no larger error than 1 per cent, if the period is divided into 30 intervals. The whole analysis takes less than a half hour, when the 30 corresponding ordinates have been evaluated before.

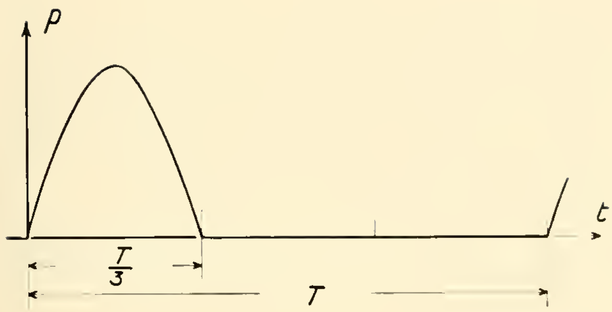

FIG. 14

TABLE 3

			ψ	ψ/n
$a_0 = 0.212$				
$a_1 = 0.191$	$b_1 = 0.330$	$c_1 = 0.380$	30°	30°
$a_2 = -0.136$	$b_2 = 0.236$	$c_2 = 0.272$	−30°	−15°
$a_3 = -0.141$	$b_3 = 0$	$c_3 = 0.141$	−90°	−30°
$a_4 = -0.017$	$b_4 = -0.030$	$c_4 = 0.035$	210°	52°
$a_5 = -0.010$	$b_5 = 0.018$	$c_5 = 0.021$	149°	30°
$a_6 = -0.028$	$b_6 = 0$	$c_6 = 0.028$	−90°	−15°

represents a highly schematic pulse curve. For the systolic hump we have used a sin-shaped half wave whose "base" corresponds to a third of the whole period. For such a function, the Fourier coefficients can easily be calculated and we obtain, if we take the height of the "systolic hump" as unity, the values given in table 3.

Figure 15 shows the three first harmonics drawn as functions of time (thin lines) and their sum (heavy line). The period is assumed to be 1 sec. We shall now see how this sum-function representing a given pressure function, recorded at, say, $z = 0$ of a rubber tube, will be distorted when we make the recording at any other point z on the tube-line. A distortion will occur for the following reasons: *a*) The three component waves will run along the line with different speeds, changing the phasic relations between the components. This is much like the distortion observed many years ago on telephone lines, when speech was blurred at long distances. *b*) The amplitudes of the components are damped in a different way, because the higher frequencies undergo a higher damping than the low ones. The lower curve of figure 15 show the result of distortion for the two distances $z = 100$ cm and $x = 200$ cm. They are obtained from the original curve above by reducing the amplitudes of the component waves by multiplication with the factor $e^{-\beta z}$ and by shifting the component waves in the positive time axis by the amount z/v. The data

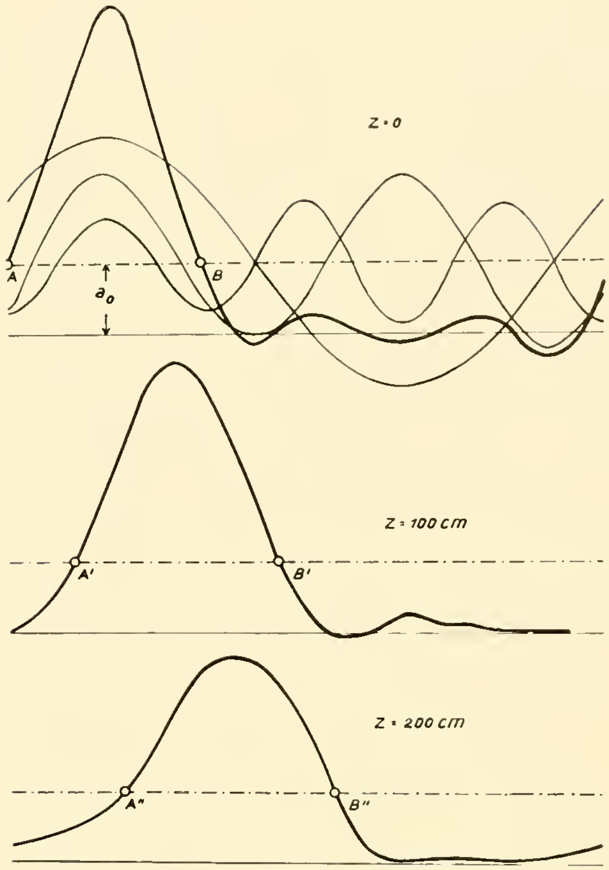

FIG. 15. Distortion of a pulse-wave composed of three harmonics at different points from the origin. The data used were 1st harmonic: $v = 860$ cm/sec $\beta = 0.0013$; 2nd harmonic: $v = 891$ cm/sec $\beta = 0.0030$; 3rd harmonic: $v = 897$ cm/sec $\beta = 0.0052$.

used for the damping constants and the velocities of the components are given in the legend to figure 15 and are those which were obtained with the thick-walled tube (see above). As can be seen from the figure, distortion is already appreciable at $z = 100$ cm, and is of course enhanced at $z = 200$ cm.

If we try in a naive way to determine the speed of propagation from the time lag of corresponding points, for example AA' AA'' or BB' BB'', we obtain, respectively, the values 923, 1030, 750, and 880 cm/sec, which are appreciably different from the velocities v_1, v_2, and v_3 of the component waves.

For the given example, the main causes of distortion are the different damping constants of the components. This is also the case in blood vessels where the dispersion (frequency dependence of E_{dyn}) is much like that of rubber. Higher dispersion would, of course, enhance the distortion.

Even though these distortions tend to invalidate

measurements of pulse-wave velocities, the errors might still be tolerable when dealing only with a purely progressive unidirectional wave. In the presence of reflected regressive waves, on the other hand, measurement of pulse-wave velocities with the abovementioned naive method becomes extremely problematical. Let us consider the extreme case of a standing wave in the strict physical sense, which is possible only in the absence of damping. If we choose the positions of the recording instruments in such a manner that there is no node of vibration between them, the recorded pressures have the same phase. In other words, the corresponding points of the pressure curves, which we suppose to be sinusoidal in this case, correspond to the same time and the calculated velocity would appear to be infinite. In actual cases we obtain, of course, values which lie between the true value and infinity. This difficulty was first pointed out by Porjé (15) and in an extensive paper by M. G. Taylor (19). It will therefore be sufficient to illustrate what we have said above with an example.

Upon a wave $p_1e^{-\beta z}\sin(\omega t - \alpha z)$ running in the positive direction within a conduit, a second wave $p_2e^{+\beta z}\sin(\omega t + \alpha z)$, running in the negative direction and due to a reflection of some kind, may be superimposed. We have therefore

$$p_z = p_1e^{-\beta z}\sin(\omega t - \alpha z) + p_2e^{+\beta z}\sin(\omega t + \alpha z) \quad (5.4)$$

If we substitute for this sum a pure sin-function with a different constant α', $v' = \omega/\alpha'$ is then the "apparent" velocity of propagation which we wish to find. We write therefore

$$p_z = A\sin(\omega t - \alpha' z)$$

If we expand this expression and compare the coefficients with those of 5.4, we obtain for α' and A the equations

$$\tan(\alpha' z) = \tan(\alpha z)\cdot(e^{-2\beta z}\cdot p_1/p_2 - 1)/(e^{-\beta z}\cdot p_1/p_2 + 1)$$
$$A = [F^2\cos^2(\alpha z) + G^2\cdot\sin^2(\alpha z)]^{1/2} \quad (5.5)$$

with $F = p_1e^{-\beta z} + p_2e^{+\beta z}$; $G = -p_1e^{-\beta z} + p_2e^{+\beta z}$. For $p_1 = p_2$ and $\beta = 0$, that is, for the extreme case of a standing wave, $\tan(\alpha' z)$ will vanish, that means that $\alpha' z = 0$ or π. In the first case α' becomes zero (unless $z = 0$ or $v' = \infty$) and $A = 2p_1\cos(\alpha z)$. The pressure function in the tube is therefore given by

$$p_z = 2p_1\cos(\alpha z)\sin\omega t$$

This is the expression for a standing wave with the nodes z_k given by the condition $\cos(\alpha z_k) = 0$.

For a numerical example we put $p_1/p_2 = 10$; that is to say, we suppose that at $z = 0$ the reflected component amounts to 10 per cent. With the same values of $\beta = 0.0013$ and $\alpha = 0.0073$ for the fundamental angular frequency $\omega = 6.28$ (which we used for the example in fig. 15) we obtain, at $z = 100$ cm for $\tan(\alpha' z)$, the value 0.688 from (5.5) and therefore $\alpha' z = \text{arc tan } 0.688 = 0.600$; $v' = \omega/\alpha'$ becomes therefore $6.28/0.006 = 1046$ cm/sec instead of $v = 860$ cm/sec, which we had supposed to be the true velocity. To be precise, we obtain this velocity $v' = 1046$ cm/sec if we make the recording at two points near $z = 100$ cm. If we were to make the recording near $z = 0$, we would obtain, under the same conditions, $\tan(\alpha' z) = (9/11)\tan(\alpha z)$ or approximately $\alpha'/\alpha = 0.816$, which leads to $v' = v/0.816 = 860/0.816 = 1054$ cm/sec, which is not much different from the first case.

We see from this example that even a relatively small amount of reflected wave can falsify the determination of pulse-wave velocity made in the usual manner. This is all the more annoying because the presence of strongly reflected waves seems now to be well established. Compare the papers of Hamilton & Dow (2, 4), Porjé (15), and Wetterer (23). Even refinement of the method with the help of harmonic analysis shows merely that we obtain different apparent velocities for the different harmonics, but which of these lie nearest to the true value we can only guess.

6. REFLECTION

Until now we have described only single progressive waves in conduits free from reflection, with the exception of the remarks in the last few paragraphs. A single progressive wave can, at least theoretically, only exist in an infinitely long homogeneous conduit, or in a conduit of finite length provided with some device to absorb the wave at its termination. As these conditions do not exist, we have to describe any stationary state by assuming two wave trains, one of which runs in the positive and the other in the negative z-direction. We must therefore replace expression 3.10 for pressure by

$$p = P'e^{j\omega t - \gamma z} + P''e^{j\omega t + \gamma z} \quad (6.1)$$

where

$$\gamma = \beta + j\alpha$$

and for current

$$i = I'e^{j\omega t - \gamma z} + I''e^{j\omega t + \gamma z} \qquad (6.2)$$

With 4.1 we obtain from these expressions

$$-\frac{\partial p}{\partial z} = \frac{1}{Q}(j\omega\rho + R_2)(I'e^{j\omega t - \gamma z} + I''e^{j\omega t + \gamma z}) \qquad (6.3)$$

But dp/dz can also be obtained by differentiation of 6.1 with respect to z, and we get

$$-\frac{\partial p}{\partial z} = P'\cdot\gamma e^{j\omega t - \gamma z} - P''\gamma e^{j\omega t + \gamma z} \qquad (6.4)$$

Comparing the coefficients on the right of 6.3 and 6.4 we obtain

$$\begin{aligned} P'\cdot\gamma &= (I'/Q)\cdot(j\omega\rho + R_2) \\ -P''\cdot\gamma &= (I''/Q)\cdot(j\omega\rho + R_2) \end{aligned} \qquad (6.5)$$

Writing Z for the complex quantity $(j\omega\rho + R_2)/(Q\gamma)$, we obtain for 6.2 the equation

$$i = \frac{P'}{Z}e^{j\omega t - \gamma z} - \frac{P''}{Z}\cdot e^{j\omega t + \gamma z} \qquad (6.6)$$

Then, if we divide by $e^{j\omega t}$, that is to say, if we consider amplitudes only, we obtain the important equation:

$$I = \frac{P'}{Z}\cdot e^{-\gamma z} - \frac{P''}{Z}\cdot e^{+\gamma z} \qquad (6.7)$$

which relates the amplitudes of pressure and current along the conduit and is much used in electrical engineering, for transmission lines. If we replace the exponentials by the hyperbolic functions

$$\sinh z = \tfrac{1}{2}(e^z - e^{-z}) \qquad \cosh z = \tfrac{1}{2}(e^z + e^{-z}) \qquad (6.8)$$

we obtain for 6.7

$$I_z = I_0 \cosh(\gamma z) - \frac{P_0}{Z}\cdot\sinh(\gamma z) \qquad (6.9)$$

where I_0 denotes the current amplitude and P_0 the pressure amplitude, at an arbitrarily chosen origin within the tube, and I_z the current amplitude at a point z. A similar equation holds for the pressure amplitudes:

$$P_z = P_0 \cosh(\gamma z) - I_0 Z \sinh(\gamma z) \qquad (6.10)$$

Equations 6.9 and 6.10 permit calculation of the amplitudes at a given point z from the input amplitudes at $z = 0$. An analogous pair of equations is used for the inverse problem

$$I_0 = I_z \cosh(\gamma z) + \frac{P_z}{Z}\sinh(\gamma z) \qquad (6.11)$$

$$P_0 = P_z \cos(\gamma z) + I_z Z \sinh(\gamma z) \qquad (6.12)$$

We can terminate a conduit of finite length l with any real or complex resistance W_1. A purely real resistance might be difficult to realize in practice. As an example of a complex resistance we might use a rubber balloon at the end of the tube line. (See APPENDIX 1.) By definition we have

$$P_1 = I_1 W_1 \qquad (6.13)$$

If we make especially $W_1 = Z$, we obtain

$$I_0 = I_1[\cosh(\gamma\cdot l) + \sinh(\gamma l)] = I_1\cdot e^{\gamma l} \qquad (6.14)$$

and likewise

$$P_0 = P_1 e^{\gamma l} \qquad (6.15)$$

In this case the complex input impedance P_0/I_0 is equal to the output impedance—using the terminology of electrical engineers—and is independent of the length of the conduit, which might even be made infinitely long without altering the reasoning. In other words, this means that a line terminated by an impedance Z behaves like an infinitely long conduit without reflection. The impedance Z is called the surge impedance of the conduit. It depends only upon the characteristic data of the conduit, such as the radius, wall thickness, elasticity, etc., but not upon its length.

Because many sources of reflection at constrictions, junctions, marked curvatures, etc., are present in the arterial system, evaluation of Z is of great interest. Let us therefore look at the expression $Z = (R_2 + j\omega\rho)/(Q\gamma)$. For the thick-walled tube which we used for a previous example, R_2 was found to be $0.6 + \omega\,0.06$ for $\omega = 15$ (see 4.5), that is to say, for a frequency of 2.4 it would be 1.5, whereas $\omega\rho$ would be about 15, so that R_2 is about ten times smaller than $\omega\rho$. If we neglect the friction of the liquid in a first approximation, we obtain

$$Z = j\omega\rho/(Q\cdot\gamma) \qquad (6.16)$$

from 3.13 we have

$$\gamma^2 = \beta^2 - \alpha^2 + 2j\alpha\beta = (-\omega^2 v_0^2 + \omega^3 C)/(v_0^4 + \omega^2 C^2)$$

and therefore

$$\gamma = j\omega[(v_0^2 + j\omega C)/(v_0^4 + \omega^2 C^2)]^{\frac{1}{2}} \qquad (6.17)$$

Inserting this expression in 6.16 we obtain finally

$$Z = \frac{\rho}{Q}(v_0^2 + j\omega C)^{1/2} \tag{6.18}$$

If we further neglect wall friction, C becomes zero and we get for Z the very simple formula

$$Z = \rho v_0/Q \tag{6.19}$$

This formula was first proposed by Landes (9). It is also valid for the propagation of sound waves in rigid tubes. In this case v, as we have mentioned in the first section, is conditioned by the elasticity of the liquid and Z becomes very high in comparison with the surge impedance of a soft rubber tube. Because ωC is, in most cases, much smaller than v_0^2, equation 6.19 is a fair approximation, as demonstrated by our experiments.

If Z is real, that is to say if equation 6.19 can be used, pressure and current are in phase when no reflection is present. Experiments show, in most cases, that current leads pressure in phase by about 5 to 10 degrees. If we introduce liquid friction again, we obtain instead of 6.19 the equation

$$Z = (1/j\omega Q)\cdot(R_2 + j\omega\rho)(v_0^2 + j\omega C)^{1/2} \tag{6.20}$$

Because $j\omega C$ generally amounts to not more than 10 per cent of v_0^2, we can expand the root and get

$$Z = (1/j\omega Q)\cdot v_0^2\cdot[1 + j\omega C/(2v_0^2)]\cdot(R_2 + j\omega\rho) \tag{6.21}$$

Separating the real and imaginary parts, we can put Z in the form

$$Z = A + jB \quad \text{or} \quad Z = \bar{Z}e^{j\varphi} \tag{6.22}$$

where $\tan\varphi$ is given by

$$\tan\varphi = B/A = (\omega^2\rho C - 2v_0^2R_2)/(R_2\omega C + 2v_0^2\omega\rho).$$

Let us again use $\omega C = 0.48\cdot 10^5$, $\omega = 10$, $R_2 = 1.2$ (according to equation 4.5, $v_0 = 880$ cm/sec and $\rho = 1.14$. Then $\tan\varphi = -0.0714$ corresponding to an angle of about $-4°$. That is to say, current leads pressure by about $4°$, in fair agreement with the afore-mentioned experiments, because $I = P/Z = P/\bar{Z}e^{+0.071}$.

With the help of equations 6.11 and 6.12 we are now able to find the input impedance of a line which is closed at the end $z = l$. In this case, the output impedance will be real and infinite or in mathematical expression

$$P_l/I_l = \infty \tag{6.23}$$

From this we obtain the input impedance $P_0/I_0 = Z_0$ at the origin of the line with the surge impedance Z

$$P_0/I_0 = Z\cosh(\gamma l)/\sinh(\gamma l) \tag{6.24}$$

If we suppose Z to be real we obtain, by separation of the real and imaginary parts,

$$P_0/I_0 = Z\cdot[e^{2\beta l} - e^{-2\beta l} - 2j\sin(2\alpha l)]/ \cdot[e^{2\beta l} + e^{-2\beta l} - 2\cos(2\alpha l)] \tag{6.25}$$

For the undamped line with $\beta = 0$ we would have

$$P_0/I_0 = -jZ\sin(2\alpha l)/[1 - \cos(2\alpha l)] \tag{6.26}$$

that is to say, the input impedance is purely imaginary. The current leads the pressure by 90° if $\sin(2\omega l)$ is positive and lags behind the pressure if $\sin(2\omega l)$ is negative. Figure 16 shows the input impedance plotted against the length of the tube. The ordinates are the absolute value $|P_0/I_0|$ (solid line) and the phase angle (dotted line). Z has been taken as unity for $|P_0/I_0|$. If, for example, $l = \lambda/4$, λ being the wavelength, the current is maximal at the origin of the conduit and the pressure amplitude is infinitely

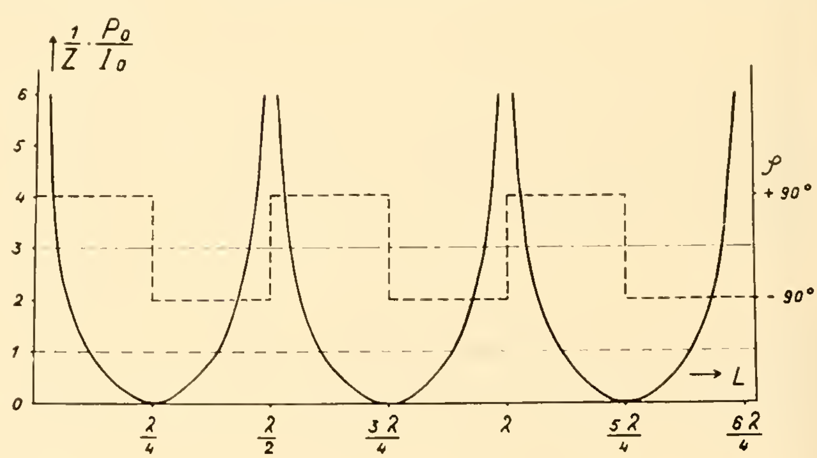

FIG. 16. Calculated input-impedance of a closed rubber tube. (Modulus P_0/P and phase φ) as a function of the tube length.

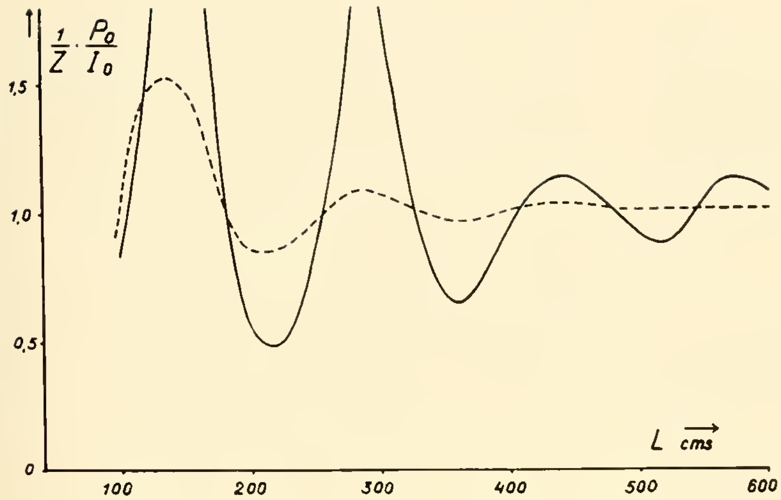

FIG. 17. Calculated input impedance with damping constants $\beta = 0.002$ and $\beta = 0.0055$.

small with respect to the current amplitude. At the closed end, of course, the current amplitude vanishes. The conditions are much like those in an organ pipe which is blown at one end and closed at the other. Standing waves can be established only if the length is an integer multiple of $\lambda/4$.

A somewhat different picture will be obtained if damping occurs. Two impedance curves calculated from equation 6.25 with damping constants $\beta = 0.002$ and $\beta = 0.0055$ are shown in figure 17. The oscillations of the input impedance with varying tube length decrease as we go to greater lengths, and the input impedance itself approaches the surge impedance as the length becomes very great. Such input impedance curves can easily be obtained experimentally if one records pressure and flow simultaneously at a given place in the conduit, designated as the origin. Figure 18 shows the result of such an experiment, where the flow has been recorded with an electromagnetic flowmeter (5). The frequency was kept constant, while the length of the line was varied by clamping the tube at different places. The dotted line corresponds to the function (6.25) with $\beta = 0.0038$. The shape of the experimental curve fits quite well with the calculated one. This is not very surprising, because equation 6.25 holds for any unidirectional wave propagation. The only qualification we have to make is that the dotted curve has been obtained using a constant β. Because we know that β depends on amplitude, the value $\beta = 0.0038$, which we had to use to fit the experiment, is therefore a kind of mean effective value.

With a damped line we can no longer obtain a true standing wave because the sum of the amplitudes of all partial waves running in the positive

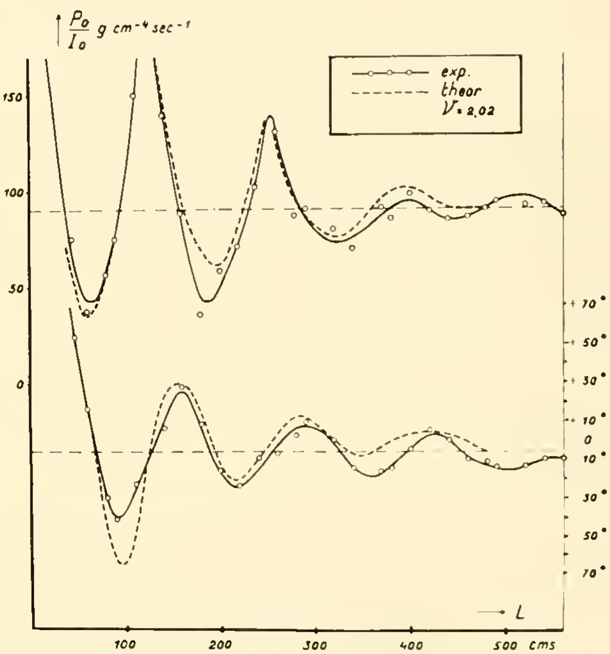

FIG. 18. Observed input impedance for the frequency = 2.02 (modulus and phase). Dotted line: calculated curve with $\beta = 0.0038$.

z-direction is always greater than the sum of the amplitudes of the reflected waves. At no point on the line, therefore, can the amplitudes cancel each other, and no nodes can be formed in the strict sense of the word. If reflection at the end of the line is incomplete, the argument holds even more strongly.

From equation 6.1 it follows, if we consider amplitudes only, that

$$P_z = P_0' e^{-\gamma z} + P_0'' e^{+\gamma z} \qquad (6.27)$$

and equation 6.7 furnishes

$$I_z = (P_0'/Z)e^{-\gamma z} - (P_0''/Z)\cdot e^{+\gamma z} \quad (6.28)$$

if we use the index $_0$ to indicate that the amplitude is taken at the origin $z = 0$. From equations 6.27 and 6.28 we obtain therefore the impedance at point Z

$$W_z = \frac{P_z}{I_z} = Z\cdot(P_0'e^{-\gamma z} + P_0''e^{+\gamma z})/(P_0'e^{-\gamma z} - P_0''e^{+\gamma z}) \quad (6.29)$$
$$= Z(P_z' + P_z'')/(P_z' - P_z'')$$

where P_z' and P_z'' are, in general, complex quantities containing the phase shift φ between pressure and flow. We will define the quantity

$$R = P_z''/P_z' \quad (6.30)$$

as the reflection coefficient and write the impedance at z in the form

$$W_z = Z(1 + R_z)/(1 - R_z) \quad (6.31)$$

For $R = 0$, that is to say, for a tube free from reflection, W becomes equal to the surge impedance Z at every point z, as already pointed out. W_z becomes infinitely large if $\bar{R}_z = +1$ or zero if $\bar{R}_z = -1$. The first case corresponds to a tube closed at z, the second to a tube open at z. The first case may be set up experimentally by clamping the tube, the second by connecting it to an open reservoir.

If we know the impedance W_z at a given point z along the tube, as from recordings of pressure and flow, we can find the reflection coefficient from

$$R_z = (W_z - Z)/(W_z + Z) \quad (6.32)$$

This possibility is of great interest in hemodynamics. If, at some peripheral point z along the arterial stem, we can make a simultaneous recording of pressure and flow, preferably with an electromagnetic flowmeter which integrates flow over the whole cross section, and if we determine the amplitudes and phases of the different harmonics with an analyzer as described in the preceding section, we shall obtain the reflection coefficient, that is to say, the ratio of the amplitudes of reflected to outgoing waves, and their respective phases as a function of frequency, provided that Z is also known at that point. Z might be roughly estimated at least from the diameter, wall thickness, and Young's modulus E or E' respectively, where care must be taken to measure E at the relative extension occurring in vivo.[7] Experiments of this kind might well be the best way to settle the old question of peripheral reflection.

When speaking of reflection, we must always keep in mind that the reflection coefficient is a function of locus, that is to say, of the coordinate z along the conduit. If we talk of the reflection coefficient of a constriction, for example, we mean the ratio of the incoming to the outgoing wave amplitude just before that constriction, but this reflection factor depends upon all the characteristics of the conduit before and beyond the constriction.

If we wish to know the input impedance of a conduit which has a reflection coefficient R_l at a certain point $z = l$ we obtain from equation 6.29

$$W_0 = (P_0/I_0) = Z(P_0' + P_0'')/(P_0' - P_0'')$$
$$= Z(P_l'e^{\gamma l} + P_l''e^{-\gamma l})/(P_0'e^{\gamma l} - P_l''e^{-\gamma l}) \quad (6.33)$$

and when $R_l = P_l''/P_l'$, we then have

$$W_0 = Z\cdot(1 + \bar{R}_l e^{-2\gamma l})/(1 - \bar{R}_l e^{-2\gamma l}) \quad (6.34)$$

With this equation we are able to calculate an unknown reflection coefficient at point $z = l$ from a measured input impedance W_0, if $\gamma = \beta + j\alpha$, that is, if the damping constant and the speed of propagation are known with sufficient accuracy. On the other hand, β and α may be found from input impedance when the reflection factor $\bar{R}_1$ at $z = l$ is known; for example, when $\bar{R}_l = +1$ for a tube clamped at $z = l$. This method proved to be quite useful for the determination of β. Indeed, the β-values given in figure 11 were obtained in this way. The determination of $\alpha = \omega/v$, on the other hand, can be obtained more precisely by direct determination of phase velocity from recordings at different places along a sufficiently long tube which is practically free from reflections.

The way in which the complex equation 6.34 can be solved for γ, that is to say for α and β, has been described in APPENDIX 2. As the result of such a calculation the reflection factor will be obtained in the form $\bar{R} = a + jb$, which can be stated in the more convenient form $\bar{R} = P''/P' = |\bar{R}|\cdot e\psi$. This means that the pressure of the reflected wave leads the pressure of the incoming wave by the phase ψ (which may also be negative).

We shall now apply these theoretical considerations to a few examples and compare the results with experiments carried out by the author.

If a second conduit of surge impedance Z_2 is joined to the first, with surge impedance Z_1, the reflection just before the joint will be

$$\bar{R} = (Z_2 - Z_1)/(Z_2 + Z_1) \quad (6.35)$$

[7] A technic similar to that used by Peterson (14) might well be used for this purpose.

TABLE 4

	Tube I	Tube II
Mean diameter	2.84 cm	2.04 cm
Wall thickness	0.112 cm	0.193 cm
v_0	628 cm/sec	880 cm/sec
$Z = \rho\, v_0/Q$	147 g cm^{-4} sec^{-1}	307 g cm^{-4} sec^{-1}

ρ = Density of filling fluid = 1.14.

To test this formula, some experiments have been carried out with two rubber tubes, the data of which are given in table 4. The direct determination of Z as the input impedance of a tube, the length of which was 10 meters and practically free from reflection, gave a value of 130 for frequency 1 and a value of 160 for frequency 5.

If we join the larger tube I to the narrower tube II we obtain from equation 6.35 a value of -0.352 for $\bar{R}$. That is to say, the reflected wave is reversed in phase as is the case for an open end, and the amplitude of the reflected wave will be 35 per cent of that of the incident wave. The calculation of the input impedance measured 30.5 cm before the joint gave the values plotted in the complex plane in figure 19 for the frequencies 1, 2, 3, and 4 cps. The calculations were made according to the method outlined in APPENDIX 2. The "vectors" drawn to the points from the origin correspond to the absolute value or "modulus" of $\bar{R}$. Their mean value is 0.46 instead of 0.35 as calculated from the simple and approximate equation 6.35 where only real values for Z have been used. The phase is somewhat smaller than 180° suggested by equation 6.35. If we take into account the complicated calculation of the input impedance, which demands an accurate knowledge of α and β, and the approximate character of equation 6.35, the agreement with theory is not too bad.

If, on the other hand, we join the narrow tube to the large one, we obtain a reflection factor of $+0.352$. The experiment gave in this case a mean phase angle of about $+35°$ instead of 0°, and the R-values showed a strong dependence upon frequency, ranging from 0.78 at frequency 1 down to 0.35 at frequency 4 and 0.1 at frequency 4.8. Agreement with the theory was therefore quite poor.

Better and fairly interesting results were obtained with rigid cannulas of different lengths inserted into the elastic conduit. Because these results are of some interest in regard to experiments on animals, which often necessitate the use of a cannula tied into a vessel, and because they furnish some information on the influence of stenoses and other pathological changes, we will discuss them briefly.

A piece of conduit of length l and surge impedance Z' shall be inserted into a tube line of practically infinite length and surge impedance Z. The propagation constants shall be $\gamma' = \beta' + j\alpha'$ and $\gamma = \beta + j\alpha$ respectively. Z' as well as Z are assumed to be real. The reflection coefficient at the peripheral joint will then be

$$\bar{R}_2 = (Z - Z')/(Z + Z') \qquad (6.36)$$

and the impedance at the central joint nearest the source of the wave will be

$$W_1 = Z'\cdot(1 + \bar{R}_2 e^{-2\gamma' l})/(1 - \bar{R}_2\cdot e^{-2\gamma' l}) \qquad (6.37)$$

If the inserted piece is either a rigid cannula or a short

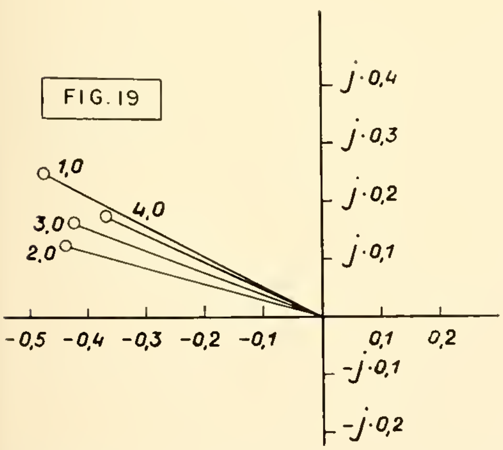

FIG. 19. Reflection at the junction of a wide tube and a narrow one, as:
. Complex R-values for different frequencies.

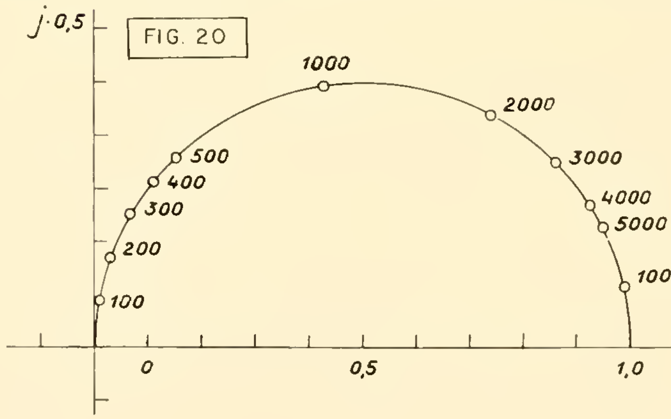

FIG 20. Calculated complex reflection coefficients of an inserted rigid cannula of length l. All the R's with different parameters ω l lie on a half circle with radius 0.5.

constriction, γ' or l are small. In this case the exponential can be expanded ($e^{-2\gamma' l} = 1 - 2\gamma' l$) and we obtain

$$W_1 = Z' \cdot [1 + \bar{R}_2(1 - 2\gamma' l)]/[1 - \bar{R}_2(1 - 2\gamma' l)] \quad (6.38)$$

Taking the value R_2 from equation 6.36 this leads to

$$W_1 = Z'[2Z' - 2\gamma' l(Z - Z')]/[2Z' + 2\gamma' l(Z - Z')] \quad (6.39)$$

The reflection coefficient at the central joint measured from the origin is

$$\bar{R}_1 = (W_1 - Z)/(W_1 + Z) \quad (6.40)$$

Taking for W_1 the value of equation 6.39 we obtain finally

$$\bar{R}_1 = [\gamma' l(Z' - Z)(Z' + Z)]/[2Z'Z + \gamma l \cdot (Z' - Z)^2] \quad (6.41)$$

As we have already mentioned, $Z' = \rho v'/Q$ holds also for the rigid cannula; v' is then the speed of propagation of a sound wave in the liquid of density ρ. Its order of magnitude is 10^5 cm/sec, whereas the propagation velocity for the elastic tube is of the order of magnitude of 10^3 cm/sec. If we use a cannula of the same cross section as that of the elastic tube $Z' \gg Z$, and we obtain for $\bar{R}_1$, after some transformations, the approximate formula

$$\bar{R}_1 = \gamma' l \cdot /[2Z/Z' + \gamma' \cdot l(1 - 2Z/Z')] \quad (6.42)$$

because $\gamma' l$ is very small, $2\gamma' l \cdot Z/Z'$ will be small of a higher order, and we may write

$$\bar{R}_1 = \gamma' l/[\gamma' l + 2Z/Z'] \quad (6.43)$$

For equal cross sections, the surge impedances are proportional to the propagation velocities, $2(Z/Z') = 2 \cdot v/v'$. For a glycerine-water mixture of density 1.14, the sound velocity will be 163,000 cm/sec, whereas the pulse wave velocity for the tube used was about 590 cm/sec; $2(Z/Z')$ was, therefore, 0.065. If we ignore damping in the rigid cannula, we can write $\gamma' = j\omega/v'$ and obtain from equation 6.43

$$\bar{R}_1 = j\omega l/(j\omega l + 2v) \quad (6.44)$$

Separating the real and imaginary parts, we get

$$\bar{R}_1 = \omega^2 l^2/(\omega^2 l^2 + 4v^2) + j \cdot 2\omega l v/(\omega^2 l^2 + 4v^2) \quad (6.45)$$

It can easily be seen that all points R lie on a circle of radius 0.5 in the complex plane. The center of the circle lies on the real axis at $x = 0.5$. The positions of the points R on the circle are functions of the parameter ωl only. Figure 20 shows such a half-circle with some points corresponding to the indicated parameters. The v value used was 590 cm/sec. This kind of representation (space-curve construction) is much used by electrical engineers.

Let us take, for example, the relatively small value $\omega l = 100$. Figure 20 gives for this a reflection coefficient of 0.09. A cannula of 10 cm length would then produce at frequency $10/(2\pi) = 1.6$ a reflected wave with an amplitude equal to 9 per cent of the incident wave with a phase shift of nearly 90°. A cannula of 5 cm length would reflect only about 5 per cent under the same conditions.

Measurements with three different cannulas of 10, 30, and 125 cm lengths, inserted into a rubber tube of the same cross section, showed in general the behavior predicted by the theory outlined above (fig. 21), taking into account the lack of precision of such measurements.

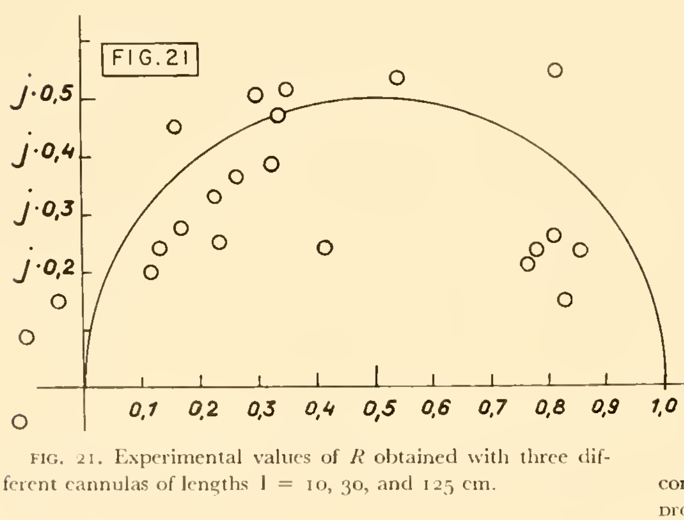

FIG. 21. Experimental values of R obtained with three different cannulas of lengths l = 10, 30, and 125 cm.

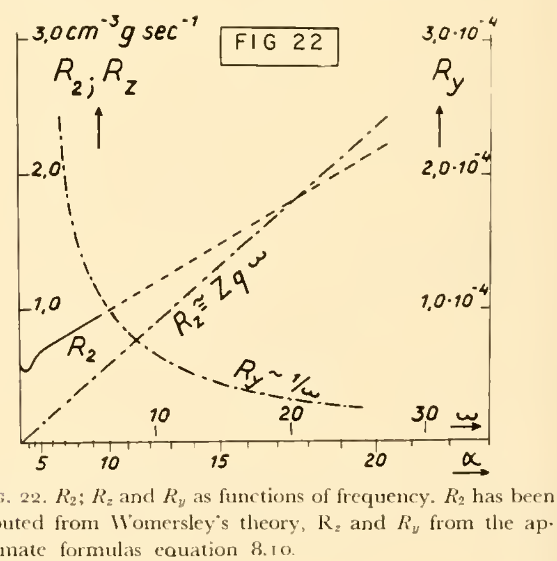

FIG. 22. R_2; R_z and R_y as functions of frequency. R_2 has been computed from Womersley's theory, R_z and R_y from the approximate formulas equation 8.10.

As an application to experimental technique, let us consider the case of a femoral artery with a pulse-wave velocity of 800 cm/sec. What will be the reflection coefficient for a cannula 5 cm long tied into it? For the angular frequency $\omega = 10$ or $\nu = 1.59$, we obtain from equation 6.45 $\bar{R} = j\cdot 0.031$; the reflected wave would therefore amount to about 3 per cent with a phase shift of 90°. But with a frequency of $\omega = 100$ ($\nu = 15.9$) we obtain $\bar{R} = 0.089 + j\cdot 0.284$, and the absolute value of $\bar{R}$ would be $\bar{R} = (0.089^2 + 0.284^2)^{1/2} = 0.296$. The reflected wave would therefore be about 30 per cent of the incoming wave, and the phase shift will be obtained from $\tan \psi = 0.284/0.089 = 3.19$ as $\psi = 72.6°$.

As a last example, ramifications shall be considered as a source of reflection. For the general case of ramification into two branches, we have to consider a conduit of surge impedance Z_1 splitting off in two branches, with surge impedance Z_2 and Z_3, respectively. In order to find the reflection coefficient just before the ramification, we must find the joint impedance Z' of the two branches. One might be tempted to put $Z' = Z_2Z_3/(Z_2 + Z_3)$ as we do in the case of two electrical transmission lines connected in parallel. This would lead to convenient formulas for the reflection coefficients, but our own attempts to check these formulas experimentally have given, so far, only negative results. This is not very surprising, because we cannot construct an actual ramification without creating some angles in the conduit. Such bends give rise to very complicated hydrodynamic conditions, even in the case of a stationary current, which have been the object of many experimental and theoretical studies in applied hydraulics. A brief account of these is given in a paper by Ansgar Müller (13). Whether or not gentle curves or sharp angles change the impedance in a conduit has not yet been systematically studied as far as we know. It seems to us that we may not use knowledge obtained exclusively from straight conduits to tackle the problem of ramifications, where changes in momentum occur.

7. HYDRODYNAMIC CONSIDERATIONS

In the previous sections we have treated wave propagation in an elastic tube as a one-dimensional problem, that is to say we considered total flow only as the product of mean velocity and cross section of the conduit, and did not worry about the velocity distribution over the cross section of the tube (velocity-profile). As early as 1878, Korteweg (6) worked out a hydrodynamic theory of wave propagation in tubes with ideally elastic walls and filled with a nonviscous, incompressible liquid. Since then, the theory has been further developed by Frank (3), Morgan & Kiely (11), Lambossy (8), and Womersley (24). Lambossy treats the case of pulsating flows of a viscous liquid in a rigid tube. He obtains a solution for velocity as a function of time and distance r' from the axis of the tube. From this solution he obtains, in addition to the velocity profile, the viscous drag acting on the surface of a liquid cylinder of radius r'. Integration furnishes the total resistance to flow and the deviation from Poiseuille's law, which we have already mentioned. Womersley, independently, obtained the same solution for a rigid tube although in a somewhat different form, and extended the theory to the elastic tube. The rather complicated functions are given in the form of tables in a more extensive paper (25). A common feature of both theories is the important statement that the type of flow depends upon the dimensionless parameter:

$$\alpha = r(\omega\rho/\eta_1)^{1/2} \tag{7.1}$$

the significance of which, for pulsating current, is similar to that of the Reynold's number for stationary flow. This is of practical importance in the designing of models. Experiments using soft rubber tubes of large diameter and low frequency are more difficult to make, and yield less accurate results than experiments on tubes with smaller bore and higher frequency. It cannot yet be stated, however, whether this statement holds true for the more complicated conditions present at sharp bends and ramifications.

We can obtain much information concerning resistance to flow (R_2) from the hydrodynamic theory. As we have already pointed out in section 4, Poiseuille's law, and therefore equation 4.4, is no longer useful to us when we change from the study of stationary flow to that of pulsatile flow.

Womersley finds, for mean flow in z-direction, the relationship

$$\bar{u} = \frac{P}{\rho v}\cdot\Phi(\alpha, k, \sigma)e^{j\omega(t-z/v)} \tag{7.2}$$

where the pressure is given by $p = Pe^{j\cdot\omega(t-z/v)}$. Φ is a complex function of the parameter $\alpha = r(\omega\rho/\eta_1)^{1/2}$, of the ratio k between wall thickness and tube radius ($k = a/r$), and of Poisson's ratio σ which we always take as 0.5. (The function Φ appears in Womersley's tables as $1 + \eta F_{10}$, where η is some other function having nothing to do with a viscosity constant.)

In order to find the value R_2, we start from equa-

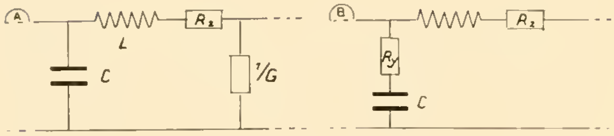

FIG. 23

tion 4.1, which we write, for the present purpose, in the form

$$R_2 \cdot \bar{u} = -\frac{\partial p}{\partial z} - \rho \frac{\partial \bar{u}}{\partial z} \qquad (7.3)$$

If we use for p the complex term from above, R_2 will also come out as a complex quantity. Dividing by the exponential, we obtain

$$\Phi \cdot R_2 \cdot P/v = j\omega P/v - j \cdot \Phi\omega P/v$$

and, finally, we get for the real part, which is the only part of interest to us,

$$R_2 = Re\{j\omega\rho(\Phi^{-1} - 1)\}$$

or

$$= -n_1(\alpha^2/r^2) \cdot \mathrm{Im}\Phi^{-1}$$

$$R_2 = -\eta_1(\alpha^2/r^2) \cdot \mathrm{Im}\{\Phi^{-1} - 1\} \qquad (7.4)$$

With $r = 1.02$ cm, $\eta_1 = 0.078$, $\rho = 1.14$, $k = 0.2$ (this is the set of values in the tables next to the sample calculation $a/r = 0.193/1.02 = 0.189$, which corresponds to our tube model), we obtain for $\alpha = 1$, which corresponds to the very low frequency $\nu = \omega/(2\pi) = 0.0105$ $\Phi = 0.0155 + j\,0.1235$ and the reciprocal $\Phi^{-1} = 1.025 - j\,8.13$. Finally R_2 becomes $0.078 \cdot 8.13/1.04 = 0.608$. That is to say, we obtain for this very low frequency practically the same value as we would obtain from equation 4.4, namely, $R_2 = 0.078 \cdot 8/1.04 = 0.600$.[8] In a similar way, we find for $\alpha = 10$ $R_2 = 1.01$. R_2 as a function of angular frequency or the parameter α is plotted in figure 22. Because Womersley calculated his tables only up to $\alpha = 10$, the dotted part of the curve is merely a guess.[9] Using a very crude approximation, R_2 can be represented by a linear relation. (Compare the discussion in section 8.) For the mentioned example, we obtained $R_2 = 0.6 + 0.06\,\omega$. We used this result previously in section 4, when discussing the influence of liquid friction on velocity of propagation and damping (see equation 4.5).

8. ELECTRICAL ANALOG OF THE ELASTIC TUBE AND ITS LIMITS OF APPLICATION

A reader familiar with the theory of electric transmission lines will see the striking resemblance between the propagation of pulse waves and electric waves along a line. This relationship was first mentioned by Landes (9). Before making extensive comparisons, we should first determine which type of electric conduit corresponds to the mechanical tube model. Let us consider a homogeneous electric line, for example a telegraph wire stretched out at a certain distance above the reconducting ground, or a one-core cable in a grounded reconducting sleeve. The cable or the telegraph wire has a definite resistance **R**, self-induction **L**, and capacity **C** per unit length (dz). The loss per unit length due to incomplete insulation may be represented by the conductivity **G**. We can therefore replace a part of the line dz by the scheme shown in figure 23*A*. For the tension u and the current i we can easily derive the differential equations

$$-\frac{\partial u}{\partial z} = \mathbf{R}_z \cdot i + \mathbf{L} \cdot \frac{\partial i}{\partial t} \qquad (8.1)$$

$$-\frac{\partial i}{\partial z} = \mathbf{G} \cdot u + \mathbf{C}\frac{\partial u}{\partial t} \qquad (8.2)$$

We look now for similar equations for our tube model. Equation 8.1 obviously corresponds to equation 4.1 in the form

$$-\frac{\partial p}{\partial z} = \frac{\rho}{Q} \cdot \frac{\partial i}{\partial t} + R_2 \cdot i. \qquad (8.3)$$

Now can we also find the mechanical equation corresponding to equation 8.2? Solving equation 3.5 for di/dz, we obtain (dropping the index z)

$$-\frac{\partial i}{\partial z} = \frac{2\pi r^3}{Ea}\frac{\partial p}{\partial t} + \frac{R_1 \cdot r^2}{E \cdot a}\frac{\partial^2 i}{\partial z \partial t} \qquad (8.4)$$

Equation 8.4 has no term with p, but only its derivative against time. Therefore the term including u in

[8] In a more general way this result can be obtained mathematically by expanding the function $F_{10} = 2\ J_1\ (\alpha\ j^{3/2})/[\alpha\ j^{3/2}\ J_0\ (\alpha\ j^{3/2})]$, where J_0 and J_1 are the Bessel functions of order zero and one. In this way we find, for small values of α, that $Im\ \{(1 + F_{10})^{-1}\} = -8/r^2$ and therefore $R_2 = \eta \cdot 8/r^2$.

[9] In this case, also, the function F_{10} can be approximated for large values of α by using the semi-convergent series for the Bessel functions J_0 and J_1. This leads to the asymptotic formula $R_2 = (\eta,\ \alpha/r^2)\ (2 \cdot \sqrt{2/x})$, where $x = 2.74$ for $\sigma = 0.5$ and $k = a/r = 0.2$, using Womersley's equation 40 with the + sign suggested by the preceding case $\alpha > 0$. A graph of R_2 values over a more extended frequency scale shows that the rise of the R_2-curve diminishes with increasing ω so that the R_2 value, say for $\alpha = 23$, would be about 1.9 instead of 2.3 as indicated by the dotted line in figure 22.

the electric analog is dropped, which means that the conductivity **G** must disappear. On the other hand we find, in the mechanical equation, a term with the composite derivative $[(R_1 r^2/Ea)\cdot(d^2i/dz\,dt)]$ which has no analog in equation 8.2. We will therefore try to work with a modified circuit according to figure 23*B* with $\mathbf{G} = 0$. In series with the capacity we connect a resistance $\mathbf{R}_y$. The decrease of current in the element dz of the transmission line corresponds then to the diagonal current driven by the tension u through the combination $\mathbf{CR}_y$. This tension is the sum of the tension $u_{\mathbf{R}_y}$ across the resistance $\mathbf{R}_y$ and the tension u_C across the capacity **C**, and we have

$$u = u_{\mathbf{R}_y} + u_C \qquad (8.5)$$

The term $-di/dz$ in equation 8.4 corresponds to the diagonal current i_y per unit length dz of the line, that is, to the current going through the side branch $R_y - \mathbf{C}$ of the substitute circuit; or, as a formula:

$$-\frac{\partial i}{\partial z} = i_y = \mathbf{C}\cdot\frac{\partial u_c}{\partial t} = \mathbf{C}\cdot\frac{\partial u}{\partial t} - \mathbf{C}\cdot\frac{\partial u_{R_y}}{\partial t} \qquad (8.6)$$

The voltage drop $u_{\mathbf{R}_y}$ is, however, $i_y R_y = -R_y di/dz$ and thus we get the electrical equations corresponding to the mechanical equations 8.3 and 8.4:

$$-\frac{\partial u}{\partial x} = \mathbf{L}\cdot\frac{\partial i}{\partial t} + \mathbf{R}_z\cdot i \qquad (8.7)$$

$$-\frac{\partial i}{\partial z} = \mathbf{C}\frac{\partial u}{\partial t} + \mathbf{C}\cdot\mathbf{R}_y\frac{\partial^2 i}{\partial z \partial t} \qquad (8.8)$$

The difference between these equations and the mechanical one lies only in the different meanings of the constants. Therefore, the substitute circuit (fig. 23) that we chose was practical. To simplify for the reader the change from one system to the other, we have put corresponding values together in table 5. In the first column, we find the terms for electrical values and some of their combinations. In the second column, we see the corresponding mechanical values as obtained by means of comparison with equations 8.7, 8.8, and 8.3, 8.4, respectively. The difference between the third and the second column is only the introduction of the velocity v_0 for the undamped case. The last column contains the dimensions of the mechanical constants for the tube line. For the electrical analog, as well as for the elastic tube, the product $\mathbf{R}\cdot\mathbf{C}$ of resistance and capacity, respectively, and the product of viscosity and reciprocal elasticity $1/E$ have the dimension of time.

Our electric model has, however, a great practical disadvantage, as previously acknowledged by Taylor (21). From the second column of table 5, we see that

TABLE 5

L	$\frac{\rho}{r^2\pi}$	$\frac{\rho}{r^2\pi}$	cm^{-5} g
C	$\frac{2\pi r^3}{E\cdot a}$	$\frac{r^2\pi}{\rho\cdot V_0^2}$	cm^{-1} g^{-1} sec^2
$\mathbf{R}_y$	$\frac{\eta\cdot a}{2\pi r^3}$	$\frac{\eta\cdot a}{2\pi r^3}$	cm^{-3} g sec^{-1}
$\mathbf{R}_z = R_2$*	$\frac{8\cdot\eta_1}{r^2}$	$\frac{8\cdot\eta_1}{r^2}$	cm^{-3} g sec^{-1}
$\mathbf{R}_y\cdot\mathbf{C}$	$\frac{\eta}{E}$	$\frac{\eta\cdot a}{2r\rho V_0^2}$	sec
$\frac{1}{(\mathbf{LC})^{1/2}}$	$\left(\frac{E\cdot a}{2r\rho}\right)^{1/2}$	V_0	cm sec^{-1}

* For low frequencies only ($\omega \to 0$).

there is an obvious dependence of **C** upon frequency, if the modulus of elasticity depends upon frequency. Nevertheless, this alone would not be too bad, because in most cases E depends very little on frequency, except in cases of very low frequencies not important in the physiological range. But matters are much worse for the diagonal resistance, $\mathbf{R}_y$, because η is approximately inversely proportional to the frequency ω, the product $\omega\eta$ staying more or less constant. Finally $R_z \geqq R_2$ is also inconstant, as we see theoretically from the Womersley papers mentioned in the preceding section. Taylor (21) shows that one may express the values $\mathbf{R}_z$, $\mathbf{R}_y$, **L**, and **C** in a more general way by Z and γ, that is to say, by the measurable surge impedance Z and the propagation constant $\gamma = \beta + j\alpha$. He obtains the expressions

$$\mathbf{R}_z = Re(Z\gamma) \qquad \mathbf{R}_y = Re(Z/\gamma)$$

$$\mathbf{L} = (1/\omega)\cdot Im\,(Z\gamma) \qquad 1/\mathbf{C} = -\omega\, Im\,(Z/\gamma) \qquad (8.9)$$

Re and *Im*, before the brackets, mean that one must take either the real or the imaginary part of the value in the bracket. Again we will first discuss the general course of the values considered. Z, as we know, is practically constant and real, $\alpha = \omega/v$ is almost exactly proportional to the frequency and the same too is approximately true for β. Therefore, we take $\alpha = p\cdot\omega$ and $\beta = q\cdot\omega$ and we have

$$\mathbf{R}_z = Z\cdot q\cdot\omega \qquad \mathbf{R}_y = (1/\omega)\cdot Zq/(q^2 + p^2) \qquad (8.10)$$

$$\mathbf{L} = Z\cdot p \cong \text{constant} \qquad \mathbf{C} = (p^2 + q^2)/(Zp) \cong \text{constant}$$

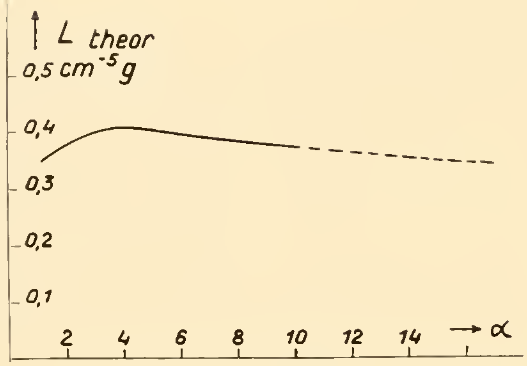

FIG. 24. Calculated values of L from equations 8.11 following Womersley's theory.

Of course, the proportionality of $\mathbf{R}_z$ with frequency is, again, a rough approximation, first because β is proportional to the frequency only in a general way and second, because Z, too, still depends a little upon frequency, showing a slight increase with it. **L** and **C** are practically constant. We might be tempted to believe that the resistance $\mathbf{R}_z$ is caused only by fluid friction and $\mathbf{R}_y$ only by wall friction. But this is not true because the damping constant β, and therefore q, is a function of both viscosities η_1, and η of the liquid, as well as of the tube wall. **L** is not absolutely constant. This might be explained from equation 8.10 by the variability of the surge impedance. In reality, there is a small interdependence between frequency and the oscillating mass of a definite part in the tube. It is also possible to obtain an expression for **L** from Womersley's theory. Taylor (21) obtains the following formula:

$$\mathbf{L} = \frac{\rho}{r^2\pi} Re\Phi^{-1} \qquad (8.11)$$

where Φ is the function already mentioned in the previous section. In figure 22 we have drawn not only the curve for R_2 calculated from equation 7.4, but also the function $R_z = Zq\omega$ and

$$\mathbf{R}_y = [Zq/(q^2 + p^2)]1/\omega$$

with $p = 1.20 \cdot 10^{-3}$ and $q = 2.9 \cdot 10^{-4}$. These values have been obtained from measurements with the thicker-walled tube used as an example several times before. For Z the real value 307 has been taken. In figure 24 the value **L** calculated from equation 8.11 has been represented as a function of the dimensionless parameter α. It increases a little from the value $\rho/(r^2\pi)$, passes through a flat maximum, and again approaches the initial value. That means that in a certain range of low frequencies, a little more of the liquid mass is in oscillation than for the higher frequencies.

A more detailed analysis has thus shown that the analogy between the elastic tube and the substitute electric circuit shown in figure 23*B* is only formal. To use such a system as the basis for analog computer studies on pulse waves, we would have to build resistances with the frequency characteristics postulated by the previous analysis. But these resistances should exhibit an ohmic character, which means that no phase shift should occur between current and tension. This might be achieved with certain expensive electronic equipment, but the whole circuit would be rather complicated. If someone succeeds in realizing such an analog, it might be used, for example, to study the propagation of a single pulse as a transient phenomenon, which is practically impossible by means of mathematics alone, even with the help of Fourier integrals or Laplace transformations. The study of single impulses in the mechanical model, using a rubber tube and with the help of recording manometers, is not of much use, because it is almost impossible to give the input pulses any specific desired shape. On the other hand, this is easy to do with electrical input pulses. Also, recording tension with a cathode-ray oscillograph is much simpler than with a recording manometer. The same is true for the recording of electric current, whereas the recording of flow in the tube model with the electromagnetic flowmeter involves rather expensive apparatus. The study of reflections due to ramification with the help of an electrical analog would not be of any use, because it would be based on the same false suppositions mentioned at the end of section 6. As a whole, not much insight can be gained from the electrical analog, because it provides only a different picture of things which are already understood. Nevertheless, its use has had merit, since it has acquainted physiologists with mathematical methods and such concepts as impedance, resistance, and so on, which have proved to be very useful in electrical engineering. The reason for our devoting so much space to all this lies in the fact that the use of analogs has become fashionable, and there is great danger that they may be used improperly. On the other hand, the recognition of common features in the different fields of science is always pleasant to the human mind.

APPENDIX 1

THE CONCEPT OF MECHANICAL IMPEDANCE

The concept of impedance was first used by electrical engineers in the treatment of problems involving alternating current. Impedance denotes the ratio of tension to current in alternating circuits. Because an alternating current or tension is defined by amplitude and phase, impedance can be most suitably represented by a complex quantity. Within the last few decades, due to the emergence of broadcasting and sound-recording technics, acoustics has become a new field of engineering and analogies with the theory of electrical currents and lines have been established (18). Also, because the physics of pulse-wave transmission is essentially homologous with the acoustics of very low frequencies, the concept of impedance can be explained using a simple example, similar to the well-known Helmholtz Resonator in acoustics.

Let us consider a rubber balloon filled with an incompressible liquid and tied to a rigid neck as represented by figure 1A. Some excess pressure p may be applied to the neck. The volume of the balloon shall be V. If a column of x cm of liquid from the neck with the cross section Q is pressed into the balloon, by the excess pressure p, its volume will be increased by the amount $v = Qx$. A restoring force of $-pQ$ will thus be created which balances the pressure p. We have thus

$$\frac{v}{V} = \frac{p}{\kappa} = \frac{Qx}{V} \tag{1}$$

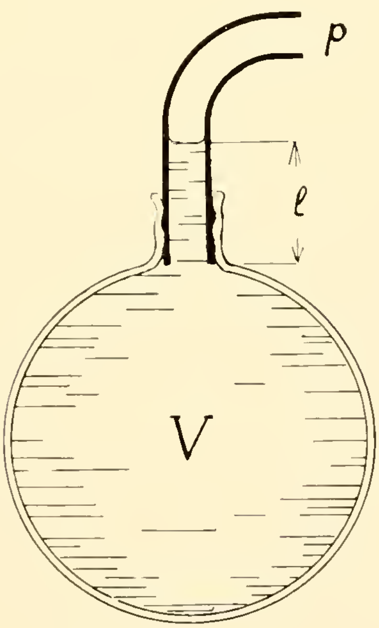

FIG. 1A

where $\kappa = pV/v$ denotes the volume elasticity. The amount of v is assumed to be small with respect to V. The restoring force is then

$$-pQ = -\frac{Q^2 x}{V} \cdot \kappa \tag{2}$$

If we change now from a constant excess pressure p to an alternating pressure $p' = p_0 e^{j\omega t}$ we have to consider a second force needed to accelerate a certain mass m of liquid. This mass corresponds approximately to the mass of liquid $m = Ql$ contained in the neck, where ρ stands for the density of the liquid, and l is the height of the liquid column in the neck. This inertial force is then $Q \cdot l \cdot \rho \cdot d^2x/dt^2$. Besides this we need another force $R\, dx/dt$ to overcome the friction in the neck, where dx/dt is the mean velocity in the neck. The dynamic equilibrium can then be expressed by the equation

$$Q \cdot l \cdot \rho \frac{d^2x}{dt^2} + R \cdot \frac{dx}{dt} + \kappa \cdot \frac{Q^2}{V} \cdot x = p'Q \tag{3}$$

A solution of this equation will be $x = x_0 e^{j(\omega t + \varphi)}$. With this we obtain from equation 3 the complex equation

$$x_0 \left(-\omega^2 Q \cdot l + j\omega R + \kappa \frac{Q^2}{V}\right) e^{j\varphi} = p_0 Q \tag{4}$$

Since we are interested in the ratio of pressure to flow we write $i = Q \cdot dx/dt$, and with $dx/dt = j\omega x_0 e^{j\omega t} e^{j\varphi} = j \cdot i_0 e^{j\omega t} e^{j\varphi}$ we obtain from equation 4

$$i_0 \left(-\frac{1}{j} \cdot Ql\rho\omega + R + \frac{\kappa \cdot Q^2}{j \cdot V \cdot \omega}\right) \cdot e^{j\varphi} = p_0 \tag{5}$$

or for the desired rate

$$W = \frac{p}{i} = \frac{p_0}{i_0} \cdot e^{-j\varphi} = R + j\left(Q \cdot l \cdot \rho \cdot \omega - \frac{\kappa Q^2}{V\omega}\right) \tag{6}$$

This equation looks much like the analogous equation

$$\mathbf{W}_l = \mathbf{R} + j\left(\omega \mathbf{L} - \frac{1}{\omega \mathbf{C}}\right) \tag{7}$$

for the electrical circuit represented by figure 2A, where **W** is the impedance of that circuit and i is the current flowing through the circuit due to the electromotive force u of a certain external power supply. **R** is the ohmic resistance, **L** the self-induction, and **C** the capacity of the circuit. Any

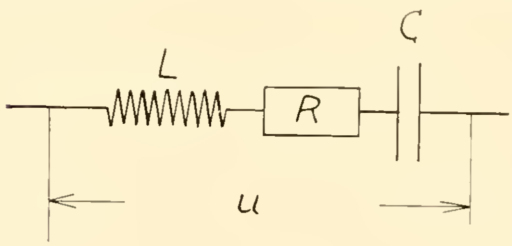

FIG. 2A

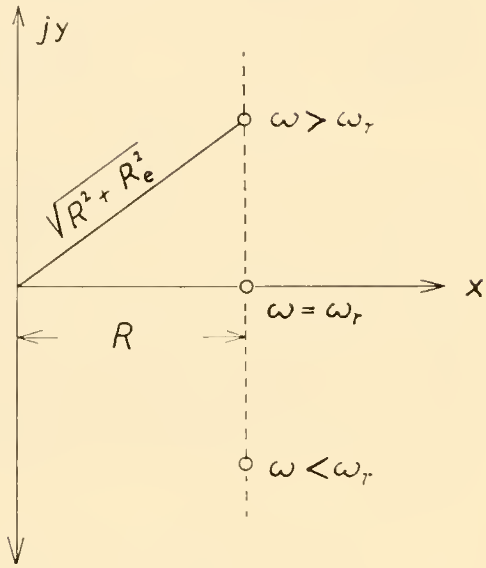

FIG. 3A

complex equation like 5 can be split into two real equations. If we use R_e as an abbreviation for $[Ql\rho\omega - (\kappa Q^2/\omega V)]$, and if we replace $e^{j\varphi}$ by $\cos\varphi + j\sin\varphi$, according to Euler's theorem we obtain:

$$i_0 e^{j\varphi} = i_0(\cos\varphi + j\cdot\sin\varphi) = p_0/(R + jR_e) \quad (8)$$

In order to separate the real and imaginary parts of the right side of the equation, we multiply numerator and denominator by the conjugate complex $R - jR_e$ of the latter. This leads to

$$i_0(\cos\varphi + j\cdot\sin\varphi) = p_0(R - jR_e)/(R^2 + R_e^2) \quad (8a)$$

From this we obtain the first real equation for the phase

$$\tan\varphi = -R_e/R \quad (9)$$

The real part of equation 9 furnishes

$$i_0\cdot\cos\varphi = p_0\,R/(R_e^2 + R^2) \quad (10)$$

With $\cos\varphi = 1/(1 + \tan^2\varphi)^{1/2}$ we get the second real equation

$$i_0 = p_0/(R^2 + R_e^2) \quad (11)$$

The highest possible amplitude of current or flow will be obtained if $R_e = 0$. This is the case when the angular frequency becomes

$$\omega = \left(\frac{\kappa Q}{V\cdot l}\right)^{1/2} \quad (12)$$

The frequency given by 12 is the resonant angular frequency of the rubber balloon with neck of length l and cross section Q.

Equation 6 permits a geometrical interpretation. For different frequencies, all the points $W = x + jy$ in the complex plane lie on a straight line parallel to the jy-axis which

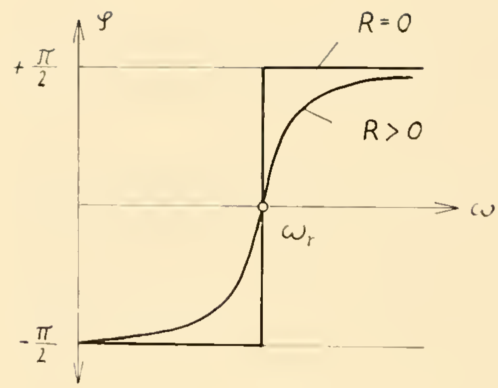

FIG. 4A

cuts the x-axis at the distance R from the origin, the corresponding frequency being the resonant frequency ω_r (fig. 3A). The distance from the origin to the point W is equal to the absolute value W of the impedance.

Figure 4A shows how the phase angle φ depends on the frequency. For the undamped case $R = 0$, the phase angle jumps from $(-\frac{1}{2})\cdot\pi$ to $+(\frac{1}{2})\pi$ at the resonant frequency ω_r. For $R > 0$ it passes continuously from $(-\frac{1}{2})\cdot\pi$ to $(+\frac{1}{2})\cdot\pi$ with increasing frequency.

The first term within the bracket in equation 6, $Q\cdot l\rho\omega$, is called inertance, while the second term, $\kappa Q^2/(V\omega)$, is called compliance. If these terms are properly chosen, a device similar to that of figure 1 might be used to match the surge impedance of a rubber tube, which would then behave like an infinitely long tube free from reflection.

APPENDIX 2

DERIVATION OF THE COMPLEX REFLECTION COEFFICIENT R

In order to find the complex reflection coefficient R for a given $\gamma = \beta + j\alpha$ from equation 6.34, we put R in the form $R = e^{2(a+jb)}$ and try to find a and b. If we insert this form for R into equation 6.34, we obtain with $\gamma = \beta + j\alpha$

$$\frac{W_0}{Z} = \frac{1 + e^{2(a+jb)}e^{-2(\beta+j\alpha)\cdot l}}{1 - e^{2(a+jb)}\cdot e^{-2(\beta+j\alpha)\cdot l}} = \frac{1 + e^{2(x+jy)}}{1 - e^{2(x+jy)}}$$

Using x for $a - \beta l$ and $y = b - \alpha l$. With the definitions

$$\frac{e^x + e^{-x}}{e^x - e^{-x}} = \text{cotanh}\,x \qquad \frac{e^x - e^{-x}}{e^x + e^{-x}} = \tanh x$$

we find

$$\frac{W_0}{Z} = -\text{cotanh}\,(x + jy)\quad \frac{Z}{W_0} = \tanh(-x - jy) = u + jv$$

When Z/W_0 is given as a measured quantity u and v are also known. Solving for x and y we obtain

$$x = -\frac{1}{4} \ln \frac{(u+1)^2 + v^2}{(u-1)^2 + v^2}$$

$$y = -\frac{1}{2} \cdot \left[(2k+1)\cdot\pi - \arctan \frac{u+1}{v} + \arctan \frac{u-1}{v} \right]$$

where k is an arbitrary integer. To y we can therefore add an arbitrary multiple of π. When x and y are obtained in this way, we find a and b from the equations

$$a = x + \beta l \qquad b = y + \alpha \cdot l + k$$

and therefore

$$\bar{R} = e^{2(a+jb)} e^{\pm 2jk} = e^{2(a+jb)}$$

REFERENCES

1. Betticher, A., V. Hardung, and J. Maillard. Eine elektronische Apparatur zur Messung der dynamischen Elastizität und Viskosität kautschukähnlicher Körper *Koll. Z.* 148: 66–73, 1956.
2. Dow, P., and W. F. Hamilton. An experimental study of the velocity of the pulse wave propagated through the aorta. *Am. J. Physiol.* 125: 60–65, 1939.
3. Frank, O. Die Theorie der Pulswellen. *Ztschr. Biol.* 85: 91–130, 1926.
4. Hamilton, W. F., and P. Dow. An experimental study of the standing waves in the pulse propagated through the aorta. *Am. J. Physiol.* 125: 48–59, 1939.
5. Hardung, V. Wellenwiderstand und Impedanzen der geraden Schlauchleitung. *Arch. Kreislaufforsch.* 29: 77–88, 1958.
6. Korteweg, D J. Über die Fortpflanzungsgeschwindigkeit des Schalles in elastischen Röhren. *Ann. Phys. und Chem.*, Neue Folge, 5: 225, 1878.
7. Lambossy, P. Aperçu historique et critique sur le problème de la propagation des ondes dans un liquide compressible enfermé dans un tube élastique. *Helvet. physiol. et pharmacol. acta* 8: 209–227, 1950.
8. Lambossy, P. Oscillations forcées d'un liquid encompressible et visqueux dans un tube rigid et horizontal. Calcul de la force de frottement. *Helvet Phys. Acta* 25: 371–386, 1952.
9. Landes, G. Die Berechnung des Schlagvolumens mit Berücksichtigung der Reflexionen, verteilter Elastizität, Masse und Reibung. *Arch. Kreislaufforsch.* 15: 1–23, 1949.
10. McDonald, D. A. *Blood Flow in Arteries*, London: Edward Arnold, 1960.
11. Morgan, G W., and J. P. Kiely. Wave propagation in a viscous liquid contained in a flexible tube. *J. Acoust. Soc. Am.* 26: 323–328, 1954.
12. Müller, A. Über die Abhängigkeit der Fortpflangungsgeschwindigkeit und der Dämpfung der Druckwellen in dehnbaren Röhren von deren Wellenlänge. *Helvet. physiol. et pharmacol. acta* 9: 162–176, 1951.
13. Müller, P. A. Die Strömungsverhältnisse in einem Krümmer mit kleinem Krümmungsradius. *Arch. Kreislaufforsch.* 19: 281–312. 1953.
14. Peterson, L. H., R. E. Jensen, and J. Parnell. Mechanical properties of arteries in vivo. *Circulation Res.* 8: 622–639, 1960.
15. Porjé, I. G. Studies of the arterial pulse wave, particularly in the aorta. *Acta physiol. scandinav.* 13 (Suppl. 42), 1946.
16. Ranke, O. F. Die Dämpfung der Pulswelle und die innere Reibung der Arterienwand. *Ztschr. Biol.* 95: 179–204, 1934.
17. Rymer, T. B., and C. C. Butler. An electrical circuit for harmonic analysis and other calculations. *Phil. Mag.* 35: 606–616, 1944.
18. Stewart, G. W., and R. B. Lindsay. *Acoustics, A Text on Theory and Applications.* New York: Van Nostrand, 1930.
19. Taylor, M G. An approach to an analysis of the arterial pulse wave. I. Oscillations in an attenuating line. *Phys. Med. Biol.* 1: 258–269, 1957.
20. Taylor, M. G. A simple electrical computer for Fourier analysis and synthesis. *J. Physiol.* 141: 23P–25P, 1958.
21. Taylor, M. G. An experimental determination of the propagation of fluid oscillations in a tube with a visco-elastic wall, together with an analysis of the characteristics required in an electrical analogue. *Phys. Med. Biol.* 4: 63–82, 1959.
22. Treloar, L. R. G. *The Physics of Rubber Elasticity.* Oxford: Clarendon Press, 1949.
23. Wetterer, E. Die Wirkung der Herztätigkeit auf die Dynamik des Arteriensystems. *Verhandl. deutsch. Gesellsch. Kreislaufforsch.* 22: 26–60, 1956.
24. Womersley, J. R. Oscillatory motion of a viscous fluid in a thin-walled elastic tube. I. The linear approximation for long waves. *Phil. Mag.* 46: 199–221, 1955.
25. Womersley, J. R. An elastic tube theory of pulse transmission and oscillatory flow in mammalian arteries. *WADC Tech. Rep.* 56–614, 1957.

The rheology of blood

L. E. BAYLISS | *Department of Physiology, University College, London*

CHAPTER CONTENTS

RHEOLOGY IS THE STUDY of the properties of a material or of a system of materials— which affect the way in which it flows. Suppose that a force acts on a system in such a way as to produce a deformation or change of shape; if the system is solid, the deformation is limited, and the original shape is regained when the force is removed; if it is liquid, the deformation increases continuously so long as the force is acting, and remains when the force is removed. There are, however, many kinds of apparently solid materials in which the shape is regained incompletely, so that there is some permanent deformation; and there are many kinds of apparently liquid systems—particularly colloidal systems—in which a small force, for example, will produce only a limited deformation, which may or may not be reversed when the force is removed, while a larger force will produce a progressively increasing deformation or flow. In the process of clotting or coagulation blood clearly behaves as a system which has the properties both of a liquid and of a solid, and the study of these properties may properly be regarded as part of the rheology of blood. But when circulating in the vessels of an animal or, indeed, in any conditions in which the phenomenon of clotting is excluded, blood would appear to be an obvious liquid. It has, nevertheless, certain peculiar properties, and it is not to be regarded as an "ordinary" liquid. It is with these properties that we are now mainly concerned.

SOME FUNDAMENTAL DEFINITIONS

Suppose that a liquid is flowing from one place to another. We imagine two parallel plane surfaces within it, such that one is in motion with respect to the other while remaining parallel to it. The velocity of one plane relative to that of the other, divided by the distance between them (i.e., the "velocity gradient") is the "rate of shear" of the liquid; it is measured in centimeters per second, per centimeter distance, or in (seconds)$^{-1}$. (It is usually necessary to suppose that the planes are very close together, since the velocity gradient may vary in different parts of the liquid.) In order to create a given rate of shear, a force must be exerted, the magnitude of which will depend on the area of the planes considered; for each unit area, the magnitude of the force is the "shearing stress," which is measured in dynes per square centimeter. The ratio of the shearing stress to the rate of shear is, in ideal conditions, a quantity

which depends only on the nature and temperature of the liquid, and is defined as its "viscosity." If a shearing stress of 1 dyne per cm^2 produces a rate of shear of 1 sec^{-1}, the liquid has unit viscosity; the unit being called the "poise," after Poiseuille.

Newton in his *Principia* considered the force necessary to move a solid through a liquid at a given velocity, and assumed as an hypothesis that the one was directly proportional to the other. This implies that the rate of shear is directly proportional to the applied shearing stress, and thus that the viscosity of the liquid is a constant, independent of either. But there was no experimental justification for this until Poiseuille made his extensive series of measurements in 1840. Although he himself did not express his results in this way, they showed that the viscosities of water, of a number of other liquids, and of watery solutions of crystalloidal substances were independent of the shearing stress applied. Such fluids are thus called "ideal" or "Newtonian" in respect of their behavior when made to flow. Many kinds of colloidal solution, however, and suspensions of particles which are large enough to be visible (with or without a microscope) do not obey the Newtonian assumption; they are said to be "anomalous" or "non-Newtonian." They do not have a definite coefficient of viscosity, and the "apparent viscosity" in any particular condition of shear is said to be "shear-dependent." Blood is such an anomalous fluid, and its apparent viscosity depends on the shearing stress applied.

If it is possible to find some part of the liquid in which the two parallel planes that are in relative motion may have a finite area, the motion of the liquid is said to be "laminar" in this region; in any region where such planes can have only an infinitesimal area, the motion is "turbulent." Put in another way, in laminar flow any small element of the fluid travels in a straight line, and the course that it takes is parallel to that taken by any other small element of the fluid. In turbulent flow, elements of the fluid do not, in general, travel in straight lines. Flow will be laminar only if the rate of shear is less than some critical value, and will become turbulent when the rate of shear becomes large.

FLOW IN TUBES

In the study of circulatory phenomena in animals, we are concerned almost entirely with the relation between the pressure required to drive the blood through the blood vessels and the volume rate of flow produced. This will be determined by the dimensions of the vessels and by the apparent viscosity of the blood in the conditions considered. But, owing to the geometry of the system, certain complications may arise.

Suppose that we have a rigid tube of circular cross section. It is filled with a liquid of viscosity η and connected to a reservoir at each end; the fluid in the reservoir at one end is under a hydrostatic pressure P_1, and that in the reservoir at the other end is under a pressure P_2. Then the "pressure head" which drives the liquid through the tube is $P_1 - P_2 = P$. The liquid is assumed to be incompressible, and the flow to be laminar and steady, so that any element of the liquid moves in a straight line parallel to the axis of the tube with constant velocity. The pressure is then uniform over the cross section of the tube at all distances from its ends (if it were not, some elements of the liquid would have a velocity perpendicular to the axis), and the fall in pressure per unit length of tube (the "pressure gradient") is constant from one end to the other and has a value given by P/l, where l is the length of the tube (if it were not, the velocity parallel to the axis would not be constant). When a liquid flows through a tube, the surfaces of uniform velocity will not be plane, as in the ideal conditions just considered, but will be cylindrical; the shear occurs between concentric circular sleeves. Consider a column of liquid of radius r and unit length. The force acting on its circular ends and driving it down the tube will be $\pi r^2 \cdot P/l$; the area of its surface, where it drags against the fluid outside it, will be $2\pi r$, so that the shearing stress (τ_r) at this surface will be given by:

$$\tau_r = P \cdot r/2l \tag{1}$$

Thus the shearing stress increases from zero at the axis of the tube to a maximum value at the wall of the tube, the average value ($\bar{\tau}$) being given by:

$$\bar{\tau} = P \cdot a/4l \tag{2}$$

where a is the radius of the tube.

We now make two further assumptions: *1*) the velocity of the very thin layer of liquid which is in contact with the wall of the tube is zero. (This assumption, that the liquid does not "slip" along the wall of the tube, is justified by the most careful and accurate measurements that have been made with Newtonian fluids in rigid tubes.) *2*) The viscosity (or apparent viscosity) of the liquid is the same at all distances from the axis of the tube. We then find that

the linear velocity, u, of the liquid at any radius r is given by:

$$u_r = \frac{P}{4\eta l}(a^2 - r^2) \tag{3}$$

where η is the coefficient of viscosity, as already defined. This equation defines the "parabolic distribution of velocities": if u_r is plotted against r, the curve obtained is a parabola, with its vertex at the axis of the tube. Finally, the volume rate of flow through an elementary annulus of radius r and width dr will be $2\pi r \cdot dr \cdot u_r$. Thus the total rate of flow will be given by:

$$Q = 2\pi \int_0^a r \cdot u_r \cdot dr$$

On inserting equation 3 and integrating, we get:

$$Q = \frac{\pi a^4}{8\eta} \cdot \frac{P}{l} \tag{4}$$

This is the well-known "Poiseuille equation." Poiseuille himself deduced it from his experimental observations on the flow of various kinds of liquid through tubes of different dimensions, and used an empirical constant in place of the coefficient $\pi/8\eta$. The deduction of the equation from the Newtonian assumption, of the proportionality between rate of shear and shearing stress, was made by Wiedemann in 1856, and more precisely by Hagenbach in 1870.

If we combine equation 4 with equation 3, we get:

$$u_r = \frac{2Q}{\pi a^2}(1 - r^2/a^2) \tag{3a}$$

The mean linear velocity, $\bar{u}$, is given by: $\bar{u} = Q/\pi a^2$, and is thus one-half the maximum linear velocity at the axis of the tube, where $r = 0$. We may deduce further, that the rate of change of velocity with radius—i.e., the rate of shear—is given by:

$$D_r = \frac{4Q}{\pi a^3} \cdot \frac{r}{a} \tag{5}$$

The rate of shear at any value of the radius is, of course, $1/\eta$ times the shearing stress at that radius, is zero at the axis of the tube, and has a maximum value at the wall of the tube. It is important to remember, however, that in deriving equation 3 it is assumed that η is independent of r. When the liquid is non-Newtonian, for example, or in certain other conditions to be discussed later, this will not be justified; the distribution of velocities will not be parabolic, and the velocity and rate of shear at any value of the radius cannot be correctly calculated by means of equations 3a and 5.

According to the Poiseuille equation 4, the rate of flow, Q, is directly proportional to the applied pressure head, P. This will be true only when the pressure gradient is uniform and the flow is laminar. The first of these requirements cannot be satisfied in practice without special arrangements, although the error introduced can be made negligible; the second is satisfied only if the pressure gradient and rate of flow are less than certain limiting values.

The Kinetic Energy Correction

The fluid in the reservoirs at each end of the tube is sensibly at rest. On entering the tube, each element must be accelerated to its steady velocity u_r; this requires the expenditure of power, which can be derived only from the pressure head applied. On leaving the tube, the kinetic energy of the fluid will, in general, be dissipated in the reservoir as heat. In order to create a volume rate of flow Q, it is necessary, therefore, to apply a pressure head greater than that expected from the Poiseuille equation. The conditions at the entrance to the tube, before the parabolic distribution of velocities has been taken up, are complicated; but it is generally accepted that the value of this additional pressure head is given by:

$$p = m\frac{\rho Q^2}{\pi a^4} \tag{6}$$

where ρ is the density of the liquid and m is a constant the value of which is close to 1.10 (its precise value depends on whether the tube is cut off sharply at the ends, or is opened out into a bell-mouth, and may vary with the rate of flow). It is always desirable to ensure that the kinetic energy correction is small—i.e., that p is small compared with P. Equation 6 may be written in the form:

$$\frac{p}{P} = \frac{m\rho}{64\eta^2} \cdot \frac{a^2}{l^2} \cdot P \tag{6a}$$

The correction, therefore, will become increasingly significant as the applied pressure becomes greater. If the correction is significant, but is not applied, the rate of flow corresponding to a given pressure head will be smaller than that expected from the Poiseuille equation: the line relating rate of flow to applied pressure will become curved, concave to the axis of pressure.

Turbulence

The assumption that the flow is laminar is justified only so long as the mean linear velocity of the liquid is not too large. The critical quantity concerned is the "Reynolds Number" (*Re*), which is defined as:

$$Re = \frac{\bar{u}a\rho}{\eta} \tag{7}$$

where the quantity η/ρ is the "kinematic viscosity." (Some authors use the diameter of the tube in place of the radius, a; their values of *Re* are then twice as large as those given here.) If *Re* is small, the flow will be laminar, and if *Re* is large, the flow will be turbulent; but it is not possible to state some precise value of *Re* below which the flow will certainly be laminar and above which it will certainly be turbulent. The smooth rectilinear motion of the liquid in the tube is likely to be disturbed if the liquid in the reservoir is in motion before it enters the tube; if the end of the tube is cut off sharply and does not open out gradually in a bell-mouth; and if there are discontinuities, sharp bends, or branches in the tube. The greater the value of *Re*, the more likely it is that turbulence will start. If *Re* is greater than about 200, turbulence may occur at branches of a system of tubes, for example; but if it is less than 1000, this turbulence will not persist but will die away as the liquid flows along the tube, and the flow will be approximately laminar. If *Re* is greater than 1000, turbulence is likely to occur even in a single straight tube; although if special precautions are taken to eliminate all the factors which are likely to initiate turbulence, laminar flow may persist up to values of *Re* of 10,000 or more.

More complete treatments of the nature of fluid flow and of the techniques of viscosity measurement will be found in appropriate monographs, such as that by Barr (2).

TURBULENCE IN BLOOD. The conditions determining the onset of turbulence in blood are sensibly the same as those which determine its onset in water. In a smooth straight tube the critical value of *Re* is about 1000 (12). This value is not ordinarily attained in any part of the vascular system of an animal except the aorta. Values of several hundred may occur in the larger arteries, so that transient turbulence may be expected to occur at branches and sharp bends as, indeed, has been observed (32). The greater part of the fall in pressure, however, occurs in the smaller arterioles, and it is most unlikely that turbulence will occur in these.

VISCOSITY OF SUSPENSIONS

The effect on the viscosity of a liquid of inserting a number of spherical particles, so as to make a suspension, was studied theoretically by Einstein (14, 15). Provided the particles are so far apart that the motion of any one of them does not affect that of any other, the viscosity of the suspension is directly proportional to the total volume of particles in unit volume of suspension, and is independent of their size. Thus, if the viscosity of the suspending fluid (which we will suppose to be water) is η_w, a suspension in which the volume of the particles in unit volume of suspension (the volume fraction) is α will have a viscosity η, given by:

$$\eta/\eta_w = \eta_s = 1 + 2.5 \cdot \alpha \tag{8}$$

where η_s is the "relative viscosity" of the suspension.

If the particles are not spherical, theoretical studies by Jeffery (28) indicate that the coefficient 2.5 should be replaced by a smaller figure; in the limiting case of flat discs (to which we may approximate the red blood cells) the expected figure is 2.061 (this assumes that the flow takes place with a minimum dissipation of energy).

The simple Einstein relation between relative viscosity and volume concentration is valid, not only for suspensions but also for solutions, crystalloidal and colloidal. But it ceases to hold even approximately if the volume fraction is greater than about 0.1 (10%). If the concentration is greater than this, the observed relative viscosity is greater than that calculated, owing to the interactions between the particles. If one particle moves past another, each will exert a drag on the other even if they do not actually come into contact. If they collide, they may remain in contact for varying periods of time, and this will have two consequences: *1*) A group of 2, 3, or more particles will enclose and "immobilize" a certain volume of the suspending fluid; the effective volume fraction of the particles is thus greater than the measured volume fraction, and the viscosity of the suspension is correspondingly increased; and *2*) a certain force may have to be applied in order to drag the particles apart again; the suspension will then have non-Newtonian properties, as will be discussed in more detail later. Theoretical studies by Guth & Simha (21) and by Vand (39) show that the effect of these interactions between the particles on the relative viscosity of the suspension may be expressed by adding to the Einstein equation terms in α^2, α^3, etc. in an infinite series. The coefficients of these higher powers

of α, however, cannot be precisely evaluated without making some rather arbitrary assumptions.

Various empirical, or semiempirical, equations relating relative viscosity to volume fraction in more concentrated suspensions have been put forward. Most of them have been used to describe the relation between the relative viscosity of plasma and the protein concentration, and the relation between the relative viscosity of blood and the red cell concentration (hematocrit value): none of them, however, does so perfectly. Since the viscosity of blood is shear-dependent, it is obvious that the effect of changing the hematocrit value must be observed in some defined conditions of shear, although this has not always been done. The most suitable is the asymptotic condition which is approached when the shearing stress is very large, and the blood behaves nearly as a Newtonian fluid (see below).

Arrhenius (1) modified and extended the Einstein equation, and arrived at the expression:

$$\log \eta_s = \beta \cdot c \tag{9}$$

where c is the "mole fraction" of the suspended particles, i.e., the ratio (number of moles in disperse phase)/(number of moles in continuous phase). Roughly, if the densities of the two phases are not very different, we can put $c = \alpha/(1 - \alpha)$. Empirically, however, it was found necessary to increase the value of c by an arbitrary factor representing the volume of suspending fluid which is carried along with the suspended particles. This equation does not fit very well when applied to the viscosity of dog defibrinated blood (3). An equation of this form, however, in which the hematocrit value (i.e., α) is inserted in place of c describes adequately the viscosities of suspensions of red cells in acid citrate-dextrose solutions (23).

Bingham & White (8) and Hess (25) independently, but using the same general conceptions, different from those used by Einstein, arrived at an expression of the form:

$$\eta_s = 1/(1 - b \cdot \alpha) \tag{10}$$

where b is an arbitrary factor representing the increase in the "effective" volume fraction of the suspended particles. This equation may be used to estimate the viscosity of plasma or serum from the protein concentration, within the limits of variation likely to occur in living animals. If the protein concentration is expressed in grams per 100 ml, the value of b is 0.06. When applied to blood, however, the factor b must be made a function of α. If we make $b = 1/\alpha^{2/3}$, we get:

$$\eta_s = 1/(1 - \alpha^{1/3}) \tag{11}$$

which is the expression derived by Hatschek (22) for the flow of an emulsion so concentrated that the particles are deformed into flat polyhedra. The asymptotic minimum viscosity of dog defibrinated blood has been found to be a constant fraction of that deduced from the Hatschek expression, over a wide range of hematocrit values (3, 42). If the radius of the tube is 200μ or over, this fraction is approximately 0.6 at 37°C; for smaller tubes, it is smaller by an amount which is plotted in figure 2.

Effect of Temperature on the Viscosity of Blood

The relative viscosity of a suspension or solution should be unaffected by temperature unless the volume fraction or the shape of the suspended or dissolved particles changes; its absolute viscosity, therefore, should depend on temperature to the same extent as does that of the suspending fluid. This is true of plasma or serum, and the viscosity measured at one temperature may be corrected to some other temperature by reference to the tabulated values of the viscosity of water (27, 29).

The relative viscosity of blood, however, rises by about 10 per cent when the temperature is reduced from 37°C to about 17°C (3). This temperature effect is sensibly independent of the hematocrit value of the blood when this is greater than about 30 per cent. It is probable, though not definitely established, that the increase in the relative viscosity as the temperature is reduced is due to a small increase in the volume of each red cell, together with a change of shape towards a more spherical and less disc-like form. There is no reason to believe, however, that the rheological properties of blood are substantially altered when it is allowed to cool to room temperature. These properties are, in fact, more stable at the lower temperature, and many of the observations to be referred to subsequently have been made at about 20°C.

THE NON-NEWTONIAN FLOW OF BLOOD

Let us take a sample of blood of approximately normal composition, make it flow through a tube, and plot the relation between the volume rate of flow and the pressure head applied across the ends of the

tube. If the pressure head is sufficiently large, and the mean shearing stress within the tube (equation 2) is greater than about 50 dynes per cm^2, the plotted points will lie closely about a straight line (the kinetic energy correction must be applied, of course, if necessary, and the correction must be small, owing to the uncertainty in its exact value). This straight line, if extrapolated, will appear to indicate that the rate of flow would be zero when the applied pressure is such that the mean shearing stress is about 10 dynes per cm^2 (the exact figure varies greatly in different samples of blood). This, however, is only apparent, since if the extrapolated "intercept" pressure is applied to the tube, the blood will be found to flow quite readily, and will continue to flow even when the pressure is reduced well below this value (5, 23). In this region, the plotted points indicating the relation between the rate of flow and the applied pressure lie on a smooth curve, which is convex to the pressure axis.

Now according to the Poiseuille equation, the relation between the rate of flow of a Newtonian fluid (Q) and the applied pressure head (P) should be represented by a straight line passing through the origin of the flow and pressure axes (equation 4). Blood, therefore, is not a Newtonian fluid. If the red cells are separated from the plasma or serum, and resuspended in a simple saline solution, the plasma or serum is found to behave as a Newtonian fluid, whereas the suspension of cells is non-Newtonian; the anomalous behavior of blood is due, therefore, to the presence of the red cells. In studying these properties, we are thus concerned primarily with the effects produced by the presence of the red cells; and we are concerned with the relative viscosity of the blood with respect to that of the plasma. In a tube of given dimensions, we may write the Poiseuille equation for the flow of plasma in the form:

$$Q_p = G_p \cdot P \tag{12}$$

where the quantity G_p (which may be called the "conductance" of the tube for plasma) replaces the quantity $\pi a^4/8\eta_p \cdot \eta_w l$, where η_p is the relative viscosity of the plasma, η_w is the absolute viscosity of water, l is the length of the tube, and a is its radius. Similarly, for the flow of blood, in the same tube, we may write:

$$Q_b = (G_p/\eta^*) \cdot P \tag{13}$$

where η^* is the apparent viscosity of the blood, relative to that of the plasma, in the particular conditions of measurement; its value depends not only on the volume fraction of the red cells (the hematocrit value) as already discussed, but also on the shearing stress applied, on the radius of the tube, as will be discussed later, and on other factors, some of which have not been precisely defined. As is obvious from equation 13, the apparent relative viscosity of the blood at any particular value of the applied pressure and rate of flow is proportional to the ratio P/Q_b. Owing to the curvature of the pressure-flow line, this ratio falls steadily towards an asymptotic value as P and Q_b are made larger.

When the shearing stress is large, and the pressure-flow line sensibly straight, we may write equation 13 in the form:

$$Q_b = (G_p/\eta^*_\infty)(P - P^*) \tag{13a}$$

where η^*_∞ is defined by the slope of the straight line to which the observed pressure-flow line approximates—i.e., by the ratio dP/dQ_b when P approaches infinity—and P^* is the intercept of this line on the axis of pressure. If P is made very large compared with P^*, the mean shearing stress being not less than about 150 dynes per cm^2, and provided that the flow remains laminar, the ratio P/Q_b will be nearly constant; in these limiting conditions blood will appear to behave as a Newtonian fluid.

The reduction in the apparent viscosity of blood with increase in the shearing stress and rate of shear has been observed chiefly when the blood is made to flow through a tube; it appears to have been noticed first by Ewald (17). Brundage (9), however, observed it when blood was sheared in a rotating cylinder (Couette) viscometer; in this apparatus the shear occurs in the annular space between two concentric cylinders, the outer one being rotated at different but constant speeds, and the torque produced on the inner one being measured by means of a torsion wire. Copley *et al.* (11), again, observed it in an apparatus in which relative viscosities were measured in terms of the rate at which a sphere rolled down an inclined tube filled with blood; the shearing stress and rate of shear being varied by altering the inclination of the tube. It is not to be expected, however, that the change in apparent viscosity with a given change in shearing stress or rate of shear will be the same in all these types of viscometer. Several different factors are responsible for the effects observed.

Orientation of the Red Cells

If the particles of a suspension are not spherical, and in the limit are either thin rods or flat discs, they may become orientated when the suspension is

sheared. If the long axis of a rod lies along the axis of the tube through which the suspension is flowing, or the flat surface of a disc is parallel to the wall, there will be a minimum disturbance to the lines of flow, and the presence of the particle will have the least effect on the viscosity of the system. Such an orientation, however, is unstable, and any small departure from it would result in a rotation of the particle through 180°. Indeed, if the motion of any one particle is not seriously interfered with by the presence of neighboring particles, it may be observed to undergo continuous rotation as it passes down the tube. But its angular velocity is a minimum when it is in the state of metastable orientation along the lines of flow, and is a maximum when it is at right angles to this; there will thus be a "statistical" orientation in the direction which leads to a minimum value of the viscosity of the suspension. The difference between the maximum and minimum angular velocities will increase with increase in the rate of shear, and so also will the fraction of the particles which are in the optimum condition of orientation at any moment: the viscosity will thus be shear-dependent.

Direct microscopic observation of suspensions of small rod-shaped particles, flowing through a tube, has shown that with increase in the rate of flow the particles become increasingly orientated along the axis of the tube (16); the viscosity of the suspension also decreases with increase in the rate of shear. A similar effect has been observed in suspensions of tobacco mosaic virus, the average orientation of the particles being measured in terms of the birefringence of the suspension (36). When blood is sheared, both its optical transmittance (30, 41) and its electrical conductivity, measured in the direction of flow (12, 41), increase. These changes would be expected if the red blood cells became partially orientated along the lines of flow. It is probable, therefore, that orientation effects will contribute to the reduction in the apparent viscosity of blood with increase in the rate of shear.

Coherence Resistance and Friction

In 1912, Hess (24), having observed that the rate of flow of blood through a tube decreased, as the pressure head was reduced, more than in proportion to the reduction in pressure, suggested that this resulted from the existence of a "coherence resistance" between the red cells, independent of the rate of shear, in addition to the viscous resistance, proportional to the rate of shear. Bingham (6), independently, made the analogous suggestion that the anomalous flow properties of paints were due to "friction" between the particles of the pigment in suspension.

The essential feature of both hypotheses is the replacement of the simple Newtonian assumption, that the shearing stress (τ) is equal to the product of the viscosity (η) and the rate of shear (D), by an equation of the form:

$$\tau = \eta \cdot D + f \qquad (14)$$

where f is the "friction" per unit area. Thus D is zero unless τ is equal to, or is greater than f (f is of the nature of a "static" friction or "stiction," and D does not become negative when τ is less than f). The expected relation between the rate of flow of a suspension in which there is friction and the applied pressure head was worked out by Buckingham (10) and by Reiner (35), independently. It may be written in the form:

$$Q_b = \frac{G_p}{\eta}\left(P - \frac{4P_f}{3} + \frac{P_f^4}{3P^3}\right) \qquad (15)$$

There will be a finite pressure head P_f below which the suspension will not flow at all; if the applied pressure head is large compared with P_f, the line relating the rate of flow, Q_b, to the pressure head will approach an asymptotic straight line; this line, when extrapolated back to $Q_b = 0$, will cut the axis of pressure at $4P_f/3$.

The Buckingham-Reiner equation is not, in fact, obeyed either by blood or by paint. It has not been possible to discover a value of the pressure head below which the flow ceases. If there is such a critical pressure, it is an order of magnitude smaller than the intercept of the asymptotic straight line on the axis of pressure. This is illustrated in figure 1, in which the thick line represents the observed pressure-flow relation of a sample of dog defibrinated blood under small values of the shearing stress, the "asymptotic" line is the extrapolation of the straight line obtained under very large values of the shearing stress, and the "calculated" line is the pressure-flow relation deduced from the Buckingham-Reiner equation. Bingham accounted for this by supposing that when the applied pressure was less than the "friction" pressure, a "plug" of unsheared suspension moved down the tube within a thin layer of suspending fluid between it and the wall of the tube. The existence of such a "slippage" layer is to be inferred also from several

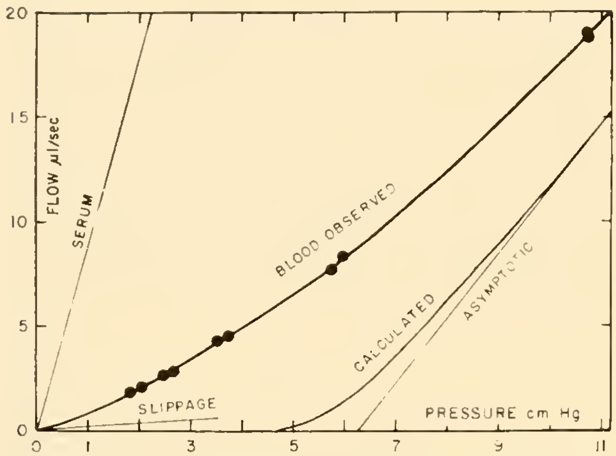

FIG. 1. The pressure-flow relation of a sample of dog defibrinated blood: hematocrit 49%; tube radius 480 μ; tube length 155 cm; mean shearing stress (dyne. cm^{-2}) = 1.38 × pressure (cm Hg). The "asymptotic" line, on extrapolation, intercepts the line of zero flow at a pressure of 6.3 cm Hg; from its slope the asymptotic relative viscosity of the blood is deduced to be 3.05. The "calculated" line is that derived from the Buckingham-Reiner equation (equation 15), the "friction" pressure being ¾ of the "intercept" pressure. The "slippage" line is the pressure-flow relation for "plug" flow within a marginal sheath 2 μ wide.

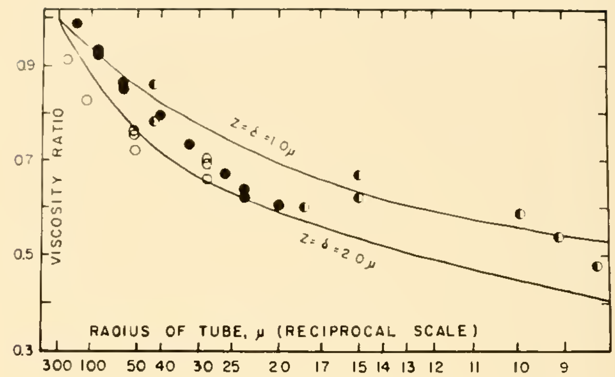

FIG. 2. The ratio of the viscosity observed in a small tube to the viscosity of the same (or a similar) sample of blood observed in a tube of radius greater than 200 μ, plotted against the reciprocal of the radius of the tube. ●: Data of Fåhraeus & Lindqvist (19): human blood, 3 samples. ⊙: Data of Kümin (31): ox blood, 5 samples. ◖: Data of Bayliss (3): dog's blood, 7 samples. The lines are calculated from equations 18 and 22.

other properties of suspensions. Whether it is sufficient, by itself, to account for the departure of the pressure-flow line of blood from that to be expected from the Buckingham-Reiner equation cannot be decided until some other aspects of the flow of blood have been discussed.

FLOW OF BLOOD IN VERY SMALL TUBES

If the apparent viscosity of blood depends only on the shearing stress applied to it, its value (as measured in terms of the pressure-to-flow ratio), at any given value of the average shearing stress in the tube, should be independent of the radius of the tube. So long as this radius is more than about 100 times the radius of the red cell, this, on the whole, is found to be true. But if the radius of the tube is made smaller than this, the apparent viscosity of the blood is found to be less than the value observed in larger tubes; and the smaller the tube, the smaller the viscosity. The effect is of considerable magnitude, as may be seen in figure 2. In a tube of radius 20 μ, for example (approximately that of the arterioles), the asymptotic apparent viscosity of blood is about two-thirds of the value obtained in large tubes, such as are ordinarily used in viscometers.

Attention was first called to this phenomenon in blood by Fåhraeus & Lindqvist (19), and it has since been observed by many others (e.g., 3, 23, 31). But it is a phenomenon which has been observed also in many kinds of suspension, such as paint (7), clay, glass beads, etc. Dix & Scott Blair (13) have termed it the "sigma Phenomenon." It has its origin in two features which are peculiar to the flow of suspensions in which the particles are large enough to be comparable in size with the radius of the tube.

The Finite Summation Correction

In these circumstances, we cannot regard the fluid within the tube as a continuous system with uniform viscous properties, and we cannot properly use the method of the infinitesimal calculus in order to deduce the relation between rate of flow and applied pressure from the relation between rate of shear and shearing stress, as is done when deriving the Poiseuille equation. Dix & Scott Blair (13), assuming for simplicity that the shear occurs in layers of suspended fluid, separated by unsheared layers of thickness δ, and applying a method of summation over finite intervals, arrived at an equation which may be put in the form:

$$\frac{Q_b}{P} = \frac{G_p}{\eta}\left[1 + \frac{2\delta}{a} + \frac{\delta^2}{a^2}\right] \tag{18}$$

The apparent viscosity of the blood will thus become smaller as a becomes smaller, and the ratio δ/a becomes larger.

The Wall Effect

The particles of a suspension cannot penetrate into the wall of the vessel in which they are contained. Imagine a plane surface within a suspension of uniformly distributed spherical particles; the quantity of suspended material, per unit volume, will be the same on each side of the plane, and the plane will pass through particles the centers of which lie on each side of it within a distance equal to their radii. If, now, this plane is made the interface between the wall of the vessel and the suspension within it, we shall have to remove not only all the particles which were on the wall side of the plane, but also all those on the suspension side through which the plane passed. Thus there will be a relative deficit of suspended material up to a distance from the wall equal to the radius of the particles. According to Vand (39), this layer in which the concentration of particles is reduced behaves hydrodynamically, when the suspension is sheared, as if it were a layer completely free from suspended material with a width 1.301 times the radius of the particles. Experimental evidence suggests, however, that the equivalent width of this hypothetical slippage layer is about one-half of that expected theoretically (26, 33, 40). In blood, therefore, we may expect its width to be some 1 μ to 3 μ.

Effect of the Marginal Sheath on the Pressure-to-Flow Ratio

When blood (or any other suspension) flows through a tube, therefore, we may expect that there will be a marginal slippage layer, or sheath, of relatively low viscosity, surrounding an axial core of greater viscosity. When a volume Q_b of blood enters the tube per second, part of it will travel in the marginal sheath and part of it in the axial core. Let the volume emerging from the sheath be Q_{sh} and the volume emerging from the core be Q_{co}. Then, since the same total quantity of blood must leave the tube in unit time as enters it, we must have:

$$Q_b = Q_{sh} + Q_{co} \tag{19}$$

There will not be a sharp boundary between the core and the sheath; but in order to simplify the analysis, it is convenient to assume that there is such a boundary, and that the hypothetical sheath contains no red cells, and has a viscosity equal to that of the plasma. The width of this boundary may be defined in one of two ways: for the moment, we define it as being such that the flow properties of the hypothetical system (i.e., the ratio Q_b/P in any given conditions of flow) are the same as those actually observed in the sample of blood used. Let the radius of the tube be a and the radius of the axial core be γa. Then, as in the derivation of the Poiseuille equation (equation 4), we have:

$$Q_{sh} = 2\pi \int_{\gamma a}^{a} r \cdot u_r \cdot dr$$

where u_r is given by equation 3. This reduces to:

$$Q_{sh} = G_p(1 - \gamma^2)^2 \cdot P \tag{20}$$

where G_p is defined by equation 12. Similarly, for the axial core, we have:

$$Q_{co} = 2\pi \int_0^{\gamma a} r \cdot u_r \cdot dr + \pi\gamma^2 a^2 \cdot u_{\gamma a}$$

The value of u_r is now defined by equation 3, after inserting the viscosity of the blood in the core; and the additional term is due to the fact that the outer margin of the core has a velocity equal to that of the inner margin of the sheath (i.e., $u_{\gamma a}$). After integration and simplification we get:

$$Q_{co} = G_p[2\gamma^2(1 - \gamma^2) + \gamma^4/\eta b]P \tag{21}$$

Thus

$$\begin{aligned} Q_b &= Q_{sh} + Q_{co} \\ &= G_p[(1 - \gamma^4) + \gamma^4/\eta b]P \end{aligned} \tag{22}$$

By using equation 13, we find:

$$1/\eta^* = (1 - \gamma^4) + \gamma^4/\eta b \tag{23}$$

If the width of the marginal sheath is z, then $\gamma = 1 - z/a$; and if z/a is small compared with 1, we may simplify equation 22 to:

$$Q_b = G_p[(1 - 4z/a)/\eta b + 4z/a)]P \tag{22a}$$

The modification of the Poiseuille equation, in order to allow for slippage, by multiplying a^4 by the quantity $(1 + 4z/a)$ was first suggested by Helmholtz, and was applied to the flow of paints by Buckingham (10). The viscosity of the blood in the axial core, η_b, will be a function of the radius, a, as given by equation 18. If, moreover, z is not small compared with a, η_b will vary with γ: the smaller the radius of the axial core, the greater will be the concentration of red cells within it, as will be discussed later.

We see from this that unless z is porportional to a—and there is no reason why it should be—the ratio of P to Q_b, and thus the observed apparent

viscosity as deduced from the pressure-to-flow ratio will fall as a becomes smaller and the ratio z/a becomes larger. This effect will be superimposed on that produced by the reduction in the viscosity of the blood itself, according to equation 18.

If we know the values of the pressure-to-flow ratios for a given sample of blood, under the same conditions of shear, in tubes of several different radii, we can deduce from equations 18 and 22 the values of z, δ, and η_b. The computation, however, is elaborate, and the experimental methods are not, at present, of sufficient precision for it to be possible to derive other than very approximate values. If one neglects the finite summation correction (equation 18), the analysis is greatly simplified, although the results may be subject to a systematic error. The quantities z and δ, however, are both probably related to the dimensions of the red cells, and are thus likely to be more or less equal in magnitude; the error is not likely to be serious except when the radius of the tube used is extremely small (say 30μ or less). The results of analyses of this kind (5, 34) indicate that in blood with hematocrit values between 40 and 50 per cent the width of the marginal sheath lies between 1μ and 5μ, and is probably between 1μ and 3μ; it is thus about the value to be expected from the wall effect. The lines drawn in figure 2 are calculated from equations 18 and 22, putting $\eta_b = 3.15$ (in a tube of infinite radius) and either $z = \delta = 1.0\ \mu$ or $z = \delta = 2.0\ \mu$.

Transit Times of Cells and Plasma and the Dynamic Hematocrit

When blood flows through a tube, the existence of a marginal sheath and an axial core has the effect of partially separating the red cells from the plasma, so that their average velocities are not the same. The relative velocities of cells and plasma will be inversely proportional to the relative "transit times," that is, to the average times taken by the cells and the plasma, respectively, to traverse the tube or system of tubes, such as an organ or tissue of an animal. These times may be measured experimentally by "labeling" suitably the cells and the plasma.

Further, in unit time the volume of cells emerging from the tube or system of tubes must be equal to the volume of cells present in each unit length of the tube, multiplied by the average velocity of the cells. Now the volume of cells in unit length of a tube will be equal to the cross-sectional area of the tube, multiplied by the hematocrit value of the blood while it is flowing in the tube. This last is called the "dynamic hematocrit"; it may be measured experimentally by suddenly stopping the flow and estimating the relative volume of cells and plasma in the tube or system ("suddenly" means in a time very short compared with the transit time). The relation of the dynamic hematocrit (α_D) to the ordinary or "bulk" hematocrit (α_o) is thus defined by the equation:

$$\alpha_o \cdot Q_b = \pi a^2 \cdot \alpha_D \cdot \bar{u}_c$$

where a is the radius of the tube, and $\bar{u}_c$ is the average linear velocity of the cells. An analogous equality must apply to the rate of emergence of the plasma, so that we have:

$$(1 - \alpha_o)Q_b = \pi a^2(1 - \alpha_D) \cdot \bar{u}_p$$

If the transit times of cells and plasma, respectively, are $\bar{t}_c$ and $\bar{t}_p$, we thus find:

$$\frac{\bar{t}_p}{\bar{t}_c} = \frac{\bar{u}_c}{\bar{u}_p} = \frac{\alpha_o}{(1 - \alpha_o)} \cdot \frac{(1 - \alpha_D)}{\alpha_D} \tag{24}$$

This is a perfectly general equation relating transit times to the dynamic hematocrit. No assumptions have been made as to the origin of the difference between the velocity of the cells and the velocity of the plasma; it might even be, as an extreme example, that the cells and the plasma travel in different channels, of different dimensions, in parallel with one another. But in so far as the difference in velocity is due only to the existence of a marginal sheath and an axial core, it is possible to deduce the relations between the dynamic hematocrit, or the relative transit times, and the fractional width of the marginal sheath (i.e., the ratio z/a or the quantity γ). But we must now define the hypothetical cell-free marginal sheath in the second of the two ways mentioned above; it must be of such a width that the volume of cells in unit length of the tube (now in the axial core only) is the same as that which actually exists in the same conditions of flow. This definition leads to a value of the equivalent cell-free marginal sheath which is not necessarily identical with that resulting from the definition used in the previous section. The matter is not of great practical importance, however, since we cannot measure either of the values, except very approximately. If the radius of the tube is a, and that of the axial core is γa, we have:

Volume of cells in unit length

$$= \pi a^2 \cdot \alpha_D = \pi \gamma^2 a^2 \cdot \alpha_{cc}$$

so that

$$\alpha_D = \gamma^2 \alpha_{co}$$

where α_D is the dynamic hematocrit, and α_{co} is the hematocrit value of the blood in the idealized axial core. By analogy with equation 19, for the total flow through the tube, we can write for the flow of red cells:

$$\alpha_o Q_b = \alpha_{sh} Q_{sh} + \alpha_{co} Q_{co}$$

Putting $\alpha_{sh} = 0$ (since it is supposed to be free from red cells) we get:

$$\alpha_{co}/\alpha_o = Q_b/Q_{co}$$

Inserting the values of Q_{co} and Q_b from equations 21 and 22 we find:

$$\frac{\alpha_{co}}{\alpha_o} = \frac{1 - \gamma^4(1 - 1/\eta b)}{2\gamma^2 - \gamma^4(2 - 1/\eta b)} \tag{25}$$

and

$$\frac{\alpha_D}{\alpha_o} = \frac{1 - \gamma^4(1 - 1/\eta b)}{2 - \gamma^2(2 - 1/\eta b)} \tag{26}$$

The corresponding expression for the relative transit times may be derived by inserting the value of α_D from equation 26 in equation 24. Alternatively, we may put:

$$\bar{u}_c = Q_c/\pi\gamma^2 a^2 = \alpha_{co} Q_{co}/\pi\gamma^2 a^2$$

and

$$u_p = Q_p/\pi a^2 = [Q_{sh} + (1 - \alpha_{co})Q_{co}]/\pi a^2$$

and then insert the values of Q_{sh} and Q_{co} from equations 20 and 21.

Thus from measured values of the dynamic hematocrit, or of the relative transit times of cells and plasma, the value of γ and hence the width of the marginal sheath may be estimated from equations 24 and 26. A method of successive approximation may have to be used, since the value of α_{co}, and thus the appropriate value of η_b, depends on the value of γ.

We may take as illustrative examples first some measurements of Fåhraeus (18) of the dynamic hematocrit of human blood flowing in glass tubes. If these are inserted in equation 26, it appears that in the two smaller tubes used, 47.5μ and 25μ in radius, the width of the equivalent cell-free marginal zone was 12μ and 10μ, respectively. Such values are not consistent with the measurements of optical transmittance (4, 38) to be discussed below, and are very much larger than those to be expected from the viscosity measurements, as discussed above. The origin of the discrepancy is not known. No measurements of transit times seem to have been made on blood flowing in glass tubes. But as a second illustrative example, we may take the measurements of Freis *et al.* (20) of the transit times of plasma and of cells between the brachial artery of a man and a large vein draining chiefly the deeper tissues of the arm; these were found to be about 10 sec and 7 sec, respectively, so that $\bar{t}_p/\bar{t}_c = 1.45$. If α_o is taken to be 45 per cent, α_D must have been 36.5 per cent. Applying equation 26, we find that this value of α_D would be obtained if all but 1 sec of the transit times was occupied in flow through a tube 10μ in radius, with an equivalent cell-free marginal sheath 2μ in width. Such a solution is a reasonable one, but of course it is not unique, and many others are possible.

ORIGIN OF THE ANOMALOUS FLOW PROPERTIES OF BLOOD

If the flow of blood along a tube, when the applied pressure is equal to or less than the "friction" pressure, results from the movement of a solid plug within a slippage layer of constant width, the pressure-flow line should be straight, as may be seen from equation 22. This is by no means so, as is illustrated for example in figure 1. We must suppose, therefore, either that the width of the slippage layer increases rather rapidly, with increase in the applied pressure, to a value some 10 times as great as that likely to result from the wall effect, or that the axial core is not a solid plug but has a finite viscosity which decreases with increase in the shearing stress, even when this is less than the value corresponding to the friction pressure.

Motion of Red Cells Toward the Axis of the Tube

Observations made on blood flowing in the small vessels of an animal have led to the idea that when a suspension is made to flow in a tube, the particles leave the region near the walls and collect near the axis. There is little evidence that this occurs generally in all kinds of suspension, and the evidence that it occurs in blood is by no means conclusive. Until recently, moreover, there was no theoretical reason to expect that such a movement should occur. Saffman (37), however, as a rider to his studies on the motion of spheroidal particles in a viscous liquid, has studied

the motion of a spherical particle in an infinite sheared liquid. If the motion of the liquid is along the x-axis (e.g., along a tube) and its velocity, u, at any point along the z-axis (e.g., at any particular radius of the tube) varies with z in a parabolic manner (as in Newtonian flow along a tube), then the particle will have a component of velocity in the z-axis, in addition to its main velocity along the x-axis (e.g., it will move towards the center of the tube). The magnitude of this component is determined by the fourth power of the radius of the particle, by the parameters defining the relation of u to z, and by the kinematic viscosity of the suspending fluid. We cannot necessarily assume that this conclusion can be applied to the flow of a relatively concentrated suspension in a tube, where account must be taken not only of the interactions between the particles, but also of the boundary conditions introduced by the wall of the tube and the reversal of the velocity gradient at the axis. But it makes it somewhat more probable that some axial movement of the red cells may occur. That it occurs, if at all, to an extent which is quantitatively insufficient to account for the curvature of the pressure-flow line, is suggested by two lines of evidence.

DIRECT OBSERVATION OF BLOOD FLOWING IN A TUBE. Study of the optical transmittance of the marginal layers of the blood in a tube, viewed tangentially, has shown that when the rate of flow is increased, the transmittance is also increased. This has been observed in suspensions of red cells in saline solutions (38), and in dog defibrinated blood (4). In the defibrinated blood, however, the magnitude of the increase was very variable as between one sample and another, and had no relation to the magnitude of the reduction in apparent viscosity with increase in rate of flow. The changes in optical transmittance may be due, in part at least, to an orientation of the cells; but the observations suggest that some axial movement of the cells probably occurs. But even if it were due entirely to an axial movement, the consequent increase in the effective width of the marginal slippage layer in the defibrinated blood was insufficient to account for the observed reduction in the apparent viscosity of the blood (using equation 23). Nevertheless, both in the suspension of red cells and in the defibrinated blood, the component of velocity of the red cells towards the axis of the tube, necessary to produce the observed apparent increase in the width of the marginal layer, was an order of magnitude greater than that to be expected from the equation developed by Saffman (37). The evidence is unsatisfactory and somewhat confused, but it does not suggest that axial accumulation of the red cells occurs to any considerable extent.

DEDUCTION FROM THE VARIATION OF APPARENT VISCOSITY WITH RADIUS OF THE TUBE. The estimates of the width of the marginal sheath, given in the previous section, were all derived from measurements made at large rates of flow. Similar calculations applied to pressure-to-flow ratios observed at very small rates of flow should indicate whether there is any change in the width with change in the rate of flow. Very few adequate measurements are at present available; but it has been concluded (5) that the width of the marginal sheath increases at most by a factor of 2 when the average shearing stress increases from 4 dynes per cm^2 (or, by extrapolation, from zero) to infinity (i.e., in the asymptotic conditions of flow). These conclusions must, of necessity, be derived from observations in tubes of small radius. It is conceivable that when the radius of the tube exceeds 100 times the radius of the red cell, the width of the marginal sheath ceases to be independent of the size of the tube, and when the shearing stress is large, becomes more or less proportional to it: the width of the sheath would then be underestimated by the method used. There is no evidence that this occurs, and it does not seem very probable.

GENERAL CONCLUSIONS

The reduction in the observed apparent viscosity of blood with reduction in the radius of the tube through which it flows may be ascribed, mainly, to the presence of a marginal sheath of low viscosity, with a width of some 1μ to 3μ. The effect does not depend on the existence of non-Newtonian properties of the blood itself, although its magnitude may be affected by them. But the disproportionate increase in rate of flow through a tube of given radius, when the applied pressure is increased, must result from these non-Newtonian properties. In tubes of relatively large radius (300μ or more), the presence of the marginal sheath has little effect on the pressure-to-flow ratio, and this will be sensibly proportional to the apparent viscosity of the blood in the axial core (equation 22a, if $z/a = 0$). From the available evidence, which is rather scanty, it seems that the change in apparent viscosity with change in shearing stress varies very greatly from one sample of blood to another. At a mean shearing stress of 1 dyne per

cm², for example, the viscosity of Kümin's ox blood (31) was 1.5 times the asymptotic value; whereas in some samples of dog blood, the same proportionate increase in viscosity occurred at $\bar{\tau}$ = 25 dynes per cm², and at $\bar{\tau}$ = 1 dyne per cm², the viscosity was 3 to 4 times the asymptotic value.

We may imagine that when a sample of blood is at rest, a large fraction of the cells—and perhaps all of them—are attached to one another by coherence forces. If a gradually increasing shearing stress is applied, the cells will be dragged apart as soon as its value exceeds the "friction" introduced by the coherence force. According to the Buckingham-Reiner conception, this force is the same between any two pairs of cells, and the "plug" will break up into separate cells. But as Maude & Whitmore (34) have suggested, it may be that at first the plug breaks up into aggregates or "clumps" of cells, and that these break up into separate cells when the shearing stress is increased still further. This implies that the coherence force between any one pair of cells is not the same as that between any other pair: as the shearing stress is increased, those with the smallest coherence are dragged apart first, and those with the largest coherence last. Thus the value of the "friction pressure" to be inserted in the Buckingham-Reiner equation will be small when the shearing stress is small, and will increase to a maximum value when the last pair of cells breaks apart; the pressure-flow line will thus rise gradually, as observed, and will not "take off" abruptly from the axis of pressure. We may consider, alternatively, that the clumps of cells will enclose and immobilize a certain volume of the suspending plasma; the viscosity of the blood will then be large, and will fall gradually as the clumps break up.

On this view, when the shearing stress applied to a tube is small, the apparent viscosity of the blood will depend largely on the magnitude and variation of the coherence forces between the red cells, about which little is known. Unless the shearing stress is very small, the axial core of blood, within the marginal sheath, will have a thin outer layer of fully separated and more or less orientated cells; within these, there will be aggregates of cells, progressively increasing in average size towards the axis of the tube; in the immediate neighborhood of the axis, these may join up into a solid plug. In the asymptotic conditions, the whole of the core will contain separated and perhaps orientated cells. In so far as the apparent viscosity of the blood is determined by the coherence forces, it should be the same in tubes of different dimensions, provided the average shearing stress is the same. But if orientation or axial accumulation of the red cells plays a significant part, the viscosity of the blood at any point in the tube may be determined partly by the rate of shear at this point. This will introduce an element of instability, since, if increase in the rate of shear lowers the viscosity, the rate of shear will be still further increased, and so on; the consequences are difficult to predict. The unexplained differences between the flow properties of different samples of blood, apparently similar in composition, may perhaps result from some such complicating effects.

REFERENCES

1. Arrhenius, S. The viscosity of solutions. *Biochem. J.* 11: 112–133, 1917.
2. Barr, G. *A Monograph of Viscometry*. London: Oxford Univ. Press, Humphrey Milford, 1931.
3. Bayliss, L. E. Rheology of blood and lymph. In: *Deformation and Flow in Biological Systems*, edited by A. Frey-Wissling. Amsterdam: North Holland Pub. Co., 1952, pp. 354–418.
4. Bayliss, L. E. The axial drift of the red cells when blood flows in a narrow tube. *J. Physiol.* 149: 593–613, 1959.
5. Bayliss, L. E. The anomalous viscosity of blood. In: *Flow Properties of Blood and Other Biological Systems*, edited by A. Copley and G. Stainsby. London: Pergamon Press, 1960.
6. Bingham, E. C. Plastic flow. *J. Wash. Acad. Sci.* 6: 177–179, 1916. *Fluidity and Plasticity*. New York: McGraw-Hill, 1922.
7. Bingham, E. C., and H. Green. Paint, a plastic material and not a viscous liquid: the measurement of its mobility and yield value. *Am. Soc. Testing Materials, Proc.* 19: 640–675, 1919.
8. Bingham, E. C., and G. F. White. Viscosity and fluidity of emulsions, crystalline liquids and colloidal solutions. *J. Am. Chem. Soc.* 33: 1257–1275, 1911.
9. Brundage, J. T. Blood and plasma viscosity determined by the method of concentric cylinders. *Am. J. Physiol.* 110: 659–665, 1934.
10. Buckingham, E. On plastic flow through capillary tubes. *Amer. Soc. Testing Materials, Proc.* 21: 1154, 1921.
11. Copley, A. L., L. C. Krchma, and M. E. Whitney. Humoral rheology: viscosity studies and anomalous flow properties of human blood systems with heparin and other anti-coagulants. *J. Gen. Physiol.* 26: 49–64, 1942.
12. Coulter, N. A., and J. R. Pappenheimer. The development of turbulence in flowing blood. *Am. J. Physiol.* 159: 401–408, 1949.
13. Dix, F. J., and G. W. Scott Blair. On the flow of sus-

pensions through narrow tubes. *J. Appl. Phys.* 11: 574–581, 1940.
14. EINSTEIN, A. Eine neue Bestimmung der Moleküldiemnsionen. *Ann. Phys.* 19: 289–306, 1906.
15. EINSTEIN, A. Berichtigung zu meiner Arbeit: eine neue Bestimmung der Moleküldimensionen. *Ann. Phys.* 34: 591–592, 1911.
16. EIRICH, F., M. BUNZL, AND H. MARGARETHA. Untersuchungen über die Viskosität von Suspensionen und Lösungen. 6. Über die Viskosität von Stäbchensuspensionen. *Kolloid-Z.* 75: 20–37, 1936.
17. EWALD, C. A. Über die Transpiration des Blutes. *Arch. Anat. u. Physiol.* 208–249, 1877.
18. FÅHRAEUS, R. The suspension stability of the blood. *Physiol. Rev.* 9: 241–274, 1929.
19. FÅHRAEUS, R., AND T. LINDQVIST. The viscosity of the blood in narrow capillary tubes. *Am. J. Physiol.* 96: 562–568, 1931.
20. FREIS, E. D., J. R. STANTON, AND C. H. P. EMERSON. Estimation of relative velocities of plasma and red cells in the circulation of man. *Am. J. Physiol.* 157: 153–157, 1949.
21. GUTH, E., AND R. SIMHA. Untersuchungen über die Viskosität von Suspensionen und Lösungen. 3. Über die Viskosität von Kugelsuspensionen. *Kolloid-Z.* 74: 266–275, 1936.
22. HATSCHEK, E. Die Viskosität der Dispersoide. *Z. Chem. Ind. Kolloide,* 8: 34–39, 1911.
23. HAYNES, R. H., AND A. C. BURTON. Role of the non-Newtonian behavior of blood in hemodynamics. *Am. J. Physiol.* 197: 943–950, 1959.
24. HESS, W. R. Der Strömungswiderstand des Blutes gegenüber kleiner Druckwerten. *Arch. Anat. u. Physiol.* 197–214, 1912.
25. HESS, W. R. Beitrag zur Theorie der Viskosität heterogener Systeme. *Kolloid-Z.* 27: 1–11, 1920.
26. HIGGINBOTHAM, G. H., D. R. OLIVER, AND S. G. WARD. Studies of the viscosity and sedimentation of suspensions. Part 4. Capillary tube viscometry applied to stable suspensions of spherical particles. *Brit. J. Appl. Phys.* 9: 372–377, 1958.
27. *International Critical Tables.* Viscosities of water and calibrating solutions. 5: 10 and 21–25, 1929.
28. JEFFERY, G. B. The motion of ellipsoidal particles immersed in a viscous fluid. *Proc. Roy. Soc. London* A. 102: 161–179, 1922.
29. KAYE, G. W. C., AND T. H. LABY. Viscosity of water. In: *Tables of Physical and Chemical Constants.* London: Longmans, Green, 1957, p. 36.
30. KRAMER, K. Ein Verfahren zur fortlaufenden Messung des Sauerstoffgehaltes in strömenden Blut an uneröffneten Gefässen. *Z. Biol.* 96: 61–75, 1935.
31. KÜMIN, K. Bestimmung der Zähigkeitskoeffizienten für Rinderblut bei Newton'sche Strömungen in verschieden weiten Röhren und Kapillaren bei physiologischer Temperatur. Inaugural Dissertation, University of Berne. Freiburg, Switzerland: Paulusdruckerei, 1949.
32. McDONALD, D. A. The occurrence of turbulent flow in the rabbit aorta. *J. Physiol.* 118: 340–347, 1952.
33. MAUDE, A. D., AND A. L. WHITMORE. The wall effect and the viscometry of suspensions. *Brit. J. Appl. Phys.* 7: 98–102, 1956.
34. MAUDE, A. D., AND A. L. WHITMORE. Theory of the flow of blood in narrow tubes. *J. Appl. Physiol.* 12: 105–113, 1958.
35. REINER, M. Über die Strömung einer elastischen Flussigkeit durch eine Kapillare. Beitrag zur Theorie der Viskositätsmessungen. *Kolloid-Z.* 39: 80–87, 1926.
36. ROBINSON, J. R. The viscosity of colloids. I. The anomalous viscosity of dilute suspensions of rigid anisometric particles. *Proc. Roy. Soc. London* A. 170: 519–550, 1939.
37. SAFFMAN, P. On the motion of small spheroidal particles in a viscous liquid. *J. Fluid Mech.* 1: 540–553, 1956.
38. TAYLOR, M. The flow of blood in narrow tubes. II. The axial stream and its formation, as determined by changes in optical density. *Australian J. Exper. Biol. & M. Sc.* 33: 1–16, 1955.
39. VAND, V. Viscosity of solutions and suspensions. I. Theory. *J. Phys. & Colloid Chem.* 52: 277–299, 1948.
40. VAND, V. Viscosity of solutions and suspensions. II. Experimental determination of the viscosity-concentration function of spherical suspensions. *J. Phys. & Colloid Chem.* 52: 300–321, 1948.
41. VELICK, S. E., AND H. G. GORIN. The electrical conductance of suspensions of ellipsoids and its relation to the study of avian erythrocytes. *J. Gen. Physiol.* 23: 753–771, 1940.
42. WHITTAKER, S. R. F., AND F. R. WINTON. The apparent viscosity of blood flowing in the isolated hind limb of the dog, and its variation with corpuscular concentration. *J. Physiol.* 78: 339–369, 1933.

Action of electrolytes and drugs on the contractile mechanism of the cardiac muscle cell

EDWARD LEONARD
STEPHEN HAJDU | *National Heart Institute, National Institutes of Health, Bethesda, Maryland*

CHAPTER CONTENTS

THIS CHAPTER is an essay on the cell physiology of cardiac muscle. It is oriented toward the problem of regulation of muscle contractility, and therefore the focus will be on a number of cations and drugs which provide insight into cellular mechanisms that affect heart muscle contractile force. The study of muscle has a long tradition, and it should be noted that investigators working primarily on cardiac muscle

frequently made contributions of more than parochial interest which opened important avenues of approach in other fields. We might mention the work of Ringer on the importance of the composition of the bathing fluid for muscle function, that of Loewi on the chemical mediation of nerve impulses, and the recent discovery that digitalis is an inhibitor of active transport processes in many kinds of tissues. By the same token the cardiac physiologist must borrow from work on noncardiac tissues, and so when the reader of this chapter on the heart discovers that veratrine causes increased potassium loss from stimulated crab nerve or that the calcium concentration of rabbit blastocytes is 0.5 mM per kg he should not conclude that the authors have a particularly whimsical or perverse turn of mind.

As for the specific sections, the first is a discussion of contractility along lines which have been so fruitful in the study of skeletal muscle, but which are more difficult to apply to heart and have therefore only recently begun to be explored. The second section is about sodium and potassium which are of great importance in cardiac muscle, not only because of their relationship to the electrical properties of the cell membrane, but also (and in this respect heart is qualitatively different from skeletal muscle) because of their influence on contractile force. These ions are discussed in section II, but they also form the central topic of section VI on stimulation frequency and contractile force as well as the section on digitalis. The alkali metals, rubidium and lithium, reviewed in section III, are of interest mainly because as chemical congeners of sodium and potassium their fate provides insight into certain aspects of cell membrane permeability and function. Calcium, discussed at length in section IV, was known by Ringer to have remarkable effects on the contraction of cardiac muscle. Although it is now appreciated that calcium influences many structures and systems of muscle (membrane, actomyosin, ATPase, relaxing factor), one may still ask how alterations in external calcium concentration influence cardiac contractility and whether calcium plays a critical role at some point in excitation-contraction coupling. Barium and magnesium, reviewed briefly in section V, provide little insight at the present time into the normal function of cardiac muscle. A chapter on the physiology of cardiac muscle would be incomplete without a discussion of quinidine, veratrum, and the cardiac glycosides, each of which has interesting effects on the cell membrane. Acetyl choline and adrenaline are not included, since they are reviewed in another chapter of this *Handbook*. No extended discussion of hydrogen ion or the anions will be found in this chapter.

The bibliography is not exhaustive, nor is it intended to be a guide for the establishment of priority for discoveries in the field. Rather an attempt has been made to select the best references for providing further background in areas the reader may wish to pursue.

I. CONTRACTILITY

Since this chapter of the *Handbook* is concerned with the effects of various interventions on the mechanical performance of heart muscle, it will be appropriate to begin with a discussion of the definition and measurement of muscular contractility. The term "contractility" does not have a very precise meaning, and Bayliss, for example, in his textbook of general physiology has a carefully written chapter on muscle in which the word is not used at all (12). The rest of the physiological literature is not so eclectic however, and "contractility" abounds, having various meanings for various investigators. Isometric tension, isotonic shortening, velocity of shortening, cardiac output, stroke work, efficiency, all have been measured in the name of contractility. The discussion of this subject that follows has been drawn largely from the work of Hill, Fenn, and others who have worked in their tradition (75, 87, 136–139, 326) mostly on skeletal muscle. Although much of this work is now well known, it deserves emphasis as background for a chapter on a type of muscle for which a rigorous biophysical experimental approach has been difficult to make.

Work Capacity and Length-Tension Curves

We may begin by considering the measurement of the work capacity of a muscle. Hill, noting that Fick had failed to devise an adequate means of measuring this capacity, made the following point (136): "In order to obtain the full tale of work out of the potential energy of a stretched elastic body as, e.g., in excited muscle, the conditions of loading must be arranged so as to be what is known in thermodynamics as 'reversible': i.e., the load at every length, during the course of the shortening, must be exactly equal to the maximum tension the muscle can exert at that length." In the simple case of a muscle lifting a weight, such conditions do not obtain, since at the onset of

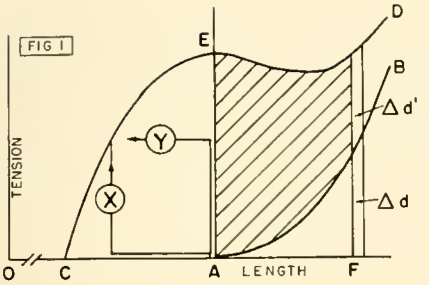

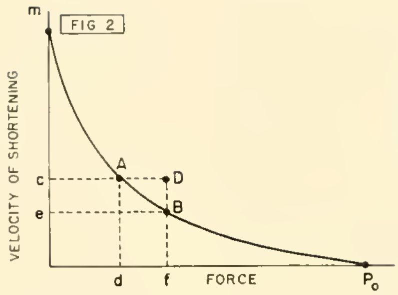

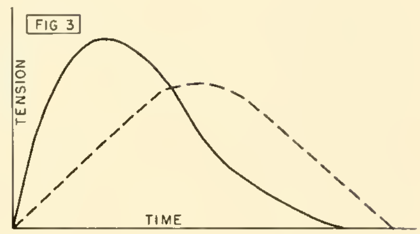

FIG. 1. Diagrammatic length-tension curve of muscle. [After Abbott & Wilkie (2).] See text for description.

FIG. 2. Relation between velocity of shortening and the mechanical load in isotonic contractions. [After Hill (137).]

FIG. 3. Diagrammatic active state curve (solid line) and isometric tension curve (dotted line) of muscle. [From Gasser & Hill (87).]

shortening the muscle would be capable of lifting a greater weight and at the termination of shortening further shortening (and therefore work) could be done if the weight suspended from the muscle were smaller. The load which muscle, in a steady state of either rest or activity, is capable of supporting at any length is given by the length-tension curve of the muscle. Therefore, applying the type of analysis useful for any engine working in cycles, Hill reasoned that the work capacity of a muscle was given by the area enclosed by the curves relating length to tension of resting and stimulated muscle. Such curves are shown diagrammatically in figure 1, adapted from a paper by Abbott & Wilkie (2). *OA* is the length of the resting, unloaded muscle; *AB* is the length-tension curve of the resting muscle; and *CED* is the corresponding curve for the tetanized muscle. The maximum work starting from any given length which can be obtained from the stimulated muscle is given by the area under the curve *CED*. For example, the obtainable work from a muscle of length *OA* is represented by the area *AEC*. For lengths greater than *OA*, one must subtract the work done in extending the resting muscle (area under curve *AB*), so that the maximum work obtainable from muscle activity is given by the area enclosed by the curves *CED* and *AB*. It can be seen, of course, that the obtainable net work (total less that done in stretching resting muscle) becomes greater as the resting length is increased. This is true up to length *OF*, the maximum obtainable work being represented by area *AEC* plus the cross-hatched area. Beyond this length, the work increment done in stretching the muscle (area Δd) becomes progressively greater than the work increment obtained when the muscle is stimulated (area $\Delta d'$). The maximal work as a function of initial fiber length was measured for frog sartorius by Doi (64), and it was found that maximum net work increased with increases in initial length up to 1.7 times the unloaded resting length of the muscle; beyond this the net maximal work declined.

We may define contractility, then, as the capacity for a muscle to do work, and this is given by a pair of length-tension curves like those shown in figure 1. It should be pointed out, however, that muscle cannot be thought of as a simple spring for which the difference between the resting and stimulated state is a difference in the elasticity of the spring. The heat changes in shortening, for example, are not those of an inert spring, since the sum of heat plus work is greater when muscle is allowed to shorten than when it is held fixed, which would be thermodynamically inconsistent with an elastic model (137). Even the final equilibrium state reached by a tetanized muscle and represented by the curve *CED* in figure 1 is not quite independent of the path taken to get there. Thus, if curve *CED* is constructed by allowing a muscle to shorten isotonically to a certain length and then develop tension isometrically to equilibrium (path *X* in fig. 1) it is frequently found that in the reverse sequence of isometric contraction followed by isotonic shortening (path *Y* in fig. 1) the muscle shortening stops before reaching the previously determined length-tension curve. [This has been observed over a wide range of lengths by Buchthal & Kaiser (36), but only above body length by Abbott & Wilkie (2). It has been noted consistently in heart muscle by Rosenblueth and co-workers (248).]

Despite the reservations just noted, much information can be obtained from a length-tension or work diagram of muscle. An estimate of obtainable work can be made from measurement of isometric tension at one length (i.e., one point on the length tension

curve). Hill (136) determined the area AEC (fig. 1) experimentally in a number of frog sartorius muscles and found that the area bore a reasonably constant relationship to the isometric tension developed by the muscle, such that the maximum work (area AEC) obtainable on stimulation at length OA was equal to $1/6\ TL$, where L was the unloaded length of the resting muscle, and T was the isometric tension developed at that length. Deviations occur at longer lengths (2). It is apparent therefore that if one defines contractility as the potential for performing work at a defined length, then isometric tension developed at that length is a fair reflection of contractility.

By keeping the working diagram in mind one can avoid the error of attributing increased work done to increased contractility, whereas in fact changes in work may only reflect changes in the working conditions of the muscle, in terms of the initial length or load. Thus, as noted above, increases in the initial length of the muscle are associated with increases in the work done without any changes in contractility. And of course under conditions of isotonic shortening the work done will vary with the load in the absence of changes in contractility. Great variations in cardiac output with diastolic volume, such as those observed by Patterson *et al.* (229), were indeed accounted for in terms of the length-tension or work diagram of cardiac muscle.

Isotonic Measurements

It has already been pointed out that work capacity cannot be determined under conditions of isotonic loading. It is also true that contractility cannot in general be estimated by the extent of isotonic shortening. It was shown, for example, by Varga (301) in a study of the effect of temperature changes on the contractile properties of glycerinated muscle fibers that the increase in shortening with increase in temperature reached a maximum plateau at a point where the isometric tension development was only about half maximum. Further increase in temperature above this point resulted in an improvement of the muscle as judged by further increase in isometric tension, but this could not have been seen in the shortening which had already reached its maximum.

Velocity of Shortening

It has been claimed that an increase in velocity of myocardial muscle shortening as indicated by rate of ejection of blood from the left ventricle must mean an increased contractility. However, a consideration of the work of A.V. Hill (137) reveals the possibility that contractility as we have defined it and velocity of shortening may vary independently. He found that if a muscle was allowed to lift a load the velocity of shortening varied inversely with the load as shown by curve mP_0 in figure 2.[1] Isometric tension for this muscle is given by the point P_0 (i.e., force where velocity of shortening is zero); the intercept on the y-axis represents velocity of shortening with no load. The curve is described by the equation

$$v = \frac{b(P - P_0)}{(P + a)} \tag{1}$$

where v is velocity of shortening, P is load, P_0 is isometric tension, a is a constant with dimensions of force, and b is a constant with dimensions of velocity. The quantity P_0/a is rather constant in various muscles. In different types of muscles b varies widely, and it increases with temperature. When P equals zero, v equals $b(P_0/a)$. A change in the velocity constant b, without a change in P_0 or a would give a curve which went through point P_0 but had a different intercept on the ordinate. This would represent a faster muscle without a change in contractility (as indicated by the same P_0). In general there is no necessary interrelationship between the velocity constant b and the force terms P_0 and a. Not only are there different types of muscles in which contractility may be comparable but velocities are different; but changes in a given muscle with, say, temperature may be such that in a certain temperature range b will increase progressively, whereas P_0 (and probably a) will increase, go through a maximum, and thereafter decline (109). This short paragraph should suffice to indicate that velocity of shortening and contractility may vary independently, and experimental interventions may affect either one or both.[2]

Active State

Having just excluded the velocity of shortening from the definition of contractility, we must proceed

[1] Velocity of shortening was constant over most of the short distance shortened, but strictly speaking "v" is the initial velocity. See ref. (2) for a modification of the Hill equation which applies over a wide range of shortened lengths.

[2] It is evident, of course, that increased velocity of shortening may contribute greatly to the stroke work of the intact heart. For example, at high rates a rapid contraction cycle will allow time for adequate filling in diastole so that despite the fast frequency stroke volume and work can be maintained (256).

to consider it again in relation to the internal dynamics of shortening and the development of the active state. For purposes of this argument the muscle can be considered as a contractile element in series with a passive elastic element. If the series elastic element were not there, and the contractile element were fixed at either end, stimulation would result in a rise and fall in tension which would faithfully reflect the contraction-relaxation cycle within this muscular element. Such is not the case when the elastic element is in series, since now the tension rise is slower by virtue of the extension of the elastic element which occurs when the muscular element is stimulated, and likewise the fall in tension is prolonged because of the release of potential energy that was imparted to the elastic element during stretching. This is shown diagrammatically in figure 3, which is taken from Gasser and Hill's description in 1924 (87). The behavior of the muscular element without the influence of the series elasticity is observed at various points in the contraction cycle by raising the tension of the elastic component by a quick stretch, thus establishing isometric conditions for the contractile element. [For the most elegant of the experimental methods for measuring active state, see reference (139).] The mechanical response under these circumstances is indicated by the solid curve in figure 3, and has been called the "active state" of the muscle. The active state in skeletal muscle rises extremely quickly to peak level very shortly after stimulation and then rapidly declines. The twitch tension (dotted curve) rises more slowly because the series elastic element allows the contractile component to shorten. It likewise falls more slowly since the series elastic elements stretched by the contractile component return to their resting length only after the active state in a single twitch has declined to zero. Tetanization of the muscle prolongs the active state, without increasing its intensity, the difference between twitch and tetanus tension being due simply to adequate time for elastic element tension to be raised to the level of the muscular element at the active state peak. Therefore, whereas all these complexities are avoided in the tetanized muscle, in the case of single twitches, be they in striated or heart muscle, isometric tension is a function *a*) of the intensity of the active state, and *b*) of the duration of the active state, in relation to the elasticity of the series noncontractile element.[3] We will consider in a later section (see section VI) an example of a decline in isometric twitch tension of heart muscle which is thought to be due to a decline in active state duration but not intensity.

[3] This introduces a complication into our definition of contractility. The measurement of maximum work capacity and its relation to isometric tension development in striated muscle was worked out with tetanized fibers, so that the active state peak was being measured. Since the heart cannot be tetanized, and since measurements of active state are impractical as a general procedure, one must be satisfied with isometric twitch tension as a reasonable measure of cardiac muscle contractility in all except detailed biophysical studies.

Efficiency

A comment should be made about the use of efficiency (work output/energy input) for evaluating myocardial function. It should be clear from the foregoing discussion that there need be no relationship between efficiency and contractility, since the work output of a muscle depends on the conditions of loading. An experimental curve relating efficiency to load for frog sartorius is shown in figure 4 (138). Efficiency is of course zero for both zero load and zero shortening, since no work is done at these extremes. It rises to a maximum when the load is 48 per cent of the isometric value. Thus any value of efficiency for this muscle of given contractility can be obtained depending on the load. Figure 5 shows the variation of work done by dog cardiac muscle as a function of load. There are no data on energy input for calculation of efficiency, but the study illustrates the main point made in this paragraph and is an example of a good biophysical investigation on heart muscle (249).

Applications to Cardiac Muscle

A discussion of cardiac contractility would not be complete without leaving the relatively idealized frog sartorius and mentioning in passing certain problems peculiar to real heart muscle. Instead of a straight strip of parallel fibers the heart is a hollow viscus made up of a syncytium of fibers running in several different directions and stimulated by a complex conduction system. The relationships between wall tension and hydrostatic pressure in tubes have recently been reintroduced to physiologists by Burton (41), and will be considered *in extenso* by other authors in this volume. They add another variable to the relation between contractility of the myocardial cell and work done by the heart as an organ. The conduction system plays an important role in the contractility of the whole heart so that, for example, abnormalities in conduction leading to marked asynchrony in contraction of different portions of the ventricle will cause

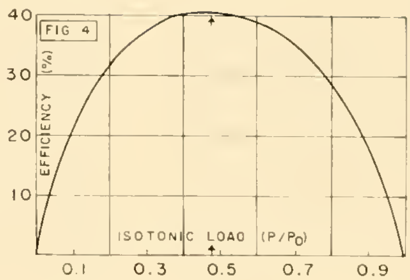

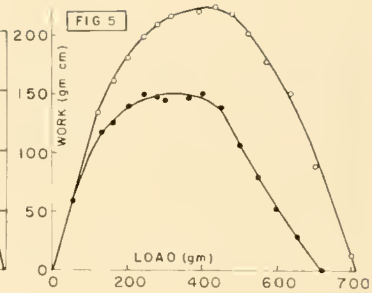

FIG. 4. Relation between efficiency and isotonic load for frog sartorius muscle. [From Hill (138).] P is actual load, P_0 is isometric tension.

FIG. 5. Work performed in after loaded contractions as a function of load. The dots show the work when the loads were applied at the length which corresponded to a tension of 55 g, and the circles that developed at the length corresponding to a tension of 120 g. [After Rosenblueth *et al.* (249).]

a diminution in the functional capacity of the organ even though the contractility of the component cells may be normal. An attempt will be made in later sections to consider direct effects on the contractility of heart tissue itself, and to separate them from alterations in shape or innervation that affect the performance of the heart as a pump.

An interesting example in which the type of analysis outlined above may be helpful is provided by experiments on cardiac oxygen consumption first reported by Evans & Matsuoka (73) and confirmed many times subsequently (6, 99, 104, 166, 167, 174, 262). The stroke work of the heart is given approximately by the product of stroke volume and arterial pressure. An increase in stroke work caused by an increase in stroke volume is associated with a very small increment in oxygen consumption; but increased stroke work caused by raising arterial pressure is accompanied by a considerable rise in oxygen consumption. In other words, work output/energy input or mechanical efficiency is lower when work is augmented by raising blood pressure than by raising stroke volume. This phenomenon could be accounted for at least in part if the heart were working in the region of the peak of its load-efficiency curve (fig. 4), since an increase in load by elevation of arterial pressure would cause a drop in efficiency. Another factor may also play a role, if it can be established that P_0 (equation 1) does not change greatly. Reference to figure 2 will show that if the heart muscle working at point A on its force-velocity curve against a load d (on the force axis) and velocity c is presented with an increased load f (on the force axis), it would then be working at point B on that curve at a considerably decreased velocity (e). However, measurements show that when the load is increased by increasing aortic pressure, the velocity of shortening is not decreased (212); and it is apparent that the heart muscle must be working on a curve which passes through point D, thus reflecting a change in contractility and/or velocity of the muscle.

Although a length-tension curve such as that shown

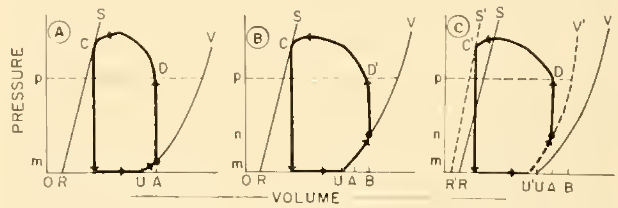

FIG. 6. Changes in dynamic pressure-volume curves of dog heart in response to an increase in inflow pressure. (See text for description.)

in figure 1 can be obtained experimentally with a cardiac muscle strip, the corresponding pressure-volume curve for an intact heart is impossible to obtain, and this section will be concluded with a discussion of the difficulties encountered. Consider an isolated perfused heart in which volumes and pressures can be measured. Referring to figure 6*A*, the cardiac cycle begins at the black dot corresponding to volume A and end diastolic pressure m, a point on the resting pressure-volume curve. The aortic diastolic pressure is at a level p. When the heart contracts, pressure rises isometrically to p (point D in the figure) and then shortening occurs to point C which is on the contracted pressure-volume curve.[4] Isometric relaxation then occurs and finally the heart returns to the original point as shown by the direction of the arrows. In this example the end-diastolic volume is OA, the stroke volume is DC, and the stroke work is the area enclosed by the arrows. Construction of the resting and contracted pressure-volume curves, UV and RS, could theoretically be accomplished as follows. For the resting curve, increase the input pressure stepwise and measure the corresponding (end-diastolic) volumes. For the contracted curve, increase the output pressure stepwise and again measure the (systolic) volume at each pressure level. However, a series of elegantly performed experiments by Rosenblueth and co-

[4] There is some doubt as to whether the ventricle reaches equilibrium with the output pressure during systole (248). That is, shortening may stop before point C is reached. See also section 1.

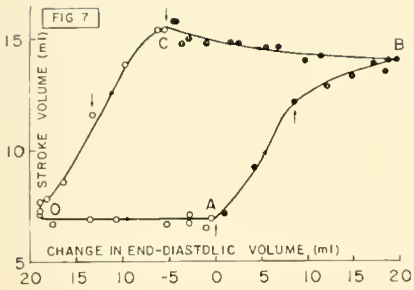

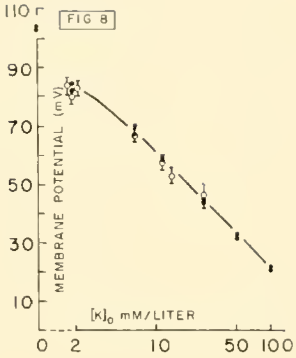

FIG. 7. Stroke volumes as a function of the diastolic volume in the course of the reaction to changes in input pressure. Between the lower pair of vertical arrows (starting at *A*) the input pressure was raised. The arrowheads on the curves indicate the sequence of changes: an increase in stroke volume, accompanied by an increase (*A* to *B*) and then a decrease (*B* to *C*) in end-diastolic volume. Between the upper pair of vertical arrows (starting at *C*) the input pressure was lowered and the ensuing changes are represented by path *CDA*. [From Rosenblueth *et al.* (248).]

FIG. 8. Relation between membrane potential and concentration of potassium in bathing medium, frog ventricle. [From Lüttgau & Niedergerke (200).]

workers (248), recently reported, calls attention to a serious pitfall which may occur in such an approach. Working with an isolated heart perfused with blood from a donor dog for good maintenance of function [see (248) and also (85) for details of the method], they obtained pressure and volume data for a cycle such as that outlined in figure 6*A*. They then raised input pressure to level *n*, as shown in figure 6*B*. As expected, the diastolic volume increased, say from *OA* to *OB*. Now, if the ventricle volume reaches equilibrium with the output pressure during systole, the stroke volume should be *D′C*. (In fact, isotonic shortening may fall short of point *C* in the first few beats.) The interesting point, illustrated by figure 6*C*, is that after a short period of time the end diastolic volume decreases, so that it may end up back at the original level *OA* characteristic of input pressure *m*. Furthermore, this is associated with more complete systolic emptying so that systolic shortening may now proceed further than *C* to point *C′*. Comparison of figures 6*A* and 6*C* shows that the heart is operating from the same diastolic volume, but the stroke volume *DC′* is greater than the original stroke volume *DC*, and stroke work (the area enclosed by the arrows) is likewise greater.[5] The dynamic pressure-volume curves of the heart in figure 6*C* are now shifted from *UV* and *RS* to *U″V″* and *R′S′* and the work capacity or contractility is increased. In other words, the mere attempt to measure the pressure-volume curves by stepwise increase in input pressure caused a change in those curves. A discussion of the possible cause and significance of this compensatory change, which allows the heart to work at greater input or output pressures without excessive increase in volume, is not within the scope of this section.[6]

[5] Fig. 7, taken from the paper of Rosenblueth *et al.* (248), shows the results of such an experiment in which stroke volume is plotted as a function of diastolic volume.

II. SODIUM AND POTASSIUM

Investigations of sodium and potassium in living tissues have occupied a central place in modern cellular physiology. The results have included information about the asymmetry of ion distributions across cell membranes, elucidation of various types of transport of ions in and out of cells, and a basis for understanding bioelectric phenomena in terms of the distribution and movement of sodium and potassium. A brief summary of some of these points will be presented, since they bear on heart muscle as well as on other tissues. The effects of alterations in the extracellular concentration of sodium and potassium on cardiac contractility will be discussed in more detail, since the response of cardiac tissue is different in some respects from that of skeletal muscle. A detailed presentation of the effects of sodium and potassium on bioelectric phenomena in the heart can be found in Chapters 11 and 12. Alterations in cellular potassium effected by various drugs or by changes in stimulation frequency are discussed in sections VI, VII, VIII, and IX.

[6] Rosenblueth *et al.* believe that the work curves plotted in fig. 6, which are based on instantaneous pressures and volumes measured in a cardiac cycle, do not touch at any point the pressure-volume curves of the resting and isometrically contracted ventricle, but always remain inside the area bounded by these curves. For this reason we are inclined to use the term dynamic pressure-volume curve to refer to the values obtained during the cardiac cycle. This leaves open the question as to what extent the shift in the dynamic pressure-volume curve represents a shift in the "equilibrium" pressure-volume curve and to what extent it might represent a closer approach of the dynamic pressure-volume curve to the equilibrium value.

Distribution of Sodium and Potassium in Muscle

It is well known that the main intracellular cation of muscle is potassium, sodium being to a large extent excluded. The actual intracellular concentrations of these ions cannot be stated with certainty because of the variability of the extracellular fluid space measurements on which calculations of intracellular values depend. For example, total sodium and potassium concentrations (meq/100 g dry tissue) have been found to be the same in both dog and cat ventricle. However, an extracellular space of 18.2 per cent was found with C^{14} mannitol in the dog heart (53); whereas a value of 25 per cent was calculated for the cat heart on the basis of chloride measurements (245). The calculated intracellular potassium concentrations were thus 151 and 139 meq per liter of fiber water for cat and dog, respectively; and sodium concentrations were 6.5 and 21.5 (recalculated from references 53, 245, 335). The variability of extracellular space measurements in the same species can be appreciated by reference to two published results on frog ventricle, one with an inulin space of 19.1 per cent, the other with a sucrose space of 24 per cent (110, 158). The problem of extracellular space measurement in cardiac tissue is magnified by the trabecular structure of the organ, which causes difficulty in blotting successive tissue samples uniformly. This factor may be even more important in the atrium with its loosely arranged muscle cells and large surface-to-volume ratio, for which an inulin space as high as 44 per cent has been reported (236). For ventricular tissue, extracellular space measurements based on the distribution of inulin or mannitol (53, 110, 134) are in fairly good agreement, and yield calculated intracellular sodium concentrations of 23.0, 27.7, and 21.5 meq per liter of fiber water for frog, rat, and dog, respectively. Other references on the tissue partition of electrolytes in heart may be found in the review by Manery (207) and in papers of Lowry (197), and Darrow *et al.* (63).

No categorical answer can be given to the question whether intracellular potassium is distributed uniformly throughout the cell with a chemical activity equivalent to that of a free solution. Studies pertinent to the point include binding of potassium to intracellular proteins (189, 299), exchangeability of radioactive potassium between cells and medium (52, 235), analysis of potassium efflux from cells (121, 122), histochemical localization of potassium within the cell (65, 90), osmotic pressure measurements (54), measurements of electrical conductivity of protoplasm (141, p. 281), and mobility of radioactive potassium in cells under the influence of an electrical gradient (118, 145).

The binding of potassium to proteins has been studied by numerous investigators (299, p. 37). Lewis & Saroff (189), using an anion impermeable membrane, found that at pH 6.4 in 0.15 M KCl, potassium was bound to myosin to the extent of about 12 ions per mole of myosin. Actin and albumin exhibited no potassium binding capacity. Potassium binding by myosin would amount to not more than 5 per cent of the total cell potassium however, and even this value might be less in the presence of cellular divalent cations.

A number of studies on the exchangeability of radioactive potassium lead to the conclusion that one cannot regard the cell as a simple sac filled with a solution of potassium ions. For example, although it is generally agreed that cellular potassium is completely exchangeable at body temperature (52, 235), at low temperatures a portion of the potassium becomes practically nonexchangeable (116, 117, 127, 287). If one portion still exchanges normally at low temperature while another portion becomes nonexchangeable, an alteration of membrane permeability cannot account for the findings; rather it appears that diffusion of a part of the intracellular potassium ion becomes restricted in the cold for some unknown reason. The work of Harris & Steinbach (121, 122) also leads to the conclusion of nonuniform behavior of intracellular potassium, since these investigators found that the potassium leached out of cells previously equilibrated with radioactive potassium had different specific activities—the potassium collected early having a high specific activity, the value decreasing progressively in the samples collected later. The nonuniformity of intracellular potassium distribution is also suggested by other evidence. Histochemical studies on the localization of potassium indicate that there appear to be potassium rich zones (65) [for contrary evidence see (90)]. The potassium concentration in certain subcellular particles such as the mitochondria may be different from that of the surrounding system (287).

Such lines of evidence have led several investigators to the view that the various intracellular ions are not uniformly distributed (119, 192, 275). Harris (119), for example, suggests that there is an outer region of the cell containing nonspecific binding sites, and an inner region with sites normally occupied by potassium. The time course of ion movement will be limited by inter-site migration and also by long paths of various lengths imposed by cellular structures.

On the other hand, it does not seem that the chemical activity of the bulk of intracellular potassium can be greatly different from what it would be in free solution, since studies on osmotic pressure of cells in which the principle cation is potassium show that the cells are in osmotic equilibrium with the medium (54), and therefore the potassium must be osmotically active. The high electrical conductiviy of the protoplasm of cells leads to the same conclusion (141, p. 281). Direct measurements of the mobility of K^{42} in the longitudinal axis of cell protoplasm also give values not greatly different from that in free solution (118, 145). Although some of these physical chemical measurements show that the bulk of the potassium must have a chemical activity the same as in free solution and the potassium is completely exchangeable under physiological conditions, nonuniform localization or binding of a certain fraction of the potassium cannot be ruled out.

Ion Concentrations and Bioelectrical Potentials

The unequal distribution of inorganic ions across the plasma membrane of living cells gives rise to an electrical potential difference between the cell interior and its environment. This has been appreciated since the time of Bernstein (15), who suggested that the membrane potential was due to the concentration difference of potassium inside and outside the cell, assuming that the membrane was permeable to potassium ions but impermeable to all other ions present. The theory required modification when Boyle & Conway (28) showed that the cell membrane of the frog sartorius was permeable not only to potassium, but also to chloride and bicarbonate ions. The changes in the membrane potential with changes in concentration of sodium and potassium in the bathing fluid were interpreted by Boyle and Conway as consistent with the theory that the muscle was in a true Gibbs-Donnan equilibrium, the muscle membrane being completely impermeable to protein and certain other multivalent anions as well as to extracellular sodium. The nondiffusibility of a fraction of intracellular anion on one side of the membrane and of sodium on the other thus gave rise to a "double-Donnan" potential, the distribution of such permeating ions as K, Cl, and HCO_3 following a relationship of the form (Nernst equation)

$$E = \frac{RT}{F} \ln \frac{[\mathrm{Cl}]_i}{[\mathrm{Cl}]_o} = \frac{RT}{F} \ln \frac{[\mathrm{K}]_o}{[\mathrm{K}]_i} \cdots \text{etc.} \qquad (2)$$

where E is the membrane potential, R, T, and F have their usual significance, and i and o refer to cell interior and extracellular space.

Although the cell membrane of the frog sartorius appears to be virtually impermeable to sodium at 4°C, this is not the case at higher temperatures, and in general resting cell membranes probably have some low degree of permeability to the sodium ion. This, combined with the fact that sodium ions are thought to enter the cell during the action potential, requires a mechanism for the active transport of sodium ions out of the cell. Therefore it is now not usually considered that the distribution of all the ions can be regarded as a true thermodynamic equilibrium involving an inert membrane with selective permeability for different ionic species (Gibbs-Donnan equilibrium). Instead, a steady state exists in which sodium diffuses into the cell at a rate determined by the magnitude of the membrane permeability for sodium and the electrochemical potential gradient of sodium across the membrane, and is then pumped out of the cell by some kind of active transport system. The pump is considered to be nonelectrogenic (see 299, p. 57), i.e., no net charge transfer across the membrane occurs with active transport. The passive diffusion of sodium into the cell can be considered to affect the membrane potential according to the equation

$$E = \frac{RT}{F} \ln \frac{[\mathrm{K}]_o + b[\mathrm{Na}]_o}{[\mathrm{K}]_i + b[\mathrm{Na}]_i} \qquad (3)$$

where b is the ratio of the membrane permeability for Na and K, P_{Na} P_K. Since b is thought to be about 0.01 for muscle and nerve, $b[\mathrm{Na}]_i$ is small compared to $[\mathrm{K}]_i$, and at high $[\mathrm{K}]_o$ and low $[\mathrm{Na}]_o$, $b[\mathrm{Na}]_o$ can be neglected also and the equation reduces to the form of equation 2 so that E is a linear function of $[\mathrm{K}]_o$. At low $[\mathrm{K}]_o$ in the physiological range, $b[\mathrm{Na}]_o$ becomes a significant fraction of the sum $[\mathrm{K}]_o + b[\mathrm{Na}]_o$ and the linear relationship between E and K_o no longer exists (142). An example of experimental data on this point is shown in figure 8. The nontransported but permeating anions, such as chloride and bicarbonate, will be distributed passively according to their electrochemical potential gradients.

It is perhaps worth pointing out that the magnitude of the potential difference across the membrane in this system is influenced by the difference in membrane permeability to sodium and potassium ions. If, for example, the membrane exhibits little selectivity between sodium and potassium in regard to passive diffusion (i.e., b becomes much larger, approaching the ratio of the diffusibility of the ions in free solution),

the membrane potential will be much lower, even though the pump is efficient enough to maintain large concentration differences of sodium and potassium on each side of the cell membrane. This appears to be the case in the erythrocyte (142). Conversely, a decrease in *b* will cause the membrane potential to approach even more closely the equilibrium potential for a potassium electrode. For a detailed discussion of these subjects the reader is referred to references 12, 28, 142, 143, 313 and also the chapter in this volume by Woodbury.

The inward current represented by the spike of the action potential is thought to be carried by sodium ions which enter the cell because of a sudden increase in membrane sodium permeability associated with excitation. Repolarization must involve a movement of ionic charge in the opposite direction—perhaps loss of cellular potassium ion, uptake of chloride ion, or both. The cell at this point has gained sodium and lost potassium, and active transport of one or both ions is required to restore the original conditions.

It follows, then, that resting muscle in the steady state should have measurable fluxes of sodium and potassium across the cell membrane, which should increase during activity. It has been shown by independent methods that potassium efflux of amphibian ventricle increases greatly with electrical stimulation. Thus, Wilde *et al.* (325) showed a phasic increase in the efflux of radioactive potassium from a cooled turtle heart which corresponded in time to the T wave of the electrocardiogram. Their elegant technique involved the continuous collection of coronary sinus effluent on a moving strip of filter paper, and had enough sensitivity and time resolution to associate the increased K efflux with the T wave. (The contraction cycle was very slow, the length of the T wave itself being of the order of 1 sec.) The potassium released by the turtle heart under these conditions was 45 pmoles per cm^2 per beat. Hajdu (110) calculated the amount of K released during the contraction of isolated digitalized frog ventricle by measuring the increase in bathing fluid potassium which occurred over the course of 30 contractions. According to his view, digitalization should have prevented any re-entry of potassium lost from the cells during this period. The resting K efflux was extremely small, and the increase per contraction was 20 pmoles per $cm.^2$ Both of these values are larger than the flux for nerve which is in the range of 2–5 pmoles per cm^2 per impulse, but this is hardly surprising considering the differences in the tissues, notably the time course of repolarization. Quantitative data on K fluxes in mammalian hearts have been more difficult to obtain, and there are no results based on either of the experimental approaches mentioned above. The available information is based on analyses of K^{42} efflux and influx curves (235, 236, 335) which the authors consider can provide only approximate data because of some intrinsic error in the kinetic analysis (335) or nonexponential time course of the flux curves (235, 236). Despite these uncertainties the data show that K flux increases with increasing heart rate, which confirms the basic finding on the amphibian hearts. The resting potassium flux in these mammalian tissues appears to be rather high. This is not necessarily due to passive leakage out of the cell with re-entry accomplished by active transport, but may be only exchange diffusion. There is as yet no evidence on this point.

Analysis of sodium flux as a function of cardiac activity has been successfully carried out for an *in situ* dog heart preparation perfused with freshly collected arterial blood (53). The hearts were loaded with Na^{24} and an efflux curve was obtained. Heart rate was increased by electrical stimulation, decreased by cooling the right atrium, and the results clearly show a linear increase in sodium flux with increasing heart rate, the sodium exchange per beat being 0.04 meq per kg heart tissue. Extrapolation of the sodium flux heart rate curve to zero shows that the sodium flux is close to zero at 0 heart rate.

Further discussion of ion fluxes and heart rate can be found in section VI.

Potassium and Cardiac Excitability

The effects of alterations in the concentration of extracellular potassium on excitability are probably secondary to the resulting changes in resting membrane potential. The relationship between cardiac resting membrane potential and extracellular potassium concentration is linear, with deviations occurring only at levels of potassium concentration below about 10 mM per liter (38, 149, 200). [Hoffman & Suckling (149) found that not only high $[K]_o$ but also very low $[K]_o$ below 0.48 mM per liter caused depolarization of dog Purkinje fibers, but the latter finding has not been observed in frog skeletal (4) or cardiac (200) muscle.][7]

[7] The changes in resting potential caused by alterations in potassium concentration which have been described by Hoffman & Suckling (149) for Purkinje fibers as well as heart muscle can be altered by alterations in the concentration of calcium. The depolarization caused by increases in potassium concentration can be reversed by increasing calcium concentration. Likewise the depolarization associated with very

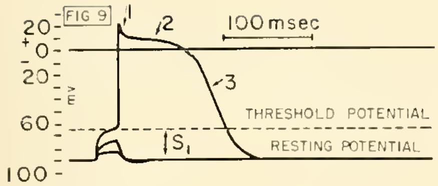

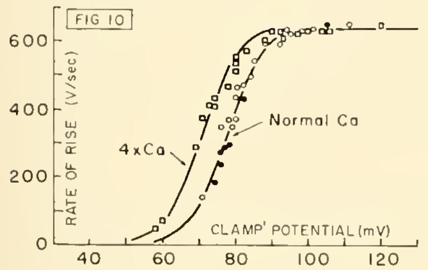

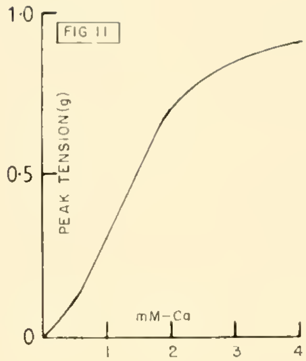

FIG. 9. Diagrammatic cardiac action potential curve. Resting potential, 90 mv. Small local depolarizations are not followed by a spike. Depolarization by an amount S_1 or more causes typical propagated response, consisting of spike and 3 phases of repolarization. *Phase 1:* rapid early repolarization; *phase 2:* plateau; *phase 3:* terminal repolarization.

FIG. 10. Effect of calcium ions on the relationship between membrane "clamp" potential and maximal rate of rise of the action potential. Open circles correspond to values obtained before, filled circles to values measured after the application of a calcium-rich solution. [After Weidmann (314).]

FIG. 11. Relation between calcium concentration in bathing fluid and peak tension of isometric twitches of isolated frog ventricle. [After Niedergerke (220).]

The effects of changing potassium on the electrical events associated with excitation can best be appreciated after reviewing one or two facts about transmembrane potentials and excitability. Reference to figure 9 will show that in order to achieve a propagated depolarization it is necessary to decrease the resting potential to a given value, the so-called threshold potential. Depolarizations to less than this value result in small local changes but no propagated depolarization. The second point, which is illustrated by figure 10, shows the relationship between the rising velocity of the action potential and the level of the previous resting potential as determined by Weidmann (314) on Purkinje fibers using a voltage clamp technique. It can be seen that as the steady level of membrane potential is lowered, the rate of rise of the action potential, which is thought to be due to the rate of inward movement of sodium current, falls until it reaches a value close to zero at a resting potential of about 60 mv. Thus, below resting membrane potentials of 60 mv in this experiment there is no inward sodium current and therefore no action potential. Returning to the effects of potassium, it can now be appreciated that any change in $[K]_o$ that leads to a decrease in resting membrane potential will cause first an increase in excitability and then an abrupt decrease. The phase of increased excitability occurs in the region in which the resting membrane potential is reduced but is still greater than the threshold potential. At such values a smaller than normal current is required to reach the threshold potential. Spontaneous rhythmicity, which is seen with increased concentrations of extracellular potassium, can be explained by depolarization of the resting membrane to potential levels close to the threshold potential.

When, on the other hand, the level of the resting potential has reached the threshold or lower, it is clear from reference to figure 10 that no sodium current and therefore no propagated depolarization can occur. The observed effects of increased potassium on the action potential, such as a diminution in the rate of rise of the action potential and a lower than normal height of the spike, are probably due to resting membrane depolarization with the associated changes just described. The diminution in conduction velocity caused by increased potassium is a reflection of the slower rate of rise of the action potential.

Effects of Sodium and Potassium on Contractility

It is generally accepted that alterations in the extracellular concentrations of sodium or potassium may be associated with changes in contractility of heart muscle. Ringer (242) showed that increasing potassium caused a decreased contractile response of the isolated frog heart, and it has since been demonstrated that the opposite effect can be produced by decreases in the concentration of extracellular potassium (47, 62, 110). Variations in extracellular sodium concentration are associated with similar changes, the basic facts having been summarized as early as 1920 by Daly & Clark (62), who stated that "lack of potassium or sodium and excess of calcium all produce increase of systolic tone in the heart." The alterations in contractility caused by such inter-

low concentrations of potassium can be eliminated by lowering the calcium concentration below normal levels. The latter effect would not seem to be a phenomenon related to the contracture which may occur in very low potassium solutions in which calcium concentration is normal since the effect is also observed in the nonmuscular Purkinje fibers.

ventions are not due to changes in membrane potential (110, 200). Not only twitch tension but also contracture tension are similarly affected. It has fallen to the lot of present-day physiologists to find out at what locus and by what mechanisms such alterations in extracellular cations act to produce changes in contractility. The incompleteness of the answer is attested to by the length of the following discussion.

One viewpoint, which has been advanced by Hajdu (110), is that contractile force is affected by an interaction between monovalent cations and actomyosin, an interaction in which the contractile protein does not distinguish between sodium and potassium. The pertinent fact in support of this idea is that depletion of intracellular monovalent cation, either sodium or potassium, by any of several means is associated with an increase in contractile force. Loss of cellular potassium can be induced by placing ventricular tissue in a potassium-free medium (110) by increasing stimulation frequency (see section VI) or by digitalization (see section IX). Cellular sodium loss occurs when a fraction of the extracellular sodium chloride is replaced by a nonpenetrating sugar or by the chloride of a cation other than sodium, such as lithium or choline. The remarkable aspect of this phenomenon is that a very small change in the intracellular ion content causes a large change in contractility. For example, a loss of 3 meq per kg of cellular potassium is associated with a change from zero to 100 per cent contractile force in the case of the isolated frog ventricle (110). Likewise, soaking of frog hearts in a solution containing about one-fourth of the normal sodium concentration is followed by a rise to maximum contractility and a loss of about 10 meq per kg of intracellular sodium ion. Another point of interest is that changes in the concentration of intracellular cation in the absence of an actual change in intracellular content (e.g., water shifts caused by alterations in the extracellular osmotic pressure) are not associated with alterations in contractility.

It should be emphasized that, since contractility can be affected by changes in either intracellular sodium or potassium, it cannot be the ratio of the two ion concentrations which is important; but it is rather the sum of the intracellular concentrations of these two cations which seems to affect contractility. Furthermore, it would appear to be not the concentration per se but the number of ions per contractile protein unit which determines the contractile response. According to this view, a reduction in the total intracellular monovalent cation, whether accomplished by loss of either sodium or potassium, should be associated with increased contractility. Two examples relating to mammalian hearts may be cited. In one, contractility is enhanced by reducing cellular sodium; in the other, by reducing cellular potassium. Hercus *et al.* (134) have shown that the soaking of isolated strips of rat right ventricle in oxygenated Krebs bicarbonate solution results in a loss of intracellular K and a gain of Na. There is actually more sodium gained than potassium lost, so that the total monovalent cation increases. If the tissue is shifted to a medium in which the sodium concentration has been reduced, there is a sharp drop in intracellular sodium concentration (134) and a striking increase in contractile response (201). A second example is provided by hearts from patients in congestive failure. Like the rat hearts soaked in Krebs solution, the concentration of potassium is decreased and sodium is increased in these tissues (43, 50, 123, 155, 208, 327). The therapeutic action of digitalis, according to the view under consideration, would be due to a decreased total intracellular cation caused by a digitalis-induced further decrease in the already abnormally low cellular potassium (see section IX and ref. 113).

Is there any other evidence to suggest that the contractile protein can be affected by small changes in monovalent cation concentration? Experiments on both extracted actomyosin and on glycerinated heart muscle fibers bear on this point. Szent-Györgyi (291) has shown that extracted actomyosin may exist in two states depending on the ATP and salt concentrations. At low ionic strength actomyosin exists as a gel, whereas at higher salt concentrations it dissociates. The addition of ATP causes syneresis of the gel (or actual shortening of actomyosin artificial "fibers"), but a very small increase in the KCl concentration, by not more than 15 per cent, causes complete dissociation of the actomyosin complex. It is thus apparent that the physical state of extracted muscle protein may be extremely sensitive to ionic strength changes of the order produced in the intact cell.

The glycerinated heart muscle fiber has also been examined with respect to ion sensitivity (32, 129, 234, 293), but the results are conflicting. The glycerinated fiber has been variously shown to *a*) suffer a great drop in contractility with small increases in sodium concentration (234); *b*) to show a great increase in rate of relaxation on perfusion with sodium solutions (129); and *c*) to exhibit little or no sensitivity to changes in concentrations of Na, K, H, or ATP (32). It is thus possible to produce glycerinated fibers which contract on the addition of ATP, but which exhibit even less

ion sensitivity than isolated actomyosin preparations. However, experiments with the isolated protein and with glycerinated fibers prepared by certain investigators seem to show that the contractile mechanism may be quite sensitive to small alterations in the ionic environment. The variability of results with glycerinated fibers emphasizes the need for careful attention to detail in the preparation of the material.

The action of monovalent cations on heart muscle contractility has been viewed in another fashion by Wilbrandt & Koller (324) and by Lüttgau & Niedergerke (200). These investigators re-examined the antagonism between calcium and the monovalent cations with respect to contractility and found that the results of a large number of experiments, in which bathing fluid, calcium, and sodium concentrations were varied independently over a wide range, could be expressed in a single curve obtained by plotting contractile force (as percentage of the maximum) against the ratio $[Ca]/[Na]^2$. This finding lends credence to the idea that the opposing actions of calcium and sodium occur at the same locus. Furthermore, despite the barriers to diffusion which calcium apparently encounters in the cell interior (see section IV), changes in calcium concentration in the bathing medium affect twitch or contracture tension very rapidly. It would therefore seem reasonable to postulate that the action of calcium (and sodium) occurs at a rather superficial site in the muscle on a link in the excitation-contraction chain rather than on the actomyosin directly. Lüttgau & Niedergerke (200) have, in fact, postulated that contraction is initiated by a calcium complex which moves from a surface site into the cell interior when the cell membrane is depolarized. According to their view, sodium ions can displace calcium from this complex, rendering it inactive. The increased calcium influx observed in the absence of extracellular sodium ion or under conditions of membrane depolarization is adduced as supporting evidence.

Their theory as originally presented seems to leave little room for the role of changes in potassium concentration on contractility. They believe that sodium is attracted to the anionic portion of the surface site calcium complex, but that potassium is probably not. In fact they suggest that the anionic moiety can even distinguish between sodium and lithium, since twitch or contracture tension is increased not only in sodium-free sucrose solutions but also in sodium-free lithium solutions, the lithium thus not being a substitute for sodium with respect to muscle contractility. The difference between sodium and lithium, however, may be explained on another basis (see section III), according to which the lithium ion never reaches the complex in short-term experiments, and therefore no conclusion can be drawn about the affinity of lithium for the complex.

In general, although the evidence suggests that calcium ions can affect contractility by an action on a relatively superficial muscle site (see section IV), the idea that sodium, specifically among the monovalent cations, has an antagonistic action at this locus needs further support before it can be accepted.

III. OTHER ALKALI METAL IONS

Lithium

Lithium is the lightest member of the alkali metal group. Although the ionic radius of lithium in crystals is the smallest in the group, it should be noted that the radius of the hydrated lithium ion is the largest among the alkali metal ions. Traces of lithium are found in mammalian organs, but no physiological role for this ion has been established. Biochemically, lithium bears some resemblance to its congener sodium. For example, lithium and sodium have no effect on, and may inhibit, a group of enzymes that require potassium for activity (265, 268). Since lithium is clearly distinguished from potassium at the enzymatic level, it is not surprising to find that cellular accumulation of lithium results in marked derangements of cellular function. It has been found by Mudge (214), for example, that substitution of lithium for sodium in the bathing fluid of potassium-deficient kidney cortex slices is associated with a marked inhibition of potassium uptake and also with a 30 to 40 per cent inhibition of respiration. Likewise, Orloff & Kennedy (227) have found that lithium interferes with acidification of the urine, and Taggart *et al.* (294) have reported that para-amino hippurate uptake by kidney slices was inhibited by lithium. Further examples of the toxicity of lithium can be found in the review by Schou (265).

The action of lithium on cells has been elucidated by studies on striated muscle and on nerve, a brief review of which will provide a basis for understanding the effects of this ion on cardiac tissue. In 1902, Overton (228) showed that the ability of frog striated muscles to conduct impulses and contract was abolished if the sodium ion in the bathing medium was replaced by sucrose. The only other cation which could maintain or restore excitability was lithium. If the lithium concentration was 35 mM per liter or less, no impairment of muscle function was observed

even after long incubations. Exposure to higher concentrations of lithium over periods of several hours caused irreversible damage to the muscle (228). Many years later it was shown by Hodgkin & Katz (144) and by Huxley & Stämpfli (154) that not only resting potentials but also action potentials of nerve fibers were unaltered when the bathing medium sodium was replaced by lithium. However, prolonged exposure to lithium solutions over periods of many hours is associated with depolarization of the cell membrane which in the experience of Gallego & Lorente de No (82) begins about 2 hours following exposure to lithium and is progressive thereafter. The recent studies of Keynes & Swan (173) on frog sartorius muscle show that the efflux of lithium ion from the frog muscle is more than 10 times slower than the efflux of sodium under similar conditions; and though sodium efflux is diminished in potassium-free solutions the movement of lithium is not affected by external potassium. Furthermore, whereas sodium can be transported out of the cell against an electrochemical gradient, a lithium loaded muscle cannot eject lithium into an outside solution in which all the sodium is replaced by lithium. All this evidence, taken together, strongly suggests that lithium efflux is completely or for the most part passive, and that active transport of lithium out of the cell is negligible if it exists at all.

Some active transport of lithium by frog skin (341) has indeed been demonstrated, but certainly in the case of the frog skin lithium transport is quite small compared to that of sodium. Maizels (202) has shown that in human red blood cells the inward passive movements of sodium and lithium have roughly equal rate constants, but there is little or no active outward movement of lithium.

From the studies cited above, one may emerge with the following picture of lithium action. At least in the case of striated muscle and nerve, it appears that lithium shares with sodium low cellular membrane permeability when the membrane is in the resting state. In view of the fact that the action potential is thought to be due to an inward sodium current which occurs as a result of a sudden change in membrane permeability during depolarization, and in view of the fact that the action potential in lithium solutions is indistinguishable from that in sodium, it appears that during activity the membrane becomes highly permeable not only to sodium but also to lithium. In contrast to the passive membrane qualities, it appears that the cellular capacity for transporting lithium out of the cell against an electrical and chemical potential gradient is very small compared to that for sodium. Because of the low cell membrane permeability for lithium the replacement of external sodium by lithium does not result in any immediate cellular depolarization, but a finite permeability to lithium combined with a negligible cellular capacity for pumping lithium out of the cell results in a slow accumulation of lithium, a decrease in intracellular potassium, and a progressive depolarization of the cell membrane.

The effect of replacing sodium by lithium on the contractility of the heart is rather promptly seen, in contrast to the results in skeletal muscle. Thus many investigators (110, 191, 223, 342) have found that in lithium solutions the contractile force of isolated heart is increased and may be followed shortly thereafter by contracture. The difference between heart and skeletal muscle in this respect is probably related to the fact that in ion-free solutions heart muscle loses rather readily a certain fraction of the intracellular cation, and, as we have noted previously (section II), monovalent cation loss from cardiac muscle is associated with increased tension and finally contracture. The lithium solution (if heart muscle membrane has a low permeability to lithium as do those of nerve and skeletal muscle) is therefore in this respect like an isomotic nonelectrolyte solution, and both intracellular sodium and potassium will be lost without a corresponding gain in cellular lithium. The early effects of lithium on contractility of heart muscle are probably related to this phenomenon. Later, as more and more potassium is lost, the cellular membrane potential will decrease to low levels as it does in nerve and skeletal muscle. [For references on the effects of lithium on the electrocardiogram which appear in papers on clinical lithium toxicity, the reader is referred to the review by Schou (265).]

Rubidium

Just as lithium and sodium have certain properties in common, the remaining available members of the alkali metal group, rubidium and cesium, are to some extent comparable to potassium in certain of their properties. The gross chemical similarities between the rubidium and potassium ion can be appreciated at several levels of complexity. For example, enzymes activated by potassium can frequently be activated by rubidium or ammonium (265). In whole animal studies it has been noted that the disappearance rates of a tracer dose of rubidium injected simultaneously with radioactive potassium into blood plasma are quite comparable (37) and many investigators during the past half century have found that solutions of rubidium chloride can depolarize nerve or muscle membranes in a

fashion somewhat comparable to solutions of potassium chloride (260 and references cited therein). On the other hand, rubidium cannot be substituted for potassium in the animal economy, and if rats, for example, are fed diets in which potassium is replaced by rubidium death occurs after several weeks (241). Examination of such animals before the terminal stages of the experiment shows that although plasma rubidium concentration is lower than that of potassium, muscle rubidium is higher than potassium; the ratio of intracellular to extracellular potassium concentration is about 44, that for rubidium is 118. And indeed in cesium-fed animals the ratio is 185. Relman *et al.* (241) used these findings as evidence against the idea that the distribution of muscle potassium was determined solely by its electrochemical potential gradient without the contribution of any active transport. Clearly the distribution of rubidium across the cell membrane could not be explained in this fashion, and could come about only by virtue of active rubidium uptake or binding of rubidium by muscle tissue. Further light on this problem was provided by the studies of Lubin & Schneider (198), who showed that if muscles which had been depleted of potassium in the cold were transferred to solutions at room temperature containing equal concentrations of rubidium and potassium, a net accumulation of rubidium greatly in excess of potassium occurred over a period of 3 hours. Such results could be explained *a*) by assuming rubidium binding by the muscle, or *b*) by assuming that muscle transported both rubidium and potassium actively across the membrane into the cell, and that passive rubidium efflux was much lower than that of potassium, or *c*) by assuming that active influx of rubidium was much greater than that of potassium. Experiments by Lubin & Schneider (198) and also by Sjodin (277) showed that permeability of the cell membrane of frog sartorius muscle for rubidium was much less than that for potassium. Lubin and Schneider's conclusion was based on efflux of tracer potassium and rubidium from muscle at zero degrees under conditions in which active transport was minimal. Sjodin's findings were based both on membrane potential measurements and also on flux measurements. Sjodin also found that if a muscle was placed in a solution containing rubidium ions at a concentration of 100 mM per liter, an immediate drop in membrane potential from a normal of 75 to approximately 45 mv was observed, and then the membrane potential declined progressively over the next 7 hours to a level of about 15 mv. The initial depolarizing action of rubidium is due to the addition of a new cation to which the muscle membrane is to some extent permeable. [For a quantitative treatment based on the Goldman constant field equation, see (277).] The subsequent progressive decline in membrane potential is due to the slow accumulation of rubidium and loss of potassium.

The peculiar actions of rubidium are perhaps most simply explained, then, by postulating a membrane transport mechanism which distinguishes poorly, if at all, between rubidium and potassium, so that both rubidium and potassium are accumulated actively. This fact, combined with the observed much lower cell membrane permeability coefficient for rubidium than for potassium, will result in a net increase in intracellular rubidium to concentrations exceeding that of potassium. Such is the case for frog skeletal muscle, but the results should not be extrapolated freely to other tissues. Whereas the data on frog skeletal muscle strongly indicate that the rubidium permeability coefficient is considerably smaller than that for potassium, studies of Love & Burch (194) indicate that this great difference does not exist for human red blood cells, in which rubidium is concentrated to the same extent as potassium. Thus the use of Rb^{86} as a "tracer" for potassium may be justified for red blood cells, but would obviously not reflect the behavior of potassium in skeletal muscle. No careful studies exist at the present time to show where cardiac muscle fits into this picture.

IV. CALCIUM

Effect of Calcium on Contractility

It has been known for many years that cardiac contractility is markedly influenced by variations in calcium concentration. Ringer in 1883 observed that the contractions of the isolated frog heart disappeared in a calcium-free salt solution and were restored by the addition of calcium. He also noted that a further increase in calcium concentration "rounds the top, and also broadens the trace of the beat." The effect of calcium on the staircase phenomenon was observed by Moulin & Wilbrandt (213), and Hajdu (111a), and are described in section VI. The relationship between twitch tension and external calcium concentration at a given frequency of stimulation has been examined recently by several investigators. A curve for isolated frog heart is shown in figure 11. A comparable curve for frog ventricle was obtained by Payne & Walser (230). The relationship for mammalian heart muscle obtained by Reiter *et al.* (239, 240) is similar, except that there is no

plateau such as that seen in figure 11 at calcium concentrations as high as 10 mM per liter.

The speed with which calcium ions can increase twitch tension has been shown beautifully by Weidmann (316) in experiments on isolated turtle ventricles. The turtle heart was perfused through the coronary artery with a low calcium Ringer's solution and was stimulated to beat once per minute in the cold. By means of a second small catheter, which was placed in the coronary artery cannula, it was possible to inject a bolus of concentrated calcium chloride over a period of 2.5 sec. The normal contraction cycle of turtle ventricle at these low temperatures was long enough so that the calcium could be injected after the onset of contraction, but before the end of the contraction cycle. The results of such experiments show that calcium injected after the onset of contraction increases the twitch tension of that contraction.

The effect of calcium ions can be seen not only in a normal twitch but also in contractures caused, for example, by high concentrations of potassium chloride. Niedergerke (219) has shown that between 0 and 4 mM per liter calcium chloride the tension of strips of frog ventricle in a potassium chloride contracture increases with the concentration of calcium in the bathing medium. The effects of calcium on the contractility of heart muscle are thus well documented but the mechanism of calcium action is not understood at the present time. In the sections that follow, an attempt will be made to summarize the information in the literature that bears on this question. Since the information in the case of heart muscle is frequently meager or nonexistent, appropriate data from other tissues will be discussed.

Calcium and the Electrical Properties of Excitable Tissue

The effects of increasing calcium in excitable tissues have been studied at great length, and in general it has been found that the effects include *a*) increase in current strength needed for stimulation, *b*) slowing of spontaneous rhythm, and *c*) block of conduction of impulses (33). The effect of increased calcium ion in decreasing irritability of amphibian hearts was observed very early (for references, see 103), and was confirmed in the case of cat papillary muscle by Greiner & Garb (103) in 1950. With the use of microelectrode techniques the basis for some of the previously observed results has now been elucidated. For example, Weidmann (314) has shown in the case of Purkinje fibers that in increased calcium solutions the threshold potential is decreased. The threshold potential in his experiments was the membrane potential at which propagated depolarization occurred in response to a 50 msec square pulse. Similar results in a different preparation and with a different experimental protocol were obtained by Frankenhaeuser & Hodgkin (79) in studies on giant squid axons. They found, starting with fibers that were hyperpolarized 41 mv above the usual resting potential, that the higher the external calcium concentration the greater was the depolarization needed to achieve peak sodium conductance. Since sodium conductance must increase to a certain critical level for propagated depolarization to occur, these results also indicate that in high calcium a greater depolarization is required before a propagated impulse occurs (i.e., threshold potential is lowered and the distance *S* in figure 9 is increased), and thus excitability is diminished. By the same token however, since the threshold potential is lowered, the tissue following stimulation becomes re-excitable at a relatively early stage of repolarization. Perhaps, this can explain the results of Grumbach and co-workers (106) who noted that ventricular fibrillation of isolated rabbit heart could be induced by sudden increases in extracellular calcium concentration. Comparable changes in dog heart had previously been observed by Butcher *et al.* (42). An alternative explanation for the arrhythmias that may be seen with increased calcium which is favored by Brooks *et al.* (34, p. 298) is that the marked decrease of threshold potential caused by the increased calcium creates local conduction blocks thought to be favorable for the development of fibrillation.

The effects of calcium ions on the rate of rise of the action potential are very interesting. It has already been noted that if the resting membrane potential is lowered the rate of rise of the action potential is likewise lowered. The effect of increasing calcium is to shift the curve to the left along the membrane potential axis [fig. 10 (79, 314)]. Frankenhaeuser and Hodgkin have pointed out that both with respect to this phenomenon and to the effect on threshold potential increasing calcium is equivalent to hyperpolarizing the resting membrane.

Some of the effects of calcium on the phases of the action potential which follow the spike have been studied by Hoffman & Suckling (149). Increasing the calcium concentration in the bath of isolated papillary muscle causes an increase in the speed of the initial phase of repolarization (phase 1) which occurs before the plateau (phase 2). Repolarization continues without the delay characteristic of a

plateau phase, but the rate is slower than that of the rapid repolarization (phase 3) which normally follows the plateau. Low calcium has the opposite effect in that the plateau of papillary muscle becomes increased in duration, but the terminal repolarization phase is not altered. In the complete absence of calcium and magnesium a remarkable prolongation of the plateau to durations as long as several seconds has been observed in both auricular and papillary muscle. A phenomenon which may be related to this was observed by Garb (83), who found that with calcium concentrations of less than 0.27 mM per liter the presence of strontium chloride in concentrations not exceeding 10 mM per liter was associated with a great prolongation of the RT interval of the electrogram of his cat papillary muscle preparation. The T wave under these circumstances was often inverted but not widened. It appears then that as in the case of the calcium- and magnesium-depleted preparations the effect here was to cause a great prolongation of the plateau without any significant change in the rate of repolarization when it finally occurred. Brooks *et al.* (34) have suggested that the strontium in this low calcium experiment displaces tissue calcium from sites in the fiber membrane essential for normal repolarization.

Exposure of cardiac tissue to very low concentrations of calcium may cause a transient increase in excitability followed by a decrease to the point of complete loss of propagated responses in spite of a normal resting potential (149). The maximum rate of rise of the action potential is decreased by low extracellular calcium concentrations.

In summary, it is clear from the above discussion that calcium is most important for the normal function of the excitable membrane. Although it has little effect on the resting membrane potential under normal conditions, it does modify resting potential changes induced by alterations in extracellular potassium concentration (see footnote 7). The most important actions of calcium on electrical events, however, are on excitability, spike, and repolarization phenomena as described in the preceding paragraphs.

Chemical State of Calcium in Living Tissue

There are few reliable measurements of calcium ion concentration in muscle. Fenn *et al.* (76) reported a value of 0.9 mM per kg of fiber water for cat and rat striated muscle. The fiber water calculations were based on a chloride space measurement of extracellular fluid. Gilbert & Fenn (92) have shown that the calcium content of muscle varies widely, according to the condition of the tissue. They found that the calcium concentration of freshly dissected frog sartorius muscle was 1.63 mM per kg, but increased to 2.84 mM per kg after a short period of immersion in Ringer's solution. An even greater deviation from the freshly dissected tissue value was found if the muscle was cut into small pieces, the concentration of calcium in this muscle being about twice that of the controls immersed in Ringer's solution. These investigators concluded that dead or damaged tissue takes up calcium from the surrounding medium. Measurements of calcium concentration in other tissues include a value reported by Keynes & Lewis (172) of 0.5 mM per kg for squid axoplasm, extruded from the nerve sheath to eliminate the surface membrane and connective tissue. These authors found calcium concentrations of 1 mM per kg in rabbit blastocytes. The value of 9.0 mM per kg reported by Sekul & Holland (267) for rabbit atria obviously requires some explanation in the light of the above values for other tissues. Since the atria had been soaked in Ringer's solution, it is possible that the soaking and also the contribution of the cut edges of the atrium account for the high calcium measured. The large fraction of connective tissue in atrium is probably another factor, as will become clear from the discussion below.

Recent studies on the kinetics of radioactive calcium movement in isolated tissues have thrown light on the distribution of calcium among the various phases of tissue. It was found by Niedergerke (220), for example, in efflux experiments on strips of frog ventricle, which had been soaked for 12 hours in radioactive calcium, that calcium efflux could be divided into two parts, a rapid phase occurring during the first 30 min, and a second phase presumed to represent intracellular radioactive calcium which was released from the cell very slowly. The rapidly moving radioactive calcium which was lost in the first 30 min of soaking in nonradioactive solution amounted to 1.37 mM per kg of tissue. This was three and one-half times the amount expected in the heart extracellular fluid, assuming the extracellular phase to be 25 per cent of the tissue volume. These results suggested that the rapid phase calcium represented not only the tracer distributed in extracellular fluid, but also a moiety bound to connective tissue or to a surface site of the heart muscle cell from which it could exchange readily with the surrounding medium. A more quantitative approach to this problem in frog sartorius muscle has been made by Gilbert & Fenn (92) by

TABLE 1. *Calcium Partition in Muscle*

		μM Ca/gm
	Connective Tissue Space	
Rapid Ca^{45} efflux	1. Aqueous*	.16
	2. Bound to connective tissue†	.25
	Muscle Fibers	
	3. Surface bound‡	0.1 + 0.03
Slow Ca^{45} efflux	4. Myoplasm, exchangeable	.33
No Ca^{45} efflux	5. Myoplasm, nonexchangeable	Not determined

* This represents the Ca^{45} in the extracellular fluid. The extracellular fluid volume was based on a sucrose space of 16%. † This fraction was based on Ca^{45} distribution in tendon and the assumption that the tendon and muscle connective tissue were comparable with respect to calcium binding capacity. ‡ This represents the total surface-bound Ca^{45} less the amount bound to connective tissue. The 0.03 figure is calculated from the sudden increase in Ca^{45} efflux which occurs when the tissue is shifted from a calcium-free medium into a solution containing calcium. It is thought to be a superficial moiety of "self-exchanging" calcium which is capable of exchanging with any calcium that exists in the bathing fluid but which is rather firmly bound to surface sites in the absence of calcium.

analysis of an experimentally obtained calcium uptake curve of the muscle. A somewhat more complete analysis along the same lines was made by Shanes & Bianchi (272). In their experiments Ca^{45} efflux curves from frog sartorius muscles were obtained. Their results are presented in table 1. The efflux curve is divided into a fast and slow phase. The fast phase is considered to represent *1*) Ca^{45} in the extracellular fluid; *2*) a moiety bound to connective tissue; and *3*) a so-called surface-bound calcium which, since the connective tissue space moiety is accounted for in *2*, is assumed to be bound to the surface of the muscle fibers. The rest of the tissue calcium is, then, in the myoplasm, and this accounts for the slowly exchanging muscle calcium. A fraction of the tissue calcium is nonexchangeable under the conditions of the experiment.

Harris (120), on the basis of iontophoresis experiments, also concluded that calcium ions become bound to surface sites of skeletal muscle because of its low mobility in an electric field.

The studies noted above indicate that calcium is bound to connective tissue and quite likely muscle surface. There is also a good deal of qualitative evidence to suggest that calcium is bound to intracellular protoplasmic components as well. It has already been noted that cut muscle binds more

TABLE 2. *Ca^{45} Equilibration in Tissues*

Tissue	Reference	Equilibration, % of Extracellular Specific Activity
Rabbit atrium	(267)	2–4% in 4 hr
Squid axoplasm	(146)	20% in 8½ hr
Frog skeletal muscle	(272)	38% in 4 hr
Frog skeletal muscle	(120)	10–25% in 16–20 hr
Frog skeletal muscle	(57)	45% in 6 hr
		25% in ½–8 hr*
		100% in 6–10 hr†
Rat skeletal muscle	(57)	100% in 2 hr‡

* In vivo, resting frogs. † In vivo, jumping frogs. ‡ In vivo, active rats.

calcium than intact muscle (92). This has also been found for breis of frog muscle (317); and it has been reported that no ultrafiltrable calcium can be obtained from a suspension of finely cut up rat muscle (318). An attempt to construct a more quantitative picture of the state of calcium within living tissue has been made by Hodgkin & Keynes (146) who studied the movement of a microvolume of Ca^{45} injected into the axoplasm of an intact squid nerve. They found that the mobility of the injected calcium was less than 1/45 of what it would have been in free solution. Their conclusion is that the ratio of ionized to total calcium in the cell cannot be more than about 0.02 and assuming a total axon calcium concentration of 0.4 mM per kg the free calcium concentration in squid nerve should be less than 0.01 mM per kg.[8] Hodgkin and Keynes argue that if calcium were distributed according to the Nernst equation, the ratio of intracellular to extracellular calcium should be more than 100. The actual value for squid axon derived from their experiments would be about 0.01/11, so that clearly the system is far from equilibrium with respect to calcium. A similar viewpoint is presented by Gilbert & Fenn (92). It would thus appear both from this reasoning and from the observations that damaged tissues accumulate calcium, that the cell interior maintains a very low free calcium ion concentration compared to its environment. Not only does the cell membrane have a low permeability to calcium ion (as will be elucidated in the next section) but the cell must have the capacity

[8] One might contend that the micro-injection of calcium into the cytoplasm of a living cell would not provide an accurate reflection of the mobility of the naturally occurring calcium. It is known for example that such injections cause gelation or clotting of the cytoplasm of certain tissues; however, in the case of the squid axon the calcium apparently liquefies the squid axoplasm. For references on this interesting subject the reader is referred to the paper of Chambers & Kao (49).

TABLE 3. *Ca^{45} Influx* of Resting Tissue*

Tissue	Reference	Influx
Frog ventricle	(221)	Slow, no quantitation
Rabbit atrium	(267)	0.024 pmoles/cm²/sec
Guinea pig atrium	(338)	0.015 pmoles/cm²/sec
Squid axon	(146)	0.076 pmoles/cm²/sec
Frog sartorius	(16)	0.094 pmoles/cm²/sec
Frog sartorius	(92)	0.8 mM/liter/hr

* Influx into cell, based on analysis of the slow component of Ca^{45} flux.

to eject, by some kind of active transport, calcium which passes the membrane barrier.

Movements of Calcium In and Out of Cells

CELLS AT REST. It has been observed for a variety of tissues bathed in artificial media that the entry of calcium into the interior of the tissue cells is extremely low. This can be appreciated by reference to table 2 which shows the percentage equilibration of Ca^{45} in the tissue after long periods in radioactive calcium solution. [The in vivo results of Cosmos (57) will be discussed below.] It should be noted that certain of the investigators in this group found an upper limit to the specific activity of Ca^{45} achieved in tissue and concluded therefore that a portion of the intracellular calcium was nonexchangeable with the external calcium. Information on Ca^{45} influx for resting tissue is presented in table 3. The most complete data are those of Hodgkin and Keynes, and since their measurements were made on axoplasm extruded from squid nerves these values are unique in representing direct measurements of intracellular content in contrast to values derived by analysis of the slow component of Ca^{45} influx or efflux curves. One fact which emerges from the squid axon data is the extremely low permeability of the resting membrane to calcium, the apparent permeability coefficients of potassium, sodium, and calcium being in a ratio of 1:0.025:0.001.

CELLS DURING ACTIVITY. *Calcium movement during stimulation under normal conditions.* It had been shown several years ago that no change could be observed in the total calcium concentration of striated muscle following a prolonged period of stimulation (76). An increased exchange of calcium between active muscle and a Ca^{45} labeled environment was demonstrated by Cosmos (57), who showed that specific activity of calcium in stimulated muscle was greater than that of corresponding control muscles between the 3rd and 4th hours of a prolonged experiment in which the experimental muscle was stimulated for a total period of 6 hours. The curious feature of these results, however, was that between 4 and 6 hours the specific activity of the control muscles increased and reached the level of the experimental muscles, leveling off to a value of about 45 per cent exchange. The most significant aspect of Cosmos' work is the finding that in contrast to the apparently nonexchangeable moiety of tissue calcium found in experiments with muscles in vitro, if the radioactive calcium was injected into the whole animal and the muscles were analyzed at intervals thereafter, it was found that all the muscle calcium exchanged with the isotope after 6 to 10 hours in the case of frogs stimulated to jump, and within a period of about 2 hours in the case of spontaneously active rats (see table 2).

There is general agreement that Ca^{45} influx increases as a result of stimulation. This has been shown for guinea pig atrium, rabbit atrium, frog sartorius, and squid nerve (16, 146, 267, 328). However, there is no agreement on the question of changes in calcium efflux during stimulation, Woodward (338) and Shanes & Bianchi (273) having demonstrated an increased efflux for frog sartorius, other authors having found no change (120, 146, 267). In view of the increased Ca^{45} specific activity equilibration during muscular activity demonstrated by Cosmos (57) and the agreement that Ca^{45} influx increases with stimulation, one should expect a corresponding increase in efflux over long periods of stimulation if the muscle approaches a steady state with respect to calcium ion exchange.

Calcium flux during stimulation under abnormal conditions. Before discussing this topic it would be well to emphasize certain points elucidated in previous sections. It was pointed out that most of the cellular calcium is bound and there must be a very low concentration of free ionic calcium within the cell. The electrochemical gradient for calcium strongly favors movement of the ion from bathing fluid into the cell, and this gradient is maintained by a low membrane permeability to calcium and by some kind of active process for ejecting calcium. In general, then, changes in calcium influx may occur because of alteration in the electrochemical gradient or change in membrane permeability; and changes in efflux will reflect a change in the active ejection of calcium, either because of an alteration in the amount of calcium made available to the transport mechanism or a variation in the activity of the mechanism itself. It should be remembered that since there are doubtless several different moieties of bound

calcium, alterations in the state of these calcium complexes may influence certain of the factors mentioned above. In our present state of knowledge we can do no more than enumerate the calcium flux changes that have been observed, and it will remain for future investigators to determine the relationship of these changes to the contractile process. Calcium influx is influenced by the following interventions.

1) Cell membrane depolarization. Depolarization of excitable tissue membranes by high concentrations of potassium is associated with increased influx of calcium (16, 146, 221). This has been observed in frog heart, frog sartorius muscle, and squid nerve. The occurrence in nerve as well as in muscle obviously eliminates contracture as the cause of the increased influx. Since the electrical gradient in the depolarized state is less favorable for calcium influx, it would appear likely that increased membrane permeability for calcium occurs under these conditions.

2) Muscular contraction. Prolongation of muscular contraction or production of contracture is associated with increased calcium influx, and this is independent of the membrane potential, since it may occur in even potassium-free solutions in which the membrane is hyperpolarized. Such results have been reported with frog heart contracture produced by ouabain (296), potassium-free bathing fluid (296), and sodium-free bathing fluid (221). Increased calcium influx has also been observed in frog sartorius when nitrate ion replaces chloride as the major anion in frog Ringer solution. Under these conditions, associated with an increased twitch tension due to a prolongation of the active state (140, 160), there is a 60 per cent increase in calcium influx. Since nitrate ion does not alter the calcium influx of the unstimulated muscle, the increased flux is clearly related to the nitrate-induced prolongation of the active state (16). Such calcium changes in cardiac tissue might not be expected, since the reaction of isolated toad heart to nitrate is a decrease in contractility and therefore apparently active state duration is not increased (218).

3) Ionic composition of bathing fluid. Hodgkin & Keynes (146) have found that the calcium influx in the case of the squid axon is greater in magnesium-free solution than in normal sea water. Niedergerke (221) believes that calcium moves into the cell in combination with an anionic carrier, and that sodium competes with calcium for the carrier. Thus, he would explain the increased influx of calcium in sodium-free solutions on this basis rather than on the basis of the contracture which occurs under these conditions. Experiments on nerve would therefore be of interest in this regard.

One can do no more than add to the list of unexplained phenomena the observations that calcium efflux is diminished in low sodium or low potassium solutions (222) and during ouabain-induced contracture (323).

Locus of Action of Calcium on Contractility

The previous discussion has dealt for the most part with the subject of calcium and the cell membrane. Even in this respect it has not been complete. There is space to mention only in passing the fact that alteration in external calcium concentration may cause changes in the uptake of potassium by the heart (238) and in the potassium content of the heart (239). The calcium ion may be extremely important in the structure of various membranes, including those of red blood cells (21, 86, 203), smooth muscle (29), and heart sarcosomes (51). In addition to membrane effects there are several intracellular loci at which calcium ion could affect contractility. For example, it is known that microinjection of calcium chloride induces muscle contraction (131); calcium affects the contractility of actomyosin threads (128); it affects ATPase activity (10) and is extremely important for the activity of relaxing factor (13, 89, 163, 215).

It is apparent, then, from studies on isolated components of muscle that a variety of structures and systems may be affected by the calcium ion. Another approach which may be more useful for the present discussion is to consider what happens to intact heart muscle deprived of calcium. On this basis there appear to be two sites sensitive to variations in extracellular calcium. One is the cell membrane itself. Although the cell membrane is resistant to calcium deprivation (211, 297), it does become inexcitable at very low concentrations of calcium (78, 149). The second site is some calcium-sensitive mechanism responsible for propagation of excitation from the membrane to the contractile protein. This site is apparently very sensitive to calcium since variations in extracellular calcium concentration very rapidly cause changes in twitch tension, and at low calcium concentrations at which membrane depolarization is still normal twitch tension disappears (297). There is certain evidence which suggests that this site is located in a relatively superficial region of the muscle cell. It was shown by Boehm (19) that heart muscle which loses all contractility

when placed in a calcium-free solution gradually regains this as calcium ion diffuses from the cell interior outward. Replacement of the bathing solution by another calcium-free solution causes disappearance of contractility again, so that the process is not some sort of accommodation independent of calcium ion. The rapidity with which calcium ion increased contractility in the turtle heart in the experiment by Weidmann, cited earlier (see first of this section), also showed that contractility can be influenced by calcium acting on a relatively superficial site of the heart muscle. The prompt release of Ca^{45} from frog sartorius muscle following a 12-sec stimulation shows that contraction is associated with the mobilization of a superficially located calcium moiety (273).

All these pieces of evidence are consistent with the idea that at least one link in the excitation-contraction cycle is calcium-sensitive. It has been suggested by some investigators that initiation of contraction is actually mediated by calcium, or a calcium complex moving from a superficial locus into the cell interior (16, 200, 213). In the case of heart muscle, if the amount of calcium at this locus influences contractility, then it must change readily with changes in extracellular calcium concentration to which cardiac contractility is so sensitive.[9] It will be of interest to determine whether the increased calcium influx associated with stimulation (267, 328) varies with contractile force and with changes in the concentrations of extracellular calcium.

V. OTHER ALKALI EARTH METAL IONS

Magnesium

Magnesium ions block neuromuscular transmission in concentrations which do not stop nerve conduction or the response of muscle to direct stimulation. This action of magnesium may be reversed by increasing calcium ion concentration. The widespread effects of magnesium on the whole organism are summarized in a recent review by Engback (71).

The intravenous injection of magnesium salts into intact animals is followed by a progression of electrocardiographic abnormalities which have been studied by Smith and co-workers (279). As the serum concentration of magnesium rises from 2 to 5 meq per liter, there is an initial tachycardia which is followed shortly by bradycardia. There are extensive disturbances of intracardiac conduction, including *a*) progressive increase in P-R interval at 5 to 10 meq per liter magnesium; *b*) occasional S-A and A-V block of various grades, occurring above 15 meq per liter; and *c*) prolonged intraventricular conduction time (widening of QRS interval) beginning at concentrations of 5 to 10 meq per liter. The final event is cardiac arrest, at levels usually between 27 and 44 meq per liter.

Studies on isolated cardiac tissues also reflect the electrical disturbances caused by magnesium. The spontaneous beating of the frog ventricle can be stopped by the application of magnesium chloride, though the heart is said to remain responsive to mechanical or electrical stimulation (39, 210). The effect of magnesium on the spontaneous rhythm can be reversed by increasing calcium concentration (39). It should be noted that the magnesium concentration in these experiments was very high, being 64 meq per liter in the protocol presented by Burridge (39), and it is surprising that any response could be induced under these conditions. Action potentials of nerve fibers disappear completely in isotonic magnesium chloride (101).

Alterations in magnesium concentration do not have any striking effect on isolated cat papillary muscle, a tissue which is not characterized by spontaneous rhythmicity. For example, Garb (83) studied both magnesium-free solutions and 10 times the normal concentration of magnesium, and in neither case did he observe any effect on the surface electrogram of cat papillary muscle. In a study on the effects of various cations on cat papillary muscle excitability, Greiner & Garb (103) found that both calcium and magnesium decreased excitability in high concentrations, the effect of magnesium being less than that of calcium. Hoffman & Suckling (149), working with a similar preparation, found a slight drop in excitability at very high levels of magnesium. However, if the calcium was reduced, a 5-fold increase in magnesium concentration caused a shortening in the plateau of the action potential in a manner

[9] Skeletal muscle is different in this regard. Exposure to calcium-free solutions is associated with a drop in twitch tension only after a period of several hours. If calcium concentration is raised above normal, resting calcium influx is increased, but the extra calcium influx associated with contraction is not increased. The superficial calcium identified by Shanes and Bianchi, which is lost readily to the surrounding medium (see table 1) is thus not important for skeletal muscle contractility. If a superficial moiety of calcium is involved in the excitation contraction cycle of skeletal muscle it must be part of the calcium which exchanges slowly in the resting state.

similar to that described for high calcium (see section IV).

Although many opinions have been expressed on the question whether cardiac muscle contractility is depressed by magnesium ion, there is little evidence from which to draw a conclusion. For example, Smith *et al.* (279) assert that normal systole is maintained until cardiac arrest supervenes in their experiments, but this is based on the fact that the heart on observation showed a "well-defined and vigorous systole." The heart-lung preparation described by Stanbury & Farah (286) performs a given stroke work at a higher than normal filling pressure in 14 meq per liter of magnesium, and filling pressure drops on addition of calcium. Such impairment of function as this may represent could be caused by intraventricular conduction blocks (279) rather than a direct effect on the muscle. Garb finds that the isometric tension developed by cat papillary muscle is not influenced by magnesium concentrations over a range from 0 to 10 times normal (83). On the other hand, an increase of magnesium concentration by 6 mM per liter in the solution bathing an isolated frog heart caused an immediate drop in developed tension, which could be brought back to normal by increasing the duration of the square pulse used to stimulate the muscle (unpublished observations). Further studies are needed to establish at what steps in the excitation-contraction process magnesium exerts an effect.

In relationship to the last question certain complementary facts come to mind. *a*) Magnesium blocks neuromuscular transmission, and the effect can be counteracted by calcium. *b*) Neither magnesium nor calcium affect the contractile response of skeletal muscle to direct electrical stimulation. *c*) In contrast, the contractile response of cardiac muscle is very sensitive to changes in calcium, and perhaps reacts in the opposite fashion to magnesium. *d*) Magnesium appears to enter cardiac muscle more readily than skeletal muscle. The resistance of most cells to accumulation of magnesium had been noted previously (280). In recent experiments it has been found that injection of Mg^{28} intravenously is followed by accumulation of radioactivity in heart muscle to an extent 10 times greater than that in skeletal muscle. It has been shown that this is not a function of stimulation of the muscle, nor is it due to excessive accumulation in Purkinje fibers (30, 94). Skeletal muscle, then, exhibits less uptake of magnesium tracer than does heart and is not directly affected by variations in extracellular calcium or magnesium. Cardiac muscle may be more like the neuromuscular junction, both calcium and magnesium perhaps being capable of reaching superficial sites where these ions may affect steps in the excitation-contraction process.

Magnesium deficiency is encountered clinically in man, usually because of a generally poor nutritional status secondary to chronic alcoholism or gastrointestinal tract dysfunction (233). Nonspecific ST segment and T wave changes are often seen under these conditions, and sometimes a slow change back toward normal occurs during the course of therapy. The improvement is not necessarily correlated with the change in serum magnesium concentration, however, and many other factors in the clinical course may contribute to the final result.

It was observed many years ago that the magnesium concentration expressed in mg per 100 g of dry tissue was abnormally low in hearts of patients dying in congestive failure (327). Since phosphorus and potassium were also decreased, there is a possibility that the chemical findings reflect a relative decrease in cell mass. Any result which pointed specifically to magnesium loss would be of interest because of the possible relationship of magnesium to normal muscle function. [For example, magnesium inhibits calcium-activated myosin ATPase (105).]

Barium

Barium has been known, since the time of Boehm (18) in 1875, to affect electrical properties of cardiac muscle. Many workers (23, 103) have shown in both amphibian and mammalian preparations that barium chloride can initiate spontaneous activity in cardiac muscle. Other changes may also occur. For example Kleinfeld *et al.* (176) found that injection of barium chloride into the dorsal lymph sac of the frog was followed by A-V block, idioventricular rhythm, ventricular extrasystoles, and ventricular tachycardia.

The effect of barium on the cardiac action potential was shown by Kleinfeld and co-workers (176) to consist of a marked lengthening of the terminal portion of the recovery phase of the action potential. Comparable tracings were obtained by Greengard & Straub (101) from rabbit cervical sympathetic trunk B and C fibers bathed in isotonic barium chloride. It would appear that calcium (149), barium (101, 176), and strontium (101) may all prolong the terminal phase of repolarization of the action potential. This is in contrast to the effects of *a*) calcium and magnesium-free solutions, or *b*) high strontium in the presence of low calcium, which are both

associated with prolongation of the plateau; whereas terminal repolarization, when it begins, proceeds at a normal rate. (See section IV.)

It is well established that barium chloride can cause contracture of the isolated frog heart when added to the Ringer's solution (175, 321) or serum (321) bathing the tissue. If rather low concentrations of barium chloride are given (10–100 μmoles/liter) no effect is observed if the calcium concentration is normal, but contracture occurs with barium in the complete absence of calcium ion (unpublished observations). This brings to mind the findings of Thomas (295) that the addition of strontium to an isolated frog heart in the absence of calcium increases the isometric tension almost to the point of contracture. The addition of calcium reverses the strontium action. These results might be formulated according to the following scheme. There is a chemical site in the excitation-contraction process for which barium, strontium, and calcium all can compete. This site has a stronger affinity for calcium than for either of the other two cations. However, once attached to the site, the order of increasing potency for enhancing contractile force is calcium, strontium, barium. Therefore, barium or strontium in the presence of comparable concentrations of calcium has no effect because, according to this scheme, the site preferentially binds calcium. In the absence of calcium, barium or strontium is free to reach the site, where they are more effective than calcium in increasing contractility.

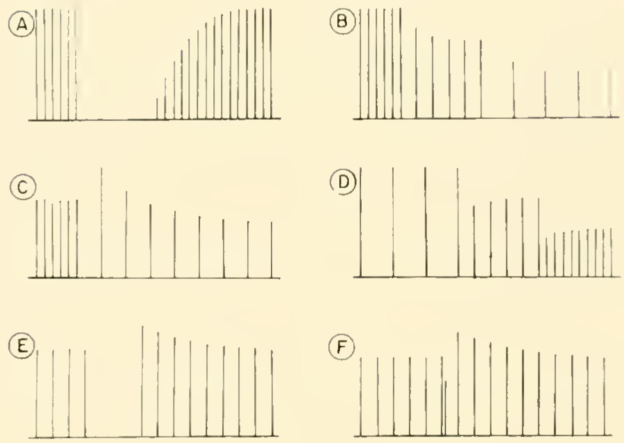

FIG. 12. Schematic diagrams of frequency-tension relationships. Continuous tracings of contractions. (See text for details.) *A:* Bowditch staircase. Following a rest period the first contractile response is small, but rises progressively with each stimulus until a plateau is reached. *B:* Bowditch staircase. The higher the stimulus frequency, the higher the tension. *C:* poststimulation potentiation, a mixture of Bowditch and reverse staircase. The first contraction after shifting from a high to low frequency is greater than before (reverse staircase). Then there is progressive drop to a new plateau characteristic of the slow stimulus frequency (Bowditch staircase). *D:* reverse staircase. The higher the stimulus frequency the lower the tension. *E:* rest contraction, an example of reverse staircase. Stimulation rate before and after the rest is the same. The first few contractions after the rest are greater than before. *F:* postextrasystolic potentiation. The first few contractions after the extrasystole are greater than before. [From Hajdu & Leonard (113).]

VI. EFFECT OF STIMULATION FREQUENCY ON CONTRACTILE FORCE

Historical Note and Definitions

The twitch tension developed by cardiac muscle is affected in large measure by variations in the frequency and regularity of stimulation. Comparable effects have been observed in smooth (60, 186) and striated muscle (243), but are much less obvious in the latter tissue. In the case of heart muscle the variations in contractile force with frequency are probably due to either pure examples or mixtures of two basic phenomena, the so-called Bowditch staircase and the reverse staircase. Postextrasystolic potentiation may represent yet a third phenomenon responsible for tension changes, or may be closely related to the Bowditch staircase as will be discussed below. The term staircase has recently been applied by Rosenblueth and co-workers to a frequency-independent stepwise change in contractile force of the heart which occurs under certain conditions following changes in inflow or output pressure (250). This is referred to in the section on contractility and will not be discussed further here.

The first correlation between stimulation frequency and contractile force was reported by Bowditch (24) in 1871. Working with an isolated frog heart, he noted that following a long period of asystole the amplitude of contractions which occurred when the heart was subsequently stimulated at a regular frequency began at a low level and increased progressively to a maximum which was then maintained at a plateau (fig. 12*A*). Later workers confirmed this observation, not only for amphibian but also for some mammalian hearts, and also made the generalization that for any regular stimulation rate a characteristic level of twitch tension was achieved (61, 114), being low at low frequency and higher at increased frequencies over a certain range (fig. 12*B*). It was clear, however, especially in the case of mammalian

heart, that an opposing phenomenon frequently operated simultaneously. This was first described by Woodworth (340) in experiments on dog heart muscle. He stimulated the muscle at a regular fast frequency until a steady twitch tension was obtained. When he shifted to a slow frequency the first one or two twitches were greater than the previous ones, rather than smaller as would have been expected on the basis of the Bowditch staircase, and then progressively declined as expected to a level characteristic of a slow rate (fig. 12*C*). [This phenomenon is sometimes referred to as poststimulation potentiation (252).] The increased amplitude of the first twitches at the slow rate led him to believe that the twitch tension was the result of two effects, "the stimulating effect of a rapid succession of contractions and the recuperative effect of a long pause." In certain animals, such as the rat, the opposing phenomenon is so dominant that even the steady state level of twitch tension decreases with increasing frequency and vice versa (14, 148, fig. 12*D*). Of the names used to refer to this opposing phenomenon "reverse staircase" will be employed in this chapter. The relative contribution of reverse staircase and Bowditch staircase for any one species may change over the observed frequency range (180). For example, even in the case of the rat for which the reverse staircase has been so frequently described, the Bowditch staircase becomes dominant at higher frequencies (unpublished observations). The so-called "rest contraction" (252) is another example of the reverse staircase phenomenon (fig. 12*E*), since the interval of rest can be regarded as a temporary shift to a lower frequency which causes an increase in twitch tension. To this already long list of phenomena must be added still another one, first observed by Langendorff in 1885 (cf. 340), namely the effect of an extrasystole in causing an increased amplitude of the following contraction (fig. 12*F*). These various force-frequency relationships are discussed below.

The Bowditch Staircase

The central fact about the Bowditch staircase is that for any frequency of stimulation there is a characteristic twitch tension. Perturbations caused by extrasystoles or by shifts in the regular frequency are followed, on the return to the control frequency, by a return to the control twitch tension. The Bowditch staircase in the frog heart has been studied by Hajdu (110). He found that, when a previously nonbeating heart was stimulated electrically, with

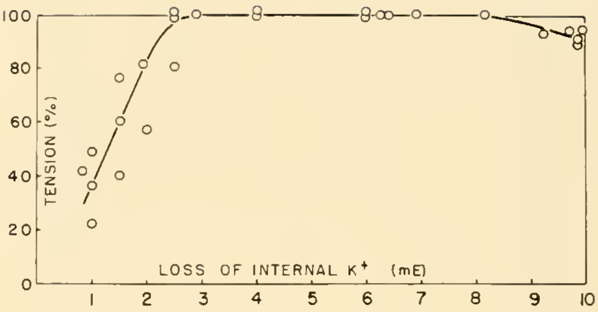

FIG. 13. Correlation between tension and loss of internal potassium. [From Hajdu (110).]

the progressive rise in twitch tension which occurred there was a progressive net potassium loss from the muscle. This can be expressed in the diagram of figure 13, which shows that over the range of 1 to 3 meq of potassium per liter of fiber water lost from a muscle cell, the twitch tension rises from a very low level to a maximum value. The higher the frequency of stimulation the greater the loss of internal potassium, but losses beyond 3 meq of potassium per liter of fiber water were not associated with any further increase in twitch tension. In summary, over the rising portion of the curve shown in figure 13, for any stimulation frequency there is a unique value for both twitch tension and cellular potassium content. Over the flat portion of the curve there is no further increase in twitch tension, but there continues to be a correlation between stimulation frequency and cellular potassium content.

In an attempt to account for these findings the following reasoning is presented. In the resting muscle at the steady state, potassium influx and efflux are of course equal. When the muscle is stimulated there is a rise in potassium efflux, which probably occurs in temporal relation to the repolarization phase of the action potential (see section II). Therefore, in the shift from rest to activity, or in a shift from a lower to a higher rate of stimulation, the increased potassium efflux would lead to a progressive net loss of potassium from the cell unless the influx was increased to a corresponding level, or unless the efflux subsequently decreased to the original level. One can conclude from the recent work of Rayner & Weatherall (236) on potassium movement in resting and stimulated rabbit auricles, that potassium efflux remains elevated during activity and that therefore a progressive net potassium loss from the cell must be prevented by an increase in the influx. The view may be taken, then, that on stimulation, potassium efflux increases, in-

ternal potassium concentration falls, and that the mechanism for transporting potassium into the cell is stimulated by the fall in potassium. The lower the potassium falls, the greater the stimulation of the potassium pump, until finally the potassium influx becomes equal to the potassium efflux so that a new steady state is achieved in which no further fall of cellular potassium concentration occurs. In summary, one postulates that the potassium pump is affected by the intracellular potassium content so that for any frequency there is a characteristic tension, potassium content, and rate of potassium transport into the cell.

Vick & Kahn (304) produced evidence confirming part of the Hajdu study by showing that a net loss of potassium from guinea pig heart occurred when the stimulation rate was increased. Brown *et al.* (35) observed no net loss of potassium from the hearts of intact dogs when stimulation frequency was increased over an approximately 2-fold range. It is possible that in their preparation the cardiac muscle "potassium pump" was more sensitive to intracellular potassium content than in the frog or guinea pig heart, so that the rise in potassium efflux with increased frequency was immediately matched by a rise in influx without a significant loss of intracellular potassium. The steady state potassium fluxes of dog cardiac muscle do increase with stimulation frequency, according to the studies of Wood & Conn (335).

A few general comments should be made about the Bowditch staircase. It is clear that any factor that alters the contractile force of cardiac muscle will affect the force-frequency relationship. In the case of the frog heart there is a comparatively small change in twitch tension with frequency directly after the heart has been removed from the animal, but after a period of several hours washing in Ringer's solution the twitch tension varies greatly with alterations in frequency. This is the characteristic quality of the washed or "hypodynamic" frog heart. High twitch tension, which does not fall when stimulation frequency is lowered, occurs in the presence of low extracellular sodium or potassium, or high extracellular calcium. Among the most effective agents for inducing a maximal twitch tension which is insensitive to frequency changes over a wide range are digitalis and cardioglobulin, a cardiotonic protein system recently isolated from mammalian blood plasma (112, 188).

Although the stepwise changes in tension with changes of frequency can be correlated with changes in intracellular potassium, there is no evidence that the potassium change is directly responsible for the altered contractility. Some authors, for example (213, 218a, 289), are inclined to attribute the increased tension of the Bowditch staircase to an accumulation of cellular calcium, rather than a diminution in potassium. A net accumulation of calcium with changes in stimulation frequency has not yet been shown. In any case, both ions have effects on the function of muscle. Small changes in potassium concentration, for example, produce marked alterations in the shortening of actomyosin threads. The dramatic effects of calcium on muscular contractility are likewise well known (see section IV). At the present time, a choice between the two ions cannot be made. Furthermore it cannot be said whether the variations in contractility with frequency reflect a change in the milieu of the contractile protein, or a change in excitation-contraction coupling.

The biophysics of the Bowditch staircase phenomenon has been investigated by Ritchie & Wilkie (243) in the case of skeletal muscle. These workers found that previous stimulation of a frog sartorius caused an increase in the duration of the active state (see section I for a discussion of the active state), and they believe that this accounts for the staircase phenomenon and the posttetanic potentiation which can be seen in frog skeletal muscle. On the other hand, the increased twitch tension that occurs with increasing frequency in cat papillary muscle has been attributed to an increase in the intensity rather than in the duration of the active state (1).

Reverse Staircase

The essential fact about the reverse staircase is that following a twitch a comparatively long period of time is required before cardiac muscle regains full contractility (31, 276). This is illustrated by the curves shown in figure 14 (31). Cardiac tissue was stimulated at a regular frequency. Then a test pulse was given at varying intervals following a normal beat and the amplitude of contraction was recorded. It can be seen in the experiments cited that about 5 sec was required for maximum amplitude to be reached, and it is likely that if isometric tension rather than isotonic shortening had been measured, the plateau would not have occurred until an even longer interval had passed. This curve of recovery of contractility is not significantly altered by variations in the previous stimulation frequency over a range from 60 to 120 beats per min (but it is difficult to generalize this conclusion over a wide frequency range, since the

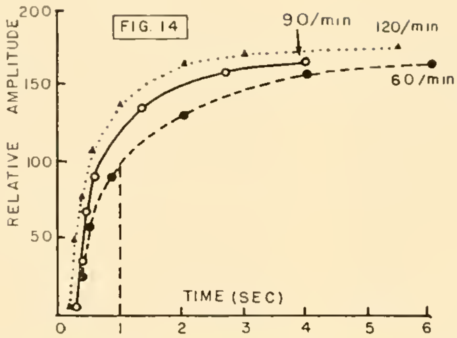

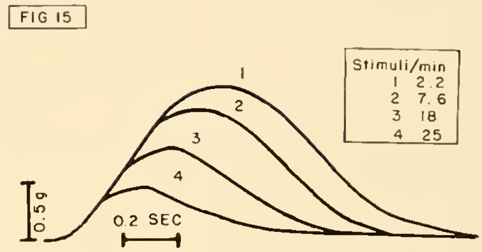

FIG. 14. Recovery of cardiac contractility following stimulation. Three recovery curves are shown at basal stimulation frequencies of 60, 90, and 120 per min. See text for further description. [After Braveny & Kruta (31).]

FIG. 15. Superimposed records of isometric contraction curves of frog ventricle at different basal stimulation frequencies, demonstrating the similarity of the rising phase of the four curves. [After Niedergerke (218a).]

Bowditch staircase will cause significant changes in the maximum twitch tension). Referring again to figure 14, it can be seen that for a heart beating at 60 per min (1 sec interval between stimuli), each stimulus interrupts the rising recovery curve of contractility, the amplitude of contraction being indicated by the dotted line in the figure. It is clear then that a prolongation of the interval between stimuli will find the muscle fiber more fully recovered, and the twitch tension will be correspondingly higher. The curve of recovery of contractility is different in different animals, being greatly prolonged for example in the rat heart (148, 180). The reverse staircase of rat heart becomes less prominent after bathing in Krebs solution for long periods of time, and it is usually not obvious in frog or guinea pig heart (unpublished observations). Many factors can change the rate of recovery of contractility. For example, the reverse staircase is intensified (recovery prolonged) in hypoxic frog heart (218a) and in rabbit atrium treated with fluoroacetate (169). But the basic phenomenon of interest, the slow recovery of contractility in cardiac muscle, occurs under conditions in which hypoxia or fatigue can hardly be invoked as explanation. Figure 15 shows contraction-relaxation curves in a range where the reverse staircase is prominent. It can be seen that the initial rate of rise of tension appears similar at different frequencies, and the smaller peak tension at the higher frequencies appears to occur because relaxation sets in earlier (218a).

None of the published studies on the reverse staircase provides any clue about the cause of the phenomenon. Speculations have ranged from the idea that during rest time is provided for certain metabolic reactions to achieve cellular recovery (168, 169, 340) to the postulation of a potentiating substance (252). Recently it has been suggested that the increased contractile force observed after a rest is correlated with the ability of the cell to maintain a low intracellular sodium at low stimulation frequencies (176a). It is possible that just as the increased tension of the Bowditch staircase depends on the high frequency loss of intracellular potassium, the increased tension of the reverse staircase depends on a loss of intracellular sodium due to increased extrusion at low frequencies.

Postextrasystolic Potentiation

An example of postextrasystolic potentiation is shown in figure 12*F*. Woodworth, exploring the earlier findings of Langendorff found that two or more extrasystoles had a greater stimulating effect than one, that the effect persisted on the average for about eight subsequent beats, and that the earlier in the contraction cycle the extrasystole occurred the greater was the potentiating effect. These observations were later confirmed by others (45, 46, 84, 147, 206, 276).

Postextrasystolic potentiation has been thought by many (45, 46, 231, 263) to be an example of the Bowditch staircase. An analysis of the problem can be facilitated by reference to an experiment on cat papillary muscle, published by Hofmann *et al.* (147), which is similar to an earlier one of Garb & Penna (84). Figure 16 is a schematic diagram to show the essential part of the experiment. It represents a continuous tracing of contractions induced by stimulation at an average frequency of 1 per sec. Whereas the stimulation was regular in the first and last part of the tracing,

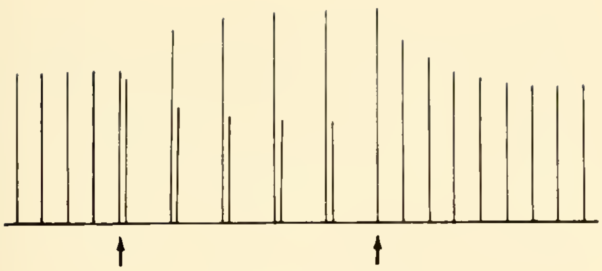

FIG. 16. See text for description.

in the section bounded by the two arrows the average frequency was maintained by stimulating at a regular rate of one half per sec, and following each regular contraction with an extrasystole. It can be seen that when the shift was made to the irregular frequency the tension of the postextrasystolic contractions rose progressively to a plateau, and dropped back when regular stimulation was resumed. This rise in tension is partly due to reverse staircase, since the interval between any extrasystole and the following contraction is almost 2 sec rather than 1 sec as in the control period, and the effect of the reverse staircase would be to cause a greater tension after the longer rest period. However, the rise in tension is progressive for several beats, and the reverse staircase (i.e., recovery of contractility) is not expected to change from beat to beat. It seems likely, therefore, that an additional factor contributes to the rise in tension, either the postulated potassium shift of the Bowditch staircase or a completely different phenomenon. In the former case the progressive rise in the tension of the postextrasystolic contractions would be associated with a *pari passu* drop in cellular potassium until a new steady state level is reached. Since the average frequency remains the same during the experiment, the development of a lower steady state level of cell potassium could occur only if potassium loss during an extrasystole, following close on a normal beat, is greater than during a regularly spaced contraction at the same average frequency. No information on this aspect of the Bowditch staircase is currently available, and so the choice between an unknown or a potassium mechanism cannot be made at this time.

Hofmann believes that postextrasystolic potentiation is not associated with potassium shifts, in part because he could find no change in resting membrane potential during the potentiation period, and he believes that a net efflux of potassium from the cell should be associated with a temporary rise in the potassium concentration immediately surrounding the fiber large enough to cause a drop in the membrane potential. This assumption is certainly not supported by the finding of an unchanged membrane potential during the administration of glycosides, where it is well known that a considerable potassium loss occurs.

VII. QUINIDINE

General

Quinidine has dramatic effects on both the electrical and contractile properties of heart muscle. The electrical effect, as expressed by Love (195) in 1926, is a lengthening of the effective refractory period of heart muscle, that is to say, quinidine reduces the maximum frequency at which atrial muscle can respond to stimulation. The other well-known action of quinidine is a reduction of the twitch tension of isolated heart muscle preparations (150, 185, 216, 246). The concentration of quinidine used in the studies on contractility has generally been higher than the plasma concentration achieved in the therapeutic use of the drug, but in some cases (e.g., ref. 150) the concentration is about the same as that found in certain instances of clinical toxicity due to quinidine (9). The plasma concentration of quinidine at which 75 per cent of a series of patients with auricular fibrillation reverted to a normal rhythm ranged from 4 to 9 mg per liter (282). Tissue concentrations may be as much as 10-fold higher than plasma levels (312).

Electrical Changes

Intracellular microelectrode techniques have yielded information which provides a basis for the action of quinidine on refractory period and conduction. Weidmann, working with Purkinje fibers, showed that in the presence of 10 μg per ml quinidine sulfate (a high dose, which was just short of causing conduction block) the rate of rise of the action potential and the height of the spike were both diminished. A "normal" response in the presence of quinidine could be obtained if the membrane was hyperpolarized to a resting potential of 120 mv before stimulation (314). In contrast to calcium, which shifts the maximum rate of rise versus resting potential plot to the left (see fig. 10), quinidine (as well as cocaine and procaine amide in the case of the Purkinje fiber) shifts the curve in the other direction. Johnson (156) also found that the rate of rise of the action potential was diminished in the presence of quinidine (3–4 μg per ml), the effect

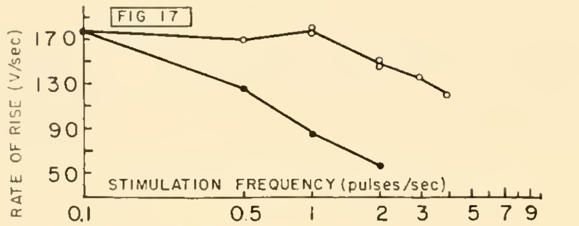

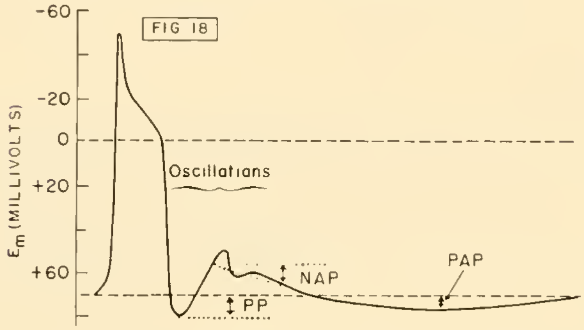

FIG. 17. Effect of quinidine on the relation between stimulation frequency and rate of rise of the action potential. Open circles: control. Closed circles: in 10 μg/ml quinidine sulfate. [From Johnson & McKinnon (157).]

FIG. 18. Diagram of nerve action potential. *PP:* positive potential. *NAP:* negative afterpotential. *PAP:* positive afterpotential. [From Shanes (271).]

on the height of the spike being variable. His experiments were performed on guinea pig ventricular muscle. Similar results were obtained by Vaughan Williams (302, 303), using guinea pig atria and a quinidine concentration of 9 μg per ml. He observed not only a decreased rate of rise of the AP and a diminished spike height, but also noted that although the beginning of repolarization was normal the terminal phase was prolonged. Johnson & McKinnon (157) in a careful study on guinea pig right ventricle, in which results were based on a well-fixed microelectrode remaining in position throughout the course of an experiment, found that the maximum rate of rise of the action potential decreased with increasing frequency of stimulation above a critical level. This relationship is shown in figure 17. It can also be seen in this figure that in the presence of 10 μg per ml of quinidine sulfate the decrease in the maximum rate of rise in the action potential began to occur at lower frequencies.

Vaughan Williams (302) has pointed out that the physiological studies discussed above provide some insight into the mechanism of action of quinidine. As stated earlier, a tissue will not respond to stimulation with a propagated depolarization unless the rate of change of the membrane potential induced by the stimulus is above a certain minimum. This rate depends on many factors, including the magnitude of the resting potential. The higher the resting potential, the higher the rate of rise of the action potential (see fig. 10). Below a critical resting potential no propagated action potential can be produced. Consider, then, a muscle which has contracted and is recovering. The membrane has been depolarized and must now repolarize to a critical value before the muscle can respond to another stimulus with a sufficiently fast rate of rise of the action potential for a propagated depolarization. But since quinidine slows the rate of rise, the quinidine-treated muscle must repolarize further than the normal before the muscle can respond, and this of course means more time elapses before the muscle is ready for another stimulus. In addition, the tail of the repolarization phase in quinidine is somewhat prolonged. Thus not only must the repolarizing membrane reach a higher membrane potential before a propagated response can occur in quinidine, but the time taken for it to reach this level is prolonged compared to the normal. These two factors, then, combine to produce the prolongation of the effective refractory period which occurs in the presence of quinidine. The absolute refractory period, on the other hand, that is the time interval from the peak of the action potential to the point when a local nonpropagated response can occur, is not prolonged in quinidine, since the early phase of repolarization does not appear to be affected by the drug in the concentrations used in the above studies.

Effect of Quinidine on Ionic Concentration and Fluxes in Muscle

IONIC CONCENTRATIONS. Gertler *et al.* (91), in experiments on rabbits, found that after 0.12 g of quinidine gluconate twice daily for 5 days the intracellular cardiac potassium concentration had increased from 108 to 124 meq per liter cell water (calculated on the basis of chloride space measurements), and the intracellular sodium concentration had decreased from 13.6 to 6.8. Both changes were statistically significant. Holland found that the net potassium loss from isolated rabbit atria stimulated at 200 per min for 5 min in low potassium Ringer's solution was 3.81 mM per kg wet tissue for seven control atria, and 3.27 for five atria in 5×10^{-5} M quinidine (150).

IONIC FLUXES. Holland & Klein (152) showed that the potassium efflux from rabbit atria after 20 min in quinidine (concentration not stated) was decreased by 40 to 50 per cent, and that the flux returned to normal

within 20 to 40 min after quinidine was removed from the bathing medium. It would thus appear that quinidine interferes with the passive loss of potassium from the cell. The data on potassium influx are conflicting. Holland and Klein in their study observed an increased potassium influx. On the other hand, Kärki (165) found that cold stored red blood cells, when brought to a higher temperature, have a lower than normal potassium uptake in the presence of quinidine.

EFFECTS OF EXTERNAL POTASSIUM CONCENTRATION ON QUINIDINE ACTION. The effect of quindine can be counteracted by decreasing the potassium concentration in the extracellular fluid. This was shown by Armitage (8) in experiments on perfused rabbit heart and isolated rabbit atria. He found that the effects of 30 μg per ml of quinidine on both the rate and amplitude of the heart beat could be reversed by lowering the potassium concentration to $^1/_4$ normal. Similar results were reported by Holland (150), who showed that the effect of quinidine on both twitch tension and effective refractory period of isolated rabbit atria could be counteracted by lowering the potassium.

DISCUSSION. The increased cardiac potassium shown in quinidine-treated rabbits (91), the abnormally low loss of potassium from isolated cardiac tissue on rapid stimulation (150), and the diminished potassium efflux in the presence of quinidine all support the idea that quinidine has an effect on the permeability of the cell membrane to potassium. The diminution in the rate of rise of the action potential in quinidine is quite likely associated with a decrease in the influx of sodium during depolarization. Since changes in resting membrane potential have not been reported, the results might suggest that quinidine has a peculiar effect on the phasic changes in cell membrane permeability that occur during activity. Thus, we have already seen that the slowing of the rate of rise of the spike could be interpreted in terms of a diminished cell membrane permeability to sodium, which normally increases greatly during this period. Similarly, the prolonged phase 3 (terminal repolarization phase) of the action potential in the presence of quinidine and the diminution of potassium efflux observed in stimulated muscle might be explained in the terms that the normal increase in permeability of the membrane to potassium, that is thought to occur in phase 3, is inhibited in the presence of quinidine.

There are not enough data at the present time to explain the depressing action of quinidine on contractility. Gertler's evidence that the intracellular concentration of potassium in quinidine-treated rabbit hearts is increased provides a possible mechanism for the decreased contractility, since it has been previously noted that increased intracellular monovalent cation content is associated in the frog heart with a decreased contractility (see sections II and V). To date, no correlation between the magnitude of the quinidine effect and the change in intracellular potassium concentration has been made. The reversal of the quinidine action on contractility by immersing the tissue in a low potassium medium can be explained by assuming that the external potassium concentration is so low that the "potassium pump" is no longer saturated, resulting in a diminution of potassium influx and a consequent lowering of intracellular potassium from the high levels characteristic of the exposure to quinidine. The arguments for the idea that stimulation is associated with the movement of calcium from some superficial muscular site into the cell interior have already been presented (see section IV). It is possible that quinidine, with its apparent action on membrane permeability, might cause changes which would limit the diffusibility of the calcium ion and depress contractility by this mechanism.

Effect of Quinidine on Metabolism

Partly because of the effect of quinine on the malaria parasite, the interest in the metabolic action of quinidine has been great. A sampling of the literature may be found in references 135, 185, 300, and 310. These particular papers were chosen because they are descriptions of experiments with heart tissue, and the concentrations of drugs used were not more than 10 to 20 times the therapeutic concentration of the drug in plasma. Webb *et al.* (310) for example, in studies on rat ventricle and auricle, found that in the presence of quinidine endogenous oxygen uptake was diminished, anaerobic glycolysis was diminished, but there was no inhibition of the increased oxygen uptake that occurred on the addition of various carbohydrate substrates. On the other hand, Uyeki (300) found that not only was endogenous oxygen uptake of rat heart slices diminished but also the oxidation of various carbohydrate substrates was inhibited. Uyeki also found that calcium-activated ATPase activity was diminished, and in homogenate studies he presented evidence that phosphorylation was also inhibited by quinidine at 5×10^{-4}M. The homogenate

concentration of quinidine may bear some reasonable relationship to the concentration of quinidine achieved in tissue, if one accepts the data of Wegria & Boyle (312) that tissue concentrations may be 10 times that of the plasma.

On the other hand, Lee (185) found that with quinidine in a concentration of 3×10^{-4}M, which was sufficient to depress the contractility of cat papillary muscle, there was no significant effect on the oxygen consumption of cat heart slices. Hess & Haugaard (135) in studies on rat heart slices and homogenates found that oxygen uptake and glucose utilization were depressed in the presence of 5×10^{-4}M quinidine. They found, however, that procaine which has somewhat similar actions to quinidine, at least on the rate of rise of the action potential (314), had little metabolic effect.

It would appear then that although quinidine can be shown to affect a variety of enzyme systems, there remains a question as to whether the concentrations required are reached in the therapeutic situation, and whether the characteristic pharmacological action of the drug is mediated by any of the enzymatic effects observed. If, however, the effect of quinidine is primarily on the phasic alterations in cell membrane permeability to sodium and potassium which occur during stimulation, the physicochemical mechanism for this action still remains to be worked out.

VIII. VERATRUM ALKALOIDS

Summary of General Effects on Heart

The veratrum alkaloids act on a wide variety of nervous and muscular tissues. The result of these actions in the whole animal is a complex series of respiratory and cardiovascular responses (179). The present section will be confined to the direct action of the veratrum alkaloids on cardiac tissue. Reference will be made to recent work on other types of tissue, insofar as the results may throw light on the mechanism of action of the veratrum alkaloids.

The major effects of the veratrum alkaloids on the heart are first a positive inotropic action and secondly a striking alteration in certain of the electrical properties. Whereas the positive inotropic effect is frequently masked in the whole animal because of reflex changes in heart rate and blood pressure, it is readily observed in isolated heart tissue. The positive inotropic effect of the veratrum alkaloids was demonstrated early for amphibian heart, and was even more readily observed in hearts made hypodynamic either by exposure to low calcium solutions or by prolonged washing (179, p. 404). The positive inotropic action of veratrine (a mixture of veratrum alkaloids) was also demonstrated in mammalian heart-lung preparations, more readily if the heart was in failure (179).

The effects of veratrine on the electrical properties of the isolated heart include bradycardia, or occasionally tachycardia at low dosages, and at larger doses extrasystoles which may finally end in fibrillation. Veratrine diminishes conduction velocity and may cause partial A-V block (179). It has been said that veratrine may initiate spontaneous beating in inactive strips of cardiac muscle (179). Such a veratrine response can be found in a publication of a tracing of isotonic contractions registered by a strip of left auricle from a guinea pig (253). In fact, this tissue was not perfectly quiescent, and in the presence of 14 μg per ml of veratrine no response was seen until a spontaneous contraction occurred. Following this single contraction, a series of beats occurred at high frequency until finally the strip of tissue ended in contracture.

Electrophysiological Details

EFFECT ON EXCITABILITY AND RELATED PHENOMENA. For conflicting early work on excitability and refractory period of amphibian cardiac muscle, the reader is referred to Krayer & Acheson's review (179, p. 407). Information for mammalian tissue comes from the work of Matsuda *et al.* (34, 209) on isolated rat auricle and ventricle, and on dog ventricle. These authors found that both the absolute refractory period and the relative refractory period were increased in the presence of veratrine. Like other authors (93) they found that conduction in the A-V bundle was markedly slowed. These workers point out (34) that there is a period in the cardiac cycle corresponding approximately to the relative refractory period in which cardiac tissue may respond to electrical stimulation of given strength and duration with multiple beats or fibrillation. This so-called vulnerability appears to be increased in the presence of veratrine.

MEMBRANE POTENTIAL CHANGES. In contrast to nerve and skeletal muscle the effects of veratrine on the action potential of cardiac muscle have not been studied extensively. Matsuda *et al.* (209) have shown that mammalian cardiac muscle in the presence of veratrine may remain partially depolarized for a long

time following a normal spike, and during this period repetitive brief spikes may occur.

This type of phenomenon has been studied extensively in nerve and skeletal muscle (see for example references 3, 74, 181, 269). The reader is referred to figure 18 for terminology of the various components of the action potential. The veratrine response in these tissues is characterized frequently but not always by the production of a large and prolonged negative afterpotential. The question is whether the repetitive firing which occurs in the presence of veratrine is correlated with or caused by the size of the negative afterpotential. In some instances a good correlation has been obtained between the size of the negative afterpotential and the occurrence of repetition (181). In other cases no necessary correlation has been noted (74). In some of the work of Shanes (269, 271) on the squid axon it would appear that in the presence of veratrine the normal oscillations of membrane potential which occur following repolarization do not become damped but, on the other hand, may progressively increase in amplitude to the point where they become adequate as stimuli and initiate spikes. It is clear that the factors involved in the production of repetitive activity are not yet fully understood, and further discussion is beyond the scope of this review. Suffice it to say that in certain tissues (such as some of the nerve preparations studied) the oscillatory phenomena in the presence of veratrine are prominent without a tremendously increased negative afterpotential, whereas in the case of the mammalian heart the striking feature is the delay in repolarization.

Finally the work of Shanes *et al.* (274) on impedance changes following the spike in squid nerve in the presence of veratrine should be mentioned, since the results may provide further information on the mode of action of the drug. These investigators found that the negative afterpotential following the spike in the squid axon is accompanied by an increase in measured conductance. The cause of the conductance increase could perhaps best be explained by an increase in the permeability of the membrane to sodium ions, although there was some objection to this because the quantitative relationships between the observed change in conductance and the magnitude of the negative afterpotential (3 mv) was considerably different from the predicted value.

Effects on Contractility and Ion Movements

CONTRACTILITY. It was established early that the prolongation of the contractile response of striated muscle in the presence of veratrine was due to a tetanus caused by the repetitive firing which occurred. Such an explanation for the observed prolongation of systole in cardiac tissue (179, p. 412) was not very palatable, since cardiac muscle is said not to be capable of tetanization. Whereas this may be true in the general case, one may ask what happens to the mechanical response of cardiac muscle if repolarization is delayed for, say, several seconds. Rosenblueth *et al.* (251) gave a categorical answer to this question as a result of studies on turtle ventricle in veratrine. They found no necessary correlation between mechanical and electrical events in this tissue. They concluded that the potential changes and the contraction were largely independent and felt that whereas the spike triggered the contraction process, the time course of contraction was probably governed by factors other than the potential changes. On the other hand, Kavaler (170) has found in the case of mammalian ventricle that prolongation of repolarization by a voltage clamp is associated with prolongation of the contractile response. It is interesting that whereas this is the case for ventricular tissue, prolongation of depolarization in the case of the atrium is not associated with a prolonged mechanical systole (171). We may conclude then that at least in certain cases prolonged depolarization may be associated with prolonged contractile response. Another factor which quite likely contributes to prolongation of mechanical systole has to do with the loss of potassium from veratrinized cardiac muscle, which is described in the next section. Suffice it to say at this point that potassium loss from cardiac muscle whether induced by digitalis, veratrine, or a potassium-free bathing medium is associated with prolonged contraction because of slowed relaxation. The positive inotropic effect caused by veratrine is presumably also due to the cellular changes associated with the potassium loss, as has been suggested in the case of digitalis (see section IX).

POTASSIUM MOVEMENTS. It was first shown by Szent-Györgyi *et al.* (292) that stimulation of skeletal muscle in the presence of veratrine was associated with a large loss of potassium from the tissue. Similar results were obtained by Shanes (270) for nerve, who found that the net potassium lost from crab nerve during stimulation in the presence of low concentrations of veratrine (insufficient to induce a repetitive response to stimulation) was almost twice the potassium lost in the control preparation. Large potassium losses were also observed in the case of cardiac tissue by Hajdu (111) and by Vick & Kahn (304) who concluded on

the basis of indirect evidence that the potassium loss was secondary to an increased efflux rather than to a diminished influx. The action of veratrum in increasing efflux appears to occur only during activity and is probably associated with the prolonged depolarization and/or repetitive stimulation.

In summary, the primary action of veratrine on isolated cardiac tissue is on events following a normal spike. Repolarization is greatly prolonged, and during this phase repetitive small spikes may also occur. These events are associated with an excessive loss of cellular potassium which leads to an increased contractile force and finally to slowed relaxation and even contracture. The prolonged repolarization itself may also contribute to the prolongation of mechanical systole, although this phenomenon alone is not associated with such an effect in all types of cardiac tissue. Veratrum apparently has no effect on potassium movements or contractility of unstimulated cardiac muscle.

IX. DIGITALIS

Metabolism

When a muscle is stimulated to contract and is then allowed to return to its resting state, the event may be viewed as two cyclic processes, one being the shortening and lengthening of the contractile protein, the other being the hydrolysis and subsequent resynthesis of a high energy phosphate compound (such as ATP). The second cycle provides the energy for the cyclic change in the protein, and it does not matter for the argument how or at what point in the cycle the phosphate bond energy is transferred to the contractile protein. This energy-providing cycle has been called "energy liberation" by Wollenberger (333). The maximum work obtainable from the operation of the contractile protein cycle depends on many factors which can be summed up as the ability of the protein to utilize the available energy. In other words, following the usage of Wollenberger, all the steps in the energy cycle are part of the process called "energy liberation"; whereas what the contractile protein does with the energy made available to it is called "energy utilization."

The effect of cardiac glycosides on the failing heart may be discussed by considering whether cardiac failure in terms of the above frame of reference is due to impairment of energy utilization or energy liberation. In the case of the latter, the defect could be in either ATP synthesis or ATP hydrolysis. If ATP synthesis were impaired, the concentration of ATP in failing heart muscle should be below normal and the therapeutic effect of the glycosides should be associated with a rise in the ATP concentration. Although information on this point is not available for human low output failure, in a variety of experimental conditions characterized by an impaired cardiac performance which improves with digitalis [failing heart-lung preparation (332, 333), hypodynamic guinea pig atrium (81)], ATP and CP (creatine phosphate) concentrations are not depressed and do not rise on digitalization. (For exceptions see 20, 102.)

If heart failure were caused by a subnormal rate of ATP hydrolysis, the therapeutic effect of the glycosides should be associated with a parallel increase in ATP splitting (and also oxygen consumption, assuming no oxygen debt) and obtainable muscle work. Therefore the calculated efficiency (work output/energy input) of the treated muscle would not be different from that of the failing muscle. This is not the case, Peters & Visscher (232) having found that in the failing heart-lung preparation operating at constant diastolic volume the administration of cardiac glycosides caused increases of 63 to 153 per cent in the mechanical efficiency. Qualitatively similar results for human heart failure have been published by Bing and co-workers (17). The defect in human low output failure and in experimental conditions characterized by a favorable response to digitalis appears then to be an impairment not in energy liberation but in the ability of the contractile system to convert energy into useful work. The glycosides increase the capacity of the contractile protein for "energy utilization" which is reflected in an increased mechanical efficiency; and any increase in oxygen consumption associated with administration of the glycosides is secondary to an increase in mechanical work rather than to a primary action of the glycosides on the "energy liberation" cycle.

A large number of studies have been made to determine whether cardiac glycosides have a demonstrable effect on the metabolism of tissue slices or homogenates. There is general agreement that the glycosides do not affect oxygen consumption of mitochondria (183) or homogenates (88, 255, 258, 331, 332). The data on tissue slices are conflicting and throw little light on the problem under discussion, especially considering the normally depressed state of muscle slices incubated in bicarbonate-free media (59a, 247). Studies on the effect of glycosides on radioactive phosphate turnover of muscle have been compromised by the fact that extracellular inorganic

phosphate does not exchange readily with the bulk of the intracellular phosphate (22, 124). [For further details on these points see reference 113.]

Action of Glycosides on Muscle Proteins and Models

In an attempt to define the locus of action of the cardiac glycosides, many investigators have examined the effect of glycosides on a variety of muscle fractions or models of the contractile mechanism. These studies will be enumerated briefly.

1) G-F transformation of actin. It was found in 1949 (153) and subsequently confirmed (58, 281, 334) that the rate of polymerization of solutions of globular actin to form the long chain called F actin was increased in the presence of strophanthin or digitoxin. However, Wollenberger (334) made an important contribution to the problem by comparing the effects of pairs of glycosides which were structurally similar but one of which had no pharmacological activity in whole animals. Both members of two such pairs increased the rate of polymerization to the same extent, showing that there was no correlation between in vivo pharmacological activity and the effect on the isolated protein. In the absence of such a correlation it is difficult to conclude that the observed effect is related to the pharmacological action of the drug. Many of the studies enumerated below cannot be judged because of the absence of control observations with a pharmacologically inactive glycoside.

2) Actomyosin viscosity. Addition of glycosides causes a very small decrease in the viscosity of actomyosin solutions, but both pharmacologically active and inactive compounds have the same effect (306, 309). The drop in viscosity induced by ATP is not affected by cardiac glycosides (68, 309).

3) Muscle enzymes. ATPase activity is either increased or decreased by ouabain, depending on the purity of the preparation (68, 133). Digoxin appears to have no effect on myosin ATPase activity, provided the preparation is free of myokinase, but does enhance the conversion of ADP to ATP which occurs in the presence of myokinase (237). Strophanthin has little or no effect on the activity of adenosine deaminase prepared from mouse myocardium (217), but ouabain in very large doses inhibits deaminase activity of guinea pig heart preparations (7).

4) Potassium binding. The only investigator who has made a correlation between in vivo pharmacological activity and any effect on isolated contractile proteins has been Waser (308), who has shown that moderate concentrations of cardiac glycosides cause increased potassium binding by isolated actomyosin. He also showed that these drugs decreased the thixotropy (tendency to form a gel on standing) of actomyosin (306, 307). In none of these studies did pharmacologically inactive glycosides have a corresponding action.

5) Shortening of actomyosin threads and bands. Mallov & Robb (204) first showed that the ATP-induced shortening of threads of skeletal muscle actomyosin was increased by addition of a cardiac glycoside. This was later confirmed for both skeletal (25) and heart (244) muscle actomyosin. Kako & Bing (162a) showed that the contractility (% shortening vs. load) of actomyosin bands prepared from hearts of patients with congestive failure was significantly lower than that of normal hearts. In the presence of digoxin plus 10^{-3}M Ca the contractility of the failure protein increased to the normal range.

6) Glycerol-extracted muscle. The divergent results obtained with this preparation (69, 178, 288) probably reflect the differences caused by small variations in the glycerination procedure (see also section II).

In summary, glycosides have effects on various properties of muscle cell proteins, but to date Waser is the only investigator who claims a correlation between a protein effect and in vivo pharmacological activity.

Site of Glycoside Action

It was stated at the beginning of this section that glycosides are thought to act by altering the capacity of the contractile protein to utilize the chemical energy made available to it. This might occur by some direct action of the drug on the contractile protein, as suggested by some of the results noted in the previous section, or it might be brought about indirectly by a change in the cellular chemical environment induced by the drug. There is a large body of literature indicating that the glycosides can induce cellular chemical changes by interfering with normal membrane transport of inorganic ions (see next section). It becomes pertinent to ask, then, whether the glycosides can enter the cell interior where interaction with the contractile protein might occur, or whether they do not penetrate beyond the cell membrane. It is clear from a number of studies that glycosides bind to certain proteins, including actomyosin (70, 298, 305), and their rapid disappearance from the blood suggests that they are accumulated preferentially by a tissue phase (284). Binding to serum albumin fractions has been reported also (107, 254), but this seems to be due to something associated with salt fractionation of the albumin (either a small change in the albumin or

coprecipitation of another molecule), since no binding to albumin can be demonstrated using starch block electrophoresis for separation (284).

There is no certainty, however, that the glycosides enter the cell. The only studies available involve fractionation of cellular components by homogenization and differential centrifugation, with estimation of the amount of glycoside associated with each fraction (126, 257, 285). No conclusions can be drawn, since the results are conflicting. (See ref. 113.)

The solution to this problem would appear to require another approach, such as an attempt to determine the cellular locus of digitoxin by radioautography.

Membrane Transport

In contrast to the variable effects of cardiac glycosides on separated cellular protein components, there is a consistent body of evidence showing that glycosides have a profound effect on the plasma membrane of intact cells.

GLYCOSIDE-INDUCED NET POTASSIUM LOSS FROM MUSCLE. It was shown by Wood & Moe (336) that administration of lanatoside increased the cardiac potassium A-V difference in dog heart-lung preparations. They showed that potassium was lost slowly from both the heart and lungs during the control period, and that the rate of potassium loss was increased significantly by lanatoside, not only in toxic but also in therapeutic doses. Furthermore, there was a positive correlation between the increase in mechanical efficiency caused by the glycoside and the rate of increase of potassium concentration in the venous blood. A net tissue potassium loss induced by glycosides has since been demonstrated for isolated frog (110, 164) and guinea pig (289, 304) hearts by measuring the resultant increase in potassium concentration in the perfusion solution. Comparable results in intact animals and human subjects have been obtained, now that the technique of coronary sinus catheterization makes it possible to measure coronary arteriovenous potassium concentration differences without exposing the heart. Studies utilizing this method have not included measurement of coronary blood flow, estimates of cardiac net potassium changes being based on the coronary arteriovenous concentration difference alone. Harris and co-workers (115) showed that the administration of K-strophanthoside to intact dogs was followed by a rise in both arterial and coronary sinus blood potassium concentration; in some but not all cases the potassium increase in coronary sinus blood was said to be significantly greater than in the arterial blood. Since the chances of detecting a net cardiac potassium loss by this method would be best if the drug induced an intense loss over a short period of time, Regan *et al.* (238) administered to dogs the fast-acting acetylstrophanthidin which caused a peak effect on ion movements at about 6 min. They consistently found a potassium loss from the heart under these conditions, and Hellems *et al.* (132) from the same laboratory reported similar findings in seven patients with cardiac failure. With slower acting glycosides such consistent differences have not been found (100).

MECHANISM OF THE POTASSIUM LOSS. The glycoside-induced potassium loss could be caused by an inhibition of the active process which normally transports potassium into the cell, or it could be due to an increased potassium leakage out of the cell. Based on a comparison of the action of digitalis and veratrum on the isolated frog heart, Hajdu (110, 111) suggested that the glycosides decreased the rate of potassium reentry during the recovery phase of the contraction cycle. Similar conclusions were reached by Vick & Kahn (304) in studies of the potassium release from guinea pig hearts during alternating periods of rapid and slow beating in the presence of ouabain or veratridine. Support for this view has recently been obtained by means of potassium tracer measurements, a decrease in the influx with no change in efflux being reported for both frog ventricle (266) and guinea pig auricle (235) when glycosides are administered. These studies, in which influx is found to be slowed while efflux remains unchanged, were of course made in the unsteady state when a net loss of potassium from the cell must have been occurring as a result of the action of the glycosides. Eventually a new steady state must be reached in which efflux and influx are equal and intracellular potassium concentration is stabilized at a new level. Conn (51a) has measured potassium flux across the cell membrane in the heart of an intact animal after such a presumed new steady state has been reached during a period of continuing glycoside action in which digitoxin was administered to dogs in a dosage of 0.2 to 0.4 mg daily for 10 to 14 days. K^{42} transfer rates between cell and interstitial fluid in these digitalized dogs were significantly below normal, being 4.25 ± 0.25 (SEM) meq K per kg per min for the controls and 3.74 ± 0.15 for the experimental group. The combined results of the isotope studies, then, show that potassium influx is diminished as a result of digitalis administration, and that after

new steady state conditions are reached the transmembrane rate of potassium movement continues to be depressed.

It is thus seen that cardiac glycosides depress the active cell membrane mechanism responsible for the uptake of potassium. This aspect of glycoside action is not limited to muscle. Schatzman (264) has shown that cardiac glycosides inhibit the potassium uptake and sodium extrusion of previously cold-stored red blood cells. Inhibition of red cell potassium influx by glycosides has been confirmed by others (95, 96, 159, 162, 283, 290). A correlation between potency of this effect and in vivo pharmacological activity has been shown by Kahn (161). Sodium-potassium exchange in the renal tubule also appears to be affected by glycosides (226). Also interesting is the fact that cardiac glycosides inhibit active transport of certain anions. Chloride transport by the isolated bullfrog gastric mucosa is diminished by strophanthidin (55), and the uptake of iodide by slices of mammalian thyroid tissue is profoundly inhibited by ouabain in concentrations of about 10^{-6}M (330). The thyroid effect seems to correspond to the in vivo pharmacological activity of these compounds on the heart, since dihydrodigoxin, for example, has not only low cardiotonic activity but also low potency with respect to inhibition of iodide uptake.

The broad tissue and ionic spectrum of glycoside action suggest the possibility that the cellular mechanism for transporting different ions consists of a part which is common to many cells and an additional part which confers ionic specificity to the system. The cardiac glycosides, then, would appear to act on the nonspecific part of the system.

GLYCOSIDE-POTASSIUM ANTAGONISM. It is generally accepted that potassium ions inhibit the action of digitalis, and it was suggested by Loewi (193) in 1917 that intravenous administration of potassium salts might abolish glycoside toxicity. This approach was used in clinical medicine by later investigators (72, 259). Sampson *et al.* (259), for example, showed that the ectopic beats caused by toxic doses of digitalis in humans were abolished by the oral administration of enough potassium acetate to cause a 10 to 30 per cent rise in serum potassium concentration usually within 1 hour. Conversely, with depletion of body potassium signs of digitalis poisoning occurred at a lower drug dosage than that characteristic of the potassium-repleted state (196). Increasing extracellular potassium concentration is associated with an increase in the minimum lethal dose of glycosides in guinea pigs (130), with an inhibition of the effect of glycosides on the rhythm of the embryonic duck heart (80), with a diminution in toxicity for isolated rabbit heart (11), and with a decreased glycoside effectiveness in the heart-lung preparation (40). In many of these cases the potassium effect is on cardiac rhythm rather than contractility. If the rhythm is controlled, variations in extracellular potassium concentration over the range observed in clinical usage do not cause alterations in the effect of the glycosides on contractility (84a, 187). On the other hand, large changes in external potassium concentration do inhibit the action of glycosides (48) on contractility, and have also been shown to reverse the characteristic action of the glycosides on ion fluxes in red blood cells (96), kidney (226), and thyroid (330).

The nature of this potassium inhibition of glycoside action is not understood. It appears that potassium uptake by glycoside-treated tissues is enhanced by increasing extracellular potassium. This does not occur in the absence of glycoside, suggesting that the active transport system is normally "saturated" at normal extracellular potassium concentrations and is regulated by other factors probably related to intracellular ionic composition. It is believed by some that glycoside molecules and potassium ions compete for a critical site on the membrane transport system and that high concentrations of potassium can displace the glycoside (96). There is no other working hypothesis at the present time, but the possibility should be noted that the glycoside-inhibited transport system might be affected independently by potassium.

CHANGES IN MUSCLE IONIC COMPOSITION CAUSED BY GLYCOSIDES AND THEIR RELATIONSHIP TO THE POSITIVE INOTROPIC ACTION OF THE DRUG. The effects of digitalis on ionic transmembrane fluxes have been demonstrated only recently, but many years before this was known Calhoun & Harrison (44) showed that the potassium concentration of hearts from dogs given toxic doses of digitalis was diminished. They even considered that this alteration in ionic composition was the basis for the therapeutic action of the drug, and suggested that digitalis "may act in such a way as to readjust the ionic balance" of the failing heart.

During the ensuing years many workers measured tissue potassium concentrations in an attempt to determine whether therapeutic as well as toxic amounts of glycoside caused a loss of potassium from the heart (5, 27, 91, 108, 110, 151, 164, 225, 311, 337). The results were often conflicting, difficulties arising from the fact that a small loss of potassium was not easy to

detect by tissue analysis. However, measurements of potassium changes in the extracellular phase (reviewed in the first part of this section) leave little doubt that therapeutic amounts of digitalis do cause cellular potassium loss.

Hajdu's analysis of changes in sodium, potassium, and water of digitalized frog hearts, which was based on both tissue and bathing fluid measurements, showed that the tissue lost 13.7 ± 0.8 meq K per liter of fiber water and gained 2.0 meq of Na. The cells lost water along with potassium, such that the sum of the intracellular concentrations of sodium and potassium (meq liter fiber water) was not significantly altered by the glycosides; but the amount of sodium plus potassium expressed as meq per kg dry weight of the cells had clearly decreased. Similar results for digitalized dog heart have recently been reported by Kyser *et al.* (182), who found a drop in cardiac muscle potassium, but an actual rise in concentration because of concomitant water loss. The increase in contractility which occurs whenever the intracellular monovalent cation content is diminished by any of several means (see Section II) led Hajdu (110) to postulate that this diminution accounts for the glycoside positive inotropic effect.

There is another kind of evidence which provides indirect support for the idea that the diminution in intracellular potassium is causally related to the positive inotropic action. Many years ago, Weizsäcker (319) showed in a group of carefully designed experiments that the time of onset of contracture, after strophanthin was added to the medium perfusing a frog heart, depended not on the duration of action of the drug but on the number of contractions which occurred in the presence of the drug. For example, at a frequency of 15 per min it required 30 min and 490 contractions for systolic arrest, whereas at a frequency of 35 per min toxicity was apparent in only 14 min after approximately the same number of contractions. Similar conclusions have been reached by later workers (261, 322). Since increasing the contraction rate increases efflux (see Section VI), it is clear that the onset of the glycoside positive inotropic action occurs earlier in a maneuver which hastens the net loss of cellular potassium.

GLYCOSIDES AND CALCIUM. Ever since Ringer's observation that increases in the bathing fluid concentration of calcium strengthen the contraction of the isolated frog heart, the generally similar action of calcium and cardiac glycosides on cardiac contractility has been of great interest to investigators. It seemed that calcium enhanced the action of the glycosides. For example, Werschinin (320) in 1910 found that systolic arrest of a perfused frog heart following the addition of strophanthin was more complete and appeared earlier when the calcium concentration of the perfusion fluid was twice normal. Many workers after this maintained that the activity of the glycosides as reflected by toxicity in intact animals was enhanced by high serum calcium concentrations (26, 67, 97, 98, 190, 278). Were calcium and digitalis synergistic in their action or were the above observations simply due to the additive effect of two agents each of which increased contractility by different mechanisms?

An early approach to this question was made by Konschegg (177), who found that frog heart contractility which had been abolished in a calcium-free medium was restored by strophanthin. He suggested that cardiac glycosides could act in the absence of calcium and could perhaps serve as a substitute for calcium. Loewi (193) pursued the same experimental approach, but used sodium oxalate in the medium in order to be more certain of the absence of calcium from the perfusion medium. Under these conditions the heart exhibited no twitch tension, and the addition of strophanthin caused contracture without restoring the twitch. He recognized that there was still a small amount of calcium ion in the bathing fluid, and believed that strophanthin acted by increasing the sensitivity of the heart to calcium.

Without entering into the controversy which centered around Loewi's contention, and recognizing that even in the absence of glycosides heart muscle contractility varies with changes in calcium, it may be helpful to consider two possibilities. One is that glycosides act by altering the intracellular concentration of calcium, thereby increasing contractility. The other is that glycosides increase contractility through a mechanism which does not involve a change in intracellular calcium. In this case it still might be possible for glycoside effect on this mechanism to be altered by variations in calcium. A choice between the two main possibilities can be made then according to whether or not intracellular calcium concentration is changed by cardiac glycosides. For a positive inotropic effect the expected intracellular change would be an increase in calcium. If it could be shown that the glycosides can act in the complete absence of external calcium, this should constitute evidence that the inotropic action is not due to an increase in intracellular calcium. In at least three papers published several years after Loewi's work it was claimed that the glyco-

sides could act in the absence of external calcium. This view was first stated by Mandelstamm (205), who stated that in a calcium-free medium the glycoside effect was still detectable, causing an increase in contractile force, a plateau of tension, a prolongation of the total duration of contraction, and even contracture. Of course the fact that Mandelstamm obtained muscle twitches showed that the bathing fluid was not completely free of calcium. More helpful were the investigations which showed a difference in speed of onset of calcium and digitalis actions on contractility (77, 224). Nyiri & DuBois (224) expressed their conclusions as follows: "The digitalis action, therefore, takes place in the regular way and at the regular speed in the presence or absence of calcium. In the absence of this ion, however, we do not see the effect because the heart muscle has lost its inotropic property. At any time that we re-establish the contractility of the muscle fiber in the course of the digitalis poisoning, the effect of the corresponding time appears." In other words, since it appears that the steady progression of glycoside action can occur in the absence of external calcium, the mechanism of action cannot be to cause directly a net gain of intracellular calcium. Even in these experiments there may have been traces of calcium in the perfusion medium due to contaminating amounts in other salts or in the glycoside preparations. When care is taken to exclude ionic calcium from the perfusion fluid and the glycoside preparation by addition of EDTA, toxic concentrations of glycosides have no detectable effect (113), but addition of calcium causes immediate contracture (unpublished observations). This indicates that the primary action of glycosides on the muscle cell, which normally is cumulative during the first 10 min of exposure, occurs in the virtual absence of external calcium ion, the positive inotropic action becoming apparent immediately on the addition of calcium. The same conclusion can be drawn from the work of Caviezel & Wilbrandt (48) who showed that if one allows for the inotropic action of calcium in the absence of digitalis, variations in the concentration of calcium have no effect on the activity of cardiac glycosides on heart muscle contractility. The effect of the glycosides in inhibiting transmembrane potassium transport in red blood cells (199) and skeletal muscle (329) is likewise unaffected by variations in calcium concentration. The evidence reviewed up to this point shows that the primary action of digitalis on heart muscle cannot possibly involve the calcium ion, but it does not rule out a primary action that causes some change within the fiber, as a result of which calcium accumulates. Such a change could develop in the absence of calcium, but one must postulate a capacity for the glycoside-treated cell to take up calcium extremely rapidly in view of the immediate effects observed on shifting from a calcium-free to a normal perfusion medium [unpublished observations and (224)].

It is probable that the glycosides have no direct effect on calcium fluxes in heart muscle. It has been reported that Ca^{45} influx is unchanged by nontoxic doses of glycosides (125, 296); the diminution of efflux observed in digitalized frog heart was at a contracture-causing dose (323). The changes observed with contracture-causing concentrations of glycosides (125, 296, 323) are probably secondary to other cellular alterations.

Membrane Potential

The effects of digitalis on the electrical events of the cardiac cycle appear to be as follows. Initially an increase in the magnitude of the spike is sometimes observed (339). This change is transient, and is followed by a decrease in spike amplitude. Thus, normally, the spike describes a change in potential from −90 mv to a positive value of about 30 mv, whereas in the presence of toxic concentrations of glycosides the spike decreases to the point where the "positive overshoot" disappears and even the zero potential level is no longer reached (56, 339). Dudel & Trautwein (66) have found that the glycosides cause a diminution in the rate of rise of the action potential spike. The most marked effects of the glycosides, however, are on the repolarization phase. Following a transient increase in the total duration of the action potential there is marked shortening, due mostly to a decrease in the time taken for repolarization (66, 339).

The meaning of these findings in terms of cellular ion movements is not known at this time, but it is perhaps worth considering them in the light of a hypothesis outlined by Cranefield & Hoffman (59). As a result of the depolarization of the cell membrane, the outflow of potassium would be expected to increase since the ion is no longer held back by a large intracellular electronegativity. However, the membrane does not allow completely free diffusion of K^+, and so efflux is still comparatively slow during the plateau (phase 2). The outflow is sufficient, however, to cause the accumulation of some K^+ at the extracellular surface of the membrane and this by some mechanism increases P_K which starts the rapid K^+ outflow of phase

3 and the return of the membrane potential to normal. Thus, any factor which tends to raise [K^+] at the membrane should increase P_K and diminish the time needed for repolarization; whereas, a low external [K^+] should lengthen this time. Consistent with the theory are the findings that *a*) in a K-free medium repolarization is greatly prolonged (184); *b*) close intra-arterial injection of K^+ shortens the action potential (315); and finally *c*), interventions which cause accumulation of K^+ at the outer surface of the membrane, either by inhibiting the rate of re-entry (digitalis) or diminishing the time available for re-entry between contractions (high frequency), also are associated with a shortened action potential.

Dudel & Trautwein (66) have reported that cardiac glycosides cause an increase in the membrane resistance of the Purkinje fibers of the cat during both rest and activity. This finding suggests that in addition to an effect on active transport the glycosides alter the permeability of the cell membrane. The data of Glynn (96) on red cells are consistent with such a conclusion.

REFERENCES

1. Abbott, B. C. and W. F. H. M. Mommaerts. A study of inotropic mechanisms in the papillary muscle preparation. *J. Gen. Physiol.* 42: 533, 1959.
2. Abbott, B. C. and D. R. Wilkie. The relation between velocity of shortening and the tension-length curve of skeletal muscle. *J. Physiol.* 120: 214, 1953.
3. Acheson, G. H. and A. Rosenblueth. Some effects of veratrine upon circulated mammalian nerves. *Am. J. Physiol.* 133: 736, 1941.
4. Adrian, R. H. The effect of internal and external potassium concentration on the membrane potential of frog muscle. *J. Physiol.* 133: 631, 1956.
5. Aikawa, J. K. and E. L. Rhoades. Effects of digitoxin on exchangeable and tissue potassium contents. *Proc. Soc. Exper. Biol. & Med.* 90: 332, 1955.
6. Alella, A., F. L. Williams, C. Bolene-Williams, and L. N. Katz. Role of oxygen and exogenous glucose and lactic acid in the performance of the heart. *Am. J. Physiol.* 185: 487, 1956.
7. Angkapindu, A., A. W. Stafford, and R. H. Thorp. The influence of cardiac glycosides on the deamination of adenosine and the adenine nucleotides. *Arch. internat. pharmacodyn.* 119: 194, 1959.
8. Armitage, A. K. The influence of potassium concentration on the action of quinidine and of some antimalarial substances on cardiac muscle. *Brit. J. Pharmacol.* 12: 74, 1957.
9. Bailey, D. J., Jr. Cardiotoxic effects of quinidine and their treatment. *A.M.A. Arch. Int. Med.* 105: 13, 1960.
10. Bailey, K. Myosin and adenosinetriphosphatase. *Biochem. J.* 36: 121, 1942.
11. Baker, J. B. E. The influence of calcium and potassium ions on the toxicity of ouabain. *Brit. J. Pharmacol.* 2: 259, 1947.
12. Bayliss, L. E. *Principles of General Physiology* (5th ed.). London: Longmans, 1959.
13. Bendall, J. R. Further observations on a factor (the 'Marsh' factor) effecting relaxation of ATP-shortened muscle-fibre models, and the effect of Ca and Mg ions upon it. *J. Physiol.* 121: 232, 1953.
14. Benforado, J. M. Frequency-dependent pharmacological and physiological effects on the rat ventricle strip. *J. Pharmacol. & Exper. Therap.* 122: 86, 1958.
15. Bernstein, J. Untersuchungen zur Thermodynamik der bioelektrischen Ströme. Erster Theil. *Pflüger's Arch. ges. Physiol.* 92: 521, 1902.
16. Bianchi, C. P. and A. M. Shanes. Calcium influx in skeletal muscle at rest, during activity, and during potassium contracture. *J. Gen. Physiol.* 42: 803, 1959.
17. Bing, R. J., F. M. Maraist, J. F. Dammann, Jr., A. Draper, Jr., R. Heimbecker, R. Daley, R. Gerard, and P. Calazel. Effect of strophanthus on coronary blood flow and cardiac oxygen consumption of normal and failing human hearts. *Circulation* 2: 513, 1950.
18. Boehm, R. Über die Wirkung der Barytsalze auf den Thierkörper nebst Bemerkungenuber die Wirkung des Wasserschierlings auf Frosche. *Nauny-Schmiedebergs Arch. exper. Path. u Pharmakol.* 3: 216, 1875.
19. Boehm, R. Über das Verhalten des isolierten Froschherzens bei reiner Salzdiät. Experimentelle Beiträge zur Theorie der Ringerschen Flüssigkeit. *Nauny-Schmiedebergs Arch. exper. Path. u Pharmakol.* 75: 230, 1914.
20. Bogatzki, M. and H. Staub. ATP-System und übriger Phosphatstoffwechsel im normalen und akut-insuffizienten Herzmuskel unter der Behandlung mit Herzglykosiden. *Ztschr. ges. exper. Med.* 127: 425, 1956.
21. Bolingbroke, V. and M. Maizels. Calcium ions and the permeability of human erythrocytes. *J. Physiol.* 149: 563, 1959.
22. Bollman, J. L. and E. V. Flock. Phosphocreatine and inorganic phosphate in working and resting muscle of rats, studied with radioactive phosphorus. *J. Biol. Chem.* 147: 155, 1943.
23. Boulet, L. and M. A. Boulet. Effets antagonistes du baryum et du potassium sur le coeur. *Compt. Rend. soc. biol.* 139: 1106, 1945.
24. Bowditch, H. P. Über die Eigenthümlichkeiten der Reizbarkeit, welche die Muskelfasern des Herzens zeigen. *Arb. Physiol. zu Leipzig* 6: 139, 1871.
25. Bowen, W. J. Effect of digoxin upon rate of shortening of myosin B threads. *Fed. Proc.* 11: 16, 1952.
26. Bower, J. O. and H. A. K. Mengle. The additive effect of calcium and digitalis. *J.A.M.A.* 106: 1151, 1936.
27. Boyer, P. K. and C. A. Poindexter. The influence of digitalis on the electrolyte and water balance of heart muscle. *Am. Heart J.* 20: 586, 1940.

28. BOYLE, P. J. AND E. J. CONWAY. Potassium accumulation in muscle and associated changes. *J. Physiol.* 100: 1, 1941.
29. BOZLER, E. AND D. LAVINE. Permeability of smooth muscle. *Am. J. Physiol.* 195: 45, 1958.
30. BRANDT, J. L., W. GLASER, AND A. JONES. Soft tissue distribution and plasma disappearance of intravenously administered isotopic magnesium with observations on uptake in bone. *Metabolism* 7: 355, 1958.
31. BRAVENY, P. AND V. KRUTA. Dissociation de deux facteurs: restitution et potentiation dans l'action de l'intervalle sur l'amplitude de la contraction du myocarde. *Arch. internat. Physiol.* 66: 633, 1958.
32. BRIGGS, N. F. Factors influencing contraction in glycerinated myocardial fibers. *J. Pharmacol. & Exper. Therap.* 124: 43, 1958.
33. BRINK, F. The role of calcium ions in neural processes. *Pharmacol. Rev.* 6: 243, 1954.
34. BROOKS, C. McC., B. F. HOFFMAN, E. E. SUCKLING, AND O. Orias. *Excitability of the Heart.* New York: Grune & Stratton, 1955.
35. BROWN, T., G. GRUPP, AND G. H. ACHESON. Potassium balance of the dog heart: effects of increasing heart rate and of pentobarbital and dihydro-ouabain. *J. Pharmacol. & Exper. Therap.* 129: 42, 1960.
36. BUCHTHAL, F. AND E. KAISER. *The Rheology of the Cross Striated Muscle Fibre, With Particular Reference to Isotonic Conditions.* Copenhagen: Biologiske Meddelelser, 1951, bind. 21, nr. 7.
37. BURCH, G. E., S. A. THREEFOOT, AND C. T. RAY. The rate of disappearance of Rb^{86} from the plasma, the biologic decay rates of Rb^{86}, and the applicability of Rb^{86} as a tracer of potassium in man with and without chronic congestive heart failure. *J. Lab. & Clin. Med.* 45: 371, 1955.
38. BURGEN, A. S. V. AND K. G. TERROUX. On the negative inotropic effect in the cat's auricle. *J. Physiol.* 120: 449, 1953.
39. BURRIDGE, W. A survey of some elements of cardiac excitability. *Quart. J. Exper. Physiol.* 12: 355, 1920.
40. BURSTEIN, S. G., L. L. BENNETT, F. E. PAYNE, AND J. HOPPER, JR. Effects of potassium and lanatoside-C on the failing heart in heart-lung preparations. *Fed. Proc.* 8: 20, 1948.
41. BURTON, A. C. Relation of structure to function of the tissues of the wall of blood vessels. *Physiol. Rev.* 34: 619, 1954.
42. BUTCHER, W. A., K. G. WAKIM, H. E. ESSEX, R. D. PRUITT, AND H. B. BURCHELL. The effect of changes in concentration of cations on the electrocardiogram of the isolated perfused heart. *Am. Heart J.* 43: 801, 1952.
43. CALHOUN, J. A., G. E. CULLEN, G. CLARKE, AND T. R. HARRISON. Studies in congestive heart failure: VI. The effect of overwork and other factors on the potassium content of the cardiac muscle. *J. Clin. Invest.* 9: 393, 1930.
44. CALHOUN, J. A. AND T. R. HARRISON. Studies in congestive failure: IX. The effect of digitalis on the potassium content of the cardiac muscle of dogs. *J. Clin. Invest.* 10: 139, 1931.
45. CATTELL, McK. AND H. GOLD. The relation of rhythm to the force of contraction of mammalian cardiac muscle. *Am. J. Physiol.* 133: 236P, 1941.
46. CATTELL, McK. AND H. GOLD. Relation of rhythm to force of contraction of mammalian cardiac muscle. *Am. J. Physiol.* 182: 307, 1955.
47. CAVIEZEL, R., H. KOLLER, AND W. WILBRANDT. Zur Frage des Kalium- Calcium-Antagonismus am Herzmuskel and seiner möglichen Beziehung zu Ionentransporten. *Helv et. physiol. et pharmacol. acta* 16: 22, 1958.
48. CAVIEZEL, R. AND W. WILBRANDT. Die Abhängigkeit der bleibenden Herzglykosidwirkung von der Kalium- und Calciumkonzentration während der Glykosideinwirkung auf das Herz. *Helvet. physiol. et pharmacol. acta* 16: 12, 1958.
49. CHAMBERS, R., AND C. KAO. The effect of electrolytes on the physical state of the nerve axon of the squid and of Stentor, a protozoon. *Exper. Cell Research* 3: 564, 1952.
50. CLARKE, N. E. AND R. E. MOSCHER. The water and electrolyte content of the human heart in congestive heart failure with and without digitalization. *Circulation* 5: 907, 1952.
51. CLELAND, K. W. AND E. C. SLATER. The sarcosomes of heart muscle. Their isolation, structure, and behaviour under various conditions. *Quart. J. Microscop. Sc.* 94: 329, 1953.
51a. CONN, H. L. Effects of digitalis and hypoxia on potassium transfer and distribution in the dog heart. *Am. J. Physiol.* 184: 548, 1956.
52. CONN, H. L., JR. AND J. S. ROBERTSON. Kinetics of potassium transfer in the left ventricle of the intact dog. *Am. J. Physiol.* 181: 319, 1955.
53. CONN, H. L., JR. AND J. C. WOOD. Sodium exchange and distribution in the isolated heart of the normal dog. *Am. J. Physiol.* 197: 631, 1959.
54. CONWAY, E. J. In: *Metabolic Aspects of Transport Across Cell Membranes*, edited by Q. R. Murphy. Madison, Wis.: University of Wisconsin Press, 1957, p. 73.
55. COOPERSTEIN, I. L. The inhibitory effect of strophanthidin on secretion by the isolated gastric mucosa. *J. Gen. Physiol.* 42: 1233, 1959.
56. CORABOEUF, E., C. DE LOZÉ, AND J. BOISTEL. Action de la digitale sur les potentiels de membrane et d'action du tissu conducteur du coeur de chien étudiée à l'aide de microélectrodes intracellulaires. *Compt. rend. soc. Biol.* 147: 1169, 1953.
57. COSMOS, E. Factors influencing movement of calcium in vertebrate striated muscle. *Am. J. Physiol.* 195: 705, 1958.
58. COWLE, J. B. AND R. H. THORP. Action of cortisone on the polymerization of action. *Nature, London* 171: 1067, 1953.
59. CRANEFIELD, P. F. AND B. F. HOFFMAN. Electrophysiology of single cardiac cells. *Physiol. Rev.* 38: 41, 1958.
59a. CREESE, R. Bicarbonate ion and striated muscle. *J. Physiol.* 110: 450, 1950.
60. CSAPO, A. I. AND G. W. CORNER. The antagonistic effects of estrogen and progesterone on the staircase phenomenon in uterine muscle. *Endocrinology* 51: 378, 1952.
61. DALE, A. S. The staircase phenomenon in ventricular muscle. *J. Physiol.* 75: 1, 1932.
62. DALY, I. DEB. AND A. J. CLARK. The action of ions upon the frog's heart. *J. Physiol.* 54: 367, 1920.
63. DARROW, D. C., H. E. HARRISON, AND M. TAFFEL. Tissue electrolytes in adrenal insufficiency. *J. Biol. Chem.* 130: 487, 1939.
64. DOI, Y. Studies on muscular contraction. II. The relation between the maximal work and the tension developed in

muscle twitch, and the effects of temperature and extension. *J. Physiol.* 54: 335, 1921.

65. DUBUISSON, M. Sur la répartition des ions dans le muscle strié. *Arch. internat. physiol.* 52: 439, 1942.
66. DUDEL, J. AND W. TRAUTWEIN. Electrophysiologische Messungen zur Strophanthinwirkung am Herzmuskel. *Nauny- Schmiedebergs Arch. exper. Path. u Pharmakol.* 232: 393, 1958.
67. EDENS, E. AND J. E. HUBER. Über Digitalis-bigeminie. *Deutsches Arch. klin. Med.* 118: 476, 1916.
68. EDMAN, K. A. P. Wirkung des Ouabains auf das Aktomyosin der Herzmuskulatur. *Experientia* 7: 71, 1951.
69. EDMAN, K. A. P. Action of cardiac glycosides on the ATP-induced contraction of glycerinated muscle fibers. *Acta physiol. scandinav.* 30: 69, 1953.
70. ELLENBOGEN, E., R. IYENGAR, AND R. E. OLSON. Properties of myosin from normal and failing dog hearts. *Fed. Proc.* 18: 221, 1959.
71. ENGBAEK, L. The pharmacological actions of magnesium ions with particular reference to the neuromuscular and the cardiovascular system. *Pharmacol. Rev.* 4: 396, 1952.
72. ENSELBERG, C. D., H. G. SIMMONS, AND A. A. MINTZ. The effects of potassium upon the heart, with special reference to the possibility of treatment of toxic arrythmias due to digitalis. *Am. Heart J.* 39: 713, 1950.
73. EVANS, C. L. AND Y. MATSUOKA. The effect of various mechanical conditions on the gaseous metabolism and efficiency of the mammalian heart. *J. Physiol.* 49: 378, 1915.
74. FENG, T. P. The production of prolonged after-discharge in nerve by veratrine. *Chinese J. Physiol.* 16: 207, 1941.
75. FENN, W. O. A quantitative comparison between the energy liberated and the work performed by the isolated sartorius muscle of the frog. *J. Physiol.* 58: 175, 1923.
76. FENN, W. O., D. M. COBB, J. F. MANERY, AND W. R. BLOOR. Electrolyte changes in cat muscle during stimulation. *Am. J. Physiol.* 121: 595, 1938.
77. FISCHER, H. Beitrag zur Frage des Synergismus zwischen Digitalis- und Calciumwirkung. *Nauny- Schmiedebergs Arch. exper. Path. u Pharmakol.* 130: 194, 1928.
78. FRANKENHAEUSER, B. The effect of calcium on the myelinated nerve fiber. *J. Physiol.* 137: 245, 1957.
79. FRANKENHAEUSER, B. AND A. L. HODGKIN. The action of calcium on the electrical properties of squid axons. *J. Physiol.* 137: 218, 1957.
80. FRIEDMAN, M. AND R. BINE. Observations concerning the influence of potassium upon the action of a digitalis glycoside (lanatoside-C). *Am. J. Med. Sc.* 214: 633, 1947.
81. FURCHGOTT, R. F. AND T. DE GUBAREFF. The high energy phosphate content of cardiac muscle under various experimental conditions which alter contractile strength. *J. Pharmacol. & Exper. Therap.* 124: 203, 1958.
82. GALLEGO, A. AND R. LORENTE DE NO. On the effect of several monovalent ions upon frog nerve. *J. Cell. & Comp. Physiol.* 29: 189, 1947.
83. GARB, S. The effects of potassium, ammonium, calcium, strontium and magnesium on the electrogram and myogram of mammalian heart muscle. *J. Pharmacol. & Exper. Therap.* 101: 317, 1951.
84. GARB, S. AND M. PENNA. Some quantitative aspects of the relation of rhythm to the contractile force of mammalian ventricular muscle. *Am. J. Physiol.* 182: 601, 1955.

84a. GARB, S. AND V. VENTURI. The differential actions of potassium on the therapeutic and toxic effects of ouabain. *J. Pharmacol. & Exper. Therap.* 112: 94, 1954.

85. GARCÍA RAMOS, J., J. ALANIS, AND A. ROSENBLUETH. Estudios sobre la circulación coronaria. I. Los factores extravasculares. *Arch. Inst. cardiol. Mexico* 20: 474, 1950.
86. GARDOS, G. The function of calcium in the potassium permeability of human erythrocytes. *Biochim. et biophys. acta* 30: 653, 1958.
87. GASSER, H. S. AND A. V. HILL. The dynamics of muscular contraction. *Proc. Roy. Soc. London. ser. B.* 96: 398, 1924.
88. GENUIT, H. AND W. HAARMANN. Zur Frage der Spezifitat der Digitalisstoffwechselwirkungen an Herz- und Skeletmuskulatur von Ratte und Meerschweinchen. *Nauny- Schmiedebergs Arch. exper. Path. u Pharmakol.* 196: 481, 1940.
89. GERGELY, J., G. KALDOR, AND F. N. BRIGGS. Participation of a dialyzable cofactor in the relaxing factor system of muscle. II. Studies with myofibrillar ATP-ase. *Biochim. et biophys. acta* 34: 218, 1959.
90. GERSH, I. Improved histochemical methods for chloride, phosphate-carbonate and potassium applied to skeletal muscle. *Anat. Rec.* 70: 311, 1937.
91. GERTLER, M. M., J. KREAM, J. W. HYLIN, H. ROBINSON, AND E. G. NEIDLE. Effect of digitoxin and quinidine on intracellular electrolytes of the rabbit heart. *Proc. Soc. Exper. Biol. & Med.* 92: 629, 1956.
92. GILBERT, D. L. AND W. O. FENN. Calcium equilibrium in muscle. *J. Gen. Physiol.* 40: 393, 1957.
93. GILSON, A. S., JR. AND E. IRVINE-JONES. The effects of cold and of veratrine upon the action potential of ventricular muscle. *Am. J. Physiol.* 92: 165, 1930.
94. GLASER, W. AND J. L. BRANDT. Localization of magnesium-28 in the myocardium. *Am. J. Physiol.* 196: 375, 1959.
95. GLYNN, I. M. Action of cardiac glycosides on red cells. *J. Physiol.* 128: 56P, 1955.
96. GLYNN, I. M. The action of cardiac glycosides on sodium and potassium movements in human red cells. *J. Physiol.* 136: 148, 1957.
97. GOLD, H. AND D. J. EDWARDS. The effects of ouabain on the heart in the presence of hypercalcemia. *Am. Heart J.* 3: 45, 1927.
98. GOLDEN, J. S. AND W. A. BRAMS. Mechanism of the toxic effects from combined use of calcium and digitalis. *Ann. Int. Med.* 11: 1084, 1938.
99. GOLLWITZER-MEIER, K. AND E. KRUGER. Zur Verschiedenheit der Herzenergetik und Herzdynamik bei Druck- und Volumleistung. *Pflüger's Arch. ges. Physiol.* 238: 279, 1936.
100. GONLUBOL, F., A. SIEGEL, AND R. J. BING. Effect of a cardiac glycoside (Cedilanid) on the sodium and potassium balance of the human heart. *Circulation Res.* 4: 298, 1956.
101. GREENGARD, P. AND R. W. STRAUB. Restoration by barium of action potentials in sodium-deprived mammalian B and C fibres. *J. Physiol.* 145: 562, 1959.
102. GREINER, T. The relationship of force of contraction to high-energy phosphate in heart muscle. *J. Pharmacol. & Exper. Therap.* 105: 178, 1952.

103. Greiner, T. H. and S. Garb. The influence of drugs on the irritability and automaticity of heart muscle. *J. Pharmacol. & Exper. Therap.* 98: 215, 1950.
104. Gremels, H. Zur Physiologie und Pharmakologie der Energetik des Säugetierherzens. *Nauny- Schmiederbergs Arch. exper. Path. u Pharmakol.* 169: 689, 1933.
105. Greville, G. D. and H. Lehmann. Magnesium-calcium antagonism in muscle. *Nature, London* 152: 81, 1943.
106. Grumbach, L., J. W. Howard, and V. I. Merrill. Factors related to the initiation of ventricular fibrillation in the isolated heart: effect of calcium and potassium. *Circulation Res.* 2: 452, 1954.
107. Haarmann, W., A. Hagemeier, and L. Lendle. Über die Bindung von Digitalisglykosiden und Digaloiden an die Eiweissstoffe des Blutserums. *Nauny- Schmiedebergs Arch. exper. Path. u Pharmakol.* 194: 205, 1940.
108. Hagen, P. S. The effects of digilanid C in varying dosage upon the potassium and water content of rabbit heart muscle. *J. Pharmacol. & Exper. Therap.* 67: 50, 1939.
109. Hajdu, S. Behaviour of frog and rat muscle at higher temperatures. *Enzymologia* 14: 187, 1950.
110. Hajdu, S. Mechanism of staircase and contracture in ventricular muscle. *Am. J. Physiol.* 174: 371, 1953.
111. Hajdu, S. In: *Chemical Physiology of Contraction in Body and Heart Muscle.* New York: Academic Press, 1953, p. 92.
111a. Hajdu, S. Bioassay for cardiac active principles based on the staircase phenomenon of the frog heart. *J. Pharmacol. & Exper. Therap.* 120: 90, 1957.
112. Hajdu, S. and E. Leonard. A serum protein system affecting contractility of the frog heart present in increased amounts in patients with essential hypertension. *Circulation Res.* 6: 740, 1958.
113. Hajdu, S. and E. Leonard. The cellular basis of cardiac glycoside action. *Pharmacol. Rev.* 11: 173, 1959.
114. Hajdu, S. and A. Szent-Györgyi. Action of DOC and serum on the frog heart. *Am. J. Physiol.* 168: 159, 1952.
115. Harris, A. S., J. E. Firestone, and R. A. Liptak. Relation of potassium ions in extracellular fluid to ectopic ventricular arrhythmias induced by K-strophanthoside. Proceedings of the 28th Scientific Sessions of the A.M.A. Chicago, 1955, p. 52.
116. Harris, E. J. The exchangeability of the potassium of frog muscle, studied in phosphate media. *J. Physiol.* 117: 278, 1951.
117. Harris, E. J. The exchange of frog muscle potassium. *J. Physiol.* 120: 246, 1953.
118. Harris, E. J. Ionophoresis along frog muscle. *J. Physiol.* 124: 248, 1954.
119. Harris, E. J. Permeation and diffusion of K ions in frog muscle. *J. Gen. Physiol.* 41: 169, 1957.
120. Harris, E. J. The output of ^{45}Ca from frog muscle. *Biochim. et biophys. acta* 23: 80, 1957.
121. Harris, E. J. and H. B. Steinbach. Inexchangeable Na and K in frog muscle. *J. Physiol.* 131: 20P, 1956.
122. Harris, E. J. and H. B. Steinbach. The extraction of ions from muscle by water and sugar solutions with a study of the degree of exchange with tracer of the sodium and potassium in the extracts. *J. Physiol.* 133: 385, 1956.
123. Harrison, T. R., C. Pilcher, and G. Ewing. Studies in congestive heart failure. IV. The potassium content of skeletal and cardiac muscle. *J. Clin. Invest.* 8: 325, 1930.
124. Harvey, S. C. Radiophosphorus metabolism of the guinea pig heart and the action of digitoxin and pentobarbital. *Am. J. Physiol.* 183: 559, 1955.
125. Harvey, S. C. and E. E. Daniel. Possible interrelationship of digitoxin and calcium studied with radiocalcium on the isolated guinea pig heart. *J. Pharmacol. & Exper. Therap.* 106: 394, 1952.
126. Harvey, S. C. and G. R. Pieper. Intracellular distribution of digitoxin-C^{14} in the heart. *J. Pharmacol. & Exper. Therap.* 114: 14, 1955.
127. Hashish, S. E. E. The effects of low temperatures and heparin on potassium exchangeability in rat diaphragm. *Acta physiol. scandinav.* 43: 189, 1958.
128. Hasselbach, W. and H. H. Weber. Der Einfluss des MB-Faktors auf die Kontraktion des Fasermodells. *Biochim. et biophys. acta* 11: 160, 1953.
129. Hawkins, L. W. and J. R. Smith. Effect of certain cations on relaxation of the glycerol-extracted heart muscle of frogs. *Am. J. Physiol.* 186: 304, 1956.
130. Hazard, R. and J. Hazard. Variations de la sensibilité à la digitaline en fonction de la kaliémie. *Compt. rend. soc. Biol.* 146: 832, 1952.
131. Heilbrunn, L. V. and F. J. Wiercinski. The action of various cations on muscle protoplasm. *J. Cell. & Comp. Physiol.* 29: 15, 1947.
132. Hellems, H. K., T. J. Regan, F. N. Talmers, R. C. Christensen, and T. Wada. The mode of action of acetyl strophanthidin on the failing human heart. *J. Clin. Invest.* 35: 710, 1956.
133. Helmreich, E. and K. Simon. Zur Frage der Wirkung von Digitalisstoffen auf das Aktomyosin und die Adenosintriphosphatase des Herzmuskels. *Z. Naturforsch (B)* 7: 341, 1952.
134. Hercus, V. M., R. J. S. McDowall, and D. Mendel. Sodium exchanges in cardiac muscle. *J. Physiol.* 129: 177, 1955.
135. Hess, M. E. and N. Haugaard. Studies of the effect of antiarrhythmic drugs on carbohydrate metabolism of rat heart muscle in vitro. *Circulation Res.* 6: 256, 1958.
136. Hill, A. V. The absolute mechanical efficiency of the contraction of an isolated muscle. *J. Physiol.* 46: 435, 1913.
137. Hill, A. V. The heat of shortening and the dynamic constants of muscle. *Proc. Roy. Soc. London. ser. B* 126: 136, 1938.
138. Hill, A. V. The mechanical efficiency of frog's muscle. *Proc. Roy. Soc. London. ser. B.* 127: 434, 1939.
139. Hill, A. V. The 'plateau' of full activity during a muscle twitch. *Proc. Roy. Soc. London. ser. B* 141: 498, 1953.
140. Hill, A. V. and L. MacPherson. The effect of nitrate, iodide and bromide on the duration of the active state in skeletal muscle. *Proc. Roy. Soc. London. ser. B* 143: 81, 1954.
141. Höber, R. *Physical Chemistry of Cells and Tissues.* Philadelphia: Blakiston, 1945.
142. Hodgkin, A. L. Ionic movements and electrical activity in giant nerve fibres. *Proc. Roy. Soc. London. ser. B* 148: 1, 1958.
143. Hodgkin, A. L. and P. Horowicz. The influence of potassium and chloride ions on the membrane potential of single muscle fibres. *J. Physiol.* 148: 127, 1959.
144. Hodgkin, A. L. and B. Katz. The effect of sodium ions on the electrical activity of the giant axon of the squid. *J. Physiol.* 108: 37, 1949.
145. Hodgkin, A. L. and R. D. Keynes. The mobility and

diffusion coefficient of potassium in giant axons from Sepia. *J. Physiol.* 119: 513, 1953.
146. Hodgkin, A. L. and R. D. Keynes. Movements of labelled calcium in squid giant axons. *J. Physiol.* 138: 253, 1957.
147. Hoffman, B. F., E. Bindler, and E. E. Suckling. Post-extrasystolic potentiation of contraction in cardiac muscle. *Am. J. Physiol.* 185: 95, 1956.
148. Hoffman, B. F. and J. J. Kelly, Jr. Effects of rate and rhythm on contraction of rat papillary muscle. *Am. J. Physiol.* 197: 1199, 1959.
149. Hoffman, B. F. and E. E. Suckling. Effect of several cations on transmembrane potentials of cardiac muscle. *Am. J. Physiol.* 186: 317, 1956.
150. Holland, W. C. A possible mechanism of action of quinidine. *Am. J. Physiol.* 190: 492, 1957.
151. Holland, W. C., M. E. Greig, and C. E. Dunn. Factors affecting the action of lanatoside-C on the potassium content of isolated perfused guinea pig hearts. *Am. J. Physiol.* 176: 227, 1954.
152. Holland, W. C. and R. L. Klein. Effects of temperature, Na and K concentration and quinidine on transmembrane flux of K^{42} and incidence of atrial fibrillation. *Circulation Res.* 6: 516, 1958.
153. Horvath, I., C. Kiraly, and J. Szerb. Action of cardiac glycosides on the polymerization of actin. *Nature, London* 164: 792, 1949.
154. Huxley, A. F. and R. Stämpfli. Effect of potassium and sodium on resting and action potentials of single myelinated nerve fibers. *J. Physiol.* 112: 496, 1951.
155. Iseri, L. T., L. C. Alexander, R. S. McCaughey, A. J. Boyle, and G. B. Myers. Water and electrolyte content of cardiac and skeletal muscle in heart failure and myocardial infarction. *Am. Heart J.* 43: 215, 1952.
156. Johnson, E. A. The effects of quinidine, procaine amide and pyrilamine on the membrane resting and action potential of guinea pig ventricular muscle fibers. *J. Pharmacol. & Exper. Therap.* 117: 237, 1956.
157. Johnson, E. A. and M. G. McKinnon. The differential effect of quinidine and pyrilamine on the myocardial action potential at various rates of stimulation. *J. Pharmacol. & Exper. Therap.* 120: 460, 1957.
158. Johnson, J. A. Sodium exchange in the frog heart ventricle. *Am. J. Physiol.* 191: 487, 1957.
159. Joyce, C. R. B. and M. Weatherall. Cardiac glycosides and the potassium exchange of human erythrocytes. *J. Physiol.* 127: 33P, 1955.
160. Kahn, A. J. and A. Sandow. The potentiation of muscular contraction by the nitrate-ion. *Science* 112: 647, 1950.
161. Kahn, J. B., Jr. Effects of various lactones and related compounds on cation transfer in incubated cold-stored human erythrocytes. *J. Pharmacol. & Exper. Therap.* 121: 234, 1957.
162. Kahn, J. B., Jr. and G. H. Acheson. Effects of cardiac glycosides and other lactones, and of certain other compounds, on cation transfer in human erythrocytes. *J. Pharmacol. & Exper. Therap.* 115: 305, 1955.
162a. Kako, K. and R. J. Bing. Contractility of actomyosin bands prepared from normal and failing human hearts. *J. Clin. Invest.* 37: 465, 1958.
163. Kaldor, G., J. Gergely, and F. N. Briggs. Participation of a dialyzable cofactor in the relaxing factor system of muscle. III. Substitution of pyrophosphate for the cofactor. *Biochim. et biophys. acta* 34: 224, 1959.
164. Kanda, Z., A. Sekiya, K. Sakai, N. Ueno, and T. Kamei. Studies on the potassium content of the heart muscle receiving K-strophanthin and the influence of potassium on the respiration of heart muscle. *Japan. J. Pharmacol.* 6: 105, 1957.
165. Kärki, N. T. Effect of quinidine and other antimalarial agents on the uptake of potassium ions by red cells. *Arch. internat. pharmacodyn.* 114: 243, 1958.
166. Katz, L. N. Analysis of the several factors regulating the performance of the heart. *Physiol. Rev.* 35: 91, 1955.
167. Katz, L. N., K. Jochim, E. Lindner, and M. Landowne. The effect of varying resistance-load and input-load on the energetics of the surviving mammalian heart. *Am. J. Physiol.* 134: 636, 1941.
168. Katzung, B. and A. Farah. Influence of temperature and rate on the contractility of isolated turtle myocardium. *Am. J. Physiol.* 184: 557, 1956.
169. Katzung, B., H. Rosin, and F. Scheider. Frequency-force relationship in the rabbit auricle and its modification by some metabolic inhibitors. *J. Pharmacol. & Exper. Therap.* 120: 324, 1957.
170. Kavaler, F. Membrane depolarization as a cause of tension development in mammalian ventricular muscle. *Am. J. Physiol.* 197: 968, 1959.
171. Kavaler, F. Membrane depolarization and contraction in auricle. *Fed. Proc.* 19: 109, 1960.
172. Keynes, R. D. and P. R. Lewis. The intracellular calcium contents of some invertebrate nerves. *J. Physiol.* 134: 399, 1956.
173. Keynes, R. D. and R. C. Swan. The permeability of frog muscle fibres to lithium ions. *J. Physiol.* 147: 626, 1959.
174. Kiese, M. and R. S. Garan. Mechanische Leistung, Grösse und Sauerstoffverbrauch des Warmblüterherzens. *Naunyn-Schmiedebergs Arch. exper. Path. u Pharmakol.* 188: 226, 1938.
175. Kionka, H. Die Wirkungen der Erdalkalien auf das isolierte Froschherz. *Ztschr. ges. exper. Med.* 17: 108, 1914.
176. Kleinfeld, M., E. Stein, and S. Meyers. Effects of barium chloride on resting and action potentials of ventricular fibers of the frog. *Circulation Res.* 2: 488, 1954.
176a. Koch-Weser, J. and J. R. Blinks. Dependence of interval-force relationship of mammalian heart muscle on extracellular electrolyte concentrations. *Pharmacologist* 2: 65, 1960.
177. Konschegg, A. von. Über Beziehungen zwischen Herzmittel- und physiologischer Kationenwirkung. *Naunyn-Schmiedebergs Arch. exper. Path. u Pharmakol.* 71: 251, 1913.
178. Korey, S. Some factors influencing the contractility of a non-conducting fiber preparation. *Biochim. et biophys. acta* 4: 58, 1950.
179. Krayer, O. and G. H. Acheson. The pharmacology of the veratrum alkaloids. *Physiol. Rev.* 26: 383, 1946.
180. Kruta, V. and J. Stejskalova. Rate of contractility and optimal frequency of the auricular myocardium in certain mammals. *Arch. internat. physiol.* 68: 152, 1960.
181. Kuffler, S. W. Action of veratrine on nerve-muscle preparations. *J. Neurophysiol.* 8: 113, 1945.
182. Kyser, F. A., H. Teloh, and G. C. Sutton. The effect

of digitalis and desoxycorticosterone acetate administration upon intracellular potassium ion concentration. *J. Lab. & Clin. Med.* 53: 216, 1959.

183. LANGEMANN, H., T. M. BRODY, AND J. A. BAIN. *In vitro* effects of ouabain on slices and mitochondrial preparations from heart and brain. *J. Pharmacol. & Exper. Therap.* 108: 274, 1953.
184. LEE, J. AND J. W. WOODBURY. Effect of potassium lack and digitoxin on transmembrane potentials and tension of frog ventricle. *Fed. Proc.* 17: 94, 1958.
185. LEE, K. S. Effect of quinidine on papillary muscle. *Proc. Soc. Exper. Biol. & Med.* 86: 444, 1954.
186. LEONARD, E. Alteration of contractile response of artery strips by a potassium-free solution, cardiac glycosides and changes in stimulation frequency. *Am. J. Physiol.* 189: 185, 1957.
187. LEONARD, E. AND S. HAJDU. The effect of potassium on the inotropic action of cardiac glycosides. *Clin. Research* 7: 19, 1959.
188. LEONARD, E. AND S. HAJDU. Cardioglobulin. *Clin. Research* 8: 187, 1960.
189. LEWIS, M. S. AND H. A. SAROFF. The binding of ions to the muscle proteins. Measurements on the binding of potassium and sodium ions to myosin A, myosin B, and actin. *J. Am. Chem. Soc.* 79: 2112, 1955.
190. LIEBERMAN, A. L. Studies on calcium: VI. Some interrelationships of the cardiac activities of calcium gluconate and scillaren-B. *J. Pharmacol. & Exper. Therap.* 47: 183, 1933.
191. LINDEMAN, V. F. The physiology of the crustacean heart. II. The effect of lithium, ammonium, strontium, and barium ions upon the heart rhythm of the crayfish (Cambarus Clarkii). *Physiol. Zoöl.* 2: 395, 1929.
192. LING, G. N. The role of phosphate in the maintenance of the resting potential and selective ionic accumulation in frog muscle cells. In: *Phosphorus Metabolism*, vol. II, edited by W. D. McElroy and B. Glass. Baltimore: Johns Hopkins Press, 1952, p. 748.
193. LOEWI, O. Über den Zusammenhang zwischen Digitalis- und Kalziumwirkung. *Nauny- Schmiedebergs Arch. exper. Path. u Pharmakol.* 82: 131, 1917.
194. LOVE, W. D. AND G. E. BURCH. A comparison of potassium^{42}, rubidium^{86}, and cesium^{134} as tracers of potassium in the study of cation metabolism of human erythrocytes in vitro. *J. Lab. Clin. Med.* 41: 351, 1953.
195. LOVE, W. S. The effect of quinidine and strophanthidin upon the refractory period of the tortoise ventricle. *Heart* 13: 87, 1926.
196. LOWN, B., H. SALZBERG, C. D. ENSELBERG, AND R. E. WESTON. Interrelationship between potassium metabolism and digitalis toxicity in heart failure. *Proc. Soc. Exper. Biol. & Med.* 76: 797, 1951.
197. LOWRY, O. H. Electrolytes in the cytoplasm. *Biol. Symposia* 10: 233, 1943.
198. LUBIN, M. AND P. B. SCHNEIDER. The exchange of potassium for caesium and rubidium in frog muscle. *J. Physiol.* 138: 140, 1957.
199. LUNDSGAARD-HANSEN, P. Vergleich der Wirkungen von Calcium und Digitalis auf die aktiven und passiven Kaliumbewegungen durch die Erythrocytenmembran. *Nauny- Schmiedebergs Arch. exper. Path. u Pharmakol.* 231: 577, 1957.
200. LÜTTGAU, H. C. AND R. NIEDERGERKE. The antagonism between Ca and Na ions on the frog's heart. *J. Physiol.* 143: 486, 1958.
201. McDOWALL, R. J. S., A. F. MUNRO, AND A. F. ZAYAT. Sodium and cardiac muscle. *J. Physiol.* 130: 615, 1955.
202. MAIZELS, M. Active cation transport in erythrocytes. *Symposia Soc. Exper. Biol.* 8: 202, 1954.
203. MAIZELS, M. Calcium ions and the permeability of human red cells. *Nature, London* 184: 366, 1959.
204. MALLOV, S. AND J. S. ROBB. Behavior of actomyosin threads. *Fed. Proc.* 8: 104, 1949.
205. MANDELSTAMM, M. Über den Zusammenhang zwischen Digitalis- und Calciumwirkung. *Ztschr. ges. exper. Med.* 51: 633, 1926.
206. MANDOKI, J. J. AND J. ALANIS. Efecto de la actividad rápida sobre la amplitud de la contracción del músculo ventricular. *Arch. Inst. cardiol. Mexico* 19: 79, 1949.
207. MANERY, J. F. Water and electrolyte metabolism. *Physiol. Rev.* 34: 334, 1954.
208. MANGUN, G. H., H. S. REICHLE, AND V. C. MYERS. Further studies on human cardiac and voluntary muscle. *A.M.A. Arch. Int. Med.* 67: 320, 1941.
209. MATSUDA, K., B. F. HOFFMAN, C. N. ELLNES, M. KATZ, AND C. McC. BROOKS. Veratrine induced prolongation of repolarization in the mammalian heart. XIX International Physiological Congress, 1953, p. 596.
210. MATTHEWS, S. A. AND D. E. JACKSON. The action of magnesium sulphate upon the heart and the antagonistic action of some other drugs. *Am. J. Physiol.* 19: 5, 1907.
211. MINES, G. R. On functional analysis by the action of electrolytes. *J. Physiol.* 46: 188, 1913.
212. MITCHELL, J. H., J. P. GILMORE, R. J. LINDEN, AND S. J SARNOFF. Effect of increasing aortic pressure on the performance characteristics of the left ventricle. *Fed. Proc.* 19: 119, 1960.
213. MOULIN, M. AND W. WILBRANDT. Die Wirkung von Kalium and Calcium auf das Treppenphänomen am Froschherzen. *Experientia* 11: 72, 1955.
214. MUDGE, G. H. Electrolyte and water metabolism of rabbit kidney slices: effect of metabolic inhibitors. *Am. J. Physiol.* 167: 206, 1951.
215. MUELLER, H. The action of relaxing factor on actomyosin. *Biochim. et biophys. acta* 39: 93, 1960.
216. MURNAGHAN, M. F. The antiaccelerator action of quinine on the isolated perfused heart of the cat. *Arch. internat. pharmacodyn.* 120: 312, 1959.
217. NAYLER, W. G. The effect of strophanthin-G on the rate of deamination of adenyl compounds. *Australian J. Exper. Biol. & M. Sc.* 37: 109, 1959.
218. NAYLER, W. G. AND M. McCULLOCH. The action of anions on cardiac muscle. *Australian J. Exper. Biol. & M. Sc.* 38: 117, 1960.
218a. NIEDERGERKE, R. The 'staircase' phenomenon and the action of calcium on the heart. *J. Physiol.* 134: 569, 1956.
219. NIEDERGERKE, R. The potassium chloride contracture of the heart and its modification by calcium. *J. Physiol.* 134: 584, 1956.
220. NIEDERGERKE, R. The rate of action of calcium ions on the contraction of the heart. *J. Physiol.* 138: 506, 1957.
221. NIEDERGERKE, R. Calcium and the activation of contraction. *Experientia* 15: 128, 1959.
222. NIEDERGERKE, R. AND E. J. HARRIS. Accumulation of

calcium (or strontium) under conditions of increasing contractility. *Nature, London* 179: 1068, 1957.

223. NIEDERGERKE, R. AND H. C. LÜTTGAU. Calcium and the contraction of the heart. *Nature, London* 179: 1066, 1957.
224. NYIRI, W. AND L. DUBOIS. Experimental studies on heart tonics: III. The relationships of calcium ions, hydrogen ions and digitalis. *J. Pharmacol. & Exper. Therap.* 39: 111, 1930.
225. ORABONA, M. L. AND G. MANGANELLI. Modificazioni del potassium nei tessuti di ratti sottoposti a sforzo ed in ratti trattati con digitale. *Boll. Soc. ital. biol. sper.* 30: 10, 1954.
226. ORLOFF, J. AND M. BURG. Effect of strophanthidin on electrolyte excretion in the chicken. *Am. J. Physiol.* 199: 49, 1960.
227. ORLOFF, J. AND T. J. KENNEDY, JR. Effect of lithium on acidification of the urine. *Fed. Proc.* 11: 115, 1952.
228. OVERTON. E. Beiträg zur allgemeinen Muskel und Nervenphysiologie. *Pflüger's Arch. ges. Physiol.* 92: 346, 1902.
229. PATTERSON, S. W., H. PIPER, AND E. H. STARLING. The regulation of the heart beat. *J. Physiol.* 48: 465, 1914.
230. PAYNE, J. W. AND M. WALSER. Ion association. II. The effect of multivalent ions on the concentration of free calcium ions as measured by the frog heart method. *Bull. Johns Hopkins Hosp.* 105: 298, 1959.
231. PENNA, M. AND S. GARB. Relationship of changes in ionic concentrations to the augmentation produced by extra contractions in isolated mammalian ventricular muscle. *Am. J. Physiol.* 184: 572, 1956.
232. PETERS, H. P. AND M. B. VISSCHER. The energy metabolism of the heart in failure and the influence of drugs upon it. *Am. Heart J.* 11: 273, 1936.
233. RANDALL, R. E., JR., E. C. ROSSMEISL, AND K. H. BLEIFER. Magnesium depletion in man. *Ann. Int. Med.* 50: 257 1959.
234. RANNEY, R. E. Biochemical characteristics of glycerol extracted myocardial fibers. *Am. J. Physiol.* 183: 197, 1955.
235. RAYNER, B. AND M. WEATHERALL. Digoxin, ouabain and potassium movements in rabbit auricles. *Brit. J. Pharmacol.* 12: 371, 1957.
236. RAYNER, B. AND M. WEATHERALL. Acetylcholine and potassium movements in rabbit auricles. *J. Physiol.* 146: 392, 1959.
237. READ, W. O. AND F. E. KELSEY. Effect of digoxin on myokinase activity. *Science* 125: 120, 1957.
238. REGAN, T. J., F. N. TALMERS, AND H. K. HELLEMS. Myocardial transfer of sodium and potassium: Effect of acetyl strophanthidin in normal dogs. *J. Clin. Invest.* 35: 1220, 1956.
239. REITER, M. Die Beeinflussung des Kationentransportes im Herzmuskel durch Calcium und Strophanthin in Beziehung zur inotropen Wirkung. *Pflüger's Arch. ges. Physiol.* 267: 158, 1958.
240. REITER, M. AND J. NOÉ. Die Bedeutung von Calcium, Magnesium, Kalium und Natrium fur die rhythmische Erregungsbildung im Sinusknoten des Warmblüterherzens. *Pflüger's Arch. ges. Physiol.* 269: 366, 1959.
241. RELMAN, A. S., A. T. LAMBIE, B. A. BURROWS, AND A. M. ROY. Cation accumulation by muscle tissue: the displacement of potassium by rubidium and cesium in the living animal. *J. Clin. Invest.* 36: 1249, 1957.
242. RINGER, S. A further contribution regarding the influence of the different constituents of the blood on the contraction of the heart. *J. Physiol.* 4: 29, 1883.
243. RITCHIE, J. M. AND D. R. WILKIE. The effect of previous stimulation on the active state of muscle. *J. Physiol.* 130: 488, 1955.
244. ROBB, J. S. AND S. MALLOV. Effect of ouabain on actomyosin threads. *J. Pharmacol. & Exper. Therap.* 108: 251, 1953.
245. ROBERTSON, W. VAN B. AND P. PEYSER. Changes in water and electrolytes of cardiac muscle following epinephrine. *Am. J. Physiol.* 166: 277, 1951.
246. ROHDE, E. In: *Handbuch der Experimentellen Pharmakologie*, herausgegeben von A. Heffter. Berlin: Julius Springer, 1920, p. 62.
247. RONA, P. AND P. NEUKIRCH. Experimentelle Beiträge zur Physiologie des Darmes. *Pflüger's Arch. ges. Physiol.* 148: 273, 1912.
248. ROSENBLUETH, A., J. ALANIS, E. LÓPEZ, AND R. RUBIO. The adaptation of ventricular muscle to different circulatory conditions. *Arch. internat. physiol.* 67: 358, 1959.
249. ROSENBLUETH, A., J. ALANIS, AND R. RUBIO. Some properties of the mammalian ventricular muscle. *Arch. internat. physiol.* 67: 276, 1959.
250. ROSENBLUETH, A., J. ALANIS, R. RUBIO, AND E. LÓPEZ. The two staircase phenomena. *Arch. internat. physiol.* 67: 374, 1959.
251. ROSENBLUETH, A., W. DAUGHADAY, AND D. D. BOND. The electrogram of the ventricle of the turtle's heart. *Am. J. Physiol.* 139: 464, 1943.
252. ROSIN, H. AND A. FARAH. Post-stimulation potentiation of contractility in the isolated auricle of the rabbit. *Am. J. Physiol.* 180: 75, 1955.
253. ROTHBERGER, C. J. AND A. SACHS. Rhythmicity and automatism in the mammalian left auricle. *Quart. J. Exper. Physiol.* 29: 69, 1939.
254. ROTHLIN, E. AND A. KALLENBERGER. Uber das Glykosidbindungsvermogen verschiedener Eiweissfraktionen des Blutes. *Arch. internat. pharmacodyn.* 81: 520, 1950.
255. ROTHLIN, E. AND O. SCHOELLY. Einfluss herzwirksamer Glykoside auf die Atmung des Herzens, gemessen mit der Warburg-Apparatur. *Helvet. physiol. et pharmacol. acta* 8: C69, 1950.
256. RUSHMER, R. F. Constancy of stroke volume in ventricular responses to exertion. *Am. J. Physiol.* 196: 745, 1959.
257. ST. GEORGE, S., M. FRIEDMAN, AND T. ISHIDA. Intracellular distribution of digitoxin. *Proc. Soc. Exper. Biol. & Med.* 83: 318, 1953.
258. SALOMON, K. AND O. REISSER. Zur Frage des Einflusses von Digitoxin und Strophanthin auf oxydative Vorgange in Versuchen am Modell sowie am atmenden überlebenden Herzmuskelgewebe. *Nauny- Schmiedebergs Arch. exper. Path. u Pharmakol.* 177: 450, 1935.
259. SAMPSON, J. J., E. C. ALBERTON, AND B. KONDO. The effect on man of potassium administration in relation to digitalis glycosides with special reference to blood serum potassium, the electrocardiogram and ectopic beats. *Am. Heart J.* 26: 164, 1943.
260. SANDOW, A. AND H. MANDEL. Effects of potassium and rubidium on the resting potential of muscle. *J. Cell. & Comp. Physiol.* 38: 271, 1951.
261. SANYAL, P. N. AND P. R. SAUNDERS. Relationship between

cardiac rate and the positive inotropic action of ouabain. *J. Pharmacol. & Exper. Therap.* 122: 499, 1958.

262. Sarnoff, S. J., E. Braunwald, G. H. Welch, Jr., R. B. Case, W. N. Stainsby, and R. Macruz. Hemodynamic determinants of oxygen consumption of the heart with special reference to the tension-time index. *Am. J. Physiol.* 192: 148, 1958.
263. Scarinci, V. Soluzioni di Ringer prive di potassio rimuovono la contrattura da ouabaina e restaurano la contralliltà del cuore di rana. *Experientia* 9: 187, 1953.
264. Schatzmann, H. J. Herzglykoside als Hemmstoffe für den aktiven Kalium- und Natrium-transport durch die Erythrocytenmembran. *Helvet. physiol. et pharmacol. acta* 11: 346, 1953.
265. Schou, M. Biology and pharmacology of the lithium ion. *Pharmacol. Rev.* 9: 17, 1957.
266. Schreiber, S. S. Potassium and sodium exchange in the working frog heart. Effects of overwork, external concentrations of potassium and ouabain. *Am. J. Physiol.* 185: 337, 1956.
267. Sekul, A. A. and W. C. Holland. Cl^{36} and Ca^{45} exchange in atrial fibrillation. *Am. J. Physiol.* 197: 752, 1959.
268. Sexton, A. W. and D. K. Meyer. Effects of potassium, caesium and lithium ions on sodium transport through gills of goldfish. *Fed. Proc.* 14: 137, 1955.
269. Shanes, A. M. Electrical phenomena in nerve. I. Squid giant axon. *J. Gen. Physiol.* 33: 57, 1949.
270. Shanes, A. M. Potassium movement in relation to nerve activity. *J. Gen. Physiol.* 34: 795, 1951.
271. Shanes, A. M. Electrochemical aspects of physiological and pharmacological action in excitable cells. Part II. The action potential and excitation. *Pharmacol. Rev.* 10: 165, 1958.
272. Shanes, A. M. and C. P. Bianchi. The distribution and kinetics of release of radiocalcium in tendon and skeletal muscle. *J. Gen. Physiol.* 42: 1123, 1959.
273. Shanes, A. M. and C. P. Bianchi. Radiocalcium release by stimulated and potassium-treated *Sartorius* muscles of the frog. *J. Gen. Physiol.* 43: 481, 1960.
274. Shanes, A. M., H. Grundfest, and W. Freygang. Low level impedance changes following the spike in the squid giant axon before and after treatment with "veratrine" alkaloids. *J. Gen. Physiol.* 37: 39, 1953.
275. Shaw, F. H. and S. E. Simon. The nature of the sodium and potassium balance in nerve and muscle cells. *Australian J. Exper. Biol. & M. Sc.* 33: 153, 1955.
276. Siebens, A. A., B. F. Hoffman, P. F. Cranefield, and C. McC. Brooks. Regulation of contractile force during ventricular arrhythmias. *Am. J. Physiol.* 197: 971, 1959.
277. Sjodin, R. A. Rubidium and cesium fluxes in muscle as related to the membrane potential. *J. Gen. Physiol.* 42: 983, 1959.
278. Smith, P. K., A. W. Winkler, and H. E. Hoff. Calcium and digitalis synergism. *A.M.A. Arch. Int. Med.* 64: 322, 1939.
279. Smith, P. K., A. W. Winkler, and H. E. Hoff. Electrocardiographic changes and concentration of magnesium in serum following intravenous injection of magnesium salts. *Am. J. Physiol.* 126: 720, 1939.
280. Smith, P. K., A. W. Winkler, and B. M. Schwartz. The distribution of magnesium following the parenteral administration of magnesium sulfate. *J. Biol. Chem.* 129: 51, 1939.
281. Snellman, O. and B. Gelotte. A reaction between a deaminase and heart actin, and inhibition of the effect with cardiac glycoside. *Nature, London* 165: 604, 1950.
282. Sokolow, M. and A. L. Edgar. Blood quinidine concentrations as a guide in the treatment of cardiac arrhythmias. *Circulation* 1: 576, 1950.
283. Solomon, A. K., T. J. Gill, 3rd, and G. L. Gold. The kinetics of cardiac glycoside inhibition of potassium transport in human erythrocytes. *J. Gen. Physiol.* 40: 327 1956.
284. Spratt, J. L. and G. T. Okita. Protein binding of radioactive digitoxin *J. Pharmacol. & Exper. Therap.* 124: 109. 1958.
285. Spratt, J. L. and G. T. Okita. Subcellular localization of radioactive digitoxin. *J. Pharmacol. & Exper. Therap.* 124: 115, 1958.
286. Stanbury, J. B. and A. Farah. Effects of the magnesium ion on the heart and on its response to digoxin. *J. Pharmacol. & Exper. Therap.* 100: 445, 1950.
287. Stanbury, S. W. and G. H. Mudge. Potassium metabolism of liver mitochondria. *Proc. Soc. Exper. Biol. & Med.* 82: 675, 1953.
288. Stutz, H., E. Feigelson, J. Emerson, and R. J. Bing. The effect of digitalis (Cedilanid) on the mechanical and electrical activity of extracted and non-extracted heart muscle preparations. *Circulation Res.* 2: 555, 1954.
289. Sulser, F. Die Wirkung von Herzglykosiden und Kalzium auf den Kaliumtransport im Herzmuskel. *Experientia* 15: 97, 1959.
290. Sulser, F. and W. Wilbrandt. Die Wirkung von Corticosteroiden und Herzglykosiden auf Ionentransporte am Erythrocyten. *Helvet. physiol. et pharmacol. acta* 15: C37, 1957.
291. Szent-Györgyi, A. *Chemistry of Muscular Contraction.* New York: Academic Press, 1947, p. 30.
292. Szent-Györgyi, A., Z. M. Bacq, and M. Goffart. A humoral transmission of muscular contraction in the presence of veratrine. *Nature, London* 143: 522, 1939.
293. Taeschler, M. and R. J. Bing. Some properties of contractile proteins of the heart as studied on the extracted heart muscle preparation. *Circulation Res.* 1: 129, 1953.
294. Taggart, J. V., L. Silverman, and E. M. Trayner. Influence of renal electrolyte composition on the tubular excretion of *p*-aminohippurate. *Am. J. Physiol.* 173: 345 1953.
295. Thomas, L. J., Jr. An antagonism in the action of calcium and strontium ions on the frog's heart. *J. Cell. & Comp. Physiol.* 50: 249, 1957.
296. Thomas, L. J., Jr., W. B. Jolley, and R. Grechman. Effect of potassium lack and ouabain on $calcium^{45}$ uptake in frog's heart. *Fed. Proc.* 17: 162, 1958.
297. Trautwein, W. and K. Zink. Über Membran- und Aktionspotentiale einzelner Myokardfasern des Kalt- und Warmblüterherzens. *Pflüger's Arch. ges. Physiol.* 256: 68, 1952.
298. Turbe, F. and Ch. Scholtissek. Untersuchungen mit C^{14}-markierten Digitalis-Stoff. *Nauny- Schmiedebergs Arch. Exper. Path. u Pharmakol.* 222: 206, 1954.
299. Ussing, H. H. The alkali metal ions in biology. I. The alkali metal ions in isolated systems and tissues. In:

Handbuch der experimentellen Pharmakologie (Dreizehnter Band). Herausgegeben von O. Eichler and A. Farah. Berlin: Springer, 1960.

300. UYEKI, E. M., E. M. K. GEILING, AND K. P. DUBOIS. Studies on the effects of quinidine on intermediary carbohydrate metabolism. *Arch. internat. pharmacodyn.* 97: 191, 1954.
301. VARGA, L. Observations on the glycerol-extracted *musculus psoas* of the rabbit at higher temperature. *Enzymologia* 14: 212, 1950.
302. VAUGHAN WILLIAMS, E. M. The mode of action of quinidine on isolated rabbit atria interpreted from intracellular potential records. *Brit. J. Pharmacol.* 13: 276, 1958.
303. VAUGHAN WILLIAMS, E. M. The action of quinidine interpreted from intracellular potentials of single cardiac fibers. *Lancet* 1: 943, 1958.
304. VICK, R. L. AND J. B. KAHN, JR. The effects of ouabain and veratridine on potassium movement in the isolated guinea pig heart. *J. Pharmacol. & Exper. Therap.* 121: 389, 1957.
305. WASER, P. G. Bindung von Herzglykosiden an Actomyosin. *Helvet. physiol. et pharmacol. acta* 13: C37, 1955.
306. WASER, P. G. Über die Wirkung von Herzglykosiden auf Actomyosin. *Cardiologia* 29: 214, 1956.
307. WASER, P. G. Über die Wirkungvon Herzglykosiden auf Actomyosin: 3. Thixotropieveränderungen. *Helvet. physiol. et pharmacol. acta* 15: 125, 1957.
308. WASER, P. G. Verstärkte Bindung von Kaliumionen an Actomyosin durch herzwirksame Glykoside. *Helvet. physiol. et pharmacol. acta* 15: C42, 1957.
309. WASER, P. G. AND O. VOLKART. Wirkung von Herzglykosiden auf Actomyosin. *Helvet. physiol. et pharmacol. acta* 12: 12, 1954.
310. WEBB, J. L., P. R. SAUNDERS, AND K. NAKAMURA. The metabolism of the heart in relation to drug action. VI. Metabolic actions of quinidine on rat heart muscle. *J. Pharmacol. & Exper. Therap.* 101: 287, 1951.
311. WEBB, A. M. The influence of digoxin on the potassium content of heart muscle. *J. Pharmacol. & Exper. Therap.* 65: 268, 1939.
312. WEGRIA, R. AND M. N. BOYLE. Correlation between the effect of quinidine sulfate on the heart and its concentration in the blood plasma. *Am. J. Med.* 4: 373, 1948.
313. WEIDMANN, S. The effect of the cardiac membrane potential on the rapid availability of the sodium-carrying system. *J. Physiol.* 127: 213, 1955.
314. WEIDMANN, S. Effects of calcium ions and local anaesthetics on electrical properties of Purkinje fibers. *J. Physiol.* 129: 568, 1955.
315. WEIDMANN, S. Shortening of the cardiac action potential due to a brief injection of potassium chloride following the onset of activity. *J. Physiol.* 132: 157, 1956
316. WEIDMANN, S. Effect of increasing the calcium concentration during a single heart beat. *Experientia* 15: 128, 1959.
317. WEIMAR, V. L. Calcium binding in frog muscle brei. *Physiol. Zoöl.* 26: 231, 1953.
318. WEISE, E. Untersuchungen zur Frage der Verteilung und der Bindungsart des Calciums im Muskel. *Nauny-Schmiedebergs Arch. exper. Path. u Pharmakol.* 176: 367, 1934.
319. WEIZSÄCKER, V. Über die Abhängigkeit der Strophanthinwirkung von der Intensität der Herztätigkeit. *Nauny- Schmiedebergs Arch. exper. Path. u Pharmakol.* 72: 282, 1913.
320. WERSCHININ, N. Über die systolische und diastolische Herzwirkung des g-Strophanthins. *Nauny- Schmiedebergs Arch. exper. Path. u Pharmakol.* 63: 386, 1910.
321. WERSCHININ, N. Über die Herzwirkung der Bariumionen. *Nauny- Schmiedebergs Arch. exper. Path. u Pharmakol.* 66: 191, 1911.
322. WILBRANDT, W., K. BRAWAND, AND P. N. WITT. Die quantitative Abhängigkeit der Strophanthosidwirkung auf das Froschherz von der Tätigkeit des Herzens und von der Glykosidkonzentration. *Nauny- Schmiedebergs Arch. exper. Path. u Pharmakol.* 219: 397, 1953.
323. WILBRANDT, W. AND R. CAVIEZEL. Die Beeinflussung des Austritts von Calcium aus dem Herzmuskel durch Herzglykosid. *Helvet. physiol. et pharmacol. acta* 12: C40, 1954.
324. WILBRANDT, W. AND H. KOLLER. Die Calciumwirkung am Froschherzen als Function des Ionengleichgewichts zwischen Zellmembran und Umgebung. *Helvet. physiol. et pharmacol. acta* 6: 208, 1948.
325. WILDE, W. S., J. M. O'BRIEN AND I. BAY. Time relation between potassium K^{42} outflux, action potential and contraction phase of heart muscle as revealed by effluogram. *Proc. Intern. Conf. Peaceful Uses Atomic Energy* 12: 318, 1956.
326. WILKIE, D. R. Facts and theories about muscle. In: *Progress in Biophysics*, edited by J. A. V. Butler and J. T. Randall. New York: Academic Press, 1954, p. 288.
327. WILKINS, W. E. AND G. E. CULLEN. Electrolytes in human tissue. III. A comparison of normal hearts with hearts showing congestive heart failure. *J. Clin. Invest.* 12: 1063, 1933.
328. WINEGRAD, S. The relationship of calcium uptake to contraction in guinea pig atria. *Physiologist* 3 (No. 3): 179, 1960.
329. WITT, P. N. The effect of strophanthin and calcium on potassium loss from frog sartorius muscle. *J. Pharmacol. & Exper. Therap.* 119: 195, 1957.
330. WOLFF, J. Thyroidal iodide transport. I. Cardiac glycosides and the role of potassium. *Biochim. et biophys. acta* 38: 316, 1960.
331. WOLLENBERGER, A. Metabolic action of cardiac glycosides: I. Influence on respiration of heart muscle and brain cortex. *J. Pharmacol. & Exper. Therap.* 91: 39, 1947.
332. WOLLENBERGER, A. On the energy-rich phosphate supply of the failing heart. *Am. J. Physiol.* 150: 733, 1947.
333. WOLLENBERGER, A. The energy metabolism of the failing heart and the metabolic action of the cardiac glycosides. *Pharmacol. Rev.* 1: 311, 1949.
334. WOLLENBERGER, A. Non-specificity of the effect of cardiac glycosides on the polymerization of actin. *Experientia* 10: 311, 1954.
335. WOOD, J. C. AND H. L. CONN, JR. Potassium transfer kinetics in the isolated dog heart. Influence of contraction rate, ventricular fibrillation, high serum potassium and acetylcholine. *Am. J. Physiol.* 195: 451, 1958.
336. WOOD, E. H. AND G. K. MOE. Correlation between serum potassium changes in the heart-lung preparation and the therapeutic and toxic effect of digitalis glycosides. *Am. J. Physiol.* 129: 499, 1940.
337. WOOD, E. H. AND G. K. MOE. Electrolyte and water

content of the ventricular musculature of the heart-lung preparation with special reference to the effects of cardiac glycosides. *Am. J. Physiol.* 136: 515, 1942.

338. WOODWARD, A. A., JR. The release of radioactive Ca^{45} from muscle during stimulation. *Biol. Bull.* 97: 264, 1949.
339. WOODBURY, L. A. AND H. H. HECHT. Effects of cardiac glycosides upon the electrical activity of single ventricular fibers of the frog heart, and their relation to the digitalis effect of the electrocardiogram. *Circulation* 6: 172, 1952.
340. WOODWORTH, R. S. Maximal contraction, "staircase" contraction, refractory period, and compensatory pause of the heart. *Am. J. Physiol.* 8: 213, 1902.
341. ZERAHN, K. Studies on the active transport of lithium in the isolated frog skin. *Acta physiol. scandinav.* 33: 347, 1955.
342. ZONDEK, S. G. Das Ionengleichgewicht der Zellen. Gleichreitig ein Beitrag zur Physiologie des Natriums. *Biochem. Ztschr.* 121: 87, 1921.

Physiology of cardiac muscle

ROBERT E. OLSON | *Department of Biochemistry and Nutrition, University of Pittsburgh, Pittsburgh, Pennsylvania*

CHAPTER CONTENTS

FROM THE TIME of the discovery of the circulation of the blood (95) to the present, the molecular events underlying the motion of the heart have intrigued biologic scientists. Although a large amount of intensive research has been devoted to the elucidation of these processes, it must be admitted that many biochemical phenomena underlying contractility and the adaptability of the heart muscle to varying work loads are still visualized incompletely. It is clear, however, that the ability of the heart to do work is dependent upon the capacity of the enzyme systems in cardiac muscle to convert chemical energy, available in various substrates, to mechanical work. Even the shortening and lengthening of the myofibril in the contractile cycle must be viewed in a biochemical perspective.

The function of the heart is to pump the blood at a rate commensurate with the needs of the tissues. The purpose of this chapter will be to review the pertinent data drawn from many studies of ultrastructure and cellular physiology which shed light on the biochemical mechanisms underlying this essential function.

STRUCTURE OF THE HEART

Anatomy

The mammalian heart is a globular muscular organ with four chambers and a fibrous skeleton composed of four tendinous rings surrounding its four valvular orifices. The aortic ring is the strongest and is like a cuff. The other rings are less rigid but firm enough to prevent dilatation with valvular incompetence during cardiac systole. The atrial musculature is thin, translucent, and consists of only two layers oriented at right angles to each other. The ventricular muscle, contrastingly, is thick, opaque, and composed of three layers: one superficial, one middle, and one deep. The wall of the left ventricle is two to three times as thick as that of the right ventricle and constitutes the muscular foundation around which the other chambers of the heart are built (136). The thinner-walled right ventricle is fastened anteriorly and laterally, and may be described as a crescentric pocket attached to the left ventricle. Although the two ventricles are anatomically separate, they function physically as an essentially common musculature. The three layers of the ventricles are formed by four major bundles of muscle fibers which are *1*) the superficial sinospiral bundle; *2*) the superficial bulbospiral bundle; *3*) the deep sinospiral

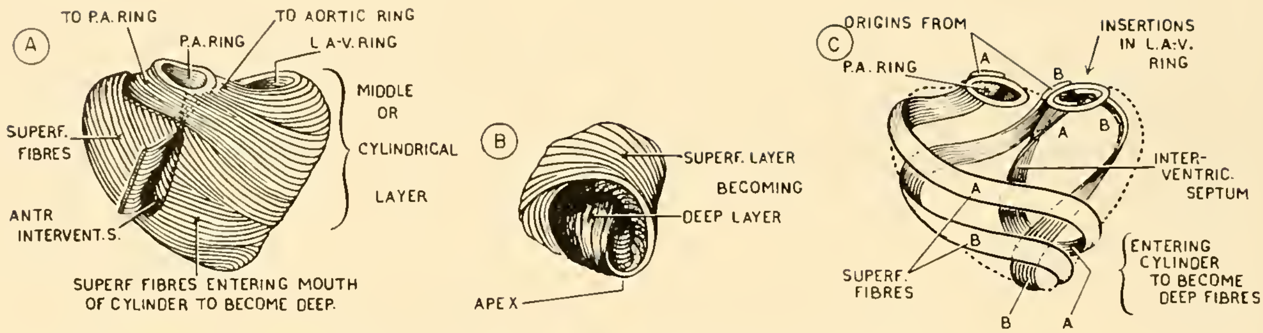

FIG. 1. Section of the mammalian heart. *A:* shows the superficial fibers of the sinospiral bundle sweeping toward the apex and entering the cylindrical layer of the left ventricle. *B:* shows the superficial fibers becoming deep while turning at the apex and proceeding at right angles beneath the middle layer to form the septum and the wall of an anterior papillary muscle. *C:* presents the full course of the superficial fibers of the sinospiral bundle as they become deep and enter the left ventricular cylinder. [From Grant (86).]

bundle; and *4*) the deep bulbospiral bundle. These bundles originate in the fibrotendinous ring structure at the base of the heart and converge in a spiral fission toward the apex where they form a vortex before running upward and returning via a spiral pathway to the opposite side of the fibrotendinous ring from which they began. As shown in figure 1 the superficial bundle and the sinospiral and the deep sinospiral bundle envelop portions of both ventricles, whereas the deep bulbospinal muscle encircles only the left ventricle. The superficial bulbospiral and sinospiral bundles originate laterally on their respective ventricles and sweep toward the apex, enveloping part of the opposite ventricle whereupon they burrow beneath the middle layer, which is comprised of the deep bundles, and return most deeply and at right angles to their original course to form the interior of the ventricles and the papillary muscles. The deep sinospiral bundle composes primarily the middle layer of the right ventricle, although its fibers ramify around both ventricles. The deep bulbospinal encircles the left ventricle at its base, does not reach the apex, and hence is unique among the bundles in being the possession of only one chamber. These relations are shown in figure 1.

Contraction of the deep and superficial layers serves to shorten the ventricles along their major axis, and contraction of the middle layer reduces their transverse diameters. According to Rushmer (206), reduction of the left ventricular cavity during systole involves only a slight decrease in length, but chiefly a reduction in transverse diameter. In contraction, the base of the heart descends toward the apex. Although this is not consistent with the usual action of a muscle acting from its point of origin (the base), it appears that one action of the sinospiral fibers is to confer rigidity on the apical portion of the septum which makes it a functional origin toward which all parts of the heart move during systole.

Vasculature of Heart Muscle

The heart muscle is nourished by the coronary arteries which terminate in a rich capillary vasculature. These capillaries form a plexus which invests the individual muscle fibers. The number of capillaries is three to four times as plentiful in cardiac muscle as in skeletal muscle and provides an average blood flow ten to twenty times as large (89). Roberts *et al.* (203) found an average of 3,342 capillaries per cubic milliliter of normal human heart muscle which had an average muscle fiber diameter of 13.9 μ and gave a minimum of one capillary for each muscle fiber. Direct coronary sinus catheterization of normal human subjects and dogs has shown that the coronary flow is about 100 ml per min per 100 g heart muscle, and that coronary arterial blood undergoes a much greater desaturation of its oxygen content than does arterial blood perfusing skeletal musculature (23, 221). Average values for oxygen content of coronary venous blood of 5 to 7 volumes per cent were found as compared to 14 to 15 volumes per cent for mixed venous blood.

Ultrastructure of Heart Muscle

The microscopic appearance of cardiac muscle is somewhat different from skeletal muscle despite the typical striated nature of both. Instead of longitudinal fasciculi of discrete muscle cells the heart is a syn-

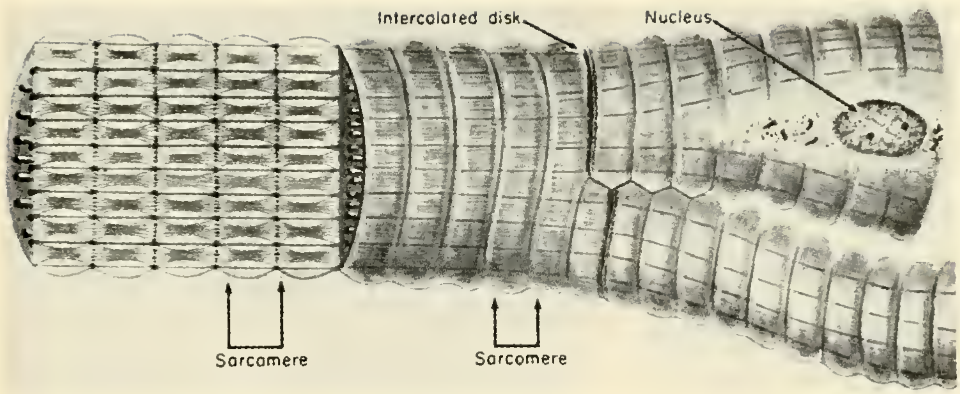

FIG. 2. A 3-dimensional view of a cardiac muscle cell. [From Licata & Roberts (136).

cytium composed of many branching fibers. A typical cardiac muscle fiber is shown in figure 2. The location of the oval nucleus is essentially central rather than peripheral as in skeletal muscle, and the intranuclear material is condensed into a reticulated framework which may change in appearance as the result of contraction and relaxation of the cell. One or more nucleoli are present. Around each pole of the tapered nucleus are accumulations of granular sarcoplasm. The sarcoplasm or muscle cytoplasm consists of a homogenous intracellular matrix which contains a variety of organelles and the myofibrils (the smallest anatomic contractile unit of the fiber).

The sarcolemma is a well-defined external limiting membrane which invests the muscle fiber but which is thinner than that found in skeletal muscle and presumably provides less resistance to the diffusion of substrates and gases in the highly aerobic cardiac muscle. The sarcolemma seems to be a procollagen which becomes collagenous at insertion points of the muscle bundles. In the electron microscope the sarcolemma of the heart appears as a double membrane separated by a clear space of 200 Å (191, 195). The inner membrane is more dense than the outer and is known as the plasma membrane.

Cardiac muscle is also characterized by intercalated discs which stain with silver nitrate and which occur at variable distances throughout the muscle, often at points of bifurcation of the fiber, shown in figure 2. The intercalated discs, when viewed in the electron microscope, appear to be jagged membranes superimposed on or merged with the Z membrane of the individual cell but spanning more than one myofibril. The Z membranes mark the boundaries of individual sarcomeres, the smallest anatomic units of the myofibril. The intercalated disc then represents the invagination and fusion of several plasma membranes. It would appear therefore that, although in the light microscope the heart appears to be a syncytium with cardiac muscle cells branching throughout the myocardium, actually the syncytial nature of the heart is more apparent than real. The myofibrils appear to terminate at the intercalated discs and support the view espoused by several anatomists (164) that the heart is in fact cellular and not syncytial in its ultimate organization.

The cross striations of skeletal and cardiac muscle are visible in both the light and polarizing microscope. These are due to periodic changes in the birefringence of the myofibrils which gives an alternating light and dark pattern to the muscle fiber as shown in figures 3 and 4. The dark A (anisotropic) band is light when viewed under a polarizing microscope, and the light I (isotropic) band is uniformly dark under polarizing conditions. The lower birefringence of the I band appears to be due to a lack of myosin in that portion of the myofibril rather than to the crosswise orientation of lipids as once thought (54). The dark A band is crossed centrally by a lighter H band and the I band is seen to be crossed by the dark Z membrane. The Z membrane appears to be a more or less helicoid continuous structure, uniting the fibrils to one another (probably with the aid of the endoplasmic reticulum) keeping them in register, and blending indistinguishably into the plasma membrane at the cell margins. The myofilaments proceed from one sarcomere to another through the Z band without interruption, although they apparently stop at the intercalated disc. When the myofibrils shorten, the noncontractile sarcolemma is thrown into periodic folds because of its points of attachment to the Z membrane.

As indicated earlier, the part of the fiber between two Z membranes is designated as the sarcomere and therefore consists of an A band and two half I bands. The sarcomere length from resting skeletal

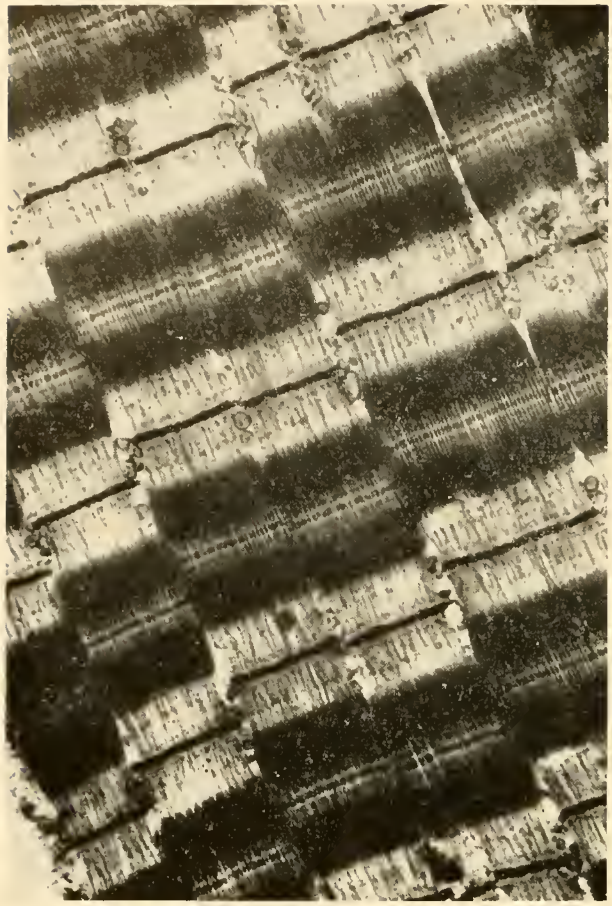

FIG. 3. Striated muscle bundles. Electron micrograph of longitudinal section of rabbit psoas muscle (by H. E. Huxley). Note the clearly delineated bands (A band = 1.5 μ). The sarcosomes are relatively few, small in size, and distributed mainly in the region of the I bands. [From Perry (191).]

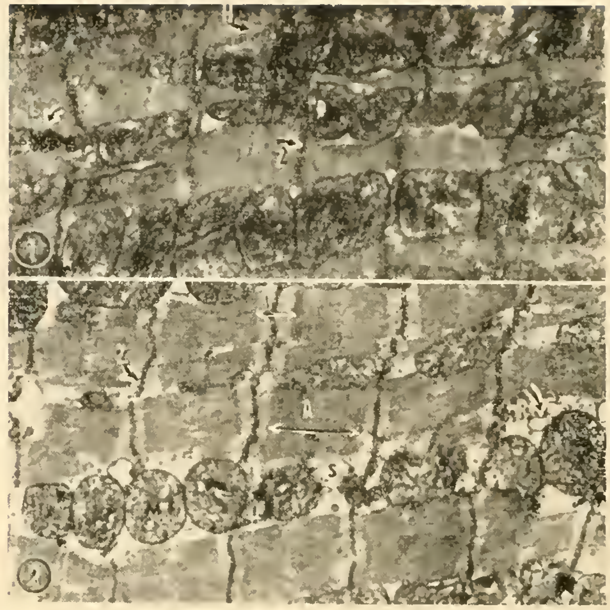

FIG. 4. Electronmicrograph of cardiac muscle from rat. From Bryant *et al.* (35).]

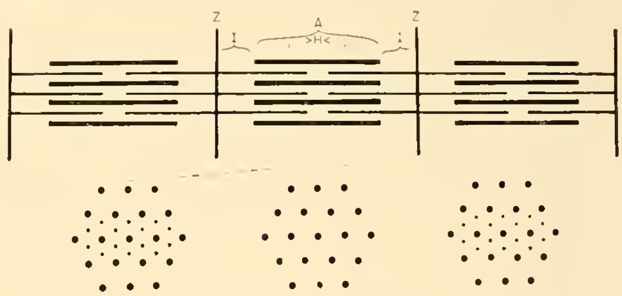

FIG. 5. Filament model of striated muscle. [From H. E. Huxley (109).]

muscle is of the order of 2 to 3 μ (190), whereas in the heart the range is from 1 to 2 μ. Myofibril diameter for both skeletal and cardiac muscles falls in the range of 0.5 to 2.0 μ (164). The cardiac muscle cells (fibers) themselves are 16 to 20 μ in diameter (196), and hence contain 200 to 300 myofibrils.

The skeletal myofibril, when examined in the electron microscope, is found to contain two types of myofilaments (107, 111): the primary filaments, approximately 100 Å in diameter and 1.5 microns in length, correspond to the A band of the fibril; the smaller secondary filaments are about 50 Å in diameter and extend to the Z membrane toward the center of the sarcomere where they are connected in the region of the H zone by very fragile S filaments. These relationships are shown in figure 5. The ultrastructure of the cardiac musculature does not differ significantly from that of skeletal muscle (123). Cardiac myofilaments also consist of thin 40 Å filaments and thicker 110 Å filaments closely related to those seen in skeletal muscle and related to the A and I bands in the same way. As in skeletal muscle the Z membrane seems to be a continuous structure across the fibril and forms a connecting bridge between individual filaments blending indistinguishably into the plasma membrane at the cell margin.

Cardiac muscle differs from skeletal muscle quantitatively in the abundance of mitochondria (sarcosomes) which lie crowded between the myofibrils as shown in figure 4. They measure 0.3 to 1.7 microns in length and 0.2 to 1.0 microns in width (164, 187). They possess a double membrane in common with other mitochondria, the inner membrane of which ramifies in numerous cristae which are the seat of the terminal respiratory chain of enzymes essential for aerobic metabolism (fig. 6) (103). The endo-

FIG. 6. Mitochondria from rat ventricle showing cristae. ×55,200. [From Siekevitz (216).]

plasmic reticulum which surrounds the sarcomeres at the level of the Z bands appears to communicate with the nucleus also. The mitochondria appear to lie in the sarcoplasm without attachment to the myofibril although, in contrast to other cells where the mitochondria can move freely in the cytoplasm, they are confined within the length of one sarcomere along the myofibrillar axis (190). Glycogen granules and, more rarely, fat droplets are also seen in normal cardiac muscle cells.

Myoglobin of Heart Muscle

Cardiac and red skeletal muscle are characterized by the presence of the red pigment myoglobin in the sarcoplasm. It is a conjugated protein containing an iron porphyrin prosthetic group which is closely related to hemoglobin. Its molecular weight is one-fourth that of hemoglobin (16,500 vs. 66,000) and it resembles but is not identical in amino acid composition with the monomer of hemoglobin, the latter being composed of four such iron-porphyrin protein

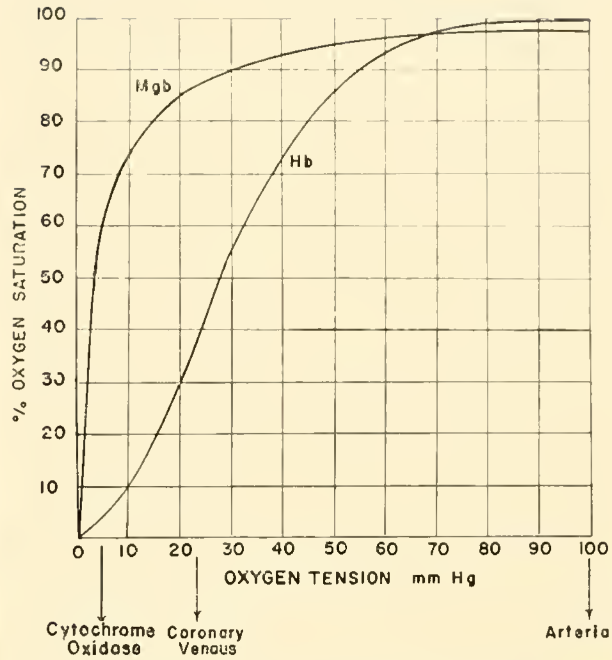

FIG. 7. Myoglobin (horse) and hemoglobin (human) oxygen dissociation curves at physiological temperature and pH [From Biorck (24).]

units. The porphyrins are identical (protoporphyrin IX) (159). The conformation of myoglobin and the specific folding of its peptide chain has been intensively studied by Kendrew (119) using X-ray diffraction methods.

The oxygen dissociation curve for myoglobin is hyperbolic in comparison with the curve for hemoglobin which is sigmoid (fig. 7). The sigmoid nature of hemoglobin's dissociation curve is due to the interaction between the four hemoprotein units in the hemoglobin molecule (42).

From figure 7 it may be seen that at coronary sinus P_{O_2}, hemoglobin is only 35 per cent saturated, whereas myoglobin is 85 per cent saturated. At the minimum effective P_{O_2} of cytochrome oxidase, the terminal electron transport enzyme (P_{O_2} = 5 mm Hg) myoglobin is still 60 per cent saturated. This signifies a limited oxygen storage function of myoglobin in heart and other red muscles, although the energy requirement of the mammalian heart is so high that the amount of oxygen stored by cardiac myoglobin would suffice to sustain only six additional cardiac beats at rest in the absence of oxygen and glycolytic energy sources. Of more significance than this oxygen storage capacity is the ability of myoglobin to facilitate the transport of oxygen through membranes (212a). This property would facilitate the

delivery of oxygen from the cell membrane to the mitochondria where terminal respiration actually occurs.

Myoglobin is found in largest quantities in muscles requiring relatively slow repetitive contractions of considerable force, maintained for long periods. Such muscular activity is characteristic of cardiac muscle and the breast muscles in larger flying birds, such as the pigeon and duck, and the leg muscles in running animals such as the horse and dog. The presence of myoglobin furthermore correlates with the presence of large numbers of mitochondria (sarcosomes) and a more aerobic metabolism. Myoglobin is not found in the leg muscles of jumping amphibia, such as the frog, and in the breast muscles of nonflying birds such as the chicken. It is also absent from the flight muscle of insects which contain large numbers of sarcosomes. These relationships suggest that myoglobin is present in those tissues where sustained activity and aerobic metabolism coincide, and rates of anaerobic glycolysis are insufficient to sustain the work requirement.

Cardiac muscle does not always contain the highest myoglobin concentration. The myoglobin content of heart muscle from young dogs is slightly higher than that of their skeletal muscle, but in adult dogs the myoglobin concentration of psoas muscle is twice as high as in cardiac muscle. Likewise, in horses the skeletal myoglobin concentration is higher than that of the heart (131). Values for myoglobin in a number of muscles are shown in the Appendix table. The content of cardiac muscle ranges from 0.40 to 1.50 per cent fresh weight. In the leg muscles of horse, dog, and man, the myoglobin concentration may be as high as 2.0 to 3.0 per cent (24).

Lipids of the Myocardium

The heart is relatively rich in complex lipids. It contains a large variety of phosphatides and related compounds, moderate amounts of cholesterol, and very little, if any, triglyceride under normal conditions. These lipids are distributed largely in the organelles of the cell. The mitochondria and microsomes (endoplasmic reticulum) have the richest content of lipid, 94 per cent of which is phospholipid and 6 per cent cholesterol (222). Since cardiac muscle is so rich in sarcosomes, the lipids of the heart reflect primarily the lipids of the cardiac sarcosome. Marinetti and co-workers (125, 151) have studied the distribution of lipids in pig heart and find that mitochondrial lipid represents approximately 60 per cent of the lipid isolated, the microsomes representing about 30 per cent, and the supernatant or the cytoplasm representing about 10 per cent. The myofibril (191) contains very little, if any, lipid. The remaining lipids are associated with granules, which can be isolated from the sarcoplasm (189) and the membrane. Ninety-one per cent of the sarcosomal lipid is phosphatide—distributed among inositol phosphatide, sphingomyelin, lecithin, plasmalogen, phosphatidal serine, phosphatidal ethanolamine, and polyglycerol phosphatide (cardiolipin) (228).

Cardiac microsomes contain more sphingomyelin and phosphatidal ethanolamine and less inositol phosphatide than do the sarcosomes. Marinetti and co-workers (150) have shown further that pig heart lecithin fraction contains 60 per cent of the diester-lecithin and 40 per cent of plasmalogen (monoester monoacetal lecithin). The fatty aldehydes appear to be mainly saturated, whereas the fatty acids associated with phospholipids of the heart are highly unsaturated.

The lipids of cardiac muscle are integral parts of tissue lipoproteins which provide a suitable matrix for the enzymatic activities of sarcosomes, microsomes, and nucleus of the cardiac muscle cell (149, 175). Stotz and collaborators (228) have shown that various purified enzymes of the sarcosome (cytochrome *b–c*, cytochrome *a–3*) have phosphatide, cholesterol and other lipids firmly attached to the enzyme micelle. Green & Järnefelt (88) have further shown that the electron transport system of the heart sarcosome can be fractionated to yield a variety of lipoproteins with enzymatic activity.

PATHWAYS OF CARDIAC METABOLISM

Metabolic processes in heart muscle may be divided into three general phases: *a*) energy liberation, *b*) energy conservation, and *c*) energy utilization. These phases are presented very schematically in figure 8 and will be discussed in detail. The phase of energy liberation includes those reactions by which the carbon-carbon and carbon-hydrogen bond energy of oxidizable substrate is liberated as free energy. The processes of glycolysis, fatty acid oxidation, and the common terminal oxidative reactions of the Krebs tricarboxylic acid cycle occur in phase 1. The net result of this biochemistry is the near quantitative conversion of the bond energy of substrate into the free energy of hydrogen electrons which are then available for transport to oxygen along a chain of electron transport enzymes located on the cristae

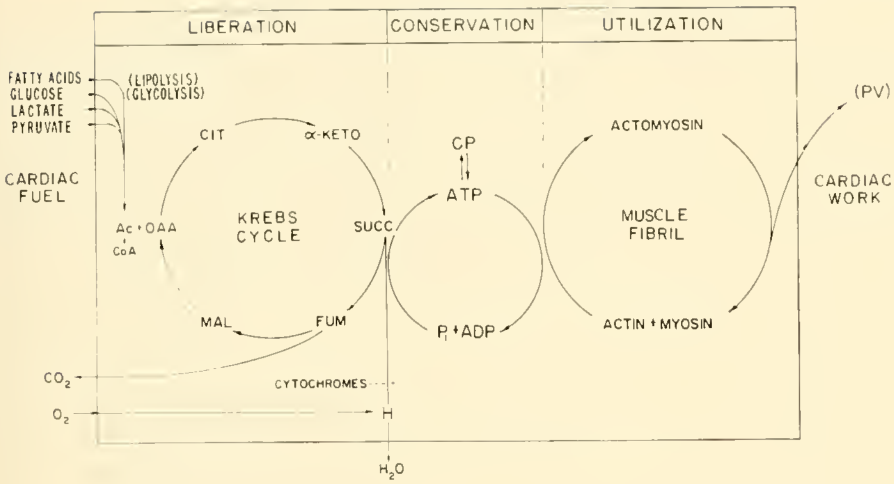

FIG. 8. Schema of energetics in cardiac muscle. [From Olson & Piatnek (181).]

of the sarcosome. The phase of energy conservation includes mainly the process of oxidative phosphorylation by which the electronic energy of hydrogen is converted into the terminal bond energy of adenosinetriphosphate (ATP) and creatine phosphate (CP). Some storage of energy as glycogen occurs at the substrate level in cardiac muscle and may also be included as a process of energy conservation.

The phase of energy utilization includes the mechanisms by which the high energy phosphate bonds of ATP are channeled into a variety of anabolic processes involving performance of chemical work and into the contractile process which results in mechanical work. Although there is considerable controversy about the model which best represents the contractile system (133, 167, 250), the model presented in figure 8 is consistent with most of the facts which have been determined experimentally and which are discussed below.

Energy Liberation

The pathways leading from oxidizable metabolite in the coronary blood to the final electron transport chain of enzymes in the cardiac sarcosome include *a*) glycolysis via Embden-Meyerhof schema, *b*) fatty acid oxidation, and *c*) terminal oxidation of fatty acid and carbohydrate carbon via the Krebs cycle. The glycolytic enzymes are found in the sarcoplasm, whereas the enzymes of fatty acid oxidation, pyruvic acid oxidation, and those of the tricarboxylic acid cycle are located in the sarcosome. The function of the electron transport enzymes themselves will be considered in the section on energy conservation.

GLUCOSE METABOLISM. The metabolism of glucose is initiated in heart muscle, as in most tissues, by the action of hexokinase, an enzyme which phosphorylates glucose with the aid of ATP to glucose-6-phosphate. Hexokinase is associated with both the soluble and the particulate portions of the cardiac muscle cell (50). The particulate hexokinase is probably associated with sarcolemma fragments and acts to facilitate the transport of glucose across the membrane. The product of the hexokinase reaction, glucose-6-phosphate, is a key metabolite because it may *a*) be converted to glycogen, *b*) be glycolyzed via the Embden-Meyerhof schema shown in figure 9, or *c*) undergo direct oxidation via the reactions of the Warburg-Dickens hexosemonophosphate shunt (55, 105, 198). Hydrolysis of glucose-6-phosphate to glucose, a reaction characteristic of liver and kidney, and dependent upon glucose-6-phosphatase, does not occur in cardiac or skeletal muscle because of the absence of the phosphatase. Pathways (*a*) and (*c*) which are pathways of less importance in the heart will be discussed subsequently.

Glycolysis. The reactions of the Embden-Meyerhof pathway are well presented in a variety of standard textbooks of biochemistry (74) and summarized in figure 9. Following the initial phosphorylation, glucose-6-phosphate undergoes an isomerization to fructose-6-phosphate catalyzed by the enzyme phosphohexoseisomerase. The second phosphorylation of glycolysis catalyzed by phosphofructokinase, and driven by ATP, converts fructose-6-PO_4 to fructose-1,6-diphosphate. Olson (182, 183) has presented evidence that strongly suggests that phosphofructokinase is the limiting enzyme of glycolysis in liver, a tissue with a relatively low glycolytic rate, and Cori (46) and Neifakh & Melnikova (169) have claimed that this same enzyme limits the maximum over-all rate of glycolysis in muscle.

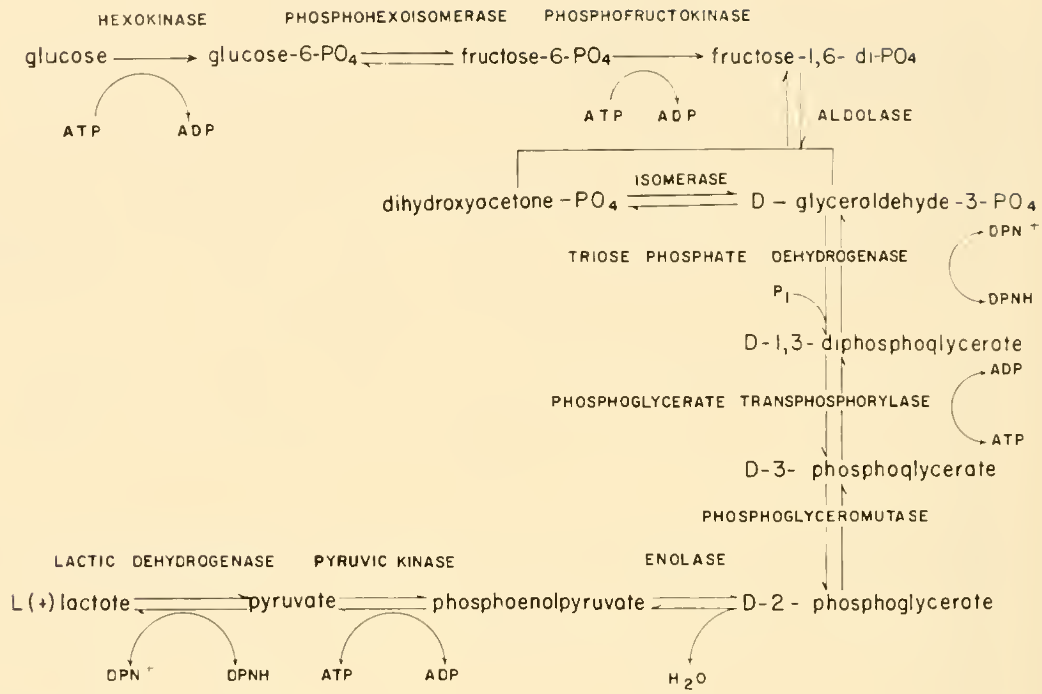

FIG. 9. The Embden-Meyerhof pathway for glycolysis.

The enzyme aldolase converts fructose-1,6-diphosphate to a mixture of two triose phosphates, dihydroxyacetone phosphate, and glyceraldehyde phosphate. A triose phosphate isomerase catalyzes the interconversion of the two. The oxidation reduction in anaerobic glycolysis involves the oxidation of D-glyceraldehyde-3-phosphate in the presence of inorganic phosphate and DPN^+ to D,1,3-diphosphoglyceric acid and DPNH. The D,1-3-diphosphoglyceric acid then reacts with ADP to yield D,3-phosphoglyceric acid plus ATP. A second mole of ATP is formed subsequently through the hydrolysis of phosphoenolpyruvic acid to pyruvic acid. In anaerobiosis (which is rare in cardiac muscle) the DPNH formed in the oxidation of D-glyceraldehyde-3-phosphate is oxidized by pyruvate to form lactate with the regeneration of DPN^+. Usually the DPNH formed aerobically via glycolytic reactions is oxidized by sarcosomal DPN^+ to initiate the transport of this hydrogen to O_2.

As noted above, two high energy phosphate bonds are derived from each mole of triose glycolyzed, i.e., four per mole of glucose. The net yield of ATP in glycolysis, however, is 2 moles of ATP per mole of glucose, since 2 moles of ATP are required by the kinases. The limited formation of ATP represents an over-all energy liberation in glycolysis of only 9 per cent of the energy content of glucose. The over-all reactions of glycolysis can be written:

$$\text{Glucose} + 2\,\text{ATP} + 2\,\text{P}_i + 2\,\text{ADP} \xrightleftharpoons[\qquad]{\text{glycolytic enzymes}} 2\,\text{lactate} + 4\,\text{ATP} \qquad (1)$$

In addition to the enzymes themselves, and their cofactors (168), it is obvious that any of the four terms on the left side of the equation may limit the rate of glycolysis (199). In the intact heart, because of the very vigorous oxidative phosphorylation occurring in the sarcosome (248), ADP is most likely to be limiting. In general, the concentrations of the glycolytic enzymes in cardiac muscle are not as high as those of skeletal muscle (Appendix table), although evidence to decide whether enzyme concentrations are actually limiting under in vivo conditions is lacking for the cardiac muscle cell.

Under aerobic conditions, which are essential for in vivo activity of heart muscle, the terminal reaction of glycolysis, i.e., the reduction of pyruvate, does not occur. In fact, lactate and glucose are simultaneously extracted from the coronary blood and metabolized to carbon dioxide and water. This suggests that the capacity of the sarcosome for hydrogen transport greatly exceeds the glycolytic rate under the usual conditions. The sarcoplasmic DPNH,

associated with glyceraldehyde-dehydrogenase and lactic dehydrogenase, must therefore react with sarcosomal DPN^+ to initiate hydrogen transport. The report that α-glycerophosphate is an obligatory intermediate in the transfer of hydrogen from soluble DPNH to mitochondrial DPN^+ in insect flight muscle has not been explored in heart muscle. von Korff & Twedt (247) have shown that heart mitochondria will oxidize lactate in the presence of added purified lactic dehydrogenase and DPN^+, and Brin *et al.* (33) have shown that L(+) lactate-U-C^{14} is oxidized to pyruvate-U-C^{14} and $C^{14}O_2$ in heart slices. These workers also showed that lactic dehydrogenase was limiting in the oxidation of lactate in heart muscle.

The glycolytic reactions are essentially reversible as indicated in equation 1. DPNH and ATP are, of course, required to regenerate hexose phosphate from pyruvate, and both are available in the cardiac muscle cell. Hexosediphosphate phosphatase is also present in heart muscle and provides reversibility to the phosphofructokinase step (fig. 10). The phosphorylation of pyruvate by ATP is accomplished with great difficulty because the equilibrium of the pyruvic kinase reaction shown below lies far to the right:

$$\text{phosphoenolpyruvate} + \text{ADP} \xrightleftharpoons{K^+} \text{pyruvate} + \text{ATP} \quad (2)$$

To circumvent this thermodynamic difficulty a system exists in cardiac muscle and certain other tissues for converting pyruvate to PEP (phosphoenolpyruvate) without employing the pyruvic kinase reaction. This sequence of reactions, known as the Utter-Ochoa cycle, is shown in figure 10, and provides the means for converting pyruvate to PEP by way of malate and oxaloacetate.

The first step, the conversion of pyruvate to malate, catalyzed by "malic enzyme," was first demonstrated in pigeon liver by Ochoa *et al.* (171). This TPNH dependent reaction occurs in the sarcoplasm. Since malate is freely diffusible, conversion of malate to oxaloacetic acid can occur in the mitochondria, by one of the established steps of the Krebs cycle. Utter & Wood (243) discovered an enzyme which catalyzes reversible reaction:

$$CO_2 + \text{phosphoenolpyruvate} + \text{GDP} \rightleftharpoons \text{oxaloacetate} + \text{GTP} \quad (3)$$

This reaction provides a means for forming phosphopyruvate from oxaloacetic acid with much more favorable equilibrium constant. The phosphoenolpyruvate-carboxykinase reaction occurs in the mitochondria and hence can make full use of oxaloacetic acid present there. The oxaloacetic acid can then be converted to PEP with the evolution of CO_2. PEP is convertible to glycogen by reversal of the reactions of glycolysis.

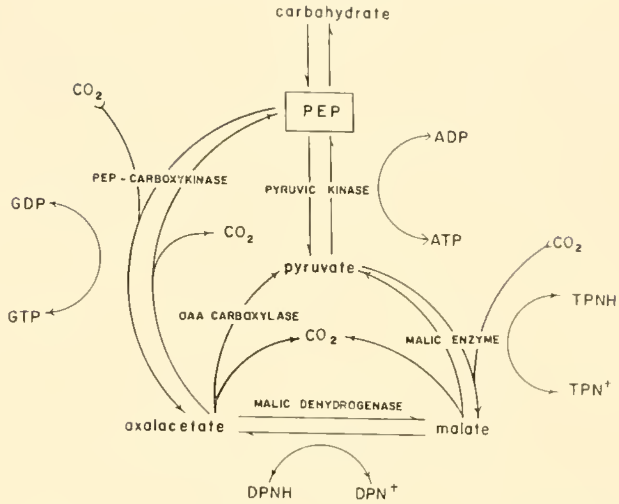

FIG. 10. Utter-Ochoa pathway for synthesis and breakdown of phosphoenolpyruvate.

Cardiac muscle contains all the enzymes concerned, although PEP carboxykinase is low in comparison with liver and kidney but high in comparison with skeletal muscle. The "malic enzyme" is present in abundant amounts in heart muscle, as is pyruvate kinase. Stadie *et al.* (223) have shown rat heart slices form glycogen from glucose, but were unable to demonstrate glycogen formation from lactate, pyruvate, or alanine. On the other hand, Lorber *et al.* (139, 140) showed that $C^{14}O_2$ could be incorporated into the glycogen of the isolated cat heart incubated with glucose and lactate. These workers found that heart glycogen acquired a substantial labeling under these circumstances in a relatively short time and the results suggest that the isolated heart has a capacity of synthesizing glycogen by the dicarboxylic acid pathway, by reversal of the pyruvic kinase reaction or by both mechanisms. Glycogen synthesized from pyruvate 2-C^{14} (239, 259) produced label in the 1, 2, 5, and 6 positions of glycogen with almost equal specific activity, suggesting that equilibration through a dicarboxylic acid had occurred prior to resynthesis.

In summary, glycolysis of glucose to pyruvate via the Embden-Meyerhof pathway is an important pathway in cardiac muscle, but is not sufficient to generate enough ATP for the energy needs of the heart nor to deliver 3-carbon compounds at the rate required in the terminal oxidation pathway. The

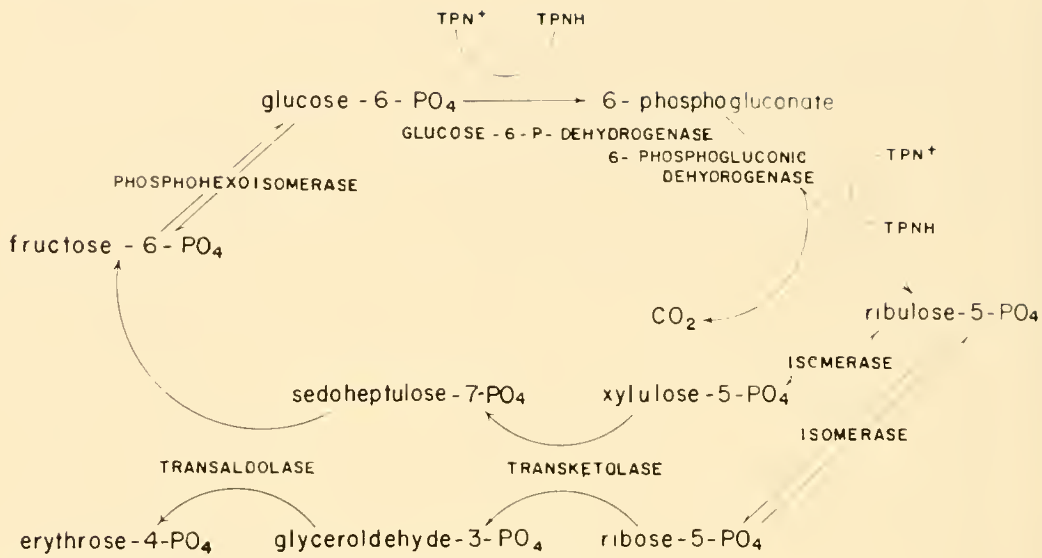

FIG. 11. The hexomonophosphate pathway (pentose shunt) for glucose oxidation.

reactions of glycolysis are reversible in cardiac muscle with the aid of the Utter-Ochoa cycle, although the synthesis of glycogen from pyruvate is not quantitatively important.

Pentose phosphate shunt. A second fate of glucose-6-phosphate in cardiac muscle is the direct oxidation via the TPN-dependent hexose monophosphate shunt. The details of the metabolism of pentose-phosphate and the proof of a pentose-hexose cycle is largely due to the work of Horecker & Mehler (105) and Racker (198). The first reaction of this cycle is catalyzed by glucose-6-phosphate dehydrogenase (named Zwischenferment by Warburg) and results in the formation of 6-phosphogluconolactone and TPNH followed by enzymatic hydrolysis of the lactone to 6-phosphogluconic acid. A second TPN-dependent dehydrogenase then converts the 6-phosphogluconic acid to ribulose-5-phosphate with the loss of a molecule of CO_2. In these two steps four electrons are transferred to TPN^+ to form two molecules of TPNH which does not merge with the hydrogen derived from DPN-dehydrogenase catalyzed oxidations destined for transport to oxygen in the sarcosome, but remains in a sarcoplasmic pool for synthetic reductions required in the formation of fatty acids, sterols, and other structural components of heart muscle. The ribulose-5-phosphate is isomerized to ribose-5-phosphate and xylulose-5-phosphate, and these pentose phosphates are converted via transketolase (which requires thiamin pyrophosphate as a coenzyme) and transaldolase to a variety of 3-, 4- and 7-carbon sugar-phosphates, and ultimately to fructose-6-phosphate. This provides the basis for a pentose-hexose cycle with a limited oxidation of glucose as shown in figure 11. The over-all reaction of this cycle is:

$$6 \text{ glucose-6-phosphate} \rightarrow 6CO_2 + 5 \text{ glucose-6-phosphate} \quad (4)$$

The quantitative extent of this shunt varies in different tissues. Glock & McLean (80) have studied the distribution of the enzymes glucose-6-phosphate dehydrogenase and 6-phosphogluconate dehydrogenase and found these enzymes plentiful in actively synthesizing tissues such as adrenal, lactating mammary gland, lymphatic tissues, and embryonic tissues, moderate in liver and low in both skeletal and cardiac muscle. A study of fetal and adult cardiac muscle by Jolley and associates (113), who employed glucose-C^{14} labeled in various carbon atoms, revealed a significant pentose shunt in rapidly growing fetal heart tissue but a negligible one in adult pig heart homogenates. The over-all glucose oxidation rate, however, was 3 to 4 times as high in adult as in fetal tissue. The need for TPNH for synthetic reactions is apparently not high in cardiac muscle.

Glycogenesis and glycogenolysis. A third fate of glucose-6-phosphate is conversion to glycogen. Although this may be viewed as a form of energy conservation (at the substrate level), it is considered in this section because of its important relationship to the pathways of glucose metabolism.

Glycogen is a highly branched polysaccharide with a molecular weight of 10^6 to 10^7, consisting of 1,4- and 1,6-α-D-glucoside residues. It occurs in heart

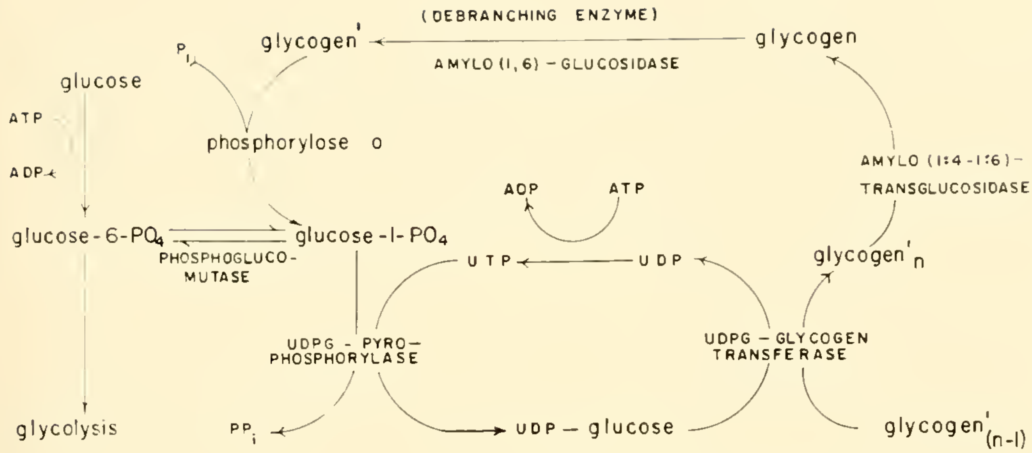

FIG. 12. Pathways for glucogenesis and glucogenolysis in cardiac muscle.

primarily as sarcoplasmic granules. The glycogen content of muscle ordinarily ranges from 0.4 to 0.6 per cent of the fresh tissue weight (220). Cardiac glycogen level is maintained very constant under a variety of conditions including those which tend to deplete glycogen in liver and skeletal muscle, such as prolonged fasting (145) and diabetes (114). Under the influence of glucose plus insulin the cardiac glycogen may rise as high as 1.2 per cent (43). After cardiac arrest or acute anoxia, due to coronary ligation, cardiac glycogen falls with the formation of lactic acid via the reactions of glycolysis. The working heart demonstrates more rapid glycogenolysis than the quiescent excised heart under anoxic conditions (28). It has been suggested by Bloom *et al.* (28, 207) (on the basis of differential extractibility of muscle glycogen by trichloracetic acid and KOH after tissue digestion) that two forms of glycogen exist in muscle tissue, one labile and extractible by TCA and one fixed to protein and extractible only after digestion. In the dog heart (43, 155) the TCA-extractible fraction is about 80 per cent of the total and appears to be more labile physiologically under conditions favoring both glycogenesis and glycogenolysis. It is possible that the labile fraction exists as free granules in the sarcoplasm, whereas the stabile fraction is bound to one of the organelles or other structure.

Glycogenesis and glycogenolysis occur via separate pathways in cardiac muscle. These are presented in figure 12. Glucogenesis from glucose-6-phosphate involves four enzymatic steps. First the glucose-6-phosphate is corrected to glucose-1-phosphate by phosphoglucomutase. The glucose-1-phosphate then reacts enzymatically with uridinetriphosphate to give UDP-glucose plus pyrophosphate. An enzyme known as UDPG-glycogen transferase then transfers a glucose residue from UDPG to an oligosaccharide to give a 1:4 glucoside of this oligosaccharide (glycogen). The branching enzyme amylo, -1:4 to 1:6-transglucosidase then creates a branch point in the glycogen molecule by transferring a glucose residue from the linear 1:4 sequence to a 1:6 linkage. In this way the glycogen molecule is built up. The UDP formed in the sequence is rephosphorylated to UTP by reaction with ATP.

Glycogenolysis is the result of the action of two different enzymes, phosphorylase and the debranching enzyme (1,6-amyloglucosidase). Phosphorylase *a*, the biologically active form of the enzyme from skeletal muscle has a molecular weight of 500,000. It is formed from the inactive phosphorylase *b*, which has a molecular weight of 250,000 (118) by an ATP driven kinase which phosphorylates the inactive enzyme and forms a dimer which is active. This reaction is shown below:

$$\text{2 phosphorylase } b + 4\text{ ATP} \xrightarrow[\text{Mn}^{++}]{\text{kinase}} \text{phosphorylase } a + 4\text{ ADP} \quad (5)$$

The reversal of this reaction, i.e., the breakdown of phosphorylase *a* to phosphorylase *b* is catalyzed by another enzyme known as the PR enzyme viz:

$$\text{phosphorylase } a \xrightarrow{\text{PR enzyme}} \text{2 phosphorylase } b + 4\text{ P}_i \quad (6)$$

The presence of PR enzyme in muscle tends to retard glycogenolysis by inactivating phosphorylase.

Epinephrine is instrumental in stimulating phos-

phorylase *a* formation by activating phosphorylase *b* kinase (230). In the liver this results in glucose output via glucose-6-phosphatase, but in cardiac muscle the only result is increased glycolysis (200). A study of the phosphorylases present in dog heart (201) has confirmed the general outlines of the enzymatic interconversions outlined above (99). It has also been shown by immunochemical studies that the phosphorylases in different tissues and species of animal are closely related but not identical.

Acute anoxia in heart muscle is a potent stimulant to glycogenolysis. Under these conditions the absence of epinephrine does not alter the rate of glycogen breakdown (28). The amount of cardiac work which can be sustained through glycolysis under these conditions is relatively small. At resting metabolic rate it may be shown that with an initial glycogen concentration of 0.6 per cent the energy requirements of the heart can be sustained through glycolysis alone for only 4.2 min. In quiescent heart muscle under conditions of complete anaerobiosis the rate of glycogenolysis is considerably slower (43). Hypothermia reduces the glycogen content of heart muscle through some obscure mechanism (112) even though total respiration is greatly reduced.

The fact that glycogen is synthesized and degraded by independent pathways in muscle brings the storage of glycogen under a variety of controls. Significant among these controls are genetic factors which may give rise to enzyme deficiencies and result ultimately in glycogen storage disease. Stetten & Stetten (227) have recently reviewed six types of glycogenoses of which at least two are applicable to the heart. One type of cardiac glycogenosis is due to a deficiency of the debranching enzyme, i.e., amylo-1,6-glucosidase (47); another more common type (Pompe's disease) has no known explanation, since the enzymes necessary for synthesis and degradation of glycogen seem to be present in normal concentration (56).

PYRUVATE OXIDATION. Pyruvate derived from glycolysis or obtained directly from the coronary blood is converted to acetyl-CoA in heart sarcosomes by an enzyme pyruvic dehydrogenase first characterized by Schweet *et al.* (213) from pig heart and pigeon breast muscle. This enzyme complex of molecular weight 4×10^6 requires five cofactors: thiamine pyrophosphate, α-lipoic acid, DPN^+, coenzyme A, and Mg^{++} ions, and catalyzes the multistage reaction sequence in figure 13.

The 2-carbon fragment formed after decarboxylation of pyruvate forms transitory compounds with

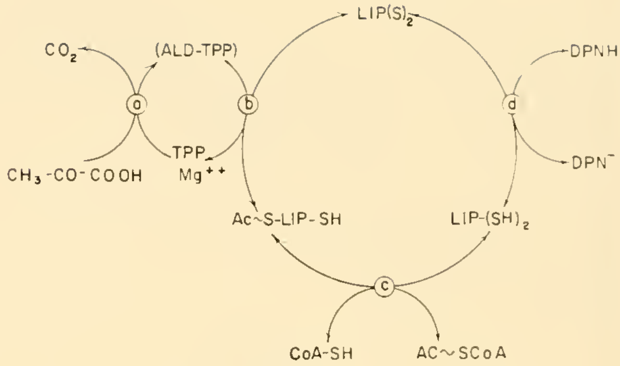

FIG. 13. The pyruvic dehydrogenase system. This enzyme system is composed of four enzymes, indicated by letter, which are as follows: (a) pyruvate decarboxylase; (b) hydroxyethylthiaminepyrophosphate-lipoic acid transacetyl reductase; (c) dihydroacetyllipoic acid-coenzyme A transacetylase; (d) dihydrolipoic acid dehydrogenase.

three coenzymes of the pyruvic-dehydrogenase complex before entry into the Krebs tricarboxylic acid cycle. The first is hydroxyethylthiaminepyrophosphate (32, 127) or "active acetaldehyde," the second is acetyl-lipoic acid (90), and the third is acetyl-coenzyme A (144) or "active acetate," representing the oxidation states of the 2-carbon fragment during the oxidation of pyruvate to acetate.

Acetyl-CoA can undergo a variety of fates in metabolism including hydrolysis to acetic acid, condensation with oxaloacetic acid to initiate the tricarboxylic acid cycle, or condensation with other molecules of acetyl-CoA or acetyl acceptors to form fatty acids, cholesterol, and other acetyl derivatives. The first and last pathways are very weak in sarcosomes so that in cardiac muscle almost all of the acetyl-CoA formed is converted to citrate by the condensing enzyme, first crystallized from heart muscle by Ochoa *et al.* (172). Cardiac muscle is the richest source of this enzyme in the animal body. Acetate can be directly activated to acetyl-coenzyme A by an enzyme in heart muscle (13, 97) which catalyzes the following reaction:

$$\text{acetate} + \text{ATP} + \text{CoA-SH} \rightleftharpoons \text{acetyl-CoA} + \text{AMP} + \text{PP} \quad (7)$$

This reaction involves the intermediate formation of an acyl-adenylate (17) and has an equilibrium constant close to 1.0. In heart muscle the reaction is forced to the right by the presence of large amounts of citrate condensing enzyme and a high level of ATP.

The final common pathway for the oxidation of acetyl groups derived from many sources is the Krebs citric acid cycle. This cycle, first advanced by Krebs & Johnson (128), is shown in figure 14. The purpose

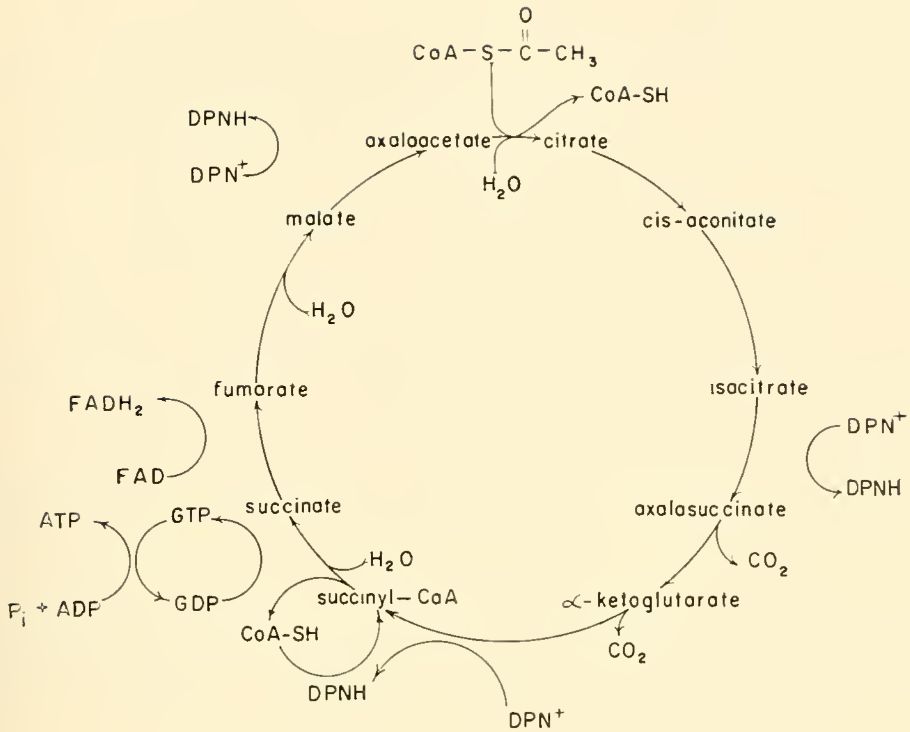

FIG. 14. The Krebs citric acid cycle.

of the cycle, as indicated earlier, is to convert the bond energy of the acetyl moiety of acetyl-CoA to 1 mole of ATP and to DPNH and $FADH_2$ bound electrons for transport to oxygen via the electron transport chain. The cycle thus accomplishes the reaction:

$$CH_3CO\text{—}S\text{—}CoA + 3DPN^+ + FAD + 3H_2O + ADP + P_i \rightarrow 2CO_2 + CoASH + 3DPNH + FADH_2 + 3H^+ + ATP \quad (8)$$

The dehydrogenases of the citric acid cycle are all contained in the mitochondrion and, with exception of succinic dehydrogenase, are all DPN-dependent. The TPN-dependent isocitric dehydrogenase (170) isolated from heart is found in the cytoplasm (212). All of the dehydrogenase of the citric acid cycle are present in heart muscle in high amount, reflecting the large number of cardiac sarcosomes as well as their richness in hydrogen transport enzymes. The cofactors for enzymes of the citric acid cycle, thiamine-pyrophosphate (TPP), coenzyme A (CoA-SH), diphosphopyridine nucleotide (DPN), and flavin-adeninedinucleotide (FAD) are all abundantly present in cardiac muscle. Comparative data for these coenzymes or their vitamin constituents for heart and skeletal muscle are shown in the Appendix table. It is obvious that depletion of these coenzymes through severe B-complex vitamin malnutrition could seriously reduce the capacity of the heart for energy production.

In the oxidation of glucose, 35 per cent of the bond energy of the molecule is released (2 moles of net ATP at the substrate level in glycolysis and 4 moles of DPNH formed in lactic and pyruvic dehydrogenations) prior to the formation of acetyl-CoA. In the Krebs cycle the remaining 65 per cent of the energy of glucose is transformed into 2 moles of ATP (formed in the phosphorylation of ADP by succinyl-CoA) 6 moles of DPNH, and 2 moles of $FADH_2$. The release and conservation of the energy stored in pyridine and flavin nucleotides is accomplished in the process of electron transport to oxygen.

AMINO ACID OXIDATION. Amino acids do not provide a major source of energy for cardiac muscle. Intracellular cardiac amino acid metabolism is not brisk and deamination is minimal. The intermolecular transfer of amino groups is particularly active in cardiac muscle, however, due to the presence in large amounts of two transaminases, glutamic-oxaloacetic transaminase (GOT) and glutamic-pyruvic transaminase (GPT). These enzymes provide a portal of entry of amino acid carbon into the tricarboxylic acid cycle at three points, i.e., alanine→pyruvate; aspartate→oxaloacetic, and glutamic→ketoglutaric

without a net oxidation of amino acid. Glutamate can be oxidized directly by glutamic dehydrogenase present in mitochondria, but the equilibrium constant favors glutamate formation (173).

FATTY ACID OXIDATION. Fatty acids and their partial oxidation products β-hydroxybutyric acid and acetoacetic acid are rapidly oxidized by cardiac muscle and, under conditions of fasting, may contribute as much as 80 per cent of the energy required by the heart. The β-oxidation hypothesis of Knoop (124), developed by feeding intact animals phenyl-fatty acids, has been elaborated in an elegant manner at the enzymatic level by Lehninger (132), Lynen (144), and Green (87) during the past two decades.

The sarcosome is the seat of the enzymes concerned with fatty acid oxidation. Fatty acids presented to the heart via nonesterified fatty acids bound to albumin (NEFA) are transported to the mitochondrion probably via the endoplasmic reticulum. An obligatory reaction for further oxidation is the conversion of these fatty acids to acyl-S-CoA derivatives by the following reaction:

$$\text{fatty acid} + \text{CoA—SH} + \text{ATP} \xrightarrow[\text{Mg}^{++}]{\text{thiokinase}} \text{acyl—S—CoA} + \text{AMP} + \text{PP} \qquad (9)$$

Three distinct thiokinases are known which carry out this reaction for fatty acids of different chain length, one for acetic and propionic acids discussed previously, one for acids of chain length C4–12 (146), and one for acids of chain length C10–18 (126). The β-oxidation of the CoA derivative then proceeds to produce two-carbon units sequentially as molecules of acetyl-coenzyme A which may undergo any of the possible fates of acetyl-CoA. In heart muscle, all but a very small percentage is oxidized to CO_2 and H_2O via the citric acid cycle.

More specifically, fatty acyl-CoA derivatives are oxidized in three steps to the corresponding β-ketoacyl derivative and then subjected to fission by the enzyme β-ketoacyl-CoA thiolase in the presence of CoA—SH to form a molecule of fatty acyl-CoA derivative two carbons shorter in length than the original, plus a molecule of acetyl coenzyme A. This process is repeated until the fatty acid is completely degraded to acetyl-CoA, viz.:

$$\text{R—CH}_2\text{—CH}_2\text{—CO—S—CoA} + \text{FAD} \xrightleftharpoons{\text{fatty acyl CoA dehydrogenase}} \text{R—CH=CH—CO—S—CoA} + \text{FADH}_2 \qquad (10)$$

$$\text{R—CH=CH—CO—S—CoA} + \text{HOH} \xrightleftharpoons{\text{unsaturated fatty acyl—CoA hydrase}} \text{RCHOH—CH}_2\text{—CO—S—CoA} \qquad (11)$$

$$\text{RCHOH—CH}_2\text{—CO—S—CoA} + \text{DPN}^+ \xrightleftharpoons{\beta\text{-hydroxyacyl—CoA dehydrogenase}} \text{R—CO—CH}_2\text{—CO—S—CoA} + \text{DPNH} + \text{H}^+ \qquad (12)$$

$$\text{RCO—CH}_2\text{—CO—S—CoA} + \text{CoA—SH} \xrightarrow{\beta\text{-ketoacyl—CoA thiolase}} \text{RCO—S—CoA} + \text{CH}_3\text{—CO—S—CoA} \qquad (13)$$

The initial oxidation of the fatty acyl-CoA derivative is FAD-dependent and hence electrons from this oxidation enter the electron transport chain at a different point than do those from the DPN catalyzed-oxidation of the β-hydroxylacyl-CoA derivative. Twenty-five per cent of the energy of a fatty acid is released during the first two oxidative steps leading to acetyl-CoA formation and 75 per cent is released during the subsequent reactions of the citric acid cycle.

The ketone bodies, acetoacetate and D(—) β-hydroxybutyrate, produced in liver as by-products of fatty acid metabolism through the action of acetoacetyl-CoA deacylase and β-hydroxybutyric acid dehydrogenase, are well oxidized by the intact heart and by heart sarcosomes. β-Hydroxybutyric acid is oxidized to acetoacetate by a DPN-dependent dehydrogenase present in sarcosomes. The acetoacetate is then activated by an acyl transferase enzyme driven by the energy-rich succinyl-CoA (225) as follows:

$$\text{succinyl—CoA} + \text{acetoacetate} \rightarrow \text{acetoacetyl—CoA} + \text{succinate} \qquad (14)$$

The acetoacetyl-CoA then undergoes cleavage by β-ketoacyl-CoA thiolase to form 2 moles of acetyl-CoA which then undergoes terminal oxidation in the citric acid cycle. No acetoacetyl-CoA deacylase is present in heart muscle so that no loss of acetoacetate can occur.

Energy Conservation

HYDROGEN TRANSPORT AND OXIDATIVE PHOSPHORYLATION. The oxidations which occur in glycolysis, in pyruvic and fatty acid oxidations, and in the reactions of the tricarboxylic acid cycle are enzymatic dehydrogenations. As noted previously, the hydrogen

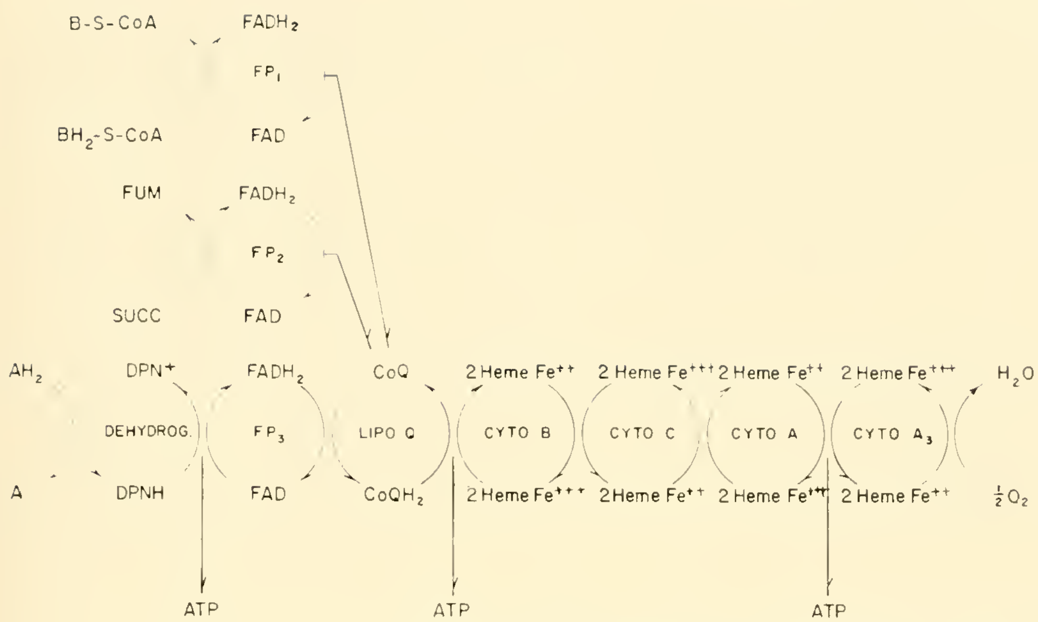

FIG. 15. Electron transport chain. The interrelated oxidation reductions of the hydrogen transport enzymes are shown. The main pathway shown at the bottom is for the DPN-linked dehydrogenases. The pathways shown above are for fatty acyl-CoA derivatives and for succinate. These are flavin-linked dehydrogenases. The indicated points for formation of ATP are tentative and are based upon evidence available at this time.

released or its electron ($H \rightarrow H^+ + e$) does not combine immediately with oxygen but reacts with a series of hydrogen transport enzymes in the electron transport chain before combining with oxygen to form water, as shown by the following over-all reaction:

$$DPNH + H^+ + \tfrac{1}{2}O_2 \rightarrow 2DPN^+ + H_2O + \Delta F(52\,kC) \quad (15)$$

The energy of this current of electrons is tapped off at three places in the respiratory chain to form energy-rich phosphate bonds. Approximately 12 kcal are required to phosphorylate ADP to ATP. The terminal bonds of ATP are then available to the cardiac muscle cell for performing cellular work of all kinds.

On the basis of studies of the effect of CN and CO on the respiration of sea urchin eggs, Warburg suggested in 1926 that an important iron-containing substance (Atmungsferment) was present in cells which transferred hydrogen to molecular oxygen. In 1925 Keilin (116) identified three iron-heme enzymes in heart muscle by their absorption spectra and named them cytochromes *a*, *b*, and *c*. Later, Keilin & Hartree (117) found a fourth, cytochrome c_1. In 1932, Warburg & Christian (251) discovered a flavoprotein which also participated in hydrogen transport. Subsequent work by many investigators (238) has revealed the presence of other hydrogen transport enzymes. Recently a novel fat soluble compound, coenzyme Q (ubiquinone), a benzoquinone (49, 167), with a long isoprenoid side chain has been found to transfer electrons between flavoprotein and cytochrome *b*.

Current research on the respective positions of these electron transport carriers has left certain controversial questions to be settled. In general, however, this outline, shown in figure 15, presents the current working hypothesis: a DPN-linked dehydrogenase transfers hydrogen from substrate to DPNH. This DPNH then transfers its electrons to a flavoprotein. The process continues by the reduced $FADH_2$ transferring its electrons to coenzyme Q, which in turn transfers them to cytochrome *b* and to the other cytochromes in turn. In electron transport by the cytochromes, one electron is transported per mole of cytochrome by oxidation-reduction of the heme iron. When the electron transport chain is operating at maximum capacity in the presence of adequate amounts of ADP and substrate, Chance & Williams (41) found that the steady-state condition of the hydrogen transport enzymes, expressed in terms of per cent reduction of the components, is DPNH 53 per cent, $FADH_2$ 20 per cent, cytochrome *b* 16 per cent, cytochrome *c* 6 per cent, cytochrome *a*, <4 per cent.

The physicochemical nature of the electron transport enzymes in the mosaic of the sarcosome has been studied by Green (88) and Stotz *et al.* (228). Through various devices, such as sonication and treatment of the insoluble sarcosomes with various lipid-emulsifying and splitting reagents such as the Tweens and bile salts, they have been able to obtain soluble lipoproteins which are enzymatically active and contain a variety of complex lipids. The lipoprotein character of these enzymes is essential for their biological activity, particularly that of oxidative phosphorylation. The lipid medium may be essential for the formation of highly labile phosphate esters during electron transport intermediate in the formation of ATP.

As the electrons traverse the chain they transfer energy at three stages by phosphorylation of ADP to ATP viz.:

$$\Delta F + P_i + ADP \rightleftharpoons ATP \tag{16}$$

The over-all P/O ratio of 3.0 for the oxidation of fatty acids and carbohydrate signifies that about 65 per cent of the chemical bond energy of the substrates is converted to high-energy bonds of ATP. Only about 10 per cent of the total energy conserved in ATP is derived from substrate level phosphorylations. The remainder occurs in the electron transport chain. The mechanisms of this process are still not completely delineated, but some progress has been made due largely to the studies of Lehninger *et al.* (133) and Chance *et al.* (39, 41, 44), who have studied this problem extensively. The mechanism by which the energy of the electron is transferred to a chemical linkage of ATP is unknown. Studies of inorganic P^{32} uptake into ATP and of the ADP-ATP exchange reaction by mitochondrial fragments have suggested, however, that one can formulate this process in three steps as follows:

$$\text{carrier}_{\text{red.}} + X \text{ (coupling molecule)} \rightarrow \text{carrier}_{\text{ox.}} \sim X + 2e \tag{17}$$

$$\text{carrier}_{\text{ox.}} \sim X + P_i \rightleftharpoons \text{carrier}_{\text{ox.}} + P \sim X \tag{18}$$

$$P \sim X + ADP \rightleftharpoons ATP + X \tag{19}$$

The enzyme catalyzing the third step, a phosphotransferase, has been isolated and purified by Lehninger (133). This formulation postulates that the energy contained in the oxidized form of the carrier is transferred to a high-energy bond between unknown intermediate (possibly an enzyme) and the oxidized form of the hydrogen carrier. This intermediate then reacts with inorganic phosphate to form another high-energy bond. The energy $P \sim X$ is subsequently transferred to ATP by reaction with ADP as shown in equation 19. The over-all reaction is:

$$2e + ADP + P_i \rightarrow 2e \text{ (lower energy)} + ATP \tag{20}$$

Dinitrophenol, an agent known to uncouple oxidation and phosphorylation, appears to act on the $\text{carrier}_{\text{ox.}}$-X complex and hence blocks ATP formation by inhibiting the reaction shown in equation 18. Packer (186) has shown that heart sarcosomes ordinarily are tightly coupled, i.e., that in the absence of the phosphate acceptor they will not transfer hydrogen and, conversely, when hydrogen is transferred, phosphorylation occurs.

The substrate succinate and fatty acid CoA derivatives transfer hydrogen directly to flavoprotein as shown in figure 15, so that these dehydrogenations result in only two high-energy phosphate bonds instead of three, since the DPN-flavoprotein transfer is missing from these two systems. The energy release in transferring two electrons from DPNH to O_2 is about 50 kcal per mole whereas the energy released from transferring two electrons from FAD from succinate to oxygen is about 35 cal per mole, the difference being essentially the value of one high-energy phosphate bond.

ROLE OF CREATINE PHOSPHATE. In muscle tissue creatine phosphate (71) serves as a high-energy phosphate buffer. A specific enzyme, creatine ATP-transphosphorylase catalyzes (138) the reaction:

$$C + ATP \rightleftharpoons CP + ADP \tag{21}$$

The structures of creatine phosphate and ATP are shown in figure 16.

The classical experiments of Lundsgaard (143) showed that muscle poisoned with iodoacetate could contract anaerobically in the absence of glycolysis, and that this action was accompanied by the disappearance of creatine phosphate and the appearance of free creatine and inorganic phosphate in equivalent amounts. He also showed that the amount of creatine phosphate consumed was proportional to the amount of muscular work done and that when the creatine phosphate was gone the muscle could no longer respond to stimulation. In cardiac muscle the creatine phosphate is present in relatively low amounts of the order of 15 to 20 mg per cent of inorganic phosphate compared to 100 mg per cent in skeletal muscle, and provides a relatively small reserve of high-energy phosphate bonds to the heart. The difference in concentration of creatine phosphate between skeletal

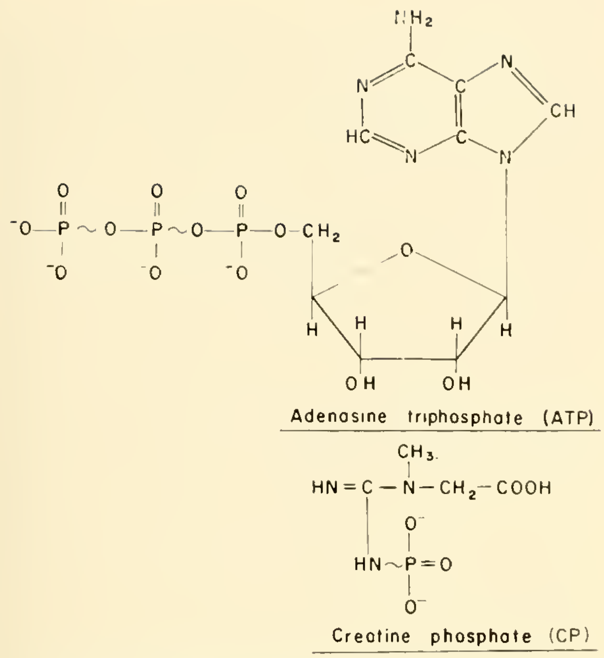

FIG. 16. Two high-energy phosphate compounds present in a cardiac muscle, ATP and CP.

muscle and cardiac muscle (6:1) is attributed by Szent-Györgyi (233) to the different requirements of skeletal and cardiac muscle. The first type can rely upon reserve energy and a strongly developed glycolytic system, whereas the second type must rely upon a steady supply of energy provided by a highly developed oxidative mechanism. The rates of formation and utilization of high-energy phosphate are more closely matched in cardiac than in skeletal muscle (181). Dinitrophenol has been shown by Fawaz and his co-workers (70) to depress the CP but not the ATP concentration of heart muscle in the heart-lung preparation, suggesting that CP is used to maintain the ATP concentration. Ligation of a coronary artery was also found to reduce the CP concentration of the heart in the heart-lung preparation, although no changes in ATP were noted within the 1 to 3 min elapsing before the onset of ventricular fibrillation. The administration of glucose was noted by Rebar *et al.* (202) to increase the content of glycogen and CP, no doubt by increasing ATP formation beyond the needs of the heart for ATP utilization.

Energy Utilization

The ATP formed in substrate oxidation is the "metabolic coinage of the cell" (232). It is this currency that pays for all of the work of the cell. In cardiac muscle most of the energy liberated is channeled into mechanical work via the contractile process. The muscle fiber must also carry out a certain amount of chemical work in activating substrates, synthesizing structural or storage materials as glycogen, protein, and lipids, and maintaining the integrity of membranes for transport of substrate and conduction of the action potential. These processes will be considered briefly under the head of chemical work.

CHEMICAL WORK. It has already become apparent that a certain amount of chemical work must be performed on most of the substrates utilized by the heart in order to make their bond energy available to the heart in subsequent reactions. This is true of glucose, fatty acids, and acetoacetate but not true of lactate, pyruvate, β-hydroxybutyrate, or glutamate. Two moles of ATP are required to store a mole of glucose as glycogen. It is beyond the scope of this presentation to consider the pathways of reactions by which proteins and lipids and sterols are synthesized (48), but these are all endergonic reactions requiring the input of high-energy phosphate bonds. The needs of cardiac muscle in this regard are not excessive, since protein turnover in muscle is low compared to visceral tissues and the muscle has no secretory activity involving a need for continuous synthesis of lipids and proteins. Dreyfus *et al.* (60) found that skeletal myosin turnover as measured with isotopic glycine in the rat was very slow for 30 days and then abruptly changed, suggesting dissolution of myofibrils at periodic intervals. Rat heart slices synthesize fatty acids and cholesterol from acetate-1-C^{14} and glucose-U-C^{14} slowly when compared with liver or kidney (179, 182). There is no doubt, however, that the variety of lipids found in heart muscle are synthesized *in situ* at slow rates.

MECHANICAL WORK. Since the pioneer work of Hill (101) and Meyerhof (156), muscle physiologists have sought a hypothesis that would adequately explain the coupling of chemical energy to mechanical work in the myofibril. Meyerhof's view that lactic acid fermentation was the direct source of energy for contraction gave way to Lundsgaard's (143) that creatine phosphate was the immediate source of contractile power. The refinements in knowledge of the intermediary metabolism of carbohydrate and of the formation of high-energy phosphate bonds has now led to the current view that ATP is the immediate source of energy for contraction as it is for all other work processes and that CP is utilized to replace ATP if the steady generation of phosphate bonds is

interrupted. Exact knowledge of the details of chemomechanical coupling remains elusive. The discovery of myosin by Weber (252) and of actin by Szent-Györgyi in 1942 (232) paved the way for the study of contractility in vitro. Currently, there are no less than six hypotheses regarding the contractile mechanism (111, 166, 229, 234, 235, 254, 255). Five of them deal with the interactions of two major contractile proteins, actin and myosin with ATP, and the sixth (8) relates this system to a third protein of the myofibril, tropomyosin. Although these three proteins (myosin, actin, and tropomyosin) appear to be the major elements in the contractile system and ATP the energy source, great controversy centers around the primary and secondary events in the contractile cycle at the molecular level. Although most of these hypotheses have been developed from data obtained in studies of skeletal muscle, the majority appear to be applicable to cardiac muscle as well. The properties of each of the contractile proteins will be discussed briefly and then the mechanisms proposed to account for contraction presented.

Myosin. Myosin from rabbit skeletal muscle was first isolated by Weber & Portzehl (253, 254) and von Muralt & Edsall (249). Myosin was discovered to have ATPase activity by Engelhardt & Ljubimova in 1939 (67). Its properties have since been studied in a number of laboratories. Estimates of its molecular weight have ranged from 1,500,000 (217) to 389,000 (162). The higher molecular weights obtained in earlier studies appear to be due to mild denaturation and aggregation of the native protein (104). Data from several recent studies (104, 130, 163, 246) give a molecular weight of about 440,000 and dimensions inferred from measurements of viscosity and diffusion of 1,200 Å by 25 Å. Skeletal myosin is thus a long narrow molecule with an axial ratio of 48. When this protein is digested with trypsin for very short periods, two discrete subunits are obtained which have been called H-meromyosin (heavy) and L-meromyosin (light) (77, 157, 236). Originally the molecular weight of H-meromyosin was estimated to be 240,000 and L-meromyosin 100,000 suggesting that 1 H-meromyosin and 2 L-meromyosins were derived from each molecule of skeletal myosin. The ATPase and actin-combining activities resided in the H-meromyosin. More recently Lowey & Holtzer (142) have presented sound evidence to show that the molecular weight of H-meromyosin is 340,000 so that it now appears that the parent molecule is composed of one of each of the tryptic digestion fragments. Kielley & Harrington (121) have also shown that guanidine HCl will depolymerize rabbit skeletal myosin into molecules of about 206,000 in molecular weight and A. G. Szent-Györgyi & M. Borbiro (236) have shown that high concentrations of urea may fragment skeletal myosin into small protomyosins of 4,600 in molecular weight which are uniform in size but variable in amino acid composition. These data suggest that myosin is a relatively unstable protein held together by many accessory as well as co-valent bonds. Studies in Olson's laboratory (66, 226) have shown that myosin isolated from dog heart is of lower molecular weight than that from rabbit skeletal muscle. Estimates of molecular weight from sedimentation and diffusion constants and light scattering measurements are in good agreement with a value of 226,000 and a size of 690 by 28 Å with an axial ratio of 24. The higher value for the molecular weight for dog heart myosin obtained by Gergely *et al.* (78) is apparently due either to contamination by actomyosin or mild denaturation (141). Cardiac myosin thus appears to be approximately half as long and half as large as skeletal myosin and does not yield the same meromyosins upon tryptic digestion. It nevertheless has an amino acid composition very similar to that of rabbit skeletal myosin and may be related to skeletal myosin as monomer is to dimer. In intact striated muscle, myosin appears to be localized in the primary filaments which compose the A band.

Actin. Actin was discovered by Banga & Szent-Györgyi in 1942 (10). Actin is extracted with more difficulty than myosin from muscle and in prolonged extractions with hypertonic salt solutions at a slightly alkaline pH the much more viscous actomyosin complex is obtained which can be dissociated in vitro by ATP to yield actin and myosin. Actin can also be obtained relatively free from myosin by extraction of an acetone powder of muscle with water. In such freshly prepared extracts, actin exists as a globular protein (G-actin) with a molecular weight of 70,000 and molecular dimensions of 290 × 24 Å. In the presence of ATP, Mg^{++} ions, and low concentrations of KCl (0.1 M) actin G dimerizes to form an aggregate of mol wt 140,000 which is 590 × 24 Å. The G-actin-dimer then further aggregates to form actin F, a long fibrous protein with a molecular weight of the order of 1,500,000 which appears as the thin secondary filaments of the sarcomere visible in the electron microscope as noted previously. Actin has been obtained from cardiac muscle and appears to be similar but not identical to skeletal muscle actin (52, 218, 219). Cardiac actin G appears to polymerize to actin F with more difficulty than that from skeletal

muscle (76). Actin F appears to be a reactant in the contractile process in vivo.

Actomyosin. As stated above, prolonged saline extraction of muscle yields solutions of actomyosin formed by interaction of the two proteins extracted from the myosin rodlets and actin filaments, respectively. If solutions of purified F-actin and myosin are mixed at ionic strength greater than 0.3, a sudden rise in viscosity occurs which is reversibly decreased by the addition of ATP. Actin combines nonstoichiometrically with 3 to 4 parts of myosin by weight to give an actomyosin gel which is insoluble at cellular ionic strength. It appears to be a macromolecule of the order of 20,000,000 in molecular weight. If such a gel is studied in vitro in the presence of low amounts of Mg^{++} ion, the addition of ATP causes synaeresis and shortening of the gel associated with the splitting of ATP. Both skeletal and cardiac actomyosin behave in this manner. It seems unlikely that such random associations between actin and myosin, as is illustrated by in vitro gel formation, occur in the intact myofibril in vivo, where these proteins appear to be highly oriented and compartmentalized.

Tropomyosin. Tropomyosin, the third major myofibrillar protein, was isolated by Bailey *et al.* (9) in 1948. Skeletal tropomyosin is a relatively small protein with a molecular weight of 53,000 (240). It is a rigid rod thought by some to be an ideal α-helix with dimensions of 12×400 Å. In pig heart the molecular weight was found to be 89,000 (241). Tropomyosin forms dissociable complexes with ribonucleic acid to form a nucleotropomyosin.

Tropomyosin has been found in a wide variety of both striated and smooth muscles in both vertebrate and invertebrate forms. In vertebrate skeletal and smooth muscle it comprises about 10 to 12 per cent of the myofibrillar protein (191) but in cardiac muscle from the pig it amounts to only 4.2 per cent (215). Although tropomyosin undoubtedly has some role in the contractile process its exact function is as yet obscure. The comparative studies of Sheng & Tsao (215) have shown that in general the tropomyosin content of smooth muscle is higher than that of striated muscle from the same species, and it has been suggested by Bailey (8) that tropomyosin plays a part in the "holding function" of such muscles. In the smooth adductor of the oyster, for example, where tropomyosin comprises about 30 per cent of the total protein, the relaxation phases is very slow in comparison with the speed of contraction (1).

Mechanism of contraction. Contraction of a muscle cell is brought about by a decrease in the length of the fibrillar units along the axis of contraction. A theory of contraction will be satisfactory only to the extent that it accounts for all the structural, biochemical, and thermodynamic phenomena observable in contracting muscle tissue. A striated structure is not essential for contraction, although striated muscle tends to contract with more rapidity and periodicity than smooth muscle. Most of the hypotheses which have been advanced have been designed to account for the molecular events which occur in striated muscle, and are relevant to the events in cardiac muscle. The hypotheses regarding the basic event in the contractile process can be divided into two groups, those that specify "folding" of one or more of the contractile proteins and those that specify "sliding" of these proteins within the sarcomere to achieve shortening. As further subdivisions, the chemical events in the contractile proteins which are alleged to occur include *a*) deformation, *b*) dissociation, and *c*) phase transition. None of these can, at this time, be said to be generally accepted. The most plausible hypothesis which is currently under consideration is one advanced independently by Huxley & Niedergerke (107) and Huxley & Hanson (111) and elaborated in later papers (106, 110), and this hypothetical mechanism will be presented in detail.

Electron microscopic studies of the ultrastructure of the muscle undergoing passive stretch or contraction down to 60 per cent of resting length reveal little if any change in the length of the A bands. All the change appears to take place in the I bands. At maximum contraction the Z membrane appears to fuse with the edge of the A band and the central H band becomes dense, to give the illusion of a reversal in striation. With maximum shortening (30% of resting length) or in contracture the A band may also shorten appreciably. These changes are shown in figure 17 and led to the view that the process of contraction was characterized by the sliding of interdigitating filaments (fig. 18).

As has been pointed out earlier, two types of filaments exist in the myofibril. The thicker ones, 100 Å in diameter coincide with the A bands of the sarcomere and have been shown to consist mainly of myosin (93, 96). The thin filaments appear to originate in the Z membrane and extend toward the center of the sarcomere where they do not, at resting length, meet the opposing thin filaments from the opposite Z membrane. There is some evidence that the thin filaments are connected in the H band by a tenuous S filament. The thin filaments appear to be composed mainly of actin (110, 111). Tropomyosin ap-

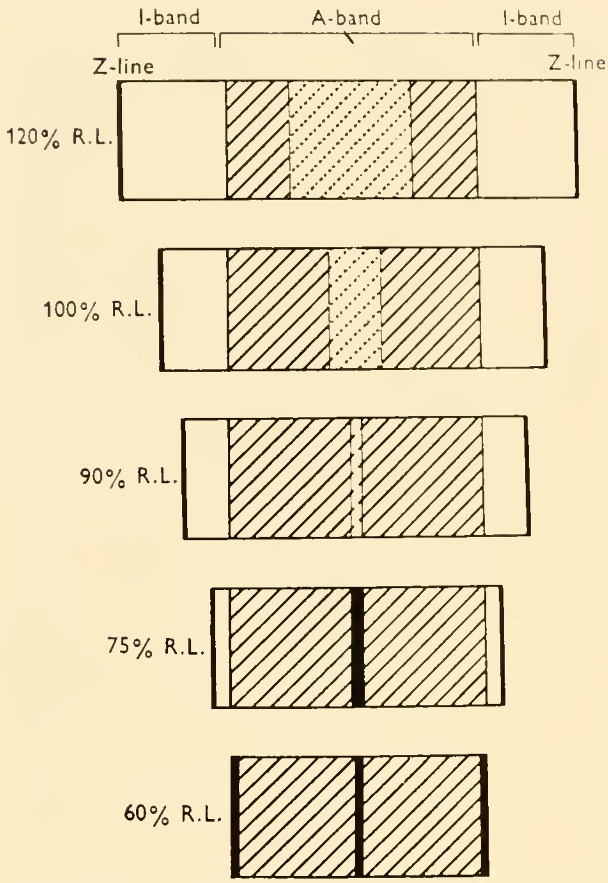

FIG. 17. Diagrammatic representation of band pattern changes during contraction. [From H. E. Huxley (110).]

pears to exist in solution in the interstices of the myofibril, particularly in the I bands. Chemical analysis of the isolated rabbit myofibril (191) indicates that the protein composition of the myofibril is as follows: myosin 50 to 55 per cent; actin 20 to 25 per cent; tropomyosin 10 to 15 per cent; other proteins 5 to 10 per cent. The identity of the protein of the Z membrane is unknown, although it is estimated to represent about 5 per cent of the myofibrillar protein.

In skeletal muscle the myosin filament is 100× 15,000 Å which would accommodate about 400 molecules of skeletal myosin. The thin filaments could be composed of a double or triple strand of F-actin. According to Huxley (106), the interaction of the filaments in the contractile process is made possible by the presence of elastic side pieces on the myosin filament which can combine with reactive sites on the active filament. Actual "feet" protruding from the thick filaments have been seen in the electron microscope which could be a double strand of myosin

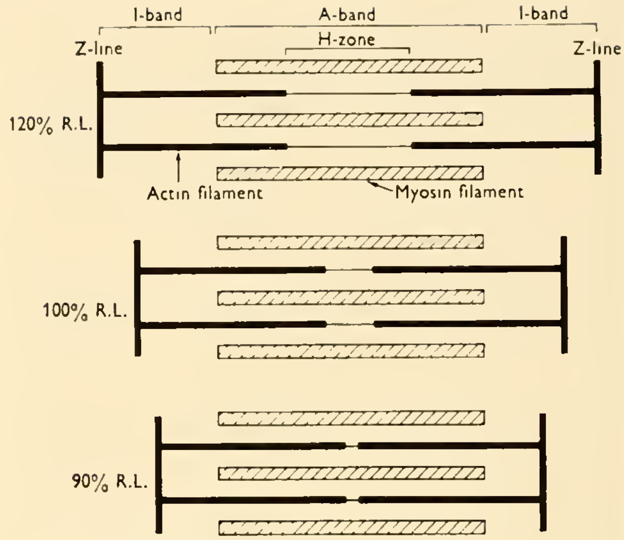

FIG. 18. Diagram showing behavior of actin and myosin filaments during changes of muscle length. [From H. E. Huxley (110).]

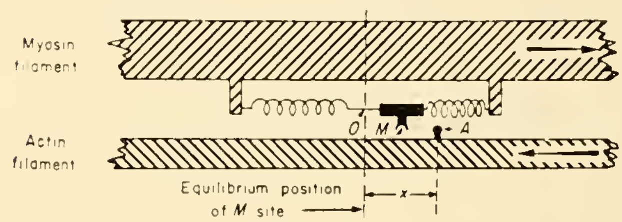

FIG. 19. Diagram illustrating a mechanism of actin-myosin combination in the sliding model. The part of a fibril which is shown is in the right-hand half of an A band, so that the actin filament is attached to the Z line which is out of the picture to the right. The arrow gives the direction of the relative motion between the filaments when the muscle shortens. [From A. F. Huxley (106).]

peptide emerging from the body of the macromolecular filament.

It is postulated that the linkages between the sliding members are formed spontaneously, but are broken only by the input of energy from metabolic sources. This is not difficult to imagine if it is supposed that the reactions are catalyzed by an enzyme which is fixed to one of the filaments or perhaps by enzymatic activity, intrinsic to one of the contractile proteins as ATPase is to myosin.

Figure 19 shows a schematic diagram of the sliding model in which the contractile elements shown are thought of as lying in the righthand half of an A band so that the nearest Z line to which the actin filament is attached is off the picture to the right. During shortening, the actin filament moves to the left relative to the myosin filament. The distance from A, the

active site on the actin filament, to 0, the equilibrium position of the sliding element on the myosin filament, is denoted by X. During steady shortening, X decreases at a constant rate. Initially, the groups M and A are detached; in response to the action potential which invades the Z membrane and the actin filaments, combination of A and M takes place spontaneously with the equilibrium in favor of the combined state. Since many A and U sites exist, any number of positions of the two filaments with regard to each other can be attained. In an average contraction many A-M linkages will be formed and broken. If the initial reaction is spontaneous and exergonic, the recovery reaction, i.e., breaking an A-M bond, will require the input of energy from an available source such as ATP. The sites on each protein are calculated to be about 100 Å apart, so as the muscle shortens more sites come into apposition.

This model also satisfies the thermodynamic data of Hill (100) obtained on striated muscle which led to his classical formulations, viz.: *1*) the hyperbolic force-velocity relationship, *2*) the proportionality between rate of heat liberation and the speed of shortening, and *3*) the proportionality between the rate of total energy liberation and the decrement below isometric tension (106, 194).

The biochemical events which may be postulated to drive the sliding model are as follows:

$$\text{actin} + \text{myosin} \rightarrow \text{actomyosin} \qquad (22)$$

The myosin is thus regarded as "energy rich" and capable of "pulling" the actin filament toward it by combining with it in the highly oriented manner imposed by the ultrastructure of the myofibril. The actomyosin bond thus formed is broken (either in more vigorous shortening or by relaxation) by reaction of the actomyosin with ATP as follows:

$$\text{actomyosin} + \text{ATP} \rightarrow \text{myosin-ATP} + \text{actin} \qquad (23)$$

The myosin-ATP complex, which may be regarded as an enzyme-substrate complex, is then split by the ATPase activity of myosin as follows:

$$\text{myosin - ATP} + H_2O \rightleftarrows \text{myosin} + P_i + \text{ADP} \qquad (24)$$

Levy & Koshland (135) have studied reaction 24 with H_2O^{18} and have produced evidence that phosphomyosin is formed transiently in this reaction. A significant and paradoxical difference between the ATPase activity of myosin and the ATPase activity of the myofibril is that extracted purified myosin ATPase is strongly inhibited by Mg^{++} (and activated by Ca^{++}), whereas both Ca^{++} and Mg^{++} activate the myofibrillar ATPase (191). The ADP formed in equation 24 is then rephosphorylated through electron transport. Although Huxley (106) prefers to write equation 23 with actin-ATP as the complex formed, the lack of ATPase activity in actin makes myosin a more likely candidate. The question of the direction of movement of the filaments must depend upon the state of activation of the Z membrane which distributes the action potential of the membrane to the contractile elements (108). It is also of interest that this model obviates the necessity of designating the time in the contractile cycle when ATP splitting occurs; it occurs during all movements of the filaments in order to permit the making and breaking of the points of attachment between actin and myosin.

The sliding model thus provides a new and stimulating hypothesis for contemplation. It is certainly not established but, at the moment, has so many attractive features that it will be studied intensively in the future. The other models which have been proposed have strengths and weaknesses which deserve mention. Szent-Györgyi (233) visualizes a folding model in which actin and myosin combine in the presence of ATP and shorten, much as actomyosin gels or glycerinated fibers do in vitro. It is unlikely, however, from the electron microscopic studies that actin and myosin combine in the myofibril as they do in vitro. More recently Szent-Györgyi (235) has suggested that muscular contraction may be a submolecular phenomenon, involving protomyosins (fragments of myosin) and the triplet state of their electrons. The triplet state occurs when an electron is raised to an excited state by the absorption of energy which reverses its spin. The excited electron is trapped because it cannot drop back to the original energy level of its partner which is spinning in the same direction and as a result the lifetime of the excited state is lengthened about a millionfold. The molecule which contains the uncoupled electrons is in an unbalanced and more reactive state, like a free radical and in Szent-Györgyi's view, molecular contraction would be a quantum mechanical process involving displacement of myosin fragments (235).

Morales & Botts (165) have suggested that the primary event in muscular contraction is a folding of a Mg-myosin complex to which ATP is adsorbed (acting as a polyelectrolyte) in an electrostatic environment altered by the passage of the action potential. The hydrolysis of ATP is visualized as occurring at the end of contraction to permit the rebuilding of the appropriate polyelectrolyte structure

for a relaxed myosin. These authors point out that relaxing factors such as EDTA, myokinase, and ATP-creatine phosphorylase either bind magnesium or elevate ATP levels. Both of these act to decrease ATPase activity and promote relaxation (36). This view postulating deformation of myosin is contradicted most directly by the observation that the A bands of muscle, which contain myosin, do not appreciably shorten under most physiological conditions.

Straub & Feuer (229) have suggested that the polymerization of G-actin to F-actin is a crucial reaction in muscular contraction. This idea, not popular in the last decade, may deserve re-examination in the light of the Huxley model with its assignment of a more important role to the actin filaments. The early hypothesis of Astbury (7) that contraction resulted from a phase change in myosin has not been confirmed experimentally. Bailey *et al.* (9) have suggested that the function of tropomyosin may be to control the rate of operation of the contractile cycle by interacting with actin. In skeletal and cardiac muscles in which the buildup and decay of tension are rapid, actin is relatively more abundant than tropomyosin. On the other hand, in those smooth muscles, in which buildup and decay of tension are slow, tropomyosin is a much more prominent constituent.

The observation of Fleckenstein *et al.* (72) and Mommaerts (161) that no observable ATP or CP breaks down during a single contraction is disillusioning, although some other labile phosphate compound may be replenishing the ATP split in a single twitch. Chance & Williams (41) have also shown that the rise in ADP following stimulation of frog sartorius muscle was low, i.e., only 0.008 μmole per gram per twitch. This represents only about 1 per cent of the calculated ATP breakdown for one twitch.

It seems likely, however, that ATP is the ultimate source of energy in muscular contraction as in other types of cellular work. The efficiency in the conversion of ATP to mechanical work in cardiac muscle varies widely from about 20 to 60 per cent, indicating that the "coupling" of ATP utilization to actomyosin function is considerably looser than the coupling of hydrogen transport to ATP formation (113). Under normal conditions the over-all efficiency of the heart thus varies from 12 to 36 per cent.

PHYSIOLOGY OF SUBSTRATE UTILIZATION

The intact beating heart may extract and utilize a variety of substrates from the coronary blood. Much

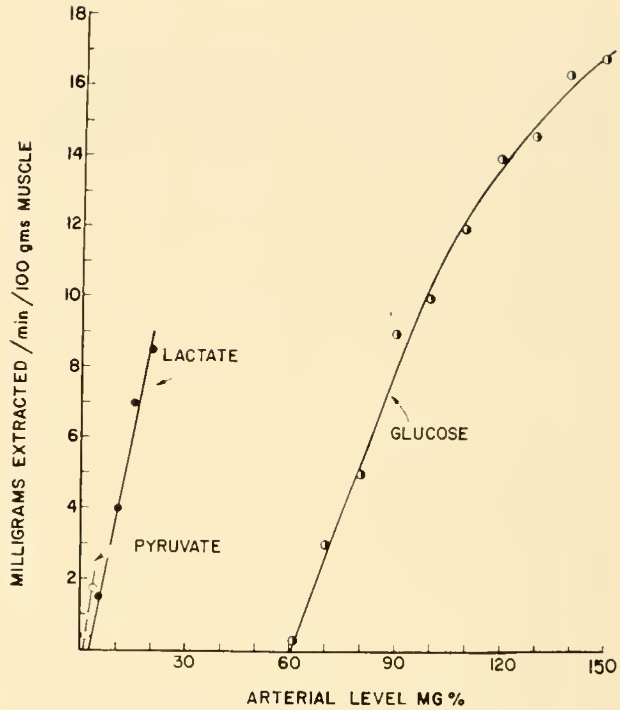

FIG. 20. Extraction of glucose, lactate, and pyruvate by muscle in vivo. These lines represent averages of large numbers of determinations upon man and dog and demonstrate the uptake of substrate at various concentrations.

evidence is available from studies of cardiac muscle homogenates and slices (33, 68, 158, 180), of heart-lung preparations (31, 139, 153, 205), isolated perfused hearts (122), and intact hearts in man and dog approached via coronary sinus catheterization (81–83), that pyruvate, lactate, glucose, acetate, acetoacetate, β-hydroxybutyrate, amino acids, and fatty acids may serve as sources of energy for heart muscle.

Under physiologic conditions glucose, lactate, pyruvate, and fatty acids (as NEFA), and to a lesser extent, acetate, ketone bodies, and amino acids are the main fuels of the heart. The extent to which each substrate contributes to the energy requirement of the heart in vivo is influenced by its concentration in arterial blood as well as by the state of nutrition and endocrine balance of the organism. Furthermore, in the intact heart there appears to be a definite threshold of extraction for some substrates. Although these are very close to zero for pyruvate (0.6 ± 0.2 mg %) and lactate (2.5 ± 0.5 mg %), the threshold for glucose extraction is considerably higher (59 ± 6 mg %). Since this threshold behavior (shown in fig. 20) is lost in cardiac muscle slices, it is probably a function of an intact cellular membrane. This is further supported by the effects of diabetes and in-

sulinization upon the threshold for glucose. Ungar *et al.* (242) and Goodale & Hackel (81) and their colleagues have shown that the threshold for glucose extraction is markedly elevated in diabetes in man and in dogs, and that insulin treatment reduces it toward normal. In addition, Hackel (92a) has shown that insulinization of normal dogs causes a marked reduction in the threshold for glucose extraction to 10 ± 3 mg per cent. It would appear that the cardiac muscle cell membrane behaves like other muscles toward glucose and insulin. Above their respective thresholds, pyruvate, lactate, and glucose are removed in proportion to arterial concentration. The regression lines for lactate and pyruvate are linear in the ranges studied, and that for glucose curvilinear as shown in figure 20, approaching a maximum extraction of about 20 mg per cent at levels of 250 mg per cent. The earlier view of Evans (68) that lactate was the primary food of the isolated heart was due to his use of blood from fasted exsanguinated animals for the perfusion medium. In such blood the lactate levels are high and the glucose levels are low.

Cardiac muscle glycogen, which appears to be derived principally from blood glucose, is maintained at very stable levels under normal conditions of cardiac work, even in the presence of hypoglycemia (53). Only with complete anoxia (102), excessive stimulation by epinephrine (29), or excess thyroxin (6) does cardiac muscle glycogen decrease. When depleted experimentally in the dog by epinephrine injections, it is replaced readily by blood glucose but not so effectively by blood lactate or pyruvate (30). Interestingly enough, cardiac glycogen may rise under certain conditions of metabolic stress accompanied by ketosis, such as severe starvation and diabetic acidosis. This occurs, presumably, because of the preferential oxidation of ketone bodies by the heart with a sparing of carbohydrate (129).

The state of nutrition of the organism influences markedly the kind of substrate used for energy production by the heart. With fasting, the heart shifts from the predominant utilization of carbohydrate to the almost exclusive utilization of fatty acids as a source of energy. Under postprandial conditions or after glucose infusions, the myocardium of both dog (81) and man (22) utilizes mainly glucose, lactate, and pyruvate as a source of energy, and the myocardial respiratory quotient approaches 1.0. After an overnight fast, the pattern of metabolism shifts to a greater dependence upon fatty acids and the myocardial respiratory quotient drops to about 0.80. Bing and associates (21), using a titrimetric method for total fatty acids in arterial and coronary sinus blood, established that the human myocardium during fasting could derive up to 67 per cent of its energy from the oxidation of fatty acids. More recently Gordon & Cherkes (84) have reported that the source of these fatty acids for myocardial oxidation is the nonesterified fatty acid (NEFA) fraction of the plasma which is albumin-bound (57). By coronary sinus catheterization of healthy postabsorptive subjects, these workers found that from 25 to 70 per cent of the myocardial oxygen usage could be accounted for by the uptake of NEFA. With prolonged fasting and diabetes mellitus, the uptake of carbohydrate by the heart is further depressed with a decrease in the extraction coefficients for glucose, pyruvate, and lactate (82) the myocardial respiratory quotient drops to 0.70, and the heart depends almost solely upon fatty acids and ketones for energy (242).

TABLE 1. *Effect of Feeding and Fasting Upon Myocardial Substrate Utilization in Man*

Condition	Fed	Fasted
A-V difference		
O_2 ml %	10.80	11.50
CBH* mM C—3/liter	1.49	0.51
NEFA† mM C–16/liter	0.01	0.12
% O_2 utilization accounted for by:		
CBH	92	30
NEFA	5	58

* CBH—Carbohydrate. † NEFA—Nonesterified fatty acids.

The shifts in usage of substrate by the human heart under conditions of feeding and overnight fasting are shown in table 1. During such transitions the uptake of total "carbohydrate" and NEFA vary reciprocally and correlate well with the observed respiratory quotients (193). Carbohydrate appears to be the preferred substrate if it is available and the animal is in the "fed" state, and is thus the "active" determinant of the fuel mixture taken up by the heart. The highly variable pattern of NEFA uptake in relation to NEFA level in arterial blood suggests that it is the "passive" partner. Under ordinary conditions, plasma amino acids do not contribute significantly to the energy production of the heart (21).

With regard to the uptake of oxygen, it has been found by Goodale *et al.* (82) that the coronary arteriovenous differences for oxygen in man vary linearly with arterial oxygen content through the range from mild anemia to marked polycythemia, as shown in figure 21. It is somewhat remarkable that the uptake of this "substrate" is also dependent upon arterial level, considering the fact that the source of demand for coronary arterial oxygen is the rate at which cytochrome oxidase is being reduced within the myocardial

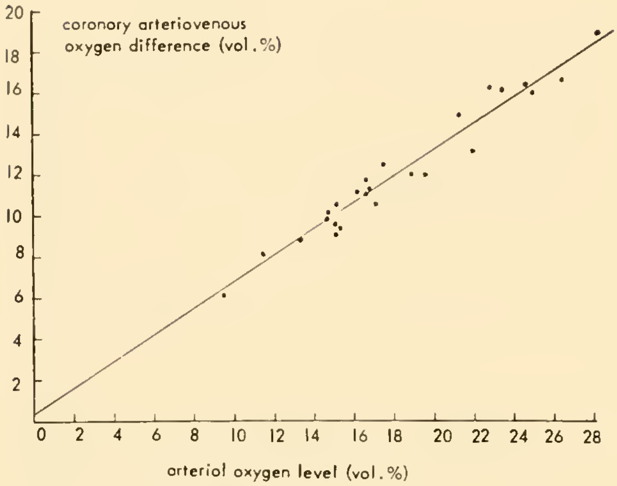

FIG. 21. Myocardial oxygen extraction in relation to arterial oxygen level in man. [Goodale *et al.* (82).]

cell. It follows from this that the mechanisms adjusting coronary flow (and hence oxygen delivery at a given oxygen content) must be extraordinarily sensitive to the needs of the hydrogen transport chain. Only under such conditions would the cardiac muscle cell "permit" the oxygen content of the arterial blood (ordinarily proportional to hemoglobin concentration) to determine the oxygen uptake and thus keep the myocardial oxygen extraction coefficient (A-V)/A constant.

It is thus seen that the heart demonstrates broad flexibility in the utilization of substrates for energy production without a change in either its work performance or work capacity. There is little evidence that total lack of arterial substrate per se occurs in any clinical situation to the extent that it embarrasses the cardiac "capacity" for work. Metabolic disturbances in heart muscle may be sufficiently marked to cause a reduction in free energy available for contraction, as noted in the next section.

PHYSIOLOGY OF SUBSTRATE EXTRACTION UNDER PATHOLOGIC CONDITIONS

The extraction of specific substrates by heart muscle, which is variable in conditions of health, may be even more variable in conditions of disease. In some situations the variations may be of such a nature that the total amount of oxidizable substrate extracted remains constant and the processes of energy production are not impaired. In other situations, the alterations in the intermediary metabolism of carbohydrate and/or fat may be so large as to impair electron transport or oxidative phosphorylation and result in restricted energy production and even cardiac failure (185). Some of these conditions will be discussed in the ensuing portion.

Hypoxia

In acute hypoxia, the oxygen supply of the normal heart is protected by a number of vascular reflexes governing coronary flow and by the excellent design of the myocardium for rapid diffusion. In dogs, made hypoxic by breathing 7 to 10 per cent oxygen, coronary sinus catheterization has shown that increased coronary flow and more complete extraction of oxygen from the coronary blood preserve myocardial oxygen delivery (63). In dogs made more severely hypoxic by breathing 3 to 6 per cent oxygen, left auricular pressure may rise just prior to death (58). Death under these conditions, however, usually results from the greater vulnerability of the central nervous system. A similar situation occurs in cyanide poisoning which produces hypoxia by inactivation by cytochrome oxidase. The heart is again less vulnerable than other critical organs because of its high content of this enzyme.

In coronary atherosclerosis, the cardiac reserve may be lowered through reduction in the efficacy of vascular adjustments to increased cardiac work loads and hypoxia. Gorlin *et al.* (85) found that coronary flow in patients with coronary artery disease did not increase after nitroglycerin, whereas marked vasodilatation occurred in normal subjects. In such patients this investigation has also noted a decrease in lactate extraction consistent with an increase in aerobic glycolysis. In experimental graded coronary occlusion (with plastic spheres) in dogs, Bing and his colleagues (20) have shown that transient reduction (10–15 min) in the extraction rates for glucose, lactate, and pyruvate (sometimes to negative values) accompany the reduction in cardiac output, coronary flow, peripheral blood pressure, and decreased myocardial oxygen consumption. Under such conditions, leading to local ischemia and infarction, the patent coronary arteries appear to be maximally dilated as indicated by a fall in coronary vascular resistance. Sarnoff (208) found that restriction of coronary flow from a main coronary artery caused a depression in the ventricular function curve (plot of stroke work versus filling pressure for that ventricle) of the left but not the right ventricle in the open-chest dog. Fawaz *et al.* (70) observed that liga-

tion of a coronary artery in the heart-lung preparation caused a prompt fall in creatine phosphate but no change in ATP during the 1 to 3 min which elapsed before the onset of ventricular fibrillation.

Chronic oxygen lack, such as occurs in anemia of long standing, is occasionally a cause for congestive failure. Despite the increased circulatory load in anemia, uncomplicated cardiac failure is a rarity in patients under 40 years of age because of the multiplicity of vascular reflexes, cited above, which act to provide adequate oxygen delivery to the myocardium. With the onset of coronary atherosclerosis, however, these protective mechanisms are partially vitiated, and electron transport may be reduced critically because of delivery of the terminal electron acceptor, O_2, at insufficient rates. In anemia, the cardiac output tends to be elevated in order to provide additional oxygen to the peripheral tissues, and this puts an additional burden upon the potentially anoxemic heart. When cardiac failure occurs in anemia it is generally of the high output type and responds to blood replacement.

Shock

The effect of acute hemorrhagic shock upon cardiac metabolism in dogs has been studied by Edwards and collaborators (64) and by Hackel & Goodale (91). In this form of oligemic stagnant anoxemia, cardiac output, stroke volume and work, and coronary blood flow are markedly reduced. In association with these hemodynamic changes, these investigators found reduced extraction coefficients for pyruvate, lactate, and glucose, although at the high arterial levels observed absolute uptake of lactate and glucose were maintained. Pyruvate uptake was abolished during both the oligemic and normovolemic phases of hemorrhagic shock despite elevated arterial values. Cardiac work efficiency dropped markedly during the oligemic phase and remained depressed after reinfusion of blood. In fact, Wiggers & Werle (257) and Sarnoff and co-workers (209) noted evidence of myocardial failure following the infusion of blood into animals with hemorrhagic shock. In regard to the precise biochemical lesion in this type of anoxemia, the data are not definitive. Bing and associates (64) postulated a loss of cocarboxylase from the myocardium to account for the failure to metabolize pyruvate, although no direct measurements of cocarboxylase were made. The continued utilization of lactate by these hearts in shock argues against a serious loss of cocarboxylase, since both pyruvate and lactate extractions are markedly depressed in thiamine deficiency in dogs (92). The marked loss of work efficiency by the heart in shock suggests uncoupling either of oxidative phosphorylation or of the contractile mechanism. Hackel & Goodale (91) have suggested that the epinephrine release accompanying hemorrhagic shock may play a key role in this alteration in cardiac metabolism, since hypotension due to spinal anesthesia does not cause the same cardiac inefficiency. Further experimental data are required before the controversy regarding the biochemical lesion in the myocardium in hemorrhagic shock can be resolved.

Beriberi

In the absence of adequate dietary thiamine, all tissues undergo depletion of cocarboxylase (thiamine pyrophosphate), the coenzyme required by the pyruvic and α-ketoglutaric dehydrogenases, and by transketolase for normal enzymatic activity. Under these conditions the oxidation of pyruvate and other carbohydrate precursors of pyruvate cannot proceed to completion, and blood pyruvate and lactate rise. A decrease in transketolase activity is probably unimportant, since the pentose shunt is normally inactive in cardiac muscle. In thiamine-deficient rats and ducks, Olson and his colleagues (180) showed that there was a relationship between the rate of pyruvate disappearance in vitro and the thiamine content of the heart slice. Although pyruvate utilization did not decline until the heart muscle cocarboxylase content had been reduced from a normal of 10 μg per g to about 2.5 μg per g, further reduction in thiamine content resulted in a precipitous drop in pyruvate utilization. Hackel *et al.* (92) showed that thiamine deficiency in dogs resulted in "dry" beriberi, with no edema and no elevation of venous pressure, despite a markedly altered myocardial metabolism. The extraction of pyruvate and lactate by the heart was markedly reduced despite high arterial levels so that only 29 per cent of the energy needs of the heart were met by carbohydrate. Furthermore, they noted that the extraction of oxygen from the coronary arterial blood varied inversely with coronary flow, a highly abnormal finding which suggested that hydrogen transport was limited in these hearts by the lack of cocarboxylase. Although most thiamine deficiency in experimental animals is dry, transient congestive heart failure has been produced in thiamine-deficient pigeons (231).

Both "wet" and "dry" beriberi occur in man.

The production of the full-blown syndrome of high-output failure in human beings with beriberi (38) requires both appreciable reduction in myocardial cocarboxylase and peripheral vasodilatation. Under these conditions of increased load and decreased cardiac reserve, congestive failure results. Cardiac catheterization of an alcoholic with high-output failure due to beriberi has revealed the same picture of depressed myocardial carbohydrate oxidation characteristic of the thiamine-deficient dog (176). The administration of thiamine, food, and bed rest usually restores these patients to normal in a few days.

Diabetes Mellitus

Insulin lack modifies the metabolic behavior of cardiac muscle without appreciably altering its work capacity. Early studies of the isolated perfused diabetic heart (69) revealed a decreased extraction of glucose without a change in lactate extraction. In cardiac muscle slices from the diabetic rat, Pearson *et al.* (188) observed a decrease in pyruvate extraction and oxidation below normal. In diabetic human subjects studied by Ungar *et al.* (242) and Goodale *et al.* (82) a decreased myocardial extraction of glucose, an increased extraction of fatty acids, and a depressed myocardial respiratory quotient in the vicinity of 0.70 was noted. The myocardial glucose extraction in diabetes is low despite markedly elevated arterial glucon levels, so that the threshold for glucose extraction is elevated and the whole curve displaced to the right. This defect in glucose uptake is rapidly corrected after insulin administration and is consistent with the permeability hypothesis of insulin action (134). Goodale *et al.* (82) also noted that pyruvate extraction was reduced in diabetes and restored after insulin administration, an observation not entirely consistent with the permeability hypothesis. Vester & Stadie (244) noted decreased pyruvate utilization and decreased oxidative phosphorylation in liver mitochondria from diabetic cats. On the other hand, Flock and associates (73) found that pyruvate given intravenously was utilized normally in diabetic dogs. The precise change in the diabetic human heart responsible for decreased pyruvate extraction is not evident. The subjects with diabetes show no hemodynamic signs of cardiac failure of metabolic origin. Thus, in diabetes mellitus there appears to be no threat to cardiac competence as a result of the defect in carbohydrate metabolism per se. The diabetic heart probably adapts itself to this biochemical lesion in carbohydrate metabolism by a greater dependence upon fat as a source of energy.

Hyperthyroidism

Of various endocrine disorders, only thyrotoxicosis has been identified as the cause of congestive heart failure. With thyrotoxicosis, failure does not usually occur in man unless there is underlying heart disease, although cases without evidence of pre-existing cardiac disorder have been cited (6, 120, 137). The tachycardia, increase in peripheral oxygen consumption, vasodilatation, and the increase in venous return, which accompany hyperthyroidism, may so increase the work of the heart as to precipitate failure at relatively high cardiac outputs of 8 to 12 liters per min at rest. Although Bing (19) reported no increase in the oxygen consumption of the myocardium in man with hyperthyroidism, convincing evidence that coronary flow and total myocardial oxygen consumption are increased in human thyrotoxicosis has been presented by Rowe and co-workers (204). The sequence of events leading to heart failure in thyrotoxicosis is not thoroughly understood. Until recently, it has been thought, on the basis of older experimental evidence showing a decrease in the concentration of high-energy phosphate compounds, ATP, and creatine phosphate (CP) in heart muscle from hyperthyroid animals (37, 152, 214), that uncoupling of oxidative phosphorylation was the biochemical lesion leading to congestive heart failure in hyperthyroidism.

The studies of Maley & Lardy (147, 148) of the effect of in vitro thyroxin addition and in vivo hyperthyroidism upon oxidative phosphorylation in kidney and liver mitochondria added support to this view of the etiology of thyrotoxic heart failure. Even the finding of Cooper *et al.* (45) that the action of thyroid hormone in uncoupling oxidative phosphorylation was due to an effect of the hormone upon the integrity of the mitochondrial membrane, rather than the intrinsic reactions of oxidative phosphorylation, did not remove the possibility that thyroid hormone in vivo might uncouple oxidative phosphorylation by altering the properties of the sarcosomal membrane in the heart. Studies by Olson & Piatnek (181), however, have cast grave doubts upon the view that cardiac failure in hyperthyroidism is due to the uncoupling of oxidative phosphorylation. Experimental hyperthyroidism was produced by these workers in dogs (181, 193) and rats (192) by feeding

them large amounts of U.S.P. thyroid powder. Values for cardiac output, coronary blood flow, and myocardial oxygen usage were augmented in dogs from 50 to 100 per cent. Determinations of the levels of total acid-soluble phosphate, inorganic phosphate, adenosine triphosphate, and creatine phosphate in the ventricles of these dogs and rats showed no decrease below normal. These results suggested that in the steady state, at augmented work loads, the processes of energy liberation and energy utilization were so balanced as to maintain the usual concentration of high-energy phosphate compounds in ventricular tissue. Further, studies of in vitro oxidative phosphorylation of heart ventricle from hyperthyroid rats and dogs have been carried out by the atraumatic polarographic method of Chance & Williams (40). High P/O values during α-ketoglutarate oxidation were obtained for both normal and hyperthyroid heart muscle, in good agreement with the studies of normal tissue by others (186). In view of these data, the mechanism of the cardiac failure in thyrotoxicosis remains obscure. It seems unlikely that the effects of hyperthyroidism are purely hemodynamic. Crispell *et al.* (51) found that protein anabolism as measured with N^{15}-glycine was depressed in hyperthyroidism. It may be that anabolic reactions leading to protein synthesis, and hence to the maintenance of the contractile proteins of the heart, may be affected in thyrotoxicosis and influence contractility of the heart. Further work is required before this enigma can be solved.

PATHOLOGIC ALTERATION IN CONTRACTILE PROTEINS

Since current views of the mechanism of contraction in cardiac muscle stress the importance of the spatial and functional relationships in the contractile cycle of the filaments of the myofibril, it follows that disturbances in the ultrastructure of the heart caused by primary disease of the muscle or alteration in the configuration of the contractile proteins may lead to cardiac dysfunction and failure. The evidence is mounting that most of the common types of cardiac failure are due to defects in energy utilization (18, 185), i.e., a failure of the myofibril to assimilate phosphate bond energy or to shorten properly in the contractile cycle. Although the biochemical lesions have not been determined with certainty in these disorders, it is considered important in the overall consideration of the physiology of cardiac muscle to mention the work which has been done to inaugurate biochemical study of this important area and to encourage additional work.

Primary Disease of Cardiac Muscle

The study of biochemical disturbances in primary diseases of cardiac muscle in man and animals has scarcely begun. No significant electron microscopic studies of the ultrastructure of the myocardium have been carried out in cases of myocarditis due to rheumatic fever, diphtheria, or bacterial or virus infections. One can only speculate from the microscopic findings that disorganization of the ultrastructure of the myofibril may incapacitate the contractile filaments. The processes of fatty degeneration and hyaline segmentation of the myocardium in extreme situations of dilatation and necrosis as a result of inflammation, circulatory occlusion, or chemical agents may interfere at several points in the normally orderly processes of energy production and utilization, and thereby induce cardiac failure. Glycogen disease, which has been mentioned briefly, results in crowding of the sarcoplasm with glycogen granules which are biochemically inert, and which ultimately embarrass the contractile mechanism by competition for space. The same may be said of neoplastic events in cardiac muscle.

Although the muscular dystrophies primarily involve skeletal muscle, there is evidence (16, 75, 211) that the dystrophic process also affects the heart and may result in congestive heart failure (75). Although study of the cardiac contractile proteins has not been carried out in muscle dystrophy of any kind, studies of the contractile proteins from dystrophic skeletal muscle from vitamin E-deficient rabbits have been made. Aloisi (5) has reported that marked changes occur in the amount and kind of myosin present in skeletal muscle during the induction of vitamin E-deficiency in the rabbit. The birefringence of the A band is lost and the quantity of myosin which can be isolated chemically is drastically reduced. Furthermore, it appears that the viscosity and solubility of the myosin are reduced so that the change associated with dystrophy is both quantitative and qualitative. One may infer that related changes may be occurring in heart muscle in this condition.

Secondary Disease of Cardiac Muscle

Congestive heart failure of the low output type generally occurs in subjects with previously normal cardiac muscle, whose hearts have been obliged to

work at a mechanical disadvantage for a period of time. The time required for the induction of failure is generally inversely related to the seriousness of the mechanical disadvantage. Cardiac failure of this type may result from congenital anomalies of the valves and great vessels, valvular disease, or hypertension. It may also occur at "normal loads" in atrophic or infarcted cardiac muscle.

In these conditions, the energy production of the heart is normal and the biochemical reactions occurring in the cytoplasm and sarcosomes proceed effectively. That failure can occur in the presence of normal oxidative metabolism has been demonstrated in the heart-lung preparation (98, 224, 245), the open-chest dog (210), the intact dog (181), and in the human subject with hypertension or valvular disease (22, 25, 83). By means of cardiac catheterization, these latter workers (25, 83) found no decrease in coronary blood flow, oxygen extraction, or substrate utilization in patients with advanced congestive heart failure with roentgenologic evidence of left ventricular enlargement. Since cardiac output in these patients was reduced, it was calculated, even assuming normal heart size, that the efficiency of the heart was low. The inability of these investigators to show any defect in myocardial oxygen consumption in failure does not support the older view of many pathologists, summarized by Harrison (94), that hypoxia within the hypertrophied cardiac muscle fiber is responsible for the failure of contractility. Further, the study of the level of ATP and CP in the myocardium of the failing heart-lung preparation by Wollenberger (258) demonstrated no depletion of these sources of free energy for contraction.

In studies of the pathologic physiology of this type of congestive heart failure, Olson (174) has studied the metabolic behavior of the failing heart in dogs subjected to cardiac valvular surgery. Chronic low output congestive heart failure characterized by edema, ascites, weakness, reduced exercise tolerance, cardiomegaly and hepatomegaly, with ultimate elevation of end diastolic filling pressures in both the right and left ventricles, was produced in dogs by avulsion of the tricuspid valve and stenosis of the pulmonary artery (12). Although initially right-sided, heart failure induced in this way eventually becomes generalized as indicated by depressed ventricular function curves in both ventricles (12) and a positive inotropic response to digitalis in both chambers (184).

The cardiac metabolism of a series of dogs in congestive heart failure due to valvular disease was compared with a series of healthy control animals. Cardiac catheterization with intubation of the pulmonary artery and the coronary sinus was performed on each animal. Values for resting cardiac output, coronary blood flow, total carbohydrate and NEFA uptake, and cardiac oxygen consumption for normal dogs and for dogs with congestive heart failure secondary to tricuspid insufficiency and pulmonary stenosis (TI/PS) are presented in table 2. It may be seen that although the cardiac output is decreased in congestive heart failure associated with valvular disease, coronary blood flow, and myocardial oxygen usage were unchanged from normal. The extractions of glucose, lactate, and pyruvate were slightly increased in the dogs with congestive heart failure so that the total contribution of carbohydrate to energy production was increased and the contribution of fatty acids reduced in the failing heart. The detailed protocols are presented elsewhere. The results of the phosphate fractionation in ventricular muscle from normal animals and those in failure are shown in table 3. No differences between groups were noted for any of the fractions studied. The fact that

TABLE 2. *Cardiac Performance and Metabolism in Normal Dogs and Dogs With Congestive Heart Failure Due to Valvular Disease*

Condition	No.	Cardiac Output Liters/min (± S.E.)	Coronary Blood Flow ml/min/100 g (±S.E.)	Myocardial O_2 Usage ml/min/100 g (± S.E.)	Oxygen Utilization				
					ml %		% usage		
					Art.	A-V	CBH*	Fat	Total
Normal	7	2.02±.12	91±9	10.9±1.2	17.8±0.9	12.7±0.4	43±11	54±10	97±8
Congestive heart failure (TI/PS)†	6	1.38±.10	98±15	10.5±2.0	14.1±0.8	10.3±0.5	63±3	37±9	100±10

* CBH—Carbohydrate. † Tricuspid insufficiency and pulmonary stenosis.

TABLE 3. *Partition of Acid-Soluble Phosphorus in Heart Muscle From Normal Dogs and Dogs in Congestive Heart Failure Due to Valvular Disease*

Group	Valvular Lesion	No.	Phosphorus in Milligrams %			
			TASP*	P_i*	CP*	ATP*
Normal	None	7	136 ±2	22.1 ±1.6	10.7 ±1.0	27.8 ±0.6
Congestive heart failure	TI/PS	7	123 ±4	22.2 ±2.4	11.2 ±2.2	26.4 ±1.2

Values for above are ± standard errors of the mean. * TASP—total acid-soluble phosphorus; P_i—true inorganic phosphorus; CP—creatine phosphate; ATP—adenosinetriphosphate.

ventricular ATP and CP levels do not change in failure due to valvular disease, in agreement with findings in the failing heart-lung preparations (258), suggests that availability of high-energy bonds for myocardial contraction are not limiting in this syndrome. Brody *et al.* (34) compared the ability of ventricular muscle from failing and nonfailing heart-lung preparations to carry on oxidative phosphorylation from pyruvate in vitro and found no difference in the P:O ratios. Similarly, no differences have been found in in vitro oxidative phosphorylation of heart muscle from intact normal dogs and those in failure in our laboratory (192). The weight of the evidence to date is that there is no biochemical defect in the reactions leading to energy liberation and conservation in the heart with low-output failure.

The study of the contractile proteins in experimental heart failure has yielded some very interesting findings. Myosin isolated from the ventricular muscle of normal animals and from those with congestive heart failure by the procedure of Szent-Györgyi (234), rigorously purified by repeated dilutions and preparative ultracentrifugations to remove any residual actomyosin, was subjected to numerous physical-chemical measurements including sedimentation (free and approach to equilibrium), diffusion (free and boundary spreading in the ultracentrifuge), viscosity, and light-scattering measurements. All the myosin preparations from normal animals appeared homogeneous by ultracentrifugation (fig. 22) and electrophoresis. Some of the data are summarized in table 4. It may be seen that although the $S_{20,w}$ intercept of the curve describing dependence of sedimentation rate upon concentration were nearly identical for myosin isolated from normal hearts (myosin C) and that isolated from failing hearts (myosin F), the slope of the dependence upon concentration (dS/dc) was markedly different for the two preparations. In three of the preparations of myosin F, a second faster moving peak appeared in dilute solution with an $S_{20,w}$ of about 9.5. Further, the intrinsic viscosities of the two myosins were markedly different. In contrast, the ATPase activities of the two preparations were not significantly different. The diffusion constant ($D_{20,w}$) for cardiac myosin A was 2.45×10^{-7} cm² sec⁻¹ and for cardiac myosin F was 0.77×10^{-7} cm² sec⁻¹. These constants, together with the light-scattering behavior, led to estimations of molecular weights of 223,000 for myosin C (as indicated previously) and 685,000 for myosin F (226). The faster moving peak in some of the myosin F preparations behaved like a polymer of myosin F.

These data are consistent with the view that an abnormal stable aggregate of myosin C is formed in cardiac failure and that this myosin F prevents the

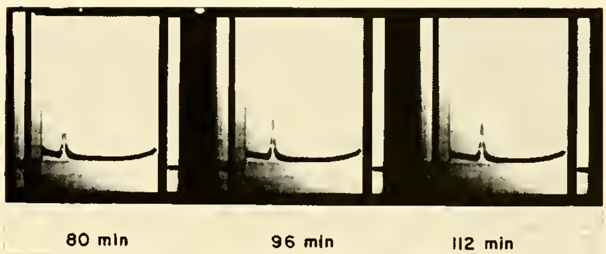

FIG. 22. Homogenous cardiac myosin from a normal dog as determined by ultracentrifugation. Conditions: protein concentration 0.44%, rotor speed 56,100 rpm. T/20.6, pH 6.8, $S_{20,w}$ 4.77. [From Olson (177).]

TABLE 4. *Properties of Cardiac Myosin From Normal Dogs and Dogs in Congestive Heart Failure*

Condition	No.	$S_{20,w}$	−dS/dc	[η]	ATPase Q_p
Normal	8	6.16±0.13*	3.10±0.16*	0.56±0.01*	382
Congestive heart failure (TI/PS)	10	6.53±0.11*	6.66±0.84*	3.65±0.03*	424

Sedimentation studies carried out on dialyzed preparations of myosin in 0.6 M KCl at pH 6.8 in a model E Spinco ultracentrifuge at 56,100 ± 7 r.p.m. at 4°C. Viscosity measurements were made in an Ostwald viscometer at 1°C. ATPase measurements were made in a glycine buffer of pH 9.2 at 25°C. over a 5-minute period.

* ± S.E. of mean.

formation of an actomyosin with normal contractile properties (178). Benson (14) found that the actomyosin content of ventricle from animals in congestive heart failure (TI PS) was reduced below normal and had certain abnormal properties, namely, decreased viscosity per unit of actomyosin and a decreased change in viscosity per unit of actomyosin upon the addition of ATP. More recently, Benson and co-workers (15) have found that the in vitro contractility of glycerol-extracted muscle strips from both the right and left ventricles of dogs with heart failure due to TI/PS was markedly reduced and that a depressed ventricular function curve similar to that observed in vivo could be constructed from the data. Since glycerol-extracted muscle retains little else than the basic contractile system and responds to ATP like isolated actomyosin, it seems reasonable to assume that the defective contractility observed by Benson and co-workers (15) must be due to an altered actomyosin fibril. Kako & Bing (115) have noted a similar decrease in the contractility of actomyosin bands prepared from failing human heart muscle post mortem when compared with control preparations. It seems reasonable to conclude that the biochemical lesion in congestive heart failure of the low-output type is located in the contractile mechanism itself, presumably because of an alteration in myosin, and hence actomyosin. The stimulus for this change may be the chronic stretch to which heart muscle working at a mechanical disadvantage is subjected. The extensive hydrogen bonding of myosin may well be disrupted under such conditions and permit aggregation to occur (65).

Much additional research is required to elucidate the molecular events underlying the heart beat in health and disease. The conception of heart failure as a manifestation of specific biochemical lesions in the myocardium, however, should lead to new investigations which will define with greater precision than is now possible the molecular pathogenesis of the various forms of the disease. It must also be remembered that although many extracardiac factors may modify the degree of manifest clinical failure in the organism, in the final analysis, the heart fails when its generation of free energy or its utilization of that energy in the process of contraction is insufficient for the circulatory load imposed.

The author would like to acknowledge the helpful suggestions of Doctor Clyde M. Williams and the clerical assistance of Miss Anna D. Francis in the preparation of this manuscript.

APPENDIX

Enzyme Differences in Heart and Skeletal Muscle

Enzyme	Species	Cardiac Muscle	Skeletal Muscle	Reference
Hexomonophosphate shunt				
Glucose-6-phosphate dehydrogenase (units/g tissue at 20°)	Rat	26.0	8.0	(79)
6-Phosphogluconate dehydrogenase	Rat	34.0	15.0	(79)
Vitamins				
Thiamine (μg/g wet wt)	Rat (male)	7.0	1.3	(160)
	Human	3.0	0.8	(237)
Riboflavine (μg/g wet wt)	Rat (male)	14.0	1.7	(160)
	Human	7.8	2.0	(237)
Nicotinic acid (μg/g wet wt)	Rat (male)	120.0	64.0	(160)
	Human	41.0	50.0	(237)
Pantothenic acid (μg/g wet wt)	Rat (male)	30.0	5.5	(160)
	Human	16.0	10.0	(237)
Pyridoxin (μg/g wet wt)	Rat (male)	1.1	1.1	(160)
	Human	0.9	1.1	(237)
Glycolytic enzymes				
Hexokinase (μl of glucose utilized/mg tissue—dry wt/hr)	Rabbit	4.1	2.6	(79)
	Rat	14.5		(11)
Aldolase (mg P released from hexosediphosphate per minute/g wet tissue)	Rabbit	0.6	7.5	(2) and (2a)
	Rat	0.6	7.5	(3) and (4)
Lactic acid dehydrogenase (units/mg dry wt acetone powder)	Rat	320.0		
	Mouse		520.0	(256) and (154)
Krebs cycle enzymes				
Aconitase (units/mg dry wt)	Rat	72.0	12.0	(256) and (197)
Fumarase (units/mg dry wt acetone powder)	Rat	96.0	62.0	(256) and (197)

APPENDIX—*Continued*

Enzyme	Species	Cardiac Muscle	Skeletal Muscle	Reference
Krebs cycle enzymes				
Malic acid dehydrogenase (units/mg dry wt acetone powder)	Rat	383.0		(256) and (154)
	Mouse		330.0	
Isocitric acid dehydrogenase (units/mg dry wt acetone powder)	Rat	56.0		(256) and (154)
	Mouse		16.0	
Myoglobin (mg/g wet wt)	Dog (2 mos)	1.3	1.1	(159)
	Dog (adult)	4.8	8.2	(159)
	Horse	4.0	6.2	(159)

APPENDIX—*Continued*

Enzyme	Species	Cardiac Muscle	Skeletal Muscle	Reference
Myoglobin (mg/g wet wt)	Rat	0.9	0.9	(59)
	Man	1.4	1.4	(59)
Cytochrome c (μg/g dry wt)	Rat	1940.0	381.0	(59)
	Man	136.0	22.0	(59)
Cytochrome a_3 (μl O_2/mg dry wt/hr)	Rat	974.0	180.0	(61)
Q O_2 (in vitro)	Rat	14.0	4.0	(62)
Transaminase (μl substrate/hr/mg dry tissue)	Rat	425.0	316.0	(26) and (27)

REFERENCES

1. Abbott, B. C. and J. Lowy. Mechanical properties of pinna adductor muscle. *J. Marine Biol. Assoc. United Kingdom* 35: 521, 1956.
2. Adelberg, E. A. Vertebrate tissues and organs: relative enzyme content. In: *Handbook of Biological Data*, edited by W. S. Spector. Philadelphia: Saunders, 1956, p. 80.
2a. Adler, F. H. Vertebrate tissues and organs: relative enzyme content. In: *Handbook of Biological Data*, edited by W. S. Spector. Philadelphia: Saunders, 1956, p. 80.
3. Adolph, E. F. Vertebrate tissues and organs: relative enzyme content. In. *Handbook of Biological Data*, edited by W. S. Spector. Philadelphia: Saunders, 1956, p. 80.
4. Aebersold, P. C. Vertebrate tissues and organs: relative enzyme content. In: *Handbook of Biological Data*, edited by W. S. Spector. Philadelphia: Saunders, 1956, p. 80.
5. Aloisi, M. Lesioni biochimiche delle proteine muscolari nella avitaminosi E. Vitamina E. Atti del terzo. Congresso Internazionale Venezia, 1955. Verona: Edizioni Valdonega, 1956, vol. MCMLVI.
6. Andrus, E. C. The heart in hyperthyroidism: A clinical and experimental study. *Am. Heart J.* 8: 66, 1932.
7. Astbury, W. T. On the structure of biological fibres and the problem of muscle. *Proc. Roy. Soc. London Ser. B.* 134: 303, 1947.
8. Bailey, K. Invertebrate tropomyosin. *Biochim. et biophys. acta* 24: 612, 1957.
9. Bailey, A., L. Johnston, and F. Moseley. Tropomyosin: a new asymmetric protein component of the muscle fibril. *Biochem. J.* 43: 271, 1948.
10. Banga, I. and A. Szent-Györgyi. Preparation and properties of myosin A and B. In: *Studies from the Institute of Medical Chemistry, University Szeged.* Basel: 1941–42, p. 5, vol. 1.
11. Bare, J. K. Vertebrate tissues and organs: relative enzyme content. In: *Handbook of Biological Data*, edited by W. S. Spector. Philadelphia: Saunders 1956, p. 80.
12. Barger, A. C., B. B. Roe, and G. S. Richardson. Relation of valvular lesions and of exercise to auricular pressure, work tolerance, and to development of chronic, congestive failure in dogs. *Am. J. Physiol.* 169: 384, 1952.
13. Beinert, H., D. E. Green, P. Hele, H. Helen, R. W. von Korff, and C. V. Ramakrishnan. The acetate activating enzyme system of heart muscle. *J. Biol. Chem.* 203: 35, 1943.
14. Benson, E. S. Composition and state of protein in heart muscle of normal dogs and dogs with experimental myocardial failure. *Circulation Res.* 3: 221, 1955.
15. Benson, E. S., B. E. Hallaway, and C. E. Turbak. Contractile properties of glycerol-extracted muscle bundles from the chronically failing canine heart. *Circulation Res.* 6: 122, 1958.
16. Berenbaum, A. A. and W. Horowitz. Heart involvement in progressive muscular dystrophy. Report of a case with sudden death. *Am. Heart J.* 51: 622, 1956.
17. Berg, P. Acyl adenylates: an enzymatic mechanism of acetate activation. *J. Biol. Chem.* 222: 991, 1956.
18. Bing, R. J. The metabolism of the human heart *in vivo*. *J. Mt. Sinai Hosp. New York* 20: 100, 1953.
19. Bing, R. J. The coronary circulation in health and disease as studied by coronary sinus catheterization. *Bull. New York Acad. Med.* 27: 407, 1951.
20. Bing, R. J., A. Castellanos, E. Gradel, C. Lupton, and A. Siegel. Experimental myocardial infarction: circulatory, biochemical and pathologic changes. *Am. J. M. Sc.* 232: 533, 1956.
21. Bing, R. J., A. Siegel, I. Ungar, and M. Gilbert. Metabolism of the human heart. II. Studies on fat, ketone and amino acid metabolism. *Am. J. Med.* 16: 504, 1954.
22. Bing, R. J., A. Siegel, A. Vitale, F. Balboni, E. Sparks, M. Taeschler, M. Klapper, and S. Edwards. Metabolic studies on the human heart in vivo. I. Studies on carbohydrate metabolism of the human heart. *Am. J. Med.* 15: 284, 1953.

23. Bing, R. J., L. D. Vandam, F. Gregoire, J. C. Handelsman, W. T. Goodale, and J. E. Eckenhoff. Catheterization of the coronary sinus and middle cardiac vein in man. *Proc. Soc. Exper. Biol. & Med.* 66: 239, 1947.
24. Biorck, G. Physiologic views on the myoglobin content and its variations. *Acta med. scandinav.* 130, Suppl. 226, 1949.
25. Blain, J. M., H. Schafer, A. L. Siegel, and R. J. Bing. Studies on myocardial metabolism. VI. Myocardial metabolism in congestive failure. *Am. J. Med.* 20: 820, 1956.
26. Blanck, F. C. Vertebrate tissues and organs: relative enzyme content. In: *Handbook of Biological Data*, edited by W. S. Spector. Philadelphia: Saunders, 1956, p. 81.
27. Blasius, W. Vertebrate tissues and organs: relative enzyme content. In: *Handbook of Biological Data* edited by W. S. Spector. Philadelphia: Saunders, 1956, p. 81.
28. Bloom, W. L. Glycogenolysis in the anoxic heart. *Am. J. Physiol.* 186: 518, 1956.
29. Bogue, J. Y., C. L. Evans, and R. A. Gregory. The effect of adrenaline together with acute anoxia upon the heart glycogen. *Quart. J. Exper. Physiol.* 29: 83, 1939.
30. Bogue, J. Y., C. L. Evans, and R. A. Gregory. Source of heart glycogen. *Quart. J. Exper. Physiol.* 27: 213, 1937.
31. Braun-Menendez, E., A. D. Chute, and R. A. Gregory. Usage of pyruvic acid by the dog's heart. *J. Physiol.* 29: 91, 1939.
32. Breslow, R. On the mechanism of thiamine action. IV. Evidence from studies on model systems. *J. Am. Chem. Soc.* 80: 3719, 1958.
33. Brin, M., R. E. Olson, and F. J. Stare. Metabolism of cardiac muscle. Comparative studies with L(+)- and D(−)-C^{14}-lactate in duck and rat tissues. *J. Biol. Chem.* 199: 467, 1952.
34. Brody, T. M., J. F. Palmer, and D. R. Bennett. Phosphorylation in cardiac muscle from failing and unfailing heart-lung preparations. *Proc. Soc. Exper. Biol. & Med.* 86: 4, 739, 1954.
35. Bryant, E. R., W. A. Thomas, and R. O'Neal. An electron microscopic study of myocardial ischemia in the rat. *Circulation Res.* 6: 699, 1958.
36. Buchtal, F., O. Svensmark, and P. Rosenfalck. Mechanical and chemical events in muscle contraction. *Physiol. Rev.* 36: 503, 1956.
37. Buell, M. V., M. B. Strauss, and E. C. Andrus. Metabolic changes involving phosphate and carbohydrate in autolyzing gastrocnemius and cardiac muscle of normal, of thyroxinized, and of adrenalectomized animals. *J. Biol. Chem.* 98: 645, 1932.
38. Burwell, C. S. and L. Dexter. Beriberi heart disease. *Tr. Assoc. Am. Physicians* 60: 49, 1947.
39. Chance, B., B. Hess, and C. M. Connelly. The respiratory chain as an indicator of intracellular ADP levels of muscle, yeast, and tumor cells. *J. Cell. & Comp. Physiol.* 46: 35, 1955.
40. Chance, B. and G. R. Williams. A simple and rapid assay of oxidative phosphorylation. *Nature, London* 175: 1120, 1955.
41. Chance, B. and G. R. Williams. The respiratory chain and oxidative phosphorylation. *Advances in Enzymol.* 17: 65, 1956.
42. Conference on Hemoglobin. Washington: National Academy of Sciences—National Research Council. Publication No. 557, 1958.
43. Conn, H. L., Jr., J. C. Wood, and G. S. Morales. Rate of change in myocardial glycogen and lactic acid following arrest of coronary circulation. *Circulation Res.* 8: 721, 1959.
44. Connelly, C. M. and B. Chance. Kinetics of reduced pyridine nucleotides in stimulated frog muscle and nerve. *Fed. Proc.* 13: 29, 1954.
45. Cooper, C., T. M. Devlin, and A. L. Lehninger. Oxidative phosphorylation in an enzyme fraction from mitochondrial extracts. *Biochim. et biophys. acta* 18: 159, 1955.
46. Cori, C. F. In: *Enzymes; Units of Biological Structure and Function.* New York: Acad. Press, 1956, p. 573.
47. Cori, G. T. Glycogen structure and enzyme deficiencies in glycogen storage disease. *Harvey Lect.* 48: 145, 1953.
48. Cornforth, J. W. Biosynthesis of fatty acids and cholesterol considered as chemical processes. *J. Lipid Res.* 1 3, 1959.
49. Crane, F. L., J. L. Glenn, and D. E. Green. Isolation of a quinone from beef heart mitochondria. *Biochim. et biophys. acta* 25: 220, 1957.
50. Crane, R. K. and A. Sols. The association of hexokinase with particulate fractions of brain and other tissue homogenates. *J. Biol. Chem.* 203: 273, 1953.
51. Crispell, K. R., W. Parsons, and G. Hollifield. A study of the rate of protein synthesis before and during the administration of L-triiodo-thyronine to patients with myxedema and healthy volunteers using N^{15} glycine. *J. Clin. Invest.* 35: 164, 1956.
52. Cruck, S. Contribution à la biochimie comparée des protéines musculaires dans les différents compartiments du coeur. *Biochim. et biophys. acta* 10: 630, 1953.
53. Cruickshank, E. W. H. and O. W. Startup. Effect of insulin on the respiratory quotient oxygen consumption, sugar utilization, and glycogen synthesis by the normal mammalian heart in hyper- and hypoglycemia. *J. Physiol.* 77: 365, 1933.
54. Dempsey, W. D., G. B. Wislocke, and M. Singer. Some observations of the chemical cytology of striated muscle. *Anat. Rec.* 96: 221, 1946.
55. Dickens F. Alternative routes of carbohydrate oxidation. *Brit. M. Bull.* 9: 105, 1953.
56. di Sant'Agnese, P. A. Diseases of glycogen storage with special reference to the cardiac type of generalized glycogenosis. *Ann. New York Acad. Sc.* 72: 439, 1959.
57. Dole, V. P., and J. Hirsch. Effect of hormones on depot fat. In: *Clinical Endocrinology*, edited by E. B. Astwood. New York: Grune, 1960 vol. 1, pp. 551–557.
58. Dow, J. W. and R. Gorlin. Pulmonary capillary pressure as an index of left atrial mean pressure in dogs. *Fed. Proc.* 9: 33, 1950.
59. Drabkin, D. L. The distribution of the chromoproteins, hemoglobin, myoglobin, and cytochrome *c*, in the tissues of different species, and the relationship of the total content of each chromoprotein to body mass. *J. Biol. Chem.* 182: 317, 1950.
60. Dreyfus, J. C., J. Kruh, and G. Schapira. Metabolism of myosin and life time of myofibrils. *Biochem. J.* 75: 574, 1960.
61. DuBois, K. P. and V. R. Potter. Biocatalysts in cancer tissue. I. Cytochrome *c*. *Cancer Res.* 2: 290, 1942.

62. DuBois, K. P. and V. R. Potter. The assay of animal tissues for respiratory enzymes. III. Adenosinetriphosphatase. *J. Biol. Chem.* 150: 185, 1943.
63. Eckenhoff, J. E. and H. H. Hafkenschiel. The oxygen content of coronary venous blood as affected by anoxia and cytochrome *c*. *Am. Heart J.* 36: 3, 1948.
64. Edwards, W. S., A. Siegel, and R. J. Bing. Studies on myocardial metabolism. III. Coronary blood flow, myocardial oxygen consumption and carbohydrate metabolism in experimental hemorrhagic shock. *J. Clin. Invest.* 33: 1646, 1954.
65. Ellenbogen, E., R. Iyengar, and R. E. Olson. Properties of myosin from normal and failing dog heart. *Fed. Proc.* 18: 221, 1959.
66. Ellenbogen, E., R. Iyengar, H. Stern, and R. E. Olson. Characterization of myosin from normal dog heart. *J. Biol. Chem.* 235: 2642, 1960.
67. Engelhardt, W. A. and M. N. Ljubimova. Myosin and adenosinetriphosphatase. *Nature, London* 144: 668, 1939.
68. Evans, C. A. L. Metabolism of the heart. *Edinburgh M. J.* 46: 733, 1939.
69. Evans, C. L., F. Grande, F. Y. Hsu, D. H. K. Lee, and A. C. Mulder. Glucose and lactate usages of diabetic heart and influence of insulin thereon. *Quart. J. Exper. Physiol.* 24: 365, 1935.
70. Fawaz, G., E. S. Hawa, and B. Tutunji. The effect of dinitrophenol, hypoxaemia and ischaemia on the phosphorus compounds of the dog heart. *Brit. J. Pharmacol.* 12: 270, 1957.
71. Fiske, C. H. and Y. Subbarow. Phosphocreatine. *J. Biol. Chem.* 81: 629, 1929.
72. Fleckenstein, A., J. Janke, R. E. Davies, and H. A. Krebs. Chemistry of muscle contraction. Contraction of muscle without fission of adenosine triphosphate or creatine phosphate. *Nature, London* 174: 1081, 1954.
73. Flock, E. V., J. L. Bollman, and F. C. Mann. The utilization of pyruvic acid by the dog. *J. Biol. Chem.* 125: 49, 1938.
74. Fruton, J. S. and S. Simmonds. *General Biochemistry* (2nd ed.). New York: Wiley, 1958.
75. Gailani, S., T. S. Danowski, and D. S. Fisher. Muscular dystrophy. Catheterization studies indicating latent congestive heart failure. *Circulation* 17: 583, 1958.
76. Gelotte, B. Myosin from cardiac muscle. *Biochim. et biophys. acta* 7: 378, 1951.
77. Gergely, J. Studies on myosin-adenosinetriphosphatase. *J. Biol. Chem.* 200: 543, 1953.
78. Gergely, J., M. A. Gouvea, and H. Kohler. Cardiac myosin. *Circulation* 14: 940, 1956.
79. Gerritsen, T. On the glucokinase activity of extracts from normal and atrophic muscles. *Biochim. et biophys. acta.* 8: 466, 1952.
80. Glock, G. E. and P. McLean. Levels of enzymes of the direct oxidative pathway of carbohydrate metabolism in mammalian tissues and tumours. *Biochem. J.* 56: 171, 1954.
81. Goodale, W. T. and D. B. Hackel. Myocardial carbohydrate metabolism in normal dogs, with effects of hyperglycemia and starvation. *Circulation Res.* 1: 509, 1953.
82. Goodale, W. T., R. E. Olson, and D. B. Hackel. The effects of fasting and diabetes mellitus on myocardial metabolism in man. *Am. J. Med.* 27: 212, 1959.
83. Goodale, W. T., R. E. Olson, and D. B. Hackel. Myocardial glucose, lactate and pyruvate metabolism of normal and failing hearts studied by coronary sinus catheterization in man. *Fed. Proc.* 9: 49, 1950.
84. Gordon, R. S. and A. Cherkes. Unesterified fatty acid in human blood plasma. *J. Clin. Invest.* 35: 206, 1956.
85. Gorlin, R., N. Branchfield, P. Bopp, and C. MacLeod. Physiological diagnosis of disordered coronary circulation. *J. Clin. Invest.* 37: 898, 1958.
86. Grant, J. C. B. Pericardium and contents. In: *Method of Anatomy* (6th ed.). Baltimore: Williams & Wilkins, 1958, chapt. 18.
87. Green, D. E. Fatty acid oxidation in soluble systems of animal tissues. *Biol. Rev. Cambridge Phil. Soc.* 29: 330, 1954.
88. Green, D. E. and J. Järnefelt. Enzymes and biological organization. *Perspectives in Biol. & Med.* 2: 163, 1959.
89. Green, H. D. Circulatory system: physical principles. In: *Medical Physics*, edited by O. Glasser. Chicago: Yr. Bk. Pub., 1950, vol. 2, p. 228.
90. Gunsalus, I. C. The metabolism of thiamin and lipoic acid. In: *Symposium on Vitamin Metabolism.* New York: National Vitamin Foundation, Inc., 1956 vol. 13, p. 6.
91. Hackel, D. B. and W. T. Goodale. Effects of hemorrhagic shock on the heart and circulation of intact dogs. *Circulation* 11: 628, 1955.
92. Hackel, D. B., W. T. Goodale, and J. Kleinerman. Effects of thiamine deficiency on myocardial metabolism in intact dogs. *Am. Heart J.* 46: 883, 1953.
92a. Hackel, D. B. Effect of insulin on cardiac metabolism of intact normal dogs. *Am. J. Physiol.* 199: 1135, 1960.
93. Hanson, J. and H. E. Huxley. Structural basis of the cross-striations in muscle. *Nature, London* 182: 530, 1953.
94. Harrison, T. R. *Failure of the Circulation.* Baltimore: Williams & Wilkins, 1939.
95. Harvey, W. *Exercitatio anatomica de motu cordis et sanguinis in animalibus*, translated by C. Leake. Springfield, Ill.: Thomas, 1930.
96. Hasselbach, W. Elektronmikroskopischen Untersuchungen um Muskelfibrille beim totler und partieller Extraktion des L-myosins. *Ztschr. Naturforsch.* 8b: 449, 1953.
97. Hele, P. The acetate activating enzyme of beef heart. *J. Biol. Chem.* 206: 671, 1954.
98. Hemingway, A. and A. R. Fee. The relationship between the volume of the heart and its oxygen usage. *J. Physiol.* 63: 299, 1927.
99. Hess, M. E. and N. Haugaard. The effect of epinephrine and aminophylline on the phosphorylase activity of perfused contracting heart muscle. *J. Pharmacol. & Exper. Therap.* 122: 169, 1958.
100. Hill, A. V. The heat of shortening and the dynamic constants of muscle. *Proc. Roy. Soc., London. ser. B* 126: 136, 1939.
101. Hill, A. V. *Muscular Activity.* Baltimore: Williams & Wilkins, 1956.
102. Himwich, H. E., W. Goldfarb, and L. H. Nahum. Changes of the carbohydrate metabolism of the heart following coronary occlusion. *Am. J. Physiol.* 109: 403, 1934.
103. Hogeboom, G. H., W. C. Schneider, and G. E. Palade. Cytochemical studies of mammalian tissues. I. Isolation of intact mitochondria from rat liver; some biochemical

properties of mitochondria and submicroscopic particulate material. *J. Biol. Chem.* 172: 619, 1948.
104. Holtzer, A. and S. Lowey. The molecular weight, size and shape of the myosin molecule. *J. Am. Chem. Soc.* 81: 1370, 1959.
105. Horecker, B. L. and A. H. Mehler. Carbohydrate metabolism. *Ann. Rev. Biochem.* 24: 207, 1955.
106. Huxley, A. F. Muscle structure and theories of contraction. In: *Progress in Biophysics and Biophysical Chemistry*, edited by J. A. V. Butler and B. Katz. New York: Pergamon, 1957 pp. 257–318.
107. Huxley, A. F. and R. Niedergerke. Structural changes in muscle during contraction. Interference microscopy of living muscle fibres. *Nature, London* 173: 971, 1954.
108. Huxley, A. F. and R. E. Taylor. Function of Krause's membrane. *Nature, London* 176: 1068, 1955.
109. Huxley, H. E. The structure of striated muscle. In: *Molecular Biology*, edited by D. Nachmansohn. New York: Acad. Press, 1960, pp. 1–16.
110. Huxley, H. E. Muscular contraction. *Endeavour* 15: 177, 1956.
111. Huxley, H. E. and J. Hanson. Changes in the cross-striations of muscle during contraction and stretch and their structural interpretation. *Nature, London* 173: 973, 1954.
112. Itzhaki, S. and E. Wertheimer. Changes in carbohydrate metabolism of cardiac and striated muscle in hypothermic rats. *Circulation Res.* 5: 451, 1957.
113. Jolley, R. L., V. H. Cheldelin, and R. W. Newburgh. Glucose catabolism in fetal and adult heart. *J. Biol. Chem.* 233: 1289, 1958.
114. Junkersdorf, P. Untersuchungen über die Phlorrhizinglucosurie. *Arch. ges. Physiol.* 200: 443, 1923.
115. Kako, K. and R. J. Bing. Contractility of actomyosin bands prepared from normal and failing human heart. *J. Clin. Invest.* 37: 465, 1958.
116. Keilin, D. On cytochrome, a respiratory pigment, common to animals, yeast, and higher plants. *Proc. Roy. Soc., London. ser. B* 98: 312, 1925.
117. Keilin, D. and E. F. Hartree. Relationship between certain components of the cytochrome system. *Nature, London* 176: 200, 1955.
118. Keller P. J. and G. T. Cori. Enzymic conversion of phosphorylase *a* to phosphorylase *b*. *Biochim. et biophys. acta* 12: 235, 1953.
119. Kendrew, J. C. Structure and function in myoglobin and other proteins. *Fed. Proc.* 18: 740, 1959.
120. Kepler, E. J. and A. R. Barnes. Congestive heart failure and hypertrophy in hyperthyroidism: A clinical and pathological study of 178 fatal cases. *Am. Heart J.* 8: 102, 1932.
121. Kielley, W. W. and W. F. Harrington. A model for the myosin molecule. *Biochim. et biophys. acta* 41: 401, 1960.
122. Kien, G. A. and T. R. Sherrod. The effect of digoxin on the intermediary metabolism of the heart as measured by glucose-C^{14} utilization in the intact dog. *Circulation Res.* 8: 188, 1960.
123. Kisch, B. *Electron Microscopic Histology of the Heart.* New York: Brooklyn Medical Press, 1951.
124. Knoop, F. Der Abbau aromatischer Fettsäuren im Tierkörper. *Beitr. chem. Physiol. Path.* 6: 150, 1904.
125. Kochen, J., G. V. Marinetti, and E. Stotz. The lipids of the myocardium, conducting bundle, and valves of beef heart. *J. Lipid Res.* 1: 147, 1959.
126. Kornberg, A. and W. E. Pricer, Jr. Enzymatic synthesis of the coenzyme A derivatives of long chain fatty acids. *J. Biol. Chem.* 204: 329, 1953.
127. Krampitz, L. O., G. Gruell, C. S. Miller, J. B. Bicking, H. R. Skeggs, and J. M. Sprague. An active acetaldehyde-thiamine intermediate. *J. Am. Chem. Soc.* 80: 5893–94, 1958.
128. Krebs H. A. and W. A. Johnson. Role of citric acid in intermediate metabolism in animal tissues. *Enzymologia* 4: 148, 1937.
129. Lackey, R. W., C. A. Bunde, and L. C. Harris. Effect on cardiac glycogen of intravenously administered sodium aceto-acetate, sodium beta-hydroxybutyrate, and sodium butyrate. *Proc. Soc. Exper. Biol. & Med.* 66: 433, 1947.
130. Laki, K. and W. R. Carroll. Size of the myosin molecule. *Nature, London* 175: 389, 1955.
131. Lawrie, R. A. The activity of the cytochrome system in muscle and its relation to myoglobin. *Biochem. J.* 55: 298, 1953.
132. Lehninger, A. L. A quantitative study of the products of fatty acid oxidation in liver suspensions. *J. Biol. Chem.* 164: 291, 1946.
133. Lehninger, A. L., C. L. Wadkins, C. Cooper, T. M. Devlin, and J. L. Gamble. Oxidative phosphorylation. *Science* 128: 450, 1958.
134. Levine, R. and M. S. Goldstein. On mechanism of action of insulin. In: *Recent Progress in Hormone Research*, edited by G. Pincus. New York: Acad. Press, 1955, vol. 11, p. 343.
135. Levy, H. M. and D. E. Koshland, Jr. Mechanism of hydrolysis of adenosinetriphosphate by muscle proteins and its relation to muscular contraction. *J. Biol. Chem.* 234: 1102, 1959.
136. Ligata, R. H. and J. T. Roberts. Histology of the heart. In: *Cardiology*, edited by A. A. Luisada. New York: McGraw-Hill, 1959, vol. 1, p. 67.
137. Likoff, W. B. and S. A. Levine. Thyrotoxicosis as the sole cause of heart failure. *Am. J. M. Sc.* 206: 425, 1943.
138. Lohmann, K. Über die enzymatische Aufspaltung der Kretinphosphorsäure; zugleich ein Beitrag zum Chemismus der Muskelkontraktion. *Biochem. Ztschr.* 271: 264, 1934.
139. Lorber, V., A. Hemingway, and A. O. Nier. Assimilation of carbon dioxide by the isolated mammalian heart. *J. Biol. Chem.* 151: 647, 1943.
140. Lorber, V., N. Lifson, H. G. Wood and J. Barcroft. The metabolism of acetate by the completely isolated mammalian heart investigated with carboxyl-labeled acetate. *Am. J. Physiol.* 145: 557, 1946.
141. Lowey, S. and A. Holtzer. The aggregation of myosin. *J. Am. Chem. Soc.* 81: 1378, 1959.
142. Lowey, S. and A. Holtzer. The homogeneity and molecular weights of the meromyosins and their relative proportions in myosin. *Biochim. et biophys. acta* 34: 470, 1959.
143. Lundsgaard, E. Untersuchungen über Muskelkontraktionen ohne Milchsäurebildung. *Biochem. Ztschr.* 217: 162, 1930.
144. Lynen, F. Functional group of coenzyme A and its

metabolic relations, especially in the fatty acid cycle. *Fed. Proc.* 12: 683, 1953.

145. MacLeod, J. J. R. and D. J. Prendergast. Glycogen in the heart and skeletal muscles in starved and well-fed animals. *Tr. Roy. Soc. Can.* 15: 37, 1921.
146. Mahler, H. R. Role of coenzyme A in fatty acid metabolism. *Fed. Proc.* 12: 694, 1953.
147. Maley, G. F. and H. A. Lardy. Metabolic effects of thyroid hormones in vitro. II. Influence of thyroxine and triiodothyronine on oxidative phosphorylation. *J. Biol. Chem.* 204: 435, 1953.
148. Maley, G. F. and H. A. Lardy. Efficiency of phosphorylation in selected oxidations by mitochondria from normal and thyrotoxic rat livers. *J. Biol. Chem.* 215: 377, 1955.
149. Mallov, S., J. M. McKibbin, and J. S. Robb. The distribution of some of the essential lipides in beef heart muscle and conducting tissue. *J. Biol. Chem.* 201: 825, 1953.
150. Marinetti, G. V., J. Erbland, and E. Stotz. The structure of pig heart plasmalogens. *J. Am. Chem. Soc.* 80: 1624, 1958.
151. Marinetti, G. V., J. Erbland, and E. Stotz. Phosphatides of pig heart cell fractions. *J. Biol. Chem.* 233: 562, 1958.
152. Mattonet, C. Chemischer Beitrag zur Frage der Herzmuskelschädigung durch Thyroxin. *Ztschr. ges. exper. Med.* 90: 237, 1933.
153. McGinty, D. A. and A. T. Miller. Studies on the coronary circulation. II. Absorption of lactic acid and glucose and the gaseous exchange of heart muscle. *Am. J. Physiol.* 103: 712, 1933.
154. Mehler, A. H., A. Kornberg, S. Grisolia, and S. Ochoa. The enzymatic mechanism of oxidation-reductions between malate or isocitrate and pyruvate. *J. Biol. Chem.* 174: 961, 1948.
155. Meyer, D. K., R. L. Russell, W. S. Platner, F. A. Purdy, and B. A. Westfall. Synthesis of glycogen fractions by heart homogenates. *Proc. Soc. Exper. Biol. & Med.* 90: 15, 1955.
156. Meyerhof, O. *Die Chemischen Vorgänge im Muskel und Ihr Zusammenhang mit Arbeitsleistung und Wännebredung.* Berlin: Springer, 1930.
157. Mihályi, E. and A. G. Szent-Györgyi. Trypsin digestion of muscle proteins. I. Ultracentrifugal analysis of the process. *J. Biol. Chem.* 201: 189, 1953.
158. Miller, O. N. and R. E. Olson. Metabolism of cardiac muscle. IV. Utilization of pyruvate and DL-lactate by duck heart. *J. Biol. Chem.* 199: 457, 1952.
159. Millikan, G. A. Muscle hemoglobin. *Physiol. Rev.* 19: 503 1939.
160. Mitchell, H. K. and E. R. Isbell. B Vitamin content of normal rat tissues. In: *Studies on the Vitamin Content of Tissues II.* Austin. Texas: Univ. Texas Publications, 1942, pp. 37–40.
161. Mommaerts, W. F. H. M. Is adenosine triphosphate broken down during a single muscle twitch? *Nature, London* 174: 1083, 1954.
162. Mommaerts, W. F. H. M. Ultracentrifugal determination of molecular weight of myosin by the Archibald procedure. *Science* 126: 1294, 1957.
163. Mommaerts, W. F. H. M. and B. B. Aldrich. Determination of the molecular weight of myosin. Interference-optical measurements during the approach to ultracentrifugal sedimentation and diffusion equilibrium. *Biochim. et biophys. acta* 28: 627, 1958.
164. Moore, D. H. and H. Ruska. Electron microscope study of mammalian cardiac muscle cells. *J. Biophys. & Biochem. Cytol.* 3: 261, 1957.
165. Morales, M. F. and J. Botts. A theory of the primary event in muscle action. In: *Currents in Biochemical Research,* edited by D. E. Green. New York: Interscience, 1956, pp. 609–627.
166. Morales, M. F., J. Botts, J. J. Blum, and T. L. Hill. Elementary processes in muscle action: an examination of current concepts. *Physiol. Rev.* 35: 475, 1955.
167. Morton, R. A. Ubiquinone. *Nature, London* 182: 1764, 1958.
168. Muntz, J. A. Effect of ions on the activity of enzymes derived from cardiac tissue. *Ann. New York Acad. Sc.* 72: 415, 1959.
169. Neifakh, S. A. and M. P. Melnikova. Enzymatic links which determine the maximal rate of glycolysis in muscle. *Biokhimiya* (English translation) 23: 410, 1958.
170. Ochoa, S. Biosynthesis of tricarboxylic acids by carbon dioxide fixation. III. Enzymatic mechanisms. *J. Biol. Chem.* 174: 133, 1948.
171. Ochoa, S., A. H. Mehler, and A. Kornberg. Biosynthesis of dicarboxylic acids by carbon dioxide fixation. I. Isolation and properties of an enzyme from pigeon liver catalyzing the reversible oxidative decarboxylation of *l*-malic acid. *J. Biol. Chem.* 174: 979, 1948.
172. Ochoa, S., J. R. Stern, and M. C. Schneider. Enzymic synthesis of citric acid. II. Crystalline condensing enzyme. *J. Biol. Chem.* 193: 691, 1951.
173. Olson, J. A. and C. B. Anfinsen. Kinetic and equilibrium studies on crystalline L-glutamic acid dehydrogenase. *J. Biol. Chem.* 202: 841, 1953.
174. Olson, R. E. Molecular events in cardiac failure. *Am. J. Med.* 20: 159, 1956.
175. Olson, R. E. In: *Discussion in Chemistry of Lipides as Related to Atherosclerosis: A Symposium,* compiled and edited by I. H. Page. Springfield, Ill.: Thomas, 1958, pp. 108–113.
176. Olson, R. E. Nutritional disease. *Fed. Proc.* 17: Suppl. 2, 24, 1958.
177. Olson, R. E. Myocardial metabolism in congestive heart failure. *J. Chron. Dis.* 9: 442, 1959.
178. Olson, R. E., E. Ellenbogen, H. Stern, and M. M. L. Liang. An abnormality of cardiac myosin associated with chronic congestive heart failure in the dog. *J. Clin. Invest. (Proc.)* 35: 727, 1956.
179. Olson, R. E., E. G. Hirsch, and M. C. Jones. Formation of fatty acids and cholesterol from radioactive acetate and glucose in rat heart, liver and hepatoma. *Fed. Proc.* 10: 230, 1951.
180. Olson, R. E., O. H. Pearson, O. N. Miller, and F. J. Stare. The effect of thiamine deficiency in rats and ducks. *J. Biol. Chem.* 175: 489, 1948.
181. Olson, R. E. and D. A. Piatnek. Conservation of energy in cardiac muscle. *Ann. New York Acad. Sc.* 72: 466, 1959.
182. Olson, R. E. Symposium on intermediary carbohydrate metabolism in tumor tissue: II. Oxidation of C^{14}-labeled carbohydrate intermediate in tumor tissue. *Cancer Res.* 11: 571, 1951.
183. Olson, R. E., J. S. Robson, H. Richards and E. G.

HIRSCH. Comparative metabolism of radioactive glucose in heart, brain, kidney and liver slices. *Fed. Proc.* 9: 211, 1950.

184. OLSON, R. E., G. ROUSH, AND M. M. L. LIANG. Effect of acetyl strophanthidin upon the myocardial metabolism and cardiac work of normal dogs with congestive heart failure. *Circulation* 12: 755, 1955.
185. OLSON, R. E. AND W. B. SCHWARTZ. Myocardial metabolism in congestive heart failure. *Medicine* 30: 21, 1951.
186. PACKER, L. Coupled phosphorylation in rat muscle sarcosomes. *Arch. Biochem. & Biophys.* 70: 290, 1957.
187. PALADE, G. E. Electron microscopy of mitochondria and other cytoplasmic structures. In: *Enzymes, Units of Biological Structure and Function* (Henry Ford Hospital). New York: Acad. Press, 1956, pp. 185–215.
188. PEARSON, O. H., C. K. HSIEH, C. H. DUTOIT, AND A. B. HASTINGS. Metabolism of cardiac muscle: utilization of C^{14}-labeled pyruvate and acetate in diabetic rat heart and diaphragm. *Am. J. Physiol.* 158: 261, 1949.
189. PERRY, S. V. The adenosinetriphosphatase activity of lipoprotein granules isolated from skeletal muscle. *Biochim. et biophys. acta* 8: 499, 1952.
190. PERRY, S. V. Relation between chemical and contractile function and structure of the skeletal muscle cell. *Physiol. Rev.* 36: 1, 1956.
191. PERRY, S. V. Muscular contraction. In: *Comparative Biochemistry, a Comprehensive Treatise*, edited by M. Florkin and H. S. Mason. New York: Acad. Press, 1960, pp. 245–340.
192. PIATNEK, D. A. AND C. W. LEE. Effect of hyperthyroidism on oxidative phosphorylation in mitochondria from the heart and liver. *Fed. Proc.* 19: 37, 1960.
193. PIATNEK, D. A. AND R. E. OLSON. Effect of hyperthyroidism upon cardiac metabolism in the dog. *Fed. Proc.* 15: 145, 1956.
194. PODOLSKY, R. J. The chemical thermodynamics and molecular mechanism of muscular contraction. *Ann. New York Acad. Sc.* 72: 522, 1959.
195. PRICE, Z., E. BILLIE, M. PRINTZMETAL, AND C. CARPENTER. Ultrastructure of the dog cardiac muscle cell. *Circulation Res.* 7: 858, 1959.
196. PRICE, K. C., J. M. WEISS, D. HATA, AND J. R. SMITH. Experimental needle biopsy of the myocardium of dogs with particular reference to histologic study by electron microscopy. *J. Exper. Med.* 101: 687, 1955.
197. RACKER, E. Spectrophotometric measurements of the enzymatic formation of fumaric and cis-aconitic acids. *Biochim. et biophys. acta* 4: 211, 1950.
198. RACKER, E. Alternate pathways of glucose and fructose metabolism. *Advances in Enzymol.* 15: 141, 1954.
199. RACKER, E. AND S. GATT. Interactions of glycolysis and oxidative pathways. *Ann. New York Acad. Sc.* 72: 427, 1959.
200. RALL, T. W. AND E. W. SUTHERLAND. Formation of a cyclic adenine ribonucleotide by tissue particles. *J. Biol. Chem.* 232: 1065, 1958.
201. RALL, T. W., W. D. WOSILAIT, AND E. W. SUTHERLAND. The interconversion of phosphorylase *a* and phosphorylase *b* from dog heart muscle. *Biochim. et biophys. acta* 20: 69, 1956.
202. REBAR, B., A. OMACHI, AND J. REBAR. Effects of glucose infusion on dog myocardial metabolism. *Circulation Res.* 7: 977, 1959.
203. ROBERTS, J. T., J. T. WEARN, AND J. J. BADAL. Capillary-muscle ratio in normal and hypertrophied human hearts. *Proc. Soc. Exper. Biol. & Med.* 38: 322, 1938.
204. ROWE, G. G., J. H. HUSTON, A. B. WEINSTEIN, H. TUCHMAN, J. F. BROWN, AND C. W. CRUMPTON. The hemodynamics of thyrotoxicosis in man, with special reference to coronary blood flow and myocardial oxygen metabolism. *J. Clin. Invest.* 35: 272, 1956.
205. RÜHL, A. Uber die Bedeutung der Milchsäure für den Herzstoffwechseln. *Klin. Wchnschr.* 13: 1529, 1934.
206. RUSHMER, R. F. Anatomy and physiology of ventricular function. *Physiol. Rev.* 36: 400, 1956.
207. RUSSELL, J. A. AND W. L. BLOOM. Extractable and residual glycogen in tissues of the rat. *Am. J. Physiol.* 183: 345, 1955.
208. SARNOFF, S. J. Myocardial contractility as described by ventricular function curves. *Physiol. Rev.* 35: 107, 1955.
209. SARNOFF, S. J., R. B. CASE, P. T. WAITHE, AND J. P. ISAACS. Insufficient coronary flow and myocardial failure as a complicating factor in late hemorrhagic shock. *Am. J. Physiol.* 176: 439, 1954.
210. SARNOFF, S. J., R. B. CASE, G. H. WELCH, E. BRAUNWALD, AND W. N. STAINSBY. Performance characteristics and oxygen debt in a nonfailing, metabolically supported, isolated heart preparation. *Am. J. Physiol.* 192: 141, 1958.
211. SCHLESINGER, P. G. AND F. POMPEU. Cardiac involvement in progressive muscular dystrophy. *Med. cir. farm.* 280: 338, 1959.
212. SCHNEIDER, W. C. AND G. H. HOGEBOOM. Biochemistry of cellular particles. *Ann. Rev. Biochem.* 25: 201, 1956.
212a. SCHOLANDER, P. F. Oxygen transport through hemoglobin solutions. *Science* 131: 585, 1960.
213. SCHWEET, R. S., M. FULD, K. CHESLOCK, AND M. H. PAUL. Initial stages of pyruvate oxidation. In: *Phosphorus Metabolism*, edited by W. D. McElroy and B. Glass. Baltimore: Johns Hopkins Press, 1951, vol. 2, p. 246.
214. SHELLY, W. B., C. E. CODE, AND M. B. VISSCHER. Influence of thyroid, dinitrophenol and swimming on glycogen and phosphocreatine levels of rat heart in relation to cardiac hypertrophy. *Am. J. Physiol.* 138: 652, 1942–43.
215. SHENG, P. K. AND T. C. TSAO. Comparative study of nucleotropomyosins from different sources. *Sci. Sinica (Peking)* 4: 157, 1955.
216. SIEKEVITZ, P. Oxidative phosphorylation in muscle mitochondria and its possible regulation. *Ann. New York Acad. Sc.* 72: 500, 1959.
217. SNELLMAN, O. AND T. ERDOS. Ultracentrifugal analysis of crystallised myosin. *Biochim. et biophys. acta* 2: 650, 1948.
218. SNELLMAN, O. AND B. GELOTTE. A reaction between a deaminase and heart actin, and inhibition of the effect with cardiac glycoside. *Nature, London* 165: 604, 1950.
219. SNELLMAN, O. AND B. GELOTTE. An investigation of the physical chemistry of the contractile proteins. *Exptl. Cell Research* 1: 234, 1950.
220. SOSKIN, S. AND R. LEVINE. *Carbohydrate Metabolism. Correlation of Physiological, Biochemical, and Clinical Aspects.* Chicago, Ill.: Univ. Chicago Press, 1946, p. 305.
221. SOSMAN, M. C. Venous catheterization of the heart. I. Indications, technics, and errors. *Radiology* 48: 441, 1947.

222. SPIRO, M. J. AND J. M. MCKIBBEN. The lipides of rat liver cell fractions. *J. Biol. Chem.* 219: 643, 1956.
223. STADIE, W. C., N. HAUGAARD, AND M. PERLMUTTER. The synthesis of glycogen by rat heart slices. *J. Biol. Chem.* 171: 419, 1947.
224. STARLING, E. H. AND M. B. VISSCHER. The regulation of the energy output of the heart. *J. Physiol.* 62: 243, 1927.
225. STERN, J. R., M. J. COON, AND A. DEL CAMPILLO. Enzymatic breakdown and synthesis of acetoacetate. *Nature, London* 171: 28, 1953.
226. STERN, H., E. ELLENBOGEN, AND R. E. OLSON. Characterization of myosin from normal and failing dog heart. *Fed. Proc.* 15: 363, 1956.
227. STETTEN, DEW., JR. AND M. R. STETTEN. Glycogen metabolism. *Physiol. Rev.* 40: 505, 1960.
228. STOTZ, E. H., M. MORRISON, AND G. MARINETTI. Components of the cytochrome system. In: *Enzymes: Units of Biological Structure and Function*, edited by O. H. Gaebler. New York: Acad. Press, 1956, pp. 401–416.
229. STRAUB, F. B. AND G. FEUER. Adenosinetriphosphate. The functional group of actin. *Biochim. et biophys. acta* 4: 455, 1950.
230. SUTHERLAND, E. W. AND T. W. RALL. Fractionation and characterization of a cyclic adenine ribonucleotide formed by tissue particles. *J. Biol. Chem.* 232: 1077, 1958.
231. SWANK, R. L. AND O. A. BESSEY. Production and study of cardiac failure in thiamine deficient pigeons. *Arch. Int. Med.* 70: 763, 1942.
232. SZENT-GYÖRGYI, A. *Studies From the Institute of Medical Chemistry* (University Szeged). Bas : Karger, 1942, vol. 2.
233. SZENT-GYÖRGYI, A. *Chemical Physiology of Contraction in Body and Heart Muscle.* New York: Acad. Press, 1953, pp. 104–106.
234. SZENT-GYÖRGYI, A. *The Chemistry of Muscular Contraction* (1st ed.) New York: Acad. Press, 1948.
235. SZENT-GYÖRGYI, A. Bioenergetics. *Science* 124: 873, 1956.
236. SZENT-GYÖRGYI, A. G. AND M. BORBIRO. Depolymerization of light meromyosin by urea. *Arch. Biochem. Biophys.* 60: 180, 1956.
237. TAYLOR, A., M. A. POLLACK, AND R. J. WILLIAMS. B Vitamins in normal human tissues. In: *Studies on the Vitamin Content of Tissues II.* Austin, Texas: Univ. Texas Publications, 1942, pp. 41–55.
238. THEORELL, H. Heme-linked groups and mode of action of some hemoproteins. *Advances in Enzymol.* 7: 265, 1947.
239. TOPPER, Y. J. AND A. B. HASTINGS. A study of the chemical origins of glycogen by use of C^{14}-labeled carbon dioxide, acetate, and pyruvate. *J. Biol. Chem.* 179: 1255, 1949.
240. TSAO, T. C., K. BAILEY, AND G. S. ADAIR. Size, shape, and aggregation of tropomyosin particles. *Biochem. J.* 49: 27, 1951.
241. TSAO, T. C., P. H. TAN, AND C. M. PENG. A comparative physiochemical study of tropomyosins from different sources. *Sci. Sinica (Peking)* 5: 91, 1956.
242. UNGAR, I., M. GILBERT, A. SIEGEL, J. M. BLAIN, AND R. J. BING. Studies on myocardial metabolism. IV. Myocardial metabolism in diabetes. *Am. J. Med.* 28: 385, 1955.
243. UTTER, M. F. AND H. G. WOOD. The fixation of carbon dioxide in oxalacetate by pigeon liver. *J. Biol. Chem.* 164: 455, 1946.
244. VESTER, J. W. AND W. C. STADIE. Studies of oxidative phosphorylation by hepatic mitochondria in the diabetic cat. *J. Biol. Chem.* 227: 669, 1957.
245. VISSCHER, M. B. The energy transformation by the heart and the mechanism of experimental cardiac failure. *Blood, Heart, and Circulation.* Washington: American Assoc. Advancement Science, Publication No. 13, 1940, p. 176.
246. VON HIPPEL, P. H., H. K. SCHACHMAN, P. APPEL, AND M. F. MORALES. On the molecular weight of myosin. *Biochim. et biophys. acta* 28: 504, 1958.
247. VON KORFF, R. W. AND R. M. TWEDT. Interaction of glycolytic and mitochondrial enzyme systems. I. Oxidation of lactate and phospholenyl pyruvate. *Biochim. et biophys. acta* 23: 143, 1957.
248. VON KORFF, R. W. Interaction of glycolytic and mitochondrial enzyme systems. II. The reaction sequences: fructose diphosphate to 3-phosphoglyceric acid; and pyruvate to lactate, carbon dioxide and water. *Biochim. et biophys. acta* 31: 467, 1959.
249. VON MURALT, A. L. AND J. T. EDSALL. Studies in the physical chemistry of muscle globulin. IV. The anisotropy of myosin and double refraction of flow. *J. Biol. Chem.* 89: 351, 1930.
250. WADKINS, C. L. AND A. L. LEHNINGER. ATP-ADP exchange reaction of oxidative phosphorylation. *Fed. Proc.* 17: 329, 1958.
251. WARBURG, O. AND W. CHRISTIAN. Über ein neues Oxydations ferment und sein Absorptions spektrum. *Biochem. Ztschr.* 254: 438, 1932.
252. WEBER, H. H. The muscle proteins and the finer structures of skeletal muscles. *Ergebn. Physiol. Exptl. Pharmakol.* 36: 109, 1934.
253. WEBER, H. H. The fine structure and mechanical properties of the myosin thread. *Pfluger's Arch. ges Physiol.* 235: 205, 1934.
254. WEBER, H. H. AND H. PORTZEHL. Muscle contraction and fibrous muscle proteins. In: *Advances in Protein Chemistry*, edited by M. L. Anson, K. Bailey, and J. T. Edsall. New York: Acad. Press, 1952, vol. 7, p. 161.
255. WEBER, H. H. AND H. PORTZEHL. The transference of the muscle energy in the contraction cycle. *Prog. in Biophys. and Biophys. Chem.* 4: 60, 1954.
256. WENNER, C. E., M. A. SPIRTES, AND S. WEINHOUSE. Metabolism of neoplastic tissue. II. A survey of enzymes of the citric acid cycle in transplanted tumors. *Cancer Res.* 12: 44, 1952.
257. WIGGERS, C. J. AND J. M. WERLE. Cardiac and peripheral resistance factors as determinants of circulatory failure in hemorrhagic shock. *Am. J. Physiol.* 136: 421, 1942.
258. WOLLENBERGER, A. On the energy-rich phosphate supply of the failing heart. *Am. J. Physiol.* 150: 733, 1947.
259. WOOD, H. G., N. LIFSON, AND V. LORBER. The position of fixed carbon in glucose from rat liver glycogen. *J. Biol. Chem.* 159: 574, 1945.

Cellular electrophysiology of the heart[1]

J. WALTER WOODBURY | *Department of Physiology and Biophysics, University of Washington School of Medicine, Seattle, Washington*

CHAPTER CONTENTS

CONTRACTION OF THE HEART is rhythmic, abrupt, maximal, prolonged, and nearly synchronous in all the cells surrounding a chamber (fig. 1). In contrast, contraction of a whole skeletal muscle is smooth, graded, and of variable duration, its component motor units twitching asynchronously. In their patterns of contraction the two types of muscle differ in ways which are consonant with their particular functions. The pattern of cardiac muscular contraction insures the efficient ejection of blood. The force exerted by a skeletal muscle can be varied smoothly and continuously over a wide range to meet the changing demands of bodily motion. The similarities between the two kinds of muscle are that they are both contractile and that, normally, the degree of activation of the contractile substance depends on the membrane potential.

In cardiac cells, the duration of contraction is proportional to the duration of the action potential; and the sequence of their contractions is determined by the characteristics of the intercellular transmission processes. Figure 1 shows simultaneous recordings

[1] Aided by Grant B-1752, from the National Institute of Neurological Diseases and Blindness, U. S. Public Health Service.

of the contractile tension of a whole frog ventricle and the transmembrane action potential from a single ventricular cell. It can be seen that the upstroke of the action potential precedes contraction and the downstroke precedes relaxation. Since the onset and duration of the action potential are about the same in all ventricular cells, it appears that this relation between electrical activity and contraction exists throughout the myocardium.

In relation to contractile activity, a survey of cardiac electrophysiology must deal comprehensively with the following questions. *a*) What mechanisms lead to the rhythmic contraction of the heart and how are these affected by the regulatory innervation? *b*) What factors determine the length of systole and diastole, and how do they vary with rate? Ancillary to this question is the problem of how changes in the membrane potential control contractile activity. *c*) Since cardiac cells are anatomically distinct and do not receive motor innervation, how is effectively synchronous contraction of all the cells achieved?

The first two questions are concerned with the temporal aspects of the control of cardiac contraction and hence with the membrane electrical properties of individual cells throughout the heart. The third question concerns the spatial aspects of the control of contraction, i.e., the mechanism whereby activity in one cell initiates activity in neighboring cells. Knowledge of the temporal and spatial aspects of cardiac electrical activity and the laws describing the flow of current in a volume conductor with known characteristics is the necessary and sufficient physical basis for understanding the electrocardiogram.

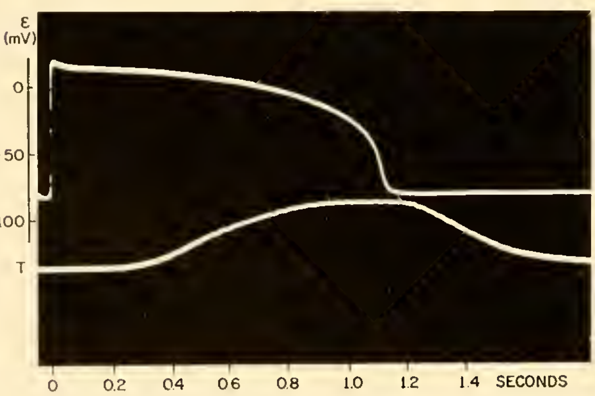

FIG. 1. Cellular transmembrane potential and contractile tension of isolated, perfused frog ventricle. Abscissa: time. Ordinates: upper trace, potential inside cell minus potential outside (ε) in millivolts; lower trace, contractile tension (T) in arbitrary (linear) units. Note the delay between the upstroke of the action potential and the beginning of contraction; and between fast repolarization and the beginning of relaxation. The time of occurrence of the action potential upstroke varies by perhaps as much as 0.2 sec from cell to cell in the intact heart, but the variation is much less in this record because the cells were excited nearly simultaneously by a current pulse. (Lee & Woodbury, unpublished data.)

Except for the extraordinarily long duration of the action potential, the electrical and excitable properties of cardiac muscle are similar to those of unmyelinated nerve and skeletal muscle. Most of our detailed knowledge of the properties of excitable membranes comes from Hodgkin and Huxley's analysis and synthesis of voltage clamp records from squid giant axons (53, 60). Knowledge of cardiac membrane properties is based on more indirect experiments that have been interpreted in the light of the behavior of the squid axon. Analysis in cardiac electrophysiology therefore requires knowledge of the corresponding changes in nerve. The aspects of nerve and cardiac electrophysiology to be considered in this chapter are: *a*) the maintenance of steady ionic and potential gradients across the cell membrane by active ion transport; *b*) the passive electrical properties of cells; *c*) the ionic conductance changes which are responsible for the excitable, all-or-nothing properties of the membrane; and *d*) the mechanism of impulse propagation from cell to cell, unique to cardiac and visceral smooth muscle.

The interpretation of the electrophysiology of cardiac cells given here is based on Hodgkin and Huxley's membrane ionic theory (cf. 53). This theory, although not universally accepted [it is sometimes termed a hypothesis (112)], is so useful in the synthesis and interpretation of such a wide range of experimental results that there is little doubt of its over-all validity. Since Tasaki's chapter on the "Conduction of the Nerve Impulse" (112) contains only a brief mention of this theory, it must be presented here so that the events in cardiac cells can be discussed coherently. Hodgkin's reviews (52, 53) and the original papers by Hodgkin & Huxley, and their colleagues (57–65) should be consulted for detailed descriptions of the ionic theory and references to the pertinent literature. A somewhat condensed and simplified treatment of the ionic theory appears in a recent textbook (135, 138). The history of electrophysiology has been covered adequately in the chapters by Brazier (5) and Tasaki (112); additional details on the history and current knowledge of cardiac electrophysiology appear in the monographs of Weidmann (129, in German) and Hoffman &

Cranefield (27, 68). Shanes (106) has exhaustively reviewed the electrophysiological literature from a viewpoint provided by the ionic theory and some of his own interesting ideas.

THE RESTING CELL MEMBRANE

The heart, like any other tissue, is composed of more or less homogeneous cell groups and the interstitial fluid bathing them. Cell plasm is separated from the interstitial fluid by a thin electrically insulating membrane. This membrane separates aqueous solutions having the same total osmotic pressure but radically different compositions. The extracellular fluid has high concentrations of Na^+ and Cl^- and a low concentration of K^+. The situation is reversed in intracellular fluid, and the anion component consists largely of organic acid radical and phosphate ions. Of course, many other substances are also dissolved in the aqueous phases, but attention here will be focused principally on Na^+, K^+, and Cl^-, since these are the only ions carrying appreciable currents through the membrane. In addition, there is a potential difference of about 80 mv (inside negative) across the membrane. Since the membrane is exceedingly thin, it is apparent that large concentration and potential gradients exist across it. Two properties of the membrane lead to the development and maintenance of the transmembrane ion and potential gradients. *a*) The membrane's structure permits ions to diffuse through it at only a minute fraction of the rate at which they diffuse through water. In most cell membranes at rest, Na^+ diffuses through the membrane much more slowly than K^+ and Cl^- do. *b*) Energy derived from metabolism is used by the cell to transport Na^+ out of it and K^+ into it. By balancing the inward diffusion of Na^+ and the outward diffusion of K^+, this active transport maintains the low Na^+ and high K^+ concentrations inside the cell and the transmembrane potential.

Since the transmembrane potential is generated by the separation of charges resulting from differential ion movements through the membrane, this discussion deals mainly with the factors governing the movements of ions. The three prime factors are *1*) the permeability of the cell membrane to ions, *2*) the ion and potential gradients across the membrane, and *3*) the active transport of ions.

Passive Ion Movements

MEMBRANE STRUCTURE (39, 103). The cell electrical membrane probably consists of alternating layers of lipids and proteins. In the lipid layer, the long thin molecules are closely packed with their long axes parallel and oriented perpendicular to the membrane surface. Each lipid layer is two molecules thick, the nonpolar ends of a pair of molecules being opposed and their polar ends being bound to the protein layers. The unit of membrane structure is probably a bimolecular lipid layer between two monomolecular protein films, 8.5 nm thick (39). Electrical and electron micrographic measurements indicate that the membrane is only about 10 nm thick; hence this structure is composed of one or at most two structural units.

Since lipids are hydrophobic, water and water-soluble compounds probably cannot penetrate a well-organized region of the membrane. It is more reasonable to assume that the lipid phase is interrupted by water-filled pores of small diameter which perforate the membrane; ions could readily diffuse through such pores. The low permeability of the membrane to ions could indicate a paucity of pores and its lower permeability to Na^+ than to K^+, and Cl^- could indicate an average pore size slightly larger than the latter two ions and slightly smaller than Na^+ [see Solomon in (100)]. Even so, all phenomena of ion transport cannot be explained on the basis of membrane porosity and it is also necessary to postulate "carriers" within the membrane. Regardless of the exact mechanism by which ions pass through the membrane, the rate of their passive penetration depends directly on the gradients of both concentration and potential. The specialized properties of the intercalated disc membrane will be considered in the section on intercellular transmission. For the discussion of intracellular events, the cardiac cell membrane may be regarded as a homogeneous structure.

MEMBRANE CAPACITANCE AND RESISTANCE (66, 88, 113, 126). A capacitor consists of two conductors separated by an insulator. A cell is a capacitor: the interstitial fluid and cell plasm are conductors, and the membrane is an insulator. The capacity of a capacitor is defined as the ratio of the charge (q) on either conductor to the potential difference ($\mathcal{E}$) between the conductors, $C = q/\mathcal{E}$. By definition, the electric potential difference between two points is the amount of work done against electrical forces to carry a unit positive charge between the points. The electrical

force acting on a unit charge placed between the conductors of a capacitor is directly proportional to the amount of charge on the conductors. Therefore, the potential difference between the conductors is also directly proportional to the charge on them, the proportionality constant being $1/C$. Since charges of opposite sign are on the conductors, the charges on one conductor will distribute themselves as closely as possible to their counter charges on the other conductor, i.e., the charges are at the conductor-insulator boundary. Capacity depends only on the geometry of the conductors and the dielectric constant of the insulating material between them. The capacity of 1 cm² of Purkinje cell membrane is about 10 μF (126).

Since ions can penetrate the membrane it obviously is not a perfect insulator. This fact can be represented by a capacitor shunted by a resistor. Thus, there must be an electromotive force in the membrane–bathing-solution system to supply charge to the membrane capacitor as fast as it leaks off through the membrane resistor. From the definitions of potential and capacity it follows that the existence of a potential difference between the interstitial fluid and the cell plasm is simply a reflection of the fact that unlike electrical charges have been separated across the membrane by nonelectrical forces. The formal expedient of representing the transmembrane potential in series with the membrane capacity (112) thus has no precise physical meaning in this system. In the absence of changing magnetic fields, potentials can arise only from separation of charges, i.e., the creation of a double layer.

Clearly, the separation of charge across the membrane creates an electric field which will exert a force on any ion within the membrane. For example, there is a net tendency for K^+ to diffuse from the inside of the cell where its concentration is high to the outside where it is low, but the excess positive charges on the outside of the membrane repel and the negative charges on the inside attract any cation within the membrane. Consequently, K^+ tends to diffuse outward due to its concentration gradient and inward due to the potential gradient. Thus, the net movement of K^+ through the membrane is determined by the difference between these two factors. If the concentration and potential gradients exert equal and opposite forces on an ion, it is distributed at equilibrium across a membrane.

ION EQUILIBRIUM POTENTIAL. Table 1 gives the approximate concentrations of Na^+, K^+, and Cl^- in the interstitial and intracellular water of the frog ventricle. The values for the intracellular concentrations are somewhat uncertain due to the difficulty of apportioning the total ion content of a tissue between the intracellular and interstitial spaces. Nevertheless, this uncertainty does not obscure the direction nor greatly alter the magnitude of the concentration gradients. In skeletal muscle, where the analysis is more precise, the ion distribution is approximately the same. Since radioactive tracer experiments show that these ions can penetrate the membrane, it is necessary to consider the forces that drive ions through the membrane.

The net diffusional flux ($\mathbf{M}_S$; unit, mole/cm² sec) of any substance (S) is proportional to the concentration gradient (grad [S]) where [S] is the concentration of S but is in the opposite direction, i.e., substances diffuse from regions of higher concentration to regions of lower concentration.[2] The ease of movement of an ion through a region is measured by the diffusion constant (D_S; unit, cm²/sec). To a first approximation the concentration gradient across a cell membrane is the difference between interstitial ($[S]_o$) and intracellular ($[S]_i$) concentrations divided by the thickness of the membrane (δ)

$$\mathrm{M}_S = -D_S \operatorname{grad}[S] = -D_S([S]_o - [S]_i)/\delta = P_S([S]_i - [S]_o) \quad (1)$$

where a net outflux is defined as positive and the expression $P_S = D_S/\delta$ (cm/sec) is defined as the permeability of the membrane to S. $\mathbf{M}_S$ is a vector whose direction is that of $-\operatorname{grad}[S]$. The one-way flux is formally defined as the net flux when the other concentration is zero, all other conditions remaining the same. The permeability of a skeletal muscle cell membrane to K^+ is of the order of 10^{-6} cm/sec and that of an equal thickness of water about 10 cm/sec, a contrast indicating the relatively great impermeability of the membrane to ions.

Equation 1 is useful for describing the movements of nonionized substances through the membrane. However, since ions are electrically charged particles and there is a voltage gradient in the membrane, the equation must be modified to take into account effects of the electric field on ion movements. It is usually assumed that the effects of concentration and potential gradients on ion fluxes are additive, i.e., that equation 1 can be made applicable to ions by adding a term on the right for the flux due to the electric

[2] Strictly speaking, activity not concentration should be used throughout this section. However, in most cases the important quantities are ratios of external to internal concentrations and these ratios are nearly equal to the corresponding activity ratios.

field. The form of this term follows from Ohm's law written in the vector form: $\mathbf{I} = -\sigma$ grad $\mathcal{E}$; where $\mathbf{I}$ is the current density (amp/cm²), σ is the conductivity of the medium (mhos/cm) and $\mathcal{E}$ is the electric potential.[3] Current density can be converted to ionic flux by dividing $\mathbf{I}$ by the valence (Z_S) of the ion carrying the current and by the Faraday (F), which converts coulombs to moles: $\mathbf{M}_S = \mathbf{I}/FZ_S$. The conductivity of an ion species in solution depends directly on the concentration of the ion, on its mobility (m_S) and on the square of the valence: $\sigma_S = Z_S^2[S]F^2m_S$. Mobility is directly proportional to the diffusion constant, since it is a measure of the same property of the ion. The diffusion constant is a measure of the ease with which an ionized substance can move through the solution when it is driven by a concentration gradient. Mobility is the measure of ease of movement when the ion is driven by an electrical gradient; hence, from energetic considerations, $m_S = D_S/RT$, where R is the universal gas constant and T the absolute temperature. Ohm's law can now be written as $\mathbf{M}_S = -(D_SFZ_S/RT)[S]$ grad $\mathcal{E}$, the flux of an ion due to a potential gradient. With the addition of the two fluxes, equation 1 becomes

$$-\mathbf{M}_S = D_S \text{ grad } [S] + (D_SFZ_S/RT)[S] \text{ grad } \mathcal{E} \qquad (2a)$$

Since [S] and $\mathcal{E}$ are independent variables, this equation cannot be integrated to give $\mathbf{M}_S$ directly in terms of $\mathcal{E}$ and [S], which are experimentally measurable, without another relationship between them. This other relationship is Poisson's law: the divergence of $-$grad $\mathcal{E}$ is proportional to the charge density, the difference between the cation and anion concentrations in any small volume. The resulting set of differential equations is so difficult to solve for any real system that some assumption is usually made concerning the variation of voltage or concentration with distance. Substitution of the assumed relationship in equation 2a permits its direct integration. Goldman's assumption (49) that the electric field is constant throughout the membrane is perhaps the most useful for calculating the fluxes through relatively impermeable membranes. This assumption is equivalent to assuming that the charge density within the membrane is negligible. The resulting flux and voltage equations describe quite accurately a number of experimental phenomena (33, 47, 55, 63, 74).

There are two convenient ways of approaching the contributions of voltage and concentration differences across the membrane to the transmembrane flux. The voltage can be considered to modify the concentrations of the ion or, conversely, the concentrations to modify the voltage difference. These approaches lead to the idea of effective concentrations or effective voltage differences. The manner in which a transmembrane voltage contributes to the effective concentration can be determined by multiplying both sides of equation 2a by the integrating factor $\exp(FZ_S\mathcal{E}/RT)$. The equation becomes

$$-\mathbf{M}_S e^{FZ_S\mathcal{E}/RT} = D_S \text{ grad } [S]e^{FZ_S\mathcal{E}/RT} \qquad (2b)$$

This is similar to equation 1 if $[S] \exp(FZ_S\mathcal{E}/RT)$ is replaced by [S]. Thus, voltage affects concentrations exponentially insofar as transmembrane fluxes are concerned.

In the converse situation, the contributions of the inside and outside concentrations of an ion to the effective transmembrane voltage follow from the condition for ionic equilibrium across the membrane, i.e., the relationship between the concentrations and the voltage at which the net flux of the ion is zero. Any membrane, no matter how convoluted, is so thin that it can be considered a plane; hence, grad [S] and grad $\mathcal{E}$ are equal to their respective derivatives with respect to x, the distance through the membrane measured from inside to outside. Setting $\mathbf{M}_S = 0$, taking $\mathcal{E} = 0$ and $[S] = [S]_o$ outside the cell and taking $[S] = [S]_i$ and $\mathcal{E} = \mathcal{E}_S$ inside the cell, integration of equation 2b gives, when solved for $\mathcal{E}_S$,

$$\mathcal{E}_S = \frac{RT}{FZ_S} \ln \frac{[S]_o}{[S]_i} \qquad (3a)$$

This is Nernst's equation. With logarithms to the base 10, a temperature of 20°C (293° absolute), values of R and F in appropriate units and $\mathcal{E}_S$ expressed in millivolts, equation 3a becomes

$$\mathcal{E}_S = \frac{58}{Z_S} \log \frac{[S]_o}{[S]_i} \text{ (mv)} \qquad (3b)$$

$\mathcal{E}_S$ is called the equilibrium potential of the ion, S.

The condition for an uncharged substance to be equilibrated across the membrane is that the concentrations on either side be equal. However, for an ionized substance, the ion concentrations on the two sides can be arbitrarily chosen and solution of the

[3] The use of the symbol $\mathcal{E}$ for the electric potential or potential difference is not common, the symbols V and E being most frequently used. All three are listed as symbols for potential or emf in the *Handbook of Chemistry and Physics* (67). $\mathcal{E}$ is used here because it seldom denotes other quantities, whereas V frequently symbolizes volume or velocity, and E nearly always stands for the magnitude of the electric field intensity $|-\text{grad } \mathcal{E}|$.

Nernst equation will give the transmembrane potential at which the distribution will be at equilibrium. Physically, $\mathcal{E}_S$ is the potential which would be generated across a membrane permeable only to S. This follows because the movement of the permeable ions through the membrane down their concentration gradient constitutes the separation of charge across the membrane. In turn, this potential gradient opposes further ionic penetration. This process continues until there is no net flux of the ion, i.e., equilibrium [see (135) for a more detailed treatment].

The Nernst equation is an expression of the condition for electrochemical equilibrium and so is immediately derivable from energetic considerations. At equilibrium for S, the sum of the concentration and electrical potential (free) energy differences per mole must be zero; the concentration energy is RT ln $[S]_i/[S]_o$ and the electrical is $FZ_S\mathcal{E}_S$.

The summation of concentration and electric potential energy difference for any [S] and $\mathcal{E}$ is called the electrochemical potential difference ($\Delta\mu_S$) between the two solutions:

$$\Delta\mu_S = FZ_S\mathcal{E} + RT \ln [S]_i/[S]_o \tag{4a}$$

From Nernst's equation (3a) it can be seen that $RT \ln [S]_i/[S]_o = -FZ_S\mathcal{E}_S$. Thus the electrochemical potential difference for S can also be written in a more meaningful and convenient form as

$$\Delta\mu_S = FZ_S(\mathcal{E} - \mathcal{E}_S) \tag{4b}$$

The variation of electrochemical potential with distance, the electrochemical gradient, is a measure of the total electrical and concentration forces acting on an ionic species. Across the membrane, the electrochemical gradient is approximated by $\Delta\mu_S/\delta$. Therefore, to the approximation used in defining permeability (equation 1), transmembrane flux is proportional to $\Delta\mu_S$. If $\mathbf{M}_S$ is expressed in the form of current density ($\mathbf{I}_S$), the flux equation becomes Ohm's law for a single ion:

$$\mathbf{I}_S = g_S(\mathcal{E} - \mathcal{E}_S) \tag{4c}$$

The proportionality constant (g_S) has the dimensions of conductance per unit area (mho/cm^2) and is called the specific conductance of S. In general, g_S varies with the voltage across the membrane and with the concentrations of ions in the vicinity of the membrane. Nevertheless, this equation is a useful representation of the fluxes through a membrane and, in particular, shows the way in which the concentrations of S on either side of the membrane alter the effective transmembrane voltage, i.e., the driving force is $\mathcal{E} - \mathcal{E}_S$, not $\mathcal{E}$.

Permeability and conductance are closely related but not identical quantities. Both are measures of the ease with which an ion can penetrate the membrane but P_S is proportional to D_S and g_S to m_S (mobility). The variation of P_S with $\mathcal{E}$ in a membrane with fixed properties can be determined by integrating the one-dimensional form of equation 2b. The solution becomes more symmetrical if the potential is taken as $-\mathcal{E}/2$ outside and $\mathcal{E}/2$ inside the membrane:

$$\mathbf{M}_S = P_S\{[S]_i e^{FZ_S\mathcal{E}/2RT} - [S]_o e^{-FZ_S\mathcal{E}/2RT}\} \tag{2c}$$

where

$$P_S = D_S\left\{\int_{x=0}^{\delta} e^{FZ_S\mathcal{E}/RT}\,dx\right\}^{-1}$$

$\mathbf{M}_S$ can be factored out of the definite integral because flux in the steady state does not vary with distance through the membrane. The permeability is determined by the value of the integral and hence depends on the variation of $\mathcal{E}$ with x in the membrane.

The foregoing discussion has been based upon the assumption that each particle's movement through the membrane is uninfluenced by the movement of any other particle. Although this assumption appears to be valid for transmembrane ionic movements during electrical activity (33, 58), there is experimental evidence that at least three K^+ interact as they move through the membrane (65) and other evidence (85) that the efflux of Na^+ is influenced by $[Na^+]_o$ (see below).

The Nernst equation can be used to determine whether an ion is distributed at equilibrium across the cardiac cell membrane. To the approximation that g_S is independent of $\mathcal{E}$, an ion is equilibrated if $\mathcal{E}_S$ is equal to the average transmembrane potential ($\bar{\mathcal{E}}$). Values of the equilibrium potentials for Na^+, K^+, and Cl^- ions are given in the right-hand column of table 1. At first glance it appears that none of these ions is equilibrated. However, the value for internal chloride concentration ($[Cl^-]_i$) given in the table was calculated from the Nernst equation with the assumption that the effective average membrane potential for Cl^- of a rhythmically beating heart is about -50 mv as compared with the diastolic or "resting" potential $\mathcal{E}_r = -80$ mv. There is considerable evidence that Cl^- distributes according to the membrane potential in both skeletal (55, 74) and cardiac muscle (73). Thus, $[Cl^-]_i$ is lower in a quiescent than in an active heart, and some of the changes in the electrical and

TABLE 1. *Approximate Steady State Na^+, K^+, and Cl^- Concentrations and Potentials in Frog Ventricular Muscle**

Interstitial Fluid $[Ion]_o$ µmole per cm³		Intracellular Fluid $[Ion]_i$ µmole per cm³		$\frac{[Ion]_o}{[Ion]_i}$	$\mathcal{E}_{ion} = \frac{58}{Z} \log \frac{[Ion]_o}{[Ion]_i}$
Na^+	110	Na^+	18	6.1	46
K^+	2.5	K^+	90	1/36	−90
Cl^-	112.5	Cl^-	15‡	7.3	−50
		Organic anions	92		
Diastolic potential	0	−80 mv		1/24§	
Mean potential†	0	−50		1/7.3§	

* Values for Na^+ from Hajdu (51) and Johnson (81); those for K^+ from Hajdu, and those for Cl^- and potentials from Brady & Woodbury (4).

† Calculated for an action potential duration of 1 sec and an interval between beats of 3 sec.

‡ Calculated from $[Cl^-]_o$ and $\mathcal{E}_{Cl}$, assuming that $\mathcal{E}_{Cl} = \bar{\mathcal{E}}$.

§ Calculated from $10^{-\mathcal{E}/58}$, the equilibrium ratio for a univalent cation.

mechanical properties of the heart accompanying the transition from rest to activity may result from net Cl^- movements.

$\mathcal{E}_K$ is 10 mv more negative than the diastolic membrane potential and 40 mv more negative than the average potential, indicating that $[K^+]_i$ is higher than would be expected from the Nernst equation. The difference between $\mathcal{E}_K$ and $\mathcal{E}_r$ is of doubtful significance considering the uncertainties in the values of both. However, the proper comparison is between $\mathcal{E}_K$ and $\bar{\mathcal{E}}$, and this difference is highly significant. $\mathcal{E}_K$ is significantly greater than $\mathcal{E}_r$ in a number of tissues including nerve (64), skeletal muscle (1), and motoneuron (38). The finding that $[K^+]_i$ is higher than the equilibrium value means that there is an influx of K^+ against the electrochemical gradient, i.e., from a lower to a higher potential energy. This influx must occur; otherwise, $[K^+]_i$ would not remain constant in the face of the relatively high permeability of the membrane to K^+ and the consequent net outward diffusional flux of K^+. This passive efflux must be equalled by an equal influx of K^+ driven by other than diffusional and electrical forces. This excess influx is called active K^+ transport.

The distribution of Na^+ is far from electrochemical equilibrium. Both the concentration and potential gradients act to drive Na^+ into the cell. From table 1 it can be seen that the cell interior must be made 46 mv positive to the outside to establish electrochemical equilibrium for Na^+. Since Na^+ can penetrate the membrane (cf 46, 54, 64, 81), unspecified forces must be driving Na^+ out of the cell. This efflux must match the influx due to the concentration and potential gradients. Dean (30) in 1941 clearly delineated the need for this active Na^+ transport and considered the implications of a simple model.

Active Na^+ — K^+ Transport

ACTIVE TRANSPORT. From the foregoing, it appears that potential and concentration gradients are not the only factors which determine the net transmembrane flux of an ion. For example, a pressure gradient across a membrane could markedly alter ion distributions because the resulting flow of water would probably drag ions with it. However, bulk flow is probably not significant in nonsecretory cells. Similarly, a large net flux of one solute could drag along another solute, particularly in long narrow membrane pores (65). In addition, Ussing (124) has proposed a mechanism which would increase, equally, the efflux and influx of an ion independently of electrochemical gradient. This mechanism, called exchange diffusion, requires the existence of a carrier substance in the membrane which combines selectively with an ion species and which can move through the membrane only when associated with an ion. Thus a round trip of the carrier could result in the exchange of an external for an internal ion. Keynes & Swan (85) have substantial evidence from tracer experiments that exchange diffusion accounts for about half of the efflux of Na^+ from frog muscle. If the exchange efflux is subtracted from the total efflux, there still remains a considerable efflux which is not attributable to passive forces. This Na^+ efflux and a substantial part of the K^+ influx are against their respective electrochemical gradients and so these fluxes require the continuous expenditure of energy for their maintenance. Ultimately, this power must come from cellular metabolism. Any flux which is maintained by a direct expenditure of energy may be defined as active transport. However, this conceptual definition is not very useful. A limited but more useful definition is given by the Ussing flux ratio test (123). If, after any fluxes due to exchange diffusion are subtracted, an ionic species does not satisfy this equation, it is assumed to be actively transported. The flux ratio equation can be derived from equation 2c. The influx ($\mathbf{M}_S^{in}$) and efflux ($\mathbf{M}_S^{out}$) are calculated successively by setting $[S]_i$ and $[S]_o$ equal to zero in equation 2c. Both fluxes

involve the same unknown function of distance; therefore their ratio is simply

$$\frac{M_S^{out}}{M_S^{in}} = \frac{[S]_i}{[S]_o} e^{FZ_S\varepsilon/RT} = e^{FZ_S(\varepsilon-\varepsilon_S)/RT} \qquad (5)$$

All the terms in this equation can be measured experimentally. If the values obtained in a particular experiment do not satisfy equation 5, it is presumed that the ion in question is actively transported. This test is similar to the use of Nernst's equation to see if an ion is in electrochemical equilibrium. The flux ratio test is superior, however, because it will distinguish between an ion distributed at disequilibrium but in a steady state due to active transport and one that is in disequilibrium because of a nonsteady state where the concentrations are changing.

ENERGETICS. The conclusion that an ion not meeting the flux ratio criterion is actively transported is stringently limited by the fact that the power required for the transport must be less than the total power production of the cell. The transport of Na^+ in frog skeletal muscle meets this condition (46, 84). If the efflux of Na^+ in these cells is considered to be one half active and one half exchange diffusion (the passive efflux is negligible) 10 to 20 per cent of the resting metabolism is required to maintain the Na^+ efflux, provided the efficiency is 50 per cent. The minimum power required is simply the product of the active efflux and $\Delta\mu_{Na}$.

THE NA^+-K^+ EXCHANGE PUMP. Results of experiments on a number of tissues support the view that the active extrusion of Na^+ and the uptake of K^+ are at least loosely linked, the ejection of one Na^+ usually being accompanied by the uptake of one K^+. This process is frequently referred to as the Na^+-K^+ exchange pump, the Na^+-K^+ pump or simply the Na^+ pump. Hodgkin & Keynes' (53, 64) findings on Na^+-K^+ exchange in giant axons of *Sepia* form a compact summary of the direct experimental evidence that part of Na^+ efflux and of K^+ influx are active and coupled. These data confirm the theoretical reasons given above for supposing that there are active components of the Na^+ and K^+ fluxes. *a*) Na^+ efflux is a direct function of $[Na^+]_i$; Keynes & Swan (85) have recently found that at low $[Na^+]_i$'s, efflux is proportional to the third power of $[Na^+]_i$ in frog skeletal muscle. *b*) In *Sepia* Na^+ efflux is abolished by metabolic inhibitors such as DNP and cyanide. However, metabolic inhibitors do not have marked effects on Na^+ efflux in other tissues (cf. 7, 46). *c*) Metabolic inhibitors produce a decrease in the K^+ influx about equal to the decrease in Na^+ efflux, but Na^+ influx and K^+ efflux are not greatly affected. *d*) Removal of K^+ from the bathing solution reduces Na^+ efflux by about two-thirds. This is also true of frog skeletal muscle (86). *e*) Na^+ efflux and K^+ influx are temperature sensitive, having Q_{10}'s of 3 to 4. The opposite fluxes have low Q_{10}'s. All these findings indicate an active Na^+ for K^+ exchange process dependent upon a supply of metabolic energy. Coupling is suggested by the parallel changes in Na^+ efflux and K^+ influx with temperature and inhibition, and by the marked reduction in Na^+ efflux when $[K^+]_o$ is reduced to zero. Evidence for a cellular energy requirement is the great sensitivity of the active fluxes to low temperature and metabolic inhibitors (cf 7). Both a lowering of temperature and metabolic blockade reduce these fluxes because they decrease the rate at which energy can be supplied. Although substitution of Li^+ for Na^+ does not abolish excitability, Li^+ is not carried by the Na^+ pump in appreciable quantities (86). Information on the various passive and active transport processes in many different tissues is the objective of intense research effort at present (100).

Evidently the operation of a metabolically driven Na^+-K^+ pump is sufficient to maintain the low $[Na^+]_i$ and the high $[K^+]_i$, Na^+ being ejected and K^+ taken up as rapidly, on the average, as they enter and leave. In the steady state, the active fluxes of Na^+ and K^+ must be just equal and opposite to the flow of these ions down their electrochemical gradients. It is well established that nerve and skeletal muscle gain Na^+ and lose K^+ during activity (cf 53, 54). Since cardiac cells are rhythmically active, it must be supposed that they are in a steady state where the increased passive fluxes of activity are equalled by an increased rate of Na^+-K^+ pumping so that internal concentrations are not changing.

As mentioned above, the efflux of Na^+ from frog skeletal muscle varies with the cube of $[Na^+]_i$ for sufficiently low $[Na^+]_i$, so there is no difficulty in explaining the maintenance of the ionic distributions in active cardiac muscle if its Na^+-K^+ pump is similar to that in skeletal muscle. If this is true, the $[Na^+]_i$ should be somewhat higher in cardiac tissues than in skeletal muscle. Experimentally, $[Na^+]_i$ is 8 μmoles/cm^3 in skeletal muscle (85) and about 18 μmoles/cm^3 in cardiac muscle (51, 81).

Generation of the Resting Potential

It is clear, in principle, how the Na^+-K^+ pump can maintain internal ion concentrations. However, the means whereby a neutral Na^+-K^+ exchange can generate a transmembrane potential is not immediately apparent. If the pump were not operating, then the potential across the membrane would be determined by the concentrations and relative membrane permeabilities of the various ions. The voltage would assume that value at which the net charge carried through the membrane by all ions was zero, the fluxes depending on voltage (equation 2c). In squid axons the membrane is most permeable to K^+ ions and P_{Cl} is about 0.3 P_K (18). In frog skeletal muscle at rest P_{Cl} is about twice P_K (55, 74). In both tissues P_{Na} is small, 0.05 P_K or less. Since the $\mathcal{E}_K$ and $\mathcal{E}_{Cl}$ have large negative values, it would be expected that, in the absence of Na^+-K^+ pumping, a voltage would develop at about the observed resting value, somewhere between $\mathcal{E}_{Na}$ and $\mathcal{E}_K$, but closer to $\mathcal{E}_K$. For at this voltage, the net fluxes of K^+ and Cl^- would not be large, despite their relatively high permeabilities, because the driving forces would be small and the net Na^+ influx would be the same magnitude, despite its low permeability, because the driving force would be large. In this situation, the cell would be slowly losing K^+ and slowly gaining Na^+ and Cl^-. If the pump were started and if the passive net fluxes of Na^+ and K^+ were equal and opposite, then the pump would maintain the internal concentrations constant and, being neutral, would not affect the voltage. It follows from this argument that, in the steady state where all net fluxes are zero and the potential is unchanging, $\mathcal{E}_r$ is determined primarily by the relative permeabilities of the membrane to Na^+ and K^+ and secondarily by the pumping rate—e.g., the higher the value of P_{Na}/P_K, the smaller $\mathcal{E}_r$; the faster the pumping rate, the greater $\mathcal{E}_r$. In the steady state, Cl^- must be distributed in equilibrium with the membrane voltage, since it is not actively transported. Hence, Cl^- cannot affect the steady-state voltage. Eccles' (38) diagram of the driving forces and fluxes through the membrane in the steady state (fig. 2) compactly summarizes the foregoing discussion. The generation and maintenance of the resting potential by a one-for-one Na^+-K^+ exchange pump are treated in detail elsewhere (135).

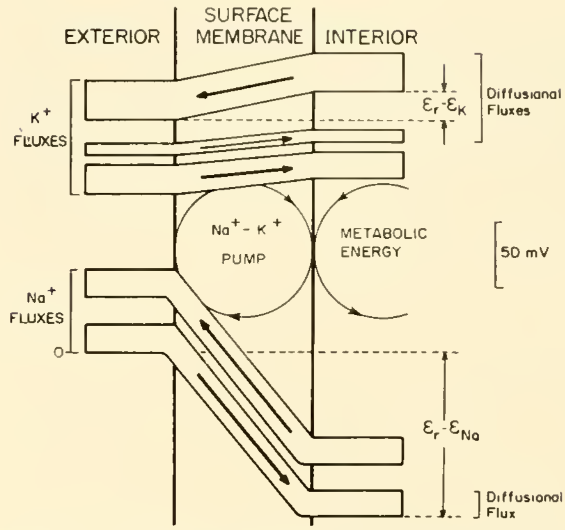

FIG. 2. Diagram of steady state passive and active fluxes of Na^+ and K^+ through the cell membrane of an excitable cell. Vertical distance represents the electrochemical potential of ion species. Downhill passive, or diffusional, fluxes exceed uphill passive fluxes. Net downhill diffusional fluxes are matched by fluxes driven uphill by the energy consuming Na^+-K^+ pump. The height of a band indicates the relative size of the flux in the direction of the arrow. $\mathcal{E}_r - \mathcal{E}_K$ and $\mathcal{E}_r - \mathcal{E}_{Na}$ are the electrochemical potential differences of K^+ and Na^+, respectively, across the membrane. Inside the cell, the electrochemical potential of K^+ is positive to the outside and that of Na^+ is negative. [After Eccles (38).]

Effects of Changes in External Ion Concentrations on Potential

If the concentration of K^+ in the interstitial fluid or in an artificial solution bathing a tissue is suddenly increased, the transmembrane potential immediately decreases. This decrease results from the rise in K^+ influx, which reduces the charge on the membrane until the increasing outflow of K^+ and inflow of Cl^- balance the increased K^+ influx. The cells are now in a nonsteady state, with the internal concentrations slowly changing. The net current through the membrane is zero, but the individual ionic fluxes are not. For moderately large cells, the imbalance in individual fluxes is so slight that the rate of change of internal concentration is measured on a time scale of hours and the voltage can be regarded as a constant in short term experiments.

The Goldman (49) constant field equation predicts quite accurately membrane voltage as a function of external ion concentrations. The equation for voltage can be derived by writing the flux for each ion (equation 2c, generally limited to Na^+, K^+, Cl^-), relating these fluxes by the condition that the total membrane current must be zero and solving for $\mathcal{E}$:

$$\mathcal{E} = \frac{RT}{F} \ln \frac{[K^+]_o + \frac{P_{Na}}{P_K}[Na^+]_o + \frac{P_{Cl}}{P_K}[Cl^-]_i}{[K^+]_i + \frac{P_{Na}}{P_K}[Na^+]_i + \frac{P_{Cl}}{P_K}[Cl^-]_o} \tag{6}$$

If it is assumed that the permeability ratios remain constant this equation accurately predicts the effects of changes in $[K^+]_o$ on $\mathcal{E}$ in a number of tissues (52, 63) but see (1) for a case where the equation does not apply and the assumptions are not true. Fitting experimental data to this equation is one way of estimating permeability ratios. Since P_K is normally much greater than P_{Na} and $[Cl^-]_i$ is quite low, it can be seen that at high values of $[K^+]_o$ the other terms in the numerator become negligible and $\mathcal{E}$ will change as rapidly as $\mathcal{E}_K$. At a normal $[K^+]_o$ the other terms are prominent and the change in voltage with $[K^+]_o$ becomes quite small. The finding that when $[K^+]_o$ is high the membrane behaves as though it were permeable only to K^+, i.e., as a potassium electrode, has been frequently interpreted to indicate that the resting potential arises from the K^+ concentration gradient and a membrane selectively permeable to K^+. However, even if K^+ were equilibrated across the membrane, there is no way of distinguishing a priori whether the membrane potential arises from a pre-existing K^+ distribution or the K^+ distribution arises from a pre-existing potential as the Cl^- distribution does. Actually, since the high $[K^+]_i$ is the result of active Na^+-K^+ transport and $\mathcal{E}$ arises because $P_{Na} < P_K$, both possibilities are irrelevant.

THE ACTIVE CELL MEMBRANE

In the preceding description of the properties of the resting cell membrane it was assumed that membrane ionic permeabilities are invariant in time, although they may vary somewhat with membrane voltage. In contrast, the membrane action potential is generated by a characteristic sequence of rapid changes in membrane permeability which are markedly dependent on voltage. In fact, the action potential is currently "explained" in terms of these changes in permeability since the underlying membrane mechanisms are not known. The sequence of the permeability changes during the action potential in the squid giant axon has been described in quantitative detail by Hodgkin & Huxley (60). Unfortunately, a similar description of activity in cardiac muscle cannot be given since the requisite data are not available, but they do suggest that the changes in permeability during the rising phase are much the same as those in squid giant axons. Hence, a brief description of the known permeability changes in giant axon membranes is a useful preface to the study of the changes in membrane permeability which may occur in heart muscle. These changes in squid axons have been recently reviewed by Hodgkin (53).

The rising phase of the action potential in most excitable tissue—including heart—is normally brought about by a large increase in P_{Na}. An increase in P_{Na} leads to an increased net flow of Na^+ into the cell, down its electrochemical gradient. This net entry of positive charges neutralizes the negative charges stored against the inside of the membrane and thus depolarizes it, i.e., reduces the magnitude of the potential.[4] If the increase in P_{Na} is large enough, the membrane charge will reverse, $\mathcal{E}$ approaching $\mathcal{E}_{Na}$. The depolarization expected from an increase in P_{Na} can be calculated from equation 6. In turn, depolarization increases P_{Na}, i.e., a reduction in membrane potential causes a specific increase in P_{Na}. This is a special property of the excitable membrane. Thus, if $\mathcal{E}_{Na} - \mathcal{E}$ is greater than zero, i.e., if the Na^+ electrochemical gradient drives Na^+ inward, then depolarization may be spontaneous.

Hodgkin (52) diagrams this regenerative sequence as follows:

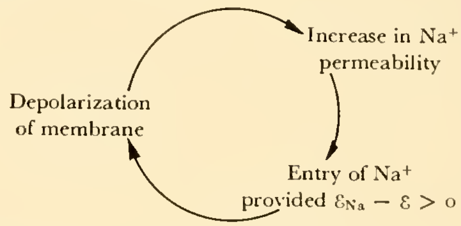

This depolarization-induced increase in P_{Na} is not maintained. Even if $\mathcal{E}$ is held constant near zero, Na^+ current quickly falls to low values owing to a fall in P_{Na}. This time-dependent decrease in P_{Na} could bring about the beginning of the recovery or repolarization phase of the action potential alone, since K^+ and Cl^- ions moving down their gradients would recharge the membrane to the resting level at a rate determined by the membrane time constant. In squid

[4] A charged capacitor is frequently said to be polarized. Thus, a reduction in resting membrane charge is called "depolarization" (more accurately but confusingly, "hypopolarization") and an increase "hyperpolarization." The rising phase of the action potential is frequently called the depolarization phase or simply depolarization. However, strictly speaking, the membrane is depolarizing only until the potential passes through zero. Thereafter, it is hyperpolarizing in the opposite sense. The phrase "a reduction in $\mathcal{E}$" should refer to hyperpolarization, i.e., $\mathcal{E}$ becoming more negative and thus decreasing; however, in common usage, "a reduction in $\mathcal{E}$" means depolarization, i.e., the phrase refers to the absolute value of $\mathcal{E}$, ($|\mathcal{E}|$). This usage generally will be followed here, but in cases where the intent is not clear from context, additional specification will be given.

axons, recovery is hastened by a delayed, depolarization-induced increase in P_K. At about the time P_{Na} begins to fall, P_K starts to increase at an appreciable rate, so that repolarization is speeded. The increased P_K persists for some time after $\mathcal{E}$ has reached the neighborhood of $\mathcal{E}_r$. Since $\mathcal{E}_K$ is considerably more negative than $\mathcal{E}_r$, $\mathcal{E}$ goes almost to $\mathcal{E}_K$ and then slowly falls back to $\mathcal{E}_r$.

The action potential is generated by the movements of Na^+ and K^+ ions through the membrane successively and respectively discharging and recharging the membrane. Hence, $\Delta\mu_{Na}$ and $\Delta\mu_K$ are the immediate sources of energy for the generation of the action potential. The ionic interchanges during an action potential slightly increase $[Na^+]_i$ and decrease $[K^+]_i$. The increased $[Na^+]_i$ stimulates the Na^+-K^+ pump, and the excess Na^+ ions are extruded over a long period of time. It should be emphasized that Na^+ pumping is not the cause of the repolarization phase of the action potential. Aside from the fact that Na^+-K^+ pumping is neutral, the process is much too slow. For example, the active efflux of Na^+ from a quiescent skeletal muscle cell in 1 sec is of the order of the influx of Na^+ during one impulse lasting about 1 msec.

An impulse is propagated by means of local current flow between active and inactive regions (see 112). Current flows in closed loops: out of the membrane at an inactive, polarized region, through the interstitial space to an adjoining active region, into the membrane and back through the intracellular fluid. Outward flow of current depolarizes the inactive membrane. If strong enough, the current eventually brings the membrane to threshold and this region also becomes active. This process is repeated at successive regions of the fiber so that the sequence of excitation and recovery moves along it continuously at a constant speed.

Membrane Current

The propagation of an impulse is accomplished by a depolarizing current supplied by an adjacent active region. With respect to a particular small patch of membrane, this depolarizing current comes from an external source and is indistinguishable from current supplied by a stimulating electrode. Any external current (I_m) flows through the membrane via two pathways (fig. 3A): the capacitor—the current (I_C) going to change the charge on the membrane—and the resistor—the current (I_i) being carried through the membrane by ions. Thus

$$I_m = I_C + I_i \tag{7a}$$

During propagation of an impulse I_m and I_C result from changes in I_i induced by voltage and time-dependent changes in membrane ionic permeabilities. Thus the study of membrane excitable properties reduces to a study of the determinants of permeability. In turn, permeabilities are estimated from measure-

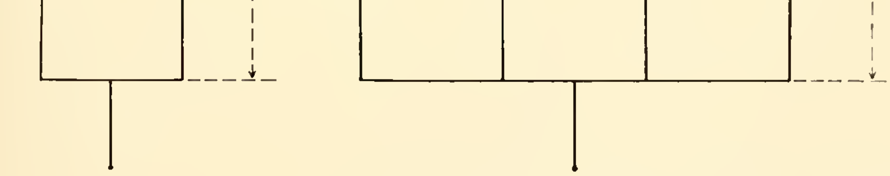

FIG. 3. Two approximate equivalent circuits for 1 cm² of cell membrane showing the division of an applied current between the various components. *A:* the external current (I_m) divides between the membrane capacitance (C_m) and resistance (R_m). Current flowing through the capacitor (I_C) charges the membrane; current through the resistance indicates the flow of ions (I_i) through the membrane. Therefore, $I_m = I_C + I_i = C_m d\mathcal{E}/dt + (\mathcal{E} - \mathcal{E}_r)/R_m$. *B:* ionic current is divided into its three major components, $I_{Na} + I_K + I_{Cl} = I_i$. R_K, R_{Cl}, and R_{Na} are the resistances to K, Cl, and Na ions, respectively; $\mathcal{E}_K$, $\mathcal{E}_{Cl}$, and $\mathcal{E}_{Na}$ are the equilibrium potentials of these ions. R_{Na} and R_K change with voltage and time, as indicated by the arrows through their symbols. [After Hodgkin & Huxley (60).]

ments of I_i and the driving forces on the ions (equations 2c, 4c).

Since it is desirable to measure I_i, it would be experimentally convenient if I_m and I_C could be eliminated or controlled. I_m can be made zero by stimulating the whole axon simultaneously so that the potential does not vary with distance along the fiber. For this purpose a long, thin electrode is inserted axially in a squid axon (fig. 4*A*). Any current from this electrode flows radially so that membrane current density is uniform. If the membrane properties are uniform, the change in $\mathcal{E}$ will be the same everywhere. This procedure is referred to as "space

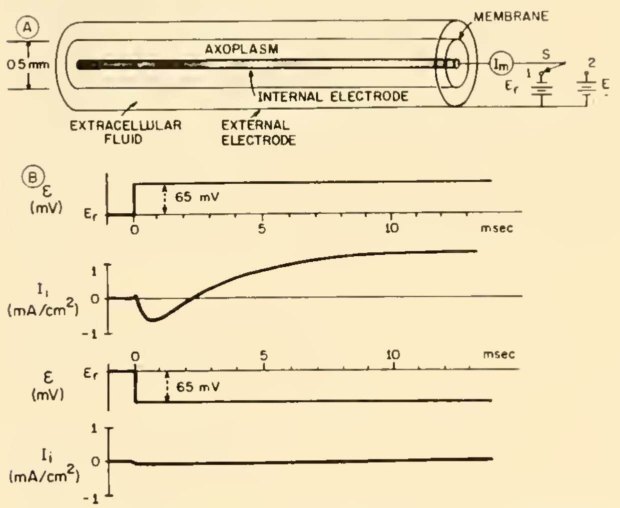

FIG. 4. Voltage clamping. *A*: principle of the voltage clamp. A squid axon is equipped with long internal and external electrodes and a fixed potential source (battery) is connected between them. Switch (S) permits a sudden change of voltage between the electrodes from one value, usually the resting potential ($\mathcal{E}_r$) to any other value ($\mathcal{E}$), typically less than $\mathcal{E}_r$. An ammeter connected in series with the battery-electrode system measures membrane current (I_m). In this simplified diagram, it is assumed that there is no resistance in the internal and external electrodes or in the junctions between the electrode and the extracellular and intracellular fluids. These idealized conditions are unobtainable in practice, and elaborate measures are required to achieve voltage clamping. [After Woodbury (137)]. *B*: typical current records from a clamped squid axon. At time zero, the switch was thrown (from position 1 to position 2 in *A*). In the upper two records $\mathcal{E}$ was 65 mv less than $\mathcal{E}_r$ so that the membrane voltage followed the time course shown in the uppermost record. The ionic current during this same period is shown immediately below. Outward flow through the membrane is defined as positive. The current surge that charged the membrane capacity to the new voltage was too large and brief to show on the record, which shows only ionic current. The lower two traces show the same experiment, except that the membrane was suddenly hyperpolarized by 65 mv at time zero. The current is small and steady throughout the hyperpolarization. Temperature, 3.8°C. [After Hodgkin *et al.* (62).]

clamping." In a space-clamped axon $I_m = 0$, so that equation 7a becomes

$$0 = I_C + I_i \left(\frac{\partial \mathcal{E}}{\partial x} = 0\right) \qquad (7b)$$

The activity resulting from a suprathreshold stimulus to a space-clamped axon is termed a membrane action potential, as opposed to a propagated action potential (62).

CAPACITATIVE CURRENT. It might be supposed that current cannot flow through a capacitor since there is an insulator in the current flow pathway. However, the flow of charges through the conductor to the surface of the dielectric pushes charges of equal sign away from the other conductor. So, although different charges are moving, the same amount of charge moves away from the capacitor as moves toward it. Hence, a current flows "through" the capacitor. A current flowing into a capacitor alters the amount of charge on it. The rate of change of charge (dq/dt) must equal the current flowing in, i.e., capacitative current is defined as dq/dt like any other current flow. There is, however, a slight difference in the meaning of the term. In the conductor, dq/dt refers to the amount of charge passing a particular cross section per unit time; in a capacitor, dq/dt refers to the rate of change of charge stored on either conductor. Since $q = C\mathcal{E}$, the current through a capacitor is $Cd\mathcal{E}/dt$. However, the membrane is not an ideal capacitor and this equation is not exact (17, 61). The error is not great for the present applications. Assuming that C_m is ideal,

$$I_i = -C_m \frac{\partial \mathcal{E}}{\partial t} = -C_m \dot{\mathcal{E}} \left(\frac{\partial \mathcal{E}}{\partial x} = 0\right) \qquad (7c)$$

In words, membrane ionic current is proportional to the time rate of change of voltage in a space-clamped axon.

Just as keeping $\mathcal{E}$ invariant with distance eliminates local current, so keeping $\mathcal{E}$ invariant in time eliminates capacitative current. Since the membrane is capable of changing its voltage via changes in permeability and in I_i, it is necessary to supply an external source or sink for I_i if the transmembrane voltage is to be kept constant. In this case equation 7c simplifies to

$$I_i = I_e \left(\frac{\partial \mathcal{E}}{\partial x} = \frac{\partial \mathcal{E}}{\partial t} = 0\right) \qquad (7d)$$

where I_e is the current supplied by the external source.

There is another, overriding advantage accruing

from holding membrane voltage constant. The regenerative interaction between P_{Na} and $\mathcal{E}$ which gives rise to the rising phase of the action potential is prevented because $\mathcal{E}$ is controlled by the experimenter and is not the consequence of uncontrolled changes in I_i. Historically speaking, it was found that holding $\mathcal{E}$ constant eliminates threshold and all-or-nothing behavior, i.e., at $\mathcal{E}$ = constant, I_i is a continuous function of time and at t = constant, I_i is a continuous function of $\mathcal{E}$. Such experiments led to the conclusion that some membrane permeabilities depend on $\mathcal{E}$ in a regenerative manner.

MEMBRANE VOLTAGE CLAMPING. The experimental procedure for holding the membrane voltage constant in space and time at a value determined by the experimenter is called voltage clamping. Figure 4*A* is a highly simplified diagram illustrating the principle of voltage clamping. A giant axon is equipped with long internal and external electrodes. If a battery is suddenly connected between these electrodes, the membrane voltage must change until it is equal to the battery voltage, the battery supplying the required membrane current. A switch is provided so that the membrane voltage can be abruptly changed from one value—usually $\mathcal{E}_r$—to any other value. An ammeter in series with one of the battery leads is used to measure the current. An idea of the factors which determine the current generated by the membrane can be obtained by substituting the equivalent circuit of figure 3*B* for the membrane in figure 4*A*.

The voltage clamp is the latest step in a sequence of increasing sophistication in experimental design. The historical and logical sequences coincide and are somewhat as follows: *a*) External electrodes were used to record propagated action potentials, a crushed end being used to secure a monophasic record. *b*) Intracellularly placed electrodes permitted the quantitative recording of resting and action potentials. *c*) Long intracellular electrodes were used to eliminate local circuit current flow, ionic current being calculated from $-C_m d\mathcal{E}/dt$ (90). *d*) Membrane voltage was held constant, permitting the direct measurement of ionic current and the elimination of regenerative interactions between $\mathcal{E}$ and I_i (19, 62).

In practice, voltage clamping is extremely difficult. Successful clamping of a "healthy" axon is attainable with present techniques only if meticulous attention is paid to the significant details (19). The experimental technique utilizes at least two internal electrodes, one of which is long (62, 90, 112, 115). One electrode is used to measure $\mathcal{E}$ and the other to supply the required current over the length of the axon. The measured membrane voltage is subtracted from the desired value. This difference is then amplified electronically and the output is applied to the current electrode in the direction which reduces the error. Electrode polarization is the principal reason for using two internal electrodes, i.e., the voltage at the internal electrode supplying current may be far different from that measured by the other electrode in the axoplasm. In "healthy" axons, spatial nonuniformity of membrane current further complicates the situation (19, 110, 115).

With $\mathcal{E}$ artificially held constant, the only independent variable in the nerve-electrode feed-back system is time. The important experimental parameters are $\mathcal{E}$ and the external ion concentrations. The experimental procedure is to measure membrane ionic current as a function of the time following a sudden shift of $\mathcal{E}$ from one value, usually $\mathcal{E}_r$, to another (fig. 4*B*). A series of such records is obtained for different values of the step voltage change (fig. 6). From these records the dependence of I_i on voltage at different times can be obtained (fig. 7). The contribution of Na^+ to I_i can be determined by measuring the effects of changes in $[Na^+]_o$ (fig. 6).

Extensive voltage-clamp experiments on squid axons have been conducted by Hodgkin *et al.* (62) and Hodgkin & Huxley (57–61). Frankenhaeuser and his colleagues (32, 33, 43) have recently obtained similar results in a study of myelinated nerve fibers. The Cole (19, 20) and Tasaki (110, 115) groups have recorded peak ionic currents considerably larger than those observed by Hodgkin and Huxley. Since these larger currents have much the same characteristics (20) as those recorded by Hodgkin and Huxley, there are no strong reasons for asserting that their analysis does not apply in principle to these "hotter" axons. Certainly, the analysis does give an accurate description of the somewhat "deteriorated" axons on which the original experiments were performed. The voltage-clamp experiments of Hodgkin *et al.* will now be described in some detail.

Ion Currents at Constant Voltage

Figure 4*B* shows a recording of the current through a membrane under a voltage clamp. At t = 0, the membrane was abruptly hyperpolarized (lower record) or depolarized (upper record) by 65 mv and then maintained at a constant voltage. In any real system, the charge on a capacity and hence its voltage cannot be changed instantaneously, since an infinite

current would be required. In practice the membrane is charged by a large, brief current. In the feed-back system used by Hodgkin and co-workers, the surge of capacitative current lasted less than 30 μsec. Following an abrupt hyperpolarization, there is a small negative (inward) current of the size to be expected from the initial membrane resistance. A depolarization, however, produces a large, diphasic variation in current (upper current curve, fig. 4*B*). If the membrane resistance remained constant, the expected effect would be a small positive current just equal and opposite to that produced by the hyperpolarization. This is the case initially, but the small initial step of outward current quickly changes into a large inward current, which reaches a peak in less than 1 msec. The current then falls gradually toward zero, reverses sign and levels off at a large, maintained, positive value. The curves obtained for other depolarizations are much the same shape if $\mathcal{E} < \mathcal{E}_{Na}$. If $\mathcal{E} > \mathcal{E}_{Na}$, the sign of the early current surge changes from negative to positive, whereas the late current is relatively unchanged. This behavior can be seen in figure 6 and is shown clearly in figure 5, where a series of currents resulting from a number of depolarizations to a value near $\mathcal{E}_{Na}$ are superimposed. For a depolarization of 117 mv it is seen that, aside from the initial step, the current is unchanging for about 0.5 msec. This curve contrasts with the records for other depolarizations. Since the resting potential was about -65 mv, depolarization of 117 mv reversed the membrane potential by about 52 mv, a value equal to $\mathcal{E}_{Na}$ within the limits of experimental error.

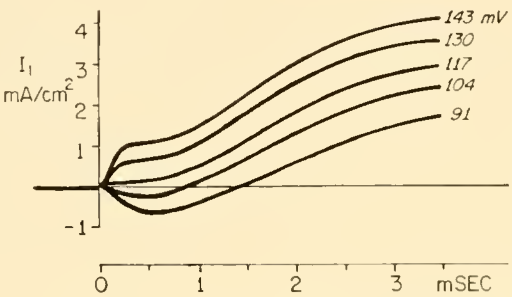

FIG. 5. Voltage clamp current records obtained when $\mathcal{E}$ was depolarized to values near the early current reversal potential. The early current was inward at depolarizations of 91 and 104 mv and outward at 130 and 143 mv. The current was small and nearly constant for 0.5 msec following a 117 mv depolarization. Normal $[Na^+]_o$; temperature, 3.5°C. [After Hodgkin *et al.* (62).]

The effects of changes in $[Na^+]_o$ furnish convincing evidence that the initial current is carried by Na^+ ions flowing down their electrochemical gradient. Figure 6 shows the effects of substituting choline$^+$ for 30 per cent of the Na^+. The left and right hand columns are membrane ionic current records taken in 30 per cent $[Na^+]_o$ before and after the records of the center column which were obtained in normal $[Na^+]_o$. In this figure, the capacitative surges have been subtracted from each current record. The curves in the two solutions are quite similar; the major difference is in the depolarizations at which the initial current reverses sign, approximately 70

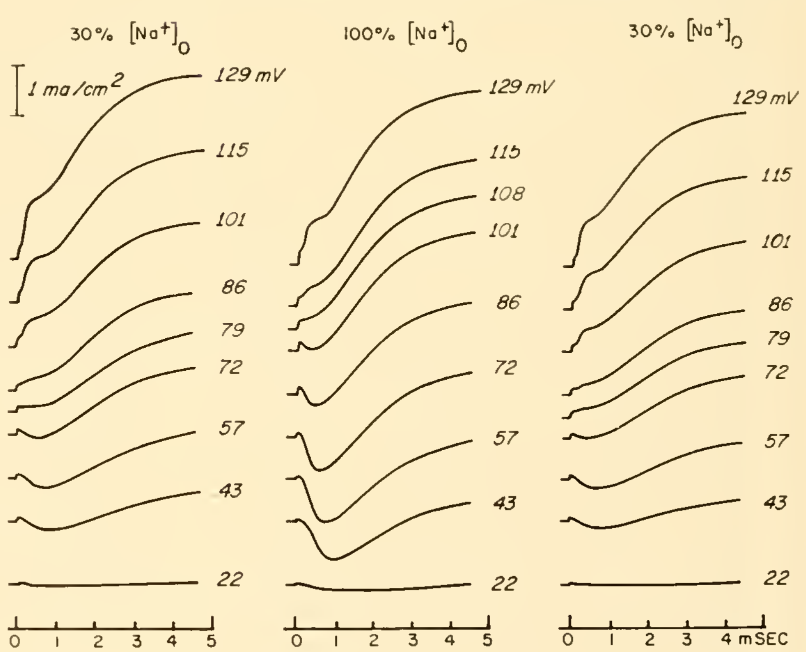

FIG. 6. Effects of altered $[Na^+]_o$ and clamping voltage on the early ionic current. Records in left and right hand columns were obtained when choline was substituted for 70% of the Na^+ in the external bathing medium. Records in middle column were obtained with axon in normal $[Na^+]_o$. The number by each curve indicates the amount by which the membrane voltage was depolarized from the resting potential at time zero. Note that in the left and right columns the early current was negative for small depolarizations and positive at large depolarizations; also that there was little early current for depolarizations of 79 mv. In normal $[Na^+]_o$ solutions, the sequence of changes in early currents was the same, but the reversal voltage was 108 mv. Temperature, 6.3°C. [After Hodgkin & Huxley (57).]

mv in the low Na^+ and 108 mv in the high Na^+ solutions. However, if the records of I_i obtained at these depolarizations are compared, they closely resemble each other. After a correction for the change in resting potential produced by altering $[Na^+]_o$, the change in the voltage at which the initial current is zero is within 1 mv of the change in $\mathcal{E}_{Na}$ calculated from the Nernst equation. This is an extremely good agreement between measured and calculated values in a biological system and strong evidence that the initial current is carried by Na^+. Although $[Na^+]_i$ was not estimated in these fibers, $\mathcal{E}_{Na}$ calculated from measurements of $[Na^+]_i$ in other fibers in similar condition was 45 to 50 mv, a value close to the zero initial current voltage.

Just as the initial inward Na^+ current has the proper direction to produce the rising phase of the action potential, the delayed rise in outward current has the proper direction and time course to produce the rapid repolarization of the falling phase in a squid giant axon. Since this outward current is still present in Cl^- deficient solutions (53), it seems likely that the prolonged outward current is carried by K^+. It is difficult to obtain direct evidence to this effect because an outward current should be little affected by changes in external concentrations of cations. There is, however, convincing tracer and other evidence that the prolonged high density outward membrane currents of depolarization are carried by K^+ (61). It will be assumed, henceforth, that this current is carried by K^+. Figure 7 shows a plot of I_i as a function of clamp voltage, I_i being measured at short times (I_{Na}) and long times (I_K). The significance of these curves will be discussed in the section on repolarization in cardiac tissue.

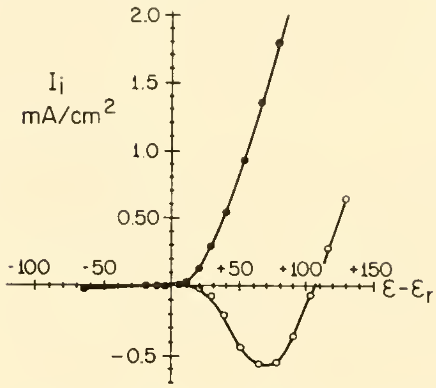

FIG. 7. Current, potential curves for short and long times after sudden changes in membrane potential of the voltage-clamped squid axon. Ordinate: membrane ionic current density, I_i (mA/cm^2), measured 0.63 msec after change in potential (open circles) and steady current measured 12 to 40 msec after change in potential (solid circles). An outward current is positive. Abscissa: difference between the clamp potential and the resting potential, $\mathcal{E} - \mathcal{E}_r$ (mv); depolarization is to the right. The curve for long times has a positive slope at all $\mathcal{E}$'s; whereas the curve for t = 0.63 msec has a positive slope for $\mathcal{E} - \mathcal{E}_r$ less than about 5 mv and greater than about 70 mv and a negative slope from 5 to 70 mv. The short time curve thus has the "N" shape often referred to as a "dynatron" characteristic. Currents are much larger for depolarizations than for hyperpolarizations. Temperature, 3.8°C. [After Hodgkin *et al.* (62).]

SEPARATION OF SODIUM AND POTASSIUM CURRENTS. In principle, the K^+ moiety of the total membrane current at a particular constant voltage ($\mathcal{E}_o$) can be obtained directly by changing the $[Na^+]_o$ until $\mathcal{E}_{Na} = \mathcal{E}_o$ and $I_{Na} = 0$. In practice it would be difficult to change $\mathcal{E}_{Na}$ by exactly the desired amount and to repeat this procedure for each $\mathcal{E}_o$. Hodgkin & Huxley (57) separated Na^+ and K^+ currents by interpolating between current records at different voltages and $[Na^+]_o$'s to get I_i at $\mathcal{E} = \mathcal{E}_{Na}$. Figure 8 shows the separation of I_i into $I_{Na} + I_K$, for a depolarization of 56 mv. Curve I_i was obtained for a normal $[Na^+]_o$ = 460 mmoles per liter. Here $I_i = I_K + I_{Na}$. Curve I_i' was interpolated from records obtained in low $[Na^+]_o$ solutions and is the current that would have been recorded with $[Na^+]_o$ reduced to a value such that $\mathcal{E}_{Na} = 56 + \mathcal{E}_r$. Since $I_{Na} = 0$ at $\mathcal{E} = \mathcal{E}_{Na}$, membrane ionic current is carried by K^+; $I_i' = I_K$. Furthermore, the difference between I_i and I_i' for a depolarization of 56 mv is the Na^+ current: $I_{Na} = I_i - I_i'$ (lowest curve, fig. 8). Similar separations are possible for all clamp voltages. The separated curves, like the total current curves, are continuous in time at a constant voltage (figs. 5 and 6) and continuous in voltage at a fixed time (fig. 7). It can be seen that I_{Na} reaches a peak then gradually falls to a value near zero even though the membrane is kept depolarized. This decline of I_{Na} in time was termed "inactivation" by Hodgkin & Huxley (59).

SODIUM AND POTASSIUM CONDUCTANCES (58). Both the inward and the outward membrane current under voltage clamp are carried by ions moving down their electrochemical gradients. The current carried by one ion species is determined by both the ease with which the ions can penetrate the membrane (permeability) and the driving force on the ion (electrochemical gradient). Since the objective is to characterize membrane properties and since the average driving force is known, a fairly direct measure of these membrane properties can be obtained by dividing the ionic

current by the driving force on the ion. From equation 4c I_{Na} can be written in the form:

$$I_{Na} = g_{Na}(\mathcal{E} - \mathcal{E}_{Na}) \tag{8}$$

where the permeability term (g_{Na}, unit, mhos/cm^2) is called the sodium chord conductance and is defined by equation 8. A similar expression can be written for all other ions. There are other ways of expressing the current through the membrane, e.g., equation 2c, so the justification for using equation 8, aside from its simplicity, is its usefulness in describing the experimental results. In this regard Hodgkin & Huxley (57) found that in normal $[Na^+]_o$, g_{Na} is constant for instantaneous changes in $\mathcal{E}$, i.e., the current-voltage curve is a straight line if the current is measured immediately after $\mathcal{E}$ is changed. Thus, at a fixed $\mathcal{E}$, g_{Na} must vary with time in the same manner as I_{Na} and similarly for g_K and I_K. The constancy of g_{Na} over brief periods indicates that conductances cannot change instantaneously, the implication being that changes in conductance result from time-consuming physical or chemical alterations in the membrane.

One consequence of the finding that conductances do not change instantaneously is a simple method for checking the reliability of the separation of I_i into I_{Na} and I_K components and the consequent calculation of g_{Na} and g_K from equation 8. It can be seen in figure 8 that I_{Na} is at its peak before I_K begins to rise appreciably. If the membrane were suddenly repolarized to the resting level at about the time of the peak I_{Na} (ca. 0.6 msec in figs. 8 and 9), g_{Na} would not have had time to change. Consequently $I_{Na} = g_{Na}(\mathcal{E}_r - \mathcal{E}_{Na})$ will be larger because the driving force has increased. The g_{Na} calculated from equation 8 for the new voltage and current should equal the g_{Na} calculated just before repolarization. The agreement between the two methods of calculating g_{Na} is good and is a further reason for defining membrane ionic currents by equation 8 (58). However, Dodge & Frankenhaeuser (33) have found it necessary to express the I_{Na} of myelinated nerve fibers in terms of a permeability and a driving force defined by Goldman's constant field integration of the membrane flux equation (equation 2c).

For any particular clamping voltage g_{Na} and g_K vary in time in the same way as I_{Na} and I_K. However, the variations of the conductances with voltage at any particular time are much less than the corresponding variation of the currents (fig. 13). Like I_{Na}, g_{Na} rises to a peak in 0.5 to 1.5 msec, depending on $\mathcal{E}$, and then falls to low values in another 1 or 2 msec. In contrast, g_K does not start rising for perhaps 0.6 msec but continues to a sustained high value (fig. 9, solid lines). The analysis of the conductance changes consequent to a rapid, maintained depolarization is the basis of the statements made above concerning the permeability changes during activity in squid nerve. Since the ionic current under voltage-clamp conditions is a continuous function of voltage and time, the behavior of the action potential of an unclamped nerve fiber should be predictable from an adequate description of the voltage and time variations of g_{Na} and g_K under voltage clamp. However, an adequate description must also include information on how a sudden repolarization alters the conductances and on the nature of the g_{Na} inactivation process. The first of these bits of information can be deduced from the data in figure 9. In marked contrast to S-shaped rising curves of both g_{Na} and g_K they fall exponentially after a sudden repolarization (dashed lines). The time constants describing the fall of the conductances depend on the final voltage.

INACTIVATION AND ACTIVATION OF SODIUM CONDUCTANCE. The activation-inactivation process is perhaps the most difficult and certainly the most crucial concept involved in understanding the genesis of the action potential and refractory period (59). Hodgkin & Huxley (60) have described hypothetically the variation of g_{Na} with time and voltage in terms of two separate but interacting rate processes. These authors supposed that a membrane channel or pathway through which Na^+ can pass relatively easily is formed when three M molecules and one H molecule are in particular positions in the membrane. Na^+ conductance was then assumed to be proportional to the number of these channels per cm^2. The probability that an M or H molecule is in the proper position for channel formation would depend on the transmembrane voltage. This variation can be explained by supposing that M and H are charged or dipolar.

The kinetics of the M substance is such that most of these molecules are not in the effective position at the resting potential—i.e., if M designates molecules in the proper position and M′, the molecules in other regions of the membrane, then the equilibrium between the two, $M \rightleftharpoons M'$, is far to the right. A large depolarization markedly increases the rate of movement from M′ to M positions and decreases the rate of movement from M to M′, so that the equilibrium shifts far to the left. The time required for this reaction to reach equilibrium following a depolarization is less than 1 msec, but is very de-

FIG. 8

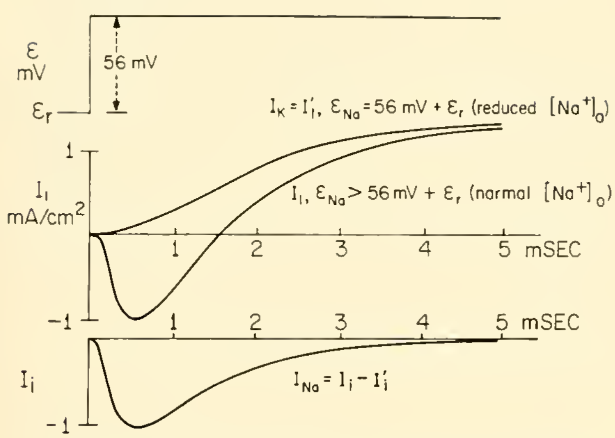

FIG. 9

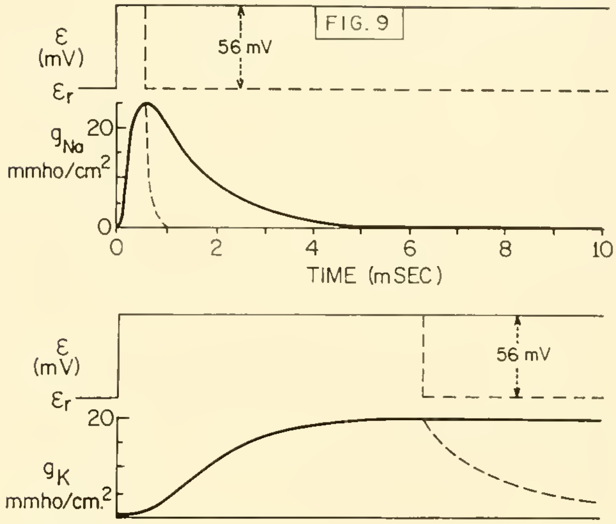

FIG. 8. Separation of ionic current at constant voltage into its component parts. Uppermost record: time course of membrane potential during current records shown below. Middle records: two superposed current curves obtained with axon in solutions with normal and with reduced concentrations of Na^+. The upper trace, actually obtained by interpolation, could have been obtained by reducing $[Na^+]_o$ so that $ℰ_{Na} = 56 + ℰ_r$. Since $ℰ = ℰ_{Na}$, I_i', is presumed to be carried entirely by K^+ ions and so $I_i' = I_K$. The lower current (I_i), obtained at normal $[Na^+]_o$, has an early component carried by Na^+ ions. If change in $[Na^+]_o$ has not altered I_K, I_{Na} is the difference between the two current records: $I_{Na} = I_i - I_i'$. The lowest tracing, with separate time scale shows this difference. Temperature, 8.5°C. [From Hodgkin (53).]

FIG. 9. Effects of sudden changes in transmembrane potential of a squid giant axon on sodium conductance (g_{Na}) and potassium conductance (g_K). First and third curves, time course of membrane potential changes; second and fourth, g_{Na} and g_K as functions of time. In both cases the membrane was suddenly depolarized by 56 mv at t = 0. The depolarization either was maintained beyond the end of the sweep (solid voltage line) or the membrane was abruptly repolarized (dashed lines) at t = 0.7 msec in first curve and at t = 6.3 msec in third curve. The resulting changes in g_{Na} and g_K are shown as solid lines for the maintained depolarizations and as dashed lines for the early repolarizations. Note that both g_{Na} and g_K increase along S-shaped curves when the membrane is depolarized but decrease along exponential curves when the membrane is repolarized. Temperature, 8.5°C. [After Hodgkin (53).]

pendent on ℰ. Since three M molecules have to move into position to form a Na^+ channel, the rise in g_{Na} following a sudden depolarization is S-shaped (figs. 9 and 13), i.e., third order kinetics.

The kinetics of the H substance are the same as those of the M substance except that the variation of the forward and backward rate constants with voltage is reversed—i.e., the reaction $H \rightleftharpoons H'$ is far to the left at $ℰ_r$ and depolarization increases the rate of movement to H'. However, the rate constants governing this reaction are slower than those governing $M' \rightleftharpoons M$, equilibrium for H taking several milliseconds (fig. 11, arrows). The fraction of H molecules in the proper position is called the amount of activation of g_{Na}. The amount of activation at $ℰ_r$ is about 0.6. Maintained hyperpolarization increases activation to 1.0 and maintained depolarization decreases it to 0 (fig. 11).

A sudden depolarization thus has two effects on g_{Na}. M molecules move rapidly into position and establish Na^+ channels at sites where H molecules have not yet moved out of position; therefore, g_{Na} rises rapidly. Even as M molecules are moving into position, however, H molecules are moving out of position, although at a much slower rate. Consequently, g_{Na} rises to a peak as M molecules align with H molecules and then falls over a period of several milliseconds as H molecules move out of position. If the membrane were suddenly repolarized after inactivation was completed, there would be little change in g_{Na} since most of the H molecules would be out of position and g_{Na} would already be near zero. Nevertheless, M molecules would start moving rapidly out of position and H molecules would begin moving slowly into position. Since, however, the M molecules would not be in position, the movement of H molecules into place (activation) would not produce an appreciable increase in g_{Na}. As this activation proceeded the peak g_{Na} subsequent to a sudden depolarization would increase until, after several milliseconds, the peak g_{Na} would again be normal. Clearly, a sudden depolarization im-

mediately following a sudden repolarization cannot produce an increase in g_{Na} any greater than that obtained immediately prior to the repolarization, i.e., proportional to the fraction of H molecules in position. This consideration suggests the experimental method actually used by Hodgkin & Huxley (59) to measure the kinetics of the activation-inactivation process—a two-step voltage experiment analogous to the classical conditioning-testing stimulus technique.

The records obtained in one such experiment are shown in figure 10. The testing stimulus is a maintained depolarization of 44 mv and the conditioning stimulus is a 31 mv hyperpolarization of variable duration. The response is the ratio of the conditioned peak inward (Na^+) current to the unconditioned peak I_{Na}. It can be seen in figure 10 that peak I_{Na} increases as the duration of the hyperpolarizing conditioning step is increased. The ratio of conditioned to unconditioned current is plotted as a function of the duration of the conditioning step in the upper curve of figure 11. The curve is exponential with a time constant of about 4 msec (arrow). The other curves in figure 11 were obtained for different values of the conditioning step voltage ($\mathcal{E}_1$). This

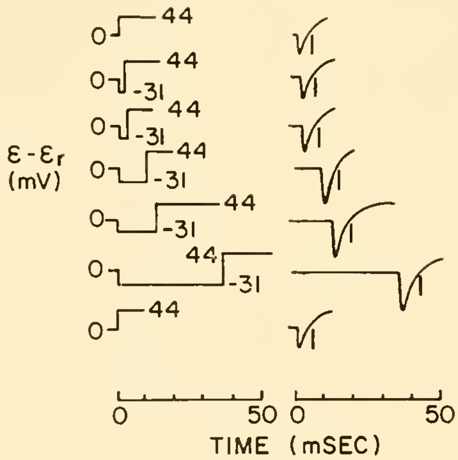

FIG. 10. Time course of activation of available g_{Na}. Left column: the time courses of membrane voltage which gave rise to the corresponding current records at right. Top and bottom current records are controls which show the I_i resulting from a depolarization of 44 mv. In intervening records, the 44 mv depolarization was preceded by periods of 31 mv hyperpolarization of progressively increasing duration. As the duration of the hyperpolarization increased, the peak I_{Na} increased. The vertical bar by each current curve is the height of the peak I_{Na} obtained in the upper record. Relative peak I_{Na} is plotted as a function of the duration of the hyperpolarizing step in fig. 11, curve labeled $\mathcal{E}_1 = -31$ mv. [After Hodgkin & Huxley (59).]

figure illustrates the major properties of the activation-inactivation system: *a*) Hyperpolarization ($\mathcal{E}_1$ negative) increases and depolarization decreases the amount of activation in the steady state. *b*) Steady-state activation is highly sensitive to voltage, as shown in figure 12 where the fractional amount of steady-state activation is plotted as a function of $\mathcal{E}$. *c*) The time required to reach a steady state also depends upon the voltage of the conditioning step; this feature is shown by the arrows in figure 11 which indicate the time constant of the exponential change in the current ratio. Hodgkin & Huxley (59, p. 505) describe these effects of voltage on g_{Na} as follows:

> The early effects of changes in membrane potential are a rapid increase in sodium conductance when the fibre is depolarized and a rapid decrease when it is repolarized. The late effects are a slow onset of a refractory or inactive condition during a maintained depolarization and a slow recovery following repolarization. A membrane in the refractory or inactive condition resembles one in the resting state in having a low sodium conductance. It differs in that it cannot undergo an increase in sodium conductance if the fibre is depolarized. The difference allows inactivation to be measured by methods such as those described in this paper. The results show that both the final level of inactivation and the rate at which this level is approached are greatly influenced by membrane potential. At high membrane potentials inactivation appears to be absent, at low membrane potentials it approaches completion with a time constant of about 1.5 msec at 6°C.

Quantitative Description of Nerve Behavior

If g_{Na} and g_K have been sufficiently characterized by the voltage-clamp analysis, it should be possible to predict the excitable properties of the unclamped nerve fiber. This possibility is strengthened by the evidence that changes in membrane permeability depend on membrane voltage rather than on membrane current—i.e., voltage clamping eliminates regenerative behavior, the shapes of the current-time curves are independent of the size and direction of the current, and current-voltage curves are continuous. To test this possibility, Hodgkin & Huxley (60) formulated mathematical descriptions of g_{Na} and g_K under voltage-clamp conditions, and with these were able to predict with astonishing success the excitable properties, potential changes, and ionic movements in a nerve fiber under many conditions.

KINETICS OF CONDUCTANCE CHANGES AT CONSTANT VOLTAGE. Hodgkin and Huxley developed the kinetic model for g_{Na} described qualitatively above to predict

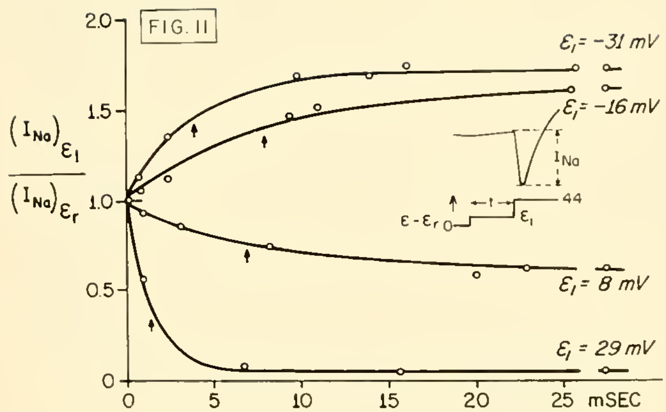

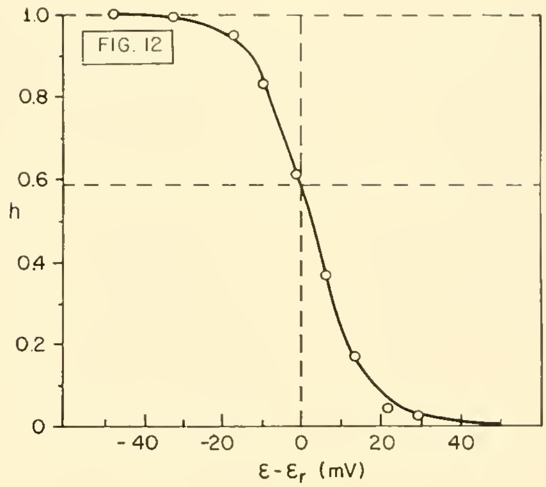

FIG. 11. Kinetics of the g_{Na} activation-inactivation process determined from conditioning, testing step voltage experiments on voltage-clamped squid giant axon. Inset shows the time course of membrane voltage and method of measuring the peak Na^+ current (I_{Na}) which developed following the testing step depolarization to $(\varepsilon - \varepsilon_r) = 44$ mv from the conditioning potential, ε_l. The ordinate is the ratio of the peak Na^+ current, $(I_{Na})_{\varepsilon_l}$, developed by the 44 mv depolarization when preceded by a depolarization of ε_l to the Na^+ current developed by the 44 mv depolarization alone, $(I_{Na})_{\varepsilon_r}$. The abscissa is the duration of the conditioning step. Curves for both plus (depolarizing) and minus (hyperpolarizing) values of the parameter ε_l are given and these values serve to identify the curves. Note that a preceding hyperpolarization increases the I_{Na} made available by a depolarization. Curve $\varepsilon_l = -31$ mv was obtained from data shown in fig. 10. Arrow by each curve indicates the time-constant of the change in $(I_{Na})_{\varepsilon_l}/(I_{Na})_{\varepsilon_r}$. The greater the absolute value of ε_l, the shorter the time-constant of the resulting changes in available I_{Na}. [After Hodgkin & Huxley (59).]

FIG. 12. Steady-state activation of Na^+ conductance as a function of transmembane potential. The open circles were obtained by measuring the values of $(I_{Na})_{\varepsilon_l}/(I_{Na})_{\varepsilon_r}$ at $t = 30$ msec for the various values of ε_l in fig. 11 and plotting this value against $\varepsilon_l = \varepsilon - \varepsilon_r$. However, the ordinate has been normalized, the quantity h having a maximum value of 1.0 for $\varepsilon - \varepsilon_r < -40$ mv. The horizontal dashed line shows the value of h at the resting potential (ε_r) shown by the vertical dashed line. Thus, at the ε_r of the axon used in these experiments, 0.6 of the maximum possible increase in g_{Na} is made available by a sudden depolarization. The solid curve is a plot of the equation $h = [1 + \exp(\varepsilon - \varepsilon_h)/7]^{-1}$, where ε_h is the value of ε at which $h = 0.5$. [After Hodgkin & Huxley (59).]

the S-shaped rise in g_{Na} on depolarization and the exponential fall on repolarization (fig. 9). The kinetics of the changes in g_K are the same except the changes are much slower. Hodgkin and Huxley postulated that a channel for K^+ ions to move through the membrane is formed when four N molecules are in place simultaneously and that the movements of N molecules into and out of each position follows first order kinetics. If n is the probability that any one of the four sites is occupied, then the total probability that a K^+ channel exists is n^4. Since each site follows first order kinetics with the rate constants depending on ε, the time course of n following a sudden depolarization is of the form $(1 - e^{-kt})$ because depolarization increases the probability that a site will be occupied. Similarly, repolarization causes a change in n of the form e^{-kt}. Since g_K is proportional to n^4, the increase in g_K on depolarization is S-shaped of the form $(1 - e^{-kt})^4$, whereas repolarization changes g_K along a curve that is proportional to e^{-4kt}. Hodgkin and Huxley described the kinetics of g_K changes by the equation

$$g_K = \bar{g}_K n^4, \quad \dot{n} = \alpha_n(1 - n) - \beta_n n \qquad (9)$$

where $\dot{n} = dn/dt$ and the rate constants α_n and β_n are functions of ε but not of time. The latter definition means that α_n and β_n instantly assume the appropriate value when ε is changed. The rate constants also depend on temperature with a Q_{10} of about 3 (60) and calcium concentration (45). Depolarization increases α_n and decreases β_n.

Similar equations were used to describe the kinetics of g_{Na} changes. If m is the probability that an M molecule is in place and h the probability that an H molecule is in place, then the total probability for the existence of a Na^+ pathway is m^3h since three M molecules and one H molecule are required. Thus, g_{Na} is described by

$$g_{Na} = \bar{g}_{Na} m^3 h, \quad \dot{m} = \alpha_m(1 - m) - \beta_m m, \quad \dot{h} = \alpha_h(1 - h) - \beta_h h \qquad (10)$$

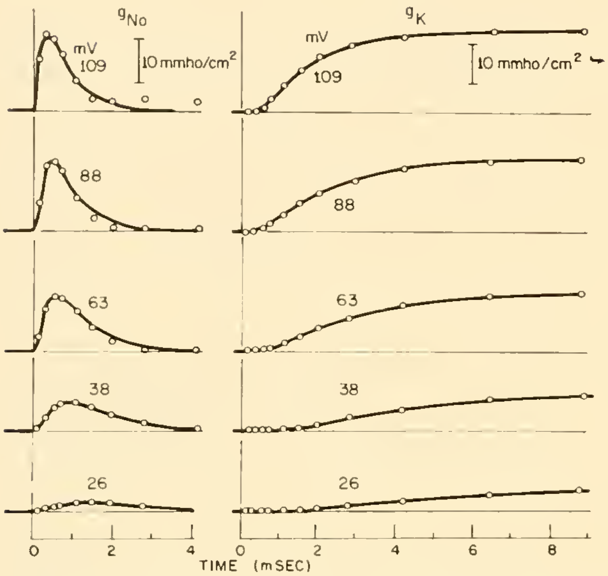

FIG. 13. Sodium conductance (g_{Na}) and potassium conductance (g_K) as functions of time in a voltage-clamped squid axon. Membrane voltage was held at the resting level until time zero when the membrane was suddenly depolarized by a fixed millivoltage denoted by the number attached to each curve. Open circles are experimental points and the solid curves were calculated from equations 9 and 10 in the text for values of the parameters which gave the best fit. The correspondence between measured and calculated values is good except at early times; the observed delay in the rise of g_K is greater than the delay in the theoretical curves. This difference can be seen for a depolarization of 109 mv. Temperature, 6°C. [From Hodgkin (53).]

As for K^+, the α and β terms are rate constants which depend on voltage, temperature and $[Ca^{++}]_o$ but not on time. Depolarization increases α_m and β_h, and decreases β_m and α_h, since m starts to increase and h to decrease following depolarization.

The equations describing g_K and g_{Na} can be easily solved for voltage-clamp conditions. Since $\mathcal{E}$ is a constant, the α and β terms are also constants and the solutions for n, m, h are exponential. Figure 13 shows the close relations between the appropriate solutions of these equations and the experimental voltage-clamp data. The circles are experimental measurements and the solid curves are solutions of equations 9 and 10 with appropriate values of the parameters. The numbers beside the curves give the depolarization from the resting level in millivolts. The fit is quite satisfactory, the principal difference being that the theoretical curves for g_K rise with somewhat less delay than the experimental curves. This difference is not obvious in the curves of figure 13 but can be seen clearly in figure 3 of (60) [cf. also (20)].

Fitting of equations 9 and 10 to the experimental data for different, fixed depolarizations provides values of the α and β terms at the different clamping voltages used. The fitted values of these parameters are reasonably well described by continuous functions of $\mathcal{E}$, e.g.,

$$\alpha_n = 0.01(-\Delta\mathcal{E} + 10) \Big/ \left[\exp\left(-\frac{\Delta\mathcal{E} + 10}{10}\right) - 1\right], \qquad (11)$$
$$\beta_n = 0.125 \exp(-\Delta\mathcal{E}/80)$$

where $\Delta\mathcal{E} = \mathcal{E} - \mathcal{E}_r$. Similar expressions describe α_m, β_m, α_h, and β_h. Equations 9, 10, and 11 describe the variations in time and voltage of R_{Na} and R_K in figure 3*B*.

PREDICTION OF THE ACTION POTENTIAL (60). With explicit expressions for the α and β terms, g_{Na} and g_K, the behavior of the membrane under space-clamp conditions can be predicted by solving equations 7b, 8, 9, 10, and 11 for $\mathcal{E}$ as a function of time. For the space clamp, I_m is a constant and the set of equations describing $\mathcal{E}$ is:

$$C\dot{\mathcal{E}} + I_i = I_m = \text{constant},\ I_i = I_{Na} + I_K + I_l$$
$$I_{Na} = \bar{g}_{Na}m^3h(\mathcal{E} - \mathcal{E}_{Na}),$$
$$I_K = \bar{g}_K n^4(\mathcal{E} - \mathcal{E}_K) I_l = \bar{g}_l(\mathcal{E} - \mathcal{E}_l) \qquad (12)$$
$$\dot{m} = \alpha_m(1 - m) - \beta_m m, \ \ldots$$

The term $I_l = \bar{g}_l(\mathcal{E} - \mathcal{E}_l)$ is the small component of the total ionic current not carried by Na^+ or K^+, $\bar{g}_l$ being a constant.

The upper curves in figure 14 are solutions of the above equations for initial depolarizations of 90, 15, 7, and 6 mv and for $I_m = 0$. The lower curves are measured action potentials recorded under comparable conditions. The two sets of curves are remarkably similar, although not identical. The most obvious difference is that the voltage of the recorded action potentials falls appreciably after the cessation of the stimulus, but the voltage of the calculated potentials falls only slightly. Other differences include sharper peaks and a more abrupt development of postspike hyperpolarization in the calculated action potentials. Another, less obvious difference is the presence of a slight hump on the falling phase of the calculated action potential. Despite these minor shortcomings, the agreement between real and computed action potentials is excellent. However, mere resemblance is not sufficient to establish the validity of equation 12 as an adequate description of nerve membrane properties. To be satisfactory, the formulation must predict *a*) the existence of a threshold depolarization (fig. 14); *b*) the nature and duration of the refractory periods; *c*) after-hyperpolarization (figs. 14 and 15); *d*) the ex-

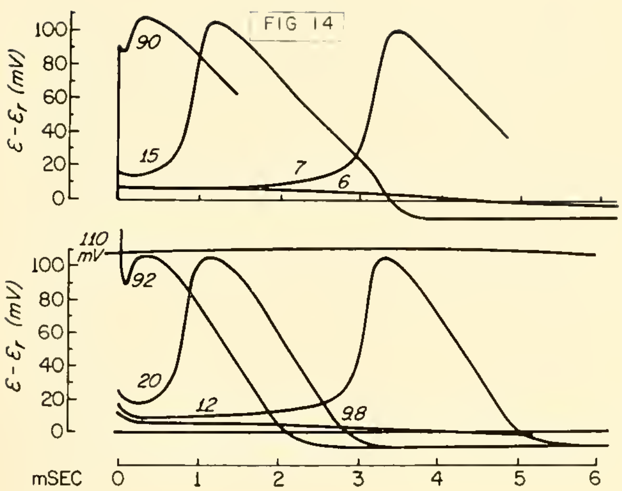

FIG. 14. Calculated (above) and measured (below) membrane action potentials of squid giant axon. Number next to each curve is the amount of charge in nanocoulombs/cm^2, displaced from the membrane by the brief stimulating current applied via long internal and external electrodes. Since membrane capacity was taken as 1.0 μF/cm^2 in the calculations, the number by each theoretical curve also indicates the initial millivoltage displacement. The upper curves are solutions of equation 12. Ordinate: displacement of transmembrane potential from the resting level, depolarization upward. Abscissa: time in milliseconds. The two sets of curves are directly comparable except for the slight curvature of the 110 mv calibration line. Calculations for a temperature of 6°C. [After Hodgkin & Huxley (60).]

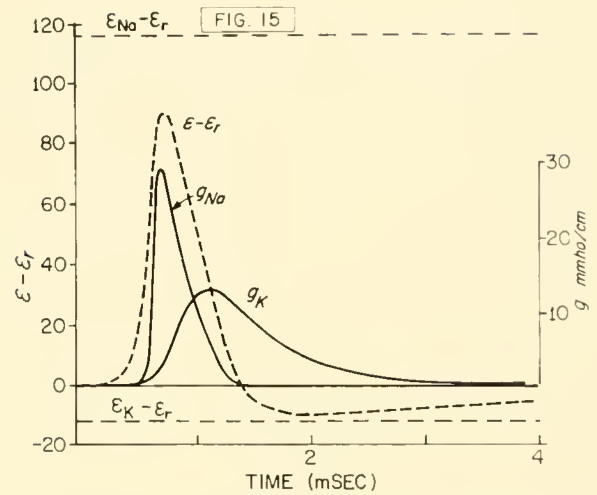

FIG. 15. Theoretical propagated action potential. Plots of transmembrane potential alteration ($\mathcal{E} - \mathcal{E}_r$), potassium conductance (g_K), and sodium conductance (g_{Na}) as functions of time at a fixed point on a squid axon during the passage of a propagated action potential. Curves are solutions of equation 12 but with I_m replaced by $-(1/r_i u^2)\partial^2\mathcal{E}/\partial x^2$, where u is conduction velocity, 18.8 m/sec and r_i is internal resistance in ohm/cm. The horizontal lines labeled ($\mathcal{E}_{Na} - \mathcal{E}_r$) and ($\mathcal{E}_K - \mathcal{E}_r$) represent the Na^+ and K^+ equilibrium potentials, respectively. Note that g_{Na} does not change appreciably until the time of the rising phase inflection point of the action potential, and that $\mathcal{E}$ approaches $\mathcal{E}_K$ during the after potential when g_K is still elevated. Calculated for a temperature of 18.5°C. [After Hodgkin (53).]

changes of Na^+ and K^+ during activity; *e*) the existence of a propagating action potential having constant velocity and amplitude (fig. 15) and that membrane resistance falls dramatically during passage of the action potential (18); and *f*) cathodal or depolarization block of conduction. This behavior is inherent in the kinetics of the g_{Na} activation-inactivation process, i.e., depolarization inactivates.

THRESHOLD AND ANODAL BREAK EXCITATION. It can be seen in figure 14 that the threshold of the theoretical action potential measured at the voltage minimum is about 6 mv. The corresponding minimum value for the nerve is about 8 mv. This agreement is more or less fortuitous, since the threshold is quite sensitive to the value of $\bar{g}_l$, which is not accurately known. However, the theoretical model closely resembles the nerve in this respect. The equation can also predict anodal break excitation, i.e., the initiation of an action potential as a result of the sudden cessation of a hyperpolarizing current. Prolonged hyperpolarization has two effects: g_K decreases and h increases (activation) so that threshold $\mathcal{E}$ becomes more negative. Thus the fall in $\mathcal{E}$ upon termination of the current will cause an increase in g_{Na} while g_K remains at its low value for a period and a regenerative response may occur. Since the resting value of h is only 0.6 (fig. 12), hyperpolarization could almost double the available g_{Na}. Thus, anodal break excitation is a possibility in any excitable tissue if h at $\mathcal{E}_r$ is appreciably less than 1.

IONIC EXCHANGE. Since the net Na^+ and K^+ currents are known at each instant, the one-way flux can be calculated if it is assumed that each ion moves through the membrane independently of any other ion. The net fluxes calculated in this way agree fairly well with the measured fluxes (83), but too little exchange of Na^+ and too much exchange of K^+ are predicted. Although a portion of the error may result from recognized simplifications in the formulation, the assumption of independent movement is now known to be incorrect for K^+ (65). Furthermore, the connective tissue sheath surrounding the squid membrane acts as a diffusion barrier to K^+ (44).

REFRACTORY PERIOD. The equations predict quite accurately the size and shape of the action potential during the refractory period (60, fig. 20). Two factors determine the refractory period—inactivation of g_{Na} (decrease in h) and the persistent increase in g_K following repolarization. Inactivation reduces the g_{Na} made available by depolarization and thus increases the depolarization required to induce a regenerative action. The delayed rise in g_K following depolarization speeds up the rate of repolarization tremendously and the slowness of g_K in falling during and after repolarization lengthens and intensifies the refractory period, because a stimulating current does not have as great an effect on $\mathcal{E}$ when g_K is above normal. Following the upstroke of the action potential, h decreases from its resting value of 0.6 to about 0.1 near the end of the spike; thereafter, h increases to its resting value in about 10 msec at 6°C. Slightly before h is minimum, g_K reaches its peak value and then decreases in a roughly exponential manner, reaching its resting level somewhat sooner than h (cf. 60, fig. 19). The absolutely refractory period ends when h becomes sufficiently high that a depolarization causes a net Na^+ influx which exceeds the above normal net K^+ efflux. The relatively refractory period lasts until g_K and h have returned to their normal values.

PROPAGATED ACTION POTENTIAL. The calculation of the response of a nerve to a current applied at a point is difficult, since membrane current is a function of distance along the fiber, $I_m = (1/r_i)\partial^2\mathcal{E}/\partial t^2$ (66, 88, 112) where r_i is the resistance of a 1 cm length of axoplasm, whereas ionic current is a function of time and voltage as given by equation 12. This expression for I_m can be substituted in the top equation of 12, but the resulting partial differential equation is extremely laborious to solve. Considerable simplification can be achieved, however, if it is assumed that the theoretical nerve model is capable of propagating an impulse of constant shape and speed (u) then, in steady-state propagation, membrane current can be expressed as a function of time, $I_m = (1/r_i u^2)\partial^2\mathcal{E}/\partial t^2$ (60, 113). Thus in a propagating action potential I_m can be expressed as a function of time; and if this expression for I_m is substituted in equation 7b to replace the top equation of 12, there results a second order ordinary differential equation in which t is the only independent variable. This equation is much easier to solve. However, since the conduction speed of the model was not known, Hodgkin & Huxley (60) tried different values of u until the calculated response resembled a propagating action potential. The result of such a calculation is shown in figure 15. The required conduction velocity was 18.8 m/sec and the comparable measured conduction velocity was 21.2 m/sec. The values of g_{Na} and g_K during the action potential are also plotted in figure 15. This figure is a quantitative plot of the membrane conductance and potential changes accompanying propagated activity. It can be seen that considerable depolarization occurs before g_{Na} begins to change, but that thereafter g_{Na} rises steeply. This passive depolarization is caused by local circuit flow into the advancing active region. This passive depolarization proceeds until threshold is reached (inflection of the $\mathcal{E}$,t curve) where membrane current flow reverses from outward to inward owing to the rise in g_{Na}. Peak g_{Na} is reached shortly before the peak of the action potential. Thereafter, g_{Na} decreases and g_K increases rapidly; the consequence is a rapid repolarization followed by the prolonged hyperpolarization, the effect on $\mathcal{E}$ of the delayed fall in g_K following repolarization. Total conductance ($g_{Na} + g_K$) follows o time course closely similar to that measured by Cole & Curtis [(18); cf. (60, fig. 16)].

MEMBRANE PROPERTIES OF CARDIAC CELLS

The transmembrane action potential of a frog ventricular cell at 20°C lasts about 1 sec, depending on the rate of stimulation (fig. 1). In contrast, the action potential of a squid giant axon at the same temperature persists little more than 1 msec (fig. 15). Nevertheless, these two excitable tissues have a number of electrophysiological features in common, e.g., high $[K^+]_i$, $[Na^+]_o$, and $[Cl^-]_o$, and low $[K^+]_o$, $[Na^+]_i$, and $[Cl^-]_i$; Na^+ for K^+ exchange pumps; resting potentials in the range 60 to 80 mv; rising phases of the action potentials brought about by a specific increase of the membrane permeability to Na^+; and inactivation of g_{Na}. These facts indicate that electrical activity in cardiac tissue and the squid axon are attributable to the same sorts of underlying mechanisms. The major difference is in the repolarization process. Repolarization in heart cells is poorly understood, since it has not been technically feasible to do voltage-clamp experiments on single cardiac cells. Pacemaker activity is not unique to cardiac cells since a continued small depolarizing current applied to a squid axon is sufficient to make the membrane model oscillate indefinitely, although trains of spikes in real axons tend to terminate (16, 77). Three aspects of the electrical properties of cardiac cell membranes are discussed.

1) There is evidence that the rising phase of the cardiac action potential is due to a specific increase in g_{Na} and that there is an activation-inactivation process. *2*) The evidence concerning the nature of the repolarization process is presented at some length. *3*) Excitation-contraction coupling, the passive electrical properties of cardiac cells, and the problem of intercellular transmission will be discussed.

In the absence of voltage-clamping techniques applicable to cardiac tissue, intracellular recording has been used to obtain most data on the nature of the cardiac action potential. Nevertheless, prior to the development of intracellular recording techniques in 1947 (87) a considerable body of information about the action potentials of heart muscle had been accumulated (cf. 13, 105). Certainly overshoot is evident in records obtained with suction electrodes (cf. 25, 26). It was, however, the advent of the Na^+ hypothesis (63) and the possibility of measuring transmembrane potentials in cardiac cells directly and quantitatively with intracellular microelectrodes that led to the recent rapid growth of knowledge of the ionic basis of cardiac excitability. S. Weidmann, in particular, has made important contributions using this technique.

Intracellular Recording

The first clear evidence of overshoot in squid axons was obtained simultaneously by Curtis & Cole (29) in the United States and Hodgkin & Huxley (56) in England just before World War II. They used glass pipettes filled with salt solution and inserted down the axis of the axon in estimating values of the transmembrane resting and action potentials.

Shortly after the war, Graham & Gerard (50) developed and Ling & Gerard (87) perfected the ultramicroscopic microelectrode or ultramicroelectrode. It is a tapering hollow glass tube drawn down to a tip diameter of about 0.2 μ and filled with an electrolyte, usually 3 M KCl (95). This electrode can be inserted transversely through the membrane in such a manner that there is little or no current leakage around the point of insertion. The "success" of an impalement depends critically on the tip diameter of the electrode. The tip diameter dividing usable from unusable microelectrodes is less than 1 μ, but depends on the tissue under study. Details of the manufacture and electrical properties of these electrodes can be found in the chapter by Frank (42).

If such a microelectrode is mounted on a micromanipulator and advanced until it touches the surface of an excised muscle, a large, steady, potential difference suddenly appears, presumably when the electrode penetrates a cell membrane. If the membrane is not damaged by the electrode insertion, i.e., if the membrane seals around the electrode, then this potential is the transmembrane potential plus an unavoidable junction potential. Nastuk & Hodgkin (95) showed that some impalements produce little membrane damage. By inserting two electrodes at two points in a cell, they found that the entry of the second electrode frequently caused only a small reduction in the voltage recorded at the first electrode. Woodbury & Brady (136) greatly improved the practicability of recording from moving tissues by mounting the tip of a microelectrode on a 25-μ tungsten wire. This technique was used to record from a human heart at surgery (137).

Considerably more information concerning the electrical properties of the cell membrane can be obtained if two electrodes can be inserted into the same cell. The passive electrical properties, the capacity (C_m) and the resistance (R_m) of 1 cm^2 of membrane and the specific resistivity of the internal medium (ρ_i) can be simply measured using this technique. The procedure is to apply a constant current through one electrode and to measure the resulting changes in membrane potential at a point near the current source and at least one other point about a space constant away. Weidmann (126) has used this technique to measure the electrical properties of Purkinje fibers during diastole. He also estimated the changes in membrane slope conductance during repolarization (125) and voltage-clamped a small region of membrane in a study of the inactivation of g_{Na} (127, 128).

Depolarization

Since the overshoot of the action potential in squid axons results from a specific increase in g_{Na}, the finding of an overshooting action potential in other tissues is presumptive evidence for the Na^+ mechanism. The first intracellular recordings of transmembrane potentials from cardiac cells were reported almost simultaneously by Coraboeuf & Weidmann (22), who worked with Purkinje fibers of dog, and by Woodbury and co-workers (140), who worked with frog ventricle. Overshoot was found in both tissues. A year later Draper & Weidmann (35) reported that the overshoot and maximal rate of rise of the action potential ($\dot{\mathcal{E}}_d$) in mammalian Purkinje tissue were directly dependent on $[Na^+]_o$. At the same time Cranefield *et al.* (25) reported that reduction of $[Na^+]_o$ reduced the size of the action potential recorded with a suction

electrode. The variation of $\dot{\mathcal{E}}_d$ with $[Na^+]_o$ would be expected from the ionic theory, since g_{Na} would be much larger than $g_K + g_{Cl}$ early in depolarization. Draper and Weidmann also found that the tissue became inexcitable when $[Na^+]_o$ was less than about 15 per cent of normal.

This indirect evidence indicates that depolarization in cardiac tissue results from a net influx of Na^+. However, some doubt was thrown on this conclusion by Coraboeuf & Otsuka's (21) finding that overshoot in guinea pig ventricle was independent of $[Na^+]_o$ except that the tissue became inexcitable at low $[Na^+]_o$ values. DeLeze (31) confirmed these results, but he also found that $\dot{\mathcal{E}}_d$ does depend directly on $[Na^+]_o$.

Working with frog ventricle, Brady & Woodbury (4) found that overshoot varies with $\mathcal{E}_{Na}$ when $[Na^+]_o$ is greater than 40 per cent of normal. There is, however, comparatively little change in overshoot if $[Na^+]_o$ is less than 50 per cent. Figure 16*A* shows superimposed traces of frog ventricular action potentials obtained for various values of $[Na^+]_o$; choline$^+$ replaced Na^+. Note the near equality of overshoot in the solutions in which $[Na^+]_o$ was 40 and 50 per cent of normal. Brady and Woodbury also observed an $\dot{\mathcal{E}}_d$ directly proportional to $[Na^+]_o$. Although the absolute values of $\dot{\mathcal{E}}_d$ varied considerably from one cell to the next, the variation with $[Na^+]_o$ was convincing in a single impalement (fig. 16*B*). The regression line relating all values of $\dot{\mathcal{E}}_d$ to $[Na^+]_o$ passed through zero, if allowance was made for experimental error (fig. 16*C*). Thus the evidence concerning effects of $[Na^+]_o$ on $\dot{\mathcal{E}}_d$ indicates that Na^+ is the depolarizing agent. On the other hand, the effects of $[Na^+]_o$ on overshoot are equivocal.

In the squid giant axon, g_{Na} is falling and g_K is beginning to rise at the peak of the action potential (fig. 15). The time when g_{Na}/g_K is maximum is earlier than this probably immediately after the inflection point. Thus, if the ionic theory is applicable to heart, nearly all membrane current is carried by Na^+ during the early rising phase. In this case, the rate of rise is proportional to I_{Na}, since $-C_m\dot{\mathcal{E}}_d = I_i \simeq I_{Na} = g_{Na}(\mathcal{E} - \mathcal{E}_{Na})$. So, if the voltage of the inflection point and g_{Na} are independent of $[Na^+]_o$, $\dot{\mathcal{E}}_d$ should vary with $\mathcal{E}_{Na}$. It is likely that g_{Na} varies directly with $[Na^+]_o$ also. Other ions must be contributing significantly at the peak since it is considerably below $\mathcal{E}_{Na}$. Thus, the failure of variations in $[Na^+]_o$ to change overshoot cannot rule out the high probability that Na^+ is the depolarizing agent [see (4) for further discussion]. Since Na^+ carries

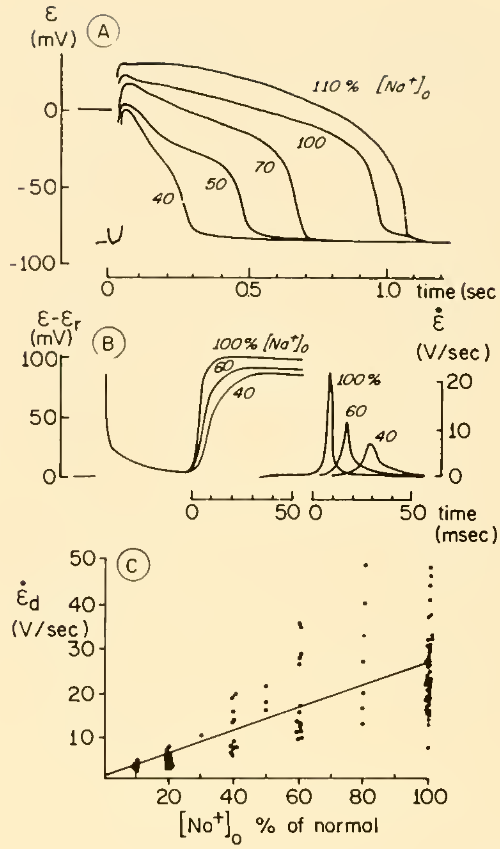

FIG. 16. Effects of changes in $[Na^+]_o$ on the transmembrane potentials recorded from cells of perfused frog ventricle. *A:* effects of $[Na^+]_o$ on overshoot and repolarization. Numbers by curves indicate percentage of normal $[Na^+]_o$ in perfusion fluid; choline substituted for Na^+. Ordinate: transmembrane potential in millivolts; abscissa: time in seconds. [After Brady & Woodbury (3).] *B:* effects of $[Na^+]_o$ on rising phase of action potential ($\mathcal{E} - \mathcal{E}_r$), on the left and rate of rise ($\dot{\mathcal{E}}$, v/sec), on the right recorded from single cell. Lowering $[Na^+]_o$ (by substituting sucrose for NaCl) reduced overshoot and rate of rise. *C:* effects of $[Na^+]_o$ on the maximum rate of depolarization ($\dot{\mathcal{E}}_d$) for a large number of cells (NaCl replaced by sucrose). The line is a least square fit of the data and the vertical axis intercept is not significantly different from zero. [After Brady & Woodbury (4).]

nearly all the depolarizing current, peak $g_{Na} \simeq -C_m\dot{\mathcal{E}}_d/(\mathcal{E} - \mathcal{E}_{Na})$. Accepting the rather high value of 30 $\mu F/cm^2$ for the C_m of cardiac tissue (122), Brady & Woodbury (4) estimated a peak g_{Na} of 10 mmho/cm^2. Hodgkin & Huxley (60) found a maximum g_{Na} of about 25 mmho/cm^2 in squid axon and Cole & Moore (19) have reported values up to 140 mmho/cm^2. A similar calculation of g_{Na} based on data from Purkinje fibers (126, 127) gives a peak value for g_{Na} of about 100 mmho/cm^2, although there is considerable uncertainty in the values of

$\mathcal{E}_{Na}$ and the voltage at which $\dot{\mathcal{E}}_d$ is maximum that were used in this calculation. Nevertheless, this high value of g_{Na} is not unexpected since Purkinje fibers are specialized for fast conduction.

ACTIVATION AND INACTIVATION OF SODIUM CONDUCTANCE. Weidmann (127) used an ingenious technique for studying the kinetics of the system carrying Na^+ in Purkinje fibers. Two closely spaced, intracellularly placed microelectrodes were used to clamp $\mathcal{E}$ for a short distance around them. The voltage measured with one electrode was used to control the flow of current through the other. $\mathcal{E}$ was clamped at some value for about 50 msec. The clamp was then released and the tissue was stimulated to produce an extrasystole. The $\dot{\mathcal{E}}_d$ of the extrasystole was then taken as a measure of g_{Na}, since the voltage at which $\dot{\mathcal{E}}_d$ was maximum was quite independent of the clamping voltage. By plotting $\dot{\mathcal{E}}_d$ against the prespike clamping voltage, Weidmann obtained an approximation to the curve relating available g_{Na} to $\mathcal{E}$—i.e., the relationship between h and $\mathcal{E}$ described by Hodgkin & Huxley (59). Figure 17 shows plots of Weidmann's measurements of these quantities in Purkinje fibers bathed in solutions with normal and 25 per cent of normal $[Na^+]$. The curves are practically identical in shape to those for squid axons, activation being maximal for $\mathcal{E} < -90$ mv and nearly zero for $\mathcal{E} > -50$ mv. Increasing $[K^+]_o$ fivefold did not alter this relationship. The time constant of activation was measured by a two-step function technique like that used by Hodgkin & Huxley (59). Although the results are not quantitatively reliable, they are remarkably similar to those obtained on squid axon. Weidmann also found that action potentials initiated during late repolarization or slow diastolic depolarization had rates of rise that varied with the membrane voltage at which they were initiated in the same manner as these rates did when the voltage was clamped. There was, however, some time displacement of the $\dot{\mathcal{E}}_d,\mathcal{E}$ curves of potentials initiated during repolarization or diastolic depolarization. He attributed this displacement to the lag in inactivation-activation equilibration behind $\mathcal{E}$ at times when $\mathcal{E}$ is changing. Thus it can be concluded that the detailed kinetics of the changes in g_{Na} during the rising phase are much the same in Purkinje tissue as in the squid axon.

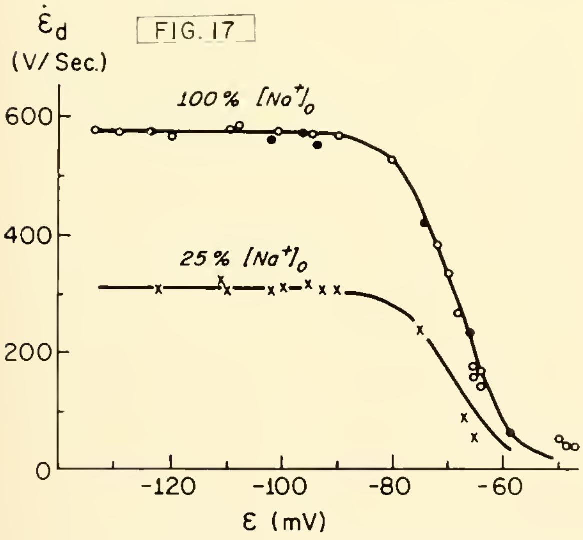

FIG. 17. Effects of initial transmembrane potential on the rate of rise of the action potential in ungulate Purkinje cells. A local region of the membrane was clamped at a fixed voltage by using an intracellular electrode measuring transmembrane potential to control the current flowing from a nearby intracellular electrode. After the membrane was maintained at the potential ($\mathcal{E}$, mv) indicated on the abscissa for 50 msec, the clamp was released and the tissue was stimulated. The maximum rate of rise of the resulting action potential ($\dot{\mathcal{E}}_d$, v/sec) was then measured and plotted as the ordinate. Reduction of $[Na^+]_o$ to 25% of normal reduced the $\dot{\mathcal{E}}_d$ at any voltage but did not alter the shape of the curve. Circles and crosses: experimental points; solid curves: graphs of the equation $\dot{\mathcal{E}}_d = (\dot{\mathcal{E}}_d)_{120}/(1 + \exp(\mathcal{E} - \mathcal{E}_h)/5)$, where $(\dot{\mathcal{E}}_d)_{120}$ is $\dot{\mathcal{E}}_d$ at $\mathcal{E} = -120$ and $\mathcal{E}_h$ is the value of h at which $\dot{\mathcal{E}}_d = 0.5\ (\dot{\mathcal{E}}_d)_{120}$. Compare with curve of h vs. $(\mathcal{E} - \mathcal{E}_r)$ in fig. 12. [After Weidmann (127).]

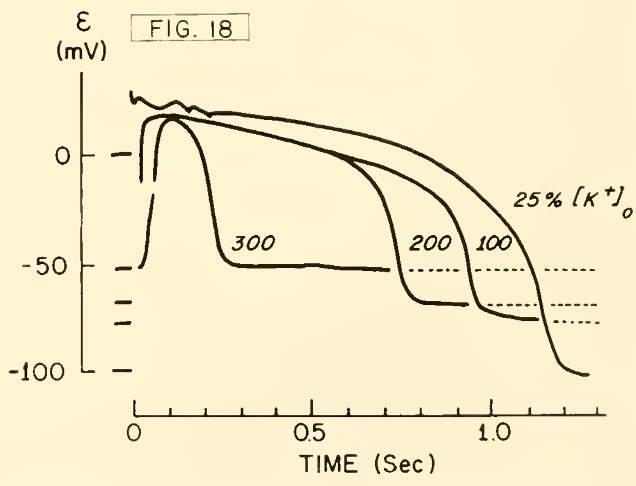

FIG. 18. Effects of changes in the concentration of potassium in the solution perfusing a frog ventricle on the transmembrane potentials of a single ventricular cell. Heart was stimulated at time zero. Number by each curve gives percentage of the $[K^+]_o$ which is normally present in the perfusion fluid. Superposed tracings of records obtained when $[K^+]_o$ had the indicated value. Note effects of $[K^+]_o$ on both resting and action potentials. [After Brady & Woodbury (3).]

Weidmann's findings serve to establish the mode of action of increased $[K^+]_o$ in making cardiac muscle inexcitable. Because P_K is relatively high, a sufficient increase in $[K^+]_o$ decreases $\mathcal{E}$ until the amount of readily available g_{Na} is reduced to a nonregenerative level. Figure 18 shows superimposed recordings of the action potentials of a frog ventricle perfused with Ringer's solutions containing different $[K^+]_o$'s. As $[K^+]_o$ increased the duration of the resting potential and action potential progressively decreased until, at a $[K^+]_o$ three times normal, excitability was lost. Overshoot was progressively, but only moderately, reduced by the increasing $[K^+]_o$ until just before block.

Repolarization

The nature of the ionic conductance changes underlying the prolonged repolarization process in cardiac muscle is the largest outstanding problem in cardiac electrophysiology immediately susceptible to experimental attack. The experimental data available are not sufficient to define uniquely the manner in which g_{Na}, g_K, and g_{Cl} (assuming that Na^+, K^+, and Cl^- carry all the current as shown in fig. 3*B*) vary during repolarization. Although no definite conclusion about the mechanisms involved is possible, a number of attractive concepts can be excluded. Throughout the following discussion it is assumed that the ionic theory, suitably modified, can account for the prolonged action potentials of cardiac muscle. However, the necessary modifications cannot yet be completely specified.

It can be seen in figures 1, 16*A*, 18, 19, 20, 21, 22, and 25 that repolarization in cardiac tissue consists of two or three distinct phases which blend into one another. The first phase is the initial spike, which is always present in Purkinje tissue (fig. 22) but which is not prominent and is sometimes absent in other cardiac tissues. A first phase appears in the frog heart, in reduced $[Na^+]_o$ (fig. 16*A*). The second phase is the prolonged plateau on either side of the minimum slope inflection point. The second phase grades slowly into the third phase of rapid repolarization. This nomenclature was introduced by L. A. Woodbury and co-workers (139) in 1951 and will be used here for descriptive purposes. When all three phases are present, their mid-points are at the successive inflection points of the repolarization process and their boundaries are at the peak of the action potential and at the succeeding points of maximum curvature. It is noteworthy that the third inflection point occurs only about 15 mv above the resting potential in the frog ventricle (cf. fig. 20*C*). Although the shape and duration of the action potential varies considerably among the various cardiac tissues, the three phases are generally present. This fact leads to the assumption that the underlying mechanisms are much the same in all vertebrate hearts, varying only quantitatively from animal to animal. Thus conclusions obtained from experiments on one type of cardiac tissue are considered to be generally applicable to other cardiac tissues.

During the second phase $\dot{\mathcal{E}}$ and hence capacitative current are negligibly small and $\mathcal{E}$ is about twice as close to $\mathcal{E}_{Na}$ as it is to $\frac{1}{2}(\mathcal{E}_{Cl} + \mathcal{E}_K)$ (table 1). Therefore, during this period, g_{Na} must be about twice as great as $g_K + g_{Cl}$. It follows that during repolarization there must be a considerable period when g_{Na} is elevated, $(g_K + g_{Cl})$ is depressed, or both. A teleological argument suggests that g_K probably decreases during the plateau. Such a decrease would reduce considerably the passive exchange of K^+ for Na^+ and thus reduce the load on the Na^+-K^+ pump. This argument does not apply to Cl^- since it is not actively transported and $[Cl^-]_i$ distributes itself so that the average net flux is zero. As mentioned above, $\mathcal{E}_{Cl}$ must be considerably smaller in magnitude than the resting potential in a rhythmically active heart. Thus the effects of Cl^- on the repolarization process are to speed early repolarization when $\mathcal{E} > \mathcal{E}_{Cl}$ and to slow late repolarization when $\mathcal{E} < \mathcal{E}_{Cl}$—the greater g_{Cl}, the greater these effects.

FACTORS AFFECTING REPOLARIZATION. One of the most striking characteristics of cardiac action potentials is the extreme variation of repolarization with the ionic composition of the bathing medium (3, 4, 8, 10, 13, 21, 25, 31, 35, 71, 73, 128, 130), with stimulus rate (4, 10, 117), and with temperature (23, 118, 121) in any one type of cardiac cell. The variation between different cell types and between species is equally striking (figs. 16*A*, 19, 21, 22, and 25). The duration of the action potential in nerve or skeletal muscle varies slightly to moderately with these same changes. As an example, the duration of the action potential (t_{AP}) of a frog ventricular cell varies from about 1.5 sec at low stimulus rates to less than 50 msec at high rates, a ratio of about 30:1.

The effects of variations in $[Na^+]_o$ on t_{AP} are shown in figure 16*A*. As expected from the ionic theory, a decrease in $[Na^+]_o$ reduces the size and duration of the action potential. In the experiments illustrated in figure 16*A*, Na^+ was replaced by

equimolar quantities of choline$^+$. If NaCl was replaced by sucrose, the effects—although in the same direction—were much smaller (4). The differences are probably due both to an appreciable contribution of Cl^- to repolarization and to an increase in g_K resulting from an acetylcholine-like action of the choline on the ventricle. These results further indicate that Na^+ current maintains the plateau. With substitution of choline, t_{AP} is directly proportional to $[Na^+]_o$, projecting to zero at an $[Na^+]_o$ of about 15 per cent of normal (4).

An increase in $[K^+]_o$ shortens t_{AP} because overshoot is reduced and, in frog ventricle, because the rate of third phase repolarization increases (3, cf. fig. 18). The latter change is not found in all tissues [fig. 19; (130)]. It would be expected that, aside from the effects of the reduced $\mathcal{E}_r$, an increase in $[K^+]_o$ would have little effect on early repolarization, since the repolarizing current flows outwardly and should be little affected by $[K^+]_o$ if the independence principle holds. However, the shortening of the action potential is clearly not due entirely to a reduction in overshoot. Weidmann (130, 131) found that a slug of K^+ injected into the coronary circulation of a turtle ventricle during the plateau phase produced early repolarization (fig. 19), indicating a direct effect of K^+ on membrane properties. He suggested three possible mechanisms of this action: *1*) The high $[K^+]_o$ increases the rate of Na^+ pumping; this explanation seems unlikely, since the pump is probably neutral. *2*) The g_K depends directly on $[K^+]_o$; this possibility is supported by the increase in repolarization rate with $[K^+]_o$ in frog ventricle (fig. 18) and the radioactive potassium studies of Carmeliet (9), but is contradicted by the slower repolarization rate of the action potential shortened by a slug of K^+ (fig. 19). *3*) An increase in $[K^+]_o$ decreases g_{Na}; a decreased g_{Na} would explain the records in figure 19 but not those in figure 18. Another possibility is that g_{Cl} depends on $[K^+]_o$ but recent experiments (8, 73) indicate that Cl^- carries about 20 per cent of the repolarizing current. Thus no definite explanation of the effects of $[K^+]_o$ on the repolarization can be selected; and it is quite possible that all cardiac tissues do not react to K^+ in the same manner.

The large effects of the interval between two successive stimuli on the duration and the near lack of effects on the shape of the action potential are shown in figure 20. Action potentials evoked successively later, during and after repolarization, have progressively greater amplitudes and durations,

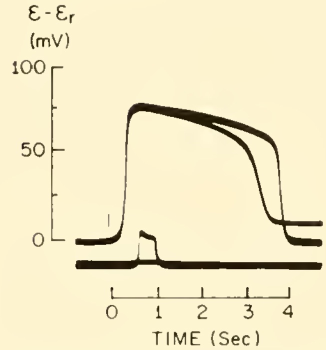

FIG. 19. Shortening of the cardiac action potential brought about by suddenly raising $[K^+]_o$ during the plateau. Preparation was tortoise ventricle perfused via the coronaries. The longer action potential is a control, evoked by a stimulus given at zero time. The shorter action potential, also evoked, was recorded when a "slug" of high $[K^+]$ solution was added to the perfusion fluid at the time indicated by the pulse in the lower record. Note that increased $[K^+]_o$ has a repolarizing action during the plateau and a depolarizing action at rest. Ordinate: change in transmembrane potential ($\mathcal{E} - \mathcal{E}_r$) in millivolts; abscissa: time after stimulus in seconds [After Weidmann (131).]

but the duration is still shorter than normal long after the threshold returns to normal. Carmeliet & Lacquet (10) have shown that, when stimuli are applied rhythmically to frog ventricle, the relationship between t_{AP} and the stimulus interval (t_s) is accurately exponential, the time constant of recovery of duration being just over 1 sec. This behavior has survival value since it provides that the diastolic and systolic periods be shortened or lengthened together, thus insuring appropriate emptying and filling times. This shortening is a characteristic property of cardiac muscle and explanation of it must be included in any hypothesis of repolarization. The t_{AP},t_s relationship arises from time dependent processes. In fact its behavior is quite similar to the activation-inactivation process for g_{Na} on a slow time scale.

SUPERIMPOSABILITY OF ACTION POTENTIALS. Brady & Woodbury (4) have pointed out an interesting characteristic of the action potentials evoked at different stimulus rates: their third phases can be superimposed by shifting them in time. This phenomenon is illustrated in figure 20*B*, where the action potentials (1 to 5) of figure 20*A* have been shifted in time so that their third phases coincide. The third phases superimpose quite well except that AP 1 is steeper than the others just before repolarization is completed. The variation between the second phases of the shortened action potentials is scarcely more than the variations of the control action potentials in figure 20*A*.

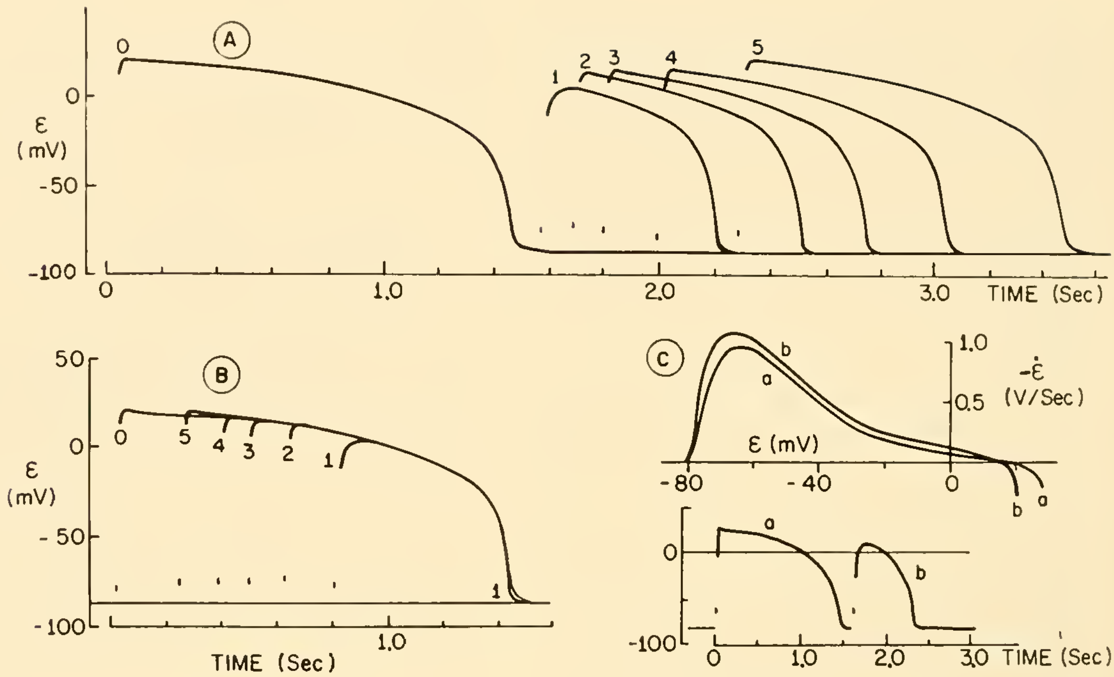

FIG. 20. Superimposability of cardiac action potentials. All potentials were recorded with an intracellular electrode from a perfused frog ventricle. *A:* effect of stimulus interval on duration of AP. Five superposed tracings, each consisting of a control, labeled 0, and other AP evoked at a particular interval after 0, labeled 1, 2, 3, 4, or 5. Vertical marks just above base line indicate the time of the second stimulus. Line 0 consists of five superimposed control tracings; the variation among the controls was about the width of the line. *B:* AP's 1 to 5 of part *A* shifted in time so that their most rapidly falling phases coincide. All the records superimpose throughout their period of overlap except that the shortest one (1) has a faster rate of repolarization for $\mathcal{E}$'s near $\mathcal{E}_r$. The early difference between 0 and 5 is little more than the variation between successive 0's. *C:* critical test of superimposability. Lower tracing shows transmembrane potential of another cell in the same ventricle as a function of time. The upper tracings show data of the same two action potentials but in this case the negative of the rate of repolarization ($-\dot{\mathcal{E}}$) is plotted as a function of $\mathcal{E}$. The two records are of the same shape but the $\dot{\mathcal{E}}$ of the *b* AP is about 20% greater than that of *a* for all $\mathcal{E}$'s. (Woodbury & Kirk, unpublished data.)

Figure 20*C* illustrates a much more sensitive test of superimposability. The lower record shows two successively evoked action potentials, the second being much shorter than the first. The upper record shows the negative of the slope of the action potential, $-\dot{\mathcal{E}}$ plotted against $\mathcal{E}$, i.e., an $-\dot{\mathcal{E}},\mathcal{E}$ diagram for the two potentials. The two curves are almost identical in shape, but the shorter one (*b*) is about 15 per cent steeper than the longer (*a*) at all $\mathcal{E}$'s. There is not this much difference in slopes between long and short action potentials in all records; rather, the figure represents the maximum deviation ordinarily seen.

The records in figure 20 indicate that, regardless of t_{AP}, repolarization is relatively stereotyped in that the sequence of events during the third phase is fixed. This fixed behavior could result if ionic conductances vary with voltage in an appropriate manner. Thus the t_s, t_{AP} relationship possibly results from largely time-dependent conductance changes during the second phase and superimposability from largely voltage-dependent conductance changes in the third phase. This latter possibility is much less attractive when examined in the light of the effects of applied currents on membrane potentials.

SLOPE CONDUCTANCE DURING REPOLARIZATION. In 1951, Weidmann (125) estimated the slope conductance of the membrane during the action potential of ungulate Purkinje cells. He polarized the membrane by flowing a current pulse several time-constants long and of strength I_s through one intracellular electrode and measured the resultant changes in membrane voltage ($\Delta\mathcal{E}$) at the end of the pulse with an adjacent intracellular electrode. I_s does not flow through the membrane with constant density

because of the cable properties of the fiber. The $\Delta\mathcal{E}$ that would be produced by a constant current density (I_m) can be calculated; $I_m/\Delta\mathcal{E}$ is proportional to $(I_s/\Delta\mathcal{E})^2$ (125). $I_m/\Delta\mathcal{E}$ is an experimental approximation of $\partial I_m/\partial\mathcal{E}$ at $I_m = 0$, a quantity closely related to the total slope conductance (G) at $I_m = 0$. G is defined as $\partial I_i/\partial\mathcal{E}$. The partial differentiation indicates that time is held constant. Since Weidmann's results have been widely quoted and nearly as widely misinterpreted, it must be emphasized that slope conductance, $G = \partial I_i/\partial\mathcal{E}$, is not the same as chord conductance, $g_S = I_S/(\mathcal{E} - \mathcal{E}_S)$. Slope and chord conductances have been repeatedly equated in the literature (e.g., 3, 68, 106) even though Hodgkin and Huxley carefully distinguished between the two when defining the chord conductances g_{Na} and g_K [(57, p. 461); see also (14; 15; 19, appendix A)].

The effects of current flow on $\mathcal{E}$ are illustrated in figure 21 and Weidmann's results in figure 22. To obtain the records in figure 21, the current was

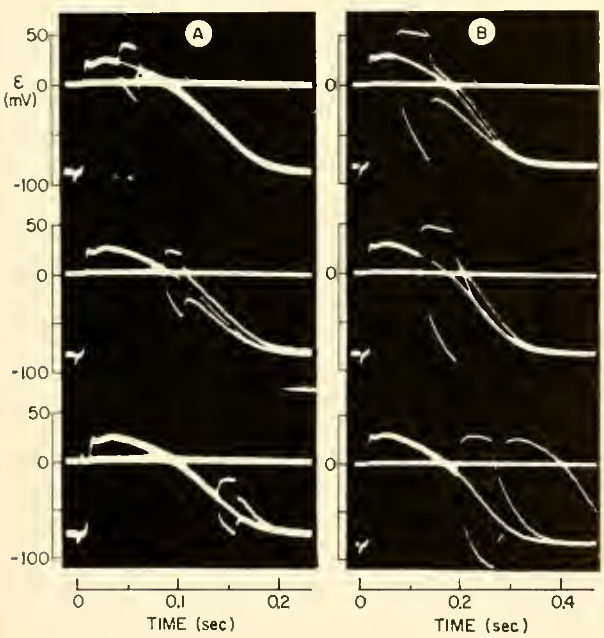

FIG. 21. Effects of polarizing current pulses on the transmembrane potentials ($\mathcal{E}$) of dog or cat papillary muscle cells. The currents were applied through several external electrodes inside a tightly fitting tube into which a length of the muscle was drawn. Transmembrane potentials were measured just outside the tube with two microelectrodes, one inside and one just outside the cell. *A*: effects of small, 20 msec depolarizing and hyperpolarizing currents applied at various times throughout the action potential. *B*: effects of large, 70 msec polarizing currents. Post-hyperpolarization excitation occurs in the lowest record. Note that in both *A* and *B* the potential changes produced by current flow are concave toward the zero current potential curve. [From Cranefield & Hoffmann (28).]

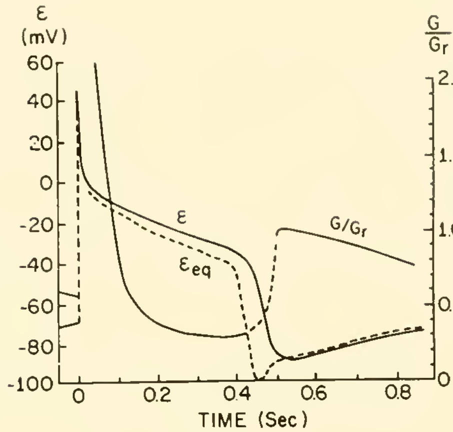

FIG. 22. Transmembrane potential ($\mathcal{E}$), relative slope conductance (G/G_r) and stable equilibrium potential ($\mathcal{E}_{eq}$) during one cycle of a spontaneously beating excised Purkinje strand. $\mathcal{E}$ was measured with an intracellular electrode; G/G_r was estimated from the potential changes produced at the recording electrode by current pulses applied via a nearby intracellular electrode. These curves are after Weidmann (129). $\mathcal{E}_{eq} = \mathcal{E} + (C_m/G)\dot{\mathcal{E}}$ was calculated from values of $\mathcal{E}$ and G/G_r graphed here and values of G_r and C_m obtained by Weidmann (126).

applied by extracellular electrodes. Although the resultant changes in $\mathcal{E}$ cannot be quantitated in terms of slope conductances, these changes do serve to characterize the membrane during activity. In figure 21*A* the current pulse was 20 msec long and the final change in $\mathcal{E}$ was 20 mv or more; in figure 21*B* the current was stronger and lasted 70 msec. Four aspects of the records in figure 21 should be mentioned. *a*) Equal currents change $\mathcal{E}$ by about the same amount at all times during repolarization. *b*) Depolarizing pulses change $\mathcal{E}$ less than equal hyperpolarizing pulses—i.e., the membrane is a rectifier which has less resistance to outward than to inward current flow. Hutter & Noble (75) found the opposite rectification in cells in Na^+-free media. *c*) The curve of $\mathcal{E}$ in time during current flow is always concave toward the $\mathcal{E}$ when no current is flowing—i.e., $\Delta\mathcal{E}$ is of the form $(1 - e^{-t/T})$ rather than $e^{t/T}$. There is one exception, the inflection in $\mathcal{E}$ following the break of current in the lower record in figure 21*A*. *d*) Statement *c* is true even for hyperpolarizations which carry $\mathcal{E}$ more negative than $\mathcal{E}_r$ (lower record in fig. 21*A* and lower two records in fig. 21*B*).

Weidmann's results were similar to those shown in figure 21, but the current was applied through an intracellular electrode so that membrane slope conductance could be estimated. Figure 22 shows $\mathcal{E}$ and G plotted as functions of time throughout a single cardiac cycle. G reaches a high value during

depolarization and then falls rapidly. It reaches its resting level, maximum diastolic conductance (G_r), in less than 100 msec and decreases to its minimum level, 0.3 G_r, just before the onset of rapid repolarization at 400 msec. During the third phase, G increases rapidly to G_r. During the slow diastolic depolarization G falls with $\mathcal{E}$. If the distinction between slope and chord conductance is kept in mind, the results shown in figures 21 and 22 severely limit the possible mechanisms of repolarization. Because of the confusion in the literature and the apparent stringency of the limitations imposed by Weidmann's data, the relationships between chord and slope conductances will be discussed further.

SLOPE AND CHORD CONDUCTANCES. The relationship between G (slope) and g (chord) conductances can be obtained by writing I_i as the sum of the individual ionic currents, writing each ionic current as the product of a chord conductance and the corresponding driving force (equation 8), and then differentiating with respect to $\mathcal{E}$. The equation for I_i is

$$I_i = g_{Na}(\mathcal{E} - \mathcal{E}_{Na}) + g_K(\mathcal{E} - \mathcal{E}_K) + g_{Cl}(\mathcal{E} - \mathcal{E}_{Cl}) \qquad (13)$$

It will be assumed that g_{Cl} is constant throughout the action potential and that g_{Na} and g_K are functions of time and voltage, possibly of the same type as in squid axons. Differentiating equation 13 with respect to $\mathcal{E}$, holding time fixed gives

$$G = \partial I_i/\partial \mathcal{E} = g_{Na} + (\mathcal{E} - \mathcal{E}_{Na})\frac{\partial g_{Na}}{\partial \mathcal{E}} + g_K + (\mathcal{E} - \mathcal{E}_K)\frac{\partial g_K}{\partial \mathcal{E}} + g_{Cl} \qquad (14)$$

Thus, generally speaking, the relationship between g and G is not simple and it is difficult to draw any unequivocal conclusions about chord conductance from measurements of slope conductance. In parallel with the definition of specific ionic chord conductance, a specific ionic slope conductance can be defined e.g., the slope conductance for Na^+ is $G_{Na} = g_{Na} + (\mathcal{E} - \mathcal{E}_{Na})\partial g_{Na}/\partial \mathcal{E}$. G_{Na} is equal to g_{Na} only if g_{Na} does not vary with $\mathcal{E}$.

There is one further complication in estimating G from experimental data. Part of the applied current may flow through the membrane capacitor even after the "transient" is "over" i.e., $\dot{\mathcal{E}}$ may be altered by an applied current. The necessary correction can be obtained by differentiating $I_m = I_i + C_m\dot{\mathcal{E}}$; equation 7a, c, with respect to $\mathcal{E}$.

$$\frac{\partial I_m}{\partial \mathcal{E}} = \frac{\partial I_i}{\partial \mathcal{E}} + C_m\frac{\partial \dot{\mathcal{E}}}{\partial \mathcal{E}} \quad \text{or} \quad G = \frac{\partial I_m}{\partial \mathcal{E}} - C_m\frac{\partial \dot{\mathcal{E}}}{\partial \mathcal{E}} \qquad (15)$$

Both terms on the right hand side of the expression for G can be measured experimentally and thus G can be calculated. The need for this type of correction is apparent in figure 21*A*. For depolarizing pulses it is intuitively apparent that the "transient" is over before the pulse is ended. Nevertheless, the final slope is considerably less than the corresponding slope at the same time in the zero current record. The difference between these two slopes ($\Delta\dot{\mathcal{E}}$), divided by the difference between the corresponding voltages ($\Delta\mathcal{E}$), is an approximation to $\partial\dot{\mathcal{E}}/\partial\mathcal{E}$. The situation is worse for hyperpolarizing pulses; here the "transient" is persisting even at the end of the pulse and calculation of G from the final $\Delta\mathcal{E}$ without using the correction indicated by equation 15 is inaccurate. However, it should be noted that estimates of G based on measurements made with two intracellular microelectrodes are subject to large errors. The corrections for the cable properties of the tissue are quite large and uncertain, particularly since the correction depends importantly on the space constant (66, 112, 122) which, in turn, depends on the membrane conductance. Nevertheless, the large corrections do not obscure the direction of the changes in G during repolarization.

The foregoing discussion shows why the long current pulse method gives an estimate of total G rather than total g. The change in $\mathcal{E}$ is measured a considerable time after the application of the current. If the voltage-dependent conductance changes in the heart are like those in the squid axon in requiring time to reach completion, the final $\mathcal{E}$ is reached only after the g changes are "completed." Since the change in $\mathcal{E}$ persists long enough to change g (if it is voltage sensitive), G rather than g is measured (19).

Weidmann's estimates of slope conductances were not corrected for the capacitative component nor can such a correction be made from his published record, which shows the superposed effects of 20 unsynchronized current pulses. However, measurements on the data obtained by I. Tanaka (111) and Cranefield & Hoffman (28, cf. fig. 21) indicate that the capacitative term is of the order of 10 to 20 per cent of the conductive term and thus is well within the limits of error of the measurements. It will be assumed, therefore, that Weidmann's results are indicative of G, but the rectifying properties of the membrane should be kept in mind.

The fall in G below its beginning diastolic value (G_r) during the plateau (fig. 22) has been interpreted to indicate that the total membrane chord conductance, $g = g_{Na} + g_K + g_{Cl}$, falls below its diastolic value (g_r). The following arguments show how this interpretation may be fallacious. The simultaneous changes in $\mathcal{E}$ and G during the slow diastolic depolarization suggest a fall in g_K. If this drop in g_K is a concomitant of the decrease in $\mathcal{E}$ (depolarization) rather than of the passage of time, then $\partial g_K/\partial\mathcal{E}$ is negative rather than zero. There is conflicting opinion on this point. Dudel & Trautwein (37) adduce powerful evidence that the slow diastolic decrease in G is due entirely to a fall in G_K. They conclude, however, that the slow depolarization results from a slow, time-dependent drop in G_K—i.e., slow depolarization is a positive afterpotential similar to that of squid axon. Shanes (106) postulates the occurrence of time-dependent changes in g_K throughout the cardiac cycle. On the other hand, Hutter & Noble (75) have found about the same relationship between $\mathcal{E}$ and G by varying $\mathcal{E}$ with an applied current in Na^+-free media as was found by Dudel and Trautwein during diastolic depolarization. It seems more likely, therefore, that the fall in G results from the decrease in $\mathcal{E}$ rather than vice versa. A further indication that g_K depends on $\mathcal{E}$ is Tanaka's (111) finding of a constant G during diastole in nonspontaneous toad atrial tissue. Thus, it is not unreasonable to suppose that $\partial g_K/\partial\mathcal{E} < 0$ at least in the neighborhood of $\mathcal{E}_r$ and, since $\mathcal{E} - \mathcal{E}_K$ is always positive, $G_K < g_K$. Similarly, depolarization increases g_{Na}; hence, $\partial g_{Na}/\partial\mathcal{E} > 0$ but $\mathcal{E} - \mathcal{E}_{Na} < 0$ so that $G_{Na} < g_{Na}$. Consequently, finding a G less than G_r during the plateau does not justify the conclusion that g is less than g_r.

SLOPE CONDUCTANCE AND CURRENT, VOLTAGE RELATIONSHIPS. Some further idea of the physical significance of slope conductance can be obtained by studying figure 23. The curve labeled $I_m = 0$ (fig. 23A) is a hypothetical relationship between I_i and $\mathcal{E}$ in the heart at a particular instant during the action potential. Voltage-clamp experiments would be the most accurate way for obtaining the actual curves. Figure 6 consists of such curves from squid axon, obtained shortly and considerably after a sudden depolarization. The $I_i,\mathcal{E}$ curve shifts continuously in time from the early curve to the late one. Another way to get an $I_i,\mathcal{E}$ curve would be to apply currents of different strengths to a cell at a fixed time during the action potential and calculate I_i by subtracting $C_m\dot{\mathcal{E}}$ from the applied current, I_m. Membrane slope conductance at any time and at any membrane voltage is defined as the slope of the $I_i,\mathcal{E}$ curve. The G, measured at various times throughout repolarization, is for $I_m \simeq 0$ (cf. 4); consequently, $I_i = -C_m\dot{\mathcal{E}}$. Since conductances are presumably changing with time and voltage, each measurement of G at $I_m = 0$ gives the slope of an $I_i,\mathcal{E}$ curve at one time and one voltage.

If the membrane voltage were set to some particular voltage, say $\mathcal{E}_1$ (fig. 23A), and then unclamped, an ionic current (I_1) would have to flow through the membrane. Since the external current has been reduced to zero, all the ionic current must go to charge the membrane capacitor; hence $\mathcal{E}$ begins to change. Since $I_i = -C_m\dot{\mathcal{E}}$, the positive current ($I_1$) will steadily decrease $\mathcal{E}$. If the $I_i,\mathcal{E}$ curve does not change with time, this process will proceed at a continually slowing rate and finally cease when I_i reaches zero at $\mathcal{E}_o$. The ($\mathcal{E}$, I_i) point describing the membrane at each instant will traverse the $I_i,\mathcal{E}$ curve from ($\mathcal{E}_1$, I_1) to ($\mathcal{E}_o$, 0). The point ($\mathcal{E}_o$, 0) is a stable equilibrium point, since displacement of the voltage from $\mathcal{E}_o$ creates a current which tends to restore the voltage to $\mathcal{E}_o$. The slope of the curve is positive, so G is positive in the region of a stable equilibrium point. The voltage-time curve is of the form of e^{-tG/C_m} as $\mathcal{E}$ approaches $\mathcal{E}_o$, showing that $\dot{\mathcal{E}}$ also decreases with time.

On the other hand $\mathcal{E}_3$ is an unstable equilibrium voltage. Although $I_i = 0$ at this point, any displacement from it would be regeneratively magnified and the voltage would quickly change until either point ($\mathcal{E}_4$, 0) or point ($\mathcal{E}_o$, 0) was reached—i.e., if for any reason the voltage decreased, an outward ionic current would develop which would additionally decrease the voltage. Thus if the I_i, $\mathcal{E}$ curve crosses zero with a negative slope, the zero current voltage is an unstable equilibrium. An unstable equilibrium voltage is the same as a threshold voltage. If the $I_i,\mathcal{E}$ curve has a negative slope but does not pass through zero (curve $I_m = 2I_m'$ in fig. 23A) no threshold is involved, but the voltage-time curve has the same form (e^{tG/C_m}) in either case. Consequently, in regions where $G < 0$, $|\dot{\mathcal{E}}|$ is increasing with time, i.e., $|\ddot{\mathcal{E}}| > 0$.

In the absence of external current, I_i can be replaced by $-C\dot{\mathcal{E}}$ on the $I_i,\mathcal{E}$ diagram. On a $-C_m\dot{\mathcal{E}},\mathcal{E}$ diagram the application of a constant negative (hyperpolarizing) current to the membrane immediately changes $-\dot{\mathcal{E}}$ by the amount I_m/C_m, since all current initially must flow through C_m. If the

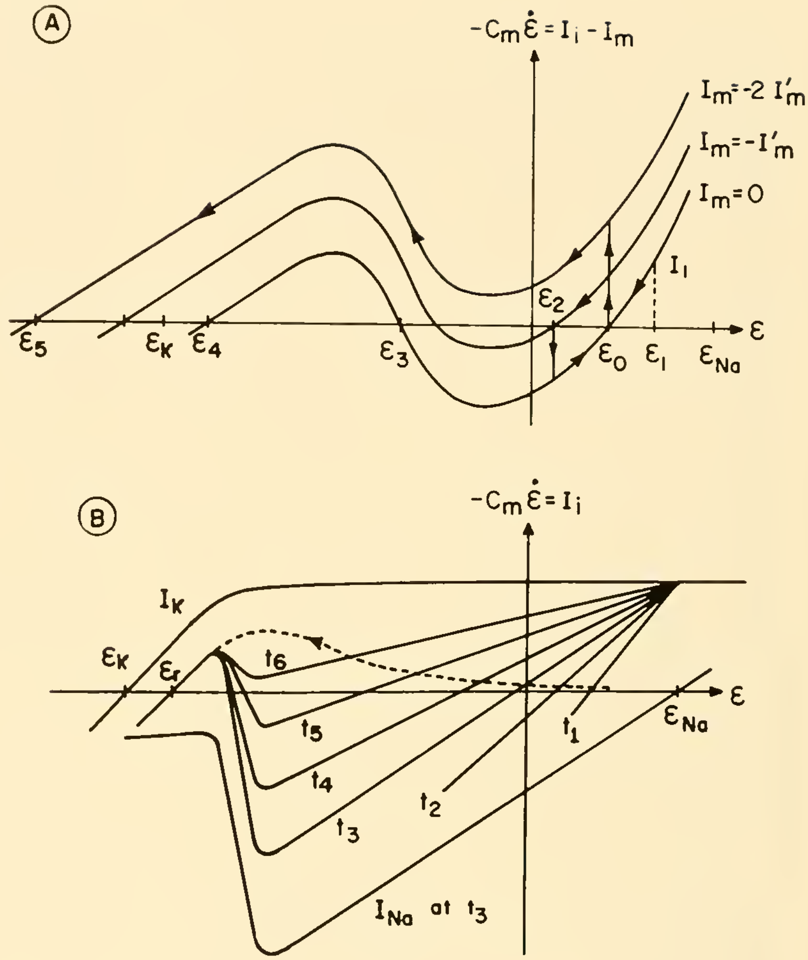

FIG. 23. Hypothetical current, potential relationships of a cell membrane at one instant in time. Ordinate: negative of capacitative membrane current, $-C_m\dot{\mathcal{E}} = I_i - I_m$. Abscissa: transmembrane voltage ($\mathcal{E}$). *A*: $-\dot{\mathcal{E}},\mathcal{E}$ curves for three values of the externally applied current (I_m). This current shifts the curve in the vertical direction. Arrows show the movements of the point ($\dot{\mathcal{E}},\mathcal{E}$) in time under various circumstances. (See text for explanation.) *B*: hypothetical $I_i,\mathcal{E}$ curves for the repolarization process in frog ventricular cells with $I_m = 0$. I_K is the curve of K^+ current, assumed unchanging in time. The $I_{Na},\mathcal{E}$ curve has the same shape at all times but its amplitude at any $\mathcal{E}$ is decreasing exponentially in time. The $I_{Na},\mathcal{E}$ curve is drawn for the instant $t = t_3$. The curves marked $t_1, t_2, \ldots, t_6$ show I_i for successively later times. Dashed line shows motion of the $\dot{\mathcal{E}},\mathcal{E}$ point. It is drawn with the same shape as the actual $\dot{\mathcal{E}},\mathcal{E}$ curve of fig. 20*C*. (See ext for explanation.)

applied current has no direct immediate effect on the membrane conductances—a not completely safe assumption (106)—the $I_i,\mathcal{E}$ curve is not altered and the $-C\dot{\mathcal{E}},\mathcal{E}$ curve is shifted vertically. The two upper curves in figure 23*A* are for two different applied currents, $-I'_m$ and $-2I'_m$. If $\mathcal{E} = \mathcal{E}_0$ before the application of $-I'_m$, the point on the $-C_m\dot{\mathcal{E}},\mathcal{E}$ plane describing $\mathcal{E}$ and $\dot{\mathcal{E}}$ of the membrane will immediately jump vertically to the $I_m = -I'_m$ curve. Thereafter, $\mathcal{E}$ will decrease toward a stable equilibrium point ($\mathcal{E}_2$) as shown by the arrows. If the current is turned off, the slope reverses in sign and the membrane will then depolarize back to $\mathcal{E}_0$. On the other hand, if $-2I'_m$ is applied, the point of minimum current rises above the zero current axis and repolarization proceeds all the way to $\mathcal{E}_5$. The repolarization rate would be rapid at first, decline to a minimum, increase to a maximum and, finally, decrease to zero at $\mathcal{E}_5$. This repolarization process has two inflection points—one at a point of minimum slope and one at a point of maximum slope—and is thus similar in shape to repolarization in the heart. The range of $\mathcal{E}$ wherein $\dot{\mathcal{E}}$ is increasing corresponds to the region of negative G. If a sudden small change in applied current is made during the repolarization from $\mathcal{E}_0$ with $-2I'_m$ flowing, $\dot{\mathcal{E}}$ would be changed in magnitude but not in sign. FitzHugh (40) has discussed the Hodgkin-Huxley nerve equations in terms of their behavior on various phase planes (e.g., $m,\mathcal{E}$; $I,\mathcal{E}$). References to the mathematical literature and a clear discussion of the usefulness of the phase plane method can be found in his paper.

POSSIBLE MECHANISMS OF REPOLARIZATION. The process of repolarization can be profitably discussed in terms of $-\dot{\mathcal{E}},\mathcal{E}$ diagrams (cf. fig. 23). For this purpose it is useful to describe the repolarization process by a family of $I_i,\mathcal{E}$ curves at different times and to determine how these vary with stimulus rate and external ion concentrations. At present no such family of curves can be specified, but certain types of curves can be excluded. The most evident $I_i,\mathcal{E}$ curve

that might be used to explain repolarization is the upper record in figure 20*C*, where $-\dot{\mathcal{E}}$ is plotted against $\mathcal{E}$ for two normal repolarizations of different durations. For $-\dot{\mathcal{E}} > 0$, these curves have the same form as the curve labeled $I_m = 2I_m'$ in figure 23*A*. The action potential would be "explained" by assuming that the $I_i,\mathcal{E}$ curve is initially like the one for squid axons at short times (fig. 7), changes rapidly at the peak of the action potential to one like figure 23*A* ($I_m = -2I_m'$) or figure 20 and remains in this form. Repolarization would then proceed along this fixed $I_i,\mathcal{E}$ curve and hence would have the correct shape. Aside from the difficulty in explaining the t_s,t_{AP} relationship from these assumptions, the fact that G measured experimentally is always positive whereas these $I_i,\mathcal{E}$ curves contain a region of negative slope rules them out. Also, a depolarizing current strong enough to change the sign of $\dot{\mathcal{E}}$ (i.e., no larger than the currents used in fig. 21*A*) would shift the $I_i,\mathcal{E}$ curve downward so that it would cross the $\mathcal{E}$ axis (i.e., as the $I_m = 0$ curve at $\mathcal{E}_o$ does in fig. 23*A*). The voltage then would approach an equilibrium value and stay there for the duration of the current. Maintained depolarizing currents prolong repolarization but not indefinitely (28).

Repolarization in squid axon is somewhat like the process described above. The $I_i,\mathcal{E}$ curve during depolarization is the early time curve in figure 7 which has two stable and one unstable equilibrium points. The system transits from the resting stable equilibrium to the active stable equilibrium when an applied current from an external source or an adjacent active area depolarizes the membrane to the unstable equilibrium or threshold point. Once threshold is reached, $\mathcal{E}$ accelerates toward the active stable point (m and $\mathcal{E}$ interacting regeneratively). However, as the active stable point is approached, g_{Na} starts to decrease owing to inactivation and g_K begins to increase, slowly at first and then more rapidly (fig. 15). These two changes act to move the unstable and the active stable points toward each other, $\mathcal{E}$ following the latter quite closely. Eventually, these points meet and vanish, leaving only one stable point which is near $\mathcal{E}_K$ (long-time curve fig. 7) but remote from $\mathcal{E}$. Repolarization then rapidly ensues along a path relatively unchanging in time. [See FitzHugh (40) for a more accurate and detailed description.]

These considerations suggest that the slow repolarization rate of heart results from a slow movement of an equilibrium point ($\mathcal{E}_{eq}$), which is stable since G is always positive (fig. 22) and that the speed of this movement gradually increases as repolarization proceeds. In the second phase when $\dot{\mathcal{E}}$ is small, $\mathcal{E}$ should be only a few millivolts more positive than $\mathcal{E}_{eq}$. If there were no membrane capacity, $\mathcal{E}$ would always equal $\mathcal{E}_{eq}$. Since there actually is capacity, $\mathcal{E}$, in FitzHugh's picturesque words (40), "pursues" $\mathcal{E}_{eq}$ as it changes slowly in time. To a first approximation, $\mathcal{E}$ is sufficiently more positive than $\mathcal{E}_{eq}$ to make I_i just large enough to charge the membrane capacitor, so that $\dot{\mathcal{E}} = \dot{\mathcal{E}}_{eq}$, i.e., $I_i = -C_m\dot{\mathcal{E}} = -C_m\dot{\mathcal{E}}_{eq}$ (fig. 23*B*). A more exact relationship between $\mathcal{E}$ and $\mathcal{E}_{eq}$ follows from the definition of G. Over a small range of $\mathcal{E}$ around $\mathcal{E}_{eq}$, $I_i = G(\mathcal{E} - \mathcal{E}_{eq}) = -C_m\dot{\mathcal{E}}$; therefore, $\mathcal{E}_{eq} = \mathcal{E} + C_m\dot{\mathcal{E}}/G$. Weidmann's experiments on Purkinje fibers (125, 126) furnish estimates of G, C_m, and $\mathcal{E}$ as functions of time throughout repolarization so that $\mathcal{E}_{eq}$ can be calculated approximately. The results of such an estimation of $\mathcal{E}_{eq}$ are plotted in figure 22 along with $\mathcal{E}$ and G/G_r as a function of time. Aside from the approximation involved in assuming G is constant over the large voltage range involved, the values of $\mathcal{E}_{eq}$ are not accurate because the graphical estimates of $\dot{\mathcal{E}}$ and G at any time during the third phase are subject to considerable error. Nevertheless, the time course of $\mathcal{E}_{eq}$ plotted in figure 22 is reasonable: $\mathcal{E}_{eq}$ stays near $\mathcal{E}$ during the second phase and then drops rapidly but does not jump to the neighborhood of $\mathcal{E}_K$ at the beginning of the third phase. Thereafter $\mathcal{E}$ and $\mathcal{E}_{eq}$ are close to each other until the succeeding depolarization.

The rapid fall in $\mathcal{E}_{eq}$ at the beginning of the third phase suggests even more strongly than does the action potential itself that g_{Na} falls rapidly, or g_K increases rapidly, or both events occur at this voltage or time. There seems little doubt that such conductance changes occur. However, if these changes are assumed to be voltage-dependent as they are in squid axon, a difficulty arises. It has already been shown that g changes of this type (g_{Na} increasing and g_K decreasing with $\mathcal{E}$) have slope conductances less than their respective chord conductances. Further analysis shows that the values of $\partial g/\partial\mathcal{E}$ have to be inordinately small in order to prevent the values of G from becoming negative at some voltages. The values of $\partial g/\partial\mathcal{E}$ required to make $\mathcal{E}_{eq}$ change as rapidly as it does would make total G become negative in this voltage range. There will be an unstable point on the $I_i,\mathcal{E}$ curve until rapid repolarization commences. However, even after the point of instability has disappeared G remains negative. A $G < 0$ is contrary to experiment. There is no sign of regenerative

repolarization in any voltage range in response to small (fig. 21*A*) or large (fig. 21*B*) hyperpolarizing current pulses. Regenerative responses would be indicated by inflections in the voltage-time curves whereas, in the records, these are always concave toward the zero current $\mathcal{E}$ curve.

If the conclusion is correct that there is no threshold for repolarization in the voltage range at the end of the second phase (-20 to -40 mv), most existent hypotheses of repolarization in cardiac muscle (4, 24, 68, 106, 130, 131) are apparently incorrect. The alternative is to suppose that the sudden changes in g at the termination of the plateau are purely time-dependent or only slightly voltage-dependent. Shanes (106) suggests a mechanism of this sort, but it is difficult to envision a mechanism which can rhythmically increase and then decrease g_K but which is not voltage-dependent. Another possibility is to suppose that g's do vary with voltage but so sluggishly that the changes in $\mathcal{E}$ produced by applied currents are too brief to change the g's very much. This possibility is contradicted by Weidmann's finding (125) that sufficiently large hyperpolarizing pulses early in the plateau can initiate an early repolarization. (cf. 28). This repolarization occurs only if $\mathcal{E}$ is maintained more negative than the resting potential for a period of time (cf. fig. 21*B*, where equally large voltage changes scarcely affect repolarization). The fact that maintenance of the voltage around $\mathcal{E}_r$ may markedly alter the ionic current flow after the end of the current pulse indicates that there are voltage-dependent g's at some times and some voltages.

The existence in the heart of a threshold for early repolarization does not contradict the above conclusions about the absence of a threshold at the voltage of the second phase since the actual threshold is more negative than $\mathcal{E}_r$. This "threshold" may be similar to the induced repolarization of squid axon (77) or frog axon (112) where a large repolarizing current may terminate activity early. This abolition response probably can occur when there is only one stable point or when all three equilibrium points are still present. In the former case no threshold is involved; any current would simply accelerate the repolarization process. However, if there are three equilibrium points, the early repolarization would have a threshold current; smaller currents would have little lasting effect on $\mathcal{E}$. The available evidence indicates that there is no true threshold for repolarization in cardiac muscle if $[Ca^{++}]_o$ is normal. One of Weidmann's records (125, fig. 5) shows a current applied at the start of the plateau carrying the voltage below resting value and initiating early repolarization. A current just insufficient to initiate early repolarization activates enough g_{Na} that, on cessation of the current, $\mathcal{E}$ is in a region of negative G and "anodal break" excitation occurs (fig. 21*B*, lower trace). A similar recording (125, fig. 6) shows a threshold at about 45 mv above maximum diastolic potential. However, in these records the current was applied during the middle of the plateau and the recording electrode was 4.2 mm from the current electrode. Hence the voltage change at the current electrode was several times bigger.

Cranefield & Hoffman (28) found that lowering the $[Ca^{++}]_o$ to one-fourth of normal decreased the amount of current required to induce repolarization. In this medium, the voltage-time curve during hyperpolarizing current flow was slightly, but definitely, inflected. This inflection indicates a regenerative process with a threshold for repolarization at about the knee of the normal repolarization curve (28, fig. 10). Weidmann (128) found that raising $[Ca^{++}]_o$ shifted the curve relating $\dot{\mathcal{E}}_d$ to initial voltage (fig. 17) toward zero voltage, i.e., the amount of g_{Na} activation at any particular voltage is increased. These findings accord with Frankenhaeuser & Hodgkin's (45) voltage clamp studies of the effects of $[Ca^{++}]_o$ variations on squid axon. In this study the effects of a rise in $[Ca^{++}]_o$ on the kinetics of g_{Na} changes were almost identical with the effects of hyperpolarization (cf. 77). A reduction in $[Ca^{++}]_o$ has the opposite effects in squid axon and probably in the heart also. It follows that the inactivation attendant on a reduction in $[Ca^{++}]_o$ will reduce the probability of anodal break excitation. Nevertheless, it is difficult on the basis of this information to deduce the mechanisms responsible for the shift from a nonthreshold- to a threshold-type behavior in the early repolarization phenomenon when $[Ca^{++}]_o$ is lowered. One possibility is that a reduction in $[Ca^{++}]_o$ reveals an underlying regenerative repolarization process which is ordinarily counterbalanced by g_{Na} activation.

The abolition of the action potential by hyperpolarization can be explained, but the possibility that this early repolarization may propagate even in normal $[Ca^{++}]_o$ is puzzling (28, 125). The spatial voltage gradient in a propagating early repolarization would be small and there would be little local current flow. If $[Ca^{++}]_o$ is low and there is a threshold, then the process could propagate at a low speed. However, the absence of an energy-yielding threshold or non-

threshold regenerative process at normal $[Ca^{++}]_o$ makes it difficult to understand how decrementless propagation could occur. An explanation of the apparent propagation of early repolarization is suggested by figure 21 (cf. 28, figs. 3 and 4). Following the termination of the hyperpolarizing pulses the $\mathcal{E}$ at which $\dot{\mathcal{E}}$ goes through zero must be $\mathcal{E}_{eq}$ and so small hyperpolarizing pulses can be used to map out the time course of $\mathcal{E}_{eq}$ to the extent that the $\mathcal{E}_{eq}$ at any time is unaffected by $\mathcal{E}$. In figure 21*A* it can be seen that $\mathcal{E}_{eq}$ is near $\mathcal{E}$ in early (top) and late (bottom) repolarization but $\mathcal{E}_{eq}$ is considerably below $\mathcal{E}$ in mid-repolarization (middle record fig. 21*A*, top record 21*B*). This time course for $\mathcal{E}_{eq}$ is similar to the one shown in figure 22. Note that in mid-repolarization hyperpolarization speeds the remainder of the repolarization process. Cranefield & Hoffman (28, fig. 8) obtained records of early repolarization at a distance of 5 mm from the polarizing electrode in which nearly all signs of electrotonic current spread had disappeared. The current flowed during early and middle repolarization. There is no sign of electrotonic spread at 5 mm during the early repolarization where $\mathcal{E}_{eq}$ is near $\mathcal{E}$ but there is some remnant in mid-repolarization where $\mathcal{E}_{eq}$ has fallen considerably below $\mathcal{E}$. Thus it seems conceivable that a large hyperpolarizing current terminating in mid-repolarization could shorten action potentials for a considerable distance because the $\mathcal{E}_{eq}$ is spontaneously moving in the same direction as the current-induced changes in $\mathcal{E}$ and because electrotonic spread is greater during this period due to the reduced slope conductance. As pointed out by Weidmann (125) and Cranefield & Hoffman (28), a 5 mm conduction distance is not great enough to permit a decision between a decrementing and nondecrementing early repolarization. No matter whether early repolarization is propagated or not, the conduction speed of normal repolarization is faster than early repolarization and eventually the latter will disappear.

HYPOTHESES OF REPOLARIZATION. Although Weidmann's (125) discussion of the ionic mechanism of repolarization in cardiac tissue appeared while the Na^+-K^+ theory for squid axons was still being formulated, he considered the possible modifications of the theory which might explain repolarization in heart. He suggested that either a long delay in the inactivation of g_{Na} or a retardation of the rise in g_K following depolarization might be responsible for the long delay in repolarization. He further ventured (125, p. 234) "that one or other of these processes may be entirely absent, or that one or other may occur in two stages." He then concluded that his impedance (slope conductance) data were compatible with a rapid but incomplete inactivation of g_{Na} and a slow rise in g_K, but not with a slow inactivation and a rapid rise in g_K. Despite the difficulties in interpreting slope conductance measurements, this conclusion seems generally valid provided the implied conductance changes are not so voltage-dependent that they give rise to negative G values.

As mentioned above, Weidmann (130) induced early repolarization of turtle ventricle by increasing $[K^+]_o$ during the plateau (fig. 19). On the basis of this finding, he suggested that normal repolarization might result from the accumulation of K^+ outside the fiber during the prolonged depolarization. From rough calculations, he concluded that existence of this mechanism was not likely unless there is a barrier to ionic diffusion lying a short distance outside the excitable membrane. He calculated that $[K^+]_o$ would increase about 0.6 mM during the action potential, but he found that a $[K^+]_o$ of 10 to 30 times normal was required to produce appreciable shortening of the duration. A rise this large during activity would require an interstitial space about 20 to 60 times smaller than the 28 per cent value used by Weidmann. Recent improvements in electron-micrographic histological techniques have shown that cardiac cells are closely packed, the spacing being only a few hundred Angstroms (6, 91, 93, 94, 107, 108). Individual cells are formed into long, thin strands about six cells in diameter. Most of the interstitial space lies between these strands and is occupied by capillaries. Using Weidmann's figures, calculation shows that the interstitial space within the strands is small enough to cause a rise of about 10 mM in $[K^+]_o$ during the action if all K^+ leaving the cells stays in this space. Thus, this mechanism cannot be definitely excluded on histological grounds.

If an increased $[K^+]_o$ is the means of repolarization during a normal action potential, then the sequence of events would be somewhat as follows. Depolarization would lead to an increased efflux of K^+ owing to the increased driving force, provided that g_K either did not decrease too much, remained constant, or increased. This net efflux of K^+ would cause a more or less gradual rise in $[K^+]_o$. In order to induce early repolarization, this increased interstitial $[K^+]$ must increase g_K or g_{Cl} or decrease g_{Na} or any combination of these. An increase in g_{Cl} is an unlikely explanation since repolarization occurs in Cl^--free media (73). Since an increase in $[K^+]_o$ increases g_K in nerve (65) skeletal muscle (47, 55) and cardiac

muscle (9, 75), an increased g_K is the most likely cause of the early repolarization. If it is assumed that P_K is proportional to $[K^+]_o$ and that $\mathcal{E}$ is given by the Goldman equation (equation 6), then the $\mathcal{E},[K^+]_o$ curve has a minimum (most negative) value at an intermediate $[K^+]_o$. Either an increase or decrease of $[K^+]_o$ from this value causes a depolarization. The higher P_{Na} is, the higher the minimum value of $\mathcal{E}$. Thus, during the early plateau, the increasing $[K^+]_o$ could cause repolarization up to the value of $[K^+]_o$ at which $\mathcal{E}$ is minimum. Any further accumulation of K^+ would depolarize. The maximum repolarization would be considerably less negative than $\mathcal{E}_r$ and the remainder of the repolarization process would require the reduction of $[K^+]_o$ to normal. This could be accomplished by enhanced Na^+-K^+ pumping and by diffusion of K^+ into the larger interstitial spaces.

This hypothesis explains the following findings concerning the nature of repolarization. *a*) The conductance changes of repolarization are nonregenerative. *b*) The third phases of action potentials of different lengths are superimposable. *c*) The potential changes produced by large depolarizing currents applied to Purkinje fibers bathed in Na^+-free media tend to fall off after about 100 msec (75).

On the other hand, the following objections can be raised. *a*) At first thought, the t_s,t_{AP} relationship could be explained by assuming that $[K^+]_o$ is slightly above normal immediately following repolarization so that less time would be required for $[K^+]_o$ to reach the same value during an immediately succeeding action potential. However, if this were the case, the conductance immediately following repolarization would be elevated and this does not accord with experiment (111, 125). *b*) Hutter & Noble (75) found that depolarization decreases membrane conductance of Purkinje fibers in Na^+-free media. They also found that increasing $[K^+]_o$ increased conductance and so it appears that depolarization causes at most a small increase in interstitial $[K^+]$. *c*) The time course of $\mathcal{E}_{eq}$ (fig. 22) during the late third phase indicates that $\mathcal{E}_K$ is not greatly different from normal. However, the calculation of $\mathcal{E}_{eq}$ is not accurate enough to give this argument much weight. *d*) Since this repolarization hypothesis requires increased turnover of K^+ and enhanced active K^+ transport, the teleological argument for economical operation makes the hypothesis less likely. *e*) Brady (personal communication, 1960) has recently repeated Weidmann's (130) experiments. He found that $[K^+]_o$ must be raised at least 20 times during the plateau to produce early repolarization in turtle ventricle. The early repolarizing action has a latency of 3 to 4 sec as compared with a latency of about 0.15 sec for a depolarizing action when the high $[K^+]_o$ solution was perfused through the coronaries during diastole. The extremely long latency for induction of early repolarization implies an even more indirect mechanism than an induced change in g_K.

Hoffman & Cranefield (68) have advocated the hypothesis that g_K is inversely proportional to the driving force on K^+ as an explanation of repolarization—i.e., depolarization decreases g_K. This, however, is a regenerative system and hence must be discounted on the basis of present evidence. Shanes (106) suggests that the inward movements of Na^+ and the outward movements of K^+ interact when the two fluxes are of the same order of magnitude. For example, such interaction could occur if Na^+ and K^+ moved through the membrane in file in the same pores (65). This ingenious mechanism is a concrete model whereby an increase in $[K^+]_o$ could lead to a decrease in g_{Na}. Such a decrease in g_{Na} could account for the early repolarization induced by an increase of $[K^+]_o$ during the plateau. Shanes also suggests that g_K decreases continuously throughout the slow diastolic depolarization, the succeeding rapid upstroke of the action potential and the plateau phase, and then increases rapidly at the time of rapid repolarization. He does not specify if these changes in g_K are dependent on time, voltage, or both. If they are voltage-dependent, the third phase is regenerative and thus suspect. If they are time-dependent, the factors that make g_K oscillate in time in this manner are not clear.

Coraboeuf *et al.* (24) have measured G during the action potential of the guinea pig ventricle. Their results are closely similar to Weidmann's observations (125) on Purkinje fibers except that $G > G_r$ during the action potential. Coraboeuf and his co-workers suggested three possible mechanisms of repolarization. The most intriguing one, attributed to Hodgkin, is that K^+ can use the Na^+ channels to a limited extent and so g_{Na} and g_K, initially high, fall simultaneously, the voltage staying constant as long as g_K is much larger than its resting value. As inactivation proceeds, g_{Na} and g_K would fall in parallel until g_K approaches its resting level. Thereafter g_K g_{Na} would rise rapidly and cause a rapid repolarization which would be aided by a voltage-dependent regenerative decrease in the remaining g_{Na} and slowed by a similar decrease in g_K. It appears that this ingenious scheme suffers from the usual defect that G goes negative during fast repolarization.

Brady & Woodbury (4) have recently proposed a

hypothesis of the repolarization process in frog ventricle quite similar to Weidmann's suggestions (125) and the hypotheses of Shanes (106) and Coraboeuf *et al.* (24), but the consequences of the hypothesis have been examined in considerably greater detail. As in other hypotheses, rapid repolarization is regenerative in this model. Despite this failure it easily integrates a number of experimental observations. Since the model was analyzed in some detail, it is perhaps worth presenting to demonstrate the nature of the phenomena which give rise to negative G's. In accord with Weidmann (125), the starting point for the hypothesis was the Hodgkin-Huxley Na^+-K^+ theory and an effort was made to explain repolarization in the heart with a minimal number of additional postulates concerning the underlying changes in conductance.

The postulates are as follows: *1*) Inactivation and activation of g_{Na} are described by two time-constants, one short and one long. More precisely, in heart the equation describing h as a function of time should be written: $\dot{h}_f = \alpha_f(1 - h_f) - \beta_f h_f$ and $\dot{h}_s = \alpha_s(1 - h_s) - \beta_s h$, where $h = h_f + h_s$ (compare with equation 9). The rate constants α_f, β_f are large so that the h_f reaction is fast, being completed in a matter of milliseconds, whereas the h_s reaction takes seconds to reach completion. More simply, there are fast and slow components of inactivation and activation in the heart instead of only a fast component as in the squid axon. This postulate is a simple explanation for the t_{AP}-t_s relationship. *2*) The kinetics of g_K change are about the same as in squid except that depolarization decreases g_K instead of increasing it; also, the changes occur somewhat more slowly than in squid axons. This mechanism would reduce Na^+-K^+ interchange during activity and could account for the double peak of the action potential seen frequently in papillary muscle from dogs and cats (fig. 21), and occasionally in frog ventricle. The principal reason for this postulate is derived from Hodgkin & Horowicz' (55) recent investigations concerning the nature of anomalous rectification in skeletal muscle. In this tissue, depolarization reduces g_K tremendously, i.e., outflux of K^+ is reduced. The functional significance of this anomalous rectification in skeletal muscle is not known, but such behavior in cardiac muscle, which is depolarized about half the time, would be efficient. Hutter & Noble (75) have recently found evidence for anomalous rectification in heart. A subsidiary assumption that g_{Cl} remains constant throughout activity is likely true, but is made here entirely for convenience.

On the basis of these assumptions, the events during a frog ventricular action potential would be as follows: After a threshold depolarization, g_{Na} and $\mathcal{E}$ increase regeneratively. However, because of fast inactivation and the relatively slow depolarization rate, g_{Na} reaches its peak value considerably before the peak of the action potential and has declined to about four times g_K plus g_{Cl} at the peak (4, 80). In Purkinje cells the initial spike on the action potential is clearly attributable to a higher peak g_{Na} with a consequent faster rate of rise and closer approach of $\mathcal{E}$ to $\mathcal{E}_{Na}$. The "reason" for this behavior in Purkinje fibers evidently is to increase conduction velocity. At the start of the plateau, fast inactivation is nearly complete and g_K is still decreasing. This circumstance could lead to first a decrease and then an increase in $\mathcal{E}$ depending on the relative rates of change of g_{Na} and g_K. Once g_K has reached its final value, $\mathcal{E}$ will slowly fall because of slow inactivation of g_{Na}. It is assumed that at the plateau voltage g_{Na} and g_K do not vary greatly with $\mathcal{E}$, so the plateau continues until $\mathcal{E}$ enters a region where one or both conductances vary rapidly with voltage. At this time repolarization speeds up because of increasing g_K and/or decreasing g_{Na}. The shape of fast repolarization is thus determined principally by the voltage dependencies of the conductances, and trailing edges will be superimposable regardless of the duration of the action potential. Slow inactivation is incomplete at the termination of the plateau, but any remaining g_{Na} is turned off by repolarization. Following repolarization, the fast moiety (h_f) increases, or activates, rapidly and hence excitability quickly returns. However, the slow moiety (h_s) reactivates slowly, with a time constant of about 1 sec (10). Thus, the overshoot of an action potential evoked shortly after the return of excitability will be nearly normal but the duration will be much shorter than normal (fig. 20*A*) because h_s has increased only slightly. After the upstroke, g_{Na} falls rapidly to a low level and fast repolarization ensues immediately. As time passes, more and more slow g_{Na} (h_s) becomes available, so that the plateau becomes higher and the t_{AP} longer. Thus the slow g_{Na} activation process accounts for the existence of a plateau and for the dependence of t_{AP} on the stimulus interval.

Like all hypotheses of repolarization which have been advanced, this scheme has major defects. Its greatest one is that the repolarization process is regenerative. Another is that the kinetics of the activation process must be different from those of the squid axon. FitzHugh (40) has demonstrated two

stable values of $\mathcal{E}$ for which $\dot{h} = 0$ in the squid, one at the resting level and the other about 50 mv more positive (depolarized). Hence, recovery to the resting state occurs only because g_K increases concurrently. Otherwise, following the upstroke, $\mathcal{E}$ reaches a plateau at the second stable state. This situation is accentuated in the heart by the postulated decrease in g_K. It is not known whether the kinetics of the g_{Na} activation-inactivation system can be modified to eliminate this deficiency without destroying other important properties of the h system. The type of change required would appear to be a reduction in the rate of change of the rate constants α_s and β_s and probably α_f and β_f with voltage. Such a change would also reduce the negativity of G during the regenerative phase of repolarization.

This scheme of repolarization in the I_i, $\mathcal{E}$ plane is represented in figure 23*B*. The lines labeled t_1, t_2,....,t_6 are instantaneous I_i,$\mathcal{E}$ curves at roughly equal time intervals of the order of 0.2 sec. These curves are the sum of I_{Na} (shown for one instant, t_3) and I_K. For the sake of simplicity g_{Cl} is taken as zero. I_K is assumed to vary linearly with $\mathcal{E}$ near $\mathcal{E}_K$, and to level off and become constant at larger depolarizations, a variation conforming roughly with Hutter & Noble's findings (75). I_{Na} is assumed to vary with $\mathcal{E}$ at any fixed time in the same manner as the I_{Na} curve at $t = t_3$ except that the magnitude of I_{Na} at any voltage decreases exponentially with time. This decreasing I_{Na}, when added to I_K, leads to the series of I_i,$\mathcal{E}$ curves shown for different times. At any time, G is positive for large depolarizations but there is a region of negative G at lesser depolarizations. $\mathcal{E}$ will pursue $\mathcal{E}_{eq}$ until the I_i,$\mathcal{E}$ curve is just tangent to the $\mathcal{E}$ axis. At this time the threshold point disappears, $\mathcal{E}_{eq}$ jumps suddenly to the left and the third phase ensues. If, prior to this time, a hyperpolarizing current is applied which carries $\mathcal{E}$ to the unstable point, early repolarization will be induced. Thus the hypothesis fails in this respect. The dashed line shows the path the $(\mathcal{E}, -\dot{\mathcal{E}})$ point would follow during spontaneous repolarization. The shape of the curve is drawn about the same as the experimental curve in figure 20*C*. Behavior of this sort is described by Moore (92) for the squid axon in isosmotic KCl.

Another set of assumptions slightly different from those shown in figure 23*B* was quantitatively analyzed by Brady & Woodbury (4). With a digital computer $\mathcal{E}$ and G were calculated as functions of time. The results of one such calculation are shown in figure 24, where calculated $\mathcal{E}$ and G/G_r are plotted against time. A measured action potential, scaled

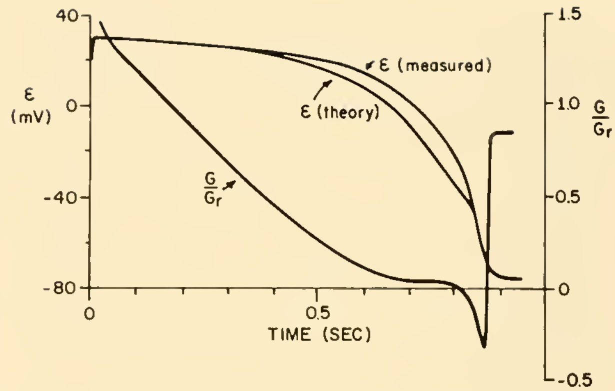

FIG. 24. Comparison of the behavior of the model of repolarization shown in fig. 23*B* with a measured action potential from frog ventricle. $\mathcal{E}$ (theory) and G/G_r were calculated from the model. For ease in comparison, $\mathcal{E}$ (measured) was scaled to the same peak height and duration as $\mathcal{E}$ (theory). The negative values of G/G_r occur just after the I_i,$\mathcal{E}$ curve becomes tangent to the $\mathcal{E}$ axis (fig. 23*B*). Left hand ordinate scale applies to potential curves and right hand ordinate scale to the G/G_r curve. Abscissa: time in sec. [After Brady & Woodbury (4).]

to the same amplitude and duration, is shown for comparison. There is reasonably good agreement between theory and experiment for $\mathcal{E}$. However, G goes rapidly and markedly negative during the third phase. The divergence between theoretical and calculated $\mathcal{E}$ probably could be eliminated by adjustment of the parameters in the equation, but the negative G in the third phase is inherent in the model.

Using an analogue computer, FitzHugh (40) made extensive calculations to demonstrate the properties of the Hodgkin-Huxley equations. He also predicted with reasonable success the behavior of squid giant axon injected with tetraethylammonium chloride (TEA). Tasaki & Hagiwara (114) found great elongation of the action potential, to 20 msec or more, when the squid axon was treated with TEA. FitzHugh predicted this behavior by assuming that the time course of the rise of g_K was more than 100 times slower than normal. Potential-time curves could be reproduced accurately, but the measured slope conductances could not be explained on this basis. Although Tasaki and Hagiwara likened the TEA-treated axon to a cardiac cell because a plateau was induced, the likeness is only superficial since, in marked contrast to heart cells, there is a distinct, sharp threshold for repolarization in this tissue. The resemblance is somewhat closer to cardiac cells in low $[Ca^{++}]$ solutions.

In summary, all the hypotheses of repolarization

described here have one or more serious defects. Further experimentation is needed to determine the process of repolarization in terms of the kinetics of the changes in membrane ionic conductances or permeabilities. Until voltage-clamping in cardiac cells becomes technically feasible, the most fruitful experimental approach seems to be to study how applied currents of different strengths, currents applied at different initial $\mathcal{E}$'s and external ion concentrations affect $\mathcal{E}$.

Despite the lack of an adequate hypothesis of repolarization, several positive statements can be made about this process. *a*) Repolarization consists of the slow movement of a stable equilibrium point with $\mathcal{E}$ pursuing it. *b*) The increased $\dot{\mathcal{E}}$ of the third phase is due to an increase in $\dot{\mathcal{E}}_{eq}$, not to a sudden jump in the position of $\mathcal{E}_{eq}$ occasioned by the disappearance of one stable and one unstable point. *c*) The slope of the $I_i,\mathcal{E}$ curve is positive for all voltages of the normal action potential at all times during repolarization (fig. 21). *d*) Reduced $[Ca^{++}]_o$ apparently changes the instantaneous $I_i,\mathcal{E}$ curves so that they have a region of negative G in the vicinity of $\mathcal{E} = 0$. These statements lead to the conclusion that the conductance changes of repolarization in heart result from rate processes which are largely time-dependent and only slightly voltage-dependent. If this conclusion is correct, then repolarization in heart is an entirely different process than in squid axon and considerably more experimental data are required to elucidate the kinetics of this relatively unknown process in heart. Any successful hypothesis must give an ionic basis for this behavior as well as explain superimposability and variation of t_{AP} with stimulus interval.

Auto-rhythmicity

Perhaps the most striking property of cardiac muscle is its spontaneous contractions. Since the contractile state is controlled by the transmembrane potential, rhythmic contraction is a consequence of rhythmic initiation of impulses. It is commonly believed that all cardiac cells are intrinsically rhythmic. In the intact heart the beat originates in a histologically specialized region, the sinoatrial node, because its intrinsic rate is the highest. Regardless of its anatomical location, the site of origin of the beat is called the pacemaker region. The distinguishing electrical characteristic of a pacemaker cell is lack of a stable equilibrium voltage—rapid repolarization being immediately succeeded by a slow diastolic

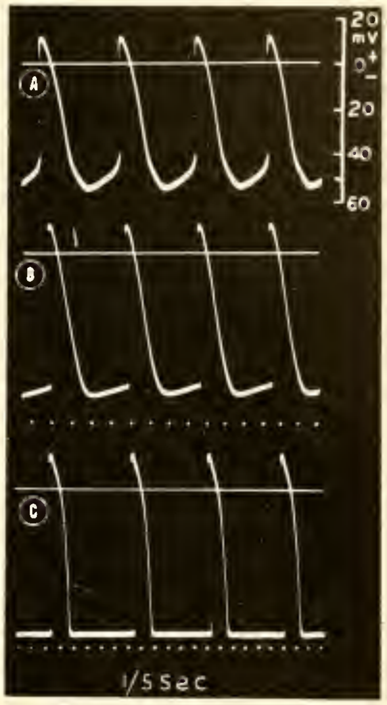

FIG. 25. Transmembrane action potentials from the sinus venosus and atrium of a frog. Ordinates: transmembrane potential in millivolts. Abscissae: time; dots are 0.2 sec apart. *A*: microelectrode recording from a pacemaker cell. Note the large diastolic depolarization and the comparatively gradual transition to the upstroke of the action potential. *B*: recording from a cell a short distance away. *C*: recording from atrial cell. Rate of all three cells is determined by the time required for the slow depolarization shown in *A* to reach threshold. [From Hutter & Trautwein (76).]

depolarization called the prepotential (2) or pacemaker potential. This depolarization contrasts to the unvarying diastolic potential of other cardiac cells. Figure 25 shows a series of intracellularly recorded transmembrane action potentials from the sinus venosus and atrium of frog (76). The potential in figure 25*A* is from a pacemaker cell. There is a comparatively gradual transition between the slow diastolic depolarization and the rapid upstroke of the action potential. In *B*, the microelectrode was in a fiber a short distance away, where there were a smaller diastolic depolarization and a more abrupt transition to the rising phase of the action potential. Simultaneous recordings from these two regions (2, 12) show that activity of the type shown in figure 25 occurs earliest; therefore, impulses are initiated in this region. Figure 25*C* is a recording from an atrial fiber in which $\mathcal{E}$ is constant during diastole. The records of figure 25 illustrate the transition from pacemaker to ordinary cardiac tissue. Presumably, re-

moval or inhibition of the normal pacemaker region allows another nearby region with a slower intrinsic rate to initiate impulses.

In the pacemaker region an impulse is set up when the slow diastolic depolarization reaches threshold voltage. Generally speaking, the rate of rise and the peak height of the action potential are less in a pacemaker than in other parts of the heart. This reduction can be attributed to the inactivation of rapidly available g_{Na} during the slow diastolic depolarization, i.e., the voltage is changing so slowly that g_{Na} is always near its steady-state value (127). Since the threshold voltage is relatively fixed, the primary determinant of the impulse discharge rate is the slope of the prepotential—the steeper its slope, the faster the rate. The slope of the prepotential is highly dependent on external ion concentrations, temperature, and the concentrations of cholinergic and adrenergic substances.

The membrane properties which lead to oscillation in heart cell potentials are not known precisely, but these properties cannot be markedly different from those of a quiescent cell membrane. Their general nature follows from a study of oscillatory behavior in the squid axon where the conductance changes during activity are precisely known. Any change that makes $\mathcal{E}_r$ about equal to the threshold voltage is likely to produce oscillations. This condition can be produced experimentally in squid axon either by applying a steady outward current to depolarize the membrane to threshold (16) or by reducing the $[Ca^{++}]_o$ to move the threshold toward the resting potential (77). In the former case, the sudden application of the current would quickly depolarize the membrane voltage to threshold and initiate an impulse. The lag in the fall of g_K during repolarization would carry $\mathcal{E}$ nearly to $\mathcal{E}_K$ for a short time. Thereafter, as g_K fell toward its resting level, the membrane potential would fall with it and another impulse would be initiated when threshold voltage was again crossed. Within limits, the greater the applied depolarizing current, the faster the rate of impulse discharge. These qualitative considerations of oscillatory behavior have been verified by solving the Hodgkin-Huxley equations on an automatic computer for different applied currents (16) and different $[Ca^{++}]_o$'s (77). Thus the oscillations occur in squid axons because the repolarization process carries the membrane potential past the resting level, which is below the threshold potential. Oscillations presumably could be obtained more naturally by increasing resting g_{Na}. An increased resting g_{Na} seems the most likely explanation of the oscillations in cardiac tissue. It appears that the Brady-Woodbury model of repolarization could be made to oscillate by increasing the resting g_{Na}. The oscillation would result because the slow activation of g_{Na} following repolarization would produce an actual increase in g_{Na}. The time course of $\mathcal{E}_{eq}$ in figure 22 during the late third phase and slow diastolic depolarization suggests that a combination of fast and slow activation is contributing to actual g_{Na} to cause a fast and then slow movement of $\mathcal{E}_{eq}$.

Trautwein & Dudel (37, 120) found that membrane slope conductance decreased during the slow diastolic depolarization, in conformity with Weidmann's measurements (fig. 22). In addition, they calculated $\mathcal{E}_K$ on the assumption that the fall in G is entirely due to a fall in g_K. This $\mathcal{E}_K$ was found to be invariant throughout slow diastolic depolarization. $\mathcal{E}_K$ measured this way agreed well with estimates of $\mathcal{E}_K$ made from a study of the action of acetylcholine. Trautwein and Dudel concluded that the pacemaker potential is an after-hyperpolarization, the increased g_K induced by the preceding repolarization slowly decreasing in time. This is the same mechanism as in squid giant axon. However, it is difficult to tell whether the decrease in membrane voltage during slow diastolic depolarization in heart is due to a decrease in g_K or vice versa. Hutter & Noble (75) have found that the slope of the current-voltage relation of quiescent cardiac muscle is the same over the voltage range of the slow diastolic depolarization as Trautwein and Dudel found during the pacemaker potential. Their interpretation is rendered less likely as an explanation of spontaneous activity by Hutter and Noble's results since the fall in g_K probably reflects the fall in voltage, not a decay in time of g_K. Nevertheless, some time-dependent process must occur during the diastolic depolarization and the possibilities seem to be a decreasing g_K, an increasing g_{Na}, or both. The possibility that a changing g_{Cl} contributes to the pacemaker potential is eliminated because Cl^- replacement only transiently affects the rate (8, 73). The decrease in G as the membrane depolarizes probably indicates a time or voltage-dependent decrease in g_K; in view of the definition of G the finding could indicate a voltage-dependent increase in g_{Na}, but Trautwein and Dudel's finding that $\mathcal{E}_K$ is constant assuming a variable g_K appears to rule out this possibility. Noble (98) has modified the Hodgkin-Huxley equations so that solutions of them are repetitive heart-like action potentials. The pacemaker

FIG. 26. Effects of vagal stimulation on the transmembrane potential of a pacemaker cell in the frog sinus venosus. Period of vagal stimulation at 20/sec is indicated by interruption in lower white line. Only the lower part of the action potential is shown; total visible voltage excursion is about 45 mv. [From Hutter & Trautwein (76).]

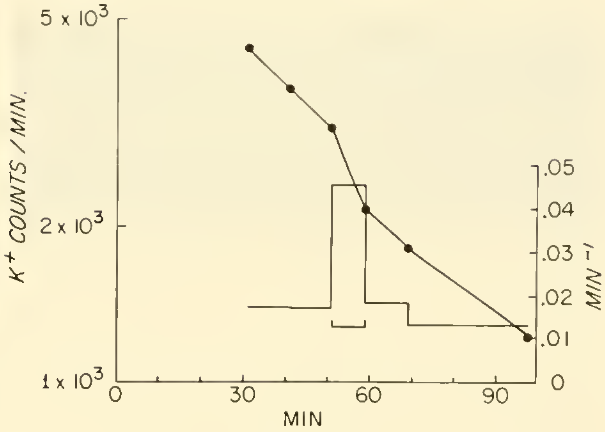

FIG. 27. Effect of vagal stimulation on the efflux of K^{42} from quiescent tortoise sinus venosus. The total radioactivity of the tissue is shown by the dots and the logarithmic ordinate scale at left. The rate constant of K^+ release by the tissue is shown by the bar graph and the linear scale at the right (min^{-1}). Abscissa: time in min. The vagus nerve was stimulated (10/sec) during the period subtended by the bracket (52–59 min). Note the quadrupling in the rate constant due to the stimulation. This effect is also shown by the increased negative slope of the tissue radioactivity curve. [After Hutter, in (41).]

potential is a positive after-potential. These action potentials have a sharp threshold for repolarization.

EFFECTS OF VAGAL AND SYMPATHETIC STIMULATION. Although the heart is spontaneously active, its rate is almost pre-emptorily controlled by vagal and sympathetic discharges in the sinoatrial pacemaker region. The mode of action of the vagal transmitter acetylcholine (ACh) is well understood. The action of epinephrine is uncertain since the evidence is conflicting (cf. 72). Figure 26 shows the effects of vagal stimulation on the transmembrane potentials of a frog sinus venosus fiber. Rapid vagal stimulation caused immediate hyperpolarization and stoppage of impulse generation (11, 76). The action persisted for the duration of the stimulation. Following cessation of the stimulation, the potential fell gradually and impulse discharge resumed at an initially slower rate. Slower vagal nerve stimulation may slow the heart rate.

Since $\mathcal{E}_{Na}$ and $\mathcal{E}_{Cl}$ are both more positive than the large negative voltage reached during vagal inhibition, the transmitter must act to increase g_K or to decrease g_{Cl}, and/or g_{Na}. There is considerable evidence that membrane conductance is greatly increased by vagal stimulation (122) and ACh (119, 120) so an increase in g_K is the probable effect of the transmitter. An increase in g_K produces a powerful inhibition since it tends to clamp the voltage at $\mathcal{E}_K$. Hutter and Harris have shown directly that ACh acts specifically to increase g_K [see (72) and Hutter in (41)]. ACh increased both the efflux and the influx of K^+ [see also (101)]. Figure 27 shows the dramatic effects of ACh on K^{42} efflux from tortoise sinus venosus. Cl^- fluxes were not appreciably affected. Evidence leading to this conclusion was furnished earlier by Trautwein & Dudel (119). They found that the equilibrium potential for ACh inhibition varied exactly as $\mathcal{E}_K$ with variations in $[K^+]_o$ and this value of $\mathcal{E}_K$ agrees with the $\mathcal{E}_K$ calculated from G and $\mathcal{E}$ during diastole (37). Woodbury and Crill (in 41) furnished less direct evidence in that the decrease in membrane resistance produced by ACh was not affected by Cl^- replacement, although Cl^- replacement in the absence of ACh caused an increase of 25 per cent or more in membrane resistance. Hoffman & Suckling (70) found that ACh dramatically shortens the atrial action potential. Action potentials elicited by direct stimulation during vagal stimulation have less overshoot and shorter durations than normal, as would be expected from an increase in g_K. The effects of ACh on heart tissue are somewhat different from its effects at neuromuscular junctions, where it produces an increase in membrane permeability to "all" ions. The differences may be reconciled if it is supposed that ACh increases membrane permeability by creating pores which are slightly larger in end-plate membranes than in cardiac muscle membranes.

The effects of sympathetic stimulation on the action potentials of a frog sinus venosus cell are shown in figure 28 (76). In this tissue, such stimulation increases the rate of discharge and the overshoot of the action potential. Hutter & Trautwein (76) also observed an increased rate of rise of the action potential during sympathetic stimulation.

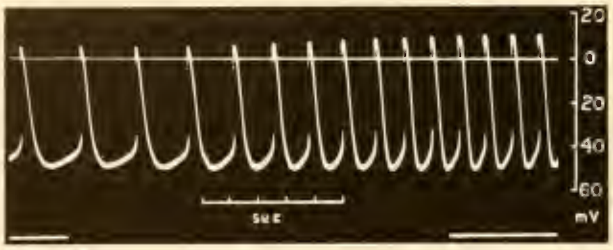

FIG. 28. Effects of sympathetic nerve stimulation on the transmembrane potential of a frog sinus venosus cell. Bath contained atropine sulphate (10^{-6}) to block cholinergic activity. Stimulation of vagosympathetic trunk at 20/sec during period of interruption of the lower white line. Ordinate: transmembrane potential in millivolts; abscissa: time in seconds. (From Hutter & Trautwein (76).]

The effects of epinephrine on various parts of the heart have also been studied (36, 48, 99, 134). The effects of sympathetic stimulation and epinephrine can be explained by assuming that the transmitter facilitates the Na^+-carrying system so that g_{Na} is always above normal. The possibility that the sympathetic transmitter decreases g_K is probably eliminated by Harris and Hutter's (cf. 72) finding that K^{42} effluxes are not affected. However, in dog atrium, application of epinephrine consistently increases the membrane potential (36). Although the mechanism is not known, sympathetic stimulation increases the heart rate.

Excitation-Contraction Coupling

Roughly speaking, depolarization turns on the contractile process and repolarization turns it off. The time from the moment of stimulation to the peak of the contractile tension is proportional to the duration of the action potential. The term "excitation-contraction (E-C) coupling" refers to the events which form the link between depolarization and contraction. When t_{AP} is altered by changing t_s, contraction time (t_c) is about equal to t_{AP} in frog ventricle (Brady, unpublished records); in cat papillary muscle t_c is about 0.5 of t_{AP} [(117); see also (102)]. Further, the Q_{10} of t_{AP} and t_c are equal in frog ventricle [see also Kaveler (82)].

The steps intervening between depolarization and contraction are not known, although a number of recent observations give some indication of the nature of the process. Huxley & Taylor (79) found that local depolarization of a frog skeletal muscle fiber membrane in the region of a Z band causes a contraction of the two half I bands on either side of the Z line—i.e., the A bands move toward the Z band and the I bands are obliterated. Equal depolarization at other regions has no effect on the contractile material. Although later evidence (78) shows that the Z band is not the main intracellular structure involved in E-C coupling in all skeletal muscle, these findings indicate that specialized structures, perhaps the endoplasmic reticulum, connect the membrane and the contractile material.

Lüttgau & Niedergerke (89) have examined in detail the well-known antagonism between Ca^{++} and Na^+ as they affect the contractile strength of frog ventricular strips. It has been long known that removal of Ca^{++} from the bathing medium abolishes contraction without appreciably affecting the action potential (cf. 13). Lüttgau and Niedergerke found that the peak tension developed during a normal contraction and during KCl-induced contractures is determined almost wholly by $[Ca^{++}]_o/[Na^+]_o^2$. Also the amount of depolarization needed to produce a given tension is reduced by a decrease in $[Na^+]_o$ or an increase in $[Ca^{++}]_o$. Lüttgau and Niedergerke interpret their findings as evidence that the contractile tension is determined by the concentration of a Ca^{++} complex (CaR) in or near the membrane and that 2 Na^+ ions can also combine with R to form an inactive complex. The effects of ions on the amount of depolarization required to produce a given tension are explained by assuming that R has a large anionic charge and that depolarization allows more negatively charged CaR complex molecules to move to the inner side of the cell membrane, where they are effective in initiating contraction. Increasing $[Ca^{++}]_o$ and decreasing $[Na^+]_o$ would increase the concentrations of the CaR complex outside and inside the membrane so that a lesser depolarization could initiate contraction despite the adverse membrane potential gradient. Thus it appears that one step between depolarization and contraction is the movement of a Ca^{++} complex to a region, presumably inside the membrane (including the endoplasmic reticulum?), where it initiates contraction; the greater the concentration of CaR in this region, the greater the tension developed, other things being equal. Further evidence for the penetration of the CaR complex during contraction is provided by the findings that the uptake of Ca^{++} in muscle is an inverse function of $[Na^+]_o$ and is a direct function of $[K^+]_o$ during contracture (96, 97, 116). Also Weidmann (132) has found that an increase in $[Ca^{++}]_o$ during the action potential increases the strength of contraction. Considerable progress in this field can be expected in the next few years.

PASSIVE MEMBRANE PROPERTIES AND INTERCELLULAR TRANSMISSION

An adequate stimulus applied to any point in cardiac tissue initiates an impulse which spreads without decrement throughout the whole muscle. Electrically, the tissue behaves like one large excitable cell. Anatomically, the tissue is composed of discrete cells, each bounded by a cell membrane (6, 91, 93, 94, 107, 108). If these cell membranes have a high electrical resistance, as do those in other tissues, then it is not clear how an active cell initiates activity in its neighbors even though the cells are closely packed (8–20 mμ spacing between membranes). The simplest possibility is that activity spreads from cell to cell by means of local currents as it does in single nerve and skeletal muscle fibers. Another possibility is some sort of synaptic transmission. In nerve and muscle fibers, current flows from an inactive normally polarized region of membrane into an adjacent active depolarized region via the extracellular fluid and returns via the intracellular fluid. This flow eventually depolarizes the inactive membrane to threshold. In turn, this portion of membrane becomes active and serves as a source for adjacent inactive membrane. If spread of activity in the heart is by local circuit flow, some regions of the cell membrane must have a comparatively low resistance to current flow, and one of these regions must be closely approximated to a like region of an adjacent cell. If these specialized anatomical and functional requirements do not obtain, intercellular transmission must be by other than electrical means, e.g., chemical.

A simple and fairly conclusive experiment helps to distinguish between the two possible means of transmission. If activity spreads by local circuit flow, a current flowed through the membrane of one cell by means of an intracellularly placed electrode must appreciably affect the transmembrane potentials of neighboring cells, i.e., the tissue would have electrotonic properties. The absence of electrotonus from cardiac tissue would establish that transmission is not electrical. The presence of electrotonus would not prove that transmission is electrical, but would make this likely as the simplest hypothesis. A more detailed consideration of electrotonic properties of long, thin cells may be found in Tasaki's chapter (112). The basic mathematical and experimental analysis was given independently by Hodgkin & Rushton (66) and by Davis and Lorente de Nó (cf. 88).

Since individual cardiac cells are only about 100 μ long and 15 μ in diameter, the existence of injury currents in cardiac tissue (cf. 25, 26, 69, 105) is presumptive evidence of low resistance electrical connections between cells and of intercellular electrotonic properties. However, the matter was settled definitely in the affirmative in 1952 by Weidmann (126), who analyzed current spread in Purkinje fibers by means of the cable equation. This analysis yielded values of specific membrane capacitance and resistance, and specific resistivity of myoplasm. The membrane capacitance was 12 μF cm^2, the membrane resistance was 2000 Ω-cm^2, and the specific resistivity of the myoplasm 105 Ω-cm, nearly twice that of Tyrode's solution. This resistivity is typical for all plasm and shows that there are no high resistance barriers to current flow in the myoplasm. The current must flow between cells since the space constant was 2.0 mm, many times the length of any cell. Therefore, it seems probable that intercellular transmission in cardiac tissue is by local circuit flow. However, the argument for local spread would be much stronger if the means by which current flows from cell to cell without appreciable loss could be given in detail. Aside from the fundamental importance of the problem, a discussion of it is of some interest because Sperelakis, Hoshiko, and their colleagues (109) have contended that the heart is not a functional syncytium, intercellular conduction occurring by means of a two-way synaptic transmitter process.

Electrotonic current spread in cardiac muscle is more difficult to measure experimentally and to interpret theoretically than similar events in nerve or skeletal muscle fibers, because current spreads in two or three dimensions in the heart but in only one dimension in nerve and skeletal muscle. Crill and Woodbury (unpublished experiments, 41) have recently measured and analyzed the spread in two dimensions of a current applied to rat atrial cell. Their main experimental findings, which confirm and extend those of Weidmann, are as follows: *a*) An intracellularly applied current produces appreciable transmembrane potential changes in what must be different cells. *b*) Current spreads about twice as far in the fiber direction as it does at right angles to fiber direction—i.e., isopotential contours are roughly elliptical with the long axis in the fiber direction (fig. 29). *c*) The decline of the steady-state potential with radial distance from the current applying electrode is steeper than exponential, as would be expected for a point current source spreading out in two dimensions (fig. 30).

If impulses spread by local current flow, then the conduction velocity should be about twice as fast in

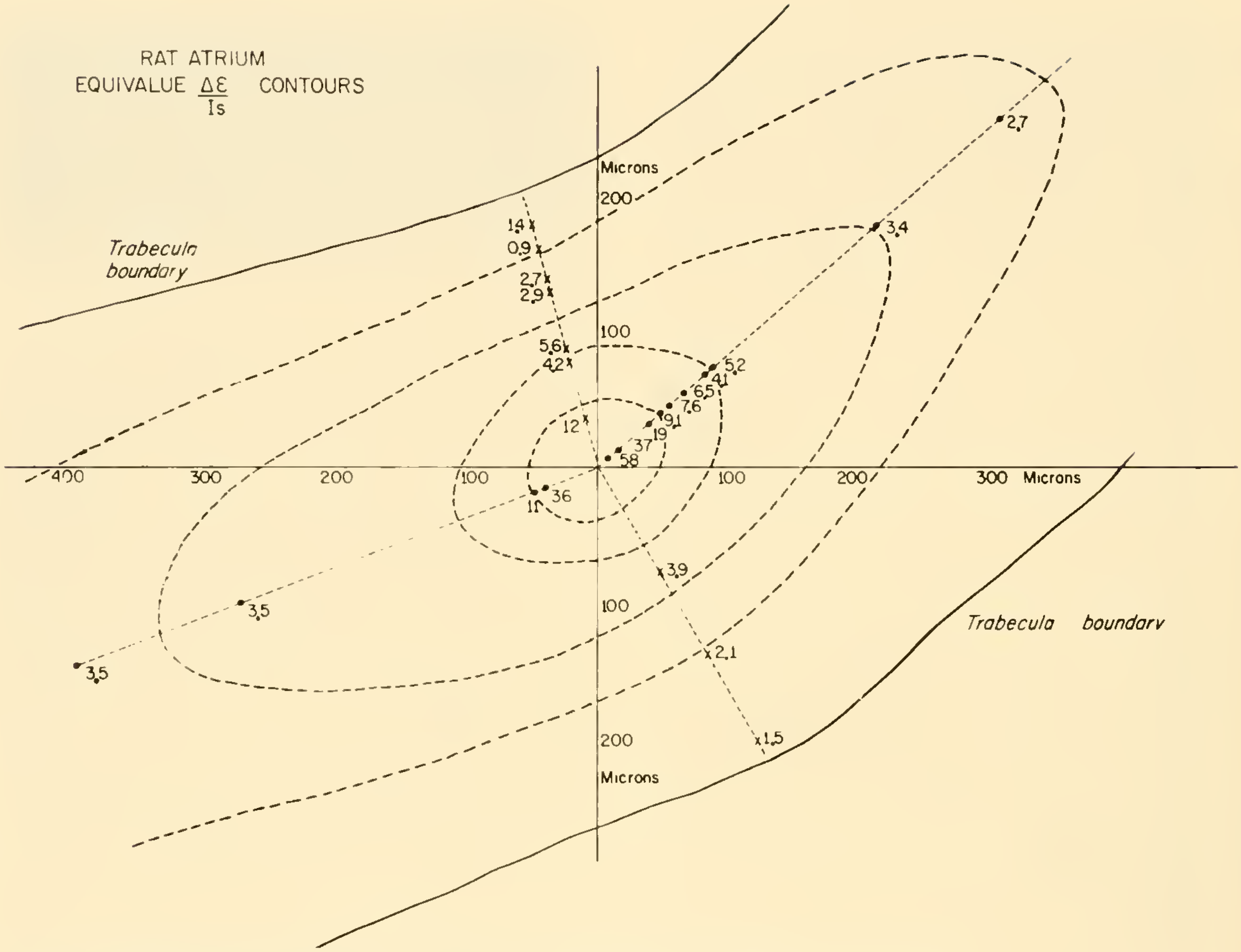

FIG. 29. Isopotential contour map of a rat atrial trabecula. A current was applied to the tissue via an intracellular electrode located at the origin. The resulting changes in potential ($\Delta \mathcal{E}$) were measured with another intracellular electrode at the points indicated by dots or X's. Dots indicate measurements made along radii parallel to trabecula edge and X's measurements along radii perpendicular to the trabecula edge. The number attached to each point is the ratio $\Delta\mathcal{E}/I_s$, where I^s is the size of the applied current, in units of mv/μA or K-ohm. Dashed lines are approximate equivalue contours. From inside to outside they are 10, 5, 3.5, and 2.5 mv/μA contours, respectively. Note the much greater spread of current in the direction parallel to the trabecula boundary than perpendicular to it. (Crill, unpublished data, 1960.)

the fiber direction as in the perpendicular direction. Draper & Mya-Tu (34) and Sano *et al.* (104) have observed conduction velocities two to four times faster parallel to the long axis of the myocardial fiber than perpendicular to it. This correlation is strong evidence for local circuit propagation. Therefore, the principal consideration is the special properties of cardiac cells which allow the flow of myoplasmic current between cells and thus accomplishes intercellular transmission by local current flow.

Structure of Cardiac Muscle

The essential features of cardiac tissue membrane structure are shown schematically in figure 31, which is based on the work of Muir (93, 94) and Sjöstrand *et al.* (107, 108). Cardiac cells are shaped and packed somewhat like bricks with dimensions of the order of 15 μ by 15 μ by 100 μ. Myofibrils (not shown in fig. 31) run the length of the cell and terminate on the cell membrane at places corresponding to Z bands on other sarcomeres. Cell surfaces parallel to the fibril axis are separated from their surrounding cells by 20 to 30 nm, whereas the membranes perpendicular to the fibrils are only 8 to 10 nm apart. The opposing membranes in these regions are thickened and greatly folded, the surface area being about 10 times the cross-sectional area. These thickened and tortuous membranes constitute the microscopically

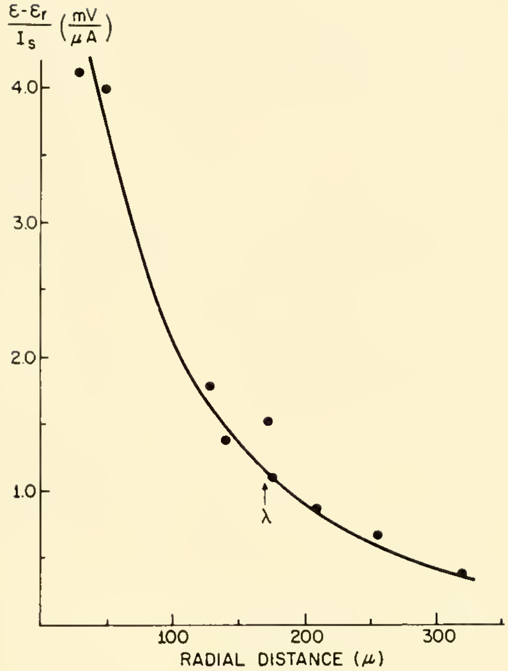

FIG. 30. Spatial decrement of electrotonic potential in a rat atrial trabecula. Ordinate: change in membrane potential per unit applied current $[(\mathcal{E} - \mathcal{E}_r)/I_s]$. Abscissa: distance from an intracellular current-applying electrode along radius parallel to the trabecula edge. Dots are points from one experiment; the solid line is the theoretical curve of voltage against radial distance for a single planar cell. The space constant (λ) is indicated by the arrow at 170 μ. The theoretical curve, a zero order Bessel function of the second kind with imaginary argument was fitted to the experimental points by trial and error. (Crill & Woodbury, unpublished data, 1960.)

visible intercalated discs. These discs frequently cross a cell in a stepwise manner, the disc membrane changing to a regular membrane when running parallel to the fibrils between steps. This structure has been formalized and schematized in figure 31 (93). Thus, different cells oppose a particular cell across the different steps. The tortuosity and close spacing of the disc membranes strongly suggest that the intercalated discs are the site at which intracellular current is transferred from one cell to the next. The increased surface area at the disc reduces transmembrane resistance and the narrow gap decreases the leakage of intercellular current into larger interstitial spaces. If the resistance of the discs is comparatively low, the multiple connections to other cells through them insure spread of the current in all directions from any one cell, but preferentially in the fiber direction (as shown by the current flow lines in fig. 31). Sjöstrand *et al.* (108) suggest that the gap between opposing disc membranes is filled with lipids rather than interstitial fluid. If true, this arrangement should aid transmission, since the poorly conducting lipids would greatly reduce flow parallel to the disc membrane but, being thin, would have a much lesser effect perpendicular to it. However, theoretical calculation (Woodbury and Crill in 41) shows that transmission is efficient even if the gap is filled with interstitial fluid.

On a grosser scale, cardiac cells are not uniformly closely packed. Bundles of closely packed cells are separated from other bundles by larger interstitial spaces containing capillaries. These bundles are no more than about six cells in diameter, so that no cell is more than three or four cell diameters from a large extracellular fluid space. These bundles merge and branch at short intervals, but tend to form even larger bundles of the order of millimeters in diameter, called "trabeculae," which in turn merge and branch in a meshwork to form the myocardium.

Analysis of Two-Dimensional Electrotonus in Atrium

Theoretical analysis of the experimentally measured two-dimensional current spread in rat atrium (Crill and Woodbury, unpublished results) gives considerable insight into the detailed electrical properties of cardiac tissue in general and of the intercalated disc in particular. The results can be best interpreted on the assumption that the intercalated discs have low or negligible resistance to transverse current flow so that the atrium is the two-dimensional equivalent of a skeletal muscle fiber; i.e., this flat tissue can be represented electrically as one large planar cell. Aside from the observed variation of current spread with direction, this simple model served to describe surprisingly well the steady-state distribution of potential as a function of radial distance (r). Theoretically, this steady-state voltage as a function of r is a Bessell function of zero order, of the second kind and with imaginary argument. The solid curve in figure 30 is such a function fitted to the variation of potential with distance measured in the fiber direction. The space constant is 160 μ. Measurements made at right angles to the fiber direction are equally well fitted by the Bessell function, but the space constant is slightly more than half of that in the fiber direction. The space constant and the area under the $\mathcal{E}$,r curve can be used to calculate values of specific membrane resistance and internal resistivity for this tissue. These were about 40 Ω-cm^2 and 1500 Ω-cm, respectively (assuming that the equivalent planar cell is 75 μ thick).

All of these values are markedly different from corresponding values in other tissues. The space con-

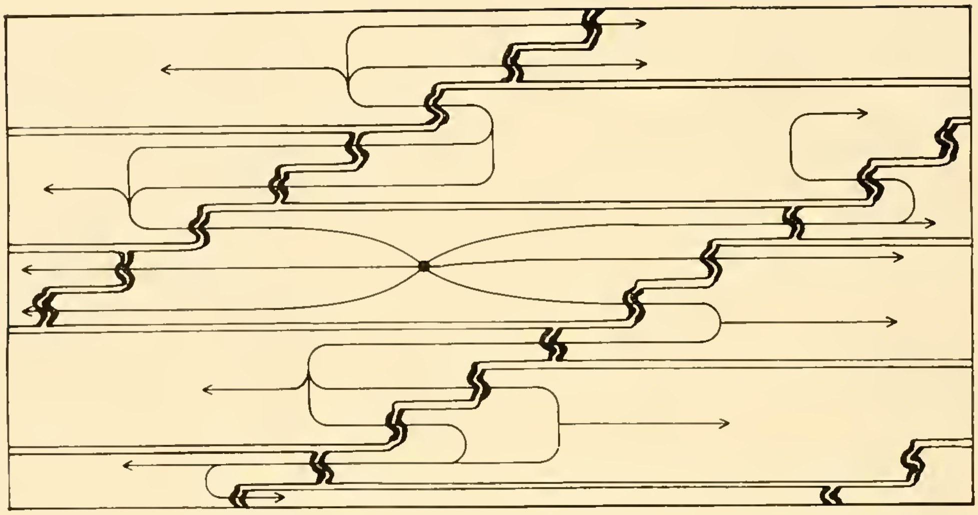

FIG. 31. Simplified and formalized diagram illustrating the electrical structure of a portion of a rat atrial trabecula. Thin straight lines represent regular, excitable cell membranes having high electrical resistance; thickened heavy lines represent intercalated disc membranes having low resistance. Each cell is completely surrounded by membrane. Large dot in center indicates location of an intracellular current electrode. Lines with arrowheads indicate the major pathways of current flow from the electrode in the intracellular fluid. Current flow through regular membranes into the extracellular fluid is small and is not shown; most of this current flows perpendicularly to the diagram to enter large extratrabecular spaces. Intracellular current flow at right angles to the fiber direction follows a zigzag path of least resistance largely through the intercalated discs. This structure accounts for the spatially nonuniform spread of current. Contractile material is not shown for simplicity.

stant is extremely short in comparison to space constants of skeletal muscle, nerve fibers, and Purkinje strands which are of the order of millimeters (66, 126). The space constant of the two-dimensional model is given by $(R_m \delta \rho_i)^{1/2}$, where R_m is specific membrane resistance (Ω-cm^2), δ is the thickness of the model cell (cm), and ρ_i is the specific resistivity of the cell fluid (Ω-cm). In the model the external resistance was assumed to be negligible. It might be supposed that the close packing of the cells makes extracellular resistance sufficiently high to invalidate the equation and give rise to a short space constant; however, no cell is more than two or three cell diameters from a large extracellular space. Hence, such a supposition is unlikely to be correct. Rather, the reason for the short space constant is a low specific membrane resistance, 40 Ω-cm^2. Corresponding values in other tissues are 1000 to 5000 Ω-cm^2. It was at first thought that this low value for heart invalidated the model, but further analysis led to the following interpretation. The theoretical model is based on the assumption that the atrium behaves like a single planar cell; but the actual tissue, though planar, has a membrane area many times greater than the surface area of the model cell. Thus the calculated specific membrane resistance is the resistance of all cell membranes throughout the thickness of the tissue under 1 cm^2 of surface area. This is true because an applied current flows through all membranes as it spreads away from the electrode (fig. 31). Consequently, the actual change in voltage produced by a current at a given distance will become less as the actual membrane area per unit surface area increases. If atrial tissue is effectively only five cell diameters thick, the actual membrane area is 20 times the surface area of the tissue. Since the calculated membrane resistance is about 40 Ω-cm^2, the actual resistance will be of the order of 20 $\times$ 40 Ω-cm^2 = 800 Ω-cm^2, a value near the usual range of values for specific membrane resistance. This interpretation also accounts reasonably for the low specific resistance of the membrane and short space constant, and hence for the low membrane resistance (280 Ω-cm^2) and high capacity (30 μF/cm^2) found by Trautwein *et al.* (122) in frog atrial strips.

The measured value of ρ_i, 1500 Ω-cm, is 15 times the value found by Weidmann (126) in Purkinje fibers. ρ_i's for other tissues (66) are about double external resistivities (ρ_e). ρ_e for mammalian tissues is about 60 Ω-cm. Thus Weidmann's value of 100

Ω-cm for ρ_i indicates that discs contribute little to the total internal resistance in Purkinje tissue. It seems unlikely that the ρ_i of rat atrial myoplasm is more than 100 Ω-cm, so most of the measured ρ_i must be attributed to disc resistance. On this basis, the average value of the disc specific resistance (R_{md}) was close to 6 Ω-cm^2, not taking into account the folding of the disc membrane. Weidmann (133) has obtained a similar but somewhat smaller value for R_{md} from measurements of the rate of diffusion of K^{42} along Purkinje fibers, indicating that current is carried through the disc membrane largely by K^+. The resting potential could be maintained across such a selectively permeable disc membrane. A separate calculation by Woodbury & Crill (in 41) gives further evidence that R_{md} may be as low as 1 Ω-cm^2. On the basis of a simplified representation of the transmembrane potentials across the disc membranes at the junction between an active and an inactive cell, these investigators calculated that R_{md} must be of the order of 1 Ω-cm^2 or less to insure efficient current transmission across the disc. In other words, to insure that most of the current leaving one cell through a disc enters the adjacent cell and does not escape into the interstitial fluid, R_{md} must be 1 Ω-cm^2 or less. Thus three completely separate approaches yield R_{md} values ranging from 1-6 Ω-cm^3. Together, these arguments constitute strong evidence for the correctness of these values and the view that disc resistance is low.

It is worth pointing out that membrane resistivities of 1 Ω-cm^2 are not unknown in cells. If disc membrane area is ten times the cellular cross-sectional area, then R_{md} is about 10 Ω-cm^2. Red blood cell membranes have resistivities of about 1 Ω-cm^2 owing to their high anion permeability. The R_m of a squid axon at the peak of activity can be as low as 6 Ω-cm^2 (19). Despite the low R_{md} disc resistance contributes substantially to the total internal resistance of atrial tissue.

The findings that the resistance of intercalated discs is low and that K^+ diffuses through them rapidly enough to account for this low resistance suggest a possible explanation of the rapid disappearance of injury potentials in cardiac muscle. It is known that increasing $[K^+]_o$ increases g_K (9, 65, 75). It seems possible that normal K^+ leakage into the interdisc space maintains there a $[K^+]$ high enough to reduce considerably disc resistance and transdisc potential. In an injured area, the membranes of the injured cells are ruptured; hence they will gradually lose their K^+. Concomitantly the $[K^+]$ in the interdisc space common to intact and injured cells would fall. In turn, this fall in $[K^+]_o$ could increase disc resistance and potential, which would have the effect of electrically isolating the intact cells from the injured ones.

REFERENCES

1. Adrian, R. H. The effect of internal and external potassium concentration on the membrane potential of frog muscle. *J. Physiol.* 133: 631, 1956.
2. Bozler, E. The initiation of impulses in cardiac muscle. *Am. J. Physiol.* 138: 273, 1943.
3. Brady, A. J. and J. W. Woodbury. Effects of sodium and potassium on repolarization in frog ventricular fibers. *Ann. New York Acad. Sc.* 65: 687, 1957.
4. Brady, A. J. and J. W. Woodbury. The sodium-potassium hypothesis as the basis of electrical activity in frog ventricle. *J. Physiol.* 154: 385, 1960.
5. Brazier, M. A. B. The historical development of neurophysiology. In: *Handbook of Physiology*. Washington: American Physiological Society, 1959, sect. 1, vol. I, p. 1.
6. Caesar, R., G. A. Edwards, and H. Ruska. Electron microscopy of the impulse conducting system of the sheep heart *Ztschr. Zellforsch.* 48: 698, 1958.
7. Caldwell, P. C. and R. D. Keynes. The effect of ouabain on the efflux of sodium from a squid giant axon. *J. Physiol.* 148: 8P, 1959.
8. Carmeliet, E. Effets de la substitution des ions chlorure sur le potentiel de membrane des fibres de Purkinje. *Helv. physiol. et pharmacol. acta* 17: C 18, 1959.
9. Carmeliet, E. L'influence de la concentration extracellulaire du K sur la perméabilité de la membrane des fibres de Purkinje de mouton pour les ions ^{42}K. *Helv. physiol. et pharmacol. acta* 18: C 15, 1960.
10. Carmeliet, E. and L. Lacquet. Durée de potentiel d'action ventriculaire de grenouille en fonction de la fréquence. Influence des variations ioniques de potassium et sodium. *Arch. internat. physiol.* 66: 1, 1958.
11. Del Castillo, J. and B. Katz. Production of membrane potential changes in the frog's heart by inhibitory nerve impulses. *Nature, London* 175: 1035, 1955.
12. Cervoni, P., T. C. West, and G. Falk. Multiple intracellular recording from atrial and sino-atrial cells: correlation with contractile tension. *Proc. Soc. Exper. Biol. & Med.* 93: 36, 1956.
13. Clark, A. J., M. G. Eggleton, P. Eggleton, R. Gaddie, and C. P. Stewart. *The Metabolism of the Frog's Heart.* Edinburgh: Oliver & Boyd, 1938.
14. Cole, K. S. Dynamic electrical characteristics of the squid axon membrane. *Arch. sc. physiol.* 3: 253, 1949.
15. Cole, K. S. Beyond membrane potentials. *Ann. New York Acad. Sc.* 65: 658, 1957.
16. Cole, K. S., H. A. Antosiewicz, and P. Rabinowitz.

Automatic computation of nerve excitation. *J. Soc. Indust. Appl. Math.* 3: 153, 1955.

17. Cole, K. S. and R. H. Cole. Dispersion and absorption in dielectrics II. Direct current characteristics. *J. Chem. Phys.* 10: 98, 1942.
18. Cole, K. S. and H. J. Curtis. Electric impedance of the squid giant axon during activity. *J. Gen. Physiol.* 22: 649, 1939.
19. Cole, K. S. and J. W. Moore. Ionic current measurements in the squid giant axon membrane. *J. Gen. Physiol.* 44: 123, 1960.
20. Cole, K. S. and J. W. Moore. Potassium ion current in the squid giant axon: Dynamic characteristic. *Biophysical J.* 1: 1, 1960.
21. Coraboeuf, É. and M. Otsuka. L'action des solutions hyposodiques sur les potentiels cellulaires de tissu cardiaque de mammifères. *Compt. Rend. Acad. Sc., Paris,* 243: 441, 1956.
22. Coraboeuf, É. and S. Weidmann. Potentiels d'action du muscle cardiaque obtenus à l'aide microélectrodes intracellulaires. Présence d'une inversion de potentiel. *Compt. Rend. Soc. Biol., Paris,* 143: 1360, 1949.
23. Coraboeuf, É. and S. Weidmann. Temperature effects on the electrical activity of Purkinje fibres. *Helv. physiol. et pharmacol. acta* 12: 32, 1954.
24. Coraboeuf, É., F. Zacouto, Y-M. Gargouïl, and J. Laplaud. Mesure de la résistance membranaire du myocarde ventriculaire de mammifères au cours de l'activité. *Compt. Rend. Acad. Sc., Paris,* 246: 2934, 1958.
25. Cranefield, P. F., J. A. E. Eyster, and W. E. Gilson. Effects of reduction of external sodium chloride on the injury potentials of cardiac muscle. *Am. J. Physiol.* 166: 269, 1951.
26. Cranefield, P. F., J. A. E. Eyster, and W. E. Gilson. Electrical characteristics of injury potentials. *Am. J. Physiol.* 167: 450, 1951.
27. Cranefield, P. F. and B. F. Hoffman. Electrophysiology of single cardiac cells. *Physiol. Rev.* 38: 41, 1958.
28. Cranefield, P. F. and B. F. Hoffman. Propagated repolarization in heart muscle. *J. Gen. Physiol.* 41: 633, 1958.
29. Curtis, H. J. and K. S. Cole. Membrane resting and action potentials from the squid giant axon. *J. Cell. & Comp. Physiol.* 19: 135, 1942.
30. Dean, R. B. Theories of electrolyte equilibrium in muscle. *Biological Symposia* 3: 331, 1941.
31. Déleze, J. Perfusion of a strip of mammalian ventricle. Effects of K-rich and Na-deficient solutions on transmembrane potentials. *Circulation Res.* 7: 461, 1959.
32. Dodge, F. A. and B. Frankenhaeuser. Membrane currents in isolated frog nerve fibre under voltage clamp conditions. *J. Physiol.* 143: 76, 1958.
33. Dodge, F. A. and B. Frankenhaeuser. Sodium currents in the myelinated nerve fibre of *Xenopus laevis* investigated with the voltage clamp technique. *J. Physiol.* 148: 188, 1959.
34. Draper, M. H. and M. Mya-Tu. A comparison of the conduction velocity in cardiac tissues of various mammals. *Quart. J. Exper. Physiol.* 44: 91, 1959.
35. Draper, M. H. and S. Weidmann. Cardiac resting and action potentials recorded with an intracellular electrode. *J. Physiol.* 115: 74, 1951.
36. Dudel, J. and W. Trautwein. Die Wirkung von Adrenalin auf das Ruhepotential von Myokardfasern des Vorhofs. *Experientia* 12: 396, 1955.
37. Dudel, J. and W. Trautwein. Der mechanismus der automatischen rhythmischen Impulsbildung der Herzmuskelfaser. *Pflügers Arch. ges. Physiol.* 267: 553, 1958.
38. Eccles, J. C. *The Physiology of Nerve Cells.* Baltimore: Johns Hopkins Press, 1957.
39. Finean, J. B. X-ray diffraction studies of the myelin sheath in peripheral and central nerve fibres. *Exper. Cell. Res. Suppl.* 5: 18, 1958.
40. FitzHugh, R. Thresholds and plateaus in the Hodgkin-Huxley nerve equations. *J. Gen. Physiol.* 43: 867, 1960.
41. Florey, E. (Ed.) *Nervous Inhibition.* New York: Pergamon Press, 1961.
42. Frank, K. Identification and analysis of single unit activity in the central nervous system. In: *Handbook of Physiology.* Washington: American Physiological Society, 1959, sect. 1 vol. I, p. 261.
43. Frankenhaeuser, B. Steady state inactivation of sodium permeability in myelinated nerve fibres of *Xenopus laevis.* *J. Physiol.* 148: 671, 1959.
44. Frankenhaeuser, B. and A. L. Hodgkin. The after-effects of impulses in the giant nerve fibres of *Loligo.* *J. Physiol.* 131: 341, 1956.
45. Frankenhaeuser, B. and A. L. Hodgkin. The action of calcium on the electrical properties of squid axons. *J. Physiol.* 137: 218, 1957.
46. Frazier, H. S. and R. D. Keynes. The effect of metabolic inhibitors on the sodium fluxes in sodium-loaded frog sartorius muscle. *J. Physiol.* 148: 362, 1959.
47. Freygang, W. H. and R. H. Adrian. Rectification in muscle membrane. *Fed. Proc.* 19: 135, 1960.
48. Gargouïl, Y. M., R. Tricoche, D. Fromenty, and É. Coraboeuf. Effets de l'adrénaline sur l'activité électrique du coeur de mammifères. *Compt. Rend. Acad. Sc., Paris,* 246: 334, 1958.
49. Goldman, D. E. Potential, impedance and rectification in membranes. *J. Gen. Physiol.* 27: 37, 1943.
50. Graham, Judith and R. W. Gerard. Membrane potentials and excitation of impaled single muscle fibers. *J. Cell. & Comp. Physiol.* 28: 99, 1946.
51. Hajdu, S. Mechanism of staircase and contracture in ventricular muscle. *Am. J. Physiol.* 174: 371, 1953.
52. Hodgkin, A. L. The ionic basis of electrical activity in nerve and muscle. *Biol. Rev.* 26: 339, 1951.
53. Hodgkin, A. L. The Croonian Lecture. Ionic movements and electrical activity in giant nerve fibres. *Proc. Roy. Soc., London, Ser. B* 148: 1, 1958.
54. Hodgkin, A. L. and P. Horowicz. Movements of Na and K in single muscle fibres. *J. Physiol.* 145: 405, 1959.
55. Hodgkin, A. L. and P. Horowicz. The influence of potassium and chloride ions on the membrane potential of single muscle fibres. *J. Physiol.* 148: 127, 1959.
56. Hodgkin, A. L. and A. F. Huxley. Resting and action potentials in single nerve fibres. *J. Physiol.* 104: 176, 1945.
57. Hodgkin, A. L. and A. F. Huxley. Currents carried by sodium and potassium ions through the membrane of the giant axon of *Loligo.* *J. Physiol.* 116: 449, 1952.
58. Hodgkin, A. L. and A. F. Huxley. The components of membrane conductance in the giant axon of *Loligo.* *J. Physiol.* 116: 473, 1952.

59. HODGKIN, A. L. AND A. F. HUXLEY. The dual effect of membrane potential on sodium conductance in the giant axon of *Loligo*. *J. Physiol.* 116: 497, 1952.
60. HODGKIN, A. L. AND A. F. HUXLEY. A quantitative description of membrane current and its application to conduction and excitation in nerve. *J. Physiol.* 117: 500, 1952.
61. HODGKIN, A. L. AND A. F. HUXLEY. Movement of radioactive potassium and membrane current in a giant axon. *J. Physiol.* 121: 403, 1953.
62. HODGKIN, A. L., A. F. HUXLEY, AND B. KATZ. Measurement of current-voltage relations in the membrane of the giant axon of *Loligo*. *J. Physiol.* 116: 424, 1952.
63. HODGKIN, A. L. AND B. KATZ. The effect of sodium ions on the electrical activity of the giant axon of the squid. *J. Physiol.* 108: 37, 1949.
64. HODGKIN, A. L. AND R. D. KEYNES. Active transport of cations in giant axons from *Sepia* and *Loligo*. *J. Physiol.* 128: 28, 1955.
65. HODGKIN, A. L. AND R. D. KEYNES. The potassium permeability of a giant nerve fibre. *J. Physiol.* 128: 61, 1955.
66. HODGKIN, A. L. AND W. A. H. RUSHTON. The electrical constants of a crustacean nerve fibre. *Proc. Roy. Soc., London, Ser. B*, 133: 144, 1946.
67. HODGMAN, C. D. (editor). *Handbook of Chemistry and Physics* (37th ed.) Cleveland: Chemical Rubber Publishing Co., 1955, p. 3095.
68. HOFFMAN, B. F. AND P. F. CRANEFIELD. *Electrophysiology of the Heart*. New York: McGraw-Hill, 1960.
69. HOFFMAN, B. F., P. F. CRANEFIELD, E. LEPESCHKIN, B. SURAWICZ, AND H. C. HERRLICH. Comparison of cardiac monophasic action potentials recorded by intracellular and suction electrodes. *Am. J. Physiol.* 196: 1297, 1959.
70. HOFFMAN, B. F. AND E. E. SUCKLING. Cardiac cellular potentials: effect of vagal stimulation and acetylcholine. *Am. J. Physiol.* 173: 312, 1953.
71. HOFFMAN, B. F. AND E. E. SUCKLING. Effects of several cations on transmembrane potentials of cardiac muscle. *Am. J. Physiol.* 186: 317, 1956.
72. HUTTER, O. F. Mode of action of autonomic transmitters on the heart. *Brit. M. Bull.* 13: 176, 1957.
73. HUTTER, O. F. AND D. NOBLE. The influence of anions on impulse generation and membrane conductance in Purkinje and myocardial fibres. *J. Physiol.* 147: 16P, 1959.
74. HUTTER, O. F. AND D. NOBLE. The chloride conductance of frog skeletal muscle. *J. Physiol.* 151: 89, 1960.
75. HUTTER, O. F. AND D. NOBLE. Rectifying properties of heart muscle. *Nature, London* 188: 495, 1960.
76. HUTTER, O. F. AND W. TRAUTWEIN. Vagal and sympathetic effects on the pacemaker fibers in the sinus venosus of the heart. *J. Gen. Physiol.* 39: 715, 1956.
77. HUXLEY, A. F. Ion movements during nerve activity. *Ann. New York Acad. Sc.* 81: 221, 1959.
78. HUXLEY, A. F. Local activation of muscle. *Ann. New York Acad. Sc.* 81: 446, 1959.
79. HUXLEY, A. F. AND R. E. TAYLOR. Local activation of striated muscle fibres. *J. Physiol.* 144: 426, 1958.
80. JOHNSON, E. A., P. A. ROBERTSON, AND J. J. TILLE. Purkinje and ventricular membrane resistances during the rising phase of the action potential. *Nature, London* 182: 1161, 1958.
81. JOHNSON, J. A. Sodium exchange in the frog heart ventricle. *Am. J. Physiol.* 191: 487, 1957.
82. KAVELER, F. Membrane depolarization and contraction in auricle. *Fed. Proc.* 19: 109, 1960.
83. KEYNES, R. D. The ionic movements during nervous activity. *J. Physiol.* 114: 119, 1951.
84. KEYNES, R. D. AND G. W. MAISEL. The energy requirements for sodium extrusion from a frog muscle. *Proc. Roy. Soc., London, Ser. B*, 142: 383, 1954.
85. KEYNES, R. D. AND R. C. SWAN. The effect of external sodium concentration on the sodium fluxes in frog skeletal muscle. *J. Physiol.* 147: 591, 1959.
86. KEYNES, R. D. AND R. C. SWAN. The permeability of frog muscle fibres to lithium ions. *J. Physiol.* 147: 626, 1959.
87. LING, G. AND R. W. GERARD. The normal membrane potential of frog sartorius fibers. *J. Cell. & Comp. Physiol.* 34: 383, 1949.
88. LORENTE DE NÓ, RAFAEL. A study of nerve physiology. *Studies from the Rockefeller Institute for Medical Research*, Vols. 131 and 132, 1947.
89. LÜTTGAU, H. C. AND R. NIEDERGERKE. The antagonism between Ca and Na ions on the frog's heart. *J. Physiol.* 143: 486, 1958.
90. MARMONT, G. Studies on the axon membrane. *J. Cell. & Comp. Physiol.* 34: 351, 1949.
91. MOORE, D. H. AND H. RUSKA. Electron microscope study of mammalian cardiac muscle cells. *J. Biophys. & Biochem. Cytol.* 3: 261, 1957.
92. MOORE, J. W. Excitation of the squid axon membrane in isosmotic potassium chloride. *Nature, London* 183: 265, 1959.
93. MUIR, A. R. An electron microscope study of the embryology of the intercalated disc in the heart of the rabbit. *J. Biophys. & Biochem. Cytol.* 3: 193, 1957.
94. MUIR, A. R. Observations on the fine structure of the Purkinje fibres in the ventricles of the sheep's heart. *J. Anat.* 91: 251, 1957.
95. NASTUK, W. L. AND A. L. HODGKIN. The electrical activity of single muscle fibers. *J. Cell & Comp. Physiol.* 35: 39, 1950.
96. NIEDERGERKE, R. Calcium and the activation of contraction. *Experientia* 15: 128, 1959.
97. NIEDERGERKE, R. AND E. J. HARRIS. Accumulation of calcium (or strontium) under conditions of increasing contractility. *Nature, London* 179: 1068, 1957.
98. NOBLE, D. Cardiac action and pacemaker potentials based on the Hodgkin-Huxley equations. *Nature, London* 188: 495, 1960.
99. OTSUKA, M. Die Wirkung von Adrenalin auf Purkinje-Fasern von Saügetierherzen. *Pflügers Arch. ges. Physiol.* 266: 512, 1958.
100 Physiology of the cell membrane. Symposium held at the Instituto Venezolano de Investigaciones Científicas, Caracas, Venezuela, 1959. *J. Gen. Physiol.* 43 (5, pt. 2): 1, 1960.
101. RAYNER, BARBARA AND M. WEATHERALL. Acetylcholine and potassium movements in rabbit auricles. *J. Physiol.* 146: 392, 1959.
102. REICHEL, H. AND A. BLEICHERT. Excitation-contraction coupling in heart muscle. *Nature, London* 183: 826, 1959.

103. Robertson, J. D. The cell membrane concept. *J. Physiol.* 140: 58P, 1957.
104. Sano, T., N. Takayama, and T. Shimamoto. Directional difference of conduction velocity in the cardiac ventricular syncytium studied by microelectrodes. *Circulation Res.* 7: 262, 1959.
105. Schütz, E. Elektrophysiologie des Herzens bei einphasischer Ableitung. *Ergebn. Physiol.* 38: 493, 1936.
106. Shanes, A. M. Electrochemical aspects of physiological and pharmacological action in excitable cells. I. The resting cell and its alteration by extrinsic factors. II. The action potential and excitation. *Pharmacol. Rev.* 10: 59, 165, 1958.
107. Sjöstrand, F. S. and E. Andersson-Cedergren. Intercalated discs of heart muscle. In: *The Structure and Function of Muscle*, edited by G. H. Bourne. New York: Academic Press, 1960, vol. 1, p. 421.
108. Sjöstrand, F. S., E. Andersson-Cedergren, and M. M. Dewey. The ultrastructure of the intercalated discs of frog, mouse and guinea pig cardiac muscle. *J. Ultrastruct. Res.* 1: 271, 1958.
109. Sperelakis, N., T. Hoshiko, and R. M. Berne. Nonsyncytial nature of cardiac muscle: membrane resistance of single cells. *Am. J. Physiol.* 198: 531, 1960.
110. Spyropoulos, C. S. Miniature responses under 'voltage-clamp'. *Am. J. Physiol.* 196: 783, 1959.
111. Tanaka, I. Apparent membrane resistance changes during repolarization in the toad atrium. *Fed. Proc.* 18: 156, 1959.
112. Tasaki, I. Conduction of the nerve impulse. In: *Handbook of Physiology* Washington: American Physiological Society, 1959, sect. 1, vol. I, p. 75.
113. Tasaki, I. and S. Hagiwara. Capacity of muscle fiber membrane. *Am. J. Physiol.* 188: 423, 1957.
114. Tasaki, I. and S. Hagiwara. Demonstration of two stable potential states in the squid giant axon under tetraethylammonium chloride. *J. Gen. Physiol.* 40: 859, 1957.
115. Tasaki, I. and C. S. Spyropoulos. Nonuniform response in the squid axon membrane under 'voltage-clamp'. *Am. J. Physiol.* 193: 309, 1958.
116. Thomas, L. J. Increase of labeled calcium uptake in heart muscle during potassium lack contracture. *J. Gen. Physiol.* 43: 1193, 1960.
117. Trautwein, W. and J. Dudel. Aktionspotential und Mechanogramm des Warmblüterherzmuskels als Funktion der Schlagfrequenz. *Pflügers. Arch. ges. Physiol.* 260: 24, 1954.
118. Trautwein, W. and J. Dudel. Aktionspotential und Mechanogramm des Katzenpapillarmuskels als Funktion der Temperatur. *Pflügers. Arch. ges. Physiol.* 260: 104, 1954.
119. Trautwein, W. and J. Dudel. Zum Mechanismus der Membranwirkung des Acetylcholin an der Herzmuskelfaser. *Pflügers. Arch. ges. Physiol.* 266: 324, 1958.
120. Trautwein, W. and J. Dudel. Hemmende und 'erregende' Wirkungen des Acetylcholin am Warmblüterherzen. Zur Frage der spontanen Erregungsbildung. *Pflügers Arch. ges. Physiol.* 266: 653, 1958.
121. Trautwein, W., U. Gottstein, and K. Federschmidt. Der Einfluss der Temperatur auf den Aktionsstrom des excidierten Purkinje-Fadens gemessen mit einer intracellulären Elektrode. *Pflügers. Arch. ges. Physiol.* 258: 243, 1953.
122. Trautwein, W., S. W. Kuffler, and C. Edwards. Changes in membrane characteristics of heart muscle during inhibition. *J. Gen. Physiol.* 40: 135, 1956.
123. Ussing, H. H. The distinction by means of tracers between active transport and diffusion. *Acta physiol. scandinav.* 19: 43, 1949.
124. Ussing, H. H. Transport of ions across cellular membranes. *Physiol. Rev.* 29: 127, 1949.
125. Weidmann, S. Effect of current flow on the membrane potential of cardiac muscle. *J. Physiol.* 115: 227, 1951.
126. Weidmann, S. The electrical constants of Purkinje fibres. *J. Physiol.* 118: 348, 1952.
127. Weidmann, S. The effect of the cardiac membrane potential on the rapid availability of the sodium-carrying system. *J. Physiol.* 127: 213, 1955.
128. Weidmann, S. Effects of calcium ions and local anaesthetics on electrical properties of Purkinje fibres. *J. Physiol.* 129: 568, 1955.
129. Weidmann, S. *Elektrophysiologie der Herzmuskelfaser* Bern: Huber, 1956.
130. Weidmann, S. Shortening of the cardiac action potential due to a brief injection of KCl following the onset of activity. *J. Physiol.* 132: 157, 1956.
131. Weidmann, S. Resting and action potentials of cardiac muscle. *Ann. New York Acad. Sc.* 65: 663, 1957.
132. Weidmann, S. Effect of increasing the calcium concentration during a single heart-beat. *Experientia* 15: 128, 1959.
133. Weidmann, S. Sheep heart; low resistance of intercalated disks to the movement of ^{42}K. *J. Physiol.* 153: 32P, 1960.
134. West, T. C., G. F. Falk, and P. Cervoni. Drug alteration of transmembrane potentials in atrial pacemaker cells. *J. Pharmacol.* 117: 245, 1956.
135. Woodbury, J. W. In: *Medical Physiology and Biophysics* (18th ed.), edited by T. C. Ruch and J. F. Fulton. Philadelphia: Saunders, 1960, p. 2.
136. Woodbury, J. W. and A. J. Brady. Intracellular recording from moving tissues with a flexibly mounted ultramicroelectrode. *Science* 123: 100, 1956.
137. Woodbury, J. W., J. Lee, A. J. Brady, and K. A. Merendino. Transmembranal potentials from the human heart. *Circulation Res.* 5: 179, 1957.
138. Woodbury, J. W. and H. D. Patton. In: *Medical Physiology and Biophysics* (18th ed.), edited by T. C. Ruch and J. F. Fulton. Philadelphia: Saunders, 1960, p. 32.
139. Woodbury, L. A., H. H. Hecht, and A. R. Christopherson. Membrane resting and action potentials of single cardiac muscle fibers of the frog ventricle. *Am. J. Physiol.* 164: 307, 1951.
140. Woodbury, L. A., J. W. Woodbury, and H. H. Hecht. Membrane resting and action potentials of single cardiac muscle fibers. *Circulation* 1: 264, 1950.

Excitation of the heart

ALLEN M. SCHER | *Department of Physiology and Biophysics, University of Washington School of Medicine, Seattle, Washington*

CHAPTER CONTENTS

FUNCTIONAL ANATOMY

THE WAY in which the electrical impulse spreads through a particular heart is determined by the gross geometry of that heart, and by the position within it of the specialized conduction tissue that both generates and "distributes" the impulse. It is an anatomical rather than a physiological problem to discuss in detail the geometry of a great many hearts and we will presume a rather standard cardiac conformation (figs. 1, 2). The distribution of the specialized tissue in a variety of invertebrate and vertebrate hearts has been described in a number of excellent papers (1, 2, 27, 28, 35–37, 63–65, 78, 81, 83, 86–88, 93, 96, 97, 127, 129, 135–137, 139, 143, 144).

Specialized Tissue

The specialized tissue comprises two or three cell types with a fairly constant distribution through the hearts of various warm-blooded species. There are similar cells in lower forms. It includes the pacemaker cells of the sinus node, which initiate the beat of the mammalian heart, and similar cells that lie in the sinus venosus in lower forms. These pacemaker cells anatomically resemble the A-V nodal cells (see below), which are generally considered the "next" group of specialized cells and which are first in the train of cells transmitting the impulse from atrium to ventricle. The A-V nodal cells are connected to the cells of the common bundle and the right and left conducting bundles. The right and left conducting bundles also give rise to a large number of cells lining the endocardium and distributing the impulse within the

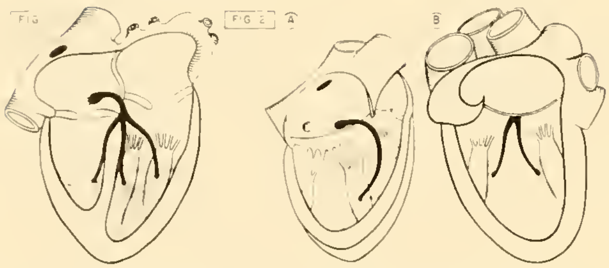

FIG. 1. Diagrammatic view of heart showing cavities of both ventricles and atria. At upper left, superior and inferior venae cavae may be seen entering left atrium. Black ellipse in this area indicates region of sinoatrial node. Atrioventricular node is indicated above tricuspid valve cusps in interatrial septum. Right bundle passes down into right ventricle; the two branches of left bundle pass into left ventricle. Numerous Purkinje branches cross ventricular cavity on both sides. [From Scher (114a).]

FIG. 2. The conduction system as seen from the right and left sides. In *A:* right bundle terminates near anterior papillary muscle on the right. In *B:* the two branches of left bundle pass to general regions of anterior and posterior papillary muscles on the left. Much of the Purkinje tissue lining the endocardium is not represented. [From Scher (114a).]

ventricles, in the various mammalian forms which have been studied.

It is common (129), although not strictly correct, to refer to all of these cells as "Purkinje cells." Properly, this term should be restricted to those cells which distribute the impulse in the ventricles, and which were originally described by Purkinje (93). The reasons why the term Purkinje fibers is extended to other cells are that some of the anatomical characteristics overlap and that the A-V nodal cells are directly connected to the Purkinje fibers of the common bundle. Furthermore, since Purkinje's description, various anatomists have found cells, which they believe to be Purkinje fibers, at a large number of locations in both the atria and the ventricles, and in a variety of hearts. These findings have somewhat weakened the specificity of the description of these cells.

Myocardial Cells

Ordinary heart muscle cells are striated like skeletal muscle. Their diameter ranges from 15 to 25μ. The length is not definitely known since available electron micrographs do not show both ends of a cell; length is probably 150μ. Within the fibers or trabeculae are slightly oval nuclei placed on transverse sections. The cytoplasm shows cross striations. The sarcolemma surrounding the nucleus contains the contractile fibrils. Submicroscopic details as well as the syncytial organization of the cells have been mentioned in Chapter 11.

Pacemaker Cells

The sinoauricular node, the pacemaker of the heart, was discovered by Keith & Flack (63) who noted tissue, similar to that previously discovered by Tawara (127) in the atrioventricular node, at the junction of the superior vena cava and auricle. A portion of their description follows:

"In the human heart the fibres are striated, fusiform, with well-marked elongated nuclei, plexiform in arrangement, and embedded in densely packed connective tissue—in fact, of closely similar structure to the Knoten [referring to the auriculoventricular node]. The special neuromuscular system lies at the junction of the free border of the appendix with the mouth of the superior cava, and extends downwards along the sulcus terminalis for a distance of about 2 cm in man. In thickness it is approximately 2 mm. The muscular fibres are small, being but a half or third the breadth of those of auricular fibres proper."

Pacemaker cells are found in the sinus venosus of the vertebrate heart and it appears that similar pacemakers exist in the hearts of all species (36, 64, 67, 86, 123). The pacemaker cells are, as indicated, about 10μ in diameter in man or the dog.

The S-A node, like the A-V node, is richly supplied with nerve endings and ganglion cells. As has been mentioned, the sinus node is the pacemaker of the heart and the electrical signs of cardiac activity for each beat commence in the node and travel thence over the remainder of the atrium.

The Atria: Atrial Conduction System

It is generally felt that (with the exception of the region around the A-V node which will be discussed below) atrial muscle is not composed of more than one functional type of cell. One source of contention is the presence or absence of an atrial conduction system or, more generally, of Purkinje fibers distributed within the atria. The atria of birds, fish, reptiles, and mammals have been studied. In the first of these a well-developed atrial conduction system has been described (35, 78, 86). Arguments have been advanced and some evidence presented that an extensive atrial conduction system exists, or that there are Purkinje cells, in the atrium in the other forms. The literature on this subject is surprisingly extensive and

guides to it have been included in the references to this chapter (27, 48, 64, 81, 83, 84, 128, 129). Some consideration will be given later to the physiological evidence on this point.

Atrioventricular Conduction System

The A-V node (127) is a mass of specialized tissue anatomically resembling the sinus node. The A-V node lies above the interventricular septum in the interatrial septum, approximately above the central portion of the tricuspid valve. There is some question about the anatomy of the cells on the border between ordinary atrial musculature and the cells of the A-V node. It appears that on this boundary there are cells which are intermediate between the atrial and the nodal cells and/or cells which are somewhat different from either and smaller. Indeed, several "nodes" have been named in this area (8, 27, 68). Also, there is some feeling that a specific internodal (S-A to A-V) pathway exists. The node, as mentioned,

FIG. 3. Distribution of the left bundle in goat heart as shown through injection. Left bundle emerges beneath the aortic valve as a single bundle. It gives rise to two branches which cross the cavity, one running to the anterior and one to the posterior papillary muscle, and to two branches which run to the endocardium between the papillary muscles. Note the numerous fibers crossing the cavity and those forming an extensive endocardial network. [From Aagaard & Hall (1).]

lies somewhat posteriorly and at the right border of the interatrial septum, but at times the node is apparently displaced from this rightward position (27). In man the node is about 2 mm in width and height and 3 mm long, and gives rise to the common bundle.

A-V Conduction System in Lower Forms

The atrioventricular ring of the turtle contains cells resembling the Purkinje fibers of other hearts (96). These cells cross the A-V ring and apparently conduct the impulse from the atrium to the ventricle. They are similar to the atrioventricular plug in the frog (16, 88) and fowl (86), and the atrioventricular bundle in the reptile (87). Concerning the last there is some disagreement (37).

Purkinje Fibers of the Ventricle

The common bundle and the right and left bundles in most animals consist of large Purkinje cells that can be easily identified histologically (17, 64, 97, 135). In the mammal the common bundle commences at the A-V node, runs to the left, and passes through the membranous septum. After passing through this septum, a little in front of the septal leaflet of the tricuspid valve, the common bundle breaks up into the left and right bundles. The right bundle moves onto the endocardial surface of the septum and proceeds, with a slight curvature, to the anterior papillary muscle of the right ventricle (fig. 2). Here it arborizes. The arborizations apparently run to both the septal surface and the free wall of the right ventricle. The left bundle moves through the membranous septum and spreads, fanwise, beneath the aortic valves on the left, so that no clear bundle is discernible for 1 or 2 mm below the aortic valve. The bundle then passes down the septum and gives rise to several branches which conduct the impulse into the ventricles (fig. 2). Some branches cross the basal left cavity as they pass from the septal surface to the papillary muscles on the left. In man and in the dog there appear to be two main branches of the left bundle, which run to the anterior and posterior papillary muscles, respectively. In other animals (1, 71, 136, 137) it appears that the left bundle is not so discretely separated into two branches. There may well be other branches of the left bundle in man and in dog. The subsidiary branches may lie between the two major branches as they descend the left septal surface (fig. 3). The two major branches of the left

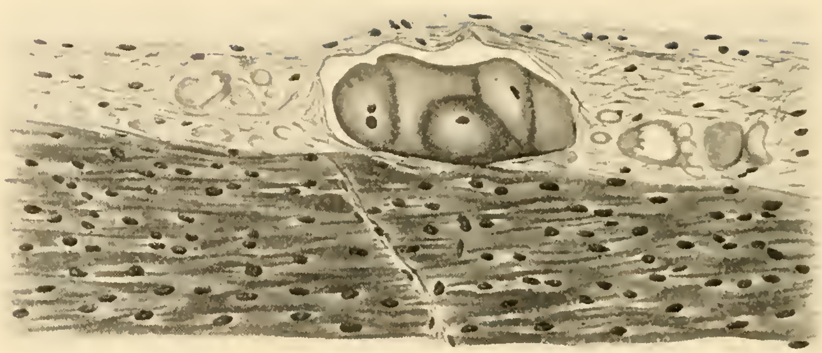

FIG. 4. Purkinje distribution near the endocardium in the goat. The dark muscle fibers below are ordinary myocardium; the lighter ones above are the specialized cells which line the endocardium. Oriented toward the bottom and to the right is a small strand of Purkinje tissue penetrating the muscle. Note the gray circles and tubes around the large subendocardial layer. These are portions of the sheath which surrounds many of the specialized cells. No sheath surrounds the small fibers which penetrate the muscle. [From Aagaard & Hall (1).]

bundle terminate near the anterior and posterior papillary muscles. The bundles give rise to numerous Purkinje fibers subendocardially on the right and left.

Many of the finer ramifications of this Purkinje network can be seen as small strands of muscle crossing the cavities between the trabeculae, particularly on the left and in the apical region of the heart. The specialized tissue is more clearly identifiable, both grossly and histologically, in the ungulates. Portions of it can, however, be grossly identified in the dog and in man. For instance, the right bundle is often readily apparent to the moderately trained eye, as are the branches of the left bundle. The fine fibers which cross the cavities are also clearly identifiable. In the ungulates, the larger branches of the Purkinje system are encased in a connective tissue sheath which can be injected with dyes to delineate a large part of the course of the Purkinje fibers. It has, however, been shown (1) that many of the fine Purkinje branches which penetrate the muscle in the ungulates are not surrounded by this sheath (fig. 4). It is undoubtedly necessary that the sheath disappear before Purkinje fibers can excite the myocardium. The characteristics of Purkinje fibers in the birds and various mammalian species have been summarized by Truex & Copenhaver (135) with particular reference to the glycogen content.

"In comparison with cardiac muscle fibers, Purkinje fibers are usually larger, contain fewer myofibrillae, have more interfibrillar sarcoplasm, and give a distinctly clearer less compact appearance. The center of the fiber, being devoid of myofibrillae, is filled with a granular sarcoplasm in which the nuclei are usually in groups of two or more. . . until recently it was assumed that the Purkinje fibers of the conduction system were comparatively rich in glycogen, whereas the cardiac muscle had only a meager amount or no glycogen."

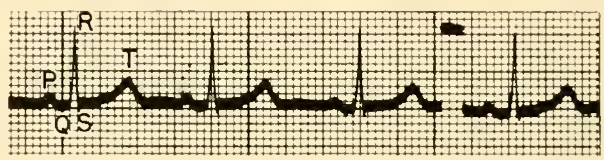

FIG. 5. Normal lead II electrocardiogram. Initial, low, rounded deflection about 1 mm high and 2 mm long is the P wave. Second deflection, about 10 mm high and 1 mm wide. shows a rapid rise and fall and is the QRS complex. Third, peaked deflection, about 3.5 mm high and 6 mm long, is the T wave. Sequence is repeated three times. Standardization at right, 1 mv. Small black vertical lines are 40 msec apart; larger lines (five spaces) are 200 msec apart; heaviest lines are 1 sec apart. [From Winsor (146).]

They go on to give data concerning relative amounts of glycogen in myocardium and Purkinje tissue. In their own studies Purkinje fibers were found to be about twice the size of ventricular myocardial fibers in the sheep (30.9μ vs. 12.6μ), pig (37.2μ vs. 14.3μ), calf (26.5μ vs. 11.1μ) and beef (43.6μ vs. 15.0μ), whereas in man the relation was closer to 1:1 (20.6μ vs. 16.1μ). The relations in cat and monkey were similar to that in man. Truex and Copenhaver further comment on the frequency of Purkinje fibers in the moderator band in various species. The glycogen content was quite variable in their specimens. It is worthwhile in passing to note that the existence of a conduction system in the dog and in man was quite recently denied by some anatomists (47) who had at one time a considerable following.

Accessory Pathway for A-V Conduction

In Kent's studies (64) he stated that the A-V node and its Purkinje branches are not the sole connection between the atria and ventricle. He found an apparent

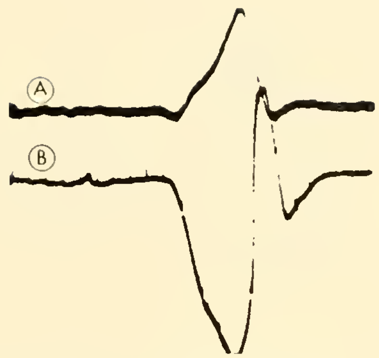

FIG. 6. *A:* lead II QRS in the dog. *B:* simultaneous unipolar record of electrical activity high in posterior interventricular septum. *B* shows an initial negative (downward) deflection caused by receding activity in apical ventricle. As activity approaches electrode, voltage goes through zero to a positive value. Depolarization in this septal region (final, fast, negative-going deflection) begins at about time of S wave in the electrocardiogram. A small potential from Purkinje tissue precedes the QRS deflection by about 22 msec on *B*. The lower negative-positive-negative potential is recorded in the very last ventricular regions to be excited. With a slow recording system, the initial negative-going portion and the terminal negative-going portion might be confused. Local activity occurs during the latter period, but the potential shape provides no clear proof of this. [From Scher & Young (119).]

A-V connection composed of ordinary myocardial cells. This connection has since been the subject of some controversy (65).

Other Anatomical Details

The following additional structural details are important in the consideration of ventricular electrical activity in man or the dog. The right wall is generally no more than 3 or 4 mm thick; the left wall is much thicker, up to 15 mm, except in infants whose two ventricular walls are about equally thick. The endocardial Purkinje network is more widespread in the central and apical portions of the wall and septum bilaterally. This network is sparse or nonexistent in the basal septum.

EXCITATION OF THE HEART

Electrical activity of the heart produces potentials at the body surface which are referred to as an electrocardiogram. The shape of the recorded complex varies with a number of factors and a normal record is presented for reference (fig. 5). The P wave signals atrial depolarization; the QRS, complex ventricular depolarization; and the T wave, ventricular repolarization.

All our direct knowledge of the pathway of cardiac excitation is derived from animal experiments, most of them on dogs. Although the various components of the canine electrocardiogram last about one-half as long as do those of the human cycle, it is customary to consider results obtained in dogs as applicable to man. This extrapolation is justified by two facts: *1*) human and canine hearts are anatomically similar, both grossly and histologically, and *2*) electrocardiograms of similar shape can be recorded from both hearts if the differences in heart position are taken into account (125, 126, 146). It might seem possible to determine the pathway of cardiac excitation by studying the body surface electrocardiogram. It is, however, implicit in Green's theorem in electricity and magnetism (60), and has been stated by Helmholtz (55) and Lorente de Nó (73), that if one knows only the potential distribution at the surface of a body, one cannot determine a unique internal generator. For this reason it is theoretically impossible to determine the exact pathway of excitation by knowing only the potentials which occur at the body surface, or even at the surface of the ventricles. Since the cardiac anatomy is so well known, prediction of a likely pathway of excitation of anatomical grounds might seem possible. This prediction could then be verified by deriving from it, at least qualitatively, electrocardiograms which could be compared with those actually recorded. Attempts to formulate such a prediction have been made by various experts. They have been successful (46) but never entirely so. For this reason it appears to be necessary to trace the pathway of excitation through the heart.

In the case of a thin-walled chamber like the atrium, it has been assumed, undoubtedly correctly, that the wall can be considered a sheet, and that no details are needed on what happens between the endocardial and epicardial surfaces. In the case of the thicker walls of the ventricles, however, no such assumptions can be made. If we place an electrode on or near cardiac muscle and record the potential difference between this electrode and another electrode at a distance, the recorded potential will be positive if the net sum of activity is approaching the electrode, i.e., if the recording locus "sees" more approaching than receding activity (14, 32). A negative potential will be recorded if the net sum of activity is receding from the recording point. It might seem that potentials of this sort would enable us to completely plot the activation of a thin strip of muscle,

and indeed, in the studies of atrial excitation to be cited below, a great deal of success has been achieved with this technique. In contrast, this use of positive and negative potentials is of much more restricted value in the case of a larger and more complicated mass of myocardium like the ventricles. Indeed some serious errors are possible (fig. 6). The use of potential shape as an indication of sequence of activity is unreliable, since if an electrode records a positive potential at a particular instant we can only say that activity is approaching, we do not know from which direction, or how close. In the unipolar potential we would expect to see a rapid negative-going potential as the wave passed the recording site, and a continuation of negativity as it retreated from the recording site. The attempt has been made to use this negative-going portion of an extracellularly recorded lead to determine the instant of local activity. This particular instant, however, is often not clearly and unequivocally discernible on such a unipolar record. Further, the negative-going phase can be superimposed on a negative or on a positive potential.

In the above discussion the unipolar record is considered as taken between an exploring electrode and a truly distant point which averages all potentials. In the open-chest animal (30) the "unipolar" record may in fact be a "bipolar" between the exploring electrode and the place where the heart makes contact with the body. Also, the conductivity of the surrounding media may grossly alter unipolar potentials.

Ideally, an intracellular record may be substituted for the extracellular unipolar record. Here the rapid depolarization phase, lasting less than 1 msec, is an accurate indication of local activity. Unfortunately, use of intracellular electrodes is not a practical method of studying thick masses of muscle. One substitute for attempting to read the inflection point on a unipolar extracellular record would be to take the first derivative of the record. This derivative should indicate the most rapid rate of change of potential at the recording point, and should give a brief spike potential which reaches its peak as the wave passes the recording point. An approximation of this derivative can be achieved by recording the potential between two electrodes which are very close to one another in the muscle. The derivative of the unipolar record is, of course, the rate of change of voltage with respect to time (dv/dt). The approximation which is made by taking the voltage change between two close electrodes is to determine as closely as possible the rate of change of voltage with distance (dv/dx). The accuracy of this approximation depends entirely on the assumption that a propagated wave of activity passes the two points and moves in a consistent direction not parallel to the line joining the points. It has been verified several times that this space derivative indicates the instant of local activity (40, 75, 106, 114).

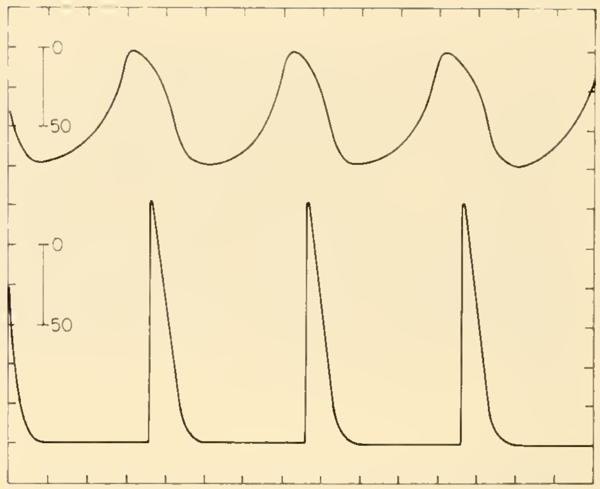

FIG. 7. *Upper trace:* potentials recorded by ultramicroelectrode in the pacemaker region. *Lower trace:* potentials simultaneously recorded by second ultramicroelectrode in normal atrial tissue. [After West *et al.* (142).]

The Cardiac Pacemaker; Excitation of Atrium

One property of cardiac tissue is automaticity—the ability to beat rhythmically without external stimuli. The cells with the most rapid inherent rhythm are called pacemaker cells. In cold-blooded animals, pacemaker activity seems to be possible for all parts of the heart, but in intact warm-blooded animals pacemaker activity is normally confined to the S-A and the A-V nodes (fig. 7). Other parts of the Purkinje system may also normally generate impulses, but it is not certain that all portions of the mammalian heart can do so normally. However, it is clear that with even minor departures from the normal state extrasystolic (i.e., abnormal) beats may originate at both atrial and ventricular sites. The pacemaker with the highest inherent rhythm will ordinarily dominate the heart rate, and the impulses conducted from it will depolarize slower pacemakers faster than they can generate impulses. Normally, the dominant pacemaker is the S-A node. The A-V node is the pacemaker with the second highest inherent rate; if the S-A node fails or is abnormally slowed, the A-V node will usually control the heart rate.

As has been previously indicated, the sinus node has a characteristic intracellular potential with a

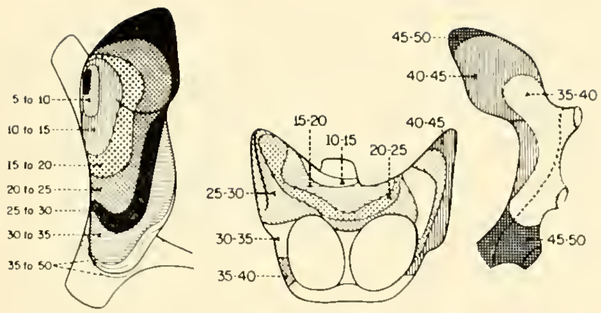

FIG. 8. Pathway and mode of atrial activation. *Left:* right atrium and right atrial appendage viewed from right. Activity begins in sinus node (black) and progresses toward borders of atrium. *Center:* activation of atria viewed from anterior aspect. *Right:* activation of left atrium and appendage. Shading shows areas activated within each 5-msec period. Duration of P wave was 50 msec. [After Puech (92).]

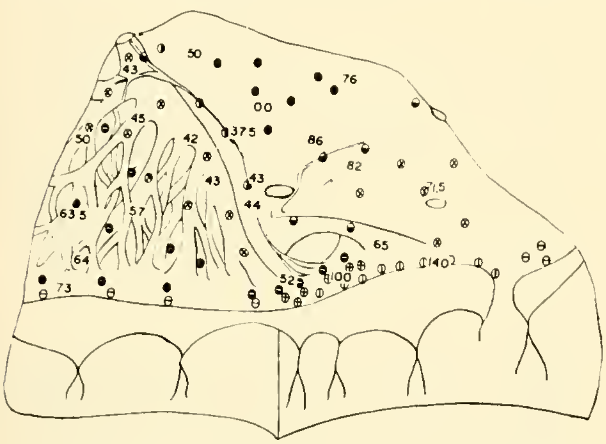

FIG. 9. A view from the interior of the rabbit's right atrium. Trabeculated area is at the left as indicated. Numbers indicate the instant of activity in milliseconds after depolarization of the sinus node. Note that activity spreads approximately radially from the sinus node, which is in the upper central region of the figure. The shapes of action potentials recorded are indicated by the various symbols in the figure. Note along the atrioventricular margin on the right (circle with vertical line) the region of the common bundle. Immediately upstream from this (circle with cross) are cells from an intermediate region along the A–V conduction pathway, which the experimenters termed nodobundle cells. Above these (black circle with horizontal white line) are cells which the researchers considered to be the first link in the A–V transmission system and which they termed atrial-nodal cells. Note further that these atrial-nodal cells extend from the trabecular region into the A–V nodal region. [From Paes de Carvalho *et al.* (82).]

diastolic depolarization to threshold (7, 20, 134, 140–142). Prior to study with the intracellular electrode Lewis (71) had shown that the S-A node is the site of earliest negativity, and other workers (11, 19, 95) had demonstrated that an electrode in this region shows a potential slightly earlier than the firing of ordinary atrial muscle. The process by which the S-A and A-V nodes generate impulses is not known. It is possible that these cells differ from others in being more permeable to sodium when at rest and consequently gradually depolarize at the end of each cycle to the level at which rapid depolarization takes place.

Activity in the atrium commences in the S-A node and spreads outward like the wave produced when a stone is dropped into still water (21, 71, 82, 92). The plots of atrial excitation by Lewis (71) and more recently by Brendel and co-workers (21), Puech (92), and Paes de Carvalho and co-workers (82) agree closely (figs. 8, 9). From the region of the S-A node, the wave of atrial depolarization proceeds at a velocity of slightly less than 1 m per sec toward the borders of the two atria and of the interatrial septum.

Among the theories which constantly recur in the anatomical literature are those concerning the existence or absence of a specialized conduction system in the atrium (see above). The belief that such a conduction system is present in birds has led individuals with a strong interest in comparative physiology to feel that there must be such a system in other species. There seems to be no compelling evidence for such a system in "gross" plots of atrial excitation in mammals. However, Paes de Carvalho and his co-workers (82) believe that potential shapes similar to those recorded from the A-V nodal and other specialized cells (i.e., potentials showing diastolic depolarization, etc.) can be found throughout the atria. These investigators also report evidence for rapid conduction between the S-A and A-V nodes in tissue which they refer to as the S-A ring bundle in the rabbit (fig. 9). It is possible that this rapid conduction occurs along the long axes of the fibers rather than in specialized tissue. In other disputed studies it has been claimed that certain small strategically placed cuts in the interatrial septum will disrupt A-V conduction. Since the potentials found by Paes de Carvalho *et al.* (82) are reminiscent of pacemaker (S-A and A-V) cells it seems pertinent to ask whether pacemaker activity occurs in the atria when neither the S-A node nor the A-V node is present. In certain animal experiments and in certain human lesions complete atrial standstill may occur if both nodes are removed or inactive (despite the fact that isolated ventricular Purkinje fibers may act as pacemakers). Also, the human heart with complete A-V block and without a sinus pacemaker may show no clear atrial potentials. On the other hand, atrial

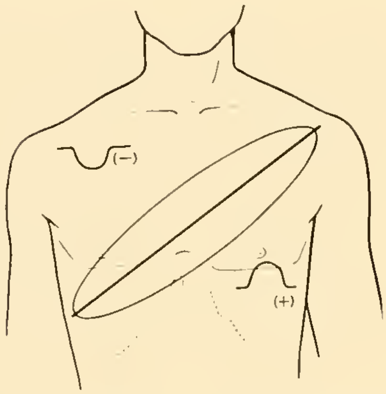

FIG. 10 Shapes of P waves which would be recorded at various places at body surface. Since general direction of atrial activation is from right arm toward left leg, electrodes on upper part of body will see a negative potential during atrial activation; those on the lower part will see a positive potential. There will be a plane, as indicated on drawing, where an electrode would record both positive and negative activity. [From Scher (114a).]

arrhythmias often appear to originate in nonsinus sites (coronary sinus, left atrium).

The initial elliptical shape of the depolarized area in the atria has been considered to indicate that many cells within the sinus node are simultaneously acting as pacemakers. It has also been thought that after this initial pacemaker activity, the spread of excitation is a rather random phenomenon. As stated above, there is good evidence for a greater space constant for myocardial fibers along their long axis, and there is a greater conduction velocity in this direction (figs. 8 and 9). The present plots of atrial excitation do support the idea of a greater velocity parallel to the fiber direction. In the plots of right atrial activation by Puech (92) and Brendel *et al.* (21) the conduction velocity is greater along the length of the fibers than perpendicular to them. The conduction velocity in the mammalian atrium appears to be about 0.8 m per sec.

If we consider the position of the atria in the body, electrodes placed almost anywhere on the precordium (except near the right shoulder) will record a positive potential as the atria depolarize. Conversely, lead VR and esophageal leads will record a negative P wave (fig. 10). The P wave usually has a smooth rounded contour, although it may at times be notched or peaked; it has an average duration of 90 msec in man and an amplitude of less than 0.25 mv. It is about half as long in the common domestic small animals which are studied experimentally.

Atrial Repolarization

Repolarization of the atrium in the dog and in man normally occurs during the depolarization of the ventricles, and the repolarization potential is concealed by the much larger ventricular potentials. There is thus an isoelectric period between the end of atrial depolarization and the beginning of ventricular depolarization, although, as will be discussed, portions of the atrioventricular conduction system are depolarizing during this time. Infrequently, the ventricular potentials do not conceal the atrial repolarization potential (referred to as the T_a wave), and it may be seen as a very small mirror image of the P wave. It is probable, although there is no direct evidence to support this contention, that repolarization of the atrium progresses in a direction similar to that followed by depolarization. Since the electrical charges in repolarization are oppositely arranged across the boundaries between resting and active tissue, the resultant potentials have a polarity opposite that seen during depolarization. The small size of the repolarization complex probably reflects the slow potential changes in the cells during repolarization.

Atrioventricular Conduction

The P wave of the human electrocardiogram is followed by a period of approximately 80 msec during which no potentials are recorded electrocardiographically (fig. 5). This P-R interval is followed by the QRS complex which signals ventricular depolarization. During this interval the impulse is confined within the A-V node and peripheral portions of the A-V conduction system, as first shown by Hering (56). In many clinical conditions, the P-R interval is prolonged (first degree A-V block) or the P waves may not always be followed by QRS complexes (second degree A-V block). At times, the P wave and the QRS complex are completely independent, indicating that the atria and ventricles have separate rhythms (third degree A-V block). Until very recently there was no knowledge of A-V nodal function enabling us to decide when the various structures along the A-V conduction pathway are activated or labeling the anatomic site which fails to conduct the A-V nodal block.

The period between the end of the P wave and the beginning of the QRS complex is commonly referred to as the period of "A-V nodal delay." This term probably originated from the feeling that the upper

portion of the interventricular septum was the first portion of the ventricle to be activated. Hypothetically, the electrical impulse had only to travel through the connective tissue boundary in this region—a distance of 1 mm or less—before ventricular excitation began. It thus seemed that, since so long a time was consumed in going so short a distance, there must be a true delay, i.e., a period when the impulse was moving little or not at all. The time which must be accounted for by conduction within the A-V node has been decreased by the realization that the Purkinje fibers excite the ventricle nearer to the apex than previously thought (see below). A portion of the atrioventricular interval is thus consumed by conduction in the bundles and other peripheral Purkinje

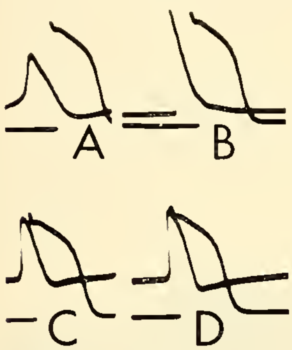

FIG. 11. Intracellular records from sinus node, atrial muscle, A–V nodal region, and common bundle. For timing purposes, large potential which has lowest base line is repeated and is taken near common bundle. Small potential, *A*, which begins earliest is from sinus nodal region. It shows a diastolic prepotential and slow rate of depolarization with lack of overshoot. Potential *B* has a resting potential slightly smaller than that of common bundle but depolarizes to about the same extent. This is from ordinary atrial muscle and occurs somewhat later than potential from sinus node. *C*: potential from upper A–V node shows a smaller amplitude and a small diastolic prepotential after rapid repolarization. A similar potential with a diastolic prepotential, phase *D*, is seen occurring somewhat later and closer in time to the depolarization of the common bundle. This potential is from the mid A–V node. [From Hoffman *et al.* (58).]

tissue. The A-V conduction time has been increased by the realization that the atrial cells in the A-V nodal region are actually excited about two-thirds of the way through the time interval occupied by the P wave (92). As will be seen below, the electrical impulse may at times travel very slowly through the tissues which link the atrium and ventricle, but there appears to be no evidence that the impulse stops or that any chemical transmission is involved. The term delay therefore seems inappropriate, implying as it does a period during which nothing happens. Despite the fact that newer knowledge has indicated the incorrectness of this term, it probably will continue to be used for convenience.

Recently both intracellular and extracellular electrodes have been used to study A-V nodal conduction, but the information so far derived provides only imperfect answers. Hoffman and co-workers (57, 58), Sano and co-workers (107, 110), and Matsuda and co-workers (74), who studied mammals, and Inoue (59), who studied the frog, are generally agreed concerning the shape of the intracellular action potentials (figs. 11, 12) recorded from the A-V node itself. *a*) The resting and action potentials are smaller than those in the rest of the atrial or ventricular musculature. *b*) The rate of change in voltage during the period of initial depolarization is less rapid than in other muscle. *c*) The action potential has a shorter duration than that from the fibers of the bundle of His and is usually of about the same duration as the action potential from ordinary atrial musculature. Sano and co-workers (107), using an ingenious marking technique with the intracellular electrode, were able to demonstrate histologically that these potentials were indeed from the A-V nodal region. They further feel that the A-V nodal potential has a step on the rising phase and that potentials without this step are from "transitional tissue."

Despite the excellence of these intracellular studies, there remain unanswered questions concerning the shapes of the recorded action potential. In some

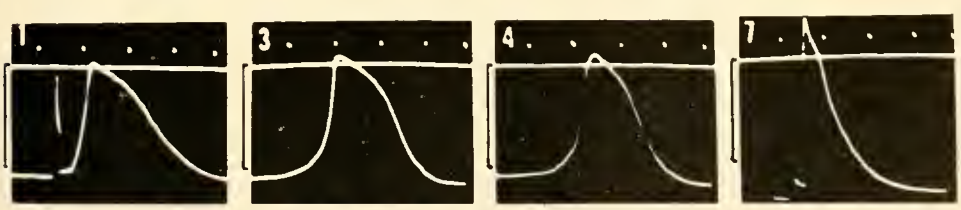

FIG. 12. Potentials from the A-V node recorded by Sano and co-workers. Trace 1 from ordinary atrial muscle; trace 7 from the common bundle. Traces 3 and 4 from the A-V node, and are distinguished by a "step." [From Sano *et al.* (107).]

records (fig. 12) a step-like prepotential of 40 to 100 msec duration precedes the rapid depolarization phase. Is this prepotential due to current flow from one or more bordering cells? Can the nodal cells actually respond to a stimulus of over 40 msec duration, or is the effective threshold, like that of ordinary myocardium, no different for a 10 msec stimulus than for a longer one (22)? If this latter condition were true, the step would not be functional although it might be characteristic. Also, are we to believe that one cell along the A-V pathway requires 40 msec to become depolarized when the entire period between the firing of atrial cells in the nodal region and the firing of ventricular cells may normally be no longer than 60 msec in some of the animals used? Can the step be due to distant cells? Similar speculation applies to the diastolic prepotential seen in other records. The diastolic prepotential of the nodal cells would be expected were they functioning as pacemaker cells, but like the "step" discussed above, it does not appear that this characteristic serves an essential function in some records. Strangely, the diastolic prepotential of the nodal cells has reached what might well be threshold when the cell is fired by a conducted impulse.

The possibility further exists that the small size of nodal cells makes it difficult to pierce them without causing a "leak" which produces some characteristics of these shapes. As will be indicated below, similar critical questions exist with respect to the extracellular potentials recorded in this region. All of the mentioned characteristics of intracellular A-V nodal potentials are consonant with the concept, discussed below, of slow conduction in small fibers which may have difficulty in exciting large fibers. Although no measurements of velocity were presented in these studies, Hoffman *et al.* (58) indicate that when an intracellular electrode was moved 1 mm along the slowest conducting portion of the A-V nodal system, time intervals of 20 to 70 msec were noted between the rapid phases of depolarization at the two sites. This might be construed as indicating a conduction velocity as low as $\frac{1}{70}$ or $\frac{1}{20}$ m per sec.

Extracellular action potentials have been recorded from the A-V nodal region by several groups of investigators. Van der Kooi and co-workers (138)

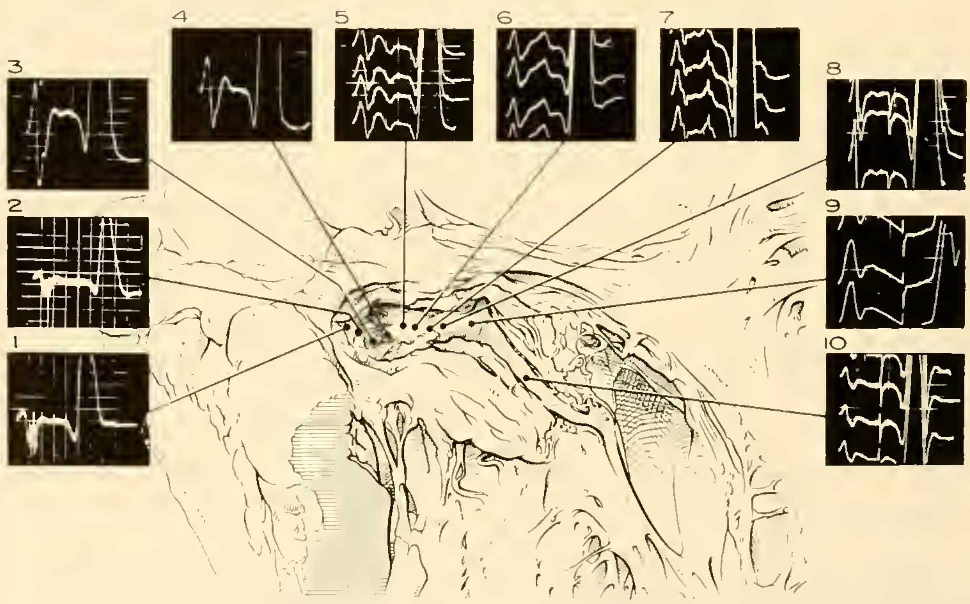

FIG. 13. A sketch of the atrioventricular conduction system in the cow showing the sites at which recording electrodes were placed and the electrograms recorded at these sites. At position 1, a small multiphasic atrial potential is found followed by a small positive-going potential. This positive "hump" increases slightly in positions 2 and 3 and is much bigger in position 4, where it begins to approach a positive-negative potential. In position 5 the potential is markedly positive-negative and at position 6 markedly positive. Here it is followed by a rapid negative-going deflection which appears to be the influence at this locus of the common bundle potential. Position 7 shows a positive common bundle potential, perhaps superimposed on some A-V nodal activity; the common bundle potential becomes positive-negative at positions 9 and 10. A similar figure has been published by Scher and co-workers (116). [From Pruitt & Essex (91).]

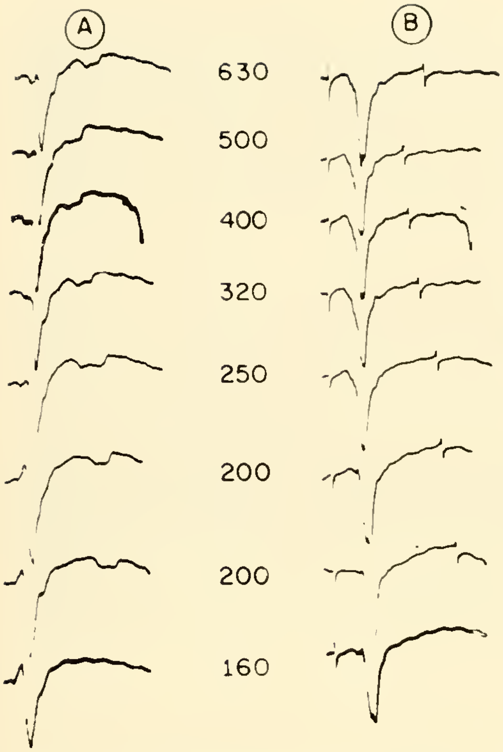

FIG. 14. Effects of stimulation at several frequencies on A–V nodal and bundle potentials. Column *A* shows a negative-going A–V nodal potential which follows a large negative atrial potential. The recording electrode was within the A–V node. Column *B* illustrates potentials recorded 2 mm away, near origin of common bundle. Small negative potential following atrial potential in *A* and positive-going potential preceding rapid depolarization of common bundle in *B* are due to activation of A–V node. Magnitude of A–V nodal potential in both *A* and *B* can be seen by comparison with potentials recorded at interstimulus interval of 160 msec, which show neither A–V nodal nor bundle activity (complete block). Atrial potentials in *A* are of 2 mv magnitude; time pips are at 20 msec. [From Scher *et al.* (116).]

obtained a polyphasic deflection in bipolar recordings from the perinodal region in the dog. They felt this potential was from the A-V node. Pruitt & Essex (91), who studied the calf and dog, believe such a potential at times originates from atrial fibers immediately above the A-V node or from the atrionodal junction; however, their records are generally unipolar. The significance of a particular potential shape in a bipolar record from the nodal region appears obscure. Scher and co-workers (116), also working with dogs, were unable to find in the perinodal region any potentials of the type reported by van der Kooi and co-workers. The extracellular potentials recorded from the A-V node by Pruitt and Essex, and by Scher and his co-workers appear to be

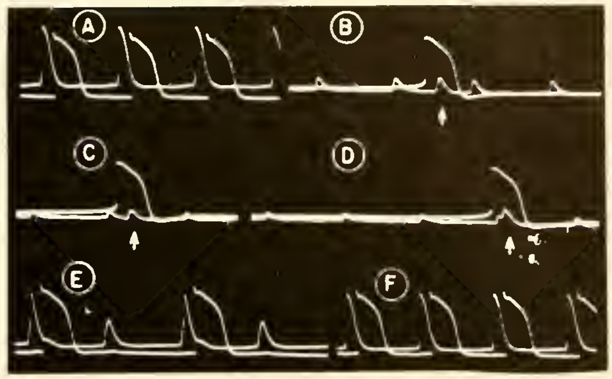

FIG. 15. Transmembrane action potentials recorded from a single fiber of the A–V node (*upper trace*) and another single fiber in His bundle (*lower trace*). *A*: control; *B* to *E*: acetylcholine effect; *F*: after elimination of acetylcholine. [From Cranefield *et al.* (33).]

identical. The potential from the A-V node was referred to by the former group as a "slow potential" and by the latter as a nodal "hump." In unipolar records it consists of a slowly changing potential which is negative in the upper A-V node, positive-negative in the mid-nodal region and positive in the lower node. The potential is unique in its lack of a rapid negative-going phase (except at the nodobundle junction where it is terminated by the rapid negative-going bundle potential (figs. 13, 14). This potential occupies the period of about 20 msec between the excitation of atrial fibers at the upstream nodal region and the excitation of the common bundle. The results of these two studies differ remarkedly from those reported by Alanis and co-workers (3), who are not specific concerning either the type of electrode used or the number of animals studied. Indeed, since these investigators, in contrast to Pruitt and Essex, and Scher *et al.*, used no histologic controls, there is no assurance that the potentials they report originated in the A-V node.

In Pruitt and Essex' study vagal stimulation increased the width and altered the form of the nodal "hump." They believe that vagal stimulation acts within the node itself. In the study by Scher and co-workers rapid stimulation usually increased the interval between the atrial potential and the potential from the A-V node (fig. 14). The site of first degree A-V nodal block under most conditions was at the junction between atrial and nodal cells. At times, however, the nodal potential also increased in duration. The conclusions of Scher and co-workers about the location of first degree A-V block agree with those of Hoffman and co-workers (58) and

Cranefield and co-workers (33). The latter group found that acetylcholine acts on the same atrionodal junction when it slows conduction (fig. 15). In the studies of Scher *et al.* (116) there was rarely, if ever, block between the A-V node and the bundle of His. The sensitive junction during forward and retrograde conduction was between atrial and nodal fibers. Rosenblueth & Rubio (103) have presented indirect evidence for other conclusions. In a study by Sano *et al.* (108) evidence was presented that complete retrograde A-V block can occur in the ventricular portion of the A-V conduction system. There is no necessary conflict between this study and that of Scher *et al.*, since the latter group only studied hearts in which retrograde conduction occurred.

In several studies, hypotheses based on the geometry of the A-V region have been advanced to account for the slow conduction. It appears likely that the small size of the fibers in the boundary between the A-V node and the atrium, as well as of those within the node, accounts in part for the slow conduction velocity, and that there may be a region where small fibers, or a small bundle of fibers, has difficulty in exciting either large fibers or a large bundle of fibers. It is further probable, as stated by Pruitt & Essex (91), that the random orientation of the nodal fibers with respect to one another leads to cancellation of some potentials even though a wavefront is moving from the atrionodal to the nodobundle junction. It is also possible that the cell-to-cell connections influence conduction velocity. It was estimated by Scher and co-workers that the velocity in the atrionodal junction is about .05 m per sec and in the node 0.1 m per sec.

Potentials from the A-V Region in the Frog Heart

As indicated previously, the region of the A-V ring in a number of cold-blooded animals contains cells which link the atrium and ventricle. Inoue (59) has placed intracellular electrodes into this region in the frog heart. The potentials which he recorded appear to be similar to those reported by Sano and Matsuda and their co-workers (see above).

Summary

Some questions may be raised concerning the shapes of potentials recorded extracellularly. As stated above, several hypotheses have been advanced to account for the peculiarities of these records. The reason for the lack of rapid negative-going spikes as the atrionodal and nodal cells fire is a matter for speculation, as is the fact that in some studies there does seem to be a period when virtually no potential changes are recorded.

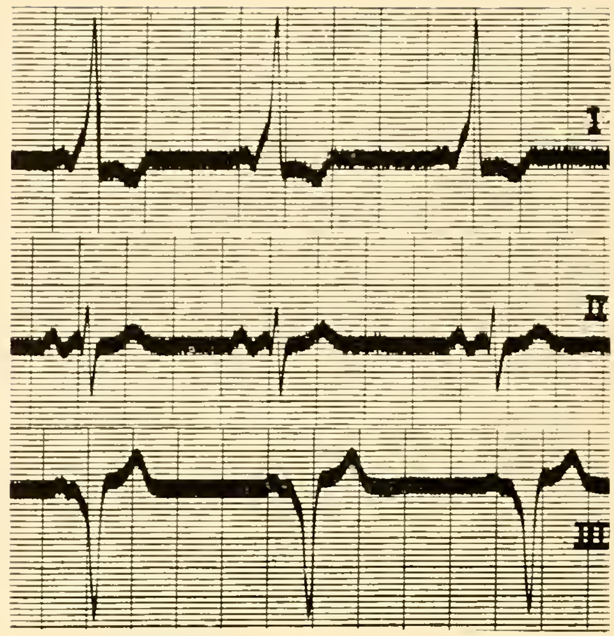

FIG. 16. Electrocardiogram of the Wolff-Parkinson-White syndrome; leads I, II, and III from above down. Note that the P wave is continuous with the QRS complex, and that the QRS complex shows an initial slow deflection (heavy line in lead I) which is generally referred to as a delta wave. The latter portion of the complex is quite similar to late portion of a normal electrocardiogram. [From Wolff *et al.* (147).]

From all the studies cited, it appears that conduction from the atrium to the common bundle involves no basic mechanisms differing from those which generally obtain in cardiac muscle. Conduction is continuous, although velocity is not constant in all portions of the system. Conduction is not one-way (as is synaptic transmission), since an impulse can be conducted from ventricle to atrium. Conduction does not involve chemical transmission from cell to cell as does synaptic transmission.

Wolff-Parkinson-White Syndrome: Alternate A-V Conduction Pathways

A clinical condition known as the Wolff-Parkinson-White syndrome (100, 124, 147) has led to much speculation concerning A-V conduction. In this syndrome, the interval between atrial firing and ventricular firing is markedly reduced (fig. 16). A

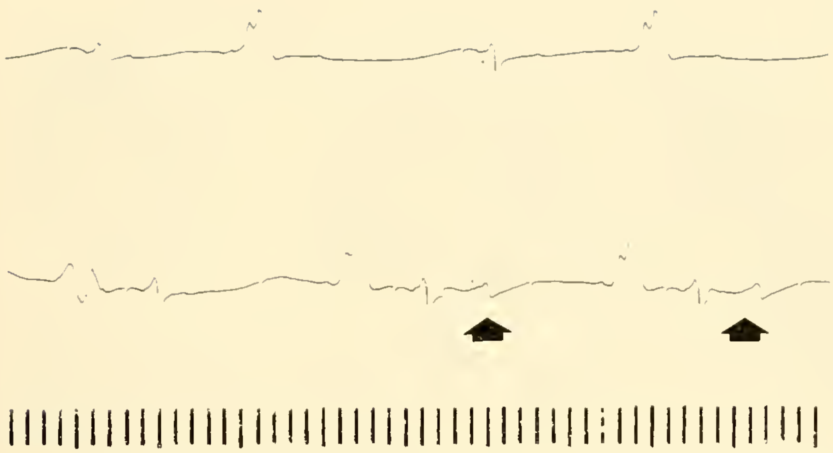

FIG. 17. During normal excitation an electrode in the region of the upper A-V node records nothing following atrial activity. When the sinus node is driven at a rapid rate, and A-V block is produced, a spike-like potential (indicated by arrows) appears following the atrial record. Initial sequence in top record is stimulus, atrial depolarization, ventricular depolarization. Records are sequential. (Scher A. M., unpublished.)

number of explanations have been offered. Among these are *a*) the existence of an accessory conduction pathway from atrium to ventricle, the "bundle of Kent" (64); *b*) ephaptic conduction from atrium to ventricle across the boundary between the chambers; *c*) mechanical coupling of some sort between atrium and ventricle; and *d*) ability of the A-V node to "accelerate" its conduction rate under appropriate conditions (18, 90). The experimental evidence does not appear to support any of these theories; the theory of accelerated A-V conduction appears to be based on experiments which involved coupled beats and are not pertinent. Of the other three theories, the existence of a bundle of Kent (64) has at times been confirmed but at other times vigorously denied, and it remains to be proved that such a bundle, if it exists, would have a conduction velocity of the proper magnitude to advance rather than retard the instant when the ventricles become activated. The best possible guess regarding the origin of this syndrome seems to be a coupling of beats across the interventricular septum in some as yet undetermined fashion. It is possible for a ventricular extrasystole to be coupled to the previous normal beat and it does not therefore seem unlikely that a ventricular beat can in some unknown fashion be coupled to previous atrial depolarization. In the classical Wolff-Parkinson-White beat the ventricular complex appears to be in part extrasystole and in part normal, so that a combination of normal excitation and coupled (or conducted) abnormal excitation appears to exist.

Dual A-V Conduction System

In studies by Moe and co-workers (77), later repeated by Rosenblueth (101), the conclusion was reached that there might be two processes or pathways for A-V conduction. This conclusion was reached because of two apparently distinct and separate times for activation of the ventricle when the atrium was stimulated at varying rates and a like phonomenon for retrograde atrial activation when the ventricle was similarly stimulated. The variable which was altered to give these results was stimulation frequency. Another piece of evidence was the existence of "echoes." When the ventricle was stimulated the wave of activation passed to the atria and then "echoed" back to the ventricle, usually with a different transmission time. In the studies by Scher and co-workers (116) the echo phenomenon was noted and was found to occur in a very circumscribed group of cells in the region of the A-V node. Further, when A-V conduction was studied with extracellular electrodes, no evidence was found for a separate pathway since, whatever the time required for A-V conduction, the impulse was confined to the same specialized tissue pathway. The echo phenomenon appears to be a property of the A-V nodal region; and the stepwise variation in A-V conduction time would also appear to be a function, although an unexplained one, of the ordinary A-V conduction pathway.

In this and other aspects of its behavior, the atrioventricular conduction system behaves like a network of cells with multiple interconnections. These interconnections are ordinarily more than adequate to allow the impulse to be transmitted from the atrium to the ventricle. During normal atrioventricular conduction none of the network properties are really apparent. If the system is put under stress by disease, anoxia, mechanical damage, rapid stimulation, or alterations of the ionic environment, these

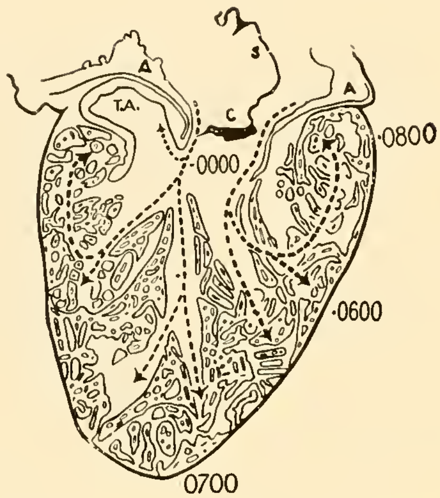

FIG. 18. Time of activity after the earliest recorded point in the toad's ventricle. Note that on the left the earliest activity is in the center of the ventricles, and that there is later activity at both the apex and the base. *A:* auricular muscle passing into A-V ring; *C:* endocardial cushion; *S:* auricular septum; *TA:* commencement of bulbus arteriosus. Arrows indicate deduced direction of activation. [From Lewis (70).]

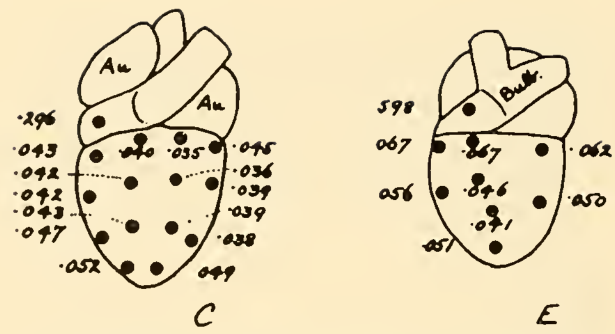

FIG. 19. Surface activation in the toad. The time reference is the beginning of the R wave in the body surface electrocardiogram. In the heart shown at the left the base was activated before the apex, but in that at the right, the base was activated after the apex. In both, the central portion of the ventricular wall was first area activated, and the bulbus arteriosus was activated very late. [From Lewis (71).]

properties may become quite obvious. One such property is the generation of echoes. The production of first degree A-V block by rapid stimulation, which delays the firing of some cells and changes the duration of potentials recorded extracellularly, also involves an alteration of the conduction characteristics of the A-V conduction system. In some experiments, an electrode in the upper A-V node recorded no clear potentials from other than atrial cells. With rapid stimulation (fig. 17) a spikelike potential may appear as first degree block develops. Here a group of cells, which did not normally show signs of firing in concert, are driven to fire simultaneously by the rapid stimulation. Another example is found in certain patients in whom a sinus beat which is or is not transmitted to the ventricles can markedly alter the A-V nodal rhythm (69, 102). A non-nodal similar phenomenon is found in the fact that conduction in turtle ventricle may become one-way if a pressure block is caused in a mass of muscle (9, 62). These properties may not be unique to the A-V conduction system, but they are here most apparent.

Conduction in the Common Bundle and Its Branches

The velocity of conduction in these "cables" has been measured at 2.0 m per sec in the false tendon of the kid by Draper & Weidmann (39) and by Weidmann (140). Curtis & Travis (34) calculated a velocity of about 4 m per sec for the false tendon of the kid at 40°C. Pruitt & Essex (91) confirm this measurement. Scher and co-workers calculated a velocity of 1.7 m per sec in the right bundle of the dog (115).

Ventricular Activation

As with atrial activation, the earliest detailed studies of ventricular activation were conducted by Lewis (71, 72). His papers are classics in the development of our understanding of electrophysiology and electrocardiography. His reasoning is lucid, his expression exact, and his contribution must be read by any serious worker in the field. As will be discussed, Lewis plotted the time of activation of many points over the surface of the canine heart and attempted to deduce the pathway followed by the wave of activity within the muscle.

In other studies he observed that cutting the epicardium between a stimulating and a recording electrode (both on the epicardium) did not alter the conduction time between the points if they were sufficiently removed from one another. From this Lewis reasoned that the impulse was not traveling along the epicardium but must indeed be going first from the epicardium to the endocardium, then along the endocardium, and finally from the endocardium to the epicardium. Such a course demanded a conduction velocity along the endocardium more rapid than that measured on the ventricular surface (0.4 m per sec). From experiments such as this he calculated conduction velocities of 0.3 to 0.5 m per sec and 1.5 to 2 m per sec for Purkinje fibers and ordinary

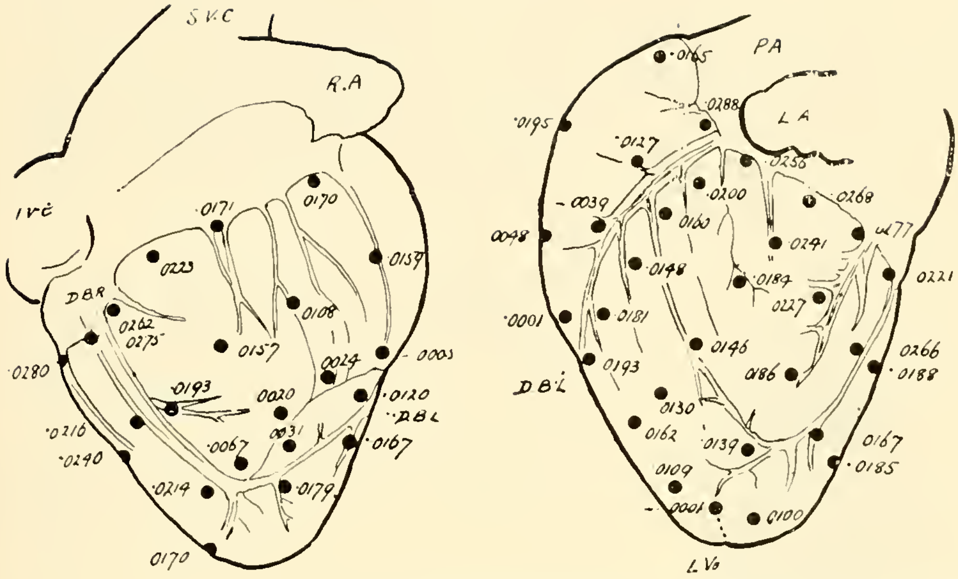

FIG. 20. Activation time over surface of right and left ventricles seen from the sides; two different dogs. *Left:* the earliest activity was at the right border of the cardiac outline; latest activity at the base of the right ventricle (upper left portion of fig.). This figure shows predominantly the free wall of the right ventricle. *Right:* the distribution over the left ventricle. The earliest activity occurred just to the right of the anterior descending branch of the coronary artery and near the apex of the ventricle, and the latest activity was generally near the base. Activity tended to be later on the posterior and lateral portions of the heart. [From Lewis (72).]

ventricular myocardium, respectively. These estimations were close to those later measured directly.

Excitation of the Ventricular Surface

Several early investigators attempted to plot the sequence of excitation of the ventricles of small hearts (24, 26, 70, 71). Lewis found the earliest excitation in the toad ventricle (fig. 18) in its central region and the wave appeared to spread from there toward both apex and base. A similar pattern is illustrated in figure 19. In all cases the apex and base were activated within 20 msec (26). The problem of activation of the ventricular surface (43, 45, 145) has been difficult to study in small hearts and has been most easily resolved in the large canine heart. A study in guinea pigs has, however, been conducted by Dower & Osborne (38), who found that the surface of the right ventricle was activated earlier than the surface of the left. A number of excellent studies have been carried out on the surface excitation of the ventricle in large mammals. Particularly important are the studies by Lewis (71), Harris (53), Sodi-Pallares & Calder (126) and Schaefer & Trautwein (113, 114) [see also Katz (61)].

Lewis' plot of the surface activation of the dog ventricle (fig. 20) is similar to that for the toad. Some points in the center of the heart, particularly over the trabecular region of the right ventricle, become active earlier than any other surface points. The base of the heart tends to be excited later than the central region and than the apical regions, but in some hearts 5 msec separates the earliest point on the apex from the last on the base. A somewhat different picture is presented by Sodi-Pallares (fig. 21). From these small time differences, certain authors did attempt to derive a complete pattern of ventricular activation.

Figure 22 shows a plot of ventricular surface excitation in the monkey from Harris' work (53). The time differences are roughly the same as, or perhaps slightly greater than, those for the dog. The earliest area is in the center of the trabecular region on the right with a similar area on the anterior central left ventricle. Surrounding these earliest points are points activated later, which extend down to the apex and laterally in the right ventricle. The latest points activated are at the basal regions of the left and right ventricle. In the posterior section there are much smaller time differences, but again the base is later.

Barker *et al.* (13) studied surface activation in the human heart. They found the earliest points on the anterior right ventricular surface near the A-V

groove. These points were activated approximately 10 msec after the beginning of a positive potential in the lead II electrocardiogram. The earliest points on both the left and the right were near the origins of the papillary muscles anteriorly. In their experiments there was at times a tendency for both the base and the apex to be activated later than the center of the ventricles; however, on the anterior surface the apex was activated later than the base, whereas on the posterior surface the base was activated later than the apex. These investigators found unexplained variability in their results when the measurements were repeated in the same individual at intervals of days. Groedel & Borchardt (50) recorded potential shapes from several sites on the human heart, as did Nylin & Crafoord (80).

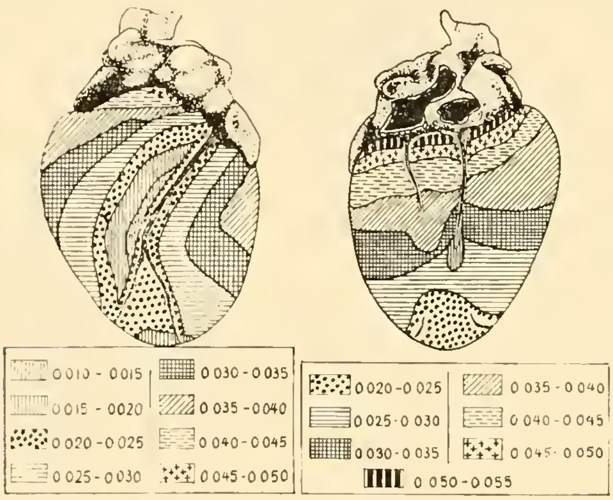

FIG. 21. A scheme for the activation of the surface of the dog ventricle presented by Sodi-Pallares. He finds the earliest activity just to the right of the anterior descending branch of the coronary artery. From this area there is a movement to the right. There is also early depolarization in the apical area. On the back, the earliest activity occurs, at between 20 and 25 msec, near the apex, and the base of the heart is depolarized last. [From Sodi-Pallares & Calder (126).]

Excitation of the Ventricular Walls

In the late 1940's a number of laboratories (40, 41, 98, 99, 104, 117, 126) began to explore the inner layers of the canine ventricular myocardium with penetrating electrodes (referred to as needle electrodes and plunge electrodes). Some of these electrodes had one or two recording tips, and the electrode was moved in and out of the wall to determine the time of activity at various depths. In other studies, multipolar electrodes which could record from the various depths without being moved were used. Recording equipment varied from pen-writers to multichannel oscilloscopes. The results of many of these studies are summarized in a symposium (54) and in a text (126), although some must be read in the original literature. Many of these papers stress the finding that in the dog the impulse does not move in a straightforward fashion from endocardium to epicardium. The impulse may arrive first at a point several millimeters within the wall and spread toward both endocardium and epicardium, or it may show reversals of direction near the endocardium. In the several studies, the amount of tissue excited from within outward has been estimated as 20, $33\frac{1}{3}$, and

FIG. 22. Spread of surface excitation in the monkey's heart. *A:* ventral surface; *B:* dorsal surface. Numbers indicate the time of excitation at the marked points on the surface as compared to the earliest point at which activity was recorded. Note that the earliest activity on both sides is toward the center of the anterior ventricle on both the left and the right. Also, the latest activity recorded on the anterior surface is near the base of the heart. The posterior base of the heart is activated somewhat earlier. The base is activated later than the apex anteriorly and posteriorly. Note that all surface points are excited within a very short period of time, the maximum time difference is 13 msec; the QRS of the electrocardiogram has about three times this duration. [From Harris (53).]

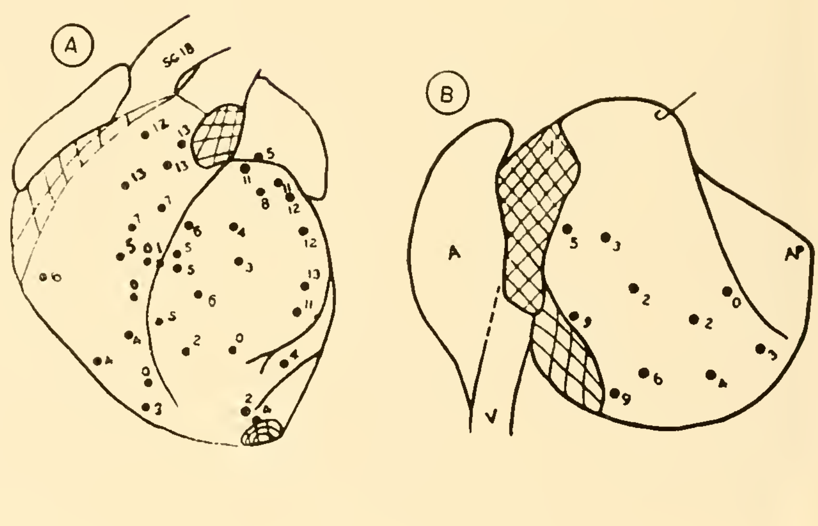

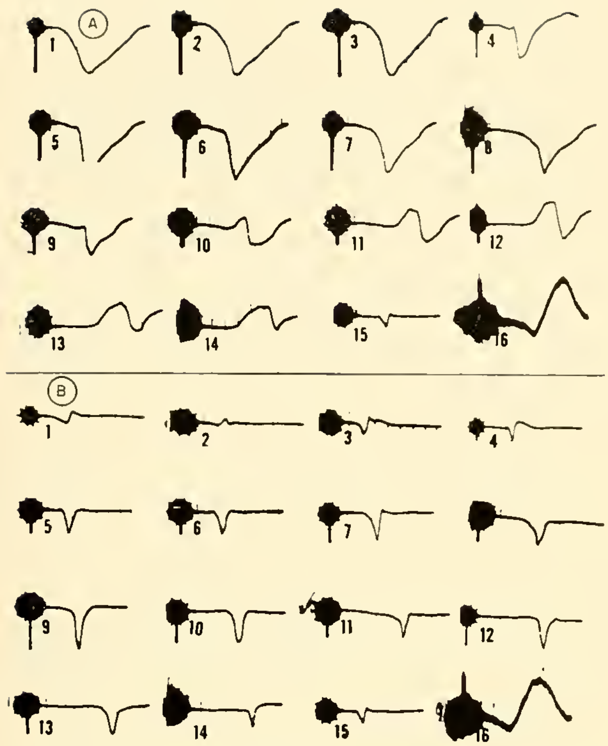

FIG. 23. Potentials recorded from endocardium to epicardium in the mid-lateral left ventricular wall of the rhesus monkey. *A:* unipolar potentials; *B:* bipolar potentials. Terminals 1, 2, and 3 of the unipolar record show characteristic central left cavity records. Terminal 15, from which no unipolar record was taken, was at the epicardial surface. Bipolar channel 1 records the potential difference between unipolar records 1 and 2, and bipolar channel 2 records the potential difference between 2 and 3, etc. Channel 15 records the fixed time-reference potential, and channel 16 the lead II QRS. Time pips at 5 msec intervals. Downward bipolar records indicate movement of the wave from inside out. [From Scher & Young (117).]

60 per cent of the wall thickness. Scher and coworkers have tended to minimize the importance of the reversals of direction within the wall and of the endocardially directed portion of the activation wave, although many examples of this phenomenon have been presented in data published by this group (119, 120). There is often no evidence for Purkinje penetration along an electrode in the dog or monkey heart (fig. 23). They have also stressed the fact that activation under the papillary muscles and some trabeculations originates in the middle of the wall and moves toward both surfaces. Durrer & van der Tweel (41) state, "In the area where most of our experiments were performed, the area bounded by a line 1 cm apical of the sulcus atrioventricularis, the left side of the ventricular septum and the lateral

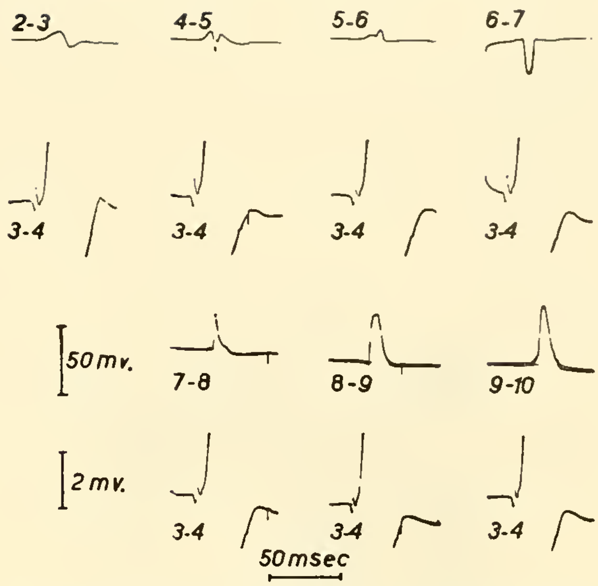

FIG. 24. Bipolar potentials recorded at 1 mm intervals within the left ventricular wall of the dog heart. First and third lines show potentials recorded at various positions from inside out in the wall; these are compared with the potential recorded at a fixed place in the wall, between terminals 3 and 4. Potentials recorded at this point make up the second and fourth line of traces. Note that the potentials are downward on 4–5, upward on 5–6, downward on 6–7, and finally upward on 7–8, 8–9, and 9–10. This indicates that conduction was moving from inside out only between 5 and 6, and between 7 and 10. The small spike at the beginning of 3–4, the reference, is considered due to intramural Purkinje fibers. [From Durrer & van der Tweel (41).]

part of the left ventricular wall between the insertions in the papillary muscles—the depth most frequently found was two-fifths of the diastolic thickness of the wall. In some instances only two or three of 8 terminals showed successive activation." [See fig. 24.]

Durrer and his colleagues found it more difficult to estimate Purkinje penetration on the apical portion of the ventricular wall. They obtained the same results (earliest activation within the wall rather than on the endocardial surface) near the base of the heart with the exception that 21 per cent of the places examined in that region showed no Purkinje penetration. These investigators apparently feel that Purkinje penetration in the goat is similar to that which they believe exists in the dog (see below).

Sodi-Pallares states his results somewhat differently. "For purposes of didactic discussion, the muscular mass comprising the free walls of the ventricles may be considered to consist of an inner $\frac{2}{3}$ (sub-endocardial) and another $\frac{1}{3}$ (sub-epicardial). Propagation through the former is rapid, figures of 1 or 2

meters per second being commonly found . . . the impulse travels through the outer or sub-epicardial third of the wall at speeds of only 300 to 400 mm per second (126)."

He further feels that the apical portions of the free wall are activated earlier than the basal portions (fig. 21) and thinks that the subendocardial layers are depolarized in such a fashion that they give rise to no potentials in leads outside the region. This idea has also been strongly advanced by Prinzmetal and colleagues (89). Sodi-Pallares feels that, because of Purkinje penetration into the wall, a number of closed volumes of muscle are activated from Purkinje strands. Since these are closed volumes, they give rise to no potentials in external leads.

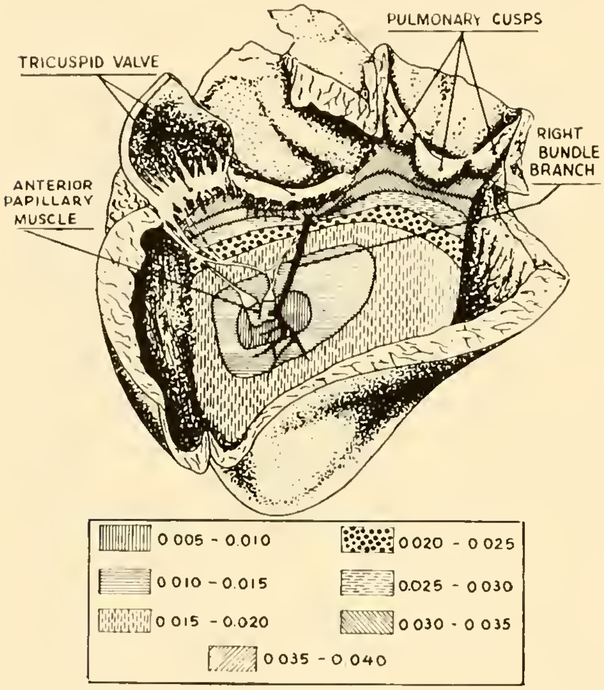

FIG. 25. Activation of the right surface of the interventricular septum recorded by Sodi-Pallares. Earliest activity was recorded near the base of the anterior papillary muscle, from this region the activity spread radially towards the lateral, inferior, and superior borders of the septum. [From Sodi-Pallares & Calder (126).]

The question of Purkinje penetration has ramifications beyond the electrophysiological and anatomical. It has been claimed that, because of Purkinje penetration, only the outermost ventricular layers contribute to the normal QRS complex and therefore that lesions of most of the inner wall will be undetectable electrocardiographically.

The work of Prinzmetal and his colleagues deserves some comment. All of the early papers in a very large series stressed the fact that most of the inner layers of the wall were silent and were depolarized before the beginning of the peripheral electrocardiogram. The faulty reasoning on which this claim was based has been analyzed *in extenso* (119). A final paper in the series (85) re-examined the major claim (excitation of inner layers before the beginning of QRS) and found it to be incorrect. In the various papers from this laboratory between $33\frac{1}{3}$ and 80 per cent of the wall was considered to be simultaneously activated.

In the hearts of ungulates, where penetration of Purkinje fibers can be clearly shown histologically, the excitation of the wall is quite different from mural activation in the dog. As has been shown by Hamlin & Scher (51) in the goat, the direction of activation

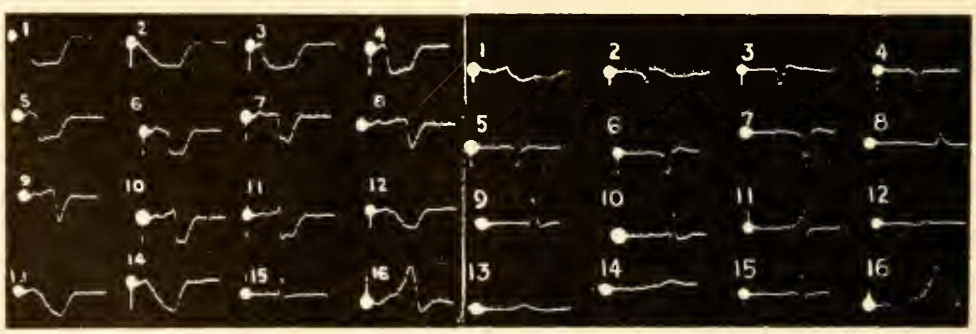

FIG. 26. Simultaneous oscillographic records from multipolar electrode across apical septum (1–14). Negative potentials gave downward deflection. Unipolar records on left; bipolar on right. Channel 15, fixed time reference; channel 16, lead II ECG. Time pips are 5 msec apart. Potentials on the first 14 channels of unipolar records average 40 mv. Bipolar records show difference between adjacent unipolars (one minus two, etc.). Activity proceeds from both endocardial surfaces toward center of septum. [From Scher *et al.* (121).]

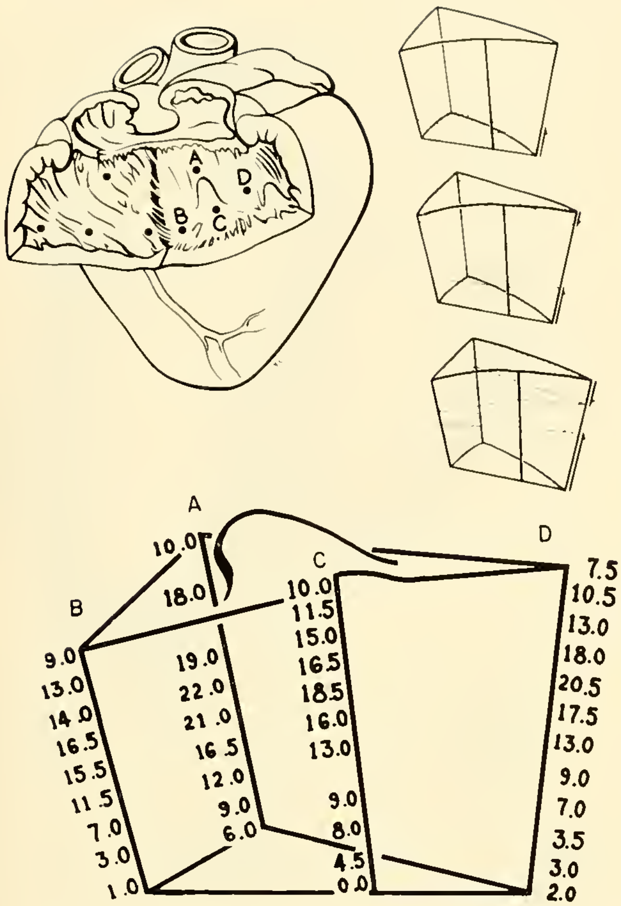

FIG. 27. Diagram showing excitation times along four insertions into interventricular septum. Position of the electrodes is indicated on sketch of heart at upper left. Times of local activation shown in block of tissue bounded by electrodes at bottom of figure. Advance of wave front through tissue shown in three small drawings at upper right. Hatched areas indicate volume of tissue excited 5, 10, and 15 msec after time reference. Note double envelopment of septum. [From Scher *et al.* (121).]

reverses many times, so that depolarization in the wall has no clear direction and there is little if any difference between the times of activation of points on the endocardium or epicardium, or within the wall (fig. 37). Depolarization of penetrating Purkinje fibers in the goat leads to small "pips" superimposed on the early portions of unipolar or bipolar intramural records. When an electrode insertion showing such pips is examined histologically, the Purkinje fibers are found at the proper location. In the dog, such pips are at times recorded, usually within 3 mm of the endocardium; staining techniques which delineate the Purkinje fibers show specialized tissue at these recording sites.

Activation of the Interventricular Septum

This region has been studied in several laboratories, the first detailed investigations being performed by Rodríguez and her co-workers (98, 99). Certain of their findings have been confirmed by Burchell and co-workers (23), Scher and co-workers (121), and Amer *et al.* (5). The following points are generally agreed upon. Activation of the septum begins near the terminations of the bundles in its central portion (fig. 25). In the apicobasal direction, the wave moves both toward the apex and toward the base, and the base is activated last. It was noted in these studies that the direction of activity was from left to right, that a large movement was directed from apex to base and that the mean pathway of excitation was indeed directed basally. Amer and colleagues (5) conducted a detailed study of the excitation of the septal surface, bilaterally, in the perfused dog heart. They found the earliest activity to be nearly simultaneous on both surfaces, just above the anterior papillary muscle on the right and in a large region near the midline on the left.

Some studies have included exploration within the muscular mass of the septum (121). These differ somewhat in their final conclusions. In one case it is claimed that the septum is excited virtually entirely from the left, and that the right bundle activates only the "right septal mass," which is maximally between 20 and 30 per cent of the total septal mass. It is further suggested that the two electrical septal masses are functionally independent and that the septal mass is not syncytial from the electrical point of view. Sodi-Pallares and his co-workers feel that at times the impulse may take 20 msec to cross the "boundary" between the right and left masses of the septum (fig. 29). In the study by Scher and co-workers (121) the septum was found to be predominately excited from the left, although at times as much as 45 per cent of the canine septum was excited from right to left (figs. 26, 27). Furthermore, when an extrasystole was started on the septal surfaces, there was no region of delay in the septum, there was no partition of the septum into electrically separate masses, and the septum was a functional syncytium. As a result of the controversy existing on these points, special studies were undertaken by Scher and Rodríguez (unpublished observations), who found that the septum is indeed a functional syncytium, that there is no partition, and that a sizable portion of the septum is excited by the right bundle. These data are supported by the studies of Amer *et al.* (5) discussed

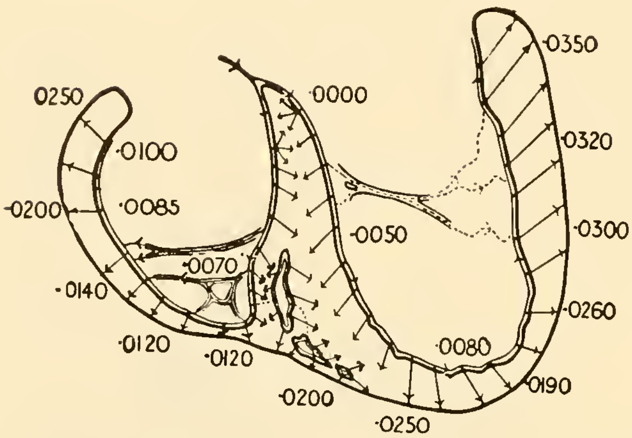

FIG. 28. A scheme illustrating the direction taken by the excitation wave on both sides of the heart as deduced by Lewis. He considered (incorrectly) that the wave of excitation passed down the muscle in the interventricular septum and then up around the free walls. He also felt (correctly) that there was inside-out spread of activity in the free walls and that the septum was enveloped from both sides towards the center. [From Lewis (71).]

above. The discrepancy between the highest figure cited by one group (30%) and the lowest cited by the other (40%) for the amount of the septum excited from the left seems small, and the major disagreement concerns the question of a functional barrier to conduction in the septum.

Details of Ventricular Excitation in Two and Three Dimensions

Using his plots of ventricular surface activation as a rough guide and adding to them his demonstration that there was a sizable inside-out component to mural depolarization, Lewis deduced a two-dimensional map of ventricular depolarization (fig. 28) which greatly influenced later authorities and was generally accepted (71). Lewis felt that the wave of activity moved down the septum from the atrioventricular junction, along the septal surface. He thought that the Purkinje fibers then conducted the activity upwards along the mural endocardium, so that the basal portions of the free walls were the last to be depolarized. In the illustrations he presented for the dog, and in his deductions (based largely on the dog) concerning the human heart, initial activity is depicted as directed apically in the septum followed by activity which moves basally in the walls. The latest regions to be depolarized are in the lateral left wall, which is depolarized later than the basal right wall.

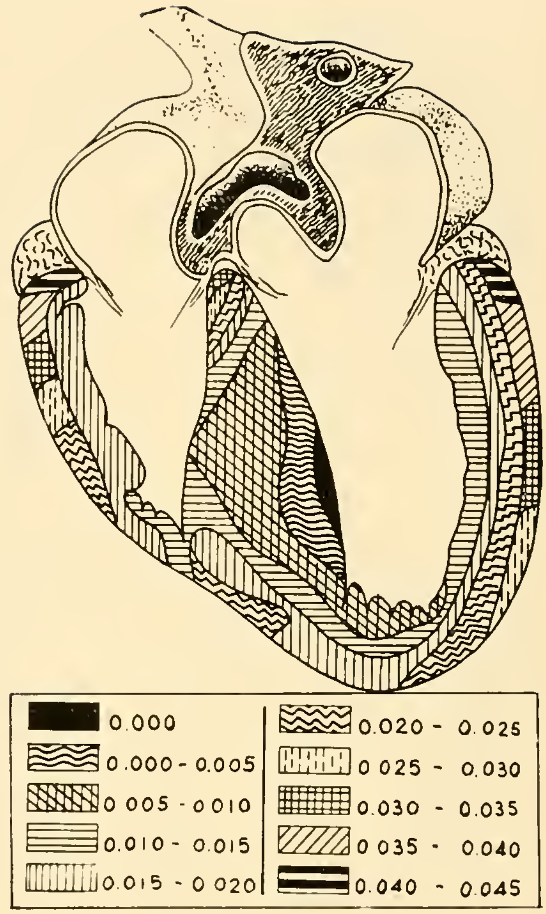

FIG. 29. A pattern of ventricular excitation as presented by Sodi-Pallares. Note that the septum is shown depolarized from left to right, although in the apical areas there is some movement from right to left and from apex to base. Near the apex of the free wall activity moves entirely from inside out. In the lateral aspects of the left wall, and in most of the right wall, activity moves from apex to base, as if there were some barrier to movement from inside out. [From Sodi-Pallares & Calder (126).]

Sodi-Pallares and collaborators (126) have produced a somewhat more detailed and somewhat contradictory picture of two-dimensional ventricular depolarization in the dog (fig. 29). Although they do not state whether this picture results from detailed measurements or from limited measurements plus some deduction, it is probable that the material is in part deduced. It should be noted that in figure 29 the septum is depolarized from left to right. The free walls are generally depolarized in a fashion similar to that which will be discussed in connection with the studies by Scher *et al.* (117, 119). It should however be noted that the basal epicardial layers of the wall are excited by a wave which moves up the

wall rather than from inside out and that there appears to be some barrier to inside-out movement of the wave in these basal regions.

Map of Ventricular Activation

Ventricular activation [(fig. 30) (117, 119)] apparently commences somewhat earlier on the left than on the right. As indicated above, the left bundle separates into two separate branches and it is possible, although by no means proved, that activity commences in two separate areas supplied by the anterior and posterior branches of the bundle, respectively. On the right, activity begins earliest at the septal termination of the right bundle, in the region of the anterior papillary muscle of the right ventricle. In addition to the fact that earliest activity is usually found on the left, a greater volume of tissue is usually activated early on the left. Septal activity on the left moves toward the center of the septum, as does that on the right as well. These two waves of activation thus tend to cancel. The preponderance of activity moving from left to right is important in the production of the initial deflections of the electrocardiographic complex. Branches of the Purkinje system run from the septal terminations of both bundles to the free wall. On the left these bundles are rather close to the endocardium; on the right, one or more branches of the bundle cross the cavity. The activity moves out along these branches to the endocardium and the periendocardial regions of the free walls almost immediately after the beginning of septal excitation.

Since most of the apical mural endocardium is now excited, the major direction of movement available to the depolarizing impulse is toward the epicardium. The impulse moves toward the epicardium throughout the major portion of the QRS complex. If we think of this impulse as a wave directed from the inside out in the wall and remember that the terminations of the Purkinje fibers on the right are somewhat anterior, we can see that initially the wave will be directed to the right and anteriorly at this region. On the left, however, there is activity directed anteriorly, apically, and posteriorly in the apical portion of the left wall. Because the right wall is thin, the wave of activity breaks through to its surface early in the QRS complex and, for this reason, the right wall ceases to be electrocardiographically important. The thicker left wall, particularly posteriorly, and the posterior right wall, however, are not activated so

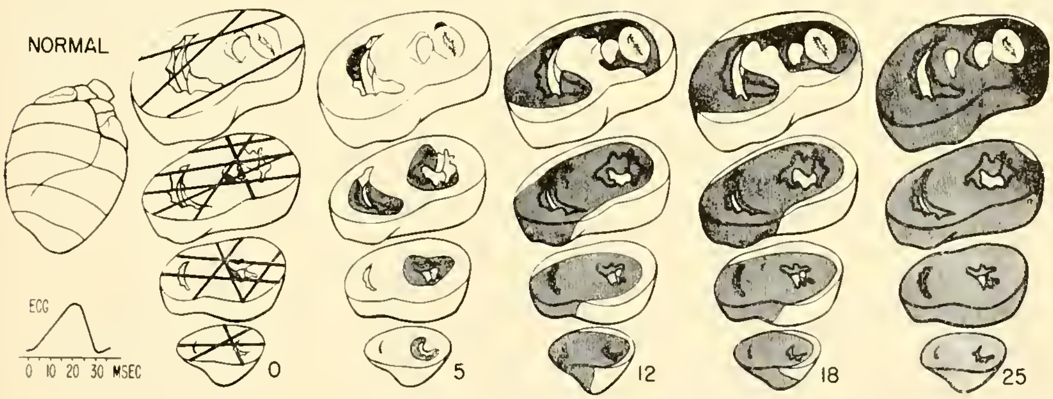

FIG. 30. Pathway of normal ventricular excitation in dog as plotted by noting extent of depolarization 0, 5, 12, 18, and 25 msec after beginning of QRS complex. Simultaneous lead II electrocardiogram is shown. At 0 msec, small amount of muscle bordering left cavity is active. This volume of muscle is too small to give a deflection in peripheral electrocardiogram at this amplification. At 5 msec after beginning of QRS, an incomplete and irregular cone of activity surrounds left cavity, mostly on septal aspect, and a smaller cone surrounds right cavity. By 12 msec after beginning of QRS, these two cones have united in lower three sections and have joined slightly in upper section. Heart now contains a cone of depolarized muscle within an incomplete cone of muscle which is still in resting state. Notice breakthrough of electrical activity anteriorly on right. This leaves activity in posterior and leftward portion of ventricles unopposed. This pattern of excitation continues during next 6 msec. Picture at 18 msec is generally unchanged, although amount of muscle depolarized is, of course, larger; the fraction of posterior and left portions of the ventricle in resting state has become smaller. At 25 msec after beginning of QRS complex, only a small amount of muscle in posterior and lateral portion of left wall and of basal septum remains to be excited. Dark lines on the first drawing indicate the positions of electrodes used to plot this pattern of activity. [From Scher (114a).]

early and the mean direction of activity thus sweeps to the left and posteriorly.

Eventually, the wave completely depolarizes all apical portions of the right and left ventricles, leaving unexcited a basal and posterior portion of the left ventricle. In addition, there is a change in the direction in which the wave of activation in the septum moves. The apical portions of the septum are depolarized from both surfaces, but the leading edge of the boundary between resting and active tissue is directed basally. Also, there appears to be less Purkinje tissue on the right than in the left, so that the basal portion of the septum is often excited by a wave moving from left to right and toward the base of the heart late in the QRS complex. The latest activity is thus directed posteriorly, slightly leftward, and basally in the wall and basally in the septum. The velocity of conduction across the septum and in those portions of the wall where there is no evidence of Purkinje penetration has been calculated by measuring the time and distance between successive positions of the wave front. The velocity averages 0.37 m per sec. Along the endocardium the velocity of spread cannot be calculated, since many endocardial points are simultaneously activated by the highly branched Purkinje system. A detailed picture of the activation as directly measured in the dog is given in figure 30.

Conduction During Ventricular Extrasystoles

The data concerning excitation of the canine ventricles already discussed are explained by the anatomy of the conduction system—the locations of its terminations and its extensive branching—and by the conduction velocities of 1 to 2 m per sec and 0.3 to 0.4 m per sec for Purkinje fibers and myocardial fibers, respectively. Studies of conduction during extrasystoles provide a means of checking this explanation. Scher & Young (118) stimulated various ventricular points at a rate slightly higher than the sinus rate. The conduction velocity was about 1.0 m per sec near the endocardium and parallel to it in the apical regions of the heart, and about 0.3 m per sec within much of the thickness of the walls and septum, and along the basal endocardium. The pathway of excitation was such that it was explained by the endocardial and mural velocities stated, and the electrocardiographic complexes recorded in lead II were in accord with the pathway (fig. 31).

Durrer and van der Tweel (41) found that with epicardial stimulation the wave traveled with constant velocity to the endocardium. With endocardial stimulation, they generally observed a straight inside-out spread, even in regions where reversals of polarity during normal beats had indicated Purkinje fiber penetration. During some extrasystoles the normal

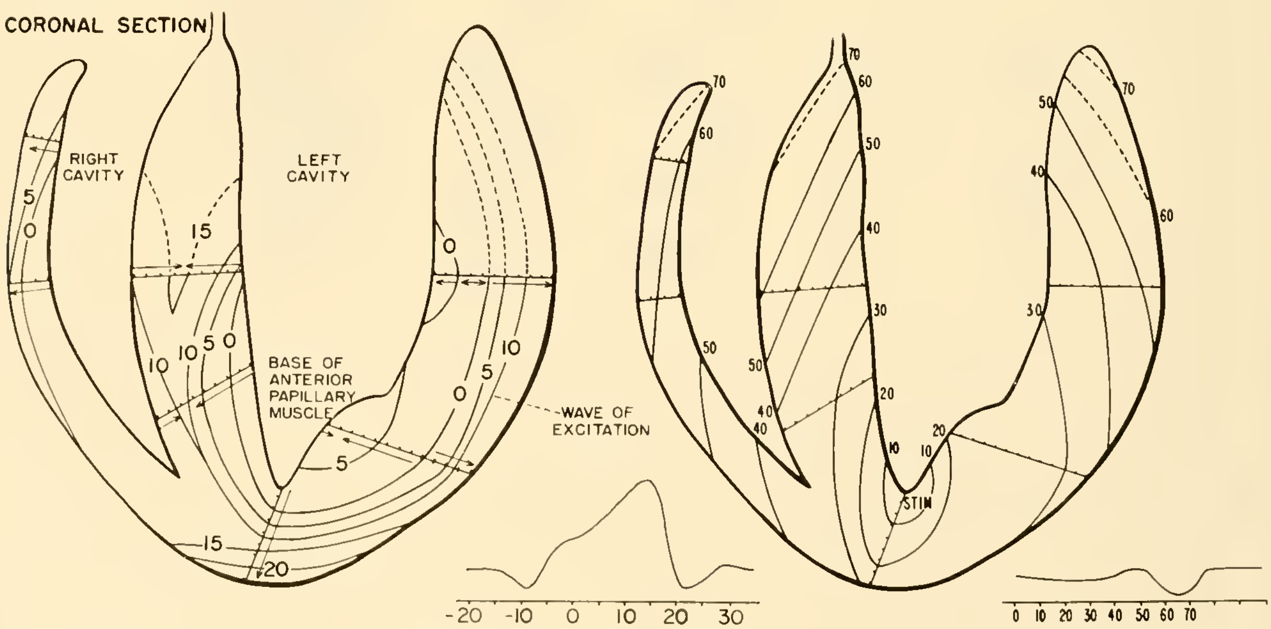

FIG. 31. Successive positions of depolarizing wave front for coronal section of heart in normal beat (left) and in premature systole which originated at apical endocardium (right). Electrode terminals 1 mm apart. Arrows above and below each drawing indicate the approximate position of the line connecting the lead II terminals. [From Scher & Young (118).]

reversals of polarity were preserved, and these results were thought to reflect direct stimulation of the Purkinje fibers.

As indicated earlier, a variety of experiments indicate that conduction in the atria is more rapid along the long axes of the fibers. Similar data has been supplied for the ventricles by Sano and coworkers (109), who found velocities generally 2 to 10 times higher parallel to the fiber direction than perpendicular to it.

Ventricular Activation and the QRS Complex

The shape of the ventricular complex recorded at the body surface is determined by the pattern of ventricular activation, the particular ECG lead which is recorded, and the position of the heart within the chest. Direction of the activation wave will therefore vary with respect to recording points on the body surface according to the position of the heart; also the activation process undoubtedly varies from individual to individual with such anatomic features as wall thickness, distribution of Purkinje tissues, etc. A detailed discussion of the electrocardiogram will follow in the next chapter. However, a brief description of the origin of the human ventricular (QRS) complex seems appropriate here. The consideration is directed toward the potentials recorded at conventional sites on the body surface. As is explained in the preceding chapter, the "V" designation on an electrocardiographic lead means that the potential is recorded between a body surface point and a terminal which averages the potential of the two upper extremities and the left leg. In considering the relation of depolarization to potentials recorded at the body surface, it must be remembered that the right ventricle lies anteriorly and the left posteriorly. The septum is tilted slightly forward apically, and the base-to-apex axis of the heart is often quite parallel to the diaphragm. In this presentation, data from the dog heart are transposed to the human and the duration of the QRS complex (40 msec in the dog) is extended to 80 msec.

As indicated earlier, the initial phase of ventricular

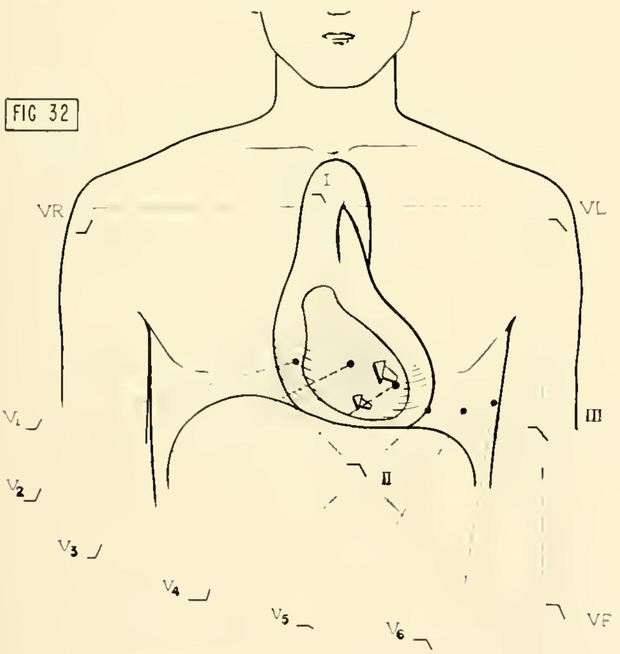

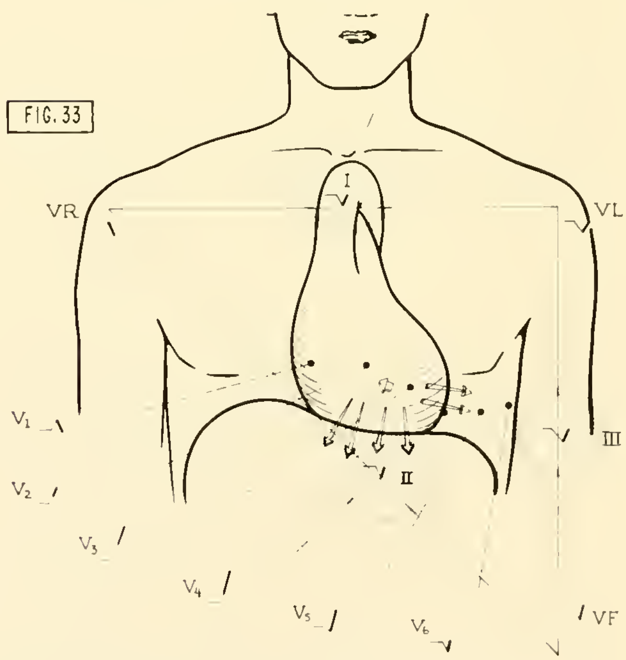

FIG. 32. Mean direction of activity during earliest portion of QRS transposed from canine to human heart. First activity goes from left to right in septum. Because of position of septum in human chest, this results in negative deflection in all bipolar limb leads, positive deflection in VR and in leads on right side of precordium (V_1 through V_4), and negative deflection in V_5, V_6, VL, and VF. [From Scher (114a).]

FIG. 33. When about one-quarter of QRS interval has passed, activity is proceeding from left to right in septum, and activity from inside out in wall has begun. Total activity is such that potentials are near zero in all limb leads, both bipolar and unipolar, and in V_1 and V_6. Other leads on chest are positive because activity proceeds toward the apex and free left wall. [From Scher (114a).]

activity in the dog is usually directed from left to right in the septum and results from earlier and/or greater initial left-to-right activity. This activity, transposed to the human heart, would produce a wave directed to the right, toward the head (since the left side of the septum lies caudally), and possibly slightly anteriorly (fig. 32). This wave will produce an initial negative deflection in all limb leads, termed the Q wave. For the leads on the precordium, the picture is also clear. The leads on the right side of the chest (V_1 and V_2) face the positive side of the wave front and record an upward deflection, while those on the far left (V_5 and V_6) record a negative deflection.

Immediately after invasion of the septum begins (fig. 33), rapid conduction through the Purkinje system results in an irregular pattern of inside-out spread in the walls; the transition from the first phase of activity to this second and major phase of ventricular activity is smooth and gradual. Within the septum, left-to-right activity predominates slightly. Arrows drawn perpendicular to the advancing wave front depict the instantaneous vector of depolarization. At 5 msec after the beginning of QRS in the dog (by extrapolation 12 msec after the beginning of QRS in man), the average direction of these arrows indicates a pattern of activity directed slightly forward to the right and from base to apex. Such a pattern will result in negative deflections in leads II and III, and little or no deflection in lead I, which may be positive or negative at this time. The potentials in the leads on the anterior chest surface will differ slightly from those occurring during the earlier phase, since the leads on the right will now "see" both approaching (left to right) and receding (base to apex) activity. The approaching activity will be in the right wall and on the left side of the septum; the receding activity in the left wall and in the right septum. At this time, there may be little or no potential in these leads and a positive deflection in V_3.

At 15 msec after the onset of QRS in the dog, i.e., almost halfway (35 msec in man) through QRS

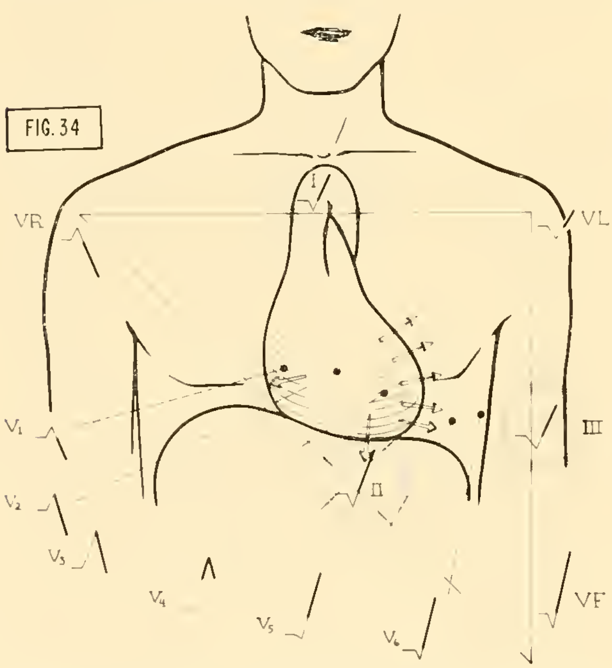

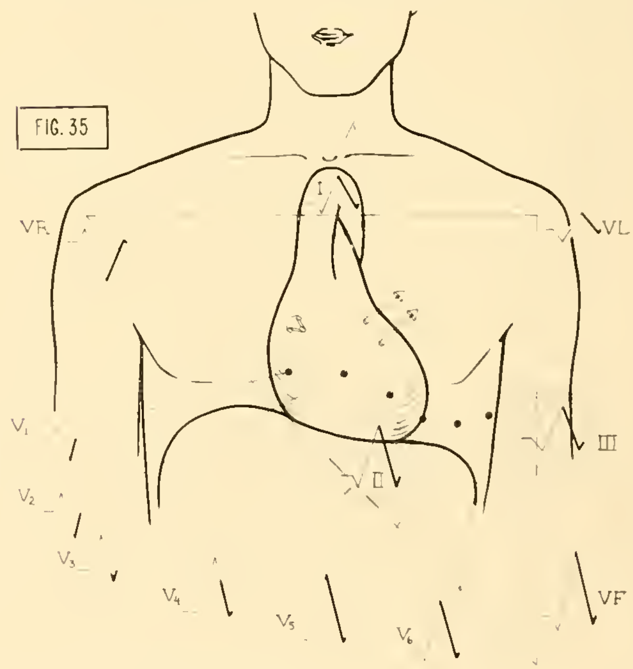

FIG. 34. At about the middle of QRS interval, breakthrough of activity to anterior right ventricle has left forces moving to left posteriorly relatively unopposed. The result is a negative deflection in lead VR and positive deflections in all other limb leads. The leads on far right of chest (V_1 and V_2) now see negative activity; potential at V_3 is near zero, and potentials at V_4, V_5, and V_6 are positive. [From Scher (114a).]

FIG. 35. During terminal portion of QRS complex, activity is directed to left and posteriorly in basal left ventricle and basally in upper septum. This condition results in potentials which are small in all leads. Deflection in VR is positive, deflections in all other limb leads are negative. Potentials are now returned to zero from negative peak in V_1 and V_2 and from positive peak in V_4, V_5, and V_6. This activity results in slight negative potentials in V_3, V_4, V_5, and V_6. [From Scher (114a).]

(fig. 34), union of the two separate masses of activated tissue around the ventricle has produced strong forces directed posteriorly, to the left, and inferiorly. The breakthrough of activity to the anterior right wall has greatly reduced the left-to-right component, and over-all activity is directed apically, posteriorly, and to the left in the apical, lateral, and anterior left wall. Some opposing inside-out activity persists in the basal right wall. At this time, positive deflections will appear in all standard limb leads, and the leads on the left side of the chest will "see" approaching activity. The continuation of this pattern results in the eventual disappearance of the wave front anteriorly, on the right, and in the central and apical portions of the heart. Overlying precordial leads will therefore record negative potentials.

The over-all pattern of activity immediately following the above, i.e., about midway through QRS, is a continuation of the movement toward the thin slice of lateral posterior left ventricle, which remains in the resting state, and a smaller movement toward the basal septum. Depolarization reaches the apex of the heart on the right, and some muscle in the apical region of the left ventricle remains to be depolarized. The net result is a wave moving posteriorly, leftward, and slightly toward the apex. Again, the limb leads will be positive. The chest leads except V_5 and V_6 (on the far left) will, however, show negativity.

After depolarization of the apical regions is complete (25 msec after the beginning of QRS in the dog and about 60 msec in the human), i.e., for the last quarter of the QRS complex, a wave moves from the inside out in the walls near the base of the left ventricle, particularly posteriorly and from apex to base in the septum. This wave is relatively ineffective in causing potentials in lead I, although leads II and III should show a negative potential; the potentials in the chest leads will be small but generally negative (fig. 35).

In figure 30 it can be seen that the depolarization process exhibits a great amount of symmetry around the longitudinal axis of the heart. At various instants, activity is proceeding in opposite directions in the lateral walls and/or in the septum. This symmetry of depolarization leads to "cancellation" of much of the cardiac electrical activity as recorded from the body surface. It has been estimated that the recorded potentials are 5 to 10 per cent of what might be expected if there were no cancellation (112). Any condition which alters the sequence of ventricular depolarization in a manner to reduce this cancellation will, of course, produce an increase in the magnitude of the potentials recorded in one or more leads. This is true of bundle branch block and many types of infarction, and also of impulses arising in abnormal sites.

To summarize, we may divide ventricular activation into three phases, remembering that they succeed one another smoothly and are not separate. The first phase is one of predominant activity from left to right and anteriorly in the septum. The second, consisting of inside-out activity in the wall plus double invasion of the septum, produces very strong forces directed from base to apex, somewhat posteriorly and to the left. The final phase is the activity—directed from apex to base, leftward, and posteriorly—resulting from activation of the basal posterior left wall and the basal septum.

Ventricular Repolarization

In most electrocardiographic leads in man the T wave has the same electrical polarity as the QRS complex, i.e., is usually upright when the QRS is upright. Since the electrical charges across the cell boundaries are oppositely arranged during repolarization and depolarization, the polarity of the record would be opposite if repolarization followed the depolarization pathway. Repolarization therefore does not follow the same pathway and, indeed, the pathway tends to be the reverse. It is important in this connection to consider whether repolarization is electrically propagated.

In studies with the intracellular electrode (140) repolarization of a fiber was induced by appropriate stimulation (i.e., by stimuli causing the inside of the fiber to become negative). Induced repolarization could propagate through a single fiber. In cardiac tissue in low calcium solutions, induced repolarization might propagate through several fibers. It is, however, doubtful that repolarization normally is propagated in the ventricles. Calculations of the density of current flow indicate that the current flowing during repolarization is less than 1 per cent of that flowing during depolarization. Such a small current probably cannot initiate a propagated wave.

If repolarization is not propagated, we may wonder why the configuration of the T wave is consistent under normal conditions. Several factors have been thought to control the sequence of repolarization; among them are temperature and pressure. According to one theory, the pressure differential within the walls favors initiation of repolarization in the outer layers, and repolarization occurs later near the

endocardium (10). Another theory considers the repolarizing wave to "move" from apex to base because of temperature differences, the apex being warmer due to its proximity to the liver.

Potentials within the right and left cavities of the human heart are negative during repolarization. Sodi-Pallares and co-workers (75) interpreted these findings as indicating that the T wave normally results from a spread of repolarization from the outside to the inside of the left wall. He believed further that electrical forces from other portions of the ventricles cancel one another, and that the right wall and the septum are electrically silent during repolarization, i.e., have no clear-cut direction of repolarization but repolarize at random. Available data do not allow complete acceptance of any theory concerning ventricular repolarization, although the normal "pathway" of repolarization is apparently independent of, although statistically generally opposite to, the pathway of depolarization. In a careful study Reynolds & Vander Ark (94) found a general correlation between the direction of ventricular recovery and the polarity of T waves recorded on the epicardial surface. When the T wave was negative or negligible, the epicardium recovered later than the endocardium. When the T waves were positive, recovery was delayed in the deeper layers. It should also be noticed that acute injury produced by the ligation of the coronary arteries caused an earlier recovery in the deeper layers, sometimes extending to the surface. (This is important in connection with studies of myocardial injury discussed below.)

Ventricular Activation in the Ungulate Heart

The pathway of ventricular excitation in the ungulate heart has been determined in part by Durrer & van der Tweel (41) and by Hamlin & Scher (51). In the ungulate heart, as indicated previously, there is a widespread penetration of Purkinje fibers into the depth of the free wall. This leads to a nearly simultaneous activation of much of the depth of the free wall and in this respect, particularly according to the latter investigators, the ungulates are quite different from the dog and monkey. In some experiments Durrer found that even when extrasystoles were started at the endocardium, the epicardial layers were excited in an epicardial-endocardial direction, pointing to a very extensive Purkinje penetration (fig. 36).

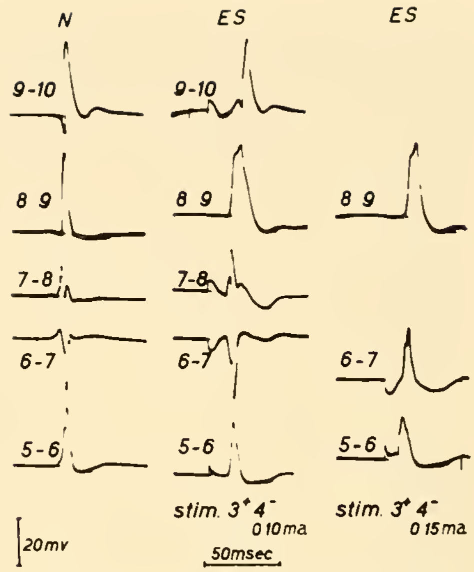

FIG. 36. Records of normal (*N*) and extrasystolic (*ES*) activity in a goat's heart. During normal activity, deflections on channels 5–6, 7–8, 8–9, and 9–10 are upright, indicating movement from inside out (from endocardium to epicardium) at these sites; downward deflection appears on channel 6–7. With endocardial stimulation at low current, virtually this pattern was reproduced; at a higher current (on the far right), however, activity was entirely from inside out. [From Durrer & van der Tweel (41).]

Three-Dimensional Activation in the Goat (*Fig. 37*)

During the earliest portion (5 msec) of the QRS complex, activity is found in a cup-shaped zone around the apex of the left ventricular cavity including the endocardial portions of the septum and the free wall. This activity is moving to the left in the septum and, since it occurs in a buried area within the free wall, is moving towards both the endocardium and the epicardium. Within the next 10 msec the apical third of the septum is excited from both the left and the right ventricular endocardial surface. It is interesting to note that there is double envelopment of the septum from both endocardial surfaces as in the dog. Most of the free walls of the ventricles are also activated during this period, in what has been described as a "single burst" of depolarization. Only a small apical and basal region of the free wall, particularly of the left ventricle, remains to be excited. This portion of the wall is excited during the next 3 to 5 msec, along with the middle third of the interventricular septum. The final 15 msec of the QRS complex and some period beyond its end are occupied by activation of the basilar portion of the interventricular septum. This basilar portion is excited

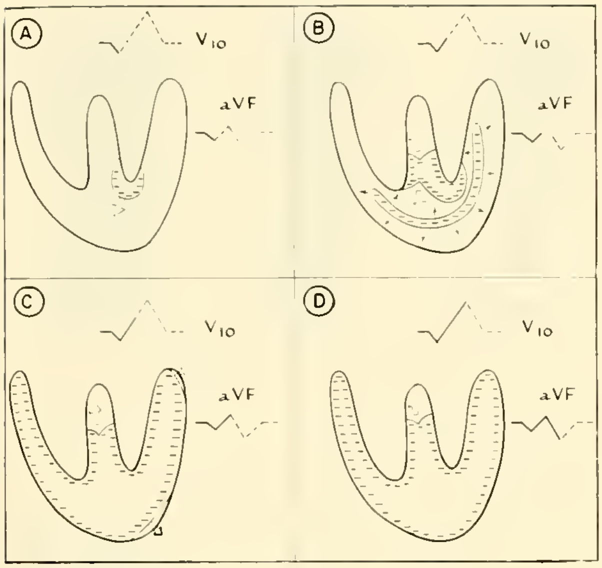

FIG. 37. The boundary between active and resting muscle at four instants in time during depolarization of the ungulate ventricle. *A:* an initial phase of activity is directed from left to right at the left and apical portion of the junction between septum and free wall. *B:* this left-to-right septal activity is joined by activity from right to left in the septum, and there is also simultaneous activation of a large portion of the wall, between endocardium and epicardium. The activity in the wall is moving towards both the epicardium and the endocardium. *C:* very rapidly thereafter most of the wall is depolarized, and only a small apical portion and a high basal portion of the left wall remain to be depolarized in addition to the septal region, which is being depolarized by a wave moving from apex to base. *D:* the final phase of ventricular activation involves a movement of the wave towards the base of the septum. Leads V_{10} and AVF are shown in their approximate positions with respect to the heart. [From Hamlin & Scher (51).]

by a wave moving towards the base and somewhat toward the right, since left-to-right activity preponderates in this portion of the septum as in its more apical portion. Interestingly, the widespread Purkinje fiber penetration in the goat is so efficient in conducting the impulse that the QRS complex may be of virtually normal duration when extrasystoles are started at a single ventricular focus (52) or when one bundle is cut.

Derivation of the Ventricular Electrocardiogram in the Ungulate

Figure 37 shows the approximate position of the boundary between depolarized and resting muscles at four instants during ventricular activation in the goat. Leads aVF and V_{10} are shown in approximate position with respect to these boundaries. The excitation of the apical region of the septum and of the left ventricle, which occurs during the first 5 msec of the goat electrocardiogram, generates negative potentials in aVF and V_{10}. The excitation of the interventricular septum that follows is directed from both endocardial surfaces toward the center, and the activation of the wall is directed both endocardially and epicardially. There is so much cancellation during this activity that only a very small potential or, generally, an isoelectric period is seen in the electrocardiogram. During the next period the septum is activated from both surfaces by a wave which moves from apex to base and results in basally directed activity. At this time the wall has been almost entirely activated, except for a small posterior basal region on the left. In these regions, as in the septum, activity is moving toward the base of the heart and positive potentials are seen in both aVF and V_{10}. This late activation of the basal septum (and wall) gives rise to a major deflection in the electrocardiogram, because of the cancellation of potentials generated during activation of much of the apical portion of the heart. This same apical portion gives rise to the major electrocardiographic deflections in such animals as the dog and monkey, and undoubtedly in man.

ABNORMAL EXCITATION

Bundle Branch Block

Bundle branch block results from failure of transmission either in the right or left conduction bundles, or in their terminal ramifications. The usual cause is probably myocardial damage from infarction or fibrosis from long-standing cardiac disease, although right bundle branch block may occur in normal young persons. The term "complete bundle branch block" is an arbitrary designation for beats originating in the A-V node but having a total QRS duration of over 120 msec in man.

The pattern of ventricular excitation in complete left bundle branch block in the dog is shown in figure 38; to produce this pattern, the left bundle was cut immediately under the aortic valve. Figure 39 indicates the changes resulting from right bundle branch block. Here the right bundle was cut in its course down the right side of the interventricular septum. As might be expected, after the main bundle

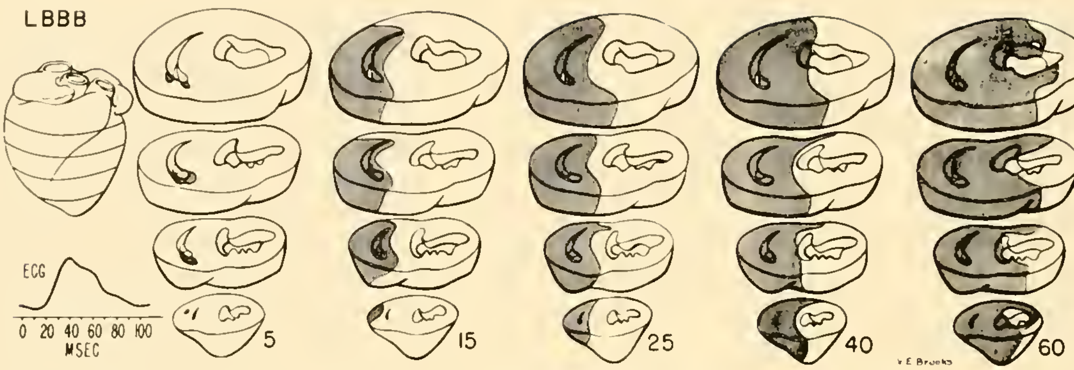

FIG. 38. Ventricular depolarization after left bundle branch block. This figure should be compared with fig. 30, which shows a normal depolarization pattern. Shaded area represents portion of myocardium depolarized up to the instant indicated at bottom of column, and this is compared with lead II electrocardiogram. Note that activity begins around right cavity, proceeds gradually across septum as depolarization of right free wall is completed, and has reached approximately center of septum at 25 msec after beginning of QRS. Activity continues across septum through 40 msec, and even at 60 msec after beginning of QRS, lateral left ventricle is not completely excited. Note that both septal activation and activation of left wall are altered by bundle branch block. Increased time required to excite septum and left wall accounts for prolongation of depolarization in complete left bundle branch blocks. This figure, like fig. 30, represents activity in the dog heart in which the duration of normal QRS is 40 msec or less. [From Becker *et al.* (15).]

was interrupted, the normal double envelopment of the septum was replaced by one-way activation from the unblocked side, and activation of the free wall began at the sites first reached by spread of depolarization across the septum. The wave of excitation utilized the endocardial Purkinje fibers and traveled along the endocardium on the side of the block at about 1 m per sec (15, 44). In normal conduction, simultaneous excitation of many endocardial points by the branched Purkinje system leads to an apparently infinite endocardial conduction velocity.

Prolongation of the QRS complex in bundle branch block results both from the increased period of time required to activate the septum (5, 15, 44) and from the greater time required to activate the blocked free wall. The change in the activation of the free wall during right bundle branch block in the dog is shown in figure 39. Normally, it requires about 18 msec to activate the right mural endocardium, and a large central area is activated within a few milliseconds by the branching Purkinje system. After block, the impulse reaches the wall at the inferior and posterior junctions of the wall and the septum, and spreads anteriorly and superiorly. The smooth progression of the wave is altered as it breaks through the septum superiorly. The total time required to activate the free wall after block is 35 msec (44). Similar changes in mural activation are seen after left bundle branch block (29, 130).

In the dog, complete right bundle block doubles the duration of QRS; complete left bundle branch block increases it two and one-half times. Comparable durations of the QRS in man would be 160 and 200 msec for complete right and complete left block, respectively. A clinical diagnosis of complete block is based on far less prolongation of the QRS complex, i.e., 120 msec or more. In complete right bundle branch block we would expect that the initial left-to-right septal activation would be present and that the loss of the early activity on the right septum (right to left) would be partly counterbalanced by the elimination of early inside-out activation of the free wall (left to right). Such appears to be the case. The free right wall is the last portion of the heart to be activated, a situation which produces late positive deflections in V_1 and V_2, and aVR. Grant (49) believed that these conditions are met only rarely in clinical examinations and concluded that truly complete right bundle branch block is extremely uncommon. Complete left bundle branch block is more common and is accompanied by clear signs of right-to-left activation of the septum and left ventricle. In bundle branch block, as in ventricular ectopic beats, those portions of the ventricular myocardium which depolarize first tend to repolarize first, and, similarly, the last areas to fire recover latest. Consequently, the T wave tends to become a mirror image of the QRS complex; leads in which the QRS is upright show a downward T wave, etc.

In conditions clinically described as complete

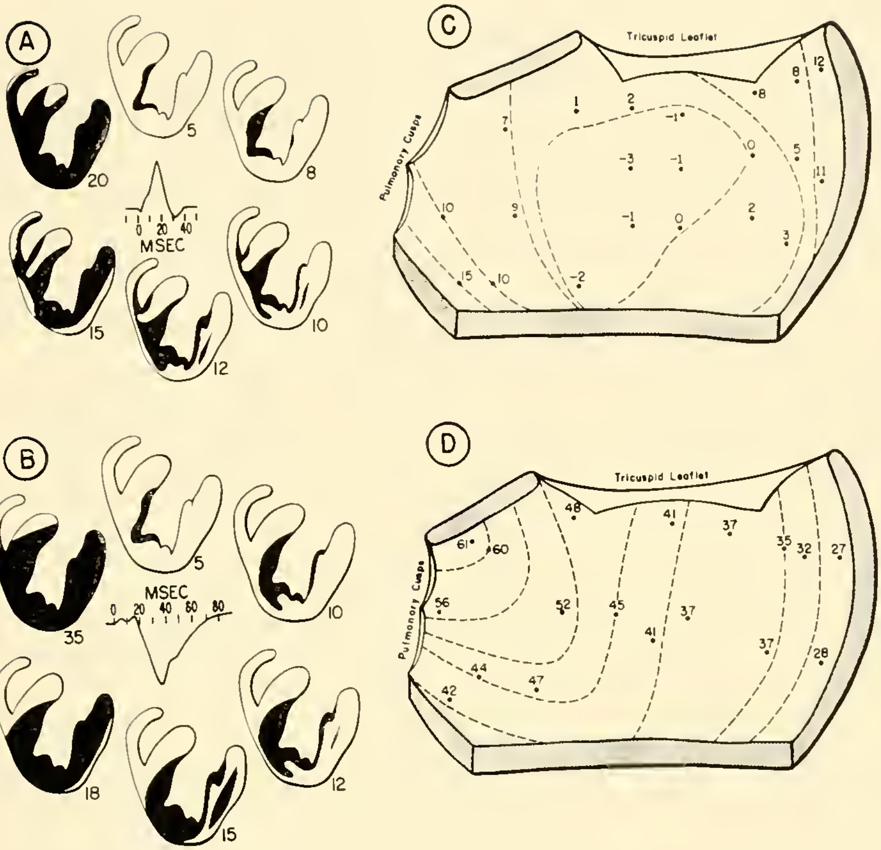

FIG. 39. Pattern of ventricular depolarization before and after right bundle branch block. *A* and *B:* sagittal sections through right and left ventricles showing pathway as measured by nine multipolar insertions. Small numbers show position in heart of depolarization wave at various stages of depolarization. *A:* normal depolarization; normal lead II QRS is shown at center. *B:* pattern of ventricular depolarization during right bundle branch block (same insertion as in *A*). Lead II QRS is typical of canine right bundle branch block. *C* and *D:* pattern of activation of right mural endocardium as viewed from inside right cavity. Shaded areas indicate junction of right wall and septum. Numbers indicate time of depolarization in milliseconds after onset of QRS. Dotted lines approximate wave front position at 5 msec intervals. *C:* normal depolarization. *D:* pattern of activation after right bundle branch block. [From Erickson *et al.* (44).]

bundle branch block, the QRS may have a duration as short as 120 msec. The mechanism of such prolongation (which is not equivalent to that produced by cutting the bundle in the dog) is not at all clear. Possibly damage to fine strands of the Purkinje network (arborization block) or even frank myocardial damage might lead to such lengthening of the QRS. In unpublished experiments in dogs, Gould has cut the strands of the right bundle which run to the free right wall. He finds some prolongation of QRS and other changes, but this procedure does not duplicate any known clinical lesion.

Flutter and Fibrillation

The arrhythmias, involving greatly increased heart rate, flutter and fibrillation, are of interest to us since they represent "pathological" types of conduction resulting from modifications of the normal physiology of myocardial cells. It appears to many observers that flutter and fibrillation are different degrees of the same arrhythmia and that the two can arise from a very fast heart beat referred to as paroxysmal tachycardia. Flutter is generally confined to the atrium. It consists of a very rapid sequential depolarization of the atria—so fast that the rate verges on 300 beats per min. Fibrillation involves even higher rates, at times greater than 500 beats per min.

The mechanism of these two conditions has greatly interested physiologists and electrocardiologists, and a heated controversy has existed concerning this mechanism. Lewis (71) considered fibrillation to result from a "circus movement" of the layer of excitation. He used as a model a type of conduction which can be seen in the muscle of the jellyfish, where a circulating wave can be induced to progress around a ring of muscle. Models of this condition have been created in other animals (76). If a portion of tissue on the superior vena cava is damaged by clamping with forceps, an impulse started at one side of the damaged region may proceed around the ring, return to the original site, be conducted slowly through the damaged region, and find the initial site again excitable. Other theories have been offered as alternatives to the "circus theory" (122). In the two main alternates, a rapidly firing focus and multiple ectopic foci are suggested as the source of

periodic excitation. Some studies have been concerned with ionic changes during fibrillation (66). It appears questionable that flutter and fibrillation are ordinarily induced by changes in the ionic environment of the cells, or at least that such changes are necessary precursors of these arrhythmias.

Certain interesting aspects of fibrillation suggested to Lewis that some orderly sequence of events must lead to this condition of complete disorder. In the first place, a certain volume of tissue is necessary for fibrillation to occur. The cat's atrium cannot be made to fibrillate by electrical stimulation, and the cat's ventricle will fibrillate only transiently and recover spontaneously. The dog's atrium will generally fibrillate transiently and recover spontaneously, but if the dog's ventricle begins to fibrillate, heroic measures are required to end the condition. The critical nature of tissue volume has also been observed in lower animals. The frog's heart usually will not fibrillate, but a large turtle's ventricles may be made to fibrillate by rapid electrical stimulation. Cooling the heart tends to increase the incidence of fibrillation, and certain ionic changes or addition of hormones and chemicals to bathing solutions inincrease the tendency to fibrillation. Greatly increasing the extracellular concentration of potassium is effective, as is addition of hormones which increase the tendency toward occurrence of ectopic impulses.

An important relevant point is the clinical observation that the Q-T interval shortens as the heart rate increases. This phenomenon has been extensively investigated (25, 132) by means of the intracellular electrode. If a cardiac cell is stimulated near the end of repolarization, the record during the next beat will show a decreased duration of the action potential and a slightly decreased rate of initial depolarization. If the stimulation is repeated before the end of the shortened complex, the action potential will again shorten and the rate of initial depolarization will again decrease. The decreased slope of initial depolarization leads to slowing of the conduction velocity (12).

In the normal myocardium, the conduction velocities fall between 300 mm and 800 mm per sec, about 240 mm of muscle are in the depolarized state at any one time and therefore completely refractory. (This distance is the length of a depolarized segment of a long piece of muscle with the duration of action potential and conduction velocity stated; $L = V \cdot D$.) In ventricular muscle, which conducts at 300 mm per sec, the length of the depolarized segment would be about 90 mm; in Purkinje tissue, about 600 mm. Since normal ventricular conduction utilizes myocardial and Purkinje tissue, the length of the depolarized segment in either the atrium or the ventricle is probably greater than that of any pathway normally found in the human heart. If, however, the action potential becomes continuously shorter at the same time that the velocity becomes continuously slower, the length of the depolarized segment will decrease. When this decrease occurs, it is possible for the wave to "catch its own tail." Once this has happened, the process can be repeated. Each successive completion of the circuit can result in a slower conduction velocity, a decreased action potential duration, and a shorter pathway for the circus wave until, finally, it has a very short pathway. At this time, there could be a large number of circus pathways on the myocardium, possibly undergoing continuous change. In support of this hypothesis it has been reported that, during the early stages of fibrillation in the cooled heart, certain frequencies are repeated on the electrical record and that these finally disappear as fibrillation continues (6).

When Sano and co-workers studied ventricular fibrillation with ultramicroelectrodes, they found some synchrony of activity early in fibrillation but none later (111). There were also some changes in the action potential and an irregularity in the magnitude and configuration of the action potential during fibrillation. Records obtained with both intracellular and extracellular electrodes indicate that once fibrillation has been established, the situation is one of complete chaos.

Myocardial Injury; Ischemia and Infarction

PHASE 1. If a region of myocardium is partially deprived of oxygen, the first change observed electrocardiographically is an alteration of the T wave. Apparently the region of ischemia cannot repolarize normally. Possibly the ischemic region remains depolarized after adjacent regions have returned to the resting state. An overlying electrode will therefore record a negative T wave that is usually larger than normal. A similar change in the T wave is seen during recovery from an infarction. It should be noted that the T wave is a most labile portion of the electrocardiogram and less reliable for diagnostic purposes than other portions of the ventricular complex. Changes similar to those resulting from ischemia arise also from benign causes. If the entire heart is uniformly deprived of oxygen, T wave changes may appear in all leads.

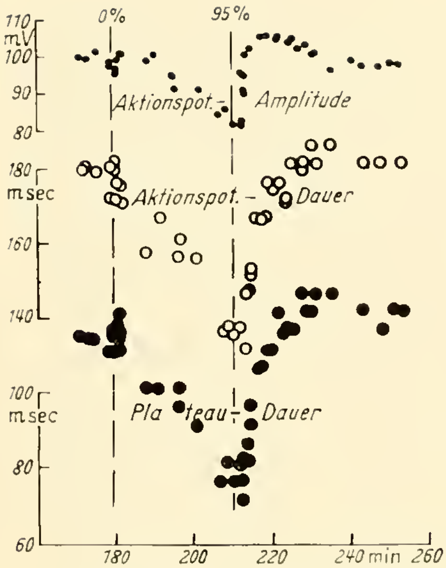

FIG. 40. The effects of oxygen lack on the action potential of heart muscle. Transition from 95% to 0% oxygen leads to decrease of amplitude and duration of the action potential. [From Trautwein & Dudel (133).]

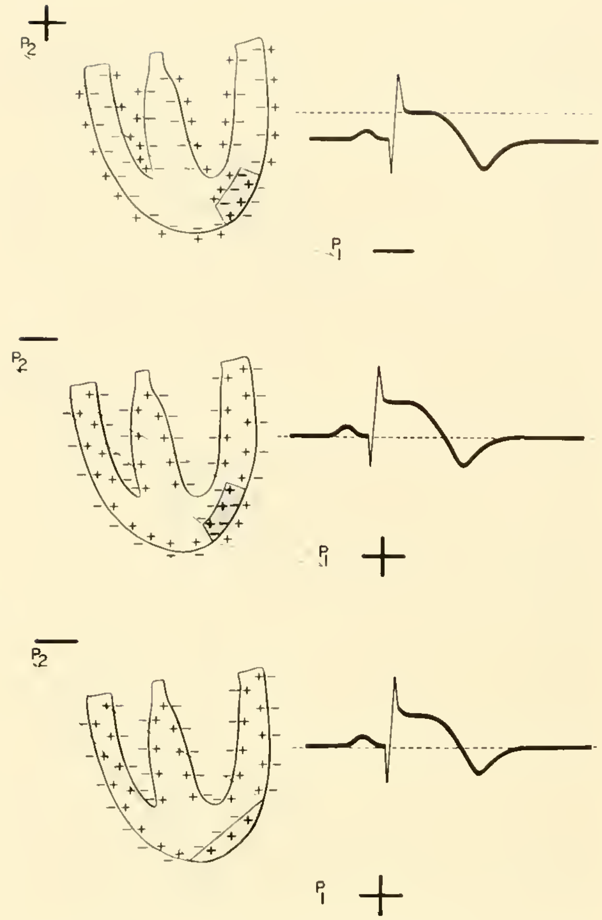

FIG. 41. Three possible mechanisms for S-T segment changes. In the top drawing, the base line is depressed at rest, i.e., during the T-Q interval. Since the injured cells are partially depolarized during this period, current flows into them. When all cells are uniformly depolarized during the S-T interval, the base line is at true zero. In the second case, the base line is normal at rest but elevated during the S-T interval due to a shortening of the action potential duration in the injured cells. In the third case, the injured cells cannot depolarize. A wave of activity reaches the border of the injured region but cannot invade it, so that the S-T segment is elevated. The second of these states occurs early in experimental infarction and is followed by the first.

PHASE II. When a blood vessel supplying the ventricular myocardium is completely occluded by a thrombus or the deposition of atheromatous plaques in the vessel wall, and when no collateral circulation exists, the cells previously supplied by this vessel will be completely deprived of oxygen. A complicated series of events will ensue, all of them causing the same change in the relationship between the S-T and T-Q segments.

The first change which takes place is a shortening of the intracellular action potential. This occurs within a few seconds after the tying of a ligature in an experimental animal, as has been demonstrated by several investigators (105, 133, fig. 40). When the action potential is shortened, the injured cells depolarize normally but repolarize more rapidly than do adjacent normal cells. For this reason, during the period of repolarization, i.e., during the S-T segment of the electrocardiogram, current flows from the injured cells to the adjacent normal cells (since, by definition, current flow is from positive to negative). This flow then leads to a change in the S-T segment, which becomes elevated in unipolar leads facing the area of the infarct. This elevation is a primary change in the S-T segment; it is transient, however, and recovery from this phase occurs within a few minutes (figs. 40, 41).

While this change is still in effect (and during the period of recovery), a second change takes place: a decrease in the steady potential of the injured cells. Since the steady potential of the injured cells is now lower than that of the adjacent uninjured cells, current flows from the normal cells into the injured ones during electrical diastole. (This current is frequently referred to as the "current of injury.") This condition produces a depression of the T-Q segment of the electrocardiogram in unipolar electrodes facing the area of injury. At first this depression adds to the true S-T segment shift mentioned previously, but it continues after the initial change disappears. The

input capacitors of the electrocardiographic recorder prevent its use to discriminate between a shift in the T-Q segment and a shift in the S-T segment. In the clinical literature, both of these changes are referred to as "S-T segment elevation" in electrodes facing the injury. (Electrodes facing the rear of the injury record the opposite changes.) At present, there seems to be no need to discriminate among these various causes of "S-T segment elevation" during acute and chronic occlusion of the vessels, and such a discrimination would present overwhelming technical problems.

A later change has been described by Durrer *et al.* (42) and by Conrad *et al.* (31). At this time, some cells in or near the "infarcted" region fail to depolarize normally, depolarizing much later than they normally would. [See also Trautwein (131).] A unipolar electrode facing the area of injury thus sees approaching (positive) activity immediately after the QRS complex. Again, this change produces a true S-T segment elevation, but it has not been demonstrated that the increase in conduction time is equal to the S-T interval (200 msec). It would have to be of this duration if it were to account for the changes in the S-T segment. Possibly, this change and the second change, which is a true T-Q depression, exist together during the period of chronic injury in patients, although there is no direct evidence at present.

PHASE III. After the initial phases of ischemia and injury have disappeared, the S-T segment and T wave may return to normal. The diagnosis of such chronic infarcts is a difficult problem for the practitioner and may be important in determining whether a patient should be treated or should limit his activity. The major problem exists with regard to the QRS complex. In many cases, a sizable portion of the myocardium will have been replaced by scar tissue which is, of course, electrically silent. If the conduction system has not been impaired by the infarction, the duration of the QRS complex may be normal; if a large amount of myocardium is missing, the complex will be changed, i.e., it will lack the potentials previously contributed by the infarcted region. An electrode which faces the infarcted region and which previously recorded approaching (positive) activity from that region will record less positivity than normal, or it may record a negative deflection. If the area of infarction is in a part of the heart which is normally depolarized early, this increased negativity may either produce an initial negative deflection or increase the magnitude of a negative deflection which would normally occur in the lead facing the region. An initial negative deflection is referred to as a Q wave, and an abnormal Q wave is the most common diagnostic sign of chronic infarction. Q waves are not abnormal per se; the abnormality is frequently definable only in terms of the magnitude or duration of the wave in a particular lead. Some portions of the body surface normally show Q waves. Although this sign is useful, if it is the sole criterion of infarction, a diagnosis obviously can be made only when the infarction lies in regions which are depolarized early in QRS.

Several recent textbooks of electrocardiography have described successful techniques for the detection of an infarction which affects the later portions of the QRS complex. Some large infarcts may damage the conduction system, thus causing a prolongation of the QRS complex. It may be important to differentiate such prolongation from that seen in bundle branch block, since the latter may be present and innocuous in an otherwise healthy heart. The value of a control electrocardiogram taken before any reason exists to suspect myocardial damage should be apparent.

It is interesting that, during the period after infarction, a fixed relationship between changes in the S-T segment and T wave is often observed; those leads which show elevated S-T segments show a negative T wave. Although the mechanism has not been directly determined, a possible explanation is available by extrapolation from observations by Durrer *et al.* (42) and Bayley (14), as well as Conrad *et al.* (31). Since depolarization is delayed in some cells in the infarcted region, might not these cells also repolarize late? Late depolarization would elevate the S-T segment and late repolarization would cause a negative T wave over the region. That is, the wave of repolarization would approach a lead over the infarction so slowly as to give a large negative deflection. (Remember that approaching repolarization produces a negative potential.)

REFERENCES

1. AAGAARD, O. C. AND H. C. HALL. Über Injektionen des "Reizleitungssystems" und der Lymphgefässe des Säugetierherzens. *Anat. Hefte* 51: 359, 1914.
2. ABRAMSON, D. I. AND S. MARGOLIN. A Purkinje conduction network in the myocardium of the mammalian ventricles. *J. Anat.* 70: 250, 1936.

3. ALANIS, J., E. LOPEZ, J. J. MANDOKI, AND G. PILAR. Propagation of impulses through the atrioventricular node. *Am. J. Physiol.* 197: 1171, 1959.
4. ALANIS, J., C. RODRÍGUEZ, AND A. ROSENBLUETH. El automatismo del nodo aurículo-ventricular. II. La acción de la adrenalina y del simpático. *Arch. Inst. cardiol.* (*México*) 25: 571, 1955.
5. AMER, N. S., J. H. STUCKEY, B. F. HOFFMAN, R. R. CAPPELLETTI, AND R. T. DOMINGO. Activation of the interventricular septal myocardium studied during cardiopulmonary bypass. *Am. Heart J.* 59: 224, 1960.
6. ANGELAKOS, E. T. AND G. M. SHEPHERD. Autocorrelation of electrocardiographic activity during ventricular fibrillation. *Circulation Res.* 5: 657, 1957.
7. ARVANTAKI, A. *Propriétés Rythmiques de la Matière Vivant. II. Etude Expérimentale sur le Myocarde d'Hélix.* Paris: Hermann, 1938.
8. ASCHOFF, L. Die Herzstoerungen in ihrer Beziehung zum spezifischen Muskelssystem des Herzens. *Zentralbl. Path. u. path. Anat.* 21: 433, 1910.
9. ASHMAN, R. AND R. HAFKESBRING. Unidirectional block in heart muscle. *Am. J. Physiol.* 91: 65, 1929.
10. ASHMAN, R. AND E. HULL. *Essentials of Electrocardiography.* New York: Macmillan, 1957.
11. ATHANASION, D. AND H. GAPFERT. Untersuchungen über das Sinus-elektrogramm des kaltbluterherzens. *Arch. ges. Physiol.*, 245: 265, 1941.
12. BAMMER, H. Die Beziehungen zwischen der Reizfrequenz und der Geschwindigkeit der Erregungsbreitung im Herzmuskel. *Ztschr. ges. exper. Med.* 121: 488, 1953.
13. BARKER, P. S., A. G. MACLEOD, AND J. ALEXANDER. The excitatory process observed in the exposed human heart. *Am. Heart J.* 5: 720, 1930.
14. BAYLEY, R. H. The electric field produced by an eccentric dipole in a homogeneous circular conducting lamina. *Circulation Res.* 7: 272, 1959.
15. BECKER, R. A., A. M. SCHER, AND R. V. ERICKSON. Ventricular excitation in experimental left bundle branch block. *Am. Heart J.* 55: 547, 1958.
16. BIDDER, F. Über functionell verschiedene und räumlich getrennte Nervenzentra im Froschherzen. *Arch. Anat. Physiol.* 163, 1852.
17. BITTENCOURT, D., D. M. LONG, Y. K. LEE, AND C. W. LILLEHEI. Intravital staining of the atrioventricular bundle with iodine compounds during cardiopulmonary bypass. *Circulation Res.* 7: 753, 1959.
18. BORDUAS, J. L., L. RAKITA, R. KENNAMER, AND M. PRINZMETAL. Studies on the mechanism of ventricular activity. XIV. Clinical and experimental studies of accelerated auriculoventricular conduction. *Circulation* 11: 69, 1955.
19. BOZLER, E. The initiation of impulses in cardiac muscle. *Am. J. Physiol.* 138: 273, 1943.
20. BRADY, A. J. AND H. H. HECHT. On the origin of the heart beat. *Am. J. Med.* 17: 110, 1954.
21. BRENDEL, W., W. RAULE, AND W. P. TRAUTWEIN. Die Leitungsgeschwindigkeit und Erregungsausbreitung in den Vorhöfen des Hundes. *Arch. ges. Physiol.*, 253: 106, 1950.
22. BROOKS, C. MCC., B. F. HOFFMAN, E. E. SUCKLING, AND O. ORIAS. *Excitability of the Heart.* New York: Grune & Stratton, 1955.
23. BURCHELL, H. B., H. E. ESSEX, AND R. D. PRUITT. Studies on the spread of excitation through the ventricular myocardium. II. The ventricular septum. *Circulation* 6: 161, 1952.
24. BURDON-SANDERSON, J. AND F. J. M. PAGE. On the time-relation of the excitatory process in the ventricle of the heart of the frog. *J. Physiol.* 2: 384, 1879.
25. CARMELIET, E. AND L. LACQUET. Durée du potentiel d'action ventriculaire de grenouille en fonction de la frequente influence des variations ioniques de potassium et sodium. *Arch. internat. physiol.* 66: 1, 1958.
26. CLEMENT, G. Über eine neue Methode zur Untersuchung der Fortleitung des Erregungsvorganges im Herzen. *Ztschr. Biol.* 58: 110, 1912.
27. COHN, A. E. On the auriculo-nodal junction. *Heart* 1: 167, 1909–10.
28. COHN, A. E. Cardiac Muscle. In: *Special Cytology*, edited by E. E. Cowdrey. New York: Hoeber, 1147, 1932.
29. CONRAD, L. L. AND T. E. CUDDY. Activation of the free wall of the right ventricle in experimental right bundle branch block. *Circulation Res.* 7: 173, 1959.
30. CONRAD, L. L. AND T. E. CUDDY. The influence of boundary conditions on the amplitude of R and other accession potentials in leads from the ventricular wall. *Circulation Res.* 8: 82, 1960.
31. CONRAD, L. L., T. E. CUDDY, AND R. H. BAYLEY. Activation of the ischemic ventricle and acute peri-infarction block in experimental coronary occlusion. *Circulation Res.* 7: 555, 1959.
32. CRAIB, W. A study of the electrical field surrounding active heart muscle. *Heart* 14: 71, 1927.
33. CRANEFIELD, P. F., B. F. HOFFMAN, AND A. PAES DE CARVALHO. Effects of acetylcholine on single fibers of the atrioventricular node. *Circulation Res.* 7: 19, 1959.
34. CURTIS, H. J. AND D. M. TRAVIS. Conduction in Purkinje tissue of the ox heart. *Am. J. Physiol.* 165: 173, 1951.
35. DAVIES, F. The conducting system of the bird's heart. *J. Anat.* 64: 129, 1930.
36. DAVIES, F. AND E. T. B. FRANCIS. The conducting system of the vertebrate heart. *Biol. Rev.* 21: 173, 1946.
37. DAVIES, F., E. T. B. FRANCIS, AND T. S. KING. The conducting (connecting) system of the crocodilian heart. *J. Anat.* 86: 152, 1952.
38. DOWER, G. E. AND J. A. OSBORNE. Surface activation of guinea pig ventricle determined by intracellular electrodes. *Am. J. Physiol.* 195: 396, 1958.
39. DRAPER, M. H. AND S. J. WEIDMANN. Cardiac resting and action potentials recorded with an intracellular electrode. *J. Physiol.* 115: 74, 1951.
40. DURRER, D. *Experimenteel Onderzoek Naar Het Verloop Van Het Activatieproces in de Hartspier.* Amsterdam: Scheltema & Holkema, 1952.
41. DURRER, D. AND L. H. VAN DER TWEEL. Excitation of the left ventricular wall of the dog and goat. *Ann. New York Acad. Sc.* 65: 779, 1957.
42. DURRER, D., A. A. W. V. LIER, R. TH. V. DAM, E. JONKMAN, AND G. DAVID. The intramural electrocardiogram of myocardial infarction. IIIrd World Congress Cardiol. 355, 1958.
43. ERFMANN, W. Ein Beitrag zur Kenntnis der Fortleitung des Erregungsvorganges im Warmblüterherzen. *Ztschr. Biol.* 61: 155, 1913.
44. ERICKSON, R. V., A. M. SCHER, AND R. A. BECKER. Ventricular excitation in experimental bundle-branch block. *Circulation Res.* 5: 5, 1957.

45. Eyster, J. A. G., W. J. Meek, and W. E. Gilson. Spread of impulse over the ventricles in the mammalian heart. *Am. J. Physiol.* 123: 60, 1938.
46. Gardberg, M., and R. Ashman. The QRS complex of the electrocardiogram. *A.M.A. Arch. Int. Med.* 72: 210, 1943.
47. Glomset, D. J. and A. T. A. Glomset. A morphological study of the cardiac conduction system in ungulates, dog, and man. *Am. Heart J.* 20: 389, 1940.
48. Goormaghtigh, N. Die eigenartige Struktur der Herzohren. *Arch. Kreislaufforsch.* 1: 377, 1937.
49. Grant, R. P. *Clinical Electrocardiography.* New York: McGraw Hill, 1957.
50. Groedel, F. M. and P. R. Borchardt. *Direct Electrocardiography of the Human Heart.* New York: Brooklyn Medical Press, 1948.
51. Hamlin, R. L. and A. M. Scher. The ventricular activation process and genesis of the QRS complex in the goat. *Am. J. Physiol.* 200: 223, 1961.
52. Hamlin, R. L., C. R. Smith, and R. W. Redding. Time-order of ventricular activation for premature beats in sheep and dogs. *Am. J. Physiol.* 198: 315, 1960.
53. Harris, A. S. The spread of excitation in turtle, dog, cat and monkey ventricles. *Am. J. Physiol.* 134: 319, 1941.
54. Hecht, H. H. (editor). The electrophysiology of the heart. *Ann. New York Acad. Sc.* 65: 653, 1957.
55. Helmholtz, H. F., quoted in R. Lorente de Nó, *A Study of Nerve Physiology* (2) New York: Rockefeller Institute, 1957, 387.
56. Hering, H. E. Nachweis dass die Verzögerung der Erregungsüberleitung zwischen Vorhof und Kammer des Säugetierherzens im Tawara'schen Knoten erfolgt. *Arch. ges. Physiol.* 131: 572, 1910.
57. Hoffman, B. F., A. Paes de Carvalho, and W. C. Mello. Transmembrane potentials of single fibers of the atrioventricular node. *Nature* 181: 66, 1958.
58. Hoffman, B. F., A. Paes de Carvalho, W. C. Mello, and P. F. Cranefield. Electrical activity of single fibers of the atrioventricular node. *Circulation Res.* 7: 11, 1959.
59. Inoue, F. Slow potential and conduction delay in the atrioventricular region in the frog's heart. *J. Cell. & Comp. Physiol.* 54: 231, 1959.
60. Jeans, J. *The Mathematical Theory of Electricity and Magnetism* (5th ed.). Cambridge: University Press, 1901.
61. Katz, L. N. The genesis of the electrocardiogram. *Physiol. Rev.*, 27: 429, 1947.
62. Katz, L. N. and A. Pick. *Clinical Electrocardiography*, Chapt. 16, Part 1, The Arrhythmias. Philadelphia: Lea & Febiger, 1956.
63. Keith, A. and M. Flack. The form and nature of the muscular connections between the primary divisions of the vertebrate heart. *J. Anat.* 41: 172, 1907.
64. Kent, A. F. S. Researches on the structure and function of the mammalian heart. *J. Physiol.* 14: 233, 1893.
65. Kistin, A. D. Observations on the anatomy of the atrioventricular bundle (bundle of His) and the question of other muscular atrioventricular connections in normal human hearts. *Am. Heart J.* 37: 849, 1949.
66. Klein, R. L. and W. C. Holland. Factors affecting the incidence of atrial fibrillation. *Am. J. Physiol.* 193: 235, 1958.
67. Koch, W. Neuere Befunde am Sinusknoten der Hufticre. *Deutsche med. Wchnschr.* 36: 688, 1910.
68. Koch, W. Über die Bedeutung der Reizbildungsstellen (kardiomotrischen Zentren) des rechten Vorhofes beim Säugetierherzen. *Arch. ges. Physiol.* 151: 279, 1913.
69. Langendorf, R. and A. Pick. Concealed conduction. *Circulation* 13: 381, 1956.
70. Lewis, T. The spread of the excitatory process in the toad's ventricle. *J. Physiol.* 49: 36, 1915.
71. Lewis, T. *Mechanism and Graphic Registration of the Heart Beat* (3rd ed.). London: Shaw, 1925.
72. Lewis, T. The excitatory process in the dog's heart. II. The ventricles. *Proc. Roy. Soc., ser. B* 206: 181, 1915.
73. Lorente de Nó, R. *A Study of Nerve Physiology*, v. 2, New York: Rockefeller Institute, 1947.
74. Matsuda, K., T. Hoshi, and S. Kameyama. Action potential of the atrioventricular node. *Tohoku J. Exper. Med.* 68: 8, 1958.
75. Medrano, G. A., A. Bisteni, R. W. Brancato, F. Pileggi, and D. Sodi-Pallares. The activation of the interventricular septum in the dog's heart under normal conditions and in bundle-branch block. *Ann. New York Acad. Sc.* 65: 804, 1957.
76. Mines, G. R. On dynamic equilibrium in the heart. *J. Physiol.* 46: 349, 1913.
77. Moe, G. K., J. B. Preston, and H. Burlington. Physiologic evidence for a dual A-V transmission system. *Circulation Res.* 4: 357, 1956.
78. MacKenzie, I. and J. Robertson. Recent researches on the anatomy of the bird's heart. *Brit. M. J.* 2: 1161, 1910.
79. Nagayo, M. Ueber die Glykogengehalt des Reizleitungssystems des Säugetierherzens. *Verhandl. deutsc. pathol. Gesellsch.* 12: 150, 1908.
80. Nylin, G. and C. Crafoord. Das vom Menschenherzen in vivo simultan vom linker und rechten Ventrikel abgeleitete Elektrogramm. *Cardiologia* 6: 136, 1942.
81. Pace, D. Dix années de recherches sur le tissu specifique du coeur. *Arch. mal. coeur* 17: 193, 1924.
82. Paes de Carvalho, A., W. C. de Mello, and B. F. Hoffman. Electrophysiological evidence for specialized fiber types in rabbit atrium. *Am. J. Physiol.* 196: 483, 1959.
83. Pannier, R. Le tissu Purkinien des oreillettes du chat. *Arch. biol.* 50: 271, 1939.
84. Pannier, R. and N. Goormaghtigh. Sur l'existence de faisceau Purkiniens dans l'oreillette droite. *Compt. rend. soc. de biol.* 127: 1114, 1938.
85. Pipberger, H., L. Schwartz, R. A. Massumi, S. M. Weiner, and M. Prinzmetal. Studies on the mechanism of ventricular activity. XXI. The origin of the depolarization complex with clinical applications. *Am. Heart J.* 54: 511, 1957.
86. Prakash, R. The heart and its conducting system in the common Indian fowl. *Proc. Natl. Inst. Sc. India* 22: 22, 1956.
87. Prakash, R. The atrioventricular bundle in the heart of the banded krait, Bungarus fasciatus. *Proc. Natl. Inst. Sc. India* 22: 255, 1957.
88. Prakash, R. The heart and its conducting system in the tadpoles of the frog, Rana tigrina (Daudin). *Proc. Zool. Soc.* 7: 27, 1954.
89. Prinzmetal, M., C. McK. Shaw, Jr., M. H. Maxwell, E. J. Flamm, A. Goldman, N. Kimura, L. Rakita, J. L. Borduas, S. Rothman, and R. Kennamer. Studies on the mechanism of ventricular activity. VI. The depolarization complex in pure subendocardial infarction; role of

the subendocardial region in the normal electrocardiogram. *Am. J. Med.* 16: 469, 1954.

90. Prinzmetal, M., R. Kennamer, E. Corday, J. A. Osborne, J. Fields, and L. A. Smith. Accelerated conduction. *The Wolff-Parkinson-White Syndrome and Related Conditions*. New York: Grune & Stratton, 1952.
91. Pruitt, R. D. and H. E. Essex. Potential changes attending the excitation process in the atrioventricular conduction system of bovine and canine hearts. *Circulation Res.* 8: 149, 1960.
92. Puech, P. *L'activité Electrique Auriculaire Normale et Pathologique*. Paris: Masson, 1956.
93. Purkinje, J. E. Mikroskopisch-neurologische Beobachtungen. *Arch. Anat. Physiol. u Wissensch. Med.* 12: 281, 1845.
94. Reynolds, E. W. and C. R. Vander Ark. An experimental study on the origin of T-waves based on determinations of effective refractory period from epicardial and endocardial aspects of the ventricle. *Circulation Res.* 7: 943, 1959.
95. Rijlant, P. La conduction dans le coeur du mammifère. *Arch. internat. physiol.* 33: 325, 1931.
96. Robb, J. S. Specialized (conducting) tissue in the turtle heart. *Am. J. Physiol.* 172: 7, 1953.
97. Robb, J. S., C. T. Taylor, and W. G. Turman. A study of specialized heart tissue at various stages of development of the human fetal heart. *Am. J. Med.* 5: 324, 1948.
98. Rodríguez, M. I., A. Anselmi, and D. Sodi-Pallares. Activación de las paredes libres ventriculares. I. Activación endocárdica. *Arch. Inst. cardiol. México* 23: 624, 1953.
99. Rodríguez, M. I., D. Sodi-Pallares, and A. Anselmi. Activación de las paredes libres ventriculares. II. Activación del espesor de las paredes libres. *Arch. Inst. cardiol. México* 23: 756, 1953.
100. Rosenbaum, F. F., H. H. Hecht, F. N. Wilson, and F. D. Johnston. The potential variations of the thorax and the esophagus in anomalous atrioventricular excitation. *Am. Heart J.* 29: 281, 1945.
101. Rosenblueth, A. Two processes for auriculo-ventricular and ventriculo-auricular propagation of impulses in the heart. *Am. J. Physiol.* 194: 495, 1958.
102. Rosenblueth, A. El automatismo del nodo auriculoventricular. *Arch. Inst. cardiol. México* 25: 171, 1955.
103. Rosenblueth, A. and R. Rubio. La influencia de la frecuencia de estimulación sobre los tiempos de propagación aurículo-ventricular y ventrículo-auricular. *Arch. Inst. cardiol. México* 25: 535, 1955.
104. Rothman, S., E. Gerlach, M. Prinzmetal, L. Rakita, and J. L. Borduas. Studies on the mechanism of ventricular activity. XIII. Genesis of the depolarization complex in the mammalian heart. *Am. J. Physiol.* 178: 557, 1954.
105. Samson, W. E. and A. M. Scher. Mechanism of S-T segment alteration during acute myocardial injury. *Circulation Res.* 8: 780, 1960.
106. Sano, T., O. Masaru, and T. Shimamoto. Intrinsic deflections, local excitation and transmembrane action potentials. *Circulation Res.* 4: 444, 1956.
107. Sano, T., T. Minoru, and T. Shimamoto. Histologic examination of the origin of the action potential characteristically obtained from the region bordering the atrioventricular node. *Circulation Res.* 7: 700, 1959.
108. Sano, T., E. Ohtsuka, and T. Shimamoto. Unidirectional atrioventricular conduction studied by microelectrodes. *Circulation Res.* 8: 600, 1960.
109. Sano, T., N. Takayama, and T. Shimamoto. Directional difference of conduction velocity in the cardiac ventricular syncytium studied by microelectrodes. *Circulation Res.* 7: 262, 1959.
110. Sano, T., M. Tasaki, M. Ono, H. Tsuchihashi, N. Takayama, and T. Shimamoto. Resting and action potentials in the region of the atrioventricular node. *Proc. Japan Acad.* 34: 558, 1958.
111. Sano, T., H. Tsuchihashi, and T. Shimamoto. Ventricular fibrillation studied by the microelectrode method. *Circulation Res.* 6: 41, 1958.
112. Schaefer, H. The general order of excitation and of recovery. *Ann. New York Acad. Sc.* 65: 743, 1957.
113. Schaefer, H. and W. Trautwein. Über die elementaren elektrischen Prozesse im Herzmuskel und ihre Rolle für eine neue Theorie des Elektrokardiogramms. *Arch. ges. Physiol.*, 251: 417, 1949.
114. Schaefer, H. and W. Trautwein. Weitere Versuche über die Natur der Erregungswelle im Myokard des Hundes. *Arch. ges. Physiol.* 253: 152, 1951.

114a. Scher, A. M. In: *Medical Physiology and Biophysics* (18th. ed.), edited by T. C. Ruch and J. F. Fulton. Philadelphia: Saunders, 1960.

115. Scher, A. M. Direct recording from the A-V conducting system in the dog and monkey. *Science* 121: 398, 1955.
116. Scher, A. M., M. I. Rodriguez, J. Liikane, and A. C. Young. The mechanism of atrioventricular conduction. *Circulation Res.* 7: 54, 1959.
117. Scher, A. M. and A. C. Young. Ventricular depolarization and the genesis of QRS. *Ann. New York Acad. Sc.* 65: 768, 1957.
118. Scher, A. M. and A. C. Young. Spread of excitation during premature ventricular systoles. *Circulation Res.* 3: 535, 1955.
119. Scher, A. M. and A. C. Young. The pathway of ventricular depolarization in the dog. *Circulation Res.* 4: 461, 1956.
120. Scher, A. M., A. C. Young, and A. L. Malmgren. Multichannel recording apparatus for physiological studies. *Rev. Sc. Instr.* 26: 603, 1955.
121. Scher, A. M., A. C. Young, A. L. Malmgren, and R. V. Erickson. Activation of the interventricular septum. *Circulation Res.* 3: 56, 1955.
122. Scherf, D. and A. Schott. *Extrasystoles and Allied Arrhythmias*. New York: Grune & Stratton, 1953.
123. Schonberg, S. Über Veränderungen im Sinusgebiet des Herzens bei chronischer Arrhythmie. *Frankfurt. Ztschr. Path.* 2: 153, 1909.
124. Sodi-Pallares, D., A. Bisteni, and G. A. Medrano. Estudios sobre el síndrome de Wolff-Parkinson-White. *Arch. Inst. cardiol. México* 25: 676, 1955.
125. Sodi-Pallares, D., R. W. Brancato, F. Pileggi, G. A. Medrano, A. Bisteni, and E. Barbato. The ventricular activation and the vectorcardiographic curve. *Am. Heart J.* 54: 498, 1957.
126. Sodi-Pallares, D. and R. M. Calder. *New Bases of Electrocardiography*. St. Louis: Mosby, 388, 1956.
127. Tawara, S. *Das Reizleitungssystem des Saugethierherzens*, Jena: Gustav Fischer, 1906.
128. Thorel, C. Vorläufige Mitteilung über eine besondere Muskelverbindung zwischen der cava superior und dem Hisschen Bundel. *Munchen med. Wchnschr.* 56: 2159, 1909.

129. TODD, T. WINGATE. Specialized systems of the heart. *Special Cytology*, edited by E. E. Cowdrey. New York: Hoeber, 1932, 1173.
130. TRAUTWEIN, W. Experimentelle Untersuchung zur Theorie des Schenkelblock-EKG. *Ztschr. ges. exp. Med.* 117: 204, 1951.
131. TRAUTWEIN, W. Über die Veränderungen der elementaren Daten der elektrischen Erregungswelle des Herzens bei der Insuffizienz des Myocards. *Arch. ges. Physiol.* 252: 573, 1950.
132. TRAUTWEIN, W. AND J. DUDEL. Aktionspotential und Mechanogramm des Warmblüterherzmuskels als Funktion der Schlagfrequenz. *Arch. ges. Physiol.* 260: 24, 1954.
133. TRAUTWEIN, W. AND J. DUDEL. Aktionspotential und Kontraktion des Herzmuskels im Sauerstoffmangel. *Arch. ges. Physiol.* 263: 23, 1956.
134. TRAUTWEIN, W., V. GOTTSTEIN, AND K. FEDERSCHMIDT. Der Einfluss der Temperatur auf den Aktionsstrom des excidierten Purkinje-Fadens, gemessen mit einer intracellularen Elektrode. *Arch. ges. Physiol.* 258: 243, 1953.
135. TRUEX, R. C. AND W. M. COPENHAVER. Histology of the moderator band in man and other mammals with special reference to the conduction system. *Am. J. Anat.* 80: 173, 1947.
136. UHLEY, H. N. AND L. M. RIVKIN. Peripheral distribution of the canine A-V conduction system. *Am. J. Cardiol.* 5: 688, 1960.
137. UHLEY, H. N. AND L. M. RIVKIN. Visualization of the left branch of the human atrioventricular bundle. *Circulation* 20: 419, 1959.
138. VAN DER KOOI, M. W., D. DURRER, R. T. VAN DAM, AND M. S. VAN DER TWEEL. Electrical activity in sinus node and atrioventricular node. *Am. Heart J.* 51: 684, 1956.
139. WALLS, E. W. Dissection of the atrioventricular node and bundle in the human heart. *J. Anat.* 79: 45, 1945.
140. WEIDMANN, S. *Elektrophysiologie der Herzmuskelfaser.* Bern: Huber, 1955.
141. WEST, T. C. Ultramicroelectrode recording from the cardiac pacemaker. *J. Pharmacol. & Exper. Therap.* 115: 283, 1955.
142. WEST, T. C., G. FALK, AND P. CERVONI. Drug alteration of transmembrane potentials in atrial pacemaker cells. *J. Pharmacol. & Exper. Therap.* 117: 245, 1956.
143. WHITE, P. D. AND W. J. KERR. The heart of the sperm whale with especial reference to the A-V conduction system. *Heart* 6: 207, 1917.
144. WIDRAN, J. AND M. LEV. The dissection of the atrioventricular node, bundle and bundle branches in the human heart. *Circulation* 4: 863, 1951.
145. WILDE, W. S., C. E. DRAWE, AND R. ASHMAN. The sequence of excitation of the surface of the turtle ventricle. *Am. J. Physiol.* 129: 497, 1940.
146. WINSOR, T. (editor) *Electrocardiographic Textbook.* New York: Am. Heart Assoc., 1956.
147. WOLFF, L., J. PARKINSON, AND P. D. WHITE. Bundle-branch block with short P-R interval in healthy young people prone to paroxysmal tachycardia. *Am. Heart J.* 5: 685, 1930.

Electrocardiography

HANS SCHAEFER
HANS G. HAAS | *Department of Physiology, University of Heidelberg, Heidelberg, Germany*

CHAPTER CONTENTS

THE ELECTROCARDIOGRAM (ECG) is the record of a superposition of electromotive forces which originate during the activation process in the individual heart muscle fibers. Action currents from the heart were recorded very early in the history of physiology. In 1855, Koelliker & Müller (295) first demonstrated what they called the negative deflection of a beating frog heart. The first actual recording of a frog ECG was made by A. D. Waller (505) in 1887, and that of a human heart, in 1889. The era of modern electrocardiography, however, started with Einthoven (182), who, by the invention of the string galvanometer, was able to record small voltages of short duration. His recording techniques have not been much improved

since they were first published. After Einthoven's initial successes, many workers started a thorough investigation of electrocardiographic data, beginning with a detailed study of the action currents from isolated frog hearts. Burdon-Sanderson, Samojloff, Boruttau, and Bayliss were some of the names closely connected with the early development of electrocardiography. Nevertheless, this entire field of research stagnated for nearly 30 years, until the introduction, by Wilson *et al.* (528), of local leads and the zero electrode in unipolar recordings. In the last decade, a rapid development of the theoretical basis of electrocardiography has occurred, mainly under the influence of physicists, who applied the principles of field theory to the problems of recording. It is the result of much ingenious endeavor by collaborating physicians, physiologists, and physicists that we are now able to operate with mathematically and physically correct concepts.

The electrocardiogram has a twofold peculiarity: on the one hand it is a highly theoretical topic, the physical complexity of which covers the most difficult problems in medicine; on the other hand, the value of this branch of medical science consists exclusively of its application to clinical medicine. The ECG poses no problems, the investigation of which might lead to the advancement of our basic scientific knowledge in physiology or physics. The conditions under which the normal and abnormal ECG originates are most complex in nature, and their elucidation leads only, under optimal conditions, to the statement that the well-known laws of electrical fields and the electrophysiological behavior of single cells, as reviewed in the preceding chapter, are sufficient for the interpretation of the intricacies of electrocardiographic curves. Whatever an electrocardiographer may expect as the result of his scientific endeavor can scarcely be more than a contribution to the questions concerning the translation of an ECG into the language of physiological events, such as the spread of excitation waves and their respective velocities and pathways, duration of local action potentials, their deviations and local differences, and production of excitation in pacemakers. From things like these, perhaps, an indirect conclusion may be possible concerning heart contraction, its mechanical forces, work performance, and imminence of heart failure or recovery. But whatever an ECG may indicate, it certainly is no indicator at all of the function of the heart, which can only be determined by the analysis of stroke volumes ejected at known pressures (408). We definitely know that the ECG can be nearly normal in mechanically ineffective hearts, and, conversely, that greatly disturbed ECG curves may be recorded from an individual with mechanically intact circulation. Even in hearts with scarcely perceptible mechanical movement, the ECG may remain nearly normal (433, 469), though a minimal mechanical movement can always be seen as long as electrical events can be recorded (184). So the very purpose of an ECG is to give information about the direction and velocity of the excitation wave, the inhomogeneities of the excitation process in the various parts of the heart, and the focus which generates this traveling excitation wave. All other conclusions drawn from an ECG are indirect. Observations, theories, and derivations which do not lead to information of this kind are useless.

Interpretation of an electrocardiographic curve is based on three fundamental elements: the theory of derivation, the form of an individual action potential, and the spread of myocardial activation. If these three items were completely known, the ECG of a particular heart would be predictable in every detail. It is our aim in the following sections of this chapter to show how difficult the study of derivation of potentials is. The form of the thorax, the magnitude of the heart and its position and movement during the cardiac cycle, as well as the inhomogeneity of the field in which the heart is embedded, are so complicated that a strict physical solution of the simple problem as to how the electromotive forces of the heart lead to the recorded surface potential seems for the present (and, as we believe, for the future) impossible. In the absence of such a solution, we may use simplified models which permit prediction of the electrical behavior of the heart, at least within certain limits. The action potentials produced by the various myocardial fibers interfere in producing a common electric field. If the potential production in every fiber were the same in pattern and strength, the problem could be handled in a reasonably simple way by making certain assumptions. But the action potential patterns are quite different in the various parts of the heart. Only a marked inhomogeneity in the form of single fiber action potentials can explain the form of the T wave. The spreading process, moreover, cannot be described completely without knowledge of the anatomical structure of the muscular walls, and this is imperfectly known. Even if this knowledge were exhaustive, our problem would still be far from solved: we need detailed knowledge of the way the excitation wave travels across the heart walls, including directions, propagation times, and resulting local latencies.

All this is impossible to achieve. So, every inter-

pretation of the ECG is based upon a model which simplifies the physiological and physical conditions as much as necessary to permit a clinically relevant and relatively simple mathematical formulation. We should always bear in mind that the ECG is primarily a clinical, diagnostic method that must be translated into the simple language of muscular function (contractile force) or prognosis of function under the influence of trauma, drugs, etc. Because, for the most part, translation into such physiological data cannot be achieved, the ECG is merely a toy for some scientists. No basic problems of general interest can be solved on the playground of electrocardiographic research, excluding the problems of production of the potential at the fiber membrane. Our endeavor, therefore, will be to demonstrate how far and to what purpose modern electrocardiographic research serves elementary clinical application. [For further background, see monographs (1–74).]

1. TECHNICAL REMARKS

The basis of every electrocardiographic diagnosis is the record. The reliability of recording systems depends on the properties at the surface of the body of the electrical events generated by the heart. With the usual leads, the ECG has an average potential variation of 1 mv, but recording of potentials accurately to 0.1 mv is necessary (438). Most recording systems possess sensitivities of about 1 mv per cm. The time course of the ECG is comparatively slow, so that a recording velocity of 25 to 50 mm per sec is sufficient. The accuracy of the curve, however, depends mainly on the frequency range of the event to be recorded and of the recording system. Fourier's analyses of the ECG reveal a maximal frequency range of 0 to 140 cps (212), but, in general, the frequencies between 0.3 and 60 cps are responsible for all waves and notches found in a usual record, and 0.5 to 20 cps for all of clinical importance (211).

It is no problem to construct amplifiers with such a frequency band, whereas the construction of adequate recording systems is much more difficult. The best direct writer is doubtless the "mingograph," which utilizes a moving beam of ink spurted out of a very tiny glass cannula. Systems of this kind move at speeds up to a critical frequency of 200 cps, whereas the stylus technique, at its best, reaches an upper frequency of 100 cps.

Evaluation of an ECG is a somewhat tedious procedure. A great variety of techniques and evaluation devices, therefore, have been invented, even going so far as to put the ECG into a computing machine, which analyzes it in all possible directions in an extremely short time.[1] Details are beyond the scope of this review.

2. THE IDEAL ELECTRIC FIELD OF A SINGLE CARDIAC FIBER

The ECG is originated by sources of electrical potential within the muscular wall of the heart; it is, in most cases, picked up by electrodes more or less remote from the heart. We therefore record, in the ordinary ECG, peculiarities of an electric field. The theory of such a field is extremely complicated, because of the irregular body surface, the inhomogeneous conductivity of the thorax, the eccentric position of the heart as the source of the field, and the comparatively large diameter of the heart—large, that is, when compared with every electrode distance possible. Nevertheless, a description of the field of the body surface must start with the simple physical rules which determine the field under ideal conditions. Such conditions are: a homogeneous medium of infinite boundaries, with a central dipole as a source representing the heart. A first step in adapting this ideal condition to reality can be the assumption of a regular, spherical boundary of the medium, thus representing an approximation of the boundaries of the thorax.

The very first papers on the dipole theory of the heart (161) started with the assumption that the electrical source, i.e., the heart, may be represented by a physical dipole consisting of two equal spheres. The fields which are determined by such a doublet of spherical charges of opposite sign are somewhat similar to the fields of single muscular fibers, in spite of their completely different geometrical form.

It was Wilson *et al.* (530) who introduced a more realistic model of the heart as a source of electric potential. Figure 1 gives a more correct model of the electrical charges producing the field in the case of a single active fiber which is closed at both ends (410). If, in such a fiber, the potential difference across the membrane is equal at any point along the fiber, no potential field is generated in the surrounding medium (homogeneous double layer). This is true in the resting as well as in the "completely" activated state. If, however, an excitation wave has entered the fiber, so that one part of the fiber (the right in fig. 1) is still resting,

[1] Research going on at the National Bureau of Standards, Washington, D. C. (336, 370, 478).

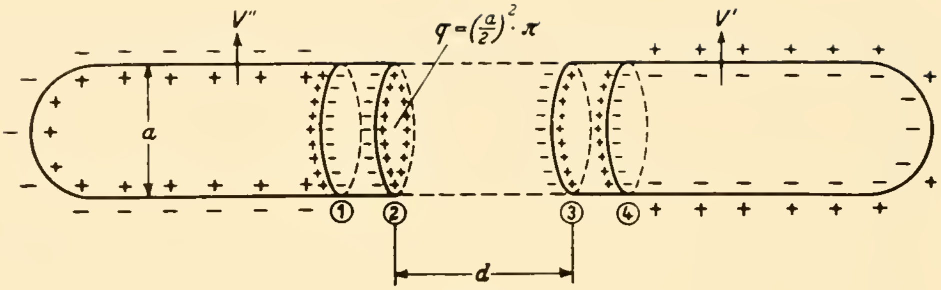

FIG. 1. Model of an elementary dipole: a myocardial fiber. The right part of the fiber is at rest, the left maximally excited. Both parts of the fiber may be reduced to electrical ineffectiveness by adding charged discs, 1 and 4, having the same potential difference across their surfaces as the membrane of the fiber. The two now completely closed, though oppositely charged, parts of the fiber no longer develop an electric field. The addition of discs 1 and 4 is neutralized, however, by the addition of two more discs, 2 and 3, of opposite polarity but the same potential difference as disc 1 or 4. These two discs, 2 and 3, now produce the same electric field as the action potential. The area between the discs is disregarded here, but it may be analyzed in the same manner, with the same result, by cutting it into infinitesimally small slices. V' and V'' are the respective membrane potentials of the resting and the excited membrane. The potential recorded is determined according to fig. 2. [From Schaefer (58).]

one part (the left) already completely activated, we may perform the following theoretical operation. Let the membrane potential of the resting fiber be V', of the activated fiber V'', in both cases as viewed from the inside to the outside of the fiber. The resting potential V' appears to be positive, the activated membrane potential V'' ("overshoot") negative. The resting as well as the activated part of the fiber may be completed to an over-all closed surface of constant membrane potential by inserting a disc (1 and 4 in fig. 1), so that these parts of the fiber become electrically inactive. The introduction of the closing disc (1) must be compensated for electrically by a second disc, (2), of equal area but opposite charge. This disc 2 is thus the only charge acting to produce an electrical field. The same procedure is utilized with the resting part of the fiber, which opens toward the active portion. It is closed by disc 4, the charge of which is electrically compensated for by the charge of disc 3. The result is that the electrical disturbance at the region of activation may be represented by two discoid charges. Each of these two discs represents a dipole, which is composed of two surfaces carrying opposite charges. A dipole of this type is characterized by the magnitude of the area and the dipole moment m per unit area, which is defined as

$$m = \frac{V}{4\pi} \tag{2.1}$$

when V is the potential difference between the two surfaces of each disc. The potential difference of these discs is measured in the direction of the traveling excitation wave, i.e., in figure 1 from left to right. Under these circumstances the potential differences of the disc 1 to 4, V_1 to V_4, are

$$V_1 = V''; \quad V_2 = -V_1; \quad V_3 = -V_4; \quad V_4 = -V'$$

This moment m introduces the real membrane potential V into the calculation, its magnitude being well known from experimentation. This is important, because all electrocardiographic records are made using electrodes that lie far away from the heart on the conductive medium that surrounds the electrically active fibers. If we consider the distribution in such a homogeneously resistive medium of the potential originated by discoid charges like those of figure 1, and their dipole moments per unit area, a very simple equation can be written, which describes the local potential V_p at any point p of the field (without regarding the sign):

$$V_p = m \cdot \Omega \tag{2.2}$$

where Ω is the solid angle under which the charged discs appear, looking from the electrode (fig. 2). The surface q of the disc determines, to a great extent, the local field potential; it is, however, contained in the value of the solid angle Ω, which is directly proportional to the surface q of the dipole.

In figure 1, the two discs 2 and 3 develop two different moments m_2 and m_3, which may be added without appreciable error, if the exploring electrode is sufficiently remote from the fiber.[2] In this case the

[2] "Sufficiently remote" means that the distance between the exploring electrode and the center of the disc is great compared with the dimensions of the myocardial fiber.

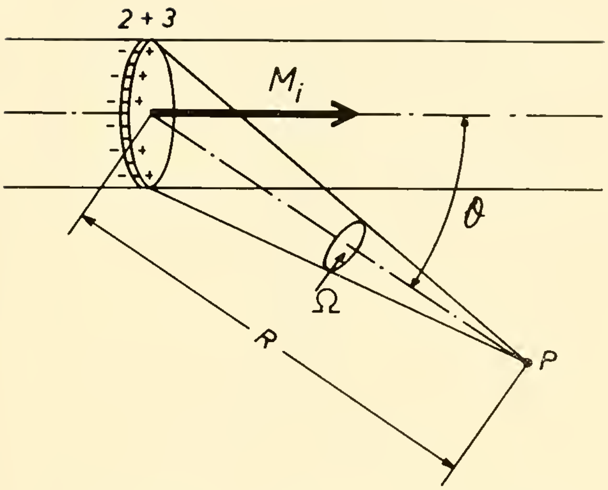

FIG. 2. The amount of potential recorded at P from the charge at discs 2 and 3 of fig. 1, the potential differences of which are summed. The potential is proportional to the solid angle Ω, under which the discs appear from the electrode point P. M_i is the individual total moment of the two discs.

fiber during the "accession" process may be represented by only one single discoid charge with the square unit moment

$$m = m_2 + m_3 = \frac{V}{4\pi} \qquad (2.3)$$

where $V = -V'' + V' = |V''| + |V'|$ is the spike potential of the monophasic action potential, counted in its absolute value.

In figure 1 we closed the two ends of the fiber by two discs, 1 and 4, a procedure which apparently does not take into account the fact that between the resting and the active portion of the fiber a certain part of the fiber is in a transient state. Nevertheless, a correct solution is possible if one extends the principle of figure 1 to a subdivision of the fiber into infinitely small slices, to each of which the same procedure is applied (233). The general result of such a consideration is that the dipole moment of the single fiber can be represented by the simple expression of equation 2.3, where V equals the difference between the membrane potentials at the beginning and the end of the fiber.

For many purposes equation 2.2, containing the solid angle Ω, is difficult to apply. Especially if vectorial concepts are introduced, the dipole must be represented by its total moment M_i[3] which takes into account the fact that the field potentials are proportional to the surface q of the charge.

$$M_i = q \cdot m \qquad (2.4)$$

This moment M_i can be represented by a vector which stands perpendicular to discs 1 to 4 and lies along the fiber directed from − to +, its length indicating the scalar value of M_i. Since the membrane resting and action potentials of the various cardiac fibers are nearly identical, the length of the vector is dependent only upon the cross section of the fiber, when identical instants of the depolarization process are compared.

Using the total moment M_i, a second expression of the local field potential generated by a single fiber may be given:

$$V_p = M_i \cdot \frac{1}{R^2} \cdot \cos\theta \qquad (2.5)$$

where R is the distance between the exploring electrode and the center of the disc, and θ the angle between $\overrightarrow{M_i}$ and the "lead line," joining the exploring electrode and the dipole center (fig. 2).

The foregoing equations are valid only in infinite homogeneous, linear resistive media. If the medium has a boundary, the flow lines are forced to run parallel to the boundary and are thereby compressed, leading to a higher density of lines near the boundary and therefore to higher local potentials. Simple equations for such limited fields can be derived only for spherical forms. Even in cylinders they are rather complicated (145, 362). The following is the equation for the potential V_p at the point P inside a spherical medium (151):

$$V_p = q \cdot m_i \left(\frac{1}{r^2} + \frac{2r}{R^3}\right) \cos\theta \qquad (2.6)$$

where r is the distance between the exploring electrode and the dipole, R is the radius of the sphere, $m_i = V/4\pi$, if V is the spike potential, and q is the cross section of the fiber. Figure 3 gives a picture of the equipotential lines. The potentials at the surface of the sphere $(r = R)$ follow the much simpler equation

$$V_p = M_i \cdot \frac{3}{R^2} \cos\theta \qquad (2.5a)$$

or, in the form of equation 2.2

$$V_p = 3 \cdot m_i \cdot \Omega \qquad (2.2a)$$

This means that the potentials at the surfaces of the sphere are three times as great as they could be if

[3] The index i to M refers to the individual fiber, the moment of which is represented by M_i.

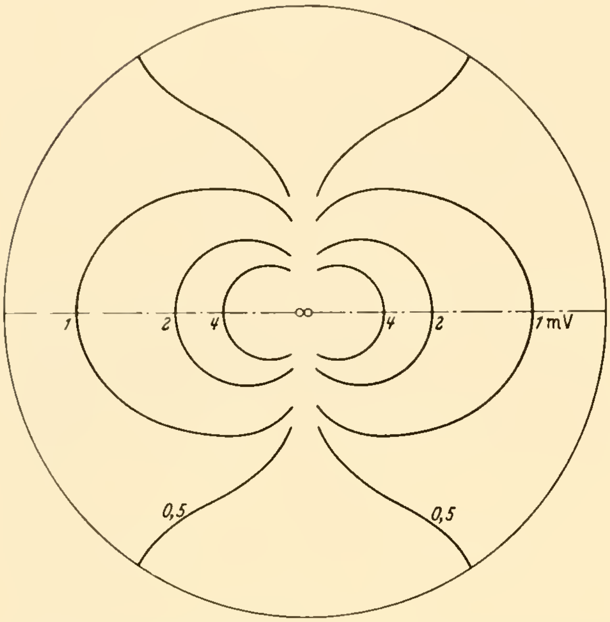

FIG. 3. Equipotential lines in a spherical, limited electric dipole field of homogeneous conductivity. The dipole is indicated by the two circles and lies in the center of the sphere. The sign for the values of one side is opposite that for the other. [From Schaefer (58).]

recorded at a similar distance from the dipole from an interior point in an infinite medium. Calculations for special dipoles in a tank model are given by Nelson (357).

The physics of the field are those of a stationary current. There are apparently no whirlpools detectable, since the algebraic sum of derivations forming a closed circle is zero (18). There is no evidence that the potential distribution is distorted either by impedances or by nonlinear resistance properties (437).

The meaning of "potential" V_p in equations 2 and 5 of this section needs a more detailed explanation. The value of V_p is identical with the potential difference between the reference electrode and a very remote point of the field. As may be seen from figure 4, the potential of a very remote point is identical with a potential to be found at the point between the dipole charges. This potential may be called the "mid-dipole potential," but the term "zero potential" is commonly used. The term "zero potential" may be misunderstood. It does not mean a "potential" of zero value in the meaning of the potential theory (140). The use of the word "zero" in connection with the ECG indicates that an electrode lies in a certain area of the potential field reaching from a point of mid-dipole potential between the poles or discs to the

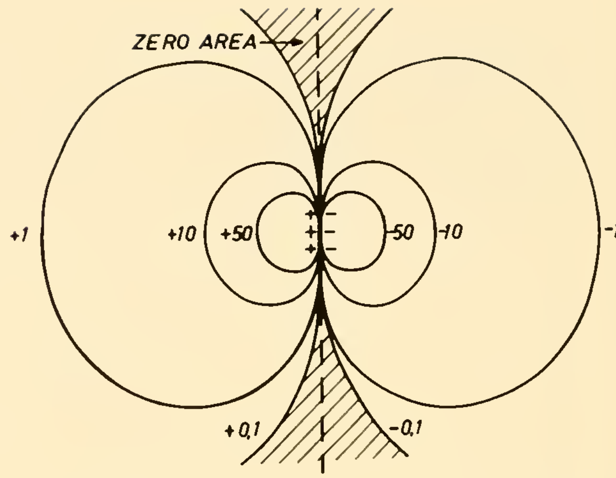

FIG. 4. Definition of a zero area in an infinite dipole field. (See text.)

infinitely remote boundaries of the field (204). If, for practical purposes, "zero" is assumed at any point of the field where the potential difference against the plane of symmetry is less than a certain percentage (e.g., 0.1) of the dipole potential difference, we find a "zero area" which may be symbolized in figure 4 as a shaded area. Every electrode lying in this area may be assumed to be at zero potential in this practical sense.

Every recording system consists of two electrodes, the potential differences of which are led to the input of an amplifier. If the two electrodes are both put on arbitrary points of the field or of the body surface, the record measures the difference $V_{p1} - V_{p2}$ of the potentials at the points P_1 and P_2. Such a record is called "bipolar."

If one of the two recording electrodes is put on the zero area of the field, the potential difference recorded between this and a second, "different" electrode, is called a "unipolar potential."

Zero electrodes may easily be defined in an ideal field of infinite extension. In the practice of electrocardiography, however, the use of unipolar leads is complicated, because we never know the site of the zero area, and this area changes its position within the cardiac cycle. Also the distances within the body are too short to develop sufficiently large zero areas. The difficulties in defining zero potentials of the entire heart will be discussed later. There are several possible ways to solve the zero potential problem, at least approximately (57). Under greatly simplified assumptions, a zero electrode may be constructed, if the three electrodes of the classical Einthoven lead system (R, L, F) are combined over equal resistances

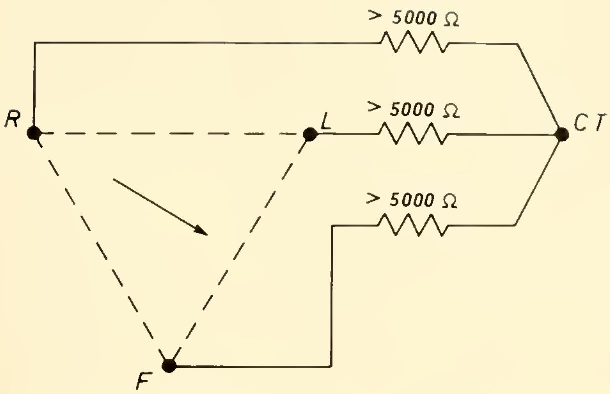

FIG. 5. The commonly used network to gain a zero potential electrode, called central terminal (CT).

of more than 5000 ohms to one point (fig. 5). This point has the mid-dipole potential if the field is homogeneous and if the dipole lies exactly in the center of an equilateral triangle, the angles of which are formed by the three electrode points R, L, F. This follows from the original concept of the Einthoven triangle (528). It has been proved all too often that this concept introduces errors of considerable magnitude into the ECG. [Examples of a much broader literature (99, 147).] Nevertheless, there are general solutions possible, by replacing the resistances in the network of figure 5 by resistance values calculated for certain electrode positions and certain thorax configurations. Such networks, however, are not interchangeable, neither from one electrode combination to another one nor from one patient to the next (335). They are therefore, practically speaking, inapplicable to clinical electrocardiography. Here, the simple procedure of Wilson (fig. 5) is still in use, in spite of its errors. The zero point is called the "central terminal" (CT).

3. VECTOR THEORY OF THE ELECTROCARDIOGRAM

In the production of the ECG very many individual fibers are involved. The activation time, anatomical site, and direction of their excitation waves can scarcely be analyzed in detail. Every theory of the ECG is therefore based on simplifications. Analysis of the excitation process going on in the heart may be performed in two different ways: one is to gain as much detailed information as possible about the various parts of the heart, their interaction, and their local electrical events. We may call data of this kind "partial or local derivations" of the excitation process. The second way is to represent the totality of the heart's excitation by one single measurement ("total derivation"—see section 6). Which of the two types a specific derivation really represents depends merely upon the position of the electrodes.

An ECG is thus the potential difference recorded by unipolar or bipolar leads put on the body surface. Under ideal conditions these potential differences can be calculated or graphically constructed by the projection laws of the dipole vectors, but simple equations or constructions are only possible if the body is replaced by a spherical conductor of homogeneous conductivity, with the dipole lying in the center of the sphere. Even for a cylindrical model of the thorax the mathematics are very complicated and completely inapplicable to practical electrocardiography using realistic thoracic models. We nevertheless have had to develop the simple equations, partly for historical reasons, and partly because modern and exact solutions are based on the theoretical understanding of the ideal case. The simplified concept is indicated in figure 6. If one considers a cross section through the sphere, going through the center, we may put three electrodes on the spherical boundary, all electrodes being equidistant from each other and lying in the same plane of this cross section. They form an equilateral triangle. Under these, and only under these conditions, the well-known projection laws of Einthoven will be observed: the relative magnitude of the bipolar derivations of the ECG, named I, II, and III, respectively, are proportional to the cosine of the angle between the instantaneous dipole moment and the line connecting the electrodes of each derivation. The simple derivation of these projection laws from equations 2.2 and 2.5 may be omitted here. The construction of figure 6 gives only the relative magnitude of the derived potentials. The absolute values depend mostly upon the distance between electrodes and dipole or, in other words, upon the radius of the sphere. They may be calculated as the differences between the unipolar potentials of each electrode, as they are given in equation 2.5a.

The Einthoven concept (183) started from the assumption that the electromotive forces of the heart could be represented by one single vector centered in an equilateral triangle (fig. 7). The figure, however, shows clearly that not even the geometrical assumptions of the triangle concept are valid for the anatomical properties of the human body. Several corrections have been made, but there is only one correct solution of the problem, the Burger triangle (see section 6, fig. 18).

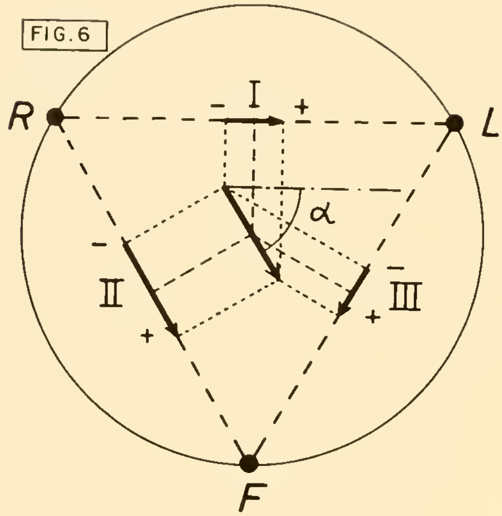

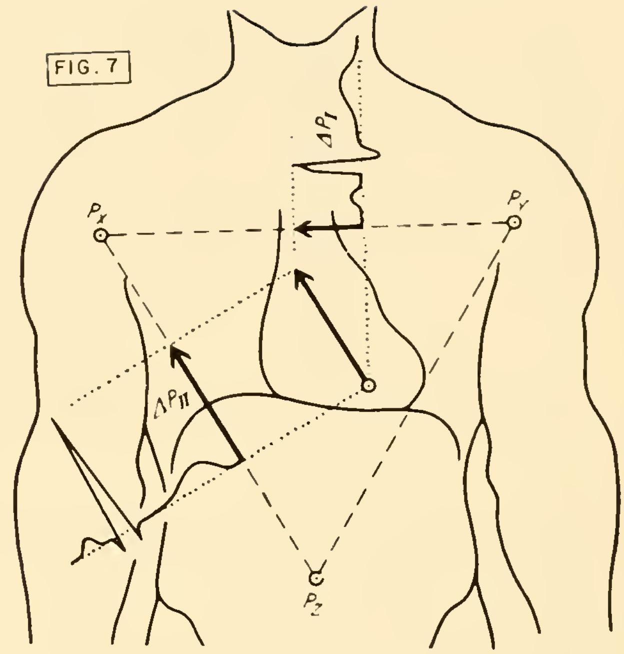

FIG. 6. The Einthoven triangle. The resultant vector of all heart fiber potentials, lying at the center of an equilateral triangle, is recorded by the three standard leads with potential differences proportional to the projections of the vector on the electrode lines. R, L and F: right and left arms and left leg as electrode sites; α is the angle of the vector with the horizontal.

FIG. 7. Demonstration of the invalidity of the Einthoven triangle. Even if one assumes the dipole to be centered in the chest, the electrode at the left leg does not form an equilateral triangle with the electrodes at the arms. The projections indicated in the figure therefore cannot be valid. [From Schaefer (58).]

We are never able to record the heart vector directly except by means of vectorcardiography, which will be discussed later. In classical electrocardiography derivations are recorded, i.e., potential differences between two electrodes. These derivations may be regarded as the projections of the heart vector on the lead line. In the reverse sense, if the lead lines and their projections are known, we may reconstruct the heart vector. Under the conditions of the spherical thorax model of figure 6, the lead lines of Einthoven electrodes are identical with the line connecting the electrodes. When a unipolar system is used, the lead line is identical with the connection between electrode and dipole center. All derivations are proportional to the projection of the heart vector on these lead lines. For comparing bipolar and unipolar leads, however, a constant factor must be used to convert one kind of derivation into the other. If the Einthoven derivation I (horizontal) is compared with a unipolar horizontal lead, the latter records a potential difference V_u which is compared with the magnitude of the derivation I V_I

$$V_u = V_I/3^{1/2}$$

Details can be found in the literature (150).

The assumptions basic to the use of the Einthoven triangle are not actually realized. It therefore seems necessary to derive generally acceptable solutions which describe the potential differences and their correct interpretation even under the extremely complicated anatomical conditions existing in the human body. All modern solutions are based on the Helmholtz theorem (253, 472). The meaning of this theorem is symbolized in figure 8. In the interior of the thorax a charged surface (double layer) Q may be assumed, which produces a current through a recording instrument connected with the thorax by two surface electrodes. The electromotive force (emf) of Q is called V, and the current going through the instrument is called j. If we now replace the galvanometer by a battery with the same emf as that of the intrathoracic surface Q, the battery will produce the same current strength i through Q, which Q itself actually produces in the circuit with the galvanometer.

FIG. 8
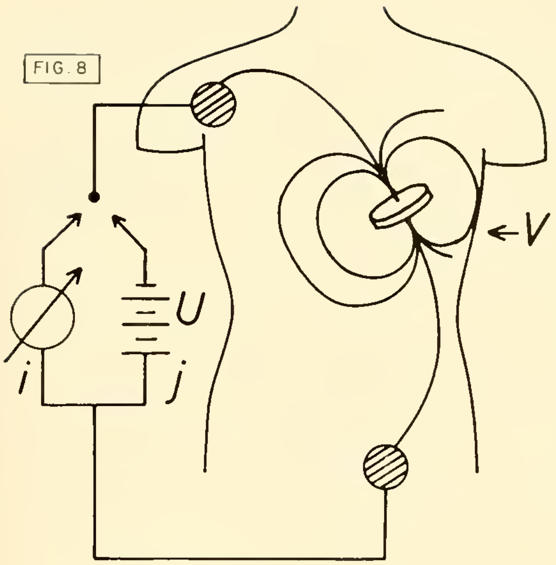

FIG 9
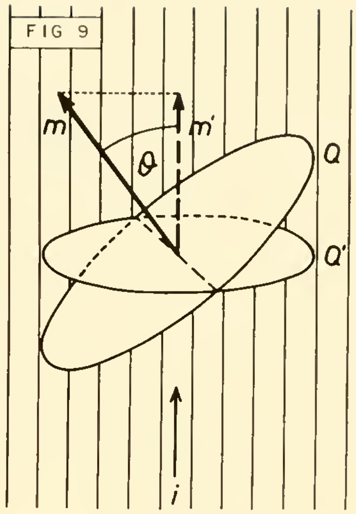

FIG. 10
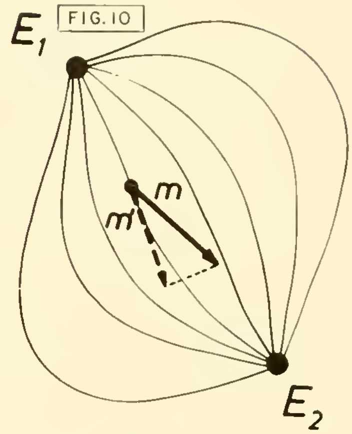

FIG. 8. Demonstration of the Helmholtz theorem. (See text.)

FIG. 9. A charged disc (membrane) of area Q representing an electromotive force which is recorded by the galvanometer of fig. 8 in an amount relative to its projection Q′ on a plane perpendicular to the current flow of the lead field. θ is the angle between the flow lines and the moment m of the disc. This means that m is represented in the record only as the smaller voltage m′. (See text.)

FIG. 10. Principle of "lead field." The flow lines of a current entering the body at two arbitrary points, E_1 and E_2, are shown. If a dipole V, represented by its vector, is recorded with the same electrodes, the recorded potential is proportional to the projection m′ of the moment m on the flow line penetrating the region of the dipole.

In a more general formulation, if U is the emf of the battery, and i the current generated by U and penetrating Q, we find

$$U \cdot j = V \cdot i \tag{3.1}$$

If r is the resistance in the recording system, $j \cdot r$ is the actually measured part of the voltage V of Q:

$$W = j \cdot r = V \cdot i \cdot \frac{r}{U} \tag{3.2}$$

If the resistance r is high compared with the internal resistance of the body (a condition existing in every modern recording instrument), the expression U/r is practically equal to the total amount of current driven by the external battery U through the whole body, i_o. Therefore:

$$W = V \cdot \frac{i}{i_o} \tag{3.3}$$

If $i_o = 1$, the formula is transformed into

$$W = V \cdot i \tag{3.4}$$

The interpretation of equation 3.4 leads to the following concept: i is the current, a percentage of the total current i_c, which penetrates the surface Q. If the current lines of i run parallel to Q, no current penetrates the surface, i.e., no part of the voltage on Q is picked up by the electrodes and recorded by the galvanometer. If the current lines run perpendicular to Q, the maximum current penetrates the surface, and thus the galvanometer records a maximum of the potential V. This leads, in general, to the relation indicated in figure 9, that the current i is proportional to the projection of the surface Q on a plane perpendicular to the direction of the current flow. Since $V = 4\pi \cdot m$ (equation 2.1), the recorded potential difference W is proportional to the "dot" (scalar) product of the vectors $\vec{m}$ and $\vec{i}$, if $\vec{m}$ represents the dipole moment per unit area, and $\vec{i}$ the vector of the local current strength.

$$W = 4\pi\,(\vec{m} \cdot \vec{i}) \tag{3.5}$$

(The sign of the potential difference is neglected.) For our purposes it is more suitable to replace the moment m by M_i/q, so that

$$W = 4\pi \left(\frac{\vec{M_i}}{q} \cdot \vec{i}\right) = 4\pi \left(\vec{M_i} \cdot \frac{\vec{i}}{q}\right) \tag{3.6}$$

where $\vec{i}$ q is the current density penetrating the active cross section of the myocardial fiber. The term $\vec{i}$/q may be called $\vec{L}$ (= "lead vector"). The recorded potential W thus equals (if we neglect the constant factor 4 π) the scalar ("dot") product of the lead vector $\vec{L}$ and the dipole moment $\vec{M}_i$, and therefore the product of the projection of $\vec{M}_i$ on $\vec{L}$ and the magnitude of $\vec{L}$. Expressed in a simpler manner, this product is identical with the product of the absolute values of $|M_i|$ and $|L|$ and the cosine of the angle between $\vec{M}_i$ and $\vec{L}$. Obviously the physically determined lead vector replaces the geometrically determined lead line, i.e., the connection of the bipolar electrodes or the connection between a unipolar electrode and the zero point of the vector. Translated into pictorial language, equation 3.6 means: the recorded potential of the electromotive surface Q depends upon *a*) the magnitude of the dipole moment M_i (i.e., the membrane potential in the case of our myocardial fiber, times the surface Q or the cross section of the fiber); *b*) the angle between $\vec{M}_i$ and the direction of $\vec{L}$ (fig. 10); *c*) $\vec{L}$ itself, and this involves the site and distance of the electrodes. The more remote the electrodes, the more scattered the flow lines of the current i_o introduced into the body (see fig. 22). The portion recorded of M_i therefore is greater the nearer M_i lies to one of the electrodes. These relations are valid for every configuration of the field, every electrode position, and every peculiarity of the conductive medium, be it homogeneous or not.

The currents introduced into our consideration in figures 8 and 10 of course do not exist in reality. They only serve as a tool to demonstrate the mode of recording potential differences on myocardial fibers in the thorax. We therefore may replace the current lines of our analysis by lines symbolizing the configuration of what we call a "lead field." This means that for each point in the interior of the body a vector $\vec{L}$ may be defined, the direction and length of which indicates one factor of the dot product determining the recorded potential of equation 3.6. This lead field, dependent in its configuration upon the position of the electrodes and the form of the body, replaces the simplified model of the projection laws in figure 6. To every point of this field a lead vector can be ascribed, the scalar product of which, with the moment M_i, immediately gives the amount of potential recorded for M_i at the given electrode positions. The first outline of this theory was given by Burger & van Milaan (141–143), and a detailed description by McFee & Johnston (340–342).

It may be mentioned that the bipolar ECG recorded from a strip of parallel muscle fibers may be correctly interpreted as the difference between two monophasic action potentials recorded at the sites of the two bipolar electrodes ["Differenzkonstruktion," (56, 69, 433, 435)]. This principle remains valid even when the muscle strip is inserted into a volume conductor. As soon as many strips going in various directions act together to build up an electric field, as in the intact heart, the principle of forming the difference between two monophasic action potentials is no longer applicable. It may be replaced by a "multiple difference construction" (56), but this leads to such complicated procedures that no simple and correct construction can be obtained by such methods. The superimposition of dipoles can be handled in an appropriate manner only on the basis of a vectorial concept.

4. SUPERPOSITION OF DIPOLES AND THEIR FIELDS

The interaction of numerous muscular fibers can be calculated in a sufficiently exact manner, only to the extent that the vectors $\vec{M}_i$ of each fiber are known in respect to their site and time of appearance, and only insofar as the simple law of vectorial addition remains applicable. It should be pointed out here that, in general, this applicability does not exist. For the majority of lead systems, multiple dipoles cannot be represented, in a model, by one single dipole (363). Either complicated mathematics have to be used (536) or a lead system adopted which corrects the multiple sites of electric sources by virtue of its lead field (see sec. 5). A correct vectorial addition of the various dipole moments would be possible only if one and the same lead vector $\vec{L}$ were valid for all different points of the myocardium. In such a case only the projection of the sum of all individual dipole moments on the lead vector equals the sum of the projections of the individual fibers. This condition is approximately met in every derivation in which the dimensions of the heart are small compared with the electrode distance. This is valid in the special "ideal" case of a centered dipole in a homogeneous sphere with electrodes put on the surface of this sphere. In such cases, the superposition of individual dipole moments can be constructed through the parallelogram of forces. Figures 11 and 12 indicate the most common cases of such a superposition in two examples. If such a superposition is extended to all myocardial fibers, the result is the "heart vector."

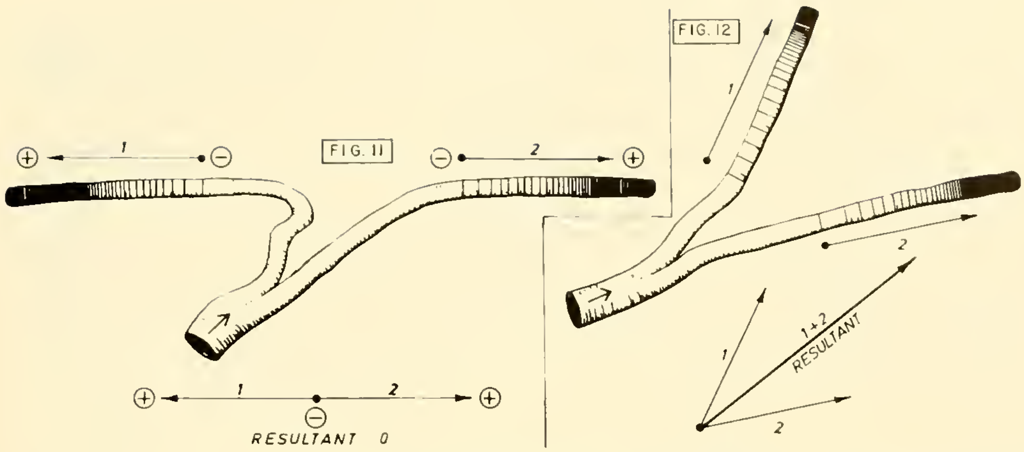

FIG. 11. Vectorial addition of two fiber dipoles showing complete cancellation of the potentials.
FIG. 12. The same as fig. 11, but with a resultant emf larger than the single component.

The heart vector can be characterized by its magnitude, direction, and position. The magnitude depends upon the number of simultaneously active fibers, their individual electric moments (including the magnitude of their cross section, which influences M), and the degree of divergence of the individual fibers. If, in an extreme case, all fibers were to start from a central point symmetrically in all directions, the fields of these fibers would cancel each other completely and no electric field would occur, in spite of a great activity of the muscle mass of the heart. This cancellation of fields takes place in every heart. As will be shown later, the fibers diverge to a considerable degree, and, in some hearts, diverge so strongly that nearly no QRS complex remains This phenomenon of cancellation may be called "physiological low voltage" (410).

The direction of the heart vector is determined by the result of this cancellation as well, because some fibers do not find a canceling counterpart, so that these alone in the total pattern of individual vectors remain as components of the resultant heart vector. Its direction therefore corresponds to the average direction of the uncanceled fibers. Every disturbance in the spread of excitation during the ventricular activation will immediately disturb this balance of vectorial addition, and thereby change the direction and magnitude of the vector. The direction of the heart vector can be completely described only in a three-dimensional space, by determining the angles in zenith (elevation) and azimuth on the sphere. In practice, these data are replaced by the angles which the projections of the vector on the three planes form with the horizontal or the transverse line. The sense in which the angles are counted may be seen in figure 58. The classical derivations of Einthoven's extremity leads record only the frontal projection of the vector. The angle which the frontal projection of vector forms with the horizontal line is the Einthoven angle α.

The "position" of the vector is irrelevant in the ideal case of a parallel lead field. If this condition is not realized, the position has to be determined by methods which will be discussed later.

5. LIMITS OF APPLICABILITY OF SIMPLE VECTORIAL CONCEPT

The vectorial composition of the heart vector, according to figures 11, 12, and its projection on a lead line are correct in the ideal case, in which the medium has a homogeneous conductivity, the field has a boundary of simple configuration (sphere), the heart is centered in the sphere (all surface electrodes having the same distance from it), and the dimensions of the heart are small compared with the dimensions of the field, so that all myocardial fibers may be assumed to be concentrated in the central point of the sphere. Inasmuch as these assumptions are invalid, for exact application the vectorial concepts need corrections for which, in most cases, the mathematics are extremely difficult.

Two problems arise out of this difficulty. The first one is: if and how far the cardiac potentials can be represented by one single resultant vector of fixed location, the changes of direction and magnitude of which interpret changes in the interior of the heart. The second problem is: how the heart vector projects

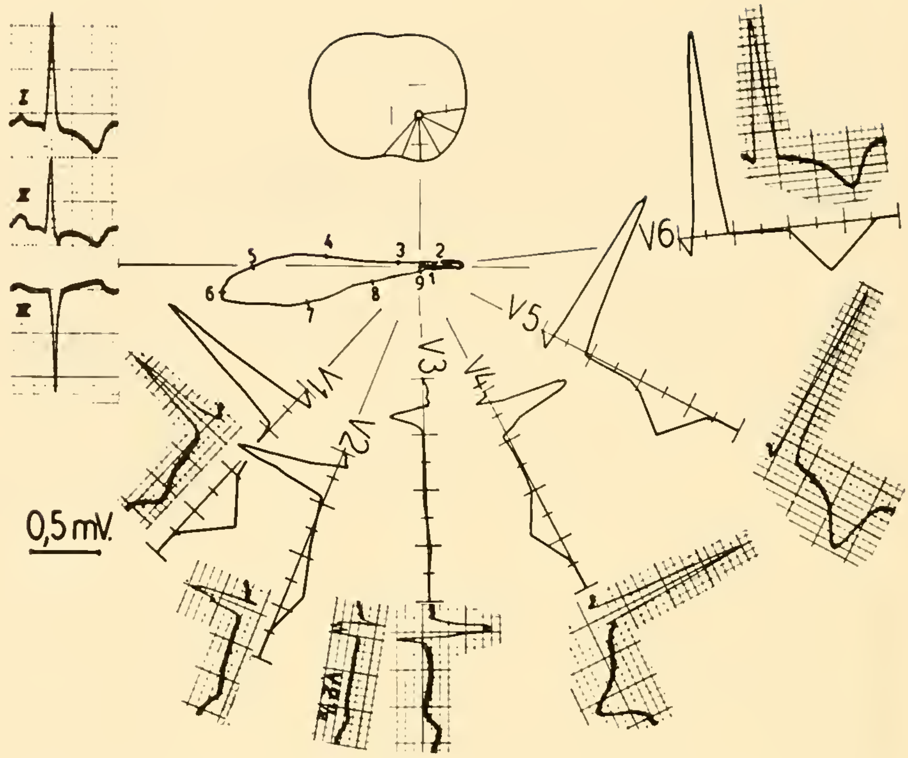

FIG. 13. Construction (prediction) of precordial records from a vector loop recorded with the rectangular bipolar electrode system of fig. 20 (Duchosal cube). Both the constructed and the actually recorded tracings are given. Left ventricular hypertrophy of a man, 65 years old. To the upper left the standard ECG. [From Duchosal & Sulzer (15).]

itself on the lead line of a derivation and how this line can be determined.

The Single Dipole Concept of the Electrocardiogram

There is nearly complete agreement that the single fiber may be regarded as a dipole. But it is very uncertain how far the superposition of all simultaneously generated fields of the various fibers may be regarded as the field of one single resultant dipole, which may be represented by one resultant vector. It must be decided whether such a single dipole concept is valid for all possible derivations or for special electrode arrangements only. Many attempts have been made to prove the general correctness of this assumption. In 1949, Duchosal & Sulzer (15) started an investigation in which the form of a record taken with precordial unipolar leads was predicted from a vector loop recorded with a rectangular bipolar electrode system, the electrodes of which were relatively far away from the heart (fig. 13). In the report of this investigation it has been stated that unipolar electrodes situated in a circle around the thorax, at the height of the heart mass center, tended to find "mirror patterns" with certain electrode positions, the connection of which went in most cases through the heart center (fig. 14). This result is one of the most frequently cited tests for the single dipole concept. If a single vector of fixed location exists, it really should be expected that for each electrode position used a second one may be found with the same form but opposite polarity of the ECG. This is identical with the possibility of finding two electrode positions, the lead vectors of which lie in a strictly opposite direction (fig. 15). The mirror pattern technique has been repeated several times by various authors and with similar results (130, 200, 320, 352, 430, 461). The best generally valid method to determine mirror patterns has been described by Frank (199).

Though mirror patterns do exist, and cancellations are possible, it can scarcely be doubted that the dimensions of the heart are great compared with the dimensions of the thoracic field. It was claimed at a very early stage in electrocardiographic research that, from precordial electrodes, a "partial derivation," or partial ECG, can be recorded (29). This should be expected from the fact that, viewed from a precordial electrode, fibers in the remote parts of the heart appear under a much smaller solid angle than those in the proximal parts. The latter therefore prevail in the record [nondipolar fraction (130) or proximity potentials]. We should mention, however, that in Frank's opinion (203) even the strictly precordial electrodes do not show peculiarities in the form of

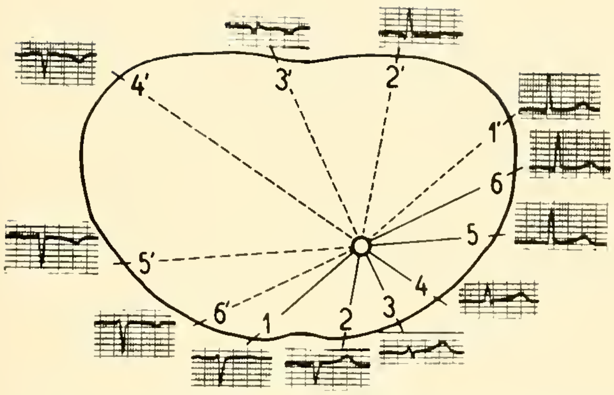

FIG. 14. Mirror patterns of the ECG. Demonstration of mirror patterns at opposite points of the thorax. The tracings were recorded with unipolar electrodes at the points indicated [From Duchosal & Sulzer (15).]

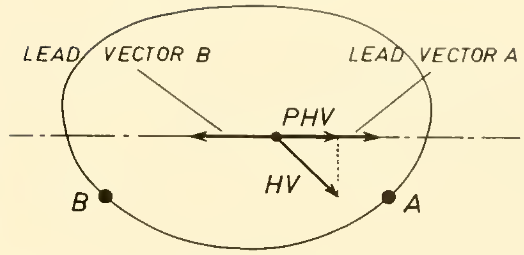

FIG. 15. Mirror patterns are observed if the lead vectors of the two unipolar electrodes A and B are strictly opposite to each other, as indicated. The heart vector HV projects itself on the two lead vectors with the same amount PHV, but is recorded with opposite polarity.

proximity potentials, but this view is denied by most authors. The details of these proximity potentials will be dealt with later. Nevertheless, it should be stated here that even under ideal experimental conditions, using an isolated cat heart in a homogeneous infinite field, proximity potentials are detectable in unipolar leads with the exploring electrode lying at a distance from the heart surface twice the diameter of the heart (238). The distribution of proximity potentials varies during the excitation process and is different in depolarization and repolarization. This leads to the fact that the error in a "single fixed-location dipole" concept can be diminished by assuming that the dipole position shifts during the cardiac cycle. [Migration of zero point, Nullpunktswanderung (23, 307, 308).] After all, the assumption of a migrating vector is nothing more than a hypothesis to explain the incorrectness of a "single fixed-location dipole" concept. The whole problem of locating the heart vector on an "electric center" is complicated (200) and only of theoretical interest. Such a location is without a physical meaning if the lead field is unknown. No one will deny that one single vector of one fixed position is merely a simplification which never can be valid in a strict sense. The attempt, therefore, to locate the electric center by means of simple or corrected electrode systems often leads to divergencies between the dipole location and the anatomical mass center of the heart (351, 443).

The Image Surface

Even if one accepts the "single fixed-location dipole" concept, a number of difficulties remain in the way of interpreting the ECG in a physically correct manner. These difficulties derive from the fact that the medium surrounding the heart is neither homogeneous nor of a regular and geometrically simple surface, nor is the dipole position centered. This bears the consequence that the simple projection laws are invalid, as mentioned above. The method designed to overcome this situation was the construction of lead vectors. The lead vector reconciles the anatomical data with the physical laws of projection: a projective reconstruction of the heart vector as a single fixed-location dipole becomes possible again in an exact manner, if the lead vectors are experimentally provided.

The usual method of constructing lead vectors may be briefly discussed. One first makes a model of the medium in question (e.g., the thorax). The model is filled with a homogeneous resistive medium (saline). An artificial dipole is put into the model, at a point at which the heart vector is supposed to lie, i.e., the mass center of the heart. The artificial dipole is moved into the three axes of space and the unipolar potential recorded at P for each of these three positions. The result of the record at P can now be easily translated into the construction of a lead vector, so that the dipole projection on this vector gives, in any case, the recorded voltage at P (143, 197, 249, 298).

To eliminate all the difficulties arising from the irregular shape of the field and the eccentric position of the heart, lead vectors are constructed for numerous unipolar surface electrodes, for a given shape of the thorax, and a presupposed position of the dipole. These lead vectors are drawn from a single common origin, which corresponds to the dipole location. The tips of these lead vector arrows may be projected onto a closed surface. This surface is called the "image surface" of this model and this single dipole location (143, 145, 197, 249, 298). This same image

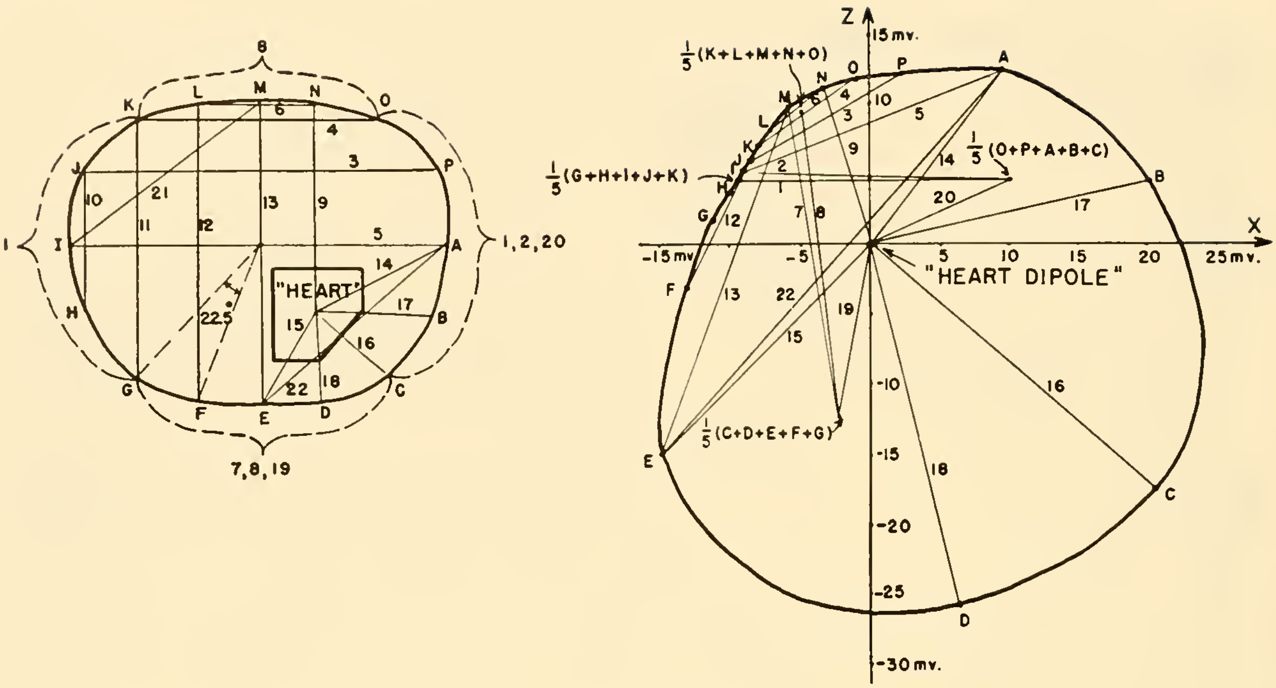

FIG. 16. Image surface (space) of a set of thoracic electrodes and some of their combinations. The anatomical picture of the electrode positions is shown on the left. On the right, these same electrode positions are shifted so that, in the case of unipolar derivations, their connections with the heart dipole form the lead vector of every electrode. In case of bipolar derivations, the lead vector is equal to the line connecting the two electrodes on the image surface. The potentials recorded at each electrode are the scalar (dot) product of the projection of the dipole moment on the lead vectors and the length of the lead vectors. [From Heim (249).]

surface allows vectorial operations such as projections for every electrode combination, e.g., for bipolar as well as for unipolar leads. Even the effect on the derived potential of multipolar lead connections can be calculated (fig. 16).

The mass center, however, is not always the "best" location of the dipole, so that complicated methods have been invented to improve this location, gaining a "best" dipole position from a combination of mirror patterns of the human thorax and correcting factors taken from the spatial image of a model of this same thorax (200, 206). Another method consists of putting an artificial dipole into the living body. In dogs, the dipole can be introduced into the heart (116, 281). In man, dipoles have been put into the esophagus immediately behind the heart (78, 257), and in one case even into the right ventricle (149). A third method is to put the dipole at any point in the interior of a human corpse (121, 527). It is evident that, in all cases, the dimensions of the heart and the peculiar distribution of its individual dipoles are completely neglected. This is the only serious objection to the validity of the lead vector and image surface constructions. With the aid of such methods, a fairly correct prediction of potentials recorded by any desirable electrode position is possible. Nevertheless, in spite of the great experimental effort put into such determinations, there remains an error in such predictions of ±15 per cent. These errors occur because the large diameter of the heart cannot be taken into account by a procedure based on the "single fixed-location dipole" concept. Consequently, it is probable that no correcting system exists which is able to compensate for all anatomical deviations from the conditions of the "ideal" vector field, and which consists in the application of lead vector projections.

Lead Fields

The preceding section showed the limits of certain accepted interpretations of the ECG with the aid of lead vectors and projections, on the basis of the single fixed-location dipole concept. It therefore was a decisive step forward to apply the Helmholtz theorem to ECG analysis in such a form that the anatomical peculiarities are taken into account and the various

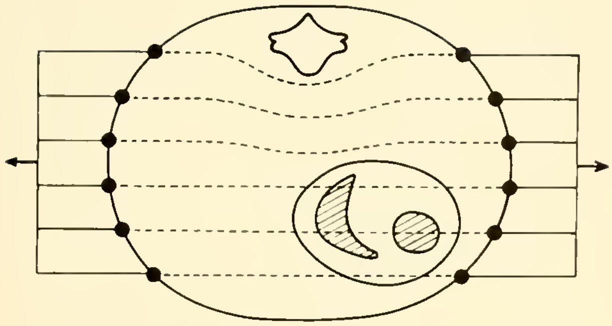

FIG. 17. Ideal lead field penetrating the heart with equidistant flow lines. This field records all individual fiber potentials with the same lead vector, i.e., with the projection of the fiber dipole on the parallel flow lines. All fibers are therefore recorded with the same relative amplitudes.

parts of the heart considered individually. If we reconsider figure 10, a correct projection of a vector originated in the heart is possible as soon as we are informed about the lead field of a given electrode combination. Theoretically, one could interpret the ECG of the total heart by knowing both the lead field penetrating the heart as well as the distribution and direction of the individual electromotive forces. In reality, however, a lead field of complicated geometrical structure will always inject practical difficulties into the interpretation of an ECG record. The only way to overcome this difficulty would be to introduce lead fields with parallel and equidistant flow lines. Using some simplifying assumptions in such a field, and a multipole electrode combination, we may achieve a simpler interpretation of the record (fig. 17). Such a field records every single fiber dipole in the heart with the same lead vector, i.e., with a projection on one and the same lead direction, and with a relative magnitude which is the same for all parts of the heart. Such a system, therefore, would allow determination of a single resultant vector, which would represent all fiber activities occurring in the cardiac muscle. Only thus could the "heart vector" be determined correctly. Unfortunately, such a lead field can be realized only in an approximate manner. The obstacle is the inhomogeneous conductivity of the thoracic media. (In fig. 17, this inhomogeneity is taken into consideration only for the vertebral column. The big inhomogeneities of the lung are omitted.) We know that even big changes in the conductivity of the media surrounding the heart, e.g., metal or rubber shields at the heart's surface (256, 276, 285, 325) or opening of the chest wall (353), lead only to slight changes in the form of the ECG. This fact is incompatible with the assumption that a parallel lead field may ever be obtained with electrode combinations of such simple form as shown in figure 17. The flow lines seem to enter the heart preferably through a very restricted area, mostly in the direction of the mediastinum. The form of the mediastinal conductor seems to indicate that a parallel lead field might be achieved in the sagittal direction with a minimum of distortion, if a multiple electrode system were used. A suitable arrangement of this kind has been described (382).

The assumption of a homogeneous medium in the thorax is invalidated also by the blood filling the cavities of the heart. The conductivity of the blood exceeds ten times that of the intrathoracic tissues. This fact influences the potentials of the various fibers in different ways, depending on their direction: in radially directed fibers the dipole moment is augmented; in fibers tangential to the cavities it is diminished (128). A similar influence will be found on the lead field: the lead lines are compressed in the cavities. A parallel, equidistant lead field, as could be gained in models with a homogeneous medium, principally cannot be achieved with the heart *in situ*.

For the lead field concept, the same restrictions of its applicability have to be made as for the lead vectors and the image surface: we do not know any simple method to determine lead fields in living man. Measurements have not yet been made in corpses. In living man, only one report is available of determination of the lead field of the retrocardial space in the esophageal area (257). Thus our knowledge of the lead fields is based merely on experiments with models in which the flow lines of a certain electrode position were determined by an analogous hydraulic model: instead of a current, a fluid was made to flow across the torso, and the stream lines were photographed. The flow lines were made visible by crystals of dye [fluid mapper (343)]. The theory of the lead field has been outlined in several papers (129, 245, 340–342, 382).

Discussion of the Vectorial Concept

It seems necessary to emphasize the antagonism between the lead field and the image surface. The latter transforms the geometrical electrode site into a "corrected" position, and is valid for any electrode combination, but only for one dipole of a fixed location in a thorax of a given form. The lead field however is valid only for one special electrode combination and a given thorax form, but remains valid for any dipole position or even for any combination

of several dipoles. It is evident, therefore, that both methods of obtaining "correct" leads require simplifications with resulting limitation of their validity. Thus the image surface seems to be extremely sensitive to changes in the location of the dipole (197, 200), which has to be chosen more or less arbitrarily. The anatomical data of the heart are fully neglected. The lead fields, on the other hand, are constructed on the theoretical basis of simple hydraulic or electric models. The enormous complexity of the real situation in the thorax is never taken into account. Models, either of the lead field or the image surface and lead vectors, do not provide a solution with general validity; they remain applicable only for that individual thorax form and heart position from which they are taken. If, therefore, a corrected lead system is to be utilized to record the ECG of a given person, a highly complicated mathematical and experimental procedure has to be put into operation, which by itself excludes a broad clinical application. Nevertheless, a practical application could be to use only such electrode systems as have proved, in such experimental research, to have a statistical minimum of deviation from the "best" method of recording the electrical events of the heart. The question remains, however, what the "best" method is and what kind of electrical events the investigator wishes to receive.

The best method depends upon the purpose of the record. There are two such purposes: the investigation of the resultant heart vector as the equivalent representation of all active fibers, and the derivation of local events by their proximity potentials. It is obvious that proximity potentials can only be picked up by "precordial" leads or leads near the heart, e.g., in the esophagus. The theory of such electrode systems will be given in the next section. If, however, the resultant heart vector is to be recorded, the influence of proximity potentials should be eliminated. This is the case if, and only if, the lead field penetrates the heart in parallel and uniform flow lines. The electrode combination is best, which most nearly realizes this condition. If possible, therefore, we should test all electrode systems with respect to their lead fields.

6. DIFFERENT LEAD SYSTEMS

It is not the aim in this review to enumerate or even discuss the details of electrocardiographic practice. For one thing, theoretical reasons for choice of a certain lead position are usually not available.

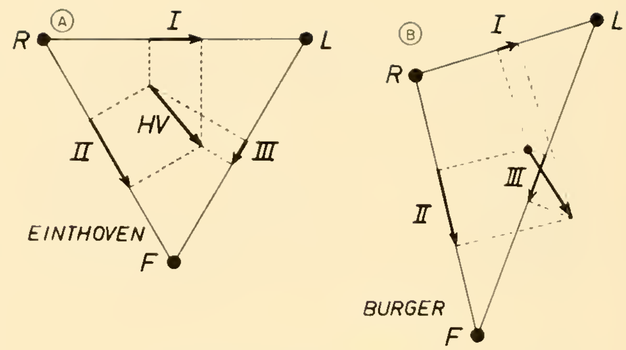

FIG. 18. Comparison between an Einthoven and a Burger triangle of the same subject. *A*: the projection of a given heart vector HV on the three leads is I, II, III. These projections do not represent the actual ratio of the amplitudes recorded with the leads. These are correctly given in *B* where the projections I, II, and III are drawn on the sides of a "distorted" triangle. The Burger triangle may be electronically reduced to a correctly equilateral triangle by subdividing the lead connections by resistances. The corrections in *B* are based on torso models, which do not take into account the inhomogeneities of the field.

Decision as to which of the different lead systems may be the best cannot be drawn out of a comparison of their results, as it is unknown whether several systems which yield equal results reveal a common error or a common truth. The question therefore depends merely on the result of model experiments. The models used so far, however, are rather simplified homogeneous torsos which disregard individual deviations from thorax to thorax, the large differences in conductivity of lung and mediastinum, and the fact that the normal ECG is led off by flow lines which apparently do not penetrate the heart-lung boundary. Nevertheless, these model experiments are, for the time being, the only way to compare the correctness of leads.

A rather comprehensive work comparing nearly all lead positions has been done by Schmitt & Simonson (428, 429, 431). In these papers, the lead vectors for the different electrode combinations are given. Before we discuss these results, we should briefly mention what principal differences exist in the various leads and how they can be put into a general order.

Regarding technique, we may distinguish between unipolar, bipolar, and multipolar leads. Each of these lead systems may be used in two ways. First, one could try to determine the position and magnitude of a "heart vector," representing all electric sources of the heart with the same weight. We will call such systems "total leads" or "heart vector leads" in the following lines. The second aim of both unipolar and

bipolar leads is the derivation of parts of the heart by recording partial derivatives or proximity potentials. We may call such systems "local leads." The nature of their electrical arrangement favors use of multipolar systems as total leads and bipolar or unipolar systems, as local leads.

Total or Heart Vector Leads

BIPOLAR DERIVATIONS IN ONE PLANE. The most common leads of this type are the classical Einthoven extremity leads, put on both arms and the left leg and usually marked with the letters R, L, F. Under "ideal" conditions, the projection laws are those demonstrated in figure 18*A*. More realistic conditions, however, as revealed by a homogeneous torso model, lead to a correction: the Burger triangle (126, 142, 524). This triangle, for a single case given in figure 18*B*, consists of the three lead vectors of the extremity leads and is valid for one single heart vector in a fixed location. The length of each side of the triangle represents the amplitude factor: the recorded potential is the scalar product of this length, as a vector, and the projection of the heart vector. This means, regarding figure 18 *B*, that in lead I (R to L) the recorded heart vector is relatively much smaller than that in the other leads. The reason apparently is that the points which mark the real electrode positions are the region where the extremities join the thorax; these points do not actually form an equilateral triangle.

It is a physical platitude that in the Einthoven triangle the sum of all leads I + II + III equals zero for each moment. (That II is ordinarily introduced with its negative value stems from the inverse polarity which the common technique uses to record this lead.) This remains true for the Burger triangle as well, so that the three lead vectors form a closed geometrical figure, if put together.

The Einthoven and Burger triangles only record the heart vector projections in the frontal plane, if one disregards a slight inclination of the plane of the triangle away from the frontal plane. There is a second lead system for recording in a single plane, the Nehb triangle (356), the electrode positions of which are the sternal end of the right second rib (R), the projection of the heart apex on the left posterior axillary line (L), and the heart apex (F). The long axis of the heart lies in the plan thus formed. A horizontal triangle has been described by Blasius (112). Yet it is questionable whether derivations like those of Nehb really are total heart vector leads, because, in the clinical use of the Nehb triangle, it seems to pick up preferably events, such as infarcts, in the posterior wall of the heart. The explanation could be that the lead line RL in Nehb's triangle is minimally represented in other lead systems, but lies in the direction of all vectors developing after local disturbances in the posterior part of the left ventricle. Such events would naturally be evidenced in a total heart vector, but would project themselves minimally in an orthogonal lead system.

THREE-DIMENSIONAL BIPOLAR SYSTEMS. All other lead systems of the bipolar type are oriented three-dimensionally. In order to compare and describe these systems, it is first necessary to discuss the nomenclature. The three axes in space, x, y, and z, are directed as indicated in figure 19. There are other symbols used as well, but in this paper we should like to adopt these. The electrodes vary both in their craniocaudal and their circumferential position. The lead vectors thus achieved must be described by their magnitude and their elevational and azimuthal angles (see fig. 58). The elevational angles are designated in accordance with the usual Einthoven angle α, which is negative upward. The positions anatomically fixed for certain standard leads will be mentioned later. If a rotation is to be described appropriately, a convention must be established regarding the side of the plane to be viewed (248). In this chapter the notations are such that the frontal plane is viewed from the front, the sagittal plane from the left, and the horizontal plane from above the patient (390). (See table 1*b*.)

Several attempts have been made to determine the sagittal component of the heart vector, the most prominent of which are the two cubic systems of Duchosal & Sulzer (15) and Grishman & Scherlis (28), and the Wilson tetrahedron (163, 527) (fig. 20). These systems show rather considerable deviations in their respective potential differences and patterns even in analogue derivations (198), and the deviations in the torso model are, with the best system, (Wilson's tetrahedron) as much as 15 per cent! There are, however, more optimistic voices (306). A system which offers some advantages is the Condorelli system, the lead axes of which coincide with the axes of symmetry of the electrical heart field (480). Whatever the situation might be, the "best" lead system, determined by comparison with the simplified (homogeneous) torso model and therefore having restricted reliability only, seems to be a combination of electrodes known as the SVEC system (standard vector electrocardiogram) (431).

The SVEC system in its best corrected form (called

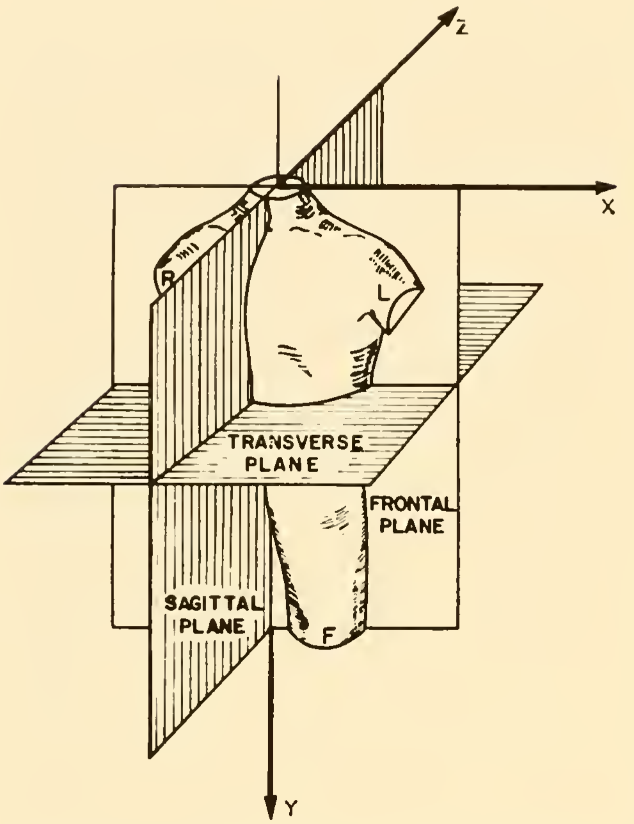

FIG. 19. A rectangular coordinate system defining three planes commonly used in electrocardiography. The axes of this figure are used throughout this monograph. [From Frank (198).]

III) consists of the following electrode combinations: component x combines, with equal weight, lead I and a lead at the height of the fifth interspace at the sternum, which reaches from a surface point of an azimuth of 60° to an azimuth of 300° (nearly point B and H in fig. 16). The component y is recorded between the head and left leg, the component z is derived by a weighted combination of four chest and four back electrodes, the details of which may be seen in figure 21. Somewhat simpler systems have been described by Frank (202) and many others (72, 251, 271, 382, 492, 518).

UNIPOLAR SYSTEMS OF NONLOCAL CHARACTER. A unipolar lead may serve as a heart vector lead, if it is remote from the heart. The condition which permits it to act as a total lead is that the lead field penetrating the heart must be approximately parallel and uniform. Numerous unipolar lead positions have been described, the value of which is often dubious. There is really only one practical argument for choosing leads differing from the orthogonal orientation. If the partial vector of a certain group of heart fibers is directed so that the angles between the fiber and the orthogonal axes are maximal and equal (which corresponds to an angle of 55°), this vector projects itself with a factor cosine of 0.575. In such a case, only about 58 per cent of the vector is represented in each of the lead records.[4] As the ECG is always the result of superimposing fields, it might happen that such minimally recorded potentials would be masked by others. For every heart vector position there exists an "optimal" lead vector running in the same direction as the heart vector (23). This may be the reason why the unipolar limb leads are so often used clinically as a supplement to the standard Einthoven leads (24). In "unipolar limb leads" the elevational angles of the lead vectors lie in between those of the Einthoven leads. These leads are commonly marked as VR, VL, and VF (V means voltage and is used as the symbol for all unipolar leads with CT as reference electrode). The angles of elevation are: VR −150° and 30°, VL −30° and 150°, VF 90° and −90° reading from positive to negative polarity in these leads, whereas the Einthoven leads have elevational angles of: I 0° and 180°, II 60° and −120°, III 120° and −60°, again reading from positive to negative polarity of the leads. [For details see (24, 305, 450).]

Goldberger proposed a procedure named "augmented unipolar limb lead," which involves connecting one lead (e.g., VR) with the combination of the two others (VL and VF). These leads are symbolized with aVR (VR against VL + VF), aVL and aVF.[5] The lead vectors of these are given in table 1a. They are useful even though their basic theory incorrectly assumes the presence of an ideal field.

The most commonly used unipolar leads are those of Wilson, with the classical electrode positions standardized by various national cardiological societies (529). Most of these leads can be regarded as heart vector leads, although the records from them usually deviate to some extent from the vector loop recorded with an orthogonal corrected system (15, 200), and

[4] It may be mentioned that, in a planar system, the minimal projection corresponds to an angle of 45° with a cosine of about 0.708. Therefore, the minimal projection is still 70 per cent of the vector. As can be seen, the derivations in space may record a much smaller percentage of a vector than derivations which are in the same plane with the vector.

[5] "Augmented" means that these leads record a potential which is 50% larger than that recorded with the use of a CT as indifferent electrode. However, the method introduces serious deviations from the simple projection laws, because the "reference" electrode combination no longer has zero potential.

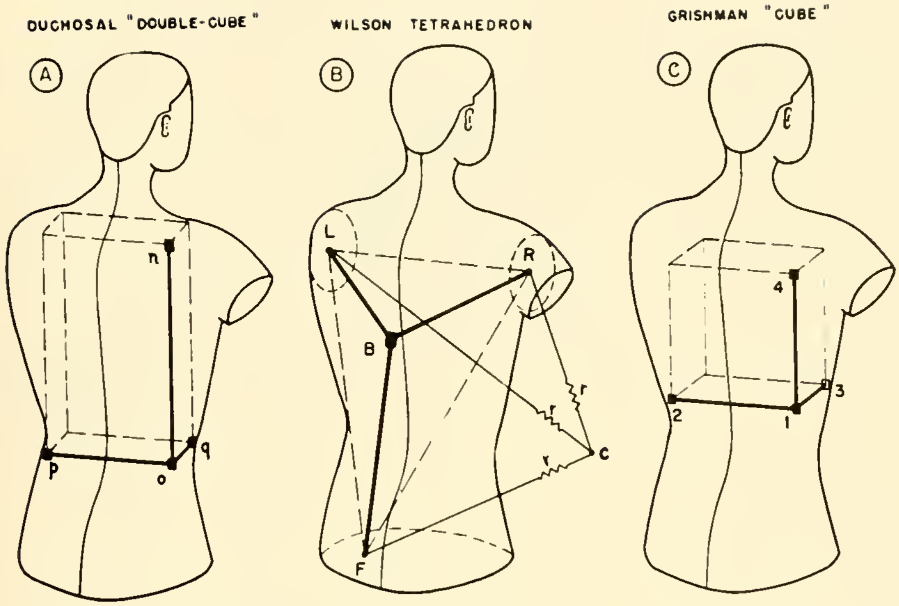

FIG. 20. Illustrates the electrode arrangements of three commonly used systems. R, L, and F in *B* are the standard limb electrodes. The left and right "cubic" systems are bipolar; the tetrahedron is a unipolar system, where all derivations are recorded with the CT as reference point. [From Frank (198).]

proximity potentials of 30 per cent and higher may be found. This corresponds to the fact that calculations of the heart vector in a completely uncorrected system are fairly reliable, the strictly precordial leads excepted (118). A theoretical basis for the discrimination of "heart vector" and "local" peculiarities of unipolar leads will be given next.

COMPARISON OF DIFFERENT TOTAL OR HEART VECTOR LEADS. The most important quality of a lead, for clinical application, is its lead vector. Only such leads as have identical lead vectors can be regarded as equal. A comparison between various systems (e.g., of orthogonal character) is possible only if one knows their lead vectors. Determinations of the lead vectors of various electrode systems can be made only in torso models. The results of such investigations show how closely the various lead systems approach the ideal (e.g., orthogonal) condition and to what extent the results of such systems may be compared with each other. In table 1 such a comparison is listed (428, 431). The result is that the SVEC III system is by far the most correct, both concerning lead vector directions and standard deviations, which are minimized by the corrections of this system. Comparisons of various lead systems have often been made (80, 122, 144, 164, 168, 198, 207, 293, 308, 348, 368, 372, 400, 457, 460, 462). The results are too detailed to be reviewed here, but it is surprising to what extent derivations with comparable lead lines give similar results, even when the electrode positions are rather different (481).

Local Leads. Theory of Unipolar Leads

ELECTRODE SYSTEMS. A "local" lead may be defined as a lead, the lead field of which penetrates the heart in an extremely divergent manner. For such leads, the concept of a single uniform heart vector is not applicable. They are used therefore with the intention of recording electrical events in local areas of the heart. There are two completely different methods of recording local processes. First, the lead field of a given lead selects the individual vectors of those fibers which run in the direction of the field lines. Second, a local lead close to the heart picks up the potential of those parts of the heart which lie proximal to the recording electrode ("proximity lead"). This happens because the field lines of the lead field, in the case of unipolar records from an infinite medium, are divergent and penetrate every part of the field with a density which is inversely proportional to the square of the distance from the electrode (fig. 22). The mathematical expression for this fact has been given in equation 2.5. Unfortunately, in limited fields this simple relationship is not valid. The invalidity may be explained in a twofold manner. First, in a spherical medium and with surface electrodes (fig. 23), the field lines of the lead field are no longer straight lines; they diverge in the complicated form indicated in figure 22. Second, the influence of the distance between electrode and a local (individual) dipole is also complicated. For eccentric dipole positions, the simple equations 3.5 and 3.6 are no longer valid, either. Mathematical treatment of eccentricity, which could lead

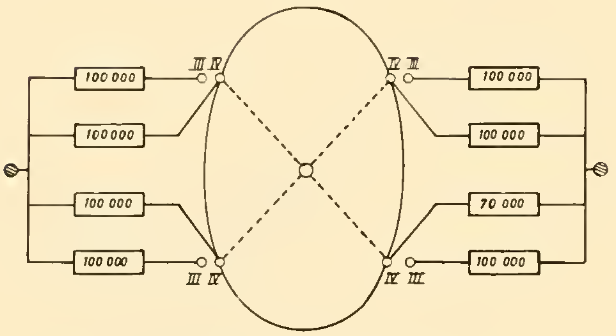

FIG. 21. The combination of electrodes for the sagittal (Z −) component of the ECG in the SVEC III system. Two anterior and two posterior pairs of electrodes at the height of the IIIrd and IVth intercostal spaces at the sternum, and with azimuthal angles of 30, 150, 210, and 330°, are combined over the resistances indicated to a central anterior and a central posterior point. This electrode combination is supposed to have a nearly parallel and uniform lead field in the antero-posterior direction and much resembles the derivation of Reynolds *et al.* (382).

to a correct description of the potential distribution to local leads, is rather complicated (113, 195, 196, 250, 523) and must be omitted here. It scarcely seems applicable to analyses of human precordial or local leads.

There are several lead systems, the lead fields of which reveal a certain local character of the lead. The one most frequently used is the unipolar precordial lead system. As shown in figure 23, the flow lines penetrate the heart in a highly divergent manner, so that parts nearest to the electrode show the higher density of the flow lines when compared with the more remote ones. There is, however, no sharp distinction possible between locally derived potentials and those recorded with a minimal amplitude from more remote areas. "Locally" and "generally" derived potentials are simply idealized terms, meaning that the nearer the part in question lies to the electrode, the more its potential prevails in the total pattern.

The second system of more or less local character is the "close bipolar system" using short distances between electrodes. Figure 24 indicates the lead field of such electrodes as being strongly curved and showing a considerable density at only short distances from the surface. Yet we have no information as to how deep a sufficiently dense part of the lead field penetrates into the interior of the chest. Neither experiments nor calculations are available. It is obvious, however (fig. 24), that even at a short distance from the electrodes the field becomes quite uniform with nearly equidistant flow lines, though these lines are still curved. The

TABLE 1*a*. *Lead Vectors of Common Electrocardiographic Leads*

Lead	Strength	Per cent SD	Azimuthal Angles, Mean	Elevational Angles, Mean	Angular SD, Degrees From mean	Angular SD, Degrees From ideal
I	1.08	20.4	98.3 (90)	−14.8 (0)	10.3	20.1
II	1.16	12.3	89.5 (90)	+63.0 (+60)	6.8	7.6
III	1.44	14.2	272.2 (270)	+67.5 (+60)	7.9	14.1
aV_L	1.16	18.8	91.4 (90)	−47.7 (−30)	9.4	22.3
aV_R	0.86	14.8	270.3 (270)	−25.9 (−30)	10.1	11.5
aV_F	1.17	11.5	2.7	+84.1 (+90)	6.8	9.1
V_1	1.19	46.0	334.0	−22.2	26.6	
V_2	1.40	47.2	12.0	−22.3	25.0	
V_3	1.42	52.6	34.2	−9.5	26.0	
V_4	1.21	48.4	45.0	+2.0	26.7	
V_5	1.09	42.8	67.7	+1.4	27.7	
V_6	0.91	27.9	95.6	−3.7	28.1	

Azimuthal and elevational angles in the sense of fig. 58*D*. With the key of these values, all records taken with these leads can be used to determine the heart vector. [From Schmitt (428).]

TABLE 1*b*. *Lead Vectors of Orthogonal Lead Systems**

	Strength	Per Cent SD	Azimuthal Angles, Mean	Elevational Angles, Mean	Angular SD, Degrees From mean	Angular SD, Degrees From ideal
Duchosal-Sulzer						
X	0.81	40.7	113.4 (90)	+11.0 (0)	19.2	30.6
Y	0.78	22.6	34.5	−76.5 (90)	12.1	17.5
Z	0.76	44.3	354.8 (0)	+16.3 (0)	19.5	25.8
Wilson-Burch						
X	1.14	20.3	98.2 (90)	−15.4 (0)	10.0	19.9
Y	1.20	17.4	186.2	−59.7 (90)	10.8	32.3
Z	0.60	39.0	6.7 (0)	+27.2 (0)	16.9	35.5
E. Frank						
X	1.12	15.2	86.8 (90)	−2.1 (0)	8.9	9.8
Y	1.16	6.9	3.4	−85.0 (90)	5.6	7.5
Z	1.09	16.5	358.0 (0)	+8.8 (0)	9.7	16.5
SVEC III						
X	1.33	10.2	90.1 (90)	−3.6 (0)	5.8	6.8
Y	1.41	3.0	216.8	−86.4 (90)	1.5	3.9
Z	1.00	4.0	359.9 (0)	+1.0 (0)	2.3	2.5

* See fig. 20.

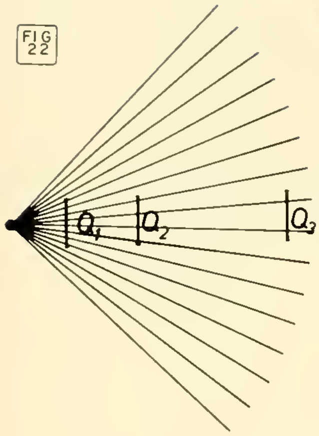

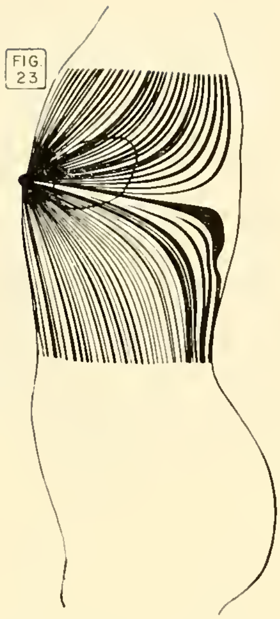

FIG. 22. Lead field of a unipolar electrode in a homogeneous field, of "local" character, as far as events in the neighborhood of such electrodes are concerned. The "different" unipolar electrode lies in an infinite homogeneous medium, the field lines of its lead field diverging symmetrically into all directions; the "indifferent" electrode may be regarded as infinitely remote. The potentials recorded from three membranes Q_1, Q_2, and Q_3 are inversely proportional to the square of the distance (and proportional to the number of flow lines penetrating the active cross section of these sources).

FIG. 23. Lead field of a unipolar chest electrode, i.e., from an electrode on the surface of the field. The flow lines are strongly curved and the relation between recorded potential and square of distance of fig. 22 is no longer generally valid. The flow lines of the lead field have been produced in a fluid model by streaming stained fluid entering the field through the electrode point ("fluid mapper"). [From McFee & Johnston (341).]

closer the electrodes lie together, the greater difference exists between lead field densities in neighboring and remote parts of the heart. The potential differences recorded are very low with short electrode gaps and may even be so small that such electrodes do not yield sufficient input to the ordinary ECG amplifiers, even though they lie very near the heart's surface.

Records from close bipolar electrodes have no essentially different features: for example, the QRS complexes have nearly the same durations as in total leads. The proximity features of the record, nevertheless, are remarkable. There are some peculiarities of the records which cannot be explained by the single dipole assumption (98, 405). Thus, the latency of the peaks of Q, R, and S, respectively, behave differently from what would be expected of a rotating

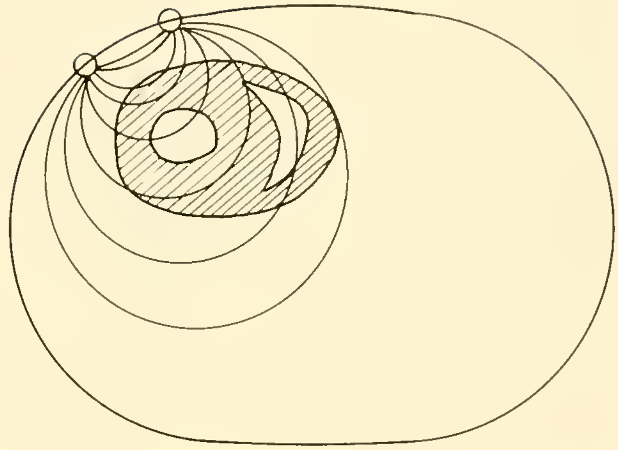

FIG. 24. Lead field (schematically drawn) of a close bipolar lead. The field lines show a considerable density only near the electrodes. At greater distances, the lines become less curved and more nearly uniform; and their direction, where they penetrate the heart, is approximately parallel to the line connecting the electrodes, at least for the greater part of their flow.

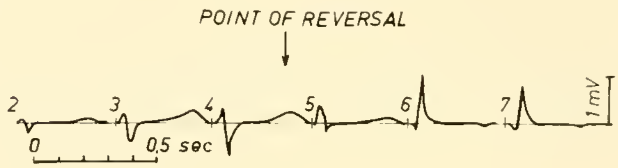

FIG. 25. Tracings from close bipolar chest leads (distance 3 cm), with horizontal electrode positions varying from the right margin of the heart (no. 2) to the left (no. 7). The records are taken thus: the electrode pair is shifted 3 cm toward the left side of the chest between each tracing. With each move, the right electrode (as viewed from the subject) is placed where the left member of the pair had previously been. Between 4 and 5 (approximately over the heart center), the main deflection is reversed. P is omitted in all records. The QRS duration is nearly the same as in the standard leads. [So-called "Herzbild" of Ernsthausen & Kienle (18).]

dipole. The main deflection (R) of the records is inverted, if the bipolar leads are moved from left to right or from above downward to a certain line (fig. 25). Interpretation of this behavior has been attempted on the assumption that excitation waves, starting in the center of the heart and running in divergent directions, build up these local fields with their opposite potential gradients (18). However, this interpretation can scarcely be adopted in this general formulation.

Another system has been described by Fattorusso *et al.* (191) and Thaon *et al.* (482) consisting of "concentric" electrodes (a ring-shaped indifferent with a centered recording electrode). The lead field

of such a recording electrode consists of very short and strongly curved flow lines, the density of which diminishes rapidly as the distance increases at a ratio of about $1:r^4$ (r = distance) (58). Such an electrode records very small amplitudes, probably from very small regions. Therefore, the total duration of the QRS is distinctly lower than that of standard leads, and the latencies vary from position to position. However, there has been almost no experimental work done with this electrode.

STANDARD UNIPOLAR LEADS OF "LOCAL" CHARACTER. The only commonly used electrodes which may have a certain local effect are the Wilson electrodes on the precordial part of the chest (528). We therefore discuss the theory of these electrodes in detail. Wilson's first aim in introducing unipolar precordial electrodes apparently was to avoid the potential variations of the second electrode, which might, he believed, interfere with its own potential pattern. This belief was based on the single dipole concept. He therefore put the second "indifferent" electrode on a very remote part of the body, e.g., on one leg. The invention of the CT as reference point was a step toward a more correct solution of the problem. But soon the lead field concept proved such derivations to be of a local character (see fig. 23). Because the heart is imbedded in the mediastinum, the flow lines of the lead field do not have a good chance to diverge; rather they are forced by the lung resistance to run along the mediastinal borders. Therefore it is not surprising to hear that even in precordial leads the influence of the proximity potentials is comparatively small. The local character of such electrodes is restricted by still another factor. Figure 23 shows the flow lines in the sagittal plane being bent very strongly along their way through the heart. There is no one prevailing direction in the flow lines, not even that one directed strictly toward the electrodes. Therefore, no single direction of the excitation waves is favored. From a bundle of muscle fibers which run parallel to the chest wall, only minimal potential is recorded. There is only one kind of excitation preferably recorded: waves which run directly toward the electrode or directly away. Assuming the heart to consist of a bulk of fibers running "at random," such fibers would be selected. Provided the unipolar electrode is positive against the CT, the majority of these fibers develop excitation waves running to the electrode. In case of negativity, the waves run away from the electrode. If an electrode is attached close to the heart, the recorded potential pattern usually

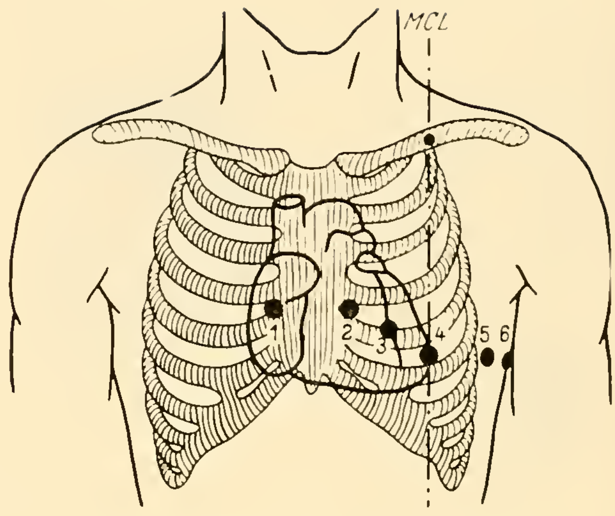

FIG. 26. Standard positions of the Wilson chest leads V_1–V_6.

is determined by the interference of approaching and receding waves which run in the direction of the lead field and near the electrode.

Considering the standard positions of unipolar leads, as Wilson proposed them, only some of these leads can contain a noticeable amount of a local derivation. The standard positions are shown in figure 26. Evaluation of their proximity potentials may be given in the following manner. Potentials to be recorded from various parts of the heart are easily calculated for the ideal conditions of a perfect spherically radiate lead field, assuming "random" distribution of fiber directions for all parts of the heart. As figure 27 demonstrates, the mass of the ventricle can be subdivided into spheric sectors of a given solid angle θ viewed from the electrode, and a certain thickness d. Similar distribution of fiber directions assumed, the potential to be recorded from such spheric sectors can be calculated. The rough estimation of figure 27 leads to the conclusion that from the Wilson point V_5, the left ventricle is recorded with 72 per cent of the total potential, the right ventricle only with 28 per cent. From point V_2, the relative percentages are 46 and 54 per cent. Thus, even in a precordial electrode quite close to the right ventricle, this part of the heart contributes only a little more than one-half of the potential of the record. In some extremely favorable electrode positions the small muscle mass of the right ventricle may be recorded with the same relative weight as the left ventricle, but, considering the relative masses of the ventricles, no real local derivation can be gained under normal circumstances (58).

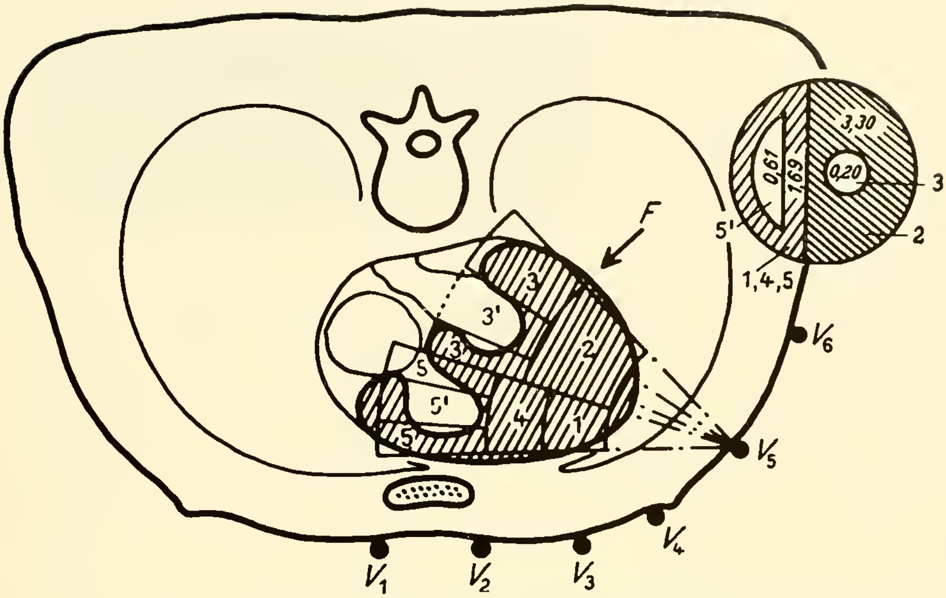

FIG. 27. Demonstration of the proximity effect of the Wilson chest lead V_5. The heart is roughly divided into five compartments, each of which forms the part of a spheric shell with various solid angles and thicknesses. The figure to the right shows how these compartments are projected on the sphere F, seen from the electrode. The amount of potential which (assuming random distribution and direction of the individual fibers in the compartment) each compartment contributes to the record V_5 equals the product of solid angle and thickness. The various compartments then contribute the following percentile potentials of the record:

Compartment	Thickness	Relative Solid Angle	Product	One Ventricle in % of the Whole Heart
1	9	2.3	21	
2	13.5	3.5	47	left = 72%
3	15	3.3	50	
4	8.5	2.3	20	right = 28%
5	15	1.7	25	

Even in V_5, the right ventricle is represented with one-fourth of the whole potential difference of the record! [From Schaefer (58).]

"INFORMATION" GAINED BY THE VARIOUS ELECTRODE SYSTEMS. Against the background of the preceding sections, the problem of information given by any certain lead system may be discussed. The word "information" here means that the electrocardiographic record contains symbols which can be transformed into language describing physiological events. In the first place, the direction of local potentials (of their vectors) is of interest. The more the lead field is curved, however (see fig. 23), the more uncertain is every statement concerning the site and direction of the fibers which react in an abnormal manner. The quantitative problem of the muscle masses participating in the potential pattern (fig. 27) is a second handicap to interpretation. If in a record the potential differences belonging to the left and to the right heart are equal, no information can be gained about the localization of events in one of the two parts of the heart, even in case of heavy distortions. If the proportion of potentials recorded is not so well balanced, and a distortion of the potential pattern is observed, the probability of course is greater that the distortion belongs to events in the preferentially derived part of the heart. Nevertheless, abnormal events in large, but remote, parts of the heart have the same influence on the total potential production as abnormal events in small, but near, parts. The decision as to which of these two possibilities is realized in a peculiar case can only be made with other indirect or empirical signs. One single exception exists: if the direction of a very large bundle of muscle fibers is known, an electrode position at which the lead field flow lines pass the bundle parallel to its fibers is "optimal" in recording events in that special bundle. Such conditions may exist only during the repolarization process or in the ST displacement, for reasons to be discussed later.

So, data which allow a physiological interpretation of local events are only occasionally embodied in local leads, and gained only by the strictly precordial

leads V_1 to V_3 and by local leads very near to the heart.

SPECIAL LEADS. LEADS FROM THE SURFACE AND THE INTERIOR OF THE HEART. Because of the difficulties in getting "local" recordings, many attempts have been made to bring electrodes as near as possible to the heart. One of the earliest attempts of this kind has been the esophageal lead (96). A small electrode is swallowed by the patient and, by virtue of the calibrated length of the attached wire, its position relative to the heart is well known. The second electrode is usually a CT. The results have been reviewed by various authors and are of more clinical than theoretical interest (10, 61, 91, 289). The ECG has also been recorded from the stomach (244, 274). The lead fields of the esophageal electrodes have been investigated, so that an explanation of the curves can be given (131, 352). This explanation is more or less identical with that of the other leads near the heart and shall be given in connection with them.

The intrapulmonary leads, introduced into the lung by a bronchial catheter (216, 402), show results similar to those from the esophagus. If the electrode positions are mapped in the fashion of figure 13, the intrathoracic derivations fit perfectly well into the picture, their lead lines (electrode to heart center) being drawn and compared with the records of the neighboring lead lines from the chest surface (367). The only advantage of electrodes like these is the high atrial potential, so that both from intrapulmonary and esophageal leads abnormalities in the atrial rhythm are optimally recorded (515).

The theory of such leads can be developed most clearly using the patterns of direct surface electrodes of the heart. Many electrophysiologists have experimented with such electrodes on animals. In the last few years, surface electrodes have been used even in man, during open-chest operations (30, 67, 95, 278, 279). The procedure of putting electrodes on the heart's surface in animals has been commonly done by electrophysiologists for a long time. The interpretation of such curves is much more complicated than most of these authors apparently realize. We therefore discuss their theory in common with the theory of all leads deriving potentials in direct contact with myocardial fibers.

7. LEADS IN DIRECT CONTACT WITH THE MYOCARDIUM

Whenever one or two of the exploring electrodes touch the surface of the heart or penetrate into its

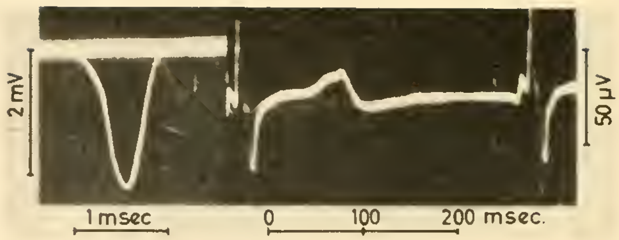

FIG. 28. Action potential from the surface of a dog's ventricle with close bipolar microelectrodes of a distance of 0.2 mm. The left record (R wave) is taken with low sensitivity (gauge to the left) and high speed, the right with high sensitivity and lower speed, to show the T wave. The QRS in the right record consists of some short but low extrinsic potentials, too small to be seen in the left record. The areas of R and T are nearly equal (90 and 85 microvoltsec); T is discordant. R (*left record*) is recorded as inverted, for technical experimental reasons. [From Haas *et al.* (234).]

muscular wall, a maximum of "proximity" potentials is recorded. The theory of such direct leads is of importance because records from such leads have been used to determine the spread of the excitation process.

First we shall consider the case of a bipolar electrode system with a rather narrow distance. Such a pair of electrodes records the potential gradient of the resultant electrical field at its site. The resultant field is preferably composed of flow lines stemming from the very nearest myocardial fibers; but flow lines from more remote fibers do interfere in a confusing manner and can never be completely eliminated. If the electrode distance is very short (less than 1 mm) and the contact to the myocardium very close, the amount of potential arriving from remote fibers is quite small. This can be demonstrated by the potential pattern. Figure 28 shows a record taken by such electrodes. The total duration of the R wave is nearly identical with the duration of the upstroke in monophasic action potentials recorded by intracellular electrodes (412). If the fibers were isolated in the air, the bipolar derivation would yield the first derivative of the monophasic action potential. But even if the electrodes are put directly on the epicardium, the distance to the next fiber is of the order of magnitude of 50μ, and the potential recorded is distorted by the flow lines of the developed electrical field. As figure 29 shows, the arrangement of fibers near the surface is strongly asymmetrical. If a pair of electrodes is put on the surface, the recorded potential will be triphasic, a first deflection downward indicating that the dipole is approaching the electrodes, a second main and upward deflection indicating the passage

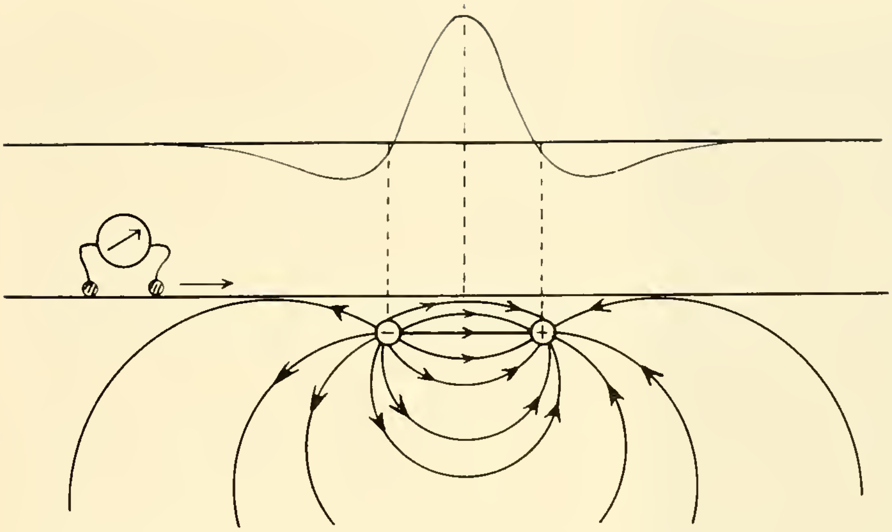

FIG. 29. A dipole moves along a myocardial fiber directly below the epicardial surface. The field is asymmetrical, and a pair of closely spaced electrodes is supposed to pick up the potential gradients of the field. Instead of moving the dipole, we may move the electrodes across the fixed dipole field. The potential recorded is drawn at the top of the figure. Each point on the record corresponds to a certain electrode position. If the dipole moves below the fixed electrodes, the same picture is obtained, with the *abscissa* indicating velocities instead of distances.

of the dipole below the electrodes, and a third deflection being the receding phase (160). Records of this type permit determination of the moment when the center of the dipole (or, in our case, the center of the depolarization process) passes the midpoint of the electrode distance: it is the summit of the recorded spike. The smaller the electrode distance, the more correct is the determination, because fewer fibers contribute to the recorded potential. This bipolar technique with "contiguous" electrodes is the only one apt to record local excitation directly below the electrodes. Distances between the electrodes of less than 1 to 2 mm are desirable to obtain correct results (412).

The unipolar potential recorded in close contact with the surface is much more difficult to interpret. Here we never get a preferably local potential, since the duration of the QRS complex is always nearly identical with that recorded by total lead systems. There is not even a marked spike of short duration superimposed, so that the total mass of the heart participates in the potential to nearly the same extent as the proximal parts of the heart. There is no strictly local derivation possible with unipolar electrodes! This is easy to understand if one considers the theory outlined earlier: if the lead field is spherically radiate (fig. 22), the local potential depends upon the solid angle under which the active cross sections of excited fibers appear. Since many fibers are active simultaneously, the momentary distribution of these excitatory processes governs the potential pattern. The sum of all individual solid angles ω_i, under which the different active fibers i appear, is a solid angle Ω as well, regardless of the irregularity of its shape. The potential recorded is then

$$V_p = m \cdot \sum \omega_i = m \cdot \Omega$$

Let us call this solid angle Ω the "weighted active cross section," weighted, because each fiber contributes proportionately less the more remote it is from the electrode. The polarity depends upon the direction of the excitatory wave, whether it runs toward the electrode or away from it. Parts of the heart, the fibers of which run in opposite directions, develop potentials of opposite polarity and cancel each other. If a definite polarity is recorded, it represents the influence of the prevailing direction of the weighted active cross section. When the unipolar potential is positive, as against the CT or any other indifferent electrode, the fibers run predominantly toward the electrode during depolarization. (During repolarization, of course, all polarities are of opposite sign.) A bundle of nearby fibers prevails over a remote bundle because of its larger solid angle. But the effect of a small amount of very near fibers may be counterbalanced easily by a large mass of remote fibers with a great solid angle Ω. The unipolar record therefore reveals always the prevalent direction in the activation of fibers, plus the effects of mutual cancellations of waves running in opposite directions.

If under comparable field conditions the ECG of a big (hypertrophic) heart is compared with that of a smaller one, the hypertrophied heart has a somewhat larger potential (219), because it appears under a somewhat larger solid angle. If the electrode is put on the heart's surface, no such effect can be demonstrated (56), because now the solid angle under which

FIG. 30. Superposition of extrinsic and intrinsic potential in a unipolar record from the ventricular surface of a dog. The intrinsic deflection starts far behind the top of the R wave with a slur at the beginning of the very rapid downstroke. [From Schaefer (58).]

the heart muscle mass appears has reached its maximal value of 2π.

The solid angle Ω, under which the active cross section of a fiber bundle appears from the surface electrode, can never exceed the value of 2π, according to a hemisphere, and in most cases is much less. The unipolar potential therefore becomes $V_p = m \cdot \Omega = (V/4\pi) \cdot \Omega$, and amounts maximally to one-half of the intracellular action potential V, i.e., 100/2 = 50 mv. In most cases it is much less, but may go as high as 25 mv. This means that the weighted active cross section of fibers sending their excitation waves towards the electrode has a solid angle of about π. The nearest fibers influence the total potential pattern with a very characteristic event, the "intrinsic potential" (322, 531). In the record, a sudden and very steep downstroke occurs, indicating that the bulk of nearby fibers is about to be activated. The downstroke (fig. 30) may be finished in such a short time as 3 to 5 msec. This shows that the shell of active cross sections around the electrode suddenly disappears, as the depolarization wave front reaches the electrode. The heart mass around the electrode is then totally active and without any membrane potential differences. The intrinsic downstroke is usually followed immediately by a local potential of opposite sign, indicating that a certain number of fibers are now activated by excitation waves running away from the electrode. Thus the zero point of the downstroke indicates that moment in time at which the weighted active cross section of the approaching fibers equals exactly the corresponding cross section of the receding fibers.

In the older literature it is often claimed that summit of the spike of the unipolar action potential is recorded at the "time of arrival" of the excitation at the electrode point. This, however, may be quite wrong, as simultaneous recordings with unipolar and close bipolar electrodes have shown (413, 501). In most cases, the beginning of the downstroke is induced by depolarization of relatively remote but large muscle masses, the excitation waves of which had been approaching the electrode. Only the starting point of a "very sudden" downstroke may be more or less correct as a measure of the local activation time. For that reason, we regret to say that many classical determinations of the time course of ventricular activation cannot be accepted.

As unipolar electrodes are often used nowadays in close contact with the heart, even in man (30), it seems necessary to discuss briefly how curves so obtained are to be interpreted. The first argument to contest is that only certain parts of the heart contribute to a unipolar potential. This is true neither for extremity leads nor for a direct electrode on the heart's surface. Even from the epicardial surface of the heart, a resultant electromotive force is recorded which is more or less identical with the force represented by the heart vector. The amount of proximity potential, in other words, is smaller than expected by many authors. Therefore, although Groedel claims that the precordial potential contains a high local effect because of its similarity to the epicardial record taken from a point exactly below the precordial point, the correct conclusion should have been drawn in the opposite direction: even the epicardial record is largely determined by the resultant heart vector with comparatively small proximity influences (94).

The interpretation of unipolar surface derivations is difficult. If a record from the caval surface is purely negative, it may be that the bulk of fibers having direct contact with the electrode conduct their excitation waves strictly away from the electrode, as at the sinus node region (239, 278) or at the site of origin of an extrasystolic beat (416). The same record, however, would be obtained where the inner surface layer of fibers runs parallel to the surface and therefore perpendicularly to the lead vector: their potentials will not be recorded, and the record

is thus determined by the big muscle masses of the more remote parts of the ventricular wall, which lead away from the electrode. The latter is obvious at many points of the endocardial surface. In experiments of Durrer *et al.* (178, 179), the bipolar potential with leads perpendicular to the surface is very low and polyphasic, a fact which can be explained only by a conduction parallel to that surface. The reports of various authors (397, 526), that the endocardial surface in the unipolar record only has a negative deflection, therefore may easily be explained. The bulk of the fibers in the ventricles is excited by waves running toward the epicardial surface, corresponding to the specific conduction system which runs near the endocardial surface and branches from there into the myocardial spindles. The same is true for results of Prinzmetal *et al.* (377), who found that the cavity, intramural and surface potentials of an infarct region may be equally negative; because in this region the approaching waves are deleted, and the distant receding waves command the potential pattern in all lead positions. However, if only the inner part of the ventricular wall is damaged, the epicardial electrode shows a positive potential (337). Positive or negative deflections depend solely upon the amount of fibers with excitation running toward the electrode or away from it.

Such a theory, which proves itself to be applicable and useful, is the modern variant of what Lewis called the "theory of limited potential differences" [(321); see also (175)].

8. SPREAD OF ACTIVATION THROUGHOUT THE HEART, IN RELATION TO A THEORY OF P AND QRS

As has been shown in the introduction, the spread of the excitation wave is of fundamental importance to the explanation of an electrocardiographic curve. The resultant electric field depends upon the mode of interference of the various cardiac muscle fibers concerning position, direction, and time of activation. Therefore, any itemized analysis would first require complete knowledge of anatomical details. We will shortly mention such facts as are known, and elucidate the ECG pattern. The anatomy of the conductive tissue (11, 171, 269) has been given in the preceding chapter. Second, the time course of the spread of activation has to be known. This is the topic of the following section.

The explanation of the electrical signs during atrial activation is relatively simple. Under normal conditions the excitation wave starts at the sinus region and proceeds from there nearly linearly to all parts of the atria, the auricles included (124, 322, 378) (fig. 31). The velocity of the wave varies within the limits of 0.4 to 1.2 m per sec (124, 171), a result which agrees with earlier and recent experiments. In the extreme parts of the auricles, the fibers apparently run in a somewhat curved manner, but the main part of atria and auricles is excited by a wave front progressing from the sinus node on an approximately radial pathway. The most remote points of the auricles are reached within a latency time of about 60 msec in dogs (124, 378). This means that the latest fiber is depolarized during the fall of the P wave, shortly before it ends. The P wave therefore may be regarded as the superposition of excitation waves in the atrial and auricular fibers. (See section 10 and fig. 49 for nomenclature.)

The highly diverging individual excitation waves imply a high degree of cancellation. This, and the small muscular mass of the atria, are the reasons why the P wave is very small. On the other hand, none of the radial pathways of the wave front is strongly bent. The thickness of the atrial walls is much more homogeneous than that of the ventricles. All these data collaborate in making the P wave as smooth and simple as it is. Only in cases of marked dilatations or local hypertrophies, does broadening and splitting, or augmentation of the amplitude occur, a finding well known to the clinician as "mitral" or "pulmonary" P wave.

Only a few of the many fibers radiating outward from the sinus node are responsible for atrioventricular conduction (396). Once the A-V node is activated, the excitation spreads along the specific conducting system. Details of this conduction are given in the preceding chapter by Scher. During the PR segment, excitation proceeds in a very small bundle of fibers, which has a comparatively negligible cross section. The potential produced by such an excitation wave is therefore too low to be recorded. One can calculate the average amount of fibers necessary to produce a detectable potential. Even under optimal conditions, at least 4000 normal myocardial fibers have to be active to produce a measurable potential in a precordial lead. In an extremity lead, the number will be ten times as much (58, p. 456). That means that the cross section of a bundle, the action potential of which may be recorded by optimal precordial or conventional extremity leads, has to be at least 1 mm^2 in the former case and 10 mm^2 in the latter. The cross sections of

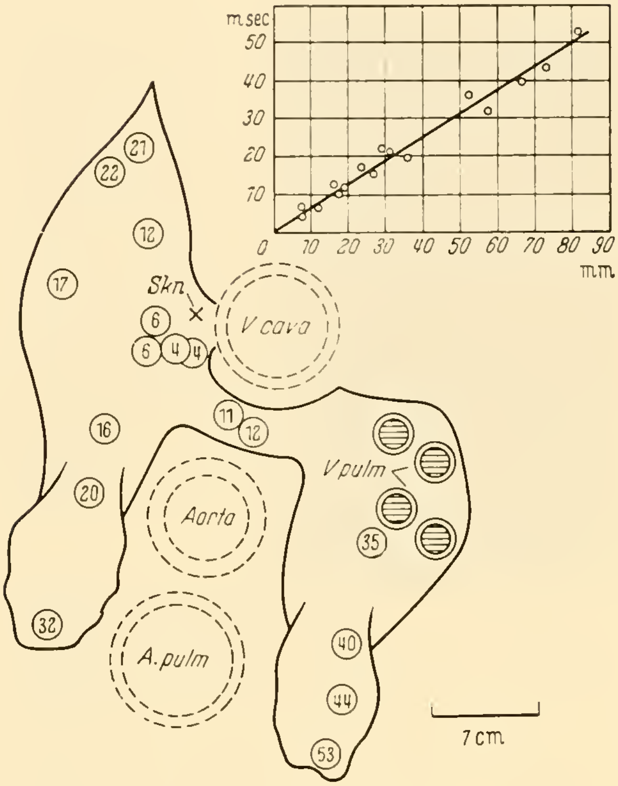

FIG. 31. Pathway of the atrial excitation waves. The atria of a dog are seen from above, with the auricles. The figures in circles indicate the latencies observed at the various points, against the earliest visible excitation at SKn, the sinus node. *Inset*: the latencies are plotted against the distances from the sinus node. The propagation takes place radially on nearly straight lines from the sinus. [From Brendel *et al.* (124).]

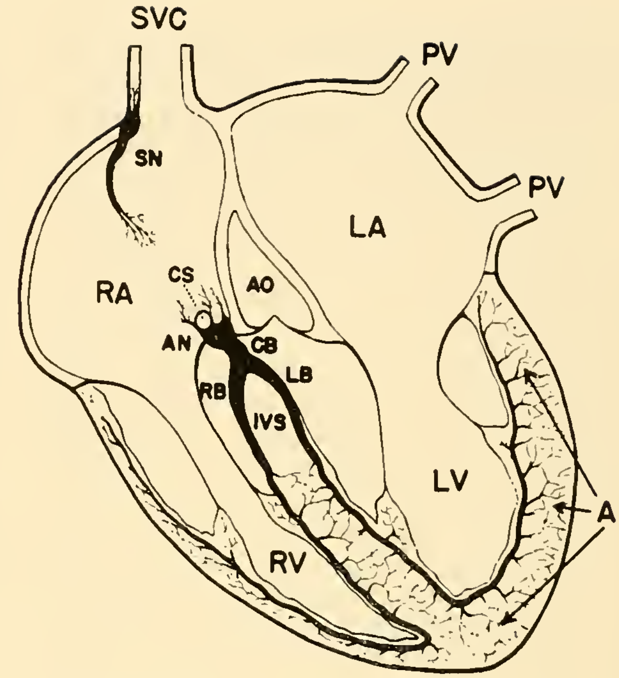

FIG. 32. Diagram showing distribution of specialized heart muscle. RA and LA, right and left atria; RV and LV, right and left ventricles; IVS, interventricular septum; AO, ascending aorta; CS, coronary sinus; SVC, superior vena cava; PV, pulmonary veins; SN, sinus node, AN, atrioventricular node, CB, common bundle, RB and LB, right and left bundle branches; A, the peripheral Purkinje net. [From Katz (39).]

the bundle of His are about 10 mm^2 maximally, calculated from the data of Read *et al.* (379), and scarcely more than 1 mm^2 according to the findings of Glomset & Glomset (224). These cross sections, therefore, are just at or below the borderline of a recordable potential for extremity leads. In precordial leads it should perhaps be detectable, but no special attempt has ever been made to discriminate it from the large potentials of atria or ventricles. In direct unipolar derivations, the action potential of the His bundle can be detected only when there is close contact between bundle and electrode (82). Any clinically reliable information about the action potential of the bundle therefore will scarcely be gained by the conventional lead systems. As long as the excitation travels in the bundle alone, the ECG is mute, if the atria are not still producing potentials in their lateral parts. The details of this propagation process have been described in the preceding chapter (260, 296, 415).

The essence of the spread of excitation in the ventricles, which is by no means known in every detail, lies in the following facts. The excitation wave is first propagated through the more or less unbranched bundles of His down to a midpoint region on the septum between the ventricles, where the first big branches leave the system and the excitation enters the mass of the ventricular wall (fig. 32). Propagation into the myocardium is effected thus: the conduction fiber converts itself into an ordinary myocardial fiber (360), which branches several times, producing a cone-like system (387, 389). The specific form and site of the conductive tissue exhibits now a doublefold divergence. First, the excitation front spreads from that midpoint region in all directions, so that at the surface of the heart the excitation occurs earliest at a central point and spreads in the form of concentric rings. Second, myocardial activation starts near the endocardial surface—how near, is still a matter of controversy. But at the point at which the conduction system branches, as experiments to be described later have shown, a divergent wave runs from the specific system in both directions,

thus forming excitation waves of opposite direction with a cancellation of their electric fields. There are several sets of observations which elucidate this general pattern in more detail. Unfortunately, all these details are only concerned with the hearts of animals, mostly dogs. There is only a small amount of information available which deals with the human heart. But the similarity between the anatomy of human and dog hearts does allow generalization of the conclusions drawn from experiments in dogs. These indicate that a considerable synchronization of all parts of the ventricle is effected by the fact that *1*) the conducting system connects all points of the ventricle on the shortest pathway with a centrally situated point of distribution, at which point the specific system branches; *2*) this system conducts with a comparatively high velocity of about 2.5 m per sec, diminishing in an "intermediate" part to about 1.0 m per sec and reaching then, in the bulk of the myocardial fibers, perhaps much slower rates (171). These facts govern the total duration of QRS.

Direction of Excitation Wave Recorded With Bipolar Electrode Combinations at the Surface

The simplest way to determine the pattern of propagation along the ventricular wall would be by direct measurement of propagation velocities and directions. This, however, can be done only with a minimum of three different electrodes closely placed on a bundle of myocardial fibers. As the orientation of such bundles can never be observed directly in the interior of the ventricular wall, only surface measurements promise reliable results. However, the distance between such electrodes must be smaller than 1 mm, if the behavior of single fibers is to be observed. Any record in which the local R wave or spike potential exceeds even 1 msec cannot be regarded as a true picture of the elementary processes in the myocardium, because too many unsynchronized fibers contribute to the potential.

The first measurements of this kind with close bipolar electrodes showed small local action potentials of a duration as short as 1 msec (412). A "compass-electrode" was used, with which several directions of conduction could be derived. The electrode position yielding the maximal amplitudes could be defined as being parallel to the direction of the excitation process. The time difference between the peaks of two potentials recorded with closely paired electrodes was an exact measure of the propagation velocity (fig. 33). With a series of such measurements, the propagation at the surface of a dog's heart could be investigated, and the result shows that the propagation waves run more or less uniformly in a direction which seems to start from a common central region, the so-called "source" (Quellpunkt) on the anterior surface of the heart. In figure 34, the directions of the propagation waves are shown in the form of a map; figure 34*B* shows one experiment and its original result. Arrows demonstrate the directions of the waves. The velocities ranged between 0.5 and 1.7 m per sec, with an average of 0.9 m per sec. These observations have been repeated with sufficiently accurate technique only by Meda (344) in frog hearts and with rabbits by Taccardi (479), who achieved similar results. Only Draper & Mya-Tu (171) report much slower conduction velocities in strands of ventricular tissue. Taccardi found that the excitation wave traveled in one direction only over very short distances, about 4 mm. This has been confirmed in recent experiments (234). It seems certain that the distance over which there is uniform propagation of myocardial excitation is limited to a few millimeters ("length of free way"). As soon as excessive electrode distances are used, the electrodes touch different muscular bundles and high apparent propagation velocities are recorded (466, 467).

Latencies at the Ventricular Surface

The above results have been confirmed by measurements of local latencies at the epicardial surface. Lewis *et al.* have investigated these latencies with amazingly precise results, in dogs (323), many other animals (321), and even in man (321). A rather comprehensive series of papers has dealt with the same problem more recently. Unfortunately, most of them recorded the intrinsic deflection in unipolar leads, a method of only restricted value, so that the results are not as accurate as one could wish them to be (64, 81, 388, 397). The intrinsic deflection is by no means synchronous with the arrival of the excitation wave at the electrode (413, 467, 501). Therefore, close bipolar electrodes provide the only method for obtaining conclusive results. All measurements made with such electrodes, to date, agree that the latencies of superficial local excitations are minimal in a region on the anterior surface of the dog's heart (64, 237, 412, 420); and in cats (58), rabbits (501), and guinea pigs (169), the same result has been found. This means that the "source" region of figure 34 bears the shortest latency. The differences in latency time, however, are rather small, and very

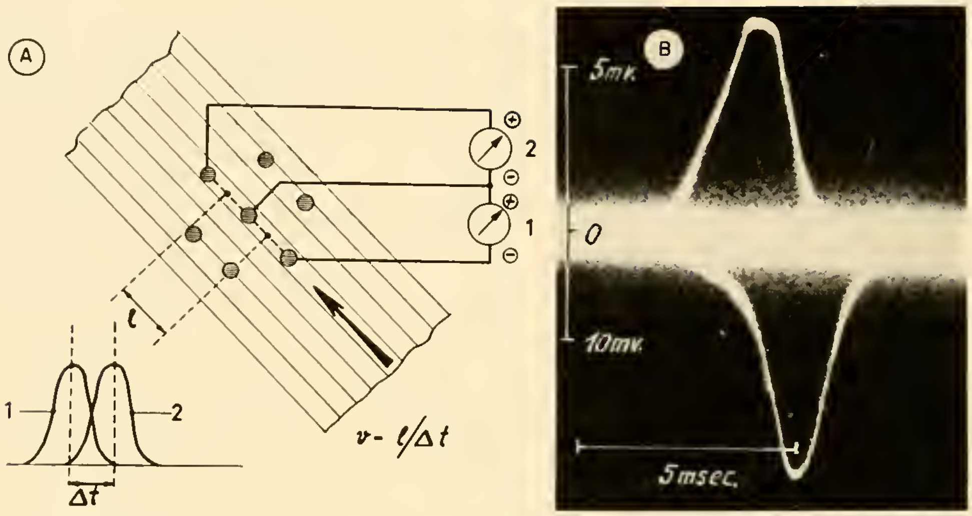

FIG. 33. *A*: schematic drawing of the "compass-electrode," placed on the epicardial surface of a dog's heart. Two amplifiers are connected in the manner indicated. Various connections may be made by the use of a gang switch. If the records are obtained from connections parallel to the muscle fibers, the potentials and the peak-to-peak distance will reach a maximum, as in the record below. The excitation velocity v may be calculated from the symbols given. [From Schaefer (407).] *B*: original record made with the electrodes illustrated in *A*. For convenience the two action potentials are recorded with opposite polarity. Cathode-ray oscilloscope. [From Schaefer (407).]

FIG. 34. Map of the direction of surface excitation. *A*. one experiment on the posterior surface of a dog's heart, with the technique of fig. 33 (Experiment of Trautwein). *B*: the results of several experiments on the anterior surface of a dog's heart. [From Schaefer & Trautwein (412).]

high apparent velocities would be calculated from such latencies and the distances at the surface. Since the muscular propagation velocity is relatively slow, a synchronizing mechanism apparently exists, which leads the excitation wave on a more direct route to the various parts of the ventricles. This mechanism is assumed, of course, to function through the Purkinje system, but there is no exact proof of this assumption. Figure 35 gives an idea of the spreading process, which indeed seems to imitate the propagation of an ink spot on a blotting paper, as Lewis previously stated in reference to the atria.

In spite of the extreme importance of such measurements, nobody has ever tried to measure the propagation process in the human heart by a reliable method. There have been some observations made with unipolar recordings, evaluating the intrinsic deflection (95), but the results deviate greatly from those obtained from the dog's heart, insofar as the earliest excitation wave recorded appeared near the base of

the heart. The interpretation of such records is rather uncertain. In a recent paper by Torrésani (67), the results coincide much more with the behavior of the dog heart: the latencies are minimal near the interventricular septal region, and the lateral parts of the left ventricle are the latest activated. The book by Groedel & Borchardt (30) does not include any information on this, as the intrinsic deflections are not visible in the records printed. Some papers of Jouve *et al.* (278, 279), although they do not contain an evaluation of latencies, do seem to indicate, as far as the records can be read, that the shortest latencies of the intrinsic deflection are found near the pulmonary conus, and at least over the right ventricle. Between dog and man no important differences in the surface and intramural potentials seem to exist (277). Therefore we may draw our conclusions from experiments on dogs and apply them to the theory of the human ECG.

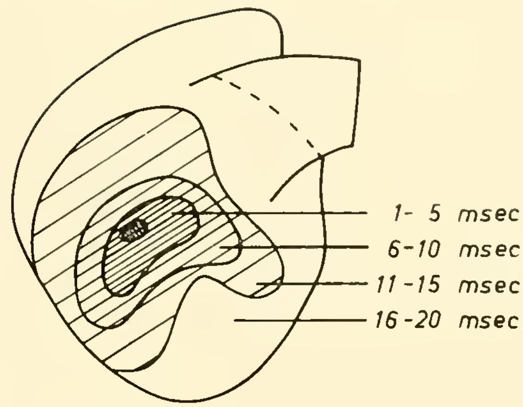

FIG. 35. The latencies at the surface of the cat's heart. The figures give the range of latencies in the area indicated, in milliseconds. [Experiment of Harris (237).]

Latencies Across the Ventricular Wall

The behavior of superficial excitations can scarcely explain the formation of the QRS complex. Although Durrer (16) was seriously skeptical about our statement, we still are convinced that the directions of the epicardial excitation waves are a kind of indicator for the propagation process within the musculature of the ventricles, because we cannot imagine how, in a geometrically reasonable way, excitation in the ventricular wall could run in an essentially different direction to the waves in the surface fibers. This argument is fully corroborated by the result of intramural derivations. Such derivations, however, have been difficult to evaluate concerning their biological reliability. The results presented by the laboratories of Scher and Durrer (176–179, 414–420), however, seem to indicate that the distortions are not too serious. If a needle with multiple electrode points along its axis is put through the heart, latencies may be recorded either by taking bipolar records with narrow electrode distances (176–179, 237, 414–420, 467, 468) or by using unquestionable intrinsic deflections in unipolar records (139, 321, 377, 397, 467, 468). The latter, however, may be recorded only after some time of waiting, until the distortion by the injury has disappeared. The results of both methods are quite similar. They may be listed as follows:

1) The propagation of the excitation wave proceeds in two directions: one (as in the classical concept) from the endocardial to the epicardial surface; a second one from a midpoint of the heart toward the apex and the base, in two opposite wave fronts.

2) The activation of the interventricular septum is directed from apex to base (139, 468), with an earlier activated point in the mid-anterior region at the junction of the free wall and the septum (420). This fits optimally into the surface picture, because this region lies directly below the "source" region of figure 34.

3) There is a minimal latency time in regions lying in the wall, close to but not identical with the endocardial layer. If we translate this latency picture (fig. 36) into directions of the various excitation wave fronts, we get a result like figure 37. However, we should point to the fact that such translations are always a bit questionable, since the excitation process does not take the shortest distance between the isochrones of figure 36. The only conclusion to be drawn from these measurements is that there are strong cancellation effects from excitation waves traveling in opposite directions.

4) If a needle electrode is put across the ventricular wall, there is a "reversal" point where the polarity of a bipolarly recorded potential is inverted (179) and from which the excitation waves start in opposite directions.

5) On cross sections perpendicular to the heart's axis, a similar conduction pattern can be seen: the waves start at points quite near to the endocardial surface, and spread radially in all directions (fig. 38) (417–419). A tentative drawing of the directions in which the excitation is conducted is given in figure 39. Activation of the septum is rather complicated, as all authors agree.

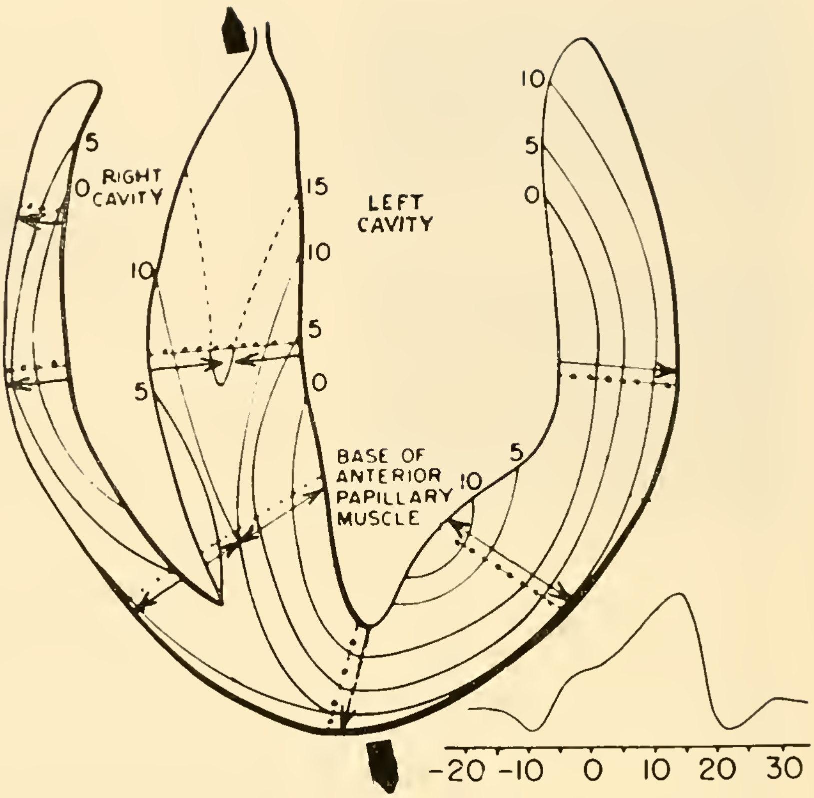

FIG. 36. Successive positions of depolarizing wave front for coronal section of a dog's heart in a normal beat. A multipole needle electrode is inserted into the ventricular wall, with terminals 1 mm apart. The latencies of bipolar records have been observed. The lines are isochrones of latencies. The black arrows indicate the line connecting the lead II electrodes. [From Scher & Young (416).]

9. GENERAL PRINCIPLES UNDERLYING INTERPRETATION OF THE ELECTROCARDIOGRAM

Areas of QRS and T and the Ventricular Gradient

In the preceding sections, our emphasis has been on the "activation" wave, i.e., the depolarization process of the myocardium. A complete theory of the ECG, however, should take into account as well the repolarization and its electrocardiographic counterpart, the T wave. The repolarization phenomenon is complicated by the different manners in which the various parts of the heart behave, whereas depolarization appears to be more homogeneous. This is one of the reasons why the physical laws of electric fields and leads, and the physiology of conduction, are difficult to correlate with the behavior of T.

Depolarization and repolarization in the heart can be considered separately because of the form of the monophasic action potential. Activation accession (i.e., the upstroke of the action potential) is very rapid compared with repolarization, which starts slowly, forms a plateau, and then returns to the base line with the maximal decline of the curve being about 1/1000 as fast as the downstroke of the depolarization process. If we construct the electric field of one single fiber during the whole cardiac cycle, the same methods can be adopted as were used previously in discussing the dipole during depolarization.

FIG. 37. Schematic translation of the isochrones of fig. 36 into intraventricular pathways of the excitation. The arrows are only an indicator of the average direction in which the wave front of the excitation proceeds.

The dipole moment M_i of a single, cylindric

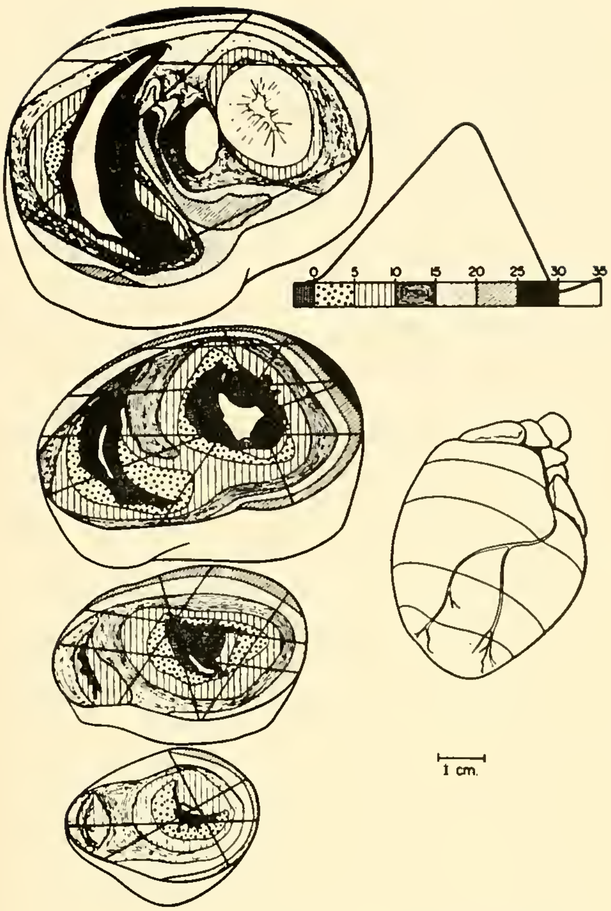

FIG. 38. A plot of total ventricular activation. Seventeen electrode tracks are shown in four cross sections of the heart. The time of activity (in milliseconds) before or after the time reference was noted at each terminal of the same electrodes which were used in obtaining fig. 36. All times are referred to the beginning of QRS in lead II, and points of equal latency are connected with each other. Tissue activated within each 5-msec interval is shaded in the same manner in all sections. Above and to the right is the lead II QRS and the shading of time intervals. [From Scher & Young (418).]

myocardial fiber of a cross section Q and a length sufficiently short is given by the formula: (see equation (2.4))

$$M_i = Q \cdot (m_2 - m_1) \tag{9.1}$$

where m is the membrane potential at the beginning (m_1) and the end (m_2) of the respective fiber. The dimension of M_i is mv · cm². M_i is the momentary value, which of course changes with time. No special assumptions are made in this connection about the form (time course) of the action potential. A good illustration of the magnitude of the development of M_i during time is the difference between the mono-

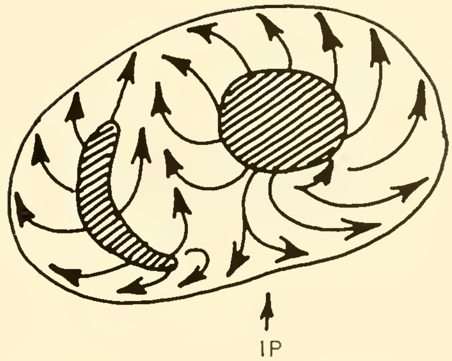

FIG. 39. Schematic drawing of the pathways along which the excitation most probably spreads, shown in a cross section perpendicular to the heart axis. IP is an inversion point, at which on the surface the excitation seems to diverge to the left and to the right.

phasic action potentials at the beginning and the end of the fiber in question (fig. 40). These momentary values are drawn in figure 40 for two distinct instances. If one considers the time course of this moment M_i for the whole duration of the excitation process, the time-voltage area of M_i equals

$$\int M_i\,dt = Q \cdot \int (m_2 - m_1)\,dt = Q \cdot \left[\int m_2\,dt - \int m_1\,dt\right] \tag{9.2}$$

if Q is considered as constant. The value of this expression is equal to the shaded area in figure 40. If $\int m_2\,dt$ equals exactly $\int m_1\,dt$, taken over the whole of the excitatory cycle, the resulting integral of M_i becomes zero. This is the case when the forms of the monophasic action potentials are completely identical. We define excitations with such an identity of their voltage curves as "homogeneous" and call a region in which all fibers behave in such an identical manner an area of "homogeneous excitation." In such an area, under the assumption of constancy in time of the cross sections of all fibers, the total shaded area for every fiber (fig. 40) would be alike and of opposite sign. Under the special assumption that the monophasic action potential has the form of figure 40 (i.e., reveals a plateau of sufficient duration), the time course of M_i shows two separate peaks, of opposite direction, the first of which may be called R, the second one T. Both belong to the single fiber, and may therefore be called local (or individual) R_i and T_i. In a homogeneous region of the heart the time-voltage areas of R_i and T_i are equal and of opposite polarity: $\widehat{R_i} = -\widehat{T_i}$. (The sign $\frown$ is generally adopted to characterize the time-voltage areas.)

The innumerable fibers of the heart act together

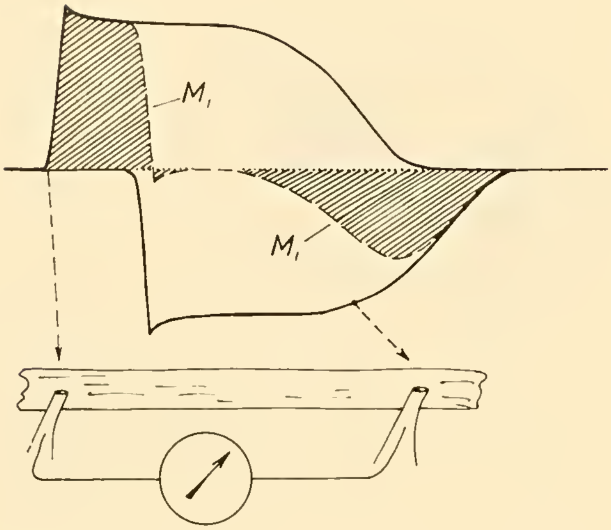

FIG. 40. The microelectrodes are inserted into a ventricular fiber, and the difference of the membrane potentials at the two points recorded. The two monophasic action potentials, as they would have been recorded between each of the electrodes and an indifferent external electrode, are drawn separately. Their difference, changing with time, is M_i. The time course of M_i is represented by the curve enveloping the shaded areas ("Differenzkonstruktion" of Schütz). The total sum of all shaded areas is zero, if the polarity is taken into account. (This assumes no ventricular gradient, and that repolarization is homogeneous all over the fiber.)

in building up a resultant electric field by spatial and temporal superposition of the individual components. The moment M_i as defined above has the nature of a vector. The addition of these vectors $\vec{M}_i$ then leads to a resultant vector, the well-known "heart vector" $\vec{M}$ (see section 4):

$$\vec{M} = \sum \vec{M}_i \tag{9.3}$$

where this sum is a vectorial sum, for a given instance. For this resultant vector, the time-voltage integral is governed by the same laws as govern the individual vector $\vec{M}_i$, i.e., the time-voltage area

$$\int \vec{M}\, dt = \int \sum \vec{M}_i\, dt = \sum \int \vec{M}_i\, dt \tag{9.4}$$

or in analogy to our previous formulation:

$$\widehat{\vec{M}} = \sum \widehat{\vec{M}}_i \tag{9.5}$$

The value of $\widehat{M}$ is commonly known as the "ventricular gradient." Under the above-mentioned conditions (homogeneous behavior of the monophasic action current), the value of $\widehat{M}$ equals zero. This means: as $\vec{M}$ is a vector entity, $\vec{M}$ can be divided into three components M_X, M_Y, and M_Z, corresponding to the three axes of figure 19. If therefore $\widehat{\vec{M}}$ (the time-voltage integral of M) disappears, every component of $\vec{M}$ forms a time-voltage integral (or area) $\widehat{M_X}$, $\widehat{M_Y}$, and $\widehat{M_Z}$, equaling zero. This form of an analysis may be called the "integrated electrocardiogram" (125).

Every individual dipole M_i builds up an electric field, the form of which can never be determined exactly, as has been shown in the preceding sections. The total field of the heart, possibly recorded by the electrocardiographic leads, is formed by the superposition of all individual fields. Now the following general statement can be made. If one records the potential difference U between arbitrarily chosen points of this field, U is the algebraic sum of all individual voltages U_i generated from the individual fibers with their dipoles M_i ($U = \sum U_i$). Correspondingly, the time-voltage integral is $\widehat{U} = \sum \widehat{U}_i$. We now make the following assumptions: *1*) The monophasic action potential should be homogeneous all over the heart. *2*) The form (e.g., the cross section) of the fiber should be constant. *3*) The anatomical (spatial) orientation and position of the fiber should remain unchanged. *4*) The relationship between source and field should be linear, e.g., a doubling of source voltage should lead to a doubling of flow lines and local potentials. Under these conditions, every individual voltage U_i is proportional to M_i with a fixed factor of proportionality. In the same way, $\widehat{U}_i$ is proportional to $\widehat{M}_i$, and equals therefore zero. Furthermore, $\widehat{U}$, as the time-voltage area of U and the algebraic sum of $\widehat{U}_i$, equals zero as well (233).

To summarize, the following relations are valid. If we suppose the individual events in the heart to be homogeneous, and assume the other three conditions mentioned, every record with every lead system would give a time-voltage area of exactly zero. This would be true for every lead, every projection of the heart vector in case of a lead field with parallel flow lines, and every local (e.g., precordial) lead. It would remain true regardless of how distorted the potential field and how peculiar the conditions of derivations might be. Now, it is well known that in fact the time-voltage area generally differs considerably from zero. Therefore one or more of the above-mentioned conditions must not be realized. Since condition 4 (the linearity condition) is at least approximately fulfilled, the deviation from the ideal points to the invalidity of conditions 1 to 3.

To understand the physiology of the ventricular gradient, we should assume for a moment a lead system which can be used to derive the total heart vector or one of its components in a correct manner. Such a system could be a lead field with parallel flow lines. From such a system recording in the three axes of space, every derivation forms a component of the heart vector, and in general we observe that the time-voltage area of the component has a definite value different from zero. This value may be regarded as a component of a spatially oriented vector. This vector is the spatial ventricular gradient ($\vec{G}_s$).[6] The gradient projects itself on each lead vector under the same conditions that apply to the heart vector. The projections are simple, if the lead possesses a parallel lead field. Where the heart vector does not project itself in such a simple manner in local leads, a projection of the ventricular gradient is not possible.

The ventricular gradient concept was propounded for the first time by Wilson, and elaborated in detail by Ashman *et al.* (84–89) in several papers. The numerical value of the gradient consists of two parts, one of which corresponds to the events of depolarization and is measured by the area of QRS in the derivations mentioned. The second part is the area of T. Recognition of the parts is possible only if and because depolarization is separated from repolarization in the ECG by a time interval (ST), during which the whole myocardial fiber and approximately the whole heart are nearly completely and constantly depolarized, indicated by the "plateau" of the monophasic action potential. We therefore have two vectors, $\overrightarrow{\widehat{QRS}}$ and $\vec{\hat{T}}$, formed by the components of the areas of QRS and T in the different projections, the vectorial resultant of which is the ventricular gradient: $\vec{G}_s = \overrightarrow{\widehat{QRS}} + \vec{\hat{T}}$. Figure 41 demonstrates this vectorial relationship.

Provided that conditions 1 to 4 are realized, $\vec{G}_s = \overrightarrow{\widehat{QRS}} + \vec{\hat{T}} = 0$, and therefore $\vec{\hat{T}} = -\overrightarrow{\widehat{QRS}}$, or, as in our figure, the vector $\vec{\hat{T}}$ is opposite to and of equal length with the vector $\overrightarrow{\widehat{QRS}}$. If in general, $\vec{G}_s \pm 0$, we can define a value $\vec{\hat{T}}e = -\overrightarrow{\widehat{QRS}}$, which is the virtual resultant of all repolarization processes and assumes these processes to be homogeneous all over the heart, and the form and the orientation of

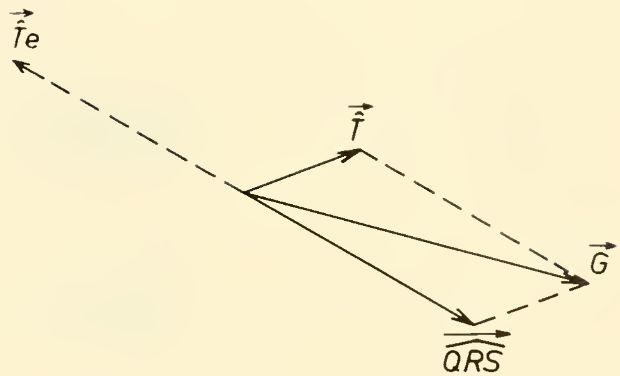

FIG. 41. The analysis of the vectorial area T, which is the vectorial sum of all time-voltage areas Q-T of all single fibers, with their inhomogeneous repolarization, $\vec{G}$, and of the fictive T-areas produced by the homogeneous repolarization process, $\vec{\hat{T}}_e$. $\vec{\hat{T}}_e$ equals $\overrightarrow{\widehat{QRS}}$, because in case of homogeneous behavior; the area of T is equal and of opposite polarity to the area of QRS ("elementary T"). The real $\vec{\hat{T}}$ is the resultant of $\hat{T}_e$ and $\vec{G}$. Since $\hat{T}_e$ is equal but opposite to $\overrightarrow{\widehat{QRS}}$, the same vectorial relations may be expressed thus: the gradient $\vec{G}$ is the vectorial sum of $\vec{\hat{T}}$ and $\overrightarrow{\widehat{QRS}}$.

the fibers to be constant. We will call this virtual vector the "elementary $\vec{\hat{T}}$".[7] This elementary $\vec{\hat{T}}$ may be regarded as that component which, together with the ventricular gradient, gives the true $\vec{\hat{T}}$. The true T area in any projection, therefore, is the result of two components, one of which depends totally upon the area of QRS. If QRS changes, e.g., if its area gets larger, T undergoes a corresponding change which has no specific significance regarding any change of the repolarization process if G remains constant. For further detail see also section 11.

The formal reasons for the existence of a ventricular gradient have already been listed above. Among these four possible reasons, the lack of linearity most probably does not play any role. The relative importance of the other three is, however, very difficult to decide. As we calculated (233), the pure geometrical factors of the beating heart, i.e., the changes in the form or relative position of the different myocardial fibers certainly contributes in some degree to the ventricular gradient; the real value of the gradient however cannot be explained by these factors alone. The only adequate explanation for the high value of the gradient is inhomogeneity in

[6] Mathematically: if we put $\vec{M} = (M_x, M_y, M_z)$, it is $\vec{\hat{M}} = (\int M_x dt, \int M_y dt, \int M_z dt) = (\hat{M}_x, \hat{M}_y, \hat{M}_z) = \vec{G}_s$.

[7] This term "elementary" means that the corresponding part of T stems from the repolarization of the individual fiber elements of the heart, irrespective of their differences in repolarization velocity.

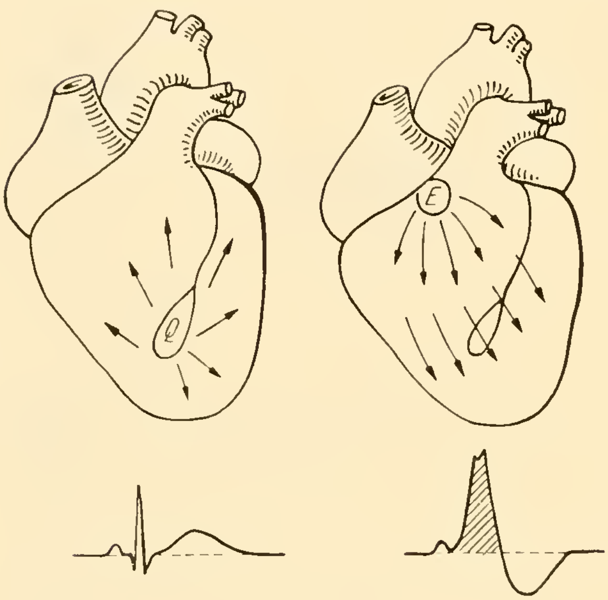

FIG. 42. Model of the differences in the excitation process in normal and ventricular ectopic beats. The extrasystolic beat has only a slight mutual cancellation of potentials and therefore a large time-voltage area of QRS and T. E: the site of the ectopic pacemaker. The arrows indicate the average direction of the excitation waves, analogous to fig. 37.

the pattern of the action potentials. The predominant role of this factor has long been known. In the very beginning of electrophysiology, scientists were aware that monophasic action potentials varied in different parts of the heart and seemed to last longer at the base than at the apex (433, 434). Such differences, however, could not be analyzed with a reliable technique until small electrodes were developed for recording local monophasic action potentials. The first attempt of this kind was made with a small sucking electrode (411), recording the events in very restricted areas. By means of intracellular electrodes it has often been found that various fibers of the heart show differently shaped action potentials (157–159, 240, 261, 262, 506, 534, 535). In dogs the action potential gets shorter from the base to the apex on the heart's surface (234). We therefore may conclude that a regular distribution of inhomogeneity exists, so that perhaps the inner layers repolarize more slowly than the outer, or the basal fibers more slowly than those of the apex. If, for example, T is flat or negative, the epicardial surface recovers with a mean delay of 11 msec, compared to the endocardial level. In positive T waves, the epicardial surface recovers 8 msec in advance (383). Since the recovery (measured by timing the refractory period) is closely related to the action potential, the positive T seems to correlate with a shorter action potential at the surface, which fits perfectly well into the general picture.

The cause of these differences in the monophasic action potential can only be speculated upon at present. Neither mechanical factors (173) nor the well-known differences in temperature between inner and outer layers (75, 187, 314, 359), nor differences in blood supply of the inner and outer layers of the heart can explain the vectorial direction and magnitude of the gradient (58, 216, 297, 371, 407). How far metabolic differences or differences in the content of calcium could be responsible, is quite uncertain.

Most probably, the inhomogeneous behavior of the action potential is due to a structural factor which we do not know in detail. This is more than likely, as even small parts of the heart, as papillary muscles (213) or muscle strips from the tortoise heart (215), show an upright, concordant T and a high ventricular gradient. All other factors mentioned above may play their limited role as well, but cannot be claimed to be the main cause of the ventricular gradient.

Amount of Cancellation of Fiber Dipoles

The area of QRS is very important for theoretical interpretation of the ECG, because it is completely independent of the degree of desynchronization of the various fibers, provided that the spatial pattern of the spread of excitation remains unchanged. The instantaneous voltage or the form and amplitude of the QRS complex, however, are highly dependent upon the mode of interaction and synchronization of individual fibers. Area and form therefore reveal totally different peculiarities of the spread of excitation which can be analyzed in detail. The area, irrespective of the total duration of QRS, is an excellent measure of the degree of cancellation resulting from the diverging excitation waves: the higher the area, the lower the cancellation of comparable muscle masses provided. The absolute voltage is a measure of the number of simultaneously active fibers and their momentary cancellation.

Quantitative relationships can be elucidated fairly well by an analysis of extrasystolic beats. In a homogeneous infinite medium under ideal conditions, the cancellation coefficient could be exactly predicted, if the directions of the individual fibers were known. But neither are the fields ideal nor do we know the structure of the heart exactly. Yet we have recorded maximal amounts of time-potential

area of a normal heart, with minimal cancellation effect in tracings of extrasystolic beats with the largest QRS areas. It has been shown (416) that in ventricular extrasystoles the intramural propagation runs more or less in one single direction, if the stimulus lines near the apex or the base and unipolar observations point in the same direction (468): the polarity in the septal region is reversed if the stimulus activates the base, and the septal wave is conducted from the base to the apex. Under optimal conditions, the time-voltage area in the frontal projection may increase to 300 μvsec (microvolt-seconds) and is up to 25 times higher in extrasystolic than in normal beats, with healthy hearts (410). This means that the total time-voltage production of the heart can be reduced to an amount of 1:25 or 4 per cent, or even less, of the maximal possible amount. "Or even less" means that even in an optimally situated ectopic focus the excitation wave does not travel in completely parallel fiber bundles, so that a certain amount of cancellation still remains. The value of 4 per cent is borderline; the average ratio of ectopic to normal beats is 10:1, if only large ventricular extrasystoles are selected. The mechanisms which govern the extrasystolic ECG are drawn schematically in figure 42.

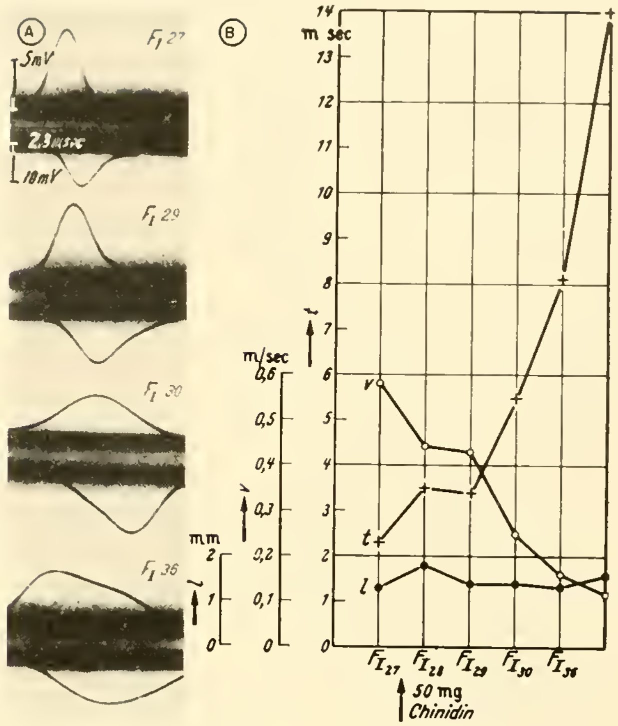

FIG. 43. Influence of quinidine on the conduction velocity and the bipolar action potential of single fibers. Action potentials at four different instances are given in the left part of the figure. The broadening of the potentials (duration t) and the increase in latency (measured according fig. 33) indicate a slowed conduction velocity v. The length l of the excitation wave (fig. 33) remains nearly constant. Strophanthine reduces these effects instantaneously to normal. [From Trautwein (485).]

Influence of Conduction Velocity Upon the QRS Complex

It is obvious that in the case of a slowing of the conduction velocity, the depolarization dipole would remain longer on the myocardial fiber, so that the time-voltage area would be enlarged inversely proportional to the velocity. If therefore a QRS complex shows an augmented area, it is unknown whether this is due to diminution of cancellation or to slowing of conduction. Only from indirect signs is discrimination possible. Every change in cancellation necessarily means that parts of the heart muscle conduct their excitation in a direction opposite to the normal. This is the case, for example, in the true bundle branch block. It has often been shown that after an experimental block the excitation wave is inverted in certain areas (486). A block, however, inevitably changes the position of the resultant vector $\overrightarrow{QRS}_s$, because it is impossible that in a certain set of dipole components a part of these components would change its direction without a change in the direction of the resultant dipole. The slowing of the excitation wave, however, if homogeneous all over the heart, would act in the same manner as if the speed of the recording instrument had been increased. $\overrightarrow{QRS}$ would be enlarged, but the vector direction unchanged. A simple test of whether the vector is changed or not may be made by a calculation of the type of QRS (see section 9). The whole consideration, of course, must assume that the area of the action potential, recorded with microelectrodes at a single point of the fiber, remains unchanged, perhaps not a valid assumption in all cases.

The propagation velocity has always been disregarded in textbooks on the ECG because we know little about processes causing the slowing of conduction. Nevertheless, it can be found experimentally that drugs like quinine act in this way (166, 485). As figure 43 indicates, the propagation velocity decreases from 0.6 to about 0.1 m per sec after injection of 50 mg quinidine. At the same time, the action potentials recorded with close bipolar elec-

TABLE 2. *Relationship Between the Size of Growing Hearts, the Heart Weight and the QRS Duration in Man*

Age, Years	*a* Observed Duration of QRS, msec	*b* Approx. Length of Ventricle, mm	*c* Male Heart, Weight, g	*d* $\sqrt[3]{\text{Weight}}$	*e* Calculated Length of Conduction Pathway in Specific System, mm	Calculated Length of Mean Direct Muscular Pathway, mm	*g* Calculated QRS Duration Related to $\sqrt[3]{\text{Weight}}$ and to Adult Value	*h* $\sqrt[6]{\text{Weight}}$	*i* Calculated QRS Duration Related to $\sqrt[6]{\text{Weight}}$ and to Adult Value
1–2	45	45	46	3.6	69	5.3	40	1.9	55
2–5	62		68	4.1	80	6.1	46	2.0	58
6–9	64	65	98	4.6	89	6.8	51	2.14	62
9–12	66	70	137	5.2	100	7.7	58	2.3	65
13–14	69		194	5.8	112	8.6	65	2.4	69
Adult	75	100	300	6.7	130	10	75	2.6	75
Hypertrophy									
600 g			600	8.4	164	12.6	94	2.9	84
900 g			900	9.7	187	14.4	104	3.0	87
Elephant	160		~18,000	26	500		290	5.1	147

The figures of rows *a*, *b* and *c* were measured directly; the rest were calculated. In *e*, the length of the specific system in the adult is assumed to be 130 mm; all other values were calculated from this value by assuming that this length is proportional to $\sqrt[3]{\text{weight}}$. *e* and *f* have a constant ratio of 130:10, which is the probable adult ratio [Schaefer (58)]. In *g* and *i*, the QRS durations were calculated by assuming the QRS to increase with the third or the sixth root of heart weight, respectively. *g* and *i* should be compared with *a*. As will be seen, the QRS duration varies in good agreement with the sixth root of heart weight. This may be explained by two assumptions: *1*) that in the growing heart, QRS increases predominantly with the heart length or the length of the specific system, and *2*) that the larger heart has the larger fiber diameters, the conduction velocity depending on the square root of the fiber diameter, whereas the diameters depend on the third root of weight. Hypertrophy within the clinically observed limits never increases QRS to more than 0.1 sec.

trodes are broadened and the QRS duration is augmented. Ouabain changes this effect suddenly back to normal (485). Adrenaline, on the other hand, shortens the QRS complex and increases the conduction velocity.

Form of the QRS Complex

Besides the area, the form of QRS is a very important indicator of the physiological events in the heart. The form may be analyzed with regard to the total duration, the polarity of QRS, i.e., the preponderance of positive (R) or negative (Q, S) deflections in the various leads, the maximal amplitudes of these deflections and the contour of the curve with respect to notches, polyphasic deformations, etc. It is not the purpose of this chapter to present a diagnostic guide, but we will try to explain the general rules governing these characteristics of the QRS.

1) The total duration of QRS is exclusively determined by the time the excitation wave takes to reach the most remote points of the heart. The very beginning and the very end of this process may happen in relatively small areas of the heart. So we know that the onset of Q is due to the activation of the papillary muscles and of the ventricular septum. There is no direct proof of this assumption, but we may conclude so from the direction of the heart vector during Q, which normally is directed cranially, slightly forward, and mostly to the left (7, 72). This agrees fairly well with the fact that the first fibers leaving the specific system run into the septum and the papillary muscles, both being activated in the direction mentioned. The last activated region is doubtless the posterior part of the base, as all latency measurements indicate (see section 8). Both portions of the heart are small, and their respective voltages low. Moreover, the momentary vectors of earliest Q and latest S do not project optimally on the same lead lines, so that beginning and end of QRS cannot be determined in one single lead: a simultaneous record of several leads with high power and high fidelity amplifiers is therefore necessary (111, 318). Quantitatively, however, these small initial or final events in QRS are of minor importance. We may therefore take the usual determinations of QRS duration (most commonly read from lead II) as its real duration. The question is how to interpret an increase in this duration.

From observations of the spread of excitation at the surface, we concluded that the excitation wave travels only over very short distances in a directly conducted manner (234, 412). If one assumes the conduction velocity of the myocardium to be of the order of magnitude of 1 m per sec or less, and the

length of the myocardial fibers over which an unbranched homogeneous wave is running to be about 10 mm or less, a simple calculation can be made, which is given in table 2 (58, p. 83). In this table we have tried to calculate the relation between heart weight and QRS duration, and to give at the same time a simple explanation for the observed magnitudes.[8] As the table shows, the QRS duration changes very little with heart weight, so that a fairly good correlation exists between QRS duration and the cube root of weight, as has been already claimed by Wilson & Hermann (525). The correlation with the sixth root of weight is even better. The reason is obvious: "hypertrophy" acts in the later stages of normal growth, as well as under pathological conditions, to augment fiber diameter, and not so much to augment fiber length. If this is correct, then every increase in the QRS duration does not indicate hypertrophy so much as an increase in conduction times. Two events lead to such an increase: the decrease of conduction velocity in either specific or regular myocardial fibers, and the block of those specific conduction pathways which provide the shortest pathways to different myocardial areas ("blocks" in the general sense). A decision may be made between these two possibilities by analyzing the direction of the heart vector. Every pure decrease in the conduction velocity would leave direction and the vector loop of the heart vector unchanged. If, however, the decrease were inhomogeneous, so that some parts of the heart were more involved in it than others, or if some pathways were blocked, the excitation wave of some fiber bundles would have to travel in the opposite direction from normal (fig. 44) and would arrive with a much higher latency. Changes in the vector direction combined with an increase in the QRS duration are due, in most cases, to blocks of the specific system or an otherwise induced inhomogeneous change of the conduction velocity.

The duration of QRS enables us to estimate the number of simultaneously active fibers. The total length of all myocardial fibers in the left ventricle alone amounts (in a normal heart weighing 130 g) to about 3.10^7 cm. The surface area of these fibers equals about 25 m^2 (326). The time of QRS during which a considerable number of fibers are active may

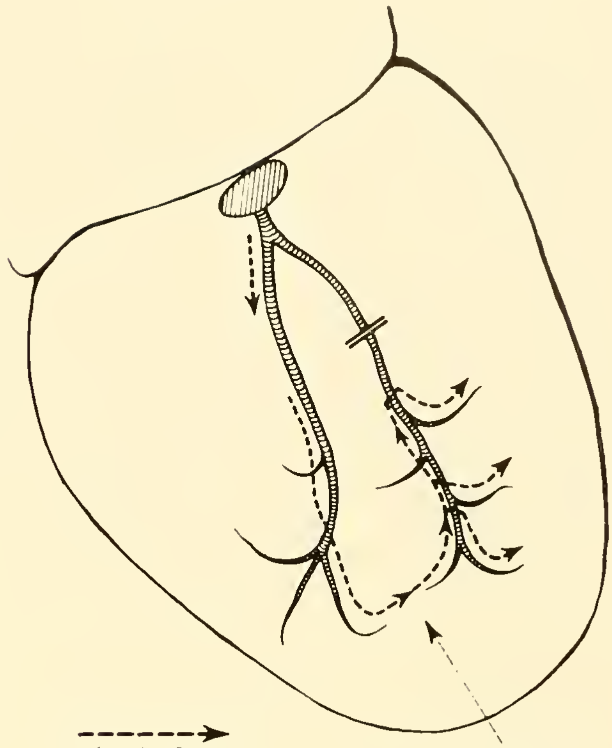

FIG. 44. Schematic drawing of the excitation pathway in a left bundle branch block. The direction of the excitation wave is inverted in the peripheral parts of the left branch, which is stimulated by a myocardial bridge, indicated by an arrow, from the right bundle. [From Schaefer (408).]

be listed as 50 msec. During this time the excitation can run over a myocardial fiber of only 5 cm in length. As 3.10^7 cm are excited, on the average, 6.10^6 fibers must be active at the same time. This number is too high for the rising and declining phases of R, and too low for the peak; and only the left ventricle is taken into account. In leads with parallel lead fields, it should be possible to calculate the absolute value of the voltage resulting from such data, and thereby the amount of mutual cancellation.

2) Changes in the vector direction can be induced by different processes: by changes in the preponderance, by changes in the direction of the excitation waves, by changes in the temporal excitation pattern of the various regions of the heart, and by changes in the anatomical position of the whole heart. The vector direction changes in all these cases, the momentary vectors as well as the vector of the QRS area. It is, therefore, of much value to be able to scan the vector directions swiftly and roughly. This is possible with the technique called "typology." Several

[8] If the myocardial conduction velocities were much less, e.g., about 0.55–0.70 m/sec, the estimated length of the myocardial fiber in table 2 would have to be reduced to about two-thirds of the values given. The principal results of table 2 remain valid, however.

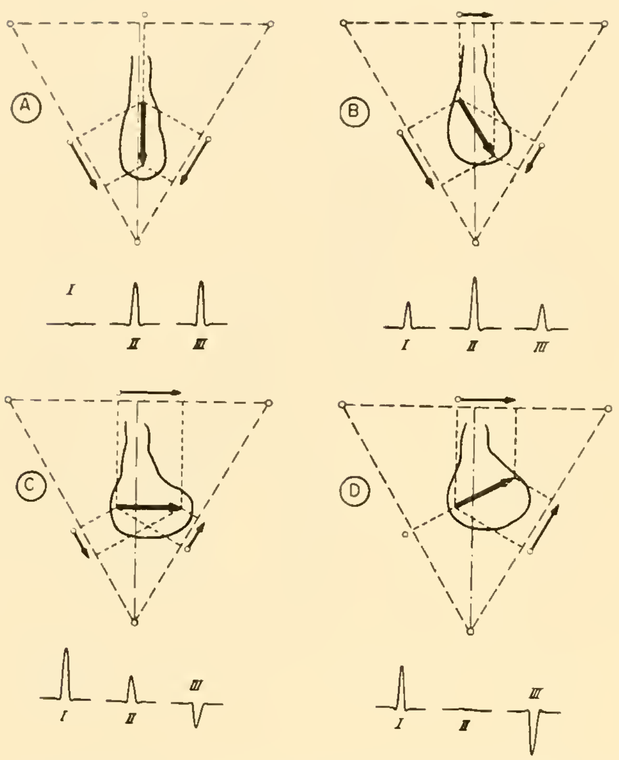

FIG. 45. Four types of vector direction of the QRS group with the respective pattern of QRS in the standard leads. [From Schaefer (58).]

formulas have been published (104, 424) for determining type in a rapid manner and describing it by an index. A rough estimation can be drawn by regarding the polarity of the main deflection in the three standard limb leads, if the typology is restricted to the frontal plane projections of the vector. The estimation of the Einthoven angle, therefore, seems to be nearly satisfactory. Figure 45 gives an idea of the appearance of such an analysis. The various mechanisms influencing the type are the following. A change in preponderance by hypertrophy augments the area at least a bit, mostly (in left hypertrophy) by augmenting the amplitude of the main deflection. A change in direction of the excitation waves always changes the area to a fairly large extent (extrasystoles, bundle branch blocks) and is always accompanied by a change in the temporal pattern. An isolated change in the latter occurs only in peripheral blocks (ramification blocks) and in a slowing of the conduction velocity. This changes the area as well; minimally in the ramification block, maximally in a reduced velocity of conduction. There is not a strict correlation between the "electrical axis" (i.e., the direction of the heart vector at its highest amplitude or of the vector of the area) and the anatomical axis (194). It is well known that the heart may rotate about its longitudinal axis, and rotations of this kind are not to be recognized in an X-ray picture. So, the relations between the two axes are fairly complicated (38).

3) The amplitude of the ECG depends among other things upon the amount of the "active cross section" (see section 7) of all fibers depolarized at a given moment, whereby the cancellation factor plays its most decisive role. The second most important factor in determining amplitude is the form of the lead field and the distance of the electrodes from the heart.

4) The contour of QRS in nearly all normal cases is smooth, and shows notching or slurring only if the record is taken with a high speed and high fidelity system (304). The reason is that propagation across the ventricular walls never passes immediately from a small to a large active cross section, or, in other words, that the number of fibers prevailing at a certain moment and producing the resultant vector increases and decreases in a continuous fashion, without abrupt changes in the amount of active tissue. This is the "normal" behavior. Notching of this type will occur only if relatively small amounts of the ventricular mass are involved in the disturbances, and single notches, now and then, lack all pathological significance (282).

The QRS complex is the result of a strong mutual cancellation. For this reason changes in conduction through even small parts of the ventricular mass lead to a marked distortion of QRS. Nevertheless, it is surprising that complete abolishment of the function of large areas, as in infarcts, may have comparatively little influence on the form and area of QRS! The QRS complex is much more an indicator of reduced conduction velocities in the specific system, or reversed directions of the spread of excitation, than of local destructions. The reason for this is not very clear, but it may be assumed that the cancellation effect takes place in between narrow limits, e.g., between the endocardial and epicardial surface of the heart, so that a complete destruction of parts of the heart does not lead to a "prevailing" of the intact remainder of the ventricles, which retains nearly all its cancellations as though normal. Only a different distribution of conduction through the specific system would alter the QRS complex decisively, as is the case with infarcts in which the specific system itself has been damaged. Summarizing we may conclude.

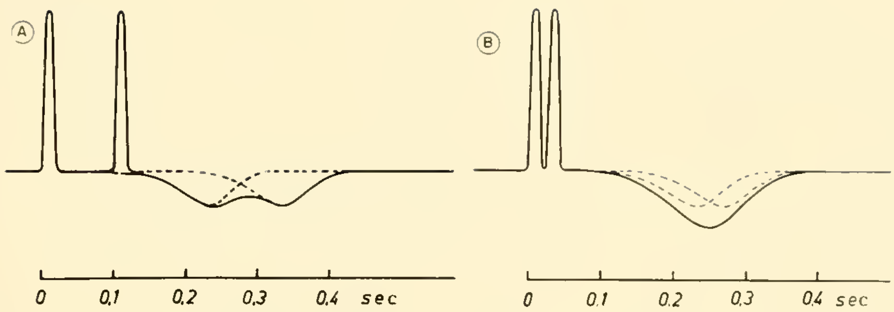

FIG. 46. The differences in the superposition of R and T of two single fibers. The desynchroniza tion of the fibers leads in both cases to a complete separation of R, whereas the T deflections are summed to a higher potential in case of short intervals (B), to a smooth cumulative curve in case of long intervals (A).

An augmentation of the QRS area may be caused by the following events: *1*) a diminution of cancellation by a reversal of excitation waves in certain parts of the heart (extrasystoles, blocks); *2*) slowing of conduction velocity; *3*) augmentation of all active cross sections of the muscular mass, i.e., a real hypertrophy.

An increase in the duration of QRS may be caused by *1*) an increase in heart weight and muscle mass; *2*) detours in the spread of excitation, with an inversion of direction in some parts of the heart; *3*) retardation of conduction velocity.

The direction of the heart vector and the type of QRS are changed by *1*) a local (not general) hypertrophy and a changed preponderance pattern of the myocardial fibers; *2*) changes in the temporal and/or spatial distribution of the excitatory processes of the single fibers; *3*) changes in the anatomical position of the whole heart.

General Principles Underlying Interpretation of the T Wave

The rules which govern the interpretation of T are completely different from those valid for QRS. The main reason is that the repolarization process is of such a long duration that shifts in the synchronization of various fibers have no influence on the form of T, whereas they have great influence on QRS. This may be exemplified as follows. In figure 46, the bipolarly recorded action potential of a very small bundle of muscle fibers is given, which shows the big differences in the time course R_i and T_i of a single fiber. If two fibers[9] were to depolarize a short time apart, the two R_i waves would be completely separated, resulting in a double-spiked potential; whereas the two T waves from these fibers would simply sum up to double their individual potentials. The T wave, therefore, does not reflect the degree of desynchronization of the various fibers. It is the result of a more or less complete superposition of all individual T_i potentials. Whereas the desynchronization of fibers increases mainly the duration of QRS, it increases mainly the (percentile) amplitude of T.

It may be of interest to have some more precise data in this respect. Let us assume that the total duration of QRST may be about 0.4 sec (the normal value for a heart rate of about 56/min, fig. 65). Then the QRS complex will have a normal duration of about 0.1 sec. This means that the earliest fiber starts its excitation with its R 0.099 sec earlier than the fiber of highest latency. The mean duration of the individual monophasic action potential therefore is $0.4 - 0.1 = 0.3$ sec. The T wave with its main, steep part has a duration of about 0.15, so that the peak of T in the earliest fiber is 0.05 sec later than the start of T in the latest fiber. Whereas the R spikes are separated by a long interval, the T waves overlap and form a smooth superposition (fig. 46). In reality, the interval between the R's in figure 46 are filled with the innumerable R_i's of the mass of the myocardium, but QRS in its form is an image of the desynchronization pattern, and T is not.

The cancellation of all individual fiber voltages remains true for T as well as for R. This means that the area of T would be reduced in the same manner as the area of QRS, if all fibers would behave homogeneously. The shape of the T wave thus reveals the pattern of repolarization of the uncancelled fibers.

If all monophasic action potentials were shorter, as their fibers approached the epicardial surface, a gradient of the repolarization velocity would exist of a quite uniform direction across the heart wall. As we found (234), the potential lasts longer, the nearer to the base it is recorded. Monophasic action

[9] The term "fiber" needs a brief definition: it is, in general, a short part of the semisyncytial structure of the heart, of a length of about 1–5 mm, through which the excitation wave usually runs unbranched, with a thoroughly homogeneous velocity of about 1 m/sec. At the cross-sectional circumference the fiber is limited by a "membrane" which gives rise to the usual resting and action potential.

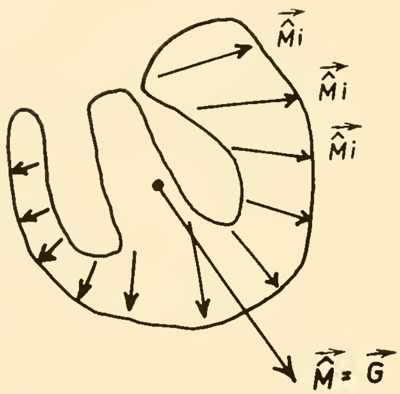

FIG. 47. Vectorial addition of the several $\overrightarrow{\widehat{M}}_i$ of fig. 40 to the ventricular gradient $\vec{G}$, which is the vectorial sum of all $\overrightarrow{\widehat{M}}_i$ originated along the single myocardial fibers, some of which are represented in the figure.

potentials at the two ends of any fiber must differ to a certain degree. In the dog heart we found that, even with very short bipolar electrode distances, the action potential recorded at the surface commonly does not have a total time-voltage area which equals zero. The area of T_i is always opposite to R, but in general a bit smaller than the area of R_i, and the quotient $Q = |\widehat{T}_i/\widehat{R}_i|$ generally is 0.85 (234). This points to the fact that inhomogeneities of repolarization occur within very small distances all over the heart's surface and most probably as well all over the ventricular walls. If, as figure 47 shows, these inhomogeneities are represented by the value of $\overrightarrow{\widehat{M}}_i$ (the area of individual fibers), all vectors $\overrightarrow{\widehat{M}}_i$ add to the resultant vector $\overrightarrow{\widehat{M}}$, the ventricular gradient, but without cancellation of such a degree as was found in QRS. This is the reason why even slight differences in local forms of monophasic action potentials of repolarization lead to remarkable values for the ventricular gradient. Or, in other words, the T wave is some kind of a special detector for differences in repolarization of the various parts of the ventricles.

There is an indirect but rather conclusive proof that differences in the action potential pattern are responsible for the gradient: every increase in frequency diminishes the differences in action potential area of different fibers (489), and correspondingly the ventricular gradient is considerably reduced by rising heart rates (86). Concerning quantitative differences between action potentials, we may give some examples. If the areas of the two monophasic action potentials differ by about 4 per cent, and the

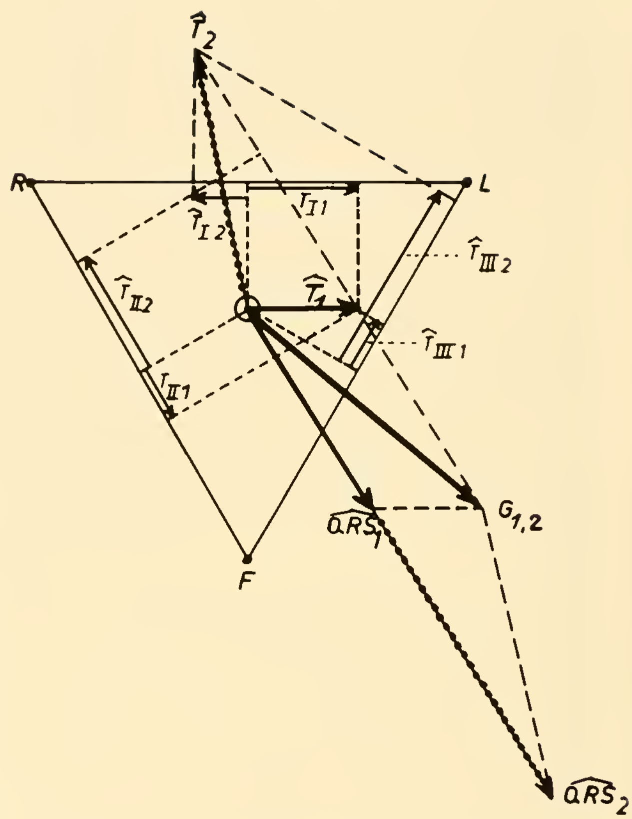

FIG. 48. The vectorial analysis of QRS and T areas and the ventricular gradient in the Einthoven triangle, under the assumption that the area of QRS is doubled for some reason, whereas the gradient remains constant. Doubling of $\widehat{QRS}$ induces not only a marked increase of $\widehat{T}$, but at the same time a shift in the direction of the $\widehat{T}$ vector. (The vectors with doubled $\widehat{QRS}$ are marked with dots.)

number of fibers not involved in mutual cancellation of R_i were of the degree mentioned above, namely 1:25 or 4 per cent, the ventricular gradient would have the same time-voltage area as QRS. This seems to be true for the human heart. Very small alterations in repolarization can cause big percentile changes of T.

As the area of T depends, among other things, upon the area of QRS, every increase of $\widehat{QRS}$ leads to a marked change in the $\widehat{T}$ vector, and therefore in its polarity in some leads. This may be illustrated by figure 48, where QRS is doubled in area, which involves a doubling of the "individual" $\widehat{T}$ and, if all inhomogeneities remain constant, the resulting $\overrightarrow{\widehat{T}}$ changes its position from an Einthoven angle α of $5°$ to $-110°$, so that the T wave in leads I and II becomes negative. Such an inversion of T does not

indicate more than the change in QRS indicates, and of course is no sign of abnormal myocardial processes. In extrasystoles (216), in the WPW syndrome (105) and bundle branch blocks (365), G may remain normal, indicating that changes of T are only conditioned by the changes of QRS. Where repolarization is distorted by refractoriness (in premature beats and some extrasystoles) G will change (484).

Only changes of T without concomitant changes of QRS, therefore, bring about primary alterations of the ventricular gradient ultimately due to mechanisms which influence the inhomogeneities of repolarization. As has been pointed out before, a dilatation of the heart could reduce the inhomogeneities by equalizing all mechanical and thermal differences between the various parts of the heart. The movements of the heart (elevations and rotations) are certainly reduced as well, when the heart is enlarged. This will lead to a flattening of T and a reduction of the ventricular gradient. The most important changes of T, however, are caused by new inhomogeneities in the monophasic action potentials which change the direction of $\vec{G}_s$, and increase its numerical value in most cases. Such changes are induced mostly by "local" events, which alone lead to an inhomogeneous behavior of the muscle cells. Therefore local metabolic differences, caused by local ischemic damage, local inflammation, etc., are the important reasons for strong alterations of the magnitude and the direction of $\overset{\approx}{T}$.

A peculiar cause of a diminished ventricular gradient is the loss of the plateau (ST interval), which itself has to be ascribed to disturbances of the ionic exchange, especially to an accumulation of potassium in the extracellular space. In such cases, the records show constant decline in voltage during the whole repolarization, every difference between action potentials and plateaus of different fibers being reduced. Such a loss of plateau always leads to a change in the contour of T. The T wave becomes a small, long lasting, and (in the case of a linear decline of the action potential) constant, negative deflection starting at the end of S. In such cases, it is very difficult to find a correct line of reference. The determination of the T area therefore becomes erroneous.

Summarizing, it becomes clear that T and the ventricular gradient respond most strongly to local changes or damage, since only these induce an augmentation or change in the inhomogeneities of the repolarization. If, therefore, a previously local area of damage spreads and becomes generalized, the ECG may look more normal than before, in spite of an impaired heart (41).

10. DESCRIPTION OF THE PQRS PART

Any attempt to describe the normal ECG meets with two difficulties: defining "normality" and selecting methods of description which present all information contained in the ECG in the shortest, but nevertheless most comprehensive, form.

The form of the ECG varies considerably from person to person and even in the same person during the day. The reason is that functional differences in the spread of excitation, the local excitation process, and the inhomogeneity of repolarization (because of differences in the autonomic innervation) exist. The strongly diverging excitation waves cancel their respective fields to such a degree that even small individual differences or small changes in the spread of excitation lead to large differences in the potential pattern. In addition, differences in the anatomical properties of the thoracic surface, conductivity distribution, heart position, etc., lead to a great variety in the form of the lead fields, the direction and magnitude of the lead vectors, and the magnitude and direction of the heart vector itself. Individual variability, therefore, is very large, and a single normal form does not exist. We do not even know its borderlines (449, 454), because "normality" obviously can be defined only from the point of view of the heart's function or anatomical structure, which cannot both be judged in all cases. Moreover, the separation of disturbances in the peripheral circulation from those of the heart is frequently somewhat intricate. As a matter of fact, it is not unusual to find an ECG pattern which we are accustomed to regard as abnormal in apparently healthy and even young persons (452, 502).

A reliable presentation of electrocardiographic data can avoid a tiring enumeration of facts only by presenting the electrical events of the heart in their simplest form: as the temporal change of the heart vector, recorded as the "vector loop."

The vectors and the vector loop are nevertheless insufficient to interpret in an easily understandable manner all information available in the ECG. All details concerning the time course are more concealed than disclosed in vector loops, even when time marks are given. As the spread of excitation is the most important physiological event in the heart,

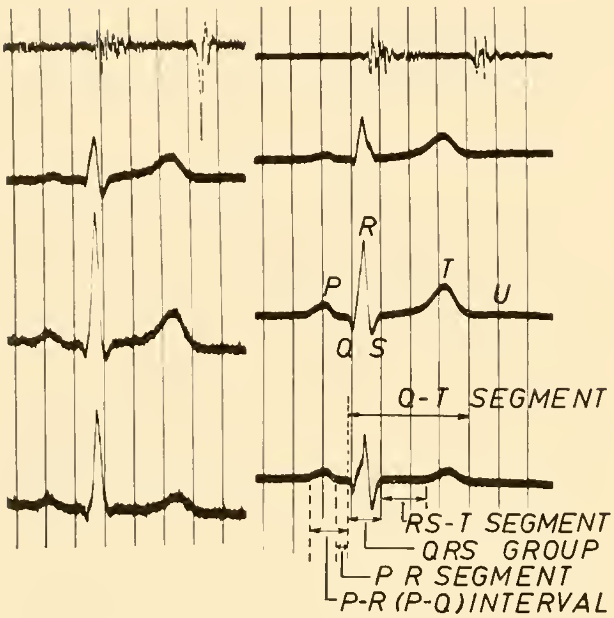

FIG. 49 Two normal ECG in standard leads. *Upper row*: heart sounds. *Time marks*: 0.1 sec.

and as it is reflected predominantly (though not exclusively) in the time course of the ECG, a description of voltages as a function of time is still one of the most important things electrocardiography can supply. This is the main reason why some authors are so reluctant to ascribe great clinical value to the vectorcardiogram (7). Also, the ventricular gradient is not directly represented in the vector loop. The same is true for all proximity potentials, because the vector loop has a physical meaning only in the absence of such potentials. We therefore need a double analysis of the ECG: by the conventional curves and by their vectorial counterpart.

Nomenclature (529)

A normal ECG curve taken from a conventional (standard) extremity or Einthoven lead is given in figure 49. The sequence of deflections was named by Einthoven with the symbols P, Q, R, S, T, U. Some of these deflections are combined in groups or complexes: the QRST group, the QRS complex. Parts of the curve are called "segments," e.g., PQ segment, ST segment, counting from the end of P to the beginning of QRS or from the end of S to the beginning of T. Special difficulty lies in the identification of the QRS deflections. The current use is merely a descriptive nomenclature, in which the first sharp, downward deflection after the P wave (if followed by an upward deflection) is labeled Q, the first upward deflection is R, the second downward, S. If there is only one downward deflection, it is labeled QS. If more than the Q, R, and S deflections are present, the upward deflection following S is labeled R′, a downward deflection following R′ is S′ (if necessary, R″ and S″ may follow). If one of the deflections is comparatively small, it is sometimes written with a small letter. For example, rS means that a small positive deflection is followed by a large negative one. The normal pattern in extremity leads, then, is qRs. The P wave of atrial depolarization is occasionally followed by an opposite polarity, low-voltage, and long-lasting wave; the repolarization wave of the atria, clearly distinguishable from QRS only in cases of complete A-V block. It is labeled Tp. If necessary, a polyphasic P wave may be subdivided into Qp, Rp, Sp, R′p, S′p. This, however, will be practically restricted to atrial esophageal leads.

A peculiar difficulty is sometimes met in the determination of the zero line or level of reference. Since, in the majority of ECG tracings, the QRS complex is superimposed on the Tp or Ta deflection, the best level of reference for QRS is the level at the beginning of the first of its deflections. For the ST segment however, this "zero" level may be wrong. There is no correct procedure applicable in all cases. The best reference point, recommended by the international societies, is the level at the beginning of QRS for the determination of the ST junction (i.e., the point where S ends and the steep deflection is replaced more or less abruptly by the more gradual slope which precedes the first limb of T). For the ST segment, the best reference line is the isoelectric level T-P or U-P, when this can be determined. But often a persisting U wave is superimposed on the beginning of P. In this case, the beginning of QRS is the best (though not unquestionably correct) zero level.

A special nomenclature has been adopted to describe the various vectors of the ECG. Whenever the vectors are measured in space, they carry the index s: $\overrightarrow{QRS_s}$, $\overrightarrow{T_s}$. If their time-voltage areas are concerned, the symbol A_{QRS} or A_T is sometimes used, and if observed in space, the index s is added. In some papers (as in this chapter) the area is indicated by the symbol $\widehat{QRS}$ or $\widehat{T}$, with s as index in case of spatial values. If the areas are measured in a plane, the indices f for frontal, h for horizontal, and sa for sagittal are used here: $\widehat{QRS}_f$, e.g., means time-voltage area of QRS, taken as frontal projection of its vector. The ventricular gradient is marked with

TABLE 3.* *Normal Adults, 20 Years Old and Over, Supine*†

Lead	P				Q				R				S				RS or QR				S-T				T			
	No. Cases	Min	Max	Mean	No. Cases	Min	Max	Mean	No. Cases	Min	Max	Mean	No. Cases	Min	Max	Mean	No. Cases	Min	Max	Mean	No. Cases	Min	Max	Mean	No. Cases	Min	Max	Mean
I	475	0	2.5	0.69	505	0	2.0	0.27	505	0.7	19.4	5.51	505	0	6.4	1.27	63	3.0	20.6	8.54	100	−0.3	0.9	0.11	505	−0.5	5.6	2.20
II	475	0	3.0	1.07	505	0	4.0	0.38	505	0.5	28.0	9.41	505	0	8.2	1.36	63	8.0	32.0	15.14	100	−1.0	1.0	0.21	505	0	8.0	2.67
III	475	−0.8	2.0	0.56	505	0	4.0	0.48	505	0	22.0	5.56	505	0	13.0	1.29	63	3.2	25.0	10.62	100	−0.6	0.8	0.04	505	−2.0	5.5	0.77
V_R	32	−1.0	−0.5	−0.63	62	0	8.0	2.48	62	0	3.0	0.90	62	0	11.0	3.01	62	3.5	12.0	6.50	32	0	0	0	62	−4.0	−0.5	−1.65
V_L	32	−0.5	0.5	0.07	62	0	1.5	0.16	62	0	7.0	1.21	62	0	7.0	2.04	62	0.5	8.5	3.37	32	0	0	0	62	−1.0	1.5	0.29
V_F	32	0	2.0	0.72	62	0	2.0	0.30	62	0	15.0	6.82	62	0	6.5	0.74	62	3.5	16.5	7.77	32	0	0	0	62	0	4.6	1.40
aV_R	411	−1.5	−0.1	−0.79	552	0	16.8	2.38	552	0	4.1	0.94	552	0	15.7	3.76									479	−5.5	−0.2	−2.40
aV_L	411	−1.0	1.4	0.51	552	0	3.5	0.27	552	0	10.1	2.61	552	0	11.3	1.35									479	−4.0	6.6	0.78
aV_F	411	−1.8	1.7	0.74	552	0	3.0	0.38	552	0	20.0	4.73	552	0	7.1	0.81									479	−0.6	5.2	1.85
V_1	371	−1.1	2.2	0.57	567	0	0	0	567	0	15.5	3.09	567	0.8	26.2	9.44	63	6.6	35.0	14.99	33	0	0.5	0.01	542	−4.0	12.2	0.84
V_2	371	−0.7	2.0	0.60	594	0	0	0	594	0	23.0	5.96	594	0	39.2	14.09	63	13.0	55.0	26.82	33	0	1.0	0.09	542	−2.6	18.0	4.70
V_3	371	−0.5	2.0	0.61	567	0	1.5	0.01	567	0.7	54.6	8.93	567	0	27.5	9.51	63	11.1	54.6	24.12	33	0	2.0	0.20	542	−2.0	21.0	5.16
V_4	371	−0.2	2.3	0.60	594	0	4.0	0.13	594	1.8	46.0	13.78	594	0	28.8	5.93	63	9.0	51.6	26.16	33	0	1.0	0.03	542	−0.5	17.0	5.06
V_5	371	0	2.4	0.56	567	0	3.4	0.43	567	0.4	33.6	12.01	567	0	16.1	1.96	63	10.0	36.4	19.31	33	0	0	0	542	0	11.0	3.83
V_6	371	0	1.8	0.54	564	0	2.7	0.44	564	2.0	22.6	9.68	564	0	14.3	1.00	33	7.0	24.5	13.93	33	0	0	0	512	0	6.9	2.80

* This table is taken from *Nomenclature and Criteria for Diagnosis of Diseases of the Heart and Blood Vessels*, fifth edition, published by the New York Heart Association. It is based on normal series studied by Kossmann & Johnston; Kossmann & Goldberg; Wilson & Nyboer; Vaquero, Limón & Limón; Deeds & Barnes; Myers, Klein, Stofer & Hiratzka; Sokolow & Friedlander; Kneese de Melo. [Reprinted from Kossmann (297).]

† Size of the electrocardiographic deflections in the bipolar extremity, augmented unipolar extremity, and unipolar precordial leads, is given in tenths of a millivolt.

G. It is always a time-voltage integral, *per definitionem*. It is indicated by f, h, sa, s in the same manner as $\widehat{QRS}$ or $\widehat{T}$.

The Normal P Wave (54, 77, 297, 374)

The P wave corresponds to atrial activation and is very small in the standard surface leads, where the amplitude seldom exceeds 0.1 mv and never is higher than 0.5 mv in normal hearts (table 3). In orthogonal leads, P is maximal along the y axis (on the average 0.11 mv with a maximum of 0.24 mv) (399). The reason is obvious: the muscle mass of the auricles is too small to produce a very strong electric field. This is even more the case with the sinus region, from which the directly recorded monophasic action potentials are well known (see preceding chapter), whereas the ECG most probably never contains any sign of the sinus action. In high amplifications and high fidelity records a very low initial portion of P may be ascribed to the sinus (473), but this assumption seems at least uncertain. The amplitude of P is maximal in the standard extremity lead II; the resultant vector of the atrial fibers coincides therefore more or less with the anatomical axis of the heart as a result of the symmetrical structure of both atria. The oblique position of the heart under these circumstances leads to the fact that the right atrium is activated in a preferably craniocaudal direction, the left in a right-to-left direction, as has been observed in man (517). The vector of P (193, 401) runs in the horizontal projection from the back to the front, with an azimuthal angle (after fig. 58) of

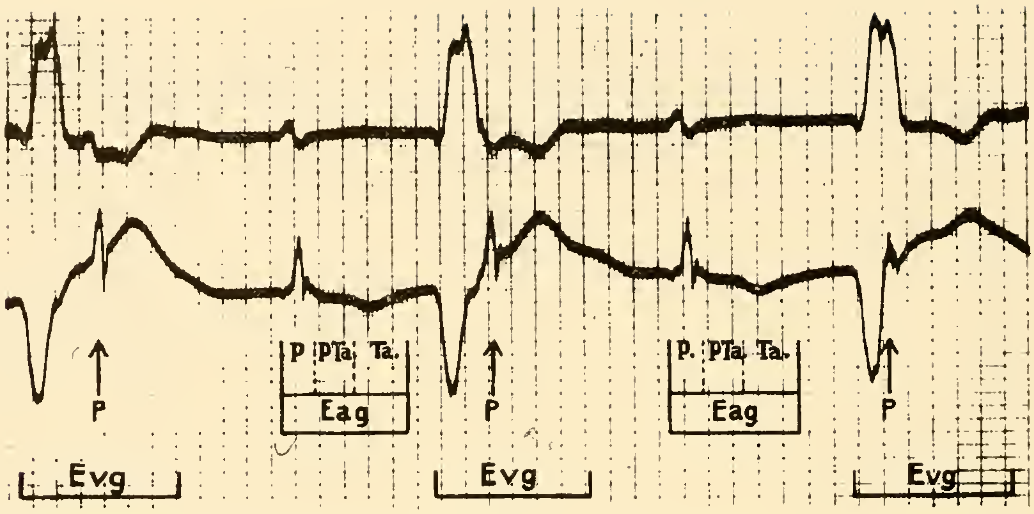

FIG. 50. Demonstration of the atrial T (T_a) in a case with complete A-V block. *Eag:* electroatriogram. *Evg:* electroventriculogram. [From Holzmann (34).]

about 45°; in the frontal plane it has an angle α varying in wide limits between 0° and 80° (366), and lies in the majority of cases at about 60° (541). In the sagittal plane it has an elevation of 70 to 80° measured in a clockwise rotation from the right end of the z axis, looking at the sagittal plane from the right side of the erect subject (193, 497). The vector has a relatively constant direction during the whole atrial systole, but shows a rounded contour of its frontal vector loop projection in most cases of a left atrial hypertrophy (108).

The duration of P depends on both the distance of the most remote auricular point from the sinus node and the conduction velocity. The total duration of P is maximal in leads deriving the y axis (0.096 sec), and shorter along the x and z axis (0.079 and 0.072, respectively) (374). In an isolated auricle, the conduction time is increased by stretching the muscle fibers, most probably by lengthening the conduction path (258). In left atrial enlargement, the P wave is also prolonged over the normal value of 0.1 sec ("mitral" P). It is always slightly notched especially in cases of dilated left atria. In right atrial enlargement the P wave is often tall and sharply pointed, but there are frequent exceptions of these rules. The mitral P may be due at least in some cases to a left atrial hypertrophy, whereas the tall pointed P is most frequently found in pulmonary heart disease ("P pulmonale"). It is very important in regard to the theory behind the ECG that the explanation for these facts is uncertain. We may assume that strong dilatations or hypertrophy in mitral defects may favor an atrial hypertrophy with a prolonged conduction time, so that the area of P is increased.

In the normal ECG, the atrial complex is largely obscured by ventricular activation. There are two possibilities for separation of atrial and ventricular potentials: by putting electrodes on or near the atrial surface (e.g., by esophageal leads), whereby the atrial component of the ECG is augmented, the ventricular part, however, is by no means reduced; and by observing the isolated atrial activity in atrioventricular block. We obtained our precise knowledge of the whole atrial complex from observations with block (fig. 50). It became clear that the P wave is followed by Tp (or Ta). This Tp is always opposite to P, so that the "atrial gradient," an analogue of the ventricular gradient, is always small if not zero and averages 2 μv sec (106), whereas the area of P alone is about 4 μvsec (155). There is, in other words, only a small inhomogeneity, if any, in atrial repolarization, since these small gradients may perhaps be explained by a shift in the atrial position during atrial systole.

The monophasic action potential of atrial fibers has no, or only a very short, "plateau." Correspondingly, Tp develops directly after P, without an isoelectric interval. This means that QRS is always superimposed on Tp, and that the PQ interval cannot be strictly isoelectric (210, 232). The larger P, the deeper the PQ displacement (423).

The QRS Complex

The main part of the spread of excitation is preceded by the activation of the septal and papillary regions, which causes the very first vectors of the ventricular activation to go upward and sometimes to the right, or, more often, to the left, so that standard

leads I and II start with negative deflections, the Q waves, or directly with R. In the frontal plane, the normal form of QRS never shows a deep Q in any lead. This means that the heart vector, as long as it runs in an upward direction, never develops a high voltage. If a deep Q is found, the differentiation between normal and abnormal still offers considerable difficulties (225, 338), but if Q_{III} is very deep, the spread of excitation may be regarded as abnormal. By experience, it is known that posterior wall infarcts and coronary sclerosis are the usual conditions causing a deep Q_{III} (Pardee-Q). The limit is usually defined thus: Q should not exceed one-fourth of the highest R wave. A deep S wave, however, is very common and apparently without clinical significance (192). An S in all leads points to late activation of comparative large muscle masses in the posterior portion of the base (fig. 51). Only if S is extremely deep and prevailing in all leads, the probability is very high that the heart is abnormal (263, 267, 503).

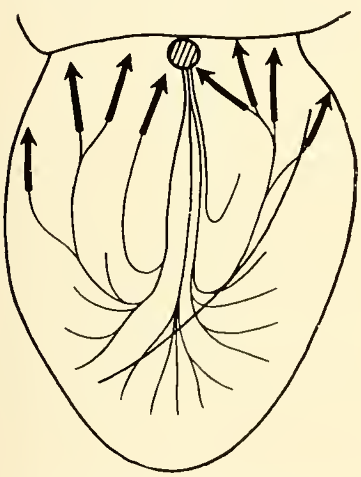

FIG. 51. Schematic drawing of the excitation waves producing the S deflection. These waves occur in the last-activated parts of the ventricular base. [From Schaefer (58).]

The Einthoven extremity leads record the projections of the heart vector on lead lines in the frontal plane only. Wilson for the first time introduced leads into electrocardiography which should be able to detect the projections of the heart vector on a horizontal plane, the unipolar precordial leads (fig. 52). The electrode positions he chose are by no means the best, because records from them contain fairly high proximity potentials which are, however, too small to give detailed information about local events. The position of the electrodes was pictured in figures 26 and 27. The records are not uniform but resemble each other in different persons much more than do the extremity leads. The rule is that in V_I the rS pattern prevails and that the R becomes larger and dominates more and more as the electrode is shifted to the left. There is a "transitional zone" usually between V_3 and V_5, around the apex region, where the positive and negative deflections are nearly equal. After V_5, the deflection is converted into a predominantly positive one. V_6 resembles, more or less, lead I, since they have in common the horizontal position of the lead vector. A quantitative description of the relative voltages in the precordial leads is given in figure 53. The average values are listed in table 3. The S deflection indicates that, at that instant, most of the "active cross section" is activated in a direction away from the electrode.

The normal values for amplitude, form, vector position, and duration of QRS vary within wide limits. Table 3 shows the averages to be expected in normal hearts. Figures like these, however, are of a restricted value, because the combination of certain values for Q, R, and S characterize the ECG, and this cannot be taken from such tables. We therefore

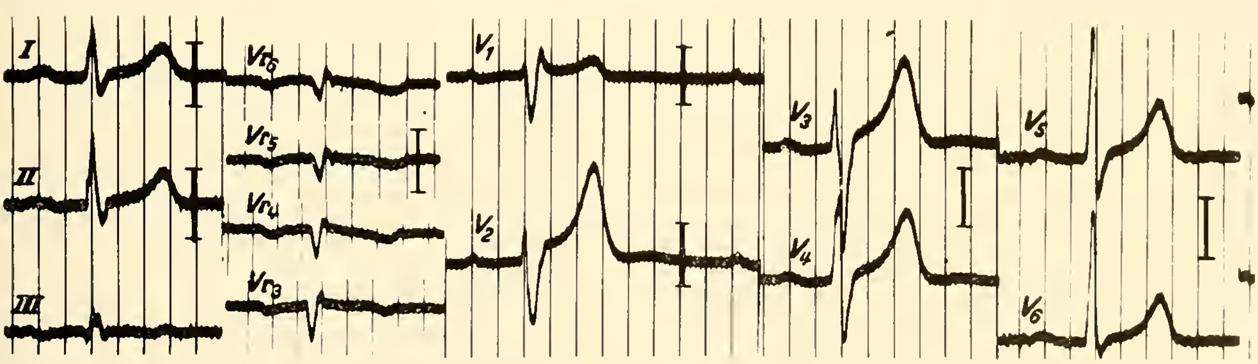

FIG. 52. Normal chest leads. V_{r6}–V_{r3} are included. The calibration shows 1 mv. To the left are the standard leads.

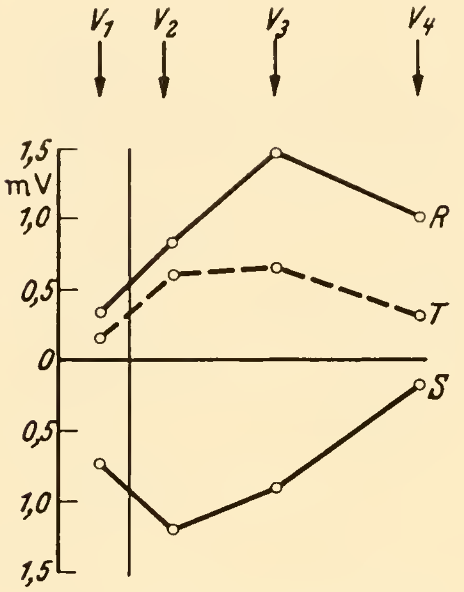

FIG. 53. The potential distribution of the R, S, and T deflections in the Wilson precordial leads V_1–V_4, in 100 normal persons. [From Holzmann (34).]

consider it more useful to give the vectorial data for QRS. The total duration of QRS should not exceed 0.1 sec in one of the leads. Yet it makes a difference whether QRS shows a tall, narrow R with low but broad Q or S waves, or whether the main deflection is itself broadened. Only in the latter case could a deviation from normal be assumed if borderline values for the total duration are found. The duration of QRS depends, as do all durations in the ECG, upon the heart rate. Figure 54 gives the relationships. These values are valid for the extremity lead with the longest duration of the respective deflection. [For details of the major literature see the textbook by Lepeschkin (47). For the most important collections of normal data see the following references (47, 79, 83, 154, 230, 246, 297, 350, 364, 448, 449).] A survey of the most important electrocardiographic data is given in table 4.

Vectorial analysis of QRS can be properly done only by recording the vector loop. Nevertheless, many attempts are made to interpret conventional ECG tracings as vectorial data. The simplest procedure is to estimate the sector in which the vector of a deflection lies, by comparing the direction and magnitude of this deflection in several different leads (221, 540, 541). In some respects, the typological index (see section 9) belongs among these methods. If, however, more than one vector is determined, the procedure is quite arbitrary. One could, of

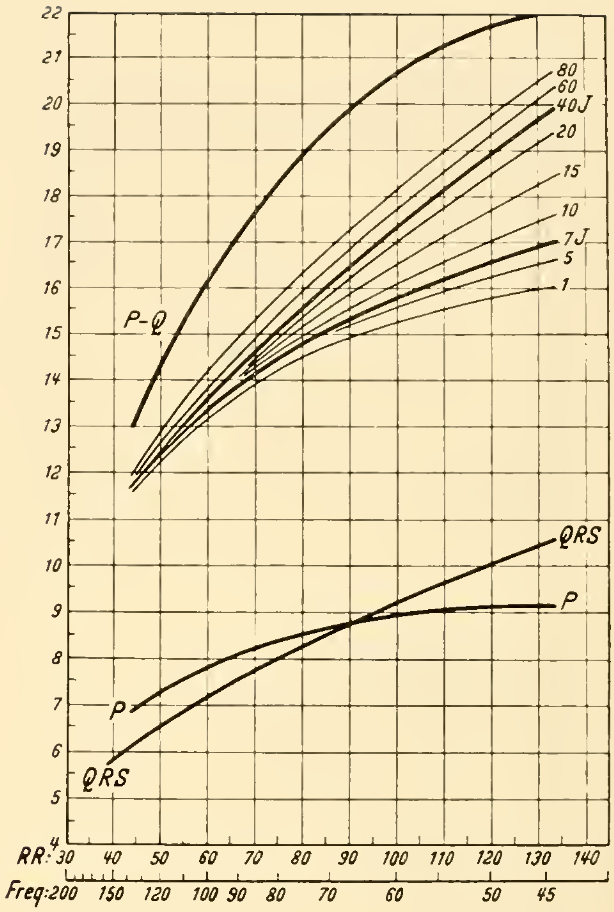

FIG. 54. Relation between heart rate (*abscissa*) and duration of P, P-Q interval, and QRS. The upper curve represents the upper normal limit of the P-Q interval, below this line the average values in different age groups. *Ordinate* in 1/100 sec. The data are based on a small series and may not be reliable. [From Lepeschkin (46).]

course, determine a vector of Q or of a small S. The peaks of Q or S, however, are the random result of a rotating heart vector, which projects itself on every lead vector at a certain instance with a maximal voltage. Such vectors Q or S are distinguished from any vector position only by the choice of the lead in which by chance the deflection appears to be maximal. The range of the angles that such Q and S vectors reveal is therefore very large (366) and apparently without any physiological meaning. The direction of the main deflection (R), however, shows a very regular behavior. The axis of R or electrical axis shows a migration with increase in age. In the frontal projection, it migrates from a value (α) of $+100°$ to $+0°$ between birth and the age of 60 years. In the horizontal plane, the direction of R migrates from 50° to 130°, i.e., from an anterior to a posterior

TABLE 4. *Mean Durations and Standard Deviations of the Normal Orthogonal Electrocardiogram**

	No. of Persons	Mean, sec	Standard Error, sec	Range, sec
1. Total P wave duration	133	0.102±0.013	0.001	0.068–0.141
2. P-R (P-Q) interval	133	0.135±0.024	0.002	0.101–0.211
3. P-R segment (end P — beginning QRS)	133	0.047±0.017	0.001	0.010–0.093
3. Q-T duration	133	0.367±0.028	0.002	0.283–0.444
4. Q-T duration corrected†	133	0.41±0.027	0.002	0.34–0.52
5. QRS duration	100	0.093±0.01	0.001	0.074–0.113

* Recorded with the SVEC III system (see fig. 21). [Data from Pipberger & Tanenbaum (374) and Pipberger (368).]

† Corrected Q-T duration was calculated by dividing the actual Q-T duration by the square root of the preceding P-R interval.

direction (angles in fig. 58). The T vector (frontal) shows a completely different form of migration, starting with 0° value (α), and after having reached 60° the vector turns back again and ends at the position 0° at the age of 60 years. In the horizontal plane, the vector starts with 120° and turns to the front, reaching 50° at the age of 60 years (497). With healthy persons between the age of 30 and 50 years, the main QRS axis in 97 per cent of cases has been found to be between 0° and 90° (α), with an average of 43° (310) or 47° (357). The magnitude of the angles α is distributed on a Gauss probability curve with the mean both for QRS and T angles for all groups of people between the ages of 5 and 50 at the same angle of about 45° (538). However, with another method to be described immediately, a shift to a more horizontal position of the vector in the course of age is apparent (498).

This other method for calculating vector positions in a fairly simple manner involves determining the so-called "null contour" of potential distribution at the surface of the thorax (34, 228). The procedure of such determinations is as follows: one observes a unipolar ECG at various points on the thorax, and locates certain electrode positions at which the recorded time-voltage area is minimal. One connects these points and thus gets a "transitional zone," on one side of which the polarity of the main deflection of the ECG is reversed as compared to the other. This zone in most cases has an elliptic form. This ellipse

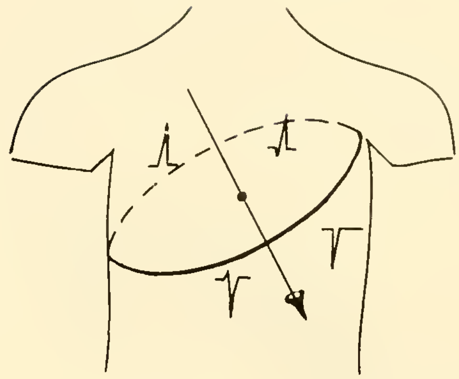

FIG. 55. Illustration of the null-contour method to determine the direction of a vector in space. The plane is determined which separates the predominantly positive from the negative QRS groups. The vector stands perpendicular to this plane.

can be regarded as a plane of zero potential though the thorax to which the vector QRS is perpendicular (fig. 55). The error in this method is rather high, as observed with a cylindrical model (205). This is not surprising, because in such observations the distortion of the electrical field exerts its greatest effect. Nevertheless, the "null-contour method" is not much inferior to determinations of the heart vector with conventional leads, without the lead vector correction.

The theory of the null contour is closely correlated to the potential distribution at the surface of the thorax. This may be seen in figure 56, in which the intersection of the null contour plane with a horizontal cross section of the thorax is shown and the isopotential lines are drawn in a somewhat arbitrary manner. The potential distribution is, of course, the result of the distorted field. In an ideal field, the source and sink of the surface potential distribution would never lie so close together. Such fields lead to gross misinterpretations in the position of a heart vector by assuming it to be derived from parallel homogeneous lead fields.

The vectors of the QRS areas can be determined, of course, with every corrected lead system. Their spatial values are listed in tables 5 and 6. We should admit however, that the vectorial presentation of the time-voltage areas has only a restricted physiological meaning, insofar as QRS is concerned. The areas integrate the whole spread of excitation to an average direction of momentary vectors and thereby conceal even the limited information given by the vector loop. The very purpose of such time-voltage integrations can only be to have a better understanding of how T is generated. The method which best presents

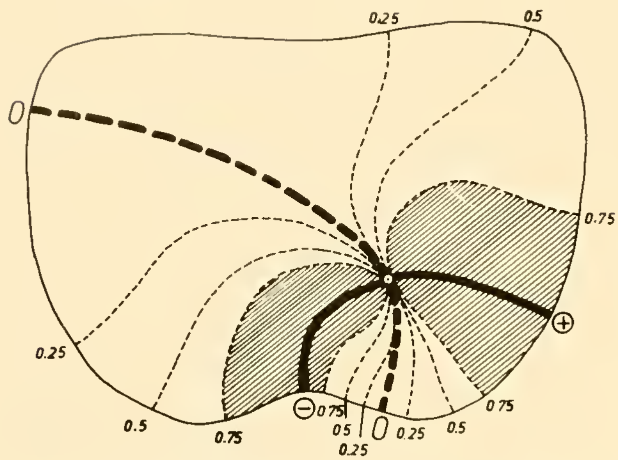

FIG. 56. Potential distribution in the cross section of a thorax, calculated from the surface time-voltage areas of QRS of normal hearts. The figures indicate the amount of time-voltage area as fractions of the maximal area, recorded with unipolar electrodes at given points on the thoracic circumference. The null line is strongly curved. The shaded parts show those areas which contain relatively high voltages. [From Böckh & Schaefer (118).]

TABLE 5. *Spatial, Azimuthal, and Elevational Angles of QRS and T Areas, and Ventricular Gradient**

Item	Azimuth		Elevation		Magnitude, μvsec	
	Mean	SD	Mean	SD	Mean	SD
			areas			
QRS	118	19.10	31.6	13.04	43	21.8
T	43	15.04	54.9	17.69	68	43.4
Ventricular gradient	66	17.90	36.2	15.50	97	62

* Measured according to fig. 58*D*. Magnitudes are given in microvolt-sec. The group of 18 normal young men is rather small, but no larger series is available in the literature. [From Simonson *et al.* (459).]

all information to be gained from a vectorial analysis doubtlessly is the record of the vector loop.

The Vector Loop

The vector loop (4, 7, 12, 15, 25, 28, 35, 37, 59, 72, 109, 247, 385, 386) does not reveal any new information which could not be gained by detailed analysis of conventional ECG records, but it does present such information in a plastic three-dimensional and illustrative form. The main handicap for clinical application of vector loops is the fact that the empirical foundation for interpretation is still rather small.

TECHNICAL REMARKS. The practice of vectorcardiography, starting with graphical constructions of vectors by Einthoven (183) and later by Mann (332) (who called such constructions "monocardiograms"), soon abandoned these rather complicated procedures. Schellong (59) and, at nearly the same time, Sulzer & Duchosal (475) developed a technique of recording the vector directly in its projection on a plane. If one takes bipolar or unipolar leads, the vectors of which stand perpendicular to each other, but lie in the same plane, and connects these leads to two pairs of plates in a cathode-ray tube, the spot of the oscilloscope follows a curve which describes the time shift in position of the vector peaks relative to the zero point (fig. 57). This curve may be regarded as the chronological summation of all vector peaks during the movement of the heart vector. If this vector loop is timed, e.g., by interruptions of the recording electron beam, the conventional ECG could be reconstructed as a voltage vs. time record, because the projection laws still hold and it is permissable to apply them in this manner. In recording the loop, a certain difficulty arises in fixing the sense

TABLE 6. *Statistics of Magnitude and Direction of the Frontal Projections of QRS Areas (A_{QRS}) and Ventricular Gradient (after Ashman)*

Vector	Subjects, Age, Years	No., Sex	Size, μv sec			Direction, Degrees (Einthoven's Angle α)		
			Mean ($\bar{x}$)	SD (S_x)	Range ($\bar{x} \pm 2S_x$)	Mean ($\bar{x}$)	SD (S_x)	Range ($\bar{x} \pm 2S_x$)
A_{QRS}	Adults 15–50	80 M	21.8	10.3	1.2–42.4	41.7*	31.6	−21.5–104.9
		84 F	22.0	8.5	5.0–39.0			
	Children 2–14	35 M, 43 F	16.6			61.1	20.5	20.1–102.1
Ventricular gradient	Adults 15–50	80 M	47.1	18.1	10.9–83.3	44.8	18.7	7.4–82.2
		84 F	45.4	14.7	16.0–74.8	33.8	18.3	−2.8–70.4
	Children 2–14	38 M, 43 F	46.4	14.9	16.6–76.2	48.0	12.5	23.0–73.0

[From Kossmann (297).] * 157 adults only.

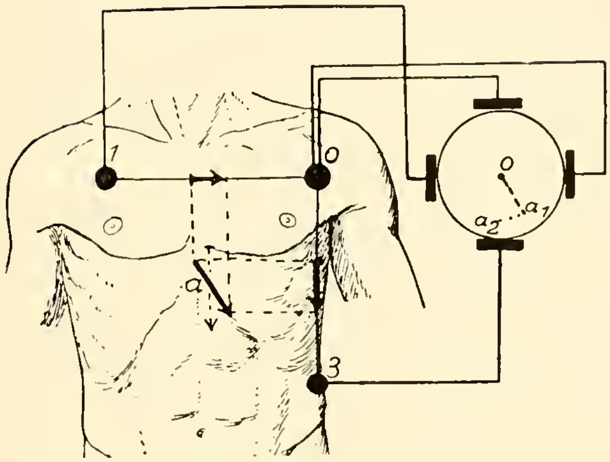

FIG. 57. Method of recording vectorcardiograms. The potential differences of two orthogonal lead systems are led to a cathode-ray oscilloscope in the manner indicated, so that the spot of the oscilloscope is shifted into a position determined by the vectorial addition of the two lead voltages, both regarded as vectors lying in the direction of their lead lines. (From Schellong (59).]

of rotation (clockwise, counterclockwise). This is done by giving timing signals of asymmetrical wave form (521). Special techniques have been developed to separate the loops of the P, QRS, and T waves of the ECG (243).

Description of vectors requires that conventions be established regarding the side from which the loops are viewed. This notation has been given in section 6. Tabulated functions are available (231) for conversion of angles from plane projections into their spatial values. The different lead systems of course offer considerable differences in angles and amplitudes. This has been discussed in section 6. For some detail see table 1 and the paper by Pipberger (369). A good and simple electrode combination has been given by Frank (202). One may find even such simple triaxial electrode combinations as V_2 (for z), V_6 (for x), and VF for the y axis (90) or of the Einthoven frontal plane derivations in comparison with a back electrode (201). In these lead combinations, the location of the dipole has considerable influence on the correctness of the vector analysis (201). Such errors arising from this variable can be theoretically corrected only in torso models; nevertheless, they are of little clinical concern since "normal" limits are not very well defined.

The spatial analysis of the vector is doubtless of great importance. The frontal plane projection alone contains too little information, even in respect to amplitudes. Many hearts show low voltages in the frontal plane leads, and normal voltages in the sagittal direction. Spatial vector positions, moreover, are extremely valuable for interpreting excitation processes, local hypertrophies, etc., so that a spatial, three-dimensional representation of electrocardiographic data is indispensable. The spatial orientation can be derived from two-plane projections. The difficulties in presenting a plastic picture of these orientations, nevertheless, are great. It is therefore advantageous to view this orientation in a stereoscopic device (45a, 59, 97, 427).

The stereoscopic presentation of vectorial data is, by virtue of its technical procedure, a subjective one. If an objective analysis of the stereoscopic data is to be made, the projections on the three planes of space must be described, and there is a convenient method for such a description, using electronic resolvers. Such a system is fed through the voltages of an orthogonal lead system (i.e., a system with lead vectors of equal length and a strictly orthogonal orientation). The voltages are electronically mixed, in such a manner that the lead system is virtually rotated around its three axes. By such a rotating procedure it is possible to determine the position of the system in which the axis of a given complex (P, QRS, T) appears minimal, so that the observer seems to look at the peak of the axis from a point in line with its direction. The rotation angle can be read directly from calibrated dials (127, 132, 375, 427). Electronic computers can record directly the angles of the momentary vector position (339).

THE NORMAL QRS VECTOR LOOP. The QRS loop in most cases shows a distinct longitudinal axis which forms certain angles with the orthogonal axes of the lead system. Various authors give rather different figures for the mean values of these angles (79, 137, 246, 366, 368, 446, 453, 498, 500, 537). Some results are listed in tables 7, 8, and 9. The longitudinal axis lies in the frontal and sagittal plane between 35° and 75° (reckoned in the manner of fig. 58) and in the horizontal plane between the limits of 110 and 140°. The angles vary with age, showing a trend to diminish in all planes. In this respect, they resemble the angles of the R deflection (498).

The sense of rotation of $\overrightarrow{QRS}$ in normal adults in the frontal plane depends on the axis of the loop: those with low values of α usually rotate counterclockwise, whereas the rest usually rotate clockwise. In the horizontal plane, the loop is characterized by an initial anterior deflection, and is then inscribed in a counterclockwise direction, to the left and poste-

TABLE 7. *Tabulation of Mean Results and Standard Deviations of the Normal Orthogonal Vectorcardiogram**

Rotation of QRS-Loops (No. of Cases)	Frontal†	Left Sagittal	Horizontal
	Clockwise 61, counterclockwise 17, figure 8 or linear 22	Counterclockwise 100	Counterclockwise 100
Maximal QRS vectors			
a. Direction	41±14.9°, SE 1.5° (100)	55±36.7°, SE 3.7° (100)	127±40.6°, SE 4.1° (100) (no Gaussian distribution)
b. Magnitude	1.30±0.37 mv, SE 0.034 mv (100)	1.12±0.41 mv, SE 0.04 mv (100)	1.17±0.37 mv, SE 0.034 mv (100)
Maximal width of QRS-loops	0.33±0.20 mv, SE 0.023 mv (100)	0.74±0.34 mv, SE 0.034 mv (99)	0.89±0.31 mv, SE 0.034 mv (100)
Length of width ratio of QRS-loops	6.3±6.4, SE 0.6 (100) Range 1.1–41.5	1.8±1.0, SE 0.1 (99) Range 0.4–6.3	1.5±0.8, SE 0.08 (100) Range 0.5–5.9
Maximal T vectors			
a. Direction	44±12.2°, SE 1.2° (99)	131±20.5°, SE 2.1° (97)	52±21.7°, SE 2.2° (98)
b. Magnitude	0.36±0.13 mv, SE 0.012 mv (98)	0.34±0.13 mv, SE 0.017 mv (97)	0.36±0.15 mv, SE 0.017 mv (98)
QRS-T-angle (measured between maximal QRS and maximal T vectors)	14±9.3°, SE 0.9° (99)	94±42.0°, SE 4.3° (97)	14±45.4°, SE 4.6° (98)
Maximal P vectors			
a. Direction	64±19.8°, SE 2.2° (82)	96±26.7°, SE 3.0° (77)	84±27.7°, SE 3.4° (77)
b. Magnitude	0.16±0.06 mv, SE 0.006 mv (79)	0.15±0.06 mv, SE 0.006 mv (76)	0.13±0.034 mv, SE 0.006 mv (67)

* The loops have been recorded with the SVEC III system; the data are corrected after the author's instruction. Angles as in fig. 58. [From Pipberger (368).]

† SE = standard error. Number of subjects for each measured item is given in parentheses. Ranges between lowest and highest values were indicated only when the distribution appeared asymmetric or when the range could not be defined properly by the means and standard deviations.

TABLE 8. *Maximal Vectors of the QRS and T Loop in Space Are Given with Their Projections on the Frontal and Sagittal Plane**

	Maximal Vector in Frontal Plane				Maximal Vector in Sagittal Plane			
	QRS		T		QRS		T	
	Angle	Length	Angle	Length	Angle	Length	Angle	Length
Minimal	+20	0.31	0	0.10	+66	0.21	+77	0.05
Maximal	+89	1.73	+84	0.56	+129	1.47	+144	0.52
Average	+66	0.99	+46	0.28	+107	0.87	+124	0.23

* Equilateral tetrahedron (Wilson) as reference system. Angles as in fig. 58. The table includes data from only 66 of the 75 individuals in the series. The 66 had typical elliptical loops; the other 9 had the less usual rounded loops. [From Burch *et al.* (137).]

TABLE 9. *Angles of the Long Axis of the QRS Loop, Measured According to Fig. 58, in Their Projection on the Three Planes**

	Mean	Standard Deviation	Largest Observation	Smallest Observation
a. Frontal plane (angle α)				
Duchosal	65.69	±10.49	80.00	23.00
Grishman	40.41	±16.01	70.00	16.00
b. Horizontal plane				
Duchosal	+84.13	±4.57	+98.00	+72.00
Grishman	+86.70	±5.74	+109.00	+76.00
c. Sagittal plane				
Duchosal	90.28	±2.45	95.00	83.00
Grishman	90.69	±4.55	100.00	78.00

* Reference system: the Grishman cube and the Duchosal system (fig. 20). [Values from Young *et al.* (537).]

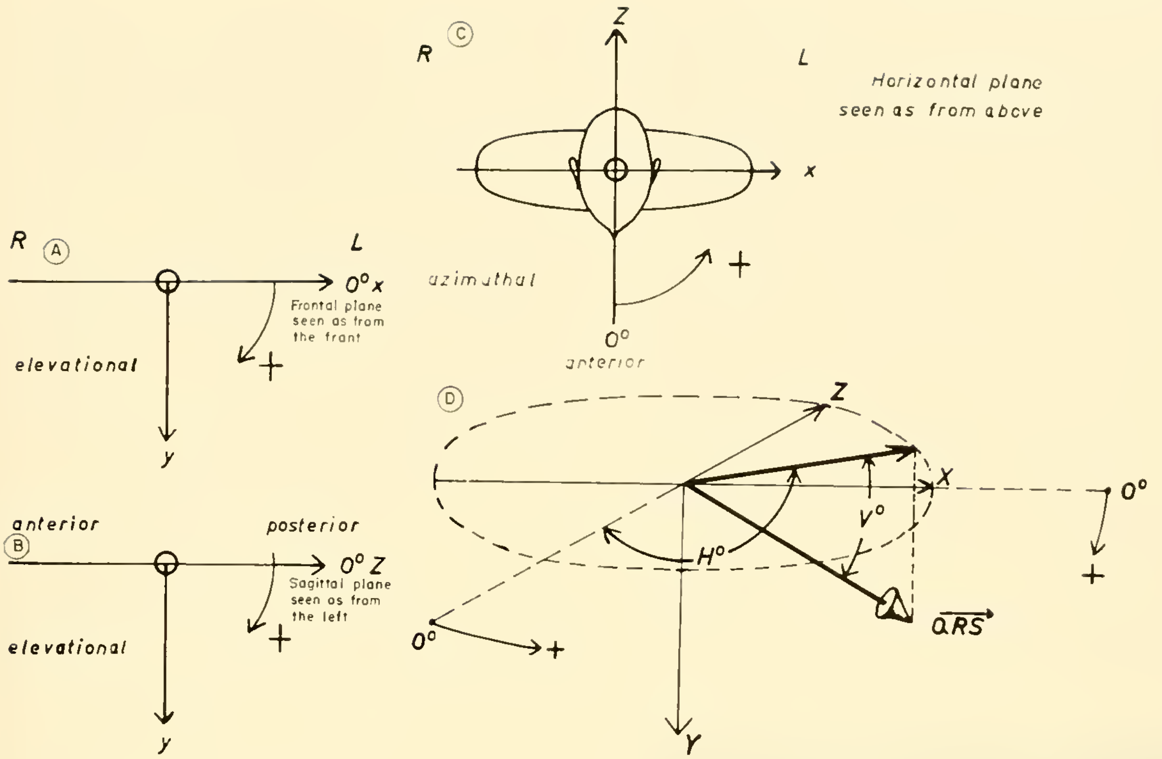

FIG. 58. The axes and positions of angles in vectorial data, as used throughout this monograph. *A–C*: the axes and angles in the projections on the 3 planes commonly used. *D*: the azimuthal (H) and elevational (V) angles as counted in a stereoscopic description.

riorly. In the sagittal plane, viewed from the left, the loop shows an initial deflection anteriorly and usually superiorly, and then turns in a counterclockwise direction inferiorly and posteriorly (422). In figure 59 some examples of normal loops are given. Rather extreme types have been selected to show the range of normality. The problem of describing the vector loops in a manner that will permit easy standarization is by no means solved. The projections of the spatial vector loop on the three conventional planes in space are arbitrarily chosen, from the viewpoint of biology. So the form of such loop projections can scarcely be standardized in a reliable manner. The best way to analyze the form of the loop and to describe detailed information it contains would be to determine angles of certain instantaneous vectors of the loop, distinguishable from all other vector positions by some unmistakable characteristic. Fortunately, such vectors can be defined in most cases. Nearly every loop has an instant of maximum amplitude and the vector of this maximal voltage can be regarded as the longitudinal axis which, however, can be correctly defined only in a three-dimensional model. If one can look at the loop broadside, the broadside width of the loop can be determined, being defined as the greatest width of the loop perpendicular to the longitudinal axis. The ratio of the width of the loop to its length in the broadside view may be called "openness," the average value of which ranges between 0.5 and 0.6 (444). Unfortunately, not all loops reveal a clear longitudinal axis. There are round loops which display a circular outline regardless of their plane of projection.

An often described peculiarity of normal QRS loops is that they usually lie in a single plane. If, therefore, the reference system of orthogonal electrodes is rotated electronically, one finds certain positions in which the loop will appear as a straight line, the edgewise view of the loop's plane. If the view is directed perpendicular to this plane, the loop appears in its broadside view. This peculiarity allows characterization of the loop in a relatively general and simple way. We may, looking at the reference system from the front, first rotate the system in either direction around the y axis until the frontal projection of the loop appears with its smallest view. By additional rotation of 90° in the positive direction, the most open loop obtainable by azimuthal rotation

about the y axis is pictured, and the final angle θ necessary to produce this view measured. With θ set at this reading, the system is then rotated in the craniocaudal direction around the newly established x' axis to produce again an edgewise view. With added 90° of rotation, the loop is again seen broadside, and the elevational angle α recorded (444).

The loop (if planar) may be simply described by its "polar vector" in the following way. The polar vector stands perpendicular to the plane of the loop and, starting from the zero point, is drawn on the side from which the rotation is seen to be counterclockwise. The length of the vector indicates the area of the loop (146). The projection of this polar vector on the horizontal plane has an azimuthal angle between 90° and 180° (it appears backward and to the left). The angle of the vector with respect to the y axis is between 0° and −90°; the vector being directed upward, and the loop therefore oriented downward (146). (Angles measured as in fig. 58.)

Viewed from the "edge" of its plane, the loop may be analyzed in the following way. The distance between two parallel lines enclosing the narrowest view of the loop obtainable by either azimuthal or elevational rotation may be called the "edgewise width." The ratio of this edgewise width to the longest vector in the broadside view is called the "planarity." Its average values lie between 0.11 and 0.13 (347, 444). These data alone would permit an ample description of the loop; however, the electronic devices necessary to resolve the ECG in such a manner are not available in many laboratories. Moreover, such a description of the loop's plane does not contain any information about the form of the loop (the openness excluded), the direction of the maximal vector (the electrical axis), and the time course of all electrical changes. Therefore, the planar projections of the loop in an orthogonal reference system will in most cases remain the method of preference, though the foregoing analysis is an excellent method for standardizing the general peculiarities of such loops.

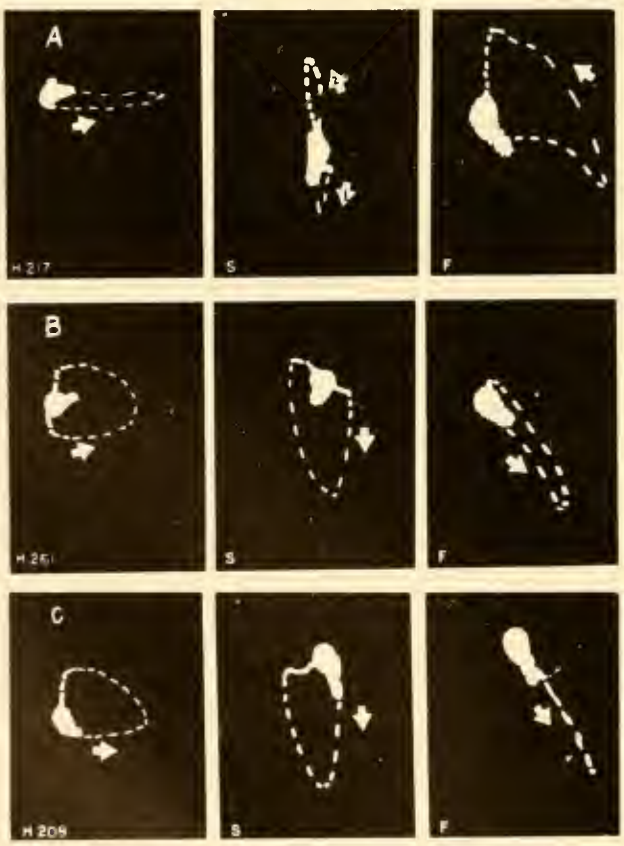

FIG. 59 Some examples of normal loops, recorded with the Grishman cube (fig. 20). Note that the saggital plane is viewed from the right. [From Grishman & Scherlis (28).]

The normal form of the QRS vector loop is rather simple: a wide open planar loop with smooth contours, without crossovers, and invariably transcribed counterclockwise when looked at from a direction normal to its respective planes, from above and left (444).

A detailed description of the form of loops is possible in every projection of the spatial loop. One may distinguish the "initial forces" of the loop, the loop "body," and the terminal "appendage." Initial forces and appendage are arbitrarily distinguished from the body thus: the body of the loop begins when the vector passes to the left and below the zero point (537). Initial forces and appendage are more or less identical with Q and S.

An additional analysis of the loop involves measuring the time the vector needs to rotate from one-half of its maximal value in the rising phase over the peak, to one-half of the falling phase. This time lies in most cases, between the limits of 15 to 30 msec, with an average of 23 msec. The central angle subtended by this segment of the loop averages 41°, and the mean angular velocity of the rotating vector varies between 16 and 21 degrees per 10 msec, with a range between 3 and 40 degrees per 10 msec. This angular velocity seems to be a measure of normality and diminishes in cardiac patients (458).

The form of the horizontal projection of the vector loop, in combination with the surface image in the horizontal plane as shown in figure 60, explains fully the precordial lead records, as given in figure 52. The horizontal loop of figure 60 is directed mainly

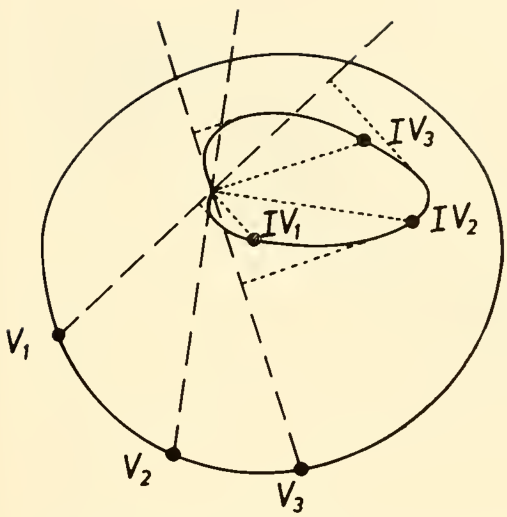

FIG. 60. The image surface of fig. 16 is taken to demonstrate the lead vectors of V_1, V_2, and V_3. An average horizontal vector loop is shown, which projects on the V_1 lead vector mainly negatively. The inversion point of the projection in all three leads is marked at the loop. In IV_2, e.g., the loop begins to project negatively in V_2.

to the left. The image points of V_1 and V_2, however, are shifted far to the right, so that the loop projects itself on the V_1 lead vector mainly away from the electrode and therefore shows an rS pattern, whereas in V_2 the first third of the loop projects in the positive direction. Only V_3 has a prevailing R.

The vector loop may be transcribed into a two-dimensional curve of usual type by recording the magnitude of the spatial vector as ordinate against time as abscissa. The curve thus registered resembles fully a normal ECG. It has been described as "Absolut-Ekg" by Hollmann, as "Manifest-Ekg" by several authors (see 358). There is only limited information incorporated in such curves. They nevertheless should be included in any complete description of vectorial data.

II. THE RS-T SEGMENT AND REPOLARIZATION

The Normal T Wave and the Ventricular Gradient

In the Einthoven standard derivations I, II, and III, T is upright in the majority of cases. Only T_{III} is likely to be negative in normal hearts, if the ventricular gradient is small or if the QRS axis is shifted to the left. In such cases, the frontal vector of the gradient lies left of $\overrightarrow{\widehat{QRS}}_f$ and the angle α of $\overrightarrow{\widehat{T}}_f$ is even smaller than that of $\overrightarrow{G}$. In the horizontal leads, especially in the Wilson precordial leads, T is upright in nearly all leads and cases (fig. 53). This is mainly due to the fact that QRS is negative in some precordial leads or exhibits at least a strong second negative deflection (s), so that total effect is to shift the T wave into the positive direction. The gradient, in addition, strengthens this positive T wave, as the gradient is directed from inward to outward, from the back anteriorly, because the outer layers show a much shorter plateau than the inner layers. The epicardial and endocardial unipolar T is positive, with gradients which (calculated from the figures) seem to be small or (in the endocardial record) zero[10] (373). If parts of the myocardial wall are cooled, the gradient and T are strongly influenced; this needs no further explanation. Curiously enough, T may be nearly normal in a heart showing no visible movement (291).

Vector analysis of T is restricted to study of the areas of T, because $\overrightarrow{G}$ has a definite meaning only in regard to areas. As a matter of fact, $\overrightarrow{G}$ is closely correlated to the position of $\overrightarrow{\widehat{QRS}}$. $\overrightarrow{G}$ is, in normal cases, of much greater magnitude than $\overrightarrow{\widehat{QRS}}$, so that the resultant vector of $\widehat{T}$ is bound to a position forming relatively small angles between $\overrightarrow{\widehat{QRS}}$ and $\overrightarrow{\widehat{T}}$. As this angle reflects, in some respects, the relative magnitude of $\overrightarrow{G}$ as compared with $\overrightarrow{\widehat{QRS}}$, it is of definite clinical value. If in vector loops the axis is determined as the line which bisects the planar vector loop into two halves, the spatial angle between QRS and T is found for a corrected orthogonal lead system to be, on the average, $56° \pm 19°$ with a range of 20° to 105° (93). With other lead systems or with the null-contour method, the angles appear to be considerably smaller and range between 43° (null contour), 18° (Grishman cube) and 28° (Tetraeder) as their average values (252). No doubt the frontal or horizontal plane projections of the QRS and T axis form much smaller angles, they are of the order of magnitude of 20° or less in the frontal plane ($19° \pm 15°$ with the corrected orthogonal system). If estimated from the plane projections, large errors in the determination of the spatial angle may occur (373).

In tables 5 and 6 the values for $\overrightarrow{\widehat{QRS}}$, $\overrightarrow{\widehat{T}}$, or $\overrightarrow{\widehat{G}}$ have

[10] In endocardial leads, QRS is nearly completely negative (qS), and T therefore positive. It is unknown, however, why the ventricular gradient appears to be zero.

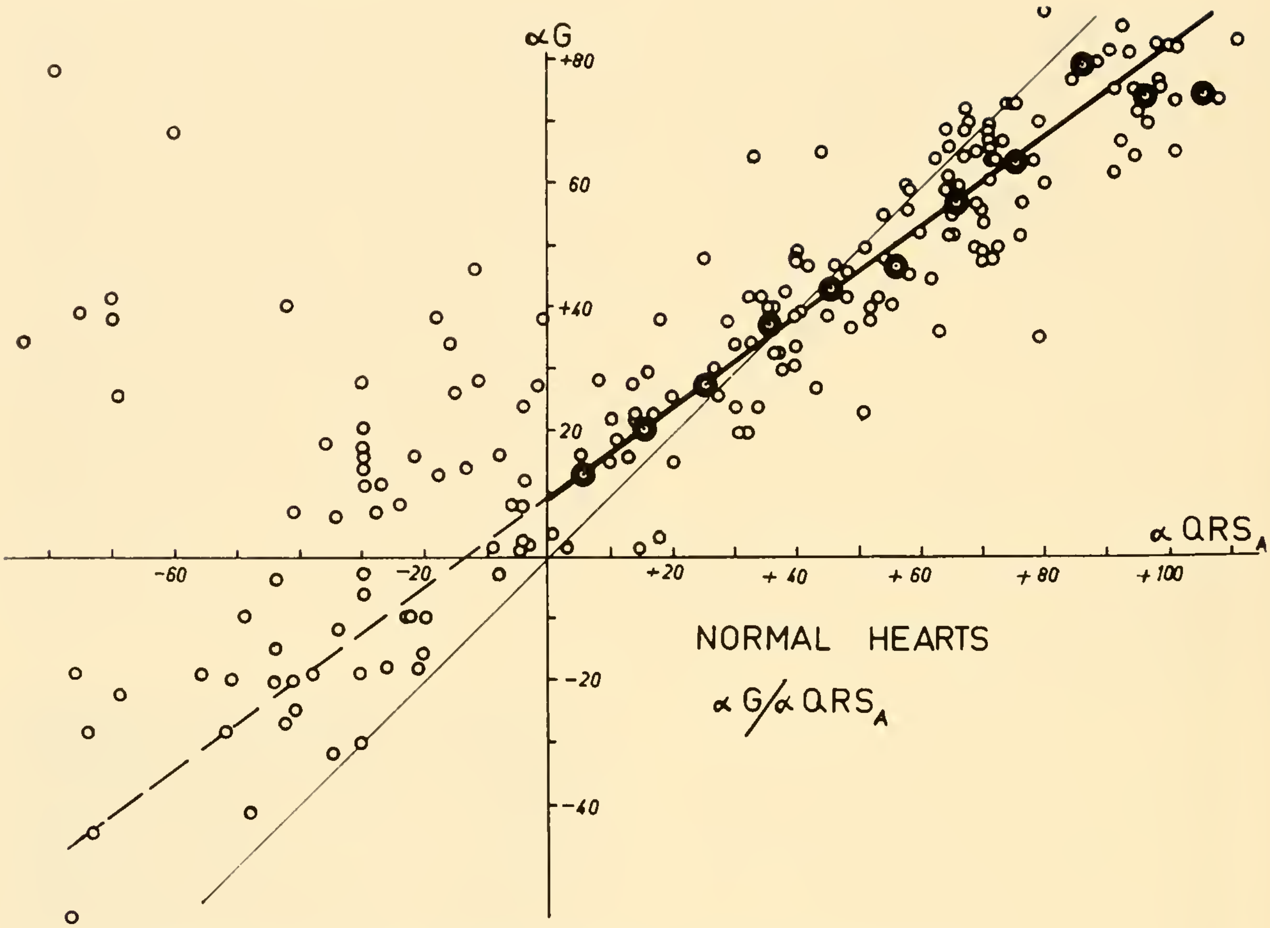

FIG. 61. Correlation between angle α of the QRS area and α of the ventricular gradient, taken for the frontal plane. The large dots are the averages. The thick line represents the equation $G = 0.72 \cdot \alpha_{QRS} + 10°$ and applies to normal subjects and to patients without clinical signs of failure. In the left ventricular strain (α_{QRS} negative) the correlation disappears almost completely. [From Gärtner & Schaefer (216).]

been listed. Since the direction of $\vec{\hat{T}}$ in the frontal plane coincides rather closely with that of $\overrightarrow{\widehat{QRS}}$, the vector of the gradient coincides with the $\widehat{QRS}$ vector as well in that plane. There is, however, a shift of the $\overrightarrow{\widehat{QRS}} - \vec{\hat{T}}$ angle in the course of age and with the direction of $\overrightarrow{\widehat{QRS}}$. As figure 61 shows, the angle α of $\vec{G}$ is smaller than that of $\overrightarrow{\widehat{QRS}}$ in high values of the $\overrightarrow{\widehat{QRS}}$ angle (right position type), but larger in small values of the $\overrightarrow{\widehat{QRS}}$ angle. Both coincide in their average value at an Einthoven angle of approximately 36° (85, 216).

In the sagittal plane, $\vec{\hat{T}}$ coincides likewise fairly well with $\overrightarrow{\widehat{QRS}}$, if measured with a tetrahedron or determined by the null contour, but it shows a high deviation from $\overrightarrow{\widehat{QRS}}$, if recorded with a corrected system: the positions are (after fig. 58) 131° for $\vec{\hat{T}}$ instead of 55° for $\overrightarrow{\widehat{QRS}}$. $\vec{\hat{T}}$ therefore is more anteriorly directed than $\overrightarrow{\widehat{QRS}}$, which is, on the average, directed somewhat toward the back (137, 368). The ventricular gradient may be calculated by a vectorial addition, since $\vec{G}$ is the vectorial sum of $\overrightarrow{\widehat{QRS}}$ and $\vec{\hat{T}}$ (fig. 45). This means that the vector of the gradient must lie between the vectors of $\widehat{QRS}$ and. $\hat{T}$ Some values for the direction of $\vec{G}$ are given in tables 5 and 6. Its frontal angle α varies, according to different authors, between 34° and 48° (85, 297, 459). The horizontal (azimuthal) angle, not well known, is on the average, 66° (459), measured as shown in figure 58.

The numerical value of $\vec{G}$ plays a decisive role in the judgment of normality. Whereas depolarization

(QRS) is a fairly stable event and changeable only by strong influences on the propagation process, T is very sensitive to even slight changes in the metabolic equilibrium of the fiber, since the action potential (especially the plateau) is, in some respects, an indicator of metabolic normality. Unfortunately, the "normal" values of $\vec{G}$ are still controversial.

The magnitude of $\vec{G}$ in space has not been determined with corrected leads, but in a small group of 18 young men (459). The area of G_s had an average value of 97 μvsec in the corrected leads, with values for $\widehat{QRS}_s$ of 43 and $\hat{T}_s$ of 68 μvsec. The group tested was too small for the establishment of satisfactory standards, as the authors indicated, but the values obtained do give some orientation. Much better known are the magnitudes of the areas in the frontal plane, of which Ashman made the first fundamental measurements. He found that the normal average of G_f is of the order of magnitude of 45 to 50 μvsec, depending largely upon the heart rate and diminishing with its increase (86). Such standard values, however, seem to be quite insufficient for the following reasons: their magnitude depends so heavily on the size of the QRS area that a linear relationship exists between these two (fig. 62) (86, 216). G_f should be, according to these observations with clinically normal persons, about twice the magnitude of $\widehat{QRS}_f$. The normal values of G_f, that is, for individuals with normal bodily performance, fall between the following limits: $G_f = 3\ \widehat{QRS}_f$ and $G_f = 1.5\ \widehat{QRS}_f$. The more G_f is diminished below $1.5\ \widehat{QRS}_f$, the higher is the probability that the heart is abnormal. The more pronounced the abnormality of the heart, as in heart failure, the lower is G_f compared to $\widehat{QRS}_f$. Unfortunately, we can never know the normal $\widehat{QRS}_f$ value of a certain heart, if QRS is itself perceivably distorted; which means, after all, that no diagnosis about normality of G is possible in such cases.

Though a correct analysis of $\vec{T}$ must include calculation of $\vec{G}$, an empirical judgment seems to be possible, since the diagnostic classification into "normal" and "abnormal" $\vec{\hat{T}}$ led to results comparable with those obtained by calculation of $\vec{G}$ and a simple inspection of the ECG (432). But if the angle between $\vec{G}$ and $\overrightarrow{\widehat{QRS}}$ is somewhat borderline at the upper limit, and if G is at the lower normal limit of its amplitude, the angle between $\overrightarrow{\widehat{QRS}}$ and $\vec{\hat{T}}$ soon surpasses the value of 90°. In such cases, T may

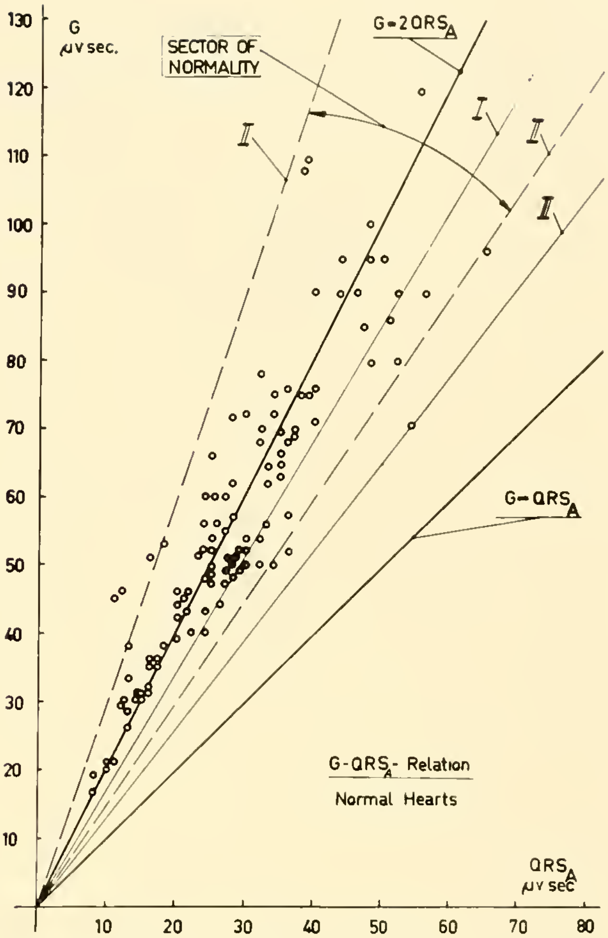

FIG. 62. Correlation between the QRS area and the ventricular gradient in normal hearts, with all values taken from the frontal plane projection. Nearly all values (7 exceptions) lie in a "sector of normality" around a line giving the relation $G = 2\ \widehat{QRS}$. Lines II are the borderlines of the sector of normality ($G = 3\ \widehat{QRS}$ and $G = 1.5\ \widehat{QRS}$). Line I separates the normal from the failing hearts. Line III gives the lowest limit of normals in our series. [From Gärtner & Schaefer (216).]

readily become negative in two standard leads (II and III) without being necessarily abnormal.

In normal hearts, the peak of T appears simultaneously in all heart vector leads. This necessarily means that the vector loop of T appears as a straight line. Only in abnormal cases does repolarization show a phase shift in different leads, the T loop developing an open, or even rounded, contour (283).

The ST Interval

As the ECG is the differential quotient of the monophasic action potential of the cardiac fibers, a

measurable voltage must be present as long as the action potential changes in time. This is always the case. The name "plateau" is only an approximate description of the facts: there is an immediate, but slow, decline of the action potential after the spike has ended. If this initial decline were homogeneous all over the heart, the resulting ST segment would be opposite in direction to the main QRS deflection. The facts, however, show that ST starts (at the so-called ST junction at the end of S, marked with J by some authors) with a slowly rising phase, which develops into the T wave without any sharp boundary. This is the natural result of the asychrony of fiber repolarization, which is present even in the very earliest moments of that process. A somewhat steeper rise of ST, forming the rising phase of T, cannot occur before repolarization starts its steep decline. The steeper this decline and the longer the plateau, the more "isoelectric" is ST and the shorter and higher is T. The behavior of the ST segment can be quantitatively evaluated by measuring the time from the ST junction until the rising phase of T reaches one-half of its spike voltage. This time should comprise less than 80 per cent of the interval between the ST junction and the top of T (47).

No other part of the ECG is subject to so many theories, interpretations, and even more misinterpretations as the ST interval. The reason is obvious. If any part of the heart is damaged, and no longer produces an action potential of its own, this part develops an injury potential at its boundaries. This potential is recorded as a superimposed monophasic distortion (433, 434). ST becomes the most important indicator of such local lesions. The interpretation of ST displacements is, however, extremely complicated and needs careful consideration. There is, in the first place, the influence of heart rate on the ST segment, intimately connected with the base line problem (section 10). In tachycardias, the P wave starts before the U wave has ended; the PQ interval is displaced by T_p, so that an apparent negative displacement of ST may be merely the result of an incorrect determination of the base line. ST is elevated in bradycardias and is depressed more and more as the frequency increases (464).

The junction does not always form a sharp angle, but shows, in many cases, a so-called saddle form. This may be found in cardiac patients, but hardly more frequently than in normals with slowly rising ST elevations, which are often found in precordial tracings from absolutely normal hearts (181, 226). Positive or negative displacements of ST, which run more or less parallel to the abscissa, are abnormal (with exceptions to be discussed).

The theory of ST displacement (58, 188, 436) should be discussed in detail, because of its clinical importance. If an excitation wave traveling along a fiber bundle reaches a region which is damaged and unable to be excited, the following will happen (fig. 63). If we assume the boundary between damaged and intact fiber to be infinitesimally small, the membrane potential difference across the boundary will produce a dipole of the same type as shown in figure 2. If the damaged fiber retains its full resting membrane potential, the dipole will show a polarity with the damaged area appearing positive compared to the normal, excited tissue. If the damaged area has no membrane potential, or a diminished one which does not change during systole, a dipole is already present at rest, the damaged area appearing negative with respect to normal; but as soon as the normal area becomes depolarized, this resting potential difference disappears. The result is the same as far as the record is concerned: during systole a negativity existing at rest seems to disappear and the damaged area appears to be more positive than the normal. This positivity endures until the end of the action potential, covering thus the whole QT segment. This potential is responsible for the ST displacement. The amount of this displacement depends on the magnitude of the solid angle subtended by the total cross-sectional area of the damaged fibers at the boundary with normal areas, as seen from the electrode. One should bear in mind, however, that such a boundary has no cancellation effect, such as is found in the spread of excitation during the QRS complex. Here, in a way similar to the generation of the ventricular gradient, relatively small areas of damaged fibers can lead to a comparatively large ST displacement. A rough estimation shows that for a displacement of 0.1 mv, about 400,000 fibers have to be damaged or inactivated, assuming no cancellation (404).

The polarity of an ST displacement and its resultant vector (fig. 64) depend fully upon the electric moment of the resting membrane potential and the anatomical directions of the fibers producing this moment and crossing the boundary between normal and damaged areas. The vector therefore does not change direction throughout the whole ST segment, as experimental evidence shows (445). It is therefore clear that similarly located injuries must produce similar vector positions and ST polarities, as experimental evidence again confirms (167). In dogs, for

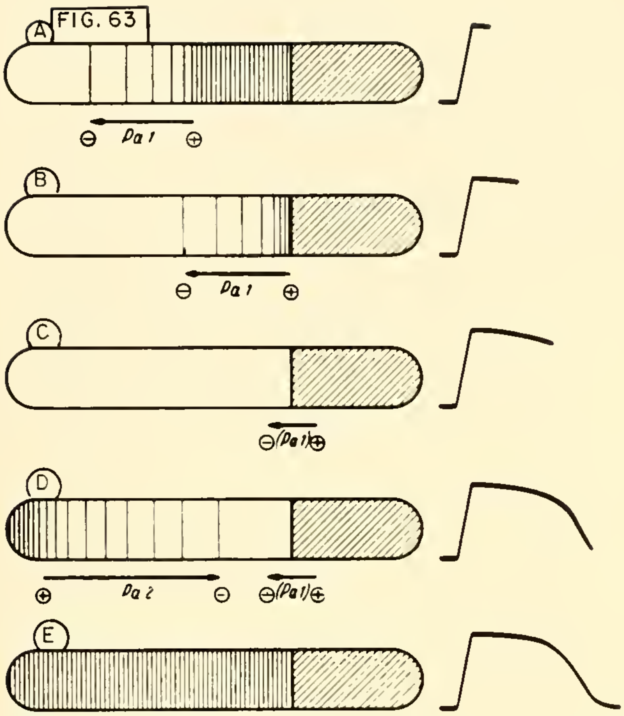

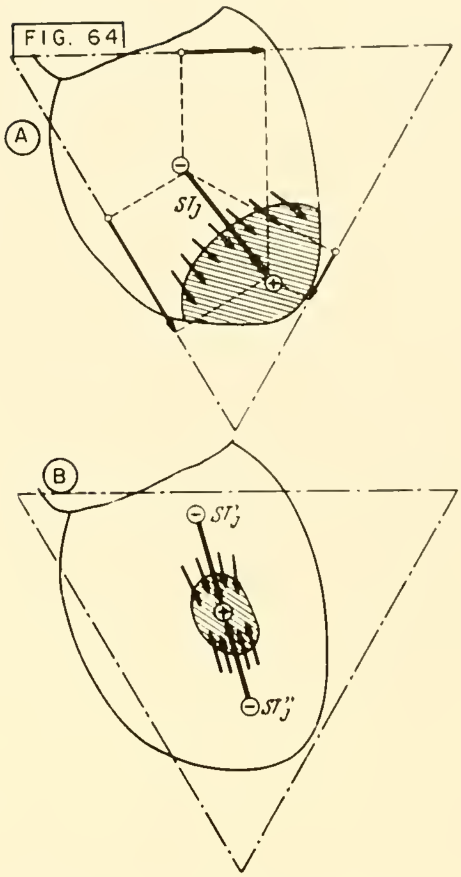

FIG. 63. Explanation of the genesis of a monophasic action potential at the boundary to an asystolic area (right part of the fiber), where two electrodes are put on the ends of the fiber. The shaded area is still (or again) resting. The arrows indicate differences of the membrane potentials along the fiber surface, with their polarities. On the right, the time course of a record is shown. P_{a1} is the potential difference during the accession, P_{a2} during the repolarization of the activity. The arrows indicate merely the distances along which the membrane potential varies. [From Schaefer (58).]

FIG. 64. *A*: resultant vector of an S-T displacement originated by injury potentials at the boundary between normal and damaged tissue. The damaged area is shadowed. The little arrows represent single fibers crossing the boundary and developing an injury potential and, during activity, a monophasic action potential and dipole moment according to fig. 63. Their resultant is shown as ST_J (integrated vector of S-T displacement). This vector projects, like other vectors, on the lead vectors of the electrodes (here on the Einthoven triangle). *B*: if the damaged area is surrounded on all sides by normal tissue, and if fiber bundles cross the boundary in the direction of the arrows, two resultant vectors develop at the two entries of the fibers into the damaged area. The total resultant will be zero (mute infarct). [From Schaefer (58).]

example, injury to the right ventricle causes an upward deflection of the base line and a depressed ST segment, whereas left ventricular injury does the opposite (354). It makes no difference whether a part of the heart remains inactive (showing an asystolic area) or the inactive part is removed. This could be demonstrated on an isolated surviving human heart (119). How much current may be recorded from a damaged or asystolic area, with a certain electrode position, depends to a large extent on how much contact the damaged area has with the optimally conducting parts of the heart's environment, such as the mediastinum and the thoracic wall (284). Moreover, a damaged area may remain "mute," even with optimal contact with conducting surfaces, if the damaged area is surrounded to an equal degree on all sides with normal tissue. In such a case, the vectors from one side of the area are

canceled by the vectors from the other (fig. 64). In general, however, the damaged area will develop only one boundary against the normal tissue, with a minimal cancellation, as seen in figure 64.

The ST displacements due to such demarcation potentials between normal and injured tissue survive for a short time only. After a 10- to 15-min period, the potential nearly completely disappears, due to the fact that the damaged fiber loses its intracellular fluid content up to the next intercalated disc (Glanzstreifen). Here a real cell boundary seems to exist, preventing the myocardial fiber from losing more of its intracellular fluid. The boundary between normal and injured tissue is thus replaced by a boundary between normal myocardial fibers, the limits of which are now the intercalated discs. The emptied, injured parts of the fiber become electrically inactive. If a new injury is sustained, destroying the membrane once more behind the intercalated disc, a new injury potential occurs (398). This is the reason why the ST displacement disappears comparatively rapidly and can only be restored by a newly occurring injury.

The QT Duration: "Electrical Systole"

The very end of T is determined by the moment when the repolarization of the latest repolarizing fiber is completed. The whole QT duration therefore depends on two factors: the amount of asynchrony, which may be calculated from the duration of the QRS complex and is nearly identical with it, and the total duration of the action potential of the average myocardial fiber. One could estimate, therefore, that QT equals the duration of the longest local action potential plus the duration of QRS. The magnitude of the ventricular gradient ($G = 2\ \widehat{QRS}$) indicates that the inhomogeneities in the duration of the action potentials are of the same order of magnitude as the desynchronization in the beginning of all local excitatory processes. However, it is always possible that the longest action potential may be the last to start, so that the simple equation: QT duration = QRS duration + action potential time is subject to considerable error. Since T is normally monophasic, it may be argued that differences in duration of individual action potentials are distributed at random over all possible local conduction latencies.

The duration of QT depends mainly on the heart rate. Many formulas have been given to calculate this duration, but none of these fits all data. This is

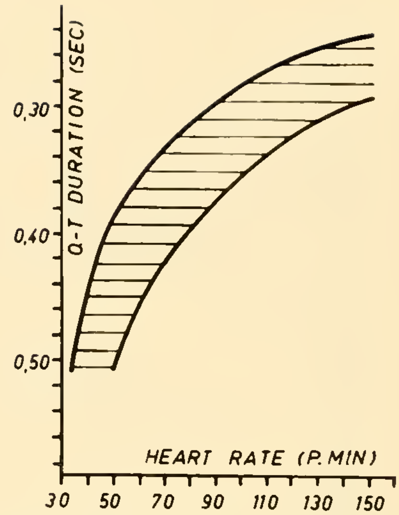

FIG. 65. Correlation between heart rate and duration of Q-T. The limits of normal values are given, in some approximation and according to the majority of authors.

not surprising, because change of rate can be induced by various processes which influence the action potential in different ways. For example, heating the heart shortens the relative QT duration, whereas an increase in the sympathetic tone increases the relative QT duration. "Relative duration" means the "normal" duration for a given rate (fig. 65). Cooling lengthens, and acetylcholine and vagal tone shorten, the relative duration of QT. Such effects reflect changes in the single fiber action potentials. In analysis of human ECG's intraindividual QT changes are described by a different formula than that for interindividual changes (218).

The formulas describing this correlation between QT duration and heart rate contain either the RR interval, its square root, or its cube root, as one of the factors. The simplest formula (and one of the best) is: $QT = 0.39\sqrt{RR}$ (241). No theory explains the mathematical form of such correlations, which therefore remain essentially empirical. Thus it seems wise to represent the frequency effect by an empirical correlation (fig. 65). The correlation is even better if the duration of QRS is subtracted from the QT time (corrected QT duration, Lepeschkin). Since the QT duration in a single fiber depends linearly on the frequency (447), a linear correlation could be expected for the whole heart as well. But QRS and the desynchronization and inhomogeneities of repolarization apparently interfere in a complicated manner. Values for portions of the QT time, as, for example, the time between Q and the top of T, have been given by Lepeschkin (315).

The adaptation of QT to a change in frequency occurs immediately after a change of one single preceding diastolic interval. Therefore it is extremely unlikely that the energy available or liberated by the heart beat is responsible for this adaptation. Nor is there any "purpose" in shortening or lengthening of QT. The mechanism most probably is due to the accumulation of potassium at the outer surface of the myocardial fiber, because K shortens the action potential. The reconveyance of K into the cell takes time and energy. The longer the time, the smaller the remainder of external potassium. Therefore, the QT duration reflects an equilibrium process between the potassium remaining outside and shortening QT and the forces of re-entry into the cell. We understand that sudden changes in the frequency lead to a slow adaptation of the QT duration (242), until the new equilibrium is established.

Electrical and mechanical events are independent of each other within wide limits. The term "electrical systole" therefore is incorrect: systole is a mechanical event, depending on circulatory conditions, like aortic pressures, and their interference with the contractile mechanism of the heart. It is often, but not always, true that QT is nearly as long as the mechanical systole, and that T ends synchronously with the beginning of the second heart sound. Proof that this is not generally true may be seen in the kangaroo, whose QT duration is about 50 per cent shorter than its mechanical systole (471). Details of the electromechanical relations will be discussed later (section 13).

12. THE U WAVE (316, 317)

During mechanical diastole, in many cases, a low potential difference is recorded, lasting in cases of tachycardia to the onset of P or even longer. This so-called U wave reaches the voltage of 0.05 mv or more in about 3 per cent of normals, and is maximal in the Einthoven lead II (299). It is sure that this wave cannot be related to monophasic action potentials during the contraction of any fiber of the heart. It must be the result of a completely different type of cellular potentials, the afterpotentials (441). Positive afterpotentials, which may occur during the diastolic phase, are known only in Purkinje fibers, where they play the role of pacemaker potentials and may be ascribed to a gradual decrease in membrane potassium conductance, combined with increased sodium permeability (487). Such positive afterpotentials, however, are unknown in the bulk of ventricular fibers and cannot be the source, on quantitative grounds, of events detectable in the ECG. The "active cross section" of Purkinje fibers is too small to evoke a sufficiently strong electric field. Negative potentials, due to stretching, therefore seem to be the only source of potential differences observed in the ECG during diastole.

We are far from having a complete theory of the U wave. The most likely explanation is that negative afterpotentials in big muscle masses most probably are the source of the U wave potential, but these afterpotentials at the same time must be distributed inhomogeneously over the heart (406). Otherwise, neither the amount of potential difference nor its polarity could be explained, since homogeneous negative afterpotentials would lead to a very small and discordant (downward) U wave. The coupling between T and U, shown by the identical direction of their vectors, indicates that U depends heavily on the processes governing the ventricular gradient. The inhomogeneity of the afterpotential is apparently correlated with the anatomical direction of the myocardial fibers and the spread of their excitation, as is the case with the T wave. The greater the stroke volume, the stronger the stretching factor, but inhomogeneities may be exaggerated in empty hearts with extremely small diastolic filling. The inhomogeneity may be minimal in hearts with a medium-sized diastolic volume, the diminution of which leads to greater inhomogeneities. The augmentation however, by increasing local stretching, leads to higher absolute afterpotentials.

The preceding remarks are concerned with the U wave in normal hearts. There are, however, strong potentials experimentally evoked, of obviously metabolic origin, which are likewise marked as U because they occur during the TP segment, in which the normal U wave also happens to appear. They can be elicited by adrenaline or insulin (152, 153) and consist of an upward (positive) deflection of the same sort as the normal U. In pathological hearts, even negative U waves are found, and various types of fusions between T and U have been described (316). However, one gets the impression that all these U waves are different from the "normal" U, that metabolic processes may be the cause, but that no explanation is available for the moment. A decrease of potassium or an increase of calcium may play a certain role in the genesis of such augmented afterpotentials (441). In some clinical cases, the situation seems to be rather intricate; a discussion lies beyond the scope of this review.

13. RELATIONS BETWEEN THE ECG AND THE MECHANICAL EVENTS IN THE HEART

Time Relations in the Whole Heart

The problem of the electromechanical relations, as far as the heart is concerned, is divided into two different parts: the time relations between mechanical and electrical events, the determination of which is more or less a matter of recording technique; and the causal relations between the membrane potential and the accompanying mechanical changes. In the time relations, the mechanical latency has often been studied. It is obvious that the results depend upon the sensitivity of the mechanical recorder. In skeletal muscles, the mechanical latency is extremely short [less than 0.1 msec (227)], but such latencies have never been observed in hearts with a reliable mechanical recorder. The first phase of the latency starts with Q (which precedes every mechanical event in the ventricle) and ends with the very first movements visible in the beginning of the heart sounds or the first movement detectable at the ventricular surface. Its duration is about 15 msec. The time between the onset of Q and the start of intraventricular pressure rise (Umformungszeit, electropressor latency) is much longer: about 40 to 50 msec (123, 264, 355). It is followed by the rising pressure time of 32 msec, so that the isometric tension time, as the sum of electropressor latency and rising pressure time, lasts about 82 msec (355). The result of the subdivision, however, is controversial, because different methods lead to very different results. As a whole, the end of QRS is not precisely reflected in the mechanical events, but may coincide more or less with the beginning of a steep rise in intraventricular pressure. The mechanical latencies reported for the atria differ considerably, ranging from 50 to 90 msec in man (123).

The latencies so far discussed have been found for the heart as a whole. Local observations of both electrical and mechanical events have been made with the aid of differential mechanographs and a simultaneous record of the electrical events with close bipolar electrodes. Such records in dogs confirmed previous findings in the turtle, indicating that the mechanical events start in the septal region (apparently near the so-called source region, section 8). Local mechanical events start at the peak of the bipolar action potential recorded at that region or not more than 2 msec later, i.e., in the moment when the electrical potentials are at their maximal rate of change (189).

The question of how long mechanical systole lasts as compared with the ECG has already been discussed (section 11). The end of the systole is a secondary event and cannot yield any correlation to the electrical potentials. In small heart muscle strips, a certain correlation exists and will be discussed later. For the whole heart, the time relations are apparently indirect. Doubtlessly, a pronounced lengthening of QT, combined either with a normal or a shortened mechanical systole, is abnormal and, in the case of shortened mechanical systoles, the sign of a so-called "energetico-mechanical insufficiency" (33). The problem is, however, extremely complicated and mostly a matter of ionic balance (265), especially in the case of hypopotassemia. Decrease in serum potassium seems to lead to severe myocardial damage, an intimate interdependency between QT and metabolic conditions having been proved (73). Nevertheless, we should agree with Burch (136) that the ECG "more reliably indicates the existence, rather than the type and degree, of electrolytic disturbance." Therefore, we here omit all detailed discussion which may be read in the original papers.

Coupling of Electrical and Mechanical Events

Doubtlessly the action potential is the first step toward contraction. But we are unable to explain fully this apparently simple relationship. There is no action potential without a mechanical contraction, though it may be extremely feeble. The spread of the mechanical events even seems to imitate the path taken by the electrical excitation: in dying hearts, the contraction wave runs clearly toward the base of the heart (255). There is a real peristalsis running over the heart of the tortoise (229). In very slowly conducting hearts, the contraction, damaged by digitalis, is preceded by a wave of relaxation or distention (120), which seems to correlate with the relaxation phase preceding every contraction of skeletal muscles.

The linkage of mechanical and electrical events is fairly complicated and can be discussed here only in regard to its most important points. It may be put thus: a close correlation usually does exist, yet, at times, this correlation may appear to be completely absent. Correlations are found in the following observations. Simultaneous recordings of the action potential and contraction of small bundles show that the peak of contraction coincides more or less with the onset of the steep slope of the repolarization wave. The duration of the total action potential

diminishes nearly proportionally to the changes in duration of contraction with increasing heart rates (300, 489). The time-voltage area of the action potential varies directly with the tension developed, in anoxia and pyruvate poisoning (509). Adrenaline, the most powerful activator of contraction, increases the action potential area (508) and lengthens the plateau (Trautwein, personal communication), but both only to a rather small degree and primarily in damaged fibers. Nevertheless, it is surprising to what degree mechanical and electrical changes may vary together. A further example of this may be seen in the effects of acetylcholine, which depresses both the action potential and contraction in nearly proportional amounts (433).

In general, these correlations are overruled by the complete separability of action potential and contraction. Fleckenstein (20) argued that the mechanical state changes in close relationship with the membrane potential of the fiber. Such correlations cannot be found under all conditions. Neither is the amplitude of the action potential proportional to the strength of contraction (433), nor does a thorough correlation exist between the duration of electrical and mechanical events. A normal ECG may be found in hearts with almost no mechanical contraction although the reverse is never found! Under the influence of low temperatures, a complete dissociation between potential and contraction occurs: the plateau can be fixed for a long time in total depolarization, while the heart relaxes (426). On the other hand, using an externally induced depolarization, the membrane can be depolarized together with a synchronous contraction lasting for about 2 sec (286). There may be, but there need not be, a strict electromechanical correspondence. This may be seen under various concentrations of Ca; an increase in calcium increases the mechanical contraction strongly with an unchanged action potential (328). These few representative data indicate that in spite of an unquestionable relationship between action (membrane) potential and contraction, secondary events may interfere with an electromechanical coupling. This is the reason why correlation between electrical and mechanical events is so extremely complicated.

14. VARIABILITY OF THE ECG

The wide range of "normal" values of all electrocardiographic data is obvious in the figures of tables 3 to 9 (see section 10). This variability may be understood easily by reconsidering the generation of electrocardiographic potentials. The strongly diverging excitation waves cancel their respective fields to such a degree that even small individual differences or small changes in the spread of excitation lead to large differences in the potential pattern. The relative constancy of QRS during life indicates that only slight changes occur in the spread of excitation, because QRS is strongly bound to structural peculiarities of the heart. Only the T wave shows a high variability with nearly all variants: during daytime, food intake, bodily work, gas exchange, emotional state, etc. The variability of T can always be related to metabolic or chemical changes, and hormonal influences. The independence of changes in QRS and T, statistically proven (454), is therefore not surprising. The number of observations is so great that a quotation of special papers is impossible in this review. Only some recently published literature can be listed. The textbook by Lepeschkin will be a perfect guide to the originals.

The Individual Properties of the ECG

Individual variability may be regarded as to the interindividual and the intraindividual variations of ECG. The same person shows changes in the magnitude and direction of the various vectors with time which are at least of the same order of magnitude as those revealed by interindividual comparisons (454). After an interval of 1 week or 1 year, the variability is similar and amounts, in the horizontal plane, to 19° for 1 week interval, for the spatial QRS in conventional leads. The same angle varies interindividually by only 22°. It may be argued that the variability of the electrode positions is one of the main causes. In the whole, the ECG remains fairly constant, concerning angles and general pattern, in the same person over many years (170). Naturally, the influence of the heart rate on the ECG should be taken into consideration in all such comparisons. A factor of heredity in the determination of the ECG has often been claimed, on the basis of investigations on uniovular twins, but the results seem at best uncertain (115, 532). A somewhat curious individual factor of the ECG has been found in some colored people, who show persistent or transient T wave inversions in precordial leads, as an apparently "normal" variant. An exaggerated vagotonia may be the cause (507). [For literature, see (376).]

The diurnal variations are mainly due to the shift

in autonomic tonic innervation. They concern primarily the T wave. The type of change is subject to disagreement. Perhaps it is maximal in the afternoon to midnight (186). These variations are much higher than the changes of T during respiration, but a strict correlation with daytime records is not always present. A shift in the subjective daytime (changing the simulated diurnal cycle) had no influence on the variations of T (117). Food intake leads to some effects on the T wave, which decreases (439) and causes an increase in the R wave and a shift to the right in its axis (451). All these influences are maximal in patients with neurocirculatory disturbances (186).

Changes in the Course of Age (32, 52, 138, 165, 270, 326, 346, 452, 520)

The influence of age on the vectorial data has been mentioned already in section 10. There are some general trends in these variations in the course of age, the electrical axis of QRS shifting to the left, but by no means gradually or constantly. After the first year of life, the axis has reached a somewhat stable position (α in the frontal plane averages 60°). In the newborn child, α has a value between 120° and 150°, which corresponds to the relative hypertrophy of the right heart. In the horizontal plane, the axis shifts from an anterior direction toward the back, but also changes from posteriorly directed positions into less markedly posterior positions are reported (456). The vector having passed its acute changes of position in the first year, the elevation (angle α of Einthoven) becomes smaller year by year. This shift corresponds fairly well with progressive anatomical preponderance of the left ventricle, the weight of which increases continuously. Perhaps the rising blood pressure plays a role in this connection. The maximal vector of T does not change its position as much with increasing age as QRS does, though the average shift is in the same direction (76, 456).

There is almost no separate feature of the ECG which does not change some during a lifetime. The QT duration increases gradually, T decreases, the PQ interval and the duration of P increase. Some of these changes are due to the marked decrease in heart rate during the first two decades of life, but there are real influences of age remaining, even after correction for the frequency shift has been made (346). The QRS duration is remarkably long even in very small hearts: in the newborn child about 0.04 sec. The amplitudes are nearly those of adult hearts, if one disregards the difference in vector position. The reason is obvious: the relation of heart diameter to thorax diameter remains more or less constant during life. The duration, however, depends upon the velocity of the excitation wave, which increases with the fiber diameters and therefore accelerates with the growing heart [(58, p. 83), and see table 2].

15. VARIOUS INFLUENCES ON THE ECG

The ECG is influenced directly and indirectly by all agents which vary the frequency of the heart, the autonomic innervation, the time pattern of the action potentials, or the spread of excitation, as to its pathway and/or its propagation velocity. Very few agents are known to influence the factors which determine QRS, whereas changes in T are most common. The reason obviously is that the plateau of the monophasic action potential is extremely sensitive to all kinds of influences, because drugs, ions, hormones, temperature changes, etc. vary the action potential pattern considerably, perhaps by changing the cellular metabolism. In all such cases it is decisive to know if and to what an extent these influences are acting inhomogeneously on the heart. Every influence which does not act on all parts of the myocardium in a similar manner will alter the degree of inhomogeneity of the repolarization and thereby alter the ventricular gradient.

Some general remarks may be made in advance which might contribute to a better understanding of the various influences on the ECG. It will be shown in the following pages that most of the effects may be due to a very simple basic phenomenon: the change of ion permeability. A simplified picture of the depolarization and repolarization mechanisms may be given as follows. The magnitude of the action potential depends on the ion battery, which, in turn, depends on intact carrier mechanisms or ion pumps, which restore the ion balance as soon as it is disturbed. Every increase in extracellular potassium leads to a better and earlier repolarization; every improvement of a potassium shift into the cell lengthens the plateau. Every decrease in the intracellular potassium acts in the same direction as an increase of intracellular sodium. Acetylcholine seems to augment the potassium permeability during systole, thus reducing the plateau via an increase in the external potassium. Adrenaline seems to augment primarily the anaerobic metabolism, thus perhaps decreasing the external potassium by an improvement of potassium intake

into the cell. As the metabolism acts in the same way (perhaps by producing more intracellular hydrogen ions which in turn exchange with external potassium), a sequence of events is possible which may explain, at least to a certain extent, the multifold actions on the ECG. The picture given here is neither complete nor fully understood as far as the mechanisms acting are concerned (for detail see 162, 488, and the preceding chapter). In particular, the action of potassium brought into the heart from outside is much less marked than would be expected if the changes in repolarization were brought about by an accumulation of potassium which left the cell during the systole (512).

Bodily Work

One of the best known influences on the ECG is that of bodily work (40, 59, 311, 381, 421, 455). Its most characteristic consequences in normal hearts are a shortening of the QRS complex and of the A-V-conduction time, beyond the effect of the rising frequency. QRS always shows a decrease of at least 2 msec after heavy work. The relative QT duration (corrected for heart rate) is lengthened at first and shortened in the second phase of exercise, an effect to be observed to a maximal degree in athletes. The amount of such changes during and after exercise of course depends mainly on the amount of work performed. A widely accepted test is Master's two-step method. With such a standardized exercise, in a group of healthy persons at the age of 50 to 60, the maximal momentary spatial QRS and T vector changes show a posterior rotation of an azimuthal angle of $-6°$ for QRS, $-2.4°$ for T (average values). In the frontal projection, the maximal QRS vector is shifted to the right, the Einthoven angle showing an increase of 2.4° in QRS, 8.8° in T (455). In normal young persons, ST is never depressed (333), though in older persons a slight ST depression seems to be the rule. T is depressed nearly always in moderate exercise. During heavy (anaerobic) work (running on a treadmill), the maximal T vector increases remarkably (to 165% of its initial value) and rotates forward (20° immediately after work) and to the right (280). The difference in the behavior of T after moderate and heavy bodily work is obvious. In the latter, apparently strong inhomogeneities occur, shifting the vector direction and indicating that the ventricular gradient must rotate anteriorly and inferiorly, i.e., in a direction which is mainly identical with its normal position. The conclusion may be drawn, therefore, that the normal inhomogeneities are merely exaggerated by the exercise.

These effects most probably can be interpreted on the basis of changes in the autonomic tonic innervation on the one hand, or the oxygen supplied on the other. The strong increase in the sympathetic tone during work, indicated by the augmentation of frequency, leads to a decrease in all time factors (duration of QRS, QT, A-V-conduction time). Especially in well-trained persons, the diminution of the very strong vagal tone of the heart leads to exaggerated effects. The oxygen lack adds a second effect, increasing, for example, the antagonism between inner and outer layers of the ventricular wall insofar as the augmented oxygen requirement increases the normal differences in oxygen supply between these layers. If certain parts of the myocardium are suffering from a relative coronary insufficiency, the increased oxygen requirement magnifies this local oxygen lack, leading to local damage of the well-known coronary type, and revealing vectorial shifts of the ventricular gradient which point, in such cases, to the location of the oxygen deficiency. This can be clearly distinguished by the abnormal position of the vectors as compared with the usual effects of exercise.

Anoxia, Hypoxia, Carbon Dioxide

The effects of blood gases on the ECG are intricate (50, 148, 470, 474), for the same reason as is the influence of bodily work. Several mechanisms are affected, cellular metabolism as well as the CNS centers, the latter inducing marked changes in the autonomic stimulation of the heart. The breathing of low oxygen concentrations has been used as a suitable test for coronary insufficiencies, although the effects of breathing CO_2 and even high oxygen pressures are nearly identical (522). This indicates that the influence of blood gas concentration may act unspecifically or even indirectly. Particularly CO_2 seems to act more on the circulatory centers than on the heart itself, because vagotomy greatly reduces all effects of CO_2. However, a small effect persists which is therefore apparently of peripheral or sympathetic origin. The use of hypoxia as a test for coronary insufficiency may be understood on an historical basis. From the viewpoint of the physiologist, hypoxia alone does not sufficiently imitate the events in coronary diseases, where ischemia (i.e., simultaneous hypoxia and hypercapnia) is obviously the traumatic agent. If a dog is artificially ventilated with low oxygen tension, the mechanical performance of the heart does

not change for minutes, as in breathing CO_2 at even extremely high concentrations. The combination of hypoxia and hypercapnia, however, leads to severe cardiac failure in a relatively short time. If the CO_2 content of the perfusing fluid of an isolated cat's heart is increased, the T wave is heightened, even if the electrolyte composition of the fluid is kept constant. A reduction of coronary flow influences T in the same direction (493). Oxygen lack (by breathing air with low oxygen tension or by breathing at high altitudes) has been introduced into clinical diagnosis by Levy. It primarily influences T, and in cases where a latent coronary insufficiency is present, the vector of the ventricular gradient shifts into abnormal positions (110). In the normal heart under severe oxygen lack, T is flattened or even (in complete anoxia) inverted, and the ST segment is slightly depressed in some cases; but it has been found that hyperventilation and the loss of CO_2 may be responsible to a degree for such effects, which disappear after adding CO_2 to the inspired air. This fact indicates the necessary conclusion that all influences of hypoxia are complicated: a direct metabolic impairment is overlaid with a secondary alkalosis, if respiration is increased. The central action, developing in three phases, brings an additional factor into play. In phase I of the central action, the heart rate is increased by increased sympathetic tone. The second phase is characterized by a sudden drop in heart rate, which is centrally induced as well, but by a prevailing vagal activation. Phase III is characterized by severe cardiac disturbances, as impaired propagation, ectopic rhythms, etc. Phase II and III are never realized under clinical test conditions. They may, however, occur spontaneously at altitudes near 5000 m. The PQ time and the QRS duration are shortened, due to a fast heart rate. These effects are the simple consequence of augmented central sympathetic tone.

Theoretical explanation of anoxic effects meets with considerable difficulties. We know little, at present, about how the ST and T changes are conditioned. It is obvious that the effects must be due to changes of the monophasic action potentials. The flattening of T could be due to a decrease in the inhomogeneities of repolarization. The action potential is shortened, the plateau definitely flattened under hypoxemia (70), both of which support our assumption, because flattening of the plateau indicates diminution of inhomogeneous repolarization. The ST depression, however, cannot be explained so simply. The question is whether ST and T changes are due at all to myocardial hypoxia. In experiments with dogs, ST and T changes did not occur unless the myocardial oxygen tension, measured polarographically, was considerably reduced (403, 539) and an ST depression was not found after an application of ergot alkaloids. At the beginning of such experiments in man the ST depression is maximal, but is apparently conditioned, to a degree, by psychical processes. We therefore may argue the ST and T displacements to be the consequence of a local action of adrenaline, which is well known to augment all metabolic processes in the heart, and thereby influence the action potentials. Oxygen lack induces this adrenergic effect centrally and is supplemented in this action by other centrally activating factors. Peripheral oxygen lack fosters this adrenergic effect. If coronary flow is insufficient, these factors are strengthened so that they bring about a severe change of ST and T under conditions which would not normally lead to marked electrocardiographic changes. [For detail see (58, p. 242).] Anoxic effects therefore may be due to two completely different mechanisms: one central, acting through the sympathetic innervation; one peripheral, acting through impairment of metabolism. Both mechanisms will be discussed in the following pages.

Influence of Autonomic Innervation on the ECG

We here refer only to some questions of interest in clinical application of our problem [for literature see (47, 273, 312, 361)]. There is a very reliable indicator of the autonomic innervation available: the heart rate. Decrease in heart rate indicates an increase in vagal tone, but, unfortunately, neither increases nor decreases in the sympathetic tone are always reflected in the change of rate, because the pacemaker is preponderantly influenced by the vagus. We do know of certain reflex conditions, e.g., the central action of CO_2, where both vagus and sympathetic are activated, as revealed by their augmented action potentials, but only the typical vagal bradycardia is effectuated. There are still other factors contributing to a degree of uncertainty about autonomic effects on the ECG. First, decisive experiments have been made only with animals, for obvious reasons, but most animals have negative T waves which scarcely can be compared with man. If, in an experiment, the autonomic nerves are reflexly stimulated, the simultaneous activation of both vagal and sympathetic fibers can be scarcely avoided. Pharmacological blocking or stimulation are by no means as specific as many people seem to believe, and most of the blockers have an action of their own, e.g., as vasoconstrictors, thus inducing an

additional anoxic effect. Besides, most hormones or drugs act in a multifold manner: e.g., noradrenaline constricts vessels and induces a reflex bradycardia via a vagal activity. The only influences strictly referable to the autonomic nerves and their hormones are those on the single cell (see Chapter 12 by Scher). Here adrenaline and the stimulation of the sympathetics lengthen the action potential somewhat, although most probably only in damaged fibers, and steepen depolarization; whereas acetylcholine and vagal stimulation shorten the action potential, especially the plateau, and slow depolarization. With both effects, however, it is difficult to explain the action on the whole heart.

There are some additional and comparatively simple effects on the spread of excitation: the vagus decreases the propagation velocity, and therefore lengthens the P-Q time and the QRS duration. The sympathetic acts antagonistically, though to a comparatively feeble degree. The relative Q-T duration is unchanged or somewhat lengthened by the sympathetic. The vagus is said to shorten QT, but only relatively and apparen ly indirectly. The amplitude of QRS is increased bty the vagus and decreased by the sympathetic, as a consequence of lower or higher synchronization and cancellation of all myocardial fibers, due to changed conduction velocity. Vagal inhibition of conduction results, in strong stimulations, in complete A-V block. In the case of a permanent augmentation of vagal tone, as seen in athletes, the P-Q interval may be markedly lengthened up to 0.5 sec. The discrimination between such functional states and abnormality is easy: in functional vagotonia exercise reduces the interval to normal (102, 380).

The influence on the T wave is rather complicated, because it is difficult to isolate pure effects. Nevertheless, it is probable that the vagus augments and the sympathetic depresses the T wave. The vagal effect may be imitated by acetylcholine, and in a dog's heart is independent of changes in blood pressure or heart rate (324). These effects remain difficult to understand, because acetylcholine shortens the action and flattens the plateau, which should lead to a decreased amplitude of T. As the vagus does not enter the ventricular muscle mass with sufficiently numerous fibers, the effects of acetylcholine (which may easily penetrate into all parts of the heart) and vagal stimulation should be treated separately. It could be argued that the reflex vagal effects may be associated with a diminution of sympathetic tone. But sympathectomy does not imitate the vagal effect. So explanation of the vagal effects is impossible for the present. Sympathetic effects, however, are most probably due to local metabolic influences, which would explain the similarity between the influences of sympathetic tone and hypoxia on T. In cases of "pheochromocytoma," T may become inverted, as in severe anoxia.

The influences of adrenaline or noradrenaline are similar if not identical to those of sympathetic activity. Some details of the action of adrenaline have been mentioned earlier. Adrenaline and acetylcholine are, like their respective nerves, antagonistic and cancel their effects if given in a ratio of 10:1; adrenaline exerts the much feebler action (92). Both sympathetic (adrenergic) and cholinergic stimuli affect ion exchanges during depolarization and repolarization, as listed above. A peculiar effect of large doses of adrenaline is an augmentation of the U wave, which may be due to strong afterpotentials (152), not yet analyzed in full detail.

As a paradoxical action of acetylcholine and vagal stimulation, the asystolic atria become active under their influence. This effect is due to the repolarizing action of acetylcholine, so that generator potentials, badly damaged before, are restored (490).

Psychological Influence

Much has been written about psychological influences on the ECG. It may briefly be stated that such influences do exist, but can be interpreted as changes in the tonic autonomic innervation. The nature of such influences therefore can be predicted without difficulty and they resemble more or less the action of adrenaline (349). They are found in 40 per cent of all patients lying on an operating table (330) and may be elicited easily in hypnosis by suggestions of an anxiety-fear situation (107).

Metabolism

Metabolism has a decisive influence, especially on the T wave. The reasons are obvious. Repolarization depends heavily upon the ion pump and the velocity of relocating the potassium which passed the cell membrane during depolarization. These processes are brought about by cell metabolism. As a matter of fact, nearly all poisons and enzyme inhibitors shorten the action potential (510), in the same way as hypoxia, and most probably by permitting an augmented external potassium concentration (Trautwein, personal communication). Therefore, it is not surprising that the T wave changes rather predictably with heart

rate (is flattened in increasing rates), though the rate change may be caused by very different agents (463). Metabolism governs the actual effect. Monohalogenic acids act about in the same way. The plateau vanishes completely and the ECG consists therefore only of a diphasic curve like those of the action potential of skeletal muscle (331). How such marked effects are produced remains imperfectly understood, but may involve blocking carbohydrate metabolism, thus blocking the energy sources responsible for the return of potassium. We know that every increase in the external potassium concentration accelerates repolarization, without increase in the membrane resistivity, a fact true only of heart fibers and contrasting with the opposite behavior of resistivity in skeletal muscle and nerve. There are still some quantitative difficulties in the explanation of metabolic and other effects, as mentioned previously.

The energy metabolism has a second effect: the ion pump has to remove the Na from the interior of the fiber. Since the sodium influx into the fiber generates the depolarization potential and thereby QRS, the QRS complex should be subject to a certain degree of metabolic influence. This really is the case to some extent. In general, however, depolarization is extremely stable compared with repolarization and plateau. Changes in T may be elicited by a simple procedure as the intake of 100 to 200 g of glucose, which leads to a flattening or even an inversion of T (495). This action is not identical with the action of a concomitant hypopotassemia (494). The potassium content of the fiber seems therefore not to be the only determinant of metabolic influences. In hypoglycemic shock much more severe alterations occur, such as voltage increase and prolongation of QRS, S-T depression, flattening or inversion of T, lengthening of QT, and increase of U (235). Here, conduction seems to be altered together with a change in repolarization.

The result is that metabolism influences T in a comparatively predictable manner. The effect to be expected in most cases of impaired metabolism would be a flattening of the plateau and a shortening of the potential, as is seen in low oxygen tension. Flattening would lead to a different behavior of the T area, which in its "elementary" part would remain unchanged, but with the potential differences distributed over the whole S-T interval. It is extremely unlikely that the inhomogeneities should remain unchanged. If, at a given time, the potential is reduced, an inhomogeneity of the potential pattern cannot be of the same amount, leading to reduced potential differences and diminution of the ventricular gradient. Small magnitudes of the gradient, therefore, may be due to metabolic disturbances of an over-all distribution. Any time that a flattening of the plateau happens only in certain parts of the heart, the whole picture is reversed: the inhomogeneities are augmented, the gradient increases, and its axis is shifted. It must be said, however, that these conclusions are true only to a degree of probability, for it may occur that a local process changes the plateau in such a manner that the "normal" inhomogeneity is counterbalanced by the abnormal, and the gradient decreases. The differentiation between localized and general trauma therefore always remains uncertain, but it has been stated in clinical experience that local events influence the Q vector so that analysis may reveal an additional abnormal vector of inhomogeneity, which points directly to the site of this disturbance, e.g., an infarct (294, 514).

The picture of metabolic influences given in the preceding pages is incomplete in one way. In case of local disturbances of blood supply, the ECG changes so that a gradient will be recorded (as after infarcts), the position of which can only be explained by assuming that the plateau is lengthened in the damaged region (58, p. 301). We have neither experimental evidence for this assumption, nor any other explanation for such ECG patterns. The postextrasystolic T wave changes also raise some unanswered questions (319, 345, 484). T is changed after extrasystolic beats, and its vector is shifted to the left and upward (α becomes more negative), even if the interval between extrasystole and the following beat is lengthened. Only part of such changes can be interpreted as the consequences of prolongation of the interval.

Ions

The influence of ions (47, 103, 254, 259, 384) on the ECG of the whole heart is not fully clarified, in spite of a good understanding of their effects on a single heart fiber and its monophasic action potential. There are several reasons which account for the widely differing results. *a*) In an intact animal or in man, sufficiently large changes in the plasma content of certain ions are difficult to achieve and, if they are present, they influence not only the action potential of the single fiber, but also the conduction, thus leading to a changed pattern of interaction of the various fibers of the heart. *b*) All changes in ionic concentration produce side effects on other functions, such as liberation of hormones, activation of autonomic nerves, disturbances of the water equilibrium. *c*) In many clinical cases, not one but several ions changed

their plasma concentrations at the same time. *d*) Even the action of different ionic plasma concentrations on single fibers varies according to the type of fibers investigated (auricle, Purkinje fibers, myocardial fibers).

In most cases, in the human heart, only moderate changes of the ECG have been described. Among these, the effects of calcium and potassium prevail. The QRS vector is comparatively stable, remaining unchanged by calcium lack (100), but QRS is prolonged by an increase in plasma potassium (254). Here, as in other influences of potassium, the absolute plasma concentrations do not show a close correlation with the shift in ECG, which depends more or less on the ratio between intracellular and extracellular potassium, as altered in dogs (301). In human hypopotassemia QRS is nearly unchanged, as is also true for changes of Ca, Na, Cl, and inorganic P. In the rabbit heart, however, the results are somewhat different (477). Only a severe sodium deficiency prolongs the human QRS, because the rapidity of depolarization in single fibers is determined by the sodium influx, and is diminished by decreasing external sodium. This leads to a reduced conduction velocity and prolongation of all conduction times, QRS included.

The QT duration is unchanged by alterations in the plasma content of Na, K, Cl, and bicarbonate; calcium deficiency prolongs QT (47, 135, 391), although in man in a not very impressive manner (254). An increase of calcium above the normal level increases QT even more. Potassium prolongs QT if its concentration rises, but here, too, it is not the absolute concentration that determines the effect, but the ratio between intracellular and extracellular potassium (301). An antagonism between calcium and potassium exists only in a very narrow band of concentrations (135).

The T wave is also rather sensitive to ionic balance. T is augmented by increased potassium concentrations, with tent-shaped T waves in severe potassium intoxication. Such variations of T occur as soon as the plasma content exceeds 6.5 meq per liter (254). A diminution of plasma potassium, especially if the quotient between cellular and extracellular potassium is raised decreases T in most cases (254, 301). Changes of Na, Cl, and P, within physiological limits, produce no distinct change in T (254); however, a rise in calcium may depress it somewhat, or even invert it and round its contour. Decrease of calcium may act in a similar manner, sometimes decreasing T but increasing it in other cases. This strengthens our suspicion that so many of the clinical findings are indirect, complicated by other events, and scarcely predictable from the effects on the single fiber.

All these effects are so inconstant and depend in such a complicated manner on the concentration gradients across the membrane of the myocardial fibers, that only in hypopotassemia is a close correlation found between the plasma concentrations and the form of the ECG (172, 476). But even the effect of potassium is complicated concerning its action on the U wave: U is strongly augmented by hypopotassemia, as it is by adrenaline (see above), so that a prolongation of QT may be simulated. In the whole, we may conclude that the ECG reveals only the presence rather than the special form of an ionic disturbance (136).

Some special remarks may be made on the mechanism by which calcium acts. The lower the calcium concentration, the higher is the sodium influx into the fiber during depolarization in nerves (208, 511), and most probably also in heart muscle fiber. It is assumed that Ca interferes with the carrier mechanism which supports the Na influx. An increase of calcium, therefore, leads to a slowing of the rising phase of the action potential and thereby slows down the conduction velocity, lengthening PQ and QRS in a manner similar to that of sodium deficiency. The role calcium plays in the repolarization process is very uncertain. Results of experimental changes in Ca concentrations on the action potential are contradictory. There is some evidence that, within physiological limits, Ca does not influence the action potential at all, but greatly changes the electromechanical coupling (328, 511, 513) and most probably the conduction in the specific system.

Drugs

The action of numerous drugs on the ECG has been described in so many papers that we can refer only to the review by Lepeschkin concerning the details (47). Drugs influencing the autonomic innervation, or transmission in general, exert the same influence as that part of the autonomic system which they do not block, or which they do activate. (There are exceptions, however.) The action of cardiac glycosides requires special discussion (53). Digitalis depresses T, may even invert it, and leads to a depression of the S-T segment. In this action, four stages may be differentiated: the stage of T depression, of S-T depression, of aggrevated S-T depression with a steep upstroke of T, and of diphasic T (47). These changes, which may resemble a pathological ECG, have been

explained as the result of an increased vagal tone, because they disappear partially or wholly after atropinization (302). With strophanthine, similar though less marked effects occur. The effects are probably of peripheral origin, for the action potential is shortened and the plateau flattened. This is the consequence of a reduced potassium and sodium permeability of the muscle fiber (174). The conduction velocity is decreased for the same reason, so that the QRS duration and the P-Q interval are increased until a complete atrioventricular block exists. Although the ECG looks rather abnormal, these events cannot be interpreted as an impairment of the cardiac function as long as no blocks occur.

Quinine and quinidine have a peculiar action, in that higher concentrations strongly reduce the conduction velocity. The result is an ECG looking like a "bundle branch block," which in reality shows only an over-all slowing in the spread of excitation. The T wave may be greatly distorted, showing a characteristic widening of its summit, or even notches. The relative Q-T interval increases as a consequence of disturbed conduction. Strophanthine abolishes these effects very quickly (485).

Hypothermia

The importance of hypothermia in modern surgery justifies a brief discussion of its influence on the ECG. There is much literature on this topic, which is nearly completely referred to by modern authors (185, 222). As had been stated long ago (329), hypothermia induces a picture quite similar to that of ventricular blocks with QT prolonged much more than QRS which might be due to the prolongation of the monophasic action potential (426), but the results depend on individual factors. ST may be elevated, preferably in lead II and III, and pronounced only within narrow limits of body temperature (32°–34° C). T is augmented in such cases (222), its vector rotated clockwise in the frontal projection (220). A very unusual pattern of QRS is seen in a series of cases: QRS, which, by the way, remains surprisingly short and seldom exceeds 0.05 sec from Q to the peak of S (185), is followed by a very high deflection, mostly in the same direction as R, and increasing with falling temperature. This deflection, well known for many years, but nevertheless called "Osborn-wave" by some authors, has no connection with atrial repolarization, as has been argued, and is not an indicator of imminent ventricular fibrillation. It becomes very high at the very moment when T becomes inverted. The mechanism of this deflection is unknown. It is not conditioned by an acidosis (185). The degree of abnormality depends completely, of course, on the temperatures reached in cooling, the QRS duration increasing gradually up to 0.4 sec and QT to more than 2.0 sec in dogs in extremely low temperatures, down to 3° C. Even after cooling to 1.5° C, all dogs survived (496).

Acceleration

If a subject is exposed to acceleration forces of 3 to 4 g, surprisingly few effects are observed. An increase in pulse rate apparently is induced by baroceptor reflexes, but only minimal effects on the ECG can be observed. The electrical axes of QRS are shifted in some cases up to 25°, but in most cases the deviations are much less, and do not surpass deviations of the axes seen in deep respiration (133, here the older literature).

Further data on how the ECG is influenced by various items may be found in Lepeschkin's textbook.

The Fetal ECG, and the ECG in Pregnancy

During pregnancy, the maternal ECG (39, 47, 542) is mainly determined by the position of the heart, which shows a left axis deviation according to the shift of the anatomical axis. The axis deviation is, however, very small in most cases (15°). Q_{III} therefore is deepened. Major changes of the ECG in pregnancy, which cannot be related to the shift of the anatomical axis, are always to be regarded with suspicion (39, p. 475).

The fetal ECG can easily be recorded during the fifth month of pregnancy but never before the fourth month (47). The electrodes have to be put on the belly of the mother, and bipolar electrodes are the best. A bipolar derivation in the craniocaudal direction just above the symphysis seems to be most successful, but vaginal electrodes are also useful. The position of the fetus may be determined quite correctly by vectorial analysis (309), and twins can be identified as they were in one case after only 16 weeks of pregnancy.

16. THE THEORY OF NORMAL AND ABNORMAL RHYTHMS (60, 66, 71, 395)

The Pacemaker

The excitation of the heart starts in a circumscribed region called the pacemaker, which is normally the

sinus or Keith-Flack node. The electrical process leading to the generation of the excitation wave, the "generator potential," has been described in the preceding chapter. In regard to the whole heart, the problem rises as to how the pacemaker region is determined. Obviously, the region with the most frequent rhythmic activity commands the rhythm of the heart. Since all parts of the specific system may develop spontaneous activity (whereas the ordinary myocardial fibers never reveal a generator potential under physiological conditions), the sinus must have the most rapidly developing generator potential or the lowest threshold for the amount of depolarization required for activation, thus leading to the earliest local excitation following a previous beat. This implies, however, that every part of the heart with potentially automatic activity has been activated by the previous excitation wave, and that thereby all local membrane potentials have been depolarized and repolarized to the resting level. This being the case, every fiber of the heart with automatic rhythmic activity is forced to start at the same time from the same resting state. Thus the more slowly a particular local generator potential is developed, or the higher its threshold, the more time it will require to generate a new impulse. Local pacemakers beat more slowly the more distant they are from the sinus venosus. If the sinus is totally removed, the heart beats with a frequency reduced to about 30 per cent of the normal, although the often-quoted close relationship between the frequency and the site of local ectopic pacemakers cannot be cited here with conviction (275).

There are possible and actual conditions under which a certain region of the heart is not completely depolarized by an arriving excitation, so that this part of the heart occasionally escapes total depolarization, thus developing a generator potential which might start a local excitation at a very early moment after an ordinary beat. If this wave meets nonrefractory surrounding tissue, the next heart beat starts at this point and an extrasystolic or parasystolic beat appears. The basic mechanism which apparently protects that region of the heart from being excited is called an "entrance block."

There are several mechanisms which may possibly shift the pacemaker region temporarily away from the sinus. The first is well known and consists of a new balance between the steepness of the generator potential and the local threshold (488, 490). If, under any circumstances, a part of the heart develops a swifter diastolic depolarization, this part of the heart may become the pacemaker, if thresholds remain the same elsewhere. The strong dependency of the generator potential on the local concentration of adrenaline and acetylcholine makes it easy to explain why every change in the tonic autonomic innervation easily leads to such a shift. Most probably, right in the sinus region, the counterbalancing influence of sympathetic and vagal innervation leads to pacemaker shifts over small distances. Such shifts have been directly observed (58, p. 377; 180, 223) especially under the influence of the heart nerves (519). The various parts of the auricles are apparently innervated with a different density by vagal and sympathetic endings, so that every vagal innervation slows down the generator potential at the sinus pacemaker, thus enabling another part of the auricle to command, with its quicker generator potentials, the start of the next excitation wave.

Such fluctuations in the generator potentials apparently occur all over the heart, depending on the fluctuations in autonomic nervous activity. Other influences, as metabolic ones, will act in a similar manner, so that in longer periods the pacemaker may shift about. In normal hearts, such events are rare; in hearts with local disturbances of metabolic or ionic equilibria, however, such things occur much more easily. The time between the preceding stimulus and the moment when the membrane potential reaches the threshold may be called the local "pacemaker interval." Changes of this local pacemaker interval are then responsible for the shift of the pacemaker position, because that region takes over the pacemaker function which at this moment has the shortest local pacemaker interval. Shifts of this kind may generally be regarded as a "dissociation with interference" ("Ersatz-Rhythmus"), because two or more dissociated, i.e., independent, centers with undisturbed local frequencies interfere in playing the pacemaker. In normal hearts, such events are rare or absent, as all other parts of the heart have a much slower local rate of generator potentials than the sinus.

This is valid only in hearts in which no entrance blocks are to be found. Whenever such a block occurs, it is only a matter of chance whether the blocked part of the heart or the normal pacemaker will command the next beat. If we call the normal pacemaker "nomotopic," every shifted pacemaker "heterotopic" or "ectopic," a special form of interference is to be expected, depending on the special circumstances given at the moment of investigation. Every rhythm determined by the interference of two or more pacemakers is generally called "parasystolic," the related arrhythmia "pararrhythmia." The characteristics of

parasystolias are that the coupling of several ectopic with nomotopic beats varies, so that the duration of intervals between two consecutive ectopic beats stand in simple mathematical relationships to one another (though this may vary a bit according to changes of ectopic frequency) and that combination or fusion beats are present (60). (See below.) It should, however, be kept in mind that no explanation for what we call an entrance block is available, but that without the assumption of such a block the whole theory of parasystoles is applicable only in case of changing local generator frequencies, i.e., mainly nodal or ventricular tachycardias, which are comparatively rare.

Dissociation and Interference

In case of two or more simultaneously active pacemakers, the normal sequence of the excitation process in sinus, atria, A-V node, and ventricle may disappear. Every interruption of that sequence is called a dissociation. This dissociation may be accompanied by a complete block of the dissociated parts of the heart, due to a disturbed conduction or to unilateral conductivity (e.g., lacking the retrograde conduction from ventricle or A-V node to the auricle). In such a case the dissociated pacemakers cannot interfere and will beat completely independently of each other (dissociation with complete block). As soon as conduction takes place, an excitation wave starts from every pacemaker, so that, in certain cases, the excitation waves meet each other on their way and obliterate each other. In other cases, the more frequent pacemaker forces the other one into a refractory period and, in the simplest case, induces a complete depolarization of its rival which then remains inactive until, by a change in its generator mechanism, it develops a shorter local generator interval and thus becomes the leader of the interfering pacemakers. If, however, the slower pacemaker is protected by an entrance block against the excitation wave coming from its rival, very intricate conditions arise and the pattern of rhythm developing then can scarcely be predicted (dissociation with interference and entrance block). There is a third possibility of dissociation found when the conduction between the two pacemakers varies from beat to beat as a result of delayed conduction or even a partial block, occurring temporarily and disappearing after longer diastolic intervals. Such changes of conduction are due in most cases to changes of refractoriness, of which the well-known Wenckebach periods are an example.

If during disturbances of rhythm a heterotopic pacemaker suddenly becomes active, it "escapes" from the rhythm imposed on the heart by the ordinary pacemaker. Such an escape means either that the primary pacemaker suddenly failed to discharge, or that a hitherto absent entrance block suddenly came into action. In the former case, the arrhythmic ectopic beat would appear later than the normal beat would have been expected. In the latter case, the ectopic beat would appear too early ("premature"). If one considers that possibly a pacemaker region may not only be blocked by an entrance block, but may be unable as well to excite its environment by what is called an exit block, one recognizes that an immense number of varieties in disorders of rhythm and conduction is possible, which cannot be described here in detail.

Extrasystoles

It seems to be generally accepted that besides parasystolic disturbances of rhythms, completely different "true" extrasystolic beats do exist. Extrasystoles of this kind are always precipitated by a preceding heart beat. The question is whether such extrasystolic beats are caused at the site of their origin by a specific mechanism. Parasystoles are comparatively rare events, whereas extrasystoles with a fixed coupling to the preceding beat are often found in clinical cases. On the other hand, only the pararrhythmia can easily be explained by ordinary physiological events at pacemaker regions, if one disregards difficulties in understanding entrance block. No comparably simple explanation is available in case of true extrasystolic arrhythmias, because records of the action potential of single fibers do not support us, in case of true extrasystoles, with a simple mechanism like the generator depolarization during diastole. There are, nevertheless, several indicators of a common event at the base of both extrasystolic and parasystolic arrhythmias. The first is that pararrhythmias are converted in the same patient into true extrasystolias, with the same form of QRS for the extrasystolic beats, and therefore, most probably, with the same site of arousal of parasystolic and extrasystolic excitations (34, p. 612). Then, only regions of the heart with a clear diastolic depolarization (generator potential) usually develop extrasystoles. Adrenaline steepens the generator potential and strongly facilitates extrasystolic beats, as is well known. Anoxia (491) and stretch (173) both foster the development of generator potentials and elicit coupled extrasystoles. The same is true with

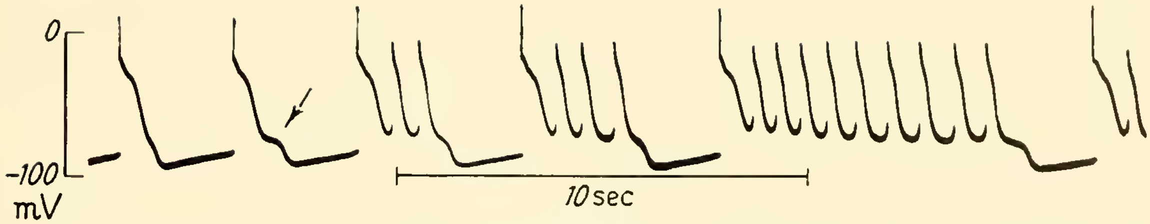

FIG. 66. Development of a paroxysmal tachycardia after aconitine in a strand of Purkinje fibers. After the third beat, a sequence of action potentials starts. They are elicited by a second plateau in the action potential (arrow) which develops rapidly in the beginning of the series, about 30 sec after the application of aconitine (0.1% in tyrode solution). Intracellular microelectrode. For theoretical explanation see fig. 67. [From Schmidt (425).]

aconitine (425), with which repolarization is slowed down shortly before the original resting level of membrane potential is reached, forming a kind of second plateau, from which an extrasystolic excitation is started (fig. 66). However, aconitine elicits extrasystoles in papillary muscles as well, though there are no pacemaker potentials there. Here, the concept of true extrasystoles seems to be reasonable. Adrenaline syncope is very similar, as judged from the ECG (190).

The explanation of all these facts offers some difficulties, because the "threshold" cannot be explained in a simple manner. We refer here to the preceding chapter, where the thresholds during the relative refractory period have been described. Usually the threshold is determined by the strength of a new depolarization necessary to start a new excitation wave (6, 70). But this definition may be unilateral in the sense that a threshold could be described as well as membrane potential changes necessary to stimulate, without any external stimulus. It is assumed that this membrane potential can be determined by short electrical stimuli, but it is by no means certain whether an automatically developed membrane potential necessarily must have the same magnitude to excite as these artificially shifted membrane potentials. The threshold most probably can be described fully only in terms of ionic events in the sense of the Hodgkin-Huxley theory, and even there certain assumptions have to be made about the properties of the membrane determining ionic permeabilities and conductances. At least, threshold is neither a certain membrane potential to be reached (even if it might differ with time) nor a certain electrotonic depolarization. Nevertheless, if we try to draw a threshold line like that in figure 67, this line does not indicate more than a formal statement of how far from excitation the fiber is at every moment. In such a formal schedule the thresholds are lowered in parasystoles as well as in extrasystoles, together with an increase in diastolic pacemaker depolarization. How both processes are

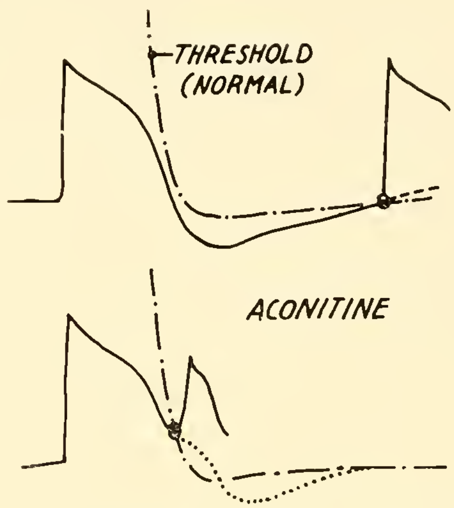

FIG. 67. Tentative explanation of fig. 66. *Abscissa*: time; *ordinate*: membrane potential. *Above*: the "threshold" of a normal fiber is shown. Threshold means in this case the membrane potential that must be reached to excite. *Below*: the threshold is unchanged, but the membrane potential crosses with its second plateau (dotted) the threshold line and leads to a new action potential.

linked together can scarcely be analyzed for the present. They both seem to depend on peculiarities of the membrane structure, though, just under the influence of aconitine, no permeability changes have been observed for K, Na, and Cl ions (425). If we assume this hypothetical basis, it merely depends on secondary or quantitative factors whether a parasystolic pacemaker comes into action or, at the same point, a coupled extrasystole appears so early in the repolarization process that the development of generator potentials and accompanying parasystoles cannot be detected. It is in this sense that we suspect extrasystoles and parasystoles to depend on the same basic process (58). It hardly can be doubted, however, that there are marked differences in form of the electrocardiographic patterns.

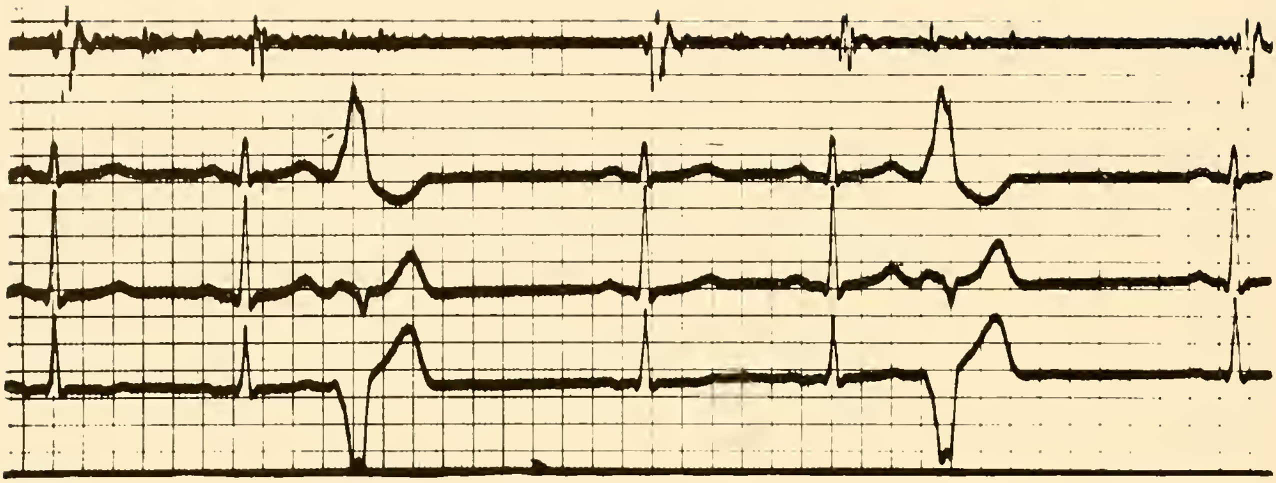

FIG. 68. Coupled extrasystoles after every second normal beat (fixed coupling). Extra beats most probably originating in the right ventricle. Trigeminus. The compensatory pause is somewhat too long.

The local disturbances giving rise to extrasystolic beats most probably are not uniform. A local impairment of cellular metabolism may lead to a local accumulation of potassium, thus lowering the threshold and shortening the fiber action potential. Perhaps an augmented sodium permeability of the damaged membrane may cause extra excitation. Such effects may occur under the influence of anoxia or of CO_2, near a hemorrhage, through an unspecific general impairment of a preparation, and after digitalis and stretch (68). If a generally augmented excitability, caused by these membrane effects, meets with a transient increase in excitability at the end of the refractory period (70, p. 59), an actual excitation is induced. Such a local augmentation of excitability may happen by putting a d-c electrode on the epicardium: with the anode(!) as the different electrode, coupled extrasystoles appear (504). This electrotonic precipitation may be the model of extrasystoles in infarcts, where the injury current may play the same role (214). Even the traction exerted by the contracting ventricle has been blamed for eliciting an extrasystole (392).

For the reasons mentioned, an extrasystole always follows a preceding normal beat at a fixed interval, as long as an ectopic focus is not spontaneously active, thus generating a parasystole. Only an "external" stimulus arising from a transient local disturbance may precipitate a single extrasystolic beat without such a coupling, but we could scarcely imagine the nature of such a local stimulus. The fixed coupling to the preceding beat is shown in figure 68. There is a second mechanism active in some cases. Every electric field developed by an excited muscle mass shifts the membrane equilibrium nearer to the threshold. This has been observed with nearly all excitable tissues (57, II: p. 349). Apparently, such an electrotonic excitation of adjacent fibers by the action current of normally excited fibers plays a role in the generation not only of extrasystoles but also of a premature excitation of ventricular fibers at the base of the heart, as in the so-called Wolff-Parkinson-White syndrome. It cannot be decided whether such electrotonic influences start from the His bundle (58) or from atrial fibers (64), but electrotonic influences are, at least, the probable cause of excitations in tissues which are already more than normally excitable as a result of local metabolic or other damage. Also, a constant injury potential, e.g., at the site of an infarct, may lead by its electrotonic effect to a locally lowered threshold with the precipitation of coupled (or even uncoupled, single) extrasystoles (68, p. 68). Two frog hearts, when put in close contact, will synchronize to each other, apparently by means of their mutual electrical fields (442).

Heart Rate, Tachycardias, and Paroxysms. Physiological Arrhythmias

The heart rate is the result of pacemaker potentials (see the preceding chapter and 488). We should like to mention here only the different mechanisms, by which the heart rate is normally controlled. There are neural, hormonal, and metabolic influences on the pacemaker. The neural influence is determined by the vagosympathetic balance and may strongly fluctuate,

with concomitant variations in heart rate, and central autonomic tone. Such fluctuations are due to central metabolic influences (CO_2!) and to a rather intricate coupling between blood pressure, baroceptors, and vasomotor activity. In respiratory maneuvers, for example, variations in heart frequency occur which surmount, to a certain extent, the ordinary baroceptor reflexes (334); but most probably, part of the respiratory arrhythmia is of central origin and due to irradiation from the respiratory centers (499). Even a 1:1 coupling between respiration and pulse rate has often been described and depends on reflex pathways from the chest (134).

Metabolic influences may be mentioned, because they might be regarded (as has been done) as a sign of reflex activity. Every dilatation of the atria may change the heart rate, accelerating the rate of the isolated heart in some (114, 483), but slowing it in other cases. We saw the heart rate decreasing in the denervated dog's heart during dilatation and under the influence of CO_2 and ischemia (unpublished observations). Even intracardiac reflexes have been postulated, as the sinus pacemaker is accelerated after pinching the ventricles in frog (440).

The amount of physiological irregularities may be measured by an index ["Rhythmiemass" of Schlomka (58, p. 344)]. To calculate this index, one measures in 16 consecutive beats the 4 longest and the 4 shortest intervals, and then takes the difference of their respective sums and divides it by 4. The rhythmicity of the heart varies from species to species, as far as it has been studied in cold-blooded animals (533).

Such bradycardias or tachycardias are by no means fully understood, though we may assume that the pacemaker potentials may account for them. The extreme tachycardias, however, found in paroxysms and often leading to atrial or ventricular fibrillation, cannot be explained with an ordinary pacemaker mechanism. As shown in figure 66 aconitine elicits a series of very frequent action potentials, which must have been started by the same mechanism responsible for the coupled extrasystoles and which, under certain circumstances, may be influenced into the production of such series of excitations. Obviously, the second beat in such a series, falling in the refractory period, changes the behavior of the membrane, so that an extremely frequent local spontaneous pacemaker is formed. Mechanical stimuli, for example, during catheterization, act in the same way (223). As soon as a part of the heart can no longer keep up with such a frequency, the muscle mass is divided into independently beating fragments and fibrillation occurs (see Chapter 12). There is no explanation available concerning what really happens at such poisoned pacemakers. The whole membrane structure must be disturbed. Perhaps Ca plays an important role in this connection (425). Every heart can be brought to fibrillation in this way, and no metabolic abnormalities are necessary, though a dilated heart is obviously more sensitive to fibrillation than a normal one (409). The generation of paroxysmal tachycardias in clinical cases is likewise unexplained. They are astonishingly regular in rhythm.

Periods. Alternans

As a rule, all beats from the same pacemaker resemble each other in their mechanical effect and action potential. In extrasystoles, the stroke volume and systolic pressure, as well as the action potential, are different from normal, but even here the monophasic action potential is nearly unchanged in many cases. Only after a very short interval is the action potential apt to be strongly diminished (433). Refractoriness may be prolonged in certain cases, so that, even with nearly normal intervals, abnormal beats occur. The refractoriness obviously differs in duration from point to point on the heart. Therefore, when ectopic foci are active, it may be only when the R-R interval is prolonged beyond a certain length in a sequence of normal beats that an ectopic extrasystolic beat can occur, originating from a pacemaker which remains refractory if it is too frequently depolarized (303).

There is another type of irregularity commonly ascribed to refractory phenomena: the Wenckebach-Luciani periods. They are characterized by a P-R interval which increases from beat to beat, until the moment when A-V conduction fails completely and a beat drops out. The equilibrium of the resting condition obviously could not be reached at the end of an interval, so that the next beat starts under somewhat impaired conditions. Raised potassium in the extracellular space could serve as an example of such impairment. But this simple hypothesis does not cover the facts, because, under such an assumption, a frequent change of the number of beats occurring between the "gaps" should be expected. We find, however, that the number of such beats, forming a "period," is rather stable. This means that some sort of an interference of two frequencies occurs, one of the two being determined by the frequency of a "functional" refractory period of the A-V conducting system (393). It seems easier to clarify the problem with a mathematical equation (393) than to explain

it in terms of physical conditions like membrane permeabilities.

The Wenckebach periods are an excellent example of what is called the formation of a period. "Period" here means that a given number of beats form a regularly repeated pattern (108). Periods of this kind may be found in the activity of every part of the heart and as ventricular extrasystolic periods as well. In such cases, one or two, or even more extrasystoles (bigeminus, trigeminus, quadrigeminus, etc.) are coupled with a normal beat, and the period ends obviously with a refractoriness (or exhaustion) of the ectopic pacemaker.

A peculiar variety of such periods is called the "alternans," which is of interest in this connection only as the "electrical alternans" (42, 60, 66). The term alternans is applicable only to such periods in which two different forms of an ECG or action potential alternate, but with a completely regular rhythm. This regularity, however, concerns only the rhythms of P or of the beginning of QRS. The behavior of parts of the heart beating later, during the conduction time from the A-V node to the utmost parts of the ventricle, cannot be stated in such records. It has been observed that cooling parts of a frog's heart leads to a mechanical alternans, obviously because the cooled parts of the heart are beating merely in a 1:2 rhythm as compared with the warmer parts (292). It is questionable whether basically different forms of a true alternans can be found, in which the single cell of the heart beats with a different amplitude of its membrane action potential, for reasons other than refractoriness. A true alternans has really been described in single cells with microelectrodes (290), so that for such a cell refractoriness cannot play any role. The mechanism of such an alternans is obscure and difficult to explain. Apparently some fundamental process responds in a 1:2 manner. In the whole heart, such events are never shown to exist. In most cases, a partial hypo- or asystole or an alternating disturbance in conduction will be found to be the cause of an electrical alternans (42). Partial refractoriness of the heart will lead to an alternating ECG pattern, if the restoration of the alternately beating parts is completed during twice the normal interval.

Besides this alternans, a pattern may be described in which the start of P and QRS is absolutely rhythmic, but the QRS form alternates on account of ectopic beats alternating in a 1:2 manner. This is a peculiar case of a coupled extrasystole, and as such is a "false" alternans, as is every bigeminus. The alternans patterns may be very complicated due to the great number of varieties possible in local refractoriness or fusion beats (313).

The ECG of Ectopic Beats

The ECG of ectopic beats is characterized by abnormalities conditioned by the abnormal spread of excitation. Hereby, the sequence of P and QRST may be changed, if the atria are excited by a backward traveling wave; or only P may be changed if the pacemaker lies between the atria and the ventricular myocardium near the A-V node; or QRST may be changed by an abnormal spread of individual fiber excitations along the ventricular wall (see fig. 42).

The diagnosis concerning the exact site of the acting pacemaker may be complicated in a single case, because P may be no longer discernible, being submerged in the electric events of the ventricular activation. Moreover, the pattern may change from beat to beat due to a change in refractoriness or to an interference of several pacemaker activities. The detail of such pictures cannot be discussed here and is of clinical interest only (516). There are, however, some facts to be mentioned which illustrate general physiological laws. The first is that after a premature beat the following interval is usually lengthened, so that the interval between a beat preceding and following the ectopic beat is approximately double that of the normal nomotopic interval (fig. 69). This prolonged postectopic interval is called the "compensatory pause." The mechanism of this pause is simple. The ectopic pacemaker starts an excitation wave running to both sides, antidromically as well as nomodromically. The antidromic volley somewhere meets either the excitation started meanwhile by the sinus, or—in case of a very early beat—the sinus itself before it becomes active. In the latter case (upper part of fig. 69), the sinus is excited by this retrograde wave and starts now with a new pacemaker potential, its start being somehow anticipated. The interval between the preceding and the following normal beat is less than twice the normal. In the former case (lower part of fig. 69), the antidromic wave meets the nomodromic wave started by the sinus somewhere between sinus and ectopic focus. Obviously, this will happen the farther from the sinus, the farther the ectopic pacemaker itself lies from the sinus. In ventricular extrasystoles, the retrograde excitation has to travel up the whole Purkinje system and His bundle, through the A-V node and the atria, which obviously takes much time. In this retrograde conduction time, the sinus has already started its next nomotopic excitation. Both waves meet in the middle

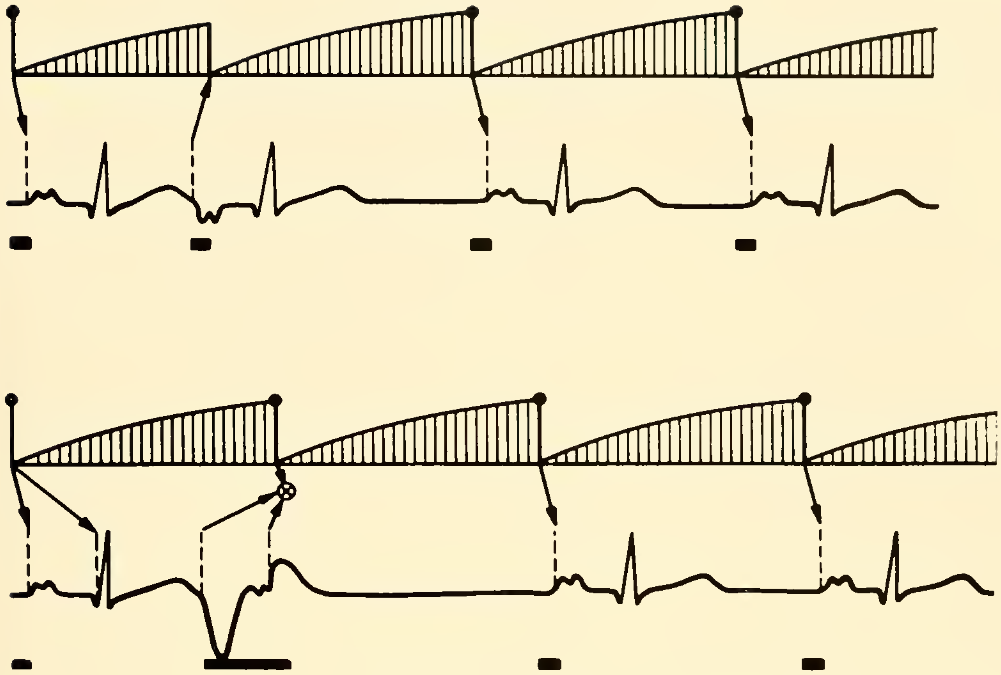

FIG. 69. Schematic drawing of the mechanism leading to the phenomenon of the compensatory pause. The distance between sinus and ectopic pacemaker is short in the upper picture (atrial extrasystole), long in the lower (ventricular extrasystole). In black brackets the time is indicated during which either the normal beat travels from sinus to the atria or from the ectopic pacemaker back to the sinus. When the antidromic volley reaches the sinus, the sinus pacemaker is stimulated and responds with an excitation, if it is not refractory. In any case, the status of membrane repolarization is brought back to a newly induced complete depolarization. The upper line in each picture indicates the local excitatory state of the sinus, which brings the sinus to excitation in reaching the threshold (black dots). If the sinus is prematurely depolarized by an antidromic volley from the ectopic center (*upper picture*), the phase of the sinus rhythm is shifted, the compensatory pause too short. If the sinus beats before the antidromic volley arrives (*lower picture*) both nomodromic and antidromic volley meet and cancel each other (*crossed circle*). The compensatory pause is correct; no shift in the sinus rhythm. [From Schaefer (58).]

of the atria, which leads to a complicated form of P. If the ectopic pacemaker beats in a very remote point of the ventricles, or shortly after the preceding normal beat, the nomotopic excitation may be just proceeding in the ventricle when the retrograde extrasystolic wave arrives, thus causing a ventricular activation which stems partly from the nomotopic, partly from the ectopic excitation. Such beats are called "fusion beats," and may be recognized by their form, which shows them to be a mixture of nomotopic and purely ectopic beats. In this latter case, the sinus remains beating in its normal rhythm without any disturbance, and the compensatory pause exactly completes the preceding ectopic interval to double the normal (58, p. 387). In comparatively rare cases, an ectopic beat is interpolated between two normal beats of normal interval. But this is possible only in bradycardias, where the refractory period of the ectopic beat ends before the normal sinus starts its next excitation. Whether or not, in this or in the former cases, the sinus is shifted in phase by the ectopic beat depends merely on chance, i.e., on the time relations between the sinus interval, the retrograde conduction time from the ectopic pacemaker to the sinus, and the interval between the ectopic and its preceding normal beat. As innumerable as the combinations in the sites of ectopic beats, in the frequency ratios of ectopic and nomotopic beats, and in the phase shifts between the two pacemakers, are the different electrocardiographic patterns.

A peculiar phenomenon has been described as "return extrasystoles" or "ventricular echoes": a ventricular extrasystole starts a retrograde excitation running to the atria, being "reflected" here and exciting again the ventricles with a second abnormal beat (60, 394).

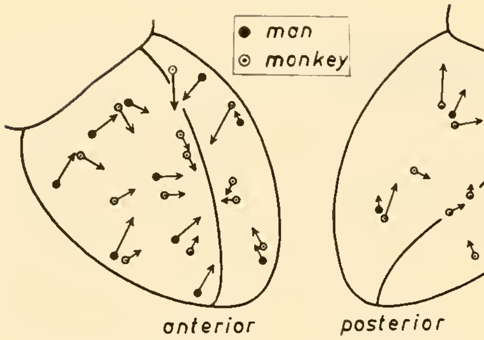

FIG. 70. Direction of the vectors of R in the frontal projection of ventricular extrasystoles (*circles*: monkey; *dots*: man). Each arrow indicates one experiment in which an extrasystole has been elicited by an external stimulus on the epicardial surface, at the site of the dots or circles. [Experiments with monkeys calculated from records of Storm, cited from Lepeschkin (46). Experiments with men from Barker, Macleod, and Alexander, cited from Schaefer (58).].

The QRST complex of a ventricular extrasystole is very different from the normal, mainly for two reasons: as mentioned before, the mutual cancellation of the fibers is greatly diminished (fig. 42) and the QRS area, therefore, highly augmented. T is altered passively by this change of QRS, and actively, also (484), and is discordant with QRS. The excitation wave runs, at least in the very beginning of its pathway, along the ordinary myocardial fibers (209). The spread is much slower than in normal beats and thus the QRS duration is increased. Only after a while does the excitation enter the Purkinje system, thus increasing in velocity but taking big detours (81). The form of QRS depends entirely on the site of the ectopic stimulus. To a certain degree, this site can be determined by vectorial analysis of QRS. We should never forget, however, that most details in this respect have been investigated in animals (236, 399, 419). Human extrasystoles have been widely interpreted in the light of certain vectorial or other theories (516). In the frontal plane, and for extrasystoles elicited at the epicardial surface, the vectorial data of the QRS area are given in figure 70, which contains experiments with monkeys and observations in man (58, p. 382). The direction of the QRS vectors is contrary, in some respects, to that of the excitation wave traveling over the heart's surface (fig. 34): the vectors point in the direction from whence the excitation starts in normal beats (58).

The activation of the ventricular wall is completely changed in ventricular extrasystoles, as has been described in Chapter 12 (416). The theory of the extrasystolic QRS seems to be clear at least in principle, if one accepts a vectorial theory based on the events in the single cardiac fiber (see sections 7 and 9). The spread of excitation in extrasystoles resembles that in experimental bundle branch block (156). Here, as well as in extrasystoles, the excitation must take a detour, which increases the conduction latencies for two reasons: the distance is increased and the velocity decreased, because much of the spread takes place in the ordinary, slowly conducting myocardium (101). There are, by the way, hitherto unsolved questions because in some experiments, after cutting the branches of the specific system, QRS is broadened; whereas in other experiments only a very small increase of QRS duration is seen (58). The incompleteness of the block may be the main reason, as some experiments (465) seem to indicate. In some cases, the pattern of a so-called bundle branch block may be in reality nothing but an over-all diminished conduction velocity (58).

The short pre-extrasystolic interval as well as the stress of a longer period of frequent extrasystolic beats involve problems of refractoriness and "fatigue," which give rise to various ECG patterns (47). So the repolarization of a premature beat has, in many cases, a different ventricular gradient (105, 410, 484), due to phenomena of refractoriness augmenting the inhomogeneities of repolarization. After a series of extrasystoles, these T changes are even more pronounced and, after a long-lasting paroxysmal tachycardia, a coronary pattern of ST and T may occur (217). Obviously, the extracellular ionic concentrations here play an important role. One should, however, be careful with the term "fatigue," because the reduction of heart rate to normal restores the T wave nearly immediately. Every shortening of the R-R interval may bring a slightly abnormal heart to a so-called reversible bundle branch block, which most probably is nothing but evidence that the pathway of excitation is temporarily blocked by refractoriness. It is even uncertain whether such "blocks" are only due to an over-all diminuition of conduction velocity. Small local changes of this velocity or refractoriness of small areas lead to considerable changes of QRS, due to alteration of the cancellation effect.

17. COMPARATIVE ELECTROCARDIOGRAPHY

The veterinary use of the ECG of domestic animals and the fact that a thorough experimental investigation of electrocardiography is only possible in experiments with animals are the main reasons why compar-

ative electrocardiography is of considerable interest. A third reason could be that, out of comparative study, a further elucidation of electrocardiographic theory could possibly be gained, insofar as the close connections between anatomical and electrocardiographic data could easily be demonstrated. The literature, however, supports us only with some (and mostly poor) figures concerning the duration of the various intervals and the patterns and magnitudes of the respective deflections. An exhaustive description of the ECG of various animals lies beyond the scope of this review. For veterinary use, some monographs are available (5, 43, 46), and the literature up to 1940 has been quoted by Schaefer (57). A collection of ECG tracings of numerous animals, from the arthropod to the elephant, is given by Zuckermann (74). The ECG of small laboratory animals (272, 288), and especially of the dog, (2, 266, 268) has been carefully described.

There are some details, remarkable beyond their descriptive value, which shall be mentioned here briefly. In the first place, the vector directions, especially of QRS, are in most animals very different from those of man. In arthropods (74), as well as in birds (287) and cattle, the main deflections of QRS in what may be called the analogue of the Einthoven leads is negative. This has been interpreted as a preferably caudocranial conduction of the excitation. According to our description of the dog's heart (fig. 34), the negativity of QRS means only that the point of distribution ("Quellpunkt") of the excitation is shifted slightly towards the apex of these hearts. The anatomy, as well as the relatively low potential, of QRS points to the fact that the principle of mutual cancellation is valid in these hearts. This shift of the distribution point therefore is not necessarily very large. Only a slight shift of this center of distribution toward the apex will cause the average direction to reverse and run toward the base (fig. 34). The reason is, of course, a similar slight difference in the anatomical distribution of the specific conducting system, which may even be hard to detect. No detailed investigation, however, has been made on the subject.

The duration of all phases of the ECG is, of course, strongly dependent on the absolute size of the heart. It is, nevertheless, surprising how small the variations are. The QT duration varies preferably with the heart rate, for obvious reasons, but, in the elephant, QT is clearly longer (0.65 sec) than it would be in man with similar heart rates, where it would be 0.5 sec. The relative bradycardia of big animals allows such prolongations of QT, but apparently there is an adaptation of QT to the highest heart rate which may occur in that particular species. The duration of QRS is determined mainly by the amount of synchronization in the various compartments of the ventricular wall. This synchronization is the more perfect the bigger the heart; but the general laws governing distribution of excitation are completely identical in small and excessively big hearts. If we extrapolate in table 2 the duration of QRS, assuming that it depends on the sixth root of the heart weight, we get for the elephant (the heart of which weighs approximately 20 kg) a QRS duration of about 0.15 sec, which is nearly the observed value of 0.16 sec.

Time relations vary, of course, with body temperature. In poikilothermic animals, figures that do not account for blood temperature are therefore useless. In homoiothermic animals, the pigeon has a QRS duration of 0.04 sec, the seagull 0.02 to 0.026 sec, a colibri, in spite of its light weight, 0.03 sec (74). Some data on domestic animals are listed in table 10. The range of QRS durations and voltages is astonishingly small.

There are some evaluations of the vectorial data, especially in the most common laboratory animals, which cannot be referred to here (see 5, 266, 327). The much bigger deviations in the field contour from ideal surfaces, compared with man, condemn all vectorial data in animals to be rather unreliable. The question of the ventricular gradient is likewise fairly unknown in animals. As far as the general pattern of QRS and T is concerned, nearly all species seem to have at least a gradient different from zero, but in many cases (as in the dog) considerably less than in man. Some animals, preferably birds, seem to have predominantly discordant T waves (74, 287) whereas in larger animals like horse and cattle, T is at least not strictly discordant. A relation between the size of the heart and its ventricular gradient has never been established and most probably does not exist: the small heart of a frog has a very big ventricular gradient, the big heart of a dog has a small one. In some animals (e.g., the boa constrictor (74)), ECG's with local leads show a very large discordant T, the ventricular gradient of which must be comparatively large in spite of a strict discordance of the T wave.

Many species show a very sensitive pacemaker, leading to marked disturbances of rhythmicity under the influence of external stimuli. In birds, the heart rate may change instantaneously between very high values and near standstill (287). The dog shows an

TABLE 10. *Some Electrocardiographic Data of Laboratory and Domestic Animals*

Animal	Mean Durations, msec				Average Amplitude in mv (Standard Leads) of Maximal Deflection			Usual Form of T	Mean Heart Rate per min	Author
	P	PQ	QRS	QT	P	R(S)	T			
Rat	17	33	26	84	0.12	0.71	0.12	Concord	346	Heise & Kimbel (242a)
White mouse		43	22		0.051	0.272			376	Lead II Lombard (326a)
Guinea pig		65	33		0.121	0.706			260	
Guinea pig	29	51	26	120					267	Lukoschek & Thiesen (327a)
Cat	40–50	70–80	40–50	130–170	0.25	0.4–0.8		Concord	180–250	Massman & Opitz (336a)
Rabbit	30–40	50–100	15–40	120	0.1	0.35	0.15	Concord.	250	Lepeschkin (47)
Dog	30–60	100	50					Variable	195	Avril (2)
Dog (anesthet.)		100	50	260	0.12	1.14	−0.07	Variable (diphas.)	100	Lombard & Witham (327)
Horse	78–155	190–381	82–140	375–574	0.41	1.74	0.98	Variable		Brooijmans (5)
Cattle	100–300	150–220	70–90	310–450	0.1	0.37	0.31		43–125	

extreme respiratory arrhythmia, apparently of central origin. The reflex tonization of the pacemaker seems to be much stronger in such animals than in man.

In the whole, the theoretical evaluation of comparative electrocardiography, promising as it would seem to be, is still nonexistent. The correlation between heart size, anatomical structure of the myocardium and the specific system, and the ECG would most probably support us with considerable information about the genesis of electrocardiographic patterns.

REFERENCES

A. MONOGRAPHS

1. Ashman, R. and E. Hull. *Essentials of Electrocardiography.* New York: Macmillan, 1954.
2. Avril, P. B. *Le champ électrique du coeur normal et pathologique. Étude expérimentale.* Paris: Masson, 1956.
3. Bayley, R. H. *Biophysical Principles of Electrocardiography.* New York: Hoeber, 1958
4. Brinberg, L. *Quantitative Vectorelectrocardiography.* Baltimore: Williams & Wilkins, 1960.
5. Brooijmans, A. W. M. *Electrocardiography in Horses and Cattle. Theoretical and Clinical Aspects.* Utrecht: Canteeleer, 1957.
6. Brooks, C. McC., B. F. Hoffman, E. E. Suckling, and O. Orias. *Excitability of the Heart.* New York: Grune, 1955.
7. Burch, G. E., J. A. Abildskov, and J. A. Cronvich. *Spatial Vectorcardiography.* Philadelphia: Lea, 1953
8. Burch, G. E. and T. Winsor. *A Primer of Electrocardiography.* London: Kimpton, 1949.
9. Cabrera, E. *Bases électrophysiologiques de l'électrocardiographie.* Paris: Masson, 1948.
10. Caniggia, A., G. Bertelli, and G. Fabrizi. *L'elettrocardiogramma esofages.* Turino: Minerva Med., 1956.
11. Doerr, W. Die Morphologie des Reizleitungssystems. In: *Rhythmusstörungen des Herzens,* by K. Spang. Stuttgart: Thieme, 1957.
12. Donzelot, E., J. B. Millovanovich, and H. Kaufmann. *Études pratiques de vectographie.* Paris: L'Expansion, 195c.
13. Doumer, E. *Les principes de l'électrocardiographie.* Paris: Masson, 1950
14. Duboucher, G. *Éléments d'électrocardiographie théorique.* Paris: Masson, 1952.
15. Duchosal, P. and R. Sulzer. *La vectocardiographie.* Basel: Karger, 1949.
16. Durrer, D *Experimenteel onderzoek naar het verloop van het activatieproces in de hartspier.* Amsterdam: Scheetema, 1952.
17. Einthoven, W. Die Aktionsströme des Herzens. In: *Handb. Physiol. VIII/2.* Berlin: Springer, 1928.
18. Ernsthausen, W. and F. Kienle. *Das elektrische Herzbild. Die Grundlagen eines neuen elektrokardiographischen Verfahrens.* München: Rinn, 1953.
19. Fattorusso, V. and O. Ritter. *Atlas d'électrocardiographie.* Paris: Masson, 1950.
20. Fleckenstein, A. *Der Kalium-Natrium-Austausch als Energieprinzip in Muskel und Nerv.* Berlin: Springer, 1955.
21. Frédéricq, H. *Aspects actuels de la physiologie du myocarde.* Paris: Presses univ. de France, 1927.

22. Gardberg, M. *Clinical Electrocardiography—Interpretation on a Physiologic Basis.* New York: Hoeber, 1957.
23. Gillmann, H. *Einführung in die vektorielle Deutung des Ekg.* Darmstadt: Steinkopff, 1954.
24. Goldberger, E. *Unipolar Lead Electrocardiography.* Philadelphia: Lea, 1948.
25. Grant, R. P. *Spatial Vector Electrocardiography.* Philadelphia: Blakiston, 1951.
26. Grant, R. P. and E. H. Estes, Jr. *The Interpretation of the ECG by Vector Methods.* Atlanta, Ga.: Emory Univ. School of Medicine, 1949.
27. Graybiel, A. *Clinical Electrocardiography.* New York: Nelson, 1950–51.
28. Grishman, A. and L. Scherlis. *Spatial Vectorcardiography.* Philadelphia: Saunders, 1952.
29. Groedel, F. M. *Das Extremitäten-, Thorax- und Partialelektrokardiogram des Menschen.* Dresden: Steinkopff, 1934.
30. Groedel, F. M. and P. R. Borchardt. *Direct Electrocardiography of the Human Heart.* New York: Brooklyn M. Press, 1948.
31. Hecht, H. The electrophysiology of the heart. *Ann. New York Acad. Sc.* 65: 653–1146, 1957.
32. Heck, W. and J. Stoermer. *Pädiatrischer Ekg-Atlas.* Stuttgart: Thieme, 1959.
33. Hegglin, R. *Die Klinik der energetisch-dynamischen Herzinsuffizienz.* Basel: Karger, 1947.
34. Holzmann, M. *Klinische Elektrokardiographie.* Stuttgart: Thieme. 1952.
35. Hurst, J. W. and G. C. Woodson, Jr. *Atlas of Spatial Vector Electrocardiography.* New York: Blakiston, 1952.
36. Huttmann, A. *Hilfstafeln zur elektrokardiographischen Diagnostik.* Darmstadt: Steinkopff, 1950.
37. Jouve, A. and P. Buisson. *La vectocardiographie en clinique.* Paris: Masson, 1950.
38. Jouve, A., J. Senez, and J. Pierron. *Diagnostic électrocardiographique.* Paris: Masson, 1954.
39. Katz, L. N. *Electrocardiography.* London: Kimpton, 1946.
40. Kienle, F. *Das Belastungs-Ekg und das Steh-Ekg.* Leipzig: Thieme, 1946.
41. Kienle, F. *Grundzüge der Funktions-Elektrokardiographie.* Karlsruhe: Braun, 1955.
42. Kisch, B. *Der Herzalternans.* Dresden: Steinkopff, 1932.
43. Kisch, B., F. M. Groedel, and P. R. Borchardt. *Comparative Direct Electrocardiography of the Heart of Vertebrates.* New York: Fordham Univ. Press, 1952.
44. Koch, E. *Allgemeine Elektrokardiographie.* Dresden: Steinkopff, 1937.
45. Kossmann, C. E. *Advances in Electrocardiography.* New York: Grune & Stratton, 1958.
45a. Kowarzykowie, H. and Z. Kowarzykowie. *Spatial Vectorcardiography.* New York. Pergamon Press, 1961.
46. Lepeschkin, E. *Das Ekg.* Dresden: Steinkopff, 1947.
47. Lepeschkin, E. *Modern Electrocardiography. The P-Q-R-S-T-U-complex.* Baltimore: Williams & Wilkins Co., 1951, vol. I.
48. Lewis, T. *The Mechanism and Graphic Registration of the Heart Beat.* London: Shaw & Sons, 1925.
49. Lutembacher, R. *Le myocarde. Physiopathologie, Cinématographies. Électrogrammes.* Paris: Masson, 1940.
50. Malmström, G. The cardiological anoxemia test, with special reference to its standardization. *Acta med. scand.*, Suppl. 195, 1947.
51. Master, A. M. *Electrocardiogram and X-Ray Configuration of heart.* Philadelphia: Lea & Febiger, 1952.
52. Nicolson, C. H. B. *Clinical Electrocardiography in Children.* New York: Macmillan, 1953.
53. Pariscenti, P. *Influenze di farmaci sul quadro ecgrafico della intossicazione digitalica sperimentale.* Milano: A. Recordati, 1957.
54. Puech, P. *L'activité Électrique Auriculaire Normale et Pathologique.* Paris: Masson, 1956.
55. Reindell, H. and H. Klepzig. *Die neuzeitlichen Brustwand- und Extremitätenableitungen in der Praxis.* Stuttgart: Thieme, 1953.
56. Rothschuh, K. E. *Elektrophysiologie des Herzens.* Darmstadt: Steinkopff, 1952.
57. Schaefer, H. *Elektrophysiologie.* Wien: Deuticke, 1940–1942, vol. 2.
58. Schaefer, H. *Das Ekg. Theorie und Klinik.* Berlin: Springer, 1951.
59. Schellong, F. *Grundzüge einer klinischen Vektordiagraphie des Herzens.* Berlin: Springer, 1939.
60. Scherf, D. and A. Schott. *Extrasystoles and Allied Arrhythmias.* London: Heinemann, 1953.
61. Segers, M. and M. Brombart. *L'Oesophage en Cardiologie.* Paris: Masson, 1953.
62. Selvini, A. *L'interpretazione razionale dell'elettrocardiogramma.* Milano: Casa Editrice Ambrosiana, 1946.
63. Sigler, L. H. *The ECG. Its interpretation and clinical application.* New York: Grune & Stratton, 1944.
64. Sodi-Pallares, D. and R. M. Calder. *New Bases of Electrocardiography.* St. Louis: Mosby, 1956.
65. Somer, E. de *Electrocardiographie expérimentale.* Paris: Masson, 1938.
66. Spang, K. *Rhythmusstörungen des Herzens.* Stuttgart: Thieme, 1957.
67. Torrésani, J. *Dérivations électrocardiographiques épicardiques chez l'homme. Contribution à l'étude de l'activation ventriculaire.* Marseille: Saint-Lambert, 1959.
68. Trautwein, W. Physiologie der Herzirregularitäten. In: *Rhythmusstörungen des Herzens*, by Spang. Stuttgart: Thieme, 1957.
69. Weber, A. *Die Elektrokardiographie.* Heidelberg: Springer, 1948.
70. Weidmann, S. *Elektrophysiologie der Herzmuskelfaser.* Bern: Huber, 1956.
71. Wenckebach, K. F. and H. Winterberg *Die unregelmässige Herztätigkeit.* Leipzig: Engelmann, 1927.
72. Wenger, R. *Klinische Vektorkardiographie.* Darmstadt: Steinkopff, 1956.
73. Wuhrmann, F. and S. Niggli. *Die Myokardose. Pathogenese, Klinik und Therapie. Mit neuen Untersuchungen über die Grundlagen der StoffwechselElektrokardiogramme.* Basel: Schwabe, 1955.
74. Zuckermann, R. *Grundriss und Atlas der Elektrokardiographie.* Leipzig: Thieme, 1957.

B. PAPERS

75. Abel, H., I. Briske, R. Engelking, W. Gartner, and H. Schaefer. L'action des gradients de température de la paroi du ventricule sur le gradient ventriculaire dans l'électrocardiogramme. *Acta cardiol.* 13: 278, 1958.
76. Abildskov, J. A. A study of the spatial vectorcardiogram

in normal subjects over the age of forty years. *Circulation* 12: 286, 1955.

77. Abildskov, J. A. The atrial complex of the electrocardiogram. *Am. Heart J.* 57: 930, 1959.
78. Abildskov, J. A., G. E. Burch, and J. A. Cronvich. The validity of the equilateral tetrahedron as a spatial reference system. *Circulation* 2: 122, 1950.
79. Abildskov, J. A., B. L. Hisey, and W. E. Ingerson. The magnitude and orientation of ventricular excitation vectors in the normal heart and following myocardial infarction. *Am. Heart J.* 55: 104, 1958.
80. Abildskov, J. A. and E. D. Pence. A comparative study of spatial vectorcardiograms obtained with the equilateral tetrahedron and a "corrected" system of electrode placement. *Circulation* 13: 263, 1956.
81. Abramson, D. I. and K. Jochim. The spread of the impulse in the mammalian ventricle. *Am. J. Physiol.* 120: 635, 1937.
82. Alanís, J., H. González, and E. López. The electrical activity of the bundle of His. *J. Physiol.*, 142: 127, 1958.
83. Albers, D. and W. Bedbur. Zur Frage der physiologischen Schwankungen der Zeitabschnitte des Kammer-Ekg. *Arch. Kreislaufforsch.* 8: 150, 1941.
84. Ashman, R. The normal human ventricular gradient. IV. The relationship between the magnitudes, $\widehat{A}$QRS and $\widehat{G}$, and deviation of the RS-T-Segment. *Am. Heart J.* 26: 495, 1943.
85. Ashman, R. and E. Byer. The normal human ventricular gradient. I. Factors which affect its direction and its relation to the man QRS axis. *Am. Heart J.* 25: 16, 1943.
86. Ashman, R. and E. Byer. The normal human ventricular gradient. II. Factors which affect its manifest area and its relationship to the manifest area of the QRS complex. *Am. Heart J.* 25: 36, 1943.
87. Ashman, R., F. P. Ferguson, A. J. Gremillion, and E. Byer. Effect of cardiac cycle length upon magnitude of ventricular gradient. *Proc. Soc. Exper. Biol. & Med.* 59: 47, 1945.
88. Ashman, R., F. P. Ferguson, A. J. Gremillion, and E. Byer. The normal human ventricular gradient. V. The relationship between AQRS and G, and the potential variations of the body surface. *Am. Heart J.* 26: 697, 1945.
89. Ashman, R., M. Gardberg, and E. Byer. The normal human ventricular gradient. III. The relation between the anatomic and electrical axes. *Am. Heart J.* 26: 473, 1943.
90. Ayala y de Landero, C. A new technique for the registration of the vectorcardiogram based on the mathematical relation between the limb and precordial leads. *Am. Heart J.* 49: 603, 1955.
91. Bain, C. W. C. The oesophageal lead. *Brit. Heart J.* 13: 485, 1951.
92. Baker, W. W. and J. M. Baker. The effects of epinephrine, norepinephrine and acetylcholine on the electrogram of the isolated frog heart. *J. Pharmacol. & Exper. Therap.* 113: 132, 1955.
93. Ball, M. F. and H. V. Pipberger. The normal spatial QRS-T angle of the orthogonal vectorcardiogram. *Am. Heart J.* 56: 611, 1958.
94. Barbato, E., A. C. Debes, T. Fujioka, F. Pileggi, E. de Jesus Zerbini, and L. V. Décourt. Direct epicardial and thoracic leads: Their relationship in man. *Am. Heart J.* 58: 238, 1959.
95. Barker, P. S., A. G. McCleod, and J. Alexander. The excitatory process observed in the exposed human heart. *Am. Heart J.* 5: 720, 1930.
96. Baur, L. Die diphasische Vorhofschwankung des gesunden und kranken Menschen bei Ableitung von der Speiseröhre. *Deutsches Arch. klin. Med.* 145: 129, 1924.
97. Baust, W. Ein einfaches Gerät zur sterischen Darstellung von Vektorgrößen, insbesondere von Vektorkardiogrammen. *Pflüger's Arch. ges. Physiol.* 260: 333, 1955.
98. Baust, W., K. D. Bock, R. Dohrmann, and H. Schaefer. Grundsächliches und Experimentelles zur Deutung des Ekg als Vektor. *Cardiologia* 25: 118, 1954.
99. Bayley, R. H. The normal potential variations on the extremity, back, and precordial electrodes with reference to central terminals of zero and nonzero potential. *Am. Heart J.* 50: 694, 1955.
100. Bechtel, J. T., J. E. White, and E. H. Estes. The electrocardiographic effects of hypocalcemia induced in normal subjects with edathamil disodium. *Circulation* 13: 837, 1956.
101. Becker, R. A., A. M. Scher, and R. V. Erickson. Ventricular excitation in experimental left bundle branch block. *Am. Heart J.* 55: 547, 1958.
102. Beckner, G. L. and T. Winsor. Cardiovascular adaptions to prolonged physical effort. *Circulation* 9: 835, 1954.
103. Bellet, S. The ECG in electrolyte imbalance. *Arch. Int. Med.* 96: 618, 1955.
104. Benedetti, P. Sugli elettrocardiogrammi cosi detti di prevalenza ventricolare. II. Proposta di un metodo di valutazione tipologica individuale del ventricologrammae. *Arch. pat. e clin. med.* 19: 317, 1939.
105. Berkun, M. A., R. H. Kesselmann, E. Donoso, and A. Grishman. The spatial ventricular gradient: intermittent Wolff-Parkinson-White syndrome, intermittent left bundle branch block and ventricular premature contractions. *Circulation* 13: 562, 1956.
106. Berkun, M. A., R. H. Kesselmann, E. Donoso, and A. Grishman. The spatial atrial gradient. *Am. Heart J.* 52: 858, 1956.
107. Berman, R., E. Simonson, and W. Heron. Electrocardiographic effects associated with hypnotic suggestion in normal and coronary sclerotic individuals. *J. Appl. Physiol.* 7: 89, 1954.
108. Bethe, A. Teilrhythmus, Alternans, Amplitude und die Grenzen des Alles-oder-Nichts-Gesetzes. *Pflüger's Arch. ges. Physiol.* 244: 43, 1940.
109. Bilger, R., H. Scharpf, and H. Reindell. Die Vorhoferregung im Vektorkardiogramm. *Klin. Wchnschr.* 37: 329, 1959.
110. Biörk, G., F. S. Jackson, and S. Rohlin. Ventricular gradient studies in positive hypoxemia tests. *Acta med. scandinav.* 132: 283, 1948.
111. Blackburn, H. W., Jr. and E. Simonson. The total QRS duration. *Am. Heart J.* 53: 699, 1957.
112. Blasius, W. Zur Methodik der Abnahme von Brustwandableitungen im Verbande gleichseitiger Dreiecke in der Horizontalebene. *Pflüger's Arch. ges. Physiol.* 261: 1, 1955.
113. Blasius, W. and R. Repges. Zur Vektoranalyse des Brustwand-Ekg im Hinblick auf die exzentrische Lage des Herzens im Thorax. *Pflüger's Arch. ges. Physiol.* 261: 8, 1955.

114. Blinks, J. R. Positive chronotropic effect of increasing right atrial pressure in the isolated mammalian heart. *Am. J. Physiol.* 186: 299, 1956.

115. Blumberger, K. Vergleichende Herzuntersuchungen bei Zwillingen. *Verh. dtsch. Ges. Kreisl.-Forsch.* 13: 150, 1940.

116. Bock, K. D. and W. Baust. Tierexperimentelle Untersuchung über die Ursachen der Fehler bei der Vektoranalyse des unipolaren Brustwand-Ekg. *Ztschr. Kreislaufforsch.* 43: 624, 1954.

117. Böckh, E. M. Ein Beitrag zur Frage der Tagesschwankungen im Ekg der Standard-Extremitäten-Ableitungen. *Ztschr. Kreislaufforsch.* 42: 420, 1953.

118. Böckh, E. M. and H. Schaefer. Weitere Untersuchungen über die Konstruierbarkeit von Ekg-Vektoren aus Brustwandableitungen. *Cardiologia* 23: 191, 1953.

119. Boden, E. and P. Neukirch. Elektrokardiographische Studien am isolierten Säugetier- und Menschenherzen bei direkter und indirekter Ableitung. *Pflüger's Arch. ges. Physiol.* 171: 146, 1918.

120. Boer, S. de Gleichzeitige direkte und indirekte Ableitung des Elektrokardiogrammes mittels zweier Saitengalvanometer bei Fröschen nach Vergiftung mit Digitalis. *Ztschr. Kreislaufforsch.* 27: 155, 1935.

121. Boer, W. den The clinical value of vectorcardiography. *Acta med. scandinav.* 144: 217, 1952.

122. Boer, W. den, H. C. Burger, and J. B. van Milaan. Vectorcardiograms of normal and premature beats in different lead systems. *Brit. Heart J.* 17. 1, 1955.

123. Braunwald, E., H. L. Moscovitz, S. S. Amram, R. P. Lasser, S. O. Sapin, A. Himmelstein, M. M. Ravitch, and A. J. Gordon. Timing of electrical and mechanical events of the left side of the human heart. *J. Appl. Physiol.* 8: 309, 1955.

124. Brendel, W., W. Raule, and W. Trautwein. Die Leitungsgeschwindigkeit und Erregungsausbreitung in den Vorhöfen des Hundes. *Pflüger's Arch. ges. Physiol.* 253: 106, 1950.

125 Briller, S. A. The integrated electrocardiogram. *Ann. New York Acad. Sc.* 65: 894, 1957.

126. Brody, D. A. The meaning of lead vectors and the Burger triangle. *Am. Heart J.* 48: 730, 1954.

127. Brody, D. A. The axostat. III. An improved form of the instrument, and its application to the establishment of spatial electrocardiographic indices in 102 normal subjects. *Am. Heart J.* 50: 610, 1955.

128. Brody, D. A. A theoretical analysis of intracavitary blood mass influence on the heart-lead relationship. *Circulation Res.* 4: 731, 1956.

129. Brody, D. A. A method for applying approximately ideal lead connections to homogeneous volume conductors of irregular shape. *Am. Heart J.* 53: 174, 1957.

130. Brody, D. A. and G. D. Copeland. Electrocardiographic cancellation: Some observations concerning the "nondipolar" fraction of precordial electrocardiogram. *Am. Heart J.* 56: 381, 1958.

131. Brody, D. A. and G. D. Copeland. The principles of esophageal electrocardiography. *Am. Heart J.* 57: 3, 1959.

132. Brody, D. A., B. P. McKay, and W. E. Romans. The axostat. I. A new instrument for the multiaxial registration of extremity electrocardiograms. *Am. Heart J.* 48: 589, 1954.

133. Browne, M. K. and J. T. Fitzsimons. Electrocardiographic changes during positive acceleration. *Brit. Heart J.* 21: 23, 1959.

134. Bucher, K. and P. Battig. Zum Mechanismus der pulssynchronen Atmung. *Helvet. physiol. et pharmacol. acta* 14: 319, 1956.

135. Bugyi, B. Über Beeinflussung der elektrischen Systolendauer durch Kalzium- und Kaliumionen. *Ztschr. ges. inn. Med.* 11: 518, 1956.

136. Burch, G. E. The electrocardiogram and disturbances in electrolyte balance. *Arch. Int. Med.* 94: 509, 1954.

137. Burch, G. E., J. A. Abildskov, and J. A. Cronvich. Studies of the spatial vectorcardiogram in normal man. *Circulation* 7: 558, 1953.

138. Burch, G. E., L. H. Golden, and J. A. Cronvich. An analysis of changes in the spatial vectorcardiogram with aging. *Am. Heart J.* 55: 582, 1958.

139. Burchell, H. B., H. E. Essex, and R. D. Pruitt. Studies on the spread of excitation through the ventricular myocardium. II. The ventricular septum. *Circulation* 6: 161, 1952.

140. Burger, H. C. The zero of potential: a persistent error. *Am. Heart J.* 49: 581, 1955.

141. Burger, H. C. and J. B. van Milaan. Heart-vector and leads. I. *Brit. Heart J.* 8: 157, 1946.

142. Burger, H. C. and J. B. van Milaan. Heart-vector and leads. II. *Brit. Heart J.* 9: 154, 1947.

143. Burger, H. C. and J. B. van Milaan. Heart-vector and leads. III. *Brit. Heart J.* 10: 229, 1948.

144. Burger, H. C., J. B. van Milaan, and W. Klip. Comparison of three different systems of vectorcardiography. *Am. Heart J.* 57: 723, 1959.

145. Burger, H. C., H. A. Tolhoek, and F. G. Backbier. The potential distribution on the body surface caused by a heart vector. *Am. Heart J.* 48: 249, 1954.

146. Burger, H. C. and J. P. Vaane. A criterion characterizing the orientation of a vectorcardiogram in space. *Am. Heart J.* 56: 29, 1958.

147. Burger, R. Über das elektrische Feld des Herzens. I. *Cardiologia* 3: 56, 1939.

148. Burnett, C. T., M. G. Nims, and C. J. Josephson. The induced anoxemia test. *Am. Heart J.* 23: 306, 1942.

149. Butterworth, S. and J. J. Thorpe. On evaluating the Einthoven triangle. *Circulation* 3: 923, 1951.

150. Cabrera, E. Le problème des dérivations bipolaires appliquées à la vectocardiographie. *Acta cardiol.* 4: 231, 1949.

151. Canfield, R. On the electric field surrounding doublets and its significance from the standpoint of Einthoven's equations. *Heart* 14: 102, 1927.

152. Cannon, P. and T. S. Jöstrand. The occurrence of a positive after-potential in the ECG in different physiological and pathological conditions. *Acta med. scandinav.* 146: 191, 1953.

153. Carlsten, A. Experimentally provoked variations of the positive after-potential in the human electrocardiogram. *Acta med. scandinav.* 146: 424, 1953.

154. Chamberlain, E. N. and J. D. Hay. The normal electrocardiogram. *Brit. Heart J.* 1: 105, 1939.

155. Chevalier, H. and M. Thaon. Le vecteur $\widehat{AP}$ manifeste (grandeur et direction) calculé sur 180 coeurs normaux entre 12 et 65 ans. *Arch. mal. coeur* 42: 333, 1949.

156. Conrad, L. L. and T. E. Cuddy. Activation of the free

wall of the right ventricle in experimental right bundle branch block. *Circulation Res.* 7: 173, 1959.

157. Coraboeuf, E., R. Distel, and J. Boistel. Potentiels cellulaires des tissus conducteur et musculaire du coeur de mammifère. *Compt. rend. soc. biol.* 147: 1757, 1953.
158. Coraboeuf, E., R. Distel, and J. Boistel. L'activité électrique normale des différents tissus du coeur de chien. *Compt. rend. acad. sci., Paris* 240: 1927, 1955.
159. Coraboeuf, E., R. Distel, and J. Boistel. L'activité électrique des différents tissus du coeur de chien. Obtention de réponses atypiques. *Compt. rend. acad. sci., Paris* 240: 2557, 1955.
160. Craib, W. H. The electrocardiogram. *Med. Research Council. Spec. Rep. Ser.* No. 147, 1930.
161. Craib, W. H. and R. Canfield. A study of the electical field surrounding active heart muscle. *Heart* 14: 71, 1927.
162. Cranefield, P. F. and B. F. Hoffman. Electrophysiology of single cardiac cells. *Physiol. Rev.* 38: 41, 1958.
163. Cronvich, J. A., J. A. Abildskov, C. E. Jackson, and G. E. Burch. An approximate derivation for stereoscopic vectorcardiograms with the equilateral tetrahedron. *Circulation* 2: 126, 1950.
164. Cronvich, J. A., J. P. Conway, and G. E. Burch. Standardizing factors in electrocardiography. *Circulation* 2: 111, 1950.
165. Datey, K. K. and P. E. Bharucha. Electrocardiographic changes in the first week of life. *Brit. Heart J.* 22: 175, 1960.
166. Dick, H. L. H., E. L. McCawley, D. V. Voiss, and J. D. Krueger. Electrocardiographic evaluation studies on Quinidine-induced changes of myocardial conduction. *Am. Heart J.* 56: 396, 1958.
167. Donoso, E., F. Wachtel, and A. Grishman. Polarity of the ST vector. *Am. J. Physiol.* 189: 219, 1957.
168. Dower, G. E. and J. A. Osborne. A clinical comparison of three VCG lead systems using resistance-combining networks. *Am. Heart J.* 55: 523, 1958.
169. Dower, G. E. and J. A. Osborne. Surface activation of guinea pig ventricle determined by intracellular electrodes. *Am. J. Physiol.* 195: 396, 1958.
170. Draper, G., H. G. Bruenn, and C. W. Dupertuis. Changes in the electrocardiogram as criteria of individual constitution derived from its physiological panel. *Am. J. M. Sc.* 194: 514, 1937.
171. Draper, M. H. and M. Mya-Tu. A comparison of the conduction velocity in cardiac tissues of various mammals. *Quart. J. Exper. Physiol.* 64: 92, 1959.
172. Dreifus, L. S. and A. Pick. A clinical correlative study of the electrocardiogram in electrolyte imbalance. *Circulation* 14: 815, 1956.
173. Dudel, J. and W. Trautwein. Das Aktionspotential und Mechanogramm des Herzmuskels unter dem Einfluß der Dehnung. *Cardiologia* 25: 344, 1954.
174. Dudel, J. and W. Trautwein. Elektrophysiologische Messungen zur Strophanthinwirkung am Herzmuskel. *Nauny-Schmiedebergs Arch. exper. Path. u Pharmakol.* 232: 393, 1958.
175. Durant, T. M. and M. J. Oppenheimer. Initial epicardial negativity and other experimental evidence relative to validity of zonal interference theory. *Am. J. Physiol.* 163: 129, 1950.
176. Durrer, I. D. and L. H. van der Tweel. Spread of activation in the left ventricular wall of the dog. *Am. Heart J.* 46: 683, 1953.
177. Durrer, D. and L. H. van der Tweel. Excitation of the left ventricular wall of the dog and goat. *Ann. New York Acad. Sc.* 65: 779, 1957.
178. Durrer, D., L. H. van der Tweel, S. Berreklouw, and L. P. van der Wey. Spread of activation in the left ventricular wall of the dog. IV. Two and three dimensional analysis. *Am. Heart J.* 50: 860, 1955.
179. Durrer, D., L. H. van der Tweel, and J. R. Blickman. Spread of activation in the left ventricular wall of the dog. III. Transmural and intramural analysis. *Am. Heart J.* 48: 13, 1954.
180. Eckervogt, F. J. Schrittmacherwechsel im Sinus-Vorhof-Bereich von Patienten. *Ztschr. Kreislaufforsch.* 43: 745, 1954.
181. Edeiken, J. Elevation of the RS-T segment, apparent or real, in the right precordial leads as a probable normal variant. *Am. Heart J.* 48: 331, 1954.
182. Einthoven, W. Die galvanometrische Registrierung des menschlichen Ekg, zugleich eine Beurteilung der Anwendung des Capillar-Elektrometers in der Physiologie. *Pflüger's Arch. ges. Physiol.* 99: 472, 1903.
183. Einthoven, W., G. Fahr, and A. de Waart. Über die Richtung und die manifeste Größe der Potentialschwankungen im menschlichen Herzen und über den Einfluß der Herzlage auf die Form des Elektrokardiogramms. *Pflüger's Arch. ges. Physiol.* 150: 275, 1913. Translated by H. E. Hoff and P. Sekelj in *Am. Heart J.* 40: 163, 1950.
184. Einthoven, W. and F. W. N. Hugenholtz. L'électrocardiogramme tracé dans le cas où il n'y a pas de contraction visible du coeur. *Arch. néerl. physiol.* 5: 174, 1921.
185. Emslie-Smith, D., G. E. Sladden, and G. R. Stirling. The significance of changes in the ECG in hypothermia. *Brit. Heart J.* 21: 343, 1959.
186. Engelbertz, P. and O. Hanke. Über tagesrhythmische Schwankungen im Elektrokardiogramm vegetativ Labiler und ihre Beeinflussung durch Nahrungsaufnahme. *Klin. Wchnschr.* 32: 790, 1954.
187. Engelking, R. and W. Bienroth. Untersuchungen über den intramuralen Temperaturgradienten des Herzens und seinen Einfluß auf das Elektrokardiogramm. *Cardiologia* 34: 147, 1959.
188. Erk, C. Über die Bedeutung der Änderungen des ST-Stückes und der T-Welle im Ekg. *Ztschr. ges. exper. Med.* 114: 590, 1945.
189. Eyster, J. A. E., W. J. Meck, and H. Goldberg. The relation between electrical and mechanical events in the dog's heart. *Am. J. Physiol.* 131: 760, 1941.
190. Fastier, F. N. Electrocardiographic features of adrenaline syncope. *J. Physiol.* 112: 359, 1951.
191. Fattorusso, V., M. Thaon, and J. Tilmant. Contribution à l'étude de l'électrocardiogramme précordial. *Acta cardiol.* 4: 464, 1949.
192. Fershing, J. and L. A. Baker. Clinical analysis of the S wave pattern ECG. *Am. Heart J.* 35: 106, 1948.
193. Fowler, N. O. and E. R. Dorney. Studies on the P loop of the spatial vectocardiogram—the normal P loop. *Am. Heart J.* 48: 36, 1954.
194. Fowler, N. O., Jr. and R. A. Helm. The spatial angle between the long axis of the QRS loop and the longitudinal axis of the ventricles. *Am. Heart J.* 46: 821, 1953.
195. Frank, E. Theoretic analysis of the influence of heart-

dipole eccentricity on limb leads, Wilson control-terminal voltage and the frontal-plane vectorcardiogram. *Circulation Res.* 1: 380, 1953.

196. Frank, E. A comparative analysis of the eccentric double-layer representation of the human heart. *Am. Heart J.* 46: 364, 1953.
197. Frank, E. The image surface of a homogeneous torso. *Am. Heart J.* 47: 757, 1954.
198. Frank, E. A direct experimental study of three systems of spatial vectorcardiography. *Circulation* 10: 101, 1954.
199. Frank, E. Measurement and significance of cancellation potentials on the human subject. *Circulation* 11: 937, 1955.
200. Frank, E. Determination of the electrical center of ventricular depolarization in the human heart. *Am. Heart J.* 49: 670, 1955.
201. Frank, E. Analysis of R, L, F, B systems of spatial vectorcardiography. *Am. Heart J.* 51: 34, 1956.
202. Frank, E. An accurate, clinically practical system for spatial vectorcardiography. *Circulation* 13: 737, 1956.
203. Frank, E. Spread of current in volume conductors of finite extent. *Ann. New York Acad. Sc.* 65: 980, 1957.
204. Frank, E. and C. F. Kay. A reference potential for unipolar electrocardiographic measurements on models. *Am. Heart J.* 46: 195, 1953.
205. Frank, E. and C. F. Kay. The construction of mean spatial vectors from null contours. *Circulation* 9: 555, 1954.
206. Frank, E., C. F. Kay, G. E. Seiden, and R. A. Keisman. A new quantitative basis for electrocardiographic theory: the normal QRS complex. *Circulation* 12: 406, 1955.
207. Frank, E. and G. E. Seiden. Comparison of limb and precordial vectorcardiographic systems. *Circulation* 14: 83, 1956.
208. Frankenhaeuser, B. and A. L. Hodgkin. The action of calcium on the electrical properties of squid axons. *J. Physiol.* 137: 218, 1957.
209. Frau, G. Die ventrikuläre Aktivierung bei durch Reiz erzeugten Extrasystolen. *Verh. dtsch. Ges. Kreisl.-Forsch.* 1952.
210. Friese, G. Über die Bedeutung der Ta-Welle für die elektrokardiographische Diagnostik. *Ztschr. Kreislaufforsch.* 43: 159, 1954.
211. Gaarz, W. and A. Weber. Zur Frage der harmonischen Kurvenanalyse des menschlichen Elektrokardiogramms. *Wiss. Veröffentl. Siemens-Konzern* 7: 287, 1928.
212. Gabler, H. Die harmonische Analyse des menschlichen Spannungs-Ekg. *Ztschr. Kreislaufforsch.* 39: 387, 1950.
213. Garb, S. and M. B. Chenoweth. Electrogram of isolated papillary muscle of the cat heart. *Am. J. Physiol.* 156: 27, 1949.
214. García-Ramos, J. El mecanismo de iniciación de las extrasistoles ventriculares en el infarto del miocardio. *Arch. Inst. cardiol. México* 24: 250, 1954.
215. Gardberg, M. and I. L. Rosen. Monophasic curve analysis and the ventricular gradient in the electrogram of strips of turtle ventricle. *Circulation Res.* 7: 870, 1959.
216. Gärtner, W. and H. Schaefer. Die Theorie und die klinische Brauchbarkeit des Ventrikelgradienten im Ekg. *Arch. Kreislaufforsch.* 27: 83, 1957.
217. Geiger, A. J. Ekg simulating those of coronary thrombosis after cessation of paroxysmal tachycardia. *Am. Heart J.* 26: 555, 1943.
218. Geppert, M. P. Die intraindividuelle QT-RR-Relation im menschlichen Ekg. *Arch. Kreislaufforsch.* 15: 64, 1949.
219. Geppert, M. P. and H. Schaefer. Statistische Untersuchungen über die Beziehungen zwischen Herzgröße und Maximalspannung von QRS im Ekg. *Arch. Kreislaufforsch.* 17: 104, 1951.
220. Gillmann, H. Vektorielle Untersuchungen über die durch künstliche Hypothermie ausgelösten Ekg-Veränderungen. *Cardiologia* 33: 21, 1958.
221. Gillmann, H. and P. Faust. Die Sektordiagraphie, eine Methode zur Dokumentation von Ekg und Durchführung elektrokardiographischer Vergleichsuntersuchungen. *Ztschr. Kreislaufforsch.* 397, 1958.
222. Gillmann, H., M Zindler, and B. Löhr. Über die Wirkung der tiefen künstlichen Hypothermie auf die Aktion des menschlichen Herzens. (Frequenz, Phonokardiogramm und Ekg). *Arch. Kreislaufforsch.* 27: 288, 1957.
223. Giraud, G., H. Latour, and P. Puech. Électrocardiographie du sinus coronaire. II. Étude ecgrapique endocavitaire des dysrythmies du sinus coronarie chez l'homme. *Arch. mal. coeur.* 47: 1008, 1954.
224. Glomset, D. J. and A. T. A. Glomset. A morphologic study of the cardiac conduction system in ungulates, dog, and man. II. The Purkinje system. *Am. Heart J.* 20: 677, 1940.
225. Goldberger, E. The differentiation of normal from abnormal Q waves. *Am. Heart J.* 30: 341, 1945.
226. Goldman, M. J. RS-T segment elevation in mid- and left precordial leads as a normal variant. *Am. Heart J.* 46: 817, 1953.
227. Göpfert, H. and H. Schaefer. Über eine dem Aktionsstrom des Muskels parallel gehende mechanische Zustandsänderung. *Naturwissenschaften* 34: 348, 1947.
228. Grant, R. P. Spatial vector electrocardiography. A method for calculating the spatial electrovectors of the heart from conventional leads. *Circulation* 2: 676, 1950.
229. Gray, S. W. Pattern of contraction and relaxation in tortoise ventricle. *Am. J. Physiol.* 162: 249, 1950.
230. Graybiel, A., R. A. McFarland, D. C. Gates, and F. A. Webster. Analysis of the ECG obtained from 1000 young healthy aviators. *Am. Heart J.* 27: 524, 1944.
231. Groeben, von der, J. Spatial representation of cardiac vectors with the aid of tabulated functions. *Am. Heart J.* 52: 562, 1956.
232. Gross, D. The auricular T wave and its correlation to the cardiac rate and to the P-Wave. *Am. Heart J.* 50: 24, 1955.
233. Haas, H. G. Ein Beitrag zur Theorie des Ventrikelgradienten. *Cardiologia* 36: 321, 1960.
234. Haas, H. G., A. Blömer, M. Ley, and H. Schaefer. Experimentelle Untersuchungen am Hundeherzen zum Problem des Ventrikelgradienten. *Cardiologia* 37: 66, 1960.
235. Hadorn, W. Untersuchungen des Herzens im hypoglykämischen Schock. *Arch. Kreislaufforsch.* 2: 70, 1938.
236. Hamlin, R. L., C. R. Smith, and R. W. Redding. Time-order of ventricular activation for premature beats in sheep and dogs. *Am. J. Physiol.* 198: 315, 1960.
237. Harris, A. S. The spread of excitation in turtle, dog, cat and monkey ventricles. *Am. J. Physiol.* 134: 319, 1941.
238. Hartmann, J., R. Veyrat, O. A. Wyss, and P. W. Duchosal. Vectorcardiography as studied on the isolated mammalian heart suspended in a homogeneous volume conductor. *Cardiologia* 27: 129, 1955.
239. Hecht, H. H. Potential variations of the right auricular

and ventricular cavities in man. *Am. Heart J.* 32: 39, 1946.

240. Hecht, H. H., L. A. Woodbury, J. W. Woodbury, and R. Christopherson. Observations on the origin of the electrocardiogram: potential variations of single heart muscle fibers in situ. *J. Clin. Invest.* 29: 820, 1950.
241. Hegglin, R. and M. Holzmann. Die klinische Bedeutung der verlängerten QT-Distanz (Systolendauer) im Elektrokardiogramm. *Ztschr. klin. Med.* 132: 1, 1937.
242. Heinen, W. and H. Loosen. Die Beziehungen der Q-T Dauer zur Frequenz im Verlaufe körperlicher Arbeit. *Ztschr. Kreislaufforsch.* 38: 713, 1949.
242a. Heise, E. and K. H. Kimbel. Das normale Elektrokardiogramm der Ratte. *Ztschr. Kreislaufforsch.* 44: 212, 1955.
243. Hellerstein, H. K., D. Shaw, and T. Sano. Dissection of the vectorcardiogram: differential vectorcardiography. *Am. Heart J.* 47: 887, 1954.
244. Helm, J. D., G. H. Helm, and C. C. Wolferth. The distribution of potential of ventricular origin below the diaphragm and in the esophagus. *Am. Heart J.* 27: 755, 1944.
245. Helm. R. A. The vectorcardiographic derivation of scalas leads. *Am. Heart J.* 46: 519, 1953.
246. Helm, R. A. The direction of mean QRS and T vectors. I. Einthoven frontal plane. *Am. Heart J.* 48: 224, 1954.
247. Helm, R. A. Theory of vectorcardiography: a review of fundamental concepts. *Am. Heart J.* 49: 135, 1955.
248. Helm, R. A. Vectorcardiographic notation. *Circulation* 13: 581, 1956.
249. Helm, R. A. The lead vectors of multiple dipoles located on a transverse plane of Frank's homogeneous torso model. *Am. Heart J.* 52: 323, 1956.
250. Helm, R. A. The effect of boundary contour on the distribution of dipole potential in a volume conductor. *Am. Heart J.* 52: 769, 1956.
251. Helm, R. A. A universal system of electrode placement for electrocardiography and spatial vectorcardiography. *Am. Heart J.* 58: 71, 1959.
252. Helm, R. A. and N. O. Fowler, Jr. Studies on the QRS-T angle. *Am. Heart J.* 46: 229, 1953.
253. Helmholtz, H. Über einige Gesetze der Verteilung elektrischer Ströme in körperlichen Leitern, mit Anwendung auf die tierisch-elektrischen Versuche. *Poggendorff's Annalen*, 1853.
254. Herndon, R. F., W. H. Meroney, and C. M. Pearson. The electrocardiographic effects of alterations in concentration of plasma chemicals. *Am. Heart J.* 50: 188, 1955.
255. Hesse, H. Elektrokardiographische Untersuchungen am sterbenden Warmblüterherzen. *Pflüger's Arch. ges. Physiol.* 250: 552, 1948.
256. Hinrichs, A. Über das Elektrokardiogramm bei der Extremitätenableitung. *Deutsches Arch. klin. Med.* 176: 391, 1934.
257. Hirsch, J. I., S. A. Briller, and C. E. Kossmann. The image tetrahedron in man determined by reciprocal stimulation of a tridimensional esophageal electrode. *Circulation Res.* 4: 599, 1956.
258. Hirvonen, L. Electrographic studies of the isolated rabbit auricle. *Ann. med. exper. et biol. Fenniae* 33, Suppl. 7, 1955.
259. Hirvonen, L. Effect of chlorides of alkali and of alkaline earth metals on the isolated rabbit auricle. *Ann. med. exper. et biol. Fenniae* 34, Suppl. 1, 1956.
260. Hoffman, B. F., A. P. de Carvalho, W. C. Mello, and P. F. Cranefield. Electrical activity of single fibers of the atrioventricular node. *Circulation Res.* 7: 11, 1959.
261. Hoffman, B. F. and E. E. Suckling. Cellular potentials of intact mammalian hearts. *Am. J. Physiol.* 170: 357, 1952.
262. Hoffman, B. F. and E. E. Suckling. Effect of heart rate on cardiac membrane potentials and the unipolar electrogram. *Am. J. Physiol.* 179: 123, 1954.
263. Hofmann-Credner, D. and R. Wenger. Beitrag zur Analyse des S 1-3-Typs im Elektrokardiogramm. *Wien. Ztschr. inn. Med.* 34: 15, 1953.
264. Holldack, K. Die Bedeutung der "Umformungs- und Druckanstiegszeit" für die Herzdynamik. *Deutsches Arch. klin. Med.* 198: 71, 1951.
265. Holzmann, M. Ekg und Elektrolyte. *Cardiologia* 31: 209, 1957.
266. Horan, L., G. E. Burch, and J. A. Cronvich. Spatial vectorcardiograms in normal dogs. *Circulation Res.* 5: 133, 1957.
267. Hörmann, J. and K. Hellwigh. Der überdrehte Linkstyp im Ekg. *Ztschr. Kreislaufforsch.* 42: 482, 1953.
268. Horwitz, S. A., M. R. Spanier, and H. C. Wiggers. The electrocardiogram of the normal dog. *Proc. Soc. Exper. Biol. & Med.* 84: 121, 1953.
269. Hudson, R. E. B. The human pacemaker and its pathology. *Brit. Heart J.* 22: 153, 1960.
270. Hupka, K. and R. Wenger. Vektorkardiographische Untersuchungen an Säuglingen mit besonderer Berücksichtigung der ersten Lebensstunden and ihre Deutung im Hinblick auf die Umstellungen vom fötalen auf den kindlichen Kreislauf. *Helv. et paediat. acta* 12: 524, 1957.
271. Hupka, K. and R. Wenger. Ein Beitrag zur Frage der vektorkardiographischen Ableitungsmethodik. *Ztschr. Kreislaufforsch.* 47: 1030, 1958.
272. Irmak, S. and R. Aykut. Vergleichende elektro-kardigraphische Untersuchungen beim Menschen und bei den Laboratoriumstieren. *München. med. Wchnschr.* 97: 460, 1955.
273. Johansson, B. and Vendsalu. The influence of adrenaline, noradrenaline and aceylcholine on the electrocardiogram of the isolated perfused guinea-pig heart. *Acta physiol. scandinav.* 39: 356, 1957.
274. Johnson, C. A. and G. H. Laing. Gleichzeitige Mechanogramme und Ekg vom unverletzten Menschen, mit Bemerkungen über die Wirkung der Magendehnung auf das Ekg. *Am. Heart J.* 20: 160, 1940.
275. Jourdan, F., R. Froment, and C. Finas. Les caractères du rythme nodal. (Leur détermination par l'observation prolongé du rythme nodal expérimental.) *Arch. sci. physiol.* 5: 93, 1951.
276. Jouve, A., J. Corriol, M. Albouy, and P. Vélasque. Variations du champ électrique cardiaque à la surface du thorax avant et après isolement partiel de la masse ventriculaire. *Arch. mal. coeur* 48: 463, 1955.
277. Jouve, A., J. Corriol, P. Vélasque, R. Benyamine, and G. Peytavy. Étude comparée des dérivations épicardiques et intra-murales chez l'homme et le chien. *J. physiol., Paris* 49: 223, 1957.
278. Jouve, A., J. Corriol, P. Vélasque, R. Benyamine, and R. Peytavy. Comparaison des dérivations précordiales chez l'homme. *Cardiologia* 33: 45, 1958.
279. Jouve, A., J. Corriol, P. Vélasque, R. Benzamine,

and R. Peytavy. Les dérivations épicardiques ventriculaires chez l'homme. *Acta cardiol.* 13: 247, 1958.

280. Kahn, K. A. and E. Simonson. Changes of mean spatial QRS and T vectors and of conventional electrocardiographic items in hard anaerobic work. *Circulation Res.* 5: 629, 1957.

281. Kaindl, F., K. Polzer, and F. Shuhfried. Vergleichende Überprüfung der gebräuchlichen vektorkardiographischen Ableitemethoden im Tierversuch. *Wien. Ztschr. inn. Med.* 34: 319, 1953.

282. Karni, H. S. High-frequency feature in the vectorcardiogram. *Am. Heart J.* 56: 98, 1958.

283. Karni, H. S. The diagnostic significance of the differential repolarization of the precordial leads. *Cardiologia* 36: 257, 1960.

284. Katz, L. N., A. Bohning, I. Gutman, K. Jochim, H. Korey, F. Ocko, and M. Robinow. Concerning a new concept of the genesis of the electrocardiogram. *Am. Heart J.* 13: 17, 1937.

285. Katz, L. N., E. Sigman, I. Gutman, and F. H. Ocko. The effect of good electrical conductors introduced near the heart on the electrocardiogram. *Am. J. Physiol.* 116: 343, 1936.

286. Kavaler, F. Membrane depolarization as a cause of tension development in mammalian ventricular muscle. *Am. J. Physiol.* 197: 968, 1959.

287. Kisch, B. The electrocardiogram of birds. (Chicken, duck, pigeon.) *Exper. Med. & Surg.* 9: 103, 1951.

288. Kisch, B. The heart rate and the ECG of small animals. *Exper. Med. & Surg.* 11: 117, 1953.

289. Kistin, A. D., W. D. Brill, and G. P. Robb. Normal esophageal and gastric ECG's. Description, statistical analysis and bearing on theories of "electrocardiographic position." *Circulation* 2: 578, 1950.

290. Kleinfeld, M., E. Stein, and J. Magin. Electrical alternans in single ventricular fibers of the frog heart. *Am. J. Physiol.* 187: 139, 1956.

291. Klewitz, F. Über die T-Zacke am stillstehenden Herzen. *Z. Biol.* 67: 279, 1917.

292. Koch, E. Herzalternans durch partielle Abkühlung des Ventrikels. *Z. exp. Path. Ther.* 21: 19, 1920.

293. Koechlin, M. R. Conditions d'application de la vectocardiographie spatiale. *Compt. rend. acad. sci., Paris,* 242: 2402, 1956.

294. Koehler, E. and K. Spang. Über den Ventrikelgradienten beim Myokardinfarkt. *Arch. Kreislaufforsch.* 20: 138, 1953.

295. Koelliker, A. and H. Müller. Nachweis der negativen Schwankung des Muskelstroms am natürlich sich contrahierenden Muskel. *Verh. phys.-med. Ges. Würzb.* 6: 528, 1856.

296. Kooi, M. W. van der, D. Duner, R. T. van Dam, and L. H. van der Tweel. Electrical activity in sinus node and atrioventricular node. *Am. Heart J.* 51: 684, 1956.

297. Kossmann, C. E. Clinical Progress: The normal electrocardiogram. *Circulation* 8: 920, 1953.

298. Kossmann, C. E. Lead vector projections. II. Determination of the image surface in man. *Ann. New York Acad. Sc.* 65: 1088, 1957.

299. Koulumies, R., R. Lumme, and A. Telkkä. Studies on the U-wave of the electrocardiogram. *Ann. med. int. Fenniae.* 42: 208 1953.

300. Kraft, H. G. and O. Wiegmann. Über die Abhängigkeit der elektrischen und mechanischen Tätigkeit des Herzstreifenpräparates des Frosches von der Schlagfrequenz. *Z. Biol.* 109: 210, 1957.

301. Kühns, K. Über den Einfluß des Kalium-Ions auf Elektrokardiogramm und Herzsystolendauer. *Ztschr. Kreislaufforsch.* 44: 4, 1955.

302. Kuppi, H. Das Digitalis-Ekg und seine Reversibilität unter Atropin. *Z. inn. Med.* 9: 837, 1954.

303. Langendorf, R., A. Pick, and M. Winternitz. Mechanisms of intermittent ventricular bigeminy. I. Appearance of ectopic beats dependent upon length of the ventricular cycle, the "rule of bigeminy." *Circulation* 11: 422, 1955.

304. Langner, P. H., Jr. The value of high fidelity electrocardiography using the cathode ray oscillograph and an expanded time scale. *Circulation* 5: 249, 1952.

305. Langner, P. H., Jr., J. M. Benjamin, Jr., and S. R. Moore. Certain inevitable relationships among the "unipolar" extremity leads. *Circulation* 5: 878, 1952.

306. Langner, P. H., Jr., E. J. Dewees, and S. R. Moore. A critical and comparative analysis of methods in electrocardiography employing mean QRS and T vectors. *Am. Heart J.* 46: 485, 1953.

307. Langner, P. H., Jr. and S. R. Moore. Location of the electrical center of ventricular repolarization. *Am. Heart J.* 52: 335, 1956.

308. Langner, P. H., Jr., R. H. Okada, S. R. Moore, and H. L. Fies. Comparison of four orthogonal systems of vectorcardiography. *Circulation* 17: 46, 1958.

309. Larks, S. D. and K. Dasgupta. Fetal electrocardiography, with special reference to early pregnancy. *Am. Heart J.* 56: 701, 1958.

310. Larsen, K. and T. Skulason. Das normale Ekg. III. Die Stellung der elektr. Achse bei 100 Gesunden im Alter von 30–50 Jahren. *Nord. med.* 29: 125, 1943.

311. Laurentius, P. Das Belastungs-Elektrokardiogramm. *Arch. Kreislaufforsch.* 10: 346, 1942.

312. Leitner, S. J. and H. Steinlein. Untersuchungen über den Einfluß des vegetativen Nervensystems auf das Ekg. *Arch. Kreislaufforsch.* 13. 62, 1944.

313. Lepeschkin, E. Electrocardiographic observations on the mechanism of the electrical alternans of the heart. *Cardiologia* 16: 278, 1950.

314. Lepeschkin, E. Role of temperature gradients within ventricular muscle in genesis of normal T wave of electrocardiogram and ventricular gradient responsible for it. *Fed. Proc.* 10: 81, 1951.

315. Lepeschkin, E. Components of Q-T and Q-U intervals of the electrocardiogram in normals. *J. Appl. Physiol.* 9: 443, 1956.

316. Lepeschkin, E. The U wave of the ECG (Symposium). *Circulation* 15: 68, 1957.

317. Lepeschkin, E., L. N. Katz, H. Schaefer, A. M. Shanes, and S. Weidmann. The U wave and afterpotentials in cardiac muscle. *Ann. New York Acad. Sc.* 65: 942, 1957.

318. Lepeschkin, E. and B. Surawicz. The measurement of the duration of the QRS interval. *Am. Heart J.* 44: 80, 1952.

319. Levine, H. D., B. Lown, and R. B. Streeper. The clinical significance of postextrasystolic T-wave changes. *Circulation* 6: 538, 1952.

320. Levine, R. B., O. H. Schmitt, and E. Simonson. Electrocardiographic mirror pattern studies. II. The statistical

and individual validity of the heart dipole concept as applied in ECG analysis. *Am. Heart J.* 45: 500, 1953.

321. Lewis, T. Interpretations of the initial phases of the electrocardiogram with special reference to the theory of "limited potential differences." *Arch. Int. Med.* 30: 269, 1922.
322. Lewis, T., J. Meakins, and P. D. White. The excitatory process in the dog's heart. I. The auricles. *Phil. Trans. B.* 205: 375, 1914.
323. Lewis, T. and M. Rothschild. The excitatory process in the dog's heart. II. The ventricle. *Phil. Trans. B.* 206: 181, 1915.
324. Liebow, I. M. and H. K. Hellerstein. Factors influencing the T wave of the electrocardiogram. *Am. Heart J.* 41: 266, 1951.
325. Lindner, E. and L. N. Katz. The relative conductivity of the tissues in contact with the heart. *Am. J. Physiol.* 125: 625, 1939.
326. Linzbach, A. J. Die Muskelfaserkonstante und das Wachstumsgesetz der menschlichen Herzkammern. *Virchows Arch. path. Anat.* 318: 575, 1950.
326a. Lombard, E. A. Electrocardiograms of small mammals. *Am. J. Physiol.* 171: 189, 1952.
327. Lombard, E. A. and C. Witham. Electrocardiogram of the anesthetized dog. *Am. J. Physiol.* 181: 567, 1955.
327a. Lukoschek, P. and J. Thiesen. Das normale Meerschweinchen-EKG. *Ztschr. Kreislaufforsch.* 43: 172, 1954.
328. Lüttgau, H. C. and R. Niedergerke. The antagonism between Ca and Na ions on the frog's heart. *J. Physiol.* 143: 486, 1958.
329. Lutz, W. Elektrokardiographische Beobachtungen bei Auskühlung des Warmblüters. *Ztschr. Kreislaufforsch.* 36: 625, 1944.
330. Mainzer, F. L'influence de l'anxiété sur l'électrocardiogramme: Son importance dans l'électrocardiographie pratique. *Cardiologia* 32: 362, 1958.
331. Maltesos, C. Über die Wirkung von Monojodessigsäure auf die elektrische Tätigkeit des Herzens. *Z. Biol.* 95: 205, 1934.
332. Mann, H. A method of analyzing the electrocardiogram. *Arch. Int. Med.* 25: 283, 1920.
333. Manning, G. W. The electrocardiogram of the Z-step exercise stress best. *Am. Heart. J.* 54: 823, 1957.
334. Manzotti, M. The effect of some respiratory manoevers on the heart rate. *J. Physiol.* 144: 541, 1958.
335. Marchand, N., S. A. Briller, and C. E. Kossmann. General networks for central terminals in electrocardiography and vectorcardiography. *Circulation* 12: 838, 1955.
336. Martinek, J., G. C. K. Yeh, and R. Carnine. A new system for electrocardiographic recording, analysis and diagnosis. *IRE Trans. on Med. Electronics* ME-6: 112, 1959.
336a. Massman, W. and H. Opitz. Das Katzen-EKG *Cardiologia* 24: 54, 1954.
337. Maxwell, M., R. Kennamer, and M. Prinzmetal. Studies on the mechanism of ventricular activity. IX. The "mural-type" coronary QS wave. *Am. J. Med.* 17: 614, 1954.
338. Mazer, M. and J. A. Reisinger. Criteria for differentiating deep Q_3 electrocardiograms from normal and cardiac subjects. *Am. J. M. Sc.* 206: 48, 1943.
339. McFee, R. A trigonometric computer with electrocardiographic applications. *Rev. Scient. Instruments* 21: 420, 1950.
340. McFee, R. and F. D. Johnston. Electrocardiographic leads. I. Introduction. *Circulation* 8: 555, 1953.
341. McFee, R. and F. D. Johnston. Electrocardiographic leads. II. Analysis. *Circulation* 9: 255: 1954.
342. McFee, R. and F. D. Johnston. Electrocardiographic leads. III. Synthesis. *Circulation* 9: 868, 1954.
343. McFee, R., R. Stow, and F. D. Johnston. Graphic representation of electrocardiographic leads by means of fluid mappers. *Circulation* 6: 21, 1952.
344. Meda, E. Sui fenomeni elettrici elementari del miocardio. *Arch. fisiol.* 55: 298, 1955.
345. Meyer, P. and C. Schmidt. Troubles post-extrasystoliques de la répolarisation. *Arch. mal. coeur* 1949: 1175.
346. Michel, D. Die Lebenswandlungen der menschlichen Herzstromkurve. *Verh. dtsch. Ges. Kreisl.-Forsch.* 24: 104, 1958.
347. Milnor, W. R. and C. A. Bertrand. The normal vectorcardiogram and the classification of abnormalities. Second World Congr. Cardiol. Washington. D. C., 1954.
348. Milnor, W. R., S. A. Talbot, and E. V. Newman. A study of the relationship between unipolar leads and spatial vectorcardiograms, using the panoramic vector cardiograph. *Circulation* 7: 545, 1953.
349. Mitchell, J. H. and A. P. Shapiro. The relationship of adrenaline and T-wave changes in the anxiety state. *Am. Heart J.* 48: 323, 1954.
350. Mori, H., K. Nakagawa, J. C. Dahl, O. H. Schmitt, and E. Simonson. A quantitative study of initial and terminal QRS vectors in a group of normal older men. *Am. Heart J.* 59: 374, 1960.
351. Morin, G., A. Jouve, M. Albouy, P. Vélasque, and G. Bergier. Sur la détermination du point origine de la boucle cardiovectographique chez le chien. *Compt. rend. soc. biol.* 144: 1177, 1950.
352. Morton, R. F., W. E. Romans, and D. A. Brody. Cancellation of esophageal electrocardiograms. *Circulation* 15: 897, 1957.
353. Nahum, L. H. A critical evaluation of electrocardiography. *Trans. Am. Coll. Cardiol.* 2: 168, 1952.
354. Nahum, L. H., W. F. Hamilton, and H. E. Hoff. The injury current in the ECG. *Am. J. Physiol.* 130: 202, 1943.
355. Nazzi, V., G. Ricco, and A. Meda. La systole ventriculaire étudiée au moyen de la méthode polygraphique. *Cardiologia* 24: 319, 1954.
356. Nehb, W. Zur Standardisierung der Brustwandableitungen des Ekg. *Klin. Wschnschr.* p. 1938, 1807.
357. Nelson, C. V. Effect of the finite boundary on potential distributions in volume conductors. *Circulation Res.* 3: 236, 1955.
358. Niggli-Meier, A. Vektorielle Messungen aus den Einthovenschen Extremitätenableitungen, mit besonderer Berücksichtigung des sog. "Manifest-Ekg." *Cardiologia* 29: 254, 1956.
359. Nims, L. F., B. Kartin, H. M. Chernoff, and L. H. Nahum. Heart temperature and its relation to the T-wave. *Fed Proc.* 7: 86, 1948.
360. Nonidez, J. F. The structure and innervation of the conductive system of the heart of the dog and rhesus monkey, as seen with a silver impregnation technique. *Am. Heart J.* 26: 577, 1943.
361. Nordenfelt, O. Über funktionelle Veränderungen der P- and T-Zacken im Ekg. Experimentelle Untersuchun-

gen mit Ergotamin und Amylnitrit, sowie klinische Beobactungen. *Acta med. scandinav.* Suppl. 119, 1941.

362. Okada, R. H. The image surface of a circular cylinder. *Am. Heart J.* 51: 489, 1956.
363. Okada, R. H. An experimental study of multiple dipole potentials and the effects of inhomogeneities in volume conductors. *Am. Heart J.* 54: 567, 1957.
364. Packard, J. M., J. S. Graettinger, and A. Graybid. Analysis of the electrocardiograms obtained from 1000 young healthy aviators: Ten year follow-up. *Circulation* 10: 384, 1954.
365. Pantridge, J. F. Observations on the ECG and ventricular gradient in complete left bundle branch block. *Circulation* 3: 589, 1951.
366. Peñaloza, D. and J. Tranchesi. The three main vectors of the ventricular activation process in the normal human heart. I. Its significance. *Am. Heart J.* 49: 51, 1955.
367. Pieri, J., A. Jouve, J. Casalonga, P. Nicolai, and C. Ambrosi. Étude comparée des dérivations de surface et des dérivations intrathoraciques chez l'homme. *Acta cardiol.* 13: 327, 1958.
368. Pipberger, H. V. The normal orthogonal electrocardiogram and vectorcardiogram. *Circulation* 17: 1102, 1958.
369. Pipberger, H. V. Current status and persistent problems of electrode placement and lead systems for vectorcardiography and electrocardiography. *Progr. Cardiovascular Diseases* 2: 248, 1959.
370. Pipberger, H. V. and E. D. Freis. A project of the United States Veterans Administration for the electronic computation of electrocardiographic data. 11th Ann. Conf. Electric. Tech. in Med. Biol. Minn., 1958.
371. Pipberger, H. V., R. Kälin and P. H. Rossier. Vektorkardiographische Untersuchungen an Hypertonikern bei massiven Blutdrucksenkungen durch Hexamethonium. Ein Beitrag zur Theorie des Ventrikelgradienten. *Cardiologia* 27: 166, 1955.
372. Pipberger, H. V. and L. S. Lilienfield. Application of corrected electrocardiographic lead systems in man. *Am. J. Med.* 25: 539, 1958.
373. Pipberger, H. V., L. Schwartz, R. A. Massumi, and M. Prinzmetal. Studies on the nature of the repolarization process. XIX. Studies on the mechanism of ventricular activity. *Am. Heart J.* 53: 100, 1957.
374. Pipberger, H. V. and H. L. Tanenbaum. The P wave, P-R interval, and Q-T ratio of the normal orthogonal electrocardiogram. *Circulation* 18: 1175, 1958.
375. Pipberger, H. V. and C. R. Wood, Jr. A simplified method for the resolution of the orthogonal electrocardiogram. *Circulation Res.* 6: 239, 1958.
376. Powell, S. J. Unexplained electrocardiograms in the African. *Brit. Heart J.* 21: 263, 1959.
377. Prinzmetal, M., R. Kennamer, and M. Maxwell. Studies on the mechanism of ventricular activity. VIII. The genesis of the coronary QS wave in through-and-through-infarction. *Am. J. Med.* 17: 610, 1954.
378. Puech, P., M. Esclarissat, D. Sodi-Pallares, and F. Cisneros. Normal auricular activation in the dog's heart. *Am. Heart J.* 47: 174, 1954.
379. Read, J. L., E. S. Hegre, and S. Russi. Reaffirmation of the auriculoventricular conduction system in man. *Circulation* 7: 42, 1953.
380. Reindell, H. Kymographische und elektrokardiographische Befunde am Sportherzen. I. Untersuchungin Ruhe. *Deutsches Arch. klin. Med.* 181: 485, 1938.
381. Reindell, H. Kymographische und elektrokardiographische Befunde am Sportherzen. II. Das Ekg nach Belastung. *Deutsches Arch. klin. Med.* 182: 506, 1938.
382. Reynolds, E. W., Jr., J. F. Cordes, P. W. Willis, and F. D. Johnston. The use of the lead-field concept in the development of leads satisfactory for vectorcardiography. I. The sagittal lead. *Circulation* 14: 48, 1956.
383. Reynolds, E. W., Jr., and C. R. Vander Ark. An experimental study on the origin of T-waves based on determinations of effective refractory period from epicardial and endocardial aspects of the ventricle. *Circulation Res.* 7: 943, 1959.
384. Reynolds, T. B., H. M. Martin, and R. E. Homann. Serum electrolytes and the ECG. *Am. Heart J.* 42: 671, 1951.
385. Rijlant, P. Spatial vectorcardiography. *Acta physiol. et pharmacol. neerl.* 6: 153, 1957.
386. Rijlant, P. Électrocardiogrammes vectoriels et vectocardiogrammes normaux et pathologiques chez l'homme. *Acta cardiol.* 13: 11, 1958.
387. Robb, J. S. A study of the detail of muscle insertions in the heart. *Bull. internat. A. M. Mus.* 30: 84, 1949.
388. Robb, J. S. and R. C. Robb. The excitatory process in the mammalian ventricle. *Am. J. Physiol.* 115: 43, 1936.
389. Robb, J. S. and R. C. Robb. The normal heart. (Anatomy and physiology of the structural units.) *Am. Heart J.* 23: 455, 1942.
390. Robertson, D. On consistency in convention of "view" in vectorcardiography. *Am. Heart J.* 53: 247, 1957.
391. Rodeck, H. Der Ca-K-Ionenantagonismus bei konstant gehaltenem Ca-K-Verhältnis untersucht an Herzfrequenz und Elektrokardiogramm. *Pflüger's Arch. ges. Physiol.* 250: 91, 1948.
392. Rosenbaum, M. and E. Lepeschkin. The effect of ventricular systole on auricular rhythm in auriculoventricular block. *Circulation* 11: 240, 1955.
393. Rosenblueth, A. Mechanism of the Wenckebach-Luciani cycles. *Am. J. Physiol.* 194: 491, 1958.
394. Rosenblueth, A. Ventricular "echoes." *Am. J. Physiol.* 195: 53, 1958.
395. Rothsberger, C. J. Normale und pathologische Physiologie der Rhythmik und Koordination des Herzens. *Ergeb. Physiol.* 32: 472, 1931.
396. Rothberger, C. J. and D. Scherf. Zur Kenntnis der Erregungsausbreitung von Sinus auf den Vorhof. *Ztschr. ges. exper. Med.* 53: 792, 1926.
397. Rothman, S., E. Gerlach, M. Prinzmetal, L. Rakita, and J. L. Borduas. Studies on the mechanism of ventricular activity. XIII. Genesis of the depolarization complex in the mammalian heart. *Am. J. Physiol.* 179. 557, 1954.
398. Rothschuh, K. E. Über den funktionellen Aufbau des Herzens aus elektrophysiologischen Elementen und über den Mechanismus der Erregungsleitung im Herzen. *Pflüger's Arch. ges. Physiol.* 253: 238, 1951.
399. Samet, P., W. H. Bernstein, and R. S. Litwak. Electrical activation and mechanical asynchronism in the cardiac cycle of the dog. *Circulation Res.* 7: 228, 1959.
400. Sangiorgi, M., V. Corsi, L. Cofano, and E. Salvo. A comparative study of some vectorcardiographic methods based on the use of unipolar leads, bipolar leads between

electrically symmetrical points and bipolar leads. *Acta cardiol.* 15: 101, 1960.
401. Sano, T., H. K. Hellerstein, and E. Vayda. P vector loop in health and disease as studied by the technique of electrical dissection of the vectorcardiogram. (Differential vectorcardiography.) *Am. Heart J.* 53: 854, 1957.
402. Savjoloff, V. V. Intrapulmonale Ableitungen der Aktionsströme vom menschlichen Herzen in situ. *Ztschr. Kreislaufforsch.* 20: 584, 1928.
403. Sayen, J. J., W. F. Sheldon, G. Peirce, and P. T. Kuo. Polarographic oxygen, the epicardial ECG and muscle contraction in experimental acute regional ischemia of the left ventricle. *Circulation Res.* 6: 779, 1958.
404. Schaefer, H. Die theoretischen Grundlagen des Ekg. *Verh. dtsch. Ges. Kreisl.-Forsch.* 18: 11, 1952.
405. Schaefer, H. Bemerkungen zu F. Kienles "Grundzüge der Funktions-Elektrokardiographie." *Ztschr. Kreislaufforsch.* 45: 462, 1956.
406. Schaefer, H. The U wave and afterpotentials in cardiac muscle: Panel discussion. *Ann. New York Acad. Sc.* 65: 954, 1957.
407. Schaefer, H. The general order of excitation and recovery. *Ann. New York Acad. Sc.* 65: 743, 1957.
408. Schaefer, H. In: *Die Funktionsdiagnostik des Herzens. V. Freiburger Symposium.* Berlin: Springer, 1958, p. 13.
409. Schaefer, H. Die Einwirkung des elektrischen Stroms auf wichtige innere Organe. *Deutsches. Ztschr. ges. gerichtl. Med.* 47: 5, 1958.
410. Schaefer, H. and W. Gärtner. Über die absolute Größe elektrokardiographischer Potentiale. *Pflüger's Arch. ges. Physiol.* 255: 251, 1952.
411. Schaefer, H., A. Peña, and P. Schölmerich. Der monophasische Aktionsstrom von Spitze und Basis des Warmblüterherzens und die Theorie der T-Welle des Ekg. *Pflüger's Arch. ges. Physiol.* 246: 728, 1943.
412. Schaefer, H. and W. Trautwein. Über die elementaren elektrischen Prozesse im Herzmuskel und ihre Rolle für eine neue Theorie des Ekg. *Pflüger's Arch. ges. Physiol.* 251: 417, 1949.
413. Schaefer, H. and W. Trautwein. Weitere Versuche über die Natur der Erregungswelle im Myokard des Hundes. *Pflüger's Arch. ges. Physiol.* 253: 152, 1951.
414. Scher, A. M., J. Lihkane, M. I. Rodriguez, and A. C. Young. "Slow" potential change in the atrioventricular node. *Science* 127: 873, 1958.
415. Scher, A. M., H. J. Rodriguez, J. Lihkane, and A. C. Young. The mechanism of atrioventricular conduction. *Circulation Res.* 7: 54, 1959.
416. Scher, A. M. and A. C. Young. Spread of excitation during premature ventricular systoles. *Circulation Res.* 3: 535, 1955.
417. Scher, A. M. and A. C. Young. The pathway of ventricular depolarization in the dog. *Circulation Res.* 4: 461, 1956.
418. Scher, A. M. and A. C. Young. Ventricular depolarization and the genesis of QRS. *Ann. New York Acad. Sc.* 65: 768, 1957.
419. Scher, A. M., A. C. Young, A. L. Malmgren, and R. V. Erickson. Activation of the interventricular septum. *Circulation Res.* 3: 56, 1955.
420. Scher, A. M., A. C. Young, A. L. Malmgren, and R. R. Paton. Spread of electrical activity through the wall of the ventricle. *Circulation Res.* 1: 539, 1953.
421. Scherf, D. and A. I. Schaffer. The electrocardiographic exercise test. *Am. Heart J.* 43: 927, 1952.
422. Scherlis, L., R. P. Lasser, and A. Grishman. Spatial vectorcardiography: The normal vectorcardiogram. *Am. Heart J.* 42: 235, 1951.
423. Schlegel, R. Über die Beziehungen zwischen der Breite von P und der Senkung der PQ-Strecke im Extremitäten-Ekg. *Ztschr. Kreislaufforsch.* 43: 772, 1954.
424. Schlomka, G. Über die Beziehungen zwischen Muskelmassenverhältnis der Herzkammern und Ekg-Typ *Deutsches Arch. klin. Med.* 193: 555, 1948.
425. Schmidt, R. F. Versuche mit Aconitin zum Problem der spontanen Erregungsbildung im Herzen. *Pflüger's Arch. ges. Physiol.*, 271: 526, 1960.
426. Schmidt, R. F. and T. T. Chang. Aktionspotential und Mechanogramm von Purkinje-Fäden in tiefer Temperatur. *Pflüger's Arch. ges. Physiol.* 272: 393, 1961.
427. Schmitt, O. H. Cathode-ray presentation of three-dimensional data. *J. Appl. Phys.* 18: 819, 1947.
428. Schmitt, O. H. Lead vectors and transfer impedance. *Ann. New York Acad. Sc.* 65: 1092, 1957.
429. Schmitt, O. H. Twenty electrocardiographic lead systems: their transfer impedances and correction coefficients. *Fed. Proc.* 17: 143, 1958.
430. Schmitt, O. H., R. B. Levine, and E. Simonson. Electrocardiographic mirror pattern studies. I. Experimental validity tests of the dipole hypothesis and of the central terminal theory. *Am. Heart J.* 45: 416, 1953.
431. Schmitt, O. H. and E. Simonson. Symposium on electrocardiography and vectorcardiography. The present status of vectorcardiography. *Arch. Int. Med.* 96: 574, 1955.
432. Schröder, R. and N. Sumruatruamphol. Über den Wert des Ventrikelgradienten für die klinische Elektrokardiographie. *Ztschr. Kreislaufforsch.* 48: 769, 1959.
433. Schütz, E. Elektrophysiologie des Herzens bei einphasischer Ableitung. *Ergeb. Physiol.* 38: 493, 1936.
434. Schütz, E. Der monophasische Aktionsstrom. *Verh. dtsch. Ges. Kreisl.-Forsch.* 12: 15, 1939.
435. Schütz, E. Zur Physiologie des Elektrokardiogramms. *Verh. dtsch. Ges. Kreisl.-Forsch.* 18: 50, 1952.
436. Schütz, U. and G. Schütz. Experimentelle Analyse der ST-Senkung des Ekg. *Ztschr. Kreislaufforsch.* 38: 66, 1949.
437. Schwan, H. P. and C. F. Kay Capacitive properties of body tissues. *Circulation Res.* 5: 439, 1957.
438. Schwarzschild, M. H., I. Hoffman, and M. Kissin. Errors in unipolar limb leads caused by unbalanced skin resistances, and a device for their elimination. *Am. Heart J.* 48: 235, 1954.
439. Sears, G. A. and G. W. Manning. Routine electrocardiography: postprandial T-wave changes. *Am. Heart J.* 56: 591, 1958.
440. Sedefeiyan, A. and H. Winterstein. Intrakardiale Reflexe. *Rev. fac. sci. univ. Istanbul Ser. B.* 10: 215, 1945.
441. Segers, M. Le rôle des potentiels tardifs du coeur. *Mém. Acad. roy. Méd. Belg.* 1: 1, 1941.
442. Segers, M. Phénomènes des synchronisations au niveau du coeur. *Arch. internat. physiol.* 54: 87, 1946.
443. Seiden, G. E. The electric heart center for the QRS complex in cardiac patients. *Circulation Res.* 4: 313, 1956.
444. Seiden, G. E. The normal QRS loop observed three dimensionally obtained with the Frank precordial system. *Circulation* 16: 582, 1957.
445. Selvini, A. Analisi vettoriale delle tenzioni bioelettriche

prodotte dal cuore di sana con punta lesa. *Folia cardiol.* 6: 1, 1947.

446. Shillingford, J. and W. Brigden. The vectorcardiogram in 100 healthy subjects. *Brit. Heart J.* 13: 233, 1951.

447. Siebens, A. A., B. F. Hoffmann, J. L. Gilbert, and E. E. Suckling. Effect of rate on excitability of dog's ventricle. *Am. J. Physiol.* 166: 610, 1951.

448. Simonson, E. The distribution of cardiac potentials around the chest in one hundred and three normal men. *Circulation* 6: 201, 1952.

449. Simonson, E. The normal variability of the electrocardiogram as a basis for differentiation between "normal" and "abnormal" in clinical electrocardiography. *Am. Heart J.* 55: 80, 1958.

450. Simonson, E. and A. Keys. A quantitative comparison of unipolar limb leads. *Circulation* 1: 954, 1950.

451. Simonson, E. and A. Keys. The effect of an ordinary meal on the electrocardiogram. Normal standards in middle-aged men and women. *Circulation* 1: 1000, 1950.

452. Simonson, E. and A. Keys. The effect of age and body weight on the electrocardiogram of healthy men. *Circulation* 6: 749, 1952.

453. Simonson, E. and A. Keys. The spatial QRS and T vector in 178 normal middle-aged men. Body weight, height, relationship of QRS and T and preliminary standards. *Circulation* 9: 105, 1954.

454. Simonson, E. and A. Keys. Repeat variability of spatial QRS and T vectors. *Circulation* 10: 850, 1954.

455. Simonson, E. and A. Keys. The electrocardiographic exercise test: Changes in the scalar ECG and in the mean spatial QRS and T vectors in two types of exercises; effect of absolute and relative body weight and comment on normal standards. *Am. Heart J.* 52: 83, 1956.

456. Simonson, E. and A. Keys. The effect of age on mean spatial QRS and T vectors. *Circulation* 14: 100, 1956.

457. Simonson, E., O. H. Schmitt, and H. W Blackburn, Jr. The effect of leads utilized upon discrepancies between spatial vectors recorded by SVEC and by mean vector methods. *Circulation Res.* 3: 532, 1955.

458. Simonson, E., O. H. Schmitt, H. W. Blackburn, Jr., and R. B. Levine. The speed of ventricular activation measured in the spatial vectorcardiograms. *Circulation Res.* 3: 409, 1955.

459. Simonson, E., O. H. Schmitt, J. Dahl, D. Fry, and E. E. Bakken. The theoretical and experimental bases of the frontal plane ventricular gradient and its spatial counterpart. *Am. Heart J.* 47: 122, 1954.

460. Simonson, E., O. H. Schmitt, and R. B. Levine. Comparison of spatial instantaneous ECG vectors, measured with the SVEC, with mean vectors derived from conventional ECG leads. *Circulation Res.* 3: 320, 1955.

461. Simonson, E., O. H. Schmitt, R. B. Levine, and J. Dahl. Electrocardiographic mirror pattern studies. III. Mirror pattern cancellation in normal and abnormal subject. *Am. Heart J.* 45: 655, 1953.

462. Simonson, E., O. H. Schmitt, and H. Nakagawa. Quantitative comparison of eight vectorcardiographic lead systems. *Circulation Res.* 7: 296, 1959.

463. Sjöstrand, F. Experimental variations in the T-wave of the ECG. *Acta med. scandinav.* 138: 191, 1950.

464. Sjöstrand, F. The relationship between the heart frequency and the ST-level of the ECG. *Acta med. scandinav.* 138: 201, 1950.

465. Smith, L., R. Kennamer, and M. Prinzmetal. Studies on the mechanism of ventricular activity. IV. Ventricular excitation in segmental and diffuse types of experimental bundle-branch block. *Circulation Res.* 2: 221, 1954.

466. Sodi-Pallares, D., E. Barbato, and A. Delmar. Relationship between the intrinsic deflection and subepicardial activation. *Am. Heart J.* 39: 387, 1950.

467. Sodi-Pallares, D., A. Bisteni, G.A. Medrano, and F. Cisneros. The activation of the free left ventricular wall in the dog's heart. *Am. Heart J.* 49: 587, 1955.

468. Sodi-Pallares, D., M. I. Rodriguez, L. O. Chait, and R. Zuckermann. The activation of the interventricular septum. *Am. Heart J.* 41: 569, 1951.

469. Somer, de E. Sur le rapport entre l'électrocardiogramme et la contraction cardiaque. *J. physiol. et pathol. gén.* 36: 1083, 1938.

470. Somer, de E. Manifestations ECG de l'asphyxie. *Arch. intern. méd. exper.* 13: 451, 1938.

471. Spörri, H. Starke Dissoziation zwischen dem Ende der elektrischen und mechanischen Systolendauer bei Känguruhs. *Cardiologia* 28: 278, 1956.

472. Stallmann, F. Über die Ableitetheorie des Elektrokardiogramms. *Arch. Kreislaufforsch.* 25: 291, 1957.

473. Stephanopoli de Comnène, J., B. Bladier, F. Colombani, and J. Bonifaci. Studies of the atriogram. *Am. Heart J.* 50: 666, 1955.

474. Stewart, H. J. and H. A. Carr. The anoxemia test. *Am. Heart J.* 48: 293, 1954.

475. Sulzer, R. and P. W. Duchosal. Planographie. Nouvelle méthode d'enregistrement électro-cardiographic selon deux dérivations simultanées. *Arch. mal. coeur* 31: 682, 1938.

476. Surawicz, B., H. A. Braun, W. B. Crum, R. L. Kemp, S. Wagner, and S. Bellet. Quantitative analysis of the electrocardiographic pattern of hypopotassemia. *Circulation* 16: 750, 1957.

477. Surawicz, B., E. Lepeschkin, H. C. Herrlich, and B. F. Hoffman. Effect of potassium and calcium deficiency on the monophasic action potential electrocardiogram and contractility of isolated rabbit hearts. *Am. J. Physiol.* 196: 1302, 1959.

478. Taback, L., E. Marden, H. L. Mason, and H. V. Pipberger. Digital recording of electrocardiographic data for analysis by a digital computer. *IRE Trans. Med. Electronics* ME-6: 167, 1959.

479. Taccardi, B. The spread of the excitation over small areas of the ventricular surface. IIIe Congrès mondial de Cardiologie, Bruxelles. Résumes des Communications. 1958, p. 37.

480. Testoni, F. and A. Giancotti. Vector analysis of Condorelli's leads. *Cardiologia* 25: 277, 1954.

481. Testoni, F. and N. B. Narbone. Vectorcardiographic studies on the symmetry of the cardiac electrical field in normal subjects and in patients with heart disease. *Cardiologia* 35: 1, 1959.

482. Thaon, M., G. Minot, R. Damoiselet, and J. Thevenet. Contribution à l'étude de la double électrode à éléments concentriques dite "électrode circulaire." *Acta cardiol.* 7: 327, 1952.

483. Tiitso, M. Über die Bedingungen des Zustandekommens des chronotropen Effektes der Dehnung des rechten Vorhofs beim Hunde. *Pflüger's Arch. ges. Physiol.* 242: 685, 1939.

484. Tobien, H. H. Untersuchungen über den Ventrikelgradienten bei Kammer-Extrasystolen. *Ztschr. Kreislaufforsch.* 48: 809, 1959.

485. Trautwein, W. Über die Veränderungen der elementaren Daten der elektrischen Erregungswelle des Herzens bei der Insuffizienz des Myocards. *Pflüger's Arch. ges. Physiol.* 252: 573, 1950.

486. Trautwein, W. Experimentelle Untersuchung zur Theorie des Schenkelblock-Ekg. *Ztschr. ges. exper. Med.* 117: 204, 1951.

487. Trautwein, W. Zur Frage der spontanen Erregungsbildung im Herzen und über Faktoren, die diese beeinflussen. *Verh. dtsch. Ges. inn. Med.* 65: 503, 1959.

488. Trautwein, W. Elektrophysiologie der Herzmuskelfaser. *Ergeb. Physiol. exptl. Pharmakol.* 51: 131, 1961.

489. Trautwein, W. and J. Dudel. Aktionspotential und Mechanogramm des Warmblüterherzmuskels als Funktion der Schlagfrequenz. *Pflüger's Arch. ges. Physiol.* 260: 24, 1954.

490. Trautwein, W. and J. Dudel. Hemmende und "erregende" Wirkungen des Acetylcholin am Warmblüterherzen. Zur Frage der spontanen Erregungsbildung. *Arch. ges. Physiol., Pflüger's* 266: 653, 1958.

491. Trautwein, W., V. Gottstein, and J. Dudel. Der Aktionsstrom der Myokardfaser im Sauerstoffmangel. *Pflüger's Arch. ges. Physiol.* 260: 40, 1954.

492. Trethewie, E. R. Simplified (ABC) electrocardiography. *Cardiologia* 25: 331, 1954.

493. Trethewie, E. R. and M. M. Hodgkinson. The influence of CO_2 and pH on the ECG of the isolated perfused heart. *Quart. J. Exper. Physiol.* 40: 1, 1955.

494. Tumiotto, G., A. Oliva, G. C. Cattini, and L. L. Barbieri. Contribution à l'étude des correlations existant entre le metabolisme cardiaques et l'électrocardiogramme. Modifications électrocardiographiques consécutives à l'administration de glucose. *Acta cardiol.* 11: 480, 1956.

495. Tumiotto, G., A. Oliva, G. C. Cattini, and G. Cappelli. Elektrokardiographische Veränderungen durch Trauben- und Fruchtzuckerbelastung bei Herzgesunden und Herzkranken. Einfluß von ATP auf die beschriebenen Vorgänge. *Cardiologia* 28: 327, 1956.

496. Tysinger, D. S., Jr., J. T. Grace, and F. Gollan. The electrocardiogram of dogs surviving 1.5° centigrade. *Am. Heart J.* 50: 816, 1955.

497. Unghvary, L. Die Lageveränderung der elektrischen Achsen in Ebene und Raum während der Entwicklung des Herzens und ihr Zusammenhang mit den Brustwandableitungen. *Ztschr. Kreislaufforsch.* 38: 674, 1949.

498. Urschel, D. L. and P. C. Abbey. Mean spatial vectorcardiography. The influence of age, sex, body build, and chest configuration on the QRS vector in normal individuals. *Am. Heart J.* 46: 496, 1953.

499. Vanremoortere, E. A propos de l'origine centrale de l'arythmie respiratoire. *Acta cardiol.* 4: 384, 1949.

500. Vastesaeger, M. and J. Rochet. Les propriétés du vectocardiogramme spital de l'homme normal, ses variations physiologiques. *Trav. Lab. l'Institut Solvay Physiol.* 29: 55, 1944.

501. Veyrat, R. La composition des potentiels électriques recueillis en dérivation unipolaire à la surface du coeur. *Helvet. physiol. et pharmacol. acta* 11: 395, 1953.

502. Viscidi, P. C. and A. J. Geiger. ECG observations on 500 unselected young adults at work. *Am. Heart J.* 26: 763, 1943.

503. Vizcaino, M., D. Sodi-Pallares, and E. Cabrera. Algunas consideraciones sobre el tipo electrocardiográfico S1, S2, S3. *Arch. Inst. cardiol. México* 14: 261, 1945.

504. Walker, S. M. Ventricular coupling induced by anodal or cathodal polarization during continuous direct currents in dog ventricle. *Am. J. Physiol.* 196: 209, 1959.

505. Waller, A. D. On the electromotive changes connected with the beat of the mammalian heart and of the human heart in particular. *Phil. Trans. B* 180: 169, 1889.

506. Ware, F., Jr., A. L. Bennett, and A. R. McIntyre. Membrane potentials in normal, isolated, perfused froghearts. *Am. J. Physiol.* 190: 194, 1957.

507. Wasserburger, R. H. Observations on the "juvenile pattern" of adult negro males. *Am. J. Med.* 18: 428, 1955.

508. Webb, J. L. and P. B. Hollander. The action of acetylcholine and epinephrine on the cellular membrane potentials and contractility of rat atrium. *Circulation Res.* 4: 332, 1956.

509. Webb, J. L. and P. B. Hollander. Metabolic aspects of the relationship between the contractility and membrane potentials of the rat atrium. *Circulation Res.* 4: 618, 1956.

510. Webb, J. L. and P. B. Hollander. Effects of enzyme inhibitors on the contractility and membrane potentials of the rat atrium. *Circulation Res.* 7: 131, 1959.

511. Weidmann, S. Effects of calcium ions and local anaesthetics on electrical properties of Purkinje fibres. *J. Physiol.* 129: 568, 1955.

512. Weidmann, S. Shortening of the cardiac action potential due to a brief injection of KCl following the onset of activity. *J. Physiol.* 132: 157, 1956.

513. Weidmann, S. Effects of increasing the calcium concentration during a single heart-beat. *Experientia* 15: 128, 1959.

514. Welsch, A. and H. Wieland. Über die klinische Brauchbarkeit des Ventrikelgradienten. Untersuchungen beim rechtstypischen Ekg. *Ztschr. Kreislaufforsch.* 42: 262, 1953.

515. Wenger, R. Die Bedeutung des Oesophagus-Ekgs für die Diagnostik von Rhythmusstörungen. *Wien. klin. Wchnschr.* 67: 408, 1955.

516. Wenger, R., H. Engelhart, and H. Mösslacher. Die verschiedene Bedeutung von Kammerextrasystolen. *Ztschr. Kreislaufforsch.* 48: 665, 1959.

517. Wenger, R. and D. Hofmann-Credner. Observations on the atria of human heart by direct and semidirect electrocardiography. *Circulation* 5: 870, 1952.

518. Wenger, R. and K. Hupka. A new vectorcardiographic lead system. *Am. Heart J.* 57: 340, 1959.

519. Wenger, R. and E. Wick. Auricular conduction in a case of wandering auricular pacemaker. *Am. Heart J.* 49: 116, 1955.

520. Wenger, R., E. Wick, and W. Swoboda. Das Vektorkardiogramm bei Kindern und Jugendlichen. *Arch. Kinderh.* 146: 99, 1953.

521. Whipple, G. H. A simple technique for registering the direction of rotation of vectorcardiographic loops. *Am. Heart J.* 44: 384, 1952.

522. Whitehorn, W. V. and J. W. Bean. Cardiac changes induced by O_2 at high pressure, CO_2 and low O_2, as manifest by the electrocardiogram. *Am. J. Physiol.* 168: 528, 1952.

523. Wilson, F. N. and R. H. Bayley. The electric field of

an eccentric dipole in a homogeneous spherical conducting medium. *Circulation* 1: 85, 1950.

524. Wilson, F. N., J. M. Bryant, and F. D. Johnston. On the possibility of constructing an Einthoven triangle for a given subject. *Am. Heart J.* 37: 493, 1949.

525. Wilson, F. N. and G. R. Herrmann. Relation of QRS-interval to ventricular weight. *Heart* 15: 135, 1930.

526. Wilson, F. N., J. G. Hill, and F. D. Johnson. The interpretation of the galvanometric curves obtained when one electrode is distant from the heart and the other near or in contact with the ventricular surface. *Am. Heart J.* 10: 163, 1934.

527. Wilson, F. N., F. D. Johnston, and C. E. Kossmann. The substitution of a tetrahedron for the Einthoven triangle. *Am. Heart J.* 33: 594, 1947.

528. Wilson, F. N., F. D. Johnston, A. G. McLeod, and P. S. Barker. Electrocardiograms that represent the potential variations of a single electrode. *Am. Heart J.* 9: 447, 1934.

529. Wilson, F. N., C. E. Kossmann, G. E. Burch, E. Goldberger, A. Graybiel, H. H. Hecht, F. D. Johnston, E. Lepeschkin, and G. B. Myers. Report of committee on electrocardiography, American Heart Association, Recommendations for standardization of electrocardiographic and vectorcardiographic leads. *Circulation* 10: 564, 1954.

530. Wilson, F. N., A. G. McLeod, and P. S. Barker. The distribution of the currents of action and of injury displayed by heart and muscle and other excitable tissues. *Univ. Mich. Studies. Ann Arbor Sc. Ser.* 18: 58, 1953.

531. Wilson, F. N., F. F. Rosenbaum, and F. D. Johnston. Interpretation of the ventricular complex of the ECG. *Advances Int. Med.* 2: 1, 1947.

532. Wise, N. B., W. J. Comeau, and P. D. White. An electrocardiographic study of twins. *Am. Heart J.* 17: 701, 1939.

533. Wolf, H. Die Genauigkeit der Herztätigkeit in der Tierreihe. *Pflüger's Arch. ges. Physiol.* 244: 181, 1940.

534. Woodbury, J. W., J. Lee, A. J. Brady, and K. A. Merenclino. Transmembranal potentials from the human heart. *Circulation Res.* 5: 179, 1957.

535. Woodbury, L. A., J. W. Woodbury, and H. H. Hecht. Membrane resting and action potentials of single cardiac muscle fibers. *Circulation* 1: 264, 1950.

536. Yeh, K., J. Martinek, and H. de Beaumont. Multipole representations of current generators in a volume conductor. *Bull. Math. Biophys.* 20: 203, 1958.

537. Young, E., L. Wolff, and J. Chatfield. The normal vectorcardiogram. I. *Am. Heart J.* 51: 713, 1956.

538. Zao, Z. Z. A utilitade do sistema de referencia circular das derivacões das extremidades na rotina clínica. *Arch. bras. Cardiol.* 7: 7, 1954.

539. Zao, Z. Z. Studies on the nature of the S-T segment changes. I. S-T changes influenced by varying concentrations of oxygen in experimental coronary artery occlusion in the dog. *Am. Heart J.* 58: 88, 1959.

540. Zao, Z. Z., G. R. Herrmann, and M. R. Hejtmancik. Spatial vector electrocardiography: method and average normal vector of P, QRS, and T in space. *Am. Heart J.* 56: 195, 1958.

541. Zárday, I. von. Elektro-Kardio-Axonogramm. *Z. klin. Med.* 140: 514, 1942.

542. Zatuchni, J. The ECG in pregnancy and the puerperium. *Am. Heart J.* 42: 11, 1951.

Physiologic consequences of congenital heart disease[1]

HIRAM W. MARSHALL
H. FREDERIC HELMHOLZ, Jr. *Mayo Clinic and Mayo Foundation, Rochester, Minnesota*
EARL H. WOOD[2]

CHAPTER CONTENTS

DURING THE LAST 100 YEARS a multitude of papers and case reports have appeared in the literature on congenital heart disease. However, there was very little correlation and integration of this material until the time of Dr. Maude Abbott (1), whose work provided the basis of our modern understanding of the various congenital anomalies of the heart. When, in 1938, Gross & Hubbard (124) performed the first successful operation for ligation of a patent ductus arteriosus and, in 1945, Gross & Hufnagel (125) and Crafoord & Nylin (72) first successfully corrected coarctation of the aorta, it brought the realization that accurate diagnosis of congenital cardiac defects had become imperative because certain properly selected patients could now be helped by surgical treatment. Tremendous added momentum to this field was given by the operation for supplementing the blood going to the lungs in cases of congenital pulmonary stenosis, first reported by Blalock & Taussig (32) in 1945.

Physiologic studies of congenital cardiac defects have depended in large measure on development of the technique of intracardiac catheterization. Forssmann (107) in 1929 introduced a catheter into his right atrium from his left arm, but only subsequent to the studies of Cournand & Ranges (70) was general interest in the method aroused. It soon became evident that important contributions to intracardiac hemodynamics in congenital malformations of the heart were possible. Great progress has been made in elucidating the physiologic effects of congenital cardiac defects in the past decade.

[1] This study was supported in part by Research Grant H-3532 from the National Institutes of Health, United States Public Health Service.

[2] Career Investigator, American Heart Association.

It is the purpose of this chapter to describe currently available information and concepts concerning the physiologic consequences of congenital cardiovascular anomalies and to point out some of the problems that remain. In addition, the techniques used to carry out hemodynamic studies in these patients will be discussed. First, however, a brief review of the various types of congenital cardiac defects will be presented.

TYPES AND ANATOMY OF CONGENITAL CARDIAC DEFECTS

No attempt will be made to discuss the embryologic basis for congenital defects or to discuss in detail the anatomic alterations that result. There are a number of excellent books and reviews of these subjects (89, 90, 150, 186). A classification of the various defects with a brief discussion of their anatomic alterations follows.

The true incidence of congenital heart disease in the general population at birth is not known. Fontana (106) found that the average incidence of congenital heart disease from necropsy material of all age groups from eight institutions was 1 per cent. This, however, may represent some degree of selection, and the true incidence is probably less than this. MacMahon and colleagues (171) reported that congenital heart disease is found in about 0.35 per cent of all live births.

Anomalies of the Great Vessels

ARTERIAL ANOMALIES. *Coarctation.* Coarctation of the aorta occurs as a single malformation in approximately 6 per cent of congenital cardiac malformations. It is characterized by a deformity of the aortic media causing narrowing, usually severe, of the aortic lumen. In the majority of instances the coarctation is downstream to the junction of the ductus arteriosus with the aorta, the ductus obliterates normally, and there is no abnormality of the pulmonary circulation. A well-developed collateral circulation bypasses the coarctation. Occasionally the ductus arteriosus remains patent and may join the aorta either proximal or distal to the coarctation. Occasionally the coarctation may occur proximal to the origin of the left subclavian artery, and in this instance there would be a pressure difference in the two arms. Rarely the coarctation may be in the usual location but with the right subclavian artery arising anomalously distal to the coarctation. Eighty per cent of patients with coarctation have a congenital bicuspid aortic valve.

Patent ductus arteriosus. Normally the ductus arteriosus, a channel that short circuits blood from the pulmonary artery to the aorta during fetal life, becomes obliterated shortly after birth. Sometimes this fails to occur, giving rise to the clinical entity, patent ductus arteriosus. This malformation is found in approximately 8 per cent of congenital cardiac malformations. As a consequence of the shunt from the aorta to the pulmonary arterial system, there usually is dilatation of the pulmonary arteries and the left side of the heart. As previously mentioned, a patent ductus may be associated with coarctation of the aorta, the coarctation occurring either proximal or distal to the ductus. Another of the more common combinations of defects is patent ductus arteriosus associated with a ventricular septal defect.

Vascular rings. Vascular rings are anomalies of the aortic-arch system. A vascular ring is of consequence if it interferes with the function of the trachea or the esophagus; it may result in death if the obstruction is not relieved surgically. This is a rare anomaly, which occurs in less than 1 per cent of all types of congenital cardiovascular defects.

The commonest types of vascular rings are *a*) anomalous origin of the right subclavian artery as the fourth branch of an otherwise normal aorta; to reach its destination it must cross the midline behind the esophagus from left to right; *b*) functioning double aortic arch; and *c*) single functioning right or left aortic arch passing behind the esophagus to reach the descending aorta which is on the contralateral side.

Persistent truncus arteriosus. Persistent truncus arteriosus is a relatively uncommon defect comprising less than 2 per cent of all congenital cardiovascular defects. It is characterized by a single functioning arterial vessel leaving the heart, and this vessel receives the blood above a ventricular septal defect from both ventricles. This vessel gives origin to the coronary, systemic, and pulmonary circulations. The pulmonary arteries may arise independently and directly from the truncus arteriosus, or secondarily from a main pulmonary artery that arises from the truncus. In one type no pulmonary arteries as such exist, the lung being supplied by bronchial arteries. Fifty per cent of patients with truncus arteriosus have a right aortic arch.

An aorticopulmonary septal defect is a variation of persistent truncus arteriosus in which only a small communication exists between the ascending aorta

and the pulmonary artery. In this condition the aortic and pulmonary valves are normally formed, but a fistulous opening exists between the ascending aorta and the main pulmonary artery. Functionally, this condition resembles patent ductus arteriosus and may give clinical signs readily confused with those of that condition.

Anomalies of coronary arteries. The coronary arteries may be abnormal in origin or in distribution. One or both may arise from the pulmonary artery. The commonest arrangement in which the pulmonary artery communicates with the coronary arterial system is that wherein the left coronary artery arises from the pulmonary artery, whereas the right coronary originates from the aorta. The incidence of this anomaly is less than 1 per cent. Rarely a coronary artery may arise from a cardiac chamber. The clinical picture of anomalous origin of the left coronary artery follows roughly the pattern of hypoxia due to acquired coronary insufficiency in adults. When the right coronary artery arises from the pulmonary artery there are as a rule no disturbances in cardiac function; however, when both coronary arteries arise from this site, a rare condition, death occurs shortly after birth.

Pulmonary arteriovenous fistula. This anomaly is a direct communication between the pulmonary arterial system and the pulmonary venous system. This allows venous unsaturated blood to enter the pulmonary veins and thus the systemic circulation. When the fistula is large and there is sufficient venous blood entering the systemic circulation, cyanosis, clubbing of digits, and secondary polycythemia are manifest.

Aortic-sinus aneurysm. Aneurysm of an aortic sinus is rare, most commonly involving the right and less commonly the posterior sinus. It is doubtful whether congenital aneurysms of the left aortic sinus ever occur.

The aneurysm usually presents toward the right atrium or the right ventricle and may communicate congenitally with either of these chambers, or there may be no communication on a developmental basis. Acquired communication between the aorta and one of the atria or ventricles may appear spontaneously or as a complication of bacterial infection of the aneurysm.

The functional disturbance from an aneurysm of an aortic sinus that communicates with one of the right-sided cardiac chambers is comparable to that from patent ductus arteriosus, and peripheral signs suggesting aortic insufficiency may be prominent.

VENOUS ANOMALIES. *Anomalous pulmonary venous connections.* Pulmonary veins may drain anomalously into the right atrium or one of its tributary veins instead of the left atrium. Such anomalous venous connection may be partial or complete. The complete form represents nearly 2 per cent of all cases of congenital cardiovascular defects. In partial anomalous venous connection some of the pulmonary veins communicate normally with the left atrium and others communicate anomalously with the right atrium or one of its tributary veins. In complete anomalous connection all the pulmonary veins are connected to the right atrium or one of its tributary veins; none drain directly into the left atrium. In the latter anomaly an atrial septal defect is present, which is the only route whereby blood can reach the left side of the heart for distribution to the systemic circulation. In partial anomalous venous connection there is pulmonary recirculation of oxygenated blood, and the condition has functional characteristics similar to those of atrial septal defect.

In complete anomalous pulmonary venous connection there is not only an arteriovenous but also a venoarterial shunt. In this condition there is relatively complete mixing of pulmonary venous and systemic venous blood, and arterial hypoxemia is always present; however, when the pulmonary flow is high, cyanosis may not be evident. Death during early infancy is common, particularly if there is some obstruction to pulmonary venous drainage. However, if the pulmonary venous pathway is not restricted and a large atrial septal defect is present, such patients may attain adult life without being aware of the presence of this rather severe hemodynamic anomaly.

Cor triatriatum is a rare congenital anomaly usually associated with partial obstruction to drainage of the pulmonary veins into the left atrium; it comprised less than 0.3 per cent of one series of 357 cardiac malformations (106). In this condition the pulmonary veins empty into an accessory chamber lying superior to the true left atrial chamber and communicating with it by means of an opening which is usually small. The narrow opening between the accessory chamber and the true left atrium constitutes a point of partial obstruction to pulmonary venous flow, functionally resembling mitral stenosis. The accessory chamber is believed to represent the common pulmonary vein of the embryo which failed to become incorporated into the left atrium as it normally should.

Variants of cor triatriatum include a connection of this accessory chamber to one of the tributary veins of the right atrium and thus functionally re-

sembling a total or a partial anomalous pulmonary venous connection.

Anomalous systemic venous connections. Occasionally, in addition to a normal right superior vena cava, there may be a persistent left superior vena cava. The latter vein joins the left extremity of the coronary sinus, which is dilated, and the blood is carried into the right atrium. This condition by itself is of no functional significance; however, rarely one or more pulmonary veins may connect to the persistent left superior vena cava. The coronary sinus may occasionally open into the left atrium alone or may communicate with both atria.

Venous obstruction. Congenital obstruction of the major systemic veins rarely occurs; however, one or more pulmonary veins may be atretic. In these instances it is usually possible to trace fibrous strands to the left atrium but there is no lumen.

Intracardiac Anomalies

VENTRICULAR SEPTAL DEFECT. Ventricular septal defects are probably the most common congenital cardiovascular anomaly, occurring in approximately 15 per cent of all types of congenital cardiovascular defects. They may occur in either the membranous or the muscular portion of the ventricular septum. Occasionally a ventricular septal defect is associated with a deformity of the adjacent aortic valve, producing aortic insufficiency. Mitral insufficiency also has been described in association with a ventricular septal defect (57). In rare instances the ventricular septal defect is located so as to establish a communication between the left ventricle and the right atrium instead of the right ventricle as is usually the case.

The size of the ventricular septal defect is extremely variable. It may be so small that it has no functional significance, or the ventricular septum may fail to form so that the ventricular part of the heart is common to both circulations. The latter condition is called cor triloculare biatriatum or common ventricle and occurs in approximately 2 per cent of all cases of congenital cardiovascular defects. Usually two vessels leave the heart and, except in rare cases, there is transposition of the great vessels. This condition is functionally similar to that in the normal turtle heart.

INTERATRIAL COMMUNICATIONS. A patent, valve-competent foramen ovale is said to be present in 25 per cent of the population and hence it is not usually considered a true congenital defect. A true atrial septal defect allows passage of blood across the atrial septum in both directions.

Atrial septal defects are one of the six most common congenital cardiovascular anomalies, occurring in approximately 7 per cent of all cases, and are among the commoner types of congenital cardiac anomalies seen in adult life. The usual form of atrial septal defect is a valvular incompetence of the foramen ovale for one or more of three reasons: the valve of the foramen may be short, the foramen may be unusually large, or the valve of the foramen may be perforated. Occasionally an atrial septal defect is associated with acquired rheumatic mitral stenosis, constituting the so-called Lutembacher syndrome (167).

In addition to valve-incompetent foramen ovale, defects in other areas of the atrial septum may occur as a result of incomplete development of the septum primum or the septum secundum. A condition occasionally encountered in cases of atrial septal defect is the so-called superior vena caval syndrome (239). This syndrome consists of a defect high in the atrial septum near the superior vena cava and a partial anomalous connection of the pulmonary veins directly to the superior vena cava or to a point near the junction of the superior cava and the right atrium. Rarely, as is true of the ventricular septum, the interatrial septum may fail to develop, thus resulting in a common atrium.

TETRALOGY OF FALLOT. Although this anomaly is a combination of intracardiac defects, it is usually considered a single entity (99). It is the most common malformation causing cyanosis that allows the patient to survive beyond 2 years of age. It is also one of the most common malformations, occurring in nearly 9 per cent of patients with congenital cardiovascular disease. The anatomic complex is characterized by biventricular origin of the aorta above a ventricular septal defect, a thick right ventricle and an anatomic barrier to the flow of blood to the lungs. The anatomic barrier may be caused by one or more of three conditions: *1*) stenosis or atresia of the pulmonary artery, *2*) stenosis or atresia of the pulmonary valve, and *3*) stenosis or atresia of the subpulmonary tract in the right ventricle. A right aortic arch and a right descending aorta occur in about 25 per cent of patients with tetralogy of Fallot. The association of right aortic arch with tetralogy of Fallot is sometimes called "Corvisart's disease" (67). An atrial septal defect is not infrequently associated with this complex, in which case it has been termed "pentalogy of Fallot."

STENOSIS OR ATRESIA OF INTRACARDIAC VALVES. Any of the four intracardiac valves may be stenotic; however, the most commonly affected is the pulmonary valve, stenosis of which occurs as a single defect in more than 2 per cent of congenital cardiovascular anomalies. It can also occur in complexes such as tetralogy of Fallot, and is frequently associated with an atrial septal defect or with the usual type of ventricular septal defect.

In addition to stenosis of the pulmonary or aortic valves there may be a localized fibrous collarlike narrowing in the outflow tract of the right or the left ventricle. Rarely, stenosis of the infundibular ostium of the right ventricle is the only abnormality. In the usual case there is an associated ventricular septal defect. Subaortic stenosis, on the other hand, is more likely to occur as a single abnormality, and the resulting functional disturbances are similar to those of acquired aortic stenosis.

"Valvular atresias" account for approximately 4 per cent of all congenital cardiovascular defects, atresia of the aortic valve apparently being the most common and atresia of the tricuspid valve the least common.

Atresia of the tricuspid orifice, as the name implies, is characterized by absence of the usual inflow orifice to the right ventricle. The great veins communicate properly with the atria. The only outlet for blood from the right atrium is through an atrial septal defect, which usually takes the form of a patent foramen ovale. The left atrium represents a common mixing chamber for venous and oxygenated blood, and from this chamber blood enters a large left-sided ventricular chamber through a wide mitral orifice. A ventricular septal defect is present in most cases. The arterial connection with the ventricles varies from normal to transposition, or a truncus arteriosus may be present. There may be pulmonary or subpulmonary stenosis in some cases, whereas in others there is no barrier to the flow of blood to the lungs.

In atresia of the mitral orifice the route of the circulation is opposite in direction to that in tricuspid atresia. Oxygenated blood from the left atrium flows usually through an opening in the atrial septum into the right atrium. The pathway of exit for left atrial blood is usually inadequate, and thus there exists a barrier to pulmonary venous blood drainage. The mixture of pulmonary and systemic venous blood in the right atrium flows through a large tricuspid orifice into the ventricular portion of the heart. In some cases there are two ventricles and a ventricular septal defect, and in other instances there is a common ventricle. Transposition of the great vessels is frequently associated. Survival beyond infancy is uncommon.

Pulmonary atresia was mentioned previously in connection with tetralogy of Fallot. In pulmonary atresia with intact ventricular septum the atresia is at valve level, the leaflets of the pulmonary valves being fused to form a fibrous diaphragmlike membrane. The right ventricular chamber is usually small and the right ventricular wall is thick, out of all proportion to the size of the chamber. An opening in the atrial septum is the route by which venous blood that enters the right atrium escapes into the left atrium. The blood supply to the lungs is usually via a patent ductus arteriosus. This malformation rarely if ever allows the patient to live beyond early infancy.

Atresia of the aortic orifice is characterized by fusion of the aortic leaflets to form an imperforate diaphragm at the level of the aortic valve. The ventricular septum is usually intact. In some cases aortic and mitral atresia may coexist. In most cases, however, there is a small, but normally developed mitral valve. Whether or not mitral atresia coexists, the normal outlet for the left side of the heart is closed and the blood is shunted from the left atrium to the right, usually through a valve-incompetent foramen ovale. The right atrium and right ventricle thus become, in essence, a common atrium and a common ventricle, respectively. The systemic circulation is supplied through the pulmonary artery by way of a patent ductus arteriosus. Survival beyond early infancy is rare.

INCOMPETENCE OF INTRACARDIAC VALVES. Incompetent intracardiac valves are usually associated with other intracardiac anomalies or are part of a developmental complex. Examples of these are insufficiency of the aortic valve in the presence of ventricular septal defect and the developmental complex, common atrioventricular canal, which is a defect in development of the atrioventricular valves from the embryologic endocardial cushion. Insufficiency of the pulmonary valve rarely if ever occurs as a congenital defect.

PERSISTENT COMMON ATRIOVENTRICULAR CANAL. Persistent common atrioventricular canal, which occurs in nearly 2 per cent of all congenital cardiovascular defects, may be considered to appear in the complete form and the partial form (253). In the complete

form, mitral and tricuspid valves as such are not present. There is only a common atrioventricular orifice and valve, so that venous and arterial blood intermix as they traverse the atrioventricular canal. There is also a defect in the atrial septum immediately above the common valve. In the partial form there is a defect in the lower part of the atrial septum but the tricuspid valve is properly formed. The mitral valve shows a cleft in its anterior leaflet. In a rare case of the partial form the atrial septum is normally formed but there is a cleft in the mitral valve. Those patients with a defect in the atrial septum suffer predominantly from the arteriovenous shunt, whereas in the rarer type of partial form with an intact atrial septum the functional disturbance is that of mitral regurgitation resulting from the deformity of the mitral valve. With the complete form survival beyond infancy is uncommon, whereas with the partial form some patients survive to adult life.

EBSTEIN'S MALFORMATION OF THE TRICUSPID VALVE. Ebstein's malformation of the tricuspid valve (87) is rare; it occurs in less than 1 per cent of congenital cardiovascular defects and is characterized by attachment of the septal and posterior leaflets of the tricuspid valve to the right ventricular wall at its apex. The anterior leaflet is normally attached to the annulus fibrosus. The abnormal valvular attachment may result in tricuspid regurgitation or cause the tricuspid orifice to be reduced in size. One feature of the abnormal valvular attachment is that the greater portion of the right ventricle forms a large, common receiving chamber with the right atrium. The only portion of the right ventricle that functions as such is the anatomic outflow portion of this chamber. An atrial septal defect is commonly associated with Ebstein's malformation via which a relatively large right-to-left shunt may occur. Patients with Ebstein's malformation usually survive to adulthood, the average survival period being about 25 years.

ENDOCARDIAL SCLEROSIS. Endocardial sclerosis was present in 5 per cent of a series of 357 cases of major cardiac malformations reported from the Mayo Clinic (106). It is characterized by elastic and collagenous thickening of the mural endocardium. Usually the left ventricle is involved and the left atrium may be involved as well. The valves on the affected side of the heart may be stenotic, but as a rule they are normal. The endocardial thickening of the left ventricle probably prevents normal excursion of the ventricle during diastole and so causes a progressive impediment to pulmonary venous drainage. The effects on the pulmonary circulation and right ventricle are similar to those that would be caused by mitral stenosis. Survival beyond infancy is uncommon.

Conduction Defects

Abnormalities of rhythm of the heart are not uncommon. Usually, however, the arrhythmias are secondary to some underlying cardiac condition.

SINUS ARRHYTHMIA. Sinus arrhythmia is present to some degree in most children more than 4 or 5 years of age and in most adults. This is a rhythmic variation of heart rate occurring synchronously with respiration. The heart rate increases toward the end of inspiration and slows toward the end of expiration. It is apparently due to alteration in the vagal tone transferred from the central respiratory mechanism.

HEART BLOCK. Depression of the conducting mechanism of the atrioventricular node results in a delay of the wave of excitation passing from atria to ventricles. This is referred to as atrioventricular block. A 2-to-1 block or complete heart block is less frequently encountered than minor degrees of heart block (147). Ninety-five per cent of the higher grades of heart block occurring in childhood appear to be congenital in origin. These may be associated with congenital heart disease, particularly corrected transposition of the great vessels which may coexist with ventricular septal defect, single ventricle, aortic atresia, and the like. Many of the patients show evidence of left ventricular hypertrophy. This is to be expected since the slow ventricular rate produces a lengthening of the heart muscle in the prolonged diastole, and this leads to hypertrophy. In children, isolated heart block causes very few symptoms. Most of them lead normal, active lives although a few tire easily. It apparently is rare for Stokes-Adams attacks to occur in congenital heart block.

WOLFF-PARKINSON-WHITE SYNDROME. In 1930, Wolff, Parkinson, and White (265) first described an electrocardiographic entity consisting of a short P-R interval and a wide QRS, as is seen in bundle branch block. This anomaly is considered to be due to either an accessory pathway around the atrioventricular node, such as the bundle of Kent, or an accelerated spread of the impulse through the atrioventricular node and bundle. One complication is the frequent occurrence

of paroxysmal tachycardia. Approximately 12 per cent of these cases are associated with congenital heart disease.

Abnormalities of Position

DEXTROCARDIA. When dextrocardia is associated with complete situs inversus or the mirror picture of normal organ arrangement, the heart is usually functionally normal and anatomically a mirror image of the normal. It is generally recognized that dextrocardia with a mirror image of the atria and ventricles without an associated situs inversus usually is associated with serious intracardiac malformations. Also, the rare isolated levocardia with an otherwise complete situs inversus is often associated with intracardiac defects.

There are patients, however, without associated situs inversus in whom the heart functionally is normal. In these instances, although the heart is on the right, the relationships of the atria and ventricles are normal, that is, the right atrium and right ventricle are to the right of the left atrium and left ventricle, and the venae cavae enter the heart on the right side. In these cases the condition is usually termed "dextroversion of the heart"; the term "dextrorotorsion" also has been suggested.

COMPLETE TRANSPOSITION OF THE GREAT ARTERIES. Complete transposition of the great vessels is characterized by origin of the aorta from the right ventricle and origin of the pulmonary artery from the left ventricle. The two great vessels lie parallel to each other, the aorta in front of the pulmonary artery. This creates a narrow vascular shadow in the roentgenogram when the great vessels are viewed from the front.

The venous connections of the heart are normal; therefore, the abnormal arterial connections lead to a profound circulatory disturbance in that venous blood does not have a direct route to the lungs. Unless there is some communication between the two circulations, life after the umbilical cord is divided is not possible. The usual communication is in the form of a patent foramen ovale, a ventricular septal defect, a patent ductus arteriosus, or combinations of these. The bronchial arteries may also serve as a route by which venous blood is carried to the lungs. This malformation has a tendency to occur in males. Survival beyond infancy is uncommon.

CORRECTED TRANSPOSITION OF THE GREAT VESSELS. In corrected transposition of the great vessels the aorta communicates with the left ventricle and the pulmonary artery with the right ventricle, but the aorta is anterior to the pulmonary artery as it is in complete transposition of the great vessels. The transposition may thus be considered as "corrected" since there is no functional disturbance in spite of the anatomic abnormality. A ventricular septal defect is usually present in corrected transposition of the great vessels. In rare instances the ventricular septum may be intact and there may be no other cardiac abnormality; when such is the case, the patient has no cardiac disability. The anatomic and hemodynamic alterations found in the various forms of this condition have recently been reviewed in detail by Schiebler and co-workers (210).

METHODS OF STUDY

Clinical Methods

The rapid increase in understanding of the pathology and hemodynamics of the various forms of congenital heart disease has, in recent years, permitted a much more accurate appraisal of the clinical findings obtained by observation with the aid of the stethoscope, the electrocardiogram, the roentgenogram, and the fluoroscope. As a result, physicians have developed to a much higher degree their ability to assess, on the basis of clinical findings alone, the physiologic and pathologic situation in patients with congenital heart disease and frequently are able to arrive at an accurate diagnosis without recourse to detailed hemodynamic studies.

Cardiac murmurs can give insight into the presence and nature of various shunts or malfunction of various heart valves. The quality of the heart sounds may give information concerning intracardiac and great-vessel pressures; for example, an abnormally split and accentuated pulmonary second sound is usually due to delayed and forceful closure of the pulmonary valve associated with pulmonary hypertension. In some instances it is of value to study the heart sounds and murmurs with a phonocardiogram, and to relate the sequence of various sounds and murmurs to the electrical activity of the heart by means of the simultaneously recorded electrocardiogram. The recent development of intracardiac phonocardiography (161) permits even better evaluation of the known hemodynamic aberrations that occur in congenital heart disease and provides some indication as to the site of origin and hence possible causes of these murmurs. Electrocardiographic studies have also proved in-

valuable in assessing the hemodynamic and pathologic alterations occurring in congenital heart disease. Sodi-Pallares (225) has developed to a high degree the use of the electrocardiogram in evaluating systolic and diastolic overload patterns of the right and left ventricles. Disturbances in conduction are best evaluated by electrocardiographic studies. Intracardiac electrocardiograms (130) have proved of value in this regard and can also give information as to the site in the heart in which the catheter-tip electrode is located.

The accuracy of radiologic examination has also benefited from the elucidation that has occurred in the past decade regarding the hemodynamic and pathologic alterations associated with given defects. One example is the ability of the radiologist, by examination of the peripheral lung fields, to estimate with some degree of confidence whether increased or decreased blood flow through the pulmonary arterial segments is present.

In general, as a result of increased knowledge of the hemodynamic alterations that occur in congenital heart disease and the correlation of these alterations with clinical findings, clinicians have greatly increased their ability to evaluate these defects. With certain exceptions, however, these clinical techniques are of limited value to the physiologist in carrying out basic studies of the hemodynamic alterations, and in the patient with complicated or unusual defects the clinician must resort to hemodynamic studies to obtain a diagnosis of the defect or defects present.

Intracardiac Catheterization

Cardiac catheterization has played an invaluable role in the diagnosis of congenital cardiac defects as well as in providing the means for accurate investigation of the hemodynamic alterations associated with various disease complexes. The increased ability of clinicians to diagnose many cardiac defects that has resulted from correlation of clinical findings with objective hemodynamic studies and surgical findings has made it unnecessary for many patients with congenital cardiac defects to undergo cardiac catheterization. The skilled clinician reserves the procedure of diagnostic cardiac catheterization chiefly for two types of patients: *1*) the patient who is relatively asymptomatic and in whom the clinician is unable to decide whether a congenital cardiac defect is present, and *2*) the patient with a complex combination of defects in whom, because of the complicated nature of the resulting hemodynamic alterations, the clinician is unable to make a definitive diagnosis. These patients also present a challenge to the hemodynamic laboratory and require the best equipment as well as highly trained individuals to attain a definitive diagnosis in a high percentage of the patients studied.

Since cardiac catheterization is a basic and valuable technique for many hemodynamic and other studies in human as well as animal investigations, a rather detailed discussion of various aspects of this procedure will be presented.

PRESSURE RECORDING. Measurement of physiologic variables directly concerned with the heart and circulation in man requires that these variables be determined on the intact, preferably unanesthetized person. Therefore, direct measurements of many of the variables must commonly be made through small needles or long, narrow-bore flexible tubes. Since variables such as blood pressure have both static and dynamic components, high-fidelity recording of them under such circumstances requires close attention to the frequency and damping characteristics of the instruments used. Adequate instrumentation must be capable of faithful reproduction of both the static component and all dynamic components of a magnitude to be of practical importance.

The highest frequencies of the dynamic components of practically important magnitudes in a complex wave form, such as an arterial pressure pulse, are not accurately known. It is generally considered, however, that instruments with a uniform dynamic sensitivity to the tenth harmonic of the fundamental frequency of such complex wave forms are suitable for high-fidelity recording of the wave concerned. By this criterion, since the heart rate of human beings seldom exceeds 240 beats per min, an instrument with a uniform sensitivity from 0 to 40 cycles per sec should be adequate for the recording of arterial blood pressure and most other physiologic variables associated with the cardiovascular system. Recent direct evidence indicates that manometer systems with a uniform dynamic response over the frequency range from 0 to 10 cycles per sec will record the pressure variations in the circulatory system in man without significant amplitude distortion (235, 267).

A manometer system suitable for direct recording of blood pressure should possess the following characteristics: high natural frequency; high stability; linear calibration; usability with long leads; insensitivity to movement, temperature, and humidity; imperviousness to electrolyte solutions; simplicity

of operation; and construction for ease of sterilization and removal of air bubbles entrapped in the hydraulic system (266). Strain-gauge manometers of the unbonded type, adapted for recording of blood pressure, more nearly approach fulfillment of these requirements than do other manometers now available from the stocks of commercial suppliers. A recent review of strain-gauge manometers and their application to recording of intravascular and intracardiac pressures has appeared (235).

The most serious difficulty in the problem of attaining high-fidelity recordings of intracardiac and great-vessel pressures by means of catheter-manometer systems is the avoidance of artifacts generated by the motions of the catheter caused by the heartbeat. Such artifacts cannot be eliminated when conventional catheter-manometer systems are used (270). They can be minimized, however, by the use of miniature manometers mounted at the catheter tip (94, 227). Such a miniature manometer has also been used with success as an intracardiac microphone for intracardiac phonocardiography (226).

Determination of Blood Gases

MANOMETRIC METHODS. Van Slyke & Neill (250) published a gasometric technique for determination of the oxygen and carbon dioxide content of blood, which later was modified by Sendroy and associates (218) and by Roughton and co-workers (201). This technique or modification of it is commonly used for determination of percentage saturation of blood with oxygen. This requires that both the oxygen content and the oxygen capacity (in volumes per cent) of the blood be measured so that, after appropriate corrections for the oxygen in physical solution, the percentage of hemoglobin saturated with oxygen can be estimated.

The principal advantage of this method is its accuracy, for with good techniques oxygen content can be determined within ± 0.1 volume per cent. This method, however, is time consuming, and it is usually true that the values from such analyses are not available until after the cardiac-catheterization procedure has been completed. Another disadvantage is that the number of samples of blood that can be obtained and analyzed from various sites in the heart and great vessels is severely limited.

POLAROGRAPHIC OXYGEN ELECTRODE. An inert metal such as platinum, gold, or mercury negatively charged in an electrolyte solution will give up electrons to dissolved oxygen gas, reducing it to H_2O_2 or OH^-. The current measured passing into solution from the electrode is directly related to the availability of oxygen at the metal surface. Bare platinum and dropping mercury have been widely used in the 60 years since the technique was first described, but for blood oxygen tension (pO_2) the proteins interfered with analysis.

Stow and associates (233) developed a membrane-covered electrode for measuring blood carbon dioxide, and in 1956 Clark (59) introduced the use of the membrane-covered electrode for the measurement of blood oxygen tension. The membrane, which is a suitable plastic permeable to oxygen but impermeable to protein molecules, protects the electrode from the "poisoning effect" caused by most biologic fluids. The electrode is usually incorporated in an airtight cuvette which can be temperature controlled and in which the blood in contact with the membrane interface can be stirred. Various techniques have been developed to accomplish this (157, 219, 228).

The polarographic electrode has been used to measure the oxygen content of whole blood (180), the principle being to inject a measured amount of blood into a larger volume of solution which frees the oxygen from the hemoglobin, releasing it into solution where the rise in pO_2 is proportional to the oxygen content of the original blood. For this purpose, ferricyanide and carbon monoxide have been used. The accuracy available is principally dependent on calibration of the electrode.

SPECTROPHOTOMETRIC METHODS. It is possible to determine the oxygen saturation of blood by means of widely used spectrophotometric methods. The physical basis of these methods rests on the difference in absorption, by oxygenated and reduced hemoglobin, of red light at a wavelength of about 640 mμ, and on their similarity in absorption of infrared light at a wavelength of about 800 mμ. These measurements are usually made on light transmitted through blood, although reflected light also has been successfully used.

A number of instruments and procedures are available for photometric determination of the oxygen saturation of blood.

Hemoreflector. This instrument and its use have been described in detail by Zijlstra (287). The intensity of light (600–680 mμ) reflected from a 0.5 ml-sample of whole blood diluted to 1 ml is measured. The instrument consists of a glass-bottom cuvette for the blood sample that is held in a revolvable turret housed in

the same cabinet as the source of light, photocells and control circuits, and a separate sensitive galvanometer for indication of the output of the photocell assembly.

Beckman DU spectrophotometer with special cuvettes. This widely used spectrophotometer allows accurate measurement of the optical density of samples of blood to relatively monochromatic light of selected wavelengths. For these procedures the blood is placed in special cuvettes and usually hemolyzed. Nicholson and colleagues (182) have described a cuvette in which the thickness of the blood film is 2.4 mm; in another cuvette, described by Nahas (179), the thickness of the blood film is 0.1 mm.

An excellent discussion of the techniques and theory of spectroscopic determination of the oxygen solution of blood is given by Drabkin (84).

Oximetry. An oximeter is a photoelectric photometer for measurement of the fraction of hemoglobin in blood that is in the oxygenated state. One type, the ear oximeter, is designed to measure the oxygen saturation of blood circulating in a particular tissue, usually the pinna, of an intact animal or human being. A second type, the cuvette oximeter, is designed to measure the oxygen saturation of blood outside the body during or soon after withdrawal from various sites in the vascular system.

Oximeters are classified on the basis of whether they are relative- or absolute-reading instruments. The former usually measures the light transmitted or reflected by blood at only one spectral region (about 640 mμ) and is usually adjusted during operation to indicate a known value for the oxygen saturation of the blood being analyzed. This type measures only changes in oxygen saturation that may occur after this initial adjustment and cannot make an independent (absolute) measurement of the actual saturation. An absolute-reading oximeter measures light transmitted or reflected by blood at two wavelengths; an initial adjustment to indicate a known value of oxygen saturation is not required, so that the instrument can make an independent (absolute) measurement of the oxygen saturation of the blood being analyzed.

The cuvette oximeter has the advantage that whole blood can be drawn directly from arterial or venous sampling sites through the cuvette for analysis. Use of the single-scale recording assembly also allows nearly instantaneous determination of the blood oxygen saturation. Determinations on flowing blood are of primary importance for cardiac catheterization, studies of pulmonary function, monitoring or study of extracorporeal pump-oxygenator assemblies, and any application that requires dynamic measurements. Also multiple samples may be obtained, since the blood can be collected in a sterile syringe and reinfused into the patient's blood stream after the analysis has been made.

It has been shown that the accuracy of cuvette oximetry in determination of the oxygen saturation of whole blood is comparable to that of a spectrophotometer used on hemolyzed blood, which is limited to in vitro applications (271). The application in diagnostic cardiac catheterization of a cuvette oximeter utilizing the reflection principle has recently been described (36).

The application of gas chromatography to the determination of blood gases has been perfected in recent years and offers distinct advantages in simplicity and speed of analyses for many applications (166, 196).

Calculation of Blood Flows and Shunts

Development of applications of the direct Fick principle for determination of blood flow using the technique of intracardiac catheterization has simplified determination of cardiac output in man. This method is the one generally used today. The equation for calculation of cardiac output is as follows:

$$\dot{Q}b = \frac{\dot{V}_{O_2}}{Ca_{O_2} - C\bar{v}_{O_2}}$$

where $\dot{Q}b$ is the cardiac output in liters per minute, $\dot{V}_{O_2}$ is oxygen consumption in milliliters per minute, Ca_{O_2} is the oxygen content of the blood leaving the lungs, and $C\bar{v}_{O_2}$ is the oxygen content of mixed venous blood returning to the lungs. In order to obtain a representative sample of mixed venous blood, the venous blood usually is withdrawn from the pulmonary artery.

This equation can also be used to determine systemic ($\dot{Q}s$) and pulmonary ($\dot{Q}p$) blood flows when the blood flow to one of these systems is greater as a result of shunted blood. The equations would then be:

$$\dot{Q}p = \frac{\dot{V}_{O_2}}{Cpv_{O_2} - Cpa_{O_2}}$$

and

$$\dot{Q}s = \frac{\dot{V}_{O_2}}{Csa_{O_2} - C\bar{v}_{O_2}}$$

Cpv_{O_2} and Cpa_{O_2} are the oxygen contents of pulmonary-vein and pulmonary-artery blood samples,

respectively, and Csa_{O_2} and $C\bar{v}_{O_2}$ the oxygen contents of systemic-artery and mixed venous blood, respectively. Since the oxygen saturation of inferior vena caval blood is usually higher than that in the superior vena cava, it is the practice in this laboratory, for patients with shunts at atrial level, to take the average of the oxygen saturation of blood from the inferior and superior venae cavae for the mixed venous saturation for determining systemic blood flow. It is usually not possible to obtain the oxygen saturation of pulmonary-vein blood for determination of pulmonary blood flow. If there is no right-to-left shunt present, systemic arterial oxygen saturation may, for practical purposes, be considered the same as that in the pulmonary veins. If a right-to-left shunt is present and pulmonary ventilation is assumed to be normal, the pulmonary venous oxygen saturation can be taken to equal 98 per cent of the oxygen capacity of the blood plus 0.3 volume per cent for that in physical solution while breathing 20 per cent oxygen.

For many years the application of the Fick principle has provided the classic indirect means of measuring blood flow. Other methods have been judged on the basis of their agreement with Fick measurements. Careful workers have recognized the importance of "the steady state" as being necessary for reliable determinations. Until recently, however, apparently few doubts have been entertained regarding the validity of the conventional application of Fick's law. In the past few years, provocative articles have appeared in the literature concerning the justification of some of the assumptions made.

Under the influence of the cardiac cycle, the respiratory cycle, and other causes, the lung volume and pulmonary blood volume periodically change. Since in practice the oxygen uptake can be measured only at the mouth or nose, the variable buffer capacity for oxygen of the alveolar space and the pulmonary blood may interfere with the accurate short-term measurement of the uptake as referred to the blood flowing to and from the lungs. Fishman *et al.* (104) have pointed out that in order to avoid this type of error it is essential that the amount of oxygen within this buffer reservoir be the same at the beginning and at the end of the period of observation.

Visscher & Johnson (252) pointed out that the usual procedure of sampling blood at a constant rate may not yield a sample of the same oxygen content as the average content of all the blood that flows past the sampling site in the collection period. This undesirable situation can occur whenever both the rate of flow and the oxygen content of the blood passing the sampling site vary during the sampling period. A more general and rigid description of the factors that may cause errors in conventional applications of the Fick principle has been given by Stow (232). It is certain that the criteria for accurate measurement of blood flow by the Fick principle are seldom if ever completely fulfilled in studies of intact animals or men. However, it is believed that in most circumstances the errors are not so large as to invalidate the method (269).

The volume of a shunt may be easily estimated when it is unidirectional by obtaining the difference in the calculated systemic and pulmonary blood flows. When the shunt is bidirectional, calculation of the actual volume of blood crossing the defect in the right-to-left and left-to-right directions is practically impossible. In the presence of unidirectional shunts the proportion of pulmonary venous blood contributing to pulmonary-artery flow, that is, left-to-right shunt, and of systemic venous blood contributing to systemic blood flow may be estimated as follows:

$$Q_{\%LR} = \%\ \text{left-to-right shunt} = \frac{Cpa_{O_2} - C\bar{v}_{O_2}}{Cpv_{O_2} - C\bar{v}_{O_2}} \times 100$$

and

$$Q_{\%RL} = \%\ \text{right-to-left-shunt} = \frac{Cpv_{O_2} - Csa_{O_2}}{Cpv_{O_2} - C\bar{v}_{O_2}} \times 100$$

in which $Q_{\%LR}$ is expressed as a percentage of the pulmonary flow and $Q_{\%RL}$ as a percentage of systemic flow, and the various C's with subscripts have been defined previously.

It frequently is not possible to measure the oxygen saturation of blood in the pulmonary veins. If there is no right-to-left shunt the oxygen saturation of systemic arterial blood is assumed to be the same as that in the pulmonary veins. When there is a right-to-left shunt resulting in desaturation of systemic arterial blood, and if pulmonary disease as a source of unsaturation has been ruled out, then it is permissible, if pulmonary ventilation is adequate, to assume that the pulmonary-vein blood was normally saturated (98%) prior to dilution by the shunt. There are inaccuracies in these calculations, but they do seem to indicate the magnitude of intracardiac shunts with sufficient accuracy for most practical purposes.

CALCULATION OF VASCULAR RESISTANCE. Vascular resistance may be described as impedance to blood flow through a given portion of the circulation; this is usually a total circuit, that is, pulmonary or sys-

temic, but may be a region such as the forearm, or an organ such as the kidney. Although there is considerable debate regarding the exact anatomic location and physiologic basis of vascular resistance, the concept appears to have practical value. It has been recognized in the field of nonbiologic hydraulics that resistance of multiple-pipe systems can be calculated by application of the principles of Ohm's law. Circulatory resistances, by analogy, are calculated in a similar manner. Thus, the simplest formula for calculating resistance is:

$$\text{resistance} = \frac{\text{mean pressure gradient}}{\text{blood flow}}$$

In recent years many workers in this field have made use of Aperia's formula so as to give the result in absolute units. Resistance then is expressed as:

$$\frac{\text{Pressure differences (dynes/cm}^2)}{\text{Flow (ml/sec)}} = \text{dynes sec cm}^{-5}$$

or

$$R = \frac{(P_1 - P_2)\cdot 1332}{\dot{Q}}$$

where R = resistance in dynes sec cm^{-5}, $P_1 - P_2$ = the pressure loss across the resistance circuit in millimeters of mercury, 1332 is the factor for conversion to dynes, and $\dot{Q}$ = blood flow in milliliters per second through this circuit.

In practice, the exit (venous) pressure for the systemic circuit is so small in relation to the entering pressure that it is often disregarded and the mean systemic arterial pressure is used in place of the pressure loss. In the pulmonary vascular bed this is not true and the actual pressure loss across the pulmonary vascular bed should be measured.

Just exactly what is measured by "resistance" remains problematic. According to Poiseuille's law, which is strictly applicable only to steady (nonpulsatile) flow of a Newtonian fluid through rigid tubes, resistance varies directly with the vessel length and blood viscosity, and inversely with the cross-sectional area. Other factors being equal and unchanged in the same patient, changes in resistance are presumed to reflect changes in cross-sectional vascular area. A decrease in resistance could be due to increased vascular distention of a passive nature resulting from an increase in transmural pressure or due to true vasodilatation. The exact mechanism and significance of a measured decrease in vascular resistance are frequently difficult to interpret with certainty.

CALCULATION OF VALVE AREAS. Taylor and co-workers applied hydraulic formulas to the study of the relationship of the flow through a patent ductus arteriosus to the size and the pressure gradient across the ductus (248).

Gorlin & Gorlin (118) have made use of similar hydraulic principles in calculating the valve areas from available hemodynamic data. The formula, an adaptation of the standard equation for hydrokinetic orifices (76), is fully discussed in Chapter 20.

Indicator-Dilution Curves

An indicator-dilution curve is a plot of concentration of a substance at a given site in the circulation against time following its injection at another site in the blood stream.

Measurement of cardiac output from such dilution curves was first advocated by Stewart (230) in 1897. The use of an indicator-dilution method for measurement of blood volume was popularized by the work of Keith and co-workers (148) and others during World War I, and in more recent years the use of indicator-dilution techniques for measurement of blood flow has been established on a firm basis by the work of Hamilton and colleagues (127); these methods have also been applied to the diagnosis and investigation of various forms of cardiovascular disease (181, 242).

The diagnostic as well as the investigative value of these techniques has gradually received progressively widespread recognition (25, 39, 74, 140, 175). The rate of this progression has, however, been greatly accelerated in the last 2 or 3 years with more general availability of suitable instrumentation and, particularly, the introduction of foreign gases for use as indicators in these techniques. The first of these was nitrous oxide (177), which was rapidly followed by the use of radioactive gases, krypton 85 (165, 207), I^{131} ethyl iodide (10, 54), and more recently, hydrogen (60) and hydrogen plus ascorbic acid (61, 62). Thermal dilution (100) and external scanning techniques (135, 189) have also been applied to the diagnosis of congenital heart disease.

The use of foreign gases as indicators in these dilution techniques has contributed greatly to the ease of application of the techniques by opening up a bloodless method of what in fact amounts to *a*)

sampling blood from the right side of the heart through the expedient of analyzing for the gas in the air equilibrated with this blood in the lungs and then expired, and *b*) "injecting" the foreign-gas indicator into the left atrium by the expedient of introducing the gas into the inspired air, where it is equilibrated in the lungs with the blood which flows to the left side of the heart.

The development of miniature detectors suitable for introduction into the vascular system for recording of the indicator concentration in blood at desired sites in the circulatory system has also expedited the application of these techniques (26, 60, 100).

Although the advent of these new types of detectors and new indicators, particularly of the gaseous types, has in many instances greatly facilitated various applications of these techniques, these applications are basically closely similar to those previously described, irrespective of the type of indicator and detector used. An important exception to this general statement is the application of gaseous indicators to the detection of blood traversing the pulmonary circulation but bypassing aerated alveoli (56, 113). This type of arteriovenous shunt can be detected by dyes or other nongaseous indicators only when the transit time of the shunted blood is significantly shorter than that of blood traversing normally aerated alveoli. Since under this circumstance the transit times of the shunted and the nonshunted blood from the right to the left side of the circulation may be closely similar, this type of shunt would escape detection by the usual nongaseous indicator-dilution methods. Since with this exception the methods are basically closely similar, this discussion of the application of indicator-dilution techniques to the study of congenital heart disease will be carried out from the viewpoint of the use of an indicator dye injected at any desired site or sites in the circulation, with its concentration being recorded continuously and simultaneously in the blood stream at any other desired site or sites in the circulation. As implied above, the use of conventional dye techniques in these applications has the disadvantage that the required direct access to the injection and sampling sites in the circulation by suitable catheters or needles may, in some applications, pose considerable technical difficulties. The techniques do, however, have the advantage that methods for obtaining quantitative information as to the relative and particularly the absolute magnitudes of systemic, pulmonary, and shunt flows have been developed and are for the most part more readily applicable than are the gaseous-indicator and intravascular-detector techniques.

A number of indicators, such as saline solution, various "blue" dyes and other dyes, and radioactive substances, with the corresponding detecting and recording systems, have been employed (82). Besides causing no cardiovascular disturbance and being readily measurable with precision, an indicator suitable for most quantitative purposes should not be lost from the blood stream during its passage through the segment of the circulation under study.

Application of oximetric methods to continuous recording of changes in the concentration of indicator in the blood stream was first demonstrated by Matthes (174) in Germany in 1936. Intensive use of earpiece and cuvette oximeters for continuous recording of dye-dilution curves in investigations of cardiovascular physiology in health and disease has been under way since 1950 (273). Other photometric methods for continuous recording of dilution curves have also been introduced. This discussion will deal with the continuous recording of indicator-dilution curves in the blood stream by means of an oximeter or a densitometer, although the same principles will apply to other types of dilution curves or methods of recording. In this regard the oximeter is used as a dichromatic densitometer (112), whereas the term "densitometer" connotes a monochromatic device which utilizes, that is, measures, the light transmitted through blood at only one rather than two spectral regions as does the oximeter. The importance of the use of a dichromatic instrument to avoid large possible errors due to nonspecific variations in the optical density of blood that occur with changes in rate of blood flow, carbon dioxide tension, and other factors has recently been emphasized (224, 234).

For the purposes of this presentation, dilution curves are separated into arterial dilution curves and venous dilution curves (268). An arterial dilution curve is defined as a recording of the concentration of an indicator from any site in the arterial circulation or from the left side of the heart (244). A venous dilution curve is defined as a recording of the concentration of an indicator at any site in the right side of the heart or the venous circulation (245).

NORMAL ARTERIAL INDICATOR-DILUTION CURVE. In dilution curves recorded by oximetry an increasing concentration of indicator usually is recorded as a downward deflection, corresponding to the decreasing light transmission of the blood. Thus after an interval

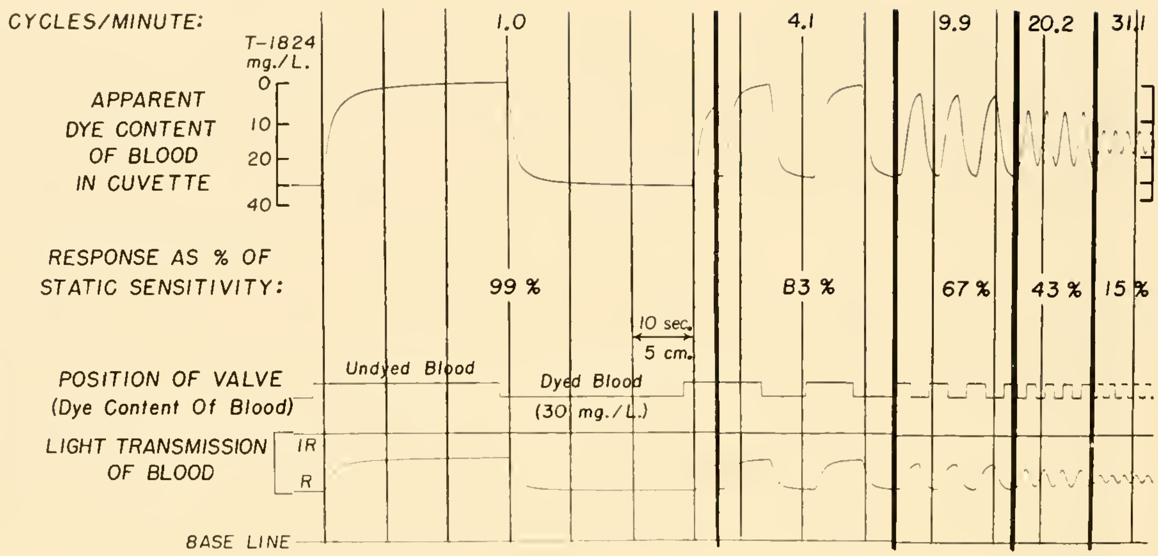

FIG. 1. Response of cuvette oximeter to variations in dye content of whole blood of equal amplitude and variable frequency. Square-wave variations in dye content of whole blood were produced by drawing blood at constant rate through mechanically operated two-position valve system. In one position of valve, blood containing 30 mg of Evans blue per liter was drawn into cuvette system; in the other position undyed blood entered system. Apparent dye content of blood, determined by cuvette oximeter, is shown above actual dye content as fixed by position of valve. Note *1*) delay and distortion in response of cuvette-oximeter system to change in dye content, and *2*) decrease in amplitude of response of system to same change in dye content of blood as frequency of variations in dye concentration increased. Blood flow through cuvette, which was attached to a 20-gauge needle (5 cm long, 0.6 mm in internal diameter), a system identical to that used for recording arterial dilution curves, was 26.5 ml/min. [From Fox *et al.* (109).]

(appearance time) equal to the shortest traversal time of the indicator particles to the sampling site, dye is detected at the sampling site. Successively greater numbers of particles then rapidly arrive at the sampling site until a maximum (peak concentration) is reached, whereupon their number decreases, the rate of decline being slower than that of the increase. Before the number of particles declines to zero, it increases again because of arrival of the more slowly moving particles on their first circulation, coinciding with arrival of the faster particles that have already made one complete circulation and are appearing at the arterial sampling site a second time. A second peak (recirculation peak) occurs when the maximal amount of recirculating indicator arrives at the sampling site.

It has been stated that a recording of the dilution of an indicator during its initial traversal of a circulation provides more information concerning the status of this circulation than does observation of any other single physiologic variable (273). From such a dilution curve one can determine such factors as *a*) volume rate of flow through this circulation, *b*) volume of the system between injection and sampling sites, *c*) fastest and mean circulation times through the system, and *d*) presence or absence of abnormal circulatory pathways, as well as magnitude of the flow through such pathways when present.

A number of excellent recent reviews of indicator-dilution curves have been published that discuss the theoretic implications in determining blood flow and volume (82, 112).

Records of rapidly changing concentrations of indicator in the blood are affected by the dynamic-response characteristics of the particular detecting instrument and recording assembly used. The dynamic-response characteristics of various cuvette-oximeter assemblies have been studied by Fox and co-workers (109) (fig. 1). At a frequency of 10 cycles per min these recording assemblies show a definite decrease in response. Ultimately the relatively poor dynamic response of instruments, such as the cuvette oximeter or densitometer, is determined chiefly by the hydraulic components of the system, namely, the volume of the detecting chamber and the length and internal diameter of the connecting tubes and the linear velocity of blood flow through them, rather than by the dynamic-response characteristics of the

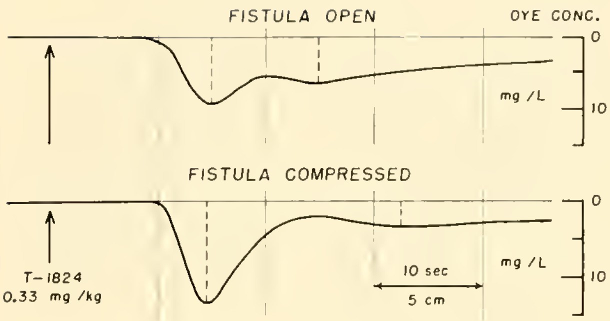

FIG. 2. Dye-dilution curves recorded after injection of dye into antecubital vein of 15-year-old youth having a femoral arteriovenous fistula. Upper curve was recorded with fistula open, and lower curve with flow to fistula abolished by manual compression. To be noted are similar appearance times of the two curves with markedly different peak concentrations and systemic recirculation times (intervals between broken lines). Upper curve reflects increased cardiac output and reduced recirculation time owing to rapid flow of blood via shortened vascular pathway through fistula.

electric components of the transducer and recording system.

Proper design of these hydraulic components and use of high rates of blood flow through the system allows a more faithful recording of dilution curves.

BASIC DILUTION-CURVE PATTERNS ASSOCIATED WITH VARIOUS STATES OF THE CIRCULATORY SYSTEM IN MAN. The effect of a striking change in cardiac output can be illustrated by comparing dilution curves recorded immediately before and after manual occlusion of a femoral arteriovenous fistula in an otherwise healthy man (fig. 2). The bottom curve, with the fistula occluded, is normal. A downward deflection occurs with increasing concentration of the dye. The second concentration peak is caused by the dye's recirculating after its first traversal of the systemic circulation. The interval of 18 sec between the two concentration peaks is related to the total circulation time, that is, the time required for the blood to make a complete traversal of the vascular system.

The upper curve, recorded when the fistula was open, shows the effect of a very high cardiac output. The amplitude of the curve is reduced since the dye is diluted in a greater volume of blood, and all the time components are reduced since the velocity of blood flow is increased by the high cardiac output, the systemic recirculation time being decreased by almost 50 per cent.

As would be expected, characteristic alterations in the dilution curves are produced in patients with congenital heart disease associated with left-to-right or right-to-left shunts or combinations of the two. The characteristic curves and the basis for their production are shown diagrammatically in figure 3. The top panel represents the normal situation. The dye is injected into the venous circulation, it traverses a normal pulmonary circulation, and a normal

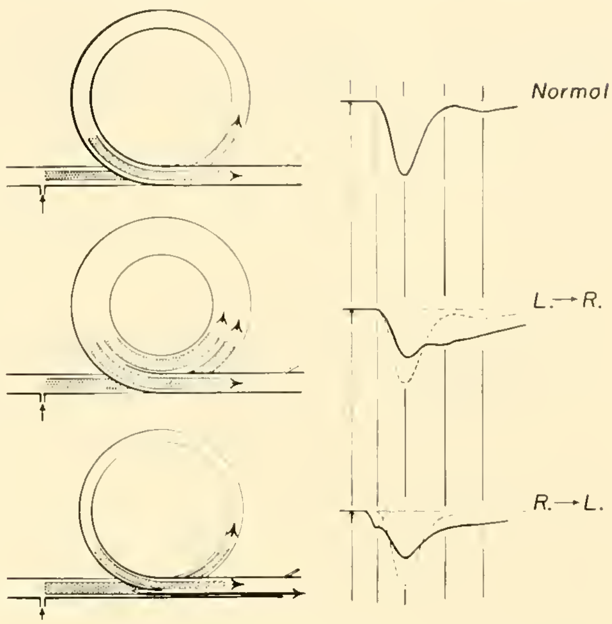

FIG. 3. Diagram representing major differences from normal of dilution curves characteristic of left-to-right and right-to-left shunts. Distribution of paths of different traversal times has been simplified (upper panel) to a single circuit, representing normal pathway from venous to arterial circulation. Normal dilution curve obtained from such a circulation, when indicator is injected rapidly into venous circulation (at arrow) and resultant dye-blood mixture is sampled from a systemic artery, is shown at right. Middle panel represents circulation characterized by increased pulmonary blood flow due to large left-to-right shunt. Indicator is not cleared rapidly but recirculates via defect through central circulation. A constant fraction (dependent on the magnitude of the left-to-right shunt and the systemic flow) leaves this central pool on each circulation. Dilution curve inscribed at right reflects this situation and may be contrasted with normal (*broken line*). Maximal deflection is reduced, because indicator is dispersed and diluted in the large volume of the central circulation and the high pulmonary flow. Disappearance phase is prolonged owing to slow clearance of dye from central pool. Circulation in cases of right-to-left shunt, which is usually associated with reduced pulmonary flow, is illustrated in bottom panel. A portion of indicator passes directly to arterial circulation via defect without traversing longer normal circulatory pathway through lungs and arrives at arterial sampling site before portion that traverses central circulation. Dilution curve inscribed to right demonstrates this early arrival of the portion of indicator shunted right to left by shortened appearance time and abnormal initial deflection superimposed on build-up portion of curve.

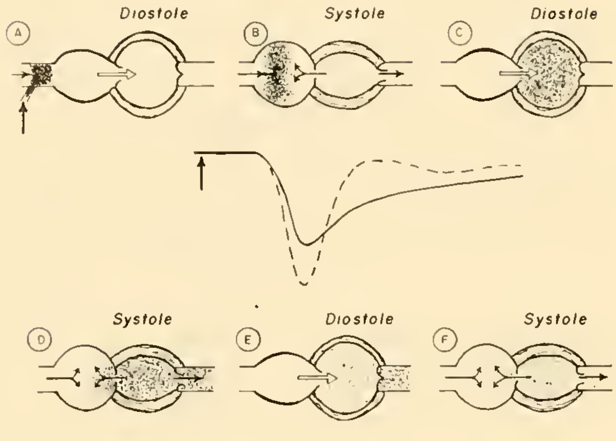

FIG. 4. Diagrammatic illustration of effect of valvular regurgitation on passage of indicator through cardiac chambers. In center of figure are illustrated normal (*broken line*) and abnormal (*solid line*) dilution curves associated with severe valvular regurgitation. Indicator is injected at inflow to cardiac chamber (*panel a*). When it flows into atrium during next ventricular systole (*panel b*) it is diluted by the volume of blood regurgitated into ventricle during succeeding diastole (*panel c*), and during subsequent systole (*panel d*) a portion of dye-blood mixture is regurgitated back into atrium and a portion is ejected forward into aorta; this process is repeated during successive cardiac cycles (*panels e* and *f*) so that time required for dye to be cleared from cardiac chambers is markedly prolonged.

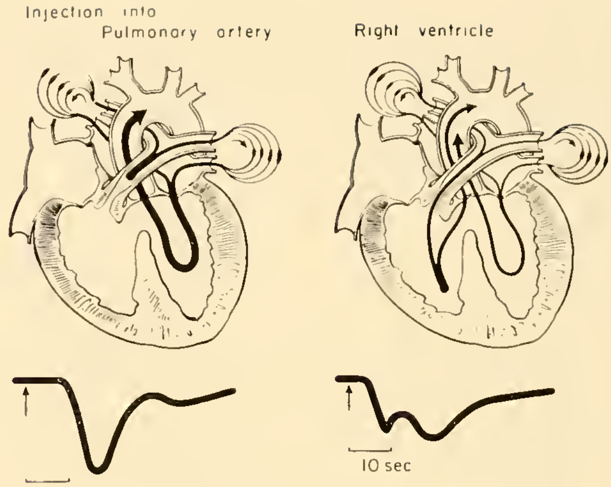

FIG. 5. Method of localizing right-to-left shunt by indicator-dilution curves in case of pulmonary stenosis and right-to-left shunt through ventricular septal defect. *Below:* arterial dilution curves after injection (*arrows*) into pulmonary artery and right ventricle. When dye is injected downstream to shunt, as into pulmonary artery (*left*), an essentially normal dye curve results; when dye is injected upstream to shunt, part escapes tc left side of heart via ventricular septal defect and appears prematurely in systemic artery to produce early abnormal deflection of curve. Dye traversing normal pathways appears later, and characteristic double-humped curve results. Difference in these two curves localizes shunt to right ventricle.

curve is obtained at the sampling site in the systemic artery.

The middle panel illustrates the situation with a left-to-right shunt such as would occur in atrial or ventricular septal defect or in aortic-pulmonary communication. Pulmonary blood flow is increased owing to recirculation of the blood through the lungs via the defect. The resulting dilution curve is decreased in amplitude owing to the increased volume of blood in which the dye is diluted as a result of the high pulmonary flow. The curve also shows disproportionate prolongation of the disappearance slope due to recirculation of the dye-blood mixture through the lungs. A similar pattern may be recorded in patients who have significant regurgitation at one or more of the valves in the circulatory system between the injection and sampling sites. In such patients the dilution curve is distorted partly by the changes in flow and volume of the circulation accompanying the frequently associated congestive heart failure and partly by slow clearance of dye from the heart due to backward as well as forward flow of dye-blood mixture across the incompetent valve (fig. 4). A simple, useful method for estimating the magnitude of left-to-right shunts on the basis of the degree of distortion of the disappearance slope has been described by Carter and associates (52).

The lower panel in figure 3 illustrates the situation with a right-to-left shunt. When the dye-blood mixture reaches the defect, a portion is shunted right to left and enters the systemic circulation directly. These dye-blood particles therefore arrive at the sampling site before those that traverse the longer normal circulatory pathway through the lungs. An abnormal initial deflection is produced and the characteristic double-humped contour associated with a right-to-left shunt results.

This characteristic distortion caused by a right-to-left shunt may be used to localize the site of shunts by injecting dye into a site in the right heart that is downstream to the chamber from which the shunt is occurring. An essentially normal dilution curve is recorded at an arterial sampling site (fig. 5). If the catheter is then withdrawn to the chamber from which the shunt is occurring and the injection repeated, an abnormal initial deflection appears on the dilution curve characteristic of a right-to-left shunt, thus localizing the defect to this chamber.

A simple, useful method for calculating the magni-

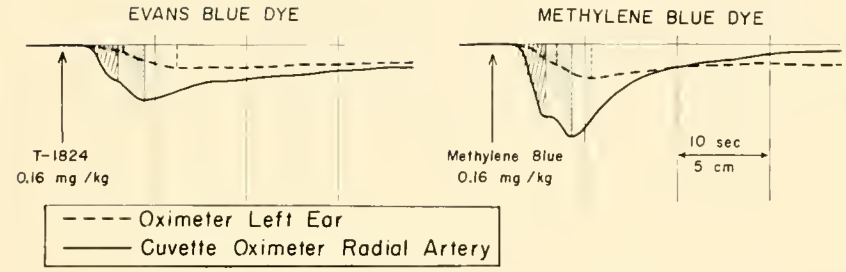

FIG. 6. Arterial dilution curves recorded by cuvette and ear oximeters following injection of indicator into superior vena cava of a girl, age 5, with ventricular septal defect, right-to-left shunt, and pulmonary hypertension. Method for determining magnitude of right-to-left shunt has been applied to cuvette-oximeter curve. Triangles are constructed by drawing vertical lines to peaks of humps, build-up time of secondary hump being taken as 44 per cent of maximal concentration time (time from injection to secondary peak). Area of first or shunt triangle (*slanted lines*) is divided by sum of areas of two triangles shown. In this instance, proportion was 25%. [From Fox & Wood (112).

tude of the right-to-left shunt from the dye curve, giving values that correlate well with those calculated from the values for oxygen saturation of venous and arterial blood, has been devised by Swan and associates (243) (fig. 6).

NORMAL VENOUS INDICATOR-DILUTION CURVE. The recently developed dye, indocyanine green, makes possible accurate recording of dilution curves in the venous circulation either upstream or downstream from the injection site, independent of the variations in the oxygen saturation of the blood (108, 111).

Venous dilution curves recorded upstream from the injection site in a patient and a dog without intracardiac shunts are shown in figure 7. After injection of dye into the pulmonary artery the dye-blood mixture was sampled from the right ventricle, coronary sinus, and venae cavae on the venous side, and also from the radial artery. In the right ventricular curve one notes, in addition to the small deflection and generalized damping of the curve, the delayed appearance of the dye at this sampling site as compared to its appearance in the radial artery. The dilution curve recorded from the coronary sinus, owing to the rapidity of flow and relatively small capacity of this bed, is similar to an arterial dilution curve. Also it is seen that the right ventricular "mixed venous curve" resembles a composite of the superior and inferior caval curves and that, as a result of the relatively much smaller blood flow from this site, the effect of the coronary-sinus curve on the "mixed venous curve" is not apparent. The dynamic response of the sampling and recording systems used for the transcription of these venous dilution curves was too slow to follow the rapid variations in indicator concentration that occur with the heartbeat. The effects of variations in the dynamic response of the recording system on the contour of dilution curves recorded from the pulmonary artery of a normal dog are illustrated in figure 8. The current practically useful techniques for detection and quantitation of left-to-right shunts or valvular regurgitation by methods involving sampling from the central circulation require only that the areas encompassed by these curves be measured accurately (223). Measurement of these areas does not necessitate accurate reproduction of rapid variations in concentration occurring with each heartbeat; therefore instruments with a relatively slow dynamic response can be used successfully in these methods.

The second channel into the heart required for simultaneous injection of indicator and recording of resultant dilution curves from multiple selected sites on the right side of the heart can be provided in one of three ways via the peripheral veins: *1*) a right heart catheter with double lumen, *2*) two right heart catheters, or *3*) a right heart catheter containing a second very small catheter for injection of the indicator. Because of greater flexibility, the latter two methods are preferred (274).

LOCALIZATION AND QUANTITATION OF LEFT-TO-RIGHT SHUNTS. Venous sampling techniques are especially useful in the detection and quantitation of left-to-right shunts (110, 206). They are more sensitive for this than studies of blood oxygen content or even of blood oxygen saturation by cuvette oximetry, since oxygen is normally present in venous blood but the presence of any early-appearing dye on the right side of the heart is abnormal. The indocyanine green dye

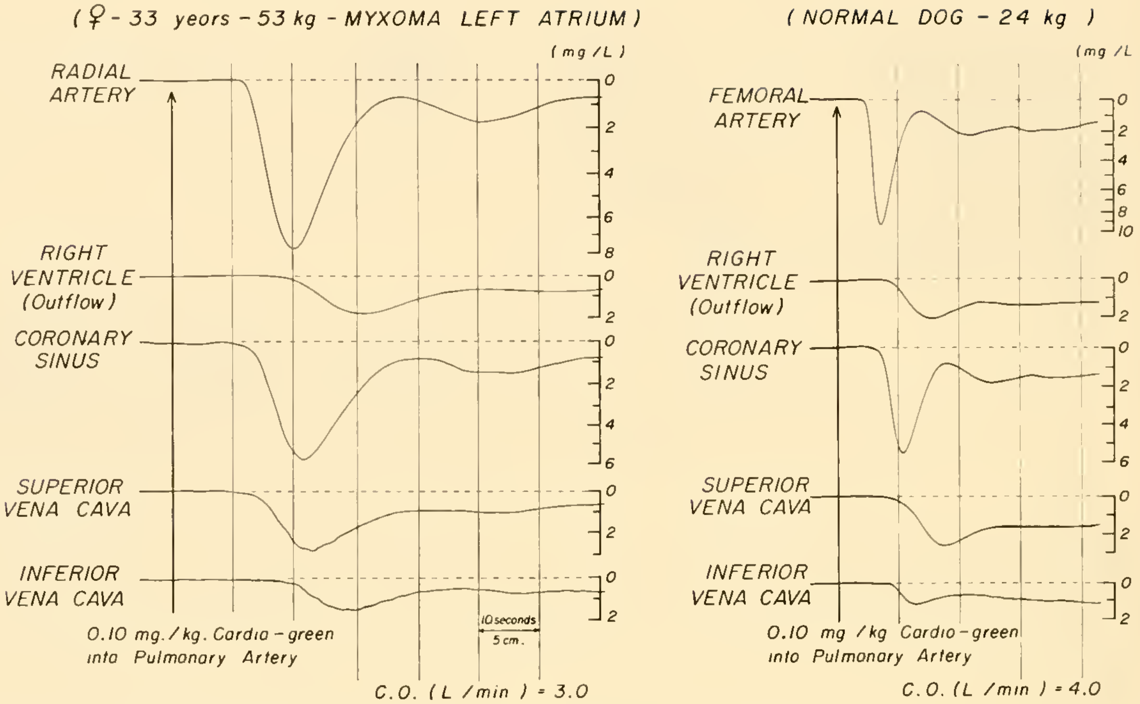

FIG. 7. Comparison of systemic arterial and venous dilution curves recorded from various sites on right side of heart in patient without arteriovenous shunt (*left*) and in normal anesthetized dog (*right*). Instant of dye injection into pulmonary artery is indicated by vertical arrows. Note that curves recorded from coronary sinus are similar to curves recorded from systemic artery. In contrast, curves recorded from other venous sites resemble badly damped versions of parent arterial curve. Probably this modification is due to differences in volumes and rates of flow through various vascular beds involved, which cause differences in degree of longitudinal dispersion of indicator particles. Note also that curve from right ventricular mixed venous blood resembles a composite of superior and inferior caval curves and that, because coronary flow is much smaller than systemic, effect of coronary-sinus curve on right ventricular mixed venous curve is not apparent. Dilution curves shown here were cut from photostats of original photographic record and realigned, correcting for effect of dead space of sampling systems, so that true time relationships of dilution curves recorded at various sampling sites are illustrated.

technique seems equal or superior to methods using gaseous indicators, for example, N_2O (174), Kr^{85} (53, 207), or radioactive serum albumin (73).

Following successive sudden single injections of indocyanine green into a lobar pulmonary artery, the concentration of the dye is recorded continuously from the main pulmonary artery and then at sites progressively more upstream—right ventricle, right atrium, and venae cavae. If there is a left-to-right shunt across any of the possible defects, the shunted dye-blood mixture will be detected in the pulmonary artery in an abnormally short interval. When during these repeated injections into the lobar artery a sampling site in the right side of the heart is found at which the abnormal, early-appearing portion of the dilution curve is absent, then the left-to-right shunt has been localized to the cardiac chamber immediately downstream to this site (274). A dilution curve simultaneously recorded from a systemic artery aids in demonstrating that the appearance of dye in the pulmonary artery is indeed abnormally early. Localization of a left-to-right shunt via a ventricular septal defect by this technique is illustrated in figure 9.

The pulmonary and systemic flows as well as the magnitude of the shunt can be calculated from such curves without the necessity of measuring either the gaseous content of blood or the respiratory gas exchange (274).

Pulmonary blood flow (Q_p) is calculated from the systemic arterial curve by the technique of Ramírez and co-workers (195), which relates the initial (forward-triangle) portion of the curve to the total area that the curve would have subtended had its disappearance slope not been distorted by early recirculation of dye-blood mixture via the shunt (fig. 10). From the ratio of the forward-triangle

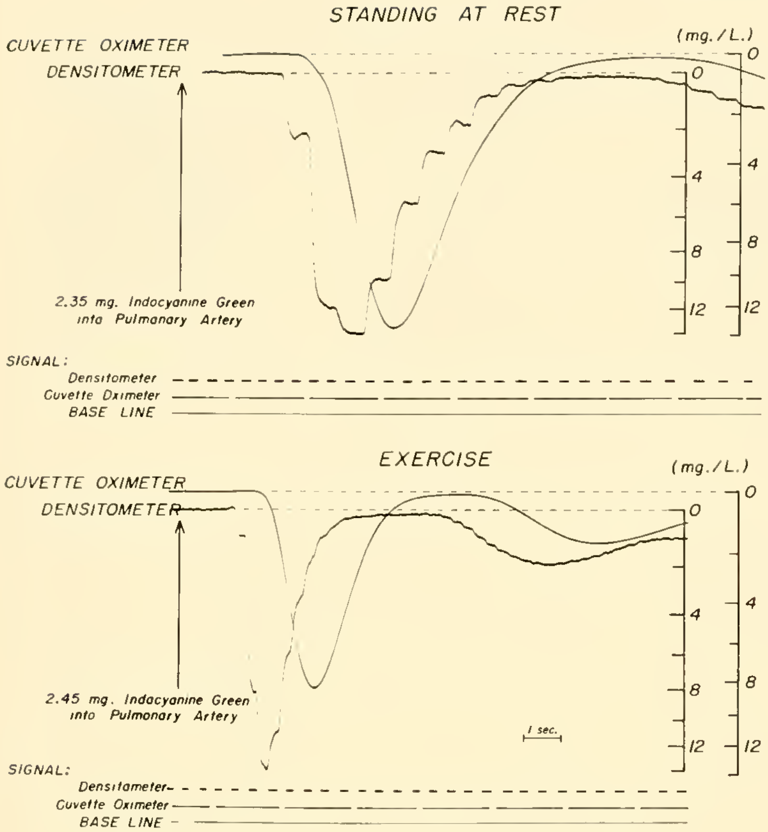

FIG. 8. Indicator-dilution curves recorded simultaneously by phototube densitometer and cuvette oximeter connected in parallel to a common catheter sampling from root of aorta. Calibration scales are on right. Interruptions in signal lines indicate passage of each milliliter of blood through instruments. *Above:* for a normal dog standing at rest *Below:* for same dog during exercise at 10 km/hour on horizontal treadmill. Note in curve recorded by densitometer using a galvanometer with a natural frequency of 30 cycles/sec that variations in concentration of dye-blood mixture with each heartbeat are clearly shown, whereas variations are not visible in curve from cuvette oximeter recorded with galvanometer with natural period of 4 sec. [From Marshall, R. J.: Factors modifying the contours of indicator-dilution curves. *Circulation Res.* (In press).]

portion of the curve caused by early-appearing dye recorded at the pulmonary artery to the initial portion of the curve recorded simultaneously at the systemic artery, the magnitude of the left-to-right shunt can be calculated as the fraction of the pulmonary flow composed of shunted blood (F_{L-R}). Then by multiplying the pulmonary blood flow (Q_p) by the fraction of unshunted blood ($1-F_{L-R}$), the systemic blood flow (Qs) may be determined. Measurements from the curves and equations required for these calculations are illustrated in figure 10. This method has been validated by comparison of the values for systemic, pulmonary, and left-to-right shunt flow by the dye technique with values determined in close temporal relationship by conventional application of the direct Fick method (265).

LOCALIZATION AND QUANTITATION OF VALVULAR REGURGITATION. The characteristic distortion of an arterial dilution curve produced by valvular regurgitation has been described. Localization of an incompetent valve by dilution curves recorded at a single arterial sampling site may be accomplished by the use of multiple selected injection sites or multiple selected sampling sites, or by combinations of these techniques (284).

Localization of an incompetent valve by dilution curves recorded at a single arterial sampling site after injections at multiple selected sites requires a normal curve at the periphery after injection just beyond the first competent valve that lies downstream to the incompetent valve, and an abnormal curve after injection between this competent valve and the incompetent one.

Use of a single injection and multiple sampling sites to localize an incompetent valve is illustrated in figure 11 in a case of aortic regurgitation. After injection into the pulmonary artery, dilution curves were recorded simultaneously at the left atrium and radial artery during combined right-heart and left-heart catheterization (272). The normal contour of the left atrial curve indicates the competence of both the pulmonary and mitral valves, and absence of a left-to-right shunt. The abnormal curve recorded at the radial artery demonstrates and localizes the site of valvular regurgitation to the aortic valve.

Although in cases of severe valvular regurgitation the characteristic changes in the systemic-artery

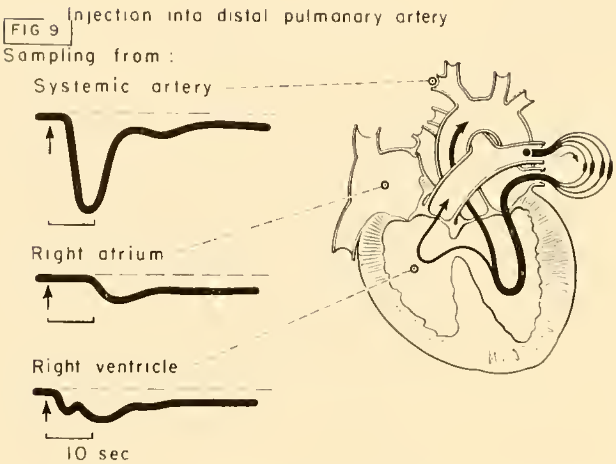

FIG 9. Method for localizing small left-to-right shunt by dilution curves recorded from selected sites in right side of heart. Indicator is injected into right or left side of heart downstream to location of left-to-right shunt. In this example, of ventricular septal defect, dye curves were recorded from systemic artery, right ventricle, and right atrium after injections into branch of pulmonary artery. Note that *1*) dye was detected in right ventricle before it appeared in systemic artery, thus demonstrating presence of left-to-right shunt, *2*) early-appearing dye was not detected from right atrium, localizing site of shunt to right ventricle, and *3*) dilution curve recorded from systemic artery was not apparently distorted by small ($< 20\%$) shunt that was present. In addition to curves shown, a fourth would be recorded from main pulmonary artery and, in case illustrated, would resemble that recorded from right ventricle.

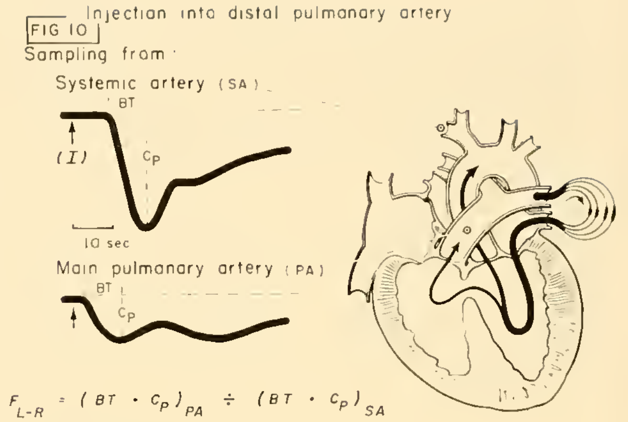

$$F_{L-R} = (BT \cdot C_P)_{PA} \div (BT \cdot C_P)_{SA}$$

$$Q_P = 47\ I/(BT \cdot C_P)_{SA}$$

$$Q_S = Q_P\ (1 - F_{L-R})$$

FIG. 10. Measurements and equations required for calculation of pulmonary blood flow, magnitude of left-to-right shunt, and systemic blood flow from dilution curves recorded simultaneously from a systemic artery (for example, radial artery) and main pulmonary artery after injection of indicator into distal pulmonary artery in patient with left-to-right shunt via ventricular septal defect. Pulmonary flow (Qp) is calculated from initial forward triangle portion of systemic arterial curve (195). Fraction of pulmonary flow composed of shunted blood (F_{L-R}) is ratio of area of forward triangle of pulmonary-artery curve $(BT.Cp)_{PA}$ to that of forward triangle of curve recorded simultaneously at systemic artery $(BT\ Cp)_{SA}$. Systemic flow Qs is calculated by multiplying pulmonary blood flow (Qp) by fraction of unshunted blood $(1\text{-}F_{L-R})$.

dilution curve are readily apparent to visual inspection, this is not always true in cases of moderate valvular regurgitation. Therefore methods have been devised to quantitate objectively the changes produced in dilution curves by valvular regurgitation. For maximal discriminatory effectiveness these methods must correct for the nonspecific changes in the dilution curve that are produced by marked variations in cardiac output and blood volume, and other factors, such as occur in congestive failure of whatever cause. The first attempt to cancel such nonspecific changes was use of the ratio of the disappearance time to the build-up time (DT/BT) by Broadbent & Wood (41).

Korner & Shillingford (155, 156) attempted to extract the nonspecific effects of flow and volume on the dilution curve by comparing the disappearance slope and the "variance" (degree of dispersion) measured from a particular curve with values for these parameters predicted from regression equations based on data obtained from normal subjects and from patients with stenotic valvular disease. The residual values for these two parameters of the curves after their extraction were then used to quantitate the degree of regurgitation. However, efforts to quantitate the volume of regurgitant flow in an individual patient are subject to gross error, due to the uncontrolled effects of variations in the volume and distensibility in the chambers upstream and downstream to the incompetent valve (173, 280).

Other attempts have been made better to locate and quantitate valvular incompetence. One of the more successful has been to inject the indicator into the cardiac chamber immediately downstream from the valve under study with sampling from the chamber immediately upstream to this valve. The presence of immediate-appearing dye indicates that the valve is incompetent (fig. 12). An index of the amount of dye regurgitated is obtained from the ratio of the areas of the curves recorded from the chamber upstream to the incompetent valve and from a simultaneously recorded arterial dilution curve (16, 281). This index is based on the assumption that there is uniform mixing of dye in the chamber into which the dye is regurgitated. It has been demonstrated, however,

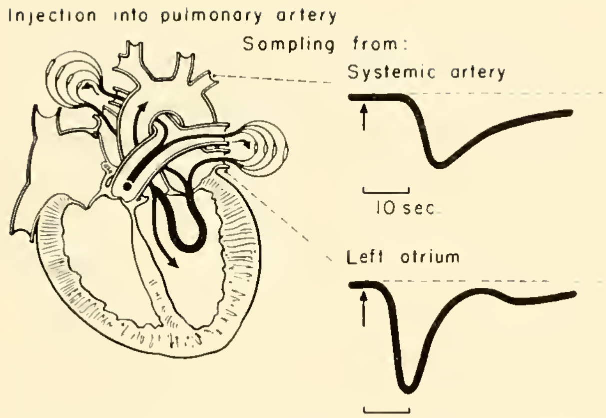

FIG. 11. Localization of regurgitation at aortic valve by dilution curves recorded simultaneously at sites proximal (left atrium) and distal (radial artery) to competent mitral valve during combined catheterization of right and left sides of heart. *At right:* after injection of dye into pulmonary artery a normal curve recorded from left atrium (*below*) indicates normality of both pulmonary and mitral valves and absence of left-to-right shunt. Abnormal curve (*above*) recorded from systemic artery indicates incompetence of aortic valve.

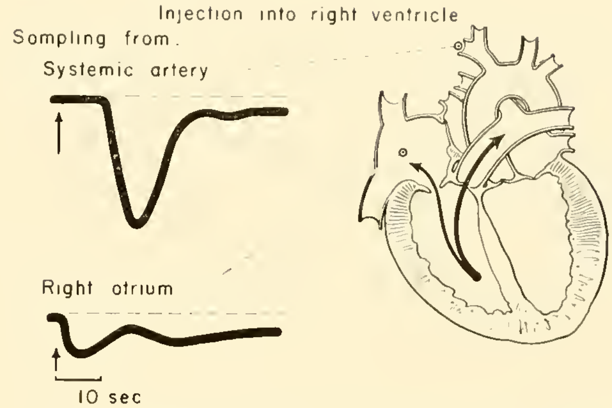

FIG. 12. Diagram of method of localizing and estimating regurgitant flow through tricuspid valve. Diagram of central circulation in tricuspid regurgitation is shown on right, and dilution curves recorded from a systemic artery and right atrium are shown on left. Vertical arrows indicate instant of dye injection. When dye is injected just downstream to incompetent tricuspid valve, a portion of dye is regurgitated through valve and is detected almost instantaneously at right atrium, producing abnormal initial concentration peak illustrated in lower curve.

that unless there is severe regurgitation, uniform mixing of regurgitated dye-blood mixture may not occur (281). Recent studies of this method in closed-chest dogs with chronic experimental aortic or mitral regurgitation indicate that under proper circumstances this upstream sampling technique provides a surprisingly accurate indication of the presence and degree of aortic or mitral regurgitation (12, 223). The accuracy obtained by these methods when applied to man is difficult to evaluate (65) (see Chapter 20).

Indicator-dilution curves have been of great value during cardiac catheterization, but probably even more basically important has been the role they play in increasing the understanding of the hemodynamics involved.

Angiocardiography

Angiocardiography, including biplane angiocardiography and cinefluorography, plays a big role in congenital cardiovascular diagnosis, especially in obtaining a picture of the gross anatomic aberrations present in a given patient (153). It also, however, may play a role in physiologic studies of congenital cardiovascular disease. Rushmer & Crystal (204) have studied the changes in the configuration of the ventricular chambers during the cardiac cycle by cinefluorographic techniques. These methods have also been applied to a study of the mechanics of ventricular contraction (205). Studies of incompetent values and of the diastolic volume of the ventricles are other areas in which cinefluorography and angiocardiography can increase the knowledge of cardiovascular hemodynamics (55).

It seems reasonable that the recent developments of image intensifiers and safer contrast media will enhance the use of this method for studies in cardiovascular physiology.

NORMAL CIRCULATION

A knowledge of the averages and ranges of normal values for pressures and blood oxygen saturations in man is mandatory as a basis for judging the significance of values obtained by similar techniques in patients with cardiovascular disease. It also seems of value to review the fetal circulation and to point out the normal changes that occur in the circulation following birth. Accordingly, this section will consist of a discussion of the fetal circulation and the hemodynamic changes occurring after birth, as well as values for cardiac output, intracardiac pressures, and blood oxygen saturations that are found in normal man during resting, supine conditions.

Fetal Circulation

By the eleventh week the heart of a human embryo has developed into a four-chambered organ with its

arterial trunks. The circulatory pattern established at this time persists throughout the remainder of fetal development. This circulatory system must function through fetal life while receiving oxygen from the mother, and must be capable of rapid accommodation to independent existence immediately after delivery of the fetus. The lungs are collapsed and have no respiratory function, and the resistance to the flow of blood through the vessels of atelectatic lung tissue is high. Since before birth the vascular resistance in the pulmonary vasculature is greater than that in the systemic circulation, most of the blood flow is diverted around the lungs. The foramen ovale and ductus arteriosus act as bypasses allowing the blood from the systemic veins to enter the systemic circulation without passing through the lungs.

If there were no interatrial communication, left ventricular output would be equal only to the amount of blood flowing through the lungs. It might be expected that under these conditions the left ventricle might not develop normally because of the small amount of blood it would pump. Patten (185) described the heart from an infant in whom the foramen ovale had sealed prematurely; the left ventricular cavity was very small and the wall was poorly developed.

Lind & Wegelius (163) have described by means of angiocardiography the blood flow through the circulatory system of human fetuses. Blood returning from the placenta flows through the umbilical vein and enters the ductus, venous, and vascular networks of the liver. On entering the vena cava this blood merges with the systemic venous blood. A larger proportion of blood from the inferior vena cava is directed across the atrial chamber, through the foramen ovale, and enters the left atrium. Most of the blood from the superior vena cava, however, passes into the right ventricle from the right atrium. Using radioisotope techniques Everett & Johnson (97) reported that only about one-fourth of the blood from each of the vena caval streams becomes mixed.

Since there is little pulmonary venous return, most of the oxygenated blood from the placenta flows directly into the left side of the heart and thence into the ascending aorta. Thus the heart and brain receive blood with maximal oxygen content. Blood flow through the pulmonary circulation probably increases as the lungs develop, but never approaches the flow through the systemic circuit, and because the pulmonary vascular resistance is greater than that in the systemic arteries (owing mainly to the collapsed lungs) a large proportion of the relatively desaturated blood entering the right ventricle and pulmonary artery is shunted through the patent ductus into the descending aorta.

The volume of blood flow through the umbilical vessels has been measured directly by several methods, and is approximately 130 ml per kg per min in a mature fetal lamb (18). This constitutes more than half the combined output of both ventricles. Pulmonary blood flow is comparatively low and amounts to only 30 ml per kg per min at the most.

The mean arterial pressure in a mature fetal lamb is about 65 mm of mercury. Pulmonary arterial pressure is just above that in the descending aorta. The pressure in the umbilical vein is about 15 mm of mercury and that in the great veins 2 to 5 mm of mercury. There is, therefore, a pressure head of 50 mm of mercury to drive blood through the placenta from the umbilical arteries to the umbilical vein, and a pressure head of 10 mm of mercury or more to drive blood through the liver from the umbilical vein to the inferior vena cava.

Postnatal Circulation

The changes that occur in the circulation at birth result from four events: *1*) removal of the placenta, *2*) expansion of the lungs, *3*) rise in partial pressure of arterial oxygen, and *4*) delivery of the fetus from a warm intrauterine environment into the cold external world. Probably the most important of these events is the "first breath," with the resultant inflation of the lungs and increased blood flow to them. On the basis of studies by Ardran *et al.* (11) in the lamb it would seem reasonable to assume that in the human infant with the first breath there is a prompt drop in pulmonary resistance with a probable increase in systemic resistance, particularly if the umbilical cord is clamped simultaneously. With this increased pulmonary flow there is an increase in left atrial pressure, and following clamping of the umbilical cord a decrease in inferior vena caval pressure. This causes the flap on the foramen ovale to be closed and prevents the venoarterial shunt through it. However, crying during the first several days of life may increase the pressure in the right atrium enough over that in the left atrium to reinstitute the venoarterial shunt and to produce transitory systemic arterial desaturation (192). The studies of Crehan and associates (75) showed that arterial oxygen saturation of infants increased rapidly, so that at 17 min after the first breath the values were within the range obtained for normal adults. Anatomic obliteration of the potential

aperture of the foramen ovale requires many weeks or years. In fact, about 25 per cent of all adults have at least probe patency of this orifice (184), a phenomenon without functional significance unless pressure in the right atrium subsequently becomes higher than that in the left. Under these conditions the interatrial communication will be restored and may even enlarge until significant quantities of venous blood are shunted into the left atrium.

In the fetus the tunica media of the ductus arteriosus is loose in structure and composed of elastic fibers and smooth muscle (142). This histologic pattern is quite different from that of the compact tunica media of the other arterial trunks. Kennedy & Clark (149) reported that functional closure of the ductus arteriosus is probably due to contraction of smooth muscle within its walls. Barclay and co-workers (17) reported angiocardiographic studies indicating that the ductus arteriosus is functionally closed 5 or 7 min after respiration begins, although contrast medium was observed to flow intermittently through the channel for a considerable period. However, Everett & Johnson (98), employing sensitive radioisotope techniques, found some reduction in ductus arteriosus flow 1 to 2 hours after birth, but a greater reduction after 9 hours. Eldridge and collaborators (93) found evidence of right-to-left shunting through the ductus arteriosus during the first several hours and days of life, since the simultaneously determined arterial oxygen saturation in the foot was frequently lower than that in the hand. Prec & Cassels (193), using dye-dilution curves as a method for determining cardiac output, also found evidence for shunting which they reasoned was probably at the level of the ductus arteriosus. These studies were done in the quiet state and were indicative of a left-to-right shunt rather than a right-to-left shunt.

Direct observations by others (4, 202), using the right-heart catheterization technique, have confirmed the patency of the ductus arteriosus and the presence of pulmonary hypertension lasting up to several days of age. Adams & Lind (4) found that the left-to-right shunt through the ductus was frequently quite large. The pulmonary hypertension observed by the above-mentioned authors was often of such a degree that pulmonary and systemic systolic pressures were equal. James & Rowe (143) later found that short periods of hypoxia with 10 per cent oxygen would increase pressure in the pulmonary artery if the arterial oxygen saturation fell to fetal levels, and Eldridge & Hultgren (92) showed that in room air, in those normal infants with a venoarterial shunt, hypoxia increased the flow through the venoarterial shunt.

Recently, interest has arisen in evaluating the effect of drugs and gas mixtures on the neonatal cardiovascular system of both animals and man (3, 6). Relatively small amounts of acetylcholine were effective in eliciting a response in newborn animals; but in humans, on the other hand, even large amounts of acetylcholine produced no drop in pulmonary-artery pressure or in heart rate. These studies suggest that the human neonatal pulmonary vascular system is capable of vasoconstriction, but as yet there is no evidence that it is capable of vasorelaxation as has been demonstrated in older patients with left-to-right shunts.

It is thus possible that the pulmonary hypertension in the newborn infant is due to two principal factors: *1*) increased resistance due to thick fetal pulmonary arteries, and *2*) increased pulmonary blood flow due to the large left-to-right shunt through the ductus arteriosus. As soon as the ductus arteriosus closes, the pulmonary hypertension apparently disappears, so that probably the anatomic nature of the fetal pulmonary arteries is not the major factor in the production of the pulmonary hypertension (5). Histologic studies of the structure of the pulmonary vessels of fetuses and infants has shown that the relative medial thickness of the muscular arteries is high during fetal life. After birth there is a pronounced drop in the relative medial thickness, which continues for about 2 weeks. A further but gradual decrease in medial thickness occurs until about 1½ years of age, when a constant level is reached which is similar to that found in older children and in adults (58).

Normal Adult Circulation

PRESSURES. Although essentially equal amounts of blood flow through the systemic and pulmonary circulations in normal man, the forces required to drive blood through these circulations are markedly different. The systemic circulation is a relatively high-resistance system requiring systolic pressures in the left ventricle of more than 100 mm of mercury to maintain a normal blood flow. Right ventricular pressure, however, is approximately one-sixth that in the left ventricle, indicating that the resistance to flow through the normal pulmonary vascular bed is much lower than that in the systemic bed.

Values for cardiac output and pressure in the right heart chambers were determined by Barratt-Boyes & Wood (20) in 26 normal subjects ranging from 13 to

44 years in age. The mean value for cardiac output in these subjects was 6.6 liters per min (range 4.4–8.9). Since cardiac output varies directly with the size of the subject, it is usually the practice to relate the cardiac output to the body surface area. In these subjects the mean cardiac output per square meter of body surface area (cardiac index) was 3.5 liters per min per m^2 (table 1). These figures are comparable to those given by others (71, 159).

The "total" pulmonary resistance of 205 dynes sec cm^{-5} was approximately one-sixth the total systemic resistance of 1130 dynes sec cm^{-5}. The pulmonary "arteriolar" resistance averaged 67 dynes sec cm^{-5}. The range of resistance values was wide (table 1).

The average and range of pressures in the right side of the heart and a systemic artery are shown in table 2. The point of reference for all pressures was taken as the midanteroposterior chest level. The pressure values for the pulmonary artery were approximately one-sixth those for the systemic artery.

No significant difference was found between the right atrial and right ventricular diastolic pressures. In this series of subjects the systolic pressure gradient across the pulmonary valve averaged 2 mm of mercury (range 0–7).

The average and range of values for blood oxygen saturation in various heart chambers and vessels in the same subjects are shown in table 3 (19). Samples of blood from the inferior vena cava were withdrawn with the catheter tip at or just above the level of the diaphragm, the catheter having been first advanced to below the diaphragm to confirm its position in the inferior vena cava and then withdrawn slightly. Samples from this position showed an average oxygen saturation of 83 per cent, whereas the oxygen saturation of superior vena caval blood averaged 77 per cent, a figure significantly less than that for inferior vena caval saturation. The mean oxygen saturation of right atrial blood equaled 80 per cent, a figure intermediate between the inferior and superior caval saturations.

There was a wide range of blood oxygen saturation values from both the right atrium and the right ventricle, apparently due to poor mixing of blood in these chambers. For example, if the catheter tip is adjacent to the orifice of the coronary sinus while sampling from the right atrium, a very low value may be obtained.

TABLE 1. *Means and Ranges of Cardiac Output and Vascular Resistances in 26 Normal Subjects While Breathing Air*

	Mean	Range (95% band)
Cardiac index, liters/min/m^2	3.5	2.8–4.2
"Total" systemic vascular resistance, dynes sec cm^{-5}	1130	952–1308
"Total" pulmonary vascular resistance, dynes sec cm^{-5}	205	154–256
Pulmonary "arteriolar" resistance, dynes sec cm^{-5}	67	44–90

TABLE 2. *Means and Ranges of Pressures in Various Heart Chambers and Vessels in 26 Normal Recumbent Subjects*

Site	Pressure, mm Hg		Maximal/Minimal Pressure, mm Hg	
	Mean	Range (95% band)	Mean	Range (95% band)
Brachial vein	8	3–13	9/7	3–15 / 2–12
Inferior vena cava	8	4–13	9/7	
Superior vena cava	8	4–13	9/7	
Right atrium	6	1–11	9/4	3–15 / 0–8
Right ventricle			24/4–10	18–36 / [(−1)–(+9)]–[4–16]
Pulmonary artery	17	11–23	22/12	15–29 / 7–17
Pulmonary-artery wedge	12	8–16	15/9	9–21 / 5–13
Radial artery	91	74–108	135/71	104–166 / 56–86

TABLE 3. *Means and Ranges of Blood Oxygen Saturation in Various Heart Chambers and Vessels in 26 Normal Subjects*

Site	% Oxygen Saturation	
	Mean	Range (95% band)
Inferior vena cava	83	77–89
Superior vena cava	77	67–87
Right atrium	80	74–86
Right ventricle	79	71–87
Pulmonary artery	78	73–83
Pulmonary-artery wedge	98	93–100
Radial artery	97	95–99

TABLE 4. *Average* Intra-Arterial Pressures (mm of Mercury) and Arterial-Pulse Propagation Times in Normal Subjects and in Patients With Coarctation of the Aorta*†

	Pressure				Ratio of Femoral to Radial Pressure		Time, sec	
	Intraradial		Intrafemoral					
	Systolic	Diastolic	Systolic	Diastolic	Systolic	Diastolic	Onset of pulse wave, femoral-radial difference	Onset to peak of femoral pulse
Normal subjects (4), aged 19–34	127 (109–144)	65 (54–85)	126 (120–134)	66 (60–69)	0.96 (0.94–0.99)	0.97 (0.91–1.06)	0.00 (−0.01–0.001)	0.15 (0.14–0.18)
Patients (21) with coarctation of aorta	196 (169–230)	96 (76–126)	113 (87–133)	81 (63–99)	0.58 (0.43–0.68)	0.85 (0.67–1.14)	0.03 (−0.01–0.07)	0.23 (0.17–0.30)

* Figures in parentheses are extreme values. † Reproduced from Brown *et al.* (45).

Variation in oxygen saturation of mixed venous blood presumably resulting from a change in cardiac output in the interval between the collection of samples was studied by Barratt-Boyes & Wood (19). In 19 subjects with an average of three samples of blood from the pulmonary artery separated by an average interval of 37 (5–147) min, the mean of the maximal variation in oxygen saturation was 3.3 per cent and the range was 0 to 10 per cent. The effects of this normal variation in oxygen saturation can be minimized when comparing the oxygen saturation values of blood from various right heart chambers by rapid consecutive sampling.

HEMODYNAMIC ALTERATIONS ASSOCIATED WITH CONGENITAL CARDIOVASCULAR DEFECTS

Obstruction of Great Vessels

COARCTATION OF THE AORTA. As early as 1870, abnormalities of the femoral arterial pulse were observed by Scheele (209) in a patient with coarctation of the aorta, and an elevation of arterial blood pressure in the cephalic portions of the body was noted by Potain (191) in 1892. It was not, however, until the development of suitable apparatus by which precise physiologic investigations might be carried out in intact man that accurate studies of the blood pressure in coarctation have been made.

Blumgart and associates (35) described the hemodynamic findings in two patients with coarctation of the aorta and noted that there was both systolic and diastolic arterial hypertension in the arms of these patients and relatively low blood pressure in the legs. Brown and colleagues (45) summarized the hemodynamic findings in 21 patients with coarctation of the aorta. Systolic pressure in the radial artery was found to be elevated in all patients with coarctation of the aorta (table 4). Radial diastolic pressure, except in one patient, was also elevated above the range of values obtained from normal subjects. In 13 of the 21 patients systolic pressure in the femoral artery was below the range of pressures encountered in the normal subjects. However, femoral diastolic pressure, except in two patients, was elevated above the normal range. The ratio of femoral to radial systolic pressure averaged 0.58 as compared to the average value of 0.96 obtained in normal subjects. The differences in the ratio of radial to femoral diastolic pressure were less marked, and the ratio fell within the normal range in 5 of the 21 patients.

The femoral arterial pulse wave has a characteristic "saw-tooth" contour (fig. 13). This difference in pulse contour from that seen in normal subjects is produced by propagation of the arterial pulse through the collateral pathways around the coarctation; usually there is relatively little transmission through the coarcted area because of its small diameter (1–2 mm). If the interval of time elapsing between occurrence of the R wave of the electrocardiogram and the onset of the radial and femoral pulse waves is determined, it is observed that the onsets of the femoral and radial pulse waves occur almost simultaneously in normal subjects. In patients with coarctation of the aorta, however, the onset of the femoral pulse wave occurs on the average 0.03 sec later than the onset of the radial pulse wave (table 4). The interval of time elapsing between the onset and the peak of the femoral pulse averages 0.15 sec in normal subjects and 0.23 sec in patients with coarctation (table 4). This represents a significant delay in the build-up of the femoral pulse wave in the latter group.

Five differences have been demonstrated between the cardiovascular dynamics existing in patients with coarctation of the aorta and those in normal subjects.

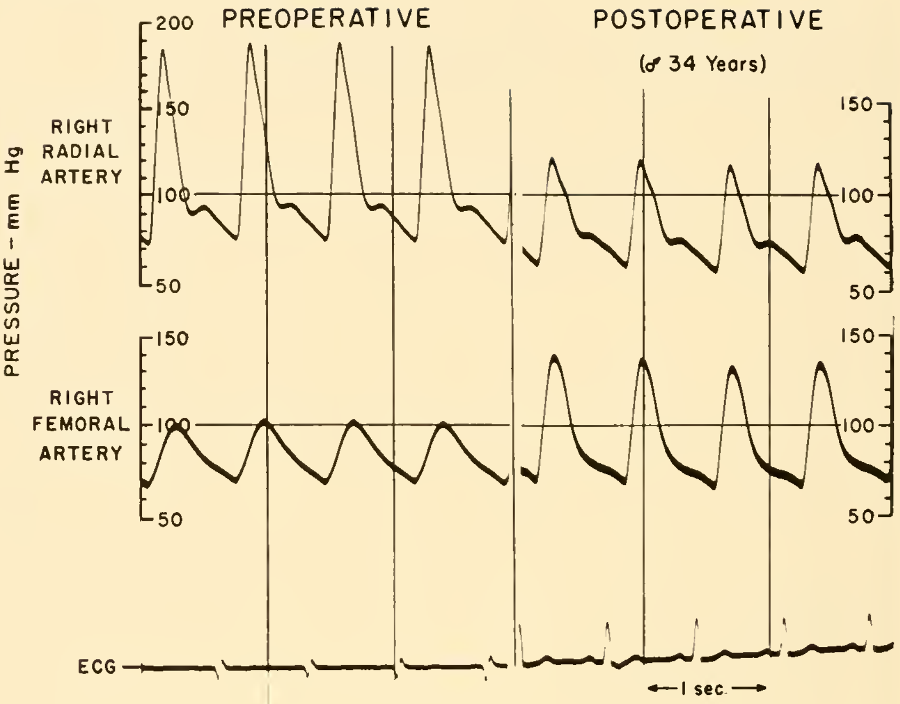

FIG. 13. Intraradial and intrafemoral arterial pulse contours in a 34-year-old man with coarctation of aorta (*left panel*). Following surgical repair of coarctation (*right panel*), pressure pulses are nearly normal. (For discussion see text.)

In these patients *a*) systolic and, in most instances, diastolic pressure in the radial artery is elevated above the range of pressures encountered in normal subjects; *b*) systolic pressure in the femoral artery is reduced or is within the range of pressures encountered in normal persons whereas diastolic pressure is, in most instances, above the normal range; *c*) as a result of these changes in radial and femoral pressure the ratio of the femoral to the radial systolic pressure in patients with coarctation of the aorta is below the range of ratios obtained in normal subjects; *d*) the onset of the femoral pulse wave is nearly always delayed beyond the onset of the radial pulse wave in patients with coarctation of the aorta; and *e*) the value for the time elapsing between the onset and the attainment of the peak in the femoral pulse wave is nearly always beyond the range of values obtained in normal subjects.

The cause of arterial hypertension in coarctation of the aorta has been studied by numerous investigators. Three theories have been postulated, either singly or in combination, to explain the blood pressure changes.

Blumgart *et al.* (35) described the dynamics of the circulation in two patients with coarctation. Since they found the arteriolar resistance in the upper extremities to be normal they concluded that the arterial hypertension above the coarctation resulted from an increased resistance to flow offered by the coarcted segment and the collaterals (mechanical theory).

From studies of blood flow in the hand and upper part of the arm, Prinzmetal & Wilson (194) and Pickering (190) came independently to conclusions that differed from the earlier notions of Blumgart *et al.* They found that there was an increase in resistance to blood flow in the upper extremities which was of general distribution, but were unable to agree upon the mechanism by which the increase was brought about. Prinzmetal and Wilson believed that the increase in arteriolar tone was due to hyperactivity of the vasomotor nerves (nervous theory), for when the vasoconstrictor activity was inhibited by application of heat the increase in the flow of blood in the hand was found to be much greater than in normal individuals or in individuals suffering from "essential" hypertension. The results of Pickering's studies were in accord with those of Prinzmetal and Wilson so far as general distribution of increased resistance was concerned. Pickering, however, was unable to show any greater increase in the flow of blood than that encountered in normal individuals either when heat was applied to the arms or when the nerves of the extremity had been injected with procaine (Novocaine). Evidence for the existence of nervous origin of the arteriolar hypertonus was lacking in his experiments, and he pointed out that there were no known nervous pathways that could lead stimuli to affect only the vasomotor system in the upper half of the body and that the view that a substance circulating

in the blood could give rise to contraction of the vessels in the upper half of the body was likewise untenable. He suggested that some abnormality of the peripheral arterioles might explain an increase in resistance in the upper extremities.

The observations by Goldblatt and co-workers (116) in 1939 that constriction of the aorta in dogs above the origin of the renal arteries would lead to the development of hypertension, whereas construction below these vessels resulted in no change in pressure proximal to the constriction, led many observers to postulate the release of a renal pressor substance (humoral theory) to explain the hypertension in coarctation. Steele (229) observed that the femoral diastolic pressure was elevated in some cases of coarctation of the aorta and interpreted this as evidence of a general increase in arteriolar tone throughout the body. Stewart & Bailey (231) and Page (183) arrived at similar conclusions. Sealy and colleagues (213), Scott & Bahnson (211) and Scott and co-workers (212) have also studied the effect of constricting the aorta in dogs and have confirmed the observations of Goldblatt and co-workers. In addition, Scott and colleagues found that transplantation of one kidney of a dog to a site above the constriction of the aorta and removal of the second kidney below the coarctation led to a return of the blood pressure to normal levels.

Genest and co-workers (114) and Tonelli *et al.* (249) observed an improvement in renal function and renal blood flow following surgical relief of coarctation of the aorta which they felt was evidence for the humoral theory in producing the hypertension.

Werkö and collaborators (259), however, pointed out that the slight decrease of renal blood flow in patients with coarctation prior to surgical correction was of the same magnitude as in patients with atrial septal defect or patent ductus arteriosus. They concluded that the decreased renal blood flow showed no relation to the origin of increased blood pressure in coarctation of the aorta.

Gupta & Wiggers (126) analyzed the changes in left ventricular, aortic, and femoral pressure pulses in dogs before and after graded constriction of the aorta. They concluded that hypertension in the aorta above a coarctation is not due solely to an increase in resistance. Equally important, they thought, were the reduced capacity and the reduced distensibility of the aortic compression chamber into which the left ventricle empties its blood during each systole. They also found some evidence that the systolic discharge from the left ventricle was increased. Gupta & Wiggers (126) also pointed out that the maintenance of femoral diastolic pressure at or above normal levels as the systolic pressure falls may be an indirect effect of damping, since damping tends to reduce pressure variations toward a mean level.

If purely mechanical factors were sufficient to account for the hypertension and if the resistance to flow through the upper limbs were normal, then the flow through these limbs would be greater than normal because of the increased perfusion pressure. On the other hand, neurogenic or humoral factors would be expected to increase the vascular resistance both above and below the coarctation.

Bing *et al.* (28) reported an increase in flow through the upper and a decrease through the lower extremity. Lewis (162), Pickering (190), and Wakim and colleagues (255) found normal values for these flows, whereas Prinzmetal & Wilson (194) found a decreased flow through the upper extremities. Although these results appear to conflict, they can probably be explained by the wide range of flow through both the upper and the lower limbs of normal people, and it seems clear that at least in the majority of patients with coarctation of the aorta the blood flow is within normal limits.

The wide range of blood flow in the forearm and calf means that no accurate prediction of the vascular resistance can be made unless both flow and pressure are measured above and below the site of the coarctation. This study was made by Patterson and co-workers (188), who found increased resistance in the forearm and normal resistance in the calf.

Bayliss (22) and Folkow (105) have demonstrated that blood vessels respond to a rise in blood pressure by increasing their tone. This occurs even when the limb is denervated and is probably a direct response of the smooth muscles of the arterioles. This finding has been confirmed in man by Patterson & Shepherd (187) and by Coles & Greenfield (63). Although this phenomenon may play a part in the increase in resistance to flow in the upper limb seen in coarctation, it would follow an increase in transmural pressure and not in itself initiate the hypertension. Such a mechanism could operate to augment the pressure, however, if mechanical factors initiated the hypertension.

Surgical removal of the coarcted segment of the aorta has generally resulted in improvement of the circulatory dynamics of these patients. Wright and collaborators (283) reported on the immediate as well as the long-term results of surgical correction of coarctation. They found, in addition to a dramatic

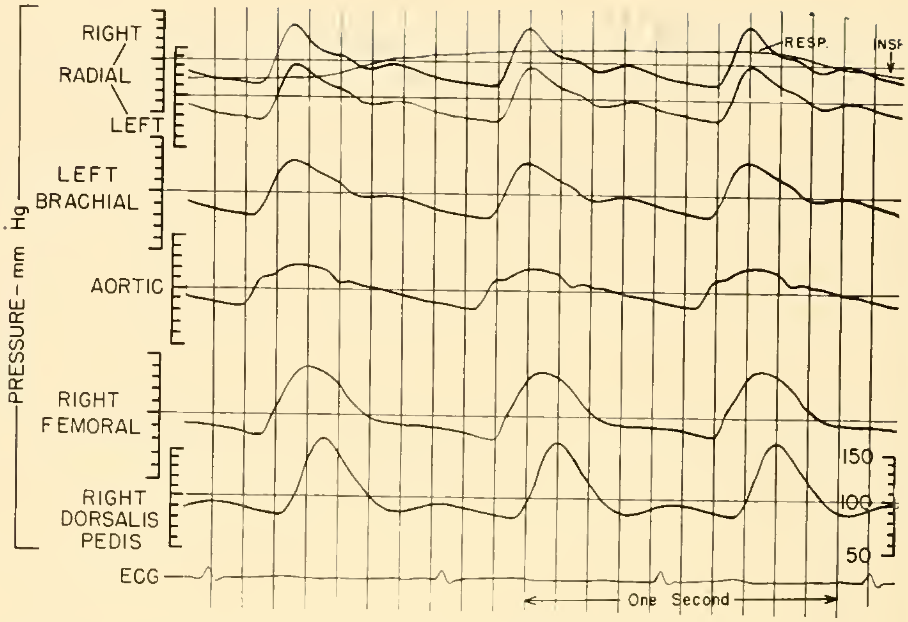

FIG. 14. Comparison of central and peripheral arterial pulses (as labeled) from a normal 31-year-old man. Note gradual increase in time interval between peak of R wave of electrocardiogram and onset of pulse wave and gradual increase in pulse pressure, especially systolic peaks, toward periphery. Anacrotic shoulder is present in aortic pulse but barely visible in femoral pulse. There is a secondary wave following primary peak but preceding dicrotic notch in brachial-radial system, and there is absence of this wave in femoral-dorsalis pedis system. The incisura, sharp and short in aortic pulse, is lost during transmission of pulse wave peripherally. Dicrotic notch, drawn out and deep in brachial-radial system, is practically nonexistent in femoral, and is so drawn out and deep in dorsalis pedis pulse that it approaches end-diastolic pressures.

immediate postoperative hemodynamic improvement, measurable continued improvement of a lesser degree occurring in succeeding years. Radial and femoral arterial pressures were within the range of normal in the majority of the patients at the time of the long-term (4–7 years) study, and none had a severe degree of hypertension.

Valvular Deformities Without Septal Defects

AORTIC STENOSIS. As stated earlier, any of the four intracardiac valves may be congenitally stenotic. A related anomaly of the aortic valve area is subvalvular stenosis. Since the hemodynamic effects are closely similar, both lesions are discussed here. Of the two, isolated subvalvular stenosis is more commonly congenital, and isolated valvular stenosis more commonly acquired.

The cardinal circulatory signs in stenosis of the aortic valve are *1*) a systolic murmur over the aortic region and large neck arteries, *2*) enlargement of the heart to the left, and *3*) the slow anacrotic ascent of the radial pulse. As long as the ventricles are able to compensate, the minute volume is not decreased, the arterial pressures are within normal ranges, and venous and pulmonary congestion is absent.

It has been found that the aortic opening must be reduced by 60 to 70 per cent of its natural size in experimental animals before the systolic discharge, the blood pressure, or the pulse form is affected (8). Much smaller degrees of stenosis, however, may produce loud systolic murmurs. Thus loud clinical murmurs, even when associated with demonstrable stenosis on subsequent postmortem examinations, are not necessarily evidence of practically significant hemodynamic impairment of cardiac ejection during life.

Usually when the left ventricle is compensated, left ventricular diastolic pressure is normal while only the systolic pressure is elevated. When aortic stenosis is moderate the pressure gradient between the left ventricle and the aorta is 20 to 50 mm of mercury, and with severe stenosis the gradient is between 50 and 100 mm of mercury or more.

The changes occurring in the aortic pressure curves with aortic stenosis are better understood by comparing them with normal arterial curves. In figure 14 pressure pulses recorded simultaneously from different

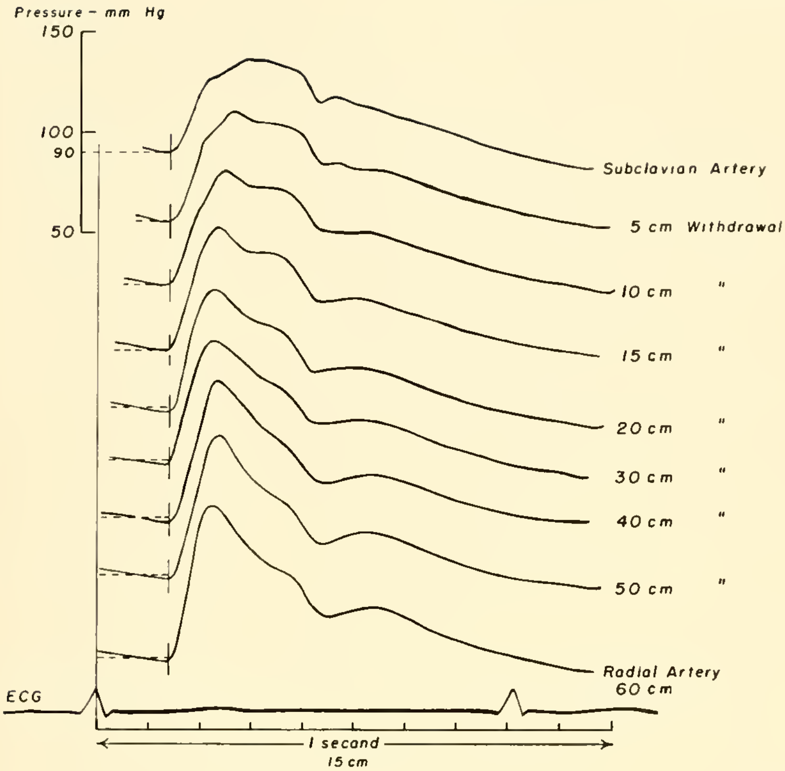

FIG. 15. Pulse contours in a healthy 30-year-old man, showing transformation of pressure pulse in subclavian-radial system. Pressure pulses were recorded consecutively during withdrawal of tip of arterial catheter from subclavian artery near aorta to radial artery in left arm. Onset of each pressure pulse is aligned for purposes of comparison. As pulse wave moves peripherally, initial wave steepens and increases in magnitude, dome-shaped systolic maximum becomes peaked, and dicrotic halt moves down and to right and becomes slurred. Low-amplitude, central postdicrotic wave is not seen after catheter has been withdrawn 10 cm or more. Prominence of radial dicrotic wave is due, in part, to change in position of dicrotic halt. Horizontal broken line intersecting onset of each pulse contour is calibration reference point (90 mm Hg). Interval of time from peak of R wave of electrocardiogram to onset of systolic upswing of each pulse wave is indicated by duration of each tracing to left side of short vertical lines, which mark onset of systole for each pulse.

sites in the arterial system of a normal man demonstrate that the wave form of the pulse changes remarkably as it moves to the periphery and that the contours recorded simultaneously from different arteries are quite different from one another.

The contour of the normal aortic pulse characteristically has an anacrotic shoulder between the onset and the maximum of systole, and this maximum is rounded or plateau-shaped. This was first demonstrated by Katz and colleagues (145). At the periphery, however, the rise of pressure to the systolic maximum is relatively more rapid, there is no anacrotic pause on the ascending limb, and the systolic maximum is peaked. The systolic pressure increases as the pulse moves to the periphery; for example, in the subject whose pulse contours are shown in figure 14 the systolic pressure in the aorta was approximately 125 mm of mercury, whereas at the radial artery it was 140 mm and at the dorsalis pedis artery 155 mm. The diastolic and mean arterial pressures decrease slightly as the pulse travels to the periphery.

The transformation of pressure pulses recorded consecutively during withdrawal of the tip of an arterial catheter from the subclavian artery near the aorta to the radial artery in the left arm is shown in figure 15. A dicrotic halt is seen in the subclavian pulse contour, which is followed by a small, postdicrotic wave. As the pulse wave moves out into the arm, the initial wave becomes steeper and larger in magnitude, the maximal pressure becomes peaked, and the dicrotic halt tends to move down and out. At the radial artery the wave that occurs between the systolic maximum and the dicrotic halt appears to be a remnant of the plateau-like maximum of the subclavian contour. The small aortic postdicrotic wave disappears shortly after the pulse wave enters the subclavian radial system (285).

In aortic stenosis the aortic pressure rises steeply at first but is soon interrupted by the anacrotic incisura, following which the pressure rises more slowly until the very end of systole (fig. 16). The initial steep rise becomes progressively shorter and the anacrotic shoulder occupies lower and lower levels as the degree of stenosis is increased. No postdicrotic wave is identifiable on the aortic contour. Wright & Wood (285) observed that the central postdicrotic wave usually is absent in patients who have significant aortic stenosis.

The aortic diastolic pressure is slightly greater than the radial diastolic pressure, as in normal persons. Unlike the normal state, however, the two contours are similar (fig. 16). An abnormal anacrotic pause is seen on the radial contour, the increase to the systolic

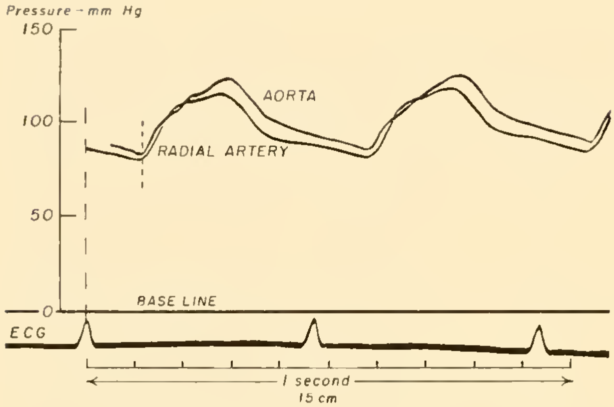

FIG. 16. Simultaneously recorded aortic and radial-artery pressure pulses in a 12-year-old boy who had severe valvular aortic stenosis. Note similarity of two contours, decreased systolic pressure, anacrotism of radial pulse (lower tracing), and absence of central postdicrotic wave of aortic contour (compared with figure 15).

maximum is greatly prolonged in both pressure pulses, and the radial systolic pressure is less than the aortic systolic pressure.

The demonstrations by Katz *et al.* (145) that an anacrotic incisura exists in the central pressure pulse, and by Feil & Katz (101) that the phenomenon occurs in patients with aortic stenosis, suggested that the turbulence started at the moment of the anacrotic incisura is transmitted as a wave to the periphery. Dow (81), who followed the changes in pressure pulses in the aorta at various distances from the aortic valve, concluded that so much resistance is developed during early systole that the central pulse assumes an anacrotic and tardus characteristic. Since the violence of ejection is reduced, characteristics of the central pulse are propagated more clearly to the periphery.

The mechanisms responsible for the transformation of pressure pulse contours during transmission to the peripheral arterial system and the explanation of the amplification of the systolic pressure remain obscure. These appear to be related phenomena in the aortic-radial and aortic-femoral systems and are difficult to explain fully by a "standing-wave" hypothesis (198). It is probable that these phenomena are related to the resonant and damping characteristics of the arterial system (158, 257).

The central aortic pressure pulse in patients with subvalvular aortic stenosis may appear normal, whereas the peripheral arterial pulse contour may be abnormal. In figure 17, pressure pulses obtained during catheterization of the left side of the heart in a patient with valvular stenosis are compared with similar contours from a patient with subvalvular stenosis. Evidence of severe obstruction to left ventricular outflow is present in both patients. The radial-artery pulses are equally abnormal in contour. The aortic contour in the patient with subvalvular aortic stenosis resembles a normal contour to a surprising degree. The postdicrotic wave on the aortic contour, which suggests a normally functioning aortic valve in the patient with subvalvular aortic stenosis, is absent in the patient with valvular stenosis. These diagnoses were confirmed surgically, and both lesions were successfully corrected. Brachfeld & Gorlin (37) found that the pulse contours in subaortic stenosis were variable. They reasoned that a tight membranous subvalvular stenosis would be hemodynamically similar to the valvular aortic stenosis, but in those cases of subvalvular stenosis in which the muscular element is of the greatest significance a somewhat different physiologic obstruction to flow is obtained. With sudden opening of the aortic valve, the violent systolic discharge subsequent to a period of isometric contraction allows a normal percussion wave to escape. With continued isotonic contraction, the hypertrophied septal portion of the outflow tract may permit the occurrence of a delayed "tidal" wave form. This secondary peak often coincides in time with the delay seen in pure valvular stenosis.

In experimental animals the pulmonary and right ventricular effects of aortic stenosis depend on the degree of stenosis and the compensatory reaction of the left ventricle (261). If both are favorable, the comparatively slight increase in blood volume is accommodated by expansion of the left atrium and the venous tributaries from the lungs. In such instances, pressures in the pulmonary artery and the dynamics of the right ventricle are not altered. If, however, the stenosis is severe, or if left ventricular compensation does not quite meet the demands, the pressure increases backward throughout the circuit and elevates pulmonary arterial pressure through augmented resistance. This may eventually lead to right heart failure.

Gorlin and associates (120) found that the "critical" area of the orifice in aortic stenosis was 0.5 cm^2. They also found that although the left ventricular stroke work was increased at rest, the pulmonary-artery wedge pressure was near normal in 80 per cent of the cases they studied. On exercise, however, the pulmonary-artery wedge pressure increased in nearly all cases, but total and effective ventricular stroke work, output and systolic pressure failed to increase and sometimes decreased. This suggests that the obstruction to outflow was such that aortic outflow

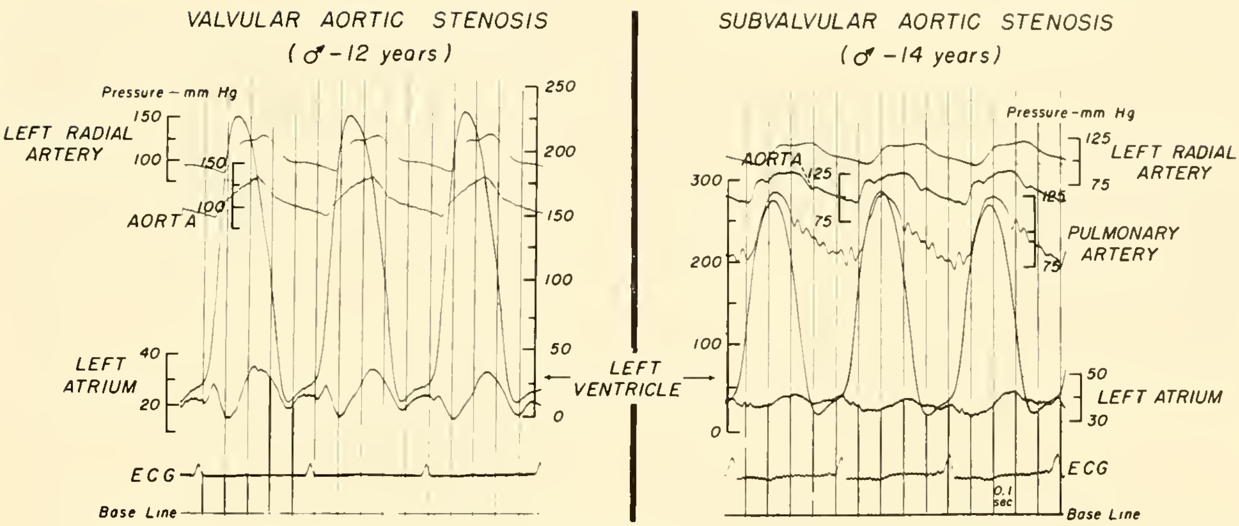

FIG. 17. Pulse contours in valvular aortic stenosis compared with those in subvalvular aortic stenosis. Simultaneously measured radial, aortic, left ventricular, and left atrial pressures were recorded during percutaneous catheterization of left side of heart. Left ventricular systolic pressure is 125 to 150 mm of mercury greater than aortic systolic pressure in both patients, indicating severe obstruction to left ventricular outflow. Pronounced anacrotism of both radial pulse contours is evident. However, aortic pressure pulse in patient with subvalvular aortic stenosis resembles normal aortic contour. In addition, a small central postdicrotic wave is easily identified.

and coronary inflow probably could not increase beyond the limit reached at rest, and hence no more work would be done.

Decreases in peripheral vascular resistance and dilatation from various causes, such as exercise, in association with a fixed minute output that patients with aortic stenosis have, are felt to be the basis for the effort syncope these patients often experience (120). Also, coronary insufficiency that is frequently found in association with aortic stenosis may be the result of a temporary increase in the disproportion between left ventricular work load and coronary flow, and of acute hypotension from systemic vasodilatation.

Further discussion of studies on aortic stenosis in experimental animals will be found in the work by Wiggers (262) and in Chapter 20, which gives a detailed discussion of stenosis and incompetence of all the intracardiac valves.

AORTIC REGURGITATION. Pure aortic insufficiency is rarely encountered as a congenital lesion. Studies of the effects of acquired insufficiency help in understanding the congenital lesion, although the latter is usually in combination with septal defects which are responsible for the major hemodynamic alterations.

Insufficiency of the aortic semilunar valve results in backflow or regurgitation of blood into the left ventricle during diastole. Blood so regurgitating competes for space with the normal inflow through the mitral orifice. Experimental work by Wiggers & Maltby (264) in 1931 demonstrated that the magnitude of the backflow depends chiefly on the size of the leak and can range from 5 per cent with small leaks to 50 per cent or more when the cusps are rendered totally deficient in experimental animals. Gorlin *et al.* (120) showed that regurgitant orifice areas of no greater than 0.5 cm^2 were capable of more than doubling total ventricular output and work.

The simultaneously recorded pressure pulse curves from the aorta and radial artery of a 24-year-old man with aortic insufficiency are shown in figure 18. The dicrotic halt of the aortic pulse contour is slurred and a well-defined postdicrotic wave cannot be demonstrated. There is a low diastolic pressure, and the radial-artery upstroke is abrupt.

The rapid rise and fall of the radial pulse wave combined with its large amplitude are generally ascribed to the rapid discharge of a large volume of blood during systole and regurgitation of a considerable volume during diastole. As Wiggers pointed out, however, measurements of the radial pulse curves demonstrate that the chief collapse occurs during systolic ejection, not during diastole. The reason for this seems to be that both central and peripheral pulses reach their maximum more rapidly than normally. This is due to the fact that the ventricle under greatly increased initial tension not only

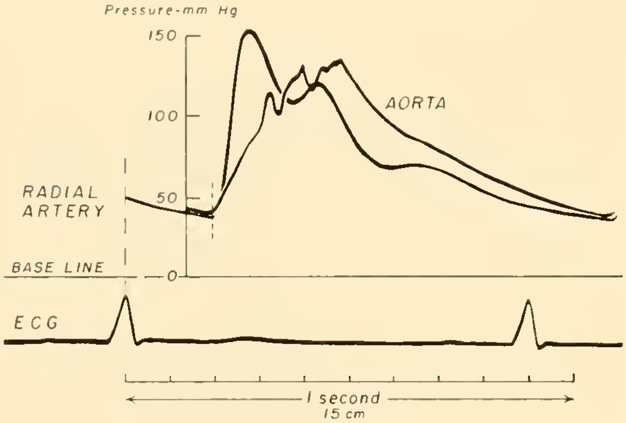

FIG. 18. Pulse contours in a 24-year-old man who had aortic regurgitation. Aortic and radial pressure pulses were recorded simultaneously, utilizing strain gauges having equal sensitivities. Contours are characterized by low diastolic pressure and wide pulse pressure. Radial upstroke is abrupt. Dicrotic halt of aortic contour is slurred, and a well-defined postdicrotic wave cannot be identified.

ejects a larger systolic volume but delivers most of this during the first half of ejection. The consequence is that comparatively less remains to be expelled during the latter half of systole, thus resulting in the systolic drop of pressure in the central and peripheral pulses. Another factor which acts to give a rapid diastolic runoff and a low diastolic pressure is vasodilatation; the calculated systemic resistance in patients with aortic insufficiency is usually a low normal (120).

The effective cardiac output is usually normal at rest and as a rule rises with exercise in contrast with that in aortic stenosis. This is accomplished at the expense of increased ventricular work by increasing the ejection volume by an amount equal to the regurgitated blood. This volume is increased in part by a prolonged period of systolic ejection resulting from the shortened phase of isometric contraction. In animal experiments an increased cardiac rate also helps to maintain a normal cardiac output. Gorlin and colleagues (120) confirmed this in man and pointed out that an increase in heart rate resulted in a decrease in the amount of blood regurgitated and, as a result, in an increase in diastolic pressure.

The increased diastolic blood volume and intraventricular tension in the left ventricle lead to enlargement of that chamber. Rosenbach (200), who first produced aortic insufficiency in rabbits, noted an initial dilatation followed by hypertrophy of the left ventricle. In human aortic insufficiency, dilatation and hypertrophy of the left ventricle are invariably found in patients with significant aortic regurgitation.

Failure of the left ventricle in aortic insufficiency usually occurs after a relatively long period of perfect or near perfect compensation. Left ventricular failure is associated with dilatation of that chamber and of the mitral orifice with consequent functional mitral regurgitation. Left-sided heart failure then results in pulmonary congestion and eventually in right-sided heart failure similar to that in mitral-valve disease.

MITRAL STENOSIS. This lesion is much more often acquired than congenital. Congenital endocardial stenosis of the left ventricle produces hemodynamic effects in the pulmonary circulation and right ventricle similar to those of mitral stenosis. Clinical mitral stenosis is characterized by two pathognomonic signs: the occurrence of a rumbling apical murmur sometimes combined with a thrill in mid-diastole or presystole, and left atrial and right ventricular enlargement. The alterations in the dynamics of the circulation depend on the degree of stenosis and not infrequently on the onset of atrial fibrillation.

In circulation models containing both a greater and a lesser circuit, the production of a severe mitral stenosis causes a decreased systolic output, a reduction in arterial pressure, an accumulation of blood in the left atrium and its tributary veins, and an increase in mean pressure in the pulmonary artery. Since the venous return is automatically diminished in such a system, venous pressure falls, the right ventricle fills less completely, and its output is diminished (261). Most of the experimental work on animals has done little more than to confirm these results. The essential changes in ventricular filling were described by Hirschfelder (132). Mild stenosis affects chiefly the rapid inflow, but this reduction of filling can be overcome by the action of an increased atrial contraction toward the end of diastole. When stenosis is severe, however, the flow during early diastole is greatly reduced, whereas the augmented atrial contraction is unable to drive any considerable volume through the narrowed valve and as a consequence systolic discharge diminishes.

The maintenance of blood flow through the narrowed mitral orifice is determined by the excess of left atrial over left ventricular pressure in diastole. The left atrial and left ventricular pressure pulses in a 49-year-old man with mitral stenosis are shown in figure 19. The individual waves contained in the usual left atrial pressure pulse are labeled. The terminology

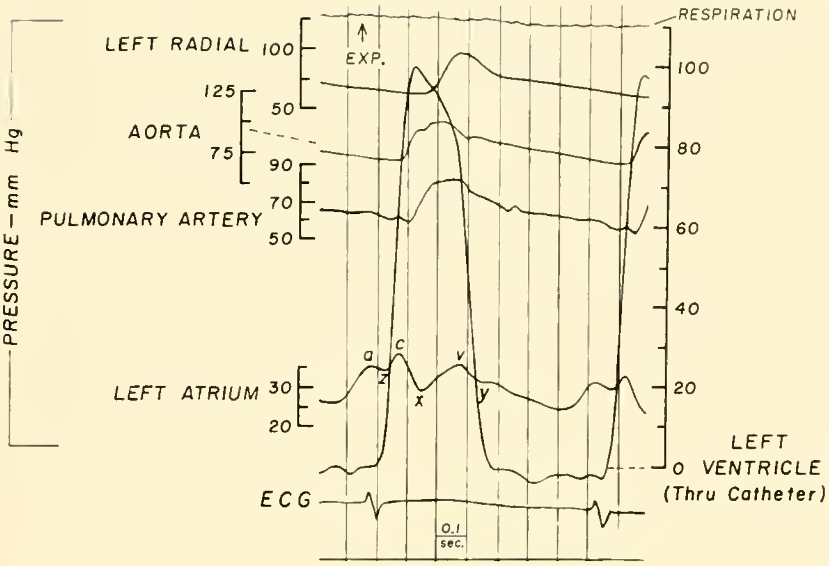

FIG. 19. Simultaneously recorded pressure pulses from various vessels and cardiac chambers in a 49-year-old man with "pure" mitral stenosis (operative diagnosis). Individual waves contained in usual left atrial pressure pulse are labeled; for explanation of these symbols see text.

used in describing these waves is that of Mackenzie (169, 170) and Wiggers (260) and is similar to that used in the description of the peripheral venous pulse. The first positive wave, the A wave, begins shortly after the onset of the P wave of the electrocardiogram and represents an increase in left atrial pressure due to atrial contraction. It is usually followed by a small dip in pressure, the Z point, just prior to the onset of ventricular systole, which is generally believed to be caused by relaxation of the atrium. The second positive wave, the C wave, appears shortly after the onset of ventricular contraction and is believed to result from closure of the mitral valve, with pushing back into the atrium of the small amount of blood contained between the leaflets, as well as from bulging of the leaflets into the left atrium, thus encroaching on its cavity. A second and larger dip in atrial pressure, the X wave, follows, and this is generally believed to result from the drawing down of the atrioventricular septum by the contracting ventricle, enlarging the atrial cavity, and thus producing a decrease in left atrial pressure. During the time that the left ventricle is ejecting blood into the aorta, the mitral valve being closed, continued inflow of blood into the left atrium produces the third positive wave, the V wave, the peak of which occurs in protodiastole. The atrial pressure then decreases rapidly to the Y point. This decrease in pressure at the onset of diastole, the "Y descent," is due to the opening of the mitral valve and flow of atrial blood into the ventricle.

In mitral stenosis, in addition to the increase in the general level of left atrial pressure, there is a more gradual descent of the V wave (Y descent) after the mitral valve opens. This results from resistance to flow across the valve. The left ventricular diastolic pressure is normal, resulting in a pressure gradient across the mitral valve. Normally, there is a minimal gradient of 1 mm of mercury or less. The gradient in mitral stenosis usually varies between 5 and 30 mm of mercury at rest, depending on the severity of the stenosis and the rate of blood flow across the valve.

For further discussion of mitral stenosis refer to the work of other investigators (88, 117, 146, 168) and to Chapter 20.

MITRAL REGURGITATION. Incompetence of the mitral valve occurs congenitally as the manifestation of a rare partial form of persistent common atrioventricular canal, in which the interior valve leaflet shows a cleft. The more usual forms of mitral incompetence are acquired.

Wiggers & Feil (263) have described in detail the immediate effects of experimentally created regurgitation of the mitral valve. Their work was confirmed by Lanari & Molins (160). Keys & Friedell (150) first demonstrated the magnitude of regurgitation by determining both roentgenokymographic (total) and Fick (stroke) outputs. They found that regurgitation varied from 25 to 100 per cent of the aortic stroke output.

The left atrial pulse contour in patients with mitral regurgitation shows typical characteristics, which are as follows (fig. 20): *1*) a high peak V wave

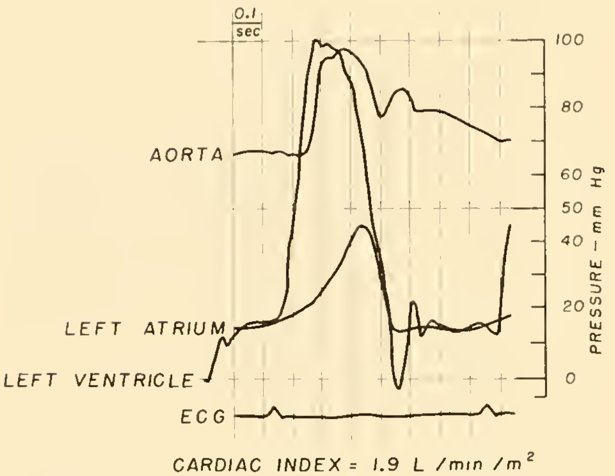

FIG. 20. Simultaneously recorded left atrial, left ventricular, and aortic pressure pulses (redrawn to identical pressure scale) from a 24-year-old man with "pure" mitral regurgitation (operative diagnosis). Note characteristic differences in contours of left atrial pulses recorded in "pure" regurgitation from those recorded in "pure" stenosis (fig. 19). For discussion see text.

is present; *2*) there is no apparent C wave, since the trough or X wave between the C and V waves is absent; *3*) if the C wave could be distinguished at the beginning of ventricular systole, its amplitude would be far exceeded by the V wave; and *4*) there is a rapid descent of the V wave at the termination of ventricular systole.

Since the pulmonary capillary (or wedge) pressure is dependent for its level on left atrial pressure, it follows that this contour of the wedge pressure pulse would also reflect the changes in left atrial pressures (66); thus hemodynamic studies using pulmonary-artery wedge pressures have been carried out (173). Gorlin and associates (119) have studied the hemodynamic status of patients with mitral regurgitation. They showed that in such patients a normal aortic output was usually maintained, but at the expense of a large increase in total left ventricular output.

McMichael & Shillingford (176) noted that any factor tending to lower the peripheral resistance and thus lessen the obstruction to aortic outflow would at the same time reduce the backflow through the mitral valve relative to the forward flow through the aortic valve. This can occur during exercise. They found that administration of amyl nitrate caused the aortic output to increase whereas the regurgitant flow decreased.

PULMONARY STENOSIS. Stenosis of the pulmonary valve, without other significant intracardiac malformations, accounts for more than 2 per cent of congenital cardiac anomalies. The essential disturbance in isolated pulmonary stenosis is an increased pressure in the right ventricle with a normal or diminished pressure in the pulmonary artery. Normally, the pressure gradient across the pulmonary valve varies from 0 to 5 mm of mercury, but with severe pulmonary stenosis this gradient may be 100 mm or more. The right ventricular pressure may actually exceed the left ventricular systolic pressure. The right ventricular hypertension leads to hypertrophy of the right ventricle. Normal cardiac output is usually maintained despite the obstruction. Eventually, however, the right side of the heart may fail and, as a result, cardiac output falls and the right ventricular diastolic, right atrial, and systemic venous pressures rise.

Numerous studies have been carried out in experimental animals on the acute effects of constriction of the pulmonary artery. The critical level of occlusion at which circulatory failure is produced has been demonstrated to be approximately 60 per cent of the cross-sectional area of the pulmonary artery (103, 246). Taquini and associates (246) found that in open-chest dogs the right ventricle was capable of attaining a pressure of approximately 60 mm of mercury without alteration of cardiac output. Up to this level the increased systolic force of the right ventricle occurred without apparent changes in the diastolic pressure or volume of the right ventricle. In general, an increase in resistance beyond this level was followed by a fall in cardiac output, a fall in left ventricular pressure and later a fall in right ventricular pressure, and by progressive failure.

Amorim and colleagues (9) studied the hemodynamic effects of acute obstruction of the pulmonary artery in normal closed-chest dogs produced by means of a balloon catheter and confirmed the findings of Taquini *et al.* (246). There appeared to be no hemodynamic change other than the increase in right ventricular pressure up to 60 mm of mercury. When the right ventricular pressure was raised beyond this level, however, a marked elevation of mean right atrial pressure and a striking decrease in cardiac output and systemic arterial pressure occurred. Pressure recordings from the right atrium and indicator-dilution techniques demonstrated the development of significant degrees of tricuspid regurgitation under these circumstances. The deterioration of right ventricular function in dogs with intact cardiac septa appears to be related *a*) to overdistention of the right ventricle, and *b*) possibly to a disproportionate

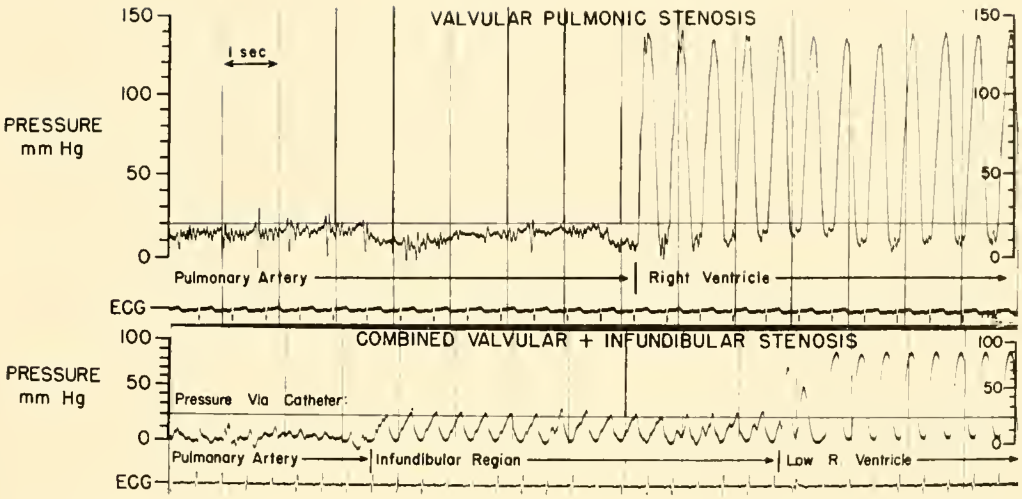

FIG. 21. Pressure recordings during withdrawal of catheter tip from pulmonary artery to low right ventricle in a patient with valvular and a patient with both valvular and infundibular pulmonic stenosis. Note small pulsations recorded from pulmonary artery. When catheter tip was withdrawn through pulmonic valve to infundibular chamber of right ventricle (*lower panel*), diastolic pressure decreased to levels obtained from low right ventricle. Systolic pressure, however, was still very low, increasing abruptly when catheter tip entered low right ventricle.

reduction in coronary blood flow to the right side of the heart caused by the fall in systemic pressure and the concomitant increase in resistance to coronary venous drainage from the right side of the heart due to the increased right atrial and ventricular pressure under these circumstances, as postulated by Visscher (251) and by Katz and co-workers (144).

These studies demonstrate the poor ability of the right ventricle to compensate for acute increases in pulmonary resistance, which is in contrast with its behavior when it has been subjected to a chronic gradual increase in pulmonary resistance.

Patients with isolated pulmonary stenosis are usually asymptomatic for a long time (21). Sooner or later dyspnea on exertion and fatigability may occur. Occasionally there is chest pain or syncope on effort, presumably due to inability of the right ventricle to increase its output during exertion. Sudden decompensation with right-sided heart failure develops commonly in such cases.

Pulmonary stenosis may be either valvular or infundibular in type, or both may be present. Hypertrophy of the right ventricle, especially the crista supraventricularis, as a result of valvular pulmonary stenosis may so narrow the outflow tract of the right ventricle that further obstruction to the flow of blood at this site is produced. Frequently, continuous recording of pressures while withdrawing an intracardiac catheter from the pulmonary artery to the right ventricle will help in determining whether the stenosis is valvular, infundibular, or both. Figure 21 shows pressure recordings from patients with valvular and with both valvular and infundibular pulmonary stenosis during withdrawal of the catheter from the pulmonary artery to the right ventricle.

PULMONARY REGURGITATION. Congenital pulmonary regurgitation is extremely rare, so that this lesion is nearly always an acquired defect secondary to bacterial endocarditis or functional regurgitation as a result of pulmonary hypertension. Two of the features common to all the varieties of pulmonic regurgitation are *1*) hypertrophy of the right ventricle, and *2*) regurgitation of blood from the pulmonary artery into the right ventricle, with the consequent production of a diastolic murmur. In many cases there is also considerable dilatation of the pulmonary artery. Dilatation and hypertrophy of the right ventricle may develop a compensatory mechanism similar to that of the enlarged left ventricle in aortic regurgitation. Right ventricular hypertrophy with relatively little dilatation may, however, have preceded the onset of pulmonary regurgitation, owing to the pulmonary hypertension associated with increased pulmonary vascular resistance that may occur in chronic pulmonary disease.

TRICUSPID STENOSIS. Either stenosis or insufficiency may result from Ebstein's malformation of the tricuspid valve, which is a rare congenital disorder. The

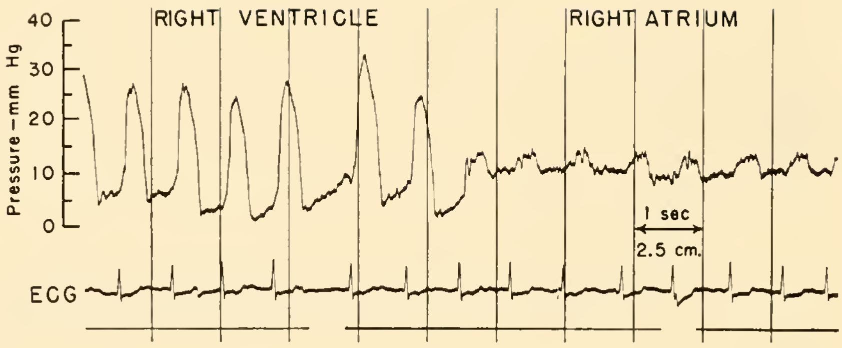

FIG. 22. Pressures obtained through cardiac catheter as tip was withdrawn from right ventricle to right atrium in a case of tricuspid stenosis and mild regurgitation. Note that even in longest cardiac cycles, atrial fibrillation being present, right ventricular diastolic pressure does not reach level of right atrial pressure. Pressure waves in right atrium with each ventricular systole (V-waves) are presumably caused by tricuspid regurgitation.

more common lesions involving this valve are acquired. With tricuspid stenosis there is an increased diastolic volume of blood in the right atrium as a result of incomplete emptying through the narrowed valvular orifice. The increased stretch of the right atrium results in a more forceful atrial contraction with at least a temporary restoration of normal cardiac output. During this process of compensation the right atrium becomes dilated and hypertrophied. Because of the limited compensatory capacity of the right atrial wall, systemic venous distention occurs early. This then seems to diminish the outflow from the right side of the heart. The effect of tricuspid stenosis is somewhat similar to that of constrictive pericarditis in that it obstructs the inflow of blood into the right ventricle.

In tricuspid stenosis the striking feature of the atrial pressure tracing is the presence of giant A waves. The right atrial pressure is elevated, usually to a mean pressure between 10 and 25 mm of mercury instead of the normal of 6 mm. There also is an abnormal pressure gradient between right atrium and right ventricle during diastole (fig. 22). Killip & Lukas (152) observed that a mean diastolic gradient of more than 1.9 mm of mercury while at rest and of more than 2.6 mm during exercise occurred in patients with tricuspid stenosis. The two major hemodynamic alterations in tricuspid stenosis were a decrease in cardiac output and an increase of right atrial pressure. Their data suggest that a tricuspid orifice smaller than 1.0 cm^2 per m^2 of body surface is associated with a decrease in cardiac output.

TRICUSPID REGURGITATION. In tricuspid regurgitation as in stenosis of the tricuspid valve, there is an increased volume of blood in the right atrium. This is due to regurgitation of blood into the right atrium during right ventricular contraction. The right atrium dilates and eventually becomes hypertrophied. Right atrial emptying is less complete than usual, and pressure is elevated.

The right atrial pressure may show many of the typical features of the left atrial pulse in mitral regurgitation. The contour of the right atrial pulse shows a diminution in the negative X wave or replacement by the ascending limb of the V wave. The V wave is elevated and descends rapidly with the onset of ventricular diastole (33, 102). However, this positive venous pulse may be absent in tricuspid regurgitation if the right atrium is greatly dilated so that the regurgitant stream has little effect on its large content.

McMichael & Shillingford (176) observed that during exercise tricuspid regurgitation increased with a corresponding fall in forward cardiac output, which is in contrast with what is seen in mitral regurgitation.

Communications Between Right and Left Ventricles and Between Pulmonary and Systemic Arteries

It is convenient to combine the discussion of these two types of defects, for although they are different anatomically their major hemodynamic effects are similar. Therefore, although most of the discussion here will be concerned with ventricular septal defects, it will, in large part, apply as well to patent ductus arteriosus and other aortic-pulmonary communications.

GENERAL CONSIDERATIONS. Since communications between the ventricles and between the pulmonary and systemic arteries are between high and low-pressure chambers and vessels, it is to be expected that the blood will flow from the left to the right side of the heart if the rest of the circulatory system is normal. This is indeed the case when the defects are small. With large defects, however, balanced shunts or even

shunts predominantly in the right-to-left direction are found.

In considering the size of the defect, it is obvious that when the opening reaches a certain size there will be an equalization of pressures in the two circulations and, in the case of ventricular septal defect, the ventricles will function as a single pumping chamber with two outlets.

Although the pulmonary vascular resistance is high in the prenatal period, this resistance normally declines rapidly after birth. With this fall in resistance some infants with ventricular septal defects die in the first few months of life from heart failure with excessive blood flow through the lungs, whereas other infants with defects of similar size respond with a return to a high pulmonary vascular resistance, survive and lead an active life for many years (34).

Another factor that has been considered important in the hemodynamics of ventricular septal defect, overriding of the aorta (the anatomic position of the defect in relation to the aorta), does not appear to play a significant role in determining the direction and magnitude of shunts across the defect.

In the past, varying degrees of severity of ventricular septal defects have been considered to be different entities, and various names to describe these entities have been in general use. For example, a very small ventricular septal defect with normal pressure in the right side of the heart has been called "maladie de Roger," and anomalies characterized by large ventricular septal defect, overriding of the aorta, and cyanosis have been termed "Eisenmenger complex." (91).

It is generally recognized now, with increased knowledge of all gradations of ventricular septal defects and associated hemodynamic alterations, that all should be regarded as ventricular septal defects of varying severity and that terms designating them as separated entities have for the most part outlived their usefulness.

AVERAGE AND RANGE OF HEMODYNAMIC DATA IN VENTRICULAR SEPTAL DEFECT. The average and range of pressures and flows in 38 patients with ventricular septal defect are given in table 5 (80). There was a wide range in the age of the patients, extending from 7 months to 44 years, 24 of whom were less than 20 years of age. Pressures in the pulmonary artery varied from normal values to values similar to those found in the systemic arterial system. In 12 patients, pressures in the pulmonary artery were within the range of normal, in 10 they were moderately elevated, and in 16 the pulmonary systolic pressures were equivalent to those found in the systemic arterial system.

TABLE 5. *Average and Range of Hemodynamic Data in 38 Patients With Ventricular Septal Defect*

	Age, years	Pressures, mm Hg			Blood Flow, Liter/min/m²	
		Right atrium	Pulmonary artery	Pulmonary-artery wedge,* mean	Pulmonary	Systemic
Avg.	21	8/3	75/40	10	8.0	4.1
Range	7/12–44	2/(−3)–19/12	18/6–151/83	3–22	1.5–17.1	2.1–7.5

* Obtained in 16 patients.

In this series the average pulmonary blood flow of 8.0 liter per min per m² was more than twice the normal value for pulmonary flow.

Values from two to four times normal were obtained in patients with normal pulmonary-artery pressures and averaged 5.6 (3.5–9.1) liter per min per m². The highest values occurred in patients with moderately elevated pulmonary-artery pressures. These flows were from 3 to 8 times normal and averaged 11.5 (7.7–17.1) liters per min per m². In those with equivalent pressure relationships between the right and left sides of the circulation, contrasting pictures were seen. In seven of these patients, less than 12 years of age, there was a high average flow of 8.2 (4.9–13.1) liters per min per m², whereas those in the older age group had an average flow of only 2.1 (1.5–3.5) liters per min per m². The relationship of the pulmonary blood flow to age is shown in figure 23. It is apparent that in patients with pulmonary hypertension (right panel) the highest pulmonary flows occur in the younger age groups (less than 12 years of age) and that the flow decreases in late adolescence and in adult life.

The largest left-to-right shunts occurred in the presence of low pulmonary resistance and gradually decreased until the pulmonary resistance was similar to systemic resistance. When the pulmonary resistance exceeded that in the systemic vascular bed, the predominant shunt was in the right-to-left direction (fig. 24).

In spite of the increased pulmonary flow seen in most patients, systemic flow was within the range of normal, the average flow being 4.1 (2.1–7.5) liters per min per m².

Pulmonary-artery wedge pressures were obtained in 16 of the patients studied. In all except one instance these values were within the range for normal

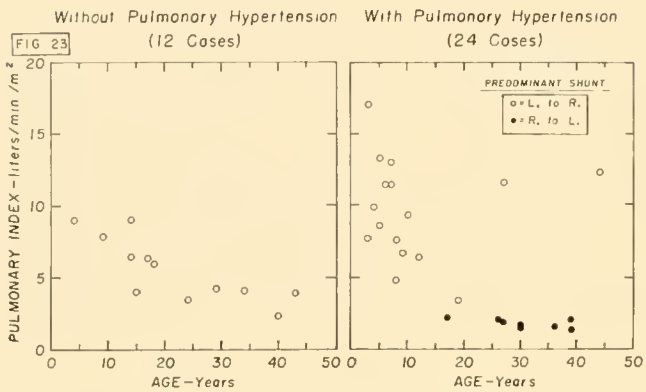

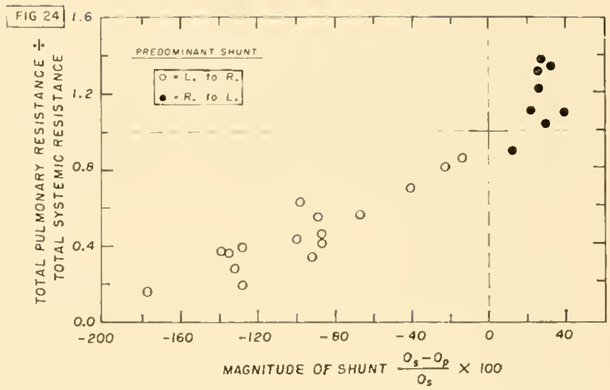

FIG. 23. Relationship of pulmonary blood flow to age in 36 patients with isolated ventricular septal defect. Note decrease in blood flow with increase in age.

FIG. 24. Relationship of pulmonary/systemic resistance ratio to direction and magnitude of shunt in 24 patients with isolated ventricular septal defect and pulmonary hypertension. Note that, as pulmonary resistance increases to levels in excess of systemic vascular resistance, left-to-right shunt decreases and is eventually exceeded by shunt in right-to-left direction.

values. Savard *et al.* (208) compared left atrial pressures measured directly during operation in 36 patients before and after closure of a ventricular septal defect (fig. 25). The data demonstrate that the left atrial pressure was significantly reduced in the majority of cases after closure of the ventricular septal defect.

FACTORS DETERMINING DIRECTION AND MAGNITUDE OF SHUNT. The hemodynamic alterations associated with a ventricular septal defect are determined chiefly by two factors: *1*) the area of the defect and *2*) the reactions of the pulmonary vasculature, that is, changes in resistance to pulmonary blood flow associated with the defect.

For purposes of simplification, ventricular septal defects may be separated into two categories, large and small, on the basis of the cross-sectional area of the defect (208, 279). Of course, there may be many defects the size of which is intermediate between these two categories.

A small ventricular septal defect is one the size of which provides a significant resistance to blood flow between the left and right ventricles. In spite of such a defect the ventricular septum still constitutes an effective, although incomplete, barrier to blood flow between the left and right ventricles. It would be expected, therefore, that the pressure in the right ventricle would be significantly lower than that in the left ventricle. Under such circumstances the magnitude of a left-to-right shunt is determined chiefly by the size of the defect, that is, the resistance to blood flow across it.

A large ventricular septal defect is defined as one

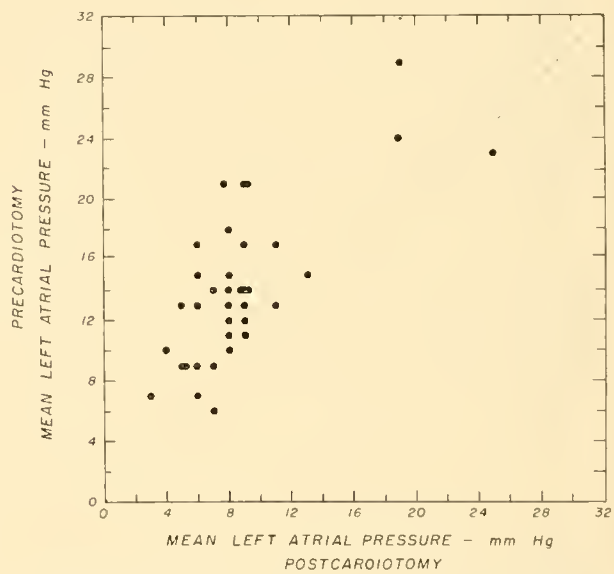

FIG. 25. Comparison of left atrial pressure recorded at operation before and after cardiotomy for closure of ventricular septal defect in 36 patients. Diagonal broken line is line of identity for preclosure and postclosure values. The fact that left atrial pressure is nearly always reduced after closure of ventricular septal defect suggests that increased left ventricular work load associated with defect had resulted in increase in left atrial pressure.

the size of which is such that the resistance to blood flow through the defect is very small, and therefore the ventricular septum is an ineffectual barrier between the left and right ventricles. Thus, in these cases, the magnitude and direction of the blood flow through the defect are determined primarily by the relative resistances to the outflow of blood from these two common-pressure chambers via the aorta on the

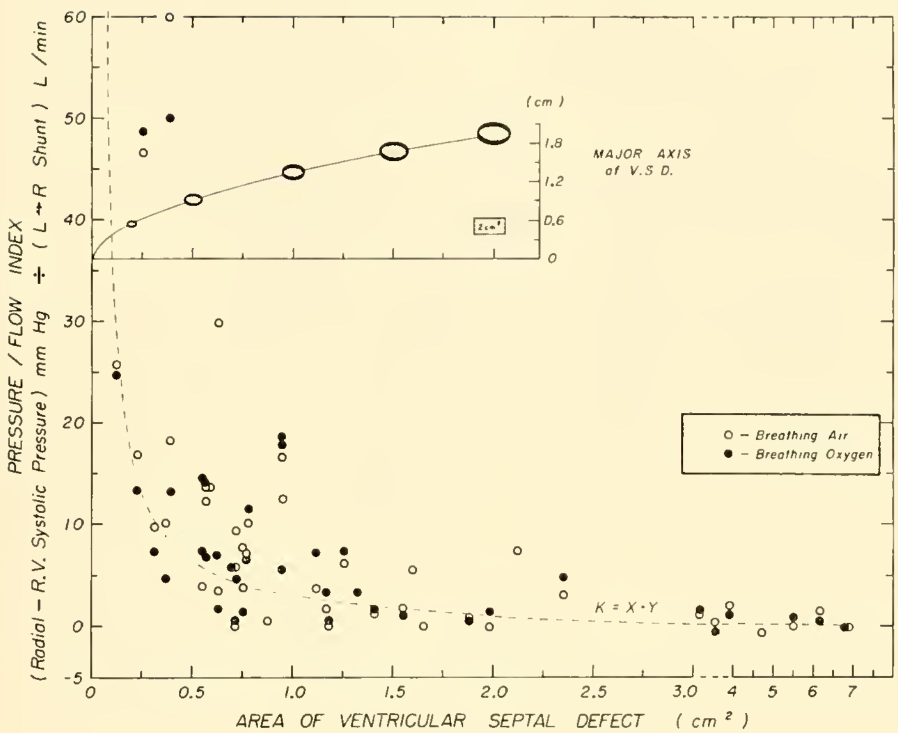

FIG. 26. Relationship between size (area) of defect and "resistance" to blood flow across ventricular septal defects. Inset shows relationship between area of ellipse in square centimeters and magnitude of major axis, which is 125% of minor axis. In series of patients studied, maximal dimension of ventricular septal defect averaged 125% of minimal dimension. Broken line indicates rectangular hyperbola, K = X·Y, in which K equals average product of *ordinate* (Y) values for pressure/flow indexes, and *abscissa* (X) values for area of defects. See text for discussion. [From Savard *et al.* (208).]

left and the pulmonary artery on the right side of the incomplete septum. The resistances to blood flow out through the aorta and the pulmonary artery are determined in turn by the degree of systemic and pulmonary vascular resistances, respectively. If pulmonary resistance is low in relation to systemic vascular resistance, a large left-to-right shunt will be present, and vice versa. Since systemic vascular resistance has been demonstrated to remain essentially normal in patients with ventricular septal defects, the alterations in pulmonary vascular resistance that are frequently associated with this disease are of paramount importance in determining the hemodynamic effects associated with the defect.

Savard and co-workers (208) have studied the hemodynamic alterations in ventricular septal defect in relation to the size of the defect measured during open cardiotomy for repair of these defects. They correlated the cross-sectional areas of the ventricular septal defects and the calculated resistance to flow across these defects (fig. 26). Their data indicate that for defects with an area of less than 1 cm^2 the resistance to blood flow across the defect increases rapidly with decrease in size of the defect, whereas the resistance to blood flow across the defects with an area of more than 1 cm^2 falls to practically zero. This confirmed the statement of Wood *et al.* (279) that no obstruction to flow would be expected in defects larger than 1 cm^2 in size.

The relationship of the estimated areas of ventricular septal defects to the ratio of the systolic pressures recorded simultaneously in the pulmonary and systemic arterial circulations is shown in figure 27. This systolic-pressure ratio has been expressed as the systolic pressure in the right ventricle divided by the systolic pressure recorded simultaneously from the radial or femoral arteries. Since in normal individuals the systolic pressure in these arteries exceeds the systolic pressure in the thoracic aorta by 14 per cent, it would be expected that this ratio would approach an average value of 0.88 for patients in whom systolic pressures in the right and left ventricles were equal. This average ratio of 0.88 is shown in figure 27 as a horizontal broken line. These data indicate that as the area of a ventricular septal defect increases toward 1 cm^2 per m^2 there is a progressive increase in the systolic-pressure ratio (that is, a decrease in pressure gradient) across the defect, and as the area of the defect approaches and exceeds 1 cm^2 per m^2 this ratio approaches 0.88, or, in other words, the pressures in the right and left ventricles approach unity with an area of more than 1 cm^2 per m^2.

It must be kept in mind, however, that the systolic pressure in the right ventricle is determined both by

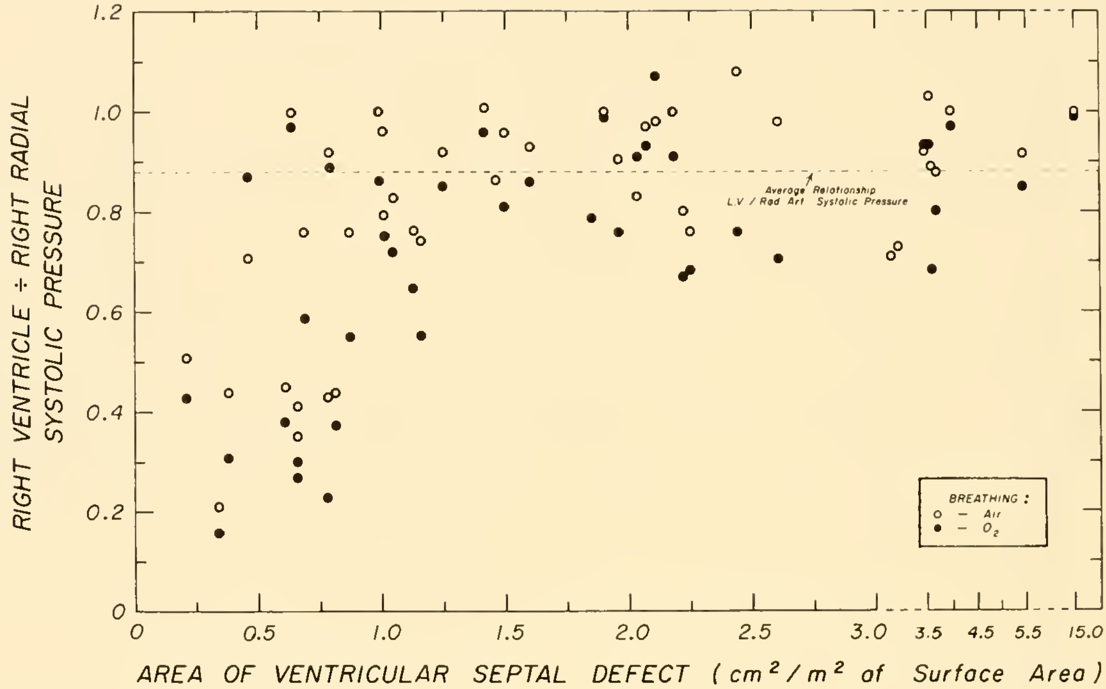

FIG. 27. Relationship between systolic pressures in pulmonary and systemic circulations and size (area) of ventricular septal defect. Horizontal broken line indicates average relationship between systolic pressure in left ventricle and that in radial artery in normal persons. It would be anticipated that in patients with equal systolic pressures in left and right ventricles, values for right ventricular/radial-artery systolic pressures would cluster along this line. Note that for patients with defects with an area of more than 1 cm^2/m^2, values for systolic pressure do scatter along this line, indicating that in this situation systolic pressures in right and left ventricles were closely similar or equal. Note also that ratios obtained when patients were breathing air (*open circles*) nearly always exceeded those obtained when breathing oxygen. This finding is a consequence of reduction of pulmonary vascular resistance associated with oxygen breathing and indicates that in the presence of lowered pulmonary vascular resistance a larger ventricular septal defect is required to elevate right ventricular systolic pressure toward level being maintained by left ventricle.

the quantity of blood flowing into it via the defect and by the pulmonary vascular resistance against which the ventricle is emptying. Thus, if the pulmonary vascular resistance is normal (that is, low), a very high blood flow through the defect will be required to equalize right and left ventricular systolic pressures and still maintain a left ventricular systolic pressure and consequently systemic arterial pressure compatible with life. Since the capacity of the left ventricle and pulmonary vascular bed to maintain a very high flow is limited, a normally low pulmonary vascular resistance is incompatible with prolonged survival in the presence of a large ventricular septal defect. Thus all surviving patients with large ventricular septal defects by necessity have an increased resistance to outflow from the right ventricle.

It would be expected that in the presence of defects in the intermediate size range of approximately 0.5 to 2.0 cm^2 per m^2 the pressure gradient between the left and right ventricles would vary from zero to a relatively large value, depending on pulmonary vascular resistance. If pulmonary vascular resistance is high in such cases, relatively little blood flow across the defect is required to equalize pressures between the ventricles so that right and left ventricular systolic pressures would be essentially equal. If, however, pulmonary vascular resistance were very low, the systolic runoff into the pulmonary artery would be very rapid, and hence a very high flow across the defect would be required to equalize right and left ventricular pressures during systole. In this situation, significant differences in the systolic pressure levels in the two sides of the heart would be expected in the presence of moderate-sized defects.

That the magnitude of the pulmonary vascular resistance may be important in determining the relative levels of right and left ventricular systolic pressures has been demonstrated by infusion of acetyl-

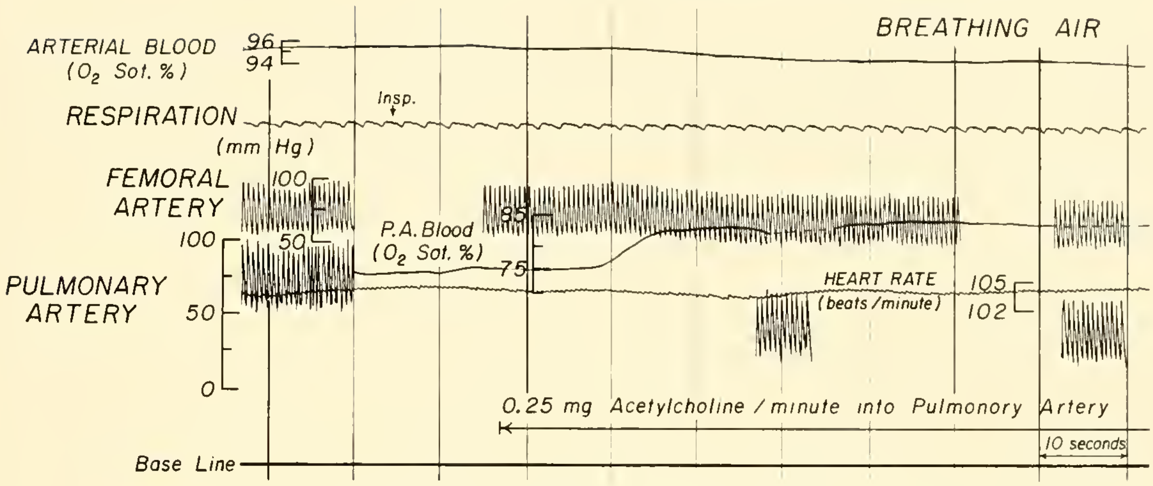

FIG. 28. Effect of continuous infusion of acetylcholine into pulmonary artery on systemic and pulmonary arterial pressures and other variables in an 8-year-old boy with large ventricular septal defect. Note that in control period, pressures in femoral and pulmonary arteries were closely similar so that right and left ventricular pressures were essentially equal. Infusion caused striking decrease in estimated pulmonary vascular resistance, from 1620 to 510 dynes sec cm^{-5}. This was associated with decrease of systolic pressure in pulmonary artery from 95 to 65, while systolic pressure in femoral artery decreased to 80 mm of mercury. The fact that heart and respiratory rates were unchanged during infusion indicates that acetylcholine was inactivated before reaching systemic arterial vessels. Area of this defect was sufficient to equalize right and left ventricular systolic pressures in control period and was such as to compromise ability of left ventricle to maintain systemic arterial pressure during infusion because of very large runoff through ventricular septal defect consequent to large decrease in pulmonary vascular resistance caused by acetylcholine. In this situation a small pressure gradient of approximately 15 mm of mercury across defect did develop. [From Shepherd *et al.* (221).]

choline into the pulmonary artery in such patients (fig. 28). When a large decrease in pulmonary vascular resistance results, there is a large increase in the left-to-right shunt (blood flow across the defect), and a significant difference in right and left ventricular systolic pressures develops.

There is a demonstrable correlation between the blood flow through small ventricular septal defects and the size of such defects (208). When the ventricular septal defect is large, however, such a relationship is no longer demonstrable (fig. 29). Systemic blood flow and vascular resistance are usually maintained in the presence of a ventricular septal defect, hence the blood flow across a large ventricular septal defect is determined primarily by the level of pulmonary vascular resistance. These concepts are in general agreement with those of Selzer (214), Wood and co-workers (279), Blount and colleagues (34), Brotmacher & Campbell (43), and Imperial *et al.* (141).

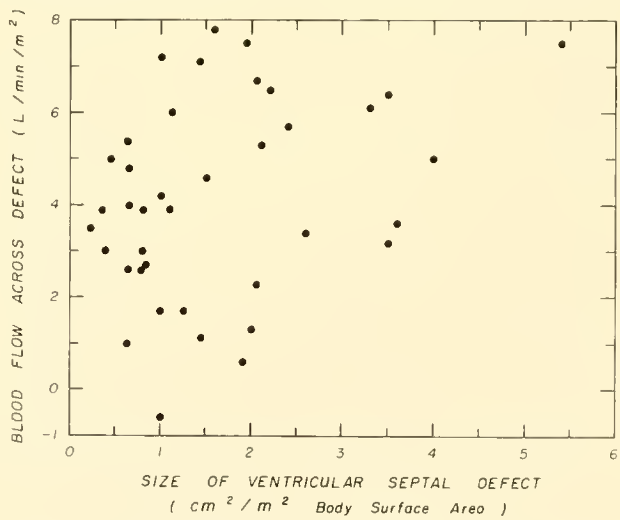

FIG. 29. Relationship of magnitude of blood flow across ventricular septal defect to size (area) of defect in 39 patients breathing air. Note that in this group of patients, most of whom had large ventricular septal defects, no relationship is apparent between these two parameters. See text for discussion. [From Savard *et al.* (208).]

The relationship of the location of the defect to the associated hemodynamic effects has been controversial. Taussig (247), in classifying ventricular septal defects as high and simple defects, claimed that the former had a more profound effect on the pulmonary circulation than did the latter. Selzer (215), however, found no correlation of location with cardiac dynamic alterations. Becu and colleagues (23) and Zacharioudakis and associates (286) were in agreement with this. Warden *et al.* (256), however, from surgical ob-

servations in 120 cases of ventricular septal defect, considered that the anatomic relationship of the defect to the orifice of the pulmonary artery is just as important a factor as size. Imperial and colleagues (141) found in their series that defects of the muscular septum had different effects from those in the membranous septum. They thought that the explanation for this was that the muscular defect may contract during ventricular systole, and on this assumption the effective size rather than the location per se is the hemodynamic determinant. In the more direct studies of Savard and co-workers (208), the data support the interpretation that the effective size of the defect is the primary determinant of its hemodynamic effects irrespective of its position in the septum.

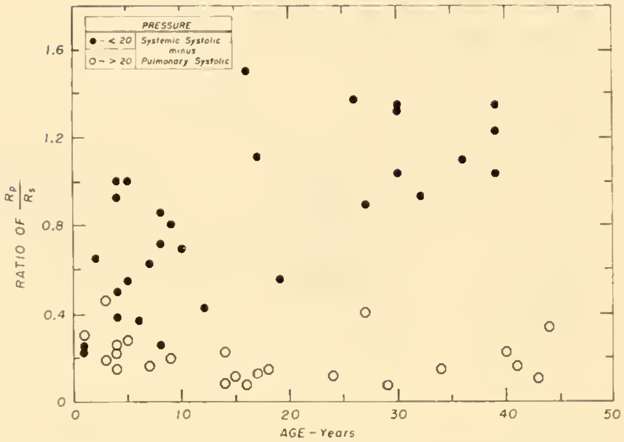

FIG. 30. Relationship of ratio of pulmonary/systemic vascular resistance to age in 53 patients with ventricular septal defect. Patients in whom systemic exceeded pulmonary systolic pressure by more than 20 mm of mercury are presumed to have small ventricular septal defects. In these patients (*open circles*) this ratio remains low, that is, vascular resistance is normal or only slightly elevated, and there is no apparent tendency for pulmonary vascular resistance to increase with age. Patients with closely similar systolic pressures in pulmonary and systemic arteries are presumed to have large ventricular septal defects. In these patients (*solid circles*) there is a significant tendency for ratio of pulmonary/systemic vascular resistance to increase with age. Note that pulmonary vascular resistance was greatly elevated to values closely similar to or in excess of those for systemic vascular resistance in all patients in this group who were more than 20 years of age.

EFFECT ON PULMONARY VASCULAR RESISTANCE. It seems logical to conclude that the changes in pulmonary vascular resistance in patients with ventricular septal defects are related to the size of the defect. If the defect is small, the pulmonary vasculature is protected, since the ventricular septum still constitutes an effective (high resistance) although incomplete barrier to blood flow from the left ventricle into the pulmonary circulation. In patients with small ventricular septal defects no increase in vascular resistance ordinarily occurs in the pulmonary circulation irrespective of the age of such patients (fig. 30). However, if the defect is large so that the ventricular septum provides an ineffective (low resistance) barrier to blood flow from the left ventricle into the pulmonary circulation, the pulmonary vasculature is subjected to very high blood flows and, in addition, to pressures equal to or approaching systemic arterial pressures generated by the forceful contractions of the left ventricle. An increase in pulmonary vascular resistance occurs in this situation and usually attains or approaches the level of systemic vascular resistance by the age of 20 years or before, as shown in figure 30.

Adams and collaborators (7) made serial observations of 20 patients with ventricular septal defect and also concluded that pulmonary resistance tends to increase progressively with time after varying intervals of "latency."

Keith and co-workers (147) noted that the association of severe pulmonary hypertension with a patent ductus arteriosus is uncommon in childhood. Since the ductus is usually considerably smaller than the aorta, the shunt (left-to-right flow) that occurs through it is, as a rule, equivalent to that which occurs via a relatively small- or moderate-sized ventricular septal defect. These authors found that 11 per cent of their series of children with patent ductus arteriosus had severe pulmonary hypertension, whereas approximately one third of their patients with ventricular septal defect had severe pulmonary hypertension. This difference in incidence of pulmonary hypertension in the two conditions is believed related to the fact that the resistance to blood flow through ventricular septal defects (which can be large) is usually less than that through a patent ductus arteriosus, the diameter of which is usually considerably less than the diameter of the aorta. Another factor is that the ductus is of variable length and the greater the length the greater will be the resistance to blood flow through the ductus.

The exact cause or causes for the increase in pulmonary vascular resistance that occurs in these patients are not known. It appears that the increase in systolic pressure in the right ventricle and pulmonary arteries that is associated with a large ventricular septal defect is an important inciting cause for the development of increased pulmonary vascular resistance. Blount *et al.* (34) have suggested that the force of ejection into the pulmonary vascular tree may

play a role in the arteriolar changes leading to an increase in pulmonary resistance. It is also possible that the magnitude of the increase in blood flow through the pulmonary vasculature associated with a large defect may be an important factor in the development of an increase in pulmonary vascular resistance.

Savard and co-workers (208) stated that the increase in blood flow associated with a ventricular septal defect may produce an increase in pulmonary vascular resistance by two mechanisms: *1*) direct effects of increased pressure and flow on the pulmonary vasculature, and *2*) a secondary effect resulting indirectly from the increased work load imposed on the left ventricle. If the work load on the left ventricle is very high, some degree of left ventricular incompetence and a consequent increase in left atrial pressure may develop. It is known that in patients with increased left atrial pressure due to left ventricular failure or mitral stenosis an elevated pulmonary venous pressure is a stimulus for the development of an increase in pulmonary vascular resistance (217). Savard and co-workers (208) showed that the left atrial pressure did tend to be increased in the presence of large ventricular septal defects and was significantly decreased after closure of these defects (fig. 25). They concluded that the possibility that an increase in left atrial pressure may be of importance in the development of the increase in vascular resistance associated with a large ventricular septal defect cannot be ignored.

It seems unlikely that elevated pulmonary vascular resistance could result solely from a direct effect of increased blood flow on the pulmonary vasculature, since it is uncommon for patients with atrial septal defects to develop pulmonary hypertension in spite of increased pulmonary blood flow which may be very high and is present from childhood into adult life.

It now is generally recognized that there are two main mechanisms which cause the increase in pulmonary vascular resistance that may occur in patients with left-to-right shunts. The first of these is related to the histologic changes in the small vessels of the lungs changes that produce obstructive anatomic lesions in the pulmonary vasculature. It is believed that in the neonatal period the normal decline in pulmonary vascular resistance proceeds in normal infants and infants with ventricular septal defect alike (58). When the fall in resistance is marked in infants with large ventricular septal defects, some die in the first few months of life from heart failure due to the excessive blood flow through the pulmonary artery and consequent heavy work load on the left ventricle. Other infants with defects of similar size apparently respond with a return to a high pulmonary vascular resistance and may survive to lead an active life for many years. It has been suggested that in some of these infants there is persistence of the fetal type of pulmonary vasculature. Usually, however, the histologic changes occurring in the pulmonary arterioles are progressive in character. Heath & Edwards (129) described six grades of structural changes varying from medial hypertrophy in arteries and arterioles to intimal fibrosis, generalized vascular dilatation, appearance of plexiform and angiomatoid lesions, and necrotizing arteritis.

The second mechanism responsible for the increased pulmonary vascular resistance in this condition is an increase in the vasomotor tone in the small vessels of the lungs. The conclusion that a component of the increase in vascular resistance associated with a ventricular septal defect is due to vasomotor tone is based on the demonstration of the capability of the pulmonary vessels to dilate in such patients. It has been shown in patients with ventricular septal defect that breathing mixtures high in oxygen content may result in a significant decrease in pulmonary-artery pressure and pulmonary vascular resistance, as illustrated in figure 31 (172). Burchell and associates (48) made similar observations in patients with patent ductus arteriosus and pulmonary hypertension. Several groups of workers have also demonstrated that infusion of acetylcholine into the pulmonary artery produces a significant decrease in pulmonary vascular resistance (128, 221).

Since the magnitude and direction of blood flow across a large ventricular septal defect are dependent on the relative resistance to flow in the pulmonary and systemic vascular circuits, it follows that the predominant flow will be in the direction of least resistance. Early in the course of this disease, pulmonary vascular resistance is much lower than systemic vascular resistance, resulting in a large flow across the defect in the left-to-right direction. As the lesions in the pulmonary arterioles progress, however, pulmonary vascular resistance increases until the resistances in both circuits are balanced. The flows across the defect then will also be balanced. Eventually the pulmonary vascular resistance can increase to the point that it exceeds the resistance in the systemic vasculature and this results in a predominant shunt in the right-to-left direction.

Swan and co-workers (240) have studied the effect

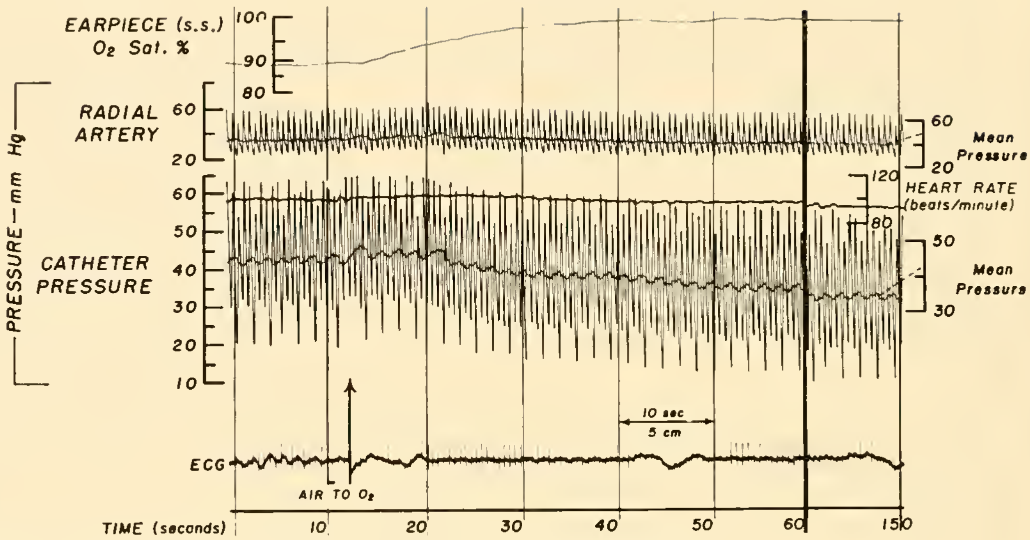

FIG. 31. Effect of change from breathing air to breathing 99.5% oxygen on systemic and pulmonary-artery pressures, heart rate, and arterial oxygen saturation in 8-month-old boy with ventricular septal defect (area 1.3 cm^2/m^2). Note that arterial oxygen saturation began to increase within 3 sec and pulmonary-artery pressure to decrease within 10 sec after change from breathing air to breathing 99.5% oxygen. Pulse and mean pressures were recorded simultaneously with double galvanometer assemblies. Decrease in pulmonary-artery pressure associated with oxygen breathing has been shown to be associated with increase in pulmonary blood flow (left-to-right shunt) and decrease in pulmonary vascular resistance.

of exercise on the pulmonary vascular dynamics in patients with intracardiac or aortopulmonary left-to-right shunts. They demonstrated that pulmonary resistance increased during exercise in patients with pulmonary hypertension and either increased or remained unchanged in patients without pulmonary hypertension. A normal decline in systemic vascular resistance during exercise was observed in both groups. This differing response of the pulmonary and systemic circuits to exercise was considered to be the underlying basis for the relatively small change in pulmonary flow during exercise in patients with large defects.

THE EISENMENGER COMPLEX. In 1897 Eisenmenger (91) described in detail a typical example of the condition that has since become known as Eisenmenger's complex. His case was that of a 32-year-old man who was cyanotic. At necropsy a large ventricular septal defect was found which was so positioned that the lumen of the aortic orifice fell half over the left ventricular outflow tract and half over the right. He discussed the "overriding aorta" at considerable length and concluded that it played no part in the physiologic disturbances of the circulation. He also stated that in otherwise uncomplicated ventricular septal defect, pulmonary hypertension resulting from obstruction in the pulmonary circulation would abolish the left-to-right shunt.

Abbott & Dawson (2) attributed the cyanosis of Eisemenger's case to a right-to-left shunt through the defect because of the overriding aorta. Taussig (247) also stated that "the essential feature of the Eisenmenger complex is that the aorta is dextroposed and overrides the right ventricle." It was not until 1947 that Bing and co-workers (30) demonstrated pulmonary hypertension at pulmonary level with bidirectional shunt in five cases of Eisenmenger's complex. Since then many studies have confirmed that pulmonary hypertension equivalent to systemic pressure is invariably present in Eisenmenger's complex (49, 216, 275). It has been found as a result of such studies that anatomic overriding of the aorta may or may not be found at necropsy in clinically undistinguishable cases, and as a result the concept has developed that Eisenmenger's complex is pulmonary hypertension with reversed or bidirectional shunt through a large ventricular septal defect (277).

That overriding of the aorta plays no significant role in the altered hemodynamics of patients with ventricular septal defect is now generally accepted (277) and thus the term seems no longer necessary (43).

Wood (275) however, uses the term "Eisenmenger

TABLE 6. *Hemodynamic Data in 57 Cases of Atrial Septal Defect*

	Age, years	Pressure, mm Hg				Arterial Blood Flow, Liter/min/m²		Shunt, % of Blood Flow	
		R.A.	R.V.	P.A.	Radial artery	Pulmonary	Systemic	Right to left*	Left to right†
Avg.	27	9/4	52/6	47/22	117/67	8.7	3.3	7	53
Range	3–58	3/1–26/15	21/0–150/13	21/6–150/80	83/54–180/108	0.8–20.7	1.1–5.6	0–60	0–80

* Expressed as % of systemic blood flow. † Expressed as % of pulmonary blood flow.

syndrome" to include all patients with a communication between the right and left sides of the heart associated with severe pulmonary hypertension and a predominant right-to-left shunt. It seems more pertinent to include all cases of a certain defect, such as ventricular septal defect, under the same name, and to realize that the cyanotic group represents merely a further progression of the pulmonary obstructive changes that may occur.

Atrial Septal Defects

Defects of the atrial septum result in an abnormal communication between the two low-pressure input chambers of the heart. The predominant flow through such defects is usually in the left-to-right direction and it is frequently large. In spite of greatly increased blood flow, pressures in the right side of the heart usually remain normal although they may increase in adulthood. The blood flow from the left ventricle is usually within normal limits. Thus the left-sided (systemic) circulation is a normal-pressure normal-volume system and that in the right side is a normal-pressure high-flow system.

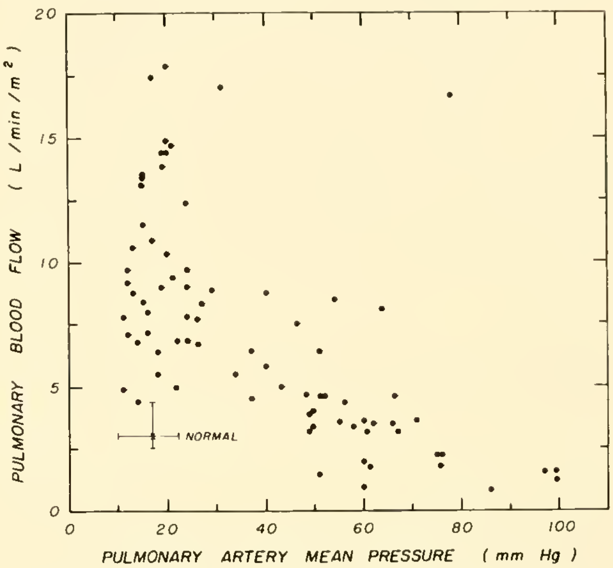

FIG. 32. Relation of pulmonary blood flow to pulmonary-artery mean pressure in 54 patients with interatrial communications. Note apparent division of data so that flow values are almost independent of pressure in those patients with a mean pulmonary-artery pressure of less than 30 mm of mercury. In patients with a mean pulmonary-artery pressure in excess of 40 mm of mercury there was an inverse relation between pressure and flow.

HEMODYNAMIC FINDINGS. The average and range of various hemodynamic values in 57 patients with atrial septal defects are shown in table 6 (258). The ages ranged from 3 to 58 years; more than one-half of the patients were between 21 and 40 years of age. The average pulmonary-artery pressure in this series was slightly elevated. Forty of the 57 patients had pulmonary-artery pressures that were normal or minimally elevated, 5 had a systolic pressure between 41 and 60 mm of mercury and 12 had severe pulmonary hypertension with systolic pressures greater than 60 mm. All 12 patients with severe pulmonary hypertension were adults; of 18 patients less than 21 years of age only one, a 4½-year-old child, had moderate elevation of the pulmonary-artery pressure.

There was no correlation between the magnitude of pulmonary blood flow and pulmonary-artery pressure in those patients without pulmonary hypertension, the pulmonary-artery pressure remaining normal or only minimally elevated despite a large pulmonary blood flow in these patients (fig. 32). However, in the group with severe pulmonary hypertension there was an inverse relation between pulmonary blood flow and mean pulmonary-artery pressure.

In this group of 57 cases the average pulmonary blood flow of 8.7 liters per min per m² was more than twice the normal flow. The systemic blood flow at rest was within the range of normal in 69 per cent of the patients in whom it was measured. Only five of the group had more than a minimal decrease in systemic flow, and all of these had pulmonary hypertension. No correlation was found between the

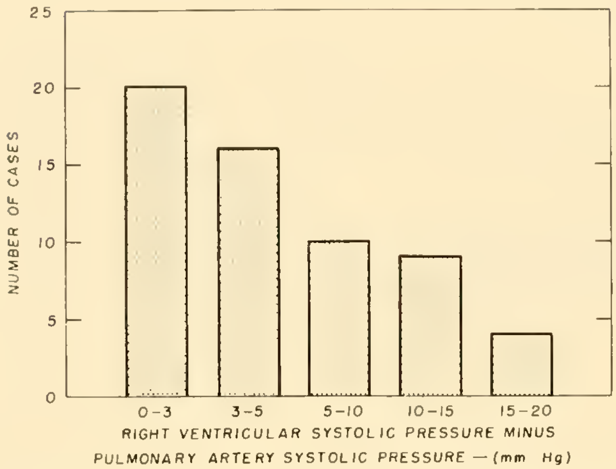

FIG. 33. Frequency distribution of magnitude of systolic pressure gradient across pulmonary valve in 59 cases of interatrial communication. Measurements were made only from records of pressures obtained as catheter tip was withdrawn across pulmonary valve and in absence of cardiac irregularities.

magnitude of the pulmonary and systemic blood flows in these patients. In patients with uncomplicated atrial septal defect the systemic blood flow remained within the range of normal despite the magnitude of pulmonary flow.

Because of the normal difference in oxygen saturation between blood from the superior vena cava and blood from the inferior vena cava, use of the saturation of superior vena caval blood as representative of mixed venous blood for the calculation of systemic blood flow will result in a systematically lower value for systemic blood flow. This may be the explanation for the report of Dexter (78) that the left ventricular output is usually reduced in patients with atrial septal defect.

Many patients with uncomplicated atrial septal defect have a lower systolic blood pressure in the pulmonary artery than in the right ventricle. Barratt-Boyes & Wood (19) have demonstrated that in the normal subject the gradient between the pulmonary artery and the right ventricle varies from 0 to 5 mm of mercury. The gradient associated with atrial septal defect, however, may be as high as 20 mm of mercury in patients in whom a normal pulmonary valve is demonstrated at operation (fig. 33).

The relative diameter of the pulmonary valve as compared to the size of the right ventricular cavity and the degree of dilatation of the pulmonary artery could affect the gradient. In patients with atrial septal defect the dilated right ventricle and pulmonary artery separated by a normal valve could produce a relative pulmonary stenosis. Weidman and associates (258) demonstrated a positive correlation between the pulmonary blood flow and the gradient. As the pulmonary blood flow increased, the gradient across the valve increased. Consequently, it is believed that the high pulmonary blood flow with the resulting dilatation of the right ventricle and pulmonary artery produces a "relative" stenosis at the pulmonary valve.

FACTORS DETERMINING DIRECTION OF SHUNTS. The reasons for the strongly predominant left-to-right shunt of blood in patients with atrial septal defect have been extensively studied. Dexter (78) found that in the presence of a small atrial septal defect, left atrial pressure was higher than that in the right atrium by usually not more than 3 mm of mercury, but when the opening was more than 2 cm^2 in cross-sectional area there was no pressure difference discernible. Although measurement of both right and left atrial pressures is difficult, a number of such studies have been carried out and, in general, are in agreement with those of Dexter. Cournand *et al.* (69) studied three subjects with atrial septal defects in whom left and right atrial pressures were recorded. In these subjects the amplitude of the pressure variations and the mean pressure in the left atrium were greater than those in the right. Little and co-workers (164) confirmed this in dogs with surgically created atrial septal defects in which the right and left atrial pressures were simultaneously recorded. They found in the dog that a left-to-right pressure gradient persisted during the entire cardiac cycle or for all but a short period before or during atrial systole. Shaffer and collaborators (220) plotted left atrial pressure against that in the right in seven cases of atrial septal defect and showed that fluctuations in the pressure gradient between the atria can occur during the cardiac cycle. Braunwald and colleagues (38) also found variations in the gradient between the right and left atria during portions of the cardiac cycle, particularly early in atrial systole and immediately after atrial systole. During these periods there may be a reversal in gradient with momentary shunting of blood from right to left. This venoarterial shunting is usually of insufficient quantity to cause demonstrable decreases in the oxygen saturation of peripheral arterial blood.

It may be assumed then that the pressure in the left atrium generally exceeds that in the right atrium. However, when there is a large atrial septal defect, the two atria can be considered to form a common pressure chamber for practical purposes and the actual pressure gradient between the right and left sides must be minimal.

In studies with dog atria, Little *et al.* (164) measured the volume-elasticity properties of the right and left atria. The amount of fluid needed to completely fill the atria without distending them was measured, and then measured amounts of additional fluid were added and the atrial pressure recorded. The right atrial system was found to have an average initial filling volume twice that of the left atrial system. The volume-elasticity curves plotted for the right and left atrial systems showed that for equal increments in volume the right atrial system was more distensible than the left. On the basis of these studies they concluded that the pressure gradient between the left and right atria is related to the different elastic properties (distensibility) of the atria. Cournand and associates (68) also attributed the pressure gradient to the smaller capacity and distensibility of the left atrium and pulmonary veins. Hickam (131), however, suggested that when the two atria communicate, that ventricle which normally operates under lower pressure more readily accepts blood and has a larger output. Since the filling pressure in the right ventricle is lower than in the left, it accepts the greater amount of blood, and the flow between the atria is left to right. Hull (136) stated that the larger tricuspid valve and the ease with which the right ventricle fills lower the pressure in the right atrium. Undoubtedly the distensibility characteristics of both atria and ventricles play a role in determining the pressure gradient between the atria. In patients with pulmonary hypertension the right ventricle becomes hypertrophied and may fail. In these cases the right ventricle becomes less distensible and the right atrial pressure may rise with failure. The right-to-left shunt may then become predominant.

The study of patients with atrial septal defect by means of indicator-dilution techniques has provided a great deal of information about the direction and magnitude of blood flow from the various pulmonary and systemic veins. Swan and co-workers (238) first demonstrated that blood from the right lung shunts preferentially across an atrial septal defect. This was done by injecting indicator into the right and left pulmonary arteries, with sampling of the resultant dye-blood mixture at a systemic artery. When indicator is injected into the right pulmonary artery the resulting dilution curve recorded from a systemic artery showed a smaller peak concentration and greater distortion of the disappearance slope than did the curve obtained following injection into the left pulmonary artery, as shown in figure 34. This anomalous drainage of relatively greater magnitude from the right lung appears

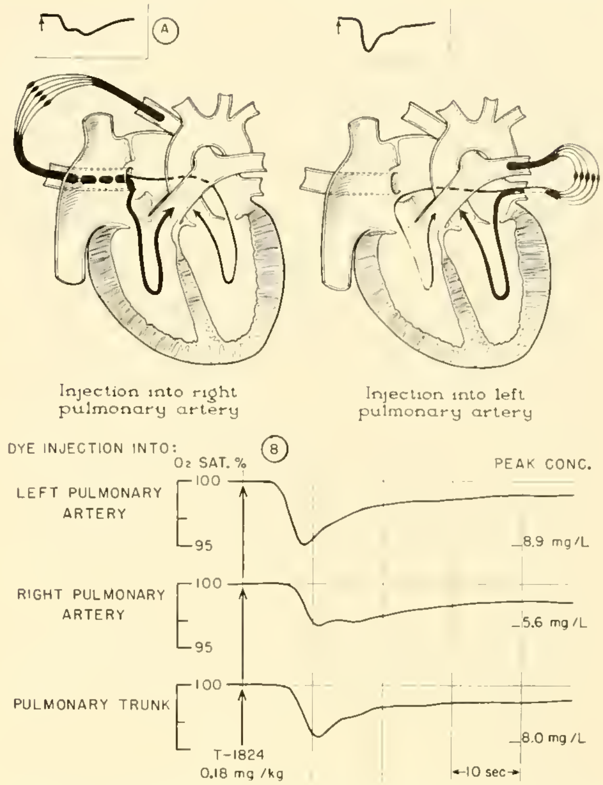

FIG. 34. Diagram of path taken by indicator dye after its injection into both right and left pulmonary arteries and resultant dilution curves recorded in systemic arterial system in a case of atrial septal defect. *a:* Diagrammatic representation of central circulation. Thick solid lines within diagram represent circulatory route taken by indicator after its injection. Relative thickness of these lines represents fraction of indicator passing to different locations from left atrium. Small insert above each diagram represents general contour of the systemic arterial dilution curve associated with each site of injection, with instant of injection indicated by arrow. Note proximity of right pulmonary veins to location of septal defect, evident from pathologic anatomic studies of this condition. *b:* Systemic arterial dilution curves recorded in a 16-year-old girl with atrial septal defect. T-1824 was injected at sites indicated to left of figure. Note smaller initial deflection and greater distortion of disappearance slope recorded following injection of dye into right pulmonary artery than into left, indicating that more of dye-blood mixture is shunted left to right from right pulmonary veins than from left. Distortion of curve recorded following injection into main pulmonary artery (*bottom panel*) is intermediate between those recorded after injection into right and left pulmonary arteries.

to be a consistent feature in the usual case of atrial septal defect and is most probably a consequence of the juxtaposition of the atrial septal defect to the orifices of the right pulmonary veins in the left atrium. Since the pulmonary veins from the left lung enter the left atrium farther from the atrial septum, less of the blood from these sites crosses the defect. Similar con-

clusions were reached by Silver *et al.* (222) in studies on dogs with artificially created atrial septal defects.

As already mentioned, there may be a reversal in gradient of left and right atrial pressures at various phases of the cardiac cycle, particularly early in atrial systole and immediately after atrial systole, with consequent momentary shunting of blood from right to left. This venoarterial shunting is usually of insufficient quantity to cause demonstrable decreases in oxygen saturation of peripheral arterial blood. It is possible, though, to demonstrate the right-to-left shunt with arterial dye-dilution techniques (236). Because of the anatomic relations of the wall of the right atrium and the cava, a natural channel for blood flow is created from the inferior vena cava to the foramen ovale (fig. 35). Consequently, that blood which shunts from right to left has been shown to be composed predominantly of blood from the inferior vena cava. Approximately 70 per cent of patients with atrial septal defect have right-to-left shunting from the inferior vena cava demonstrable by indicator-dilution curves. This preferential left-to-right shunting from the right pulmonary veins and right-to-left shunting from the inferior vena cava is evidence of incomplete mixing of blood in the two atria.

FIG. 35. Interior of heart viewed from inferior vena cava in patient with atrial septal defect. Dorsal wall of inferior vena cava is at top of picture. Note position of muscular ridge, derived from septum secundum which separates left from right atrium. A free communication exists between the atria; however, the direction of flow of a portion of the blood entering the right atrium from the inferior vena cava is directly into the left atrium, thus predisposing to right-to-left shunting of this portion of systemic venous return.

Further evidence for incomplete mixing of blood has been obtained from saturation data from the right side of the heart. Weidman and associates (258) demonstrated that samples of blood drawn from different sites in the right atrium and from the right ventricle and right atrium in rapid succession through an oximeter were different in many patients with atrial septal defects; however, this difference was not constant when rapidly successive samples drawn from the two sides of the tricuspid valve were repeated. He described two patients in whom oxygen saturation of blood withdrawn from the right ventricle was 6 to 8 per cent higher than that of samples from the right atrium; however at operation for correction of those defects the ventricular system was found to be intact in each.

In the unanesthetized patient, oxygen saturation of blood from the inferior vena cava averages 7 per cent higher than that in the superior vena cava (19); thus even in a subject with an intact septum the oxygen saturation of blood in the right atrium may be higher than that in the superior vena cava.

PULMONARY-ARTERY PRESSURE AND RESISTANCE. Despite the marked increase in pulmonary blood flow, the pressure in the pulmonary artery remains normal or only minimally elevated in many patients with atrial septal defect. The pulmonary vascular bed apparently responds to the increase in blood flow by an increase in the total cross-sectional area of the resistance vessels, with a fall in pulmonary vascular resistance. Auchincloss and colleagues (15), Rankin & Callies (197) and Bedell (24) have found that patients with intra-atrial and ventricular septal defects with normal pulmonary-artery pressures have an increased pulmonary diffusion capacity which they believe represents an increase in the size of the resting pulmonary capillary bed. Rankin & Callies (197) have measured the pulmonary capillary blood volume and found it to be increased in patients with intracardiac shunts and normal pressures in the pulmonary circulation.

Pulmonary hypertension associated with atrial septal defect differs from hypertension associated with ventricular septal defect or patent ductus arteriosus in that it is an acquired complication, rather than a necessary hemodynamic consequence of a communication between the pulmonary artery and the aorta or between the ventricles which is large enough to equalize pressures between the two circuits from birth. In the experience of Dexter (78) and Weidman and associates (258) it was uncommon to find severe pulmonary hypertension associated with atrial septal defect in patients less than 20 years of age. In certain patients, however, for reasons not understood, pul-

monary-artery pressure increases slowly or rapidly during early adult life, usually with persistence of an increased level of pulmonary blood flow. Development of hypertension in the pulmonary circuit, whether associated with increased pulmonary blood flow or not, is unlike the response of normal pulmonary vessels that are distended with but a small change in pressure, when the flow through them is increased. An increase in pulmonary hypertension in atrial septal defect with an increased pulmonary blood flow signifies an increase in pulmonary vascular resistance from values below the range of normal to values that equal or slightly exceed normal. Study of a relatively few patients seen over a period of 6 to 8 years suggests that once the level of pulmonary-artery pressure is significantly elevated, it may remain virtually the same, whereas the progression of organic change in the pulmonary vessels is manifested only by a steady decline in pulmonary blood flow. Why pulmonary hypertension develops in certain patients and not in others is uncertain. Histologic studies of the small pulmonary vessels of such patients have shown that once pulmonary hypertension is established a distinct muscular media forms in the arterioles, and the media of the muscular pulmonary arteries hypertrophies. The progression of histologic changes seems identical to that of the changes in pulmonary hypertension associated with ventricular septal defect or patent ductus arteriosus.

It has been suggested that pulmonary embolism may play a role in this phenomenon. Dexter (79), however, pointed out that pulmonary embolism is rare in the first two decades of life and begins to become apparent in the third decade. He was unable to detect any evidence that pulmonary embolism had occurred in patients with pulmonary vascular disease, and concluded that if this was a factor it must be rare.

Although, when normal, the vessels responsible for pulmonary resistance have relatively little smooth muscle as compared with similar vessels in the systemic circulation, there is evidence from the effects of hypoxia (83, 86, 96) and more recently from the effects of 5-hydroxytryptamine (203) that they are capable of constriction. That tone is present in the smooth muscle of the pulmonary vessels in some patients with atrial septal defects can be demonstrated by two different methods. First, a change from breathing air to breathing 99 per cent oxygen is accompanied in many of these patients by a fall in pulmonary vascular resistance, often by more than a third of the initial values (237). The method by which this occurs is unknown.

Second, acetylcholine chloride, a substance which when injected intra-arterially into systemic vessels causes local vasodilatation (85), has recently been used in the study of the pulmonary circulation. Its rapid destruction in the circulating blood offers the possibility that an injection can be made into the pulmonary artery in sufficient concentration to affect the pulmonary vessels without altering the hemodynamics on the left side of the heart or in the systemic circulation. Wood and collaborators (278) have used a single injection of this substance and have shown that tone is present in the resistance vessels of the lungs in some patients with mitral stenosis. Harris (128) found that rapid injections into the pulmonary artery of patients with pulmonary hypertension, some of whom had congenital heart disease, resulted in a transient fall of pressure in the pulmonary artery in slightly more than one third of the patients. Shepherd and associates (221) have administered acetylcholine chloride by continuous infusion into the pulmonary artery in patients with congenital heart disease. Figure 36 shows the effects of such an infusion in a patient with pulmonary hypertension and an atrial septal defect. During the infusion there occurred a marked decrease in systolic pressure of the right ventricle and an increase in oxygen saturation of the blood in the pul-

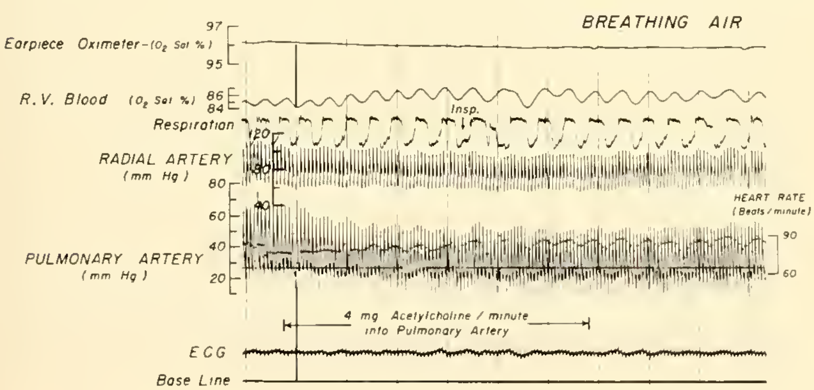

FIG. 36. Effects of continuous infusion of acetylcholine into pulmonary artery of 35-year-old woman with atrial septal defect and pulmonary hypertension. Note prompt fall in pulmonary-artery pressure associated with rise in oxygen saturation of right ventricular blood on administration of acetylcholine. Vertical time lines are at intervals of 10 sec and were 5 cm apart before photographic reduction of record.

monary artery. Shepherd *et al.* concluded that, in the absence of any change in systemic blood pressure, oxygen consumption or heart rate, acetylcholine had dilated the pulmonary vessels with a consequent decrease in resistance to pulmonary flow and an increase in the left-to-right shunt.

Whatever the cause or causes, pulmonary vascular disease, that is, obstruction to blood flow through the lungs, is a major although relatively uncommon complication of atrial septal defect. As a consequence of this obstruction of flow, pulmonary and right ventricular hypertension develop with a decrease in the left-to-right shunt and eventual progression to a predominant right-to-left shunt and deterioration of the cardiovascular status.

Partial or Total Anomalous Pulmonary Venous Connection

Partial anomalous pulmonary venous connection with or without coexisting atrial septal defect is usually hemodynamically similar to an uncomplicated atrial septal defect. Right ventricular output is high and little or no demonstrable venoarterial shunting occurs unless pulmonary hypertension develops in association with an atrial septal defect. The course of flow of blood from an anomalously connected pulmonary vein depends in part on its site of entrance to the right side of the heart. If the connection is near or into the superior vena cava, blood will flow preferentially to the tricuspid valve. If the connection is into the inferior vena cava and the atrial septal defect is in the usual position, there is a greater tendency for the anomalously drained blood to cross the defect into the left atrium because of the anatomic relation of the inferior vena cava to the foramen ovale.

TOTAL ANOMALOUS PULMONARY VENOUS CONNECTION. When all of the pulmonary veins are transposed to drain anomalously only into the right side of the heart, it is evident that the left side of the heart is bloodless unless there is a communication between it and the right side. In its simplest form this communication is a patent foramen ovale, although there may be a true atrial septal defect. It is evident on reviewing the prenatal circulation that the anomalous circulation associated with total pulmonary venous drainage causes no disturbance in the fetus, but in postnatal life a gross inefficiency in the mammalian-type circulation exists owing to the mixture of pulmonary and systemic venous blood that almost invariably occurs.

The optimal condition of the circulation with this

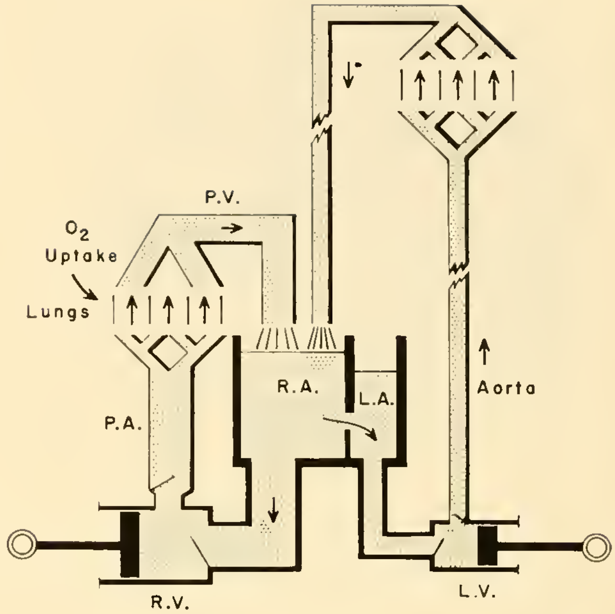

FIG. 37. Simplified diagram of circulation in total anomalous pulmonary venous connection to right atrium with high pulmonary blood flow. *R.A.*, *L.A.*, *R.V.*, and *L.V.* indicate right and left atria and ventricles, respectively, and *P.A.* and *P.V.* the pulmonary artery and veins. Note that all blood entering left side of heart must traverse atrial septal defect.

defect is represented diagrammatically in figure 37 (46). The unobstructed pulmonary veins empty into the right atrium instead of the left; the only way blood can enter the left side of the heart is through a defect in the atrial septum. From this diagram it can be seen that there is a high-pressure, normal-volume left-heart system, and a low-pressure, high-volume right-heart system. As long as there is no vascular obstruction in the lungs, the cardiac work is not excessive and, from the standpoint of cardiac-energy requirements, the situation is equivalent to that of an atrial septal defect with a large left-to-right shunt without significant pulmonary hypertension.

It is apparent that if the communication between the right and left atria were decreased below a critical level, the flow and volume of blood in the left side of the heart would be decreased. The major factor in determining the flow of blood through the right side of the heart would be the resistance offered to flow through the lungs.

Ranges of hemodynamic values. Cyanosis is not uniformly present in this condition at birth, although all infants are intermittently cyanotic. Later in life, cyanosis becomes more evident, especially during exercise. In a series of 10 cases reported by Swan and coworkers (241) the systemic arterial oxygen saturation

TABLE 7. *Average and Range of Hemodynamic Variables in 10 Cases of Total Anomalous Pulmonary Venous Connection Studied by Cardiac Catheterization*

	Age, years	Blood Flow, Liters/min/m²		Pulmonary-Artery Systolic Pressure, mm Hg	Systemic Arterial Oxygen Saturation, %
		Systemic	Pulmonary		
Avg.	19	3.7	7.8	66	85
Range	5/12–45	2.3–4.5	3.1–16.4	20–119	70–94

averaged 85 per cent, with a range from 70 to 94 per cent (table 7). However, 6 of these 10 patients studied were adults. In the patients with the more nearly normal systemic arterial oxygen saturation the pressures in the pulmonary artery were normal and these patients had the highest values for pulmonary flow.

The saturation of blood in the common venous pool (right atrium) might be expected to be the same as that in the pulmonary artery and the aorta, as pointed out in the precatheterization era by Taussig (247). Actually in this series of cases the oxygen saturations of pulmonary and systemic-artery blood were equal in four cases, whereas in the remaining cases the saturation of pulmonary-artery blood exceeded that of systemic blood by 1 to 7 per cent (fig. 38).

This difference indicates that complete mixing of blood has not occurred in the atrium and that a greater proportion of desaturated systemic venous blood passes to the systemic than to the pulmonary circulation. This situation is the result of a combination of circumstances. It has been well documented that inferior vena caval blood shunts preferentially across the interatrial communications located at the site of the foramen ovale; consequently superior vena caval blood under such circumstances passes preferentially into the tricuspid valve. If the pulmonary veins connect directly to, in juxtaposition to, or to a tributary of, the superior vena cava and if the atrial septal defect is in the usual location, then, owing to these flow patterns in the right atrium, a greater proportion of pulmonary-vein blood flows into the right ventricle than into the left ventricle via the interatrial communication. In the case of total anomalous connection to the inferior vena cava or its tributaries it would be expected that the oxygen saturation of systemic arterial blood would exceed that in the pulmonary artery. In general, however, there is a close similarity in systemic and pulmonary-artery blood oxygen saturation, the greatest difference in the oxygen saturation in this series being 7 per cent.

Factors that determine the arterial oxygen saturation. In all

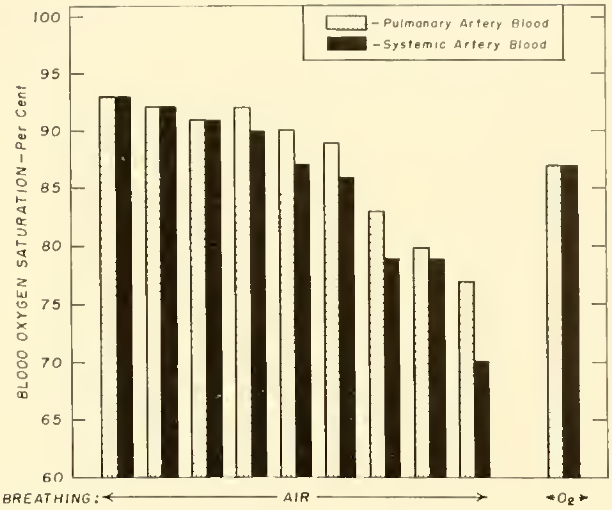

FIG. 38. Comparison of oxygen saturation of pulmonary and systemic-artery blood in 10 patients with total anomalous pulmonary venous connection. Patients 1 through 9 were studied while breathing air. Patient 10, 5 months old, was studied while breathing 100 per cent oxygen. In patients 1, 2, 3, and 10, saturation of systemic-artery blood equaled that of pulmonary-artery blood, but in the other patients oxygen saturation of pulmonary-artery blood exceeded systemic-artery value by 1 to 7% (see text for discussion). Patients 1 through 4 were not cyanotic while at rest.

types of this anomaly, all blood from both the pulmonary and the systemic circulation returns to the right atrium (fig. 37). If the pulmonary resistance is low there will be a very much greater flow of blood through the lung than through the systemic circuit. As a consequence, a great quantity of highly saturated blood from the lung returns to mix with a lesser quantity of desaturated systemic venous blood. Thus the oxygen saturation of systemic arterial blood remains high as long as the high pulmonary blood flow is maintained. As Burchell (46) has pointed out, the level of arterial blood saturation will be dependent, at any specific blood hemoglobin content and in the presence of healthy lungs, on only two factors: *1*) the amount of oxygen extracted by the tissues, and *2*) the pulmonary blood flow. This may be expressed as follows:

$$\text{Ca} = \frac{\text{Qp Cpv} - \dot{V}o_2}{\text{Qp}} = \text{Cpv} - \frac{\dot{V}o_2}{\text{Qp}}$$

where Ca and Cpv equal the oxygen content of systemic arterial and pulmonary venous blood (ml/liter), respectively, Qp equals pulmonary blood flow (liters/min) and $\dot{V}o_2$ equals the oxygen consumption (ml/min).

The assumptions are that there are normal oxygena-

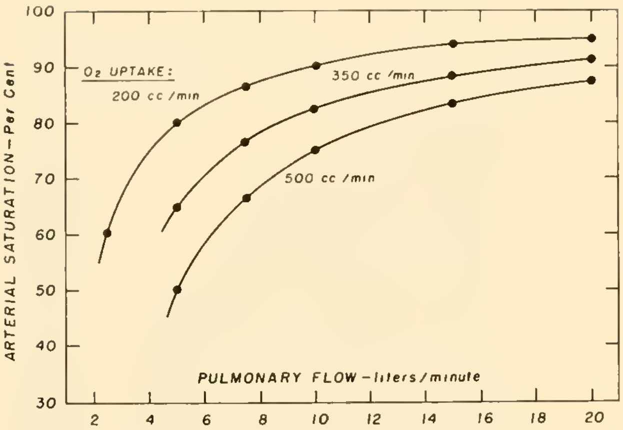

FIG. 39. Calculated relationship between pulmonary blood flow and arterial oxygen saturation in total anomalous pulmonary venous connection to right atrium at assumed values of 200, 350, and 500 ml/min for oxygen uptake. Assumptions made are discussed in text. Oxygen capacity of blood = 200 ml/liter.

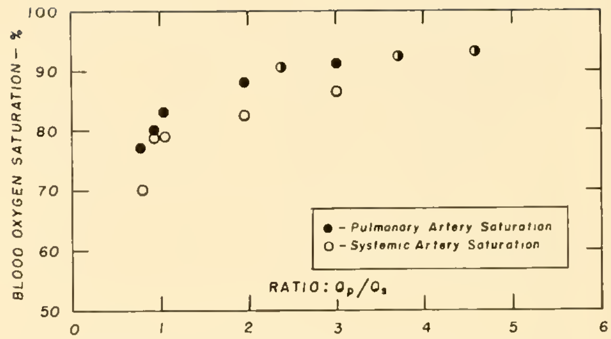

FIG. 40. Relation of systemic and pulmonary-artery blood oxygen saturations to the ratio of pulmonary flow (Qp) to systemic flow (Qs) in eight patients with total anomalous pulmonary venous connection. Two values are given for each patient (*open and solid circles*, respectively). When values coincide, case is represented by a circle with one segment closed. Note positive correlation between magnitude of pulmonary blood flow and level of blood oxygen saturation.

tion of the blood in the lungs and complete mixing of blood in the right atrium. As has been shown, the latter assumption is not strictly correct; however, in general it is accurate enough to allow one a general understanding. If this assumption is overlooked, one may calculate the arterial oxygen saturation for any hemoglobin content of the blood, metabolic rate and pulmonary flow (fig. 39). When high pulmonary flows are present, the arterial saturations will be high, approaching normal. The upper curve shows calculations based on an arbitrary resting oxygen uptake of 200 ml per min. The lower curve shows the predicted arterial oxygen saturation when the oxygen uptake is 500 ml per min, such as might occur with mild exercise.

The relation between pulmonary blood flow and systemic arterial oxygen saturation in eight patients with total anomalous pulmonary venous connection is shown in figure 40. It is apparent that these data fit well with the theoretic curves. In this series of cases a reduced pulmonary flow was always associated with increased pressure in the pulmonary artery, and from this it may be deduced that a reduction in systemic arterial oxygen saturation is associated with an increase in pulmonary vascular resistance.

When any condition, such as exercise, increases the metabolic rate the arterial oxygen saturation would be expected to decrease also, and this has been found to be so. Burchell (46) reported that in four patients with high pulmonary flows the systemic arterial oxygen saturation decreased from rest to exercise from 90 to 86, 91 to 86, 92 to 91, and 92 to 84 per cent, respectively. In one patient with low pulmonary flow and a saturation of 76 per cent at rest, the saturation dropped to 40 per cent with exercise.

Persistent Common Atrioventricular Canal

There is a wide possibility for hemodynamic alterations in patients with persistent common atrioventricular canal, depending on the degree of the anatomic malformation that is present in an individual case. Many patients with this defect die in early infancy and in this respect are similar clinically and probably hemodynamically to patients with large ventricular septal defects. On the other hand, patients may live to adult life and be relatively asymptomatic. This situation would be more like that seen in patients with atrial septal defect.

When the communication is mainly between the atria one would expect to find relatively normal pressures in the right side of the heart and a high pulmonary blood flow. If the communication is principally between the two ventricles, pressures in the right ventricle and pulmonary artery would be elevated, and if the pulmonary vascular resistance were not severely increased, the pulmonary blood flow would be increased.

HEMODYNAMIC FINDINGS. Seventeen cases of proved persistent common atrioventricular canal were studied by Wakai *et al.* (254). In this series were 7 adults ranging in age from 21 to 28 years and 10 children whose ages ranged from 4 months to 13 years. The systemic blood flow was normal in all cases when ex-

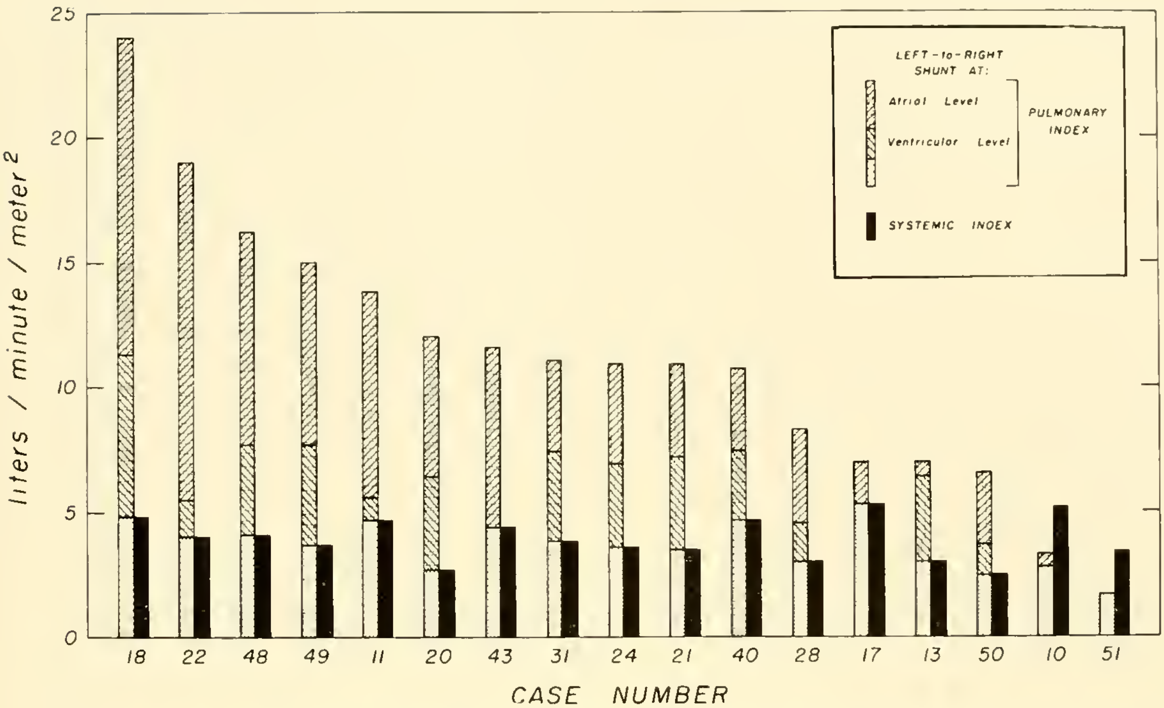

FIG. 41. Magnitude of pulmonary and systemic blood flows in 17 cases of persistent common atrioventricular canal. Note that cardiac index is within range of normal in spite of large left-to-right shunts and that the left-to-right shunt usually occurs at both atrial and ventricular levels.

pressed in terms of body surface area. The pulmonary flow, also expressed in terms of body surface area, exceeded the systemic flow in all but two cases (fig. 41). The increased pulmonary blood flows were due to large left-to-right shunts occurring at both atrial and ventricular levels, but in most cases chiefly at atrial level. Only in one case was there a predominant shunt at ventricular level.

The relationship between the ratio of pulmonary to systemic vascular resistance and the net intracardiac shunt in these 17 cases is shown in figure 42. In the presence of a normal total pulmonary resistance and total systemic resistance, large left-to-right shunts predominate. As the total pulmonary resistance exceeds the total systemic resistance, net right-to-left shunts occur with consequent desaturation of the systemic arterial blood.

The presence of large clefts in the common atrioventricular valves could preclude complete closure of the valve leaflets during ventricular systole and produce mitral and tricuspid regurgitation. The atrial and pulmonary arterial pressure pulses in this series of cases, however, showed no evidence of regurgitation.

In patients with persistent common atrioventricular canal there is less evidence of the preferential shunting of blood from the right lung than is usually seen in patients with atrial septal defect in the region of the fossa ovalis.

In persistent common atrioventricular canal, not only are the right pulmonary veins located at a greater distance from the site of the interatrial defect than in the usual type of atrial septal defect, but a proportion of the left-to-right shunt occurs at ventricular level. These factors combine to permit mixing of the streams of blood from each lung to be more nearly complete before shunting occurs than in the usual case of atrial septal defect.

Septal Defects With Valvular Stenosis

The hemodynamic alterations occurring with isolated septal defects and isolated abnormalities of the heart valves have been discussed. Two or even more of these abnormalities may occur in the same patient, and some are combined so frequently that they are considered a single entity, such as tetralogy of Fallot. This is the name used to designate the combination of defects most commonly responsible for cyanotic congenital heart disease, namely pulmonary stenosis and ventricular septal defect plus an overriding aorta which is frequently associated with a right-sided aortic arch.

Hemodynamic alterations may be more severe or

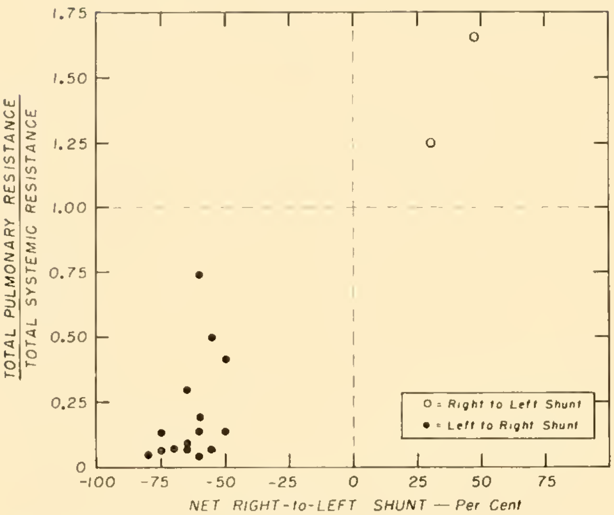

FIG. 42. Relation of ratio between calculated pulmonary and systemic vascular resistances to net intracardiac shunt in 17 patients with persistent common atrioventricular canal. Note that, as pulmonary resistance increases to levels in excess of systemic vascular resistance, left-to-right shunt decreases and is eventually exceeded by shunt in right-to-left direction.

less severe in such cases, depending on the severity of the defects, and vary widely in nature from acyanotic patients with a high pulmonary blood flow to severely cyanotic patients with a very low pulmonary flow, depending on the relative severity of the pulmonary stenosis and the size of the ventricular septal defect.

AORTIC PULMONARY DEFECT WITH VALVULAR STENOSIS. *With aortic stenosis.* Communications between the aorta and the pulmonary artery associated with aortic stenosis produce hemodynamic alterations similar to those of either of the defects alone; however, the increase in left ventricular work is considerably greater than it would be if either of these defects existed as a single lesion. When blood shunts in the left-to-right direction through the aortic-pulmonary communication, this shunted blood plus blood returning from the systemic veins traverses the pulmonary circuit, enters the left side of the heart, and is pumped by the left ventricle again into the systemic circulation. The blood flow through the left ventricle in this situation may be greater than two times the normal systemic blood flow. Since the systolic pressure generated in the left ventricle to force blood through a stenotic valve is directly related to the amount of blood flow through this valve, it is apparent that the left ventricular pressure required to drive this high flow of blood through a stenotic valve will be markedly increased. Thus the presence of aortic stenosis in patients with aortic-pulmonary communication will predispose to left-heart failure and hence to more rapid development of elevated left atrial, pulmonary-venous and pulmonary-artery pressures than is usual when these defects occur as single lesions.

Aortic-pulmonary defect with mitral stenosis. Mitral stenosis may be associated with a coexisting patent ductus arteriosus or other forms of aortic-pulmonary communication. The flow of blood through the defect is usually in the left-to-right direction. The incidence of pulmonary hypertension and increased pulmonary vascular resistance is greater because of the presence of a combination of predisposing factors. These are an elevated left atrial and pulmonary venous pressure owing to the mitral stenosis and an increased pulmonary-artery blood flow or pressure, or both, owing to the aortic-pulmonary communication. The pulmonary vascular resistance may be increased to the point that there is a reversal of the shunt, with blood flowing through the defect in the right-to-left direction. In these cases the aortic-pulmonary communication may act as an escape mechanism or "safety valve" to the high pressure created in the pulmonary vascular bed, thus preventing "overloading" of the right ventricle.

Aortic-pulmonary defect with pulmonary or tricuspid stenosis. Since the volume of blood flowing through the pulmonary and tricuspid valves is not affected directly by the presence of an aortic-pulmonary communication, no unusual multiplication of the hemodynamic effects caused by the single defects would be expected from the coexistence of either pulmonary or tricuspid stenosis with an aortic-pulmonary communication. In general, the hemodynamic alterations produced by the coexistence of these defects are the result of the simple additive effects caused by the defects when present as isolated lesions.

VENTRICULAR SEPTAL DEFECT WITH VALVULAR STENOSIS. *With aortic stenosis.* The hemodynamic alterations resulting from a ventricular septal defect in association with aortic stenosis are more severe than those caused by an equivalent-sized aortic-pulmonary communication and degree of aortic stenosis. This is due to the fact that the high pressure in the left ventricle required to force blood through the stenotic valve also acts to increase the magnitude of the left-to-right shunt through the ventricular septal defect. Both effects increase left ventricular work and contribute to the degree of pulmonary hypertension that will invariably exist if the ventricular septal defect is large.

In this condition it is apparent that the systolic blood pressure in the pulmonary artery may be sig-

nificantly higher than that in the systemic arteries, especially if there is a large ventricular septal defect with equalization of pressures between the ventricles. Blood that is shunted into the right ventricle via the ventricular septal defect will return to the left ventricle via the pulmonary veins in addition to that blood returning from the systemic veins and must either be ejected into the aorta or be shunted again into the right ventricle. The magnitude of the left-to-right shunt will depend on the relative resistance offered to the outflow of blood from the right and left ventricles. The presence of the ventricular septal defect may prevent "pressure overloading" of the left ventricle but in this situation only at the expense of an increased volume load on the pulmonary circulation as well as on the left ventricle, since the blood "escaping" from the left ventricle via the septal defect must return again to the left ventricle via the pulmonary circulation. In any event a high enough systolic pressure must be generated in the left ventricle to maintain systemic blood flow through the stenotic aortic valve. These two defects are sometimes associated with a patent ductus arteriosus plus a coarctation of the aorta upstream to the aortic end of the ductus. In this situation there is usually a very high pulmonary flow and the major blood supply to the lower part of the body is via the ductus, whereas that to the upper part is via the stenotic aortic valve. On occasion, patients with these four defects maintain a surprising degree of cardiovascular compensation into early adult life.

Ventricular septal defect with mitral stenosis. Mitral stenosis associated with a ventricular septal defect will, as in the case of mitral stenosis with an aortic-pulmonary communication, lead to a higher incidence of pulmonary hypertension and increased pulmonary vascular resistance. The predisposing factors leading to this are elevated left atrial and pulmonary venous pressures owing to the mitral stenosis, and an increased pulmonary blood flow or pressure or both owing to the ventricular septal defect. The resulting increased pulmonary vascular resistance and pulmonary hypertension will lead to an earlier development of right-heart failure than if either condition occurred alone.

Ventricular septal defect with pulmonary stenosis. The congenital anomalies, ventricular septal defect with pulmonary stenosis and the well-known complex, tetralogy of Fallot, will be discussed together, since from the hemodynamic viewpoint this latter complex is in essence a ventricular septal defect plus pulmonary stenosis. In general, the term "ventricular septal defect with pulmonary stenosis" has been used in those

TABLE 8. *Average and Range of Hemodynamic Data in 15 Patients With Ventricular Septal Defect and Pulmonary Stenosis*

	Age, years	Pressure, mm Hg		Blood Flow, Liters/min/m²		Arterial Oxygen Saturation, %
		P.A.	R.V. (syst.)	Pulmonary	Systemic	
Avg.	12	26/11	95	7.3	4.4	95
Range	5–26	13/4–50/15	64–121	3.7–20.1	2.3–12.7	89–99

patients without readily apparent cyanosis, whereas tetralogy of Fallot includes those patients who are cyanotic at rest. As in patients with ventricular septal defect, the relative volumes of blood flowing into the systemic or pulmonary circulation depend on the size of the ventricular septal defect and the relative resistance to the outflow of blood from the right and left ventricles.

In ventricular septal defect with pulmonary stenosis the resistance to the flow of blood into the pulmonary circulation is due in large part to the resistance to blood flow through the region of subvalvular or valvular stenosis upstream to the pulmonary circulation. The "overriding" aorta that is classically found in tetralogy of Fallot plays no readily demonstrable role in the direction and magnitude of the shunts. From the hemodynamic standpoint, ventricular septal defect with pulmonary stenosis and tetralogy of Fallot merely represent two stages or degrees of the same anatomic abnormalities.

Hemodynamic findings. The average and range of hemodynamic values are shown in table 8 for 15 patients with "ventricular septal defect with pulmonary stenosis" studied by Brotmacher & Campbell (44), and in table 9 for 36 patients with tetralogy of Fallot studied by Bing and co-workers (29). As would be expected, there is a wide range of values for pulmonary blood flows and pressures in the right side of the heart, as well as for the oxygen saturation of systemic arterial blood. In the series of cases studied by Brotmacher and Campbell, the average value for pulmonary blood flow was nearly double the average value for systemic blood flow, whereas the average value of 95 per cent for arterial oxygen saturation was within the range of normal. In the series studied by Bing *et al.*, however, the average pulmonary blood flow was markedly decreased, being only 1.3 liters per min per m² of body surface area, and the value for systemic arterial oxygen saturation averaged 72 per cent. Bing and associates have shown that in some of their cases the pulmonary capillary blood flow exceeded the pulmonary-artery

TABLE 9. *Average and Range of Hemodynamic Data in 36 Patients With Tetralogy of Fallot*

	Age, Years	Right Ventricular Systolic Pressure, mm Hg	Blood Flow, Liters/min/m²		Arterial Oxygen Saturation, %
			Pulmonary	Systemic	
Avg.	15	107*	1.3	3.6	72
Range	5–26	58–140	0.7–2.2	0.9–11.4	55–91

* Average of 17 patients.

flow (29), indicating that when the pulmonary stenosis is very severe the major pathway for blood flow to the lungs may be via collateral vascular channels (bronchial arteries). This was found to be particularly true in the older age groups studied.

The systolic gradient between the right ventricle and the pulmonary artery in Brotmacher & Campbell's series (44) was between 35 and 52 mm of mercury in five and between 60 and 99 mm in the remainder of the patients. The systolic right ventricular pressure was elevated in all cases, and in all but five instances it was within 20 mm of the peripheral systemic arterial systolic pressure.

Pulmonary and systemic blood flow. In patients with more severe degrees of pulmonary stenosis a right-to-left shunt is present and frequently exceeds 1 liter per min per m². A left-to-right shunt may also exist but is usually of a lesser order. The determining factor in the direction and magnitude of the shunt is the relative resistances to blood flow through the stenotic pulmonary valve or outflow tract and flow through the systemic vascular bed via the unobstructed aorta. Hemodynamically these patients are similar to patients with a large ventricular septal defect without pulmonary stenosis but with severely elevated pulmonary vascular resistance. In one instance the resistance to pulmonary blood flow is due to the stenosis, and in the other to the decreased caliber of the resistance vessels in the pulmonary vascular bed.

In tetralogy of Fallot, in addition to pulmonary stenosis and ventricular septal defect, there is overriding of the aorta which in the past has been considered an important causative factor in the cyanosis characteristic of this condition. Brotmacher & Campbell (44) have pointed out that varying degrees of overriding occur and that the degree of overriding may be secondary to the right-to-left shunt rather than primary. That overriding of the aorta may be present without cyanosis is demonstrated by many patients with tetralogy of Fallot who have had a successful valvotomy or infundibular resection and exhibit no or only minimal cyanosis following the operation. Campbell and co-workers (51) discussed some of those patients who had been recatheterized after operation and were acyanotic with an arterial oxygen saturation between 92 and 98 per cent, although it had averaged as low as 81 per cent prior to operation. Wood (276) also has described several cases of this type. On the basis of these findings, Brotmacher & Campbell (43) concluded that the presence or absence of a right-to-left shunt depends primarily on the relative resistances to blood flow in the pulmonary and systemic circuits and not on the degree of overriding of the aorta. Present-day investigators are in general agreement that the relationship of the aortic root to the ventricular septal defect plays no significant role in the altered hemodynamics (47).

Collateral pulmonary blood flow. Pulmonary arterial blood flow is greatly reduced in many patients with severe pulmonary stenosis, and in these instances, owing to the small amount of blood that is oxygenated and to the right-to-left shunt that is present, systemic arterial blood may be severely desaturated. This pulmonary blood flow may be augmented by collateral flow to the lungs via large bronchial and other accessory arteries, which are usually noted during operation in these cases. Bing *et al.* (29) calculated the pulmonary capillary blood flow, utilizing the Fick principle, by determining the output of carbon dioxide and indirectly determining the concentrations of carbon dioxide entering and leaving the pulmonary capillary bed. Although these results can be accepted as only approximations, he found that in most of the younger individuals the values for pulmonary capillary flow agreed closely with those determined for pulmonary-artery flow. In older individuals, however, pulmonary capillary flow was found to exceed pulmonary-artery flow. In those patients in whom calculations indicated the presence of extensive collateral circulation to the lungs, large bronchial arteries were found. Bing and co-workers found that this collateral blood flow frequently exceeded 1 liter per min per m². They pointed out that the collateral circulation to the lungs represents an important factor in the physiologic adjustments of these individuals to their abnormally low pulmonary-artery flow. By increasing the pulmonary blood flow the per cent of fully oxygenated blood entering the systemic circulation is increased, thus increasing the systemic arterial oxygen saturation.

Ventricular septal defect with tricuspid stenosis. Stenosis of the tricuspid valve would have no direct hemodynamic effect on the hemodynamic alterations due to a coexisting ventricular septal defect. If the tricuspid

stenosis were severe, inflow of blood to the right ventricle would be impeded and significant alterations in the systemic circulation would result. The direction and magnitude of the shunt due to the ventricular septal defect would, however, be relatively independent of these systemic effects.

ATRIAL SEPTAL DEFECT WITH VALVULAR STENOSIS. *With aortic stenosis.* This combination of defects occurs infrequently. The hemodynamic alterations produced by the atrial septal defect are not changed by the presence of aortic stenosis unless left-heart failure supervenes. When this occurs, the left ventricular diastolic pressure increases, resulting in an increase in left atrial pressure. This then results in an increase in the left-to-right shunt through the atrial septal defect. Left ventricular filling sufficient to maintain the systemic cardiac output must, however, be maintained. As a consequence, an increase in both right and left atrial pressure occurs and pulmonary hypertension also frequently develops. The mechanism of this sequence of events has not been fully elucidated

Atrial septal defect with mitral stenosis. Atrial septal defect associated with mitral stenosis has been termed the "Lutembacher syndrome." If the stenosis is congenital, blood flow into the left ventricle is impeded during fetal life so that the left atrial pressure is increased and, as a consequence, an increased proportion of blood flows into the right ventricle and the pulmonary artery and thence enters the aorta via the ductus arteriosus. At birth the right side of the heart and the pulmonary artery are large and the pressure in the left atrium usually exceeds that in the right atrium so that the shunt is in the left-to-right direction and tends to be large. Left atrial pressure must be elevated in order to maintain systemic blood flow through the stenotic mitral valve. Pulmonary hypertension is a common complication of this combination of defects.

If stenosis of the mitral valve develops later in life as a result of rheumatic endocarditis, the left-to-right shunt is increased as a result of the increased resistance to flow through the mitral valve and the concomitant elevation of left atrial pressure which must be sustained at a sufficiently high level to maintain systemic flow. The incidence of pulmonary hypertension is much higher than in uncomplicated atrial septal defect.

Atrial septal defect with pulmonary stenosis. This combination of defects is, next to the tetralogy of Fallot, the most common cause of cyanotic congenital heart disease. In patients who have pulmonary stenosis and atrial septal defect, blood may be shunted through the defect in either direction. When, as a result of severe pulmonary stenosis, the mean pressure in the right atrium increases to levels in excess of that in the left atrium, the shunt becomes partially or completely right to left. When the shunt is completely or predominantly right to left and is large, the condition clinically may resemble tetralogy of Fallot. When right atrial pressure exceeds that in the left atrium, a right-to-left shunt will occur through a valve-competent foramen ovale. Under such circumstances, if there is no demonstrable left-to-right shunt, it is impossible to be certain from hemodynamic evidence whether the pulmonary stenosis is associated with a true defect in the atrial septum or with the valve-competent type of patent foramen ovale, which is found in 25 per cent of normal individuals.

Average and range of hemodynamic variables. As would be expected, the amount of blood flow through the pulmonary circulation is extremely variable, depending on the severity of the pulmonary stenosis and the competence of the right ventricular musculature. The average and range of hemodynamic variables in 15 patients with pulmonary stenosis and atrial septal defects are shown in table 10 (42, 50). Although systolic pressures in the right ventricle and systemic artery are usually similar when patients with pulmonary stenosis have a ventricular septal defect, in atrial septal defect with pulmonary stenosis the right ventricular systolic pressure may be less than, equal to, or greater than the systemic arterial pressure (42, 50). These pressure relationships are better illustrated in table 11, which shows the differences in systolic pressures for the two groups. In five patients with pulmonary stenosis and ventricular septal defect the differences in systemic systolic and right ventricular systolic pressure are small, averaging 4 mm of mercury, with a range from -4 to 17 mm. However, in five patients with atrial septal defect, these differences were frequently quite large, averaging 44 mm of mercury, with a range of -25 to 75 mm.

Dynamics of pulmonary-artery obstruction. It is of interest that in this condition elevations in right ventricular pressure to levels in excess of systemic arterial systolic pressure may be tolerated for many years without evidence of failure of the right ventricle. The possibility that the atrial septal defect acts as a "safety valve," permitting some of the blood entering the right side of the heart to be shunted into the left atrium, has been considered.

Brecher & Opdyke (40) carried out acute studies in open-chest dogs in which the pulmonary artery could be partially occluded. They found that progressive occlusion of the pulmonary artery in dogs with intact

TABLE 10. *Average and Range of Hemodynamic Values in 15 Patients With Atrial Septal Defect and Pulmonary Stenosis*

	Age, Years	Pressure, mm Hg		Blood Flow, Liter/min		Systemic Arterial Oxygen Saturation, %
		Pulmonary artery	Right ventricle, systolic	Systemic	Pulmonary	
Avg.	13	18/8	131	4.8	4.7	83
Range	3–23	6/4–31/19	48–205	2.9–8.2	1.4–9.2	63–98

TABLE 11. *Comparison of Differences in Right Ventricular, Pulmonary and Systemic Arterial Systolic Pressures in Patients With Pulmonary Stenosis and Ventricular or Atrial Septal Defects*

Type of Defect		Difference, mm Hg	
		(S.A.-R.V.)*	(R.V.-P.A.)
Ventricular (5 patients)	Avg.	4	67
	Range	−4 to 17	44 to 78
Atrial (5 patients)	Avg.	44	47
	Range	−25 to 75	22 to 122

* S.A. = systemic artery; R.V. = right ventricle; P.A. = pulmonary artery.

septa reduced left and increased right atrial pressures. With marked stenosis, right atrial pressures exceeded left atrial pressures at all points in the cardiac cycle. They were, however, able to prevent right-heart failure by creation of an interatrial septal defect.

Amorim and co-workers (9) have studied the effect of atrial septal defects on hemodynamic alterations caused by acute partial obstruction of the pulmonary artery in dogs. These studies were carried out in closed-chest dogs in which a balloon catheter was advanced to the pulmonary artery and inflated to produce various degrees of occlusion.

In these dogs with chronic atrial septal defects, graded obstruction of the main pulmonary artery associated with right ventricular systolic pressure levels of more than 80 mm of mercury was produced without evidence of right-heart failure. A considerable decrease in the magnitude of the left-to-right shunts and an increase in the right-to-left shunts occurred which in some cases exceeded 50 per cent of the systemic blood flow. These changes were associated with only minor changes in the filling pressure of the right ventricle and no systematic changes in the systemic arterial pressure. There was no evidence for significant tricuspid regurgitation under these circumstances.

These findings contrasted with similar studies in dogs with intact cardiac septa in which obstruction of the pulmonary artery, so as to cause an increase in right ventricular systolic pressure to more than 60 mm of mercury, was associated with marked elevation of mean right atrial pressure and a striking decrease in cardiac output and in systemic arterial pressure associated with a significant degree of tricuspid regurgitation.

It appears that atrial septal defect provides a considerable increase in resistance to the hemodynamic effects associated with right ventricular hypertension caused by acute partial obstruction of the pulmonary artery. The defect in the atrial septum is in effect a "safety valve" allowing blood to shunt in the right-to-left direction, thus preventing overloading of the right ventricle.

It has also been pointed out that an increase in right atrial pressure associated with a decrease in systemic pressure and the consequent decrease in the pressure gradient across the coronary artery-coronary sinus system may decrease coronary flow. An atrial septal defect allows the blood to shunt into the left atrium and hence into the systemic circulation, thus maintaining the systemic pressure as well as preventing a marked increase in right atrial pressure. Thus the pressure gradient through the coronary vessels would be maintained in such animals in spite of a severe increase in resistance to right ventricular outflow (9).

Although it does appear that a right-to-left shunt via an atrial septal defect is protective in an acute increase in resistance to right ventricular outflow, it should be recognized that the resulting systemic arterial hypoxemia is in itself deleterious.

Atrial septal defect with tricuspid stenosis. Stenosis of the tricuspid valve increases resistance to flow of blood into the right ventricle so that an increase in right atrial pressure occurs. The left-to-right shunt through the atrial septal defect is decreased or reversed depending on the severity of the stenosis. Pulmonary blood flow never attains the high levels encountered in uncomplicated atrial septal defects and, if the tricuspid stenosis is severe, pulmonary blood flow may be decreased to less than systemic flow.

Patients who develop tricuspid stenosis as a result of rheumatic endocarditis may also develop cyanosis as a result of the occurrence of a right-to-left shunt via a valve-competent foramen ovale, present in 25 per cent of the normal population.

EBSTEIN'S MALFORMATION. The hemodynamic alterations occurring in Ebstein's malformation (87) may be considered the result of obstruction to the flow of

blood at right ventricular level. This is principally due to the reduction in size of the effective right ventricle resulting from malposition of the septal and posterior cusps of the tricuspid valve. As a result there is a decrease in the amount of blood the right ventricle can accept during diastole. In addition, tricuspid regurgitation may be present, further interfering with forward flow of blood through the right ventricle (151).

In three-fourths of the cases either the foramen ovale is patent or the fossa of the valve is fenestrated. Since the defective right ventricle cannot handle the returning blood, a large proportion is shunted through the foramen ovale into the left atrium and thence into the systemic circulation.

Keith and co-workers (147) found that in 17 cases reported in the literature the systemic arterial oxygen saturation varied from 64 to 97 per cent. Three-fourths of these patients had evidence of cyanosis at some time. Four who were exercised showed a decrease in arterial oxygen saturation. These findings are similar to those reported previously by Kilby and associates (151).

Right ventricular- and pulmonary-artery pressures are normal; the right atrial mean pressure may or may not be elevated. Usually there is a prominent A wave in the right atrial pressure-pulse tracing which is considered to result from impedance to normal emptying of the right atrium due to the "obstruction" to flow into the right ventricle (147). Right atrial pressure-pulse tracings with prominent V waves, presumably due to tricuspid regurgitation, have been shown by Gøtzsche & Falholt (121) and by Kjellberg and collaborators (153).

Continuous pressure readings obtained in a 26-year-old man during withdrawal of a catheter from the pulmonary-artery wedge position to the right atrium is shown in figure 43 (282). The right atrial pressure was elevated and showed an increased pulsation. The pulmonary-artery wedge pressure, however, was normal and lower than the right atrial pressure. There was no significant change in pressure or contour when the catheter passed the region of the tricuspid valve from the right ventricle to the right atrium as judged roentgenoscopically. The oxygen saturation of systemic arterial blood varied from 88 to 91 per cent in this patient and there was no evidence of arterialization from blood samples withdrawn from the right side of the heart.

VALVULAR ATRESIAS. Atresia of one of the valves of the heart is associated with serious hemodynamic disturbances that frequently permit survival only into early infancy. Such a defect is nearly always part of a complex anomaly, since communications between the right and left sides of the heart are necessary for survival. Since blood from the right and left sides of the heart becomes mixed, oxygen desaturation of systemic arterial blood must always be present.

Aortic atresia. In this condition the normal outlet from the left side of the heart is closed and the blood entering this side is shunted to the right, usually through a patent foramen ovale. The right atrium and right ventricle thus become, in essence, a common atrium and a common ventricle, respectively. The systemic circulation is supplied through an aortic-pulmonary communication, usually a patent ductus arteriosus. As would be expected, survival beyond early infancy is rare.

Mitral atresia. The hemodynamic alterations produced by mitral atresia are similar to those of aortic atresia. Blood entering the left atrium via the pulmonary veins is shunted to the right atrium. In this instance the systemic circulation is supplied by either a ventricular septal defect or an aortic-pulmonary communication such as a patent ductus. The prognosis as to survival is similar to that for aortic atresia.

Pulmonary atresia. Atresia of the pulmonary valve may be associated with a ventricular septal defect or rarely an interatrial communication. Survival beyond early infancy is uncommon. Usually, there is an associated patent ductus arteriosus. Systemic venous blood enters the left atrium or left ventricle via an interatrial or interventricular communication and the total pulmonary and systemic blood flow enters the systemic circulation. An aortic-pulmonary communication and a bronchial-artery collateral circulation are the only means of blood flow to the pulmonary circuit. Oxygen saturation of the systemic arterial blood is decreased and, if the ductus arteriosus is closed, may be extremely low.

Tricuspid atresia. Although there are numerous anatomic variations associated with tricuspid atresia, the intracardiac circulation is similar in all. Blood entering the right atrium from systemic veins passes into the left atrium. The left ventricle then becomes the propelling chamber maintaining, directly or indirectly, both pulmonary and systemic circulations. The right ventricle is usually diminutive, there frequently being only a small channel to the pulmonary artery. The degree of arterial hypoxemia is inversely related to the pulmonary blood flow. When a severe obstruction to pulmonary flow is present the degree of cyanosis is usually severe.

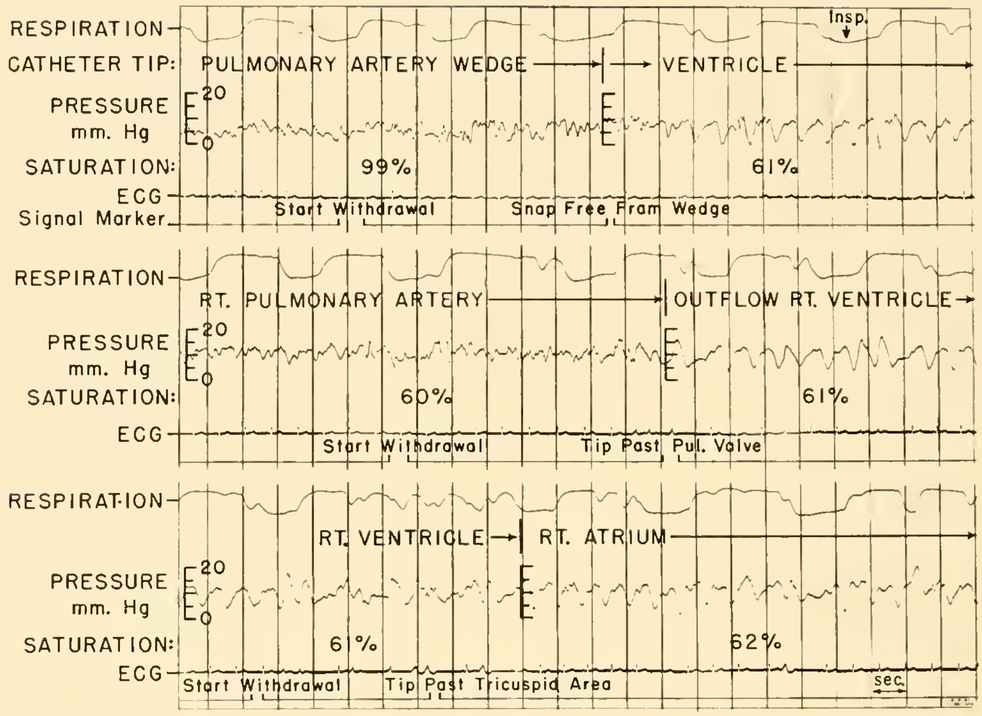

FIG. 43. Photokymographic record obtained during cardiac catheterization showing pressure relationships and other physiologic variables in a 30-year-old man who had Ebstein's malformation of tricuspid valve with severe regurgitation (functional absence) of this valve and a patent foramen ovale. *Top panel*: Withdrawal of catheter tip was begun (at signal mark) from pulmonary-artery wedge position where blood that was 99% saturated had been obtained. Catheter tip suddenly snapped free from wedge position (at signal) and passed rapidly back to outflow tract of right ventricle, at which position blood that was 61% saturated was obtained. *Middle panel*: Withdrawal of catheter tip from right pulmonary artery to outflow tract of right ventricle. Pressure levels are low for both positions and blood oxygen saturations are not significantly different. *Bottom panel*: withdrawal of catheter tip from outflow tract of right ventricle through region of tricuspid valve (as seen roentgenoscopically) to high right atrium. Note *1*) that there is no significant difference in pressure or in contour of pressure pulses in right ventricle and atrium, indicating absence of functioning tricuspid valve, and *2*) that right atrial pressure exceeds pulmonary-artery wedge (left atrial) pressure so that flow through defect in atrial septum would be chiefly in right-to-left direction.

Right-to-Left Shunts

In the presence of venoarterial shunts, venous blood that is low in oxygen saturation mixes with blood of high oxygen saturation that has traversed the pulmonary circulation, has returned to the left side of the heart and is destined for the systemic circulation. As a consequence, the amount of oxygen in the blood entering the systemic circulation is decreased.

The clinical consequence of hypoxia is commonly the occurrence of cyanosis. Cyanosis is usually apparent to most observers when saturation of capillary blood is reduced to 80 to 90 per cent of normal (64, 115). Several considerations, however, make it hazardous to assume either that arterial unsaturation is the cause of slight peripheral cyanosis or that normal arterial saturation is present in the absence of cyanosis. Cyanosis usually becomes evident when the concentration of unsaturated hemoglobin in capillary blood is increased to approximately 5 g per 100 ml. In patients with severe anemia, therefore, cyanosis may not be evident in spite of severe arterial hyperemia.

Visible cyanosis may occur in the presence of normal arterial oxygen saturation if tissue extraction of oxygen per unit of blood flow is increased sufficiently to cause capillary unsaturation of this degree. Slowing of superficial blood flow due to cold with consequent increase in tissue extraction of oxygen and a widened arteriovenous oxygen difference (stagnant hypoxemia) provides an example of this variety of cyanosis. Another important cause of stagnant hypoxemia with

a normal arterial oxygen saturation is the slowed peripheral circulation that may accompany heart failure.

Arterial hypoxemia resulting from venoarterial shunting causes physiologic alterations in the circulatory system. Various compensatory mechanisms result which enable the individual better to tolerate the arterial hypoxemia. Many of these adaptive mechanisms are also present in high-altitude dwellers. The following discussion will be concerned mainly with the adaptive mechanisms that occur with hypoxia, and some mention will also be made of studies carried out in high-altitude dwellers.

VALUES ENCOUNTERED. Burchell and colleagues (49) noted that among persons with cardiac malformations that permit venoarterial shunts, the oxygen saturation of systemic arterial blood varies widely, but when such persons are in a good state of nutrition it usually is more than 70 per cent. Marked decreases in arterial oxygen saturation may occur when they exercise. Values of less than 25 per cent for arterial oxygen saturation have been encountered in several such patients in this laboratory when they were walking in a fully conscious state on a treadmill.

In studies of the circulation of men at high altitudes, Husson & Otis (139) found that man does not seem to dwell permanently at altitudes where his arterial oxygen saturation would be much below 70 per cent. They have shown that when man is chronically exposed to hypoxia the combined oxygen in his arterial blood will increase, because of the increased carrying capacity, only until the hypoxia is so severe as to cause a saturation of 70 per cent.

DETERMINANTS OF ARTERIAL OXYGEN SATURATION. The major factors that determine the arterial oxygen saturation in individuals with venoarterial shunts are the pulmonary blood flow and the amount of oxygen extracted by the tissues (oxygen consumption).

An increase in pulmonary blood flow increases the volume of fully saturated blood contributing to systemic flow, whereas a reduction in oxygen consumption allows a higher oxygen saturation of systemic venous blood returning to the heart. Both factors tend to increase the oxygen content of the venoarterial mixture that enters the arterial supply to the body. The possibility of an adaptive mechanism whereby a threshold value below which the oxygen tension of arterial blood would act as a stimulus for an increase in systemic flow has not been established in patients with venoarterial shunts (49). Extensive investigations have been carried out at high altitude concerning the effect of the hypoxemia on cardiac output. The work of Asmussen & Consolazio (14) and of Grollman (123) indicated that an increase in systemic flow occurred early in the acclimatization period. Grollman, from observations on hypoxia produced by mixtures of oxygen and nitrogen, concluded that the stimulus came at rather specific levels of hypoxia (when the oxygen in the inspired mixture dropped to 11.6%). Such a stimulus threshold was supported by observations of Asmussen & Chiodi (13), who found that the oxygen in the inspired air had to be low enough to reduce the arterial oxyhemoglobin to 70 to 80 per cent of normal in order to produce an increase in the cardiac output. In individuals acclimatized to low barometric pressure in a low-pressure chamber for several days, Houston & Riley (134) found an increased cardiac output as one of the less significant compensating mechanisms. A recent review of the circulatory adaptations to hypoxia of types other than the result of venoarterial shunts has been published (154). Although changes in systemic blood flow may cause temporary alterations in arterial oxygen saturation in individuals with venoarterial shunts, systemic blood flow by itself is not one of the primary determinants of the level of arterial oxygen saturation in such individuals.

The level of arterial blood oxygen saturation in such patients is primarily dependent on the volume of pulmonary blood flow. The higher this flow, the higher will be the oxygen saturation of arterial blood. For example, patients with tetralogy of Fallot who have very low pulmonary blood flow uniformly have low oxygen saturation of the arterial blood whereas, in contrast, patients who have total anomalous pulmonary venous connection to the right atrium with complete venous admixture, but with very high pulmonary flows, frequently have an arterial oxygen saturation of more than 90 per cent and consequently may be acyanotic. However, if the pulmonary flow is reduced in these patients to the point where it is equivalent to systemic flow, arterial desaturation appears to the degree that cyanosis will become evident (49).

As an example, consider a patient in whom there is complete mixing of pulmonary and systemic venous blood and the pulmonary blood flow is three times as large as systemic flow. If 5 liters of systemic venous blood (6.7 g of reduced hemoglobin per 100 ml) were completely mixed with 15 liters of fully oxygenated blood from the lungs, arterial blood would contain only 1.7 g of reduced hemoglobin per 100 ml. If pul-

monary blood flow were just twice the systemic flow, the reduced hemoglobin would increase only to 2.5 g per 100 ml. If, however, pulmonary and systemic flows were equal, the mixed blood in the arteries would contain 3.4 g of reduced hemoglobin per 100 ml, and well over 5 g per 100 ml at the capillary level, assuming that capillary blood has 3.5 more grams of unsaturated hemoglobin per 100 ml than arterial blood. As a rule, then, if pulmonary blood flow exceeds the systemic flow by more than twofold, cyanosis when at rest is not likely even with complete mixing of the total systemic and pulmonary venous return.

An increase in oxygen consumption (an increase in the amount of oxygen extracted by the tissues) results in a decrease in the oxygen saturation of venous blood and, as has been pointed out, a decrease in the arterial oxygen saturation. Exercise, for example, increases the metabolic rate and thus decreases the arterial oxygen saturation.

It would be a useful adaptation to a state of chronic hypoxemia if the body would find a means of carrying on its basal activities with a diminished consumption of oxygen. That such an adaptation may actually occur was suggested by Bing *et al.* (31), who reported that in 28 of 30 patients with tetralogy of Fallot who were chronically hypoxemic from congenital heart disease the basal metabolism was either significantly below or at the lower limits of normal. Values as low as −48 per cent for the basal metabolic rate were recorded, and the average for the group was −23.

In contrast to these results, normal or slightly elevated values for basal oxygen consumption in congenital cyanotic heart disease have been obtained by Holling & Zak (133), Burchell and co-workers (49), Ernsting & Shephard (95), Davison and colleagues (77) and Husson & Otis (139). Thus most of the evidence indicates that no diminution in basal oxygen requirement occurs in chronic hypoxia resulting from congenital cyanotic heart disease.

COMPENSATORY EFFECTS RESULTING FROM ARTERIAL HYPOXEMIA. It is well known that individuals who are chronically hypoxemic tend to develop a polycythemia with a concomitant increase in the oxygen-carrying capacity of the blood. The mechanism by which the increase in concentration of blood hemoglobin is brought about is still obscure, nor is there general agreement as to its importance in the over-all picture of acclimatization (122).

Data showing the magnitude of the increase in oxygen-carrying capacity of the blood in man residing at various altitudes have been summarized by Hurtado (137). Husson & Otis (139), in an excellent discussion of this subject, have suggested the possibility that hypoxia more severe than that represented by an arterial saturation of 70 per cent fails to stimulate any further increase in hemoglobin.

The mountain dweller gains from an increased oxygen capacity because removal of a given amount of oxygen from the blood by the tissues produces less of a drop in the saturation, and hence the tension of oxygen supplied to the tissues as well as the oxygen saturation of venous blood returning to the heart is increased. The arterial oxygen saturation, since it is determined almost solely by the ventilation, will not be affected by an increased oxygen-combining power of the blood. The individual with hypoxemia resulting from a venoarterial shunt will gain even more than the altitude dweller from an increased oxygen capacity, since in effect this increases his pulmonary blood flow which, if the rate of oxygen consumption is constant, is the major determinant of his arterial oxygen saturation.

A normal individual who is exposed to an altitude that produces an arterial saturation of 75 per cent, whose oxygen-carrying capacity is 20 volumes per cent, and whose oxygen consumption and cardiac output are such that his arteriovenous oxygen difference is 5 volumes per cent will have a mixed venous saturation of 50 per cent. If his oxygen capacity were increased to 30 volumes per cent, leaving other variables as before, his arterial saturation would remain at 75 per cent and the mixed venous saturation would be increased to 58 per cent.

However, consider an individual who lives at sea level has an oxygen capacity of 20 volumes per cent but who has a right-to-left shunt of such magnitude that his arterial blood consists of a mixture of equal parts of blood that has passed through the lungs and mixed venous blood and who has an arteriovenous difference of 5 volumes per cent. With normally saturated blood leaving the lungs, the saturations of arterial and mixed venous blood would be 75 and 50 per cent, the same as in the case of the normal individual at altitude. If the oxygen capacity of the individual with the shunt is then increased to 30 volumes per cent, the arterial oxygen saturation would increase to 83 per cent and mixed venous saturation to 67 per cent.

Adaptations are, by their nature, compromises in that concessions must be made in return for the advantages gained. In this respect, there is evidence that polycythemia is a predisposing factor in the formation of pulmonary and cerebral thrombi (27, 199). The

importance and probability of occurrence of such undesirable side effects must of course be taken into account in any complete evaluation of an adaptive mechanism, especially when individual cases are concerned. Burchell and co-workers (49) observed that polycythemia was not a uniformly necessary requirement for the well-being of the hypoxemic patient suffering from congenital heart disease of the cyanotic type.

Numerous investigators have shown that individuals who are chronically hypoxic from prolonged residence at high altitudes have an increased ventilation which is greater the higher the altitude (154). There is also evidence that individuals who are hypoxemic because of circulatory shunts also ventilate more than normal (138). The hyperpnea of the altitude dweller constitutes for him an important adaptation. If at 15,000 feet, for example, an individual did not increase his ventilation above that for sea level, his alveolar (and arterial) oxygen tension would be about 40 mm of mercury. The increase in ventilation that usually occurs in the individual acclimatized to this altitude is such as to increase his arterial oxygen tension by about 20 mm of mercury and his arterial saturation to about 90 per cent, an increase which is really significant as an adaptive mechanism. The individual with shunt hypoxemia, however, can increase the oxygenation of his arterial blood but little by hyperpnea. His pulmonary venous blood will be about 98 per cent saturated even with normal ventilation, and although increasing the ventilation will raise the oxygen tension of his blood, it will alter the percentage of saturation only insignificantly because of the flatness of the dissociation curve in this region (139).

Husson & Otis (139) have pointed out that the presence of a right-to-left shunt introduces a problem of carbon dioxide elimination as well as a problem of oxygen uptake. With a normal resting ventilation the pulmonary venous carbon dioxide tension will be normal but the arterial carbon dioxide tension will be higher and the arterial pH lower than normal because of the admixture of venous blood. A normal arterial carbon dioxide tension and pH can be maintained only by hyperventilation of the proper magnitude. With no increase in ventilation, a normal pH but elevated carbon dioxide tension could be maintained by an increase in the alkaline reserve. They observed, as did Morse & Cassels (178), that the average congenital cyanotic individual appears to be in a state of metabolic acidosis that is only partially compensated for by increased ventilation. Husson & Otis (139) noted that the acidosis observed in some congenital cyanotic individuals may be considered as an advantageous adaptation insofar as delivery of oxygen to the tissue is concerned, although it may be disadvantageous in other regards.

SUMMARY

The application of existing and the development and application of new hemodynamic techniques have greatly improved the understanding of the hemodynamic alterations associated with various congenital cardiac defects and the compensatory mechanisms that frequently maintain, to a surprising degree, the functions of the circulatory system despite the defect or defects present. This information, in addition to contributing importantly to the accuracy of diagnosis and the efficacy of treatment of congenital heart disease, has also contributed significantly to the understanding of the physiology of the normal circulatory system and its reactions to stress.

The authors are indebted to many of their professional and technical colleagues at the Mayo Clinic who assisted in the collection and analysis of the data upon which this chapter is mostly based. Deserving of particular mention are Drs. H. B. Burchell, H. J. C. Swan, J. T. Shepherd, Mr. William Sutterer, Miss Lucille Cronin, and Mrs. Jean Frank.

REFERENCES

1. Abbott, M. E. In: *Atlas of Congenital Cardiac Disease.* New York: Am. Heart Assoc., 1936.
2. Abbott, M. E. and W. T. Dawson. The clinical classification of congenital cardiac disease, with remarks upon its pathological anatomy, diagnosis and treatment. *Internat. Clin.* 4: Suppl 34, 156–188, 1924.
3. Adams, F. H., L. Hirvonen, J. Lind, and T. Peltonen. Physiologic studies on the cardiovascular status of newborn pigs: Effect of adrenaline, noradrenaline, acetylcholine and serotonin. *Études Neo-natales* 7: 53–61, 1958.
4. Adams, F. H. and J. Lind. Physiologic studies on the cardiovascular status of normal newborn infants (with special reference to the ductus arteriosus). *Pediatrics* 19: 431–437, 1957.
5. Adams, F. H. and J. Lind. Fetal and neonatal circulation: Observations in humans. In: *Symposium on Congenital Heart Disease*, edited by A. D. Bass and G. K. Moe. Washington, D.C.: Am. Assoc. for Advancement of Science, 1960, p. 51.
6. Adams, F. H., J. Lind, and L. Rauramo. Physiologic

studies on the cardiovascular status of normal newborn infants: Effect of adrenaline, noradrenaline, 10% oxygen and 100% oxygen. *Études Néo-natales* 7: 62–70, 1958.

7. Adams, P., R. C. Anderson, P. Allen, and C. W. Lillehei. Physiologic changes in ventricular septal defect following intracardiac surgery. *Circulation* 16: 857, 1957.
8. Allan, G. A. A schema of the circulation with experiments to determine the additional load in the apparatus produced by conditions representing valvular lesions. *Heart* 12: 181–201, 1925.
9. Amorim, D. de S., H. W. Marshall, D. E. Donald, and E. H. Wood. Effect of atrial septal defects on hemodynamic alterations caused by acute partial obstruction of pulmonary artery. *Circulation Res.* In press.
10. Amplatz, K. and J. F. Marvin. A simple and accurate test for left-to-right shunts. *Radiology* 72: 585–586, 1959.
11. Ardran, G. M., G. S. Dawes, M. M. L. Prichard, S. R. M. Reynolds, and D. G. Wyatt. The effect of ventilation of the foetal lungs upon the pulmonary circulation. *J. Physiol.* 118: 12–22, 1952.
12. Armelin, E., L. Michaels, H. W. Marshall, D. E. Donald, and E. H. Wood. Detection of retrograde passage of indicator from aorta to left ventricle in dogs. *Physiologist* 3 (No. 3): 10, 1960.
13. Asmussen, E. and H. Chiodi. The effect of hypoxemia on ventilation and circulation in man. *Am. J. Physiol.* 132: 426–436, 1941.
14. Asmussen, E. and F. C. Consolazio. The circulation in rest and work on Mount Evans (4,300 M.). *Am. J. Physiol.* 132: 555–563, 1941.
15. Auchincloss, J. H., Jr., R. Gilbert, and R. H. Eich. Pulmonary diffusing capacity in valvular and congenital heart disease. *Circulation* 16: 858, 1957.
16. Bajec, D. F., N. C. Birkhead, S. A. Carter, and E. H. Wood. Localization and estimation of severity of regurgitant flow at the pulmonary and tricuspid valves. *Proc. Staff Meet. Mayo Clin.* 33: 569–577, 1958.
17. Barclay, A. E., J. Barcroft, D. H. Barron, K. J. Franklin, and M. M. L. Prichard. Studies of the foetal circulation and of certain changes that take place after birth. *Am. J. Anat.* 69: 383–406, 1941.
18. Barclay, A. E., K. J. Franklin, and M. M. L. Prichard. *The Foetal Circulation, and Cardiovascular System, and the Changes that They Undergo at Birth.* Oxford: Blackwell, 1944.
19. Barratt-Boyes, B. G. and E. H. Wood. The oxygen saturation of blood in the venae cavae, right-heart chambers, and pulmonary vessels of healthy subjects. *J. Lab. & Clin. Med.* 50: 93–106, 1957.
20. Barratt-Boyes, B. G. and E. H. Wood. Cardiac output and related measurements and pressure values in the right heart and associated vessels, together with an analysis of the hemodynamic response to the inhalation of high oxygen mixtures in healthy subjects. *J. Lab. & Clin. Med.* 51: 72–90, 1958.
21. Barritt, D. W. Simple pulmonary stenosis. *Brit. Heart J.* 16: 381–386, 1954.
22. Bayliss, W. M. On the local reactions of the arterial wall to changes of internal pressure. *J. Physiol.* 28: 220–231, 1902.
23. Becu, L. M., R. S. Fontana, J. W. DuShane, J. W. Kirklin, H. B. Burchell, and J. E. Edwards. Anatomic and pathologic studies in ventricular septal defect. *Circulation* 14: 349–364, 1956.
24. Bedell, G. N. Comparison of pulmonary diffusing capacity in normal subjects and in patients with intracardiac septal defects. *J. Lab. & Clin. Med.* 57: 269–280, 1961.
25. Bender, F., F. Hilgenberg, and G. Jungehülsing. Fortlaufend registrierte Farbstoffverdünnungskurven bei erworbenen und angeborenen Herzfehlern. *Ztschr. Kreislaufforsch.* 46: 845–854, 1957.
26. Bender, F. and H. H. Seifert. Zur diagnostischen Anwendung eines Photozellenkatheters. *Ztschr. Kreislaufforsch.* 47: 260–267, 1958.
27. Berthrong, M. and D. C. Sabiston, Jr. Cerebral lesions in congenital heart disease: A review of autopsies on one hundred and sixty-two cases. *Bull. Johns Hopkins Hosp.* 89: 384–401, 1951.
28. Bing, R. J., J. C. Handelsman, J. A. Campbell, H. E. Griswold, and A. Blalock. The surgical treatment and physiopathology of coarctation of the aorta. *Ann. Surg.* 128: 803–824, 1948.
29. Bing, R. J., L. D. Vandam, and F. D. Gray, Jr. Physiological studies in congenital heart disease. II. Results of preoperative studies in patients with tetralogy of Fallot. *Bull. Johns Hopkins Hosp.* 80: 121–141, 1947.
30. Bing, R. J., L. D. Vandam, and F. D. Gray, Jr. Physiological studies in congenital heart disease. III. Results obtained in five cases of Eisenmenger's complex. *Bull. Johns Hopkins Hosp.* 80: 323–347, 1947.
31. Bing, R. J., L. D. Vandam, J. C. Handelsman, J. A. Campbell, R. Spencer, and H. E. Griswold. Physiological studies in congenital heart disease. VI. Adaptions to anoxia in congenital heart disease with cyanosis. *Bull. Johns Hopkins Hosp.* 83: 439–456, 1948.
32. Blalock, A. and H. B. Taussig. The surgical treatment of malformations of the heart in which there is pulmonary stenosis or pulmonary atresia. *J.A.M.A.* 128: 189–202, 1945.
33. Bloomfield, R. A., H. D. Lauson, A. Cournand, E. S. Breed and D. W. Richards, Jr. Recording of right heart pressures in normal subjects and in patients with chronic pulmonary disease and various types of cardiocirculatory disease. *J. Clin. Invest.* 25: 639–664, 1946.
34. Blount, S. G., Jr., H. Mueller, and M. C. McCord. Ventricular septal defect: Clinical and hemodynamic patterns. *Am. J. Med.* 18: 871–882, 1955.
35. Blumgart, H. L., J. S. Lawrence, and A. C. Ernstene. The dynamics of the circulation in coarctation (stenosis of the isthmus) of the aorta of the adult type: Relation to essential hypertension. *Arch. Int. Med.* 47: 806–823, 1931.
36. Bossina, K. K., G. A. Mook, and W. G. Zijlstra. Direct-reflection oximetry in routine cardiac catheterization. *Circulation* 22: 908–912, 1960.
37. Brachfeld, N. and R. Gorlin: Subaortic stenosis: A revised concept of the disease. *Medicine* 38: 415–433, 1959.
38. Braunwald, E., A. P. Fishman, and A. Cournand. Time relationship of dynamic events in the cardiac chambers, pulmonary artery and aorta in man. *Circulation Res.* 4: 100–107, 1956.
39. Braunwald, E., H. L. Tanenbaum, and A. G. Morrow. Dye-dilution curves from left heart and aorta for localization of left-to-right shunts and detection of valvular in-

sufficiency. *Proc. Soc. Exper. Biol. & Med.* 94: 510–512, 1957.

40. Brecher, G. A. and D. F. Opdyke. The relief of acute right ventricular strain by the production of an interatrial septal defect. *Circulation* 4: 496–502, 1951.
41. Broadbent, J. C. and E. H. Wood. Indicator-dilution curves in acyanotic congenital heart disease. *Circulation* 9: 890–902, 1954.
42. Broadbent, J. C., E. H. Wood, and H. B. Burchell. Left-to-right intracardiac shunts in the presence of pulmonary stenosis. *Proc. Staff Meet. Mayo Clin.* 28: 101–106, 1953.
43. Brotmacher, L. and M. Campbell. The natural history of ventricular septal defect. *Brit. Heart J.* 20: 97–116, 1958.
44. Brotmacher, L. and M. Campbell. Ventricular septal defect with pulmonary stenosis. *Brit. Heart J.* 20: 379–388, 1958.
45. Brown, G. E., Jr., A. A. Pollack, O. T. Clagett, and E. H. Wood. Intra-arterial blood pressure in patients with coarctation of the aorta. *Proc. Staff Meet. Mayo Clin.* 23: 129–134, 1948.
46. Burchell, H. B. Total anomalous pulmonary venous drainage: Clinical and physiologic patterns. *Proc. Staff Meet. Mayo Clin.* 31: 161–167, 1956.
47. Burchell, H. B. Studies in pulmonary hypertension in congenital heart disease. *Brit. Heart J.* 21: 255–262, 1959.
48. Burchell, H. B., H. J. C. Swan, and E. H. Wood. Demonstration of differential effects on pulmonary and systemic arterial pressure by variation in oxygen content of inspired air in patients with patent ductus arteriosus and pulmonary hypertension. *Circulation* 8: 681–694, 1953.
49. Burchell, H. B., B. E. Taylor, J. R. B. Knutson, and E. H. Wood. Circulatory adjustments to the hypoxemia of congenital heart disease of the cyanotic type. *Circulation* 1: 404–414, 1950.
50. Callahan, J. A., R. O. Brandenburg, and H. J. C. Swan. Pulmonary stenosis and interatrial communication with cyanosis: hemodynamic and clinical study of ten patients. *Am. J. Med.* 19: 189–202, 1955.
51. Campbell, M., D. C. Deuchar, and R. Brock. Results of pulmonary valvotomy and infundibular resection in 100 cases of Fallot's tetralogy. *Brit. M. J.* 2: 111–122, 1954.
52. Carter, S. A., D. F. Bajec, E. Yannicelli, and E. H. Wood. Estimation of left-to-right shunt from arterial dilution curves. *J. Lab. & Clin. Med.* 55: 77–88, 1960.
53. Case, R. B., H. W. Hurley, and P. Keating. Detection and measurement of circulatory shunts by use of a radioactive gas. *Progr. Cardiovascular Dis.* 2: 186–195, 1959–1960.
54. Case, R. B., H. W. Hurley, R. P. Keating, P. Keating, H. L. Sachs, and E. E. Loeffler. Detection of circulatory shunts by use of a radioactive gas. *Proc. Soc. Exper. Biol. & Med.* 97: 4–7, 1958.
55. Chapman, C. B., O. Baker, J. Reynolds, and F. J. Bonte. Use of biplane cinefluorography for measurement of ventricular volume. *Circulation* 18: 1105–1117, 1958.
56. Chidsey, C. A. III, H. W. Fritts, Jr., A. Hardewig, D. W. Richards, and A. Cournand. Fate of radioactive krypton (Kr^{85}) introduced intravenously in man. *J. Appl. Physiol.* 14: 63–66, 1959.
57. Civin, W. H. and J. E. Edwards. Pathology of the pulmonary vascular tree. 1. A comparison of the intrapulmonary arteries in the Eisenmenger complex and in stenosis of ostium infundibuli associated with biventricular origin of the aorta. *Circulation* 2: 545–552, 1950.
58. Civin, W. H. and J. E. Edwards. The postnatal structural changes in intrapulmonary arteries and arterioles. *A.M.A. Arch. Path.* 51: 192–200, 1951.
59. Clark, L. C., Jr. Monitor and control of blood and tissue oxygen tensions. *Tr. Am. Soc. Artif. Int. Organs* 2: 41–48, 1956.
60. Clark, L. C., Jr., and L. M. Bargeron, Jr. Left-to-right shunt detection by an intravascular electrode with hydrogen as an indicator. *Science* 130: 709–710, 1959.
61. Clark, L. C., Jr., and L. M. Bargeron, Jr. Detection and direct recording of left-to-right shunts with the hydrogen electrode catheter. *Surgery* 46: 797–804, 1959.
62. Clark, L. C., Jr., L. M. Bargeron, Jr., C. Lyons, M. N. Bradley, and K. T. McArthur. Detection of right-to-left shunts with an arterial potentiometric electrode. *Circulation* 22: 949–955, 1960.
63. Coles, D. R. and A. D. M. Greenfield. The reactions of the blood vessels of the hand during increases in transmural pressure. *J. Physiol.* 131: 277–289, 1956.
64. Comroe, J. H., Jr., and S. Botelho. The unreliability of cyanosis in the recognition of arterial anoxemia. *Am. J. M. Sc.* 214: 1–6, 1947.
65. Conn, H. L., Jr. Use of indicator-dilution curves in the evaluation of acquired heart disease. *Progr. Cardiovascular Dis.* 2: 166–185, 1959–1960.
66. Connolly, D. C. and E. H. Wood. Hemodynamic data during rest and exercise in patients with mitral valve disease in relation to the differentiation of stenosis and insufficiency from the pulmonary artery wedge pressure pulse. *J. Lab. & Clin. Med.* 49: 526–544, 1957.
67. Corvisart, J.-N. *An Essay on the Organic Diseases and Lesions of the Heart and Great Vessels* (from the clinical lectures of J.-N. Corvisart, translated by Jacob Gates). Boston: Bradford & Read, 1912.
68. Cournand, A., H. D. Lauson, R. A. Bloomfield, E. S. Breed, and E. de F. Baldwin. Recording of right heart pressures in man. *Proc. Soc. Exper. Biol. & Med.* 55: 34–36, 1944.
69. Cournand, A., H. L. Motley, A. Himmelstein, D. Dresdale, and J. Baldwin. Recording of blood pressure from the left auricle and the pulmonary veins in human subjects with interauricular septal defect. *Am. J. Physiol.* 150: 267–271, 1947.
70. Cournand, A. and H. A. Ranges. Catheterization of right auricle in man. *Proc. Soc. Exper. Biol. & Med* 46: 462–466, 1941.
71. Cournand, A., R. L. Riley, E. S. Breed, E. de F. Baldwin, and D. W. Richards, Jr. Measurement of cardiac output in man using technique of catheterization of right auricle or ventricle. *J. Clin. Invest.* 24: 106–116, 1945.
72. Crafoord, C. and G. Nylin. Congenital coarctation of the aorta and its surgical treatment. *J. Thoracic Surg.* 14: 347–361, 1945.
73. Crane, M. G., J. E. Holloway, J. McEachen, C. Sears, and R. Selvester. Localization of intracardiac shunts using instantaneous injection of RIHSA with two-site sampling. *Intern. J. Appl. Radiation.* 5: 218, 1959.
74. Crane, M. G., J. E. Holloway, C. H. Sears, J. A. McEachen, R. H. Selvester, and J. C. Woodward.

Localization of intracardiac shunts by two-site sampling. *Circulation* 16: 870, 1957.

75. Crehan, E. L., R. L. J. Kennedy, and E. H. Wood. A study of the oxygen saturation of arterial blood of normal newborn infants by means of a modified photoelectric oximeter: Preliminary report. *Proc. Staff Meet. Mayo Clin.* 25: 392–397, 1950.
76. Daugherty, R. L. *Hydraulics*. New York: McGraw-Hill, 1937.
77. Davison, P. H., G. H. Armitage, and W. M. Arnott. The mechanisms of adaptation to a central venous-arterial shunt. *Brit. Heart J.* 15: 221–240, 1953.
78. Dexter, L. Atrial septal defect. *Brit. Heart J.* 18: 209–225, 1956.
79. Dexter, L. Pulmonary hypertension developing in atrial septal defect. In: *Pulmonary Circulation*, edited by W. R. Adams and I. Veith. New York: Grune & Stratton, 1959, p. 227.
80. Divertie, M. B. *A Study of the Hemodynamic Derangements Associated With Isolated Ventricular Septal Defect*, Thesis, Graduate School, Univ. of Minnesota, 1957.
81. Dow, P. The development of the anacrotic and tardus pulse of aortic stenosis. *Am. J. Physiol.* 131: 432–436, 1940.
82. Dow, P. Estimations of cardiac output and central blood volume by dye dilution. *Physiol. Rev.* 36: 77–102, 1956.
83. Doyle, J. T., J. S. Wilson, and J. V. Warren. The pulmonary vascular responses to short-term hypoxia in human subjects. *Circulation* 5: 263–270, 1952.
84. Drabkin, D. L. Spectroscopy: Photometry and spectrophotometry. In: *Medical Physics* (vol. 2), edited by O. Glasser. Chicago: Yr. Bk. Pub., 1950, p. 1039.
85. Duff, F., A. D. M. Greenfield, J. T. Shepherd, and I. D. Thompson. A quantitative study of the response to acetylcholine and histamine of the blood vessels of the human hand and forearm. *J. Physiol.* 120: 160–170, 1953.
86. Duke, H. N. Observations on the effects of hypoxia on the pulmonary vascular bed. *J. Physiol.* 135: 45–51, 1957.
87. Ebstein, W. Ueber einen sehr seltenen Fall von Insufficienz der Valvula tricuspidalis, bedingt durch eine angeborene hochgradige Missbildung derselben. *Arch. Anat. u. Physiol.* 238–254, 1866.
88. Edwards, J. E. The Lewis A. Conner Memorial Lecture. Functional pathology of the pulmonary vascular tree in congenital cardiac disease. *Circulation* 15: 164–196, 1957.
89. Edwards, J. E. Congenital malformations of the heart and great vessels. In: *Pathology of the Heart* (2nd ed.), edited by S. E. Gould. Springfield, Ill.: Thomas, 1960.
90. Edwards, J. E., T. J. Dry, R. L. Parker, H. B. Burchell, E. H. Wood, and A. H. Bulbulian. In: *An Atlas of Congenital Anomalies of the Heart and Great Vessels*. Springfield, Ill.: Thomas, 1954.
91. Eisenmenger, V. Die angeborenen Defecte der Kammerscheidewand des Herzens, *Ztschr. klin. Med.* 32 (Suppl.): 1–28, 1897.
92. Eldridge, F. L. and H. N. Hultgren. The physiologic closure of the ductus arteriosus in the newborn infant. *J. Clin. Invest.* 34: 987–996, 1955.
93. Eldridge, F. L., H. N. Hultgren, and M. E. Wigmore. The physiological closure of the ductus arteriosus in newborn infants: A preliminary report. *Science* 119: 731–732, 1954.
94. Ellis, E. J., O. H. Gauer, H. E. Essex, and E. H. Wood. Applications of a miniature manometer recording from intracardiac end of a cardiac catheter. *Am. J. Physiol.* 159: 568, 1949.
95. Ernsting, J. and R. J. Shephard. Respiratory adaptations in congenital heart disease. *J. Physiol.* 112: 332–343, 1951.
96. Euler, U. S. von, and G. Liljestrand. Observations on pulmonary arterial blood pressure in the cat. *Acta physiol. scandinav.* 12: 301–320, 1946.
97. Everett, N. B. and R. J. Johnson. Use of radioactive phosphorus in studies of fetal circulation. *Am. J. Physiol.* 162: 147–152, 1950.
98. Everett, N. B. and R. J. Johnson. A physiological and anatomical study of the closure of the ductus arteriosus in the dog. *Anat. Record* 110: 103–110, 1951.
99. Fallot, A. Contribution à l'anatomie pathologique de la maladie bleu (cyanose cardique). *Marseille-méd.* 25: 77–420, 1888.
100. Fegler, G. The reliability of the thermodilution method for determination of cardiac output and the blood flow in central veins. *Quart. J. Exper. Physiol.* 42: 254–266, 1957.
101. Feil, H. S. and L. N. Katz. The transformation of the central into the peripheral pulse in patients with aortic stenosis. *Am. Heart J.* 2: 12–17, 1926.
102. Ferrer, M. I., R. M. Harvey, M. Kuschner, D. W. Richards, Jr., and A. Cournand. Hemodynamic studies in tricuspid stenosis of rheumatic origin. *Circulation Res.* 1: 49–57, 1953.
103. Fineberg, M. H. and C. H. Wiggers. Compensation and failure of the right ventricle. *Am. Heart J.* 11: 255–263, 1936.
104. Fishman, A. P., J. McClement, A. Himmelstein, and A. Cournand. Effects of acute anoxia on the circulation and respiration in patients with chronic pulmonary disease studied during the "steady state". *J. Clin. Invest.* 31: 770–781, 1952.
105. Folkow, B. Intravascular pressure as a factor regulating the tone of the small vessels. *Acta physiol. scandinav.* 17: 289–310, 1949.
106. Fontana, R. S. *A clinical and pathologic study of congenital cardiac disease at the Mayo Clinic (1920–1954), with a review of anatomically verified cases of congenital cardiac malformations collected from the literature* Thesis, Graduate School, Univ. of Minnesota, 1958.
107. Forssmann, W. Die Sondierung des rechten Herzens. *Klin. Wchnschr.* 8: 2085–2087, 1929.
108. Fox, I. J., L. G. S. Brooker, D. W. Heseltine, H. E. Essex, and E. H. Wood. A tricarbocyanine dye for continuous recording of dilution curves in whole blood independent of variations in blood oxygen saturation. *Proc. Staff Meet. Mayo Clin.* 32: 478–484, 1957.
109. Fox, I. J., W. F. Sutterer, and E. H. Wood. Dynamic response characteristics of systems for continuous recording of concentration changes in a flowing liquid (for example, indicator-dilution curves). *J. Appl. Physiol.* 11: 390–404, 1957.
110. Fox, I. J. and E. H. Wood. Applications of dilution curves recorded from the right side of the heart or venous circulation with the aid of a new indicator dye. *Proc. Staff Meet. Mayo Clin.* 32: 541–550, 1957.
111. Fox, I. J. and E. H. Wood. Indocyanine green: physical

and physiologic properties. *Proc. Staff Meet. Mayo Clin.* 35: 732–744, 1960.

112. Fox, I. J. and E. H. Wood. Blood flow measurement by dye-dilution technics and indicator-dilution technics in study of normal and abnormal circulation. In: *Medical Physics* (vol. 3), edited by O. Glasser. Chicago: Yr. Bk. Pub., 1960, pp. 155–177.
113. Fritts, H. W., Jr., A. Hardewig, D. F. Rochester, J. Durand, and A. Cournand. Estimation of pulmonary arteriovenous shunt-flow using intravenous injections of T-1824 dye and Kr^{85}. *J. Clin. Invest.* 39: 1841–1850, 1960.
114. Genest, J., E. V. Newman, A. A. Kattus, B. Sinclair-Smith, and A. Genecin. Renal function before and after surgical resection of coarctation of the aorta. *Bull. Johns Hopkins Hosp.* 83: 429–438, 1948.
115. Geraci, J. E. and E. H. Wood. The relationship of the arterial oxygen saturation to cyanosis. *M. Clin. North America* 35: 1185–1202, 1951.
116. Goldblatt, H., J. R. Kahn, and R. F. Hanzal. Studies on experimental hypertension. IX. The effect on blood pressure of constriction of the abdominal aorta above and below the site of origin of both main renal arteries. *J. Exper. Med.* 69: 649–674, 1939.
117. Gorlin, R. The mechanism of the signs and symptoms of mitral valve disease. *Brit. Heart J.* 16: 375–380, 1954.
118. Gorlin, R. and S. G. Gorlin. Hydraulic formula for calculation of the area of the stenotic mitral valve, other cardiac valves, and central circulatory shunts. *Am. Heart J.* 41: 1–29, 1951.
119. Gorlin, R., B. M. Lewis, F. W. Haynes, and L. Dexter. Studies of the circulatory dynamics at rest in mitral valvular regurgitation with and without stenosis. *Am. Heart J.* 43: 357–394, 1952.
120. Gorlin, R., I. K. R. McMillan, W. E. Medd, M. B. Matthews, and R. Daley. Dynamics of the circulation in aortic valvular disease. *Am. J. Med.* 18: 855–871, 1955.
121. Gøtzsche, H. and W. Falholt. Ebstein's anomaly of the tricuspid valve: A review of the literature and report of 6 new cases. *Am. Heart J.* 47: 587–603, 1954.
122. Grant, W. C. and W. S. Root. Fundamental stimulus for erythropoiesis. *Physiol. Rev.* 32: 449–498, 1952.
123. Grollman, A. Physiological variations of the cardiac output of man. VII. The effect of high altitude on the cardiac output and its related functions: An account of experiments conducted on the summit of Pike's Peak, Colorado. *Am. J. Physiol.* 93: 19–40, 1930.
124. Gross, R. E. and J. P. Hubbard. Surgical ligation of a patent ductus arteriosus: Report of first successful case. *J.A.M.A.* 112: 729–731, 1939.
125. Gross, R. E. and C. A. Hufnagel. Coarctation of the aorta: Experimental studies regarding its surgical correction. *New England J. Med.* 233: 287–293, 1945.
126. Gupta, T. C. and C. J. Wiggers. Basic hemodynamic changes produced by aortic coarctation of different degrees. *Circulation.* 3: 17–31, 1951.
127. Hamilton, W. F., J. W. Moore, J. M. Kinsman, and R. G. Spurling. Studies on the circulation. IV. Further analysis of the injection method, and of changes in hemodynamics under physiological and pathological conditions. *Am. J. Physiol.* 99: 534–551, 1931–1932.
128. Harris, P. Influence of acetylcholine on pulmonary arterial pressure. *Brit. Heart J.* 19: 272–278, 1957.
129. Heath, D. and J. E. Edwards. The pathology of hypertensive pulmonary vascular disease: A description of six grades of structural changes in the pulmonary arteries with special reference to congenital cardiac septal defects. *Circulation* 18: 533–547, 1958.
130. Hellerstein, H. K. Contributions of cardiac catheterization to electrocardiography. In: *Intravascular Catheterization*, edited by H. A. Zimmerman. Springfield, Ill.: Thomas, 1959, p. 474.
131. Hickam, J. B. Atrial septal defect: A study of intracardiac shunts, ventricular outputs and pulmonary pressure gradient. *Am. Heart J.* 38: 801–812, 1949.
132. Hirschfelder, A. D. The volume curve of the ventricles in experimental mitral stenosis, and its relation to physical signs. *Bull. Johns Hopkins Hosp.* 19: 319–322, 1908.
133. Holling, H. E. and G. A. Zak. Cardiac catheterization in diagnosis of congenital heart disease. *Brit. Heart J.* 12: 153–182, 1950.
134. Houston, C. S. and R. L. Riley. Respiratory and circulatory changes during acclimatization to high altitude. *Am. J. Physiol.* 149: 565–588, 1947.
135. Huff, R. L., D. Parrish, and W. Crockett. A Study of circulatory dynamics by means of crystal radiation detectors on the anterior thoracic wall. *Circulation Res.* 5: 395–400, 1957.
136. Hull, E. The cause and effects of flow through defects of the atrial septum. *Am. Heart J.* 38: 350–360, 1949.
137. Hurtado, H. In: *Standard Values in Blood*, edited by E. C. Albritton. Philadelphia: Saunders, 1952, p. 121.
138. Husson, G. S. and A. B. Otis. Physiological adaptation to chronic hypoxia. B. Resting pulmonary ventilation. *U.S.A.F. School of Aviation Medicine Rept. No. 55–76*, 1955.
139. Husson, G. and A. B. Otis. Adaptive value of respiratory adjustments to shunt hypoxia and to altitude hypoxia. *J. Clin. Invest.* 36: 270–278, 1957.
140. Hyman, A. L., A. C. DeGraff, Jr., and A. C. Quiroz. Double catheter dye technique for detection of left-to-right shunts. *Surg. Forum Proc.* 10: 450–453, 1959.
141. Imperial, E. S., C. Nogueira, E. B. Kay, and H. A. Zimmerman. Isolated ventricular septal defects: An anatomic-hemodynamic correlation. *Am. J. Cardiol.* 5: 176–184, 1960.
142. Jager, B. V. and O. J. Wollenman, Jr. An anatomical study of the closure of the ductus arteriosus. *Am. J. Path.* 18: 595–605, 1942.
143. James, L. S. and R. D. Rowe. The pattern of response of pulmonary and systemic arterial pressures in newborn and older infants to short periods of hypoxia. *J. Pediat.* 51: 5–11, 1957.
144. Katz, L. N., K. Jochim, and A. Bohning. The effect of the extravascular support of the ventricles on the flow in the coronary vessels. *Am. J. Physiol.* 122: 236–251, 1938.
145. Katz, L. N., E. P. Ralli, and S.-N. Cheer. The cardiodynamic changes in the aorta and left ventricle due to stenosis of the aorta. *J. Clin. Invest.* 5: 205–227, 1928.
146. Katz, L. N. and M. L. Siegel. The cardiodynamic effects of acute experimental mitral stenosis. *Am. Heart J.* 6: 672–682, 1931.
147. Keith, J. D., R. D. Rowe, and Peter Vlad. In: *Heart Disease in Infancy and Childhood.* New York: Macmillan, 1958.
148. Keith, N. M., L. G. Rowntree, and J. T. Geraghty.

A method for the determination of plasma and blood volume. *Arch. Int. Med.* 16: 547–576, 1915.

149. KENNEDY, J. A. AND S. L. CLARK. Observations on the ductus arteriosus of the guinea pig in relation to its method of closure. *Anat. Record* 79: 349–371, 1941.
150. KEYS, A. AND H. L. FRIEDELL. Quantitative measurement of valvular efficiency of the human heart. *Proc. Soc. Exper. Biol. & Med.* 40: 556–559, 1939.
151. KILBY, R. A., J. W. DUSHANE, E. H. WOOD, AND H. B. BURCHELL. Ebstein's malformation: A clinical and laboratory study. *Medicine* 35: 161–185, 1956.
152. KILLIP, T. III, AND D. S. LUKAS. Tricuspid stenosis: Physiologic criteria for diagnosis and hemodynamic abnormalities. *Circulation* 16: 3–13, 1957.
153. KJELLBERG, S. R., E. MANNHEIMER, U. RUDHE, AND B. JONSSON. *Diagnosis of Congenital Heart Disease* (2nd ed.). Chicago: Yr. Bk. Pub., 1959.
154. KORNER, P. I. Circulatory adaptations in hypoxia. *Physiol. Rev.* 39: 687–730, 1959.
155. KORNER, P. I. AND J. P. SHILLINGFORD. The quantitative estimation of valvular incompetence by dye dilution curves. *Clin. Sc.* 14: 553–573, 1955.
156. KORNER, P. I. AND J. P. SHILLINGFORD. Further observations on the estimation of valvular incompetence from indicator dilution curves. *Clin. Sc.* 15: 417–431, 1956.
157. KREUZER, F., T. R. WATSON, JR., AND J. M. BALL. Comparative measurements with a new procedure for measuring the blood oxygen tension in vitro. *J. Appl. Physiol.* 12: 65–70, 1958.
158. KROEKER, E. J. AND E. H. WOOD. Beat-to-beat alterations in relationship of simultaneously recorded central and peripheral arterial pressure pulses during Valsalva maneuver and prolonged expiration in man. *J. Appl. Physiol.* 8: 483–494, 1956.
159. LAGERLÖF, H. AND L. WERKÖ. Studies on the circulation in man. II. Normal values for cardiac output and pressure in the right auricle, right ventricle and pulmonary artery. *Acta physiol. scandinav.* 16: 75–82, 1949.
160. LANARI, A. AND M. E. MOLINS. Insuficiencia mitral experimental. *Medicina, Buenos Aires* 9: 165–194, 1949.
161. LEWIS, D. H., G. W. DEITZ, J. D. WALLACE, AND J. R. BROWN, JR. Intracardiac phonocardiography in man. *Circulation* 16: 764–775, 1957.
162. LEWIS, T. Material relating to coarctation of the aorta of the adult type. *Heart* 16: 205–261, 1933.
163. LIND, J. AND C. WEGELIUS. Angiocardiographic studies on the human foetal circulation: A preliminary report. *Pediatrics* 4: 391–400, 1949.
164. LITTLE, R. C., D. F. OPDYKE, AND J. G. HAWLEY. Dynamics of experimental atrial septal defects. *Am. J. Physiol.* 158: 241–250, 1949.
165. LONG, R. T. L., E. BRAUNWALD, AND A. G. MORROW. Intracardiac injection of radioactive krypton: clinical applications of new methods for characterization of circulatory shunts. *Circulation* 21: 1126–1133, 1960.
166. LUKAS, D. S. AND S. M. AYRES. Determination of blood oxygen content by gas chromatography. *J. Appl. Physiol.* 16: 371–374, 1961.
167. LUTEMBACHER, R. De la stenose mitrale avec communication interauriculaire. *Arch. mal. coeur* 9: 237–260, 1916.
168. LYONS, W. S., R. G. TOMKINS, J. W. KIRKLIN, AND E. H. WOOD. Early and late hemodynamic effects of mitral commissurotomy. *J. Lab. & Clin. Med.* 53: 499–516, 1959.
169. MACKENZIE, J. *The Study of the Pulse: Arterial, Venous and Hepatic and of the Movements of the Heart*, London: Pentland, 1902, p. 197.
170. MACKENZIE, J. *Diseases of the Heart* (4th ed.). New York: Oxford, 1925, p. 461.
171. MACMAHON, B. T. MCKEOWN, AND R. G. RECORD. The incidence and life expectation of children with congenital heart disease. *Brit. Heart J.* 15: 121–129, 1953.
172. MARSHALL, H. W., H. J. C. SWAN, H. B. BURCHELL, AND E. H. WOOD. Effect of breathing oxygen on pulmonary artery pressure and pulmonary vascular resistance in patients with ventricular septal defect. *Circulation* 23: 241–252, 1961.
173. MARSHALL, H. W., E. WOODWARD, JR., AND E. H. WOOD. Hemodynamic methods for differentiation of mitral stenosis and regurgitation. *Am. J. Cardiol.* 2: 24–60, 1958.
174. MATTHES, K. Untersuchungen über den Gasaustausch in der menschlichen Lunge. 1. Mitteilung: Sauerstoffgehalt und Sauerstoffspannung im Arterienblut und im venösen Mischblut des Menschen. *Arch. exper. Path. u. Pharmakol.* 181: 630–639, 1936.
175. MCDONALD, L. Indicator-dilution curves in diagnosis of congenital heart disease. *Proc. Roy. Soc. Med.* 52: 689–693, 1959.
176. MCMICHAEL, J. AND J. P. SHILLINGFORD. The role of valvular incompetence in heart failure. *Brit. M. J.* 1: 537–541, 1957.
177. MORROW, A. G., R. J. SANDERS, AND E. BRAUNWALD. The nitrous oxide test: An improved method for the detection of left-to-right shunts. *Circulation* 17: 284–291, 1958.
178. MORSE, M. AND D. E. CASSELS. Arterial blood gases and acid-base balance in cyanotic congenital heart disease. *J. Clin. Invest.* 32: 837–846, 1953.
179. NAHAS, G. G. Spectrophotometric determination of hemoglobin and oxyhemoglobin in whole hemolyzed blood. *Science* 113: 723–725, 1951.
180. NEVILLE, J. R. Polarographic determination of oxygen content and capacity of blood. *Fed. Proc.* 17: 117, 1958.
181. NICHOLSON, J. W. III, H. B. BURCHELL, AND E. H. WOOD. A method for the continuous recording of Evans blue dye curves in arterial blood, and its application to the diagnosis of cardiovascular abnormalities. *J. Lab. & Clin. Med.* 37: 353–364, 1951.
182. NICHOLSON, J. W. III, G. G. NAHAS, AND E. H. WOOD. Spectrophotometric determination of T-1824 in whole hemolyzed blood. *J. Appl. Physiol.* 4: 813–818, 1952.
183. PAGE, I. H. The effect of chronic constriction of the aorta on arterial blood pressure in dogs: An attempt to produce coarctation of the aorta. *Am. Heart J.* 19: 218–232, 1940.
184. PATTEN, B. M. The changes in circulation following birth. *Am. Heart J.* 6: 192–205, 1930.
185. PATTEN, B. M. *Human Embryology*. Philadelphia: Blakiston, 1946.
186. PATTEN, B. M. *Human Embryology* (2nd ed.). New York: Blakiston, 1953, p. 656.
187. PATTERSON, G. C. AND J. T. SHEPHERD. The blood flow in the human forearm following venous congestion. *J. Physiol.* 125: 501–507, 1954.
188. PATTERSON, G. C., J. T. SHEPHERD, AND R. F. WHELAN. The resistance to blood flow in the upper and lower limb

vessels in patients with coarctation of the aorta. *Clin. Sc.* 16: 627–632, 1957.

189. Paul, M. H., A. M. Rudolph, and M. D. Rappaport. Temperature dilution curves for the detection of cardiac shunts. *Circulation* 18: 765, 1958.

190. Pickering, G. W. The peripheral resistance in persistent arterial hypertension. *Clin. Sc.* 2: 209–235, 1935.

191. Potain, O. Quoted by T. Lewis. Material relating to coarctation of the aorta of the adult type. *Heart* 16: 205–261, 1933.

192. Prec, K. J. and D. E. Cassels. Oximeter studies in newborn infants during crying. *Pediatrics* 9: 756–763, 1952.

193. Prec, K. J. and D. E. Cassels. Dye dilution curves and cardiac output in newborn infants. *Circulation* 11: 789–798, 1955.

194. Prinzmetal, M. and C. Wilson. The nature of the peripheral resistance in arterial hypertension with special reference to the vasomotor system. *J. Clin. Invest.* 15: 63–83, 1936.

195. Ramirez de Arellano, A. A., P. S. Hetzel, and E. H. Wood. Measurement of pulmonary blood flow using the indicator-dilution technic in patients with a central arteriovenous shunt. *Circulation Res.* 4: 400–405, 1956.

196. Ramsey, L. H. Analysis of gas in biological fluids by gas chromatography. *Science* 129: 900–901, 1959.

197. Rankin, J. and Q. C. Callies. Diffusion characteristics of the human lung in congenital and acquired heart disease. *Circulation* 18: 768, 1958.

198. Remington, J. W. and E. H. Wood. Formation of peripheral pulse contour in man. *J. Appl. Physiol.* 9: 433–442, 1956.

199. Rich, A. R. A hitherto unrecognized tendency to the development of widespread pulmonary vascular obstruction in patients with congenital pulmonary stenosis (tetralogy of Fallot). *Bull. Johns Hopkins Hosp.* 82: 389–401, 1948.

200. Rosenbach, O. Quoted by C. K. Friedberg. In *Diseases of the Heart* (2nd ed.). Philadelphia: Saunders 1956, p. 685.

201. Roughton, F. J. W., R. C. Darling, and W. S. Root. Factors affecting the determination of oxygen capacity, content and pressure in human arterial blood. *Am. J. Physiol.* 142: 708–720, 1944.

202. Rowe, R. D. and L. S. James. The normal pulmonary arterial pressure during the first year of life. *J. Pediat.* 51: 1–11, 1957.

203. Rudolph, A. M. and M. H. Paul. Pulmonary and systemic vascular response to continuous infusion of 5-hydroxytryptamine (serotonin) in the dog. *Am. J. Physiol.* 189: 263–268, 1957.

204. Rushmer, R. F. and D. K. Crystal. Changes in configuration of the ventricular chambers during the cardiac cycle. *Circulation* 4: 211–218, 1951.

205. Rushmer, R. F. and N. Thal. The mechanics of ventricular contraction: A cinefluorographic study. *Circulation* 4: 219–228, 1951.

206. Russell, J. L., D. E. Donald, R. N. Moersch, and H. W. Marshall. Localization and quantitation of left-to-right shunts via experimental cardiac defects. *Proc. Staff Meet. Mayo Clin.* 33: 553–561, 1958.

207. Sanders, R. J. Use of a radioactive gas (Kr^{85}) in the diagnosis of cardiac shunts. *Proc. Soc. Exper. Biol. & Med.* 97: 1–7, 1958.

208. Savard, M., H. J. C. Swan, J. W. Kirklin, and E. H. Wood. Hemodynamic alterations associated with ventricular septal defects. In: *Symposium on Congenital Heart Disease*, edited by A. D. Bass and G. K. Moe. Washington, D. C.: Am. Assoc. for Advancement of Science, 1960, pp. 141–164.

209. Scheele, O. Quoted by T. Lewis. Material relating to coarctation of the aorta of the adult type. *Heart* 16: 205–261, 1933.

210. Schiebler, G. L., J. E. Edwards, H. B. Burchell, J. W. DuShane, P. A. Ongley, and E. H. Wood. Congenital corrected transposition of the great vessels: A study of 33 cases. *Pediatrics* 27: 851–888, 1961.

211. Scott, H. W., Jr., and H. T. Bahnson. Evidence for a renal factor in the hypertension of experimental coarctation of the aorta. *Surgery* 30: 206–217, 1951.

212. Scott, H. W., Jr., H. A. Collins, A. M. Langa, and N. S. Olson. Additional observations concerning the physiology of hypertension associated with experimental coarctation of the aorta. *Surgery* 36: 445–459, 1954.

213. Sealy, W. C., W. DeMaria, and J. Harris. Studies of the development and nature of the hypertension in experimental coarctation of the aorta. *Surg. Gynec. & Obst.* 90: 193–198, 1950.

214. Selzer, A. Defect of the ventricular septum: Summary of twelve cases and review of the literature. *Arch. Int. Med.* 84: 798–823, 1949.

215. Selzer, A. Defects of the cardiac septums. *J.A.M.A.* 154: 129–135 1954.

216. Selzer, A. and G. L. Laqueur. Eisenmenger complex and its relation to the uncomplicated defect of ventricular septum: Review of thirty-five autopsied cases of Eisenmenger's complex, including two new cases. *A.M.A. Arch. Int. Med.* 87: 218–241, 1951.

217. Semler, H. J., J. T. Shepherd, and E. H. Wood. The role of vessel tone in maintaining pulmonary vascular resistance in patients with mitral stenosis. *Circulation* 19: 386–394, 1959.

218. Sendroy, J., Jr., R. T. Dillon, and D. D. Van Slyke. Studies of gas and electrolyte equilibria in blood. XIX. The solubility and physical state of uncombined oxygen in blood. *J. Biol. Chem.* 105: 597–632, 1934.

219. Severinghaus, J. W. and A. F. Bradley. Electrodes for blood pO_2 and pCO_2 determination. *J. Appl. Physiol.* 13: 515–520, 1958.

220. Shaffer, A. B., E. N. Silber, and L. N. Katz. Observations on the interatrial pressure gradients in man. *Circulation* 10: 527–535, 1954.

221. Shepherd, J. T., H. J. Semler, H. F. Helmholz, Jr., and E. H. Wood. Effects of infusion of acetylcholine on pulmonary vascular resistance in patients with pulmonary hypertension and congenital heart disease. *Circulation* 20: 381–390, 1959.

222. Silver, A. W., J. W. Kirklin, and E. H. Wood. Demonstration of preferential flow of blood from inferior vena cava and from right pulmonary veins through experimental atrial septal defects in dogs. *Circulation Res.* 4: 413–418, 1956.

223. Sinclair, J. D., C. P. Newcombe, D. E. Donald, and E. H. Wood. Experimental analysis of an atrial sampling technic for quantitating mitral regurgitation. *Proc. Staff Meet. Mayo Clin.* 35: 700–709, 1960.

224. Sinclair, J. D., W. F. Sutterer, I. J. Fox, and E. H. Wood. Dilution curves of increased optic density of

blood produced by injection of transparent solutions. *Physiologist* 3 (No. 3): 144, 1960.

225. Sodi-Pallares, D. *New Basis of Electrocardiography*, edited by R. M. Calder (English translation). St. Louis: Mosby, 1956.
226. Soulié, P., F. Bouchard, and P. Laurens. L'enregistrement intracardiaque des vibrations de fréquence acoustique et des pressions à l'aide du micromanomètre. *Bull. Acad. nat. méd.* 143: 56–68, 1959.
227. Soulié, P., P. Laurens, F. Bouchard, C. Cornu, and E. Brial. Enregistrement des pressions et des bruits intracardiaques à l'aide d'un micromanomètre. *Bull. et mém. Soc. méd. hôp. Paris.* 2: 713–724, 1957.
228. Sproule, B. J., W. F. Miller, I. E. Cushing, and C. B. Chapman. An improved polarographic method for measuring oxygen tension in whole blood. *J. Appl. Physiol.* 11: 365–370, 1957.
229. Steele, J. M. Evidence for general distribution of peripheral resistance in coarctation of the aorta: Report of three cases. *J. Clin. Invest.* 20: 473–480, 1941.
230. Stewart, G. N. Researches on the circulation time and on the influences which affect it. *J. Physiol.* 22: 159, 1897.
231. Stewart, H. J. and R. L. Bailey, Jr. The cardiac output and other measurements of the circulation in coarctation of the aorta. *J. Clin. Invest.* 20: 145–152, 1941.
232. Stow, R. W. Systematic errors in flow determinations by the Fick method. *Minnesota Med.* 37: 30–35, 1954.
233. Stow, R. W., R. F. Baer, and B. F. Randall. Rapid measurement of the tension of carbon dioxide in blood. *Arch. Phys. Med.* 38: 646–650, 1957.
234. Sutterer, W. F. A compensated dichromatic densitometer for indocyanine green. *Physiologist* 3 (No. 3): 159, 1960.
235. Sutterer, W. F. and E. H. Wood. Strain-gauge manometers: application to recording of intravascular and intracardiac pressures. In: *Medical Physics* (vol. 3), edited by O. Glasser. Chicago: Yr. Bk. Pub., 1960, pp. 641–651.
236. Swan, H. J. C., H. B. Burchell, and E. H. Wood. The presence of venoarterial shunts in patients with interatrial communications. *Circulation* 10: 705–713, 1954.
237. Swan, H. J. C., H. B. Burchell, and E. H. Wood. Effect of oxygen on pulmonary vascular resistance in patients with pulmonary hypertension associated with atrial septal defect. *Circulation* 20: 66–73, 1959.
238. Swan, H. J. C., P. S. Hetzel, H. B. Burchell, and E. H. Wood. Relative contribution of blood from each lung to the left-to-right shunt in atrial septal defect: Demonstration by indicator-dilution technics. *Circulation* 14: 200–211, 1956.
239. Swan, H. J. C., J. W. Kirklin, L. M. Becu, and E. H. Wood. Anomalous connection of right pulmonary veins to superior vena cava with interatrial communications: Hemodynamic data in eight cases. *Circulation* 16: 54–66, 1957.
240. Swan, H. J. C., H. W. Marshall, and E. H. Wood. The effect of exercise in the supine position on pulmonary vascular dynamics in patients with left-to-right shunts. *J. Clin. Invest.* 37: 202–213, 1958.
241. Swan, H. J. C., E. Toscano-Barboza, and E. H. Wood. Hemodynamic findings in total anomalous pulmonary venous drainage. *Proc. Staff Meet. Mayo Clin.* 31: 177–182, 1956.
242. Swan, H. J. C. and E. H. Wood. Localization of cardiac defects by dye-dilution curves recorded after injection of T-1824 at multiple sites in the heart and great vessels during cardiac catheterization. *Proc. Staff Meet. Mayo Clin.* 28: 95–100, 1953.
243. Swan, H. J. C., J. Zapata-Diaz, and E. H. Wood. Dye dilution curves in cyanotic congenital heart disease. *Circulation* 8: 70–81, 1953.
244. Symposium on Diagnostic applications of indicator-dilution technics. *Proc. Staff Meet. Mayo Clin.* 32: 463–508; 509–553, 1957.
245. Symposium on diagnostic applications of indicator-dilution curves recorded from the right and left sides of the heart. *Proc. Staff Meet. Mayo Clin.* 33: 535–577, 1958.
246. Taquini, A. C., J. D. Fermoso, and P. Aramendia. Behavior of the right ventricle following acute constriction of the pulmonary artery. *Circulation Res.* 8: 315–318, 1960.
247. Taussig, H. B. *Congenital Malformations of the Heart.* New York: Harvard, 1947.
248. Taylor, B. E., A. A. Pollack, H. B. Burchell, O. T. Clagett, and E. H. Wood. Studies of the pulmonary and systemic arterial pressure in cases of patent ductus arteriosus with special reference to effects of surgical closure. *J. Clin. Invest.* 29: 745–753, 1950.
249. Tonelli, L., F. Baisi, and E. Malizia. Pre- and postoperative renal function in coarctation of the aorta and its relationship to the genesis of hypertension. *Acta med. scandinav.* 148: 35–50, 1954.
250. Van Slyke, D. D., and J. M. Neill. The determination of gases in blood and other solutions by vacuum extraction and manometric measurement. I. *J. Biol. Chem.* 61: 523–573, 1924.
251. Visscher, M. B. The restriction of the coronary flow as a general factor in heart failure. *J.A.M.A.* 113: 987–993, 1939.
252. Visscher, M. B. and J. A. Johnson. The Fick principle: Analysis of potential errors in its conventional application. *J. Appl. Physiol.* 5: 635–638, 1953.
253. Wakai, C. S. and J. E. Edwards. Developmental and pathologic considerations in persistent common atrioventricular canal. *Proc. Staff Meet. Mayo Clin.* 31: 487–500, 1956.
254. Wakai, C. S., H. J. C. Swan, and E. H. Wood. Hemodynamic data and findings of diagnostic value in nine proved cases of persistent common atrioventricular canal. *Proc. Staff Meet. Mayo Clin.* 31: 500–513, 1956.
255. Wakim, K. G., O. Slaughter, and O. T. Clagett. Studies on the blood flow in the extremities in cases of coarctation of the aorta: Determinations before and after excision of the coarctate region. *Proc. Staff Meet. Mayo Clin.* 23: 347–351, 1948.
256. Warden, H. E., R. A. DeWall, M. Cohen, R. L. Varco, and C. W. Lillehei. A surgical-pathologic classification for isolated ventricular septal defects and for those in Fallot's tetralogy based on observations made on 120 patients during repair under direct vision. *J. Thoracic Surg.* 33: 21–44, 1957.
257. Warner, H. R. A study of the mechanism of pressure wave distortion by arterial walls using an electrical analog. *Circulation Res.* 5: 79–84, 1957.
258. Weidman, W. H., H. J. C. Swan, J. W. DuShane, and

E. H. Wood. A hemodynamic study of atrial septal defect and associated anomalies involving the atrial septum. *J. Lab. & Clin. Med.* 50: 165–185, 1957.

259. Werkö, L., J. Ek, H. Bucht, and J. Karnell. Cardiac output, blood pressures and renal dynamics in coarctation of the aorta. *Scandinav. J. Clin. & Lab. Invest.* 8: 193–200, 1956.

260. Wiggers, C. J. *The Pressure Pulses in the Cardiovascular System.* New York: Longmans, 1928, p. 47.

261. Wiggers, C. J. *Physiology in Health and Disease* (4th ed.). Philadelphia: Lea, 1944.

262. Wiggers, C. J. *Circulatory Dynamics, Physiologic Studies.* New York: Grune, 1952, p. 72.

263. Wiggers, C. J. and H. Feil. The cardio-dynamics of mitral insufficiency. *Heart* 9: 149–183, 1921–1922.

264. Wiggers, C. J. and A. B. Maltby. Further observations on experimental aortic insufficiency. IV. Hemodynamic factors determining the characteristic changes in aortic and ventricular pressure pulses. *Am. J. Physiol.* 97: 689–705, 1931.

265. Wolff, L., J. Parkinson, and P. D. White. Bundle-branch block with short P-R interval in healthy young people prone to paroxysmal tachycardia. *Am. Heart J.* 5: 685–704, 1930.

266. Wood, E. H. Special instrumentation problems encountered in physiological research concerning the heart and circulation in man. *Science* 112: 707–715, 1950.

267. Wood, E. H. Physical response requirements of pressure transducers for the reproduction of physiological phenomenon. *Commun. & Electronics* 23: 32–40, 1956.

268. Wood, E. H. Use of indicator-dilution technics. In: *Symposium on Congenital Heart Disease*, edited by A. D. Bass and G. K. Moe. Washington, D. C.: Am. Assoc. for Advancement of Science, 1960, p. 209.

269. Wood, E. H., D. Bowers, J. T. Shepherd, and I. J. Fox. O_2 content of "mixed" venous blood in man during various phases of the respiratory and cardiac cycles in relation to possible errors in measurement of cardiac output by conventional application of the Fick method. *J. Appl. Physiol.* 7: 621–628, 1955.

270. Wood, E. H., I. R. Leusen, H. R. Warner, and J. L. Wright. Measurement of pressures in man by cardiac catheters. *Circulation Res.* 2: 294–303, 1954.

271. Wood, E. H., W. F. Sutterer, and L. Cronin. Oximetry. In: *Medical Physics* (vol. 3), edited by O. Glasser. Chicago: Yr. Book Pub., 1960, p. 416.

272. Wood, E. H., W. Sutterer, H. J. C. Swan, and H. F. Helmholz, Jr. The technic and special instrumentation problems associated with catheterization of the left side of the heart. *Proc. Staff Meet. Mayo Clin.* 31: 108–115, 1956.

273. Wood, E. H., H. J. C. Swan, and H. F. Helmholz, Jr. Recording and basic patterns of dilution curves. Normal and abnormal. *Proc. Staff Meet. Mayo Clin.* 32: 464–477, 1957.

274. Wood, E. H., H. J. C. Swan, and H. W. Marshall. Technic and diagnostic applications of dilution curves recorded simultaneously from the right side of the heart and from the arterial circulation. *Proc. Staff Meet. Mayo Clin.* 33: 536–553, 1958.

275. Wood, P. Congenital heart disease: A review of its clinical aspects in the light of experience gained by means of modern techniques. *Brit. M. J.* 2: 639–645, 1950.

276. Wood, P. *Diseases of the Heart and Circulation* (2nd ed.). Philadelphia: Lippincott, 1956.

277. Wood, P. The Eisenmenger syndrome or pulmonary hypertension with reversed central shunt. *Brit. M. J.* 2: 701–709, 1958.

278. Wood, P., E. M. Besterman, M. K. Towers, and M. B. McIlroy. The effect of acetylcholine on pulmonary vascular resistance and left atrial pressure in mitral stenosis. *Brit. Heart J.* 19: 279–286, 1957.

279. Wood, P., O. Magidson, and P. A. O. Wilson. Ventricular septal defect with a note on acyanotic Fallot's tetralogy. *Brit. Heart J.* 16: 387–406, 1954.

280. Woodward, E., Jr., H. B. Burchell, and E. H. Wood. Dilution curves associated with valvular regurgitation. *Proc. Staff Meet. Mayo Clin.* 32: 518–525, 1957.

281. Woodward, E., Jr., H. J. C. Swan, and E. H. Wood. Evaluation of a method for detection of mitral regurgitation from indicator-dilution curves recorded from the left atrium. *Proc. Staff Meet. Mayo Clin.* 32: 525–535, 1957.

282. Wright, J. L., H. B. Burchell, J. W. Kirklin, and E. H. Wood. Congenital displacement of the tricuspid valve (Ebstein's malformation): Report of a case with closure of an associated foramen ovale for correction of the right-to-left shunt. *Proc. Staff Meet. Mayo Clin.* 29: 278–284, 1954.

283. Wright, J. L., H. B. Burchell, E. H. Wood, E. A. Hines, Jr., and O. T. Clagett. Hemodynamic and clinical appraisal of coarctation 4 to 7 years after resection and end-to-end anastomosis of the aorta. *Circulation* 14: 806–814, 1956.

284. Wright, J. L. and E. H. Wood. Localization of valvular regurgitation. *Proc. Staff Meet. Mayo Clin.* 32: 491–495, 1957.

285. Wright, J. L. and E. H. Wood. Value of central and peripheral intra-arterial pressures and pulse contours in cardiovascular diagnosis. *Minnesota Med.* 41: 215–222, 1958.

286. Zacharioudakis, S. C., K. Terplan, and E. C. Lambert. Ventricular septal defects in the infant age group. *Circulation* 16: 374–383, 1957.

287. Zijlstra, W. G. *A Manual on Reflection Oximetry and Some Other Applications of Reflection Photometry.* Assen, Holland: Van Gorcum, 1958.

The control of the function of the heart

STANLEY J. SARNOFF
JERE H. MITCHELL
Laboratory of Cardiovascular Physiology, National Heart Institute, Bethesda, Maryland

CHAPTER CONTENTS

AN INCREASED UNDERSTANDING of the integrated function of an organism is predicated, at least in part, on understanding the function of its component organs. A determination of the extent to which an organ makes intrinsic readjustments to varying conditions, i.e., autoregulates, is a desirable and helpful precursor to a more refined analysis of the effects of extrinsic influences.

"Broadly speaking, there are two main avenues of approach in the attempt to unravel the complicated processes which determine the function of any individual organ. On the one hand, we may study its reaction in the intact animal to comparatively small environmental changes—a method of inestimable value, since it is one which may readily be applied to man; on the other hand, we may remove the organ and study its reaction under grossly artificial conditions. In the former case, we sacrifice simplicity and full control to a close approximation to normality in environment; in the latter case, we sacrifice normality in environment in order to obtain greater simplicity and a higher degree of experimental control. The former may be referred to as the analytic method of experimentation, the latter as the synthetic. On the one hand, we attempt to dissociate the medley of influences which share in determining the normal function of the organ, and to relegate to each its particular office in maintaining this normality; on the other hand, we attempt to associate these influences in such a degree and in such a manner as to bring the isolated organ back to an environment and function comparable to the normal."

This general statement by Starling & Verney (115) still seems to have merit in establishing the general guidelines for continuing investigation in physiological research. It will serve as the basic pattern of presentation in this chapter.

The inadequacies of communication have rarely been more apparent in a scientific discipline than in cardiovascular physiology, or so it seems. To mitigate this, at least somewhat, it appears wise to designate at the outset the specific meaning of certain terms. The term "autoregulation" will be used to describe phenomena occurring in an organ which are not attributable to nervous or chemical influences originating outside that organ and which phenomena can reasonably be construed as being of value to the performance of the total organism. The term "myocardial contractility" will be used in a specific manner. When, from any given end diastolic pressure or fiber length, the ventricle produces more external stroke work and more external stroke power (stroke work per systolic second) an increase in ventricular contractility is said to have taken place and vice versa. Implicit in this definition is an increased rate of development of tension when contractility increases. Specifically excluded is any increased work that may be done as the result of afterload from the same end diastolic length, since the rate of development of tension is not increased under such circumstances prior to the application of the afterload (36, 37). The term "ventricular function curve" (VFC) will be used to designate *a*) the relation between mean left atrial pressure and left ventricular stroke work (VFC_{LA}), *b*) the relation between left ventricular end diastolic pressure and left ventricular stroke work (VFC_{LV}), and *c*) the relation between changes in left ventricular myocardial fiber length and changes in left ventricular stroke work (VFC_{FL}). When the terms stroke work and stroke power are employed they will always refer to external stroke work and external stroke power. The term "filling pressure" will be used to indicate mean atrial pressure. The term "pressure-length relation" will be used to indicate a curve describing the relation between changes in the length of a selected segment of left ventricular myocardium and simultaneous changes in left ventricular diastolic pressure (58). The methodology and methods of calculation used in the individual experiments discussed will be alluded to only where it seems especially desirable, since such information can be obtained in the source material referred to.

Cardiac as well as skeletal muscle will, within certain limits, contract more forcefully from a longer initial length. As will be observed from the outline above, this fundamental fact will serve as the point of departure in the analysis of the system complex under consideration.

I. PERFORMANCE CHARACTERISTICS IN THE ISOLATED HEART (INTRINSIC MECHANISMS)

A. *The Ventricle*

HETEROMETRIC AUTOREGULATION. One type of intrinsic response exhibited by the ventricle of the isolated heart is the well-known Frank-Starling mechanism. This endows the ventricles with performance characteristics such that the heart ejects whatever volume is put into it. For, if inflow is augmented and end diastolic pressure and fiber length are thus increased, the ventricle contracts more forcefully and expels an augmented stroke volume. This occurs on a beat-to-beat basis. Because this basic mechanism employs a change in initial fiber length, it is designated as heterometric autoregulation.

In 1878 Waller (121) suggested that when "the left ventricle is forced to work against a higher pressure, it has to be filled abundantly and under high pressure." Fick (38), in 1882 and Blix (11), in 1895 disclosed the fundamental relationship between the initial length of skeletal muscle and the force of its subsequent contraction. In the same year Frank (39) published his exciting observations on the dynamics of cardiac muscle, a treatise now more readily available to English speaking investigators as a result of the translation of his work by Chapman and Wasserman (40). Starling and his co-workers (113) subsequently began the first major attempt to systematize the pertinent operating parameters relating to the mammalian heart into a cogent and useful generality, and the result of their efforts came to be known as Starling's law of the heart. The advent of this work was greeted with enthusiasm not only by physiologists but also by those interested in the clinical aspects of circulatory problems, since it promised to be a valuable conceptual tool in making many observed phenomena more readily comprehensible. This initial enthusiasm was, however, gradually replaced by a growing disillusionment with the over-all helpfulness of the concept for two main reasons. The first is that many who attempted to use this concept did so with an inadequate appreciation of the essential operating parameters. More important, however, were those investigations demon-

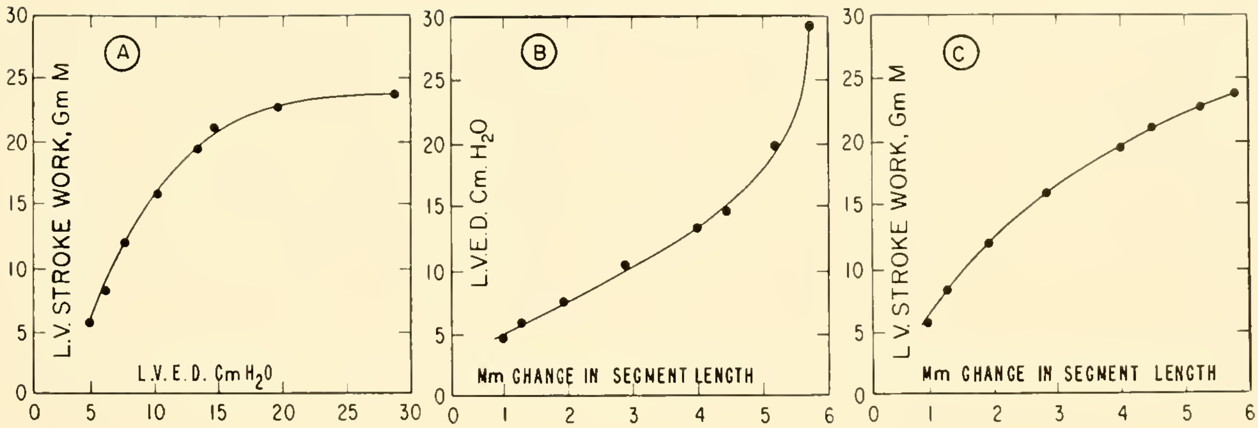

FIG. 1

strating that under certain circumstances the heart could be induced to contract more forcefully and produce more external work even though its end diastolic volume and filling pressure were lower. Such phenomena were construed by many as a violation of the relationship elaborated by Starling. He can be expected to have been aware of the studies performed in his own laboratory by Anrep (3) in 1912, and Patterson (71) in 1915, studies which demonstrated that catecholamines can cause the mammalian heart to contract more forcefully from a smaller end diastolic volume, and he certainly made his position clear with regard to this matter (112, 113).

In 1952, a broad-scale reinvestigation of the problem was initiated using the relationship between filling pressure and the external stroke work of the heart in the open-chested anesthetized dog (96). The plot of this relation, a ventricular function curve, is at least one definitive manner of describing myocardial contractility. It became clear that if the biochemical environment of the myocardium and the physical parameters are not altered a consistent and reproducible relation between filling pressure and external stroke work can be obtained in any given heart. It became equally clear that no single ventricular function curve can adequately explain the performance characteristics of a given heart, since it was possible to shift from one curve to another as the result of certain interventions, such as giving or withdrawing catecholamines (96, 98). That is to say, a family of curves rather than a single curve could readily be elicited. In retrospect, it seems that the authors were then faced with the simple alternative of abandoning the Frank-Starling concept, as had been done by some, or of retaining its basic merits while helping to broaden it so as to have it embrace the spectrum of observed phenomena. The latter of these alternatives was chosen for two main reasons. The first is that to have abandoned Starling's law would have left them without any organized system of thought with which to attempt to appreciate cardiac phenomena. Of greater importance, however, was the conviction that the ability to elicit changes in myocardial contractility over the whole range of filling pressures made possible not only the more precise definition of those influences which do alter contractility, but also provided the basis for a broader appreciation of the physiological significance of such observed effects (96, 98).

Relation between left ventricular end diastolic (LVED) pressure, myocardial segment length, and stroke work. The three curves plotted in figure 1 show certain of the static variables relevant to a consideration of heterometric autoregulation. Curve *A* shows the relation between LVED pressure and stroke work (VFC_{LV}). Curve *B* shows the relation of changes in the length of a segment of left ventricular myocardium to changes in LVED pressure (pressure-length curve). Curve *C* shows the relation between changes in ventricular segment length and changes in stroke work (VFC_{FL}). As anticipated from the postmortem ventricular pressure-volume curve (53, 96), the curve expressing the relation between fiber length and stroke work (*C*) has a more nearly linear relation than does either the curve relating LVED pressure to stroke work or the curve relating LVED pressure to fiber length. Such observations support the desirability of continuing to think of the fiber length–stroke work relation as the most appropriate and biologically meaningful point of departure in the analysis of the control of cardiac function even

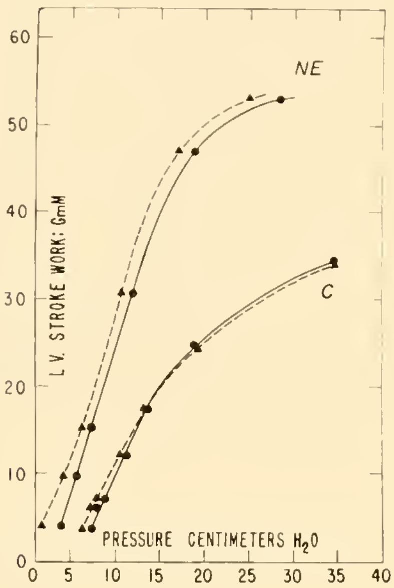

FIG. 2

though, as is often the case, other values may be more convenient to determine experimentally.

The relations expressed by these curves constitute a descriptive analysis of what is meant by heterometric autoregulation. As end diastolic pressure increases there is an increase in stroke work which is large relative to the pressure increase (curve *A*). If one assumes the steep portion of the curve to be that which is normally operative (as for example in the various phases of the respiratory cycle), then it may be seen that large changes in ventricular stroke work can be obtained without extensive changes of the pressure necessary to fill the ventricle or the pressure in the atrium and veins behind it. This fact is facilitated by the upward concavity of curve *B*, i.e., the relatively large changes in fiber length brought about by small pressure changes in the ventricle on the lower, sensitive portion of this curve.

Changes in myocardial contractility. Figure 2 shows two ventricular junction curves obtained from a heart paced at a constant rate of 140 per min. The first curve (*C*) was obtained before and the second curve (*NE*) was obtained during the administration of 0.36 gamma per min of norepinephrine. The dashed lines connect the points relating mean left atrial (LA) pressure to LV stroke work; the solid lines connect points relating LVED pressure to LV stroke work. Both VFC_{LA} and VFC_{LV} are shifted to the left during norepinephrine. From any given LVED pressure, the left ventricle produces not only more stroke work but also more stroke power and, in each instance, high speed tracings reveal that the rate of development of tension is greater from any given LVED pressure during the administration of norepinephrine. An increase in contractility has, therefore, taken place. It was noted that as long as the norepinephrine infusion was maintained, the left ventricle continued to exhibit heterometric autoregulation along the curve *NE*. When the norepinephrine was withdrawn, the heart again exhibited heterometric autoregulation along curve *C*. It is, in fact, fair to say that each heart continually exhibits heterometric autoregulation on one or another of its ventricular function curves. The shift from one curve to another will be determined by whether an intervention which can cause such a shift is imposed. Numerous other adrenergic agents, such as metaraminol (97) and mephentermine sulfate (123), have also been found to shift the VFC_{LA} to the left even though aortic pressure is held constant throughout and the increase in stroke work is accomplished solely by increasing stroke volume. The use of ventricular function curves as a means of describing alterations in the performance characteristics of the heart appears to have been found useful in the analysis of the effects of digitalis (30), hypothermia (65), surgical interventions on the heart (117, 120), and an evaluation of the toxicity produced by agents used to achieve cardiac arrest (63).

HOMEOMETRIC AUTOREGULATION. A second type of autoregulation occurs in the ventricle of the isolated heart (99, 104). Unlike heterometric autoregulation which occurs immediately, it requires at least several beats to develop fully and occurs after an increase in ventricular activity such as that associated with increase in aortic pressure or heart rate. As a result of the increase in myocardial contractility that follows such an activity increase, the heart maintains an LVED pressure and fiber length more nearly like that which obtained prior to the activity increase than it would have if this type of autoregulation had not taken place. It is therefore referred to as homeometric autoregulation. As a result, the heart is endowed with performance characteristics, such that it can expel the same or nearly the same stroke volume against a wide range of resistances without more than a brief invasion of its heterometric reserve.

In 1912, Anrep observed that when aortic resistance was elevated in the heart-lung preparation, ventricular volume at first increased but then subsequently declined. An influence appeared to him to be operating soon after the initial dilatation which

caused the heart to return toward its initial volume. He stated that when adrenaline had been given previously, ventricular volume returned to its control value during the period of increased aortic resistance, presumably while the ventricle was ejecting comparable stroke volumes and doing more stroke work (3–5). Starling, in whose laboratory Anrep's experiments were performed, made similar observations and attributed these phenomena to the presumed improvement in myocardial metabolism which accompanies the increase in coronary flow when the aortic pressure is elevated (72, 112, 113). Any apprehension concerning the possibility that the hazards of biventricular oncometry were operating was dispelled by the observations made in the tortoise heart by Kosawa (56), Peserico (73), and Stella (116). In 1938 Müller (68) examined the response of the heart to an increased aortic pressure, both in the intact heart and the isolated left ventricle, and concluded that two processes were operative. The first was active immediately, demanding an increase in the heart volume and utilizing elastic forces; the second occurred within 1 to 2 min and enabled the heart to work against the same high pressure with a smaller volume, demonstrating a marked positive inotropic effect. In 1956, Stainsby *et al.* (111) presented data obtained from the isolated supported canine heart preparation as well as from nonisolated hearts (13); they showed that when the work of the ventricle was increased by increasing aortic pressure it produced more stroke work from any given filling pressure than when the increase in work was induced by increasing stroke volume. Further, with stroke volume held constant at each of several different levels, when the aortic resistance and pressure were then elevated, the ventricle could produce substantial increases of external stroke work with little or no increase in filling pressure. Similar findings were observed by Braunwald *et al.* (13). These data in the canine heart were consonant with the findings of Kosawa, Peserico, and Stella in the tortoise.

Numerous problems of fundamental interest and importance devolved from these considerations. In 1959 a major finding was contributed by Rosenblueth and colleagues (82). Those investigators studied the right ventricle of the isolated dog heart while keeping coronary perfusion (aortic) pressure constant, and while observing changes in the combined volume of both ventricles by oncometry. They stated that when the resistance to right ventricular ejection was increased, the combined ventricular volume first increased but then declined while the right ventricle ejected a comparable stroke volume against the higher pressure. Although it was apparently not possible in their experiments to ascertain what changes in coronary flow actually took place during the transition from one state to another, these experiments nevertheless indicated that an increase in coronary perfusion pressure is not a necessary concomitant of the increase in myocardial contractility observed when the resistance to right ventricular ejection is elevated.

Hemodynamic factors eliciting homeometric autoregulation. 1) Aortic pressure (Anrep effect). The effect on LVED pressure of abruptly increasing the resistance to ventricular ejection can be seen in figure 3, which shows tracings from experiments in which left coronary flow was either controlled or independently varied in an isolated supported heart preparation (104). Figure 3*A* shows high speed tracings shortly before and 1 min after abruptly imposing a sustained increase in aortic resistance. Stroke volume changed only slightly, from 9.6 to 9.0 ml, and total coronary flow remained essentially the same. The left ventricle increased its stroke work from 8.2 to 15.2 g-m without an increase of end diastolic pressure. It required 52 msec to raise its pressure from end diastolic to 40 cm H_2O while facing the low resistance, and only 39 msec to produce the same pressure increment when facing the high resistance. The middle set of tracings (fig. 3*B*) also shows a pattern of increased ventricular contractility when a high resistance to ejection is imposed. Again, in this instance, stroke volume changed little, from 11.3 to 10.6 ml. Stroke work increased from 9.5 to 16.4 g-m, whereas coronary flow was essentially unchanged. When ejecting against the higher resistance, and while producing more stroke work, the LVED pressure was 2.4 cm lower. There was a more rapid development of pressure at the beginning of ventricular systole, and a shorter systolic ejection time as well as a more rapid decline of ventricular pressure after the incisura; a longer diastolic time appeared just as when sympathetic stimulation is applied (see below).

Figure 3*C* shows data from experiments in which an attempt was made to induce a change in contractility by altering coronary flow while keeping the resistance to ventricular ejection constant. The tracing in the left panel was obtained without pumping the coronary flow and with a screw clamp on the left coronary inflow tubing tightened so as to limit the total coronary flow to the level shown. Without altering aortic resistance, the screw clamp on the coronary tubing was then removed; coronary flow

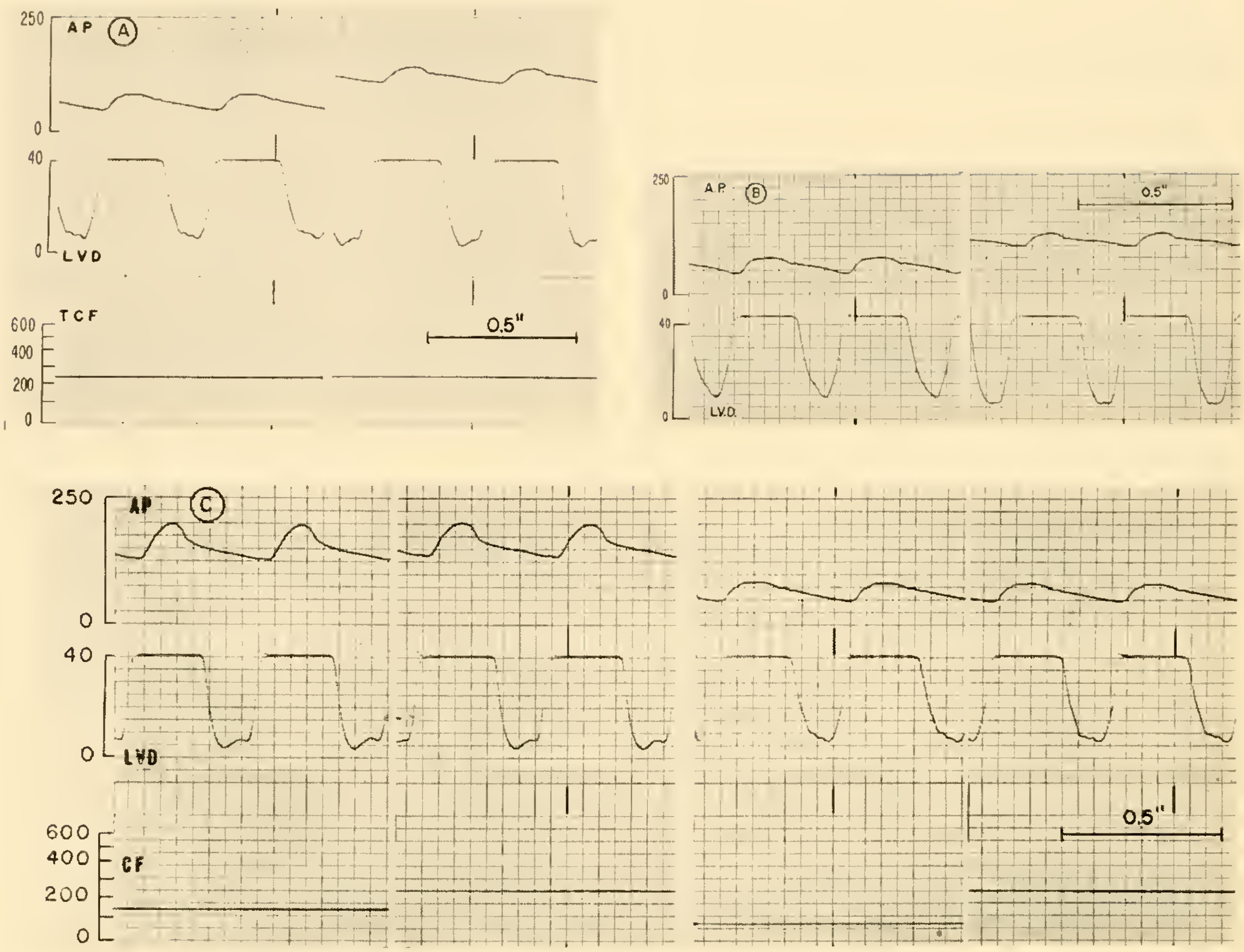

FIG. 3*A*, *B*, *C*. AP = aortic pressure in mm Hg; LVD = left ventricular diastolic pressure in cm H_2O; TCF = total coronary flow in ml/min. CF = total coronary flow in ml/min.

rose to the level shown in the second panel. No change in contractility was observed. Shortly thereafter, in the same experiment, the aortic resistance was lowered and the spontaneous, unrestricted coronary flow observed (third panel). Coronary flow was then pumped (fourth panel) at the unrestricted flow rate which had been observed when aortic resistance and pressure were high. Once again, a change in ventricular contractility was not apparent. These data are not construed as indicating that an adequate coronary flow is unimportant since, in any heart, a restriction of coronary flow below a critical level will decrease contractility (23). Rather, these data indicate that when coronary flow is adequate, a change in contractility can take place in which a change in coronary flow is not the primary determinant.

Figure 4*A* shows the results of an experiment in which changes in the end diastolic length of a selected segment of left ventricular myocardium were recorded simultaneously with changes in LVED pressure (58, 103). The left ventricular stroke work was increased over a comparable range either by increasing stroke volume while keeping aortic systolic pressure approximately constant (solid lines), or by increasing aortic pressure while keeping stroke volume approximately constant (dashed lines). When stroke work was increased by increasing stroke volume, both end diastolic pressure and end diastolic segment length rose. When work was increased by increasing aortic pressure there was little rise in end diastolic pressure and a slight decrease in end diastolic segment length. These data indicate that the ventricular myocardium had, if anything, become slightly less extensible, not more so, and that when work was increased by increasing aortic pressure, the

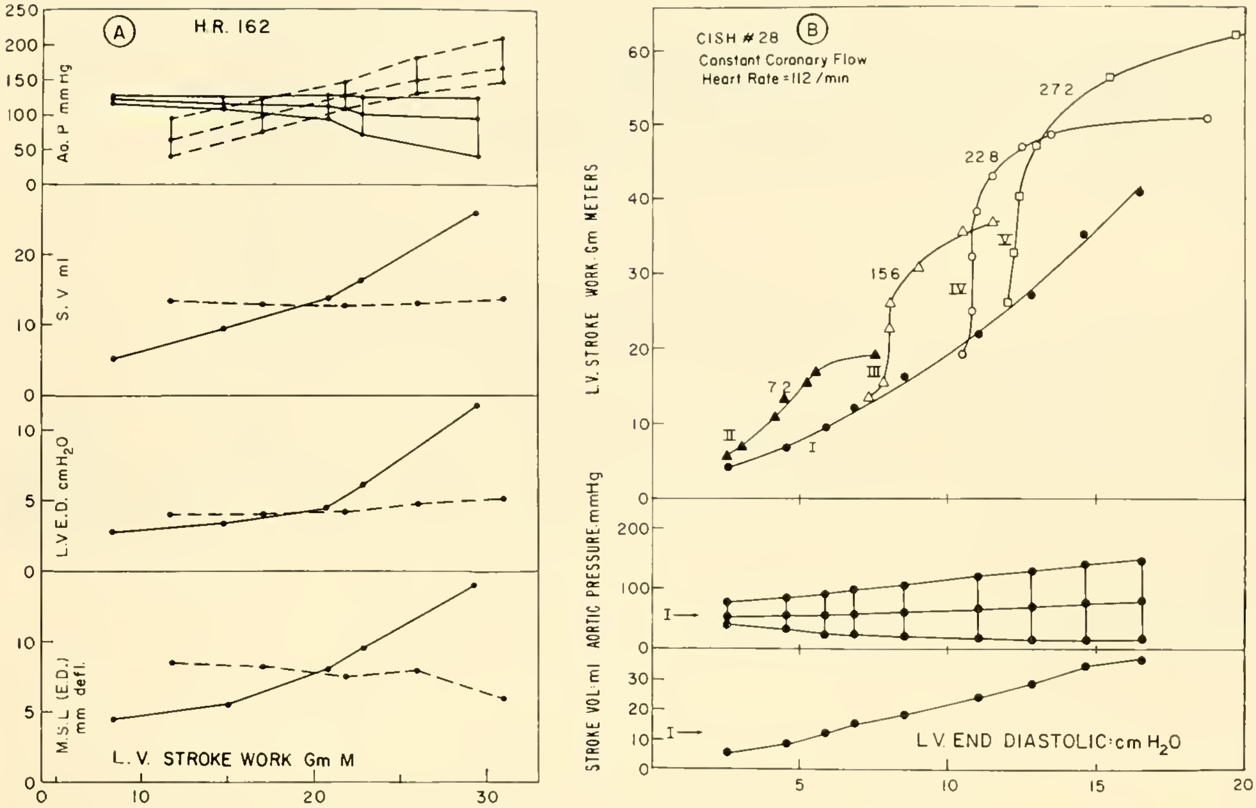

FIG. 4A, B. AoP = aortic pressure; SV = stroke volume; LVED = left ventricular end diastolic pressure; MSL (ED) myocardial segment length at end of diastole.

increased work was not taking place from a longer initial fiber length. The finding of a decreased myocardial extensibility under circumstances of increased coronary perfusion pressure is consonant with the recent evidence obtained by Horres *et al.* (51) and the intimations put forth by Salisbury and colleagues (93), indicating that a more tumescent myocardium is less extensible.

Figure 4*B* shows the range over which these phenomena can occur even when coronary flow is not allowed to vary appreciably as the result of changing aortic pressure. The run labeled I was conducted with mean aortic pressure held approximately constant and stroke work increased by increasing stroke volume as indicated in the two bottom panels. Then, at each of four different stroke volumes (runs II, III, IV, and V), stroke work was increased solely by increasing aortic pressure. Figures to left of the curves indicate the stroke volumes performed. In runs III, IV, and V there was a substantial range of stroke work which could be accomplished with little change in LVED pressure. It was of interest to note that the larger the value at which stroke volume was held constant, the steeper was the function curve when aortic pressure was increased.

The transient phenomena that occur immediately after the increase and subsequent decrease of resistance to left ventricular ejection are shown in figure 5 (upper left). The heart rate was held constant at 160 per min. Stroke volume was 11.1 ml during the low aortic resistance and 10.3 ml during the high aortic resistance. Left coronary flow was constant. There are four distinct phases. In phase 1, immediately after increasing the aortic resistance, LVED pressure rises along with the elevation of aortic pressure. The beginning of phase 2 (first arrow) occurs shortly thereafter and is signaled by the decline in LVED pressure while aortic pressure continues to rise. This decline in LVED pressure continues until the new equilibrium level is reached (phase 3). When the imposed aortic resistance is suddenly removed, LVED pressure drops sharply (second arrow) and to the lowest level observed in the sequence (beginning of phase 4); thereafter, in phase 4, it gradually returns to the level which obtained prior to the increase in aortic resistance.

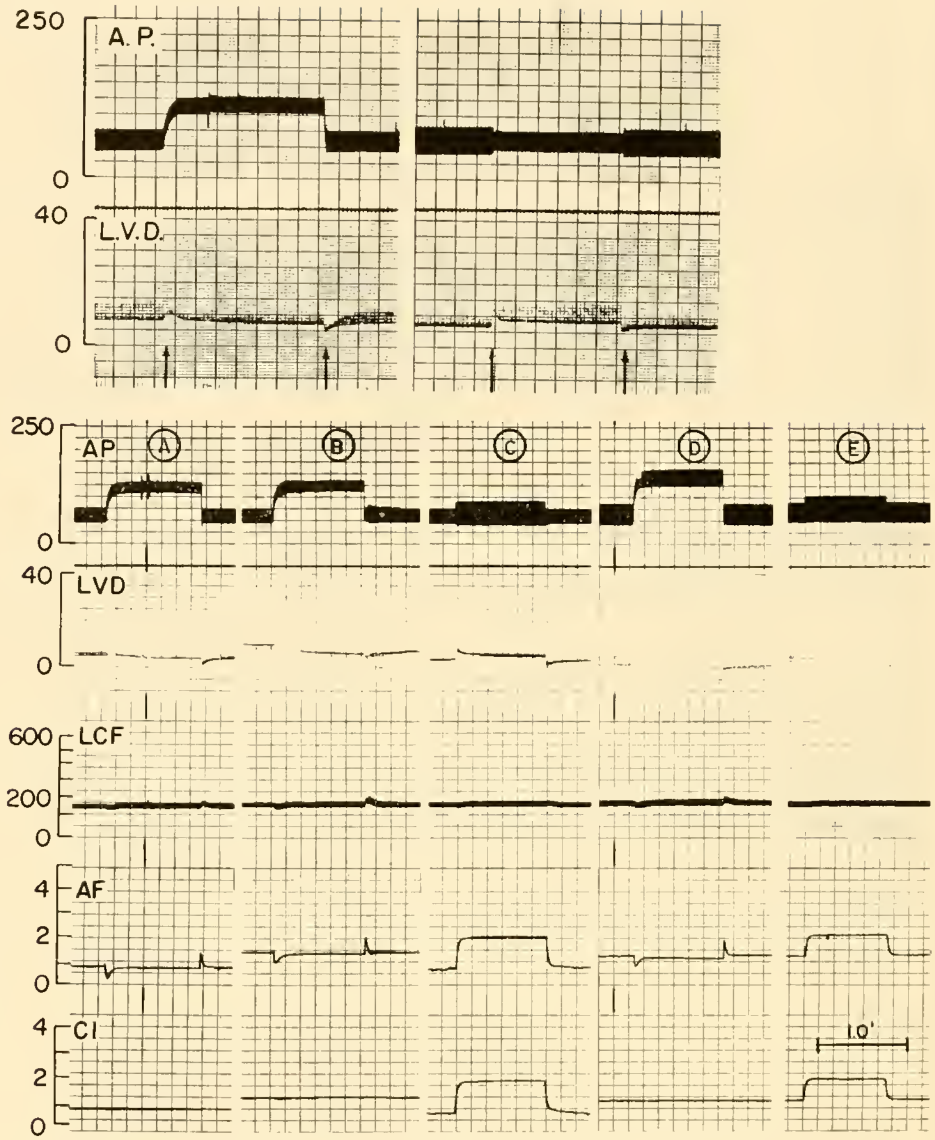

FIG. 5. LCF = left coronary flow in ml/min, AF = aortic flow (cardiac output minus right coronary flow) in liters/min, CI = cardiac (left ventricular) inflow.

Figure 5 (lower, *A*, *B*, and *D*) shows the simultaneous values for cardiac inflow, aortic flow (cardiac output minus right coronary artery flow), and left coronary artery flow before, during, and after an increase in aortic resistance. During phase 1, when LVED and aortic pressures are rising, aortic flow is diminishing while cardiac inflow is essentially unchanged. The rise in LVED pressure would thus appear to be accompanied by an increased ventricular volume since, during this phase, more blood seems to be entering the heart than is leaving it. At the onset of phase 2, as LVED pressure declines, aortic flow rises to its phase 3 plateau while inflow remains the same. At the moment when the increased aortic resistance is removed (beginning of phase 4), aortic flow is suddenly augmented while inflow remains unchanged and LVED pressure falls abruptly to its low point. At this time it would appear that the ventricular volume is diminishing, since more blood appears to leave the ventricle than is entering it. At the point of the onset of phase 2 an increase in contractility is occurring, since LVED pressure and volume are falling while stroke volume, aortic pressure, and external stroke work are rising. Further, at the very beginning of phase 4, when LVED pressure is substantially lower than prior to the increase in aortic resistance, it would appear that an increase in contractility has taken place, since the ventricle is putting out a substantially larger stroke volume against the same aortic pressure than it did in the control period. With

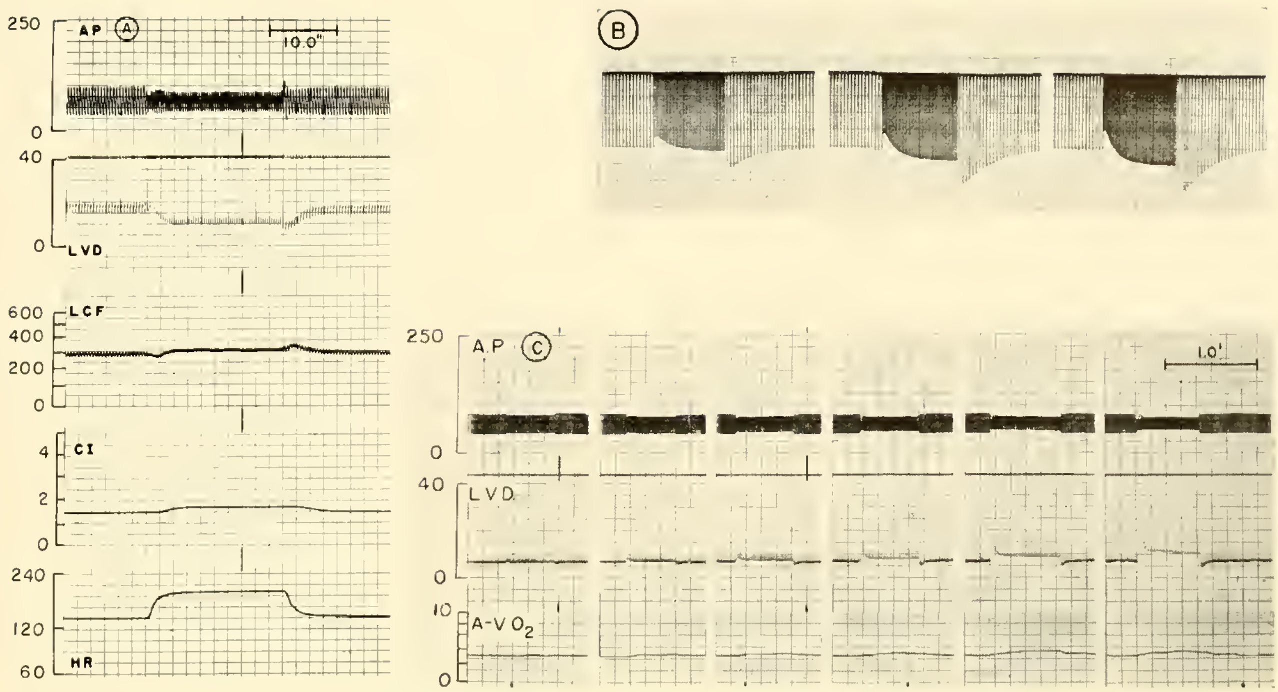

FIG. 6. HR = heart rate. A-V O_2 = coronary arteriovenous oxygen difference in volumes per cent.

regard to the tracings shown in figure 5 (lower), it should be noted that, due to the positioning of the aortic flowmeter, the "volume transients" observed were related not to the ventricle alone but to the left atrium and ventricle plus aorta.

Over a certain range, the work produced by striated muscle which encounters an afterload (an increased resistance to shortening at some interval after it has begun to contract from a given initial length) will be greater than when it is not so afterloaded (36, 37). This is an inherent property of muscle in any given biochemical state and does not, as far as is known, require an alteration in its state to exhibit this phenomenon. This may, of course, contribute to the increased work produced in the first beat after an increased aortic resistance is suddenly applied. Homeometric autoregulation is not meant to encompass this aspect of cardiac muscle performance but rather refers to the increased contractility which develops (phase 2) in the subsequent beats after the increased resistance is applied. The rate of development of tension cannot and, in fact, is not increased on the first beat, since the ventricle has no way of sensing that it is to encounter an afterload until the aortic diastolic pressure is at least equaled by that in the ventricle. In subsequent beats the rate of development of tension is increased (fig. 3) and it is only then that an increase in contractility is said to have taken place.

2) Heart rate (*Bowditch effect*). The patterns of response observed after an abrupt change of heart rate without a change in aortic resistance are shown in figure 5 (upper right), and more particularly in figure 6*A*. In the former the heart rate was abruptly changed from 124 to 163 and back to 131 while cardiac output and total coronary flow were held constant. In the latter, shortly after the increase in rate there is, in phase 1, a rise in LVED pressure as when the aortic resistance is increased. The first few beats after the increase in rate are weaker than the subsequent ones as evidenced by the aortic pressure tracing. This pattern indicates a diminished cardiac output while inflow remains constant, thus demonstrating that the rise in LVED pressure is paralleled by an increase of ventricular volume. At the onset of phase 2, LVED pressure declines while the aortic pulse is augmented briefly and a new equilibrium state is reached (phase 3), during which there is a slightly higher cardiac inflow and, presumably therefore, a higher cardiac output. At the onset of phase 4, when returning to the initial rate, it is clear, from the lower LVED pressure, wider aortic pulse, and maintained inflow that an increase in contractility had taken place during the period of increased heart rate.

Depending on the initial heart rate, the state of the heart and the stroke volume, the LVED pressure may not return to or below its initial level during the interval when heart rate is increased (fig. 5, upper right). However, the stigmata of an increasing contractility (the decline of LVED pressure during phase 2) and of an increased contractility (LVED pressure lower than control value at beginning of phase 4) were always observed when a period of relative tachycardia was imposed. Further, the changes observed were a function of the extent of the increase in heart rate imposed. This is shown in figure 6*C*, an experiment in which the heart rate was increased 10, 20, 30, 40, 50, and 60 beats per min from a control level of 128 beats per min. It was observed that the greater the heart rate change, the larger were the changes observed during phases 2 and 4. It was also found that, with coronary flow held constant, the greater the change in rate, the greater was the widening of the coronary A-VO_2 difference (fig. 6*C*).

Figure 6*B* shows the change in developed tension resulting from changing the stimulus rate in a preparation consisting of a strip of rat right ventricle in oxygenated Krebs' solution. Since resting tension did not change, an increase in contractility is indicated by a greater downward deflection. In the tracing shown in figure 6*B* the rate was changed from 30 to 60 (left), 30 to 90 (middle), and 30 to 108 (right) per min; in each instance the rate was then promptly returned to 30 per min. The pattern of changes observed in figure 6*A* and figure 6*B* are similar in that an increased contractility had been induced in both by an increased rate. Figure 6*B* also relates to figure 6*C*; in both, the greater the increase in rate, the greater was the relative increase in contractility induced as evidenced by phases 2 and 4.

3) Stroke volume. The transient phenomena observed when abruptly changing cardiac inflow are shown in *C* and *E* of figure 5 (lower). In this experiment the inflow was abruptly increased without changing either aortic resistance, heart rate, or coronary flow (see below).

Possible mechanisms involved in homeometric autoregulation. 1) Tension time index (TTI). Rosenblueth *et al.* (82) stressed "the influence of previous activity" on the contractility of the right ventricle. They state: "We suggest that whenever the work of the heart increases, this increment determines a further increase in the subsequent contractions and this influence is important enough to overcome that of the initial volume or length," and, "Any increase of work augments the amplitude of the following contractions." Subsequently, however, it was shown (104) that the homeometric influence on the contractility of the ventricle was related to the manner in which its activity was increased rather than the increase in work, per se. Examples of this are shown in figure 5 (lower). In the first three panels work was increased 100, 110, and 145 per cent, respectively, the first two increases being accomplished by elevating aortic pressure and the third primarily by increasing flow with only a slight elevation in pressure. The exhibition of homeometric autoregulation was clearly more pronounced in the first two. In the latter two panels of figure 5 (lower), later in the same experiment, work was increased 130 per cent by elevating aortic pressure (fourth panel) and 86 per cent, predominantly, by increasing flow (fifth panel). Again, the homeometric effect was more pronounced when pressure was increased than when flow was increased. Further, it was possible to induce homeometric autoregulation in the heart even when work was decreased as shown in figure 7, an experiment in which aortic resistance was abruptly increased and cardiac inflow decreased, such that a fall in stroke work from 18.9 to 13.8 g-m occurred. Coronary flow rose and arteriovenous O_2 difference narrowed, resulting in an increased O_2 consumption even though stroke work fell as in similar experiments reported previously (100). The phase 1 transient and the initial beats of the phase 4 transient are of no value in such an experiment, since a variable effect on these can be obtained, depending upon the point in the cardiac cycle when the changes of inflow and aortic resistance are made and the extent to which they are simultaneous. The findings in phase 2 and most of phase 4, however, are informative. The continuing decline in LVED pressure during phase 2 indicates an increasing ventricular contractility for an appreciable period after the new, lower stroke work level had been achieved. The continuing rise in LVED pressure after removing the imposed intervention shows a reversal of the change in contractility that had taken place.

An analysis of those hemodynamic variables influencing the oxygen consumption of the heart revealed that the variable which most closely correlates with myocardial qO_2 is not the work of the heart but rather the amount of tension developed by the myocardium as indicated by the area under the systolic portion of the pressure curve per minute (100). It was observed in those studies that an increase of aortic pressure or heart rate required the heart to produce a large increase in the total tension de-

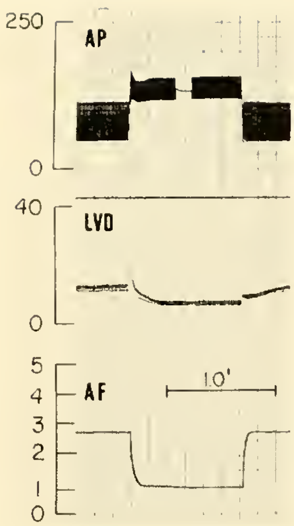

FIG. 7

veloped per minute. A greater relative increase in stroke volume, with mean aortic pressure and heart rate held constant, resulted in a much smaller augmentation of the total tension developed. As shown above, increases of rate or aortic pressure produced the exhibition of a marked homeometric influence, whereas with the augmentation of stroke volume this was relatively less well developed. It seems not unreasonable to suggest, therefore, that an increase in the amount of tension developed by the myocardium per unit of time may be that cardiodynamic factor which elicits homeometric autoregulation.

2) Ionic concentration changes. Bowditch (12) in 1871 described phenomena in the frog heart which he referred to as "treppe" or staircase. Shortly after the onset of stimulation, the heart exhibited successively stronger contractions with each succeeding stimulus until, several beats later, a plateau was reached; subsequent increases in rate produced the same effect. A common variant of the Bowditch staircase is shown in figure 6*B*; after the change of rate in the isolated rat ventricle strip, an increase in contractility became apparent, i.e., a stronger contraction from the same initial tension. The greater the rate change imposed, the greater was the increase in contractility at the new rate and the stronger were the first few contractions after the return to the control rate. The similarity between the patterns observed in figure 6*B* with those observed in figures 6*A* and *C* support the position put forth by Rosenblueth *et al.* (83) that the Bowditch staircase effect is operative in the adequately supported canine heart, a position consonant with the experiments of Braunwald *et al.* (14) in which it was observed that the higher the heart rate the shorter was the period of time required for the ventricle to eject a given volume.

Bowditch put forward the idea that each contraction leaves behind it a more favorable state for the ensuing contraction and thus, the higher the rate, the more favorable is the condition for contracting. The available evidence relating to the biochemical mechanism by which this takes place can be found in the recent review of Hajdu & Leonard (43), and indicates that potassium leaves the myocardial cell with each contraction and reenters it in the interval between contractions. Thus, the higher the rate and the shorter the period of diastole, the less would be the opportunity for re-entry of potassium relative to efflux and the lower the intracellular potassium in the new equilibrium state, a condition known to increase contractility (43). It has, in fact, recently been demonstrated (17, 27) that a potassium loss will occur in the perfused canine heart when tachycardia is imposed.

A certain similarity is to be noted between the cardiodynamic pattern elicited when activity is increased either by increasing heart rate or by increasing aortic pressure (fig. 5, upper). In both, phase 2 shows that an increase in contractility is taking place soon after the beginning of the intervention; in both, phase 4 shows that an increased contractility has occurred during the intervention. This similarity of patterns suggests that changes in intracellular ionic concentration may take place as a result of the change in the character of the contractions as well as by the length of the interval between them. This view presupposes that a more forceful contraction can either increase ionic efflux during the contraction or, perhaps less likely, so predispose the membrane as to alter net ionic flux in any given time interval between contractions. In any case it now seems clear that, over a wide range, an increase in the amount of tension developed by ventricular myocardium can produce a biochemical rearrangement which leaves behind it a more favorable condition for subsequent contractions, and that this phenomenon is not wholly dependent upon an increased coronary flow.

3) Norepinephrine. In any given isolated heart preparation, an aortic resistance can be selected against which the ventricle is unable to eject the same or nearly the same stroke volume without requiring an elevated LVED pressure. Figure 8*A* shows such an instance. Between panels 1 and 2 aortic resistance was abruptly increased. During the administration of norepinephrine (panels 3 and 4), the same aortic resistance increase did not then require an appre-

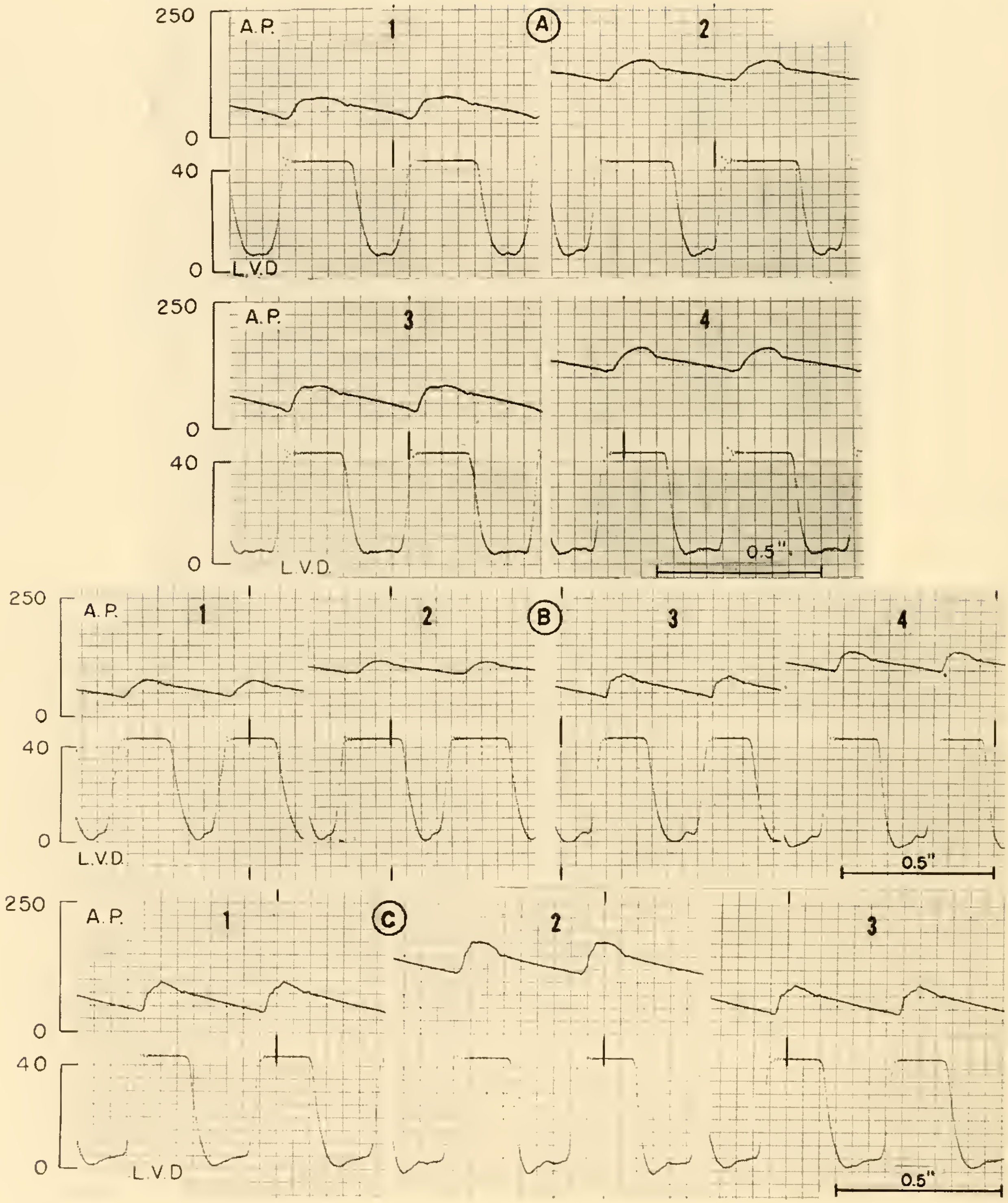

FIG. 8

ciable LVED pressure increase. In this study heart rate was held constant and the stroke volumes were 13.6 ml in panel 1, 14.0 in 2, 13.6 in 3, and 13.7 in 4. Figure 8.1 is also informative in that the alterations in ventricular activity brought about by increasing aortic resistance appear to resemble those brought about by the administration of norepinephrine. A comparison of panels 1 and 2 and of panels 1 and 3

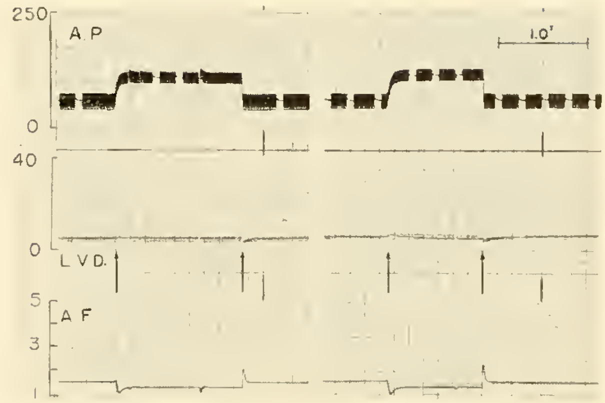

FIG. 9

reveals certain similarities. Both the increased aortic resistance and the norepinephrine made the rise and decline of ventricular pressure steeper, shortened the total period of systole (from beginning of rise of ventricular pressure to the incisura) and shortened the period required for the systolic ejection of comparable volumes. It is further found that when a ventricle is able to meet an increased aortic resistance without increasing LVED pressure (fig. 8*B*, left), the subsequent administration of norepinephrine may enable it to meet the same or even a greater resistance increase from a lower LVED pressure. Such an instance is shown in figure 8*B* (right). Figure 8*C* shows a similar phenomenon and also shows particularly clearly the accentuation of the ventricular pressure dip in early diastole that was frequently encountered when an increased aortic resistance was imposed.

Slow speed tracings of the type shown in figure 9 are also informative. It shows the same imposed aortic resistance increase with and without norepinephrine infusion in the same experiment. Without the norepinephrine infusion (right panel), the pattern was as previously described. During the norepinephrine (left panel), the LVED pressure transients were less well defined. In experiments of this type it was found that by increasing or decreasing the norepinephrine infusion rate, the left ventricle could be made to vary the rapidity with which it passed through phase 2 and arrived at the new equilibrium level in phase 3.

These findings on the effect of norepinephrine confirm those of Anrep (3) but are not in agreement with those of Rosenblueth *et al.* (82) in that the level of catecholamine present appeared to be of importance to the exhibition of homeometric autoregulation by the ventricle. First, in some instances a heart which was in relatively poor condition, as indicated by its LVED pressure, would show little or sometimes no apparent homeometric autoregulation; when norepinephrine was infused a response could then be obtained. Second, the higher the level of circulating norepinephrine, the greater was the increased resistance against which the ventricle could eject a comparable stroke volume without an elevated end diastolic pressure (fig. 8). Third, norepinephrine influenced the myocardium in a manner such that it would respond to a sudden increase in pressure not only more adequately but also more rapidly (fig. 9). Such findings are not only consonant with the observation that norepinephrine shifts the ventricular function curve to the left and makes it steeper (fig. 2), but also invites consideration of the possibility that increased ventricular activity either increases the locally available myocardial norepinephrine or facilitates its utilization during homeometric autoregulation.

Significance of homeometric autoregulation. Whatever the mechanism or mechanisms by which homeometric autoregulation is accomplished, the resulting increase in contractility has two important consequences. The first is that it permits the ventricle beating at any given rate to eject the same stroke volume against a wide range of resistances without requiring an increased LVED pressure or fiber length. Thus, over certain ranges, it acts in such a manner as to conserve heterometric autoregulation for changes in stroke volume (fig. 4). Second, the increase in contracility, especially that aspect of it which is exhibited as a more rapidly developed ventricular pressure, diminishes the proportion of the total cardiac cycle that systole would otherwise require. This is a particular advantage when heart rate is increased since, if such a phenomenon did not occur, the diastolic interval would be so constrained that ventricular relaxation would be incomplete before the next systole (67), ventricular filling impaired, and coronary flow limited. In this connection, it was of particular interest to note the frequency with which the heart, when its rate was suddenly increased, exhibited *pulsus alternans* in the first few beats but became regular again as the increase in contractility became manifest (fig. 6).

INFLUENCE OF OXYGEN AVAILABILITY ON VENTRICULAR PERFORMANCE. The ventricle will produce less external stroke work from any given filling pressure when the blood flow to the myocardium is unduly restricted (shift of VFC_{LA} to the right). Under these circumstances, when mean atrial pressure rises,

LVED pressure also rises. As might be expected, the divergence between a control VFC and one obtained during restricted coronary blood flow is larger at the higher filling pressures and stroke works; with severer degrees of coronary blood flow restriction not only will the plateau of the curve be lower but a descending limb characteristic of the failing heart will appear (23). With such techniques it has also been possible to demonstrate acutely induced unilateral ventricular failure (23).

The observation that anemia also shifts VFC_{LA} to the right, in spite of the then obtaining higher coronary blood flow, is evidence that, during coronary flow restriction, a major influence producing the depressed function is the limited oxygen availability rather than the accumulation of metabolites (24).

B. The Atrium

HETEROMETRIC AUTOREGULATION. The studies of Blinks, who used a more highly refined technique for studying atrial contractility than had previously been available, have dissolved any possible reservations as to whether the force of atrial contraction is a function of its end diastolic pressure and volume (fiber length) just as is the case with the ventricle (10). He further demonstrated a shift of the atrial function curve to the left under the influence of catecholamines and also showed that, while under this influence, a change in atrial distensibility did not take place (10a). Further evidence for heterometric autoregulation in the atrium is seen in figure 11*A* (beats 1–19), a tracing obtained during the rapid infusion of blood. As the infusion progressed and the atrial pressures became elevated, atrial systole produced a progressively larger increment in both the ventricular end diastolic pressure and segment length indicating an augmented force of atrial contraction.

Evidence on which to base a judgment as to the presence or absence of homeometric autoregulation in the atrium is not presently available.

EFFECT OF ATRIAL SYSTOLE ON LVED PRESSURE AND FIBER LENGTH. The significance of atrial systole for ventricular filling was first shown by Harvey (46) and later by Gesell (42), and Wiggers & Katz (126). Harvey stated, "At this same time when the auricles alone are beating, if you cut off the tip of the heart with a scissors, you will see blood gush out at each beat of the auricles. This shows how blood enters the ventricles, not by the suction or dilatation of the ventricles, but by the beat of the auricles."

Recently it has become possible not only to make a more definitive analysis of the influence of atrial systole but also to designate those circumstances under which atrial systole will produce more or less diastolic lengthening of the ventricular myocardium (58). The extent to which atrial systole can contribute to the lengthening of the ventricular myocardial fibers can be seen in figure 10. In this record, obtained from a dog with surgically induced heart block, there are four atrial contractions for each ventricular contraction; the results of each atrial contraction can be readily observed in the absence of disturbances produced by ventricular activity. Each atrial contraction, which produced only a small pressure rise in the ventricle, caused a substantial increase in myocardial segment length. The observed increases in segment length thus induced were an appreciable proportion of the total segment shortening which took place during systole.

The extent to which the level of ventricular diastolic pressure will modify myocardial elongation due to atrial systole is shown in figure 11. Figure 11*A* shows 41 consecutive beats during a rapidly administered infusion. Figure 11*B* shows two beats at the beginning and two beats at the end of a rapid infusion of blood. In both, at the beginning of the infusion, when ventricular diastolic pressure is low, the small increment in end diastolic pressure consequent to atrial systole is accompanied by a substantial segment length elongation. At the end of the infusion, when the ventricular diastolic pressure is high, atrial systole causes a greater rise in pressure but a much diminished increase in segment length. This relationship is expressed in the pressure-length curve of the ventricle (fig. 12) which shows the plot of ventricular diastolic pressure and changes in myocardial segment length during diastasis (58). Two successive runs (circles and squares) were obtained by the stepwise infusion of blood. When the diastolic pressure in the ventricle is low, a small increment in pressure produces a relatively large increase in myocardial segment length (sensitive part). Conversely, at the higher ventricular diastolic pressures only small increases in segment length are produced by a similar or even greater pressure increment (insensitive part).

In the study of Lind and his colleagues (57), who used contrast media for demonstrating the atrial contribution to ventricular filling in human heart block, it was suggested that the atrial beats which occurred early in diastole made a substantial contribution to ventricular filling, whereas those which occurred late in diastole contributed little to ventric-

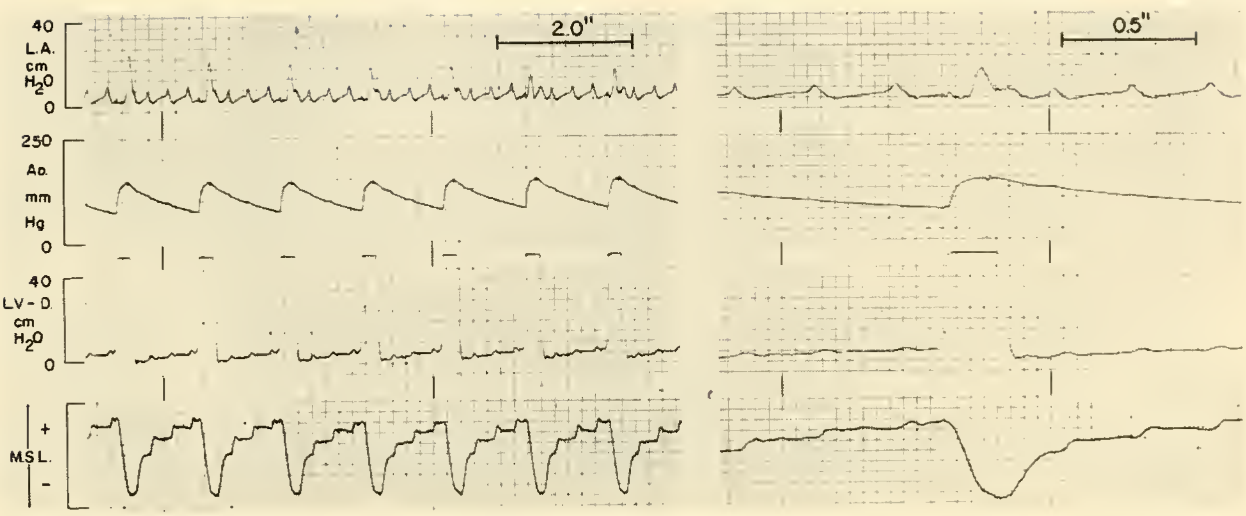

FIG. 10. LA = left atrial pressure; Ao = aortic pressure; LV-D = left ventricular diastolic pressure; MSL = changes in myocardial segment length; + = elongation; — = shortening.

ular filling "because the atrioventricular pressure difference is small." It would appear from the data shown above that the more likely explanation is the position of the ventricle at that time (late diastole) on a higher part of its pressure-volume as well as its pressure-length curve.

The extent to which atrial systole can contribute to the end diastolic elongation of ventricular myocardium, when coupled with the dependence of the ventricle's stroke work on initial fiber length, indicates the substantial extent to which variations in the vigor of atrial systole could provide the stimulus for greater or lesser amounts of ventricular stroke work.

MITRAL VALVE CLOSURE. The mechanism of closure of the atrioventricular valves has been the subject of considerable speculation. It has recently been established that not only can the mitral valve be closed solely as the result of atrial activity but that autonomically induced changes in atrial activity can influence whether or not the valve closes (106a). This will be discussed below.

II. NEURONAL EFFECTS ON THE PERFORMANCE CHARACTERISTICS OF THE HEART (EXTRINSIC INFLUENCES)

A. *Influence of Cardiac Sympathetic Nerve Stimulation on the Ventricle*

CONTRACTILITY. Supramaximal stimulation of the isolated left stellate ganglion, while heart rate is held constant by atrial pacing, produces the changes shown in figure 13*A*. During the interval between the arrows at top of the first channel, the isolated left stellate ganglion was stimulated. The prompt elevation of cardiac output and systolic, mean and diastolic aortic pressures is accompanied by a fall of mean left and right atrial pressures and a widening of the PA-LA pressure difference. As found by Shipley & Gregg (108), left stellate ganglion stimulation sometimes does not cause an appreciable change in heart rate. In such animals when observations on myocardial contractility are made either with or without a controlled rate the results are the same. In some experiments the elevation of arterial pressure is small during stellate ganglion stimulation, the increased contractility being evidenced primarily by a fall in mean atrial pressure (105).

The fall in left atrial pressure during stellate ganglion stimulation is consistently accompanied by a lowering of left ventricular end diastolic pressure. The more rapid development of tension, the more rapid myocardial shortening, the augmented aortic pressure, the shorter duration of ejection, and the more rapid relaxation are consistent and noteworthy (105). Changes of the type observed can be seen in figure 19 (lower).

In figure 13*B* the dashed lines show the relation between mean left atrial pressure and left ventricular stroke work during control period (*C*) and during stellate ganglion stimulation (*SS*); the solid lines show the relation between left ventricular end diastolic pressure and stroke work during control period (*C*)

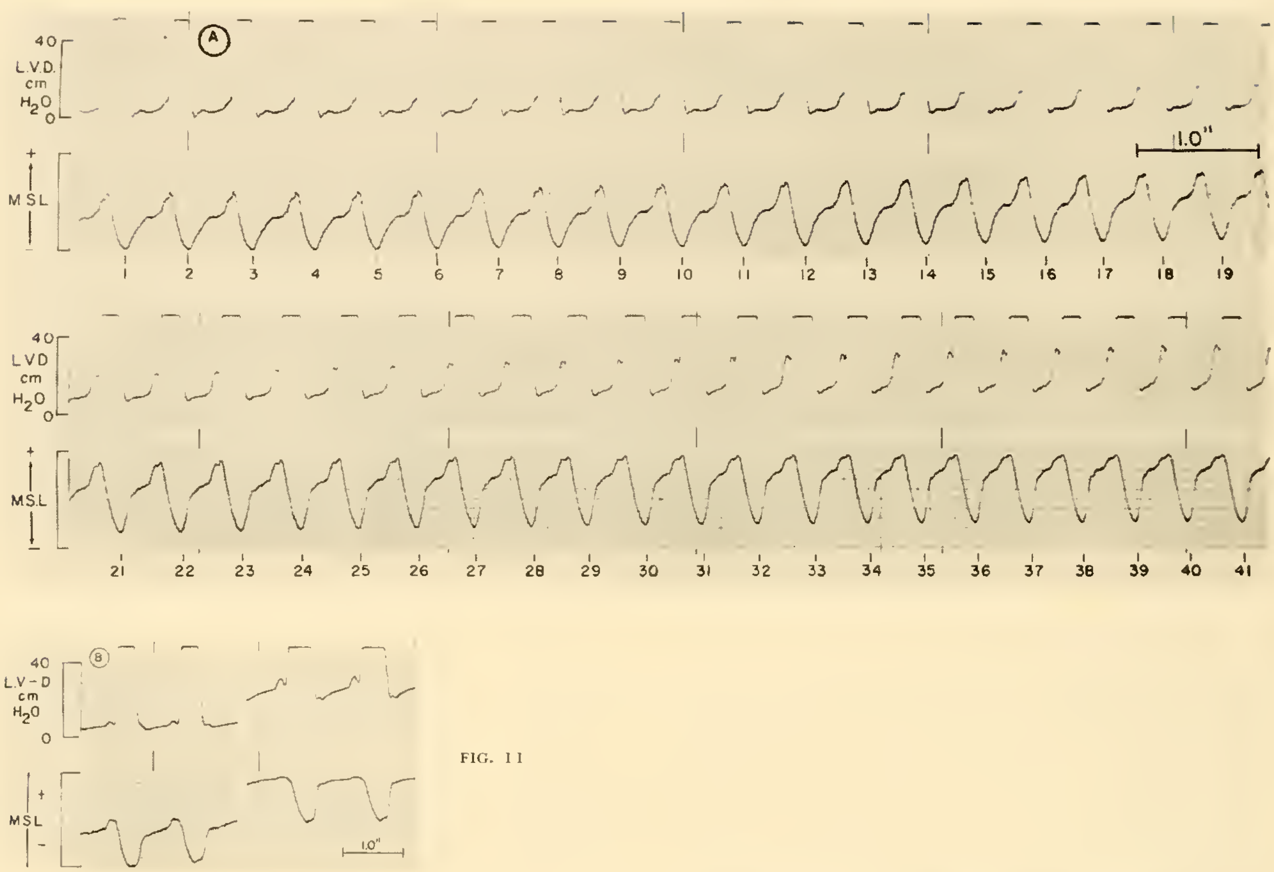

FIG. 11

and during stellate ganglion stimulation (*SS*). During stimulation a shift of the ventricular function curve to the left was observed when either mean left atrial pressure (VFC_{LA}) or left ventricular end diastolic pressure (VFC_{LV}) is plotted against stroke work just as when norepinephrine is administered (fig. 2).

The shortening of systole observed during stellate stimulation, while the ventricle produces an increased work from any given end diastolic pressure, indicates a greater increase in stroke power than in stroke work. In the experiment shown in figure 13*B*, during stellate stimulation the shortened duration of ventricular systole from any given end diastolic pressure was such that the increase in power was an average of 25 per cent greater than the increase in work. The increase in stroke work produced during stellate stimulation is consistently accompanied by a shortening of systole (105).

Figure 14*A* demonstrates the type of response obtained when applying frequency graded stimulation to the left stellate ganglion. The heart rate was held constant by atrial pacing. The rami to the right stellate ganglion and both vagi were sectioned. The

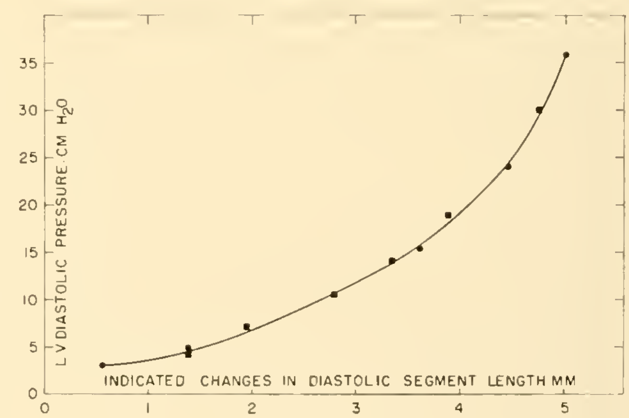

FIG. 12

isolated left stellate ganglion was stimulated at 7 volts with an impulse duration of 10 msec. The number at the top of each segment of tracing shows the impulse frequency used. Each time the stimulus frequency (with supramaximal voltage) is increased from zero up through 4 per sec, the fall in left and right atrial pressures and the rise in aortic pressure is accompanied by an increased cardiac output and, since heart rate is held constant, by a proportional

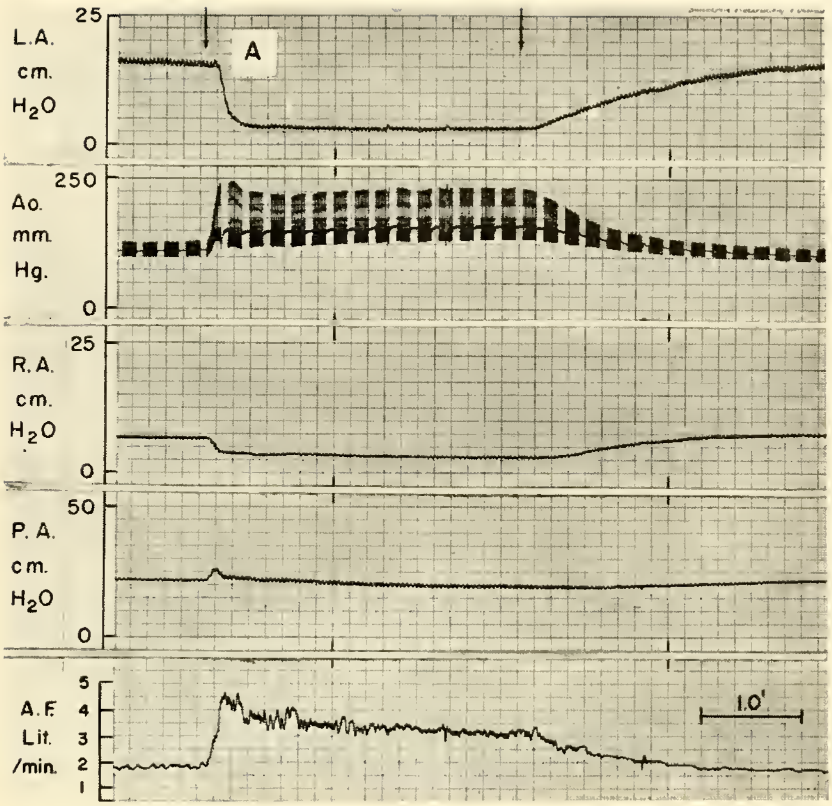

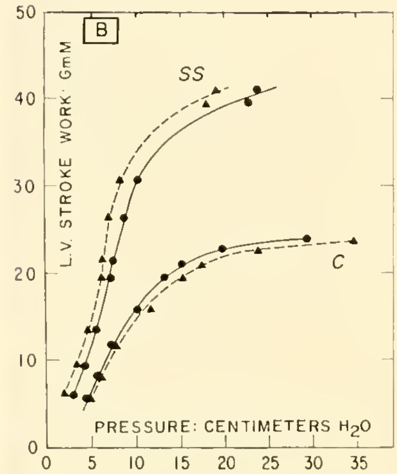

FIG. 13. LA = mean left atrial pressure, RA = mean right atrial pressure, PA = mean pulmonary artery pressure, AF = total aortic flow (cardiac output minus coronary flow).

increase in stroke volume. The calculated external ventricular stroke work thus rises with each increase in stimulus frequency while mean atrial pressure falls. The same type of result is also obtained when the stimulus voltage is varied from zero to the level of maximal response while the stimulation frequency is held constant.

At the end of the series of observations shown in the left panel of figure 14*A*, stellate stimulation was stopped and an interval of 6 min allowed to pass; during this period each of the hemodynamic values returned to control levels. An infusion of 100 ml of blood was then made. This resulted in a modest elevation of atrial and arterial pressures, cardiac output, stroke volume, and stroke work, as can be seen by comparing the first segment of the left panel of figure 14*A* (before infusion) with the first segment of the right panel (after one infusion). The same series of frequency graded stimuli were then once again applied with the results seen in the right panel of figure 14*A*. This sequence of interventions was repeated until six sets of six points each were obtained. Heart rate was held constant throughout.

The plot of mean left atrial pressure against left ventricular stroke work (VFC_{LA}) resulting from these data is shown in figure 14*B* (left). The number adjacent to each curve indicates the stimulus frequency. Worthy of note is the magnitude of the changes in the ventricular work produced at a given mean left atrial pressure level under the influence of left stellate stimulation (especially since only a portion of the cardiac sympathetic nerves were stimulated) and also the systematic manner in which the position of the curve shifts with the change in the frequency of cardiac sympathetic nerve stimulation. One hour and fifteen minutes later the experiment was repeated, and the resulting curves are shown in figure 14*B* (right). The effects of left stellate stimulation on the performance of the right ventricle (VFC_{RA}) are similar to the effects observed on the left ventricle (105).

It remained to be demonstrated whether the systematic alteration in myocardial contractility produced by an increasing frequency of cardiac sympathetic nerve stimulation is accompanied by a graded liberation of catecholamine in the heart. Recently acquired data (109a), from a type of experiment in which

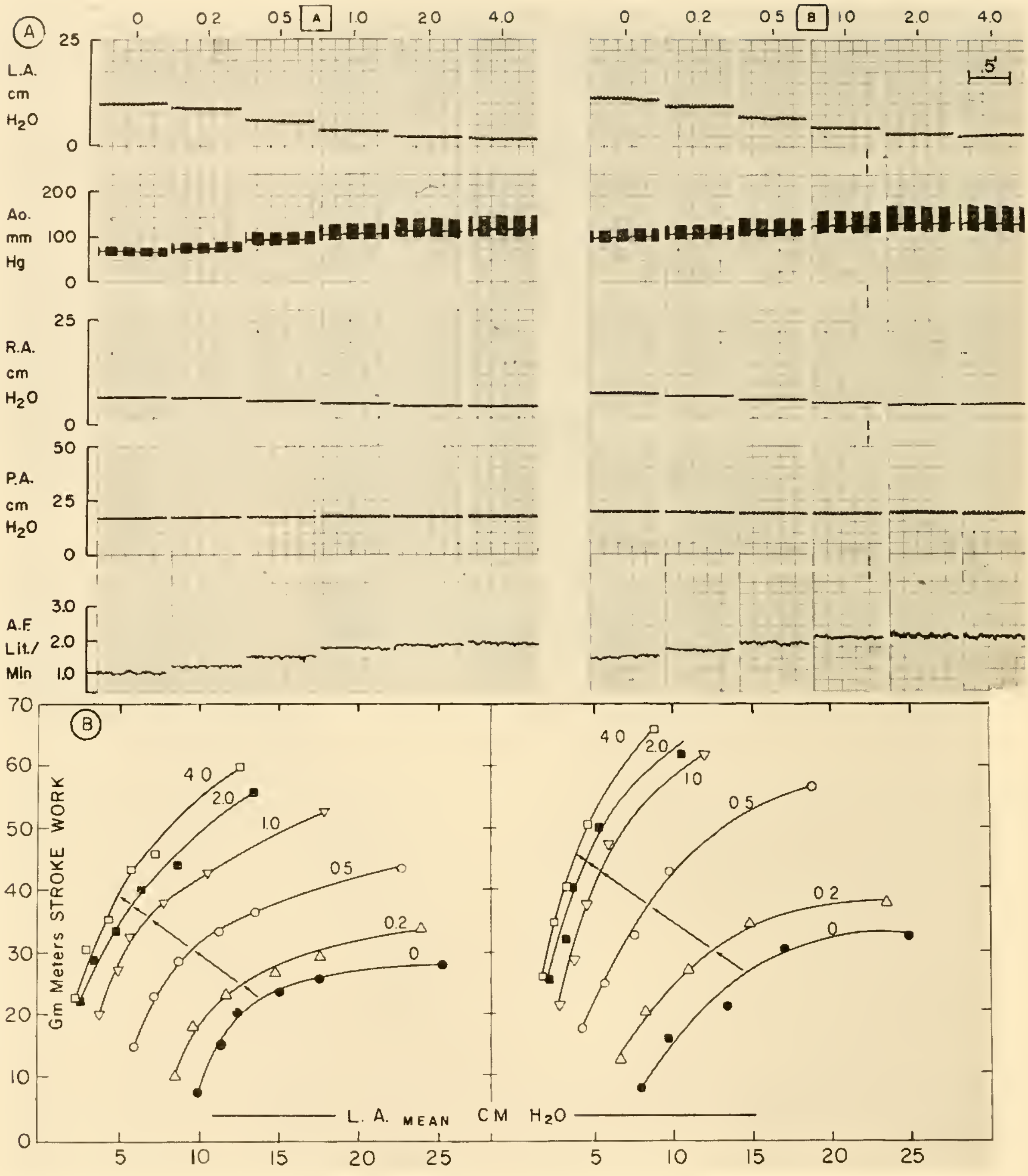

FIG. 14

cardiac output and heart rate are held constant and the total coronary venous outflow is metered, sampled, and analyzed by the trihydroxyindole technique of Lund (61), as modified by Crout (31), show clearly that a graded increase in the frequency of cardiac sympathetic nerve stimulation produces a graded increase both in the coronary venous concentration and total efflux of catecholamine from the heart. It seems not unreasonable to assume that there is a similar directional variation of catecholamine concentration in the myocardium as the stimulation frequency is increased.

END DIASTOLIC PRESSURE-LENGTH RELATION. As shown above, the administration of catecholamines or cardiac nerve stimulation increases the vigor of ven-

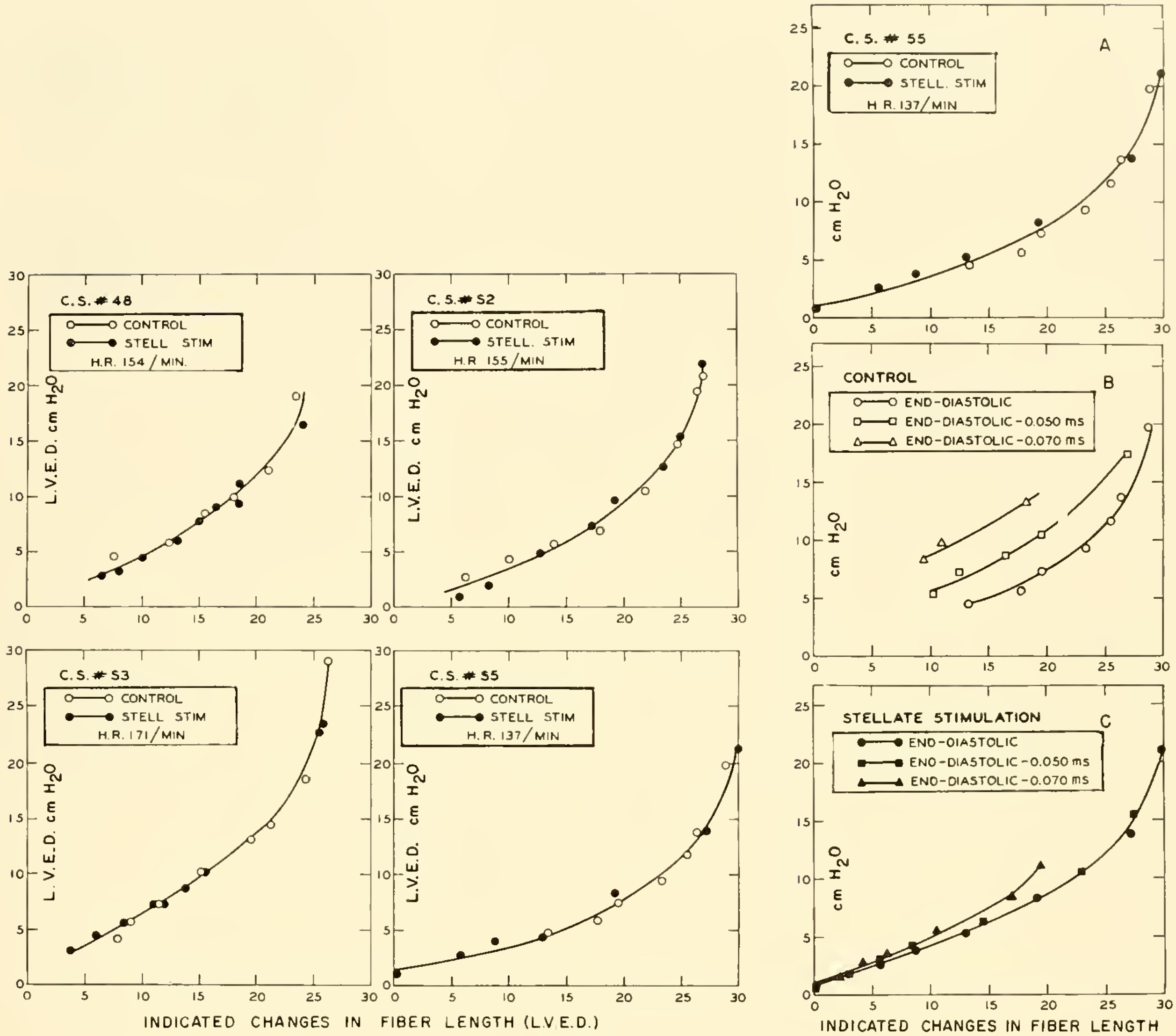

FIG. 15

tricular contraction and the ventricle will, under these influences, contract more forcefully from any given filling or end diastolic pressure as shown in figures 13 and 14. The early studies of Anrep (3) and other more recent studies (28, 29, 55, 96, 105) indicate that a changed myocardial extensibility cannot, of itself, account for the increased ventricular contraction. However, whether or not the augmented stroke work is produced solely by a more forceful contraction from a given end diastolic fiber length, or whether a change in the relation between ventricular end diastolic pressure and fiber length contributes to the observed augmentation, has only recently been established (67). In figure 15 (left) curves are shown comparing the relation between changes in left ventricular diastolic pressure and simultaneous changes in myocardial segment length at the end of diastole (after atrial systole) before and during stellate stimulation in four dogs. Figures on abscissae represent millimeter deflection on tracing. A 1-mm segment length change was equal to a 6-mm tracing deflection. The relation between left ventricular end diastolic pressure and segment length is unmodified by stellate stimulation at the heart rates studied. The same results were obtained when plotting the pressure-length curves from points in diastole prior to atrial systole (at or near equilibrium) before and during stellate stimulation when an adequate diastolic period was present (67).

It must, however, be emphasized that the relation between ventricular pressure and myocardial segment length at end diastole may involve factors

in addition to extensibility. The term extensibility refers to the change in length of a segment of myocardium when subjected to stress (uniform distending pressure). It is concerned with a static property of the tissue under examination and does not vary with the rate of application of stress (118). If diastole is abbreviated, the relation between pressure and segment length may also be determined by whether full relaxation has taken place and the extent to which inertial and viscous factors have been dissipated. Thus, when diastole is curtailed, the myocardial segment length may be shorter for any given ventricular end diastolic pressure even though no change in the extensibility of relaxed ventricular myocardium has taken place.

It was consistently observed that, at any given heart rate, stellate stimulation provided for the earlier onset of ventricular relaxation as the result of a shortened systole. Such sympathetic activity thus allowed a longer interval for ventricular relaxation to become complete before the onset of the ensuing systole. Figure 15 (right) shows data from an experiment which emphasizes the importance of this phenomena. In panel *A* the relation between left ventricular end diastolic pressure and changes in myocardial segment length was not altered by stellate ganglion stimulation. In the absence of stellate stimulation (panel *B*), 50 msec prior to systole the myocardial segment was substantially shorter at any given pressure and this effect was even more marked at 70 msec prior to the onset of systole. During stellate stimulation (panel *C*), 50 msec prior to the onset of systole, there was no change in the pressure-length relation and at 70 msec prior to systole the myocardial segment was only slightly diminished in length at any given pressure. It can be assumed that, in this experiment, had the heart rate or stroke volume been increased or the heart further depressed (14) to a point where diastole was shortened, by as little as 50 msec, the relation between pressure and segment length at the end of diastole would have shifted to the left (as shown in panel *B*). Subsequent stellate stimulation would have appeared to produce an increased ventricular diastolic extensibility whereas, in fact, by shortening systole, it would simply have permitted time for inertial and viscous factors to be dissipated and for relaxation to be complete. That this is an important operative consideration is indicated by the tracing in figure 16. In this study both stellate ganglia were isolated, and the atrium was paced at 210 per min throughout. In the left panel, with the heart deprived of sympathetic efferents from both stellate ganglia, the mean aortic pressure was 138 mm Hg, stroke volume 9.2 ml, and left ventricular stroke work 17.3 g-m. Diastole was limited to 69 msec out of a total cycle time of 296 msec. In the right panel during left stellate ganglion stimulation the mean aortic pressure was 155 mm Hg, stroke volume 12.4 ml, and left ventricular stroke work 26.1 g-m. Thus, left stellate ganglion stimulation not only increased the force of contraction from a lower end diastolic pressure but doubled diastolic time, thereby increasing the time available for a more complete ventricular relaxation. This problem has been well formulated by Buckley *et al.* (18–20), who described the observed phenomena in terms of mechanical impedance (ratio of ventricular pressure to ventricular inflow). In the isolated mammalian ventricle, norepinephrine was found to decrease mid-filling impedance and to provide a lengthened time available for filling when impedance was at its lowest. The data shown in figures 15 and 16, wherein the observed changes were induced by stellate stimulation, are compatible with the findings of Buckley and indicate that sympathetic pathways are capable of producing the same type of change in the *in situ* heart.

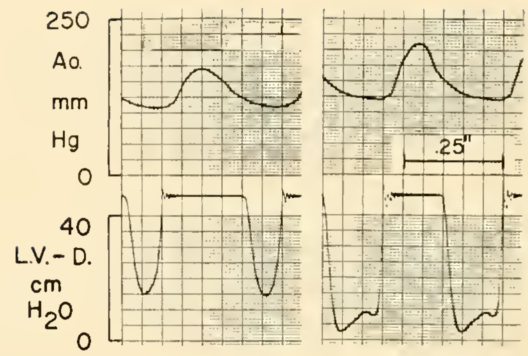

FIG. 16

These findings are also consonant with the studies of Lundin (62) on isolated frog muscle bundles, with those of Ullrich (119), who used the isometrically contracting canine left ventricle, and with the more recent studies of Rosenbleuth *et al.* (81) on the canine right ventricle. They are also in agreement with the observations of Blinks (10a), who found no change in the pressure-volume relation of isolated mammalian atria when exposed to concentrations of epinephrine which produced a marked positive inotropic effect. The results shown above appear to be at variance with the experiments of Rushmer *et al.* (84, 87), who found an increased "distensibility" during epi-

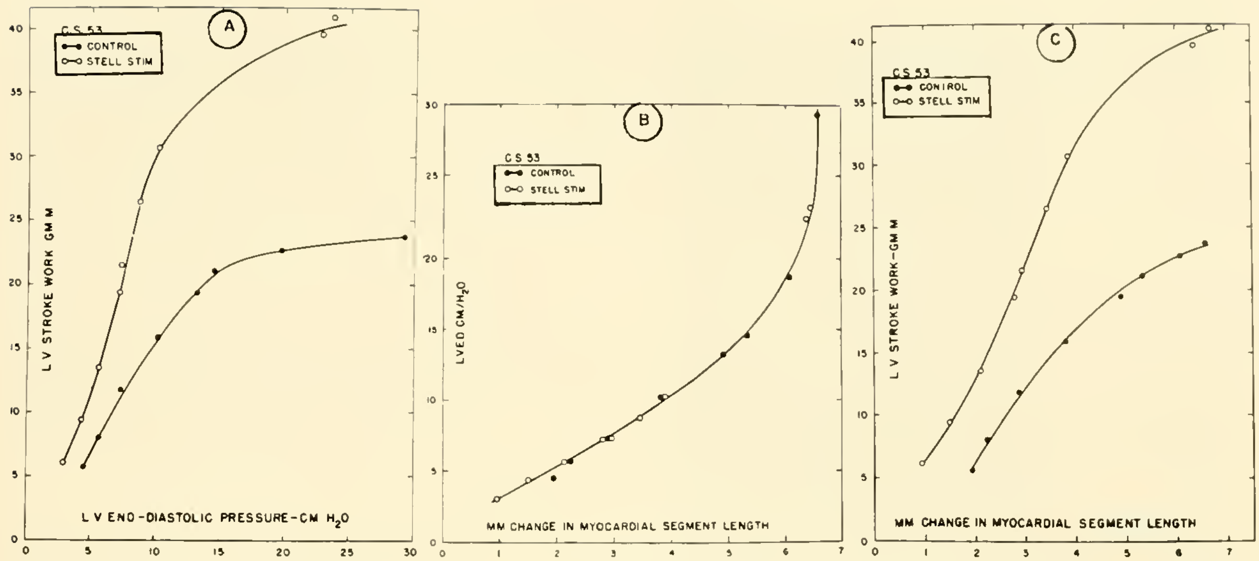

FIG. 17

nephrine infusion, and with those of Katz *et al.* (54), who suggested that norepinephrine produced an "increase in ventricular diastolic tone."

The shortening of systole and the consequent lengthening of diastole resulting from sympathetic stimulation would appear to be of great importance at high rates and/or large stroke volumes, since both tend to shorten the ratio of diastole to total cycle time (14, 60, 79). The positive inotropic effect of sympathetic efferent impulses and the consequent shortening of systole is, therefore, a most appropriate concomitant of the tachycardia induced by sympathetic chronotropic influences, since the positive inotropic effect provides means whereby the "normal" ventricular pressure-length relation is more likely to be retained at high heart rates. Such a view is reminiscent of the 1920 studies of Wiggers & Katz (125), who found that the length of systole during accelerator nerve stimulation and during the action of epinephrine was markedly less than that indicated by the theoretical curve for what these values should have been at the increased rates. They concluded "that the accelerator nerves have a specific effect on the ventricular musculature which operates to reduce the contraction period."

The lack of a change in the relation between ventricular end diastolic pressure and myocardial segment length during stellate stimulation (when diastole is initially adequate) shows that, under such stimulation, the ventricle contracts more forcefully from any given fiber length as well as from any given ventricular end diastolic pressure (67, 105). This is depicted in figure 17 which shows *A:* the relation between LVED pressure and LV stroke work before (solid circles) and during (open circles) stellate ganglion stimulation, *B:* the relation between changes in LVED pressure and changes in myocardial segment length before (solid circles) and during (open circles) stellate stimulation, *C:* the work produced from any given myocardial segment length before (solid circles) and during (open circles) stellate stimulation. In this study heart rate was held constant by atrial pacing and both vagi had been sectioned. Data for the curves shown in panels *A*, *B*, and *C* were obtained simultaneously.

More complete systolic emptying from any given end diastolic pressure or length during stellate ganglion stimulation is evident from the results described above; i.e., stellate stimulation induced the delivery of a substantially greater stroke volume as well as stroke work from any given left ventricular end diastolic segment length or pressure. This observation is in support of the early experiments of Anrep (3), and of Patterson (71), the clearly stated position of Starling (112, 114), the experiments of Cotten & Maling (28), the series of studies by Rushmer and his colleagues (84, 85, 88–91), and the recent oncometer experiments of Kelso & Randall (55) as well as earlier experiments from that laboratory (77, 80).

SYNCHRONICITY OF VENTRICULAR CONTRACTION. Unlike a piston pump in which the positive stroke produces an elevated pressure in a rigid housing,

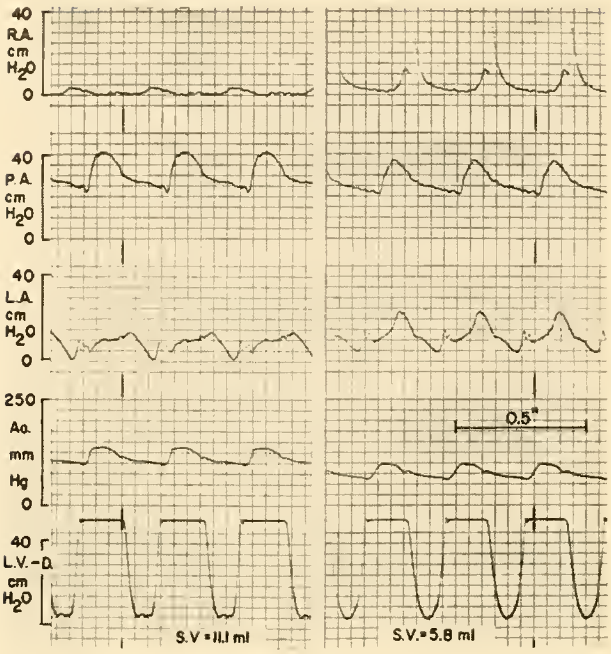

FIG. 18

pressure in the heart is produced by the sequential and progressive development of tension in the various segments of the myocardium which comprise the pump chamber while other segments are as yet uncontracted and are readily extensible. When these segments contract independently of any programmed sequence, no external work is accomplished as, for example, with ventricular fibrillation. Conversely, the extent to which the myocardial fibers contract synchronously will influence the external work produced when the over-all stimulus to the contraction of each fiber is constant. A corollary of this is that a greater stimulus to contraction (fiber length) would be required to produce the same external work when the contraction is less synchronous than when it is more so.

Figure 18 shows the results of an experiment in which the stimulus was abruptly shifted from the atrium to the ventricle. Heart rate and catecholamine background were not altered. During atrial stimulation (left panel) the duration of ventricular systole (from the beginning of ventricular systole to the aortic incisura) was 190 msec, stroke volume 11.1 ml, stroke work 18.3 g-m, and the rate of doing work 96.4 g-m per systolic second. In contrast, during ventricular stimulation (right panel) the duration of ventricular systole was 220 msec, stroke volume 5.8 ml, stroke work 5.8 g-m, and the rate of doing work 26.4 g-m per systolic second. These observations are consonant with those findings (50) indicating that the conduction velocity in the bundle of His is substantially greater than that in nonspecialized conducting tissue (16). The more leisurely and well-defined diastolic interval and the shorter period required for systole (especially in relation to the stroke volume, stroke work, and stroke power produced), when the ventricle contracts more synchronously, are noteworthy. This type of experiment, in which the observed changes were induced without altering the catecholamine background, indicates the extent to which influences which alter synchronicity can modify the external stroke work and stroke power produced from any given end-diastolic pressure as the result of modifying the rate of development of tension in the myocardium.

If this explanation is correct, namely, that the degree of synchronicity with which the ventricle contracts can appreciably modify the external stroke work and stroke power it produces from any given end diastolic pressure, then these data may aid in the interpretation of the altered ventricular dynamics observed when sympathetic stimulation is applied. For, when cardiac sympathetic stimulation results in more external stroke work and power being produced from any given end diastolic pressure or fiber length, and the rise and fall of ventricular pressure are steeper, the ventricular contraction gives every appearance of being a more synchronous one. In view of the fact that there is a more rapid propagation of the wave of depolarization during catecholamine stimulation (16), it is to be suspected that an increased synchronicity is contributing to the observed findings, making it unwise to consider the altered performance to be due solely to increased contractility of each fiber. From the findings in figure 18 it is to be expected that the VFC_{LV} as well as VFC_{LA} would be shifted to the right when the heart is paced by ventricular rather than by atrial stimulation, and evidence that this is so has recently been obtained (42a).

B. Influence of Cardiac Sympathetic Nerve Stimulation on the Atrium

Evidence which indicates that the atrium as well as the ventricle contracts with more vigor during sympathetic stimulation is shown in figure 19. In figure 19 (upper) are left atrial, left ventricular diastolic, and aortic pressure tracings from a dog in which atrioventricular block had been surgically induced. The atrium was paced at a constant rate. The control tracing is the left panel and that during

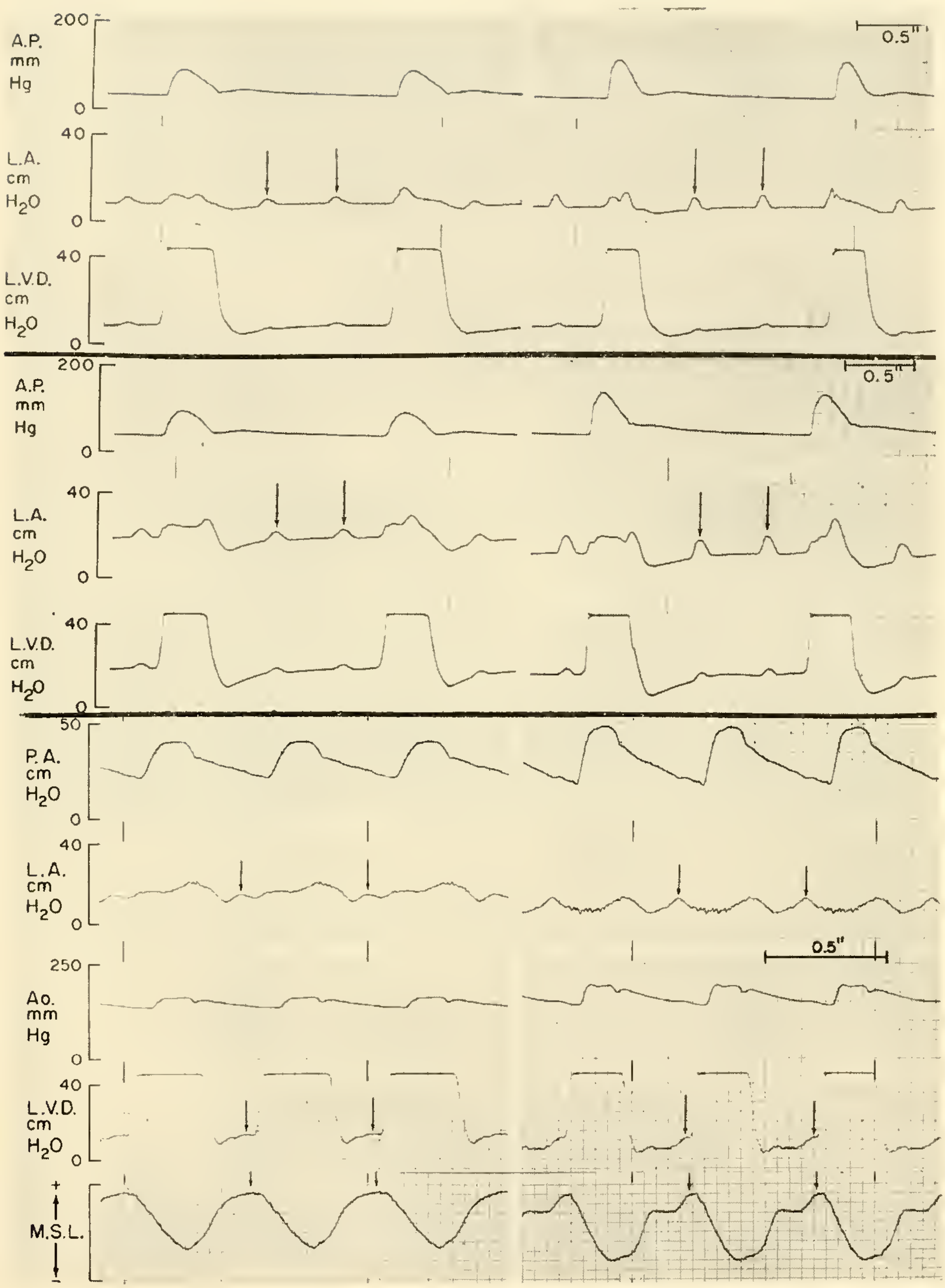

FIG. 19. LA = left atrial pressure; PA = pulmonary artery pressure.

stellate ganglion stimulation is the right panel. An increased amplitude of the atrial "a" wave contour is observed during stellate stimulation. It is also observed that the duration of atrial systole is shortened suggesting that atrial as well as ventricular power is augmented by sympathetic stimulation. The same results are obtained after the intravenous administration of norepinephrine (fig. 19, middle). The left tracing is the control study, and the right tracing during the intravenous administration of norepi-

TABLE 1. *Changes in Cardiac Cycle Due to Stellate Ganglion Stimulation Heart Rate Constant at 116/min** (*Total cycle time = 520 msec*)

	Control	Stellate Stimulation	Change
			%
Duration of atrial systole, msec[a]	120	87	−28
Duration of ventricular systole, msec[b]	270	207	−23
Duration of ventricular diastole, msec[c]	250	313	+25
A-R interval, msec[d]	495	365	−26
Increment in LVED (cm H_2O) produced by atrial systole	2.0	6.5	+225
Duration of isometric contraction msec[e]	105	55	−48
Relaxation time, msec[f]	93	75	−19

* Analysis of tracing shown in fig. 19 (lower).
[a] From beginning of increase in atrial pressure until beginning of rise in ventricular pressure. [b] From beginning of rise in ventricular pressure until aortic incisura. [c] From beginning of aortic incisura to the rise in ventricular pressure. [d] A-R interval; from beginning of rise in atrial pressure to lowest point of ventricular diastolic pressure ("relaxation point"). [e] From beginning of rise in ventricular pressure until beginning of rise in aortic pressure. [f] From aortic incisura until lowest point of ventricular diastolic pressure.

nephrine. In the tracings shown in figure 19 (lower) mild efferent vagal nerve stimulation was used so as to slow the normally conducting paced heart to a rate approximating that of the unanesthetized resting dog. This mild vagal activity was held as a constant background throughout the course of the experiment. The control tracing is at the left; that during stellate stimulation is at the right. In each tracing the arrows indicate the left atrial "a" wave, the atrially induced increase in left ventricular end diastolic pressure, and myocardial segment length. Table 1 shows the values for each of the components analyzed. It is clear from these tracings that during stellate stimulation the atrial contraction produces a larger end diastolic increment of both ventricular pressure and segment length. The greater rise in end diastolic ventricular pressure can only be attributed to the more vigorous atrial contraction; the greater elongation of the myocardial segment is attributable not only to the more forceful atrial contraction but also to the lower position on the ventricle's pressure-length curve (fig. 12) brought about by the more complete systolic emptying in the previous beat.

C. *Influence of Efferent Vagal Nerve Stimulation on the Ventricle*

Some of the hemodynamic consequences of efferent vagal nerve stimulation, while the heart rate is maintained constant by atrial pacing, are shown in figure 20 (upper left). During periods of stimulation of the distal cut end of the left vagus nerve (signals at *A* and *B*) mean right and left atrial pressures rise while aortic pressure, cardiac output, and stroke work fall. That the magnitude of the response is a function of the vagal impulse frequency used is shown in the data in figure 20 (upper right); the observed responses increase in a stepwise manner as the stimulation frequency is increased from 0 to 6 per sec. These effects are blocked by the administration of atropine. It should be noted that the carotid sinus pressure was maintained constant throughout the course of this experiment in order to control the reflex sympathetic influences emanating from this area (see section III).

These data could be explained in three different ways: *1*) that despite the lack of available anatomic evidence for vagal innervation of the ventricle (32, 70) vagal stimulation can in some way influence the force of ventricular contraction from any given end diastolic pressure; *2*) that changes in mean left atrial pressure do not, during vagal stimulation, indicate similar directional changes in left ventricular end diastolic pressure; or *3*) that changes in left ventricular myocardial extensibility during vagal stimulation could account for the observed phenomena. The last possibility has been excluded by observations showing that vagal nerve stimulation does not modify the end diastolic pressure-length curve (67). Relevant to number *2*, experiments have been done in which data were gathered in such a manner as to relate both mean left atrial pressure and left ventricular end diastolic pressure to the stroke work of the left ventricle before and during vagal stimulation (105). The results of one such experiment are shown in figure 20 (lower). In panel *A*, the relation of left ventricular end diastolic pressure and left ventricular stroke work before (solid circles) and during (open circles) stimulation of the distal cut end of the left vagus nerve (6.7 volts, 15 per sec) is shown. No change in left ventricular contractility occurred, i.e., the left ventricle produced as much work from any given end diastolic pressure during vagal stimulation as without it. These observations are in accord with the apparent lack of vagal fiber distribution to the ventricular myocardium. Mean aortic pressure ranged from 58 to 165 mm Hg when the control values were obtained and

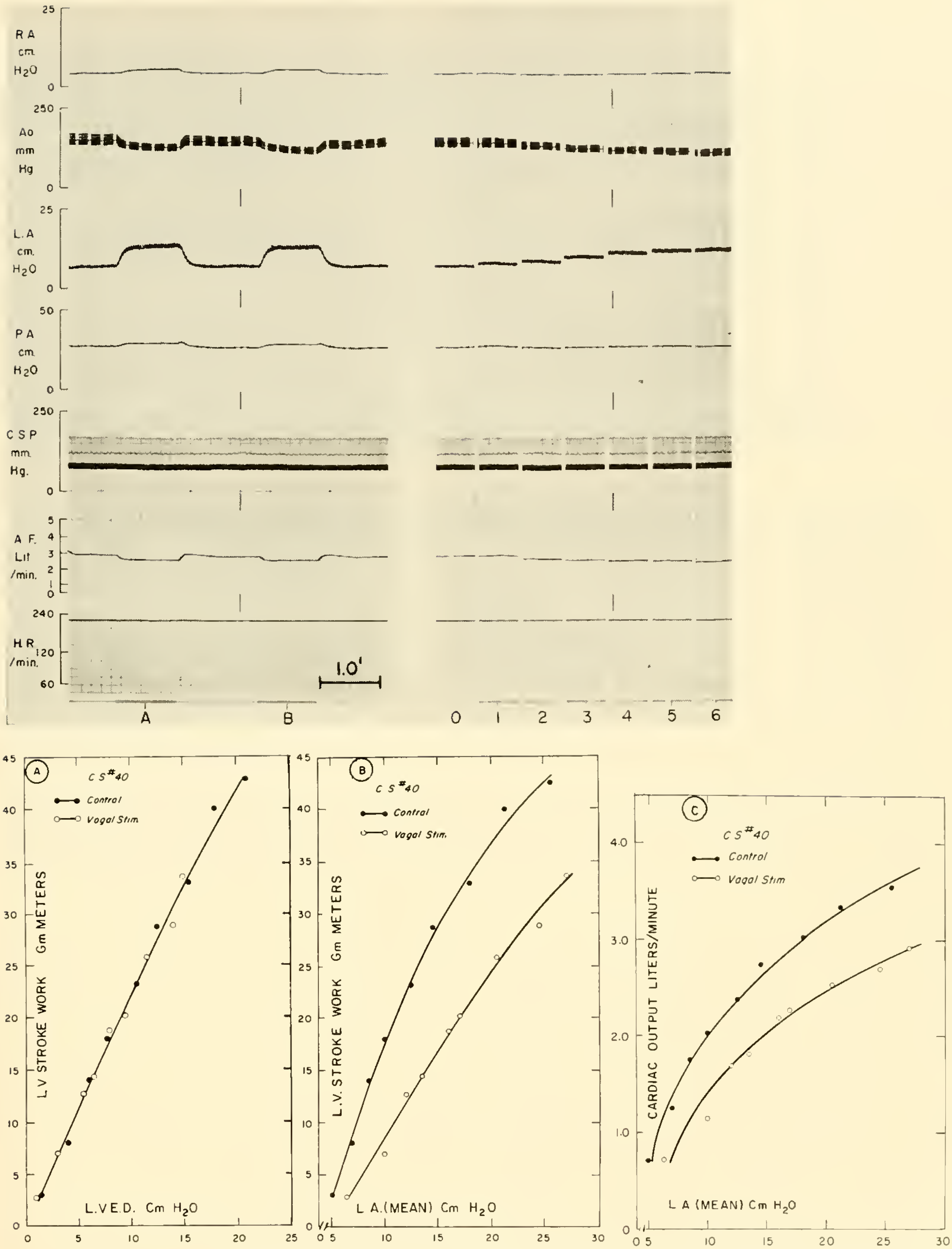

FIG. 20. CSP = carotid artery pressure (maintained constant by bilateral carotid artery perfusion).

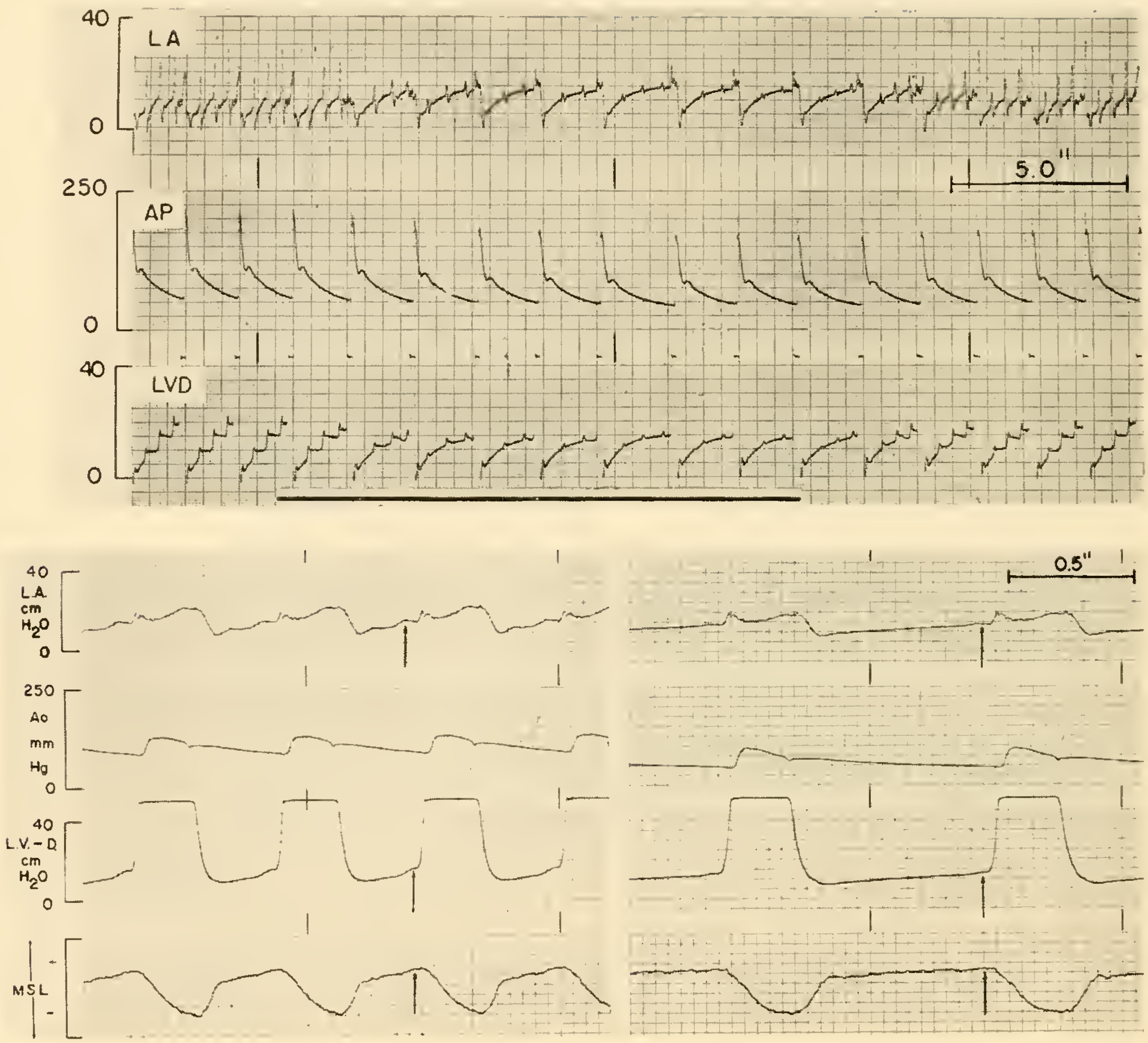

FIG. 21. LA = left atrial pressure.

from 54 to 156 mm Hg while the vagus was stimulated. In panel *B*, the relation between mean left atrial pressure and stroke work (VFC_{LA}) was shifted to the right. Schreiner *et al.* (109) did not find evidence that efferent vagal stimulation altered the relationship between mean atrial pressure and stroke work and concluded that such stimulation does not modify the contractility of the ventricle, a conclusion reaffirmed by the above experiments. It is not entirely clear, however, why they did not obtain a higher mean left atrial pressure for any given level of left ventricular stroke work as shown in figure 20.

The above experiments on vagal stimulation are not consonant with the experiments of Wang *et al.* (122) or with the suggestion of Peterson (74) that vagal fibers produce a negative inotropic effect on the ventricle. They do support the recent observations of Carlsten *et al.* (21) in man suggesting that vagal stimulation does not influence the ventricular myocardium and are in essential agreement with the experiments of Gesell (42), who attributed the changes in arterial pressure during vagal stimulation to the diminished contribution of the atrium to ventricular filling.

D. Influence of Efferent Vagal Nerve Stimulation on the Atrium

In view of the above it appeared worthwhile to make a direct and detailed re-examination (42, 124)

of the extent to which vagal stimulation can alter atrial contractility. This was done in hearts both with and without heart block. Figure 21 (upper) shows the changes induced in the amplitude of the atrial "a" wave and the consequent changes in left ventricular diastolic pressure before, during, and after distal vagal nerve stimulation in a heart block preparation. During stimulation indicated by signal at bottom, atrial pressure was higher and left ventricular pressure lower in late diastole in spite of a longer diastole. This response is also observed in the dog without heart block and in which the heart rate is either maintained constant or allowed to decrease during vagal stimulation as in figure 21 (lower). The control tracing is at the left, and the arrows in the third beat indicate the atrial "a" wave and the consequent increase in left ventricular end diastolic pressure and myocardial segment length. The tracing at the right is during stimulation of the efferent vagus nerve. In addition to the bradycardia produced in the unpaced heart, the atrial quieting also diminished the end diastolic augmentation of both the ventricular pressure and myocardial segment length.

E. Effect of Autonomic Nerve Stimulation on the Atrial Transport Function (Relation between Mean LA Pressure and LVED Pressure)

The atrium performs much like a booster pump, the function of which is to augment the transfer of fluid from the feed line into the primary or power-generating element of the system. There are two main consequences when the action of a booster pump is increased or decreased. The first is that more or less fluid will be forwarded into the main pump, provided that the latter does not have a stop which limits input. This effect was demonstrated in sections II B and II D. The second effect is that for a given input into the main pump, the pressure in the feed line behind the booster pump will be lower when the activity of the booster pump is increased and higher when booster pump activity is diminished.

The pressure in the atrium not only provides for the progress of blood into the ventricle but is also the central pressure head which must be exceeded by the pressure of the blood in the veins feeding into it. From the point of view of integrating the heart with the total organism it is, therefore, pertinent to inquire whether a change in the activity of the atrium modifies the mean pressure in it for any given end diastolic pressure, stroke work, and cardiac output (67a). Figure 22 shows the plot of mean left atrial pressure

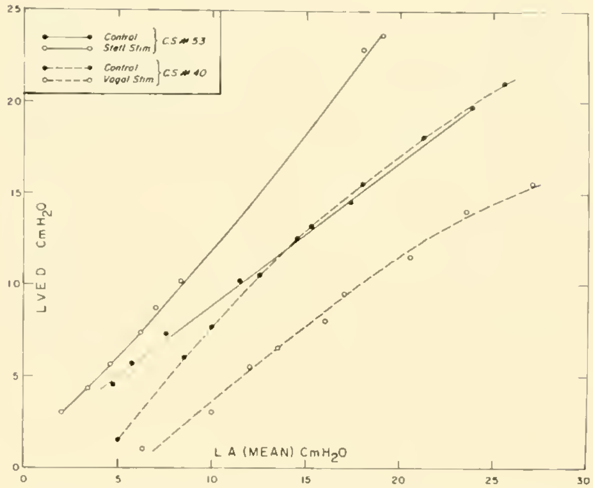

FIG. 22. LVED = left ventricular end diastolic pressure; LA (mean) = mean left atrial pressure.

against left ventricular end diastolic pressure before and during autonomic nerve stimulation. The continuous line joining solid dots shows the relation during a control run in which mean left atrial pressure, left ventricular end diastolic pressure, and stroke volume were intermittently increased by the infusion of blood. The continuous line joining open circles shows the effect of left stellate ganglion stimulation on this relation. The dashed line joining solid dots shows the control curve in another experiment and the dashed line joining the open circles shows the effect of efferent vagal nerve stimulation on this relation. During cardiac sympathetic nerve stimulation the mean left atrial pressure is lower for any given left ventricular end diastolic pressure than in the control run. Conversely, during efferent vagal nerve stimulation the mean left atrial pressure is higher for any given left ventricular end diastolic pressure than in the control run. Changes in atrial contractility contribute substantially to these altered relations. At any given heart rate during cardiac sympathetic nerve stimulation the atrium contracts more vigorously and empties more completely. This decreases residual atrial volume and places the atrium on a lower portion of its pressure-volume curve, so that for any given ΔV it requires a smaller ΔP. Conversely, during efferent vagal nerve stimulation atrial contractility is decreased and emptying is less complete. Therefore, residual atrial volume is increased, and the atrium is placed on a higher portion of its pressure volume curve, thus requiring a large ΔP for any ΔV. Further, the shorter the time required for atrial systole, the longer the period during which the atrium will be relaxed and therefore more

distensible. The net results of these altered atrial dynamics are shown in figure 21 (upper). During efferent vagal nerve stimulation the atrial "a" waves are diminished, the mean atrial pressure is increased, and ventricular end diastolic pressure decreased in spite of a longer diastole.

Whereas the relation between ventricular end diastolic pressure and stroke work is determined only by the performance characteristics of the ventricle, the relation between mean atrial pressure and stroke work is determined by the performance characteristics of the atrium as well as the ventricle. The importance of these considerations is exemplified by the plot of mean left atrial pressure against cardiac output in figure 20 (lower, panel *C*), an experiment in which it was demonstrated that efferent vagal nerve stimulation had no effect on the performance characteristics of the ventricle (fig. 20, lower, *C*). When the transport function of the atrium was inhibited by vagal stimulation, mean left atrial pressure had to be 2 cm H_2O higher in order to maintain a cardiac output of 1 liter per min. At 2 liters per min it had to be 5 cm H_2O higher and at 3 liters per min it had to be 11 cm H_2O higher. Since such data indicate the importance of a normally functioning atrium, it invites consideration of the possibility that when an elevated venous pressure is observed, failure of the atrium as well as the ventricle may be a contributing factor (67a).

F. Effect of Autonomic Nerve Stimulation on Closure of the Mitral Valve

The mechanism of closure of atrioventricular valves has not been one which can be described with certainty. One authoritative view (64) summarizes the present status with the statement "undoubtedly the most important factor in all valve closure is a change in polarity of the pressure differential across the valve orifice. In the case of the atrioventricular valves the rise in ventricular pressure (through contraction of the ventricle) above that in the atrium is the most important factor in closure." There is little basis for disputing McKusick's first sentence; the second one, as will be shown below, may be open to question.

Henderson & Johnson (47) in 1912, after studying excised heart valves, postulated that a ventricular systole not preceded by an atrial systole would produce regurgitation because the valve leaflets had not been apposed by the jet effect through the valve. Although we agree with the end result of their analysis we nevertheless concur with Wiggers' objection to their explanation (127). Evidence that the activity of the atrium is relevant to AV valve closure is to be found in the experiments of Prinzmetal *et al.* (76), who observed the atrium to enlarge after experimentally inducing atrial fibrillation. After inducing atrial fibrillation, Daley *et al.* (33) were able to recover from the atrium more of the dye which had been injected into the ventricle than during normal rhythm. The frequency of tricuspid regurgitation in patients with atrial fibrillation (69) also indicates the importance of atrial systole for AV valve closure. Although it may be objected that the hearts of such patients are diseased, this objection loses some of its weight when the regurgitation appears with the onset of fibrillation and disappears when normal sinus rhythm is re-established in the same patient (69).

From the point of view of both demonstrable evidence and the conceptual analysis of the problem, Little (59, 107) has contributed more to the understanding of tricuspid valve closure than any other single investigator. He observed that, subsequent to atrial systole, when pressure in the right atrium is falling, the pressure in the right ventricle is, after a brief decline, well maintained. Further, he appreciated the significance of his observations. However, even Little entertains a certain dichotomy in regard to this question for, although he does mention that "the reversal of the normal atrioventricular pressure gradient as a result of atrial relaxation results in at least a momentary backflow of blood into the atrium," he nevertheless concludes that "the increase in ventricular pressure resulting from atrial systole is sufficient to reverse the atrioventricular pressure gradient before the onset of ventricular contraction."

The tracings from the left atrium and ventricle shown in figures 10, 23, and 28 are relevant to this problem and afford the basis for a certain degree of conceptual simplification. In figure 10, which shows tracings from a ventricle on the low or sensitive part of its pressure-length curve, attention is drawn to the stepwise and plateau-like elevation of ventricular pressure after each atrial beat. Further, the sustained increase in ventricular segment length subsequent to each atrial systole is noteworthy. In figure 23*A* the upward arrow indicates the tracing of left atrial pressure, and the downward arrow indicates a superimposed tracing of left ventricular diastolic pressure. An unequivocal ventriculo-atrial pressure gradient, at times amounting to more than 8 cm H_2O, is established as a consequence of atrial systole and what must certainly have been mitral valve closure. As

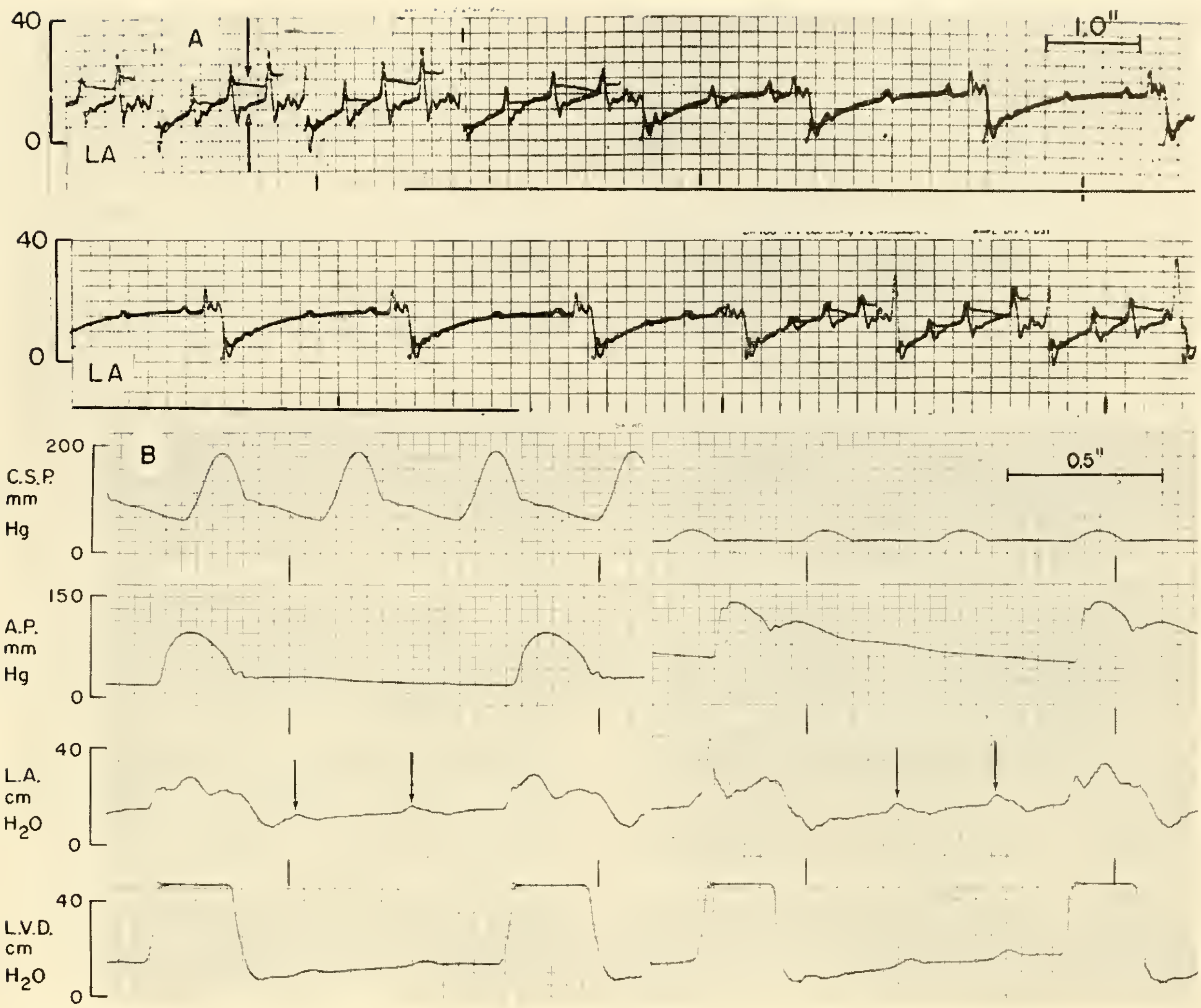

FIG. 23

can be seen, such closure took place in the absence of any ventricular activity. That mitral valve closure was a direct result of the consequences of atrial activity is clear from the subsequent portion of the same tracing. That is, the diminution of atrial systole during efferent vagal nerve stimulation (interval shown by the signal) eliminated the valve closure as evidenced by the abolition of the ventriculo-atrial pressure gradient. After cessation of vagal stimulation the original pattern returned.

When, in the dog with heart block, the control atrial and ventricular tracings are such as to indicate that mitral valve closure is not taking place after each atrial systole, atrially induced closure of the mitral valve can often be induced by stimulation of the stellate ganglion and the resulting augmentation of atrial systole. Although this is not a consistent finding, as can be seen from figure 19 (upper), it is frequently observed. Examples of atrially induced mitral valve closure by reflex sympathetic stimulation is shown in figure 23*B*. During carotid hypertension (sympathetic inhibition), evidence of atrially induced mitral valve closure was not present (left panel). When the carotid pressure was lowered (sympathetic stimulation), the pattern indicative of valve closure took place (right panel). Similar results are shown in figure 28. Figure 19 (lower) suggests that the ability of the atrium to induce mitral valve closure is not limited to conditions of atrioventricular dissociation. In the right panel of that figure, during stellate ganglion stimulation, the peak of atrial systole precedes the onset of ventricular systole by 60 msec, then declines substantially while

LVED and myocardial segment length remain increased until ventricular systole begins.

The ability to induce or abolish closure of the mitral valve by varying the activity of the atrium is strong evidence in support of Little's position (106a) that the atrium may be of importance to valve closure. We believe that the matter can be more simply expressed in terms of the rate of development of a ventriculo-atrial pressure gradient. Increasing the vigor of contraction of atrial systole not only increases the rate of the pressure buildup in the ventricle, but the atrium, like the ventricle, also relaxes more rapidly under sympathetic stimulation, thereby increasing the rate of decline of the pressure in it. These two factors combine to increase the rate of development of the VA pressure gradient and thus promote mitral valve closure.

G. Summary of Effects of Cardiac Autonomic Nerve Stimulation

The central nervous system has available direct efferent pathways to the heart over which it can, at any given heart rate, systematically regulate the ventricle's contraction by either of two means: *1*) It can control the atrial contraction over a wide range, augmenting the atrial contraction by sympathetic stimulation and diminishing it with vagal stimulation. The ventricle is thereby presented with more or less blood at the end of diastole, its end diastolic pressure and fiber length are modified, and a consequent alteration is made in the vigor of its contraction. This can occur in the absence of any change in the contractile characteristics of the ventricle. *2*) The central nervous system, by way of cardiac sympathetic efferents, can directly cause the ventricle to contract more or less forcefully from whatever end diastolic pressure and fiber length has been obtained. The magnitude of the observed changes is noteworthy.

A more precise appreciation of the net effect of sympathetic impulses on the heart beating at any given rate is as follows: the more forceful ventricular contraction resulting from sympathetic stimulation produces more complete systolic emptying and, consequently, a lower diastolic impedance to ventricular inflow, i.e., the more complete systolic emptying places the ventricle on a more sensitive portion of its ventricular pressure-length and pressure-volume curve. It is in this circumstance, in which even a small increase in pressure produces a larger fiber length increase, that a more vigorous atrial systole propels blood and elevates ventricular end diastolic pressure.

It remains to consider the altered timing of events which accompanies these phenomena. Reference is made to table 1 in which it can be seen that sympathetic stimulation substantially reduced the total period of the heart's active state (from the beginning of atrial systole to the "relaxation" point, i.e., lowest pressure in diastole). The shortening of the duration of each of the components of the heart's activity during sympathetic stimulation resulted in a longer ventricular diastole, thus allowing both a longer period for inflow and a longer interval during which ventricular relaxation can become complete. The cardiac sympathetic nerves may thus be construed, in an important sense, as the guardian of diastole, a view implicit in the experiments of Wiggers in 1927 (128).

The shorter the diastolic interval, the more important it is for blood to enter the ventricle at an increased rate, thus, not only does the contribution of atrial systole become most important at high heart rates, but it may in addition be expected that the extent to which the atrial systole becomes shorter as well as more forceful will also help to determine the extent to which it can contribute to ventricular filling under these circumstances.

The alteration of the mechanical events of the cardiac cycle consequent to sympathetic stimulation correlates well with observed electrical phenomena; that is, the increased conduction velocity observed in the atrium, at the atrioventricular node, and in the ventricle (16, 50). There is also a shortening of the total refractory period and, with administered catecholamines, an increased excitability (16). Since increasing the synchronicity of the ventricle's contraction results in the production of more stroke work and stroke power from any given LVED pressure (fig. 18), it would appear unwise to attribute the increased ventricular work and power produced under sympathetic stimulation solely to a direct effect of the catecholamines on the myocardial fibers without making allowance for the obvious increase in the synchronicity with which they contract. This aspect of ventricular performance is construed to be a matter of importance (42a, 105).

The net effect of efferent vagal impulses, at least with the intensities of vagal stimulation used in these experiments, was to diminish the vigor of atrial contraction; they did not directly modify ventricular contractility.

H. The Nervous Control of the Frank-Starling Mechanism: Principles of the Innervated Heart

As a formal means of broadening the basic Frank-Starling relationship and of integrating it with the

activity of the central nervous system in relation to acutely induced changes, two concise statements now appear to be appropriate for the heart operating at any given rate and aortic pressure, and in the absence of abnormal conditions such as hypoxia and acidosis. *1*) If the effective catecholamine stimulus remains constant, the contraction of the ventricle varies directionally with its end diastolic pressure and fiber length; if the end diastolic pressure and fiber length remain constant, the contraction of the ventricle varies directionally with the effective catecholamine stimulus. *2*) The central nervous system has direct neural connections to the heart by means of which it can vary the left ventricular end diastolic pressure and fiber length while keeping the effective catecholamine stimulus constant (atrial systole), means by which it can vary the effective catecholamine stimulus, or both.

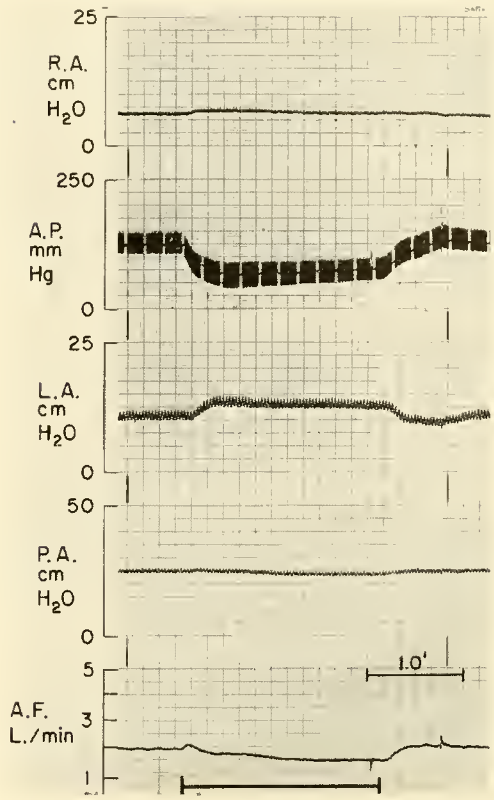

FIG. 24

III. INFLUENCE OF THE CAROTID SINUS ON THE PERFORMANCE CHARACTERISTICS OF THE HEART

The conventional view of the reflex function of the carotid sinus has been that it primarily influences heart rate and peripheral arteriolar resistance (49). That the carotid sinus can influence the pressure-volume relation of visceral veins was established by Alexander (2), whose position was supported by experiments with peripheral venous micro-balloons (94, 95, 102) and the definitive experiments of Bartelstone (8).

More recently, attention has been focused on the changes in the contractility of the ventricle and atrium which can be reflexly induced by carotid sinus stimulation (106).

A. Carotido-Ventricular Reflex

When either the right or left carotid sinus nerve is stimulated while heart rate is held constant, results like those shown in figure 24 are obtained. Bilateral cervical vagotomy had been done, therefore the changes observed can be attributed to a reflex alteration in sympathetic activity. The heart rate was held constant at 178 per min by left atrial pacing, and both carotid sinus nerves were stimulated at 3.5 volts, 25 per sec, and 5 msec impulse duration during the interval indicated at the bottom. During stimulation, mean left atrial pressure rises while aortic pressure, stroke volume, and calculated stroke work falls. The PA-LA pressure difference narrows. The directional changes observed are similar to those seen when stellate stimulation is withdrawn.

Using a preparation in which carotid artery pressure can be varied independently of systemic pressure (106), an examination can be made of the effects of changing carotid artery pressure on myocardial contractility while heart rate is held constant. In this study both vagi are sectioned in the neck, and both stellate ganglia are intact. In figure 25*A* the panel to the left (*A*, *B*, *C*, *D*) shows the hemodynamic effects of acutely changing carotid perfusion pressure (CSP). The changes in aortic flow which occur in the first 30 sec after the pump induced change in carotid pressure are not reliable. Initially, when the carotid pressure is high and pulse pressure large, aortic flow, aortic pressure, and left ventricular stroke work are low in the presence of an elevated left atrial pressure. When carotid perfusion pressure is lowered, aortic flow and pressure and left ventricular work rise substantially while mean atrial pressures fall. It is noteworthy that the increase in the left ventricular stroke work, even at a lower filling pressure, is several times the observed increase in peripheral vascular resistance. This result is a reproducible one and, as shown in the segmented panel at the right in figure 25*A* (*E*, *F*, *G*, *H*, and *I*), is a gradable effect. That is, the relation between filling pressure and external

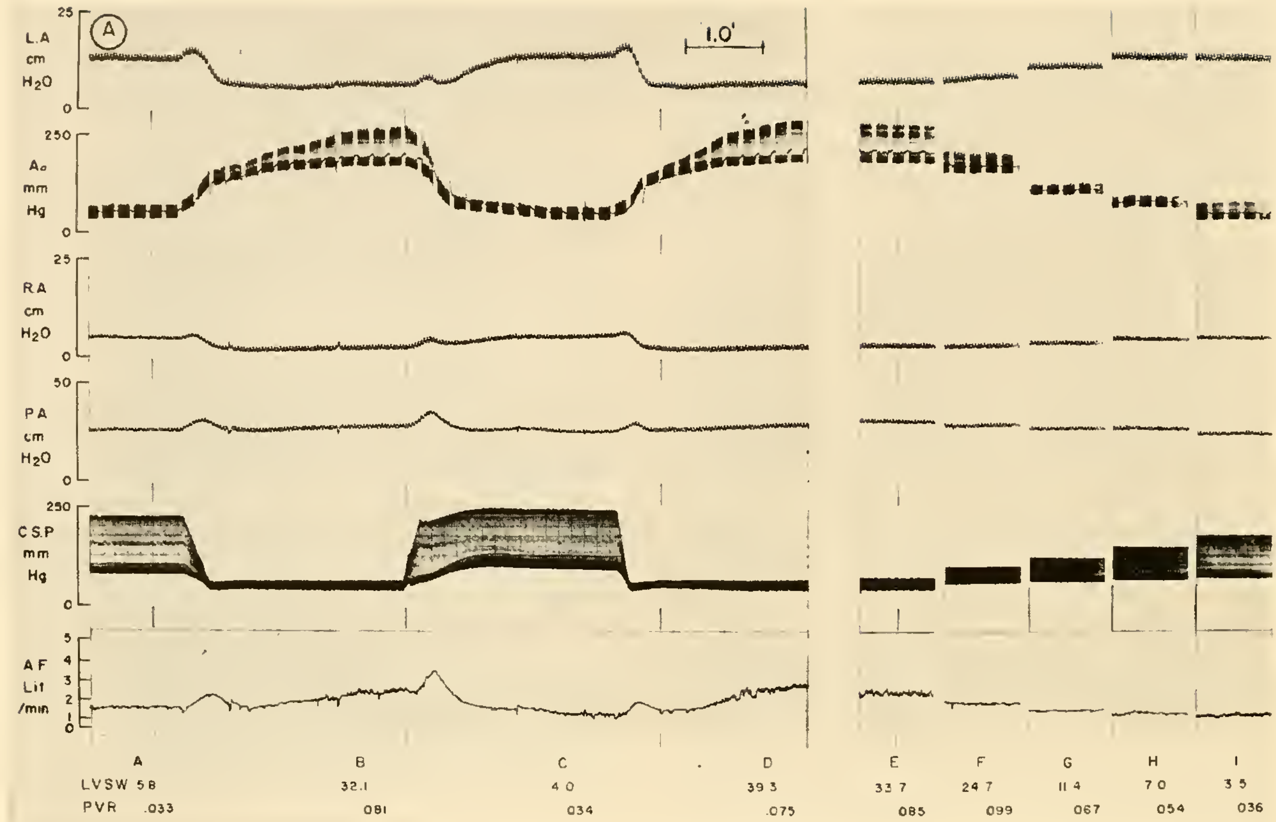

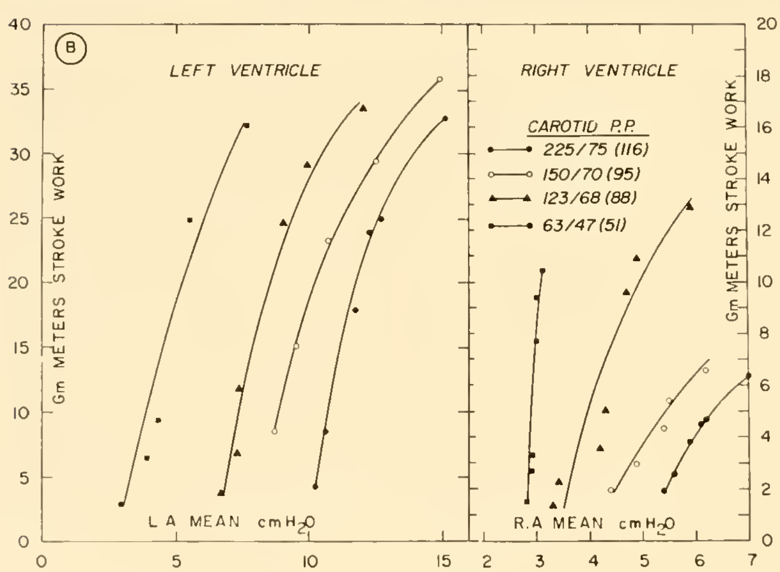

FIG. 25. CSP = carotid artery pressure (generated by pump). LA = mean left atrial pressure. LVSW = left ventricular stroke work. PVR = calculated total peripheral vascular resistance (mm Hg mean aortic pressure divided by aortic flow in ml/min).

stroke work can be reflexly manipulated in a stepwise manner by making graded changes in the carotid perfusion pressure in much the same way that comparable changes can be induced by grading the frequency of left stellate stimulation.

By using the type of sequence shown at the right in figure 25*A* and the same over-all approach used in the previously described experiments when examining the effect of graded stellate stimulation (fig. 14), the effect of carotid perfusion pressure on the position of the ventricular function curve (VFC_{LA}) can be observed. Figure 25*B* (left panel) shows that when the

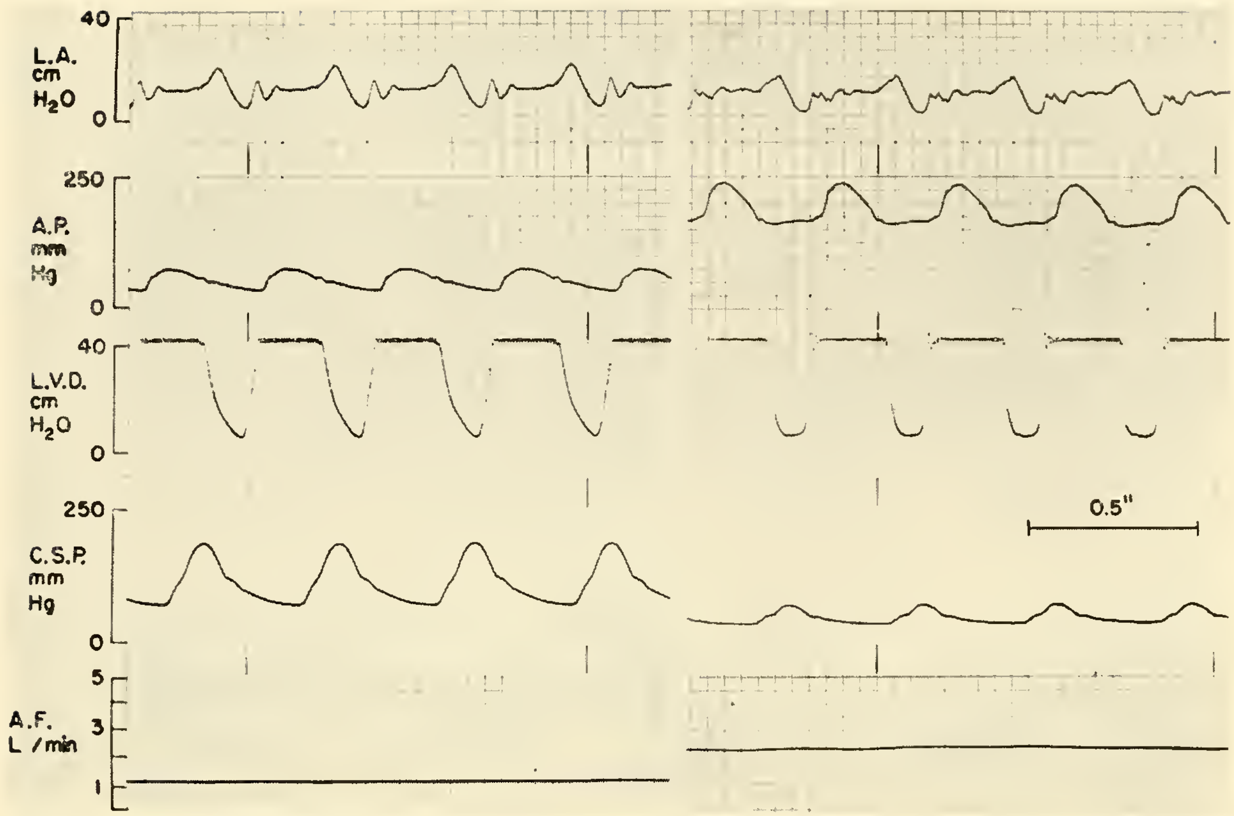

FIG. 26

carotid pressure is high, the VFC_{LA} is shifted to the right; when carotid pressure is low, the VFC_{LA} is shifted to the left. At intermediate carotid pressures, the VFC_{LA} is situated correspondingly. The carotid pressures and corresponding symbols are shown at the top (right). Once again, the magnitude of the observed changes in stroke work at any given mean atrial pressure is of interest. Figure 25*B* (right panel) shows similar results for the VFC_{RA}.

As shown above, at any given heart rate, a sympathetically induced change in mean left atrial pressure reliably indicates a similar directional change in left ventricular end diastolic pressure. Direct evidence that the ventricle does produce more external work from any given left ventricular end diastolic pressure under the influence of carotid hypotension is shown in figure 26. The tracing at the left was taken during high carotid artery pressure, and that at the right during low carotid artery pressure. Lowering the carotid pressure resulted in a doubling of stroke volume and the production of six times as much stroke work from the same end diastolic pressure. Of particular interest is the observation that during carotid hypotension there is a more synchronous type of ventricular contraction and a more rapid rate of relaxation, thus allowing for a longer diastolic interval, changes similar to those observed with stellate stimulation. The observed effects of carotid stimulation on the heart are diminished or abolished by sectioning stellate ganglion rami or by ganglionic blockade (106). It might be argued that the increase in ventricular contractility observed when carotid pressure is lowered can be attributed to the higher aortic pressure acting through the mechanism of homeometric autoregulation (section 1). However, it has recently been determined that a marked increase in ventricular contractility is also observed when carotid hypotension is induced and aortic pressure as well as heart rate is kept at the same level (J. P. Gilmore & J. H. Siegel, unpublished observations). Such experiments confirm the suggestion by Sarnoff & Berglund (96), and by Agostoni *et al.* (1) that carotid sinus stimulation can shift the VFC and are consonant with the observations of Carlsten *et al.* (22) in man, which led those authors to postulate a reflexly induced cardiac inotropic effect arising from the carotid sinus.

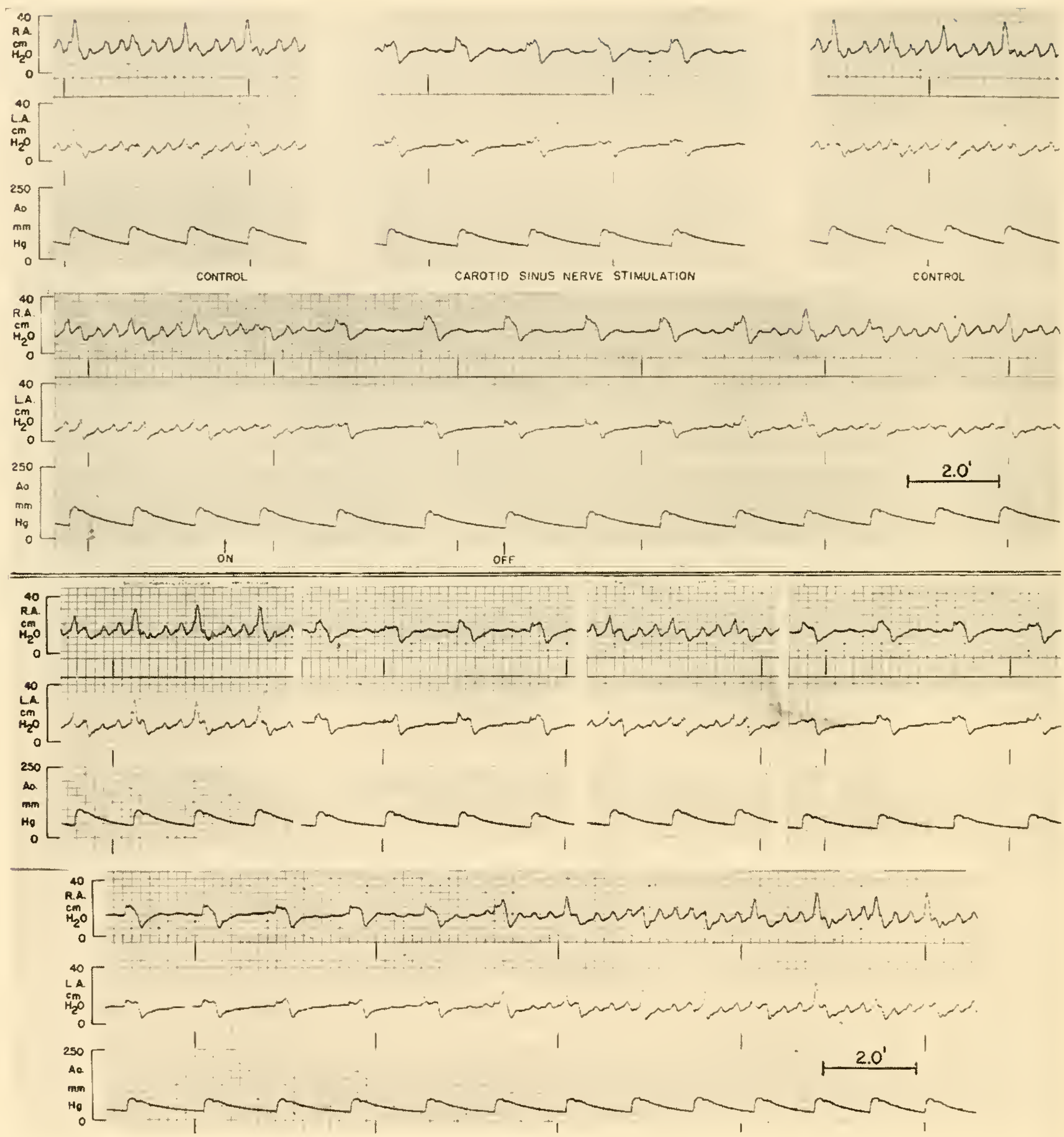

FIG. 27

The relatively modest effect on ventricular dynamics recorded by Cotten & Moran (29) with a right ventricular strain gauge arch would not appear to be compatible with the present data. A simple means of relating the experiments described above to the studies of Charlier (26) is not immediately apparent.

B. Carotido-Atrial Reflexes

THE CAROTIDO-VAGO-ATRIAL REFLEX. In experiments on this reflex the sympathetic chain from the stellate ganglion down through T-5 is removed intact on both sides. This is done so that any change in the atrial "a" wave which occurs can be attributed to reflex

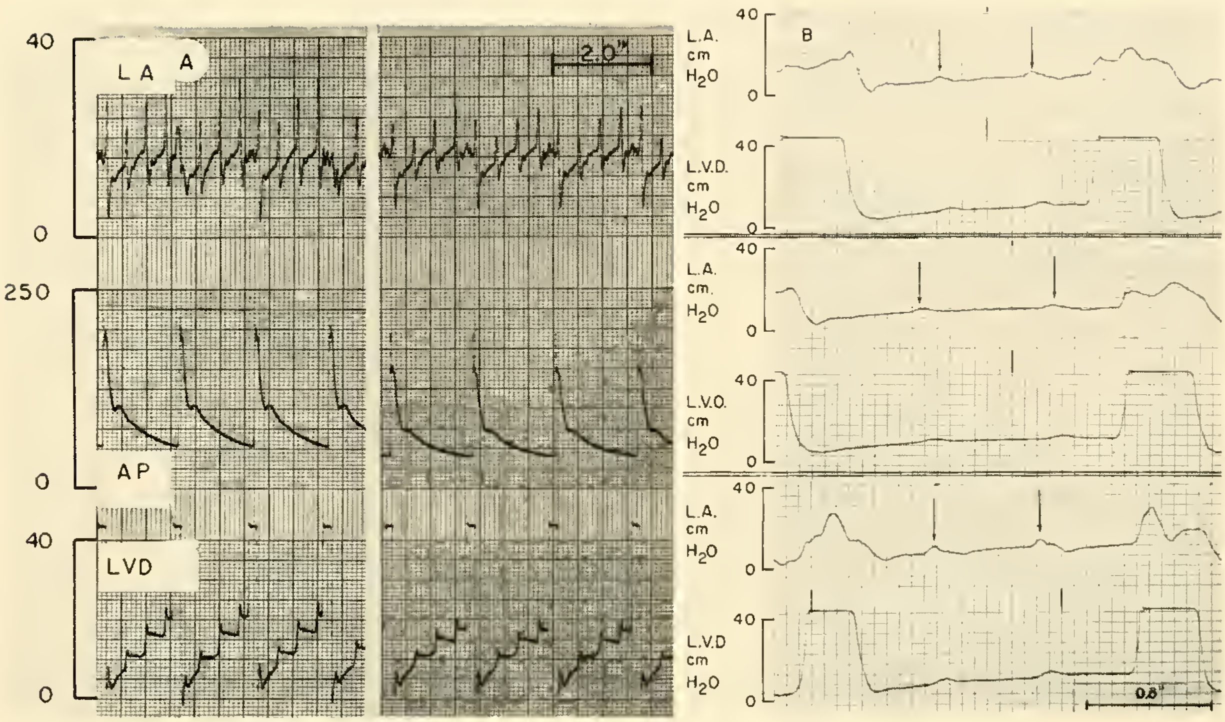

FIG. 28A. LA = left atrial pressure.

efferent vagal activity, provided of course that the observed changes are within one circulation time. Figure 27 (upper) illustrates the depressant effect of carotid sinus nerve stimulation on the "a" wave of the paced atrium in a dog with surgically induced heart block. Two or three atrial "a" waves appear in the interval between each ventricular beat. The segmented panel at the left is the control tracing; the middle, that during stimulation of the carotid sinus nerve; and the right is again a control tracing. The long lower tracing shows the rapidity of the onset and wearing off of this effect. In figure 27 (lower) the blocking of the response with atropine demonstrates that the response is achieved by vagal efferent fibers. The upper set of four panels are from left to right: control, carotid sinus nerve stimulation, control, and carotid sinus nerve stimulation. The stimulation was then maintained during the 70-sec interval until the beginning of the long lower panel (below) 12 sec before which 4.0 mg of atropine sulfate was administered intravenously.

The depression of the atrial "a" wave observed with carotid sinus nerve stimulation is comparable to changes obtainable with direct vagal stimulation.

THE CAROTIDO-SYMPATHO-ATRIAL REFLEX. In experiments on this reflex a bilateral cervical vagotomy is done so that the effects of changing carotid pressure or of carotid sinus nerve stimulation on the contraction of the atrium can be attributed to a sympathetic efferent pathway. The dog with surgically induced heart block is used. In figure 28A the left panel is the control tracing, and the right panel is the tracing 12 sec after beginning of left carotid sinus nerve stimulation. Carotid sinus nerve stimulation depresses the "a" wave of the paced atrium and its reflected effect on left ventricular diastolic pressure.

The interplay between sympathetic and parasympathetic influences on the atrium in a heart block preparation is shown in figure 28B. The atrium was not paced. In the upper panel of this figure, the atrial "a" wave was diminished by keeping carotid pressure high. To this was added sufficient efferent vagal nerve stimulation so as to all but abolish the atrial "a" wave as well as produce atrial slowing (middle panel). With the vagal stimulus kept constant, the carotid pressure was then lowered; the increased "a" waves and re-established atrial rate are shown in the lower panel. The slowing of the ventricular rate produced by vagal stimulation (middle panel) in the dog with heart block confirms the 1906 experiments of Erlanger (35).

C. Function of the Carotid Sinus

During the course of these investigations a pattern of the baroceptor's functional role has been evolved which brings together a variety of observations in a manner that seems to have an appealing unity. This position holds that a dominant physiologic responsibility of the carotid sinus in circulatory regulation is to augment or diminish the contraction of the ventricle. The basis for this is as follows:

1) Carotid hypotension diminishes venous distensibility. The net effect of such a change, if it alone occurs, is an increased ventricular end diastolic pressure and fiber length, and thus an augmented ventricular contraction. Splenic contraction would have the same effect.

2) Carotid hypotension augments and shortens the atrial contraction by means of the carotido-vagoatrial and the carotido-sympatho-atrial reflexes. The net effect of such an atrial augmentation, if it alone occurs, is an increased ventricular end diastolic pressure and fiber length and thus an augmented ventricular contraction.

3) At any given heart rate carotid hypotension directly augments the stroke work and stroke power produced by the ventricle from any given end diastolic pressure or fiber length.

4) Since carotid hypotension directly augments ventricular stroke power by shortening the systolic time for any given amount of work produced and also produces a more rapid rate of relaxation, it thus provides for a longer interval of diastolic filling than would otherwise occur. This factor becomes especially important at high heart rates.

5) The more complete systolic emptying consequent to carotid hypotension places the ventricle on a lower and more sensitive portion of its diastolic pressure-length curve. As a result there will be more filling and a greater fiber elongation produced by any given atrial systole than if the more complete systolic emptying had not taken place.

6) The increased peripheral vascular resistance during carotid hypotension maintains a higher aortic pressure at any given stroke volume and heart rate than would otherwise be present. In addition to maintaining an adequate pressure for coronary perfusion, the higher aortic pressure produces an increased ventricular contractility through homeometric autoregulation (Anrep effect).

7) Tachycardia, per se, increases ventricular contractility through homeometric autoregulation (Bowditch effect) in addition to the concomitant inotropic influence of the increased sympathetic outflow.

8) Whatever catecholamines are secreted by the adrenal medulla in response to a lowering of carotid sinus pressure would be expected to reinforce the effects enumerated above.

The intended purpose of synthesizing the available information in this manner is not to disparage the importance of changes in heart rate per se or to minimize the importance of regional changes in peripheral vascular resistance. Rather, the purpose is to invite a re-evaluation of the proper role of the carotid sinus in circulatory regulation. It seems fair to insist that to view the carotid sinus as a sense organ which acts primarily to safeguard blood flow to the vital organs, such as the brain and heart, is no longer a tenable position. It would seem much more appropriate to cast it in the role of a sensing element which helps to regulate blood flow to all the tissues of the organism in accordance with their activity and metabolic requirements (44, 78, 101). To a substantial extent the baroceptor operates much like a voltage regulating element in an electrical system; i.e., it causes an appropriate variation of input so as to maintain a constant voltage when the current requirements of the system it is supplying are changed. An example of its operation in this manner was obtained recently in experiments in which it was demonstrated that local muscular activity effectively produces a functional sympathectomy in the vascular bed of the active area (78a); under such circumstances it can be shown that when carotid pressure is elevated, thus inhibiting the stimulatory action of its reflex autonomic activity, the blood flow through the active muscular area is lower, the venous pO_2 and pH from it are decreased, and the arteriovenous O_2 difference across it is widened, each by substantial amounts relative to what these values are when carotid pressure is lower (78a).

D. Reflex Changes in Heart Rate and Contractility

It would almost appear that the medullary centers appreciate the extent to which tachycardia encroaches on the time available for diastole (14, 60, 79, 125) and thus do not have the temerity to impose tachycardia without providing simultaneous inotropic safeguards against a time-limited diastolic ventricular relaxation as well as the restricted period for coronary inflow which would otherwise take place. A simultaneous increase of both heart rate and stroke volume further intensifies the need for a more forceful and synchro-

nous type of ventricular contraction, since an increased stroke volume also impinges on diastole if the performance characteristics of the ventricle remain unmodified (14, 79). The pertinent literature, limited though it may be in terms of well-controlled experiments, does not reveal examples of a physiologically operative reflex that evokes tachycardia which does not, either directly or indirectly, also simultaneously evoke an increase in contractility. One might predict that, if it occurs, it must be rare. It is equally difficult to imagine that any operative reflex will produce an increase in the ventricular work produced from any given end diastolic pressure without simultaneously producing an increase in ventricular power. At the very least, it is now clear that carotid sinus hypotension produces not only its well-known tachycardia but also simultaneously modifies the performance characteristics of the left ventricle so as to augment both the stroke work and stroke power it produces from any given LVED pressure.

E. Interrelation of Intrinsic Mechanisms and Extrinsic Influences

It is clear that the left ventricle of the isolated heart exhibits an increased contractility through homeometric autoregulation when its activity is increased simply by increasing the aortic pressure (fig. 3). It is also clear that, starting at any given level of aortic pressure, sympathetic stimulation increases contractility in advance (fig. 13) and independently of an increased aortic pressure (105). Both must, therefore, be playing a role in producing the observed increase in ventricular contractility induced by carotid hypotension. It seems peculiarly appropriate to the operation of the carotid sinus that its cardiac and peripheral vascular effects interrelate so as to reinforce each other and, further, that an increase in the norepinephrine background resulting from sympathetic stimulation facilitates the intrinsic mechanism of homeometric autoregulation.

It is now apparent that the Bowditch staircase effect is operative in the adequately supported canine heart and thus that an increase in rate will, of itself, either increase contractility or protect against the extent to which contractility might otherwise diminish. It is also clear that, at any given heart rate, sympathetic stimulation increases contractility. Both must, therefore, be playing a role in producing the observed increase in contractility when carotid pressure is lowered in the normal organism. Again, it is appropriate for the operation of the carotid sinus that these effects are reinforcing rather than opposing.

Since the carotid sinus can, both directly and indirectly, reflexly modify both the filling and the contractility of the ventricles by such diverse means and over such wide ranges, it invites a consideration of its participation as one significant influence in the control of cardiac output in varying states.

IV. CARDIOVASCULAR RESPONSE TO EXERCISE

A. Changes in Cardiac Output and AV Oxygen Difference

The greatest demands normally made on the cardiovascular system are during heavy exercise when oxygen consumption and cardiac output reach their peak values. The maximal oxygen intake has been used as an effective measure of circulatory capacity (66); the circulatory determinants in achieving the maximal oxygen intake are cardiac output and arteriovenous oxygen difference (129). In recent studies in man, from standing rest to a workload producing the maximal figure, the oxygen consumption increased 9.6 times; the cardiac output, 4.3 times, and the arteriovenous oxygen difference, 2.2 times (66). The increase in cardiac output was achieved by a doubling of both stroke volume and of heart rate.

Although the relative roles of increased heart rate and increased stroke volume in determining the cardiac output response to exercise have recently been challenged (90–92), it now seems clear that, at least in leg exercise in the upright position, an increase in stroke volume is as important as the increase in heart rate (66). Even if, as thought by Rushmer *et al.* (90, 91), stroke volume were only maintained during exercise, it is highly unlikely that this same stroke volume would get either into or out of the ventricle if, at the increased heart rates, a simultaneous increase of myocardial contractility had not also occurred. More directly, a plot of the relation between left ventricular end diastolic volume and stroke work during rest and exercise does, in fact, reveal an increased contractility after exercise is begun (25). To maintain that an increase in heart rate is the primary means by which the organism augments its cardiac output during exercise, without specific reference to a simultaneous influence on the performance characteristics of the ventricle, is not in accord with the available information.

As mentioned above, the widening of the arterio-

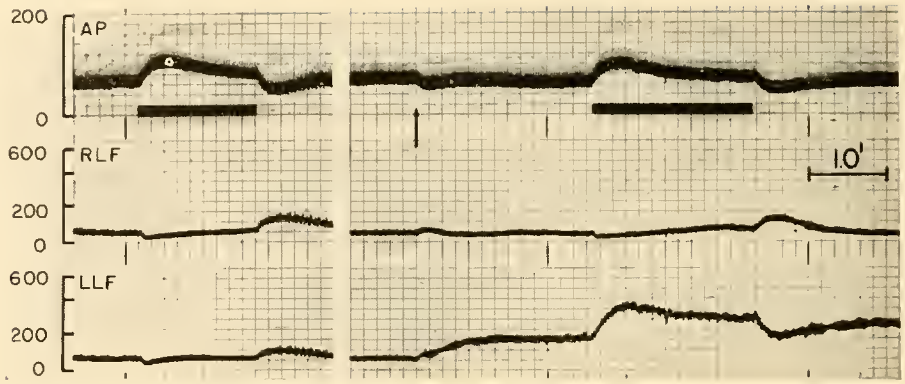

FIG. 29. RLF and LLF = blood flow in ml/min through right and left external iliac arteries.

venous oxygen difference also plays an important role in achieving the maximal oxygen intake. The arteriovenous oxygen difference during heavy exercise is about 14.5 ml per 100 ml (6, 41, 66) and is obtained by encroachment on the mixed venous oxygen content. This encroachment on the mixed venous content is, in turn, made possible by two mechanisms: one is the extent to which blood perfusing working tissue can surrender its oxygen (7); the other is a proportional shunting of blood away from inactive areas, and is discussed below.

B. Peripheral Vascular Control

An important means of widening the AV oxygen difference during exercise is the ability proportionally to shunt blood from inactive areas (34, 66). Relevant to this, and central to the understanding of circulatory regulation in varying states, is the demonstration that in an area of increased activity the vascular bed becomes functionally sympathectomized (78a). The existence of this phenomenon allows the central nervous system to distribute a general increase in the sympathetic outflow to the peripheral vascular bed, as for example during carotid hypotension, without impairing blood flow to an area of increased activity, since the vascular bed of the latter is unresponsive to such stimulation. This has been demonstrated to be so whether the sympathetic stimulation to an extremity is accomplished by the intra-arterial injection of norepinephrine, direct stimulation of the sympathetic nerves supplying the active area, or reflexly increased sympathetic activity induced either by lowering carotid pressure or by stimulation of the central cut end of the vagus nerve (78a). Figure 29 shows one example of this phenomenon. In the left panel, with both legs at rest, stimulation of the central cut end of one vagus nerve (indicated by bar in the upper channel) produces an intense vasoconstriction in both lower extremities as evidenced by the relation between pressure and flow in both during the stimulation. In the right panel, at the arrow, exercise is begun in the left lower extremity. Then afferent vagal nerve stimulation is repeated. The right lower extremity, still at rest, again responds with vasoconstriction as it did previously. Flow through the exercising left lower extremity is, however, now pressure dependent. This type of experiment indicates that functional sympathectomy occurs when local muscular activity is increased. As might be expected, it was also observed that the degree of immunity from the influence of sympathetic impulses varies with the intensity of the activity. The biochemical means by which local vessels are rendered nonreactive to sympathetic stimulation during increased activity of the organ they supply is one of the most important, unanswered questions in the physiology of the circulation.

V. THE ARCHITECTURE OF CIRCULATORY REGULATION

The circulation is comprised of: *1*) two input sensitive pumps, conduits through which each propels blood to the tissues, permeable conduits through which chemical exchange with the tissues is effected, and conduits through which the blood is returned to the other pump. There are, of course, also the conduits of the lymphatic system. *2*) Central activation elements in the circulatory centers which, by means of evoking a variety of efferent nerve impulses, can vary the rate of the pumps, can vary their stroke work and power (both by a direct effect on the pumps and by varying the input into them), can vary the resistance to flow through the efferent conduits, and can vary the pressure-volume relation of the conduits returning blood. *3*) A local peripheral vascular mechanism whereby the conduits leading blood to an

area of increased energy requirement are rendered gradably immune to instructions from the circulatory centers when the latter request an increased resistance to flow.

The combination of elements outlined above can be considered the command system of the circulation. By the relatively simple expedient of maintaining an adequate pressure head from which the various tissues of the organism can each select a flow appropriate to its activity and energy requirement (44, 78, 101), this command system has the capability of sustaining the competence of the total organism in the face of widely varying conditions and challenges. The extent to which it will be successful in so doing will, however, depend upon the availability and appropriateness of the information fed into the integrating network to which the command system is subservient.

Before proceeding to this aspect of the matter, however, it seems appropriate to evaluate here the role of Starling's law of the heart in circulatory regulation and the manner in which it participates as part of the command system. This can be most readily appreciated by posing two separate questions. *1*) "Is the heart of the normal, unanesthetized, active organism operating in accordance with Starling's law of the heart?" The answer to this is clearly in the affirmative. The continuing beat-to-beat operation of Starling's law of the heart, with both the right and left ventricles operating on the curves then obtaining, provides a convincing explanation of how the ratio between systemic and pulmonary blood volumes is constrained within such narrow limits for the lifetime of the organism. Unlike homeometric autoregulation, which requires at least several beats to fully develop, the beat which follows immediately after an increase of end diastolic pressure and fiber length produces more external work than the one immediately before it. As shown most convincingly by Brecher (15) there are substantial variations in venous return throughout the respiratory cycle. The variations of venous return to the right and left ventricle cannot be the same with respect to both amount and time, and they are, in fact, often reciprocating with each other to varying degrees. Further, the importance of changes in left ventricular volume relative to its stroke work throughout the respiratory cycle, and also the fact that this relationship still obtains after changing the circulatory state by inducing exercise, has been firmly established (25). Hamilton (45) cites the early work of Henderson & Prince (48), and supports the position established by Berglund (9) in a statement which, in many ways, is difficult to improve upon. He said, "I believe that the Starling law does play a very important role in everyday life and that that role is to preserve the balance between the pumping of the right and the left ventricle. This balance must be exact and, since the two ventricles are subject to the same hormonal and nervous influences, they each act as a control for the other. They have to follow each other from curve to curve and, so far as I can think at present, only a delicate adjustment of strength of contraction to degree of filling serves as an hypothesis to explain their maintained balanced output . . . "

But the importance of the continuing beat-to-beat operation, even of the simple Starling law, in the intact organism cannot be restricted to the single function of maintaining the pulmonary blood volume within endurable limits, as vital as that may be to the continuing existence of the organism. For if it is to be assumed that Starling's law is not otherwise operative to an important extent in the normal organism, to what end is there a venous pumping action in muscles, what significance does reflexly induced venoconstriction have, to what end is it possible for the atria to vary so markedly the amount of blood they propel into the ventricles as the result of their reflexly controlled contractility? On the basis of known mechanisms, these phenomena achieve physiologic significance only to the extent that they influence ventricular filling, stroke work, and stroke volume. Those who come to the conclusion that the generality elaborated by Starling is of importance mostly because it is informative about the heart failure syndrome but "has only limited application to the normal human heart," (75) have the unequivocal responsibility of assigning some other biologically meaningful significance to these phenomena.

2) The second question is "Does the simple operation of Starling's law of the heart of itself account for the observed changes in cardiac output with varying states, for example, exercise?" The answer to this is clearly no, nor have we ever put forward the contrary view. It is difficult, therefore, to understand those quixotic attempts to abolish a position which doesn't exist by showing that the ventricle may not enlarge or even may become smaller during exercise or with a change in posture (86, 90–92). The positive position that is maintained is that the central nervous system has available to it both direct and indirect pathways by means of which it can continuously provide varying degrees of gain for the fundamental Frank-Starling relation, and that the exploitation of these available

pathways does play a highly important role in the control of cardiac output. This mechanism is in addition to, but can hardly be held to be operating to the exclusion of the fiber length-stroke work relation.

Lastly, it remains to consider the elements concerned with the gathering of information on the basis of which it is possible for the integrating network appropriately to exploit the command system. In this presentation, the carotid sinus has been put forth as one important type of information gathering element. It is hardly to be imagined that there are not many others which are important and which differ from each other not only qualitatively but also in the relative dominance that each may acquire under varying circumstances. Centrally placed chemoreceptors must surely play an important role; the powerful and diffuse reflex sympathetic effects observed after stimulation of the central cut end of the vagi can be thought likely to have some significance other than that of simply conveying a noxious stimulus even though a nerve carrying pain is, of course, a significant information gathering element. Peripherally placed receptors in muscles have also been suggested (52). It would be difficult to imagine that the senses of sight, hearing, smell, taste, and touch do not also have access to the command system of the circulation. The helpful work of Rushmer and his colleagues (90, 91, 110) has done much to elucidate the pathways over which supratentorial influences can activate and exploit the command system of the circulation in the ambient experimental organism, a basic fact of importance apparent to any physician who has measured the heart rate and blood pressure of the so-called labile individual. The effects of emotion, frustration, and conditioning on the circulation, an expanding area of investigation, must yield increasingly profitable data not only in the understanding of normal physiology but in the understanding of disease processes. It is to be expected that information gathering elements which reflexly produce an anticipatory augmentation of the circulation will be of special interest. When, as the result of visual, olfactory, auditory, tactile, or painful stimulation, the circulatory rate is increased in advance of the actual need for an increased metabolic support of peripheral tissues, such a reaction has obvious survival value under situations of physical conflict or flight, and is teleologically appropriate. Whether or not a circulatory architecture that has been evolved in relation to an adaptation to varying physical challenges is also as appropriate in an organism where the stresses are predominantly of the emotional type will be one of the interesting questions to be more precisely attacked in the ensuing decades. The immediacy of a second important question is, in some ways, even more keenly felt. Namely, to what extent will a circulatory architecture which, in its total evolutionary history, has adapted to a 1 *g* environment function adequately in the absence of gravity.

In any case it has been our goal herein to systematize certain of the criteria by means of which a more effective and detailed examination of the command system of the circulation can be made, and to exhibit one example of the large effects to be obtained from the stimulation of one important information gathering element. It would be our hope that the effects of such an attempted systematization might be to facilitate a more critical and effective evaluation of other information gathering elements both above and below the tentorium.

Grateful acknowledgment is made to *Circulation Research* and *American Journal of Cardiology* for permission to reproduce many of the figures used in this chapter.

REFERENCES

1. Agostoni, E., J. E. Chinnock, and M. de Burgh Daly. The effects of stimulation of the carotid sinus baroreceptors upon the pulmonary arterial blood pressure in the cat. *J. Physiol.* 137: 447, 1957.
2. Alexander, R. S. The participation of the venomotor system in pressor reflexes. *Circulation Res.* 2: 405, 1954.
3. Anrep, G. V. On the part played by the suprarenals in the normal vascular reactions of the body. *J. Physiol.* 45: 307, 1912.
4. Anrep, G. V. Regulation of the coronary circulation. *Physiol. Rev.* 6: 596, 1926.
5. Anrep, G. V. Lane Medical Lectures: Studies in cardiovascular regulation. *Stanford Univ. Publication* 3: 205, 1936.
6. Asmussen, E., and M. Nielsen. The cardiac output in rest and work determined simultaneously by the acetylene and the dye injection methods. *Acta physiol. scandinav.* 27: 217, 1952.
7. Asmussen, E., and M. Nielsen. Cardiac output during muscular work and its regulation. *Physiol. Rev.* 35: 778, 1955.
8. Bartelstone, H. J. Role of the veins in venous return. *Circulation Res.* 8: 1059, 1960.

9. BERGLUND, E. Ventricular function VI. Balance of left and right ventricular output: Relation between left and right atrial outputs. *Am. J. Physiol.* 178: 381, 1954.
10. BLINKS, J. R. Method for study of the contraction of isolated heart muscle under various physical conditions. *Circulation Res.* 9: 342, 1961.
10a. BLINKS, J. R. Physical factors and the action of sympathomimetic amines on myocardial contractility. In preparation.
11. BLIX, M. Die Länge und die Spannung des Muskels. *Skandinav. Arch. Physiol.* 5: 173, 1895.
12. BOWDITCH, H. P. Über die Eigenthümlichkeiten der Reizarkeit, welche die Muskelfasern des Herzens zeigen. *Berichte Königl. Sächs. Ges. Wissen.* 23: 652, 1871.
13. BRAUNWALD, E., S. J. SARNOFF, R. B. CASE, W. N. STAINSBY, AND G. H. WELCH, JR. Hemodynamic determinants of coronary flow: Effect of changes in aortic pressure and cardiac output on the relationship between myocardial oxygen consumption and coronary flow. *Am. J. Physiol.* 192: 157, 1958.
14. BRAUNWALD, E., S. J. SARNOFF, AND W. N. STAINSBY. Determinants of duration and mean rate of ventricular ejection. *Circulation Res.* 6: 319, 1958.
15. BRECHER, G. A. *Venous Return.* New York: Grune & Stratton, 1956.
16. BROOKS, C. McC., B. F. HOFFMAN, E. E. SUCKLING, AND O. GRIAS. *Excitability of the Heart.* New York: Grune & Stratton, 1955.
17. BROWN, T., G. GRUPP, AND G. A. ACHESON. Potassium balance of the dog heart: Effect of increasing heart rate and of pentobarbital and dihydro-ouabain. *J. Pharmacol. & Exper. Therap.* 129: 42, 1960.
18. BUCKLEY, N. M., E. OGDEN, AND D. S. LINTON, JR. The effects of work load and heart rate on the filling of the isolated right ventricle of the dog. *Circulation Res.* 3: 434, 1955.
19. BUCKLEY, N. M., E. OGDEN, AND R. C. MCPHERSON. The effect of inotropic drugs on filling of the isolated right ventricle of the dog heart. *Circulation Res.* 3: 447, 1955.
20. BUCKLEY, N. M., M. SIDKY, AND E. OGDEN. Factors altering the filling of the isolated left ventricle of the dog heart. *Circulation Res.* 4: 148, 1956.
21. CARLSTEN, A., B. FOLKOW, AND C. A. HAMBERGER. Cardiovascular effects of direct vagal stimulation in man. *Acta physiol. scandinav.* 41: 68, 1957.
22. CARLSTEN, A., B. FOLKOW, G. GRIMBY, C. HAMBERGER, AND O. THULESIUS. Cardiovascular effects of direct stimulation of the carotid sinus nerve in man. *Acta physiol. scandinav.* 44: 138, 1958.
23. CASE, R. B., E. BERGLUND, AND S. J. SARNOFF. Ventricular function II. Quantitative relationship between coronary flow and ventricular function with studies on unilateral failure. *Circulation Res.* 2: 319, 1954.
24. CASE, R. B., S. J. SARNOFF, AND E. BERGLUND. Ventricular function VII. Changes in coronary resistance and ventricular function resulting from acutely induced anemia and the effect thereon of coronary stenosis. *Am. J. Med.* 18: 397, 1955.
25. CHAPMAN, C. B., O. B. BAKER, AND J. H. MITCHELL. Left ventricular function at rest and during exercise. *J. Clin. Invest.* 38: 1202, 1959.
26. CHARLIER, R. Le rôle des régions sinusales et cardio-aortiques dans la regulation reflexe du débit cardiaque. *Acta cardiol.* 3: 1, 1948.
27. CONN, H. L., AND J. C. WOOD. Acute effects of quinidine on K exchange and distribution in the dog ventricle. *Am. J. Physiol.* 199: 151, 1960.
28. COTTEN, M. DEV., AND H. M. MALING. Relationships among stroke work, contractile force and fiber length during changes in ventricular function. *Am. J. Physiol.* 189: 580, 1957.
29. COTTEN, M. DEV., AND N. C. MORAN. Effect of increased reflex sympathetic activity on contractile force of the heart. *Am. J. Physiol.* 191: 461, 1957.
30. COTTEN, M. DEV., AND P. E. STOPP. Action of digitalis on the nonfailing heart of the dog. *Am. J. Physiol.* 192: 114, 1958.
31. CROUT, J. R. *Determination of Catecholamines in Urine. Standard Methods of the American Association of Clinical Chemistry.* New York: Academic Press, III: 1960.
32. CULLIS, W., AND E. M. TRIBE. Distribution of nerves in the heart. *J. Physiol.* 46: 141, 1913.
33. DALEY, R., I. K. R. MCMILLAN, AND R. GORLIN. Mitral incompetence in experimental auricular fibrillation. *Lancet* 2: 18, 1955.
34. DONALD, K. W., J. M. BISHOP, AND O. L. WADE. A study of minute to minute changes of arteriovenous oxygen difference, oxygen uptake, and cardiac output and rate of achievement of a steady state during exercise in rheumatic heart disease. *J. Clin. Invest.* 33: 1146, 1954.
35. ERLANGER, J. Ueber den Grad der vaguswirkung auf die Kammern des Hundeherzens. *Arch. ges. Physiol.* 127: 77, 1909.
36. FENN, W. O. A quantitative comparison between the energy liberated and the work performed by the isolated sartorius muscle of the frog. *J. Physiol.* 58: 175, 1923.
37. FENN, W. O. The relation between the work performed and the energy liberated in muscular contraction. *J. Physiol.* 58: 373, 1923.
38. FICK, A. *Mechanische Arbeit und Warmeentwicklung bei der Muskelthätigkeit.* Leipzig: F. A. Brackhaus, 1882.
39. FRANK, O. Zur Dynamik des Herzmuskels. *Ztschr. Biol.* 32: 370, 1895.
40. FRANK, O. On the dynamics of cardiac muscle. Translated by C. B. Chapman and E. Wasserman. *Am. Heart J.* 58: 282, 1959; and 58: 467, 1959.
41. FREEDMAN, M. E., G. L. SNIDER, P. BROSTOFF, S. KIMELBLOT, AND L. N. KATZ. Effects of training on response of cardiac output to muscular exercise in athletes. *J. Appl. Physiol.* 8: 37, 1955.
42. GESELL, R. A. Cardiodynamics in heart block as affected by auricular systole, auricular fibrillation and stimulation of the vagus nerve. *Am. J. Physiol.* 40: 267, 1916.
42a. GILMORE, J. P., J. H. MITCHELL, R. J. LINDEN, S. K. BROCKMAN, AND S. J. SARNOFF. A comparison of cardiovascular hemodynamics during atrial and ventricular stimulation; observations on ventricular myocardial synchronicity. *Circulation Res.* In press.
43. HAJDU, S., AND E. LEONARD. The cellular basis of cardiac glycoside action. *Pharmacol. Rev.* 11: 173, 1959.
44. HAMILTON, W. F. The Lewis A. Conner Memorial Lecture. The physiology of the cardiac output. *Circulation* 8: 527, 1953.
45. HAMILTON, W. F. Role of the Starling concept in regulation of the normal circulation. *Physiol. Rev.* 35: 161, 1955.

46. Harvey, W. *Anatomical Studies on the Motion of the Heart and Blood* (3rd ed.). Springfield, Ill.: Thomas, p. 40, 1949.
47. Henderson, Y., and F. E. Johnson. Two modes of closure of the heart valves. *Heart* 4: 69, 1912.
48. Henderson, Y., and A. L. Prince. Relative systolic discharges of the right and left ventricles and their bearing upon pulmonary congestion and depletion. *Heart* 5: 217, 1914.
49. Heymans, C., and E. Neil. *Reflexogenic Areas of the Cardiovascular System.* Boston: Little, Brown 1958.
50. Hoffman, B. F., P. F. Cranefield, J. H. Stuckey, N. S. Amer, R. C. Coppelletti, and R. T. Domingo. Direct measurement of conduction velocity in *in situ*: Specialized conductory system of mammalian heart. *Proc. Soc. Exper. Biol. & Med.* 102: 55, 1959.
51. Horres, A. D., F. Brown, R. Denes, and H. Kolder. The effects of coronary perfusion on ventricular volume distensibility. *Physiologist* 3 (No. 3): 82, 1960.
52. Iaria, C. T., U. H. Jalar, and F. F. Kao. The peripheral neural mechanism of exercise hyperpnoea. *J. Physiol.* 148: 49, 1959.
53. Isaacs, J. P., E. Berglund, and S. J. Sarnoff. Ventricular function III. The pathologic physiology of acute cardiac tamponade studied by means of ventricular function curves. *Am. Heart J.* 48: 66, 1954.
54. Katz, A. M., L. N. Katz, and F. L. Williams. Registration of left ventricular volume curves in the dog with the systemic circulation intact. *Circulation Res.* 3: 588, 1955.
55. Kelso, A. F., and W. C. Randall. Ventricular changes associated with sympathetic augmentation of cardiovascular pressure pulses. *Am. J. Physiol.* 196: 731, 1959.
56. Kosawa, S. The mechanical regulation of the heart beat in the tortoise. *J. Physiol.* 49: 233, 1915.
57. Lind, J., C. Wegelius, and H. Lichtenstein. The dynamics of the heart in complete A-V block. An angiocardiographic study. *Circulation* 10: 195, 1954.
58. Linden, R. J., and J. H. Mitchell. Relation between left ventricular diastolic pressure and myocardial segment length and observations on the contribution of atrial systole. *Circulation Res.* 8: 1092, 1960.
59. Little, R. C. Effect of atrial systole on ventricular pressure and closure of the A-V valves. *Am. J. Physiol.* 166: 289, 1951.
60. Lombard, W. P., and O. M. Cope. Effect of posture on the length of systole of the human heart. *Am. J. Physiol.* 49: 140, 1919.
61. Lund, A. Simultaneous fluorimetric determination of adrenaline and noradrenaline in blood. *Acta pharmacol. et toxicol.* 6: 137, 1950.
62. Lundin, G. Mechanical properties of cardiac muscle. *Acta physiol. scandinav.* 7: suppl. 20, 1944.
63. McGuire, H. H., Jr., L. H. Bosher, Jr., and R. W. Ramsey. Exploration into narcosis for surgical cardioplegia. *Tr. Am. Soc. Artificial Internal Organs* 6: 323, 1960.
64. McKusick, V. A. *Cardiovascular Sound in Health and Disease.* Baltimore: Williams & Wilkins, 1958.
65. McMillan, I. K., R. B. Case, W. N. Stainsby, and G. H. Welch, Jr. The hypothermic heart: Work potential and coronary flow. *Thorax* 12: 208, 1957.
66. Mitchell, J. H., B. J. Sproule, and C. B. Chapman. The physiological meaning of the maximal oxygen intake test. *J. Clin. Invest.* 37: 538, 1958.
67. Mitchell, J. H., R. J. Linden, and S. J. Sarnoff. Influence of cardiac sympathetic and vagal nerve stimulation on the relation between left ventricular diastolic pressure and myocardial segment length. *Circulation Res.* 8: 1100, 1960.
67a. Mitchell, J. H., J. P. Gilmore, and S. J. Sarnoff. The transport function of the atrium: Factors influencing the relation between mean atrial pressure and ventricular end diastolic pressure. *Am. J. Cardiol.* In press.
68. Müller, E. A. Die Anpassung des Herzvolumens an den Aortendruck. *Pflügers Arch. ges Physiol.* 241: 427, 1939.
69. Muller, O., and J. Shillingford. Tricuspid incompetence. *Brit. Heart J.* 16: 195, 1954.
70. Nonidez, J. F. Studies on the innervation of the heart. *Am. J. Anat.* 65: 361, 1939.
71. Patterson, S. W. The antagonistic action of carbon dioxide and adrenalin on the heart. *Proc. Roy. Soc. ser. B.* 88: 371, 1914.
72. Patterson, S. W., H. Piper, and E. H. Starling. The regulation of the heart beat. *J. Physiol.* 48: 465, 1914.
73. Peserico, E. The influence of mechanical factors of the circulation upon the heart volume. *J. Physiol.* 65: 146, 1928.
74. Peterson, L. H. Some characteristics of certain reflexes which modify the circulation in man. *Circulation* 2: 351, 1950.
75. Pickering, G. Starling and the concept of heart failure. *Circulation* 21: 323, 1960.
76. Prinzmetal, M., E. Corday, I. C. Brill, R. W. Oblath, and H. E. Kruger. *The Auricular Arrhythmias.* Springfield, Ill.: Thomas, 1952.
77. Randall, W. C., and W. G. Rohse. The augmentor action of the sympathetic cardiac nerves. *Circulation Res.* 4: 470, 1956.
78. Rein, H. Die physiologischen Verkumpfungen Von atmung und Kreislauf. *Nauheimer Fortbildungs-lehrgange* 11: 14, 1935.
78a. Remensnyder, J. P., J. H. Mitchell, and S. J. Sarnoff. Functional sympatholysis during muscular activity: observations on oxygen uptake. *Circulation Res.* In press.
79. Remington, J. W., W. F. Hamilton, and Ahlquist, R. P. Interrelation between the length of systole, stroke volume, and left ventricular work in the dog. *Am. J. Physiol.* 154: 6, 1948.
80. Rohse, W. G., M. Kaye, and W. C. Randall. Prolonged pressor effects of selective stimulation of the stellate ganglion. *Circulation Res.* 5: 144, 1957.
81. Rosenblueth, A., J. Alanis, and R. Rubio. Some properties of mammalian ventricular muscle. *Arch. intern. physiol. et biochem.* 67: 276, 1959.
82. Rosenblueth, A., J. Alanis, E. Lopez, and R. Rubio. The adaptation of ventricular muscle to different circulatory conditions. *Arch intern. physiol. et biochem.* 67: 358, 1959.
83. Rosenblueth, A., J. Alanis, R. Rubio, and E. Lopez. The two staircase phenomena. *Arch. internat. physiol. et biochem.* 67: 374, 1959.
84. Rushmer, R. F., and N. Thal. Factors influencing stroke volume: A cineflurographic study of angiocardiography. *Am. J. Physiol.* 168: 509, 1952.
85. Rushmer, R. F. Applicability of Starling's Law of the

heart to intact unanesthetized animals. *Physiol. Rev.* 35: 138, 1955.

86. Rushmer, R. F. Anatomy and physiology of ventricular function. *Physiol. Rev.* 36: 400, 1955.
87. Rushmer, R. F. Pressure-circumference relations of the left ventricle. *Am. J. Physiol.* 186: 115, 1956.
88. Rushmer, R. F., and T. C. West. Cardiac responses to sympathetic stimulation. *Circulation Res.* 4: 302, 1956.
89. Rushmer, R. F. Autonomic balance in cardiac control. *Am. J. Physiol.* 192: 631, 1958.
90. Rushmer, R. F., and O. Smith. Cardiac control. *Physiol. Rev.* 39: 41, 1959.
91. Rushmer, R. F., O. Smith, and D. Franklin Mechanisms of cardiac control in exercise. *Circulation Res.* 7: 602, 1959.
92. Rushmer, R. F. Postural effects on the baselines of ventricular performance. *Circulation* 20: 897, 1959.
93. Salisbury, P. F., C. E. Cross, and P. A. Rieben. Influence of coronary artery pressure upon myocardial elasticity. *Circulation Res.* 8: 794, 1960.
94. Salzman, E. W., and S. D. Leverett. Peripheral venoconstriction during acceleration and orthostasis. *Circulation Res.* 4: 540, 1956.
95. Salzman, E. W. Reflex peripheral venoconstriction induced by carotid occlusion. *Circulation Res.* 5: 149, 1957.
96. Sarnoff, S. J., and E. Berglund. Ventricular function I. Starling's law of the heart studied by means of simultaneous right and left ventricular function curves. *Circulation* 9: 706, 1954.
97. Sarnoff, S. J., R. B. Case, E. Berglund, and L. C. Sarnoff. Ventricular function V. The circulatory effects of aramine; mechanism of action of "vasopressor" drugs in cardiogenic shock. *Circulation* 10: 84, 1954.
98. Sarnoff, S. J. Myocardial contractility as described by ventricular function curves; observations on Starling's law of the heart. *Physiol. Rev.* 35: 107, 1955.
99. Sarnoff, S. J., R. B. Case, G. H. Welch, Jr., E. Braunwald, and W. N. Stainsby. Performance characteristics and oxygen debt in a nonfailing, metabolically supported, isolated heart preparation. *Am. J. Physiol.* 192: 141, 1958.
100. Sarnoff, S. J., E. Braunwald, G. H. Welch, Jr., R. B. Case, W. N. Stainsby, and R. Macruz. Hemodynamic determinants of oxygen consumption of the heart with special reference to the tension-time index. *Am. J. Physiol.* 192: 148, 1958.
101. Sarnoff, S. J. Certain dimensions of circulatory regulation with special reference to the control of cardiac output. Abstracts of Symposia, III World Congress of Cardiology, 1958, p. 84.
102. Sarnoff, S. J. Some physiologic considerations in the genesis of acute pulmonary edema. *Pulmonary Circulation.* Edited by Wright Adams and Ilza Veith. New York: Grune & Stratton, 1959.
103. Sarnoff, S. J., J. H. Mitchell, J. P. Gilmore, R. J. Linden, and S. K. Brockman. The regulation of function in the innervated heart. Hypertension—Renal, Electrolyte and Autonomic Factors. Proceedings of the Council for High Blood Pressure Research, American Heart Assoc. Edited by Floyd R. Skelton, vol. VIII, 1959.
104. Sarnoff, S. J., J. H. Mitchell, J. P. Gilmore, and J. P. Remensnyder. Homeometric autoregulation in the heart. *Circulation Res.* 8: 1077, 1960.
105. Sarnoff, S. J., S. K. Brockman, J. P. Gilmore, R. J. Linden, and J. H. Mitchell. Regulation of ventricular contraction: Influence of cardiac sympathetic and vagal nerve stimulation on atrial and ventricular dynamics *Circulation Res.* 8. 1108, 1960.
106. Sarnoff, S. J., J. P. Gilmore, S. K. Brockman, J. H. Mitchell, and R. J. Linden. Regulation of ventricular contraction by the carotid sinus: Its effect on atrial and ventricular dynamics. *Circulation Res.* 8: 1123, 1960.

106a. Sarnoff, S. J., J. P. Gilmore, and J. H. Mitchell. The influence of atrial contraction and relaxation on closure of the mitral valve: observations on the effects of autonomic nerve activity. *Circulation Res.* In press.

107. Schaefer, R. D., and R. C. Little. The first heart sound in ventricular contractions arising from the apex and base. *Proc. Soc. Exper. Biol. & Med.* 85: 639, 1954.
108. Shipley, R. E., and D. E. Gregg. The cardiac response to stimulation of stellate ganglia and cardiac nerves. *Am. J. Physiol.* 143: 396, 1945.
109. Shreiner, G. L., E. Berglund, H. G. Borst, and R. G. Monroe. Effects of vagus stimulation and of acetylcholine on myocardial contractility, O_2 consumption, and coronary flow in dogs. *Circulation Res.* 5: 562, 1957.

109a. Siegel, J. H., J. P. Gilmore, and S. J. Sarnoff. Studies on the myocardial extraction and production of catechol amines during direct cardiac sympathetic nerve stimulation. *Circulation Res.* 9: 1336, 1961.

110. Smith, O. A., R. F. Rushmer, and E. P. Lasher. Similarity of cardiovascular responses to exercise and to diencephalic stimulation. *Am. J. Physiol.* 198: 1139, 1960.
111. Stainsby, W. N., S. J. Sarnoff, E. Braunwald, R. B Case, and G. H. Welch. Effect of independent alterations of stroke value, aortic pressure and heart rate on left ventricular function. *Fed. Proc.* 15: 177, 1956.
112. Starling, E. H. *Principles of Human Physiology* (2nd ed.). Philadelphia: Lea & Febiger, 1915.
113. Starling, E. H. *The Linacre Lecture on the Law of the Heart.* (Given at Cambridge, 1915.) London: Longmans, Green, 1918.
114. Starling, E. H. On the circulatory changes associated with exercise. *J. Roy. Army M. Corps* 34: 258, 1920.
115. Starling, E. H., and E. B. Verney. The secretion of urine as studied on the isolated kidney. *Proc. Roy. Soc., London* 97: 321, 1924–25.
116. Stella, G. The oxygen consumption of the tortoise heart: its dependence on diastolic volume and on the mechanical conditions of systole. *J. Physiol.* 72: 247, 1931.
117. Stirling, G. R., P. H. Stanley, and C. W. Lillehei. The effects of cardiac bypass and ventriculotomy upon right ventricular function. *Surg. Forum, Proc.* 8: 433, 1958.
118. *Tissue Elasticity.* Edited by John W. Remington, Washington, D. C.: Am. Physiological Soc., 1957.
119. Ullrich, K. J., G. Riecker, and K. Kramer. Das Druckvolumdiagrams des Warmblüterherzens. Isometrische Gleichgewichtskurven. *Arch. ges. Physiol.* 259: 481, 1954.
120. Waldhausen, J. A., N. S. Braunwald, R. D. Bloodwell, W. P. Cornell, and A. G. Morrow. Left ventricular function following elective cardiac arrest. *J. Thoracic Surg.* 39: 799, 1960.

121. WALLER, A.: Die Spanning in den Vorhöfen des Herzens während der Reizung des Halsmarkes. *Arch. Physiol.* p. 525, 1878.
122. WANG, H., M. R. BLUMENTHAL, AND S. C. WARD. Effect of efferent vagal stimulation on coronary sinus outflow and cardiac work in the anesthetized dog. *Circulation Res.* 8: 271, 1960.
123. WELCH, G. H., E. BRAUNWALD, R. B. CASE, AND S. J. SARNOFF. The effect of mephentermine sulfate on myocardial oxygen consumption, myocardial efficiency, and peripheral vascular resistance. *Am. J. Med.* 24: 871, 1958.
124. WIGGERS, C. J. The physiology of the mammalian auricle. II. The influence of the vagus nerves on the fractionate contraction of the right auricle. *Am. J. Physiol.* 42: 133, 1917.
125. WIGGERS, C. J., AND L. N. KATZ. The specific influence of the accelerator nerves on the duration of ventricular systole. *Am. J. Physiol.* 53: 49, 1920.
126. WIGGERS, C. J., AND L. N. KATZ. Contour of ventricular volume curves under different conditions. *Am. J. Physiol.* 58: 439, 1921–22.
127. WIGGERS, C. J. *Circulation in Health and Disease* (2nd ed.). Philadelphia: Lea & Febiger, 1923, p. 77.
128. WIGGERS, C. J. The mechanism of cardiac stimulation by epinephrine. *J. Pharmacol. & Exper. Therap.* 30: 233, 1927.
129. WYNDHAM, C. H., AND J. S. WARD. An assessment of the exercise capacity of cardiac patients. *Circulation* 16: 384 1957.

Effects of nerve stimulation and hormones on the heart; the role of the heart in general circulatory regulation

ROBERT F. RUSHMER | *Department of Physiology and Biophysics, University of Washington School of Medicine, Seattle, Washington*

CHAPTER CONTENTS

A PRINCIPAL OBJECTIVE of cardiovascular investigation is the understanding of the function and control of the heart in normal people and in patients with various diseases. Analysis of the heart as a pump requires simultaneous measurements of several variables including the effective pressures, the absolute volumes of the cardiac chambers, and the velocity and volume flow of blood in and out of the heart. If these factors could be measured accurately, painlessly, and safely, normal persons would be the obvious choice for experimental subjects. Unfortunately, of these variables, only pressure can be recorded directly and continuously in human subjects under normal conditions. The changing volumes and flow of blood must be estimated from intermittent, indirect determinations involving procedures that can alter the measured variables by arousing apprehension or fear. Although volume and flow can be ascertained fairly frequently, the accuracy of many of these measurements depends upon the existence of steady-state conditions, so that the nature of the transition from one level of activity to another cannot be readily studied. Without continuous registration of the essential variables, it is often difficult to evaluate the steadiness of the control condition or the sequence of events during the response to an experimental procedure.

In recent years techniques have been developed for direct and continuous measurement of pressure, dimensions and flow in healthy unanesthetized animals during all manner of spontaneously and experimentally induced cardiovascular reactions. The cardiac responses observed under these conditions have been consistent with available information on cardiac responses in man, but have failed to conform to predictions based on a wealth of experimental data obtained from studies on the exposed heart of the anesthetized dog.

The nature of the cardiac adaptations observed in heart-lung preparations or in exposed hearts has had a dominant influence on the concepts of cardiac control for a great many years. As early as 1884 Howell & Donaldson (19) presented evidence that

the output of the heart is a reflection of venous inflow. In their experiments with the Newell Martin heart-lung preparation, increasing the inflow in canine hearts caused about a fourfold increase in cardiac output and stroke volume as the right atrial pressure was raised from 10 cm to 60 cm of blood. Otto Frank's contributions to an understanding of the factors influencing the function of the isolated heart are generally recognized, but Chapman and Wasserman's recent translation of his work (11) should broaden the appreciation of his superlative experimental techniques. Experiments by Starling (29), Straub (49), and Wiggers (54) extended and refined these observations. It is not generally realized that Starling's main contribution to the development of heart-lung preparations was an improved means of controlling resistance (22). The generalization which is commonly known as Starling's law of the heart is actually a restatement of conclusions previously enunciated by Blix and Fick for skeletal muscle and by Frank for the myocardium (see ref. 41). The experiments conducted by Starling and his colleagues were extremely well designed, meticulously executed, and beautifully described. However, the subsequent extrapolation of the results to normal humans and animals (48) was premature, since the exact nature of the cardiac response during spontaneous adjustments had not been accurately described.

The principal procedure for increasing cardiac output in experiments on heart-lung preparations was to elevate the ventricular filling pressure by one means or another. The nature of the experimental model led directly to the widely accepted concept that cardiac control is determined principally by the "venous return." "It is axiomatic that the heart can pump only as much blood as it receives. Indeed the volume of blood returned to the heart is the basic determinant of cardiac output" (56). Implicit in the assumption that cardiac output is determined by venous return is the concept that the stroke volume is increased through the Starling mechanism. If these investigators had elected to stimulate the sympathetic cardiac nerves instead of to raise or lower a venous reservoir in order to induce changes in cardiac performance, quite different concepts of cardiac control would have evolved. It might even have been considered "axiomatic" that "the quantity of blood pumped by the heart determines the amount returning to the heart, thus the cardiac output is the basic determinant of venous return."

Although it was generally recognized that changes in the "physiological state" of the myocardium could be important determinants of ventricular performance, the Frank-Starling mechanism dominated the thinking about the heart so completely that neural and hormonal regulation of cardiac performance was largely ignored for many years. This situation did not occur in the case of skeletal muscle, whose contractility likewise depends upon its resting length. In this case, the much greater dependence upon the number and pattern of nerve impulses was conspicuous even in the isolated preparation. The need for central coordinating mechanisms was more obvious than in the case of a myocardium which could perform well even without nerves.

NATURE OF INCREASED CONTRACTILITY

Neural and hormonal controls affect the myocardium by inducing changes in its "physiological state" of the sort elicited by the direct action of epinephrine. The term "increased contractility" has been applied to these changes in myocardial performance. The word "contractility" has a fairly specific definition: namely, the property or capacity of cells for shortening in response to an appropriate stimulus (7). In contrast, "increased contractility" has been used to indicate many factors in different contexts; it is rarely defined and is replete with sources of semantic confusion. For example, "increased contractility" has been applied to increased stroke volume (15), increased force of contraction (6), and increased "vigor" and "velocity" of contraction (43, 55). The ventricular function curves devised by Sarnoff and his colleagues (40) describe or define changes in contractility in terms of energy released by the heart. Changes in contractility have also been defined in terms of peak contractile tension or peak systolic pressure, rate of pressure rise or fall, duration of contraction, degree of contraction, and other facets of contraction in various combinations.

If neural and hormonal mechanisms are important in cardiac control and if they exert their influence by producing changes in contractility, this term must be more fully and accurately defined. It is also important to decide whether contractility is really a single mechanism or is a group of mechanisms arbitrarily designated by a single term. Evaluation of the nature of contractility requires analysis of many different factors—more than can be conveniently measured in human subjects. However, recently developed techniques (2) make possible continuous analysis of many different aspects of left ventricular performance in healthy active dogs (fig. 1).

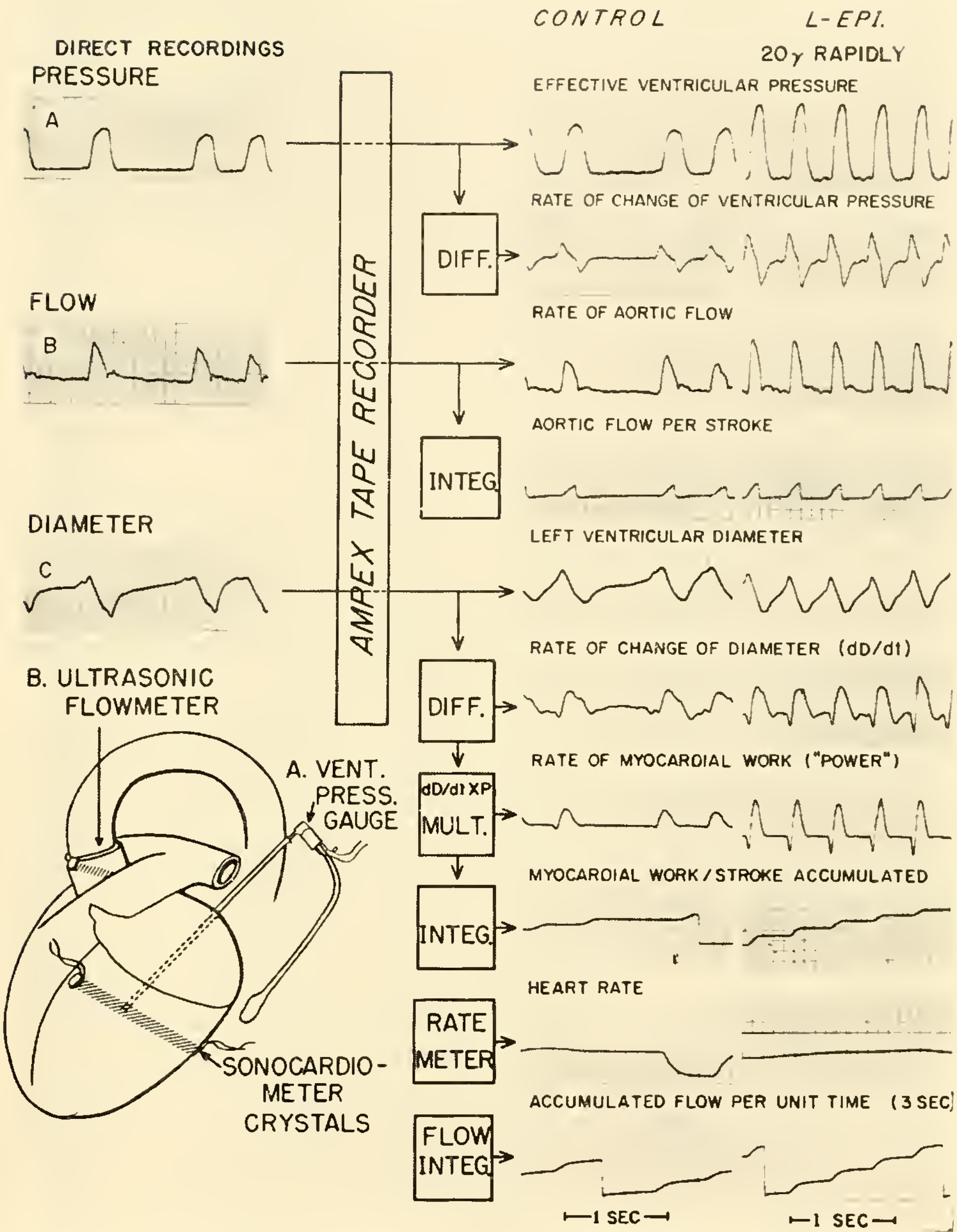

FIG. 1. *A:* effective ventricular pressure registered through an indwelling catheter by means of a miniature pressure gauge. *B:* instantaneous flow through the aorta recorded by a pulsed ultrasonic flowmeter. *C:* left ventricular diameter recorded in terms of the transit time of ultrasonic waves (3 megacycles) between two barium titanate crystals mounted on opposite sides of the chamber. These signals are stored on multichannel tape and subsequently analyzed in terms of additional functions derived by electronic analogue computers (see text). The changes in these variables produced by administration of *l*-epinephrine are shown in the right-hand column.

CHARACTERISTICS OF VENTRICULAR CONTRACTILITY

Methods of Analysis

The performance of any pump must be evaluated in terms of at least three basic parameters: pressure, flow, and dimensions. Techniques have been developed specifically to record these variables continuously and simultaneously in intact animals while they moved about.

Effective left ventricular pressure is measured

through an indwelling cannula extending posteriorly from the left atrium to the outside. A slightly longer catheter on a special miniature differential pressure gauge (2) is threaded through the lumen of the cannula, past the mitral valve orifice and into the left ventricular cavity. Pressure from a balloon in the pleural space near the left ventricular wall is impressed upon the back of the gauge, which then responds to effective left ventricular pressure (fig. 1*A*).

Left ventricular outflow is continously monitored by means of a pulsed ultrasonic flowmeter (2, 12, 13, 16, 18). In principle, the time required for a burst of 3-megacycle vibrations to pass a fixed distance diagonally across the root of the aorta is the same in either direction when the blood is stationary (fig. 1*B*). If blood is moving out of the ventricle the sound travels faster downstream than upstream and this difference in transit time is directly proportional to the mean velocity of flow across the aorta. If the dimensions of the aorta are held fixed by a rigid plastic cylinder supporting the ultrasonic crystals, the mean velocity is directly related to the instantaneous volume flow and the gauge can be directly calibrated in these terms.

Changes in cardiac dimensions have been recorded in terms of the diameter, length, and circumference of the left ventricle (2). Currently left ventricular diameter is monitored 1000 times a second as the transit time of ultrasonic bursts between two barium titanate crystals mounted on opposite sides of the chamber (fig. 1*C*). Since these sound waves travel 1.5 mm per μsec through the ventricular wall and blood, this transit time can be readily converted into distance (2, 35). Unfortunately, the complex configuration of the ventricular chamber, coupled with the fact that its different dimensions do not change by the same amounts, appears to preclude accurate computation of changes in ventricular volume from the changes in any one dimension (17). However, changes in diameter may be regarded as representing the action of a sample of myocardium which reduces that dimension during systole.

Other variables can be derived by means of electronic analogue computers. When applied to an appropriate differentiating circuit, the signals from the pressure transducer are transformed into deflections which indicate continuously the slope (rate of change) of the ventricular pressure curve. Thus, the apex of the upward deflection represents the steepest slope during the isovolumetric pressure rise, and the trough of the downward deflection represents the steepest slope of the pressure drop at the end of systole.

Applying the signal from the aortic flowmeter to an integrating circuit corresponds to adding the volume flow for each successive instant during systole, so that the peak deflection attained at the end of systole represents the total flow during the stroke. By means of another differentiating circuit, the rate of change of diameter can be derived from the sonocardiometer records. These deflections are a continuous representation of the changing slope of the diameter curve, inverted for comparison with the flow record. Since the rate of change of volume is a definition of flow, the record showing the rate of change of diameter is an expression of the extent to which the changing diameter is equivalent to a corresponding change in ventricular volume. Comparisons between the rate of change of diameter and directly registered aortic flow provide an opportunity to test the internal consistency of the observations.

The product of the rate of change of volume (flow) and the pressure is a definition of power (the rate of doing work). If the rate of change of diameter is continuously multiplied by the effective left ventricular pressure, the resulting record illustrates a function of the "power" developed by the sample of myocardium which produces the change in diameter. The area under the power curve, derived by an integrating circuit, is an expression of the "work" performed during a cardiac cycle by that sample of myocardium. The height of the step during each successive cycle during specific intervals (e.g., 5 sec) represents the accumulated work per unit time and accounts for both stroke "work" and heart rate. A more accurate indication of the "power" and "work" developed by the entire ventricle is obtained by directly multiplying the instantaneous aortic flow by the effective ventricular pressure. The heart rate is continuously registered by a rate meter triggered by the rising phase of each successive pressure pulse. The steps representing the stroke flow can be added successively during consecutive 2-sec intervals to provide an indication of the cardiac output per unit time. This value takes into account both stroke volume and heart rate.

In various combinations these primary and derived parameters have been recorded during many experimental and spontaneous adjustments in the cardiac function of intact unanesthetized dogs (36).

A Functional Description of "Increased Contractility"

To illustrate the salient features of increased contractility, the cardiac responses to administration of *l*-epinephrine (20 μg rapidly injected into a 14-kg dog) are shown at right in figure 1. This particular example was selected because the typical bradycardia was not present (36, 39, 53); the heart rate was regular at about 140 beats per min. In brief, the various recorded parameters were affected as follows: The effective left ventricular pressure reached peak values about 30 per cent higher than those during the control interval. Visual inspection indicates that ventricular pressure rose and fell more rapidly than during the control. This impression is confirmed by the larger upward and downward deflections in the next lower record, which shows the rate of change of ventricular pressure (dP/dt). The instantaneous rate of aortic blood flow reached higher peak values during systolic ejection under the influence of epinephrine. This increase in ejection velocity was not necessarily reflected in an increase in the volume ejected during each systolic interval. Often, the aortic flow per stroke was increased only slightly or remained unchanged because the duration of systole was reduced by an amount that was roughly equivalent to the increase in ejection velocity. As a result, the area under the aortic flow curves was not significantly changed. The shortening of ventricular systole by epinephrine is quite apparent in all the records.

The left ventricular diameter was slightly diminished during both diastole and systole. The stroke deflection was not appreciably altered, a finding which confirms that stroke volume was not significantly changed by the action of the epinephrine. The rate of change of diameter resembled the aortic flow. To the extent that the diameter is related to the ventricular volume, the rate of change of diameter must be related to the outflow pattern. However, a sharp downward deflection at the onset of systole did not appear in the record of aortic flow. The abrupt increase in diameter has previously been explained in terms of a sudden change in diameter without a corresponding change in ventricular volume during so-called "isovolumetric" contraction (31). The abrupt downward deflection was also prominent in the record of myocardial "power". The negative "power" deflection represented work being done on the myocardial sample between the diameter crystals as affected by contracting myocardium elsewhere in the ventricle (for example, papillary muscles, trabecular carneae). The peak "power" was increased very markedly by epinephrine, an increase reflecting the accelerated rate at which the myocardium performs work during very rapid ventricular ejection. The steps representing stroke work were only slightly higher than those during the control period in spite of the very much higher rate of "power" development. This point illustrates again that the shortening of the systolic interval very nearly compensates for the much higher deflection, leaving the area under the curve only slightly increased. However, the accumulated stroke work over each 5 sec was very much higher because the tachycardia increased the number of steps per unit time.

During the control record the heart rate was quite irregular because of sinus arrhythmia. (The indication of heart rate always lags by one cardiac cycle because the rate meter responds to the length of a completed cycle.) During the response to epinephrine, the heart rate was faster and more regular than it had been during the control period. This is an atypical response to epinephrine in the intact animal, but the record was selected because it closely resembles those obtained during sympathetic stimulation. The result of the changes in heart beat was a marked increase in both the accumulated work per unit time and the accumulated flow per unit time (2 sec).

A unifying generalization emerged from examination of many records: increased ventricular contractility is expressed primarily by large changes in "rates" and small changes in quantities (fig. 2). The increase in ventricular systolic pressure is not covered by this statement, but this increased pressure directly reflects the increased rate of ventricular ejection. The rate of change of pressure is very greatly accelerated. The quantity of blood ejected into the aorta per stroke (stroke volume) increases little or not at all, but the rate of ejection is much faster. The diastolic and systolic dimensions of the ventricle are not very different, but the rate at which the diameter changes during systole is increased. The slight increase in stroke volume is commonly accompanied by increased systolic ejection rather than by greater diastolic filling, although both may occur. The computed "work per stroke" changes relatively little although the peak "power" (rate of doing "work") is consistently increased.

Changes in the "physiological condition" of the ventricular myocardium like those illustrated in figures 1 and 2 are observed during treadmill exercise by intact dogs and during a number of procedures

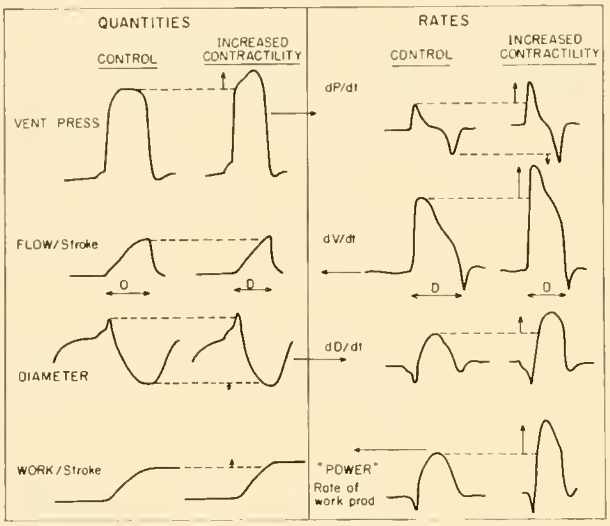

FIG. 2 Increased ventricular "contractility" is characterized in terms of the variables indicated in figure 1. Changes in quantities (i.e., pressure, flow/stroke and diameter or work/stroke) are not altered as much as the rates (i.e., rate of changes of pressure, rate of flow, rate of change of diameter, and rate of performing work, which is power), during increased contractility.

leading to changes in cardiac function rather closely simulating those of exercise. Included in the latter category are administration of epinephrine accompanied by tachycardia, administration of isoproterenol, and electrical stimulation of selected sites in the diencephalon (36, 47). The typical ventricular responses under these conditions involve at least six major components: *1*) more rapid rise in ventricular pressure during isovolumetric contraction, *2*) more rapid fall in ventricular pressure during isovolumetric relaxation, *3*) faster myocardial shortening and more rapid ventricular ejection, *4*) more complete systolic ejection, *5*) elevated peak systolic tension due in part to faster systolic ejection, and *6*) increased maximum possible isometric contraction tension. The evidence for the occurrence of the last component is the observation that, when the aorta is clamped, sympathetic stimulation of the exposed heart drives ventricular pressure to levels as high as 500 mm Hg during ventricular contractions which are almost isometric (1, 24).

Contractility, a Generic or a Specific Term

In physiological circumstances, the factors defining contractility tend to vary together even though they may involve different mechanisms. For example, a faster-rising contractile tension may reflect more nearly simultaneous excitation of the various bundles of myocardium. This mechanism would be a function of the conduction system. The shorter duration of systole indicates a more rapid repolarization of the individual muscle membranes, a function of the transmembrane ion exchanges. The faster myocardial shortening to produce more rapid ejection must involve a change in the myocardial contractile elements. The more rapid isovolumetric relaxation might involve either more synchronous repolarization or an altered rate of relaxation of the contractile elements. A more complete systolic ejection suggests either greater contractile tension or less loss of tension due to shortening owing to unknown changes at the cellular or molecular level. To lump all these factors under a single term such as "increased contractility" may obscure the issues and serve as a semantic obstacle to an understanding of the various mechanisms. Contractility must be treated as a term covering many different factors, so that we may define and understand each aspect individually. We must not close our minds to the possibility that mechanisms which are completely unsuspected at present play important roles in the control of the heart.

THE NATURE OF SPONTANEOUS CARDIOVASCULAR ADJUSTMENTS

The experimental techniques illustrated in figure 1 have been used in various combinations for continuous analysis of left ventricular performance in healthy active dogs, fully recovered from the surgical installation of the recording devices. Although it is unwise to extrapolate from dogs to man, such studies may depict circulatory response patterns that indicate what measurements should be explored in man. By comparing the continuous analysis with the available information on human reactions, one should gain some insight into the extent to which these reactions correspond to the patterns in dogs.

The most prominent feature of cardiovascular function, in dogs, under "normal" conditions is the unremitting fluctuation. The heart rate, ventricular and arterial pressures, ventricular dimensions, and flow all vary continuously. Many deviations in the records are obviously associated with such things as moving all or part of the body and altered respiratory activity a; well as with eating, exercise, and startle reactions (fig. 3). In contrast, prominent cardiovascular adaptations which cannot be attributed to any

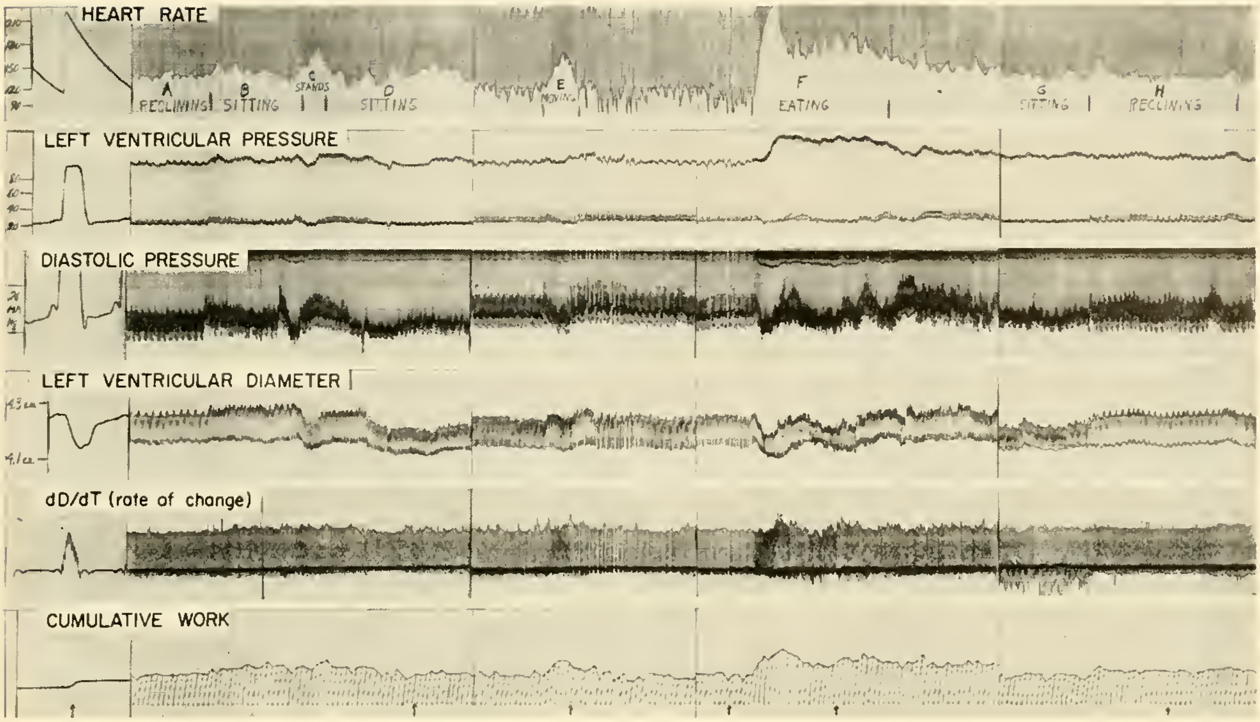

FIG. 3. In healthy alert dogs, the principal variables fluctuate continuously in response to stimuli from the external environment or from spontaneous changes in level of activity. In the dog, the changes in ventricular performance during eating are similar to those occurring during exercise and may be as pronounced.

event detected by an observer are frequently recorded. Most of the spontaneous fluctuations disappear under the influence of standard anesthetic agents, as though the cardiovascular system were completely severed from the higher levels of the central nervous system.

The cardiac responses are altered by repetition of events and by "conditioning." For example, a very prominent cardiac response can be elicited by making a loud noise—as by dropping a metal wastebasket. If this noise is repeated, the cardiovascular response is greatly attenuated, and by the third or fourth trial no vestige of a response may be observed. Even on subsequent days it may not be possible to produce a response as intense as that from the original stimulus. Similarly, the first few cardiovascular adaptations to exercise on a motor-driven treadmill show a progressive reduction in the initial overshoot (39). The responses become quite reproducible after the four or five trials in those animals that are easily trained. Some animals do not adapt well to the laboratory situation and resist all efforts at training. In these animals, the cardiac responses stabilize very slowly.

Variation in responses from animal to animal is consistently noted. Although the response patterns in a group of animals may be generally similar, they differ in important and distinctive details. In fact, with experience, the records from a specific dog can be identified in a group of records with quite remarkable accuracy. Obviously, the individual characteristics are more consistently recognized in records obtained after the animals are well trained.

In normal human subjects, certain cardiovascular variables can be recorded continuously (such as, heart rate, systemic arterial pressure, or finger volume). Such records exhibit the same type of spontaneous fluctuations under normal conditions. Very subtle changes in the environment may induce obvious changes indicating the interplay of multiple factors in cardiovascular regulation. The difficulties encountered in attempts to obtain reliable and reproducible values for systemic arterial pressure represent a case in point. Also, when finger volume is measured both intrinsic and extrinsic factors produce continuous fluctuations indicating adaptations in the calibre of the blood vessels in the finger. Individual differences in cardiovascular responses are a most challenging aspect of clinical management. Thus, there is little reason to doubt that spontaneous fluctuation of

cardiovascular function is a characteristic shared by healthy dogs and people. This aspect of cardiovascular function should be enough by itself to discourage attempts to explain cardiac control in terms of any simple generalization.

POSTURAL RESPONSES

When a healthy dog is fully relaxed and recumbent, its heart rate is relatively slow, ranging between 70 and 90 beats a minute, and pronounced sinus arrhythmia is often present. Continuous recordings of cardiac dimensions demonstrate that the left ventricle expands rapidly during diastole to reach a steady size (diastasis) early in the diastolic interval. This size persists with little change, even during atrial systole, until the next systolic contraction. Under these conditions the left ventricle functions at or near its maximal diastolic dimensions. The validity of this statement is evidenced by the fact that the filling pressure can be increased some 15 to 20 mm Hg by intravenous infusions without the diameter of the left ventricle increasing as much as a millimeter (36). In the relaxed recumbent dog, the systolic changes in the ventricular dimensions are greater than those observed in this laboratory under any other conditions, with the possible exception of the beats following extrasystolic compensatory pauses. Confirming this impression is the observation that the stroke volume recorded at the aortic root by an ultrasonic flowmeter is also as large as that under any other condition observed in these studies (13). The peak flow velocity is higher when contractility has increased (figs. 1 and 2), but the area under the velocity flow curve (stroke volume) is apparently maximal or almost maximal in the recumbent dog. Any condition—spontaneous, induced, or pathological—which produces a very slow heart rate would quite certainly produce this maximal degree of distention and a large stroke volume. It is recognized that stroke volume may increase under extremes of exertion to values well in excess of those observed during relaxed recumbency (see below).

When the animal shifts his position, sits up or stands, the left ventricular dimensions promptly diminish; at the same time the systolic deflections, peak flow velocity, and stroke volume decrease (33). Thus, the reduction in diastolic distention is accompanied by a reduction in the amount of energy released by the ventricle in a manner predictable from the Frank-Starling mechanism. In dogs, the trunk is

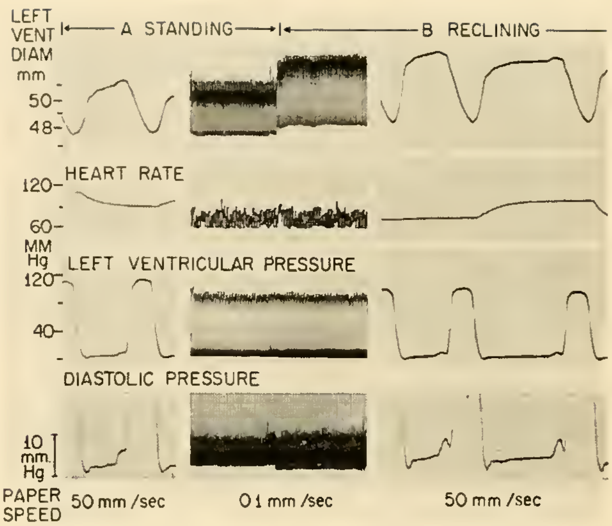

FIG. 4. When a dog lies down, the left ventricular diameter promptly increases to a higher level, associated with increased systolic deflection and stroke work in accordance with the Frank-Starling mechanism. This change in diameter is not necessarily accompanied by a change in either heart rate or effective filling pressure as nearly as this can be ascertained. This observation suggests that ventricular "distensibility" may have changed, but this cannot be definitively established (see text).

horizontal in both the recumbent and standing positions, and these changes in ventricular dimensions frequently occur without changes in diastolic filling pressure (fig. 4). Clearly, this response does not depend upon a vertical orientation of the long columns of blood even though it can be readily induced by passive tilting of the animal (fig. 5). In fact, a similar reduction in ventricular dimensions, stroke volume, and ejection velocity may occur when a recumbent dog merely lifts his head in response to a sudden noise.

In normal human subjects, the area of the cardiac silhouette on roentgenograms has consistently been observed to be maximal in the recumbent position and to be reduced promptly when the subject stands up (23, 27, 28, 30, 45). For example, Sjöstrand (45) reported that the heart volume is greater during recumbency than during standing or sitting. The diastolic volume was either unchanged or decreased when adrenaline, noradrenaline, atropine, nitroglycerin, or digitalis in toxic doses was administered. Consequently, under optimal conditions of heart filling, as exist in recumbency, the heart appears to to fill maximally with blood during diastole.

When the subject stands up, blood accumulates in the veins of the dependent parts and the quantity

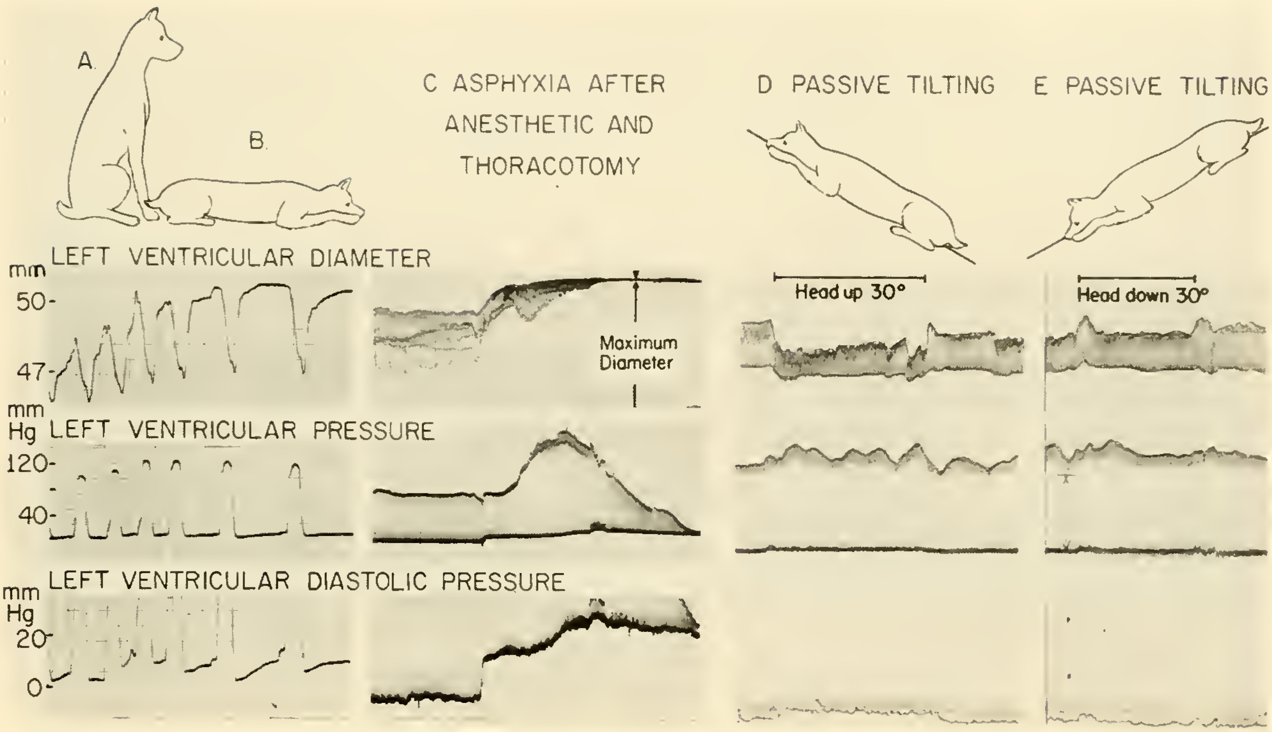

FIG. 5. When a dog reclines, left ventricular diameter increases progressively until the diastolic diameter begins to display a plateau (diastasis). After anesthesia and thoracotomy, the heart was observed to distend to a maximal size during asphyxia, and this maximum distention is comparable to the diastolic diameter in the reclining dog. The reduction in ventricular dimensions is not a result of the muscular activity because it occurs with passive tilting with the head up but not so obviously with tilting head down.

of blood in the lungs and heart is depleted. Kjellberg *et al.* (21) made several observations indicating that the left ventricle is a major source of the blood given up by the heart in this type of redistribution. Duomarco *et al.* (8) presented evidence that the venae cavae and their intrathoracic branches are all well distended when normal men are recumbent. In the erect posture the superior vena cava and its branches are distinctly collapsed above a level just above the right atrium. The depletion of blood from the superior vena cava, brachiocephalic vessels, and pulmonary veins in erect men represents a reduction in the capacity of the venous reservoirs just upstream from both ventricles. Thus the atria and the adjacent venous channels correspond in some ways to the venous reservoir in the heart-lung preparation and may be regarded as a low pressure sump from which the ventricles fill during each diastolic interval.

The Preventricular Sump

The blood that enters a ventricular chamber during each diastolic filling period comes not only from the corresponding atrium but also from considerable distances along the venous channels leading to the heart. Thus, the central veins and atria represent low pressure, variable capacity sumps just upstream from the right and left ventricular cavities. This concept of a preventricular sump corresponds to the "surge chamber" proposed by Sjöstrand (44) and elaborated by Holmgren (18). An abrupt increase in heart rate can produce a transient increase in cardiac output without a corresponding acceleration of venous flow by pumping out some of the ventricular systolic reserve capacity and by depleting some of the capacity of this sump. The augmented cardiac output can persist only for a few beats, however, if the venous inflow does not increase promptly. Thus, it is necessary to visualize a very prompt acceleration of blood flow in all parts of the circulatory tree during any transition from one level of cardiac output to another.

In standing human subjects, the collapse of the superior vena cava and the transfer of blood out of the pulmonary veins reduces the capacity of the preventricular sumps of the right and left ventricles, respectively. On this basis, cardiac output is more

apt to be limited or restricted by "venous return" in the erect than in the recumbent position. One criterion for restriction of cardiac output by inadequate venous return would be failure of the cardiac output to increase when the heart rate is accelerated (see below).

Assuming that the erect position reduces ventricular dimensions and stroke volume because venous return is limited by depletion of the preventricular sump, this mechanism would be greatly exaggerated by exposure to positive radial acceleration. When centrifugal forces act from head to foot, the increased weight of the blood tends to produce increased accumulation of blood in dependent regions. Gauer (14) employed cinefluorographic angiocardiography to study the changes in ventricular volume and stroke volume in monkeys exposed to radial acceleration up to five or six times the force of gravity. At the onset of gravitational stress the diastolic heart size and stroke volume were not reduced for a few beats, but the radiodensity of the lungs was rapidly reduced. Then the diastolic and systolic volumes rapidly diminished in a few beats until the systolic reserve volume was completely depleted, and the ventricles emptied during each stroke. From this point on, the stroke volume was a function solely of diastolic filling. This description conforms very well to the concept that stroke volume directly reflects the venous return when, under the influence of centrifugal forces, the systolic reserve volume and preventricular sumps are maximally depleted. Clearly, the cardiac output may be reduced and be limited by inadequate "venous return" during positive radial acceleration.

RELATION OF HEART RATE TO CARDIAC OUTPUT

If the heart in an intact dog is accelerated artificially through stimulating electrodes previously applied on the atrial wall, the diastolic and systolic dimensions and the systolic excursions diminish progressively as the heart rate is increased in a stepwise fashion. This observation suggests that cardioacceleration, unaccompanied by accelerated blood flow throughout the system, increases cardiac output at the expense of the preventricular sumps and the ventricular systolic reserve volume. However, induced tachycardia may indeed produce increased cardiac output, if the preventricular sumps remain adequately filled. For example, Weissler *et al.* (58) produced a tachycardia in normal recumbent subjects by administering atropine, and demonstrated a large increase in cardiac output accompanied by a fall in central venous pressure. Stroke volume was not significantly altered. Erect subjects displayed a reduction in central venous pressure and central blood volume, greater cardioacceleration produced by atropine, and reduced stroke volume. As a result, cardiac output increased only slightly. Counterpressure, applied by inflating anti-G suits over the legs and abdomen, restored in part the cardiac output and stroke volume in erect subjects.

Reduction in heart size and stroke volume with tachycardia indicates that blood is pumped out of the ventricles faster than the preventricular sumps are replenished by venous flow. The filling pressure of the heart diminishes, but, at the same time, the pressure gradient along the veins may become steeper and flow toward the heart could be accelerated by this mechanism. The pressure and the capacity of the preventricular sumps are both greater in the recumbent than in the erect positions. These considerations suggest that an inappropriate tachycardia (such as, paroxysmal tachycardia or anxiety) may produce a large increase in cardiac output in reclining subjects when the sumps are well distended. In the erect position, a similar degree of tachycardia may not increase cardiac output to the same extent.

In summary, the cardiac responses observed during changes from the recumbent to the erect position conform well to predictions from the Frank-Starling mechanism. These effects are exaggerated by exposure to positive radial acceleration. The variable capacity reservoirs, or preventricular sumps, just upstream from each ventricle, correspond functionally to the venous reservoir employed in the heart-lung preparation. Under the influence of such gravitational forces, a reduction in venous return may rather directly reduce stroke volume and even limit the increase in cardiac output which can be produced by tachycardia. An increase in heart size and stroke volume in the recumbent position occurs in both dogs and men in spite of the differences in the orientation of the long axis of body. A teleologically satisfying rationale for a greater stroke volume and cardiac output at rest than in the erect position is not obvious at present. The role of the Frank-Starling mechanism is not immediately apparent in other spontaneous cardiac adjustments such as eating, startle reactions, alerting responses, walking, running, or jumping, presumably because other control mechanisms play dominant roles.

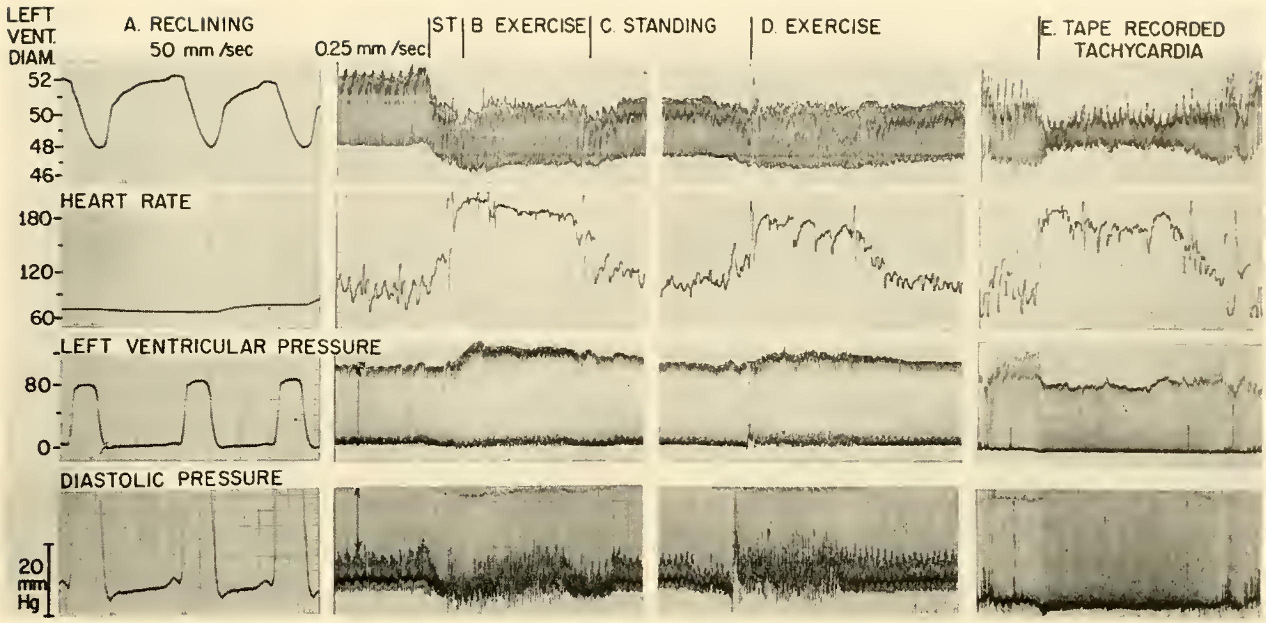

FIG. 6. If a reclining dog abruptly begins to exercise on a treadmill, the ventricular diameter first diminishes as he stands up and then changes little during the subsequent exertion. If the animal is standing during the control period, the ventricular dimensions are changed very little during moderate treadmill exercise. [From Rushmer (33).]

CARDIOVASCULAR RESPONSES TO EXERTION

The nature of the changes in ventricular performance in dogs during exertion depends to some extent upon conditions during the control period. For example, if the animal is reclining quietly on the treadmill until the moment it starts, the ventricular dimensions abruptly diminish as the animal stands, and the diastolic, systolic, and stroke dimensions are all reduced throughout the exercise and thereafter until the animal reclines again (see fig. 6). On the other hand if the animal is standing during the control period, the diastolic and systolic dimensions and stroke deflections are already diminished when the treadmill is started and change only slightly during the exertion. Under these conditions the systolic ejection may be somewhat more complete or diastolic distention slightly greater, but the over-all change is not impressive at moderate levels of exertion (fig. 6). The rate of change of diameter and the peak rate of flow are both greatly accelerated during exercise. The duration of systole is reduced, the ventricular systolic pressure is somewhat elevated, as a rule, and the rise and fall of ventricular pressure are very much steeper. The heart rate is accelerated promptly and the tachycardia is well sustained through the exertion. The cardiac output at the levels of exercise employed in these dogs is increased predominantly by accelerated heart rate without much increase in stroke volume. In other words, the changes in ventricular performance during moderate exercise correspond to the changes in contractility illustrated in figures 1 and 2 but of somewhat lesser degree.

During exertion the early diastolic pressure is lower, corresponding to a more rapid early diastolic filling—such as, a more rapid release of intrafascicular tension at the onset of diastole (34). The very low impedance to ventricular filling during early diastole is termed "diastolic suction" by some authors (5, 20). Under conditions of increased "contractility" a more synchronous relaxation of the myocardial fibers may permit a more simultaneous release of the total intrafascicular tension with a further reduction in the impedance to early diastolic filling. The increased ventricular pressure at the end of the diastolic period is clearly related to a more "powerful" atrial contraction, as though the "contractility" increased in both atrial and ventricular myocardium. Although the author previously reported that distensibility was increased by administration of epinephrine to intact dogs (38), this conclusion now seems unwarranted. Since a difference of 1 or 2 mm Hg in filling pressure may make a very great difference in ventricular volume under some conditions, this question must be

considered unresolved in intact animals where recordings are not sufficiently precise for this kind of distinction. This is not to say that occurrence of changes in myocardial distensibility has been effectively excluded in the intact animal or man. For example, the increase in ventricular dimensions with little or no sign of increased filling pressure on reclining certainly suggests that distensibility has changed (see fig. 4). Measurements of diastolic filling pressure in human subjects generally fail to include the extracardiac distending pressure because it is rarely convenient to record intrapleural pressure. Holmgren (18) reviewed the literature and reported his own data to support the conclusion that both right and left atrial pressure are essentially unchanged during the transition from rest to exercise. Sjöstrand (44) reported that the intrathoracic blood content neither increases nor decreases during work. Thus, shifts in blood from various portions of the venous system toward the heart need not be postulated. Marshall *et al.* (25) recently demonstrated that computed values for pulmonary blood volume would err consistently toward excessive values if the indicator dilution sample were withdrawn too slowly, it being possible to obtain values up to 100 per cent too large. In their experiments this factor was carefully controlled, and their values for pulmonary blood volume were either unchanged or increased less than 20 per cent under conditions of severe exertion. Kjellberg *et al.* (21) questioned the existence anywhere in the systemic circulation of blood "depots" in the usual meaning of this term. When Guntheroth (16) continuously recorded various dimensions of the liver and spleen in dogs, he found no consistent changes in the size of these organs during exercise. If there is no significant shift of blood from one part of the circulation to another, then the blood flow must accelerate so smoothly and uniformly throughout the entire circulation that little or no dislocation of blood occurs.

Ventricular Dimensions During Exertion

The available evidence clearly indicates that diastolic dimensions of the heart are not consistently increased and are often decreased during exercise. Directly recorded ventricular dimensions in dogs generally change little during treadmill exercise. Additional evidence to support this conclusion has stemmed from studies on both dogs (33, 42, 51) and men (21, 45). Indeed there is now little reason to doubt that diastolic size of the heart commonly remains unchanged or actually diminished during exercise. Systolic ejection may increase as a result of increased myocardial contractility owing to sympathetic discharge. Contrary to previous concepts, increased stroke volume is not a prominent factor in achieving increased cardiac output during a wide range of muscular exercise in most healthy dogs or men.

Constancy of Stroke Volume During Exercise

For many years the concept has prevailed that augmented stroke volume and accelerated heart rate contribute about equally to an increase in cardiac output during exercise, so that oxygen extraction in the tissues, indicated by the arteriovenous oxygen difference, is only slightly increased. The basic idea stemmed from extensive studies in which indirect Fick procedures were employed and the subjects were often trained athletes. These indirect methods, which involved use of carbon dioxide or foreign gases (acetylene, nitrous oxide, or ethyl iodide) to estimate the composition of mixed venous blood, have been largely abandoned in favor of the more accurate direct Fick method (catheterization) and indicator dilution techniques. As these newer methods have been applied to many normal but untrained persons it has become clear that, in contrast to the older view, increased oxygen delivery to the tissues during exertion is accomplished primarily by tachycardia and greater extraction of oxygen from the blood (fig. 7).

The severity of exertion is generally expressed in terms of the total oxygen consumption by the body. This practice is reasonable since the oxygen delivery to the tissues depends upon the combined effects of stroke volume and heart rate (cardiac output) and the arteriovenous oxygen difference (oxygen extraction from blood). Part *D* of figure 7 schematically summarizes data obtained in ten studies in which various investigators applied the direct Fick method or indicator dilution techniques to normal persons (33). These data include control values at rest and the changes during various levels of exercise in both erect and recumbent positions. Over a very wide range of exercise the stroke volume did not increase progressively (fig. 7). Sjöstrand (46) reached the same conclusion from his studies. However, stroke volume did increase during the transition from standing quietly to mild or moderate exercise (9), and an additional increase in stroke volume occurred during exercise so severe that the oxygen consumption had reached a plateau (i. e., at 6 to 9 mph on a treadmill

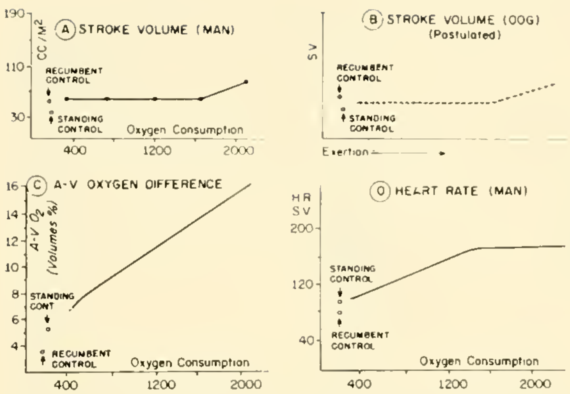

FIG. 7. *A:* in normal human subjects, the stroke volume displayed little evidence of a progressive increase with increasing severity of exercise as indicated by the oxygen consumption. *B:* judged from available evidence, the stroke volume in the recumbent dog is approximately maximal. The stroke volume is greatly diminished on standing and increases slightly or not at all over a wide range of exertion. It is postulated that stroke volume may increase as the heart rate levels off at the highest levels of exertion, as in human subjects. *C:* the oxygen extraction (arteriovenous O_2 difference) increases progressively over a wide range of exertion. *D:* in contrast, the heart rate accelerates up to a level of about 180 beats per minute and then levels off. The stroke volume is lower during standing control than during the recumbent control periods. At very low levels of exertion, the stroke volume approximates the recumbent control values and then increases very little until maximal exertion is attained.

set at a 10 to 14% grade) (26). Such exertion could be sustained for only 2½ min, so the subjects were obviously not in the steady state. In fact, they were accumulating an oxygen debt at a prodigious rate.

Stroke volume increases during exertion under certain conditions. In dogs, stroke volume is augmented during exercise when the heart rate is controlled from an external source (52). Generally speaking, any circumstance which will interfere with or reduce the extent of the cardioacceleration will be accompanied by an increase in stroke volume. Subjects exhibiting increased stroke volume during exercise for such a reason include: *a*) trained athletes, *b*) patients with chronic volume loads on the heart (4), *c*) persons with tachycardia during the control period, and *d*) patients with relatively fixed heart rates as a result of such states as paroxysmal tachycardia and complete atrioventricular block. However, the fact remains that cardioacceleration and increased oxygen extraction represent the principal mechanisms for increased delivery of oxygen during the types of exertion encountered by average normal humans and dogs in their everyday lives. A progressive increase in stroke volume in relation to the severity of exertion is not the typical response to moderate exercise by dogs or average normal persons (12, 32, 33, 35, 36, 39, 46, 47).

NEURAL MECHANISMS OF CARDIAC CONTROL

Once the techniques had been developed to describe the cardiac responses in healthy dogs during spontaneous activity, the door was open for a comparative study to determine whether the exercise response could be simulated experimentally in the same dog on the same day (36). First, the effects of increasing "venous return" by intravenous infusions, compression of the abdomen, and passive tilting were compared with the response to exercise. The changes in ventricular performance elicited by these maneuvers bore no obvious relation to the pattern during treadmill exercise at 3 mph on a 5 per cent grade. Similarly, reduced peripheral resistance brought about by an experimental arteriovenous shunt failed to reproduce the exercise response. Since contractility can be increased by catecholamines, epinephrine and norepinephrine were infused at rates based on the estimated secretion rates of the adrenal medulla during exercise. Under these conditions, the heart rate slowed and the other changes did not resemble the exercise reponse. Thus, it seemed unlikely that circulating epinephrine plays a dominant role in the response to normal exercise.

Previous experiments had indicated that the sympathetic nerves to the heart in intact dogs have a powerful influence on ventricular performance similar to that evidenced during exercise (1). As a next step, the central nervous system was explored to discover whether the patterns of cardiovascular function generally observed during exercise could be elicited by electrical stimulation of discrete areas. It was soon learned that stimulation in very small areas in the region of the H_2 field of Forel and in the periventricular gray produced changes in left ventricular performance which were very similar to the exercise responses in the same dog on the same day (fig. 8). Differences in the diastolic ventricular pressure were consistently observed; otherwise, the patterns could be reproduced with fidelity.

These areas can be consistently and reproducibly activated by weak stimuli in the same dog and in different dogs, under chloralose anesthesia or completely awake. Stimulation in these areas may be accompanied by a full-blown pattern of responses including altered respiration and running movements

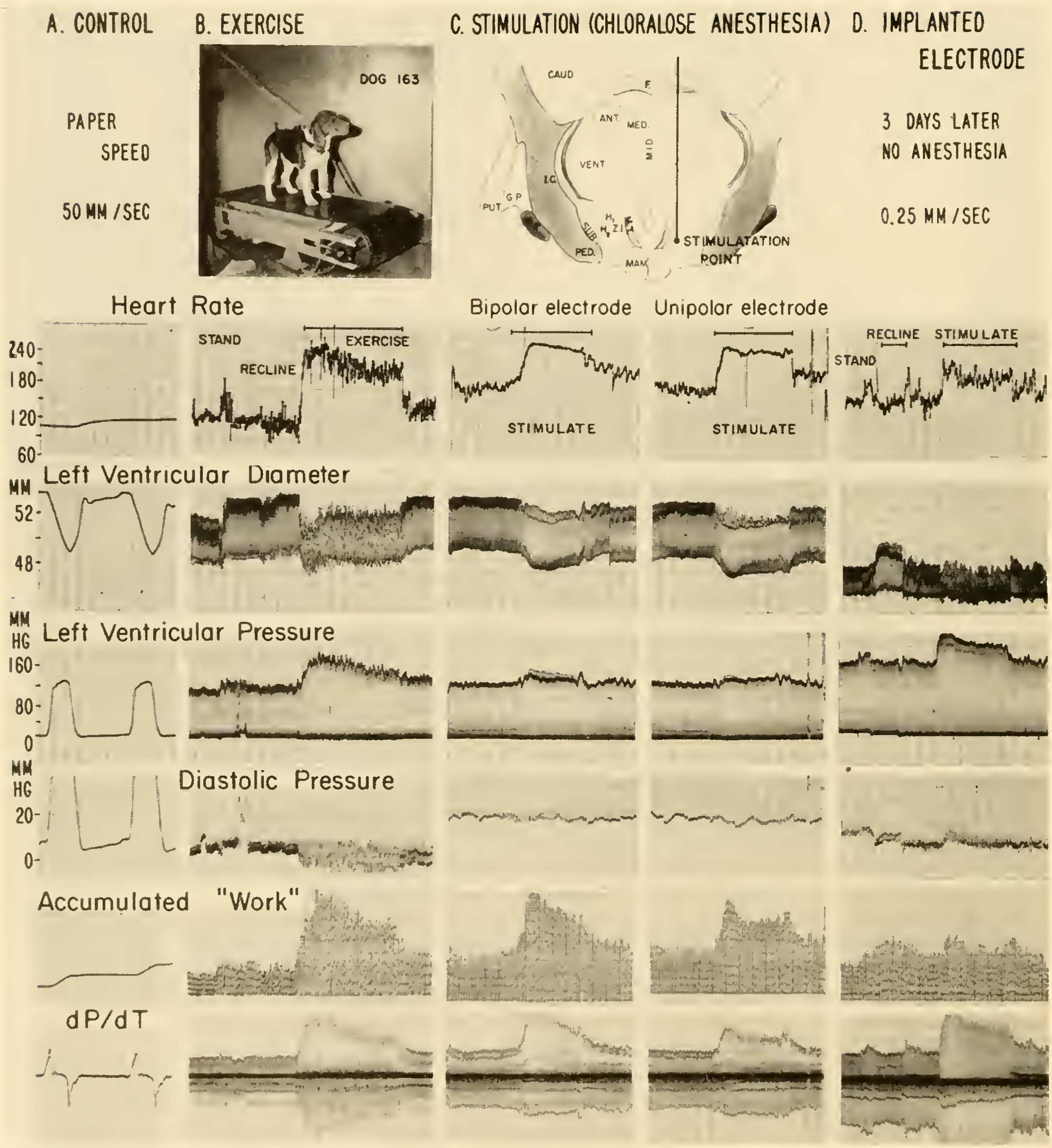

FIG. 8. Stimulation of small discrete areas in the region of the H_2 fields of Forel causes changes in ventricular performance which are similar in many respects to those observed during spontaneous exercise, both under chloralose anesthesia and after recovery from the anesthesia. (From Rushmer & Smith. *Physiol. Rev.* 39: 41, 1959.)

as well as cardiovascular adjustments. However, the cardiac response is completely independent of the respiratory and motor activities since it can be elicited without decrement after administration of syncurine to dogs under artificial respiration (57). Furthermore, certain sites of stimulation produce the same cardiovascular responses without motor activity.

The sites in the diencephalon that produce a left

ventricular response like the normal exercise responses are apparently closely related to the sympathetic vasodilator system which Uvnäs (50), Folkow (10) and their collaborators have described. This system is believed to convey impulses from higher centers in the nervous system to induce vasodilation in skeletal muscle at the onset of exercise. The distribution of blood flow through different vascular beds has been registered continuously and simultaneously by ultrasonic flowmeter. During spontaneous activity by healthy dogs the splanchnic and renal flows are altered very little, but the blood flow to the hindquarters is promptly increased at the onset of exercise. The same localized diencephalic stimulation which caused profound cardiac responses also reproduced quite closely the changes in peripheral flow distribution which had been observed during exercise on the same day. The increased flow through the terminal aorta during diencephalic stimulation apparently results from activation of the sympathetic vasodilator system for the skelectal muscles.

Clearly, there are anatomical pathways within the nervous system that carry impulses which will trigger a complete cardiovascular-respiratory response to exercise without any influence from peripheral control mechanisms. This demonstration does not prove that this is the manner in which exercise responses are normally initiated, but clearly shows the possibility of this mechanism. The diencephalon is probably a crossroads for nerve impulses coming from many portions of the cerebral cortex, so that the neural mechanisms that initiate movements of the skeletal muscle can theoretically initiate the appropriate cardiovascular-respiratory response at the same time. The cardiac contribution to this response consists primarily of cardioacceleration and increased contractility of the sort illustrated in figures 1 and 2. Note that the more rapid rate of tension development and the faster ejection velocity are consistent with a shorter systole without a reduction in stroke volume. The shortened systolic interval spares the time for diastolic filling and contributes to the effectiveness of the tachycardia in augmenting the cardiac output. On the other hand, there is no obvious role of the Frank-Starling mechanism in the responses to exertion and diencephalic stimulation.

The cardiovascular research of the future will undoubtedly focus heavily on the interactions within the central nervous system which lead to integrated responses. On the basis of past problems progress will be accelerated if a clear distinction is made between the central or integrated control mechanisms and the peripheral or local mechanisms.

INTEGRATED AND LOCAL MECHANISMS OF CARDIOVASCULAR CONTROL

Overt behavioral changes in unanesthetized animals can be induced by electrical stimulation of many different portions of the brain, including the motor cortex, cingulate gyrus, prefrontal area and amygdala. In general, stimulation in these regions also influences the cardiovascular system (37). Neuronal pathways from these areas funnel through the diencephalon, through the medulla, and terminate on the preganglionic sympathetic cell bodies in the intermediolateral cell columns of the thoracic cord. These chains of nerve fibers may or may not be interrupted by synapses, even in the medullary region, although collateral fibers are given off en route. These pathways form a basis for generalized cardiovascular responses, initiated from the central nervous system and integrated into patterns affecting widely distant portions of the autonomic nervous system. The extent of the cardiovascular response may depend upon previous experience (i.e., conditioning). This fact is evidenced by the manner in which the overshoot in the responses observed during the first treadmill exercise often diminishes rapidly so that, after a few trials, the variables promptly reach a plateau which persists without adjustment during the remainder of the exercise (39). Although it is possible that nervous impulses from receptors widely distributed through the peripheral vascular system modulate the intensity of the cardiovascular response, such a mechanism has not been definitively demonstrated. These integrated responses originating in the central nervous system bear little resemblance to those depicted in the concepts of peripheral vascular control derived from experiments on anesthetized animals and based on peripheral mechanisms. Peripheral or local mechanisms become manifest when the normal neural controls are eliminated. For example, surgical removal of the sympathetic nervous system is followed by rather severe dislocation of the peripheral vascular activity for a brief period, but after a few weeks the peripheral vessels regain a measure of control which permits quite normal activity and rapid adaptation. This observation does not mean that the sympathetic nervous system is not important in normal peripheral vascular control. It signifies instead that an additional mechanism in the periphery

permits vascular adaptation to a change in the local environment. In spite of much work on this subject, the exact nature of these peripheral vascular controls remains mysterious.

Similarly, the isolated heart displays a remarkable ability to adjust its performance in response to induced changes in the conditions under which it functions, for example, filling pressure and outflow pressure. The fact that the heart can alter its work output under experimental conditions without normal neural controls does not necessarily mean that these responses are essential or dominant during normal function. In the past, most physiological investigations of cardiac control have been conducted on anesthetized, thoracotomized dogs, a preparation in which the heart is divorced from influence by the higher levels of the nervous system nearly as effectively as it would be if the brain stem were transected above the medulla. Under these conditions, the heart responds in accordance with the Frank-Starling mechanism unless the "physiological state" of the myocardium is altered. Starling was fully aware of the profound changes in the functional properties of the myocardium induced by the administration of catecholamines or by autonomic activity. The ventricular function curves of Sarnoff and his associates represent a graphic description of this principle that the Frank-Starling relationship can be altered profoundly by changes in contractility. However, it now seems clear that changes in the myocardial contractility are far more prominent in cardiac control than the Frank-Starling mechanism, unless the neural control mechanisms are suppressed or eliminated. Removal of the neural control discloses the peripheral mechanisms which take over the cardiovascular adjustments and serve as secondary bulwarks of regulation. They do not provide such rapid or effective adjustments as the normal neural mechanisms, but they do very well indeed (see ref. 3, 41).

A great deal of semantic confusion has resulted from a failure to distinguish between the integrated neural responses and the peripheral mechanisms of control. Although both of these regulating systems are of importance and interest to physiologist and clinician alike, the neural control mechanisms normally dominate the picture under almost all normal conditions except changes in posture, as judged from currently available evidence.

SUMMARY

Cardiac output is adjusted in response to variations in requirements primarily by changes in heart rate and stroke volume. The heart rate is controlled by the reciprocal effects of the sympathetic and parasympathetic nerves distributed to the pacemaker region. Mechanisms for adjusting stroke volume have received the most attention, and are described in terms of the length-tension relationship of myocardium (Frank-Starling mechanism) and changes in the "functional state" of the myocardium ("contractility"). The term "increased contractility" has been used to denote many different characteristics of myocardial or ventricular contraction, including the rate of ejection or ejection velocity, the degree of ejection, the rate of ventricular pressure rise and fall, the ventricular tension developed, and "vigor" and velocity of contraction.

By means of direct recordings of effective left ventricular pressure, left ventricular diameter and outflow, supplemented by functions derived from these by electronic analogue computers, a graphic definition of contractility was obtained in the form of a continuous analysis of ventricular performance as affected by *l*-epinephrine. The same kind of analysis demonstrated that the length-tension relationship (Frank-Starling mechanism) was readily demonstrable during changes in posture and exaggerated by centrifugal forces. Variation in "contractility," induced primarily by sympathetic nervous activity, was clearly the dominant mechanism in the cardiac adjustments occurring during other forms of spontaneous activity by healthy alert dogs. Available evidence indicates that there is a considerable parallelism between the responses in dogs and man.

Changes in "contractility" were found to involve changes in the rates of ventricular contraction and relaxation without much change in the stroke volume or stroke work during the kinds of activity encountered in everyday living. The usual procedure for computing stroke work, from mean values for systolic pressure and for stroke volume, could easily give the same numerical values for the two sets of patterns (control and after *l*-epinephrine) in figures 1 and 2. In fact, computations of stroke work neglecting the kinetic energy involved in the increased ejection velocity underestimate true values by as much as 35 per cent.

In its most common application, the term "increased contractility" encompasses many different physiological mechanisms: the rate of excitation of the myocardial bundles, the rate of contraction of the contractile elements, the rate of recovery of the myocardial cell membrane potentials, the degree of shortening of contractile elements, and probably others which are not currently suspected. Complete description and elucidation of the various facets of

"myocardial contractility" will be an important contribution of the future and will involve analysis at the cellular and molecular levels. The mechanisms by which autonomic transmitter substances can promote these changes in myocardial function will also require extensive investigation. Since the normal cardiovascular adjustments involve changes in heart rate even more prominently than changes in stroke volume, the mechanisms by which the pacemaker activity is accelerated deserve extensive investigation. The autonomic nerve impulses which ultimately reach the heart to influence heart rate and "contractility" must be traced to their origins in the central nervous system. The factors which induce changes in myocardial fiber length (ventricular distention) must also be more explicitly determined.

The integrative functions of the nervous system in normal animals tend to overshadow the peripheral or secondary mechanisms which are revealed in the standard physiological preparations—anesthetized, thoracotomized animals. The extensive investigation of such preparations over the past 50 years has provided a clear understanding of the peripheral mechanisms of cardiac control. Such studies are no more efficient in elucidating the central integrative mechanisms than isolated nerve-muscle preparations are suitable for an analysis of the central control of fine movements of the extremities. Full blown patterns of cardiac, peripheral vascular, and respiratory responses, like those encountered during spontaneous exercise, can be elicited by electrical stimulation of discrete areas in the diencephalon. This particular region in the diencephalon serves as a pathway for nerve fibers from many different regions in the brain. Thus, the central nervous system contains anatomical provisions for the development of integrated responses involving combinations of autonomic and somatic discharges.

Eliciting these responses by electrical stimulation does not give positive assurance that these regions are involved in normal cardiac control, but does indicate that this is a possibility. A great deal of additional investigation will be required to determine the origins of the impulses and to learn the neural pathways by which they reach the effector organs of the cardiovascular system. It is equally important to determine if the observations on dogs are sufficiently applicable to human responses to warrant extrapolation of these data from one species to the other.

REFERENCES

1. ANZOLA, J., AND R. F. RUSHMER. Cardiac responses to sympathetic stimulation. *Circulation Res.* 4: 302, 1956.
2. BAKER, D. W., R. M. ELLIS, D. L. FRANKLIN, AND R. F. RUSHMER. Some engineering aspects of modern cardiac research. *Proc. Inst. Radio Engrs.* 47: 1917, 1959.
3. BERGLUND, E. Ventricular function VI. Balance of left and right ventricular output: relation between left and right atrial pressures. *Am. J. Physiol.* 178: 381, 1954.
4. BISHOP, J. M., K. W. DONALD, AND O. L. WADE. Circulatory dynamics at rest and on exercise in the hyperkinetic states. *Clin. Sc.* 14: 329, 1955.
5. BRECHER, G. A. *Venous Return.* New York: Grune & Stratton, 1956.
6. COTTEN, M. DEV. Circulatory changes affecting measurement of heart force *in situ* with strain gauge arches. *Am. J. Physiol.* 174: 365, 1953.
7. DORLAND, W. A. N. *American Illustrated Medical Dictionary*, 16th ed. Philadelphia: W. B. Saunders, 1934.
8. DUOMARCO, J. L., R. RIMINI, AND J. P. SAPRIZA. Intento de apreciación de la presión venosa efectiva por medio de la angiocardiografía. *Rev. Argent. Cardiol.* 17: 15, 1950.
9. FISHER, J. N., C. B. CHAPMAN, AND B. J. SPROULE. Effect of exercise on stroke volume in human subjects. *Clin. Res.* 8: 73, 1960.
10. FOLKOW, B. Nervous control of the blood vessels. *Physiol. Rev.* 35: 629, 1955.
11. FRANK, O. On the dynamics of cardiac muscle. Translated by C. B. Chapman and Eugene Wasserman. *Am. Heart J.* 58: 282; 467, 1959.
12. FRANKLIN, D. L., D. W. BAKER, R. M. ELLIS, AND R. F. RUSHMER. A pulsed ultrasonic flowmeter. *IRE Trans. on Med. Electronics.* ME 6: 204, 1959.
13. FRANKLIN, D. L., R. M. ELLIS, AND R. F. RUSHMER. Aortic blood flow in dogs during treadmill exercise. *J. Appl. Physiol.* 14: 809, 1959.
14. GAUER, O. H. Volume changes of the left ventricle during blood pooling and exercise in the intact animal. Their effects on left ventricular performance. *Physiol. Rev.* 35: 143, 1955.
15. GREEN, H. D. Analysis of cardiovascular activity. *Methods in Med. Research* 1: 241, 1948.
16. GUNTHEROTH, W. G. Function of liver and spleen as venous reservoirs. *Fed. Proc.* 17: 63, 1958.
17. HAWTHORNE, E. W., M. GASPAR, AND W. G. POGUE. Instantaneous dimensional changes of the left ventricle in awake dogs. *Fed Proc.* 19: 106, 1960.
18. HOLMGREN, A. Circulatory changes during muscular work in man: with special reference to arterial and central venous pressures in the systemic circulation. *Scandinav. J. Clin. & Lab. Invest.* 8 (Suppl. 24): 1, 1956.
19. HOWELL, W. H., AND F. DONALDSON, JR. Experiments upon the heart of the dog with reference to the maximum volume of blood sent out by the left ventricle in a single beat, and the influence of variations in venous pressure, arterial pressure, and pulse rate upon work done by the heart. *Phil. Trans. Roy. Soc. London* (Pt. 1) 175: 139, 1884.
20. HOWELL, W. H. *An American Textbook of Physiology.* Philadelphia: Saunders, 1896.

21. Kjellberg, S. R., U. Rudhe, and T. Sjöstrand. Effect of adrenaline on contraction of human heart under normal circulatory conditions. *Acta Physiol. Scandinav.* 24: 49, 1952.
22. Knowlton, F. P., and E. H. Starling. The influence of variations in temperature and blood-pressure on the performance of the isolated mammalian heart. *J. Physiol.* 44: 206, 1912.
23. Linderholm, H., and T. Strandell. Heart volumes in the prone and erect positions in certain heart cases. *Acta med. Scandinav.* 162: 247, 1958.
24. Manning, J. W., and C. N. Peiss. Cardiovascular responses to electrical stimulation in the diencephalon. *Am. J. Physiol.* 198: 366, 1960.
25. Marshall, R. J., Y. Wang, and J. T. Shepherd. Flow, pressure, and volume relationships in the pulmonary circulation during exercise in normal dogs and dogs with divided left pulmonary artery. *Circulation Res.* 9: 53, 1961.
26. Mitchell, J. H., B. J. Sproule, and C. B. Chapman. The physiological meaning of the maximal oxygen intake test. *J. Clin. Invest.* 37: 538, 1958.
27. Musshoff, K., and Reindell. Roentgen examination of the heart in horizontal and vertical position. I. The effects of body position on cardiac volume. *Deut. med. Wochschr.* 81: 1001, 1956.
28. Nylin, G. Relation between heart volume and stroke volume in recumbent and erect positions. *Scand. Arch. Physiol.* 69: 237, 1934.
29. Patterson, S. W., H. Piper, and E. H. Starling. The regulation of the heart beat. *J. Physiol.* 48: 465, 1914.
30. Ruosteenoja, R., E. Linko, J. Lind, and A. Sollberger. Heart volume changes at rest and during exercise. *Acta med. scandinav.* 162: 263, 1958.
31. Rushmer, R. F. Initial phase of ventricular systole: asynchronous contraction. *Am. J. Physiol.* 184: 188, 1956.
32. Rushmer, R. F. Constancy of stroke volume in ventricular responses to exertion. *Am. J. Physiol.* 196: 745, 1959.
33. Rushmer, R. F. Postural effects on the baselines of ventricular performance. *Circulation* 20: 897, 1959.
34. Rushmer, R. F., D. K. Crustal, and C. Wagner. The functional anatomy of ventricular contraction. *Circulation Res.* 1: 162, 1953.
35. Rushmer, R. F., D. L. Franklin, and R. M. Ellis. Left ventricular dimensions recorded by sonocardiometry. *Circulation Res.* 4: 684, 1956.
36. Rushmer, R. F., O. Smith, and D. Franklin. Mechanisms of cardiac control in exercise. *Circulation Res.* 7: 602, 1959.
37. Rushmer, R. F., O. A. Smith, and E. P. Lasher. Neural mechanisms of cardiac control during exertion. *Physiol. Rev.* 40, Suppl. 4, 27, 1960.
38. Rushmer, R. F., and N. Thal. Factors influencing stroke volume: a cinefluorographic study of angiocardiography. *Am. J. Physiol.* 168: 509, 1952.
39. Rushmer, R. F., and T. C. West. Role of autonomic hormones on left ventricular performance continuously analyzed by electronic computers. *Circulation Res.* 5: 240, 1957.
40. Sarnoff, S. J. Myocardial contractility as described by ventricular function curves; observations on Starling's law of the heart. *Physiol. Rev.* 35: 107, 1955.
41. Sarnoff, S. J., and E. Berglund. Ventricular function. I. Starling's law of the heart studied by means of simultaneous right and left ventricular function curves in the dog. *Circulation* 9: 706, 1954.
42. Shepherd, J. T., Y. Wang, and R. J. Marshall. Relative contribution of changes in heart rate and stroke volume to the increase in cardiac output in dogs during exercise. *Physiologist* 2 No 3: 105, 1959.
43. Shipley, R. E., and D. E. Gregg. The cardiac response to stimulation of the stellate ganglia and cardiac nerves. *Am. J. Physiol.* 143: 396, 1945.
44. Sjöstrand, T. Volume and distribution of blood and their significance in regulating the circulation. *Physiol. Rev.* 33: 201, 1953.
45. Sjöstrand, T. Regulatory mechanisms relating to blood volume. *Minnesota Med.* 37: 10, 1954.
46. Sjöstrand, T. Regulatory mechanisms relating to blood volume. *Acta physiol. scandinav.* 42 (Suppl. 145): 126, 1957.
47. Smith, O. A., R. F. Rushmer, and E. P. Lasher. Similarity of cardiovascular responses to exercise and to diencephalic stimulation. *Am. J. Physiol.* 198: 1139, 1960.
48. Starling, E. H. *The Linacre Lecture on the Law of the Heart.* London: Longmans, Green, 1918.
49. Straub, H. Dynamik des Säugetierherzens. *Deutschs Arch. klin. Med.* 115: 531, 1914.
50. Uvnäs, B. Sympathetic vasodilator outflow. *Physiol. Rev.* 34: 608, 1954.
51. Wang, Y., R. J. Marshall, and J. T. Shepherd. Stroke volume in the dog during graded exercise. *Circulation Res.* 4: 558, 1960.
52. Warner, H. R., and A. F. Toronto. Regulation of cardiac output through stroke volume. *Circulation Res.* 8: 549, 1960.
53. West, T. C., and R. F. Rushmer. Comparative effects of epinephrine and levarterenol (*l*-norepinephrine) on left ventricular performance in conscious and anesthetized dogs. *J. Pharmacol. & Exper. Therap.* 120: 361, 1957.
54. Wiggers, C. J. Some factors controlling the shape of the pressure curve in the right ventricle. *Am. J. Physiol.* 33: 382, 1914.
55. Wiggers, C. J. Studies on the cardiodynamic actions of drugs. *J. Pharmacol. & Exper. Therap.* 30: 217, 1926.
56. Wiggers, C. J. In: *Venous Return*, by G. A. Brecher. New York: Grune & Stratton, 1956, p. vii.
57. Wilson, M. F., N. P. Clarke, O. A. Smith, and R. F. Rushmer. Neural and hormonal effects on systemic arterial pressure. *Fed. Proc.* 19: 98, 1960.
58. Weissler, A. M., J. J. Leonard, and J. V. Warren. Effects of posture and atropine on the cardiac output. *J. Clin. Invest.* 36: 1656, 1957

Measurement of the cardiac output

WILLIAM F. HAMILTON | *Department of Physiology, Medical College of Georgia, Augusta, Georgia*

CHAPTER CONTENTS

THE FUNCTION OF THE HEART is to pump blood from the veins, through the lungs and out into the arterial distributing system. If we think of the veins, the right heart, and the lung vasculature as a low pressure reservoir, and the systemic arteries as a high pressure reservoir, we can say that the function of the heart is to pump blood from the low to the high pressure reservoir and thus to display before the tissues a constant supply of oxygen and nutrients as well as to transport carbon dioxide and other wastes to the lungs, liver, and kidney.

In the early history of physiology quantitation was subordinated to description in general terms. Thus to prove that the blood circulated (flowed in a circle) Harvey (72) had merely to show that a large quantity of blood passed out of the heart—something between 10 and 41 pounds of blood in half an hour—and that this quantity is more than can be drawn from the body or can be made from food and drink. He thus disposed of the Galenical tradition that blood was made *de novo* in the liver and flowed and ebbed in the arteries. Similar experiments on the veins showed that a large amount of blood was returned to the heart by one-way flow through these valved structures. These arguments were not strictly quantitative but sufficed to prove his thesis.

Stephen Hales (55) made wax casts of the distended ventricles of the horse and calculated the circulation rate as the product of the volume of the left ventricle and the heart rate. He came out with a very small figure—6 liters per min. One might expect the figure to be large because he made no allowance for residual blood. An explanation that comes to mind is the possibility that the heart was in rigor mortis (contracted) when the wax was poured in.

These early gropings in the direction of quantitation were not made in an environment that encouraged measurements of biological function. What microscopist would think of milliliters per minute when he beheld the intricate hurrying of the microcirculation, and what follower of Darwin eager to establish the truth of evolution would be interested in quantitative figures about the circulation when the gross anatomy of the heart and great vessels lent themselves to his purpose much more cogently?

Quantitation in terms of numbers was introduced into biology by the early students of metabolism and biometry. Galton used numerical measurements in describing the characteristics of populations, and his followers brought numbers into experimental biology by the use of statistical computations of the probability that differences were "significant" or due to "chance." The usefulness of this approach was self-evident and caused biologists to supplement their thinking with numerical ideas.

KINETIC ENERGY FLOWMETERS

One of the early efforts to describe the flow in an artery was that of Marey and Chauveau. In the hands of Chauveau and his pupils (92) an ingenious apparatus was developed which enabled one to record the pulsatile changes in the velocity of arterial blood. The fundamental principle is to arrange that the force of the stream moves an obstructing vane, the movement of which is proportional to the force or velocity of the stream. The movement actuates a tambour-air transmission recorder. The records made by this instrument are very nice technically and would serve if quantitatively calibrated as indications of the volume flow through the artery. The published records, however, which are easily available are not quantitatively calibrated (see fig. 1).

Later workers using the same principle employed electrical signals made by movements of the vane or bristle which was set to make changes in capacity, resistance, or electromagnetic inductance. Such a flowmeter, which has been exploited in both venous and arterial pulsatile flows, is the bristle flowmeter of Brecher (10). It is based on the mechanoelectric transducer RCA 5734, a subminiature vacuum tube that can be bought on the open market.

Pendulum or bristle flowmeters are very useful for recording pulsatile changes in arterial or venous velocity. These can be quantitated by careful calibration and the volume flow measured if the size of the vessel is known and held constant. For measuring the cardiac output it must be placed on the pulmonary artery. This sort of meter has not been used in the closed-chest animal, since it must be clamped motionless and with the bristle centered in the vessel. It is hard to see how it may become useful to measure total flow under physiological conditions.

Other methods which make use of the kinetic energy of the flowing stream take advantage of the differential pressure produced by registering a flow-dependent pressure difference between two points in a flowing stream. The pressure difference is measured by a differential manometer (see Volume II). Among devices of this sort are the venturimeter (10), the orifice flowmeter (49), and the Pitot meter (101). These instruments have been widely applied in the measurement of regional blood flow and will be described in detail in Volume II. They are mentioned in passing here not because they have been the means of measuring the cardiac output definitively but because they offer that possibility if technical difficulties may be overcome.

These difficulties are in the surgical procedures needed to insert them, the blood loss and trauma involved, and the fact that it is difficult to close the chest about them. Catheter tip Pitot meters (101) can probably be inserted into the pulmonary artery and the cardiac output measured. The same may be said of inductance or possibly of strain gauge flowmeters, both of which have been made for insertion by catheter (10). Since the mechanical effect of the flow is transduced into an electrical signal within the (e.g.) pulmonary artery, the large mass of conducting columns of fluid is avoided so that there is the possibility that the transducer may be of high frequency and hence the record may be of high fidelity. These instruments, however, have not been widely used to measure the cardiac output.

Another related approach has been introduced by Fry (43). It is based on a detailed analysis of the hydrodynamics of flow through tubes (42). The basic data used in computing the velocity (44) are the pressure differences between lateral taps from a double lumen catheter placed in the axial stream of the aorta, or the pulmonary artery. These pressure differences are those that overcome the inertia and friction of the moving column of blood between the taps and are sensed by a differential manometer. They are minimal and just about at the threshold of resolution of available pressure recorders. The equation which relates these pressure differences to velocity is quite complex and can be computed only by means of an electrical analogue. In view of the obvious artifacts of the published catheter tip pressure records from which the computations were made, it is amazing that the plot of the computation has the same appearance as the classical records of Chauveau (fig. 1), as well as records from such sophisticated instruments as the electromagnetic and sonic flowmeters. Whereas this approach has yielded considerations of great theoretical interest it is seriously to be doubted that it will compete effectively with other instantaneous methods for measuring the cardiac output.

The rotameter has been widely used to measure regional flows but has also been used to measure the total cardiac output on a few occasions (91). The principle of the instrument is to direct the stream upward through a widening tapered tube. A "float" heavier than the blood is placed in the tube. The tendency of the float to sink through the blood is counteracted by the upward force of the stream. Since the upper part of the tube is wider than the lower part, the blood passes the float in greater

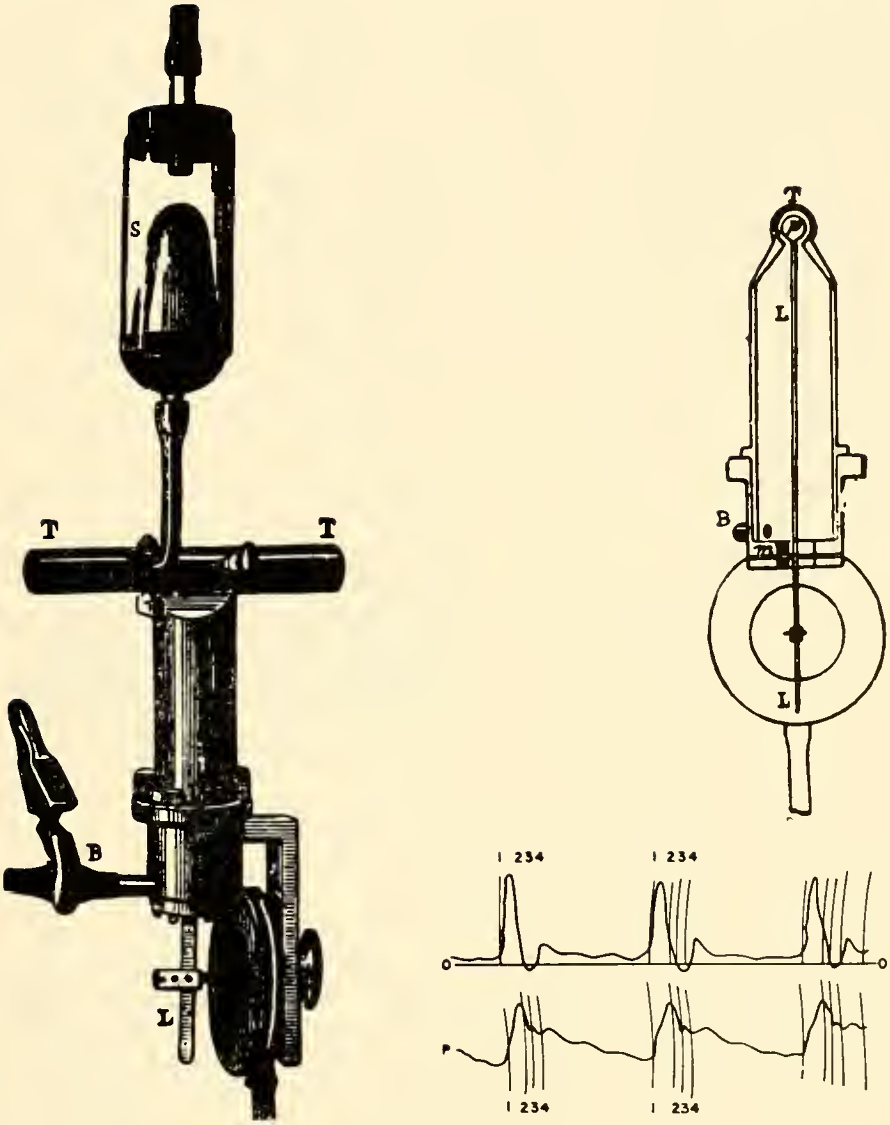

FIG. 1. Chauveau's hemodromograph. The arterial stream is directed through the tube, *T*. The lever, *L*, senses the force of the stream by means of the vane, *V*, and transmits the force to the tambour which by air transmission to another tambour inscribes the flow (upper record below). A simultaneous pressure (lower record) is made by air transmission through the pressure reducer, *S*. The rubber membrane (*M*) acts to prevent escape of blood from the cannula and as a fulcrum for the lever. [From Luciani (92).]

quantity the higher it is and the float rides higher as the flow increases. The rotameter gives a linear calibration against flow. Readings may be taken of the height of the float by eye or it may move the core of an inductance transducer to give an electrical signal of the height of the float (21).

There are three difficulties that the users of rotameters are apt to encounter. One is the fact that when a small clot or strand of fibrin lodges on the float there is a sudden and unpredictable change in the calibration. This necessitates the use of large amounts of heparin to prevent the formation of fibrin and this, in turn, causes the animal to bleed. Another is the rather high resistance of the instrument, particularly when the flows are rapid. This precludes their placement in a vein because of the resulting venous congestion. As a result of the fact that the working pressure in the arteries is so much greater than in the veins, the rotameter may be introduced into arteries. Like the bristle meter described above to measure the cardiac output, the rotameter must be placed in the course of the pulmonary artery and firmly held in a vertical position. Used in this manner it has been shown to give the same values as the Fick (123) and the dye injection methods, and results similar to those with the pulse contour method (91).

The Potter turbinometer has been used in industry. Sarnoff adapted a small model for placing in the aorta (120). It consists of a little turbine which bears a magnet that induces a current in a surrounding

coil. This current is proportional to the rate at which the turbine rotates and this in turn is proportional to the flow. It suffers the disadvantage of a high resistance to flow, positional instability, and the need for heparinization. For these reasons it is useful only in the open-chest animal under the immediate effects of surgery. The adherence of small strands of fibrin on the turbine and any backflow will stultify the calibration. Its response is slow, and it cannot measure phasic flows.

In contrast to the above, the electromagnetic and sonic flowmeters have been implanted on the aorta or pulmonary artery and have been used to measure flow after recovery from surgery and when the animal was in a normal physiological condition.

ELECTROMAGNETIC FLOWMETERS

This device depends on the principle that when a conductor moves at right angles to the lines of force of a magnetic field an electrical potential is induced. In this application of Faraday's law the conductor is a stream of fluid (blood) passing between the poles of a magnet. The induced current is led off by electrodes placed across the conduit of the stream. The current is proportional to the velocity of the stream and its polarity is determined by the direction of the stream.

The general principle of electromagnetic induction as a measure of flow is said (125) to have been suggested by Faraday in 1832, who unsuccessfully attempted to measure electric currents from the flow of the Thames in the earth's magnetic field (see fig. 2).

The application of this principle to blood flow in living animals was independently developed by Kolin (82) and Wetterer (141). Many authors have participated in the development of the method and of instruments to serve it (see 125). At first a constant magnetic field was used which resulted in a unidirectional pulsating current, necessitating bulky and unstable nonpolarizable electrodes. Difficulties in the use of these electrodes led to the use of alternating current, which avoided the need of nonpolarizable electrodes but introduced "transformer" currents which were independent of flow and were due to fluctuations in the magnetic field. These transformer currents could be eliminated in several ways, among which was the use of a phase sensitive detector to separate the transformer from the flow-induced potential. Another method of silencing the transformer current was by the use of a square wave alternating current to energize the magnet and a complex circuit to block the current induced during the instant when the magnetic field was reversed (127).

The pickup or probe developed by Spencer & Denison (127) and by Kolin (83), and Kolin & Kado (84), can be implanted in the body and used in chronic experiments allowing a degree of freedom of movement of the experimental subject. They can be applied to a human blood vessel during surgery and promise a great deal of useful information in the near future. A particularly interesting development is the coreless electromagnetic pickup which can be used on large blood vessels and which is minimal in bulk and is easily implanted (83).

A most important advantage of this method of recording the blood flow is the fact that the detailed phasic changes in the velocity and volume pulse can be accurately recorded. This will no doubt prove of value in arriving at an understanding of the cardiodynamics of ejection under different circumstances and of the nature and cause of oscillations (acceleration and retardations of flow) in the aorta and its branches. The fact that it will clearly plot the pattern of forward and backflow is of considerable importance, differentiating it from the thermostromuhr (50, 98) which gives confusing results because it does not differentiate backflow.

SONIC FLOWMETERS

The velocity of the aortic stream can also be measured by the differential speed of sound going up and downstream. This difference can be picked up as a phase difference (77) or as a simple delay. A device has been worked out in Rushmer's laboratory (2), using the delay principle, which can be implanted on the aorta or pulmonary artery and left in place with wires passing through the body wall so that changes in cardiac output can be assessed during normal activity (38). High frequency electrical pulsations of very short duration (0.2 μsec) were used to drive a piezoelectric crystal of barium titanate at 3 mc (see fig. 3). The crystal tranduces the electric pulses into ultrasonic vibrations. These are sent diagonally across the aorta to a similar barium titanate crystal which acts as receiver and is placed upstream. The current is then switched mechanically to the receiving crystal which then acts as a transmitter. The pulses are thus alternately sent upstream and downstream 400 times per sec, each crystal acting in turn as transmitter and receiver. The path of the sound waves, being diagonally across the whole aortic stream, is affected

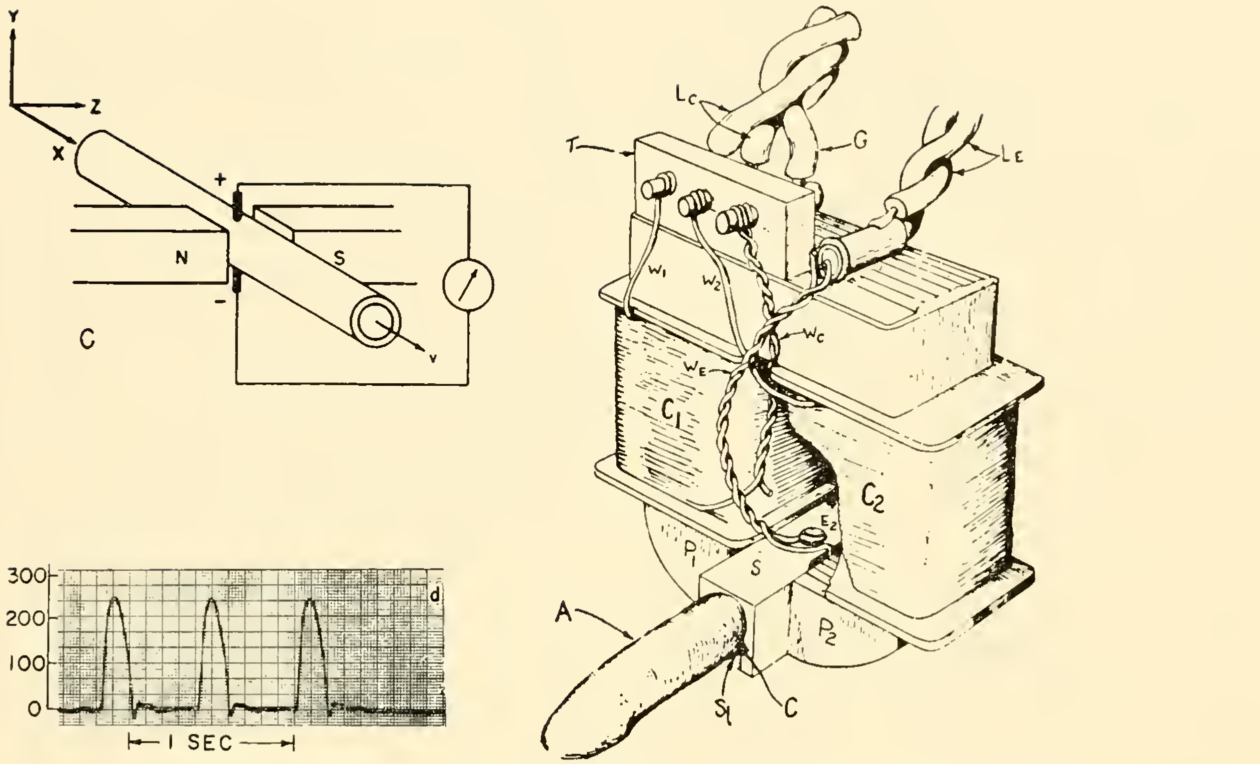

FIG. 2. (*Left, above*): flow of blood, V, in an artery between the magnet poles, n. s., induces a current in the electrodes, $+$ and $-$. *Right*: diagram of Kolin's electromagnetic flowmeter. The artery is placed in a sleeve, S, between two magnet poles, P_1, P_2. The induced current is led off over LE from electrodes E_1 (not shown) and E_2 which are in contact with the artery. *Left, lower*: pattern of aortic flow. [From Kolin (84).]

by its mean velocity. During the transit time of the sound wave a capacitor is charged at a constant rate and then discharged when the sound burst arrives at the receiving crystal. The maximum voltage of this charge measures the transit time. The transit time is slightly greater when the sound is transmitted upstream than when it is transmitted downstream. The difference in the voltages measuring the upstream and downstream transit times is filtered, amplified, and recorded so as to give a faithful measure of the instantaneous changes in the mean velocity of the blood stream. Since the mount holds the vessel to a known constant size, the flow can be derived from the velocity of the stream. The flow through the aorta (plus the estimated coronary flow) or preferably the pulmonary artery is, of course, the cardiac output.

PULSE PRESSURE METHODS

Methods for measuring the cardiac output, which have been mentioned so far, deal with some characteristic of the velocity of the stream in the aorta or preferably in the pulmonary artery. The systolic discharge, however, releases energy in another way which can give a clue to the amount of blood ejected. It stretches the aorta and thereby produces an increase in pressure therein (pulse pressure). The pulse pressure, as a measure of the stroke volume, was first suggested by Erlanger & Hooker (30). The aortic distensibility or rather the distensibility of the whole arterial tree raises the most important question in assessing the relation between stroke volume and pulse pressure. If the arterial tree were highly distensible more blood could be forced into the arteries during systole with a given change in pressure than if the vessels were less distensible. Two assumptions have been made, *1*) that arterial distensibility does not change importantly and *2*) that important changes in distensibility do occur but can be evaluated by studies of the pulse wave velocity. This possibility will be discussed first.

The relation of pulse wave velocity to absolute distensibility ($\Delta V/\Delta P$) or the amount of blood which, on

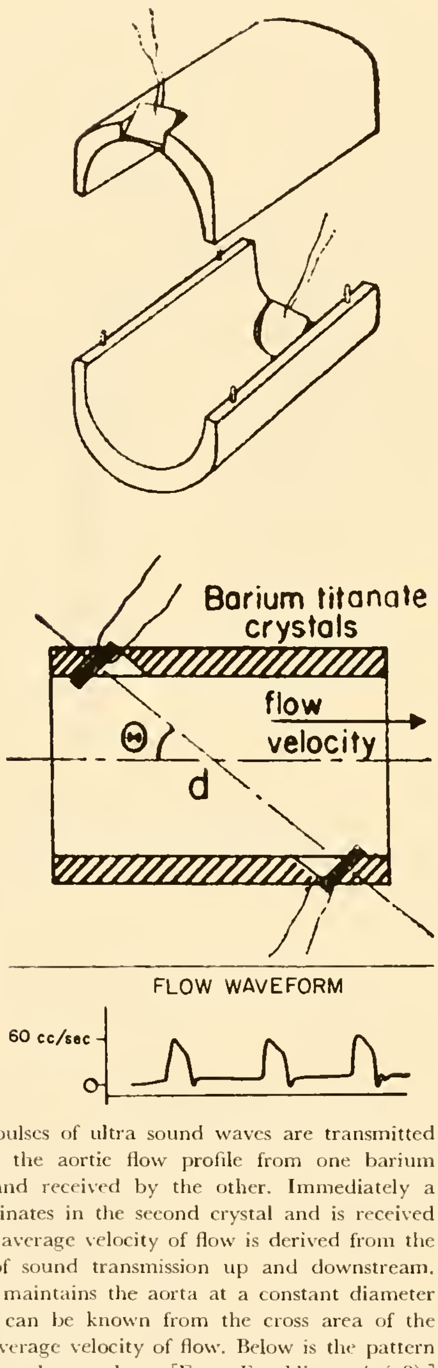

FIG. 3. Short pulses of ultra sound waves are transmitted diagonally across the aortic flow profile from one barium titanate crystal and received by the other. Immediately a second pulse originates in the second crystal and is received by the first. The average velocity of flow is derived from the time difference of sound transmission up and downstream. Since the mount maintains the aorta at a constant diameter the volume flow can be known from the cross area of the stream and the average velocity of flow. Below is the pattern of flow velocity from beat to beat. [From Franklin *et al.* (38).]

entering the arterial chamber, produces a given pressure rise is not a direct one. It depends upon the capacity of each segment of the artery at the beginning of the pulse. Pulse wave velocity then depends upon the relative distensibility of arteries and not upon their absolute distensibility. The relationship may be expressed as follows [after Bramwell & Hill (9)] $PWV = 0.357\sqrt{V\Delta P/\Delta V}$ in which ΔP is the increment in pressure in mm Hg corresponding to ΔV, the increment in volume in cubic centimeters starting from V, the initial volume of the tube. PWV is the pulse wave velocity in meters per second.

It is seen that the initial volume of the tube is a very important variable in the relationship between distensibility and pulse wave velocity. Thus if pulse wave velocity remained constant and diastolic volume were doubled, $\Delta V/\Delta P$ (absolute distensibility) would be doubled. Now the diastolic capacity is very hard to evaluate. The size of the aorta has been measured in specimens from fresh cadavers at all physiological ranges of pressure (112) (cf. fig. 4). The extreme variability ranging over twofold in people whose history was not significantly different makes it impossible to predict the size of the aorta at diastolic pressure in any given individual. Actual measurement of aortic size by aortography has not proved useful.

Another reason for believing that pulse wave velocity is not related quantitatively to absolute distensibility is that the expansion of the initial upstroke of the pulse wave is made against a preset stiffness in the wall of the artery that makes it "reluctant" to yield. This "reluctance to stretch" does not vary with different rates of rapid stretch and is therefore not viscosity as the term is usually used.

In other words, when stretched initially it is effectively more rigid than when the stretch is maintained through systole, and these forces have time to dissipate. The pulse wave velocity is set by the initial upstroke against preset resistance (65), while the amount of blood which has been taken up by the arterial tree is governed by the maintained stretch under circumstances that make the artery yield more and be more distensible than it is at the initial stretch.

Authors who have assessed arterial distensibility from pulse wave velocity have used tables of aortic size from measurements made post mortem of the undistended vessel (6). These figures are much less than those measured at diastolic pressure (112) and hence are not applicable in the calculation of absolute distensibility. Bazett *et al.* (6) have made a detailed study of different segments of the arterial tree and have calculated the distensibilities of these segments and hence of the arterial tree as a whole. The Munich school have used measurements of the aortic resonant or standing wave (see Volume II) to assess arterial distensibility (11, 142). All of these have shown agreement between their method and respiratory methods (see below) of measuring the cardiac output. Only

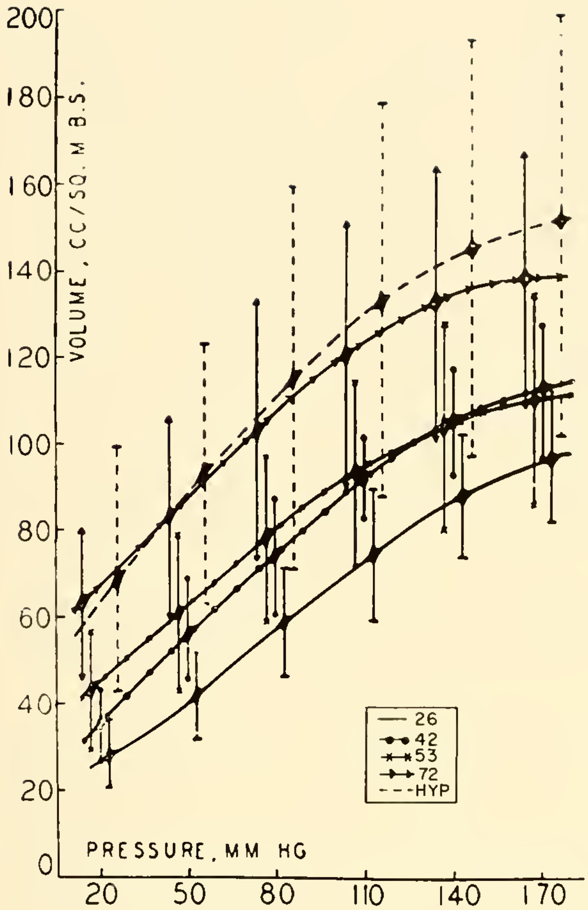

FIG. 4. The relation of the volume per m² of aortas from human cadavers at pressures ranging from 20–170 mm Hg. The different curves represent different age groups and aortas from hypertensive patients. The change in aortic capacity with change in pressure (slope) is quite constant from group to group, whereas the capacity at any one pressure may vary as much as 3-fold from group to group. [From Remington *et al.* (112).]

rarely, if ever, has the validity of methods of this type been confirmed by independent workers.

On the basis of the discussion so far it would seem that the pulse wave velocity is not very helpful in assessing absolute arterial distensibility or uptake. No other applicable method is available. It is necessary then to test the assumption that uptake does not vary in such a way as to stultify the use of pulse pressure to calculate stroke volume. Uptake may vary *a)* with pressure; *b)* with the individual under the influence of biological variability disease and age; *c)* with physiological condition; and *d)* with body size. To equalize body size all uptake figures are given per square meter of body surface.

In figure 4 are shown curves calculated from a table published by Remington *et al.* (112) in which rings cut from 48 human aortas at different levels were stretched and the aortic volume (per m²) pressure relationship calculated from the tension and length of the stretched rings. The relation of the lines indicates that regardless of previous history, age, or aortic size, the average increase in aortic volume per unit pressure rise (slope) is very similar in all the categories illustrated. The aortic volume at any diastolic pressure will vary widely, but the change in volume with pressure is more constant. It is also seen that the aortic volume changes almost proportionally with pressure from 20 to 110 mm Hg and that above this figure the distensibility gradually falls off. This indicates that at higher mean pressures the same pulse pressure would be produced by a smaller stroke volume.

The uptake of the aorta alone is much less than the stroke volume. In the first place all the branches of the aorta add their uptake. In addition, during systole the blood continues to flow through the aorta and out the arterioles. A table was constructed (112) in which the aortic uptake curve (average of fig. 4) was increased proportionately so as to give figures that would average the same as those for the stroke index as calculated by the Fick procedure. The figures are based on the comparison of practically simultaneous intra-arterial brachial pressure pulses and 83 Fick determinations.

The result of using the table on the pulse pressures shown by the 83 cases in question is given in figure 5. These results are empirical in the sense that the mean of the Fick stroke index and of the pulse pressure prediction are arbitrarily set at the same value. The scatter seems rather large on inspection but the correlation coefficient is .79 and the average discrepancy 18.6 per cent. Other methods which have been proposed give the following discrepancies when tested on these data: 34 per cent (5), 25 per cent (45), 24 per cent (89). The principal cause of the greater discrepancy between the calculation by the earlier formulas and the measured result lies in the fact that the older workers divided the pulse pressure, or some derivative of it, by a constant. This approach does not give the true relationship which at low normal arterial pressures is a proportional (linear) and constant relation between pulse pressure and stroke index. Thus at pressures below 120 mm Hg each mm Hg is produced by about 1 ml of stroke index. Above

TABLE 1. *Factors for the Prediction of Stroke Volume, per m² Body Surface, from the Pulse Pressure*

Pressure	Volume Factor	Pressure	Volume Factor	Pressure	Volume Factor
mm Hg	*ml*	*mm Hg*	*ml*	*mm Hg*	*ml*
20	0	100	81	180	140
30	10	110	90	200	148
40	21	120	100	220	155
50	31	130	108	240	161
60	42	140	115	260	167
70	52	150	122	280	173
80	62	160	128	300	179
90	71	170	134		

this pressure level a given stroke volume produces a gradually increasing pulse pressure.

Study of the plot shows that there is a group of determinations scattered rather uniformly about the line of identity and a group which includes about half of the cases of congestive failure (*C*) who display a much larger pulse pressure than would be predicted from their Fick stroke volume. It is a matter of clinical observation that pulse pressure readings are more nearly normal than are stroke volume measurements in congestive failure, but we have no clue as to what makes the arterial tree in these cases less distensible than in other diseases or than the normal.

The agreement between the stroke volume as measured by the Fick and dye dilution methods (see below) and as derived from the pulse pressure is far from perfect. However, it compares well with those derived from ballistocardiography and other methods (see below) which can be applied to the intact man and which measure the beat-to-beat variations in the stroke volume. Furthermore, since it includes measurements taken on patients with various diseases, during exercise and anxiety, it is reasonable to assume that changes in arterial distensibility, as caused by these factors, are not great enough to hide a significant relation between stroke volume and pulse pressure.

Nevertheless, improvement in calculation of stroke volume from pulse pressure may well be sought by correcting the average empirical ratio by a constant derived by a Fick or dye measurement on the particular individual. Thus if the crude pulse pressure relation as given above overestimates the stroke volume by 10 per cent in a certain individual at rest, a 10 per cent lowering of the pulse pressure figure during exercise or during the effect of tilting, or of a drug, can be expected to come closer to the true experimental figure than the uncorrected estimate.

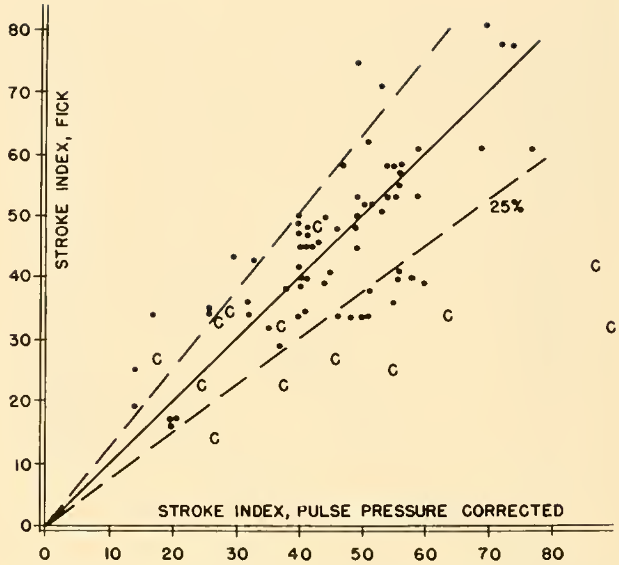

FIG. 5. Relation between stroke index as calculated from the Fick procedure and that derived from a simultaneous pulse pressure measurement. *C* = patients with congestive circulatory failure. [From Remington *et al.* (112).]

A procedure using this principle has been worked out by Warner *et al.* (136), who assumed that the arterial uptake was proportional to the systolic area (pressure × time) above end diastolic pressure, times a constant derived from a known stroke volume in the same individual under resting (steady state) conditions. Introduction of experimental conditions produces a change in the pressure pulse, the systolic area of which multiplied by the same constant gives the uptake under the new conditions. The uptake plus the systolic drainage gives the stroke volume, and the systolic drainage is the uptake times the fraction S.A./D.A. where S.A. and D.A. are the systolic and diastolic areas of the pulse curve above an arbitrary 20 mm Hg and corrected for transmission to the periphery.

PULSE CONTOUR METHOD

The best application of the pulse pressure method of calculating the cardiac output is not to man, whose variable age and susceptibility to arterial disease must necessarily cause changes in arterial distensibility. These may account for much of the scatter seen in figure 5. The laboratory dog, on the other hand, is a young animal as a result of hazards which surround him, and only rarely is he afflicted with arterial disease. The arteries from many dogs have been cut into

rings, the rings stretched, and the volume pressure relationship plotted from the circumference-tension relation (64). These curves are surprisingly uniform from individual to individual, when corrected for body size. Moreover, the slope of the plot of the uptake of the dog's aorta against pressure is the same whether the aorta is constricted on its removal from the body, relaxed after several stretches, or constricted again by epinephrine (1, 109; see also 112).

This constancy of volume uptake of the aorta under different conditions justifies considering the distending effect of the pulse pressure in a very detailed manner (64). Under different circulatory conditions the pressure pulse contour may take diverse forms, with the peak falling early or late in systole, and systole itself lasting from 80 to 120 msec. At the instant of closure of the aortic valves, each segment of the aorta and its branches will have been distended as the pulse wave passes down by very different pressure increments, ranging from zero (diastolic) to peak systolic pressure. The uptake of each segment will be conditioned by its distensibility and by the pressure at time of valve closure. The arterial uptake will, of course, be the sum of the uptake of all the segments, and the stroke volume the sum of the uptake and the arteriolar runoff during systole.

Evaluation of the stroke volume from the pulse contour in this manner will, when its results are compared with those of an independent method, prove the soundness of measuring the cardiac output from beat to beat from the pulse pressure contour, and will establish the physiological conditions under which the arterial uptake is a constant function of pressure. In order to gather data for this inquiry it was necessary to measure the uptake of aortic segments under constant conditions, i.e., postmortem. The uptake of the aorta as a whole and of the main arterial branches was ascertained as follows. All the major branches from the aorta were clamped and the smaller ones (segmentals) tied off. A large cannula was placed in the aorta via the ventricle and connected to a burette which could discharge saline rapidly into the aorta under air pressure. Optical records were taken of the pressure changes during the discharge of known amounts of saline and during "diastolic" drainage. These pressures were recorded over a wide range and the aortic uptake calculated from the injected volume minus the systolic drainage. This latter was calculated, as indicated above, from the relation of the systolic and diastolic areas of the optical pressure record. These data gave the uptake of the aorta and its branches over a wide range of pressures. Similar experiments were made by opening up in turn the leg arteries, the arteries to the viscera, and those to the head and forelegs. In this way the uptake of the several arterial beds was assessed. For the purposes of this investigation it was necessary to separate the differences in uptake of the various parts of the aorta itself. This was done by measuring the tension-circumference relationship of rings cut from various parts of the aorta and calculating the volume uptake from these. Since the uptake of the whole aorta and all its branches was known, a distribution of uptake for the arch, thoracic aorta, and abdominal aorta, together with that of the arterial branches coming from the several segments, could be estimated.

From these data, a compilation of the uptake of the aorta and its branches could be made (64). A revised form of this compilation is given in table 2 (108). All measurements are given in milliliters per square meter of body surface to account for differences in body size. This is done for convenience, since most metabolic and circulatory functions are customarily referred to body surface rather than to body weight. In the practical application of this table and table 1, it is best to read values off from a plot of convenient scales in which the tabulated values are connected by a smooth curve (fig. 6).

Quite as important as the size of the uptake of the several arterial segments is the time at which the pressure in these segments is effective in distending them to give rise to the uptake. This time is, as has been indicated above, the instant of aortic valve closure, and the pressure obtaining at this time in the several arterial segments will depend upon the shape of the systolic pressure pulse curve and the transmission time out to these segments. This is illustrated in figure 6. There are two pulses pictured; in one the pressure is about normal. At the time the valves are closed, pressure in the arch is about 39 mm Hg above diastolic; that in the thoracic aorta and the branches out to the head and forelegs (having similar transmission times) is about 52 mm Hg, whereas that in the abdominal aorta and visceral arteries is 47 and in the leg arteries 23 mm Hg. These pressures are measured from a calibrated central pressure pulse curve. The arch pressure is measured at the incisura, and the other pressures are measured at points determined earlier in the pulse contour by the transmission times as read from table 3 or from a graph plotted therefrom. Distention produced by these pressures is 7, 20, 5, and 3 ml per m^2 in the respective segments. The uptake of the arterial tree as a whole is the sum of these quantities or 35 ml per m^2 body surface.

TABLE 2. *Net Volume Uptake per m^2 Body Surface of Arterial Tree at Various Pressures*

Pressure	Arch	Head and Thoracic	Viscera and Abdominal	Legs
mm Hg	*ml*	*ml*	*ml*	*ml*
20	1.4	3.5	1.3	1.1
40	4.6	9.9	3.7	3.4
60	8.1	17.6	6.5	6.1
80	11.5	25.5	8.9	8.3
100	14.6	32.9	10.9	10.1
120	17.6	39.3	12.6	12.0
140	19.9	44.5	14.1	13.2
160	21.6	48.0	15.3	14.3
180	22.8	50.6	16.4	15.2
200	23.7	52.4	17.4	16.0
220	24.6	54.0	18.3	16.6
240	25.4	55.5	19.0	17.2

The smaller of the two pulse curves illustrates a very different set of pressure relations. At the time of semilunar closure the distending pulse pressure in the arch is effectively zero (diastolic pressure), that in the "head" system about 18 mm Hg, and that in the "visceral" system about 3 mm Hg. The pulse wave transmission at this low diastolic pressure is so slow and systole is so short that the pulse wave does not arrive at the legs before closure of the aortic valves. The uptake then is 8 ml (head) plus 2 ml per m^2 (viscera) and there is no effective uptake in the arch and legs. This means that whatever uptake may have occurred early in systole in the arch is measured elsewhere and that changes in the size of the leg arteries occur effectively during diastole.

The transmission times used in the above calculation are dependent on diastolic pressure and were measured in average-size dogs as the means of numerous observations. These are given in table 3. In addition there is a column headed Tw or transmission time weighted for drainage or arteriolar outflow. This is the average transmission time from the arch to the arterioles of the several arterial beds, each weighted for the amount of arteriolar outflow in the particular bed (see above). The "head arteries" are given the most weight because most of the drainage occurs from these arteries. The visceral arteries are given next most weight and the leg arteries the least. In using this concept in a stroke volume calculation the weighted transmission time is measured forward from the incisura. Those parts of the pulse curve occurring before $Ts - Tw$ indicate the pressures controlling systolic drainage and that afterwards (during $Td + Tw$) or $Tc - Ts + Tw$ control diastolic drainage (Tc = time of cycle).

The stroke index is the sum of arterial uptake and arteriolar outflow, or drainage during systole. Systolic drainage is evaluated according to the principle introduced by Bazett (6). Arteriolar drainage during diastole is equal to uptake, or long as end diastolic arterial pressure does not change from beat to beat. The findings of Whittaker & Winton (144) are accepted so that systolic drainage can be related to diastolic drainage in proportion to the effective pressure (i.e., the pressure above 20 mm Hg) of systole and diastole multiplied by the effective duration of these parts of the cycle. The mean effective pressure (Ps) can be computed by adding the pressures minus 20 mm Hg at regular and small intervals during effective systole ($Ts - Tw$) divided by the number of such measurements. The mean effective diastolic pressure (Pd) can be measured in an analogous manner.

The stroke index (SI) then would be

$$SI = U + \frac{Ps(Ts - Tw)}{Pd(Td + Tw)} U$$

The drainage volume, which is added to the uptake, is rarely more than 20 per cent of the stroke index and usually much less. It is questionable whether it is needful to calculate Ps and Pd meticulously. Analysis of many curves (108) has shown that the mean pressure (Ps) during effective systole ($Ts - Tw$) rarely exceeds that during effective diastole ($Td + Tw$) by more than 1 mm or so. Thus for all practical purposes $Ps = Pd$ and the systolic drainage (Ds) calculations can be simplified.

$$Ds = U \frac{Ts - Tw}{Td + Tw} = U \frac{(Ts - Tw)}{Tc - Ts + Tw}$$

$$SI = U + U \frac{(Ts - Tw)}{Tc - Ts + Tw}$$

Since flow per second is SI/Tc then

$$F_{sec} = \frac{U}{Tc - Ts + Tw}$$

The use of this formula involves estimating U, the arterial uptake per square meter, measuring the durations of systole and cycle, and the diastolic pressure. Knowing the diastolic pressure, the transmission times for the thoracic, visceral, and leg segments and for Tw can be obtained from table 2 or preferably from a plot made from the figures therein. These times can then be laid off from the incisura and pressures read at the incisura and at the moment of each

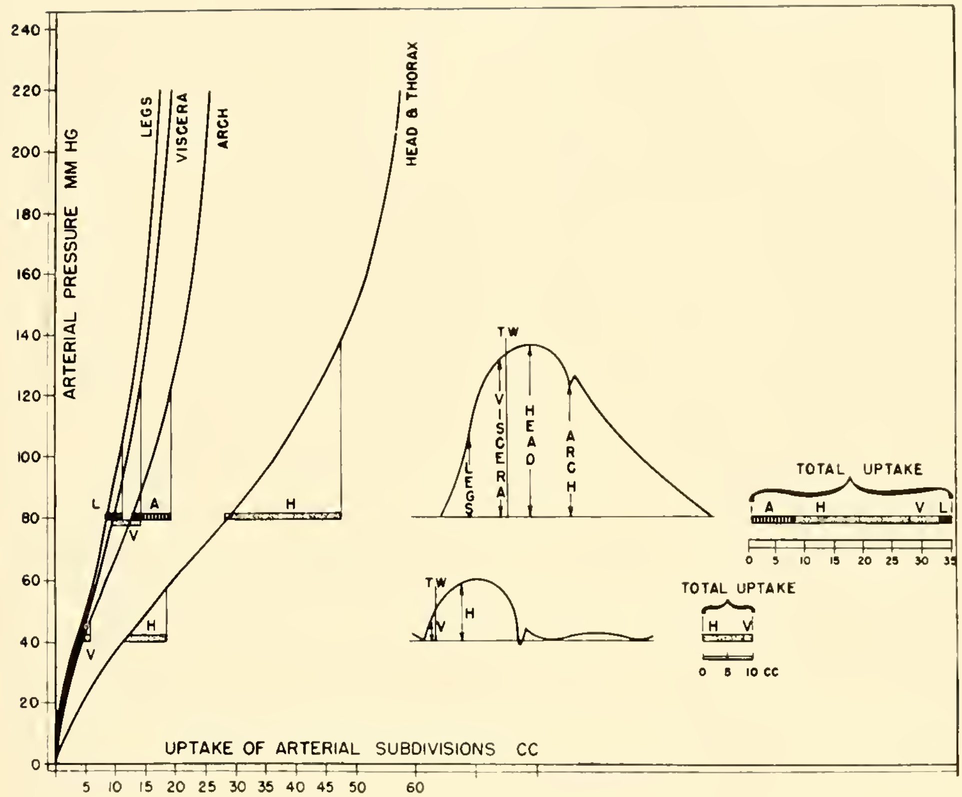

FIG. 6. *Left:* relation between capacity of the several parts of the arterial bed per m^2 and arterial pressure. *Right:* sketches to illustrate the calculation of arterial uptake and arteriolar outflow. [From Hamilton (58).]

transmission time. The uptake of each segment can be read as the difference in volume between that at diastolic pressure and at the pressures as above. Thus we will know the increase in volume of each segment as wrought by the pressure pulse at the instant of semilunar closure. The sum of these will be the arterial uptake. Substituting U, Tc, Ts, and Tw in the above formula, the flow per second per square meter can be closely approximated.

The simplified pulse contour calculation of the stroke index has been carried out many times and compared with the dye injection method and with the direct Fick procedure. The first set of observations were very encouraging, inasmuch as the correlation between the two methods was $R = 0.99$. As will be seen in figure 7 there are a few points in which the agreement between the pulse contour method and the standard method is not very good. On getting more comparisons as the method was applied to various physiological problems there appeared a rather larger number of aberrant points (fig. 8). These always showed a large contour stroke index as compared with that calculated from the Fick or dye method, as though the arteries of these dogs had become less distensible than those of normal or dead dogs. This change in distensibility was not signaled by a change

TABLE 3. *Pulse Wave Transmission Times to the Parts of the Arterial Tree at Various Diastolic Pressures for Dog of 15 kg*

Diastolic Pressure	Estimated Transmission Times			
	For uptake			For drainage
	Head and thoracic (Th)	Visceral and abdominal (Tv)	Leg (Tl)	Weighted average (Tw)
mm Hg	*msec*	*msec*	*msec*	*msec*
20	59	110	170	129
40	48	89	136	101
60	39	75	112	84
80	33	64	94	72
100	28	55	81	62
120	24	47	70	53
140	20	40	59	46
160	18	34	50	39
180	16	28	42	33

in pulse wave velocity, a fact which implies that the arteries must have become smaller. The aberrant determinations were all made on dogs that were in bad condition but not all the dogs in this condition showed the discrepancy. It was first discovered in dogs with a rotameter or pump in the great veins (29), and again in dogs suffering from electrolyte

depletion (108). Dogs *in extremis* from hemorrhagic or traumatic hypotension do not often show discrepant pulses.

The forms of these discrepant pulses show stigmata that make them recognizable on inspection. The diastolic pressure is relatively high, systole is relatively short, and there is often an early systolic peak followed by a marked preincisural drop. Perhaps the most important evidence of a discrepant pulse is the slope of the diastolic limb. If the diastolic pressure is above 40 mm Hg and the slope of diastole so flat that its prolongation to the initial upstroke cuts the anacrotic limb below one-half the pulse pressure, the pulse curve is considered one that will give a calculated stroke index that is larger than that calculated from other methods (108).

A refinement of the pulse contour method was described by which the time course of cardiac ejection could be calculated (110, 111) and compared with the cardiometer curve of Wiggers & Katz (146). The ejection curves were calculated according to the same principle as that for calculating the stroke volume, except that the uptake was figured from pressure measurements made at 10-msec intervals from the beginning of the pulse wave, and the drainage figured as in the stroke volume calculation and partitioned from interval to interval beginning at *Tw* and in accordance with the early pressures (for details of this calculation see 110 and 111). The curves plotted from this measurement agree closely in contour with those drawn by the cardiometer (73, 146) and show the large variations in the time course of ejection which cause the greatly differing pulse forms seen under different circumstances (see fig. 9).

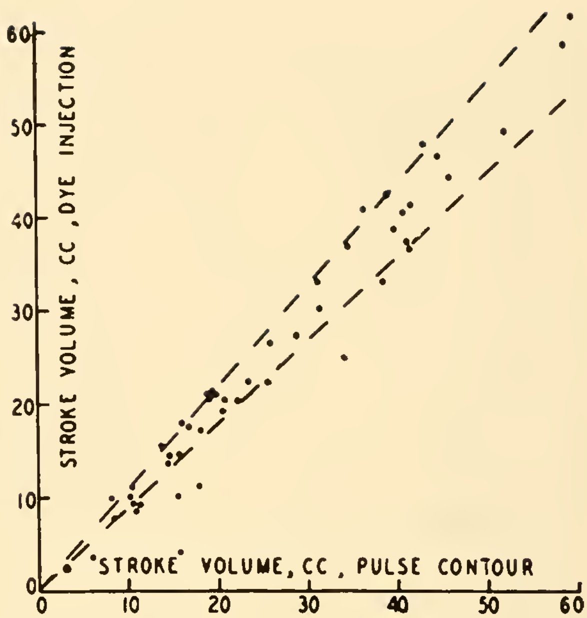

FIG. 7. Relation of stroke volume as calculated from the Fick or dye dilution methods and that calculated from the pulse contour. [From Hamilton & Remington (64).]

BALLISTOCARDIOGRAPHY

As the heart pumps blood around the circulation, it accelerates the blood from a static condition in the ventricle to rapidly moving streams in the aorta and in the pulmonary artery. The recoil from this sudden acceleration tends to move the body in the opposite direction, the two forces being equal and opposite. As the surge of blood in the great arteries reaches the arch of the aorta or the bifurcation of the pulmonary artery it is stopped in its headward course, and either mostly reversed down the aorta or surges laterally out the pulmonary branches. The impacts at the arch and pulmonary bifurcation occur during early systole, and they are in opposite direction to the cardiac recoil. There are other impacts, occurring later, but they have not been used in calculating the stroke volume.

The first attempt to record the movements of the body in response to these forces was that of Gordon, followed by Henderson and several others (for references see 59). The earliest effort to get quantitative optical records of these forces was that of Starr and colleagues (128). Using a complex equation containing terms for age, sex, as well as dimensional terms, the first two strokes of the ballistocardiogram were used in calculating the cardiac output. The equation was admittedly an empirical one of best fit and has been modified repeatedly by these and other authors (e.g., 104, 105).

There are several reasons why the relation between the ballistocardiogram and the stroke volume is hard to understand theoretically. In the first place the recoil is evident only to movements which work in accelerating blood within the great arteries. This is clear from a series of experiments on a model (25, 59) in which the driving force was cut short in early, mid, and late "systole." This driving force caused ejection to continue and the stroke volume to become greater the longer it lasted. As long as the driving force (sudden increase in air pressure surrounding a collapsible bag which acts like a heart) was of the same intensity, the recoil curve was unchanged, even though ejection lasting until late "systole" would give a much larger stroke volume than ejection cut short in early systole.

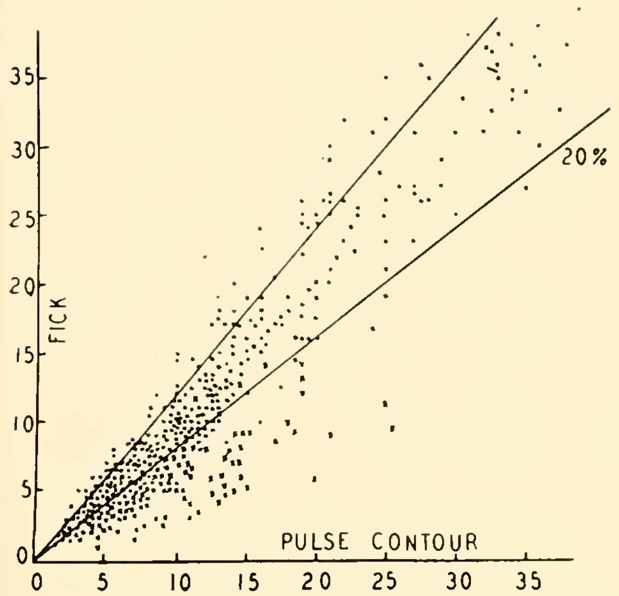

FIG. 8. Relation of stroke volume as calculated from the Fick or dye dilution methods and that calculated from the pulse contour, showing discrepant pulses (X). [From Remington (109).]

Increase in the air pressure, i.e., the force of acceleration, increased the recoil, whether the stroke volume was large (long-lasting ejection) or small. The recoil curve thus responded only to the initial acceleration of "blood" and not to the steady ejection. A cardiac contraction therefore, acting against a low aortic pressure, may give an early systolic surge of blood which, in shock (19) produces large deflections, indicating a stroke volume that is greater than normal instead of the known small stroke volume. On the other hand, in hypertension where the stroke volume is nearly normal, the initial ballistocardiographic deflections are small because the ejection is relatively slow and long maintained, giving small acceleration components and prolonged ejection at a relatively steady rate (111) which is silent for the ballistocardiogram.

Perhaps the most important basis for the ballistocardiogram's failure to have a simple quantitative relation to the forces of cardiac ejection is the fact that during systole there are many forces generated at the same time, which are contrary to each other and tend to cancel one another out. If there were none of these contrary forces operating during systole we could think of there being in the body two reservoirs: one, the heart which empties during systole, accelerates blood out into the arteries, and produces a recoil that is equal and opposite; and the other, a peripheral reservoir located at a place in the body which represents the center of gravity of the blood, being the source of a steady return to the heart through the veins. Knowing the distensibility of the major segments of the arterial tree (111, 112) it is possible to calculate the mass movements of blood from the heart (59). On the assumption that blood returns through the veins in a steady stream, there would be no accelerative forces connected with movement of venous blood and the arterial recoil forces would be alone in producing the ballistocardiogram.

Unfortunately, this is not true because when the forces which move the ejected blood out into and through the aorta are calculated in detail (59), it is seen that there are two important differences between the calculated and the recorded force curve. The calculated force curve begins much earlier and is very much larger (see fig. 10).

Two of the more important forces which may reduce and delay the recorded ballistocardiogram are accelerations of the venous stream and movements of the ventricular wall. The idea that the venous blood returns to the heart in a steady stream is not tenable. The measurements of Brecher show that there is a decided acceleration of the venous stream during systole (10). If this were not true there would be a volume of 50 or 60 ml less of blood in the thorax at the end of systole than at its beginning. On the assumption that there are 2.5 liters of air in the chest, systolic expulsion of 50 ml of blood from the thorax would lower the air pressure in the chest by 14 or 15 mm Hg if the airway were closed, or would cause a movement of 50 ml of air through the open trachea with each heart beat. There are, of course, no such changes of either pressure or volume. Measurement of the pressure change in normal man (W. F. H.) show that it is less than 0.2 mm Hg (56, 60). It consists of a lowering of pressure in early systole which is reversed by a rise in intrathoracic pressure in mid systole that cancels part or all of the lowering in early systole (see fig 11). This indicates exit of blood in early systole which is made up for before mid systole either wholly or in part. The very small air pressure change mentioned above would correspond to a volume change of 1.75 ml if the chest walls were rigid. Calculation of the equivalent elasticity of the chest walls from records made when known volume of air was added to the closed system in which the cardiopneumogram was recorded indicated that the volume change might be as high as 7.50 ml if the chest walls had the same elastic properties as air. Since the chest walls have a large mass and cannot fully respond to

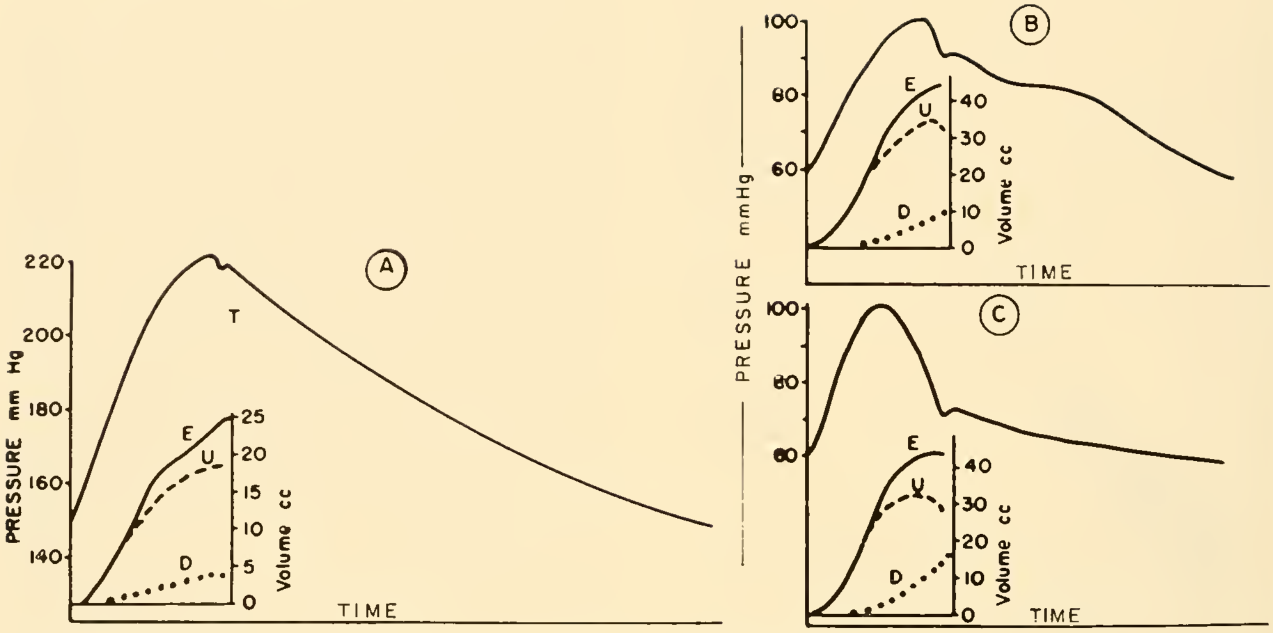

FIG. 9. Analysis of the relation between systolic ejection and the arterial pressure pulse. The uptake of successive parts of the arterial tree, as the pulse wave of distention passes down, is summated to produce the arterial uptake curve, *U*. To this is added the arteriolar outflow resulting from systolic increase in pressure *D*. *W* + *D* gives the total ejection, *E*. Diagram *A* is derived from a pulse in the presence of high resistance, *B* from one with intermediate resistance, and *C* from one with low resistance. [From Remington & Hamilton (111).]

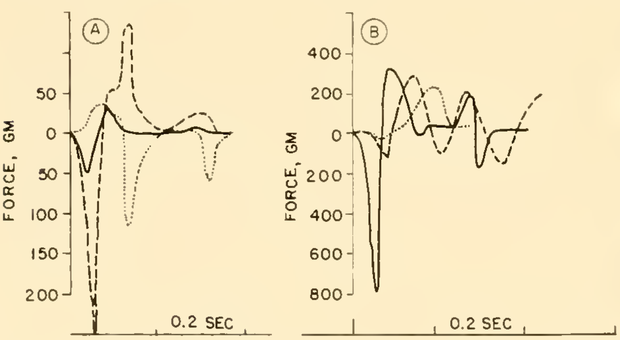

FIG. 10. Ballistocardiographic forces calculated from the forces needed to accelerate the blood that is ejected into the aorta and the pulmonary artery. *A:* solid line, forces attendant upon ejection of blood from the left ventricle; broken line, forces attendant upon movement of blood in the ascending aorta; dotted line, forces involved in moving blood down the descending aorta. *B:* solid line, summation of forces in the left diagram with, in addition, the forces attendant in moving blood from the right ventricle and through the pulmonary artery; broken line, the ballistocardiogram given by a high frequency ballistocardiograph, and dotted line by a low frequency ballistocardiograph. [From Hamilton *et al.* (59).]

transient pressure changes it seems more reasonable to accept a figure between 1.75 and 7.5 ml and closer to the smaller figure. This is acceptable on other grounds. Systolic air movements are barely percepti-

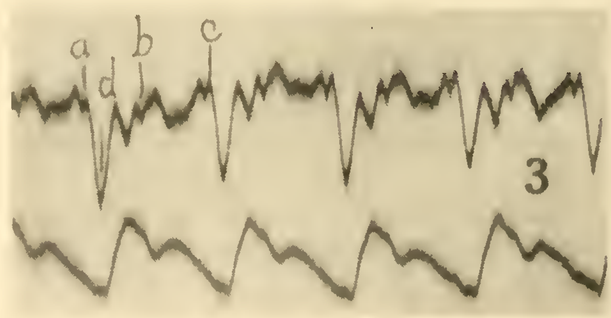

FIG. 11. Cardiopneumogram with simultaneous recording of brachial pulse. *a*) period of isometric contraction; *b*) end of systole; *c*) beginning of active systole; *d*) beginning of rapid venous return to atria. [From Hamilton (56).]

ble sensorially. As indicated by movements of a film of saliva covering the open lips or by movements of tobacco smoke through the open lips when the internal nares are closed, the glottis open, and the respiration at rest, the air movement is very small.

The fact that the intrathoracic pressure indicates that there is small net change in intrathoracic blood volume has relevance to ballistocardiography in that it implies that the stream back to the heart through the great veins pulsates as does the stream out from the heart through the arteries. Forces gen-

erated in the venae cavae and atria should cancel some of those generated in the ventricles and in the great arteries, inasmuch as the average direction of flow is opposite. Recent evidence (52) confirms the idea given in an earlier report (67), that the atria fill as the ventricles empty and vice versa (see fig. 14).

The movements of the walls of the heart probably also produce recoils that cancel and summate with recoils related to the movement of blood. When the inflow or the outflow was obstructed in dogs the ballistic waves were either diminished with their timing unaltered (134) or greatly changed in pattern (121). Elimination of pumping certainly does not eliminate ballistocardiographic forces; we must therefore conclude that the forces consequent on the movement of blood are augmented or canceled by forces originating in the movements of the cardiac walls.

In résumé it can be said that the ballistocardiograph records acceleration of blood but is silent as to flow in a steady stream; that movements of venous blood into the chest are reciprocal to the velocity pulse of the aortic stream out of the chest and produce opposite forces; that movement of the bloodless heart makes large impacts as recorded by the ballistocardiograph; and that the forces which can be shown to be necessary for moving the stroke volume into the arteries show up in the ballistocardiogram as having been delayed, distorted, and greatly diminished. For these reasons it seems best to look with skepticism at the equations which purport to calculate the stroke volume from the ballistic record (81, 105, 128) without accounting for or even mentioning the inadequacies and interferences mentioned above.

This is not to belittle the usefulness of ballistocardiography as an empirical diagnostic method and as an intriguing and difficult instrumental problem (121), but rather to point out the many things that must be incorporated into the theory of the ballistocardiogram before it can measure the stroke volume.

CARDIOMETRY

In principle the cardiometer consists of a chamber into which the heart, or better the beating ventricles, are introduced. As the ventricles change volume within the chamber there is a reciprocal change in volume of the space between the walls of the chamber and the heart. Suitable instruments can then record this change in volume from which the output of the two ventricles can be calculated. One-half of this figure is the stroke volume which multiplied by the heart gives the output per minute.

The physiological investigation of the volume changes due to the heart beat entered into its modern phase with the paper of Henderson in 1906 (73). In this paper earlier work was reviewed. It was pointed out that it had been usual to include both atria and ventricles within the cardiometer. Thus the earlier records included a series of volume changes pertaining to both atria and ventricles that might summate or cancel the effect of one another on the volume curve, making the latter very hard to interpret.

In order to avoid these complications Henderson designed his cardiometer to enclose only the ventricles. The cardiometer (see fig. 12) consisted of a rubber ball with a large opening at one end and a small one at the other. Over the large hole a rubber dam was applied which could be pierced with a hole large enough to admit the ventricles and which would close gently but airtight around the A-V groove. The smaller hole was for a tube connecting the cardiometer with a loosely covered writing tambour. The covering of the tambour was tied loosely so that pressure changes within the cardiometer would be small and have a minimal interference with cardiac action. Inadvertently this loose tying served another advantage in that the record could be made with almost no compression of the air within the system. If air is compressed even in so small a measure that it would have no appreciable hemodynamic effect, heat is generated. If this heat is not dissipated, it will cause a pressure increase that may be as much as 40 per cent greater than it would be if the heat were immediately dissipated and the pressure change were due to the compression alone.

Henderson's study of the shape of the ventricular filling curve, the influence of heart rate, filling pressure, the role of atrial contraction, and many other influences makes rewarding reading even after the lapse of more than half a century. Implicit in the shape of the cardiac volume curve are such concepts as optimal heart rate, the inadequacy of extreme tachycardia, the uselessness of atrial contraction in the presence of a normal venous pressure, and its great importance when the ventricles are not adequately filled.

Henderson's cardiometer was used by Starling (106) in documenting the "Law of the Heart" (see Chapter 15), and by means of clear cardiometer records relating diastolic size to stroke volume he hastened the acceptance of this important generalization. Wiggers & Katz (146) made technical improve-

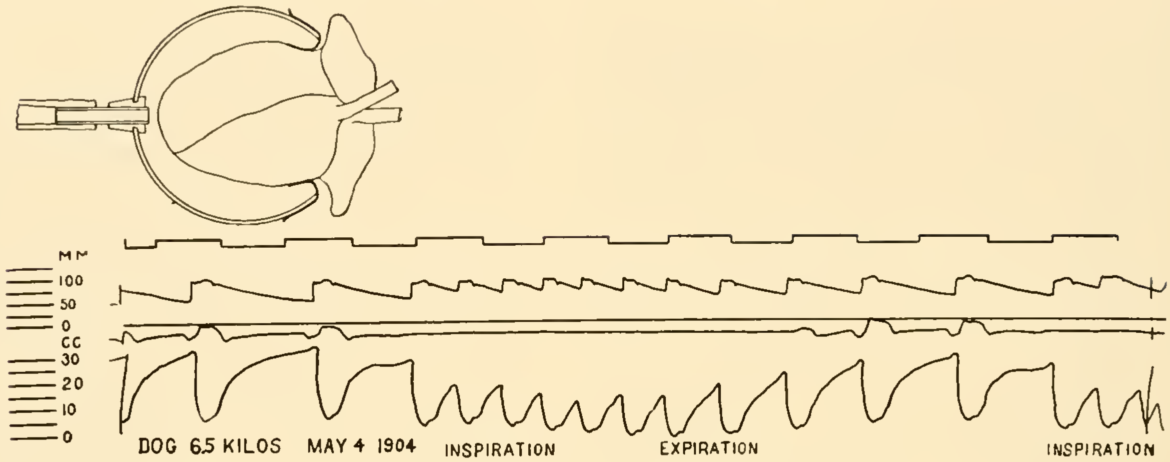

FIG. 12. Henderson's cardiometer, *left*, with calibrated record below. [From Henderson (73).]

ments in the method of recording the cardiometer curve (though they neglected the consequences of pressure change mentioned above) and, by taking simultaneous optical records of intraventricular, aortic, and atrial pressure pulses, worked out the basis for widely published diagrams of the relations between these records. These diagrams are of inestimable value in understanding and teaching cardiodynamics.

The cardiometer cannot be used in measuring the stroke volume of a heart beating normally within the closed thorax. This, of course, limits its usefulness. Nonetheless, the instrument has served very importantly in analyzing the mechanism of cardiac regulation.

X-RAY CARDIOMETRY

It has been thought possible to gain information concerning cyclic changes in the size of the heart by the use of the X ray. At first, timed short exposures were made during diastole and systole (97). From the corrected systolic and diastolic shadow areas the corresponding volumes were calculated (3, see also 70). The differences in the two volumes should give the summated stroke volumes of the two ventricles. Unfortunately, the resulting figure was nearer the stroke volume of a single ventricle, a circumstance which illustrates the essential weakness of the method. The X ray cannot visualize the ventricular roof and the pumping action which this partition does is considerable (67).

Another radiological technique which has been proposed is röntgen kymography. The outline of the heart is photographed through a set of narrow horizontal slits 1 cm apart. During the time of one or two cardiac cycles, the slits move down 1 cm. The movement of the walls of the heart are traced on the film much as would be those of a writing point on a kymograph. Connecting the systolic and diastolic points on the film permits outlining the systolic and diastolic areas and, from these areas, calculating the volumes as outlined above. This procedure, though more elegant, suffers from the same handicap in not visualizing the A-V septum. An empirical constant can, however, be applied to the kymographic movements of the left ventricular wall which gives reasonable agreement with the stroke volume as measured by dye injection (79).

The fluoroscopic image of the heart differs not only in size but also in intensity during the cardiac cycle. The intensity varies inversely with the amount of blood contained in the heart, which acts as a filter between the source of the rays and a small fluorescent screen, the luminosity of which is inversely proportional to the effective thickness of the heart. The changes in luminosity of the screen can be sensed by a photomultiplier and the proper circuity so that a graphic record is obtained of the changing volume of blood in a sector between the X-ray tube and the small fluorescent screen. The record is of admirable clarity and has a similar appearance to the mechanically recorded ventricular plethysmogram. However, the record must be calibrated empirically against known stroke volumes with the use of a phantom which produces deflections similar in amplitude to those produced by the heart (114–116).

Rushmer has pointed out that an approach to the

measurement of cardiac output by X ray would seem to be more definitive if it involves the visualization of the left ventricular cavity by means of infusions of radiopaque fluids (119). Changes in the projection of the area of the left ventricular cavity are certainly more closely related to the stroke volume than are changes in the projection of the whole heart or even of the two ventricles. Evidence brought out by this investigator showed that the effective filling pressure was not the predominant factor in determining the diastolic area of the left ventricular projection, nor was the diastolic size of this area predominant in determining the systolic change in area (stroke).

During the last 2 years this approach has been carried much further by simultaneous and equally meritorious researches in Sweden (52) and Texas (13, 14). Both groups of investigators visualized the left ventricle by injecting a relatively nontoxic radiopaque material into the right heart and studying cinefluorographic frames which showed the left ventricular outline most clearly. Each group worked out formulas for calculating the volume of the left ventricular contents from its silhouette (see also 70). Accuracy of the X-ray volume calculation was checked against casts.

Cineangiocardiographic exposures were made at 30 to 48 per sec projected life size and the formula applied to the silhouette of the radiopaque contents of the left ventricle. Twenty, more or less, of these left ventricular blood volume measurements were laboriously made during each cycle, showing filling, ejection, and isometric phases.

The Texas workers showed that the increased stroke volume of exercise was made by means of decreased systolic volume rather than an increased diastolic volume (fig. 13, 14). The Swedish workers traced the simultaneous cyclic changes in atrial and ventricular volume and showed that the atrial volume changed reciprocally with that of the ventricle (confirming what has been said above concerning ballistocardiography, cf. 59, 60, 67).

X-ray methods have led to clear insight into the relation in the intact animal between the factors which control the cardiac output such as diastolic size, systolic size, stroke volume, and heart rate as the animal changes from the resting to the active state.

In general, it may be said that the pulse pressure method, ballistocardiography, and the various forms of X-ray cardiometry which do not involve measuring the volume of left ventricular contents are methods which depend for their validity on comparison with an accepted method (see below). Comparison under one set of conditions may not validate the method under other conditions. The chief advantage of these methods is that they give data on beat-to-beat changes and do not demand a steady state as do the classical dilution methods.

DILUTION METHODS

In 1870, A. Fick wrote a much quoted but little read paragraph in the proceedings of a scientific society in the ancient university town of Wurzburg (32). This paragraph has been little read because it carries a very simple message that is self-evident, once it is grasped, and needs no careful rereading. It is much quoted because it is a turning point in the development of the quantitative measurement of blood flow, and from its central idea or principle have come many and various techniques that have given us the soundest measurements of the output of the heart and the flow of blood through organs.

Adolph Fick had an unusually analytical viewpoint in physiology. He is known at the present time in physics for his law of diffusion in fluids, published when he was 26 years old. This generalization of the relation between rate of diffusion and concentration gradient was developed mathematically in 1855, but not proven experimentally for 25 years.

In circulatory physiology he is known at the present time as the originator of the dilution principle for measuring blood flow, the so-called Fick principle being a byword on the tongue of nearly all medical students. This contribution again was not exploited by Fick nor was it experimentally tested until accurate methods of blood gas analysis had come into general use in 1886 (51) and again in 1898 (150).

As a physiologist, Fick's chief interest was in the physiology of muscular contraction, distinguishing isometric and isotonic contractions and the effect of the length of fiber on strength of contraction. This last development is the foundation of the Starling principle, a most fundamental circulatory generalization.

The principle of dilution methods in general is that if we know the amount of substance which enters or leaves a stream, and the concentration difference resulting from such entrance or removal, the size of the stream can readily be calculated. The illustration that Fick used, and most probably the only one he had in mind, involved gas transport by the blood and can be shown by the simple example that if oxygen is consumed at the rate of 240 ml per min, the arterial

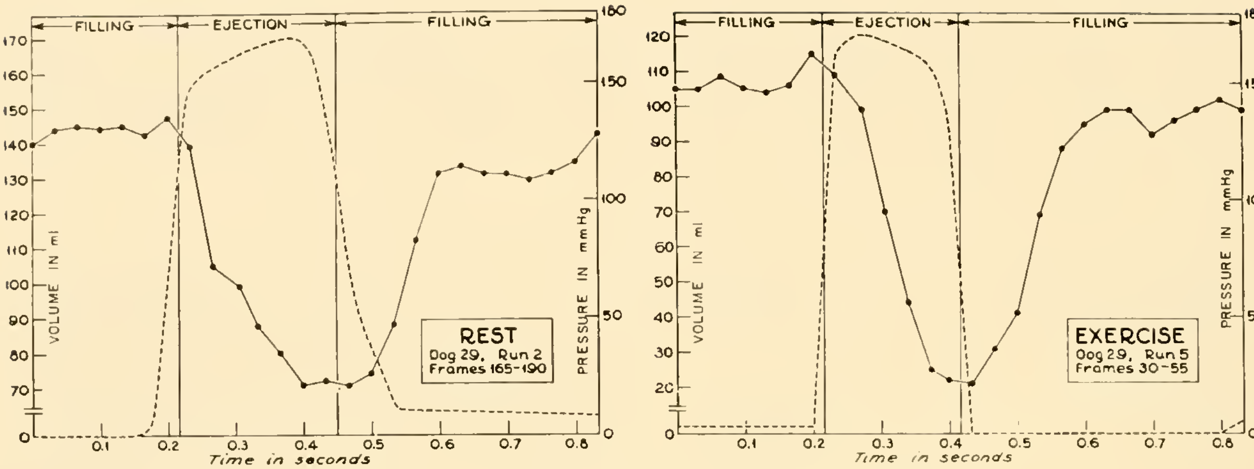

FIG. 13. Left ventricular pressure-volume curves through a cardiac cycle in the resting and exercising anesthetized dog. The successive points were calculated from the silhouette of the opacified left ventricular contents visualized cinefluorographically. [From Chapman *et al.* (13).]

blood contains 200 ml per liter and venous blood 160 ml, each liter of blood would take up 40 ml of oxygen in the lungs and it would require a flow of 6 liters per min to transport the 240 ml of oxygen to the tissues. The relation can be expressed

$$F = \frac{O}{A - V}$$

where F equals the flow per unit time, O, the oxygen consumption per unit time, and A and V the oxygen content of arterial and venous blood, respectively. This same principle is involved if a foreign substance is introduced into the blood stream either by injection or inhalation, or if a substance is removed from (or added to) the blood stream at a known rate by the function of liver or kidneys. The blood flow to the organ is to be found from the relation between the rate of removal or addition and the difference between the amount of the substance in a unit of arterial and venous blood. On this basis all the clearance methods described elsewhere in this treatise for measuring renal and hepatic blood flow, foreign gas methods, injection and infusion methods, for measuring the cardiac output or regional blood flow, are essentially dilution methods, the general principle of which was first enunciated, as a specific example, by Adolph Fick in 1870.

FICK METHOD

In measurement of blood flow through the lungs—which is the cardiac output—it is, of course, necessary to measure the oxygen in a fair sample of the venous blood which is about to enter the lungs. Blood from peripheral veins may have more or less oxygen than the average mixture from all parts of the body. Blood from the warm skin may be hardly different from arterial blood, whereas that from an active muscle (heart) may be depleted of most of its oxygen. It is necessary, therefore, to get blood from the right heart if one is to measure the pulmonary blood flow by means of the A-V oxygen difference.

All of these considerations were taken into account in the masterly and meticulous study of Zuntz & Hagemann (150). Taking advantage of the fact that horse blood coagulates slowly, these investigators inserted a rubber tube into the neighborhood of the right heart via the jugular vein and withdrew mixed venous blood samples. Comparing these with arterial blood as to oxygen and CO_2 content, and measuring the gas exchange, Zuntz and Hagemann calculated the cardiac output of their horses during rest, exercise, and digestion. The results were cumbersomely expressed in five figures. When quantitation was used in these early times it was often overmeticulous. The use of five figures to express results that could be significant only to two figures may have caused a subconscious bias against quantitative biology. Moreover, the results were descriptive rather than analytical and no general principle as to the regulation of the circulation has been derived from them.

Interest in the application of this method to the measurement of the cardiac output was suspended until the third decade of the present century. In the 1920's the method was applied by means of direct

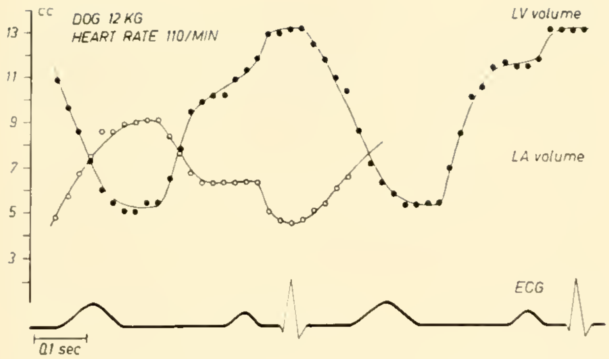

FIG. 14. Left ventricular (closed circles) and left atrial volume changes (open circles) in the dog's heart, calculated from cinefluorograms. Simultaneous ECG. [From Gribbe *et al.* (52).]

cardiac puncture in dogs in the vain search for a key (such as hydrogen ion concentration, oxygen tension or CO_2 tension) which might regulate the circulation just as the respiration was thought at that time to be regulated (cf. 57, 58, 71, 94). The search for such a simple key to the control of the circulation rate was naïve because it seems clear at the present time that the controlling role of the central nervous system, the self-regulated demands for blood on the part of active organs, and the reflex mechanisms for the homeostatic control of the arterial pressure all play a role in the complexly integrated mechanisms by which the rate of the circulation is regulated.

Even though CO_2 tension, oxygen want, or other simple key to the regulation of the circulation was not found, much interesting information was uncovered as to the effects of drugs, arteriovenous fistulas, hemorrhage, trauma, and pneumonia.

Cardiac puncture was not applied to man. The human heart and even the human artery were held inviolate until well into the present century. It was not until 1930 that Bauman & Grollman (4) punctured the right ventricle of the human heart and used the respiratory gas content of a sample of blood from this cavity together with that of arterial samples and the gas exchange to calculate the cardiac output. When these investigators found that the cardiac output by the direct puncture Fick method agreed with a favored respiratory method (see below) they carried their experiments no further, and no one since has had the temerity to repeat them.

At about this time the intrepid Forssmann (34) catheterized his own heart several times, and Klein (80) drew mixed venous blood using a catheter and calculated the cardiac output. Cardiac catheterization was used during the next decade for the visualization of radiopaque substances injected into the cardiac cavities, and a significant advance was made in the development of a nonwettable plastic catheter that minimized the danger of intravascular clotting.

The time was ripe for Cournand, Richards, and their colleagues to begin their classical work on the physiology of the circulation in health and disease (18, 113). The new techniques available from cardiac catheterization enabled these investigators to measure the pressure pulses in the cardiac chambers and great vessels as well as to take samples of mixed venous and of arterial blood, so that many of the details of hemodynamics of normal and abnormal circulations could be worked out. This pioneering work demonstrated the safety of the procedure so clearly that it was taken up in many laboratories, notably those of Bing (7), Dexter (22), McMichael (96), Stead (129), and Wood (147).

The accuracy of the cardiac output calculation depends in the first place on getting a fair sample of the mixed venous blood. As is well known from the study of the fetal circulation, blood may pass through the inferior vena cava and into the left atrium by way of the foramen ovale without mixing much with the superior vena cava stream which crosses it and enters the right ventricle. For this reason it is not surprising that Shore *et al.* (126) found that successive samples taken from the dog's right atrium might not agree in O_2 content. In man consecutive or simultaneous samples show much better agreement than those reported here. In general the effects of inadequate mixing are reduced as the site of sampling is moved downstream from the inflow tract of the right atrium to the outflow tract. The samples agree better when taken from the outflow tract of the ventricle and better still when taken from the pulmonary artery (20, 137).

Aside from the possibility that the venous stream is incompletely mixed and essentially simultaneous samples are variable in their oxygen content is the possibility that the subject is in a changing state. This is important because the fundamental assumption on which the Fick procedure is based is that the volume of oxygen taken up in the respiration equals the volume of oxygen used by the tissues. Unfortunately these quantities cannot be instantaneously measured. The gas exchange and oxygen uptake can be measured only at the mouth. The lungs are a large reservoir which in their gas capacity and in the quantity of blood which may be stagnant in the alveolar capillaries are able to take up and give off

oxygen at the capillary wall in quantities which are not reflected by the uptake at the mouth.

It is a matter of intuitive judgment which can be proven mathematically (40, 131) that the more nearly constant the general physiological condition of the subject during the time of sampling, the more adequate is the calculation of blood flow. The constancy should apply to alveolar and blood gas tensions, oxygen uptake, and respiratory quotient, and is likely to be violated when the subject exercises or changes the inspired gas mixture (anoxia) (33). In order, therefore, to insure that the oxygen uptake at the mouth is as nearly as possible like that which occurs at the tissue cells, it is necessary to hold the subject in a steady state for 10 to 15 min before the samples are taken as well as during this time.

The necessity for the steady state is emphasized when the results of calculating the blood flow with CO_2 as a reference substance are compared with those using O_2. The CO_2 results are very much more variable because slight changes in ventilation will work an easier transfer of CO_2 from lung blood to lung air than is the case with oxygen. There would thus be changes in the CO_2 content of pulmonary air that would not show at once in the expired air or in the A-V difference. Moreover, important quantities of CO_2 are combined with the tissue fluids and with sequestered plasma in the alveolar capillaries which are also released or stored with changed ventilation (12, 61).

The existence of a steady state does not rule out the general idea that oxidations may occur in the lungs or in the blood passing through the lungs. This idea was disposed of in 1913–15 when Henriques showed that the injection method (see below) measured a large enough blood flow to account in terms of the A-V difference for the gas exchange (75, 76). The question arose again in 1920 when it was suspected that lactic acid disappeared oxidatively on passage of blood through the lungs. The question received contradictory answers until the possibility of pulmonary oxidations was again laid to rest by Mitchell & Cournand (100).

There are cyclic changes in the circulation rate which depend upon respiration and the cardiac cycle (in the presence of shunts) as well as upon spontaneous vasomotor activity which are refractory to maneuvers aimed to bring about a steady state (131, 135). If the samples are taken at a constant rate, there will be no means of weighting the samples taken when the flow is fast as compared with those taken when the flow is slow. The A-V difference and oxygen uptake should be instantaneously integrated, but such a calculation can only be set down symbolically on paper. Practical tests (123) and a priori considerations (58) indicate that this concept is not likely to introduce a serious error.

In certain pulmonary diseases, the natural bronchial blood flow of 10 to 12 ml per min becomes greatly augmented. These conditions include congenital pulmonary stenosis, bronchiectasis, and situations in which a large pulmonary artery is occluded. Under such conditions numerous small branches of the bronchial artery enter the alveolar circulation and drain from the lung by the pulmonary vein. The amount of such bronchial flow may reach 20 per cent of the total flow in bronchiectasis and is said to be able to sustain life in cases of pulmonary atresia with intracardiac shunting. (Compare Chapter 14). In the absence of intracardiac shunting such blood flow serves no useful purpose and cannot be measured by the Fick procedure. It can be measured, however, as the difference between dye injection calculations made from curves taken from the pulmonary artery (excluding the bronchial circulation) and the brachial artery (including it). The dye is injected into the right atrium (40).

The most important diagnostic use of the Fick procedure is in the evaluation of intracardiac shunts in congenital heart disease. These uses will be taken up in Chapter 14.

RESPIRATORY METHODS

In the nineteenth century and the first quarter of the twentieth century it was, as mentioned above, not considered safe to enter the human heart to obtain mixed venous blood samples. At this time also, the human artery was rarely punctured. Credit is due to Loewi & von Schrotter (90) for thinking in 1903 of using the lungs as an aerotonometer to measure the tension of the mixed venous blood and hence of its gas content. Not only were these authors the first to use the lungs in this manner, but also they were the only ones to apply the principle quite impeccably. Using a balloon cannula, they blocked off a part of one lung and allowed time for complete equilibrium of the air in that part of the lung with the mixed venous blood perfusing the alveoli. The CO_2 or oxygen of this air was analyzed and its tension measured. This was applied to the relevant dissociation curve and the gas content of the mixed venous blood determined. A similar procedure using alveolar air was used to

measure the gas content of arterial blood. From the arteriovenous difference thus determined, and the gas exchange, the cardiac output could be calculated.

The procedure of Loewi and von Schrotter was cumbersome and difficult, but it could not be criticized on theoretical grounds. It was possible for them to make measurements in a steady state and allow time for complete equilibrium between lung blood and lung air to occur. Nonetheless, the method has never been tried again.

The difficulties of the Loewi and von Schrotter procedure were surmounted by making certain rather doubtful assumptions and using a simpler technique. The new technique was to rebreathe, or hold in the lungs, gas mixtures, the strength of which did not change on being exposed to lung blood. Such mixtures could be made up by trial and error until one was found, the tension of which did not change on breath holding (23). A simple way to make up such mixtures was to repeatedly rebreathe oxygen (to assure oxygenation of lung blood). After several rebreathings, each lasting 15 sec, the CO_2 tension of the rebreathed air came to a constant figure which was said to be that of mixed venous blood (74).

Originally, analyses were made of the general volume of 3 or 4 liters of rebreathed air as sampled from the rebreathing bag. Results obtained in this way may be stultified by incomplete mixing of lung air and bag air, and may further be stultified by the slowing of the evolution of CO_2 from the venous lung blood as the rebreathed air tension asymptotically approaches that of the venous blood (57). These difficulties can be avoided by insuring that the sample of rebreathed air be taken from the depths of the lung—an end expiratory or alveolar sample. Doing this uncovers other difficulties (61).

By going through the process of repeated rebreathing for 15 sec the alveolar samples reach a constant value after 3 or 4 episodes of rebreathing. If the tension reached by this plateau is that of the mixed venous blood, and that of the normal alveolar air is the tension of the arterial blood, we have established an A-V CO_2 tension difference from which the A-V content difference can readily be derived. Knowing this and the CO_2 production the cardiac output can be calculated by the Fick equation.

Unfortunately, however, the "A-V difference" levels off at different heights depending on how long the rebreathing time is made. If the repeated episodes of rebreathing are 8 sec in duration the A-V difference is 79 ± 0.9 per cent of that at 16 sec. If rebreathing episodes last 24 sec, the A-V difference is 117 ± 1.7 per cent of that at 16 sec. Moreover, it has been statistically shown (68) that it would be impossible to prove the existence of a plateau of rebreathed gas tension plotted against time of rebreathing during the period before recirculation (15 sec after the start of rebreathing). This is true, whether or not enough CO_2 has been added to the mixture to compensate for the diluting effect of residual (alveolar) air, added to the system at the beginning of each rebreathing episode.

Due to the high diffusibility of CO_2 it cannot be said that there is a failure of the CO_2 in the alveoli to reach equilibrium with the walls of the alveoli. There must be, therefore, in addition to the mixed venous blood perfusing the lungs, an appreciable quantity of arterialized fluid (blood plasma or other fluid) which remains in the lungs during the rebreathing process and absorbs CO_2 from the virtual venous inspired mixture. This has been quantitatively measured (57) and it is found that during the first 4 sec of rebreathing the stagnant arterialized fluids of the lungs absorb not only the CO_2 brought to the lungs by the venous blood but, in addition, 13 ml of inspired CO_2. At the end of 8 sec of rebreathing the lungs have absorbed the CO_2 entering the lungs together with about 1 ml of inspired CO_2. Assuming, as we must, that there is a CO_2 equilibrium between the lung and alveolar air, we have to think that the CO_2 has diffused into arterialized lung fluids.

This has been confirmed recently by Dubois *et al.* (28), who have shown that the fluid of the lung tissues combines with CO_2 in amounts similar to blood. The movement of CO_2 into the lung fluids was shown to cause the P_{CO_2} in the alveolar air to rise during breath holding much more slowly than would be predicted from the volume of air in the lungs and the rate of CO_2 output. To put the matter in other words, the amount of CO_2 required to raise the P_{CO_2} of the lung air (3 liters) by 1 mm Hg is 3.95 ml, whereas that required to raise both the lung air and lung tissue by 1 mm Hg is 4.75 ml. These experiments were done in lungs washed free of blood. The natural lung contains stagnant blood, and blood flowing backward (cf. 61). In addition to this, there is more plasma (about 30% more) in the lungs than would be expected from their erythrocyte content (46). Moreover, a large part of this plasma is sequestered probably in capillaries where it remains stagnant and capable of adding to the CO_2 combining power of lung tissue. It is believed to be stagnant because only a small part of the "extra plasma," about 5 per cent, can be accounted for by laminar flow and longer

mean transit time of plasma as compared to the rapid axial stream of cells perfusing small vessels (87).

The delay of blood (and plasma), in passing through the lungs, makes it impossible to use the lungs as a tonometer for mixed venous CO_2 tension even though mixing and bulk diffusion difficulties are eliminated by using alveolar (end expiratory) air samples. There is a constant increase in the A-V differences, as rebreathing time is prolonged, caused at first by slow mixing, slow diffusion, and slow equilibrium with arterialized fluid in the lungs, and later by recirculation of blood which has been exposed to rebreathed pulmonary air. Thus with long rebreathing time and high A-V differences the cardiac output would be calculated as low, and with short rebreathing time the figure would be high. It is small wonder that workers with this method reported variable results (57). Some believed that the circulation rate was 6 to 8 liters per min, some reported 3 to 5, whereas others reported both (53). Variations in time of exposure of air in the lungs seem to be the principal cause of the variability (5).

The work of Grollman (53) established in the minds of most physiologists of the 1930's the idea that the cardiac output was near the lower of the limits given above. Following the work of Markoff, Muller and Zuntz and that of Krogh and Lindhard (see 53), he set about to find the rate of disappearance of a foreign gas from rebreathed air and from this, and the oxygen uptake, to calculate the pulmonary capillary blood flow (cardiac output).

Grollman used acetylene rather than nitrous oxide as his foreign gas because it was more soluble in blood and because it was more easily analyzed. He was a very industrious worker and got admirably self-consistent results under varying conditions. For the normal cardiac output, the figure was 2.2 $\pm$ 0.3 liters per min per m^2 body surface. All figures must abide within these Procrustean limits in order to be acceptable at this time. Indeed, the acetylene method gave figures that agreed with the direct Fick procedure in his hands (4).

We know now as a result of many determinations of the cardiac output by the direct Fick method, as performed by Cournand, Richards, and their followers (see above), that the average basal cardiac output in man is 3.3 liters per min per m^2 instead of 2.2. The evidence is overwhelming that the larger figure is correct, for not only has it been measured many times by the direct Fick method but also figures derived from the injection method are in agreement (see below). Moreover, if we summate blood flow as measured independently through the liver, kidney, heart, brain limbs, and so on, we arrive at a figure that the aggregate flow must be of the larger rather than the smaller order of magnitude (57).

The reason for the discrepancy is not far to seek. Grollman rebreathed his gas 18 to 30 sec under the impression that the complete circulation time was of this order. This was supported by the fact that the calculation of cardiac output was the same, whether the rebreathing was carried on for 18 or 30 sec. Unfortunately, these times bracket the second rather than the first circulation, so the measurements could be too low without disagreeing.

Evidence that the total circulation time is of the order of 10 to 18 sec, with a mean at about 15 sec, is to be had from dye injection (69). Moreover, Grollman himself concedes that acetylene returns in appreciable quantities to the right heart in samples taken between 13 and 20 sec after rebreathing started. This is congruent with the experiments of Gladstone (47) and with those of Hamilton *et al.* (69) and of Werkö *et al.* (139), all of which go to show that, by hindering the entrance of acetylene into the blood and by raising the acetylene concentration of the second sample more than the first, thus changing the slope of acetylene disappearance, the Grollman method gives too low a figure for the cardiac output.

Recently Cander & Forster (12) have called attention to another error in the Grollman method. In contrast to CO_2, which in the absence of carbonic anhydrase in pulmonary tissue and fluids combines slowly, acetylene and nitrous oxide dissolve instantaneously in these fluids. This extends the effective pulmonary volume for this gas by about 10 per cent, which would lead to an underestimate of capillary blood flow by the same amount. These authors mixed about 15 per cent helium into their breath-holding mixture. This gas is quite insoluble and serves as a landmark by which changes in acetylene or nitrous oxide concentration due to bad mixing can be separated from changes due to solution in the pulmonary capillary stream. By reducing the time of breath holding and controlling mixing, and the effective lung volume, these authors seem to have developed a technique by which the foreign gas method can be used to measure the cardiac output.

The use of a foreign gas (nitrous oxide) also lends itself to measuring the cardiac output instantaneously from beat to beat. This type of measurement has certain decided advantages over other dilution methods in which the subject must be in a steady state during the time of the sampling (see above). Exploitation of

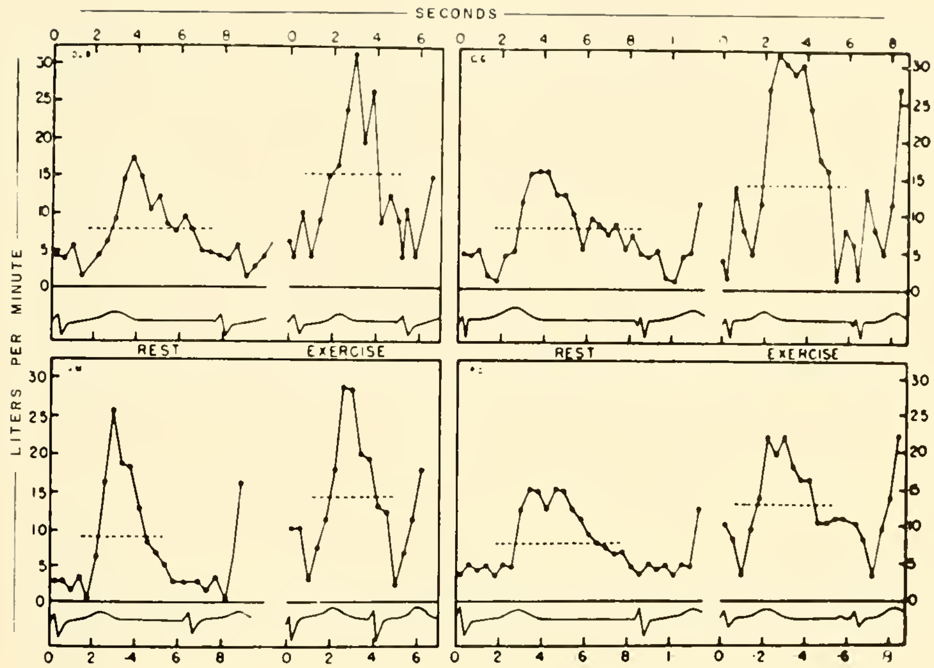

FIG. 15. Records of cyclic changes in the rate of perfusion of blood through the lungs of normal man at rest and during exercise. Data were derived from the pressure changes resulting from the absorption of nitrous oxide within a body plethysmograph. [From Lee & DuBois (88).]

this possibility is the ingenious maneuver of Lee & DuBois (88), working in Comroe's laboratory, enclosed the subject in a body plethysmograph with the idea of measuring the pressure changes resulting from the solution of nitrous oxide in the pulmonary capillary stream. The subject at first was asked to hold a breath of air inspired from the plethysmograph in his lungs with open glottis. The pressure changed very slowly due to final temperature drift and the respiratory quotient. The subject was then asked to inspire 80 per cent nitrous oxide from a bag inside of and in temperature equilibrium with the plethysmograph. The pressure in the plethysmograph began suddenly to decrease due to the reduction of gas volume from solution of N_2O_2 in the pulmonary capillary stream (see fig. 15). This reduction in pressure occurred in pulses synchronous with the surges in pulmonary capillary flow as measured by Cournand (16) from the pressure differences between the pulmonary "capillary" (wedge) pressure and the pulmonary arterial pressure. These pulsations and the minute volume flow calculated from their mean height would inincrease with exercise and would give resting values within normal limits by accepted methods.

A modification of this method has been suggested by Wasserman & Comroe (138). They require the subject to maintain the thorax at a constant size controlled by a stethogram with the glottis and mouth open to a sensitive volume recorder. Control and nitrous oxide recordings were made as described above and reproducible records of the cardiac output made which were within physiologically normal limits. Prompt improvement in the ability of most subjects to hold the chest steady was reported.

INJECTION AND INFUSION METHODS

This is another variety of the dilution method sharing that classification with the direct and indirect Fick method and with the various respiratory foreign gas methods. There are many sorts of information that may be had from the results of the injection method besides the measurement of the cardiac output. Whereas this chapter is confined in the main to discussion of the cardiac output, attention will be called here to various "extra dividends" that may be had from the use of the method. Most of these will be discussed in other chapters of this section of the *Handbook*. A detailed and clear review of the literature has recently been published (24).

The injection method or indicator dilution method

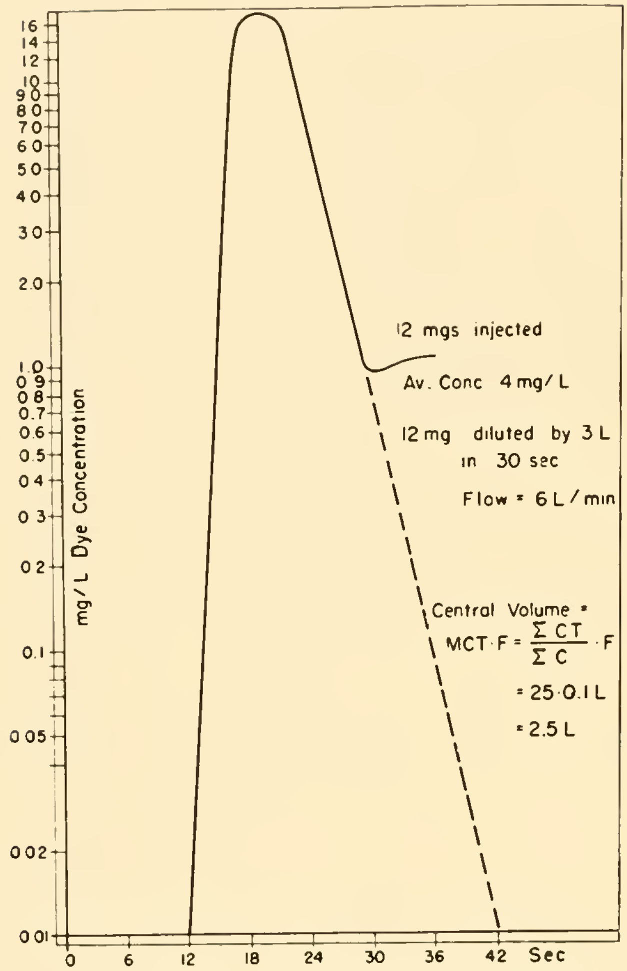

FIG. 16. Changes in arterial dye concentration after injection into a vein. Cardiac output is calculated from data given on the figure. [From Hamilton (58).]

has been widely used for localizing and evaluating congenital cardiac defects. These applications are described in Chapter 14. Its usefulness in detection and evaluation of valvular defects is discussed in Chapter 20, its application to the measurement of regional blood flow in Volume II. The time concentration curve resulting from the injection or infusion of indicators is subject to interesting theoretical analysis which is quite acceptable mathematically. This forms the proof of the intuitively acceptable idea that not only can the flow be measured by the knowing use of the method but also the capacity of the bed through which the flow takes place can be estimated with equal accuracy. These considerations are taken up in Chapter 18.

As a method for measuring the cardiac output the procedure is based on the following considerations. A dye or other indicator which does not diffuse out of the circulation is injected into the right heart or a venous tributary and appears in the arterial blood. Here the time course of its concentration may be evaluated by analyzing separate timed samples or by means of various continuous monitoring devices which will be referred to below. The injected substance begins to appear after a delay of 6 to 15 sec (appearance time). It then builds up to a peak concentration (build-up time) and rounds off. The descending limb seems to be exponential, i.e., to plot a straight line when log concentration is plotted against time. After the exponential descent has progressed for a time, which depends upon its injection and sampling sites, and upon the condition of the subject, there is a sudden deviation to the right which marks the beginning of recirculation of the indicator.

The flow (F) is calculated from this time-concentration curve by the formula $F = 60\ I/ct$, where I is the amount of indicator injected, c the average concentration of indicator during its first circulation, and t the time of passage of the dye on its first circulation. Exemplifying numbers are given in figure 16. The problem of separating the dye, which is on its first circulation, is important in establishing both c and t in such a way as to include all the indicator on its first circulation in the calculation and to avoid counting any of it twice. We prefer to regard the left heart as a simple reservoir and assume that a volume of blood within it is mixed with the indicator. At first the concentration is built up as more indicator enters than leaves. At the concentration peak, dye is leaving and entering at about the same rate. The entering stream quickly falls off in amount of indicator, and during the downslope very little is entering the left heart [see fig. 17, (78)]. The concentration of dye in the arterial effluent from the heart becomes a simple washout of the left heart and its exponential nature is thus established. If the indicator is washed out of the left ventricle and into the arteries in an exponential manner, i.e., if the amount washed out per unit time is proportional to the concentration in the left heart reservoir, the simple prolongation of the downslope past the recirculation and on as far as is significant would enclose an area describing the time concentration relations of all the indicator on its first passage and would include none on its second circulation.

Some doubt has been expressed (see Chapter 18) that the exponential extrapolation is justified. It is clear from the evidence that indicator passing through straight tubes (118), or a tubular arteriovenous network such as the pulmonary vasculature (78), does

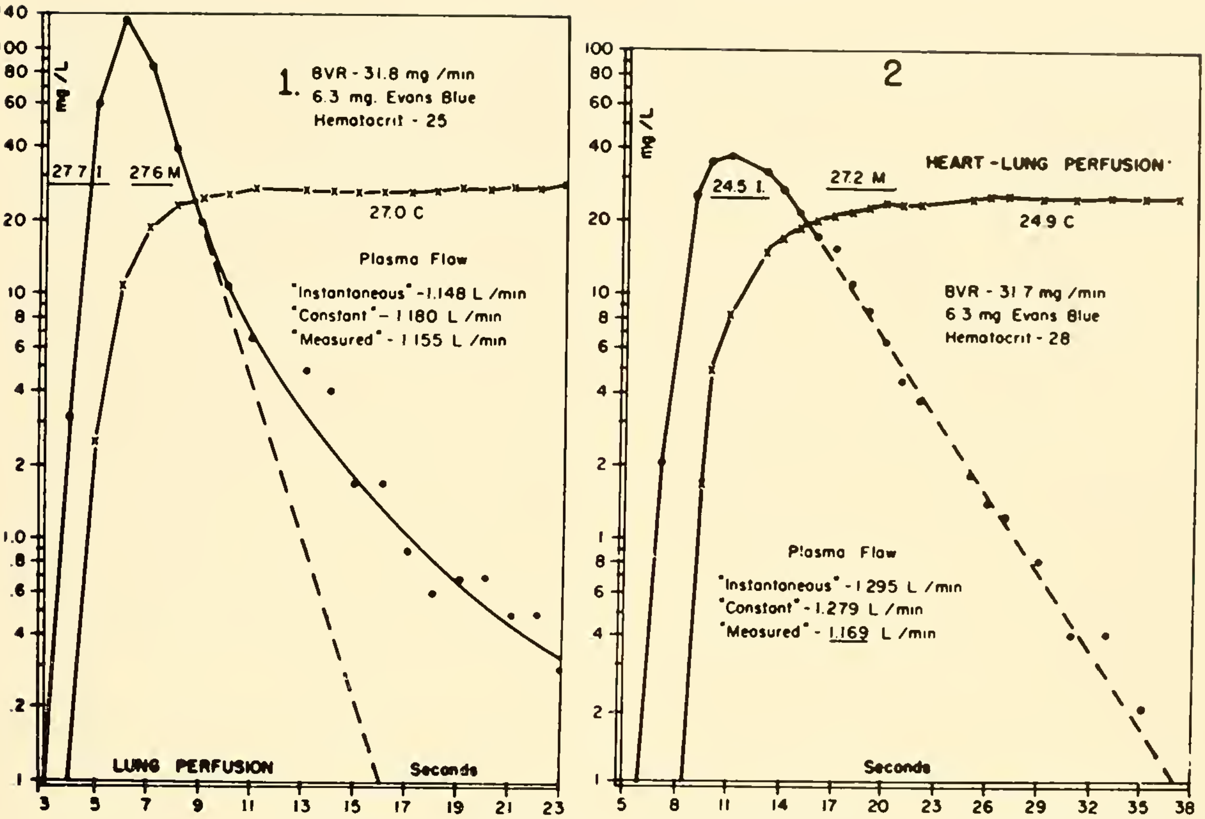

FIG. 17. Dye curves from perfusion of the heart and lungs, and from the lungs only. Simultaneous evaluation of the results of constant infusion of brilliant vital red and instantaneous injection of Evans blue (T-1824). [From Howard *et al.* (78).]

not give an exponential downslope. This may be due to the fundamental nature of laminar flow in transporting indicator (118) or to the fact that organs such as the lung and kidney have rapid and slow circulations with different flow volume relationships. When glass models are set up in parallel with different flow volume relationships the washout concentration curve is not exponential and consequently cannot be extrapolated (62). The descending curve from lungs perfused through the pulmonary artery and sampled at the pulmonary vein is also not exponential (78) (see fig. 17). Each of these curves becomes exponential when a mixing chamber is introduced in series. In the model the mixing chamber was a glass bulb (62), and in the lung perfusion experiment the perfusion was made to include the heart; the injections were made into the right atrium and the samples taken from the aorta. As soon as the curve had rounded the peak it became exponential and remained on the same course down as far as the determinations could be made, i.e., in the case of the lung experiment to $\frac{1}{100}$ the peak concentration. The mixing chamber had served to smooth out the irregularities of the curve as it left the complex system and impress upon the downslope exponential washout curve that would be expected from dye passing out of a single reservoir.

It is clear from contributions from Newman's laboratory (103) that, unless special precautions are taken to insure instantaneous mixing of dye into a glass chamber model, the volume of the chamber is not indicated by the rate of concentration change of indicator in samples of the effluent stream. This was recognized in 1932 (62) but does not alter the fact that flow through a chamber, whether mixing is complete or not, appears exponential and that the volume of the chamber and the flow through the chamber can be calculated as accurately as experimental methods will allow, on the assumption that the washout curve is exponential.

Another indication that the downstroke of the indicator dilution curve can be prolonged exponentially is the success of those who have followed this procedure. This success consists of comparison of the cardiac output, as measured by the dye injection

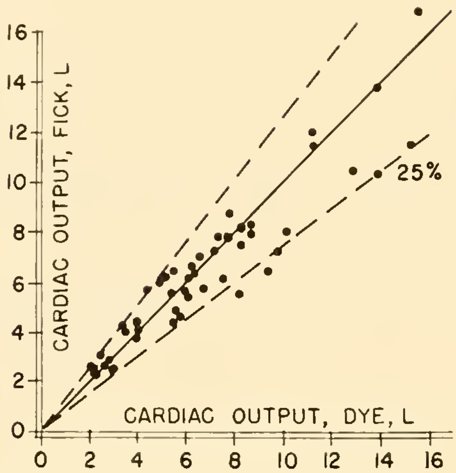

FIG. 18. Correlation of cardiac output as measured by the Fick procedure and by the injection method. [From Hamilton *et al.* (66).]

method, with that measured by the Fick procedure (27, 66, 102, 140). These comparisons show a rather wide scatter, reflecting in part the biological fluctuations in cardiac output with the longer duration of Fick respiratory sampling frustrating all attempts at simultaneity, and in part reflecting essential lack of technical precision in both methods. In spite of this scatter there is no significant difference in the average results. This in turn means that whatever fault there may be in the exponential prolongation of the downslope of the dye curve it is not enough to stultify the final answer (fig. 18).

The need that the indicator should stay in the vascular system is moot. A diffusible substance can leave the circulation in the pulmonary capillaries but, since normally there is very little interstitial fluid for it to enter, it probably is not lost in a very important quantity and much of what diffuses out of the pulmonary capillaries may very well wash back into the circulation as the indicator concentration becomes low. With normal lungs the loss is about 10 per cent, but it may be much more than that if there is pulmonary edema. Stewart (130), who was the pioneer in this field, used salt solution as did H. C. Wiggers (145) and White (143). Others have used diffusible dye, thiocyanate (63), and other substances. Diffusible substances are soon lost from the circulation, and recirculation is less of a hazard than it is when intravascular substances are used. Moreover, the determination can be repeated as many times as is desirable with diffusible substances. The fact, however, that the diffusible substance will escape into edematous lungs, even though the edema is too little to be easily detected, strikes a warning that most workers have heeded by using nondiffusible indicators.

The technique of measuring the concentration of indicator in the arterial blood has been a very important factor in the development of the method. As indicated above, Stewart (130) was the first to measure a dilution indicator quantitatively. He set up a length of artery as a part of a Wheatstone bridge so that when the blood in the artery changed its conductivity from the passage of the infused salt solution an alternating current signaled the event in a telephone receiver. On hearing the signal Stewart diverted a part of the arterial stream into a test tube thus sampling the diluted blood. The analysis consisted of diluting a sample of normal blood with the salt solution so that it equaled in conductivity the blood drawn during the sound. This would give the concentration of infused solution per liter of blood and the rate of infusion from which the rate of blood flow could easily be calculated, provided of course that the basic assumptions that no indicator is lost and none recirculated are granted.

Workers coming after Stewart, including Henriques (75, 76), Bock & Buchholz (8), took timed individual samples which were individually analyzed.

The advent of the visual colorimeter made it easy to use dyes and measure their concentration in individual plasma samples. The work done in Louisville, and already referred to, involved the use of separate samples and the visual colorimeter (62) on brilliant vital red, a dye which attaches to plasma albumin and remains intravascular, and which has the further advantage of not staining a patient an unhealthy bluish tint. In fact, patients think themselves much improved as a result of the pink color of their skin from the brilliant vital red "treatment." The blue dye, T-1824, which is similarly attached to plasma albumin, is more commonly used now because it absorbs light maximally at (625 mμ) a spectral region to which oxyhemoglobin is transparent. This property makes it measurable in the presence of hemoglobin (hemolysis in separate plasma samples) using filters or a spectrophotometer, or whole blood in a cuvette (see below).

The fact that 20 to 40 individual timed samples had to be centrifuged, pipetted, and diluted—in some cases with alcohol to eliminate fatty turbidity and adventitious protein bound color—(26), made the method seem tedious to those who had been in the habit of using the direct Fick method. This delayed the clinical use of the method until a less tedious analytical technique had been developed.

This goal has been approached in several ways. Plasma albumin (labeled with I^{131}) and cells (labeled with radioactive phosphorous, iron, or chromium) may be quantitatively injected, and collected as timed serial samples. The analysis of these separate samples can be expedited by the use of automatic serial counters which can be loaded with many samples and will register the radioactivity of successive samples without attention. If the amount of radioactivity injected and the time and activity of the separate samples are known, the indicator dilution curve may be plotted and the blood flow calculated in accordance with the principles described above.

By far the most attractive approach is to induce a change in some property of the flowing stream and arrange for self-recording of that change. Continuous automatic records of changes in conductivity were first made by Gross & Mittermayer (54) in 1926 and later by H. C. Wiggers (145) and H. L. White (143). The technique is very simple but, by the very nature of the determination, the indicator must be diffusible and hence of limited usefulness in clinical conditions.

The ease of measuring temperature with very small probes (thermo junctions, thermistors) has led Fegler (31) to take the very bold step of injecting saline at room temperature in the hope that it would pass through the circulation, gaining heat from the blood only, so that the equilibrium temperature could be used to calculate the dilution volume and hence the flow. This method, known as the thermodilution method, gives continuously recorded curves of temperature change that look surprisingly like those of dilution of a substantive indicator and are said by the author to give correct flows, calculated on the basis of the specific heat of saline, and of blood-saline mixtures—flows which are equal to simultaneous determinations by the Fick method. The allegation that heat is not gained from the tissues of the heart and lungs is bolstered by the fact that a model with air insulation is more effective than one with the air spaces flooded with water. It is argued that blood passing through the lungs is insulated by air and gains a small amount of heat. It also would not be expected to gain much heat from the walls of the heart and great vessels since it is in contact here with a relatively small surface and for a very short time.

The same principle has been modified by Fronek & Ganz (41). They inject the cool saline or dextrose solution from a catheter in an upstream jet which is rapid enough to mix with a full cross section of the blood vessel. A few millimeters downstream from the jet a thermistor is affixed to the catheter to sense the temperature change and draw, by means of a galvanometer, a thermodilution curve. Excellent checks of model experiments, regional blood flow, and cardiac output are reported. This modification of the thermodilution method is said to avoid heat exchange between point of injection and sensing. It also eliminates the exploitation of such important side issues as the circulation times and central volume.

Continuous recording of radioactivity is an approach which has been exploited and bids fair to become more and more useful as the apparatus becomes more refined. Radiation hazard is a question that deserves serious consideration, and radioactive substances with short biological half-life are to be chosen in clinical work. A physical half-life short enough to avoid accumulation of radioactive waste and long enough to use conveniently in the experiment is to be desired. Dangers of repeated injection of radioactive material are not always appreciated.

Continuous recording of the radiation from I^{131}-treated serum albumin was successfully done by MacIntyre and colleagues (93). They drew arterial blood through a small tube coiled around a counting rate meter. The calibration was done by assessing the performance of the counter when the radioactivity became constant (complete mixing with all the blood) and standardizing the relation between radioactivity in drawn blood and that of a dilution of the injected indicator.

The injection of radioactive material into a vein with a counting rate meter placed over the heart recording the concentration of radioactive material passing through the heart gives the "radiocardiogram." This shows an increase in radioactivity as the injection enters the right heart and a second rise as the blood enters the left heart (107). This could be surveyed for circulation times and other landmarks which could be empirically interpreted. Radiocardiograms have been calibrated from the deflection made by the dilution of the indicator in the total blood volume (124) and treated quantitatively so as to calculate the cardiac output though some reservation must be admitted as to the accuracy of the calibration. Curves were presented by Lammerant (86) and used to calculate the cardiac output and the "pulmonary blood volume." Actually, the calculation found the pulmonary blood volume plus one-half that in the heart.

In order to measure the mean time of passage of the indicator through a ventricle it is necessary to be able to visualize the whole curve and make certain calculations from it. Unfortunately, the first part of

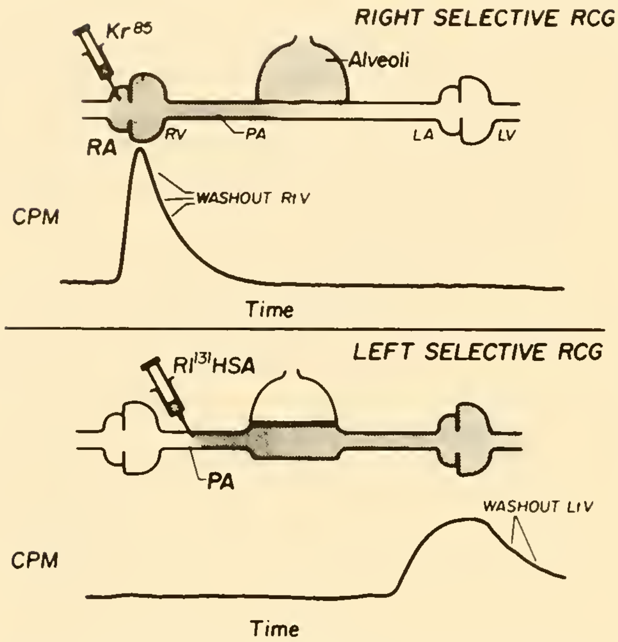

FIG. 19. Selective radiocardiography. Rate of radiation from the right ventricle is measured after injecting radioactive krypton solution into the right atrium and evaluating its passage by means of a collimated rate counter over the precordium. Since it is dissipated in the lungs no measurable amount appears in left ventricular blood. Radioactivity from the left ventricle only is evaluated by injecting a nonvolatile indicator into the pulmonary artery. [From Cournand *et al.* (17).]

the left ventricular curve and the last of the right heart curve in the radiocardiogram are superimposed and hidden. Extrapolating the right heart downslope exponentially and subtracting this from the left heart curve gives two discrete curves which were used (86) in the central blood volume calculation. This is a rather precarious procedure and it is not always possible to find a downslope of the right heart curve which can be extrapolated. This is particularly true in a patient with enlarged heart or pulmonary congestion.

Workers in Cournand's laboratory have surmounted these difficulties (17) by tracing the left heart curve from an injection into the pulmonary artery and thus eliminating the display of radioactivity from the right heart. Also a tracing from the right heart alone was made by injecting into a vein a solution of a radioactive substance which is highly volatile and is hence eliminated by the lungs before arriving at the left heart (see fig. 19). The substance of choice has been radioactive krypton (Kr^{85}).

The most widely used property of blood to make continuous tracings of indicator dilution curves is its optical density as modified by admixture of various injected substances. By means of photoelectric cells these changes are transduced into electric signals which, with or without amplification, actuate recording galvanometers.

On a priori grounds it would seem that the simplest method of influencing the optical density of a flowing stream would be to inject a transparent substance to reduce the optical density of hemoglobin by simple dilution. Experience and calculation, however, show that very large quantities of such fluid (saline, plasma dextran) would have to be injected in order to bring about the change in optical density produced by a few milligrams per liter of T-1824 at the proper wavelength. We have not found that this method has had any practical employment for measuring the cardiac output quantitatively.

The use of a dye as an indicator, the dilution of which is continuously recorded, has given rise to a great deal of fruitful work. One line of attack stems from the development of the oximeter. This instrument was based on the early researches of Matthes (95) and Kramer & Winton (85). It was further developed by Millikan (99) and Wood & Geraci (148). The oximeter is used by Wood (147) not only to measure oxygen saturation but also to inscribe dye dilution curves for measuring the cardiac output and for the diagnosis of cardiac abnormalities (see Chapter 14). The oximeter was designed to measure the blueness and hence the unsaturation of blood. It can also measure the blueness of blood to which blue dye has been added and thus quantitate the dye.

It has two photoelectric cells which are filtered so that one is sensitive to red light (about 625 mμ) and the other sensitive to infrared light (about 800 mμ). The apparatus measures the difference between the transmissions of red and infrared light by the blood sample (37, 149). This dual circuit reduces the effect of fluctuations of light transmission due to changes in the amount of hemoglobin in the light path. Since the blue dye T-1824 absorbs light at wavelength 625 mμ quite strongly, as does reduced hemoglobin, the oximetric deflection is proportional to the amount of the dye just as it is to the amount of reduced hemoglobin. Therefore, it will produce a deflection that is proportional to the amount of blue dye in the light path, provided the hemoglobin is itself completely oxygenated.

Dye dilution curves obtained in this way have been widely used in measuring the output of the heart under varying conditions, and their accuracy seems to be accepted.

A blue dye "Coomassie blue" has been suggested as

having the advantage that it leaves the circulation in 1 hour or so and can therefore be injected in large amounts without staining the patient (132, 133). It is thus possible to use a relatively insensitive pickup so that changes in oxygen saturation do not interfere badly. With this dye it is claimed that results with an ear oximeter are as accurate and reliable as those with a cuvette oximeter.

Simultaneously with the development of the use of the oximeter to record dye dilution curves, the photomultiplier tube was being adapted for the same purpose in Bing's laboratory (39). The circuity was improved independently in Newman's laboratory (103) and in the Walter Reed laboratory (122). These instruments are not set up as differential photometers and hence there is no compensation for changes in the optical density of hemoglobin either as a result of saturation changes, of quantitative differences or as a result of changing red cell orientation resulting from flow. The apparatus is quite bulky and is not conveniently used on the ear or on an unopened artery. Its advantages are its linearity and stability.

Calculation of the blood flow from the concentration of indicator downstream from a site of continuous constant infusion was the original method of Stewart (130). In fact, it is doubtful that Stewart appreciated the possibilities of instantaneous (slug) injection (24) before they were described by Henriques in 1913 (75, 76).

The calculation of the cardiac output from the arterial concentration of a continuously infused indicator demands the establishment of an equilibrium concentration plateau. At first, all the undyed blood must have left the heart and lungs, followed by blood, all of which had been homogeneously mixed with dye. If these conditions obtain before recirculation begins, a usable plateau is evident. Since the continuous infusion curve is the integral of the slug curve the infusion curve can attain a plateau only while the slug curve is maintained at zero concentration (63). This would occur only if the slug is injected into the pulmonary artery. If the infusion is made into the pulmonary artery it is thus possible to find a short plateau. If, on the other hand, an instantaneous injection is made further upstream than the pulmonary artery, dyed blood begins to recirculate before the first circulation is over and the indicator concentration will continue to mount in the arterial blood with no plateau.

There are further handicaps suffered by those who work with a constant infusion. During the build-up of the constant infusion curve there may be, as a result of respiration or of biological instability, an increase in blood flow. This would dilute the constantly infused indicator and give rise to the appearance of a plateau. Such spurious plateaus would not serve for calculating the blood flow but might easily be taken for a useful plateau (78).

Although the height of the plateau and the duration of the mean circulation time can be calculated from the early part of the concentration curve resulting from constant infusion (see Chapter 18), it is difficult and the steps are not self-evident.

It would be very convenient if an indicator could be found which would not recirculate. It has been shown in Cournand's laboratory (15, 117) that a solu-

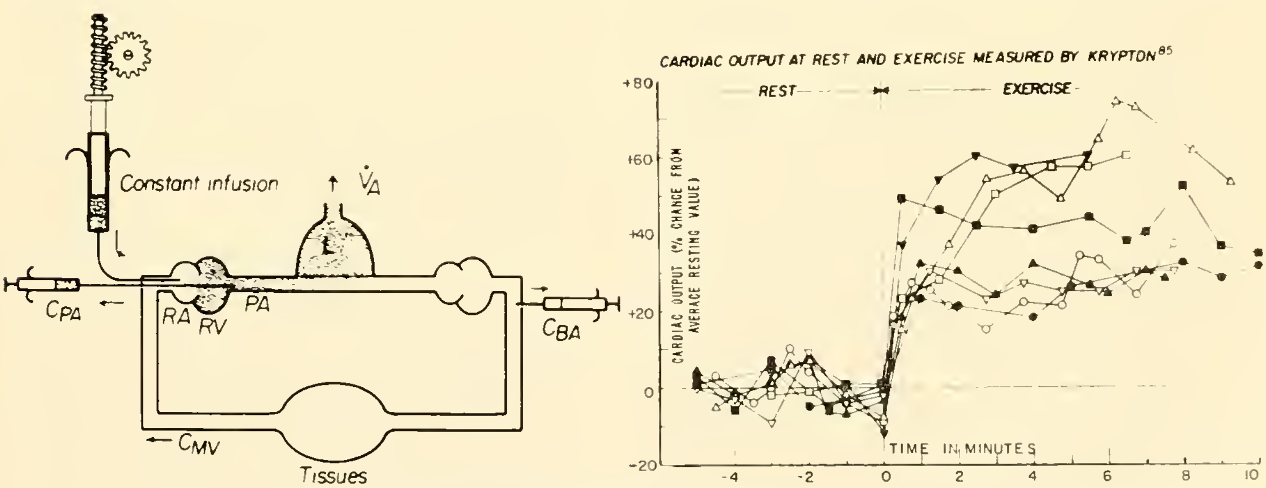

FIG. 20. The constant infusion of a solution of radioactive krypton into the right atrium gives rise to a concentration of Kr^{85} in the pulmonary artery, which can be used to measure the instantaneous cardiac output. [From Rochester *et al.* (117).]

tion of radioactive krypton (Kr^{85}) can be infused into the right atrium or into a vein and, after mixing in the right heart, can be sampled in pulmonary arterial blood. It was shown that this substance appears in low concentration in arterial blood and hence returns to the right heart in small and predictable amounts. The pulmonary arterial flow can therefore be calculated from the concentration of indicator in the pulmonary arterial blood (fig. 20).

A very similar approach has been suggested by Earl Wood's group (36, 37, 48). They had developed, for use in diagnosis of congenital heart disease, a dye which can be accurately measured in both arterial and unoxygenated (venous) blood (35). The dye ("cardio-green") absorbs light at 800 mμ, the part of the spectrum at which both reduced and oxygenated hemoglobin have the same absorption. The dye is measured with the "infrared" cell of the oximeter, but without compensating for changes in hemoglobin opacity. Using this dye it is possible to infuse it into the pulmonary artery, to record continuously by means of a photoelectric cuvette the concentration of the dye in a systemic artery (e.g., radial) and also to record the dye concentration in the mixed venous blood as it returns to the right ventricle. This makes it possible to correct for recirculated dye, taking into account transit time, and to calculate the instantaneous cardiac output.

These two infusion methods which either minimize recirculation or account for it have the advantage that they do not require a steady state in order to be applicable. They differ in this regard from the other dilution methods described above and are important advances.

REFERENCES

1. BADER, H. Über die Bedeutung der Wandmuskulatur für die elastischen Eigenschaften des Aortenwindkessels. *Ztschr. Biol.* 109: 250, 1957.
2. BAKER, D., R. M. ELLIS, D. L. FRANKLIN, AND R. F. RUSHMER. Some engineering aspects of modern cardiac research. *Proc. Inst. Radio Engrs.* 47: 1917, 1959.
3. BARDEEN, C. R. Determination of the size of the heart by means of the X-rays. *Am. J. Anat.* 23: 423, 1918.
4. BAUMANN, H., AND A. GROLLMAN. Über die theoretischen und praktischen Grundlagen und die klinische Zuverlässigkeit der Acetylenmethode zur Bestimmung des Minutenvolumens. *Ztschr. klin. Med.* 115: 41, 1930.
5. BAZETT, H. C. Observations on changes in the blood pressure and blood volume following operations in man. *Proc. Roy. Soc. London, Ser. B* 90: 415, 1919.
6. BAZETT, H. C., F. S. COTTON, L. B. LAPLACE, AND J. C. SCOTT. The calculation of cardiac output and effective peripheral resistance from blood pressure measurements with an appendix on the size of the aorta in man. *Am. J. Physiol.* 113: 312, 1935.
7. BING, R. T., L. D. VANDAM, AND F. D. GRAY, JR. Physiological studies in congenital heart disease. *Bull. Johns Hopkins Hosp.* 80: 107, 1947.
8. BOCK, J., AND J. BUCHHOLTZ. Über das Minutenvolum des Herzens beim Hunde and über den Einfluss des Coffeins auf die Grösse des Minutenvolums. *Arch. exper. Path. u. Pharmakol.* 88: 192, 1920.
9. BRAMWELL, J. C., AND A. V. HILL. The velocity of the pulse wave in man. *Proc. Roy. Soc. London, Ser. B* 93: 298, 1922.
10. BRECHER, G. A. *Venous Return.* New York: Grune & Stratton, 1956.
11. BROEMSER, P., AND O. F. RANKE. Über die Messung des Schlagvolumens des Herzens auf unblutigem Weg. *Ztschr. Biol.* 90: 467, 1930.
12. CANDER, L., AND R. E. FORSTER. Determination of pulmonary parenchymal tissue volume and pulmonary capillary blood flow in man. *J. Appl. Physiol.* 14: 541, 1959.
13. CHAPMAN, C. B., O. BAKER, AND J. H. MITCHELL. Left ventricular function at rest and during exercise. *J. Clin. Invest.* 38: 1202, 1959.
14. CHAPMAN, C. B., O. BAKER, J. REYNOLDS, AND F. J. BONTE. Use of biplane cinefluorography for measurement of ventricular volume. *Circulation* 18: 1105, 1958.
15. CHIDSEY, C. A., H. W. FRITTS, JR., A. HARDEWING, D. W. RICHARDS, AND A. COURNAND. Fate of radioactive krypton (Kr^{85}) introduced intravenously in man. *J. Appl. Physiol.* 14: 63, 1959.
16. COURNAND, A. Some aspects of the pulmonary circulation in normal man and in chronic cardiopulmonary diseases. *Circulation* 2: 641, 1950.
17. COURNAND, A., L. DONATO, J. DURAND, D. F. ROCHESTER, J. O. PARKER, R. M. HARVEY, AND M. L. LEWIS. Separate performance of both ventricles in man during the early phase of exercise as analyzed by the method of selective radiocardiography. *Tr. A. Am. Physicians* 73: 283, 1960.
18. COURNAND, A., AND H. A. RANGES. Catheterization of the right auricle in man. *Proc. Soc. Exper. Biol. & Med.* 46: 462, 1941.
19. COURNAND, A., R. L. RILEY, S. E. BRADLEY, E. S. BREED, R. P. NOBLE, H. D. LAWSON, M. I. GREGERSEN, AND D. W. RICHARDS, JR. Studies of the circulation in clinical shock. *Surgery* 13: 964, 1943.
20. COURNAND, A., R. L. RILEY, E. S. BREED, E. DEF. BALDWIN, AND D. W. RICHARDS, JR. Measurement of cardiac output in man using the technic of catheterization of the right auricle or ventricle. *J. Clin. Invest.* 24: 106, 1945.
21. CRITTENDEN, E. C., JR., AND R. E. SHIPLEY. An electronic recording flowmeter. *Rev. Sci. Instr.* 15: 343, 1944.
22. DEXTER, L., F. W. HAYNES, C. S. BURWELL, E. C. EPPINGER, R. E. SIEBER, AND J. M. EVANS. Studies of

congenital heart disease. Technique of venous catheterization as a diagnostic procedure. *J. Clin. Invest.* 26: 547, 1947.

23. Douglas, C. G., and J. S. Haldane. The regulation of the general circulation rate in man. *J. Physiol.* 56: 69, 1922.
24. Dow, P. Estimations of cardiac output and central blood volume by dye dilution. *Physiol. Rev.* 36: 77, 1956.
25. Dow, P., and W. F. Hamilton. An analysis by hydraulic models of the factors operating to produce the typical ballistocardiogram. *Am. J. Physiol.* 133: 263, 1941.
26. Dow, P., and R. W. Pickering. Behavior of dog serum dyed with brilliant vital red or Evans blue toward precipitation with ethanol. *Am. J. Physiol.* 161: 212, 1950.
27. Doyle, J. T., J. S. Wilson, C. Lepine, and J. V. Warren. An evaluation of the measurement of the cardiac output and of the so-called pulmonary blood volume by the dye dilution method. *J. Lab. & Clin. Med.* 41: 29, 1953.
28. Dubois, A. B., W. O. Fenn, and A. G. Britt. CO_2 dissociation curve of lung tissue. *J. Appl. Physiol.* 5: 13, 1952.
29. Duomarco, J. L., W. H. Dillon, and C. J. Wiggers. Comparison of cardiac output by a direct method and the Hamilton-Remington procedure. *Am. J. Physiol.* 154: 290, 1948.
30. Erlanger, J., and D. R. Hooker. An experimental study of blood pressure and of pulse pressure in man. *Johns Hopkins Hosp. Rept.* 12: 147, 1904.
31. Fegler, G. Measurement of cardiac output in anesthetized animals by a thermo dilution method. *Quart. J. Exper. Physiol.* 39: 153, 1954.
32. Fick, A. Ueber die Messung des Blutquantums in den Herzventrikeln. *Sitzungsb. der phys.-med. Ges. zu Wurzburg:* 1870, 36.
33. Fishman, A. P., J. McClement, A. Himmselstein, and A. Cournand. Effects of acute anoxia on the circulation and respiration in patients with chronic pulmonary disease studied during the "steady state." *J. Clin. Invest.* 31: 770, 1952.
34. Forssmann, W. Die Sondierung des rechten Herzens. *Klin. Wchschr.* 8: 2085, 1929.
35. Fox, I. J., and E. H. Wood. Application of dilution curves recorded from the right side of the heart or venous circulation with the aid of a new indicator dye. *Proc. Staff Meet. Mayo Clin.* 32: 541, 1957.
36. Fox, I. J., and E. H. Wood. Continuous recording of the cardiac output by a constant rate injection dye dilution technique. *Physiologist* 1 (1): 29, 1957.
37. Fox, I. J., and E. H. Wood. Blood flow measurement by dye dilution techniques. In: *Medical Physics*, edited by O. Glasser, Chicago: Yearbook Publishers, 3: 155–163, 1960.
38. Franklin, D. L., R. M. Ellis, and R. F. Rushmer. Aortic blood flow in dogs during treadmill exercise. *J. Appl. Physiol.* 14: 809, 1959.
39. Friedlich, A., R. Heimbecker, and R. J. Bing. A device for continuous recording of concentration of Evans blue dye in whole blood and its application to determination of cardiac output. *J. Appl. Physiol.* 3: 12, 1950.
40. Fritts, H. W., and A. Cournand. The application of the Fick principle to the measurement of pulmonary blood flow. *Proc. Natl. Acad. Sci.* 44: 1079, 1958.
41. Fronek, A., and V. Ganz. Measurement of flow in single blood vessels including cardiac output by local thermodilution. *Circulation Res.* 8: 175, 1960.
42. Fry, D. L. Certain aspects of hydrodynamics as applied to the living cardiovascular system. *Trans. Inst. Radio Engrs. Med. Electronics* ME-6: 252, 1959.
43. Fry, D. L., A. J. Mallos, and A. G. T. Casper. A catheter tip method for measurement of the instantaneous aortic blood velocity. *Circulation Res.* 4: 627, 1956.
44. Fry, D. L., F. W. Noble, and A. J. Mallos. An electric device for instantaneous and continuous computation of aortic blood velocity. *Circulation Res.* 5: 75, 1957.
45. Furst, T., and F. Stobeer. Experimentelle Untersuchungen über die Beziehungen zwischen Füllung und Druck in der Aorta. *Deutsches Arch. klin. Med.* 90: 190, 1906.
46. Gibson, J. G., A. M. Seligman, W. C. Peacock, J. C. Aub, J. Fine, and R. D. Evans. The distribution of red cells and plasma in large and minute vessels of the normal dog, determined by radioactive isotopes of iron and iodine. *J. Clin. Invest.* 25: 848, 1946.
47. Gladstone, S. A. Effect of posture and prolonged rest on the cardiac output and related functions. *Am. J. Physiol.* 114: 705, 1935.
48. Grace, J. B., I. J. Fox, W. P. Crowley, Jr., and E. H. Wood. Thoracic-aorta flow in man. *J. Appl. Physiol.* 11: 405, 1957.
49. Gregg, D. E., and H. D. Green. Registration and interpretation of normal phasic inflow into a left coronary artery by an improved differential manometric method. *Am. J. Physiol.* 130: 114, 1940.
50. Gregg, D. E., W. H. Pritchard, R. W. Eckstein, R. E. Shipley, A. Rotta, J. Dingle, T. W. Steege, and J. T. Wearn. Observations on the accuracy of the thermostromuhr. *Am. J. Physiol.* 136: 250, 1944.
51. Gréhant, H., and C. E. Quinquaud. Recherches expérimentales sur la mesure du volume de sang qui traverse les poumons en un temps donné. *Compt. rend. soc. biol.* 30: 159, 1886.
52. Gribbe, P., L. Hirvonen, J. Lind, and C. Wegelius. Cinecardiographic recordings of the cyclic changes in volume of the left ventricle. *Cardiologia* 34: 348, 1959.
53. Grollman, A. *The Cardiac Output of Man in Health and Disease.* Springfield, Ill.: Thomas, 1932.
54. Gross, R. E., and R. Mittermaer. Untersuchungen über das Minutenvolumen des Herzens. *Arch. ges. Physiol.* 212: 136, 1926.
55. Hales, S. Statical Essays, Haemastaticks. London: 1733, p. 230.
56. Hamilton, W. F. Filling of the normal human heart in relation to the cardiopneumogram and abdominal plethysmogram. *Am. J. Physiol.* 91: 712, 1930.
57. Hamilton, W. F. Notes on the development of the physiology of cardiac output. *Fed. Proc.* 4: 183, 1945.
58. Hamilton, W. F. The physiology of the cardiac output (the Lewis A. Conner Memorial Lecture). *Circulation* 8: 527, 1953.
59. Hamilton, W. F., P. Dow, and J. W. Remington. The relationship between the cardiac ejection curve and the ballistocardiographic forces. *Am. J. Physiol.* 144: 557, 3945.
60. Hamilton, W. F., and E. A. Lombard. Intrathoracic

volume changes in relation to the cardiopneumogram. *Circulation Res.* 1: 76, 1953.

61. Hamilton, W. F., J. W. Moore, and J. M. Kinsman. Delay of blood in passing through the lungs as an obstacle to the determination of the CO_2 tension of the mixed venous blood. *Am. J. Physiol.* 82: 656, 1927.
62. Hamilton, W. F., J. W. Moore, J. M. Kinsman, and R. G. Spurling. Studies on the circulation. IV. Further analysis of the injection method, and of changes in hemodynamics under physiological and pathological conditions. *Am. J. Physiol.* 99: 534, 1932.
63. Hamilton, W. F., and J. W. Remington. Comparison of the time concentration curves in arterial blood of diffusible and non-diffusible substances when injected at a constant rate and when injected instantaneously. *Am. J. Physiol.* 148: 35, 1947.
64. Hamilton, W. F., and J. W. Remington. The measurement of the stroke volume from the pressure pulse. *Am. J. Physiol.* 148: 14, 1947.
65. Hamilton, W. F., J. W. Remington, and P. Dow. The determination of the propagation velocity of the arterial pulse wave. *Am. J. Physiol.* 144: 521, 1945.
66. Hamilton, W. F., R. L. Riley, A. M. Attyah, A. Cournand, D. M. Fowell, A. Himmelstein, R. P. Noble, J. W. Remington, D. W. Richards, Jr., N. C. Wheeler, and A. C. Witham. Comparison of Fick and dye injection methods of measuring cardiac output in man. *Am. J. Physiol.* 153: 309, 1948.
67. Hamilton, W. F., and J. H. Rompf. Movements of the base of the ventricle and the relative constancy of the cardiac volume. *Am. J. Physiol.* 102: 559, 1932.
68. Hamilton, W. F., M. C. Spradlin, and H. G. Saam, Jr. The CO_2 of the mixed venous blood of man. *J. Physiol.* 70: 244, 1930.
69. Hamilton, W. F., M. C. Spradlin, and H. G. Saam, Jr. An inquiry into the basis of the acetylene method of determining the cardiac output. *Am. J. Physiol.* 100: 587, 1932.
70. Hamilton, W. F., Jr., P. Dow, and W. F. Hamilton. Measurement of volume of dog's heart by x-ray: Effect of hemorrhage, of epinephrine infusion, and of buffer nerve section. *Am. J. Physiol.* 161: 466, 1950.
71. Harrison, T. R., C. P. Wilson, and A. Blalock. The effects of changes in hydrogen ion concentration on the blood flow of morphinized dogs. *J. Clin. Invest.* 1: 547, 1925.
72. Harvey, W. *Anatomical Studies on the Motion of the Heart and Blood.* Leake translation. Springfield, Ill.: Thomas, 1931.
73. Henderson, Y. The volume curve of the ventricles of the mammalian heart and the significance of this curve in respect to the mechanics of the heart-beat and the filling of the ventricles. *Am. J. Physiol.* 16: 325, 1906.
74. Henderson, Y., and A. L. Prince. The CO_2 tension of the venous blood and the circulation rate. *J. Biol. Chem.* 32: 325, 1917.
75. Henriques, V. Über die Verteilung des Blutes vom linken Herzen zwischen dem Herzen und dem übrigen Organismus. *Biochem. Ztschr.* 56: 230, 1913.
76. Henriques, V. Untersuchungen über die Verbrennung in den Lungen und einige Bemerkungen über die Bestimmung der Gase des Blutes. *Biochem. Ztschr.* 71: 481, 1915.
77. Herrick, J. F., E. J. Baldes, M. G. Haugen, and W. R. Farrall. Measurement of velocity of blood by means of ultrasound. *Fed. Proc.* 15: 92, 1956.
78. Howard, A. R., W. F. Hamilton, and P. Dow. Limitations of the continuous infusion method for measuring cardiac output by dye dilution. *Am. J. Physiol.* 175: 173, 1953.
79. Johnson, S. E. Roentgen kymography considered in relation to heart output and a new heart index. *Am. J. Roentgenol.* 37: 167, 1937.
80. Klein, O. Zur Bestimmung des zirkulatorischen Minutenvolumen beim Menschen nach den Fickschen Prinzip mittels Herzsondierung. *Deutsches Arch. klin. Med.* 128: 51, 1930.
81. Klensch, H., and W. Eger. Ein neues Verfahren der physikalischen Schlagvolumenbestimmung. *Pflügers Arch. ges. Physiol.* 263: 459, 1956.
82. Kolin, A. An electromagnetic flowmeter. Principle of the method and its application to blood flow measurements. *Proc. Soc. Exper. Biol. & Med.* 35: 53, 1936.
83. Kolin, A. Electromagnetic blood flow meters. *Science* 130: 1088, 1959.
84. Kolin, A., and R. T. Kado. Miniaturization of the electromagnetic blood flowmeter and its use for the recording of circulatory responses of conscious animals to sensory stimuli. *Proc. Natl. Acad. Sci.* 45: 1312, 1959.
85. Kramer, K., and F. R. Winton. The influence of urea and of change in arterial pressure on the oxygen consumption of the isolated kidney of the dog. *J. Physiol.* 96: 87, 1935.
86. Lammerant, J. *Le Volume Sanguin des Poumons chez l'Homme.* Brussels: Editions Arscia, 1957.
87. Lawson, H. C., W. F. Cantrell, J. E. Shaw, D. L. Blackburn, and S. Adams. Measurement of cardiac output in the dog by the simultaneous injection of dye and radioactive red cells. *Am. J. Physiol.* 170: 277, 1954.
88. Lee, G. De J., and A. B. DuBois. Pulmonary capillary blood flow in man. *J. Clin. Invest.* 34: 1380, 1955.
89. Liljestrand, G., and E. Zander. Vergleichende Bestimmungen des Minutevolumens des Herzens beim Menschen mittels der Stickoxydulmethode und durch Blutdruckmessung. *Z. ges. exper. Med.* 59: 105, 1940.
90. Loewy, A., and H. von Schrotter. Ein Verfahren zur Bestimmung der Blutgasspannungen, der Kreislaufgeschwindigkeit und des Herzschlagvolumens am Menschen. *Arch. Anat. Physiol.: Physiol. Abt.* 394, 1903.
91. Longino, F. H., and D. E. Gregg. Comparison of cardiac stroke volume as determined by pressure pulse contour method and by a direct method using a rotameter. *Am. J. Physiol.* 167: 723, 1953.
92. Luciani, L. *Human Physiology.* London: Macmillan vol. I: 1911.
93. MacIntyre, W. J., W. H. Pritchard, R. W. Eckstein, and H. L. Fridell. The determination of the cardiac output by a continuous recording system utilizing iodinated (I^{131}) human serum albumin. I. Animal Studies. *Circulation* 4: 554, 1951.
94. Marshall, E. K., Jr. Studies on the cardiac output of the dog. II. The influence of atropine and carbon dioxide on the circulation of the unanesthetized dog. *J. Pharmacol. & Exper. Therap.* 29: 167, 1926.
95. Matthes, K. Untersuchungen über den Gasaustausch

in der menschlichen Lunge. I. Mitteilung Sauerstoffgehalt und Sauerstoffspannung im Arterienblut und venosen Mischblut des Menschen. *Arch. exper. Path. u. Pharmakol.* 181: 630, 1936.

96. McMichael, J., and E. P. Sharpey-Shafer. Cardiac output in man by a direct Fick method. *Brit. Heart J.* 6: 33, 1944.
97. Meek, W. J., and J. A. E. Eyster. Cardiac size and output in man during rest and moderate exercise. *Am. J. Physiol.* 63: 400, 1923.
98. Mellander, S. Venous blood flow recorded with an isothermal flowmeter. *Fed. Proc.* 17: 394, 1958.
99. Millikan, G. A. An instrument for measuring continuously the oxygen saturation of arterial blood in man. *Rev. Sci. Instr.* 13: 434, 1944.
100. Mitchell, A. M., and A. Cournand. The fate of circulating lactic acid in the human lung. *J. Clin. Invest.* 34: 473, 1955.
101. Mixter, G., Jr. Respiratory augmentation of inferior vena caval flow demonstrated by a low resistance phasic flowmeter. *Am. J. Physiol.* 172: 446, 1953.
102. Moore, J. W., J. M. Kinsman, W. F. Hamilton, and R. G. Spurling. Studies on the circulation. II. Cardiac output determinations. Comparison of the injection method with the direct Fick procedure. *Am. J. Physiol.* 89: 331, 1929.
103. Newman, E. V., M. Merrill, A. Genecin, C. Monge, W. R. Milnor, and W. P. McKeever. The dye dilution method for describing the central circulation. *Circulation* 4: 735, 1951.
104. Nickerson, J. L., and H. J. Curtis. The design of the ballistocardiograph. *Am. J. Physiol.* 142: 1, 1944.
105. Nickerson, J. L. Estimation of the stroke volume by means of the ballistocardiograph. *Am. J. Cardiol.* 4: 644, 3958.
106. Patterson, S. W., H. Piper, and E. H. Starling. The regulation of the heart beat. *J. Physiol.* 48: 465, 1914.
107. Prinzmetal, M., E. Corday, R. J. Spritzler, and W. Fleig. Radiocardiography and its clinical application. *J.A.M.A.* 139: 617, 1949.
108. Remington, J. W. Volume quantitation of the aortic pressure pulse. *Fed. Proc.* 11: 750, 1952.
109. Remington, J. W. The relation between the stroke volume and the pulse pressure. *Minnesota Med.* 37: 105, 1954.
110. Remington, J. W., and W. F. Hamilton. The construction of a theoretical cardiac ejection curve from the contour of the aortic pressure pulse. *Am. J. Physiol.* 144: 546, 1945.
111. Remington, J. W., and W. F. Hamilton. Quantitative calculation of time course of cardiac ejection from the pressure pulse. *Am. J. Physiol.* 145: 25, 1947.
112. Remington, J. W., C. R. Noback, W. F. Hamilton, and J. J. Gold. Volume elasticity characteristics of the human aorta and prediction of the stroke volume from the pressure pulse. *Am. J. Physiol.* 153: 298, 1948.
113. Richards, D. W., Jr. Cardiac output by catheterization technique in various clinical conditions. *Fed. Proc.* 4: 215, 1945.
114. Ring, G. C., M. Balaban, and M. J. Oppenheimer. Measurements of heart output by electrokymography *Am. J. Physiol.* 157: 343, 1949.
115. Ring, G. C., E. M. Greisheimer, H. N. Baier, M. J. Oppenheimer, A. Sokalchuk, D. Ellis, and S. J. Friday. Electrokymograph for estimation of heart output: comparison with direct Fick in dogs. *Am. J. Physiol.* 161: 231, 1950.
116. Ring, G. C., A. Sokalchuk, H. N. Baier, H. Rudel, M. J. Oppenheimer, S. J. Friday, and G. Navis. Electrokymograph for estimation of heart output: comparison with Stewart in dogs. *Am. J. Physiol.* 161: 236, 1950.
117. Rochester, B. F., J. Durand, J. O. Parker, H. W. Fritts, Jr., and R. M. Harvey. Estimation of right ventricular output in man using radioactive krypton (Kr^{85}). *J. Clin. Invest.* In press.
118. Rossi, H. H., S. H. Powers, and B. Dwork. Measurement of flow in straight tubes by means of the dilution technique. *Am. J. Physiol.* 173: 103, 1953.
119. Rushmer, R. F., and N. Thal. Factors influencing stroke volume: a cinefluorographic study of angiocardiography. *Am. J. Physiol.* 168: 509, 1952.
120. Sarnoff, S. J., and E. Berglund. The Potter electroturbinometer. An instrument for recording total systemic blood flow in the dog. *Circulation Res.* 1: 331, 1953.
121. Scarborough, W. R. Current status of ballistocardiographics. *Progr. in Cardiovascular Diseases* 2: 263, 1959.
122. Schadle, O. W., T. B. Ferguson, D. E. Gregg, and S. R. Gilford. Evaluation of a new cuvette densitometer for determination of cardiac output. *Circulation Res.* 1: 200, 1953.
123. Seely, R. D., W. E. Nerlich, and D. E. Gregg. Comparison of cardiac output determined by the Fick procedure and a direct method using the rotameter. *Circulation* 1: 1261, 1950.
124. Shipley, R. A., R. E. Clark, D. Liebowitz, and J. S. Krohmer. Analysis of radiocardiogram in heart failure. *Circulation Res.* 1: 428, 1953.
125. Shirer, H. W., R. B. Shackelford, and K. E. Jochim. A magnetic flowmeter for recording cardiac output. *Proc. Inst. Radio Engrs.* 47: 1901, 1959.
126. Shore, R., J. P. Holt, and P. K. Knoefel. Determination of cardiac output in the dog by the Fick procedure. *Am. J. Physiol.* 143: 709, 1945.
127. Spencer, M. P., and A. B. Denison, Jr. The square-wave electromagnetic flowmeter: theory of operation and design of magnetic probes for clinical and experimental applications. *Trans. Inst. Radio Engrs. Med. Electronics M.E.* 6: 220, 1959.
128. Starr, I., A. J. Rawson, H. A. Schroeder, and N. R. Joseph. Studies on the estimation of cardiac output in man, and of abnormalities in cardiac function, from the heart's recoil and the blood's impacts; the ballistocardiogram. *Am. J. Physiol.* 127: 1, 1939.
129. Stead, E. A., Jr., J. V. Warren, A. J. Merrill, and E. S. Brannon. The cardiac output in male subjects as measured by the technique of right atrial catheterization. Normal values with observations on the effect of anxiety and tilting. *J. Clin. Invest.* 24: 326, 1945.
130. Stewart, G. N. Researches on the circulation time and on the influences which affect it. IV. The output of the heart. *J. Physiol.* 22: 159, 1897.
131. Stow, R. W. Systematic errors in flow determinations by the Fick method. *Minnesota Med.* 37: 30, 1954.
132. Taylor, S. H., and J. M. Thorp. Properties and bio-

logical behavior of Coomassie blue. *Brit. Heart J.* 21: 492, 1959.

133. TAYLOR, S. H., AND J. P. SHILLINGFORD. Clinical application of Coomassie blue. *Brit. Heart J.* 21: 497, 1959.

134. THOMAS, H. D., W. H. FREDERICK, J. L. KNOWLES, T. J. REEVES, R. PAPPAS, AND E. E. EDDLEMAN, JR. The effects of occlusion of the venae cavae, aorta, and pulmonary artery on the dog ballistocardiogram. *Am. Heart J.* 50: 424, 1955.

135. VISSCHER, M. B., AND J. A. JOHNSON. The Fick principle: analysis of potential errors in its conventional application. *J. Appl. Physiol.* 5: 635, 1953.

136. WARNER, H. R., H. J. C. SWAN, D. CONNOLLY, R. G. TOMPKINS, AND E. H. WOOD. Quantitation of beat-to-beat changes in stroke volume from the aortic pulse contour in man. *J. Appl. Physiol.* 5: 495, 1953.

137. WARREN, J. V., E. A. STEAD, JR., AND E. S. BRANNON. The cardiac output in man: a study of some of the errors in the method of right heart catheterization. *Am. J. Physiol.* 145: 458, 1946.

138. WASSERMAN, K., AND J. H. COMROE, JR. New method for estimating pulmonary capillary blood flow in man. *Fed. Proc.* 19: 97, 1960.

139. WERKÖ, L., S. BERSEUS, AND H. LAGERLÖF. A comparison of the direct Fick and the Grollman methods for determination of the cardiac output in man. *J. Clin. Invest.* 28: 516, 1949.

140. WERKÖ, L., H. LAGERLÖF, H. BUCH, B. WEHLE, AND A. HOLMGREN. Comparison of the Fick and Hamilton methods for the determination of the cardiac output in man. *Scandinav. J. Clin. & Lab. Invest.* 1: 109, 1949.

141. WETTERER, E. Eine neue Methode zur Registrierung der Blutströmungsgeschwindigkeit am uneröffneten Gefäss *Ztschr. Biol.* 98: 26, 1937.

142. WEZLER, K., AND A. BÖGER. Über einen neuen Weg zür Bestimmung des absoluten Schlagvolumens des Herzens beim Menschen auf Grund der Windkesseltheorie und eine experimentelle Prüfung. *Arch. Exper. Path. u. Pharmakol.* 184: 484, 1937.

143. WHITE, H. L. Measurement of cardiac output by a continuously recording conductivity method. *Am. J. Physiol.* 151: 45, 1947.

144. WHITTAKER, S. R. F., AND F. R. WINTON. Apparent viscosity of blood flowing in the isolated hind limb of the dog, and its variation with corpuscular concentration. *J. Physiol.* 78: 339, 1933.

145. WIGGERS, H. C. Cardiac output and total peripheral resistance measurements in experimental dogs. *Am. J. Physiol.* 140: 519, 1944.

146. WIGGERS, C. J., AND L. N. KATZ. The contour of the ventricular volume curves under different conditions. *Am. J. Physiol.* 58: 439, 1922.

147. WOOD, E. H. Special instrumentation problems encountered in physiological research concerning the heart and circulation in man. *Science* 112: 717, 1950.

148. WOOD, E. H., AND J. E. GERACI. Photoelectric determination of arterial oxygen saturation in man. *J. Lab. Clin. & Med.* 34: 387, 1949.

149. WOOD, E. H., W. F. SUTTERER, AND L. CRONIN. Oximetry. In: *Medical Physics*, edited by O. Glasser. Chicago: Yr. Bk. Pub., vol. 3, 1960, p. 416.

150. ZUNTZ, N., AND O. HAGEMANN. Untersuchungen über den Stoffwechsel des Pferdes bei Ruhe und Arbeit. *Landwirtschaftliche Jahrb. Z. Wiss. Landwirtschaft* 27 (Ergänzungsband III): 1, 1898.

Circulation times and the theory of indicator-dilution methods for determining blood flow and volume

KENNETH L. ZIERLER | *Department of Medicine, The Johns Hopkins University School of Medicine, Baltimore, Maryland*

CHAPTER CONTENTS

AMONG THE METHODS by which the flow and volume of fluids, particularly blood, are measured are those based on the indicator-dilution principle. An indicator, in the sense used here, is a substance which permits observation of some element of volume of the fluid under study. The indicator shows the position of the element of volume in space and with respect to time, and distinguishes the indicated element from all other elements of volume.

In this chapter we shall develop the fundamental equations which make the indicator-dilution principle useful. We shall examine the assumptions underlying the principle and some effects of violation of these assumptions. We shall then inquire into some applications of the indicator-dilution principle.

MEASUREMENT OF FLOW AND VOLUME IN WELL-DEFINED SYSTEMS

Indicator-dilution methods for measurement of blood flow and volume arose from a century-old technique for measurement of "velocity" of flowing blood within the cardiovascular system, where velocity is defined as distance traversed per unit time in contrast to flow which is volume displaced through some arbitrary reference plane per unit time. In its original application by Hering (14), potassium ferrocyanide was injected intravenously and blood was collected at timed intervals from the corresponding contralateral vein. Hering tested for ferrocyanide by adding ferric chloride to serum. The first sample giving the Prussian blue reaction was, therefore, blood which had made one complete circuit from

vein to heart to pulmonary bed to heart to artery to vein. The time at which this sample of blood was obtained (zero time being the instant of intravenous injection) was called the "circulation time."

The circulation time is the time required for an element of blood to travel some standard distance. Hering did not appreciate the significance of the fact that blood does not circulate with uniform velocity. Nor did he appreciate the significance of the fact that two elements of blood starting simultaneously from the same cross-sectional plane in a jugular vein may, through ramification of the vascular network, take quite different paths of quite different lengths to return to the starting point. The circulation time is therefore a measure of some distance traversed at some velocity. Since neither the distance nor the velocity is known, the circulation time tells nothing about either; it measures only their ratio. If distance happens to be relatively constant (and this the experimenter must demonstrate), then changes in circulation time are exactly the reciprocal of changes in velocity. But what velocity is measured? As Hering, and all who followed, used the indicator principle, the circulation time is measured at the threshold of detection of indicator. It is therefore the briefest time interval, sometimes called the "appearance time." The appearance time is that time required by those particles or elements of volume that traveled the shortest route at the highest speed. If all particles travel the same path, appearance time is a function only of the highest velocity detectable. The distinction is made between the highest velocity in fact and the highest velocity detectable, because many methods used for this purpose have had poor analytical resolving power so that relatively high concentrations of indicator were required for detection. This means that the circulation time is somewhat longer than the appearance time determined by more sensitive techniques.

Two improvements in Hering's technique are noteworthy, not because they were important in advancing theory but because their antiquity may be humbling to contemporary instrumentalists who appear to have been unaware of their origin. "Vierordt arranged a number of cups on a revolving disc below the vein from which blood was to be taken. In these cups samples of the blood were received, and the rate of rotation of the disc being known, it was possible to measure the interval between the injection and appearance of the salt with considerable accuracy. Hermann made a further advance by allowing the blood to play upon a revolving drum covered with paper soaked in ferric chloride." [The quotes are from Stewart (33).]

Stewart (31) improved the method further by the introduction of a new technique which permitted measurement of circulation time through organs. A solution of sodium chloride was introduced into a blood vessel supplying an organ. A vessel draining the organ was isolated and placed over two electrodes so that the blood vessel formed one arm of a Wheatstone bridge. The galvanometer of the bridge was replaced by a telephone and the bridge balanced to yield minimum noise. When blood, diluted by the injectate, reached the outflow vessel the bridge was unbalanced, an event signaled by the howl of the telephone. The time elapsed between injection and howl was the organ circulation time. For vessels too small to be manipulated over Stewart's electrodes, he substituted for NaCl methylene blue "which at first overpowers the colour of the blood and shows through the walls of the blood vessels" (33).

For a more detailed historical background see the review by Dow (7).

Measurement of Flow

It was undoubtedly Stewart's experience with measurement of circulation time which led him to refine the method so that it would yield a measure of blood flow. Stewart (32, 34, 35) allowed a NaCl solution of known composition to run for a known number of seconds through a tube passed into a dog's left ventricle from a carotid artery. A sample of the mixture of blood and salt solution was collected from a femoral artery where its arrival was detected by the telephone howl which signaled a change in electrical resistance. To a blood blank (that is, a sample of blood obtained before injection of NaCl), NaCl solution was added until its conductivity matched that of the arterial sample. This, in effect, was a determination of the concentration of indicator in the arterial sample. The amount of indicator in the injectate and its rate of injection were known. The final concentration of indicator in blood (or, as Stewart viewed it, of blood in indicator) was achieved because the injectate was diluted by the cardiac output, that is, the amount, q, of indicator injected over time, s, was carried downstream at a rate which was the product of the cardiac output, F, with which indicator was mixed, and the ultimate concentration of indicator, c, or

$$q/s = F \times c \tag{1}$$

from which the cardiac output was calculated.

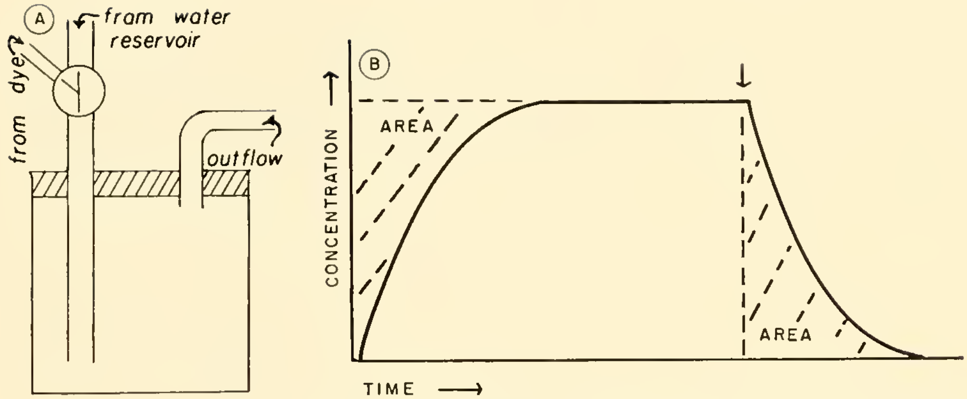

FIG. 1. *A:* principle of measurement of flow and volume by constant-injection. Water-filled beaker through which water flows at constant rate, F ml/min; into which dye is injected at constant rate, I mg/min. Outflow of dye is $F\ C$, where C is concentration of dye, milligram per milliliter. Eventually dye is distributed uniformly throughout beaker and when this occurs, despite continued injection of dye, concentration throughout beaker is constant at C_{max}. Whence inflow, I, = outflow, $F\ C_{max}$. Dye in the beaker at the time C_{max} is just reached is $C_{max} \times V$, volume of the system between site of dye injection and outflow, and this amount of dye is difference between input and output up to the time C_{max} is reached. *B:* concentration of dye at outflow as a function of time during constant-injection and subsequently. Shaded area, when multiplied by flow, F, is quantity of dye remaining in system at concentration C_{max}, and so measures volume. Plateau concentration is I/F. [From Zierler (38).]

Stewart's method was not used widely until Hamilton and his colleagues, after a lapse of several decades, systematically improved the technique, explored its possibilities, and popularized it (11, 12, 20). Hamilton used a dye which, on introduction into the blood stream, bound to serum proteins, chiefly albumin, and therefore passed out of the vascular system through capillary walls only to a negligible extent during the time over which blood flow was measured.

Over the years two forms of injection have been used, both by Stewart and by Hamilton. In one, indicator is injected very rapidly into the blood stream, so that the distribution of injection with time is simply a spike, under ideal circumstances. This will be referred to as "sudden-injection." In the other, indicator is injected continuously at constant rate. This will be referred to as "constant-injection." There are, of course, many other possible variations but only a few have been used and these to no great extent.

The principle by which sudden- and constant-injections of indicator lead to a measure of flow is simple. The arguments developed in this section and in the following section on measurement of volume follow those offered by Meier & Zierler (19) and by Zierler (38). A very similar approach is given by van der Feer (37) and by Burger and colleagues (3).

Consider first the case of constant-injection (fig. 1). Inject indicator at constant rate, I mg per min, into a system of fixed volume through which fluid flows at constant but unknown rate, F ml per min. It is obvious intuitively that after awhile the system will hold all the indicator it is going to contain, if there is no recirculation, and the rate at which indicator leaves the system will exactly equal the rate at which it is introduced into the system. The rate at which it leaves the system is the product of the measurable concentration of indicator at the outflow from the system and the unknown flow of fluid, or

$$I = F \times C_{max} \qquad (2)$$

where C_{max} is the concentration at outflow. It is called C_{max} because it is the maximum and constant (because I and F are constant) concentration at outflow. There will be from onset of injection an initial transient during which, in sequence, no indicator appears at outflow, the first measurable quantity of indicator appears, the concentration of indicator at outflow increases, in a way which we need not yet specify, until indicator is distributed uniformly throughout the system and its output equals its input.

Similarly, an intuitive argument for the case of flow measurement by sudden-injection can be made as follows (fig. 2). Indicator injected suddenly into a fluid system appears at the outflow from the system in a concentration which is some curvilinear function of time, $c(t)$. The rate at which indicator leaves the

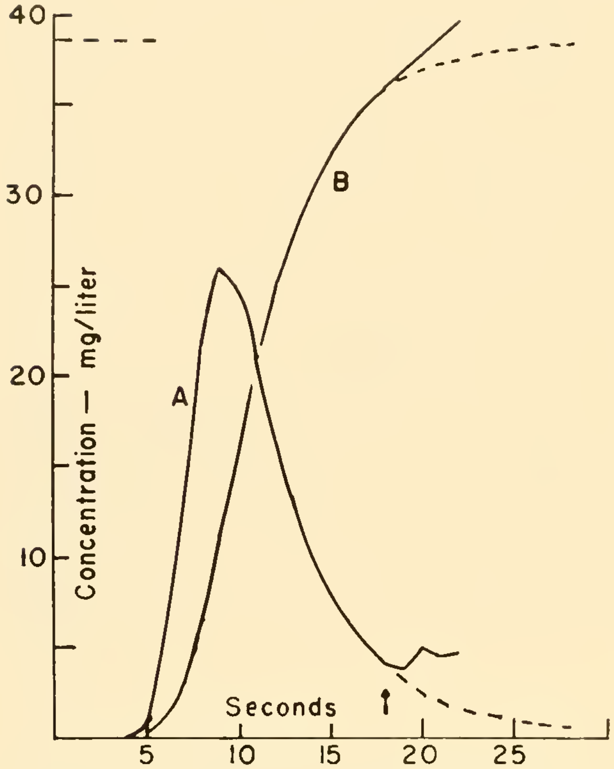

FIG. 2. *A:* concentration of indicator as function of time after sudden-injection into systemic vein, sampling from systemic artery. Recirculation of indicator begins at arrow and dashed line is extrapolation of concentration during first circulation. *B:* concentration of indicator as function of time during constant injection through same bed as *A*, to show that *B* is integral of *A* (scale factor used on concentration axis) and that recirculation is evident at same time in *B* as in *A*. Dashed line is extrapolation to plateau concentration. [From Meier & Zierler (19).]

system at any moment, *s*, is the product of its concentration at that moment, $c(s)$, and the unknown flow, *F*. Eventually the entire mass, *q*, of injected indicator must leave the system. If all products of $c(s)$ and F are summed, this sum must equal the amount of injected indicator, or,

$$q = F \int_0^\infty c(t)\, dt \tag{3}$$

F, the unknown flow, can therefore be measured from either equation 2 or 3, using constant- or sudden-injection, whichever is appropriate. Since both methods measure the same flow, combining equations 2 and 3 yields

$$q/I = \left(\int_0^\infty c(t)\, dt\right) \Big/ C_{\max} \tag{4}$$

If the magnitudes of q and I are chosen so that $q/I =$

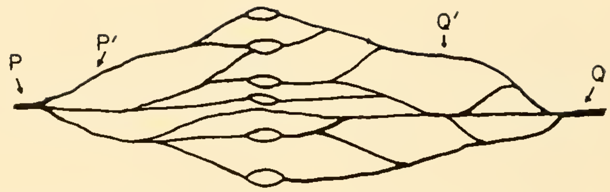

FIG. 3. Schema of vascular bed with injection sites *P*, *P′* and sampling sites *Q*, *Q′*. [From Meier & Zierler (19).]

1, $C_{\max} = \int_0^\infty c(t)\, dt$. Hamilton & Remington (13) first pointed out that constant-injection could be considered an integral of sudden-injection and that $C_{\max}$ must therefore be the integral of the concentration-time curve obtained by single injection, a point to which we shall return later.

Measurement of Volume

Measurement of flow is unequivocal, if there is no recirculation, by either sudden- or constant-injection of indicator. There has been, however, some dispute over the measurement of volume by indicator-dilution methods. We shall develop a rigorous demonstration of the relation between the volume of a system and the concentration of indicator as a function of time at the output from the system.

First consider a "closed" flow system, that is, one with a single inflow orifice, *P*, and a single outflow orifice, *Q* (fig. 3). The system contains a volume, *V*, of fluid which flows into and out of it at constant flow, *F*, in units of volume per time. The internal structure may be that of a vascular net, consisting of many branches and interlacing of vessels, but the internal structure need not be specified and the argument which follows is independent of any assumptions concerning structure. Consider that the fluid can be treated as though it were made up of many individual particles. Particles of fluid entering *P* at the same time require varying amounts of time to reach *Q*, the time required for any particle depending on the path taken and the velocity with which the particle travels. The fluid, therefore, does not have a single traversal time from *P* to *Q* but rather a distribution of traversal times. It is unnecessary to make any assumptions about the relative proportion of particles having long or short traversal times. The distribution of traversal times is determined solely by the experiment and is not part of the theoretical structure.

Several restrictions on the system must be made. *a*) The distribution of traversal times for entering particles does not change with time. Particles entering *P* at any time are dispersed when they leave at *Q*

in exactly the same manner as particles entering P at any other time. This property is called "stationarity" of flow. *b)* Flow is constant. *c)* Volume is constant. *d)* There are no stagnant pools. Fluid anywhere in the system eventually moves out of the system. (This assumption is needed only for measurement of volume; flow can be measured even if there are stagnant pools.) *e)* Flow of indicator particles is representative of the flow of total fluid, that is, the distribution of traversal times for indicator particles is the same as for fluid particles. *f)* Indicator does not recirculate. Each indicator particle, as it leaves at Q, is counted once and only once.

Indicator is injected at P. Assumption *e* demands that indicator and fluid mix completely at P. This means, for example, that for the case of constant-injection at rate I, the concentration of indicator at P is I/F. The concentration of indicator is measured at Q as a function of time.

Consider first the case of sudden-injection. Let q units of indicator be injected at P at time zero and let its concentration at Q be $c(t)$. The amount of indicator leaving the system during a small time interval, t to $t + dt$, is the concentration of indicator at Q, $c(t)$, multiplied by the volume of fluid leaving the system during this time interval, $F\,dt$. We have already seen that since all the indicator must leave the system, q equals the sum of the amounts leaving the system during all such time intervals, or

$$q = \int_0^\infty c(t)\,(F\,dt) = F\int_0^\infty c(t)\,dt \tag{3}$$

whence

$$F = \frac{q}{\int_0^\infty c(t)\,dt} \tag{5}$$

We now introduce the function

$$h(t) = \frac{F\,c(t)}{q} \tag{6}$$

Since $F\,c(t)$ is the rate at which indicator leaves the system at time t, $h(t)$ is the fraction of injected indicator leaving the system per unit time at time t; $h(t)$ is the function which describes the distribution of traversal times. It is therefore a frequency function which may be illustrated as follows:

Suppose that 12 indicator particles are introduced into the system at P at time zero. Let 2 of the 12 particles require 3 sec to travel from P to Q; 4 particles, 4 sec.; 3 particles, 5 sec.; 2 particles, 6 sec; and 1 particle, 7 sec. The frequency with which one finds particles of the kind that require 3 sec to traverse the system is thus 2/12. The frequency with which one finds particles of the kind that require 4 sec to traverse the system is 4/12, and so on. A plot of the frequency (with which each traversal time is found) against traversal time describes a frequency function, shown in figure 4.

When the concentration of indicator at Q is plotted against time, since from equation 6 $c(t) = q\,h(t)/F$, it can be considered that one is in fact plotting the frequency function of traversal times, $h(t)$, multiplied by the constant q/F. Assumption *e* states that the distribution of traversal times for indicator is the same as the distribution of traversal times for fluid particles, that is, $h(t)$ for indicator particles is the same $h(t)$ for fluid particles. Thus, from the observed plot of $c(t)$ of indicator particles versus time, one has really determined $h(t)$ for fluid particles. This fact is illustrated in figure 5.

Returning to figure 4, the sum of all frequencies, $2/12 + 4/12 + 3/12 + 2/12 + 1/12$, is 1. In terms of $h(t)$, since all fluid entering at time zero must eventually leave the system,

$$\int_0^\infty h(t)\,dt = 1 \tag{7}$$

or the area under the curve, $h(t)$ vs. t, is 1.

Combining equations 3 and 6,

$$h(t) = \frac{c(t)}{\int_0^\infty c(t)\,dt} \tag{8}$$

Thus, to determine $h(t)$ for fluid particles, each experimentally observed $c(t)$ is divided by the area under the curve $c(t)$ versus t.

To find the volume of fluid present in the system at time zero, consider that the particles of fluid which compose the volume can be distinguished by their traversal times. An element of volume, dV, is therefore made up of all those particles which, initially present at time zero, have traversal times between t and $t + dt$. The fraction of particles which require times between t and $t + dt$ to leave is $h(t)\,dt$. Some of these particles have just entered the system at time zero. Others entered the system t units before time zero and are therefore just ready to leave the system at time zero. The rest of the particles making up dV entered the system during all times between zero and t units before zero.

The rate at which all fluid particles enter the system

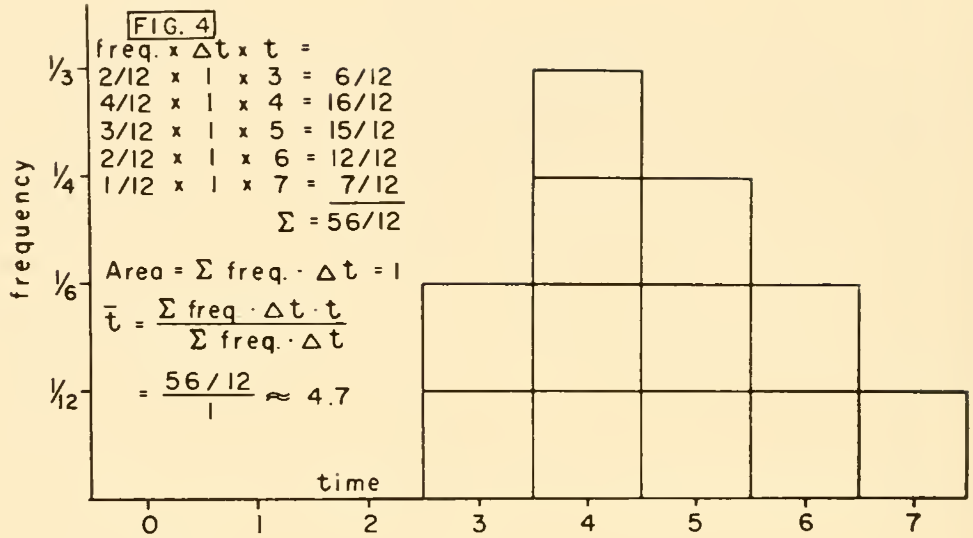

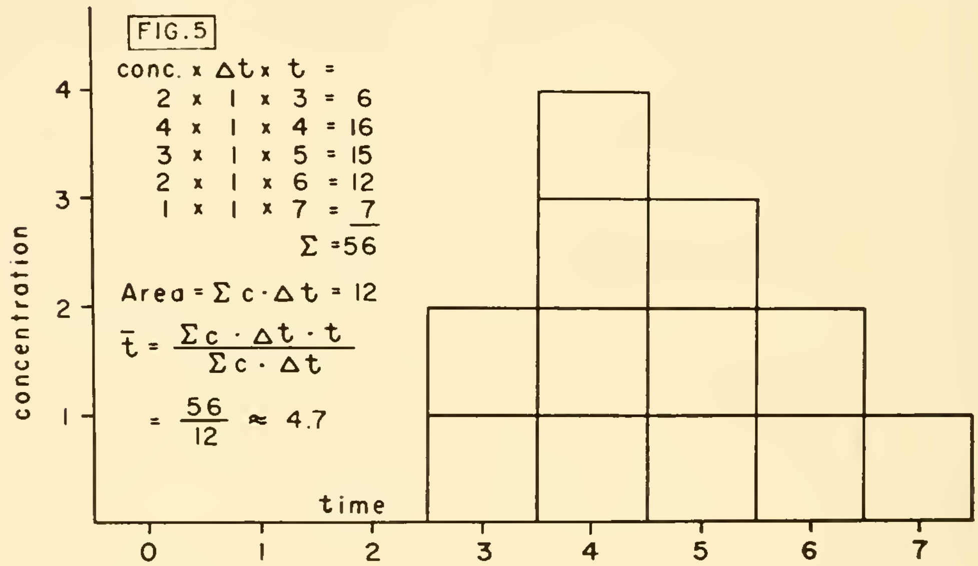

FIG. 4. A frequency histogram of times. [From Zierler (38).]

FIG. 5. Variation of concentration of indicator with time plotted as a frequency histogram. Distribution of transit times same as in fig. 4. [From Zierler (38).]

and leave it is F. The rate at which the particles making up dV leave the system is therefore $F\, h(t)\, dt$. Some of these particles leave at time zero, and particles of this traversal time continue to leave the system until time t, at which instant all such particles will have been eliminated.

The volume of such particles, dV, is the time required for them to leave, t, multiplied by the rate at which they leave, $F\, h(t)\, dt$, or $dV = t\, F\, h(t)\, dt = F\, t\, h(t)\, dt$.

To find the volume of the system, simply add up all elements dV, or

$$V = F \int_0^\infty t\, h(t)\, dt \tag{9}$$

Since $h(t)$ is the frequency function of traversal times, $\int_0^\infty t\, h(t)\, dt$ is the mean of traversal times, or the mean transit time or mean circulation time, denoted by $\bar{t}$. Therefore,

$$V = F\bar{t} \tag{10}$$

which states the fundamental fact that volume = flow multiplied by mean transit time.

Those indicator particles requiring times between t and $t + dt$ to leave the system can be regarded as pushing out ahead of them all fluid particles characterized by the same traversal time. Thus, when indicator appears at Q, all fluid particles $t\, F\, h(t)\, dt$ have left the system. In terms of the observed con-

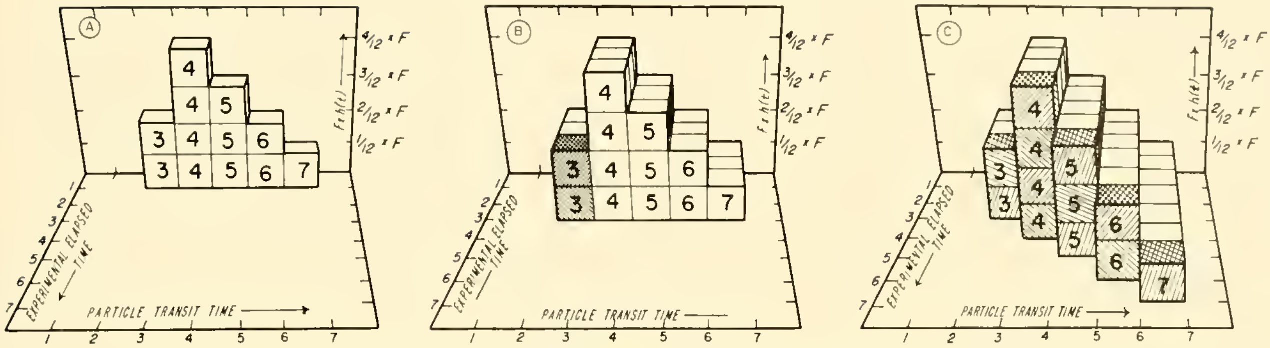

FIG. 6. Series of 3-dimensional drawings to illustrate that experimental elapsed time is identical with indicator transit time and that $V = F\bar{t}$. *A:* distribution of transit times through system (same distribution as fig. 4). Total flow during first time unit following injection of indicator. White cubes in this and subsequent drawings are untagged particles. Number on face of each cube indicates its transit time. *B:* total flow during first three time units following injection of indicator. Fastest indicator particles (shaded cubes) have just appeared. *C:* by the end of the seventh time unit all indicator particles have pushed out of the system all untagged particles of the same transit time. The total number of cubes is therefore the volume of the system. Height of each column (of cubes of the same transit time) is $F\,h(t)$, length is t, and width is dt. Volume of each column is therefore $F\,t\,h\,(t)dt$. Sum of volumes of all columns is total volume of system, $F \sum t\,h(t)\,dt$. [From Zierler (38).]

centration of indicator, from equation 8, since $h(t) = c(t)/\int_0^\infty c(t)\,dt$,

$$dV = F\,t\,h(t)\,dt = \frac{F\,t\,c(t)\,dt}{\displaystyle\int_0^\infty c(t)\,dt}$$

Summing for all such time intervals

$$V = F\,\frac{\displaystyle\int_0^\infty t\,c(t)\,dt}{\displaystyle\int_0^\infty c(t)\,dt} \tag{11}$$

where

$$\int_0^\infty t\,c(t)\,dt \Big/ \int_0^\infty c(t)\,dt = \bar{t}$$

It is important to remember that the derivation of equations 9, 10, and 11, which describe the relationship between volume, flow, and mean transit time, requires no assumptions about the form of $h(t)$ which is determined solely experimentally by the observed curve of $c(t)$ versus time. Development of the relation between mean transit time and volume is illustrated in figure 6.

There has been some misunderstanding of the definition of mean transit time. Hamilton *et al.* (10) originally and incorrectly defined the mean time as that time which divided in half the area under the concentration-time curve following sudden-injection. This, of course, is the "median" time and differs from the mean time in all but symmetrical curves. Hamilton *et al.* (12) soon corrected the error but it appeared persistently in the works of some others for more than a decade.

$\bar{t} = \int_0^\infty t\,h(t)\,dt$ is literally the mean or average value of t. This formula for the mean is not familiar to many biologists who are more accustomed to seeing it expressed as $(\sum_{i=0}^{n} t_i)/N$, where N is the total number of observations of t. The identity of the two expressions for $\bar{t}$ may be illustrated by considering a population of t in which the value t_0 appears a_0 times, the value t_1 appears a_1 times, and so on. Clearly, $\bar{t} = (a_0t_0 + a_1t_1 + \cdots + a_nt_n)/(a_0 + a_1 + \cdots + a_n) = (a_0t_0 + a_1t_1 + \cdots + a_nt_n)/N = t_0(a_0/N) + t_1(a_1/N) + \cdots + t_n(a_n/N) = \sum_{j=0}^{n} t_j(a_j/N)$. a_j/N is exactly the frequency with which the time t_j occurs, that is, it is the fraction of the total observations which includes t_j. It is therefore equivalent to $h(t)\,dt$.

In hydraulic engineering the volume of water in conduits has been measured by an indicator dilution method known as Allen's method (1), although Allen acknowledged his indebtedness to Stewart. Like Stewart, Allen added salt to the flowing system and measured the change in conductivity at some distant point. However, it was intrinsic in the conduit system that the appearance time was long and dispersion of the saline indicator was small so that no great error was introduced by using any time during the arrival of salt at the sampling site. Allen, in fact, tested the appearance time, the time at which peak concentration occurred and the mean time in the equation volume = flow × time, and found that the mean time

did not yield a solution for volume which agreed best with the known volume of his test system. Empirically, Allen chose the time at which peak concentration appeared. Since the mean time is the only time which is formally correct, Allen's result must be attributed to experimental error in either his independent measure of flow or volume, or in his measure of time. It may have been caused by dispersion of indicator at the site of introduction because, as will be shown later, this leads to an overestimate of mean transit time.

We turn now to consideration of measurement of volume by constant-injection of indicator. Indicator is introduced into the system at P (fig. 3), at constant rate, I, in units of mass·time^{-1}. Assumption e (page 589) again demands that indicator and fluid mix completely at P. Therefore, the concentration of indicator at P is I/F, where F is flow in units of volume·time^{-1}.

We have already seen that the concentration of indicator at the outflow, $C(t)$, increases with time to a maximum, C_{max}, which equals I/F (equation 2). This is so because indicator particles, entering the system at concentration I/F, gradually displace all indicator-free elements until every element of volume within the system contains indicator at concentration I/F. When the concentration at outflow finally reaches I/F, the concentration of indicator throughout the volume, V, must also be I/F. This means that there is within the system a mass of indicator, M, distributed over V at concentration I/F, or

$$M/V = I/F \tag{12}$$

Since I is known and F is calculated from equation 2, $I/F = C_{max}$, if M can be determined we have a solution for V. M is determined as follows:

The amount of indicator in the system at any time, t, is

$$\begin{aligned} M(t) &= (\text{input up to time } t) - (\text{output up to time } t) \\ &= It - \int_0^t F\,C(t)\,dt \\ &= \int_0^t [I - F\,C(t)]\,dt \\ &= F\int_0^t \left[\frac{I}{F} - C(t)\right] dt \\ &= F\int_0^t [C_{max} - C(t)]\,dt \end{aligned} \tag{13}$$

The concentration of indicator within the system at any time, t, is

$$\frac{M(t)}{V} = \frac{F}{V}\int_0^t [C_{max} - C(t)]\,dt \tag{14}$$

The limit of this concentration, as we have seen, is $C_{max} = I/F$. Therefore

$$\lim_{t\to\infty} \frac{M(t)}{V} = \frac{F}{V}\int_0^\infty [C_{max} - C(t)]\,dt = C_{max}$$

Whence,

$$V = \frac{F}{C_{max}}\int_0^\infty [C_{max} - C(t)]\,dt \tag{15}$$

$\int_0^\infty [C_{max} - C(t)]\,dt$ is the area between the line C_{max} and the curve $C(t)$, that is, the area above the concentration-time curve for constant-injection up to the line C_{max} extended back to zero time.

Relationship Between Equations for Sudden- and Constant-Injection

Equation 10 stated that for the case of sudden-injection, volume = flow × $\bar{t}$. Equation 15, developed for the case of constant-injection, states that volume = flow × $(1/C_{max}) \int_0^\infty [C_{max} - C(t)]\,dt$. Since we are dealing with the same volume and flow whether indicator is injected suddenly or constantly, it must be true that $(1/C_{max}) \int_0^\infty [C_{max} - C(t)]\,dt$ is also the mean transit time, but the identity is not obvious. To prove it we proceed as follows.

We introduce the function $H(t)$, which is the integral of $h(t)$, the distribution function.

$$H(t) = \int_0^t h(s)\,ds \tag{16}$$

We must now relate the cumulative distribution function, $H(t)$, to the observed concentration at outflow, $C(t)$.

When indicator is introduced at the inflow at constant rate, I, the concentration of indicator at outflow, $C(t)$, is determined by I and F and by the frequency function of traversal times, $h(t)$. Consider the contribution to the rate at which indicator leaves the system at time t made by indicator introduced into the system during the time interval occurring between s and $s + ds$ time units before t. The amount of indicator introduced during this time interval is $I\,ds$.

Recall that $h(t)$ was defined in equation 6 as the fraction of injected indicator (for sudden-injection) leaving the system per unit time at time t. But, be-

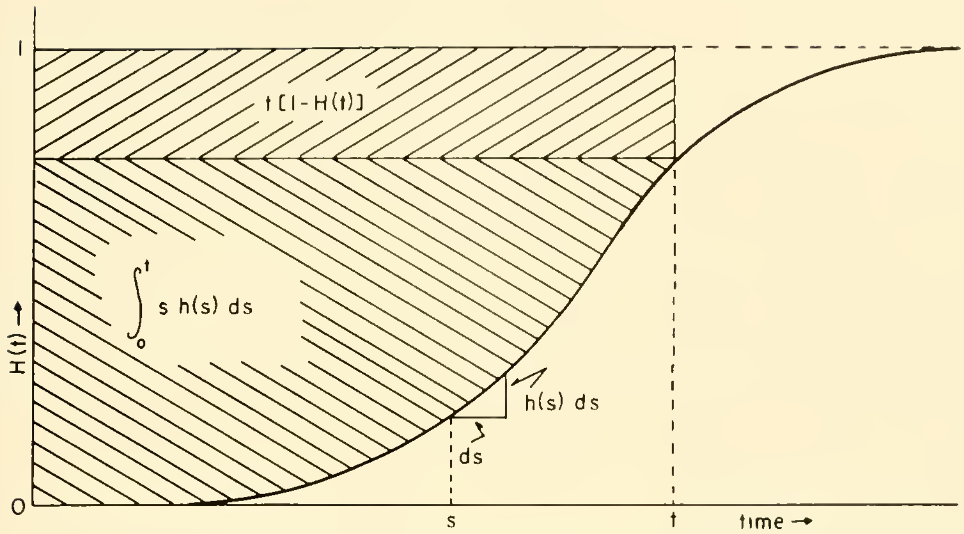

FIG. 7. Graphic representation of fact that $\int_0^\infty [1 - H(t)]\, dt$ is mean transit time. $\int_0^t [1 - H(s)]\, ds$ is sum of the two shaded areas, of which $\int_0^t s\, h(s)\, ds$ is the lower. For the limit of the lower area to remain finite as $t \rightarrow \infty$, the area of the upper rectangle must approach zero, which it does. [From Meier & Zierler (19).]

cause, from assumption e, the distribution of traversal times for indicator particles is the same as for fluid particles, of those fluid particles which entered the system at time zero, the fraction leaving per unit time is $h(t)$. Of the indicator introduced during the interval between s and $s + ds$ time units before t, that is, in the vicinity of time $t - s$, the fraction eliminated per unit time at time t is $h(s)$. Therefore, of the indicator, $I\, ds$, introduced between s and $s + ds$ time units before t, the amount leaving per unit time at time t is $h(s) \cdot I\, ds$.

Summing for all such time intervals before t, the rate at which indicator leaves at t is $\int_0^t I\, h(s)\, ds$. But the rate at which indicator leaves the system is also $F\, C(t)$. Therefore

$$C(t) = \frac{I}{F} \int_0^t h(s)\, ds \tag{17}$$

Combining equations 16 and 17,

$$C(t) = \frac{I}{F}\, H(t) \tag{18}$$

or

$$H(t) = C(t)/C_{\max} \tag{19}$$

Incidentally, since $\int_0^\infty h(s)\, ds = 1$, $\lim_{t\to\infty} H(t) = 1$. Therefore, as t becomes large, $C(t)$ approaches I/F.

Substituting $H(t)$ for $C(t)/C_{\max}$ in equation 15,

$$V = F \int_0^\infty [1 - H(t)]\, dt \tag{20}$$

We must now prove the identity of $\int_0^\infty [1 - H(t)]\, dt$ with $\bar{t} = \int_0^\infty t\, h(t)\, dt$. This is seen by an integration by parts:

$$\int_0^t [1 - H(s)]\, ds = t[1 - H(t)] + \int_0^t s\, h(s)\, ds$$

or

$$\int_0^\infty [1 - H(s)]\, ds = \lim_{t\to\infty} t\, [1 - H(t)] + \int_0^\infty s\, h(s)\, ds$$

Figure 7 illustrates the graphic meaning of the parts of the integral. It is evident from figure 7 that the integrals must both be finite or both infinite (which would yield infinite volume) and that for the case of finite integrals $\lim_{t\to\infty} t\, [1 - H(t)] = 0$. Because the volume must be finite,

$$\int_0^\infty [1 - H(s)]\, ds = \int_0^\infty s\, h(s)\, ds = \bar{t} \tag{21}$$

Since the derivation of equation 15, from simple consideration of input-output relations, is independent of equation 10, the identity shown in equation 21 is an independent demonstration of the basic relationship, volume = flow multiplied by mean transit time.

From equations 6 and 17,

$$C(t) = \frac{I}{F} \int_0^t \frac{F}{q}\, c(s)\, ds = \frac{I}{q} \int_0^t c(s)\, ds \tag{22}$$

and

$$\frac{d\,C(t)}{dt} = \frac{I}{q}\,c(t) \tag{23}$$

Equations 22 and 23 emphasize that the concentration at outflow during constant-injection, $C(t)$, is a constant, I/q, multiplied by the concentration at outflow following sudden-injection, $c(t)$. This means that the time course of the concentration curve following sudden-injection coincides with the time course of the transient or rising phase of the concentration curve during constant-injection. When no indicator appears at the outflow site, both concentrations are zero. The instant some indicator appears so that $c(t)$ just assumes a non-zero value, $C(t)$ also just assumes a non-zero value, that is, appearance time is the same for both. When $c(t)$ reaches its maximum value, i.e., when its first derivative is zero, $C(t)$ will simultaneously have a flex point. When $c(t)$ returns to zero, $d\,C(t)/dt$ becomes zero and $C(t)$ reaches its maximum, or plateau, value, $C_{\max}$. Irregularities in one curve, say $c(t)$, will appear as simultaneous irregularities in the other. For example, when recirculation is apparent in $c(t)$ it will also be apparent in $C(t)$. Manipulation of one curve, for example, in an effort to exclude the effect of recirculation, is as simple or as difficult for the other curve. The choice between sudden- and constant-injection techniques, therefore, lies not in the formal treatment of the data but in the individual experiment.

EFFECTS OF VIOLATION OF THE ASSUMPTIONS: RELATION OF THE MODEL TO REAL VASCULAR SYSTEMS

The System Is not Closed

The stipulation, from which the equations were derived, that the system be closed, that is, that it have a single input and single output, may not often be met in real vascular systems. Let us return to consideration of the vascular net illustrated in figure 3. A single artery, P, divides into a number of branches, one of which is P'. There is also a confluence of venous channels, one of which is Q'. Ultimately all venous effluent passes through Q. We have so far examined only the case of injection at P and sampling at Q.

Supposing there are many inputs and but one output. This is the case of injection at P' and sampling at Q. Because all the indicator must exit at Q, the equations developed for measurement of flow are still valid. However, the volume measured by the closed-system equations includes some portion of other input channels. From the argument leading to equation 10, $V = F\,\bar{t}$, it follows that one is required to find sites P'', P''', and so on along all input channels such that the mean transit time from P'' to Q, from P''' to Q, and so on, is exactly the same as that observed from P' to Q. The volume of the system defined by $F\,\bar{t}$ therefore begins at P', P'', etc. The proof is straightforward.

Let the flow past site P' be f_1, past P'' be f_2 and so on. Then there is a volume, beginning at P', $v_1 = f_1\,\bar{t}$, and there is a volume, beginning at P'', $v_2 = f_2\,\bar{t}$, and so on. Summing these volumes to find the total volume,

$$V = v_1 + v_2 + \cdots + v_n = f_1\,\bar{t} + f_2\,\bar{t} + \cdots + f_n\,\bar{t} = F\,\bar{t}$$

Now consider the case of a single input and many outputs. In figure 3 this is illustrated by injection at P and sampling at Q'. The equations developed for flow again hold and equation 10 is also valid. The volume includes a portion of each output channel up to that site at which the mean transit time is the same as that determined for the sampling site actually used.

In the cases $P \rightarrow Q$, $P' \rightarrow Q$, and $P \rightarrow Q'$, the total flow passes either entrance or exit sampling site or both. Because indicator must in any of these cases mix ultimately with the total flow, the total flow can be determined. For constant injection, the limiting concentration $C_{\max}$ will always be I/F, no matter where the mixing of I and F occurs, and so flow can be measured. This is true also for the case of injection at P' and sampling at Q' (many inputs and many outputs) providing there is at least one channel inside the system through which all flow must pass and in which mixing occurs. This is the case in systems which include the normal heart, providing it can be shown that mixing of indicator and all blood is complete.

However, it is not essential that all the fluid pass through a single channel. If fluid from each input channel mixes with that from every other input channel before it leaves the system, it may still be possible to measure flow. Consider the simple intercommunicating system in figure 8.

P, P', R, Q', and Q are vascular channels in which the direction of flow is indicated by the arrows within channels. Symbols within the channels represent the fraction of flow within each channel. All the flow, F, passes through P. A fraction a of F passes through P_1' and the remainder, $(1 - a)\,F$, passes through P_2'. Of the fraction a, a fraction b passes through R_2

and a fraction $(1 - b)$ through R_1. The flow through R_2 is thus $a\,b\,F$ and, through R_1, $a\,(1 - b)\,F$. The flow through R_3 is the sum of the flow through R_1 and P_2', or $(1 - a\,b)\,F$. The flow through R_3 divides. A fraction c returns to the upper channel to join the flow from R_2. The fractions a, b, and c are each greater than zero and less than 1. If indicator is injected into the system at P_1' at constant rate, I, after the initial transients have disappeared, its steady concentration as a function of the channel in which concentration is measured, assuming mixing of fluid is everywhere complete, will be:

$$C\,(P_1') = \frac{I}{aF}\,;\; C\,(P_2') = 0;\; C\,(R_3) = \frac{(1 - b)\,I}{(1 - a\,b)\,F} = C\,(Q_2')$$

$$C\,(Q_1') = \frac{(c - b\,c + b)\,I}{(c - a\,b\,c + a\,b)\,F}$$

If sampling is at Q_1', the requirement for a useful measurement of flow is that $C\,(Q_1')$ be very nearly equal to I/F. This will be true whenever a is very nearly 1, that is, whenever nearly all the flow passes through P_1' and nearly none through P_2'. In that event, the system is obviously almost that of the case of single input-many outputs. If a is small, $C\,(Q_1')$ may still be nearly equal to I/F if c is very nearly 1, for then the system is almost that of many inputs-single output. Even if c is not close to 1, but is large compared to a and b, $C\,(Q_1')$ will be approximately equal to I/F.

However, if both a and c are small, then $C\,(Q_1')$ will differ greatly from I/F. This is to be expected, for, in such a case, only a small portion of the total flow passes through the system $P_1' \rightarrow Q_1'$.

In more complex systems, even if no single channel ever receives a major portion of the total input, $C\,(Q_1')$ may be nearly equal to I/F. For example, if one adds a second pair of communicating channels, like R_1 and R_4 in figure 8, and if at every bifurcation half the flow takes one path (i.e., $0.5 = a = b = c =$), then $C\,(Q_1')$ will exceed I/F by less than 5 per cent.

Measurement of volume in an open system is more tenuous. If, in figure 8, a and b are large, that is, if most of the fluid takes the path $P \rightarrow P_1' \rightarrow R_2 \rightarrow Q_1'$, then $\bar{t}$ will be small and the volume measured will be nearly that of the preferential channels. Unless there are many communicating branches through which fluid from the inflow channels can intermingle luxuriously, there is little likelihood that the volume measured by the equations developed so far will resemble closely the true volume of the system. The criterion for satisfactory intermingling is simply that, for the case of constant-injection, the limiting concentration of indicator in every output channel must be the same. For certain vascular beds this can be and has been tested (2).

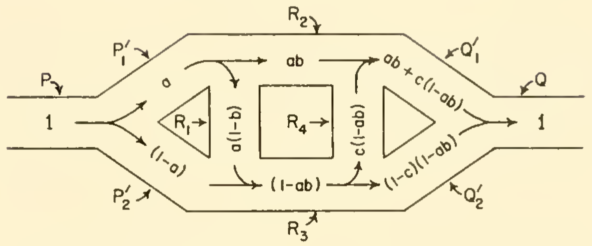

FIG. 8. Intercommunicating flow system through most of which indicator may be distributed, even if injection is only into a branch. Arrows within channels indicate direction of flow. Symbols within channels indicate fraction of flow carried by each channel.

The System Is Nonstationary

The "stationarity" condition, that is, that the distribution of traversal times for entering particles does not change with time, is violated in real vascular systems. It is certainly violated in pulsatile systems, particularly those which include the heart, and it is apt to be violated by vasomotor activity in which entering blood is distributed chiefly through one branch and then another as peripheral resistance is shifted by alterations in arteriolar diameter. In pulsatile and vasoactive systems there are not only changes in flow but also changes in volume with time. If phasic, not necessarily regular, alterations in distribution of traversal times occur many times during the evolution of the sudden-injection indicator-dilution curve, then the violation of "stationarity" may not be important. The constant-injection method will yield a measure of flow and volume in nonstationary systems because the input-output equations still hold, although there may not be a plateau concentration, but a regular or irregular oscillation about a plateau.

Flow or Volume, or Both, not Constant

The sudden-injection method cannot measure either flow or volume if flow and volume change during the course of the indicator-dilution curve, unless the changes are rapid and phasic. The constant-injection method cannot measure a changing volume but it may measure flow. If the changes in flow are slow or move from one steady flow to another,

the limiting concentration will reflect altered flow appropriately. If the changes in flow are rapid and phasic and if the mean transit time of the system is always relatively long, the limiting concentration will alter sluggishly and will measure the average flow.

Although if flow and volume vary independently, the system cannot be stationary; it is possible for flow and volume to vary together so that "stationarity" is maintained.

Flow of Indicator Particles Is not Representative of Flow of Total Fluid

If an indicator is used to measure flow and volume of distribution of biological fluids, it must be established that the distribution of transit times of the indicator is that of the fluid under study. Indicators are used frequently to estimate blood or plasma flow and volume, and both blood and plasma are heterogeneous.

In practice only one of the components of plasma is tagged, usually. For example, it is common to use as indicator certain dyes which bind chiefly to serum albumin or to use tracer amounts of albumin labeled with I^{131}. In these cases the transit times measured are those of serum albumin which may or may not be representative of blood or plasma.

Nonrepresentative behavior also arises from the fact that some substances, such as water, leave vascular systems by diffusing across capillaries. If indicator is attached to serum albumin, which diffuses across capillaries only very slowly compared to water, then, insofar as there is net water loss from the arteriolar end of capillaries, indicator will be concentrated. For the case of constant-injection, indicator leaves arterioles at concentration $= I/F$. In proximal portions of the capillaries its concentration will exceed I/F. If all water returns to the capillaries at their venular ends, concentration of indicator entering venules will again be I/F. If the water does not return completely to the venular end of the capillaries, as in edema formation, prominent lymphatic flow, or renal glomeruli, concentration of indicator in the veins will exceed I/F, where F is arterial inflow, but it will equal I divided by the venous outflow. Therefore, if there is net water movement into or out of the vascular bed under study, and indicator is albumin, the flow which is measured by the equations developed here is the venous outflow and not the arterial inflow.

The fact that water moves out of capillaries, yielding a concentration of indicator which exceeds I/F, even if only transiently (i.e., even if all the water returns to the vascular bed), means that the methods must underestimate the volume. By the sudden-injection method, the mean transit time of the indicator is less than that of water which has an extravascular circuit. In the constant-injection method, the mass of indicator in the system is estimated correctly from the equation $M = F \int_0^\infty [C_{\max} - C(t)]\, dt$, but it is no longer true that this M divided by volume is $C_{\max}$ because some portion of M exists at a concentration greater than $C_{\max}$. Some bound on the error may be calculable if there is sufficient information about the system.

For example, consider that the volume, V, is composed of a subvolume V_1, containing a mass M_1 of indicator at equilibrium concentration $C_{\max} = I/F$, and a subvolume V_2, containing a mass M_2 of indicator at an average concentration C_{supermax}, where $M = M_1 + M_2$. Then $V = V_1 + V_2 = (M_1/C_{\max}) + (M_2/C_{\text{supermax}}) = (M/C_{\max}) - M_2\,(1/C_{\max} - 1/C_{\text{supermax}})$. Thus, if a bound on M_2 is known, for example from the fact that the volume of plasma in capillaries is only, say, 1 per cent of the plasma volume of the system under study, then the error may be neglected for certain purposes. For the case of systems containing a large capillary volume the error may be important. For example, in the kidney, the concentration of tagged albumin exceeds I/F in the glomerular capillaries and in the efferent arterioles, returning almost to I/F in the peritubular capillaries.

For the case of substances which diffuse out of capillaries, flow cannot be measured by the sudden-injection method if the indicator does not flow out of the effluent sampling site. Flow can be measured by the constant-injection method and, for vascular beds, the measured flow is, in fact, plasma flow (or blood flow, depending on the analytical procedure). However, the volume measured is the volume in which indicator is distributed and therefore exceeds the plasma volume. The mean transit time, $\bar{t} = V/F$, calculated from transients of the constant-injection curve is, of course, that of indicator and not of plasma.

INHOMOGENEITY OF BLOOD AND SIGNIFICANCE OF VENOUS HEMATOCRIT

An error may occur when an indicator which tags an element of plasma is used to estimate whole blood flow and volume. The distributions of traversal times of plasma albumin and of erythrocytes are different (6, 9). Computation of whole blood flow

from measured plasma flow is valid, but whole blood volume cannot be estimated from plasma volume and venous hematocrit (19).

Let the rate at which erythrocytes flow through a vein be F_E and the rate at which plasma flows be F_P. Consider that the entire outflow from a vein is collected In one unit of time the collecting vessel will contain a volume equal to F_E of erythrocytes and a volume equal to F_P of plasma, a total blood volume, $F_B = F_E + F_P$. When the collecting vessel is subjected to centrifugation, it will be found that the hematocrit ratio (as percentage) is

$$Ht = [F_E/(F_E + F_P)]\,100 = (F_E/F_B)\,100$$

and

$$100 - Ht = (F_P/F_B)\,100$$

Whence $F_B = 100\,F_P/(100 - Ht)$, verifying that blood flow can be calculated from plasma flow and venous hematocrit ratio.

To calculate the relation between volumes, substitute the appropriate $V/\bar{t}$ for F. It will be found that

$$V_B = V_P\left[\left(\frac{\bar{t}_E}{\bar{t}_P}\right)\left(\frac{Ht}{100 - Ht}\right) + 1\right]$$

where subscripts B, P, and E refer to values for whole blood, plasma, and erythrocytes, respectively. Therefore, a single hematocrit correction factor is insufficient to convert plasma volume to blood volume. The ratio of mean transit time of erythrocytes to that of plasma must be known. By independent labeling of plasma albumin and erythrocytes, $\bar{t}_E$ and $\bar{t}_P$ have been measured simultaneously in several vascular beds (6, 9).

The equation $Ht = (F_E/F_B)\,100$ states that the venous hematocrit ratio is a function of erythrocyte flow and of plasma flow. Therefore, it should be possible to change the hematocrit ratio by changing the ratio of erythrocyte flow to total blood flow. A preliminary examination of this prediction has been made. In a group of eight determinations on four normal men, when forearm blood flow was occluded, the antecubital venous hematocrit ratio was always less, on the average by 1.5 per cent (unpublished observations).

RECIRCULATION

Recirculation of indicator is of practical importance when it occurs before all indicator particles have completed the first transit. For the case of sudden-injection, this means that before the concentration of indicator at outflow has returned to zero it is augmented by some indicator particles which have already been counted once; and for the case of constant-injection, this means that before the plateau concentration C_{max} is reached there is an increase in the slope of the curve $C(t)$ vs. t, owing to reappearance of old indicator particles. There are two reasons for trying to understand recirculation. One is that, in most cases, recirculation is a nuisance which confuses interpretation of the primary circulation curve, making it difficult to perform proper calculation of F and V. The other is that the concentration-time curve during recirculation may give some information about the channels through which recirculation occurs, as in the case of abnormal shunts.

There are two ways to handle the problems created by the presence of recirculation. One is to extend the treatment of the concentration of indicator as a function of flow and volume to include the case of recirculation. The other is to treat formally the concentration of indicator during first circulation as a separate event from the observed concentration in the presence of recirculation and, by some means, extract from the over-all concentration-time curve the concentration-time curve which applies only to the first circulation. Both of these treatments have been advanced.

Let us first examine the possibility of including concentration due to recirculation in our fundamental equations for flow and volume.

A general formal expression for an indicator-dilution curve which includes recirculation can be obtained simply by extending the argument from which equation 17 was developed. The important equation which follows, and its development, is according to Stephenson (30) as modified by Meier & Zierler (19).

Introduce indicator into the inflow of the system at rate $i(t)$, where the function is completely unspecified for the moment. During the interval s to $s + ds$ time units before t, the amount of indicator introduced is $i\,(t - s)\,ds$. The fraction of this amount eliminated per unit time at time t, or s time units later, is $h(s)$. Therefore, the contribution to the rate at which indicator leaves the system at time t made by indicator introduced between s and $s + ds$ time units earlier is the product $[h(s)]\,[i\,(t - s)\,ds]$. Summing for all such time intervals before t, the rate at which indicator leaves at time t is $\int_0^\infty i\,(t - s)\,h(s)\,ds$. But this rate is also equal to $F\,C(t)$, where $C(t)$ is the concentration at outflow. Therefore,

$$C(t) = \frac{1}{F}\int_0^\infty i\,(t - s)\,h(s)\,ds \qquad (24)$$

Equation 17, which was developed for the case of

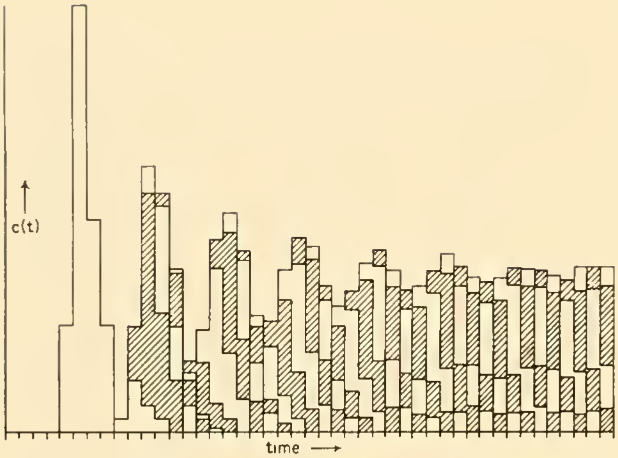

FIG. 9. Histogram of indicator concentration versus time in a recirculating system. Sudden-injection of indicator at origin. First four columns represent initial circulation and define distribution of transit times through the system. As indicator reinjects itself into the system each slug is distributed according to the frequency pattern illustrated during the first circulation. Distribution of successive reinjected slugs is marked by alternate white and shaded patterns. [From Zierler (38).]

constant-injection, is thus a special case of equation 24 in which $i(t) = 0$ for $t < 0$, and $i(t) = I$, a constant, for $t \geqq 0$.

If a quantity of indicator is injected into a closed (the primary) system (single input, single output) to which it returns repetitively by way of some other (the recirculating) system, we may analyze the concentration at outflow from the primary system as follows:

There is a distribution of transit times through the primary system, described by the function $h(t)$. There is also a distribution of transit times through the recirculating system (from output of primary system back to input of primary system) which we will describe by the function $f(t)$. There is also a distribution of transit times through the system as a whole, from input of the primary system, through output and back to input, which we will describe by the function $g(t)$.

For the case of sudden-injection, in which a quantity, q, of indicator is introduced into the system at its input, the concentration of indicator at output, $c_o(t)$, from equation 6 is

$$c_o(t) = q\, h(t)/F$$

If the concentration of indicator is measured at the input to the primary system, $C_i(t)$, there will be no indicator for $t < 0$, there will be a concentration $C_i(0)$, at time $t = 0$ when indicator is introduced suddenly into the input, and then there will reappear at the input an amount of indicator per unit time described by the distribution of transit times for the total system, $q\, g(t)$, at concentration $q\, g(t)/F$. The concentration of indicator at the input, considering now only the initial condition and the first recirculation, is

$$C_i(t) = q\, g(t)/F \tag{25}$$

where

$$q\, g(0)/F = C_i(0)$$

The rate at which indicator enters the primary system is $F\, C_i(t) = q\, g(t)$.

The concentration of indicator at the output from the primary system is expressed by the action of the distribution $h(t)$ on the input $F\, C_i(t)$. Substituting $F\, C_i(t)$ for the input function $i(t)$ in equation 24, the concentration of indicator at output from the primary system is

$$C_o(t) = \int_0^t C_i\,(t - s)\; h(s)\; ds \tag{26}$$

Equation 26 is valid for all t and for any number of repeated circulations, because every $C_i(t)$, whenever it appears, is redistributed according to $h(t)$. Equation 25 describes $C_i(t)$ only for the first circulation. During the second circulation, $C_i(t)$ is distributed once more in accordance with the function $g(t)$, so that when indicator returns a second time to the primary input, its concentration is

$$C_i(t) = \int_0^t C_i\,(t - s)\; g(s)\; ds \tag{27}$$

With each subsequent recirculation, $C_i(t)$ will be redistributed through $g(t)$. With each recirculation, indicator particles entering the primary system for, say, the nth time are dispersed more and more with respect to time (fig. 9), so that as t grows large, $C_i(t)$ tends to approach the average concentration in the system, which of course is the mass of indicator, q, divided by the total volume of the system, V_T. Therefore,

$$\lim_{t \to \infty} C_i(t) = \int_0^\infty C_i\,(t - s)\; g(s)\; ds = q/V_T \tag{28}$$

Equation 28 provides a basis for measurement of volume of certain body fluid compartments. We are not concerned with that problem in this chapter but with the use of the asymptotic behavior of $C_i(t)$, to which we shall return shortly.

If indicator is introduced into the inflow to the primary system at constant rate, I, concentration of indicator at the outflow from the primary system, from equation 18, is $C_o(t) = I\ H(t)/F$, providing there is no recirculation. As indicator recirculates, the output from the primary system, $F\ C_o(t)$, is distributed through the recirculating system by the function $f(t)$, so that the first recirculating indicator appears at the input in concentration

$$C_i(t) = \frac{I}{F}\int_0^t H\ (t-s)\ f(s)\ ds = \frac{I}{F}\int_0^t g(s)\ ds$$

For repeated distribution of $C_i(t)$ through the primary and recirculating system, the general equation for concentration at output is

$$C_o(t) = \int_0^t C_i\ (t-s)\ h(s)\ ds \qquad (29)$$

and the concentration at input is, as for sudden-injection,

$$C_i(t) = \int_0^t C_i\ (t-s)\ g(s)\ dt \qquad (27)$$

where $C_i(0) = I/F$, and $C_i = 0$ for $t < 0$

Combining equations 27 and 29,

$$C_o(t) = \int_0^t h(s)\int_0^{t-s} C_i\ (t-s-r)\ g(r)\ dr\ ds \qquad (30)$$

To return to the argument developed for equation 28 and in figure 9, the average concentration of indicator throughout the entire system at any time is the mass of indicator in the system, $I \cdot t$, divided by the total volume, V_T. Since, as was argued for equation 28, the concentration function in the system behaves as though it were a damped oscillation and, at any point in the system, approaches $I \cdot t/V_T$, the asymptotic behavior of the concentration at outflow is

$$\lim_{t\to\infty} C_o(t) = \frac{I}{F} + \int_0^\infty \frac{I\cdot(t-s)}{V_T}\ h(s)\ ds$$

$$= \frac{I}{F} + \frac{I\ t}{V_T}\int_0^\infty h(s)\ ds - \frac{I}{V_T}\int_0^\infty s h(s)\ ds \qquad (31)$$

$$= I/F + C_i(t) - I\bar{t}/V_T$$

where is the mean transit time through the primary system and F is the flow through the primary system.

Stephenson (30) has pointed out that advantage can be taken of the asymptotic behavior of the concentration function. If, in addition to constant-injection of one indicator directly into the inflow of the primary system, there is also constant-injection of a second indicator into some point of the recirculating system, then, from equation 31, the concentration of the second indicator at the primary outflow will have as its limit for large t

$$\lim_{t\to\infty} K_o(t) = K_i(t) - I\bar{t}/V_T \qquad (32)$$

where K_o and K_i are concentrations of the second indicator.

Equations 31 and 32 determine F and $\bar{t}$, and therefore V, the volume of the primary system, despite recirculation, where it is possible to inject indicators at constant rate into the primary and into the recirculating system, and to measure the concentration of both indicators at the inflow and at the outflow of the primary system. In this case, recirculation is an essential part of the scheme and is not corrected. V_T, the total volume, which appears in equations 31 and 32, is estimated independently, or simply from the limit equation 28.

Solution of equations 31 and 32 yields

$$F = I/[C_o(t) - C_i(t) + K_i(t) - K_o(t)] \qquad (33)$$

and

$$\bar{t} = V_T\ [K_i(t) - K_o(t)]/I \qquad (34)$$

where C_i and K_i are limits of the respective concentrations for large t.

Another way of treating the problem of recirculation is to solve the observed concentration-time curves for the frequency function of transit times, $h(t)$, through the primary system. This solution again requires that there be two separate injections. Let these injections be *a*) at the inflow to the primary system and *b*) at the outflow from the primary system. Injection may be sudden or constant. Consider the case of sudden-injection.

A quantity of indicator, q_a, is introduced into the inflow. During the first circulation the concentration at outflow is $C_a(t) = q\ F/h(t)$. Indicator, leaving the primary system at rate $F\ C_a(t)$, is distributed through the recirculating system in a manner described by the function $f(t)$ and re-enters the primary system where it is distributed again in the manner described by $h(t)$. The frequency function, $g(t)$, describes the over-all distribution of transit times through both the primary and recirculating systems. Therefore, indicator reappears at the outflow site at concentration $C_a(t) = \int_0^t C_a\ (t-r)\ g(r)\ dr$. The complete

expression for concentration of indicator at outflow from time zero is therefore

$$C_a(t) = \frac{q_a}{F} h(t) + \int_0^t Ca\ (t - r)\ g(r)\ dr \qquad (35)$$

Now let there be introduced into the outflow site a quantity, q_b, of indicator so that the concentration of indicator at outflow at zero time is $C_b(0)$. When this indicator reappears at the outflow site for the first time it will have been distributed through the entire system so that its concentration will be $C_b(t) = C_b(0)\ g(t)\ dt$. This distribution will in turn be redistributed in accordance with the function, $g(t)$, and the complete expression for concentration of the second indicator at outflow is

$$C_b(t) = C_b(0)\ g(t)\ dt + \int_0^t C_b\ (t - r)\ g(r)\ dr \qquad (36)$$

Equations 35 and 36 yield the measured outflow concentrations of the two indicators as a function of two unknown distributions, $h(t)$, through the primary system, and $g(t)$ through the entire system. The possibility of calculating $h(t)$ is therefore a real one.

The integrals in equations 24, 26, 27, 29, 35, and 36 are of the class called convolution integrals. They describe the fact that one function is made to pass through or is convoluted by a second function, a fact pointed out by Stephenson (30), Sheppard (27), and Zierler (38). Providing the functions meet certain requirements they can be operated upon so as to yield more tractable equations. The following are sufficient conditions for the transform.

The functions must be sectionally continuous on a finite interval. Frequency distributions of transit time, in practice, are continuous. The functions must be of exponential order as the variable t approaches infinity. This means that if the function is $h(t)$ the product $e^{-\alpha t}\ |\ h(t)\ |$ is less than some constant, A, for all t greater than some finite number T. That is, $|\ h(t)\ |$ does not grow more rapidly than $A\ e^{\alpha t}$ as $t \to \infty$, where α is a constant. Since the distribution function, such as $h(t)$, always lies between zero and one, it is satisfactory for transformation.

We introduce the function $y(s)$, the Laplace transform of the function $h(t)$, which we have shown to be suitable for Laplace transformation, where $y(s) = \int_0^\infty e^{-st}\ h(t)\ dt$. The advantage of the Laplace transformation is that the integral of the convolution of two functions becomes the product of the Laplace transforms of the two functions. Therefore, equation 35 is transformed to

$$k_a(s) = q_a\ y(s)/F + k_a(s)\ z(s)$$

Whence,

$$k_a(s) = \frac{q_a\ y(s)/F}{1 - z(s)} \qquad (37)$$

where $k_a(s)$ is the Laplace transform of $C_a(t)$ and $z(s)$ is the Laplace transform of $g(t)$.

Since $0 \leqq z(s) < 1$, equation 37 may undergo binomial expansion to yield

$$k_a(s) = \frac{q_a\ y(s)}{F}\ [1 + z(s) + z^2(s) + z^3(s) + \cdots] \qquad (38)$$

Equation 38 states explicitly, as pointed out by Sheppard (27), that the concentration of indicator at outflow is, as one expects, the algebraic sum of all convolutions of the outflow concentration through the system in its first, second, third, fourth, and so on, circuit.

The Laplace transform of equation 36 is

$$k_b(s) = C_b(0)\ dt\ z(s) + k_b(s)\ z(s)$$

where $k_b(s)$ is the Laplace transform of $C_b(t)$, and

$$\begin{aligned} k_b(s) &= \frac{C_b(0)\ dt\ z(s)}{1 - z(s)} \\ &= C_b(0)\ dt\ [z(s) + z^2(s) + z^3(s) + \cdots] \end{aligned} \qquad (39)$$

Combining equations 37 and 39, and solving for $y(s)$ with elimination of $z(s)$,

$$y(s) = A\ \frac{k_a(s)}{C_b(0)dt + k_b(s)} \qquad (40)$$

where A is the constant $F\ C_b(0)\ dt/q_a = C_b(0)/C_a(0)$. The inverse transform of equation 40 is

$$h(t) = A\mathcal{L}^{-1}\ \frac{k_a(s)}{C_b(0)\ dt + k_b(s)} \qquad (41)$$

Thus, $h(t)$, which is the desired function, is given as the product of a measurable constant and the inverse transform of a function only of observed concentrations of indicators. Equation 41 can be solved if the form of the functions is known, although at the moment it is unlikely that a formal expression of the concentration functions is known with sufficient accuracy. However, because the concentration functions are available experimentally, they can be manipulated by computer techniques and a solution for $h(t)$ obtained empirically. A preliminary report states that something along these lines has been done by Cheesman *et al.* (4).

A relatively simpler, but closely related, procedure has been used by Parrish *et al.* (22), based on an

application by Paynter (23) to a flood control problem concerned with water flow through drainage basins. The formal treatment rests on the Duhamel superposition theorem.

Consider a closed system in which any given input is distributed with time such that, for a unit step (= brief square wave) input, the output is described by the function $A(t)$, called the indicial response or admittance function. By arguments similar to those we have used previously, as in development of the convolution equation 24, if the input has magnitude dx at time s, the output will be $A\ (t - s)\ dx$. Summing for all such stepwise inputs to obtain the input, $x(t)$, yields the output

$$y(t) = x_0 A(t) + \int_0^t A\ (t - s)\ dx(s) \qquad (42)$$

or

$$y(t) = A_0\, x(t) + \int_0^t x\ (t - s)\ d\ A(s)$$

where x_0 and A_0 refer to initial conditions.

The relationship between the Duhamel integral and equations developed earlier in this chapter is obvious.

Equation 42 can be handled numerically by expressing the output as a stepwise function of the input and the admittance function. Thus

$$y(t) = \sum_{k=1}^{t} A\ (t + 1 - k)\cdot x\ (k) \qquad (43)$$

where k assumes only integer values for integer values of t. For example,

$$\begin{aligned} y(1) &= A(1)\cdot x(1) \\ y(2) &= A(2)\cdot x(1) + A(1)\cdot x(2) \\ y(\mathrm{t}) &= A(t)\cdot x(1) + A\ (t - 1)\cdot x(2) + \cdots \\ &\quad + A(1)\cdot x(t) \end{aligned}$$

Therefore, if y and x are determined experimentally, $A(1)$, $A(2)$, etc. can be calculated, and the admittance function can be described numerically.

Parrish *et al.* (22) injected proximally to the input of the system under study (the pulmonary vascular system) and measured both the input and the output concentrations of indicator as a function of time. The concentration-time curve obtained from the input constituted the input to an analog computer. The coefficients of the computer input were then adjusted until the computer output duplicated the observed concentration of indicator at output from the vascular system. A square wave was then fed through the analog and the admittance function was registered. From this distribution function the mean transit time was calculated.

All the methods described so far for dealing with systems in which recirculation occurs are complex experimentally and analytically. It would be far simpler if the shape of the distribution function were known so that its distortion by recirculating indicator could be obliterated by extrapolation of the distribution function beneath the distortion. We shall consider later some of the attempts to restrict the entire distribution function to some formal expression. For the time being we are concerned only with the downslope of the function $h(t)$.

Hamilton *et al.* (10) discovered that, when an indicator was injected suddenly intravenously in the dog and the concentration of indicator measured with time in arterial blood, the downlimb of the concentration sooner or later fitted an exponential of the form $C_o e^{-kt}$ until it was evidently interrupted by an increase in concentration attributed to the first recirculation of indicator. This means that a plot of the logarithm of indicator concentration versus linear time yields a reasonably straight line until recirculation appears. When recirculation does appear, the logarithmic downslope is simply extrapolated to very small concentrations. The extrapolated concentration-time curve is then replotted on linear coordinates, and, with recirculation thus eliminated, the area and the mean transit time of the primary curve are calculated.

This has been an extraordinarily useful artifice, although there is no convincing theoretical reason for the downlimb to assume the form $C_o e^{-kt}$. Indeed, it is a matter of experience that it by no means always does so (7).

In specific instances it may be possible to find other useful approximations. For example, in the case of measurement of blood flow through the forearm of man by constant-injection of indicator, recirculation, which must pass through the large bulk of the rest of the total body vascular bed, is a late event. Consequently, indicator, which accumulates in the total plasma volume at rate I, is almost completely distributed at its equilibrium concentration when it returns to the forearm. Therefore, the rate at which indicator re-enters the forearm is approximately $F\ I\cdot(t - b)/V_T$, where V_T is the total volume in which indicator is distributed and b is a correction for the time lag. The rate at which indicator is introduced into the forearm is therefore $i(t) = I + a\ (t - b)$, where $a\ (t - b) = 0$ for $t < 0$ and $a\ (t - b) = [t - b]\ a$ for $t \geqq 0$, where $a = F\ I/V_T$.

Substituting for $i(t)$ in equation 24,

$$C(t) = \frac{1}{F}\int_0^{\infty} [I + a\ (t - b)]\ h(s)\ ds$$

$$= \frac{I}{F}H(t) + \frac{a}{F}\int_0^{\infty} t\ h(s)\ ds - \frac{a\ b}{F}H(t) \quad (44)$$

$$\lim_{t\to\infty} C(t) = \frac{I}{F} + \frac{a\ \bar{t}}{F} - \frac{a\ b}{F} = \frac{I}{F} + \frac{I\cdot(\bar{t} - b)}{V_T}$$

It has been verified experimentally that indicator recirculating concentration in plasma to the forearm increases linearly (2). Therefore, to correct for recirculation in this system it is necessary to measure the recirculating concentration only sufficiently to establish the slope and intercept of the recirculating concentration.

Summary of Treatment of Recirculation

If recirculation is a late event so that, for the case of sudden-injection, indicator concentration has almost returned to zero before the effect of recirculation is evident, or, for the case of constant-injection, indicator concentration has almost reached plateau, then it is far simpler to make some arbitrary extrapolation of the primary concentration curve. It is obvious that under these conditions no great error will be introduced by any reasonable extrapolation. In most cases the exponential extrapolation of Hamilton *et al.* (10) is quite satisfactory.

However, if recirculation occurs early so that the downlimb of the concentration curve following sudden-injection is obscured, then no correction for recirculation can be made with confidence. Under these circumstances it is necessary to use one of the other methods which demand measurement of concentration at two sites, such as the procedure proposed by Stephenson (30). These methods, although complex, have the important advantage that they make no assumptions about the form of the distribution function.

EFFECT OF INJECTION WHICH IS NEITHER SUDDEN NOR CONSTANT

Sudden-Injection Which Is Not Truly Instantaneous

For some years it was customary to regard sudden-injection of indicator as requiring no time. That is, the injectate was delivered truly instantaneously into the vascular system where it was dissolved at once in an element of volume, dV, so that its concentration was q/dV. As dV is permitted to become as small as we please, the input concentration, q/dV, obviously goes to infinity. However, a plot of input concentration vs. time required for input must always have a finite area, for if $h_i(t)$ is the frequency distribution of injection times, then $c_i(t) = q/dV = q\ h_i(t)/F$, from equation 6, and $\int_0^{\infty} c_i(t)\ dt = q/F$, which is finite. Distribution functions of this form are essentially spikes and are known formally as delta functions.

Obviously, in practice it is impossible literally to inject instantaneously. If the mean transit time through the system is long compared to the mean time of injection, it is usually sufficiently accurate to ignore the fact that the injection is not really instantaneous. However, if the mean time of the distribution of injection is significant compared to the mean transit time through the system, then equation 6, $c(t) = q\ h(t)/F$, does not hold and the calculation of $\bar{t}$ and, therefore, volume will be erroneous.

Let $h_i(t)$ be the distribution of injection with time, where $q\ h_i(t)\ dt$ is the fraction of injectate, q, introduced into the system between time t and time t and dt. Then $q\ h_i(t)$ is the function $i(t)$ of the general equation 24, and the concentration at outflow is

$$C(t) = \frac{q}{F}\int_0^{t} h_i\ (t - s)\ h(s)\ ds \quad (45)$$

The calculation of flow from the area of the outflow concentration-time curve will still be correct. The rate at which indicator leaves the system is $F\ C(t)$. The total amount of indicator which leaves the system is $F\int_0^{\infty} C(t)\ dt$, which must equal the amount introduced, so that the equation $F = q/\int_0^{\infty} C(t)\ dt$ still applies.

However the mean time, calculated from $\int_0^{\infty} t\ C(t)\ dt/\int_0^{\infty} C(t)\ dt$, will be larger than the true mean transit time, $\int_0^{\infty} t\ h(t)\ dt$. Advantage is now taken of an important property of frequency functions.

Given the frequency function, $f_1(t)$, which is the result of the convolution of one frequency function, $f_2(t)$ on another frequency function, $f_3(t)$, or

$$f_1(t) = \int_0^{t} f_2\ (t - s)\ f_3(s)\ ds$$

then the mean time $\bar{t}_1$ of the convolution $f_1(t)$ is the sum of the mean time $\bar{t}_2$ of the function f_2 and the mean time $\bar{t}_3$ of f_3.

The important relation is illustrated in figure 10 by the use of histograms representing distribution

functions. There are three distribution functions: *1*) $h_i(t)$ is the frequency distribution of injectate, that is, of the total amount of injectate, q, a fraction $q\ h_i(t)\ dt$ is injected between time t and time $t + dt$; *2*) $h(t)$ is the distribution of transit times through the system, defined as we have used it previously throughout this chapter; *3*) $h_o(t)$ is the frequency distribution at outflow, that is, of the total quantity of injectate, q, which is eliminated eventually from the system, a fraction $q\ h_o(t)\ dt$ is eliminated between time t and time $t + dt$. $h_o(t)$ is the integral of the convolution of the injectate distribution, $h_i(t)$, upon the distribution of transit times of fluid particles, $h(t)$. That is, $h_o(t) = \int_0^t h_i\ (t - s)\ h(s)\ dt$. Remember that the area under a frequency distribution curve is unity: $\int_0^\infty h_i(t)\ dt = \int_0^\infty h(t)\ dt = \int_0^\infty h_o(t)\ dt = \int_0^\infty \int_0^t h_i\ (t - s)\ h(s)\ ds\ dt = 1$.

In figure 10*A*, injection is truly instantaneous. The entire injectate is introduced during the zero-th time interval, or $h_i(t) = 1$ for $t = 0$ and $h_i(t) = 0$ for $t \neq 0$. The area of the column representing injectate is unity. In our example, $h(t)$ is such that for $t < 5$, $h(t) = 0$, during the fifth time interval 20 per cent of the quantity introduced at zero time is eliminated from the system, an additional 40 per cent during the sixth time interval, an additional 30 per cent during the seventh, and the final 10 per cent during the eighth. The convolution of $h_i(t)$ on $h(t)$ in this case yields a distribution, $h_o(t)$, identical with $h(t)$, that is, the distribution at outflow represents the true distribution of transit times through the system. This occurs because all products of $h_i\ (t - s)$ and $h(s)$, which must appear in the convolution integral, are zero for $t < 5$ (because $h(t)$ is zero for $t < 5$) and for $s < t$ (because only $h_i(0) = h_i\ (t - t)$ is not equal to zero).

Because $h_o(t)$ and $h(t)$ are identical in the case under consideration, the mean transit time through the system $\bar{t}$ is identical with the mean time, $\bar{t}_o$, of the distribution $h_o(t)$. In the example, $\bar{t}_o = \bar{t} = \int_0^\infty t\ h(t)\ dt = \sum t\ h_o(t) = (5 \times 0.2) + (6 \times 0.4) + (7 \times 0.3) + (8 \times 0.1) = 6.3$. The mean time of the injectate is, of course, zero, in this case.

In figure 10*B*, injection is delivered as a square wave during the zero and first time intervals. That is, $h_i(t) = 0.5$ during the zero-th time interval and $= 0.5$ during the first time interval and $h_i(t) = 0$ for $t > 1$. The mean time of injectate, $\bar{t}_i$, is $\sum t\ h_i(t) = (0 \times 0.5) + (1 \times 0.5) = 0.5$. That fraction, 50 per cent, of the injectate introduced during the zero-th time interval is distributed through the system, as described by $h(t)$, so that 20 per cent

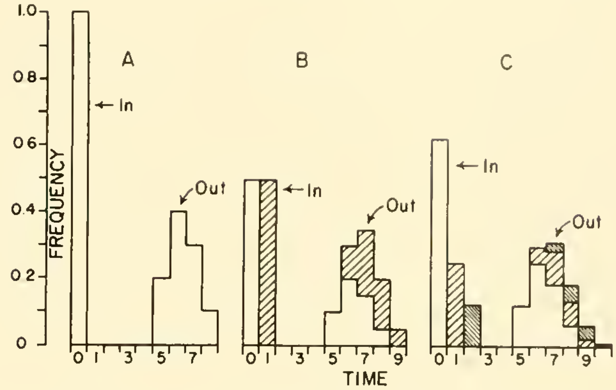

FIG. 10. Histograms of distribution of input and output of indicator versus time. Fundamental distribution of transit times through system shown in *A*. In *B* and *C* the input at each time interval (indicated successively by white column, coarsely-hatched column, and finely-hatched column) is distributed through the fundamental distribution of transit times (or input is convoluted upon the frequency function of through-put) and the output at any time is the sum of the contributions from each input column.

of it (or $0.5 \times 0.2 = 0.1$ of the total injectate) is eliminated during the fifth time interval, 40 per cent of it (or $0.5 \times 0.4 = 0.2$ of the total injectate) is eliminated during the sixth time interval. The remaining 50 per cent of injectate, injected during the first time interval, is distributed so that 20 per cent of it is eliminated five time units later, that is, during the sixth time interval, 40 per cent of it is eliminated during the seventh time interval, and so on. The total fraction of injectate eliminated during the sixth time interval is 0.2 (from the first 50% of injectate) + 0.1 (from the second 50% of injectate) = 0.3, and so on, summing for each time interval. The mean time of the output distribution, $\bar{t}_o = (5 \times 0.1) + (6 \times 0.3) + (7 \times 0.35) + (8 \times 0.2) + (9 \times 0.05) = 6.8$. The true mean transit time of fluid particles through the system is $\bar{t} = \bar{t}_o - \bar{t}_i = 6.8 - 0.5 = 6.3$, which is the result obtained from the data of figure 10*A*.

Figure 10*C* emphasizes that the form of the injectate distribution and the form of the outflow distribution are irrelevant to the problem of determining flow and volume. In figure 10*C* the injectate distribution has been selected so that it is not the square wave of figure 10*B*, but so that it yields the same value for mean time of injection $\bar{t}_i \cdot \bar{t}_i = (0 \times 0.625) + (1 \times 0.25) + (2 \times 0.125) = 0.5$. The distribution function at outflow in figure 10*C* has quite a different form from that shown in figure 10*B*, because it is the integral of the convolution of a different input on the same distribution of transit times. Never-

theless, the mean transit time at output, $\bar{t}_o = (5 \times 0.125) + (6 \times 0.3) + (7 \times 0.3125) + (8 \times 0.1875) + (9 \times 0.0625) + (10 \times 0.0125) = 6.8$, is identical with that in figure 10*B*, and the true mean transit $\bar{t} = \bar{t}_o - \bar{t}_i = 6.3$ is estimated correctly.

Therefore, the mean transit time of fluid particles through the system, $\bar{t} = \int_0^\infty t\ h(t)\ dt$, which is the datum desired, can always be calculated as the difference between the observed time of indicator particles, $\int_0^\infty t\ C(t)\ dt/\int_0^\infty C(t)\ dt$, and the mean time of the injection process. The latter may be determined experimentally, for example, by injecting into a system in which $h(t)$ is known. However, if the injection is very rapid, it may be sufficiently accurate to consider that it is a square wave.

What may seem to be an excessive amount of space has been devoted to an explanation of the fact that mean times are additive in order to make the principle clear, because uses of the principle recur in other practical aspects of the problem, particularly with those concerning the effects of collecting systems which will be considered later.

Injection at Constant Acceleration

There may be certain advantages in special situations in making the injection follow certain known functions. For example, the following interesting property occurs when injection is delivered at constant acceleration (38). Let the rate of injection $i(t) = 0$ for $t < 0$ and $i(t) = a \cdot t$, where a is constant for $t \geqq 0$.

Then,

$$C(t) = \frac{a}{F}\int_0^t (t - s)\ h(s)\ ds$$

$$= \frac{a\ t}{F}\int_0^t h(s)\ ds - \frac{a}{F}\int_0^t s\ h(s)\ ds \qquad (46)$$

$$\lim_{t\to\infty} C(t) = \frac{a}{F}(t - \bar{t})$$

The concentration of indicator at inflow is $a\ t/F$. Therefore, the difference between the concentration at inflow and concentration at outflow, after initial transients, is exactly $a \cdot \bar{t}/F$. Then if F is measured independently, $\bar{t}$ can be measured at once and more simply than by any of the other methods.

EFFECT OF COLLECTING CATHETER

If blood is led from the system under study through a device such as a catheter, the distribution of transit times through the system, $h(t)$, is convoluted upon the distribution of transit times through the catheter, $h_o(t)$. If the sudden-injection technique is used and injection is a delta function, then the observed concentration at outflow from the catheter is

$$C(t) = \frac{q}{F}\int_0^t h\ (t - s)\ h_o(s)\ ds$$

This is identical to the case in equation 44, in which an inflow distribution is convoluted through the function $h(t)$ because the sequence in which the convolution occurs makes no difference. That is $\int_0^t f\ (t - s)\ f_2(s)\ ds = \int_0^t f_2\ (t - s)\ f_1(s)\ ds$. Therefore, all the arguments used in the previous section, with reference to convolution of injection upon the distribution function of the system, apply equally to convolution of the distribution through the catheter upon the distribution $h(t)$. Again, the mean times are additive. The true mean transit time through the system (excluding the catheter) is the difference between the observed mean time, $\int_0^\infty t\ C(t)\ dt/\int_0^\infty C(t)\ dt$, and the mean time through the catheter. The latter is easily obtained, since it is simply the volume of the catheter divided by the flow through the catheter.

As was argued in the previous section, flow through the system is measured correctly by the relation $F = q/\int_0^\infty C(t)\ dt$.

Several investigators have examined the problem of the effect of catheter sampling on the shape of the indicator concentration-time curve. These studies will be considered in detail in the next section. It is important to note, however, that for the calculation of flow we are not concerned with the shape of the outflow concentration curve, only with its area, and that for the calculation of volume we need to determine only the mean time of the outflow curve (which we can do by numerical calculation) and the mean time of the catheter. The shape of the outflow curve is immaterial.

FORMAL EXPRESSIONS FOR THE DISTRIBUTION FUNCTION

In all the previous sections we have not cared what form the distribution function of transit times, $h(t)$, might take. It has been simplest and completely accurate to let the flow system (e.g., a vascular bed) determine the function for us by delivering an indicator at a concentration which is measurable experimentally as a function of time.

However, it is a legitimate object of scientific curiosity to ask whether $h(t)$ might be constrained

to fit some more specific expression, and there is the further advantage that comprehension of the distribution function might reveal something about the nature of laws governing distribution of blood through vascular nets. There are two ways to approach the problem. One is to examine the concentration-time curves obtained experimentally and, by curve-fitting, derive an empirical expression for the concentration as a function of time or some other useful relation. The other is to assume that certain given laws govern the distribution, predict the distribution function from these laws, and test the observed concentration-time curve for goodness of fit.

Empirical Expressions

Perhaps the first empirical expression is attributable to Allen (1), the hydrologist to whom reference was made earlier, who elected to treat his observed concentration-time curves (following sudden-injection) as triangles. The area is, of course, then simply $\frac{1}{2}C_p\ (T - a)$, where C_p is the peak concentration, a is the appearance time, and T is the time at which concentration returns to zero; $\bar{t}$ is simply $\frac{1}{3}\ (T + p + a)$, where p is the time at which peak concentration occurs. Allen's penstock flows must have been turbulent, since a was very long compared to $(T - a)$ and it did not make much difference what time was used in the interval a to T. These approximations, though perhaps adequate for their original purpose, are apt to be unsatisfactory for biological application owing to the large error and to the fact that recirculation obscures the curve so that T may not be estimated with confidence.

Indeed, most attempts at empirical definition of the indicator concentration-time curve have been inspired by the practical necessity of extracting the primary curve from the observed curve obscured by recirculating indicator.

Hamilton's observation, cited previously, that the downlimb of the sudden-injection curve was exponential, or reasonably close to exponential, was made on the heart-lung preparation in the dog. The exponential fit has been verified repeatedly, although not invariably, for the sudden-injection concentration-time curve obtained when indicator was distributed through the heart and pulmonary vascular bed in the intact dog and in man. However, when recirculation begins shortly after peak concentration is attained it is impossible to estimate accurately the slope of the exponential downlimb, and extrapolation by this method cannot be used. For this reason, several students of the problem asked whether or not indicator-dilution curves committed themselves, so to speak, as soon as they had written the rising limb and reached peak concentration.

To this end, Dow (5) examined a large number of indicator dilution curves obtained by sudden-injection into the cardiopulmonary circuit in dogs and in man. After testing various combinations of a number of measurable factors, Dow reported that the following formula correlated best with the area under the concentration-time curve, corrected for recirculation: $pC_p/[3 - (0.9\ p/a)]$, whence

$$F = q\ [3 - (0.9\ p/a)]/pC_p \tag{47}$$

where p is the time (after injection) at which peak concentration, C_p, occurs and a is appearance time.

Keys *et al.* (16) found that in their data on man, Dow's formula systematically underestimated flow, calculated from $F = q/\int_0^\infty c(t)\ dt$, where $c(t)$ is corrected for recirculation.

Use of p, C_p, and a in formulas designed to estimate area arises naturally from the fact that the indicator concentration-time curve approximates a linear rising phase to a peak followed by exponential decay. Concentration as a function of time in this approximation is

$$c(t) = \begin{cases} 0,\ t < a \\ c_p\ (t - a)/(p - a),\ a \leqq t \leqq p \\ c_p\ e^{-k(t-p)},\ p \leqq t \end{cases} \tag{48}$$

The area under the curve is $c_p[(p - a)/2 + 1/k]$ which is to be compared with Dow's empirical formula.

A closely related approach was taken by Hetzel *et al.* (15), who compared the area of what they called the forward triangle with the total area of the curve corrected for recirculation. The forward triangle is defined by the values which $c(t)$ assumes in equation 48 for $a \leqq t \leqq p$ and its area is $c_p\ (p - a)/2$. The ratio of the forward triangle to the total area was determined in a number of experiments in man in which indicator traversed the heart and pulmonary vascular bed. The ratio varied somewhat with the site of injection but in general was surprisingly stable at about 0.35. If equation 48 is a reasonable approximation of $c(t)$, the ratio is $k\ (p - a)/2 + k\ (p - a)$. The fact that the observed ratio was about $\frac{1}{3}$ implies that $k \approx 1/(p - a)$, and this is an anticipated result because, as we shall see later, k is related closely to $\bar{t} - a$, and $\bar{t}$ is sufficiently near p to make it plausible that some empirical correlation might be found.

Although the empirical correlations cited above may be better than nothing when one is trying to salvage data, they are the best of a bad bargain. The correlations were obtained in a specified set of experiments, in particular only in those in which recirculation was sufficiently late to permit application of Hamilton's exponential extrapolation. The necessity for their use arises in another set of conditions in which recirculation is an early event. There is no information as to whether or not the correlations from the first set of experiments can properly be applied to the second. Furthermore, none of the correlations applies to experiments in which injection or collection, or both, is from other parts of the cardiopulmonary circuit or in which other vascular beds are studied. Finally, these empirical formulas yield approximations only of the area of the curve. They therefore can be used only for estimates of flow and not of volume.

THEORETICAL APPROACHES

Conceivably, a complete description of the indicator concentration-time curve or of the distribution of transit times, $h(t)$, might require a thorough understanding of the anatomy of the bed under study, including all path lengths, the rheological properties of blood, the driving pressure, the peripheral resistance, the effect of pulsatile flow in an elastic system, the elastic response of the system, and the neural and humoral factors which affect redistribution of blood along various paths as a function of time. Very little is known about any of these, although some information may permit first approximations in certain areas. For the present, the difficulties seem insurmountable but significant attempts have been made.

Laminar Flow Through Straight Tubes and More About Catheters

When a Newtonian fluid flows through a long straight tube of uniform bore, providing the Reynolds number of the system is below a certain critical value, its behavior is described as laminar and it obeys Poiseuille's law. Several treatments of a system in which indicator is distributed through a laminar flow system have been given (24, 28, 29). The following is adopted from that of Sheppard *et al.* (28). Imagine that the cylinder of liquid is divided into concentric sleeves. Each sleeve has an inner radius r and an outer radius $r + dr$, a thickness, therefore, of dr and a length L, which is the length of the total system between inflow and outflow. The velocity of fluid in the central core is the greatest. The velocity of fluid at the wall of the container, of radius R, is zero. The velocity of fluid in all other sleeves decreases from the center to the wall in a parabolic fashion, that is, it decreases according to the square of its distance, r, from the center. Therefore, velocity, u, as a function of radius, $u(r) = u_{\max}(1 - r^2/R^2) = L/t$, where $u_{\max}$ is the maximum velocity in the central stream. It is a basic property of parabolic flow that the maximum velocity is twice the mean velocity (this follows from the fact that the volume of a cylinder is twice that of a contained paraboloid of revolution). The mean velocity is simply the flow, F, divided by the cross-sectional area of the cylinder, πR^2. Substituting for $u_{\max}$ in the equation above,

$$u(r) = \frac{2F}{\pi R^2}\left(1 - \frac{r^2}{R^2}\right) = \frac{L}{t} \tag{49}$$

The volume of a sleeve is $\pi(r + dr)^2 L - \pi r^2 L$ or $\pi \cdot 2\, r\, dr \cdot L$, and the volume of a sleeve as a fraction of total cylinder volume is $2\, r\, dr/R^2$.

Now introduce a quantity, q, of indicator into the inflow of the cylinder so that it is distributed immediately and uniformly over the entire cross-section of the inflow of the tube. Then the fraction of q in any sleeve, at any time, is the ratio of the volume of the sleeve to the volume of the cylinder, and the quantity of indicator in any sleeve is $2\, q\, r\, dr/R^2$. This quantity of indicator will reach the outflow site when it has traveled the length of the cylinder L, and since it does so at velocity $u(r)$, it will all appear at outflow between time t and $t + dt$, where $t = L/u(r)$. The quantity of fluid leaving the system between time t and $t + dt$ is $F\, dt$. The concentration of indicator leaving the system, as a function of time, is therefore the amount leaving in each sleeve divided by the quantity of fluid, or

$$c(t) = 2\, q\, r\, dr/R^2\, F\, dt \tag{50}$$

Equation 49 gives the radius r as a function of time. Differentiating equation 49,

$$du = -4\, F\, r\, dr/\pi R^4 = -L\, dt/t^2 \tag{51}$$

Substituting in equation 50 from equation 51,

$$c(t) = q\, V/2\, F^2\, t^2 \tag{52}$$

where V, the volume of the cylinder, is $\pi R^2 L$. Since $V/F = \bar{t}$, equation 52 becomes

$$c(t) = q\, \bar{t}/2\, F\, t^2 \tag{53}$$

Equation 53 must be restricted so that $c(t) = 0$ for t less than the appearance time. The appearance time is the time required by the fastest particles, those in the central stream with velocity $u_{max} = 2\ F/\pi R^2$, and is, therefore, $L/u_{max} = V/2\ F = \frac{1}{2}\ \bar{t}$.

Equation 53 also states that in parabolic flow the frequency function of transit times, $h(t)$, is $\bar{t}/2\ t^2$, since we have defined $h(t) = F\,c(t)/q$.

Equation 53 does not in fact resemble the concentration-time curve obtained with sudden-injection of indicator into a vascular bed. Unlike the experimental curve, which rises to a maximum and falls to zero, equation 53 describes a function which is monotone decreasing. Its greatest value is its initial value, occurring at appearance time $\frac{1}{2}\ \bar{t}$, and this maximum concentration is $2\ q/V$, as though all the indicator were suddenly mixed in half the volume of the cylinder. This is true because the assumptions were implicitly equivalent to stating that indicator was mixed in the volume of the contained paraboloid of revolution which is half the volume of the cylinder.

A derivation similar to Sheppard's has been made by Sherman *et al.* (29). However, instead of assuming that the velocity of the outermost sleeve was zero, they assumed that it had some positive value, u_o. The derivation, which need not be repoduced here, leads to

$$c(t) = q\ \bar{t}/2\ t^2\ (F - \pi R^2\ u_o) \tag{54}$$

which is identical with equation 53 when $u_o = 0$, and which applies only for $\bar{t}/2 \leqq t < L/u_o$. For $L/u_o < t$ and for $t < \bar{t}/2$, $c(t) = 0$.

Like equation 53, equation 54 describes a monotone decreasing function and, for the same reason, does not resemble a real indicator-dilution curve.

The unrealistic nature of equation 53 follows from the fact that the initial injectate was assumed to have been introduced at inflow into a volume $\pi\ R^2\ dx$ in which dx differed from zero by less than any arbitrarily small number, that is, the injectate had area but essentially no thickness. It was therefore distributed only as a thin skin forming the paraboloid of revolution.

Several attempts have been made to produce equations through parabolic flow systems which more nearly resemble real indicator-dilution curves. In general, the outcome depends on the exact nature of arbitrary boundary conditions which have been set by letting the injection bolus occupy a finite volume at inflow at zero time, for example, in the several solutions offered by Rossi *et al.* (24).

We will not follow their derivation but instead will treat the problem in a manner consistent with the general development used in this chapter, based on the fact that indicator concentration at outflow is the integral of convolutions. Recall equation 24,

$$C(t) = \frac{1}{F}\int_0^t i\ (t - s)\ h(s)\ ds$$

To illustrate the use of this equation for the case of parabolic flow, take the case in which indicator is introduced as a square wave, that is, the rate of injection, in units of mass/time, is constant, I, for a definite time, T. We have already established by equation 53 that $h(t)$ through a parabolic flow system is $\bar{t}/2\ t^2$, and that the appearance time is $\frac{1}{2}\ \bar{t}$.

We can therefore set boundary conditions:

$$i\ (t - s) = \begin{cases} 0,\ (t - s) < 0 \\ I,\ 0 \leqq (t - s) \leqq T \\ 0,\ (t - s) > T \end{cases} \tag{55}$$

$$h(s) = \begin{cases} 0,\ s < \frac{1}{2}\ \bar{t} \\ \bar{t}/2\ s^2,\ s \geqq \frac{1}{2}\ \bar{t} \end{cases} \tag{56}$$

These boundaries, applied to the convolution integral, lead immediately to the expressions of concentration:

$$C(t) = 0,\ t < \tfrac{1}{2}\ \bar{t} \tag{57}$$

$$\begin{aligned} C(t) &= \frac{1}{F}\int_{\bar{t}/2}^{t} I\ \frac{\bar{t}}{2\ s^2}\ ds,\ \frac{\bar{t}}{2} \leqq t \leqq \left(\frac{\bar{t}}{2} + T\right) \\ &= \frac{I}{F}\left(1 - \frac{\bar{t}}{2\ t}\right) \end{aligned} \tag{58}$$

$$\begin{aligned} C(t) &= \frac{1}{F}\int_{t-T}^{t} I\ \frac{\bar{t}}{2\ s^2}\ ds,\ t \geqq \left(\frac{\bar{t}}{2} + T\right) \\ &= \frac{I\ T\ \bar{t}}{2\ F\ t\ (t - T)} \end{aligned} \tag{59}$$

Equations 57, 58, and 59 describe concentration rising from zero to a peak (equation 58) and falling from that peak toward zero (equation 59). They are identical with one of the sets of equations developed by Rossi *et al.* (24).

If T is extended to t, equation 58 describes concentration during constant injection of indicator through a parabolic flow system and is asymptotic to I/F, as it must be if it is to be consistent with our general treatment of constant injection.

If T is decreased toward zero, the limits of equation 58 approach one another so that, for $T = 0$,

$C(t)$ vanishes. Thus, for $T = 0$ we are left with only equation 59 which has the limit $\lim_{T\to 0} C(t) = q\,\bar{t}/2\,F\,t^2$, where $\lim_{T\to 0} I\ T = q$. This result is exactly equation 53, which is therefore a special case of equations 58 and 59 for $T = 0$.

How pertinent is study of parabolic flow system to the real problem?

One obvious application is to the effect of the collecting catheter which is usually a single tube of uniform bore, though not necessarily straight. Even here, however, owing to perturbations at catheter input, if not also at output, and to the unusual rheological properties of blood, the description is not perfect. Sheppard *et al.* (28) used equation 53 and Sherman *et al.* (29) used equation 54 to examine the influence of the collecting catheter on the concentration-time curve. Sheppard *et al.* (28) also examined the effect of a collecting tube as a convoluter of a more complex input function, $i(t)$. $i(t)$ was generated experimentally by letting indicator flow through a labyrinth—a container filled with glass beads—from which it appeared as the input into a straight tube.

Sherman *et al.* (29) proposed what they called "a figure of merit" for catheter sampling systems. In order to give satisfactory resolution of indicator concentration with respect to time in systems in which rather abrupt changes occur, as in pulsatile systems, regurgitant flow, pulsatile pump models of the circulation, and so on, the smearing effect of the catheter on the concentration-time curve should be less than the interval between important changes in indicator input to the catheter. Their meritorious figure is "the volume of the catheter divided by twice the flow rate." This, of course, is exactly $\frac{1}{2}\,\bar{t}$ which is, as we have seen, the appearance time through a parabolic flow system. In terms of the convolution equation, recalling that $h(t)$ for a catheter with nonturbulent flow is $\bar{t}/2\ t^2$, then as $\bar{t}$ goes to zero, $h(t)$ disappears and the input is not distorted. The implication is that flow through the catheter should be as large as possible and the volume of the catheter as small as possible.

Do these considerations of parabolic flow systems apply to real vascular beds? Obviously, although, except for transient eddies at branches, blood flow through vascular beds is nonturbulent, it does not obey the simple law evolved here. Nevertheless, using $h(t) = \bar{t}/2\ t^2$ as a first approximation, we may ask what effect there is on indicator concentration when indicator is made to flow through tubes in parallel and in series.

Consider parabolic flow through parallel tubes. A quantity, q, of indicator is introduced at a common inflow at time zero and thoroughly mixed with inflowing fluid. It is carried immediately to one or another of parallel branches in proportion to the relative flow through each branch. Thus the rate at which indicator enters the i-th branch is $q\ F_i/F\ dt$, where F_i is flow through the i-th branch and F is total flow through the system. The fraction of indicator particles leaving the i-th branch per unit time between time t and $t + dt$ is $q\ F_i\ h_i(t)/F$, where $h_i(t) = \bar{t}_i/2\ t^2$. Indicator particles exiting from the i-th branch immediately merge with total flow, so that the contribution to indicator concentration at outflow from the i-th branch is

$$C_i(t) = \begin{cases} 0, & t < \frac{1}{2}\,\bar{t}_i \\ \dfrac{q\ F_i\ \bar{t}_i}{2\ F^2\ t^2}, & t \geq \frac{1}{2}\,\bar{t}_i \end{cases}$$

where $\bar{t}_i$ is mean transit time through i-th branch.

Contributions from all parallel branches are additive, so that the observed concentration at outflow, summed for a system of n branches, is

$$\begin{aligned} C(t) &= C_1(t) + C_2(t) + \cdots + C_n(t) \\ &= \frac{q}{2\ F^2\ t^2} \sum_{i=1}^{n} F_i\ \bar{t}_i \\ &= \frac{q}{2\ F^2\ t^2} \sum_{i=1}^{n} V_i \end{aligned} \tag{60}$$

where V_i, the volume of the i-th branch, $= F_i\ \bar{t}_i$, and where $C(t) = 0$, $t < \frac{1}{2}\,\bar{t}_2$, the shortest appearance time in the system. Since the total volume of the system $V = \sum_{i=1}^{n} V_i$, then once all branches have begun to contribute to outflow, $C(t) = q\ V/2\ F^2\ t^2 = q\ \bar{t}/2\ F\ t^2$, $t \geq \frac{1}{2}\,\bar{t}_n$, the longest appearance time in the system.

Thus, as soon as the initial transients have been completed and all branches are contributing indicator, the system of parallel tubes with parabolic flow behaves as though it were a single tube with parabolic flow, of volume V and mean transit time $\bar{t}$.

Concentration in a parallel tube system is illustrated in figure 11.

Now consider parabolic flow systems in series. The output from one tube is the input to a second tube. Concentration at output from the second tube is the integral of the convolution of the distribution function through parabolic systems.

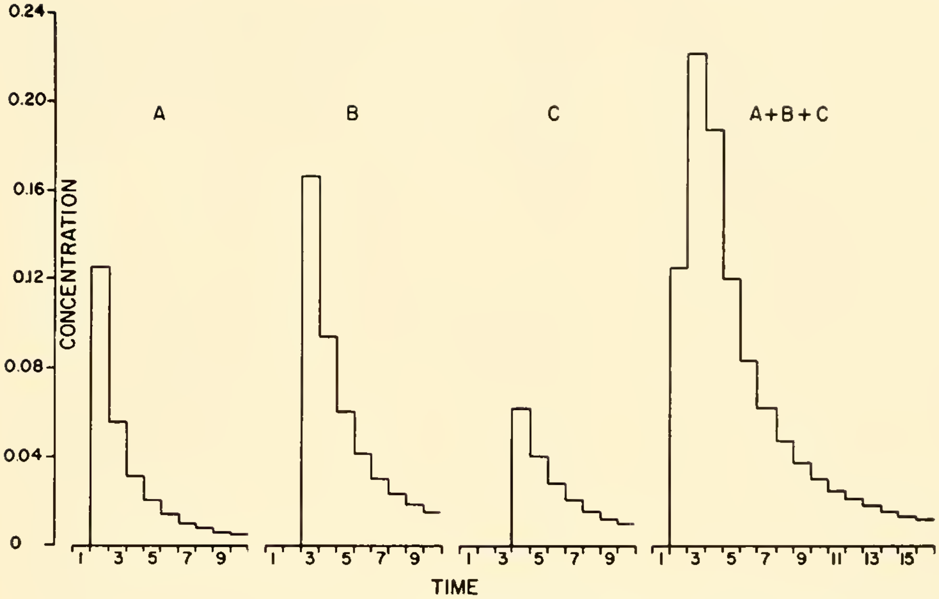

FIG. 11. Histogram of distribution of concentration of indicator as function of time through three branches, A, B, and C and through common output, $A + B + C$, of parallel branch system. Frequency function through A, B, and C is that of parabolic flow system. Mean transit time shortest through A, longest through B. Areas drawn so that $1/4$ of total flow goes through A, $1/2$ through B, $1/4$ through C. Appearance time and time at which peak concentration occurs coincide for each of the three branches, but not for the summated output, because the branches do not all have the same appearance time. The ordinate for A, B, and C is not the concentration within the individual channel but is the output from the individual channel divided by the total flow through all three channels.

Therefore,

$$C(t) = \begin{cases} 0, \ \bar{t} < \dfrac{\bar{t}_1 + \bar{t}_2}{2} \\ \dfrac{q\,\bar{t}_1\,\bar{t}_2}{4\,F_1} \displaystyle\int_0^t \frac{1}{(t-s)^2} \cdot \frac{1}{s^2} \cdot ds \quad t \geq \dfrac{\bar{t}_1 + \bar{t}_2}{2} \end{cases} \tag{61}$$

where subscripts 1 and 2 refer, respectively, to tube entered first and second. The integral in equation 61 is deceptively simple. It cannot be integrated over the limits set and its Laplace transform cannot be inverted readily. It can, however, be computed, and it appears to assume at least a quasi-exponential form.

A system of dichotomous branching or of Y-tubes is simply a combination of series and parallel tubes, the solution of which is obtained by combining equations 60 and 61. The downlimb of the resulting concentration curve will, after a sufficiently long time, assume the characteristics of the downlimb of equation 61.

Parrish *et al.* (22), by an analog computer technique to which reference was made in a previous section, obtained the admittance function of the pulmonary vascular bed in dogs and found it compatible with that of a system through which there was laminar flow, rather than with that of a system in which there was a single well-stirred pool.

Random Walk and Other Probability Functions

On the grounds that real vascular beds are randomizing nets, too complicated for assessment of the contribution of each of the factors tending to distribute indicator, Sheppard (26–28) has introduced and discussed critically the application of several probability functions.

One of the most interesting of these is the one-dimensional random walk, although it has failed to describe indicator dilution curves in several important details. The one-dimensional random walk is constructed as follows.

Consider a number, n, of chambers of equal size and shape, connected in series by tubes of negligible volume. Place indicator in the first chamber. By some means or other, the exact nature of which need not concern us, after a number of discrete jumps in random directions, an indicator particle will find its way into the second chamber. After another series of jumps the indicator particle may have

returned to the first chamber or may have advanced to the third chamber, or beyond. Now if we let fluid flow through the system in the direction from the first to the n-th chamber, the probability of indicator particles moving in the direction of fluid flow, rather than in any other direction, is increased, that is, the random walk of indicator particles tends to be in one direction or is one-dimensional. If an indicator particle must take a large number of jumps, or make many trials, in order to score a success, that is, in order to advance to the next chamber, the probability of success increases uniformly with the number of trials according to the Poisson distribution, and, since each jump requires time, the probability that a given indicator particle will escape from one chamber to the next, and so on through the series to the outflow from the n-th chamber, is a function of time. We can therefore consider transit time as a substitute for the required number of successes.

If now we let the volume of each chamber, dV, approach zero and the number of chambers approach infinity, the Poisson distribution does not apply because the number of jumps required to move from one chamber to the next becomes small. Sheppard (27) predicts a Gaussian distribution for the number of successes from one element of volume to the next. The Gaussian input to the second element of volume must pass through a Gaussian distribution in order to escape to the third element of volume, and so on. The probability of advancing from one element of volume to the next is still increased by the fact that this is the direction in which the mother fluid flows. In this way the distribution function becomes skew and the standard deviation of transit times spreads out. The standard deviation of transit times is a characteristic of the vascular bed, related to the distribution of flow through the volume. Sheppard introduces a randomizing constant, K, which is $\sqrt{2} \times$ standard deviation of transit times, as a measure of this characteristic distribution, and the dimensionless variable, τ, which is the fraction of the volume displaced by the flow from time zero to some time between t and $t + dt$. That is, $\tau = F\,t/V = t/\bar{t}$, or τ is transit time as a fraction of mean transit time. (Note that this is an equivalent definition of mean transit time. When $t = \bar{t}$, the volume displaced by the flow is exactly the volume of the system.) The indicator-distribution model which Sheppard uses is obviously related closely to that used by Einstein (8) for study of Brownian movement, and the solution, provided by Einstein in 1905 is

$$h(\tau) = \frac{e^{-(1-\tau)^2/K^2\tau}}{K\sqrt{\pi}\,\tau^{3/2}} \tag{62}$$

The exponent of e contains the factor $(1 - \tau)$, which is $(\bar{t} - t)/\bar{t}$, that is, it is a measure of the difference between the time required by those particles which take some time between t and $t + dt$ to traverse the system and the mean transit time.

Equation 62 contains two constants, K and V, the latter being implicit in the variable $\tau = F\,t/V$, where it is assumed that F can be measured correctly in the usual way from the area under the curve. The job of examining the closeness with which equation 62 describes an indicator-dilution curve boils down to empirical selection of values for K and V by curve-fitting. Despite the advantage of having not one but two constants to adjust, although some indicator-dilution curves could be well matched, in general Sheppard had to select values for V which were smaller than the known values and he had to displace the time axis to an arbitrary zero. Sheppard concludes that in real vascular beds the probability of successes is not constant as indicator moves along the system from one type of vessel to another o different diameter, and so on, whereas equation 62 depends on the assumption of constant probability of success.

Sheppard's distribution function can of course be convoluted upon others, a parabolic flow distribution, for example, which he has done successfully for certain models.

Other known probability functions might be tested. Sheppard (25) originally pointed out that sudden-injection indicator-dilution curves resemble the normal error function plotted on a logarithmic time scale. Stow & Hetzel (36) pursued this suggestion and, by analogy with the error function, offered the following expression for concentration of indicator:

$$C(t) = C_p\, e^{-k\, \ln^2 r} \tag{63}$$

where C_p is concentration at the peak of the observed curve, $r = (t - a)/(p - a)$, where a is appearance time and p is time at which C_p occurs, and k is a constant for which a value is obtained by plugging in an observed value for C at any convenient t. They reported reasonably good agreement between observed curves (through the central circulation in man) and those predicted from equation 63. The downlimb of equation 63 falls more rapidly than Hamilton's simple exponential, so that the area under the curve extrapolated by equation 63 is less than that under the curve extrapolated by Hamilton's method, and the flow estimated by the former is therefore greater.

It is difficult to accept any of these extrapolations. If a method of extrapolation yields a good fit with

an observed curve in which recirculation is not prominent, it does not follow that the same distributive law holds in those cases in which recirculation is prominent (and in which goodness of fit cannot be tested), nor that it holds for other vascular beds.

WASHOUT FROM A MIXING CHAMBER

When Hamilton *et al.* (17) discovered that the downlimb of the sudden-injection indicator-dilution curve from the dog heart-lung preparation could be fitted by a simple exponential they recognized the model which the fit described. Whenever a quantity decays exponentially, the equivalent statement is that the rate of decay is proportional to the amount remaining.

Consider a container of volume, V, filled with fluid and constantly well stirred. Introduce a quantity, q_o, of indicator into the container at zero time. Its concentration is q_o/V. Now let fluid begin flowing through the container at constant rate, F, in such a way as to mix it immediately and thoroughly with the contents of the container. Indicator remaining in the container at time t is $q(t)$ and its concentration is $q(t)/V$. The rate at which indicator leaves the container is $F\ q(t)/V$, but this is also the rate at which the quantity of indicator remaining in the container decreases, or

$$-\frac{d\ q(t)}{dt} = \frac{F}{V}\, q(t) = F\, C(t) \tag{64}$$

On integration this yields

$$C(t) = C_0\, e^{-\frac{F}{V}t} \tag{65}$$

where $C_0 = q_o/V$.

Newman and his colleagues (21) suggested that equation 65 could be used to measure the volume of the segment of the cardiovascular system through which indicator flowed. The slope, k, of the exponential downlimb is determined graphically, equated to F/V. F is determined in the conventional manner from the relation $F = q \int_0^\infty C(t)\ dt$, and V is obtained.

It is obvious, however, that equation 65 is decidedly not the usual indicator-dilution curve. It begins at time zero, at which it is maximum, and falls monotonically. If appearance time, a, is included in the model, equation 65 becomes a lag exponential of the form

$$C(t) = \begin{cases} 0, & t < a \\ C_a\, e^{-k\,(t-a)}, & t \geq a \end{cases} \tag{66}$$

where C_a is concentration for $t = a$ and is not, as we shall see, q_o/V.

When $a = 0$, k is indeed $1/\bar{t}$, not only because $\bar{t} = V/F$, and so the relation follows from the development of equation 65, but also because $\bar{t}$ of an exponential is $1/k$, as can be shown by multiplying both sides of equation 65 by t, integrating between $t = 0$ and $t = \infty$, and dividing by q/F.

This relation is not true for a lag exponential. When $\bar{t}$ is determined from equation 66, $k = 1/(\bar{t} - a)$. If k is now equated falsely with F/V, the estimate of V will be too small. For example, $\bar{t}$ is usually approximately equal to $2\ a$ for the central circulation in dog and in man. For $\bar{t} = 2\ a$, k in equation 66 equals $2\ F/V$, that is, the volume falsely estimated from the downslope k is only half the real volume.

Furthermore, as we have hinted, C_a in equation 66 is not the initial quantity of indicator divided by the volume. The proof follows.

Recall that, because all the indicator must come out eventually, $q = F\int_0^\infty C(t)\ dt = C_a\ F\int_a^\infty e^{-k\,(t-a)}\ dt$. Equating the integral on the right to $q/F\ C_a$ and integrating, $C_a = q\ k/F$. But $k = 1/(\bar{t} - a)$. Therefore,

$$Ca = q/(V - a\ F)$$

That is, the initial concentration, C_a, of an indicator-dilution curve which is a lag exponential, is greater than q/V.

Let us examine the physical meaning of this more closely. If we have two exponential curves which are superimposable, except that one is maximum at zero time and one is displaced in time so that its maximum (and first non-zero) value is at time a, then $C_0 = C_a$, where C_0 is the value of the concentration at zero time for the first curve and C_a is the value at time a for the lag exponential. Since the slope, k, is the same for the two curves, $k = 1/\bar{t}_1 = 1/(\bar{t}_2 - a)$, where subscript 1 refers to the first curve (beginning at $t = 0$) and subscript 2 refers to the second curve (beginning at $t = a$). Therefore, $\bar{t}_1 = \bar{t}_2 - a$. If the flow through the two systems is the same, then the volumes must be unequal. Then, $\bar{t}_1 = V_1/F$, $\bar{t}_2 = V_2/F = \bar{t}_1 + a$. Whence $V_2 = V_1\ \bar{t}_2/(\bar{t}_2 - a)$, that is, V_2 is larger than V_1. If the initial quantity of indicator is dissolved in V_2 so that its concentration $C_a = C_0 = q/V_1$, it cannot, therefore, be distributed evenly through V_2. Indeed this is the physical meaning of the lag in the lag exponential. During the lag period, a, a volume of fluid equal to $a\ F$, flows out of the system. The indicator is therefore distributed initially only in a quiescent volume equivalent to the difference between the total volume and the volume $a\ F$ which escapes the system.

Thus, the notions that $k = F/V$ and that the initial concentration is q/V are incompatible with a lag exponential.

One can consider the effect of connecting mixing volumes in series and in parallel. The argument is the same as that advanced earlier for parabolic flow systems. In parallel circuits, output concentrations are simply additive. As in the case of parallel parabolic flow systems (see fig. 11), the final curve will reflect the distribution of mean transit times among the members of the parallel system, and the downlimb after sufficiently long time will assume the slope of that container through which mean transit time is longest, although this might not occur until quite late. The equation describing concentration is the sum of n exponentials, each of the form of equation 66, where there are n parallel containers.

Newman *et al.* (21) have considered the effect of series connections of instantaneous mixing containers and proposed that the downslope of the concentration-time curve at outflow is determined by that container for which k is least, and, since they equate k to F/V, for which V is greatest.

We examine this proposal by applying the convolution equation 24, $C(t) = 1/F\int_0^t i(t - s)\, h(s)\, ds$. Output from the first container, of volume V_1, is, from equation 66, $F\ C_1(t) = F\ C_{a_1}e^{-k_1(t-a_1)}$, and this is the input, $i(t)$, to the second container. The subscript, 1, refers to properties of the first container. The distribution function, $h(t)$, is obtained from the relation, equation 6, $h(t) = F\ c(t)/q$. Substituting for $c(t)$ in equation 66, the distribution function, $h_2(t)$, through the second container in the series is $h_2(t) = (F\ C_{a_2}/q)e^{-k_2(t-a_2)}$. Concentration of indicator at outflow from the second container is therefore

$$c(t) = \frac{1}{F}\int_{(a_1+a_2)}^{t} F\, C_{a_1}\, e^{-k_1(t-a_1-s)} \cdot \frac{F\, C_{a_2}}{q} \cdot e^{-k_2(s-a_2)}\, ds$$

where $C_{a_1} = q/(V_1 - a_1 F)$ and $C_{a_2} = q/(V_2 - a_2 F)$.

Integration yields

$$C(t) = \frac{F\, C_{a_1} C_{a_2} e^{k_2 a_2 + k_1 a_1}}{q\ (k_2 - k_1)} \left(e^{-(k_2-k_1)(a_1+a_2)-k_1 t} - e^{-k_2 t}\right) \tag{67}$$

Equation 67 states that, for two instantaneous-mixing containers connected in series, indicator concentration at outflow is proportional to the difference between two exponentials as a function of time. The curve has an appearance time $(a_1 + a_2)$, rises to a maximum at time $t = a_1 + a_2 + 1/(k_2 - k_1)$ ln k_2/k_1, if $k_2 \neq k_1$, and falls with time, ultimately at a rate determined largely by the smaller of the values k_1 and k_2.

Equation 67 differs from that given by Newman *et al.* (21) (their equation 9), but can be reduced to the form which they offer if k_1 is set to equal F/V_1, k_2 is set to equal F/V_2, and C_{a_1} and C_{a_2} are made equal to q over the respective values of V, and a_2 equals zero, that is, they permitted the indicator to take a finite time to traverse the first container but not the second. Again, k_1 will equal F/V_1 and k_2 will equal F/V_2 only if a_1 and a_2 are zero. In the physical models which they studied, appearance time was small compared to mean time, so that the approximation which they used gave a reasonably good agreement with the observed curve. When appearance times are negligible and when $k_1 \ll k_2$, then the downslope is approximately described by $k_1 = F/V_1$, where V_1 is the larger volume, or by $k_2 = F/V_2$, where $k_1 \gg k_2$ and V_2 is the larger volume.

Newman and his colleagues have used this method for estimating volume through which indicator is injected following its sudden-injection into cardio-pulmonary or central circulatory system. The volume estimated by the slope method, $V = k/F$, is less than that estimated by the conventional method, $V = F\,\bar{t}$. Nor is it correct to say that this is so because they are measuring only the largest volume in a series of instantaneous-mixing chambers. Because appearance time is a large fraction of mean transit time their assumption that $k_1 = F/V_1$ is apt to be erroneous. Finally, if any parts of the cardiovascular system behave like instantaneous mixing chambers, they ought to be chambers of the heart, distribution through the pulmonary vascular bed can hardly fit the simple model of a single continuously stirred chamber.

We may ask what the indicator concentration-time curve looks like when an instantaneous mixing chamber is placed in series with an unspecified distribution function, $h(t)$.

$$C(t) = \frac{q\ k}{F}\int_a^t e^{-k\,(t-a-s)}\, h(s)\, ds$$

$$= \frac{q\ k}{F}\, e^{-k\,(t-a)} \int_a^t e^{k\,s}\, h(s)\, ds$$

Obviously, although the shape of the concentration-time curve cannot be predicted without knowledge of $h(t)$, it would be surprising if after sufficiently long time the downlimb did not resemble an exponential

form, but its slope would not, in general, be related to the volume through which the distribution function is exponential.

For example, if $h(t)$ is the distribution function through a parabolic flow system, $\bar{t}/2\ t^2$, then for an instantaneous mixing chamber in series with a parabolic flow system,

$$C(t) = \frac{q\,k}{F} \int_b^t e^{-k\,(t-a-s)}\,\frac{\bar{t}_2}{2\,s^2}\,ds$$

where b is over-all appearance time ($= a + \frac{1}{2}\,\bar{t}_2$) and $\bar{t}_2$ is mean transit time through the parabolic flow system. Integration yields $C(t)$ as an infinite series:

$$C(t) = \frac{q\,k\,\bar{t}_2}{2\,F}\left(\frac{e^{-k\,(t-a-b)}}{b} - \frac{e^{-k\,a}}{t} + k\,e^{-k\,(t-a)}\left[\ln t/b + \frac{k\,(t-b)}{1\,!} + \frac{k^2\,(t^2-b^2)}{2\cdot 2\,!} + \frac{k^3\,(t^3-b^3)}{3\cdot 3\,!} + \cdots\right]\right)$$

For $t = b$, $C(b) = 0$, and the limit of $C(t)$ as $t \longrightarrow \infty$ is also zero. A clearer notion of the function follows from inspection of its derivative which simplifies to

$$\frac{d\,C(t)}{dt} = \frac{q\,k\,\bar{t}_2\,e^{k\,a}}{2\,F\,t^2} - k\,C(t) \tag{68}$$

When $t = b$, $d\,C(t)/dt = q\,k\,\bar{t}_2\,e^{k\,a}/2\,F\,b^2 > 0$, that is, $C(t)$ increases from zero. It reaches a maximum value at $C(p) = q\,\bar{t}_2\,e^{k\,a}/2\,F\,p^2$, from which it will fall more slowly than a simple exponential, owing to the positive term in the right-hand member of equation 68.

MODELS CONCERNED ONLY WITH THE HEART

If indicator distribution is limited to the chambers of the heart, then Newman's model becomes more plausible, and may do very well as a first approximation despite evidence that mixing of blood is indeed not complete and immediate in the right ventricle. Interest in this application has been stimulated by clinical concern for a method with which to quantify valvular incompetence and the amount of regurgitant flow from one chamber back to another.

For the simplest case, which will suffice to demonstrate the nature of the general argument, consider that an amount of indicator, q, is introduced into a ventricle during diastole. The end diastolic volume, with which indicator is assumed to be mixed completely, is V. During systole a quantity of blood, V_E, is ejected forward and there is no regurgitation. At the end of systole there remains in the ventricle a volume $V_R = V - V_E$. During diastole, a volume equal to V_E, containing no indicator, flows from the auricle into the ventricle. The concentration of indicator at time zero, at the end of diastole, is q/V. A quantity $q\ V_E/V$ is ejected with the first systole. Therefore a quantity $q - q\,(V_E/V) = q\,[1 - (V_E/V)]$ remains in the ventricle. By the end of the first diastole this is distributed in a volume V at concentration $[1 - (V_E/V)]\ q/V$. During the second systole, a quantity $(q\ V_E/V)[1 - (V_E/V)]$ is ejected, and the quantity remaining is $q\,[1 - (V_E/V)] - q\ V_E/V\,[1 - (V_E/V)] = q\,[1 - (V_E/V)]^2$. During the i-th diastole the quantity of indicator remaining in the ventricle is $q\,[1 - (V_E/V)]^i$ and its concentration during the i-th systole is $q/V\,[1 - (V_E/V)]^i = q/V\ (V_R/V)^i$. If the heart rate is constant at, say, k beats per unit time, then the concentration of indicator at ventricular outflow during systolic ejection is $C(t) = q/V\ (V_R/V)^{t\,k}$, where for $n\ k \leqq t < (n + 1)\ k$, and n is an integer, t assumes the value of n.

As the situation is permitted to become more complicated, by introducing regurgitant flow, for example, concentration will appear as the sum of various combinations of volume, each term, in general, containing t as a factor in the exponent. (Actually, the exponent is dimensionless because k has dimension 1/time. In fact, because flow equals stroke volume and beats per unit time, $F = k\ V_E$, and k, therefore, is $1/\bar{t}$.)

A neat solution for a two-chambered system, including regurgitant flow, is given by McClure and his colleagues (18).

SUMMARY

When an indicator is introduced into a flow system in such a way as to be distributed at once throughout the inflow (for sudden-injection, concentration at inflow is $q/F\ dt$; for constant-injection, concentration at inflow is I/F), then, providing it does not recirculate before the concentration at outflow has returned to zero, the curve of its concentration as a function of time is exactly the shape of the distribution function of transit times through the system. The area under the sudden-injection indicator-concentration-time curve, in the absence of recirculation, is q/F, and so provides a measure of flow. The maximum, and plateau, concentration of

the constant-injection curve is I/F, and so provides a measure of flow. The volume of the system through which indicator is distributed is always equal to the flow multiplied by the mean transit time, providing the assumptions are met. If recirculation occurs before the concentration has returned to zero (for sudden-injection) or before the concentration has reached a plateau (for constant-injection), the problem may be handled in one of two ways. The curve reflecting events of the first circulation may be extrapolated in some arbitrary manner (say, by assuming that it is exponential) if recirculation is so late that the area under the curve (for sudden-injection) is already almost q/F. If recirculation occurs early, no arbitrary extrapolation is apt to be accurate (although flow may be estimated in restricted cases by empirical formulas) and the experiment must be redesigned to include recirculation in the theory and use one or another of the methods which depend upon sampling from two sites or injecting and sampling at two sites.

Because sudden-injection is not really instantaneous, the mean transit time of indicator particles, estimated from indicator concentration at outflow, is an overestimate of that mean transit time which is characteristic of the native fluid in the system under study. Therefore, volume is overestimated. If the mean time of the injection process is a relatively large part of the mean transit time through the system the error may be important, as in the case of measurement of plasma volume within the kidney. Similarly, the mean time of the collecting device may be long compared to the mean transit time through the bed under study and so lead to overestimate of volume. Since mean times are additive, the mean time of the injection process, measured, for example, by replicate injection into a system of known flow and volume and the mean time of the collecting device, equated to its volume divided by known flow through it, are simply subtracted from the experimental mean time of the indicator concentration-time curve. If the true mean transit time through the system proves to be, by this correction, a small difference between two large numbers, the result may be unreliable.

It is not likely that any arbitrary distribution function of transit times, stochastic or empirical, will describe the distribution function as well as the properly obtained indicator concentration-time curve. The beauty of it is that with each experiment the distribution of transit times through the bed under study is written for the investigator by the indicator-dilution curve.

REFERENCES

1. Allen, C. M., and E. A. Taylor. The salt velocity method of water measurement. *Mech. Engineering* 46: 13, 1924.
2. Andres, R., K. L. Zierler, H. M. Anderson, W. N. Stainsby, G. Cader, A. S. Ghrayyib, and J. L. Lilienthal, Jr. Measurement of blood flow and volume in the forearm of man; with notes on the theory of indicator-dilution and on production of turbulence, hemolysis, and vasodilatation by intra-vascular injection. *J. Clin. Invest.* 33: 482, 1954.
3. Burger, H. C., Y. van der Feer, and J. H. Douma. On the theory of cardiac output measurement by the injection method. *Acta cardiol.* 11: 1, 1956.
4. Cheesman, R. J., J. M. González-Fernández, and E. H. Wood. Experimental studies on a new method of analysis of indicator-dilution curves. *Physiologist* 2 (No. 3): 23, 1959.
5. Dow, P. Dimensional relationships in dye-dilution curves from humans and dogs, with an empirical formula for certain troublesome curves. *J. Appl. Physiol.* 7: 399, 1955.
6. Dow, P., P. F. Hahn, and W. F. Hamilton. The simultaneous transport of T-1824 and radioactive red cells through the heart and lungs. *Am. J. Physiol.* 147: 493, 1946.
7. Dow, P. Estimations of cardiac output and central blood volume by dye dilution. *Physiol. Rev.* 36: 77, 1956.
8. Einstein, A. On the movement of small particles suspended in a stationary liquid demanded by the molecular-kinetic theory of heat. *Ann. der Physik* 17: 549, 1905. (English translation in: Einstein, A. Investigations on the theory of Brownian movement. New York: Dover Publications, 1956.)
9. Fries, E. D., J. R. Stanton, and C. P. Emerson. Estimation of relative velocities of plasma and red cells in the circulation of man. *Am. J. Physiol.* 157: 153, 1949.
10. Hamilton, W. F., J. W. Moore, J. M. Kinsman, and R. G. Spurling. Simultaneous determination of the greater and lesser circulation time, of the mean velocity of blood flow through the heart and lungs, of the cardiac output and an approximation of the amount of blood actively circulating in the heart and lungs. *Am. J. Physiol.* 85: 377, 1928.
11. Hamilton, W. F., J. W. Moore, J. M. Kinsman, and R. G. Spurling. Simultaneous determination of the pulmonary and systemic circulation times in man and of a figure related to the cardiac output. *Am. J. Physiol.* 84: 338, 1928.
12. Hamilton, W. F., J. W. Moore, J. M. Kinsman, and R. G. Spurling. Studies on the circulation. IV. Further analysis of the injection method and of changes in hemodynamics under physiological and pathological conditions. *Am. J. Physiol.* 99: 534, 1932.
13. Hamilton, W. F., and J. W. Remington. Comparison of

the time concentration curves in arterial blood of diffusible and nondiffusible substances when injected at a constant rate and when injected instantaneously. *Am. J. Physiol.* 148: 35, 1947.

14. Hering E. Versuche, die Schnelligkeit des Blutlaufs und der Absonderung zu bestimmen. *Ztschr. Physiol.* 3: 85, 1829.
15. Hetzel, P. S., H. J. C. Swan, A. A. Ramírez de Arellano, and E. H. Wood. Estimation of cardiac output from the first part of arterial dye-dilution curves. *J. Appl. Physiol.* 13: 92, 1958.
16. Keys, J. R., P. S. Hetzel, and E. H. Wood. Revised equations for calculations of blood flow and central blood volume from indicator-dilution curves. *J. Appl. Physiol.* 11: 385, 1957.
17. Kinsman, J. M., J. W. Moore, and W. F. Hamilton. Studies on the circulation. I. Injection method: physical and mathematical considerations. *Am. J. Physiol.* 89: 322, 1929.
18. McClure, J. A., W. W. Lacy, P. Latimer, and E. V. Newman. Indicator dilution in an atrioventricular system with competent or incompetent valves. A complete analysis of the behavior of indicator injected instantaneously or continuously into either chamber. *Circulation Res.* 7: 794, 1959.
19. Meier, P., and K. L. Zierler. On the theory of the indicator-dilution method for measurement of blood flow and volume. *J. Appl. Physiol.* 6: 731, 1954.
20. Moore, J. W., J. M. Kinsman, W. F. Hamilton, and R. G. Spurling. Studies on the circulation. II. Cardiac output determinations; comparison of the injection method with the direct Fick procedure. *Am. J. Physiol.* 89: 331, 1929.
21. Newman, E. V., M. Merrell, A. Genecin, C. Monge, W. R. Milnor, and W. P. McKeever. The dye dilution method for describing the central circulation. An analysis of factors shaping the time-concentration curves. *Circulation* 4: 735, 1951.
22. Parrish, D., D. T. Hayden, W. Garrett, and R. L. Huff. Analog computer analysis of flow characteristics and volume of the pulmonary vascular bed. *Circulation Res.* 7: 746, 1959.
23. Paynter, H. M. Methods and results from M.I.T. studies in unsteady flow. *J. Boston Soc. Civil Engrs.* 39: 120, 1952
24. Rossi, H. H , S. H. Powers, and B. Dwork. Measurement of flow in straight tubes by means of the dilution technique. *Am. J. Physiol.* 173: 103, 1953.
25. Sheppard, C. W. Synthesis of dye dilution curves. *Am. J. Physiol.* 171: 767, 1952.
26. Sheppard, C. W. Mathematical considerations of indicator dilution techniques. *Minnesota Med.* 37: 93, 1954.
27. Sheppard, C. W. An electromathematical theory of circulatory mixing transients. *Proc. First National Biophysics Conference* New Haven: Yale Univ. Press, 1959, p. 476.
28. Sheppard, C. W., M. P. Jones, and B. L. Couch. Effect of catheter sampling on the shape of indicator-dilution curves. Mean concentration versus mean flux of outflowing dye. *Circulation Res.* 7: 895, 1959.
29. Sherman, H., R. C. Schlant, W. L. Kraus, and C. B. Moore. A figure of merit for catheter sampling systems. *Circulation Res.* 7: 303, 1959.
30. Stephenson, J. L. Theory of the measurement of blood flow by the dilution of an indicator. *Bull. Math. Biophys.* 10: 117, 1948.
31. Stewart, G. N. Researches on the circulation time in organs and on the influences which affect it. Parts I–III. *J. Physiol.* 15: 1, 1893.
32. Stewart, G. N. Researches on the circulation time and on the influences which affect it. IV. The output of the heart. *J. Physiol.* 22: 159, 1898.
33. Stewart, G. N. *A Manual of Physiology.* 8th ed. New York: William Wood. 1918. p. 135.
34. Stewart, G. N. The output of the heart in dogs. *Am. J. Physiol.* 57: 27, 1921.
35. Stewart, G. N. The pulmonary circulation time, the quantity of blood in the lungs and the output of the heart. *Am. J. Physiol.* 58: 20, 1921.
36. Stow, R. W., and P. S. Hetzel. An empirical formula for indicator-dilution curves as obtained in human beings. *J. Appl. Physiol.* 7: 161, 1954.
37. van der Feer, Y. The measurement of circulation time by means of an indicator. *Phys. in Med. Biol.* 3: 157, 1958.
38. Zierler, K. L. A simplified explanation of the theory of indicator-dilution for measurement of fluid flow and volume and other distributive phenomena. *Bull. Johns Hopkins Hosp.* 103: 199, 1958.

Mathematical treatment of uptake and release of indicator substances in relation to flow analysis in tissues and organs[1]

JAMES S. ROBERTSON | *Medical Research Center, Brookhaven National Laboratory, Upton, Long Island, New York*

CHAPTER CONTENTS

[1] Research supported by the U. S. Atomic Energy Commission.

THE GENERAL PRINCIPLES of the use of indicators, or tracers, have long been familiar to circulation physiologists. Measurement of blood volume, cardiac output, and regional blood flow rates, and the diagnosis of certain circulatory defects represent some of the major areas of application which have been developed with the use of dyes, gases, and other materials. In the preceding chapter, Zierler (74) discusses in detail the theory and historical development of the indicator dilution methods for determining blood flow. Several other methods such as mechanical and thermal stromuhrs are also available for measuring flow rates.

At least in part, because of the multiplicity of methods applicable to blood flow studies and to the successful uses of the older methods in circulatory studies, the relatively recent availability of isotopic tracers has had less, or at least less obvious, impact on circulatory physiology than it has had in some other branches of physiology, where the concept of the dynamic state of body constituents and numerous

studies of transmembrane transport processes may be cited as examples in which isotopic tracers have opened to investigation areas previously regarded as being inaccessible. On the contrary, the circulatory kinetic features known from the classical methods have been of value in the interpretation of tracer data obtained in studies of the turnover rates of various tissue constituents.

RELATIONSHIP BETWEEN EXCHANGE RATES AND BLOOD FLOW RATES

The blood is perhaps the most continuously busy tissue in the body. As it rushes through the capillaries, delivering food and oxygen to the other tissues while receiving various metabolic products from them, it carries chemical messages from one tissue to another and achieves numerous tasks related to the body's defense against infection, regulation of temperature, etc. With all this activity under way, it is nevertheless true that samples of the blood will show a remarkable constancy of composition with respect to most constituents. Although, for example, there is an incessant exchange of water and electrolytes between the blood and the tissues, simple chemical analyses of the blood give no indication that anything is happening. Study of the rates of exchange of many substances between the circulation and the various tissues by nontracer methods is very difficult to impossible, and such techniques as disturbing the normal state in order to observe the consequences are often open to the criticism of being "unphysiological."

Studies of isotopically labeled forms of normal constituents of the blood, particularly water and the electrolytes, however, readily demonstrate that there is in fact a rapid and continuous exchange of many of these substances between the blood and the extravascular volumes.

The rates of transfer or exchange of some substances are limited by the degree of permeability of the capillary walls. For others, however, the rates of exchange across the capillary walls are very rapid relative to the blood flow rate, so that the latter is the limiting or rate-governing process for exchange of these substances between the total blood volume (as distinct from the blood in the capillaries only) and the extravascular volumes. Thus, to the extent that the rates of exchange of substances between the circulation and the tissues are limited by the tissue blood perfusion rates, measurement of the "effective" exchange rates with tracers provides a convenient method for determining the blood flow rates. (The "effective" exchange rate measures the blood-tissue exchange and should not be confused with the true transcapillary exchange rate, which may be much faster.)

PURPOSE, SCOPE, AND LIMITATIONS OF THIS CHAPTER

The present chapter is written in the belief that much more remains to be achieved and can be achieved with isotopic tracers, particularly with radioactive isotopic tracers, in circulatory studies. The use of radioisotopic tracers in some static measurements (red cell mass, plasma volume) has become standard practice. There is even more reason to use isotopic labels in kinetic studies where, in addition to the advantages of convenience, sensitivity, and accuracy, their use extends the area of feasibility of measurement. Isotopes make it possible to work with normal constituents of the blood, to avoid disturbing physiological conditions, to utilize data obtained over long time intervals, and to study many parts of the body simultaneously and by external detection methods.

Full utilization of the advantages of isotopic tracers requires an understanding of the relationships between the labeled and the nonlabeled species of the substance being studied and, for clarity and precision, it is necessary to express these relationships in mathematical terms.

The purpose of the present chapter is to present the elementary aspects of the mathematical relationships between tracers and the substances being studied, and it is hoped that this exposition will be of particular value to novices in this field. The more sophisticated workers are referred to a book by Sheppard (59), in which advanced aspects of the subject are treated in detail, and which provides numerous references to applications of the tracer method in studies of circulatory kinetics.

The emphasis in this chapter will be on events occurring soon after the injection of labeled material into the circulation but subsequent to the first few circulation times treated by Zierler (74). Although the methods of analysis to be discussed have applications in other phases of tracer kinetics, attention will be directed to applications pertinent to blood flow rate analysis. In particular, questions of metabolic turnover of materials in tissues, metabolic pathways, and active transport are not treated Although the

importance and difficulty of data acquisition are recognized, the present discussion will be chiefly concerned with mathematical analysis and interpretation of the data.

CIRCULATORY FEATURES AFFECTING MIXING AND DISTRIBUTION

Anatomical

Except those processes which involve the formed elements of the blood and the blood vessel walls directly, the exchange of materials between the blood and the tissues occurs in the capillaries. In this context the larger vessels may be regarded merely as mixing chambers and as avenues for transportation. Purely anatomical features which promote mixing include the division of the circulating pathway into the pulmonary and the systemic circulations, and differences in the lengths of pathways to and within the various organs.

Normally all the venous blood has to traverse the pulmonary circulation before returning to the systemic circulation and, since in the pulmonary circulation all but a small fraction of the blood passes through a capillary bed, the effluent blood from a given tissue is redistributed in the next cycle to the other tissues according to the manner in which the cardiac output is fractionated, with little or no chance that preferred pathways, which would keep the circulation of one tissue separated from that of the others and delay mixing, can be maintained.

The preceding statement must be modified when substances, particularly gases, which may be quantitatively removed in one passage through the lung capillaries are under discussion. When this is the case there is in effect no recirculation of the material in the effluent blood from a given tissue. Except for the gut-spleen-liver portion of the circulation, the tissues served by the systemic circulation are arranged in parallel with respect to each other, so that for some purposes events in the lungs may be separated into components related to each of the systemic tissues in a relatively simple manner. Attempts to measure the cardiac output by nitrogen elimination from the tissues when the subject inhales pure oxygen have been based on the above concept, but have not been entirely satisfactory because the washout of air in the lungs is not fast enough to avoid obscuring the rapid components associated with tissues having high blood perfusion rate factors (50).

Because of variations in path lengths to and through the tissues, both in the pulmonary and in the systemic circulations (if these are not compensated for by corresponding variations in flow rates), a concentration peak in the arterial blood emerges greatly smeared, or prolonged, in the venous blood if the substance under consideration remains intravascular.

Dynamic

INTRAVASCULAR MIXING. Although the cardiac output is pulsed, the flow through the capillaries is practically continuous and may usually be so regarded in the analysis of tracer data.

The role of anatomical factors in promoting mixing is mentioned above. These factors are supplemented by the effects of variations in flow rates and by the nature of the flow. Flow within the circulation is usually laminar, giving a longitudinal redistribution of the blood's constituents, as is discussed by Zierler (74). The occasional occurrence of turbulent flow also produces some transverse mixing.

These mechanical effects are so rapid and violent relative to diffusion that the latter process plays only a minor role in intravascular mixing. Diffusion does play a much more important role in the transfer and exchange of substances across the capillary membranes. For some substances the transmembrane diffusion rates are much faster than the blood perfusion rates, so that the rate of transfer of these substances is flow-limited. Under some conditions, differences in hydrostatic pressure result in bulk flow. The effect of osmotic pressure differences is a more controversial subject, however, and the relative roles of diffusion and bulk flow are not clearly delineated.

EXTRAVASCULAR DISTRIBUTION. The rapidity with which the labeled form of a substance leaves the circulation is also strongly influenced by the distribution of the natural form of that substance.

Various labels of erythrocytes, iron, chromium, and N^{15}-labeled hemin, may remain in the circulation for weeks, leaving essentially only when the red cells themselves leave or are destroyed. P^{32}, which is also useful as an erythrocyte label, is less firmly bound to the cell. Although of little use in studying regional blood flow rates, labeled red cells have given valuable information on intravascular mixing times, uncomplicated by extravascular dilution. Kraintz *et al.* (39) found that sequestration of red cells in the spleen delays the achievement of uniform distribution of

labeled red cells throughout the red cell mass, so that mixing in the spleen is incomplete after 30 min, but the error in blood volume due to this is less than 5 per cent.

Other labeled-formed elements remain intravascular for much shorter periods, reflecting the shorter life spans and less strictly intravascular distribution of white cells and platelets. I^{131}-labeled plasma proteins exchange fairly rapidly (measured in hours) with extravascular proteins.

Sodium occurs in the body as an essentially extracellular ion with some 25 to 50 per cent of the body's sodium in the skeleton. In normal subjects Na^{24} introduced intravenously rapidly (10–20 min) becomes distributed in the extracellular fluid portion of the sodium space (except perhaps the cerebrospinal and intra-ocular fluids), whereas equilibration with the exchangeable portion of the bone sodium proceeds slowly. In edematous subjects, isotopic equilibrium between Na^{24} in the blood plasma and ascitic fluid or other edema fluids may not be complete at 24 hours after injection, presumably due to slow mixing in the edema fluids.

Labeled forms of water (with deuterium, tritium, or O^{18} as the label) and other substances such as urea, which are distributed in total body water, leave the circulation at rates measured in seconds and minutes (49). The early distribution of tritiated thymidine is in this category, although soon afterwards that thymidine which is not catabolyzed is incorporated in cell nuclei where it remains indefinitely.

Radioactive potassium (K^{42}) is one of the substances which disappear most rapidly from the circulation. Walker & Wilde (71) found that in the rabbit 90 per cent of intravenously injected K^{42} passes out of the circulation within 1 min. There is not complete agreement as to why the disappearance of K^{42} from the circulation is so much (4 or 5 times) faster than that of Na^{24}, D_2O (1.5 times as fast), or iodine [Sheppard & Yudilevich (60)] (6 times as fast in the lungs). Since ions of sodium and potassium are so similar in the physical properties affecting mobility, it would be reasonable to expect their diffusion rates to be about equal. Walker & Wilde (71) point out that it is ridiculous to ascribe the rapidity of disappearance of K^{42} to preferential uptake in the liver and other viscera, since 96 per cent of the cardiac output would have to pass through the viscera to account for the data. The difference in distribution of sodium and potassium is an important factor. Since the bulk of potassium is intracellular, the K^{42} which leaves the circulation promptly gets diluted in a large potassium pool, and the relative rate of feedback to the circulation from the intracellular pool is low, whereas the sodium in the interstitial fluid is much more favorably situated for feedback to the circulation. Walker & Wilde (71) discuss the possibility that potassium ions have an exclusive ability to traverse the capillary endothelial cells, and Sheppard *et al.* (61) analyze the role of incomplete mixing in K^{42} disappearance curves.

THE TRACER CONCEPT

History

The idea of labeling a few members of a group of similar objects and, from the behavior of the labeled members, drawing conclusions about the behavior of the group, is probably about as old as civilization itself. Who knows, for example, when some ingenious shepherd first put a bell on one sheep in order to make it easier to follow his flock? Possibly the first recorded tracer use is an Apocryphal story of how Daniel trapped the priests by their footprints in ashes strewn on the floor of the temple of the idol, Bel. Somewhat the same concepts are used in modern chemistry when a compound is labeled or "tagged" with radioactive atoms and its metabolic pathway is studied.

Prior to the development of isotopes as labels, other markers, particularly the dyes mentioned in the introduction, were used in circulatory studies. Their history and present uses are discussed in other chapters of this *Handbook*.

The history of isotopic methodology has been reviewed by Hevesy (32). It is of interest to note that radioactive isotopes of some of the heavy metals were used in physiological studies before the discovery in 1933 of deuterium and the first production of artificial radioisotopes in the same year. The heavy stable forms of hydrogen and nitrogen first made it possible to study the kinetic behavior of naturally occurring constituents in steady-state situations and led to the now familiar but then revolutionary concept of the dynamic state of body constituents.

The nuclear reactor, supplemented by the cyclotron, has made artificially produced isotopes of every element (including several new elements) available in quantities sufficient for use in physiological studies. With this availability, of course, the number and variety of applications have grown

commensurately, and there are now textbooks directed to applications of isotopic tracers in biology in general [Kamen (36), Hevesy (33)], and in the specialized fields of biochemistry and physiology [Sacks (54)], agriculture [Comar (16)], and clinical medicine [Veall & Vetter (70), Beierwaltes (4)].

Terminology

Some words are used with special meanings in tracer terminology; others are not always used with the same meaning by various authors. The following definitions are taken from an earlier publication (51) in which citations of the original literature providing the basis for the definitions may be found.

A *tracer* is a labeled form of a substance. Ideally, the label makes the labeled form detectable by the observer without affecting its behavior in the system being studied. In some instances an isotope of one element has been considered as a substitute tracer for a chemically similar element. Substances not normally present in the system being studied, such as colloids and inert gases, may also be treated as tracers.

The term *carrier* is used in two senses: *1*) Unlabeled material of the same or a different ("nonisotopic") element added to a sample containing a tracer as an aid in chemical processing. A logical extension of this meaning includes the unlabeled form of the substance being traced which is normally present in the system. *2*) A (usually unknown or postulated) different substance which acts as a transporting vehicle (like a shuttle or ferryboat) in getting the substance being studied through a membrane or across a phase boundary. The sense meant is usually clear from the context.

The *specific activity* denotes the ratio of the amount or concentration of the tracer to that of the total (labeled plus unlabeled) substance. Any units which define this ratio may be used. In some applications, microcuries per gram of total substance suffices to denote the specific activity; in other studies the precise location of a tracer element in a labeled molecule must be specified. The term *relative specific activity* has been used to mean the ratio of the specific activity in one chemical form to that in another. Other authors denote the "fractional amount of *S* (substance) that is tagged" the absolute specific activity, and call the radioactivity per unit amount of *S* the *relative specific activity*. The latter two terms have the same implications so far as the relative number of isotopic atoms is concerned, and in the present discussion specific activity may have either meaning.

For mathematical purposes the constituents of a living system can be represented as being located in distinguishable phases or volumes designated as *pools* or *compartments*. The boundaries of these compartments may, but do not necessarily, conform to anatomical boundaries. For example, the blood plasma is in a relatively easily defined compartment. The location of the bicarbonate pool is more difficult to define but perhaps no less clear in concept, and in some cases a shifting location, such as the cells undergoing mitosis at a given moment, may be regarded as a compartment.

Transport of a substance into and out of a compartment and chemical synthesis and degradation result in appearance and disappearance of the substance in the compartment. The term *transfer* will denote unidirectional processes of either kind when the mathematics is the same for both kinds. *Exchange* implies a one-for-one substitution of atoms or molecules, or simultaneous and equal transfers into and out of a compartment. The term *active transport* is used when energy in addition to the diffusion force (i.e., the negative value of the electrochemical potential) is involved in effecting transfers.

In an unconstrained sytem there are direct transfers of substance into each compartment from all other compartments in the system. Constrained or restricted exchange systems with the compartments connected chainwise have been designated as *catenary* (or *catenated*), or *series* systems, as contrasted with *mammillary*, *centrally exchanging* or *parallel* systems which have a single central compartment exchanging with multiple peripheral compartments and with no direct transfers between the peripheral compartments.

The term *steady state* is applied to compartments where the rates of removal of the substances being studied are equalled by their rates of replacement, so that the concentrations and amounts of the substances being studied are constant during the period of observation. Constant rates of transfer are also usually specified or implied in mathematical treatments but are not required by the definitions of steady state. In particular, the steady state includes situations where different concentrations of an exchangeable substance are maintained on opposing sides of a membrane and where the difference is greater than can be explained on a simple physical-chemical basis such as a Donnan equilibrium. Of course, during an experiment the tracer itself is

not in a steady state, but it is assumed to be introduced in an amount sufficiently small not to disturb the steady state of its unlabeled counterpart either by its quantity, by the effects of its radiations, or by its pharmacological effects.

Exchange processes produce a *turnover* of the substance in a given compartment. The *turnover time* is the time interval required for the amount of a substance transferred into or out of a compartment in the steady state to be numerically equal to the amount present in the compartment. *Turnover rate* has been used in two senses: *1*) as the reciprocal of the turnover time or fraction per unit time, giving turnover rate the dimensions of $time^{-1}$; and *2*) as the amount of the substance that is turned over per unit time, giving turnover rate the dimensions of mass/time. There being a need for both concepts, several alternative terms have been suggested, such as, for use in the first sense, "relative turnover rate" or, for use in the second sense, "flux rate." In the present discussion, use of the word *rate* (as in turnover rate, exchange rate, transfer rate, flow rate, etc.) will imply dimensions of mass/time, and the term *rate constant* will be used when dimensions of $time^{-1}$ are meant. Rates will be symbolized by ρ's and rate constants by k's.

Basic Assumptions

KINETIC IDENTITY OF LABEL AND CARRIER. Much of the misunderstanding of the relationships between a tracer and the material being traced is eliminated if it is made clear that the assumption that the tracer and the substance being traced behave identically applies only at the level of the smallest recognized units, usually atoms or molecules but occasionally larger structures such as erythrocytes.

Under conditions making the assumption of identical behavior at the unit level valid, there will, of course, remain apparent differences of behavior when large populations of these units are considered. This is not because the tracer is failing to trace properly, but because it is capable of demonstrating processes not otherwise observable. The apparent difference of behavior is, in fact, one of the important features making a tracer experiment of value in kinetic studies.

For example, the penetration of blood red cells by radioactive potassium, K^{42}, when there is no apparent movement of ordinary potassium across the same membrane, is logically interpreted as indicating that ordinary potassium likewise does move into and out of the red cells. The fact that the two rates are equal explains the apparently static situation, and it is not necessary to ascribe any special property other than detectability to the K^{42} atoms.

Similarly, if giving a labeled substance by mouth is followed by excretion of an equal amount of the substance, but by very little of the label, this shows that the material excreted was not identically the material ingested, and again is not attributable to selective handling of the labeled form. The role of tracer theory is to provide a framework whereby the behavior of the tracer, which is observable, can be explained in terms of the otherwise unobservable patterns of behavior of the substance traced.

Departures from the identity of behavior of the labeled and unlabeled forms are, of course, not impossible. The isotope effect is of importance when hydrogen isotopes are used because deuterium, D or H^2, is about twice as heavy as ordinary hydrogen, H^1, and tritium, T or H^3, is three times as heavy, atom for atom. When these isotopes are part of a large molecule, however, the weights of the labeled and unlabeled forms will not be greatly different, relatively, and the isotope effect is generally negligible. A more serious departure occurs when the label is assumed to be tightly bound to the substance being traced, but in fact is not. Hardly anyone would expect to be able to trace one constituent of an ionizable substance with a label on the other ion, but in organic chemistry, where it may be more difficult to rule out exchange reactions, more subtle problems occur. The assumption of kinetic identity between the label and its carrier implies an assumption of stability of composition of the carrier. Even in "simple" systems, for example in water, where the rate of transfer of hydrogen ions across a membrane may be quite different from the rate of transfer of hydroxyl ions or of oxygen as such, such terms as the transfer rate of the carrier may defy unambiguous definition.

ABSENCE OF DISTURBING EFFECTS. A major advantage of the radioisotopic tracers is the fact that even in the case of substances which are normally present only in trace quantities, the amount of tracer which needs to be added to give statistically valid counting rates may be so small that there is no danger that the kinetics of the system will be disturbed, particularly if a carrier-free label is used.

On the other hand, the use of radioisotopes introduces a new complication, the possibility that the

ionizing radiation will perturb the system. In general, this turns out not to be a real problem when tracers are used but in some situations, as in the use of labeled substances which concentrate in a particular organ or in a sensitive location such as cell nuclei, the possibility of getting radiation effects must be carefully evaluated.

Finally, it is essential that the material introduced as a tracer not have toxic or pharmacological properties which would disturb the system. When the substances being studied are normal constituents of the body, this is no problem, but when labeled drugs are being studied, there may be undesirable effects.

HOMOGENEITY WITHIN COMPARTMENTS. For simplicity of the mathematical considerations, it is usually necessary to regard the system being studied as consisting of a number of compartments, within each of which mixing is regarded as being immediate and perfect, giving homogeneity at all times within a given compartment. Those who know what really happens in biological systems are somewhat justified in regarding this as the most outrageous assumption made. No account is taken of the known concentration gradients within cells and across membranes. Because of the fact that it does take a definite time, measured in seconds, for the blood to complete a loop of its path from the heart to a tissue and back to the heart, mixing within the circulation obviously cannot be instantaneous. Nevertheless, analyses based on the assumption of perfect mixing have been successful as the basis for explaining the results of many tracer experiments, and the model system constructed using this assumption does provide a basis for evaluating the importance of factors which require modification of the assumptions.

MATHEMATICAL BASIS

Synopsis of Mathematical Techniques

Because many biologists who are interested in tracer methods have not had training in some of the branches of mathematics of use in developing the theoretical basis for the interpretation of the behavior of tracers, it seems appropriate to include at this point a brief introduction to pertinent selected topics in these mathematical methods. It is hoped that workers who have heretofore avoided such subjects may gain some insight into the power of the applications and be encouraged to deeper study, mathematics being one of the few subjects which can be mastered through self-study. In general, however, textbooks of applied mathematics are written for physicists, chemists, engineers, etc., and, excepting the field of statistics, there is a dearth of mathematics books concentrating on topics chiefly of interest to biologists. A recently published book by Defares & Sneddon (20) does emphasize biological applications and is recommended for further study.

LINEAR DIFFERENTIAL EQUATIONS. Differential equations are in many respects like any of the familiar algebraic equations, but there are, of course, some important differences. The distinguishing characteristic is that the rate of change of a variable is expressed in terms of the values of the variable itself. Such an equation cannot be solved by the usual algebraic techniques. In fact, the term "solved" acquires a somewhat different meaning. Whereas in algebra, solving an equation involves finding numerical or symbolic values for constants which satisfy the equation, the solution of a differential equation is usually an algebraic equation or a family of algebraic equations describing the functional relationships of the variables involved.

For example, suppose that we are asked to describe the growth of a cell population, given the information *a*) that the rate of growth is constant or, alternatively, *b*) that the rate of growth at any moment is proportional to the population at that moment. Using the symbols P for population, R for rate of growth, t for time, and K for the constant, we can answer part *a* immediately; but part *b* is more difficult. For part *a* we need only assume some starting value for P, P_0, at time zero, and note that since the rate of growth is constant, i.e., $R = K$, the number added to P in time t is simply $Rt = Kt$, so we have $P = P_0 + Kt$. It should be noted that Kt may be thought of as the result of summation of the growth which occurs in all of the shorter intervals of time which add up to t. For part *b* we may write $R = KP$, but if we are restricted to algebraic methods, this is the end of our road. In this case the rate is changing continuously, and it is not correct to use Rt to sum up the addition to the population, as doing so implies that R is constant, as it was in part *a*.

Instead, we replace R by a special symbol, dP/dt, the first derivative of P, which may be thought of as the ratio of an infinitesimally small change in P, dP, to a correspondingly very small change in t, dt, a concept consistent with our usual notion of the meaning of rate of change at any instant.

To work part *a* this way, we would have written $dP/dt = K$. In this example dP and dt may be separated and treated as if they were ordinary algebraic entities, so by rearrangement we have $dP = Kdt$. The equation can now be solved by integration, which for the present purposes may be regarded as a method for achieving the summation of many small increments. (A rigorous explanation of integration cannot be given here, but is available in the standard texts on calculus.) For the present problem it must suffice simply to state that the integral of dP is P and that of Kdt is Kt, if K is a constant. Integration also introduces another term called the constant of integration, which in this example is the starting value of P, or P_0. We thus have, as expected, the solution, $P = P_0 + Kt$.

It is apparent that any value of P_0 could be used in this equation, and in general it is true that the constant of integration may have any of a wide range of possible values. Thus another characteristic of differential equations is the infinitude of the number of solutions. A solution expressed in a form in which arbitrary values may be assigned to the constants of integration is called the general solution; a solution having definite values assigned to the constants of integration is called a particular solution.

The solution of case *b* follows the same procedure, and we begin with $dP/dt = KP$, which upon separation of the variables becomes $dP/P = Kdt$. Again the integral of Kdt is Kt, but the integral of dP/P happens to be log P, with the constant of integration being expressible as log P_0, so the solution for *b* is: $\log P = \log P_0 + Kt$. In this branch of mathematics it is "understood" that log means the logarithm to the base e $(2.718 \cdots)$, or the natural logarithm, rather than the common logarithm using the base 10. Any number could be used as the base of a logarithm scale, but e is preferred because its functions have the simplest results when subjected to the processes of differentiation and integration, not requiring a conversion constant. With this understanding, the above answer may be converted to the form: $P = P_0e^{Kt}$. When the rate of decrease is proportional to the amount present, $-K$ is used and we have: $P = P_0e^{-Kt}$. The latter equation appears frequently, as it describes the rate of radioactive decay and similar processes. It also describes the disappearance of a label from a one-compartment open system when P_0 of the label is initially present, the inflow is not labeled, the inflow and outflow rates of the substance being traced are equal, and the flow rates are constant.

In problems involving more than one compartment, a system of differential equations is used, with one equation for each compartment. In general, it is possible to reduce such a system to a single equation which will involve the second and higher derivatives of a single variable, d^2P/dt^2, d^3P/dt^3, etc. Those differential equations which involve only the first powers of these derivatives are called linear equations. The equations useful in describing the behavior of tracers in compartmented systems in the steady state are generally linear differential equations with constant coefficients and are relatively easy to solve, as differential equations go. One form of the solutions of such equations is a series of exponential terms. For example, an equation of the form:

$$\frac{d^3x}{dt^3} + a\frac{d^2x}{dt^2} + b\frac{dx}{dt} + cx = d$$

has a solution of the form:

$$x = Ae^{-\lambda_1 t} + Be^{-\lambda_2 t} + Ce^{-\lambda_3 t} + D$$

The three exponents, λ_1, λ_2, and λ_3 are the three roots of the auxiliary equation: $(-\lambda)^3 + a(-\lambda)^2 + b(-\lambda) + c = 0$. The coefficients, A, B, C, and D depend not only upon a, b, c, and d, but upon the "boundary" or starting conditions and are not readily expressed in a general form. Of course this is only one example of the differential equations method, but it is one with direct applications in tracer theory. Further examples appear in the treatment of compartmented systems which follows. Among the several textbooks which can be recommended for further study is Ford (25).

MATRICES AND DETERMINANTS. Both matrices and determinants are arrays of numbers arranged in rows and columns, but quite different properties are assigned to them and their uses are correspondingly different.

We can mention some of the most useful features here but can really hardly begin to explore the subject. For those who wish to study the methods further, an excellent but abstract approach is available in Finkbeiner (23) and a more easily followed, if somewhat chatty, approach is found in Stigant (69). A thorough treatment of determinants is available in Muir & Metzler (44).

The fundamental distinction between a determinant and a matrix is that the former represents one number and can be reduced according to an established set of rules to a single numerical value,

whereas the latter cannot be so reduced, but represents a set of values. In common with the differentiating function and other functions, matrices are operators and as such are subject to the algebra and calculus of operators. A determinant must have the same number of rows as it does of columns, but matrices are not so restricted. Both determinants and matrices are useful in solving simultaneous equations.

Let us consider the solution by determinants of two simultaneous equations:

$$\begin{cases} a_1x + b_1y = c_1 \\ a_2x + b_2y = c_2 \end{cases}$$

By the perhaps more familiar method of multiplying the first equation by b_2 and the second by b_1, subtracting the resulting second equation from the resulting first and dividing by the new coefficient of x, the solution $x = (b_2c_1 - b_1c_2)/(a_1b_2 - a_2b_1)$ is obtained. The same result is obtained by evaluating the determinants in

$$x = \frac{\begin{vmatrix} c_1 & b_1 \\ c_2 & b_2 \end{vmatrix}}{\begin{vmatrix} a_1 & b_1 \\ a_2 & b_2 \end{vmatrix}} = \frac{b_2\,c_1 - b_1\,c_2}{a_1\,b_2 - a_2\,b_1}$$

in which the denominator consists of a determinant composed of the coefficients of x and y, and the numerator is similar except that the coefficients of x have been replaced by the column of numbers constituting the right-hand members of the original system (the c's). It is apparent that evaluating the determinants by subtracting the product of the upper right and lower left numbers from the product of the upper left and lower right numbers in each case leads to the same answer as was obtained above. Similarly, the solution for y is obtained by replacing the b column in the numerator by the c column:

$$y = \frac{\begin{vmatrix} a_1 & c_1 \\ a_2 & c_2 \end{vmatrix}}{\begin{vmatrix} a_1 & b_1 \\ a_2 & b_2 \end{vmatrix}}$$

Higher order determinants, of course, require somewhat more complicated patterns for their evaluation, but the basic pattern is already established in the 2 × 2 determinant. A procedure for evaluating the 3 × 3 determinant:

$$\begin{vmatrix} a_1 & b_1 & c_1 \\ a_2 & b_2 & c_2 \\ a_3 & b_3 & c_3 \end{vmatrix}$$

is to multiply a_1 by the 2 × 2 determinant consisting of those elements not in the same row or column as a_1, i.e., $\begin{vmatrix} b_2 & c_2 \\ b_3 & c_3 \end{vmatrix}$ and evaluated as described above, minus b_1 times $\begin{vmatrix} a_2 & c_2 \\ a_3 & c_3 \end{vmatrix}$ plus c_1 times $\begin{vmatrix} a_2 & b_2 \\ a_3 & b_3 \end{vmatrix}$ giving

$$a_1(b_2c_3 - b_3c_2) - b_1(a_2c_3 - a_3c_2) + c_1(a_2b_3 - a_3b_2)$$

That portion of a determinant (or matrix) which remains when the elements in the same row and in the same column as a selected element are crossed out is called the minor of that element. Evaluation of 4 × 4 and higher order determinants may be achieved by alternately adding and subtracting the products of the elements of one row (or column) by their respective minors, in extension of the patterns described for the 2 × 2 and 3 × 3 determinants, the minor of an element of a 4 × 4 determinant being a 3 × 3 determinant, etc.

When the elements selected constitute an odd-numbered row (or column) (numbering from left to right and from top to bottom), the first product is added; if the row (or column) used is even numbered, the first product is subtracted.

The sign to be assigned to each product is given by the location of the element in the following array or an extension thereof:

$$\begin{matrix} + & - & + & - \\ - & + & - & + \\ + & - & + & - \\ - & + & - & + \end{matrix}$$

Although straightforward enough in principle, it is obvious that in practice evaluation of a 4 × 4 or higher order determinant by this procedure would involve many steps and be quite a laborious task. When real numbers (rather than symbols) constitute the array, some simplifying procedures are available. Although some of these may sound unlikely at first, their validity can be demonstrated, if not conclusively proved, by simple test examples.

Some of the rules applicable to reduction of determinants are:

a) Multiplication of each element of one row (or column) by the same number multiplies the determinant by that number.

$$m\begin{vmatrix} a & b & c \\ d & e & f \\ g & h & k \end{vmatrix} = \begin{vmatrix} ma & mb & mc \\ d & e & f \\ g & h & k \end{vmatrix} = \begin{vmatrix} a & mb & c \\ d & me & f \\ g & mh & k \end{vmatrix}$$

b) Adding or subtracting the elements of one row (or column) or multiples of these elements by a

constant to or from the corresponding elements of a second row (or column) and replacing the second row (or column) by the resulting sums or differences does not change the value of the determinant.

c) Exchanging the positions of any two rows (or columns) changes the sign of the determinant but not its absolute value. The sign resulting when the sequence of rows (or columns) is altered may be determined from the number of exchanges of pairs of rows (or columns) required to achieve the same end result.

$$\begin{vmatrix} a_1 & a_2 & a_3 \\ b_1 & b_2 & b_3 \\ c_1 & c_2 & c_3 \end{vmatrix} = -\begin{vmatrix} b_1 & b_2 & b_3 \\ a_1 & a_2 & a_3 \\ c_1 & c_2 & c_3 \end{vmatrix} = -\begin{vmatrix} a_2 & a_1 & a_3 \\ b_2 & b_1 & b_3 \\ c_2 & c_1 & c_3 \end{vmatrix}$$

d) If all of the elements except one of a row (or column) are zero, the other members of its column (or row) may be changed to zero without changing the value of the determinant.

By application of the above rules, a given determinant may be reduced to one which contains all zeros except along a principal diagonal. The following example was constructed to illustrate the use of the above rules:

$$\begin{vmatrix} 1 & 1 & 1 & 1 \\ 2 & 2 & 2 & 6 \\ 3 & 7 & 6 & 7 \\ 3 & 3 & 6 & 3 \end{vmatrix} = (2)\begin{vmatrix} 1 & 1 & 1 & 1 \\ 1 & 1 & 1 & 3 \\ 3 & 7 & 6 & 7 \\ 3 & 3 & 6 & 3 \end{vmatrix} = (2)\begin{vmatrix} 1 & 0 & 0 & 0 \\ 1 & 0 & 0 & 2 \\ 3 & 4 & 3 & 4 \\ 3 & 0 & 3 & 0 \end{vmatrix}$$

$$-(2)\begin{vmatrix} 1 & 0 & 0 & 0 \\ 0 & 0 & 0 & 2 \\ 0 & 4 & 3 & 4 \\ 0 & 0 & 3 & 0 \end{vmatrix} = (2)\begin{vmatrix} 1 & 0 & 0 & 0 \\ 0 & 0 & 0 & 2 \\ 0 & 4 & 0 & 0 \\ 0 & 0 & 3 & 0 \end{vmatrix} = (-2)\begin{vmatrix} 1 & 0 & 0 & 0 \\ 0 & 0 & 0 & 2 \\ 0 & 0 & 3 & 0 \\ 0 & 4 & 0 & 0 \end{vmatrix}$$

$$= (2)\begin{vmatrix} 1 & 0 & 0 & 0 \\ 0 & 2 & 0 & 0 \\ 0 & 0 & 3 & 0 \\ 0 & 0 & 0 & 4 \end{vmatrix} = (2)(24) = 48$$

In the first step, each member of row 2 is divided by 2, so 2 becomes a coefficient of the determinant. In the second step the first column is subtracted from each of the other three columns. The third step could be achieved by subtracting multiples of the top row from the other rows, but can also be achieved immediately using rule *d*, which may also be used for the next step. Finally, the column order and the sign are changed and the answer is the product of the numbers on the diagonal and the coefficients of the final determinant.

Returning to the subject of matrices, a few special properties may be noted. In particular, two $m \times n$ matrices may be added or subtracted by performing the corresponding operation on the pairs of elements having corresponding locations. That is, $(a_{ij} + b_{ij}) = c_{ij}$ where the subscripts i and j denote the location by row and column number. Multiplication of two matrices requires that the first have the same number of columns as the second does of rows, for in matrix multiplication each element of a row of the first is multiplied by the corresponding (sequentially) element in a column of the second, and the sum of these products is entered as the element in the product matrix at the location where the row and column used intersect. Thus,

$$\begin{bmatrix} a & b \\ c & d \end{bmatrix} \cdot \begin{bmatrix} h & k \\ w & v \end{bmatrix} = \begin{bmatrix} ah + bv & ak + bv \\ ch + dv & ck + dv \end{bmatrix}$$

The result is different if the first matrix is exchanged for the second, and this is one of the respects in which matrix multiplication differs from ordinary algebraic multiplication. The two cases of matrix multiplication are called pre- and post-multiplication (by the factor involved).

Division by matrices is not defined. Thus, to solve the matrix equation

$$[A][X] = [B]$$

for $[X]$, it is not possible to divide both sides by $[A]$. The desired result is achieved, however, by multiplying both sides by the inverse of $[A]$, $[A]^{-1}$. To understand the inverse matrix concept, it is first necessary to know about the identity matrix. As in algebra multiplication by unity does not change the value of a number, and multiplication of a number by its inverse (in this case, reciprocal) gives unity, so in matrix algebra the identity matrix is defined as that matrix which, when used as a multiplier, does not change the value of the matrix operated on, and the inverse matrix is defined as being the one which, when multiplied by the original matrix, yields the identity matrix. The identity matrix turns out to be the unit diagonal matrix, for example:

$$\begin{bmatrix} 1 & 0 & 0 \\ 0 & 1 & 0 \\ 0 & 0 & 1 \end{bmatrix}$$

One of the several available methods for generating the inverse of a matrix is illustrated in a later section of this chapter.

THE LAPLACE TRANSFORM. The Laplace transform is a mathematical device which is useful in simplifying the method of solution of many differential equations, and is particularly suitable for the solution of ordinary differential equations with constant coefficients.

such as occur in compartment theory problems. In effect, the Laplace transform converts differential equations to algebraic equations which are, of course, easier to solve. The conversion is based upon the group theory concept that if a one-to-one correlation can be established between the members of two groups, and if the rules governing the relationships among operations in the two groups are known, difficulties in performing an operation on one group may be avoided by performing the analogous operation on the second group.

The most familiar example of this kind of transformation is in the use of logarithms to convert the problem of multiplication and division of the real numbers to the problem of addition and subtraction of their corresponding logarithms.

As with the use of logarithms, the use of the Laplace transform substitutes simple operations for more difficult ones, but does not make it possible to do anything which could not be done by other methods. Also, as an analogy to the use of logarithms, it is possible to use the Laplace transform by looking up the appropriate conversions in a table, without necessarily being able to derive the conversions or even without understanding how the derivations are obtained.

An understanding of the principles, however, does give one more confidence in the use of the tabulated conversions and may help prevent their misapplication. With this philosophy in mind, the following very brief discussion of the Laplace transform is included. The present treatment largely follows that of Holl *et al.* (34).

Definition. The Laplace transform of a function of time, $F(t)$, is symbolized by: $L\{F(t)\}$, and is defined as the function $f(s)$ given by

$$f(s) = \int_0^\infty e^{-st}F(t)\,dt = L\{F(t)\}$$

if $f(s)$ exists. We can assume s to be a real number and $F(t)$ to be a continuous real-valued function of the real variable t for $t \geqq 0$. It can be shown that some of the transforms are

$$L\{1\} = \frac{1}{s};\ L\{t\} = \frac{1}{s^2}\ (s > 0)$$

$$L\{t^{-\frac{1}{2}}\} = \sqrt{\frac{\pi}{s}}\ (s > 0);\ L\{c\} = cL\{1\} = \frac{c}{s}\ (s > 0)$$

where c is any constant and $L\{e^{\beta t}\} = 1/(s - \beta)$, etc. The inverse problem arises when a function of s is given and it is required to find the corresponding $F(t)$. The inverse transform is defined by the notation

$$F(t) = L^{-1}\{f(s)\}$$

which can be obtained from the equation defining $f(s)$ by handling the operator L as if it were an algebraic variable. It can be proved that there is a unique (one-to-one) correspondence between $F(t)$ and $f(s)$ so that a table of Laplace transforms may be used in the opposite direction as a table of inverse Laplace transforms.

Example. The following example comparing the solution of a differential equation

$$\frac{dx}{dt} + 2X = e^{-2t}$$

for the initial condition $X(0) = 1$, with the method of multiplication using logarithms, is a modification of an example in reference (34).

Original problem:	
3.1416×7.2314	$\frac{dX}{dt} + 2X = e^{-2t},\ X(0) = 1$
Look up logs in table	Look up transform
Simplified problem:	
$.49715 + .85922$	$sx(s) - 1 + 2x(s) = \frac{1}{s + 2}$
Add	Solve for $x(s)$
Solution of simplified problem:	
1.35637	$x(s) = \frac{1}{(s + 2)^2} + \frac{1}{s + 2}$
Look up antilog in table	Look up inverse transform
Solution to original problem:	
22.718	$X(t) = e^{-2t}(t + 1)$

The Laplace transform method may readily be extended to a system of differential equations, and for examples the reader is encouraged to consult texts such as (34) on the subject. Sheppard (59) and Zierler (74) use the Laplace transform in problems of compartment theory and indicator dilution curves.

Notation

The symbols to be used in the following development of the analysis of compartmented systems are defined when they first appear. The most frequently used ones are collected here for reference.

S_i = amount of substance (labeled plus nonlabeled) in ith compartment
ρ_{ij} = rate of flow of substance (labeled plus nonlabeled) into ith compartment from jth compartment
x_i = specific activity (e.g., microcuries per gram) of radioactive label in S_i
x_{i0} = x_i at time zero
x_E = x_i at equilibrium (infinite time)
$k_{ij} = \frac{\rho_{ij}}{S_i}$ = fractional turnover rate constant of S_i due to flow from jth compartment
$K_i = \sum_{\substack{j=0 \\ j \neq i}}^{j=n} \frac{\rho_{ji}}{S_i} = \sum_{\substack{j=0 \\ j \neq i}}^{j=n} \frac{\rho_{ij}}{S_i}$ = total turnover rate constant for S_i in steady rate
C_{in} = coefficients of exponential terms in equations describing specific activity curves in ith compartment
λ_n = exponential constant in nth exponential term
$|C|$ = determinant of C's
$[C]$ = matrix of C's

The One-Compartment Open System and the Two-Compartment Closed System

Some of the mathematics of the one-compartment open system has already been developed as an example under the explanation given of differential equations and, of course, the one-compartment system is of fundamental importance. Since, however, the mathematics of the two-compartment closed system is only slightly more difficult, and since the one-compartment system may be regarded as a degenerate case of the two-compartment closed system, with the second compartment being infinite, the two systems may be considered together. Although the object of these considerations is to develop a procedure for deducing the properties of the system from the behavior of a tracer in it, we begin with the inverse problem of predicting the behavior of a tracer in a given system.

The two-compartment closed system may be represented by the model: $1 \leftrightarrows 2$, where the numbers designate the compartments and the arrows indicate flow rates between the compartments in the two opposing directions. In the steady state these two flow rates are equal.

If S_1 and S_2 represent the amounts of the substance being traced present in compartments 1 and 2, and ρ is the rate of flow of S, the turnover rate constants, or the fractional rates of flow for the two compartments, are ρ/S_1 and ρ/S_2. It is assumed that the same fractional rates of flow apply to the tracer so that, in the terminology of radioactive tracers, the specific activity in the outflow from each compartment at any time is equal to the specific activity within the compartment at that time. The differential equations for a tracer in a two-compartment closed system may be written as

$$\begin{cases} \dfrac{d(S_1 x_1)}{dt} = -\rho x_1 + \rho x_2 & (1) \\[2ex] \dfrac{d(S_2 x_2)}{dt} = \rho x_1 - \rho x_2 & (2) \end{cases}$$

where in addition to the symbols defined above

x = specific activity, or concentration of the labeled form of S in S.

(The equations for total substance are analogous to equations 1 and 2.)

Each of the above equations states that the rate of change (d/dt) of the amount of tracer present (Sx) is the difference between the rate of flow of tracer in, and the rate of flow of tracer out of the compartment, in conformance with the law of conservation of matter. It will be noted that the sum of equations 1 and 2 is zero, indicating that there is no change in the total tracer in the system. Equations 1 and 2 are solved as simultaneous differential equations. Several methods are applicable. One which yields the general solutions in an efficient manner involves the use of the Laplace transform. With x_{10} and x_{20} being the initial, or time zero, values of x_1 and x_2, respectively, the Laplace transforms for equations 1 and 2 are:

$$\begin{cases} \left(s + \dfrac{\rho}{S_1}\right) x_1(s) - \dfrac{\rho}{S_1} x_2(s) = x_{10} & (3) \\[2ex] -\dfrac{\rho}{S_2} x_1(s) + \left(s + \dfrac{\rho}{S_2}\right) x_2(s) = x_{20} & (4) \end{cases}$$

Solving equations 3 and 4 algebraically for $x_1(s)$ where $x_1(s) = L\,[x_1(t)]$

$$x_1(s) = \frac{\begin{vmatrix} x_{10} & -\dfrac{\rho}{S_1} \\[2ex] x_{20} & s + \dfrac{\rho}{S_2} \end{vmatrix}}{\begin{vmatrix} s + \dfrac{\rho}{S_1} & -\dfrac{\rho}{S_1} \\[2ex] -\dfrac{\rho}{S_2} & s + \dfrac{\rho}{S_2} \end{vmatrix}} = \frac{s x_{10} + \dfrac{\rho}{S_2} x_{10} + \dfrac{\rho}{S_1} x_{20}}{s^2 + \left(\dfrac{\rho}{S_1} + \dfrac{\rho}{S_2}\right) s}$$

which may be broken into the simpler fractions:

$$x_1(s) = \frac{x_E}{s} + \frac{x_{10} - x_E}{s + \dfrac{\rho}{S_1} + \dfrac{\rho}{S_2}}$$

where x_E (for "equilibrium" specific activity) is

defined as

$$x_E = \frac{S_1 x_{10} + S_2 x_{20}}{S_1 + S_2}$$

Application of the inverse transforms yields:

$$x_1 = x_E + (x_{10} - x_E)\, e^{-\left(\frac{\rho}{S_1} + \frac{\rho}{S_2}\right)t} \tag{5}$$

and similarly:

$$x_2 = x_E + (x_{20} - x_E)\, e^{-\left(\frac{\rho}{S_1} + \frac{\rho}{S_2}\right)t} \tag{6}$$

In the one-compartment open system, equation 5 alone, with $\rho/S_2 = 0$, is the general solution. Two special cases may be distinguished, *1*) if the tracer is initially present in the compartment and there is no tracer in the inflow:

$$x = x_0\, e^{-(\rho/S)t} \tag{7}$$

and *2*) if the inflow is labeled but none is initially present in the compartment

$$x = x_E\,(1 - e^{-(\rho/S)t}) \tag{8}$$

Since in a given compartment the amounts and concentrations of the tracer are directly proportional to the specific activities, these other units may be substituted for the x's in equations 5 and 6. It will be noted, however, that in general only the specific activities are equal at "equilibrium," which in this context refers to isotopic equilibrium and does not necessarily imply thermodynamic equilibrium.

Equations 5 and 6 serve to predict the behavior of a tracer in a two-compartment system in terms of the parameters of the system. Application of equations 5 and 6 to the inverse problem of deducing the parameters of the system from the observed tracer behavior is achieved as follows. The data are plotted semilogarithmically, as indicated in figure 1*A*, and smooth curves are drawn to fit the data. If the data from the two compartments approach the same value closely enough to provide an accurate estimate of x_E, x_E is subtracted from the values of the curve which approaches x_E from above and the values of the curve which approaches x_E from below are subtracted from x_E, giving the two lines shown as $(x_1 - x_E)$ and $(x_E - x_2)$ in figure 1*B*. If the data are consistent with the assumptions made for the two-compartment system, these two lines will have the same slope. Alternatively, if it has not been feasible to obtain data for a period sufficiently long to establish x_E, a plot of the difference between x_1 and x_2 should give the same slope, figure 1*C*, since from equations 5 and 6 we have

$$(x_1 - x_2) = (x_{10} - x_{20})\, e^{-\left(\frac{\rho}{S_1} + \frac{\rho}{S_2}\right)t} \tag{9}$$

The latter method has the advantage of avoiding the effect of an error in estimating x_E, but has the disadvantage of not including the check on internal consistency available if the two slopes can be compared.

Whichever method is used, the number most easily obtained to characterize the slope is the half-time $T\frac{1}{2}$. As is shown in figure 1*B*, the half-time may be obtained by determining the interval of time required for the component's value to decrease by half (as from 4 to 2 or 2 to 1, etc.). For straight lines on semilogarithmic paper, this time interval is a constant. From $T\frac{1}{2}$ the exponent or "decay factor," λ, is obtained by use of the relationship

$$\lambda = \frac{0.69315}{T\frac{1}{2}} \tag{10}$$

In the present case $\lambda = (\rho/S_1) + (\rho/S_2)$.

For very steep components, it may be difficult to estimate a single half-time accurately, but the appropriate factor corresponding to any number of half-times may be used. In particular, it is convenient to note that 10 half-times involve a diminution factor of $2^{10} = 1024$, or slightly more than three logarithmic cycles $(1/1024 = 0.0009766)$. For very gentle slopes, where the $T\frac{1}{2}$ is longer than the scale on the graph paper being used, a larger fraction, say 0.80, may be used, provided the numerator in equation 10 is changed to be the positive value of log e of the new factor, which for 0.80 is 0.22314. Alternatively, the value for $(\rho/S_1) + (\rho/S_2)$ corresponding to any reduction factor may be obtained in one setting on a log-log slide rule. Finally, if S_1 and S_2 are known from the initial and final dilutions of the tracer, or by other methods, ρ may be calculated by a rearrangement of equation 10.

$$\rho = \left(\frac{0.69315}{T\frac{1}{2}}\right)\left(\frac{S_1 S_2}{S_1 + S_2}\right) \tag{11}$$

It is not necessary to determine either S_1 or S_2 to calculate the turnover rate constants, ρ/S_1 and ρ/S_2, separately. Using the methods explained more fully in the general treatment, it can be shown that if the experimental curves are described by equations 5 and 6:

$$\frac{\rho}{S_1} = \frac{\lambda(x_{10} - x_E)}{(x_{10} - x_{20})} \quad \text{and} \quad \frac{\rho}{S_2} = \frac{\lambda(x_E - x_{20})}{(x_{10} - x_{20})} \tag{12}$$

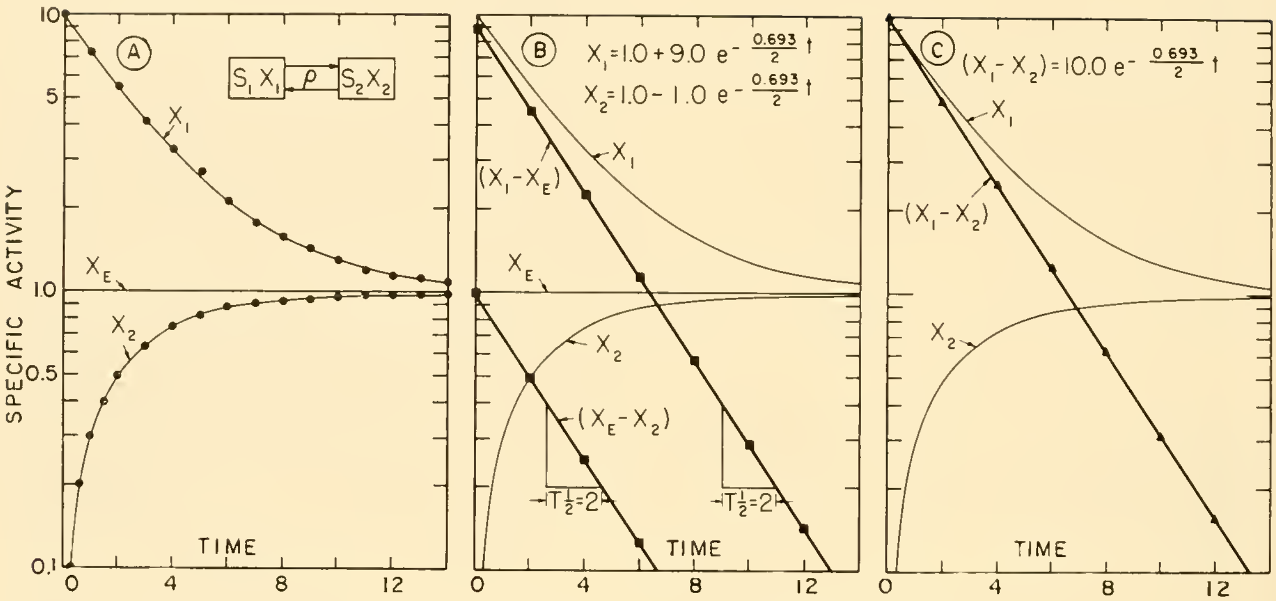

FIG. 1. Analysis of data in a two-compartment system. In *A*, a semilogarithmic plot of hypothetical specific activities in the two-compartment system is shown, with the equilibrium value, x_E, also indicated. In *B*, x_E has been subtracted from the x_1 values, giving the straight line $(x_1 - x_E)$, and similarly $(x_E - x_2)$ is another straight line having the same slope, which in both cases is measured by the half-time. An alternative method for getting the slope without using x_E is shown in *C*, where values of the lower curves are subtracted from those of the upper, giving $(x_1 - x_2)$. The use of the constants thus established to calculate the flow rate, ρ, is discussed in the text.

If $x_{20} = 0$, it is not necessary to collect data from compartment 2 in order to calculate the turnover rate constants for both compartments. Obviously, if either S_1 or S_2 is known, ρ can be calculated from the values of ρ/S_1 or ρ/S_2. [In the corresponding equations 21 in reference (51), k_{AB} and k_{BA} were inadvertently reversed.]

Failure of the points $(x_1 - x_2)$, $(x_1 - x_E)$ or $(x_E - x_2)$ to fall on a straight line on semilogarithmic paper suggests that some other model should be used as the basis for interpreting the data.

Three-Compartment and Multicompartment Systems

As is true for the simpler systems, the three-compartment systems have been completely solved in the sense that formulas are available for deducing the parameters of the system from data on the behavior of a tracer in the system [Skinner *et al.* (62), Robertson *et al.* (52), Solomon (64), Sheppard (59), Gellhorn *et al.* (27), Cohn & Brues (15)]. Perl (48) gives solutions for a four-compartment closed system. To the best of this author's information, explicit formulas have not been published for four-compartment open systems or for systems having more than four compartments.

The methods applicable to analysis of data in multicompartment systems will be discussed in this section and illustrated by application to the three-compartment systems.

Figure 2 illustrates the redistribution of an exchangeable substance which occurs in a three-compartment closed system.

EQUATIONS. A generalized form of equation 1, equation 13 describes the change in the amount of tracer in any compartment, i, attributable to exchanges and/or transfers between it and another compartment, j:

$$\frac{d(S_i x_i)}{dt} = -\rho_{ji} x_i + \rho_{ij} x_j \tag{13}$$

In this notation, ρ_{ij} is used to mean the rate of flow into i from j. The reverse order of subscript notation has been used by Solomon (64), the present author (51, 52) and others, but the convention adopted here conforms to usage in related fields, is favored by Sheppard (60), Berman & Schoenfeld (7) and Skinner *et al.* (62), and has some advantages which appear below. In those systems in which $\rho_{ij} = \rho_{ji}$, the two notations are interchangeable.

Conversion from amount equations to specific activity equations introduces many ρ_{ji}/S_i and ρ_{ij}/S_i

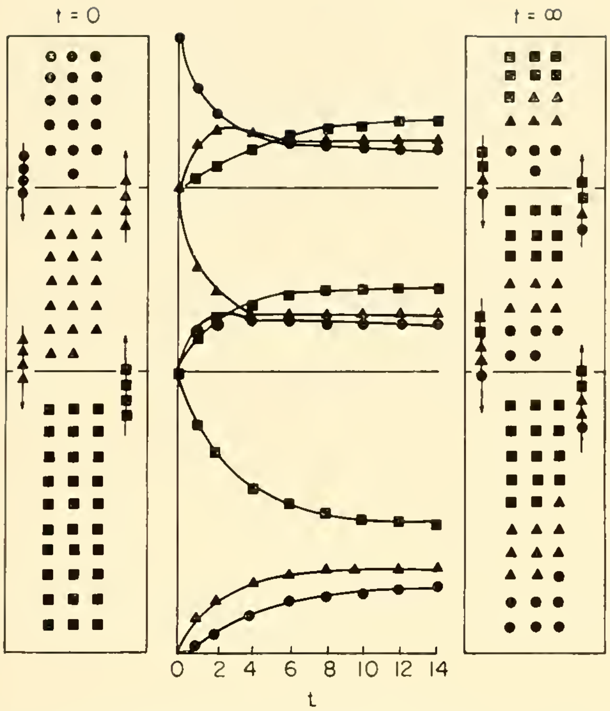

FIG. 2. Redistribution in a three-compartment system. The circles, triangles, and squares each represent a unit amount of the same substance according to whether it is initially in the top, middle, or lower compartment. The pattern at the right indicates how the substance is redistributed at equilibrium. The curves indicate the sequence by which this redistribution takes place and correspond to the curves which would be exhibited by a label introduced into the compartment indicated by the shape of the symbol and sampled in the compartment indicated by the position in the diagram. Thus the lowermost curve indicates the rate of appearance in the bottom compartment of a tracer introduced at time zero in the top compartment. A numerical analysis of this system illustrating how one set of curves yields, by matrix algebra, the flow rate constants for the system, is presented in the text.

factors in the equations when multicompartment systems are analyzed, and the form of the equations is simplified if each ρ/S factor is replaced by a single symbol. For this purpose the fractional turnover rate (or flow rate) constant, k_{ij}, is defined in terms of the rate of flow into the ith compartment by the formula: $k_{ij} = \rho_{ij}/S_i$. Because perfect mixing is assumed, the specific activity is the same for all outflows from a given compartment, and notational complexity may be avoided by collecting all of the outflow fractions, the ρ_{ji}/S_i terms, in a single symbol, K_i, the total turnover rate constant, defined by $K_i = \sum_j \rho_{ji}/S_i$. Of course, $K_i = \sum_j \rho_{ij}/S_i$ also, by definition of the steady state. In nonsteady states the turnover rate is not constant and K is not used.

The basic differential equation for the specific activity in the ith compartment of an n-compartment system is then

$$\frac{dx_i}{dt} = -K_i\, x_i + \sum_{\substack{j=0 \\ j \neq i}}^{j=n} k_{ij}\, x_j \tag{14}$$

where $j = 0$ is used to designate the inflow in open systems when the inflow is labeled and when the specific activity in the inflow is constant. For a system of n compartments there are n equation 14's, each having up to $n + 1$ terms. Equation 14 is a linear differential equation with constant coefficients and a set of n such equations has as a solution a set of n equations of the following type:

$$x_i = x_E + C_{i1}\, e^{-\lambda_1 t} + C_{i2}\, e^{-\lambda_2 t} \cdots + C_{in}\, e^{-\lambda_n t} \tag{15}$$

Equation 15 may be derived from equation 14 by the Laplace transform method, which yields the C's and λ's in terms of the k's, as is illustrated above for the two-compartment system, or equation 15 may be taken as an assumed solution and the C's and λ's calculated independently by methods described below.

Open n-compartment systems have n exponential terms in each equation 15, and x_E (the equilibrium or infinite time value of all the x's) is equal to the specific activity in the inflow, which is assumed to be constant or zero for the present discussion. In closed systems there are only $(n - 1)$ exponential terms in addition to x_E. As is illustrated above for the two-compartment closed system, the Laplace transform method may be used to derive equation 15's from equation 14's.

CALCULATION OF RATE CONSTANTS. As the starting point for this phase of the analysis it is assumed that the experimental data have been processed to the point where they are described by a set of equations of the equation 15 type. In other words, it is assumed that experimentally determined values of the C's and λ's are available. If data are available from all compartments or for closed systems, the following general procedures provide a method for calculating the rate constants, and hence the flow rates and quantities which characterize the system. The handling of incomplete data will be considered subsequently.

The relationships among the k's in equation 14 and the C's and λ's in equation 15 may be established by equating the first derivative of equation 15 to equation 14, with the right-hand members of equation 15 being substituted for the x's in equation 14. Thus the

first derivatives of equation 15 have the form

$$\frac{dx_i}{dt} = -C_{i1}\lambda_1 e^{-\lambda_1 t} \cdots\cdots + C_{in}\lambda_n e^{-\lambda_n t} \qquad (16)$$

whereas substitution of the right-hand members of the equation 15's in the equation 14's and collecting the coefficients of the exponential factors gives

$$\frac{dx_i}{dt} = (k_{i1}C_{11} \cdots\cdots - K_i C_{i1} \cdots\cdots + k_{in}C_{n1})e^{-\lambda_1 t}$$
$$+ \cdots\cdots + (k_{i1}C_{1n} \cdots\cdots - K_i C_{in} \cdots\cdots + k_{in}C_{nn})e^{-\lambda_n t} \qquad (17)$$

Not only is equation 16 = equation 17, but the coefficient of each exponential factor ($e^{-\lambda_i t}$) in equation 16 equals that of the corresponding term in equation 17. These relationships provide a basis for expressing the values of the rate constants, the k's, in terms of the C's and λ's, and for expressing the C's in terms of the k's and λ's.

The most general technique involves the use of matrix algebra. The matrix of $C\lambda$ products in equation 16 is regarded as being generated by post-multiplication of a matrix composed of the C terms in equation 15, $[C]$, by the diagonal matrix of the exponents $[-\lambda]$. Thus $[C]\,[-\lambda]$ represents

$$\begin{bmatrix} C_{11} & \cdots\cdots & C_{1n} \\ \cdot & & \cdot \\ \cdot & & \cdot \\ \cdot & & \cdot \\ \cdot & & \cdot \\ \cdot & & \cdot \\ C_{n1} & \cdots\cdots & C_{mn} \end{bmatrix} \begin{bmatrix} -\lambda_1 & \cdots\cdots & 0 \\ \cdot & & \cdot \\ \cdot & & \cdot \\ \cdot & & \cdot \\ \cdot & & \cdot \\ \cdot & & \cdot \\ 0 & \cdots\cdots & -\lambda_n \end{bmatrix}$$

Similarly, the kC products in equation 17 are generated by pre-multiplication of $[C]$ by the matrix of k's, $[k]$, from equation 14, arranged by columns of $x_1, x_2 \cdots\cdots x_n$:

$$\begin{bmatrix} -K_1 & k_{12} & \cdots\cdots & k_{1n} \\ k_{21} & -K_2 & \cdots\cdots & k_{2n} \\ \vdots & & & \\ k_{n1} & k_{n2} & \cdots\cdots & -K_n \end{bmatrix} [C]$$

The equality between equation 16 and equation 17 thus gives

$$[k]\,[C] = [C]\,[-\lambda] \qquad (18)$$

Post-multiplication of both sides of equation 18 by the inverse of $[C]$, $[C]^{-1}$, solves equation 18 for $[k]$, since by definition

$$[C]\,[C]^{-1} = [1],$$

the identity matrix, and (19)

$$[k]\,[C]\,[C]^{-1} = [k] = [C]\,[-\lambda]\,[C]^{-1}$$

The catch to this simple-appearing method is the difficulty of generating $[C]^{-1}$ when real data involving decimal fractions are used. (Matrix inversion programs are routine for modern digital computers, so this is not a problem if such a machine is available.) Also, in principle, $[C]$ requires data from all n compartments although Berman & Schoenfeld (7) and Berman *et al.* (9) have developed techniques for working with incomplete data.

A numerical example for the hypothetical model system illustrated in figure 2 will serve to illustrate the method implied in equation 19.

In the system $1 \rightleftarrows 2 \rightleftarrows 3$ having $S_1 = 15$, $S_2 = 10$, $S_3 = 8$, $\rho_{12} = \rho_{21} = 30$ and $\rho_{23} = \rho_{32} = 40$, the differential equations for specific activities are

$$\frac{dx_1}{dt} = -2x_1 + 2x_2 + 0$$
$$\frac{dx_2}{dt} = 3x_1 - (3+4)\,x_2 + 4x_3 \qquad (20)$$
$$\frac{dx_3}{dt} = 0 + 5x_2 - 5x_3$$

If in this system $x_{10} = 88$ and $x_{20} = x_{30} = 0$, the "data" will be described by

$$x_1 = 40 + 4\,e^{-11t} + 44\,e^{-3t}$$
$$x_2 = 40 - 18\,e^{-11t} - 22\,e^{-3t} \qquad (21)$$
$$x_3 = 40 + 15\,e^{-11t} - 55\,e^{-3t}$$

And

$$[C][-\lambda] = \begin{bmatrix} 40 & 4 & 44 \\ 40 & -18 & -22 \\ 40 & 15 & -55 \end{bmatrix} \begin{bmatrix} 0 & 0 & 0 \\ 0 & -11 & 0 \\ 0 & 0 & -3 \end{bmatrix}$$
$$= \begin{bmatrix} -44 & -132 \\ 198 & 66 \\ -165 & 165 \end{bmatrix} \qquad (22)$$

The inverse matrix $[C]^{-1}$ is generated as follows.

Using the method given in Birkhoff & Mac Lane (12, p. 210), in which the inverse matrix is generated by determinants, and using D for the denominator determinant, we have

$$D = (40)(11)\begin{vmatrix} 1 & 4 & 4 \\ 1 & -18 & -2 \\ 1 & 15 & -5 \end{vmatrix} = (40)(11)(264) \qquad (23)$$

$$I_1 = (11)\frac{\begin{vmatrix} A_1 & 4 & 4 \\ A_2 & -18 & -2 \\ A_3 & 15 & -5 \end{vmatrix}}{D} = \frac{15A_1 + 10A_2 + 8A_3}{1320} \qquad (24)$$

$$I_2 = (40)(11)\frac{\begin{vmatrix} 1 & A_1 & 4 \\ 1 & A_2 & -2 \\ 1 & A_3 & -5 \end{vmatrix}}{D} = \frac{3A_1 - 9A_2 + 6A_3}{264} \tag{25}$$

$$I_3 = (40)\frac{\begin{vmatrix} 1 & 4 & A_1 \\ 1 & -18 & A_2 \\ 1 & 15 & A_3 \end{vmatrix}}{D} = \frac{3A_1 - A_2 - 2A_3}{264} \tag{26}$$

In this method the coefficients of the A's form the inverse matrix, giving

$$[C]^{-1} = \begin{bmatrix} \frac{15}{1320} & \frac{10}{1320} & \frac{8}{1320} \\ \frac{3}{264} & \frac{-9}{264} & \frac{6}{264} \\ \frac{3}{264} & \frac{-1}{264} & \frac{-2}{264} \end{bmatrix} \tag{27}$$

and

$$[C][-\lambda][C]^{-1} = \begin{bmatrix} 0 & -44 & -132 \\ 0 & 198 & 66 \\ 0 & -165 & 165 \end{bmatrix} \cdot \begin{bmatrix} \frac{15}{1320} & \frac{10}{1320} & \frac{8}{1320} \\ \frac{3}{264} & \frac{-9}{264} & \frac{6}{264} \\ \frac{3}{264} & \frac{-1}{264} & \frac{-2}{264} \end{bmatrix} = \begin{bmatrix} -2 & 2 & 0 \\ 3 & -7 & 4 \\ 0 & 5 & -5 \end{bmatrix} = [k] \tag{28}$$

Comparison of $[k]$ in equation 28 with equation 20 shows that this method does generate the k's (and K's) as it should. The power of the matrix method is shown by the fact that all the k's are solved for simultaneously, whereas other methods generate them one at a time.

Access to all compartments is often not feasible, however, and it is usually necessary to work with data from only a few compartments. Useful solutions for the k's may be obtained by manipulating the equalities obtained in equations 16 and 17 to eliminate the C's for experimentally inaccessible compartments. For the three-compartment systems (including some open ones), it is possible to get all of the k's and S's, and hence the ρ's when it is assumed that only one compartment is accessible (62). This is important in circulation studies because often the only data obtainable are the tracer concentrations in the blood (or a blood fraction) and direct measurements in other body organs or tissues of interest difficult or impossible to obtain in human beings. When the tracer is a gamma-ray emitter, in vivo counting data may be valuable [Conn (17)].

In a provocative article, Bergner (5) asserts that data from a single compartment are generally inadequate for the analysis of three-compartment systems. This is partially refuted by the analysis of Skinner *et al.* (62) giving explicit formulas for these systems. In an exchange of notes between Berman & Schoenfeld (8) and Bergner (6), the disagreement seems to come down to the question of whether it is acceptable to use additional available information to associate compartment numbers and flow rates; in multicompartment systems involving nonlinear equations, Bergner (6) points out that ambiguities may remain.

If the tracer is initially confined to one compartment, the total rate constant, K_1, for the injected compartment (assumed to be compartment 1) is simply (from equations 14 and 16)

$$K_1 = \frac{C_{11}\lambda_1 + \cdots C_{1n}\lambda_n}{x_{10}} \tag{29}$$

Other rate constants generally require more computation. The procedures for several three-compartment systems are recapitulated here in the present notation.

In $1 \rightleftarrows 2 \rightleftarrows 3$, when it is assumed that the label is initially confined to compartment 1 and that only compartment 1 is accessible, numerical values for $S_1\,x_{10}$ (the amount of activity injected), x_{10}, x_E, C_{11}, C_{12}, λ_1, and λ_2 are known or obtainable by experiment. The formulas for the rate constants are [Cohn & Brues (15), Robertson (52)].

$$k_{12} = \frac{C_{11}\lambda_1 + C_{12}\lambda_2}{x_{10}} \tag{30}$$

$$k_{21} = \frac{k_{12}(\lambda_1 + \lambda_2 - k_{12}) - \lambda_1\lambda_2\left(1 - \frac{x_E}{x_{10}}\right)}{k_{12}} \tag{31}$$

$$k_{32} = \frac{x_E}{x_{10}}\frac{\lambda_1\lambda_2}{k_{21}} \tag{32}$$

$$k_{23} = \frac{\lambda_1\lambda_2}{k_{12}}\left[1 - \frac{x_E}{x_{10}}\right] - k_{32} \tag{33}$$

Once the k's are known, the ρ's are quickly computed:

$$\rho_{12} = \rho_{21} = \frac{(S_1\,x_{10})}{x_{10}}\,k_{12} \tag{34}$$

$$\rho_{23} = \rho_{32} = \frac{\rho_{12}}{k_{21}}\,k_{23} \tag{35}$$

In $1 \rightleftarrows 2 \rightleftarrows 3$, when the label is initially confined to

compartment 2, and only compartment 2 is accessible, the input data are

$$(S_2 x_{20}),\ x_{20},\ x_E,\ C_{21},\ C_{22},\ \lambda_1 \quad \text{and} \quad \lambda_2$$

The rate constants are deduced by using the following sequence of calculations [Gellhorn *et al.* (27), Robertson (52)]:

$$(k_{21} + k_{23}) = K_2 = \frac{\lambda_1 C_{21} + \lambda_2 C_{22}}{x_{20}} \tag{36}$$

$$k_{12} = \tfrac{1}{2}\left[\lambda_1 + \lambda_2 - K_2 - \sqrt{(\lambda_1 + \lambda_2 - K_2)^2 - 4\lambda_1 \lambda_2 \left(\frac{x_E}{x_{20}}\right)}\right] \tag{37}$$

$$k_{32} = \tfrac{1}{2}\left[\lambda_1 + \lambda_2 - K_2 + \sqrt{(\lambda_1 + \lambda_2 - K_2)^2 - 4\lambda_1 \lambda_2 \left(\frac{x_E}{x_{20}}\right)}\right] \tag{38}$$

$$k_{21} = \frac{\lambda_1 \lambda_2 - k_{12} k_{32} - k_{12} K_2}{k_{32} - k_{12}} \tag{39}$$

$$k_{23} = K_2 - k_{21} \tag{40}$$

Again the rates are readily calculated from the rate constants:

$$\rho_{12} = \rho_{21} = \frac{(S_2\, x_{20})}{x_{20}}\, k_{21} \tag{41}$$

$$\rho_{23} = \rho_{32} = \frac{(S_2\, x_{20})}{x_{20}}\, k_{23} \tag{42}$$

Another set of formulas is given by Solomon (65) for the case in which the paired rate constants are equal.

The method of Skinner *et al.* (62) is applicable to open three-compartment systems, and the following example is based upon their analysis. It is assumed that only compartment 1 is accessible, that at time zero the activity is confined to compartment 1, and that the inflow is not labeled. Their method is first to establish three equations which express the effects of the restrictions on the system and five constants derived from relationships among the coefficients, exponents, and rate constants. These eight equations are then solved for the rate constants in terms of the five constants.

Equations by Skinner *et al.* (62) are in terms of amounts rather than specific activities. This does not affect the exponents but, of course, the coefficients in equation 15 must be in amount units. For consistency with the present notation, $(C_{1n}\ S_1)$ will be used for H_n in the original version. The eight relationships used are in the present notation:

$$\rho_{10} + \rho_{12} + \rho_{13} = K_1 S_1 \tag{43}$$

$$\rho_{20} + \rho_{21} + \rho_{23} = K_2 S_2 \tag{44}$$

$$\rho_{30} + \rho_{31} + \rho_{32} = K_3 S_3 \tag{45}$$

$$K_2 + K_3 = \lambda_2 + \lambda_3 + (\lambda_1 - \lambda_2)\,(C_{12} S_1) + (\lambda_1 - \lambda_3)\,(C_{13} S_1) = a_1 \tag{46}$$

$$K_2 K_3 - k_{23} k_{32} = (\lambda_2 - \lambda_1)\,(\lambda_2 - \lambda_3)\,(C_{12} S_1) - \lambda_2^2 + (C_{11} S_1)\,\lambda_2 = a_2 \tag{47}$$

$$K_1 = \lambda_1 + \lambda_2 + \lambda_3 - a_1 = a_3 \tag{48}$$

$$k_{13} k_{31} + k_{12} k_{21} = a_2 + a_3 a_1 - \lambda_1 \lambda_2 - \lambda_2 \lambda_3 - \lambda_3 \lambda_1 = a_4 \tag{49}$$

$$k_{13}\,(k_{32}\, k_{21} + K_2\, k_{31}) + k_{12}(k_{23}\, k_{31} + K_3\, k_{21}) = -\lambda_1 \lambda_2 \lambda_3 + a_3 a_2 = a_5 \tag{50}$$

The above equations can be used to solve for the rate constants defined in terms of inflow rates (ρ_{ij}/S_i) but in the original version (62) the outflow rate constants (ρ_{ji}/S_i) are used, and to facilitate comparison with the original, the following is a direct conversion to the present notation for the case $\rightarrow 1 \rightleftarrows 2 \rightleftarrows 3 \rightarrow$. Equations 46, 47, and 48 are as given above, whereas the others reduce to

$$\rho_{10} + \left(\frac{\rho_{12}}{S_2}\right) S_2 = K_1 S_1 = \left(\frac{\rho_{21}}{S_1}\right) S_1 \tag{43'}$$

$$\left(\frac{\rho_{23}}{S_3}\right) S_3 + \left(\frac{\rho_{21}}{S_1}\right) = K_2 S_2 = \left(\frac{\rho_{12}}{S_2} + \frac{\rho_{32}}{S_2}\right) S_2 \tag{44'}$$

$$\left(\frac{\rho_{32}}{S_2}\right) S_2 = K_3 S_3 = \left(\frac{\rho_{03}}{S_3} + \frac{\rho_{23}}{S_3}\right) S_3 \tag{45'}$$

$$\frac{\rho_{12}\, \rho_{21}}{S_2\, S_1} = a_4 \tag{49'}$$

$$\frac{\rho_{12}\, \rho_{21}}{S_2\, S_1} K_3 = a_5 \tag{50'}$$

In this case the rate constants are then calculated from the combinations of the *a*'s indicated below:

$$S_2/S_1 = \frac{a_3\, a_5}{a_2\, a_4} \tag{51}$$

$$S_3/S_1 = \frac{a_1\, a_3\, a_4 - a_3\, a_5 - a_4^2}{a_2\, a_4} \tag{52}$$

$$\rho_{10}/S_1 = \frac{a_2\, a_3 - a_3}{a_2} \tag{53}$$

$$\frac{\rho_{03}}{S_3} = \frac{a_4(a_2 a_3 - a_5)}{a_1 a_3 a_4 - a_3 a_5 - a_4^2} \tag{54}$$

$$\frac{\rho_{12}}{S_2} = \frac{a_4}{a_3} \tag{55}$$

$$\frac{\rho_{21}}{S_1} = a_3 \tag{56}$$

$$\frac{\rho_{23}}{S_3} = \frac{a_3(a_1 a_4 a_5 - a_2 a_4^2 - a_5)}{a_4(a_1 a_3 a_4 - a_3 a_5 - a_4^2)} \tag{57}$$

$$\frac{\rho_{32}}{S_2} = \frac{a_1 a_3 a_4 - a_3 a_5 - a_4^2}{a_3 a_4} \tag{58}$$

Once the rate constants have been calculated, the conversion to rates (ρ) is readily achieved from the appropriate relationships above.

Similar analyses of two other three-compartment open systems, one having flow into the center compartment and out one of the end compartments, the other having flow into and out of the third compartment as well, are given in detail, with numerical examples, by Skinner *et al.* (62).

If data are available from additional compartments and/or the outflows, the equations used in the above procedures are simpler, and if all three compartments are accessible, all of the rate constant equations become linear.

CALCULATION OF EXPONENTIAL CONSTANTS. At the stage of model analysis, it is sometimes desirable to predict the tracer behavior from the assumed parameters of the system. The λ's in equation 15 may be calculated independently by substituting $-\lambda x_i$ for dx_i/dt in equation 14, and setting the determinant of the coefficients of the x's equal to zero.[2]

Thus, for the complete three-compartment system (fig. 3), this substitution gives:

$$\begin{vmatrix} \lambda - K_1 & k_{12} & k_{13} \\ k_{21} & \lambda - K_2 & k_{23} \\ k_{31} & k_{32} & \lambda - K_3 \end{vmatrix} = 0 \tag{59}$$

Expansion of equation 59 shows that the λ's are the three roots of a third order algebraic equation:

$$\begin{aligned} \lambda^3 &- (K_1 + K_2 + K_3)\lambda^2 \\ &+ (K_1K_2 + K_1K_3 + K_2K_3 - k_{21}k_{12} - k_{31}k_{13} - k_{32}k_{23})\lambda \\ &- K_1K_2K_3 + k_{32}k_{23}K_1 + k_{31}k_{13}K_2 + k_{21}k_{12}K_3 \\ &+ k_{21}k_{32}k_{13} + k_{31}k_{12}k_{32} = 0 \end{aligned} \tag{60}$$

[2] The basis for this substitution is the fact that the coefficients of successive derivatives, d/dt, d^2/dt^2, etc. of e^{ax} are a, a^2, etc.

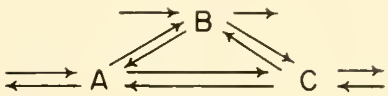

FIG. 3. Complete three-compartment open system.

The imposition of constraints such as eliminating inflows and outflows or the exchange between two compartments modifies equation 59 by eliminating some k's and by removing some ρ_{ji}/S_i terms included in the K's. For the closed three-compartment system, the last six terms in equation 60 add up to zero, and λ may be factored out of the remaining terms, leaving, for the non-zero λ's

$$\begin{aligned} \lambda^2 &- (K_1 + K_2 + K_3)\lambda + K_1K_2 \\ &+ K_1K_3 + K_2K_3 - k_{21}k_{12} - k_{31}k_{13} - k_{32}k_{23} = 0 \end{aligned} \tag{61}$$

Further reduction of the system to $1 \rightleftarrows 2 \rightleftarrows 3$ by eliminating ρ_{13} and ρ_{31} automatically eliminates k_{13} and k_{31} and imposes the requirement that $\rho_{21} = \rho_{12}$ and $\rho_{32} = \rho_{23}$, giving $K_1 = k_{12}$ and $K_3 = k_{32}$, reducing equation 61 to

$$\lambda^2 - (k_{12} + K_2 + k_{32})\lambda + k_{12}k_{23} + k_{32}k_{21} + k_{12}K_{32} = 0 \tag{62}$$

The λ's for the two-compartment open systems are also obtained as a reduced form of equation 61:

$$\lambda^2 - (K_1 + K_2)\lambda + K_1K_2 - k_{12}k_{21} = 0 \tag{63}$$

In general the λ's for an n-compartment open system are the n roots of an nth order algebraic equation, and those for an n-compartment closed system are the $(n - 1)$ roots of an $(n - 1)$th order equation. It will be noted that the λ's are determined entirely by the kinetic characteristics of the system and are not affected by variations in the initial distribution of the tracer.

CALCULATION OF COEFFICIENTS. In contrast to the case for the λ's, the absolute values of the coefficients, the C's in equation 15 do depend upon the boundary conditions such as whether or not the inflow is labeled and which compartments are labeled initially. The relative values, however, may be expressed independently of the boundary conditions. A procedure for generating the relative values of the C's is to regard the entries in equation 59 or its counterpart for other systems as the coefficients, not of the x's, but of the C's associated with a particular value of λ. The same relationships are obtained by equating corresponding terms in equation 14 and the derivative of equation 15. Thus, for the constrained three-compartment system $1 \rightleftarrows 2 \rightleftarrows 3$, the coefficients of the terms

which include the factor $e^{-\lambda_1 t}$ are determined by

$$(\lambda_1 - k_{12})C_{11} + k_{12}C_{21} + 0 = 0 \quad (64)$$

$$k_{21}C_{11} + (\lambda_1 - K_2)C_{21} + k_{23}C_{31} = 0 \quad (65)$$

$$0 + k_{32}C_{21} + (\lambda - k_{32})C_{31} = 0 \quad (66)$$

Equation 64 gives C_{21} in terms of C_{11} directly:

$$C_{21} = \frac{(k_{12} - \lambda_1)}{k_{12}} C_{11} \quad (67)$$

Solving equation 66 for C_{21} in terms of C_{31} and substituting the result in equation 67 yields

$$C_{31} = \frac{k_{32}(\lambda_1 - k_{12})}{k_{12}(\lambda_1 - k_{32})} C_{11} \quad (68)$$

Similarly, the coefficients of the terms containing $e^{-\lambda_2 t}$ are

$$C_{22} = \frac{(k_{12} - \lambda_2)}{k_{12}} C_{12} \quad \text{and} \quad C_{32} = \frac{k_{32}(\lambda_2 - k_{12})}{k_{12}(\lambda_2 - k_{32})} C_{12} \quad (69)$$

Inclusion of equations expressing the initial conditions provides the necessary basis for calculating the absolute values of the C's. For example, if the tracer is initially confined to compartment 1 in $1 \rightleftarrows 2 \rightleftarrows 3$, at time zero:

$$\begin{aligned} x_{10} &= x_E + C_{11} + C_{12} \\ x_{20} = 0 &= x_E + C_{21} + C_{22} \\ x_{30} = 0 &= x_E + C_{31} + C_{32} \end{aligned} \quad (70)$$

Combining equations 67, 68, 69, and 70 leads to

$$\begin{aligned} \frac{x_1}{x_E} &= 1 + \left(\frac{k_{12}}{k_{32}}\right)\left(\frac{k_{32} - \lambda_1}{k_{12} - \lambda_1}\right)\left(\frac{\lambda_2}{\lambda_1 - \lambda_2}\right)e^{-\lambda_1 t} \\ &\quad + \left(\frac{k_{12}}{k_{32}}\right)\left(\frac{k_{32} - \lambda_2}{k_{12} - \lambda_2}\right)\left(\frac{\lambda_1}{\lambda_2 - \lambda_1}\right)e^{-\lambda_2 t} \\ \frac{x_2}{x_E} &= 1 + \left(\frac{k_{32} - \lambda_1}{k_{32}}\right)\left(\frac{\lambda_2}{\lambda_1 - \lambda_2}\right)e^{-\lambda_1 t} \\ &\quad + \left(\frac{k_{32} - \lambda_2}{k_{32}}\right)\left(\frac{\lambda_1}{\lambda_2 - \lambda_1}\right)e^{-\lambda_2 t} \\ \frac{x_3}{x_E} &= 1 + \frac{\lambda_2}{\lambda_1 - \lambda_2} e^{-\lambda_1 t} + \frac{\lambda_1}{\lambda_2 - \lambda_1} e^{-\lambda_2 t} \end{aligned} \quad (71)$$

Electronic Computer Application

Even when only three compartments are involved, the relationships between the tracer data and the system parameters are sufficiently complicated to discourage the use of desk calculations when there are much data to process. Although various kinds of analog systems, particularly hydrodynamic systems, are of value in studying compartmented systems and in teaching the principles involved, when it comes down to calculating the results from real systems, the most effective assistance is obtained through the use of electronic computers.

The two basic types of computers, analog and digital, may be typified by the slide rule and the desk calculator. The former has the virtues of low cost, speed, and convenience, whereas a major advantage of the latter is precision. To a large extent these qualities also hold for the larger electronic counterparts of each kind of machine. The analog computers are useful for quickly determining which of several possible kinds of systems provides the best explanation for a given set of data. Once the basic model system to be used is established, the digital computers provide a higher precision than can be achieved with analog machines, or if there are ambiguities due to incomplete data available, to establish the range of possible values.

ANALOG COMPUTER METHODS. Analog computer methods may be divided into those which employ direct approaches and those which involve indirect approaches. By the direct approach is meant the use of a system in which the electrical components are arranged to give a direct analogy of the biological system, in contrast with the indirect approach in which the electrical components are arranged to solve the differential equations which describe the behavior of the labeled material in the system. The indirect approach provides greater generality but the direct approach is simpler. Since many of the problems of compartmental analysis can be treated satisfactorily by the direct approach, its use will be emphasized here. The problems for which the direct approach is inadequate can often be handled by a combination of the techniques of the two approaches without the necessity of a complete conversion to the indirect approach.

The basis for the direct approach is the fact that the equations which describe the specific activity of a tracer in certain compartmental systems are identical in form with those which describe the voltages on capacitors in resistor-capacitor (RC) circuits and other first order reactions.

Figure 4 shows the RC circuit analogs of the four-compartment series and parallel systems. In these systems capacitance is analogous to the size of the compartment and voltage to specific activity. The resistor values are inversely proportional to the flow rates. For pure RC analogies to be valid, it is essential

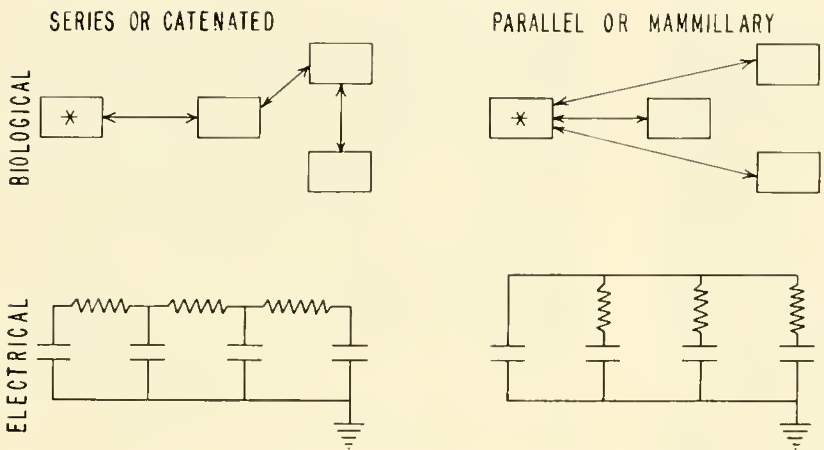

FIG. 4. Kinetic analysis of compartmental systems using electrical analogs. The analogy between the basic elements of electrical resistor-capacitor (RC) circuits and two basic types of biological compartmented systems is shown.

that the flow rates in the two opposing directions between compartments be equal. This requirement is satisfied for open systems in which the flows into and out of the system involve the same compartment. Some of the basic compartmented systems which are analyzable with RC analog circuits and typical curves obtained with an analog computer are shown in figure 5. In each case the tracer is initially present in the compartment indicated by an asterisk. It should be noted that in the two-compartment system, in which the initially labeled compartment is open, the specific activity curves cross, whereas when the second compartment is open the specific activity in the initially labeled compartment always remains the higher of the two.

The most satisfactory method for using an analog computer to obtain data fitting curves is to generate the data points electronically and to display them and the analog curves on the same oscilloscope screen, as is illustrated in figure 6, for a hypothetical four-compartment system. Once an acceptable fit is obtained, the values of the capacitor settings used are proportional to the sizes of the biological compartments. Interpretation of the resistor settings depends upon the time scale used. The electrical time units and real time units are connected through the relationship that the product of the resistance in ohms and the capacitance in farads gives the time constant in seconds, and this time constant is analogous to the average time, or the reciprocal of the turnover rate constant for the biological system. The conversion factor, α, may be determined by calculation or may be determined empirically for a given setting of the oscilloscope controls from the half-time of a single exponential curve, which in turn may be generated from the analog of a one-compartment open system, and using the relationship $k = \log_e 2/T_{\frac{1}{2}} = 1/\alpha \, \mathrm{RC}$

It is not necessary that the tracer be injected instantaneously. Figure 7 shows a curve fitted with an analog computer to data obtained when creatinine was injected in a dog by an intravenous infusion taking 30 min. In this case a constant rate of infusion was assumed, and this was simulated by a "pump" circuit giving a constant current. For more complicated inflow patterns a function generator may be needed.

The key feature of analog circuits designed for solving differential equations is the operational amplifier, which is a very high gain (100,000 and more) DC amplifier. Stacy (67) discusses the basic principles of these circuits.

The advantage of operational amplifiers is that they can be used to reproduce a given voltage at another point without drawing current from the original source. Depending upon the choice of electrical elements used in their feed-back loops, operational amplifiers may be used to add, subtract, multiply, divide, integrate, and differentiate, thus providing all of the operations needed for solving differential equations.

The use of operational amplifiers in conjunction with RC circuits makes it possible to maintain the basic simplicity of the direct analog method without the restrictions which the pure RC method imposes on flow rates. For example, Macdonald *et al.* (43) utilize a circuit for the simulation of unequal forward and reverse flow rates between two compartments in an otherwise basically RC circuit computer.

Among the illustrative examples which may be cited concerning applications of analog computers in

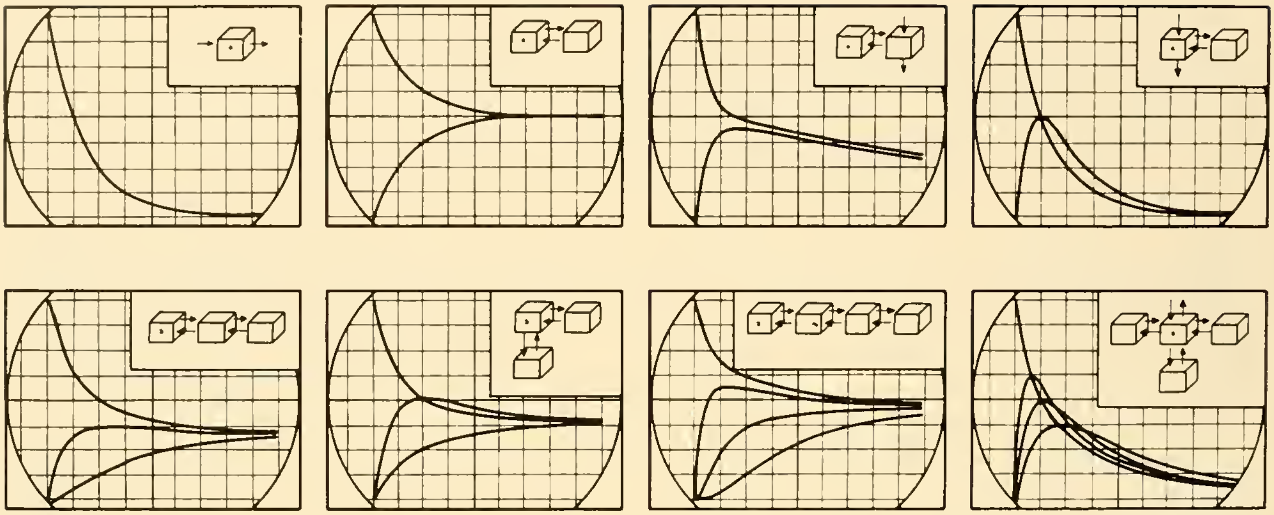

FIG. 5. Basic types of compartmented systems analyzable with RC analogs and typical curves obtained with analog computer.

compartmental system and circulatory problems are the following:

Gregg (30) discusses the use of the indirect type of analog computer to problems such as the removal by the kidney of Diodrast injected into the blood stream. Solomon & Gold (66) have used analog computers in studies of potassium transport. Warner (72) describes the use of an analog computer in studies of regulation of the circulation and the response to transient disturbances such as the Valsalva maneuver. Fish (24) discusses the general problem of compartmental system analysis by analogs, with applications to the interpretation of excretion data.

Bauer & Ray (3) used an analog computer to solve problems of strontium metabolism involving distinguishing between the uptake in bone by accretion and the uptake by exchange. Rollinson & Rotblat (53) describe a fairly elaborate electrical analog system designed to simulate the metabolism of iodine. Parrish *et al.* (47) have used an analog computer in studies of pulmonary circulation.

DIGITAL COMPUTERS. As their name implies, digital computers are essentially number-handling machines. The familiar desk calculator and the "giant brains" or electronic digital computers have in common the basic capabilities of being able to store (or "remember") numbers and to add or subtract pairs of these numbers.

Almost all other computations, multiplication, division, extraction of square roots, taking logarithms, raising to powers, etc. are achieved through sequences of basically addition operations, the larger machines differing from the smaller ones in such features as the capacity and accessibility of the memory, the degree of automation, and the speed of operations. The large machines perform tens of thousands of operations per second, so computations which would be absurd to attempt with a desk computer become entirely reasonable to achieve with an electronic computer.

In addition to performing the basic arithmetical operations, digital computers can make certain simple logical decisions such as choosing between alternative sequences of operations, stopping repetitive operations when some arbitrary condition is attained, etc.

The big job for the user of a digital computer consists of figuring out how to tell the machine what he wants it to do, or programming. The machines have built-in programs for the basic operations, so that it is not necessary to prescribe every detail, but it is necessary to establish the sequence of operations desired.

Although it is more difficult and more expensive to set up a problem on a digital computer than on an analog computer, the digital computer can handle a much wider variety of problems (including nonsteady-state conditions, for example) and gives a higher degree of precision in the answer if warranted by the data. Because of the complexity of the subject, including the differences among the variety of machines available, it is not feasible to present a complete or even an adequate discussion of the

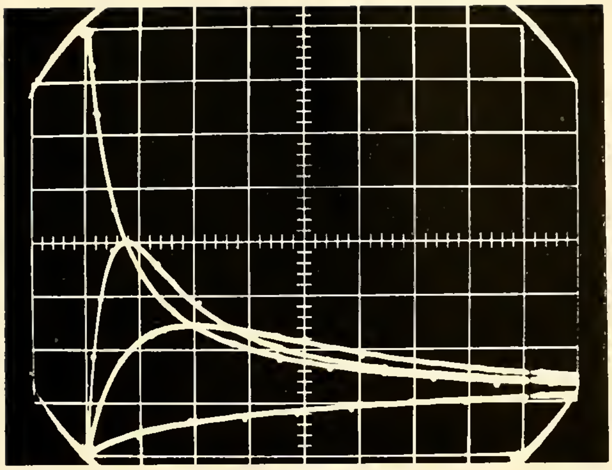

FIG. 6. Four-compartment system specific activity curves generated by an analog computer and showing data points displayed on same oscilloscope for convenience in curve-fitting.

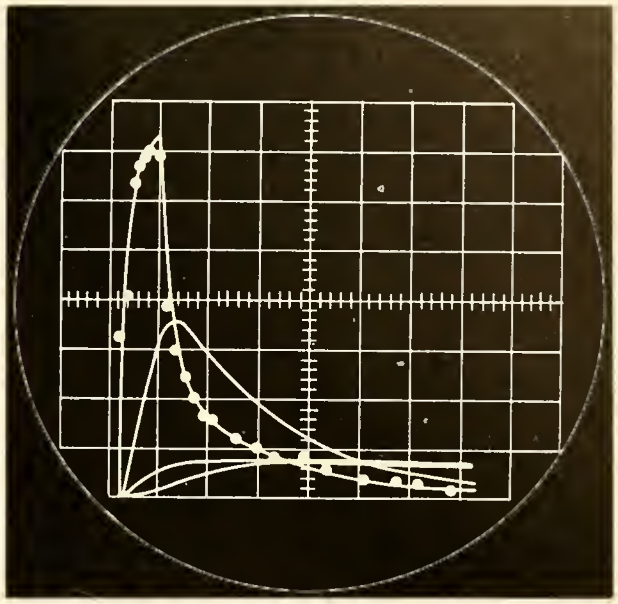

FIG. 7. Curves fitted with analog computer to concentration in plasma of creatinine injected intravenously at a constant rate during first 30 min. (Data courtesy Dr. Paul Schloerb.)

methods of programming and using digital computers here. It will have to suffice to indicate that there are several possible modes of use applicable to the analysis of tracer data.

One such use is at the stage of curve-fitting. Largely because of the accumulated effect of the random errors in real data, the attempts to achieve a true least-squares fit for multi-exponential component curves have not been entirely satisfactory. Of course, a method similar to the peeling-off technique used in graphical analysis can be used, with the least-squares method being used to give the best fit for each component, but this has been objected to on the grounds that it gives nonuniform weighting of the data points. An entirely different procedure for resolving curves into exponential components has been published by Gardner *et al.* (26). The latter method used a Fourier transform method with numerical integration being achieved with an IBM-650 computer.

Another application of digital computers to problems of compartmental analysis arises after the necessary parameters describing the curve in terms of exponential components have been achieved, and consists of transforming the parameters of the data into the parameters of the system, as indicated in principle in equation 19. Alternatively, the computer may be programmed to test a large number of possible models systematically and to select those which best fit the data.

The general principles of programming digital computers and some biological applications are discussed by Stacy (68). Sheppard (59) presents a detailed program for solving three-compartment nonsteady-state problems, written in FORTRANSIT, a "language" for giving instructions to IBM-650 digital computers. The FORTRANSIT program requires only slight modifications to FORTRAN, a more general program for use with IBM-704, -7090, Univac, and other modern high-speed machines. Each of these machines requires a translation of the FORTRAN program into its own "machine language" (using binary or octal instead of decimal numbers, etc.), but this translation is achieved automatically when cards punched to represent FORTRAN statements are used as the input for the appropriate translating machine. Berman *et al.* (9) have developed a very general program suitable for, but not restricted to, linear systems or even to compartmented systems. This program can handle up to 40 parameters, of which up to 25 may be unknowns, in a system of up to 15 compartments. A set of IBM cards with the FORTRAN statements or a set suitable for direct use with the IBM-704 is available upon request from Dr. Mones Berman, National Institutes of Health, Bethesda, Md. A good example of the kind of problem for which this program is suited, involving finding a model giving the best fit to a set of plasma and excretion data, is presented by Lewallen *et al.* (42).

ROLE OF RADIOISOTOPIC TRACERS IN DETERMINING REGIONAL FLOW RATES

When there are so many other good methods for measuring regional flow rates, it is admittedly somewhat artificial to single out those contributions which involve the use of isotopic tracer methods, and it would be desirable to treat such contributions within the context established by the other methods. This is not the place for the broad review of the literature that such comparisons would require, but it is expected that other chapters of the *Handbook* will to a large extent provide this context.

The radioactive methods do have some unique features, including susceptibility to the compartmental analysis expounded above, and determination by external detectors [Conn (17, 18), Anger & Upham (1)], which justify their separate consideration. On the other hand, in most kinetic studies which would be good examples of uses of compartmental analysis the chief interest is in other aspects of the behavior of the labeled substance, with regional flow rates being only an incidental problem, whereas in most of the studies which are directed to the problem of regional flow rates the methods of data analysis are simply extensions of other indicator dilution methods. The reader is again referred to Zierler's (74) chapter, for the theory of the Stewart-Hamilton method, but some further examples will be mentioned here. A number of articles (1, 2, 10, 13, 35, 37, 38, 40, 63) which emphasize without being restricted to the use of radioisotopic tracers in peripheral blood flow measurement are collected in the volume edited by Bruner (14). Some of the areas in which the contributions made through use of isotopic tracers are significant are as follows.

Cerebral Flow

Lassen & Munck (41) have modified and adapted the N_2O method to the use of Kr^{85} in the measurement of cerebral blood flow, and find the isotopic method equally as satisfactory. In a later report Munck & Lassen (45) recommend taking bilateral internal jugular venous blood samples because the two sides may give different results. Sokoloff (63) cites a report by Lewis *et al.* discussing the further advantages of Kr^{79}, which permits rapid and continuous measurement of total cerebral blood flow in man. In this method, cerebral blood flow is calculated minute by minute for successive minutes by the equation

$$CBF = \frac{\Delta Q_{t-1}^{t} \times f}{\int_{t-1}^{t} (C_A - C_V)\, dt}$$

where C_A and C_V are the arterial and cerebral venous concentrations as determined by counting blood flowing through a glass coil in a well-type scintillation counter, ΔQ is the change in brain counts per minute over the interval $(t\text{-}1)$ to t, f is a proportionality constant to convert brain and blood counting rates to equivalent units and CBF is the total cerebral blood flow in milliliters per minute. The mean total cerebral blood flow during the middle 6 min of the 10-min desaturation period studied was found to be 1181 ± 132 ml per min in normal young men, which is somewhat higher than corresponding N_2O results, probably reflecting some contribution from the blood flow to other tissues in the head. The Kr^{79} method had been proposed by Wechsler (73) for measurement of cerebral blood flow in humans under acceleration but he did not publish data.

Kety (37, 38) has adapted the Fick principle to the measurement of local cerebral blood flow in the cat using CF_3I^{131} and has obtained blood flow rates for 28 anatomical subdivisions of the central nervous system. The values obtained range from a low of 0.14 ml per g per min for spinal cord white matter to 1.80 ml per g per min for the inferior colliculus.

Myocardial Flow

The clinical importance of knowledge concerning the blood supply of the heart has stimulated intense interest in finding new and better methods for measuring the myocardial blood supply. For example, Hansen *et al.* (31) have used Kr^{85} for studying coronary blood flow and obtained values in normal controls comparable with values obtained using the bubble flowmeter and N_2O methods. Conn & Robertson (19) studied potassium exchange in dog heart muscle by maintaining a constant arterial K^{42} concentration and interpreting the venous K^{42} concentration curve in terms of a two-compartment open system. Assuming that the blood flow rate is the limiting process in the plasma-extracellular fluid exchange, this procedure offers another possible measurement of myocardial blood flow, but in common with other methods has the disadvantage of requiring venous catheterization. Conn (17) discusses several papers concerned with myocardial blood flow determinations by external counting methods. Bing *et al.* (11) review

the difficulties of various techniques and opine that the new tools will eventually furnish a workable method for the determination of coronary blood flow in man.

Hepatic Flow

The blood flow through the liver has been measured by Dobson & Jones (21) by observing the rate of disappearance of intravenously injected particulate matter from the blood stream.

In the dog and in mice, up to 90 per cent of intravenously injected colloidal chromic phosphate (labeled with P^{32}) can be recovered in the liver, and most of the balance in the spleen. For the first few minutes the disappearance curve is essentially exponential, with $C_t = C_0e^{-kt}$, where C_t is the concentration at any time, t, C_0 is the initial concentration, and k is the disappearance constant.

For longer time intervals (30 min or more) the disappearance curve is not a single exponential but may be resolved into three exponential components. Of these the slowest component, or "tail" of the curve, is attributed to the presence of noncentrifugable small particles in the colloidal suspension injected. At time zero this component contributes only 0.16 per cent of the radioactivity in the blood.

The two fast components of a representative curve in mice have half-times of 20 and 73 sec. The fastest component is regarded as being dependent on the liver blood flow. Since the splenic venous blood goes through the liver, the splenic blood flow is part of the hepatic blood flow. If the liver and spleen were 100 per cent efficient in removing the labeling agent from the blood, the disappearance constant, k, would measure the fraction of the circulating blood which passes through the liver in a unit time interval, but if only some fraction, η, is removed in one passage, k is the product of η and the perfusion factor. If η is low, a correction is needed to take into account the double uptake in the splenic-liver flow. In anesthetized mice, dogs, and rabbits, the efficiency factor, η, in the liver was found to be 80 to 90 per cent and in mice the spleen circulation was found to average about 4 per cent of the liver circulation, so in general the correction for splenic plus hepatic uptake is not significant in these studies. In any event, k gives the minimum perfusion factor.

A theoretically possible but unproven explanation for the second fast component involves the different rates of time required for transit of the extrahepatic portions of the circulation. Alternatively, the particles may fall into two discrete groups on the basis of the efficiency of their removal by the liver.

The above considerations justify the idealization of the system as comprising a one-compartment open system, with the blood being regarded as a uniformly mixed compartment and the liver as the only output route. Studies of the mixing times in the blood with similar but more slowly disappearing colloids containing yttrium [Gofman, cited in (21)] indicate that in rabbits the colloid is mixed with 95 per cent of the circulating blood in one-half to one minute.

The maximum and minimum blood-liver perfusion factors found with the above method in anesthetized animals were: dog 1.2 to 1.4, rabbit 1.12 to 1.3, and mouse 1.7 to 2.2 volumes of blood per minute per volume of tissue.

The minimum values in nonanesthetized rabbits and mice were lower, but the efficiency factors were not determined. Epinephrine and irradiation (19,000 to 26,000 rad delivered from radioactive yttrium) were found to lower the liver circulation.

With mice it is possible to check the results obtained using the blood-disappearance curve by comparing it with the liver-appearance curve obtained by in vivo measurements with an external counter. For animals larger than small rats, the absorption of P^{32} β^- particles in thick layers of tissue renders in vivo counting too inaccurate, but similar procedures involving gamma-emitting labels would make the in vivo technique applicable in man.

Parker & Finney (46) agree that the liver blood flow is the rate-limiting step in the removal of certain colloids from the blood for small doses of injected material, but with larger doses find it necessary to express the rate dependence on dose as follows, where C is the concentration in the plasma:

$$-\frac{dc}{dt} = kC^{0.33}$$

The doses above a critical dose are removed from the blood with a very low efficiency in a single passage through the liver, and in this circumstance blood flow is not the rate-limiting step.

Flow Rates Measured by Tissue Uptake of K^{42}

In contrast with the method described above for the liver blood flow, Sapirstein (55, 56) has capitalized on the extreme rapidity with which potassium and related ions penetrate almost all tissues [Walker & Wilde (71), Ginsburg & Wilde (28)]. Studies with K^{42} indicated that at least during the first minute after an

intravenous injection in rats, the venous drainage of K^{42} is negligible compared with its initial deposition in the organs. Analysis of the radioactivity content of various organs in animals killed 5 to 1200 sec after K^{42} injection in the femoral vein showed appreciable variation but no definite trend upwards or downwards from 5 to 60 sec. The average values found during the first minute were therefore ascribed to the fraction of the cardiac output distributed to each organ. After 3 min a downward trend was noted in the activity in the kidney. In these studies the activity in the brain was conspicuously low at all times. The extent to which this is due to depression of the cerebral circulation by the anesthesia versus inherent peculiarities of potassium exchange in the brain is not clear.

In subsequent studies the above reasoning has been applied to the determination of the blood flow rates to the hand (57) and the adrenal (58). The same principle, but using Rb^{86}, has been used by Goldman & Sapirstein (29) to measure the perfusion rate of the pituitary gland, in which exchange is much more rapid than is true for the brain.

Although at first glance the above method would seem to be open to the objection that mixing cannot be complete by the time of the first point (5 sec), further reflection shows that longitudinal mixing would be unimportant if all tissues had an extraction ratio of 100 per cent. If, however, there is a high venous return of K^{42} from the brain (or other organ), this activity is redistributed among the other tissues and the calculated perfusion rates, if expressed as fractions of the cardiac output, will be too high. If more complete data on the potassium exchange in the brain are available for the time interval concerned, a correction for cerebral flow would seem to be in order.

Regional Flow Rates by Tissue Clearance

Dobson & Warner (22) have injected Na^{24} directly into the artery supplying a limb or tissue, giving that region an initially high concentration of activity, and have characterized the circulation of the region involved by the subsequent rate of disappearance of the tracer. For the human forearm, interpretation of the data is based on a model having three compartments circulated in parallel, the washout curve having three exponential components. Comparison of the washout curves obtained similarly with I^{131} ion and I^{131}-labeled albumin has been used to estimate the relative sizes of the intravascular and extravascular pools in the tissues involved. Conn (17) discusses other aspects of the measurement of regional circulation rates by the clearance method.

SUMMARY

The elementary mathematical principles applicable to determining regional flow rates by interpretation of the behavior of tracers in steady-state compartmented systems are developed in sufficient detail for use by novices in the field. The more complicated systems, particularly nonsteady-state systems, are not treated but are referred or alluded to in the references cited. The analysis discussed is particularly suited to use with radioactive tracers, and some examples of uses of radioisotopic tracers in determining regional flow rates are discussed.

REFERENCES

1. ANGER, H. O. AND F. T. UPHAM. In-vivo counting methods in medical research. In: *Methods in Medical Research.* Chicago: Yr. Bk. Pub., 1960, vol. 8, pp. 248–253.
2. BARKER, E. S. AND J. K. CLARK. Measurement of renal blood flow by application of the Fick principle. In: *Methods in Medical Research.* Chicago: Yr. Bk. Pub., 1960, vol. 8, pp. 283–292.
3. BAUER, G. C. H AND R. D. RAY. Kinetics of strontium metabolism in man. *J. Bone & Joint Surg.* 40A: 171–186, 1958.
4. BEIERWALTES, W. H., P. C. JOHNSON, AND A. J. SOLARI. *Clinical Use of Radioisotopes.* Philadelphia: Saunders, 1957.
5. BERGNER, P.-E. E. Dynamic aspects of method in tracer kinetics. *Exper. Cell Res.* 17: 328–335, 1959.
6. BERGNER, P.-E. E. On the solution of the compartmentalized tracer system. *Exper. Cell Res.* 20: 579–661, 1960.
7. BERMAN, M. AND R. SCHOENFELD. Invariants in experimental data on linear kinetics and the formulation of models. *J. Appl. Phys.* 27: 1361–1370, 1956.
8. BERMAN, M AND R. SCHOENFELD. A note on unique models in tracer kinetics. *Exper. Cell Res.* 20: 574–578, 1960.
9. BERMAN, M., E. SHAHN, AND M. WEISS. A computer program for the fitting of data to a model. 5th National Biophysics Society Meeting, St. Louis, Feb. 1961.
10. BING, R. J. Determination of coronary blood flow. In: *Methods in Medical Research.* Chicago: Yr. Bk. Pub. 1960, vol. 8, pp. 269–275.
11. BING, R. J., H. K. HELLEMS, AND T. J. REGAN. Editorial:

Measurement of coronary blood flow in man. *Circulation* 22: 1–3, July 1960.
12. Birkhoff, G. and S. Mac Lane. *A Survey of Modern Algebra.* New York: Macmillan, 1948.
13. Bradley, S. E. Estimation of hepatic blood flow. In: *Methods in Medical Research.* Chicago: Yr. Bk. Pub., 1960, vol. 8, pp. 275–283.
14. Bruner, H. D. (editor). Peripheral blood flow measurement, I. Blood-tissue exchange methods. In: *Methods in Medical Research,* Chicago: Yr. Bk. Pub., 1960, vol. 8, pp. 222–292.
15. Cohn, W. B. and A. M. Brues. Metabolism of tissue cultures, part III; a method for measuring the permeability of tissue cells to solutes. *J. Gen. Physiol.* 28: 449–461, 1945.
16. Comar, C. L. *Radioisotopes in Biology and Agriculture.* New York: McGraw-Hill, 1955.
17. Conn, H. L., Jr. Use of external counting techniques in studies of the circulation. In: *Symposium on Use of Indicators in the Study of the Circulation.* Salt Lake City: Jan. 1961.
18. Conn, H. L., Jr. Measurement of organ blood flow without blood sampling. *J. Clin. Invest.* 34: 916–917, 1955.
19. Conn, H. L., Jr., and J. S. Robertson. Kinetics of potassium transfer in the left ventricle of the intact dog. *Am. J. Physiol.* 181: 319–324, 1955.
20. Defares, J. G., and I. N. Sneddon. *The Mathematics of Medicine and Biology.* Chicago: Yr. Bk. Pub., 1960.
21. Dobson, E. L. and H. B. Jones. The behavior of intravenously injected particulate material. Its rate of disappearance from the blood stream as a measure of liver blood flow. *Acta med. scandinav.* 144: Suppl. 273, 71 pp, 1952.
22. Dobson, E. L. and G. F. Warner. Measurement of regional sodium turnover rates and their application to the estimation of regional blood flow. *Am. J. Physiol.* 189: 269–276, 1957.
23. Finkbeiner, D. T., II. *Introduction to Matrices and Linear Transformations.* San Francisco: Freeman, 1960.
24. Fish, B. R. Applications of an analog computer to analysis of distribution and excretion data. *Health Phys.* 1: 276–281, 1959.
25. Ford, L. R. *Differential Equations.* New York: McGraw-Hill, 1933.
26. Gardner, D. G., J. C. Gardner, G. Laush, and W. W. Meinke. A method for the analysis of multicomponent exponential decay curves. *J. Chem. Physics,* 31, 4: 978–986, 1959.
27. Gellhorn, A., M. Merrell, and R. M. Rankin. Rate of transcapillary exchange in normal and shocked dogs. *Am. J. Physiol.* 142: 407–427, 1944.
28. Ginsburg, J. M. and W. S. Wilde. Distribution kinetics of intravenous potassium. *Am. J. Physiol.* 179: 63–75, 1954.
29. Goldman, H. and L. A. Sapirstein. Determination of blood flow to the rat pituitary gland. *Am. J. Physiol.* 194: 433–435, 1958.
30. Gregg, E. C. *An Analogue Computer for the Generalized Three-Compartment Model of Transport in Biological Systems.* Western Reserve University report, NYO-2906, Dec. 1959.
31. Hansen, A. T., B. F. Haxholdt, E. Husfeldt, N. A. Lassen, O. Munck, H. R. Sorenson, and K. Winkler. Measurement of coronary blood flow and cardiac efficiency in hypothermia by use of radioactive krypton-85. *Scandinav. J. Clin. & Lab. Invest.* 8: 182–188, 1956.
32. Hevesy, G. Historical progress of the isotopic methodology and its influences on the biological sciences. *Minerva nucleare* 1: 182–200, 1957.
33. Hevesy, G. *Radioactive Indicators.* New York: Interscience, 1948.
34. Holl, D. L., C. G. Maple, and B. Vinograde. *Introduction to the Laplace Transform.* New York: Appleton-Century-Crofts, 1959.
35. Hyman, C. Peripheral blood flow measurements: Tissue clearance. In: *Methods in Medical Research.* Chicago: Yr. Bk. Pub., 1960, vol. 8, pp. 256–242.
36. Kamen, M. C. *Isotopic Tracers in Biology* (3rd ed.). New York: Acad. Press, 1957.
37. Kety, S. S. Theory of blood-tissue exchange and its application to measurement of blood flow. In: *Methods in Medical Research.* Chicago: Yr. Bk. Pub., 1960, vol. 8, pp. 223–227.
38. Kety, S. S. Measurement of local blood flow by the exchange of an inert, diffusible substance. In: *Methods in Medical Research.* Chicago: Yr. Bk. Pub., 1960, vol. 8, pp. 228–236.
39. Kraintz, L., J. de Boer, E. L. Smith, and R. A. Higgins. Mixing of labeled erythrocytes in the dog's spleen. *Am. J. Physiol.* 195: 628–630, 1958.
40. Lambertsen, C. J. and S. G. Owen. Continuous, constant-rate sampling modification of nitrous oxide method for cerebral blood flow in man. In: *Methods in Medical Research.* Chicago: Yr. Bk. Pub., 1960, vol. 8, pp. 262–269.
41. Lassen, N. A. and O. Munck. The cerebral blood flow in man determined by the use of radioactive krypton. *Acta physiol. scandinav.* 33: 30–49, 1955.
42. Lewallen, C. G., M. Berman, and J. E. Rall. Studies of iodoalbumin metabolism, I. A mathematical approach to the kinetics. *J. Clin. Invest.* 38: 66–87, 1959.
43. Macdonald, J. R., E. G. Perry, L. L. Madison, and D. W. Seldin. An electrical analogue for analysis of tracer distribution kinetics in biological systems. *Radiation Res.* 6: 585–601, 1957.
44. Muir, T. and W. H. Metzler. *Theory of Determinants.* New York: Longmans, Green, 1933.
45. Munck, O. and N. A. Lassen. Bilateral cerebral blood flow and oxygen consumption in man by use of krypton-85. *Circulation Res.* 5: 163–168, 1957.
46. Parker, H. G. and C. R. Finney. Latent period in the induction of reticuloendothelial blockade. *Am. J. Physiol.* 198: 916–920, 1960.
47. Parrish, D., D. T. Hayden, W. Garrett, and R. L. Huff. Analog computer analysis of flow characteristics and volume of the pulmonary vascular bed. *Circulation Res.* 7: 746–752, 1959.
48. Perl, W. A method for curve-fitting by exponential functions. *Intern. J. Applied Radiation and Isotopes* 8: 211–222, 1960.
49. Pinson, E. A. Water exchanges and barriers as studied by the use of hydrogen isotopes. *Physiol. Rev.* 32: 123–134, 1952.
50. Robertson, J. S., W. E. Siri, and H. B. Jones. Lung ventilation patterns as determined by nitrogen elimination rates. *J. Clin. Invest.* 29: 577–590, 1950.

51. ROBERTSON, J. S. Theory and use of tracers in determining transfer rates in biological systems. *Physiol. Rev.* 37: 133–154, 1957.
52. ROBERTSON, J. S., D. C. TOSTESON, AND J. L. GAMBLE, JR. Determination of exchange rates in three-compartment steady-state closed systems through the use of tracers. *J. Lab. & Clin. Med.* 49: 497–502, 1957.
53. ROLLINSON, E. AND J. ROTBLAT. An electrical analogue of the metabolism of iodine in the human body. *Brit. J. Radiol.* 28: 191–198, 1955.
54. SACKS, J. *Isotopic Tracers in Biochemistry and Physiology.* New York: McGraw-Hill, 1953.
55. SAPIRSTEIN, L. A. Fractionation of the cardiac output of rats with isotopic potassium. *Circulation Res.* 4: 689–692, 1956.
56. SAPIRSTEIN, L. A. Regional blood flow by fractional distribution of indicators. *Am. J. Physiol.* 193: 161–168, 1958.
57. SAPIRSTEIN, L. A. AND R. S. GOODWIN. Measurement of blood flow in the human hand with radioactive potassium. *J. Appl. Physiol.* 13: 81–84, 1958.
58. SAPIRSTEIN, L. A. AND H. GOLDMAN. Adrenal blood flow in the albino rat. *Am. J. Physiol.* 196: 159–162, 1959.
59. SHEPPARD, C. W. *Basic Principles of the Tracer Method.* New York: Wiley, 1962.
60. SHEPPARD, C. W., AND D. YUDILEVICH. Radioactive tracer dilution studies in the canine heart-lung preparation. *Fed. Proc.* 19: 96, 1960.
61. SHEPPARD, C. W., R. R. OVERMAN, W. S. WILDE, AND W. C. SANGREN. The disappearance of K^{42} from the non-uniformly mixed circulation pool in dogs. *Circulation Res.* 1: 284–297, 1953.
62. SKINNER, S. M., R. E. CLARK, N. BAKER, AND R. A. SHIPLEY. Complete solution of the three compartment model in a steady state after single injection of radioactive tracer. *Am. J. Physiol.* 196: 238–244, 1959.
63. SOKOLOFF, L. Quantitative measurements of cerebral blood flow in man. In: *Methods in Medical Research.* Yr. Bk. Pub., 1960, vol. 8, pp. 253–261.
64. SOLOMON, A. K. Compartmental methods of kinetic analysis. In: *Mineral Metabolism*, edited by C. L. Comar, and F. Bronner. New York: Acad. Press, 1960, vol. I, A.
65. SOLOMON, A. K. The kinetics of biological processes; special problems connected with the use of tracers. In: *Advances in Biological and Medical Physics*, edited by J. H. Lawrence, and C. A. Tobias, New York: Acad. Press, 1953, vol. III, pp. 65–97.
66. SOLOMON, A. K. AND G. L. GOLD. Potassium transport in human erythrocytes; Evidence for a three-compartment system. *J. Gen. Physiol.* 38: 371–388, 1955.
67. STACY, R. W. Computers: analog. In: *Medical Physics*, edited by O. Glasser, Chicago: Yr. Bk. Pub., 1960, vol. III, pp. 193–201.
68. STACY, R. W. Computers: digital. In: *Medical Physics*, edited by O. Glasser. Chicago: Yr. Bk. Pub., 1960, vol. III, pp. 201–208.
69. STIGANT, S. A. *The Elements of Determinants, Matrices and Tensors for Engineers.* London: Macdonald, 1959.
70. VEALL, N., AND H. VETTER. *Radioisotope Techniques in Clinical Research and Diagnosis.* London: Butterworth, 1958.
71. WALKER, W. G., AND W. S. WILDE. Kinetics of radiopotassium in the circulation. *Am. J. Physiol.* 170: 401–413, 1952.
72. WARNER, H. The use of an analog computer for analysis of control mechanisms in the circulation. *Proc. I.R.E.* 47: 1913–1916, 1959.
73. WECHSLER, R. L. *Development of a New Method for Continuous Measurement of Cerebral Blood Flow in Humans Under Acceleration.* Bureau of Medicine and Surgery report No. NADC-MA-5202, 1952.
74. ZIERLER, K. L. Circulation times and the theory of indicator-dilution methods for determining blood flow and volume. In: *Handbook of Physiology.* Washington D. C.: American Physiological Society, 1962, sect. 2, vol. I, pp. 585–615.

CHAPTER 20

The dynamics and consequences of stenosis or insufficiency of the cardiac valves

LARS WERKÖ | *Göteborgs Universitet, Göteborg, Sweden*

CHAPTER CONTENTS

THE STUDY of valvular stenosis and regurgitation was started at the end of the nineteenth century in circulatory models and later in isolated heart preparations. The methods used were of necessity crude and the information obtained uncertain. The development of more exact manometers and their use in physiologic research, especially by Wiggers and his collaborators (68, 69, 73, 110, 111, 203, 204), signified a most important progress. However, even in those skilled hands the instruments did not always give answers that have stood the test of time. During the last decades, studies have been conducted in humans with valvular lesions due to disease and added to those made earlier in animals with experimental lesions. The necessary technical advancement to make this possible was, above all, the introduction of the technique of catheterization of the right and left heart in man (1, 16–19, 165, 166, 169), and the development of manometers, mechanical or electrical, with characteristics that made them suitable for clinical and physiologic studies. Increasing knowledge has been collected regarding the influence of alterations of valvular function on myocardial performance. As studies have been made in intact individuals with long-standing lesions, it has also been possible to register the effect of altered valvular function on the circulation as a whole and on the function of several organs that are influenced by changes in blood flow and blood pressure. The concept of the circulation in diseases with valvular deformities has been broadened. The new information thus collected has added to our understanding of the basic physiologic disturbances behind many well-known clinical syndromes. This has also created sounder foundations for effective treatment—surgical or medical—of valvular diseases.

ESTIMATION OF VALVULAR STENOSIS

Estimations have been made primarily from pressure tracings. In the case of atrioventricular valves these have been done either from the form of the atrial pressure curve or from the simultaneously obtained tracings from the ventricle and the atrium (20–22, 26, 42, 80, 98, 108, 141, 142, 146, 148, 155, 157, 165, 212, 213). In the case of stenosis of the semilunar valves some information has been obtained from

the arterial pressure record or from the simultaneously obtained ventricular and arterial tracings (16, 17, 81, 110, 151–153, 162–164).

Estimation of the degree of stenosis in a specific part of the circulation, particularly over the different valves, has been attempted through the use of various hydraulic formulas. Gorlin & Gorlin (84) derived a hydraulic formula that could be used to calculate valve areas. Dow and collaborators (52), and Silber and others (185) attempted to use a much simpler formula, based on Poiseuille's law, and calculate "valvular resistance." Rodrigo & Snellen (171), in 1953, published a critical study of the physical basis of the method employed, and concluded that the formula used for calculating valvular resistance becomes invalid if the blood flow is not laminar. The "stenotic index" derived from this formula was found to be directly proportional to the volume of flow. Accordingly, any change in cardiac output will give a change in the calculated resistance. They preferred the valve area formula for the estimation of the degree of stenosis.

The general formula for calculation of the area of certain orifices in the circulation derived by Gorlin and Gorlin reads:

$$A = \frac{F}{C \times 44.5\sqrt{P_1 - P_2}}$$

where

A	=	orifice area, cm^2
F	=	flow rate, ml/sec
C_1	=	velocity coefficient
C_2	=	orifice contraction coefficient
C	=	$C_1 \times C_2 \times 1.17$
44.5	=	$\sqrt{2g}$ = acceleration factor
$P_1 - P_2$	=	orifice pressure gradient

In each case the rate of flow must be calculated for that period when the particular valve in question is open: ventricular diastole for atrioventricular and ventricular systole for semilunar valves. Usually, empirical constants have been derived for each valve from a comparison of anatomically measured and physiologically calculated areas.

In mitral or tricuspid stenosis the general formula is altered through the insertion of the following specific values.

$$MVA = \frac{CO/DFP}{0.7 \times 44.5\sqrt{\text{``}PC\text{''}_m - 5}} \text{ or } \frac{CO/DFP}{0.7 \times 44.5\sqrt{LA_m - LV_{md}}}$$

where

MVA	=	mitral valve area, cm^2
CO	=	cardiac output, ml/min
DFP	=	diastolic filling period, sec/min
0.7	=	empirical constant, C
44.5	=	gravity acceleration factor
LA_m	=	left atrial mean pressure, mm Hg
PC_m	=	pulmonary capillary mean pressure, mm Hg
LV_{md}	=	left ventricular diastolic mean pressure, mm Hg
5	=	assumed left ventricular diastolic mean pressure, mm Hg

For tricuspid valve area, left heart pressures are exchanged for right heart values.

Rodrigo & Snellen (171) approved of the valve area formula of Gorlin and Gorlin, although the "constant" used in the formula proved to be a variable term. From mathematical considerations Rodrigo states that the acceptance of the constant provides an error of 20 per cent; when large deviations occur, this error may be as great as 40 per cent. To this mathematical error several biological sources of error must be added. The use of pulmonary artery wedge pressure instead of left atrial pressure may introduce too high a figure for pressure gradient. Of greater importance is the use of mean atrial pressure instead of diastolic pressure, which may vary considerably. To use an assumed value for left ventricular diastolic pressure likewise may cause great error in the estimation of valvular pressure gradient. The impossibility of judging exactly the presence and degree of mitral regurgitation may invalidate the flow measurements which usually estimate only the effective flow, not the total flow (which includes that lost via regurgitation) through the valve.

Ferrer *et al.* (71), in studying a case with tricuspid stenosis, obtained exact data which they used to check the formula. The results of calculation (0.58 cm^2) differed considerably from what was found at autopsy (1.65 cm^2). "The limitations of the method of Gorlin are obvious, when one considers that the engineer's formulas are applicable to hydraulic systems with fixed orifices, which are similar to short tubes and assume the absence of pulsatile flow." Many others, including the present author, likewise consider it unreliable and unsuitable for exact measurements (31).

In a recent appraisal of this formula Gorlin (83) states that the two main values of the formula, as expressed by those who are using it, were that it gave a better understanding of stenotic valve disease and that it was an aid in the occasional patient about

whom clinical opinion was in doubt. Not even Gorlin thus wants to advocate use of the formula for exact hemodynamic measurements.

In aortic or pulmonic stenosis the formula is

$$PVA = \frac{CO/SEP}{1.0 \times 44.5\sqrt{RV_{sm} - PA_{sm}}}$$

where

PVA	=	pulmonic valve area, cm^2
CO	=	cardiac output, ml/min
SEP	=	systolic ejection period, sec/min
1.0	=	empiric constant
RV_{sm}	=	right ventricular systolic mean pressure, mm Hg
PA_{sm}	=	pulmonary arterial systolic mean pressure, mm Hg

For aortic valve area right heart pressures are substituted with left heart values.

The formula for semilunar valves is less inexact than the one for atrioventricular valves, although the uncertainty introduced by the undetermined degree of regurgitation and the presence of turbulent flow decreases its applicability in hemodynamic research.

ESTIMATION OF VALVULAR INCOMPETENCE

This estimation has been made from: *a*) Pressure curves and has been used mostly in the case of atrioventricular valves where analysis of the atrial pressure tracing has shed some light on the presence or absence of incompetence (5, 167). *b*) Dye dilution curves with an indicator introduced upstream from the leaking valve and the dilution curve constructed by sampling downstream, or with indicator introduced in the chamber immediately downstream from the leaking valve with collection immediately upstream from the valve (8, 35, 36, 57, 99–101, 117, 120, 121, 129, 137, 145, 182, 183). *c*) Palpation of the leaking valve during surgery. In combination with data obtained during right heart catheterization, this has been used to calculate the regurgitant valve area and the regurgitant flow (114, 149).

Hydraulic Formula

Gorlin *et al.* (86) have derived a hydraulic formula for the calculation of the mitral regurgitant area, using the principle that total ventricular flow equals regurgitant flow plus aortic flow, where the regurgitant flow is calculated from the mitral orifice area for forward flow as determined by the surgeon at the time of operation.

The final formulas were:

$$a) \quad Fr = MVA \times DFP \times 31\sqrt{PC - 5} - CO$$

$$b) \; MRA = \frac{MVA \times DFP \times 31\sqrt{PC - 5} - CO}{SEP \times 36\sqrt{BA_{sm} - PC}}$$

where

Fr	=	regurgitant blood flow, liters/min
MVA	=	mitral valve area (forward flow), cm^2
DFP	=	diastolic filling period, sec/min
31	=	empirical constant
PC	=	pulmonary arterial wedge pressure, mm Hg
5	=	assumed left ventricular mean diastolic pressure, mm Hg
CO	=	aortic output, liters/min
MRA	=	mitral regurgitant area, cm^2
SEP	=	systolic ejection period, sec/min
36	=	empirical constant
BA_{sm}	=	brachial arterial systolic mean pressure, mm Hg

This formula has been used by Dexter and his group (149) in about 50 cases of mitral valvular disease. Areas calculated in the same individual under different circulatory states checked within 0.1 to 0.2 cm^2. Regurgitant areas ranging from 0.3 to 0.9 cm^2 were calculated. They were always less than the mitral valve forward flow area and usually about one-fourth to one-tenth the size of the aortic valve. This formula has the same error as the formula of Gorlin and Gorlin for calculating stenotic valve areas. To this are added several assumptions and the inexact method of determining the mitral valve forward flow area from palpation during surgery. Although the approach to the problem is ingenious, the derived formula has not been used for exact measurements. It seems appropriate to cite Wiggers (203), who states regarding myocardial contractility in mitral insufficiency: "Attention may be directed to the fact that since the rate of pressure increase is such an important determinant of the volume regurgitated, calculations of the size of leaking orifices from laws based on static equations do not necessarily apply to the beating heart."

Indicator Dilution Techniques

Application of the Stewart-Hamilton method for cardiac output determination (96, 97, 190) to studies of valvular backflow has been used by several investigators (33–36, 57, 63, 100, 101, 104, 116, 120, 122–124, 129, 130, 141, 142, 145, 161, 182, 183, 198, 207, 210–212). Korner & Shillingford (120–122, 154) have

proposed an indirect procedure, whereby valvular insufficiency could be evaluated from ordinary indicator dilution curves. By this technique the indicator was injected in a peripheral vein and blood collected in a peripheral artery. This method is based on the supposed invariance in the form of normal dilution curves. When mitral insufficiency was produced, the shape of the curve was altered with more rapid appearance time, lower peak concentration, and decrease of the terminal slope in proportion to the amount of insufficiency.

Figure 1 shows indicator dilution curves obtained by injecting I^{131}-tagged human serum albumin into the left atrium of a patient with pure mitral stenosis (MS) and of one with combined mitral stenosis and insufficiency (MS + MI). The effect of regurgitation is a summation of all regurgitant flows between injection and sampling sites. It should be noted that the curve will be flatter and more difficult to evaluate if the injection site is on the right side of the pulmonary circulation or even more peripherally as originally suggested. Korner and Shillingford, in their attempts to quantitate valvular insufficiency from dilution curves, also recognized the necessity of correcting for the effects of cardiac output and blood volume. They attempted to eliminate these effects by comparing the measured disappearance slope of the curve and the degree of dispersion or variance of the curve with the expected values calculated from equations relating these parameters to the cardiac output and "central" blood volume of normal individuals. Their results showed a good discrimination between valvular regurgitation and stenosis. Marshall *et al.* (142) used the method of Korner and Shillingford in 11 healthy volunteers and 30 patients with disease of the mitral valve, and showed that there was a significant correlation with the degree of regurgitation. However, a considerable overlap between results in normals and in patients with stenosis and regurgitation limits the value of the method.

Eich and co-workers (57) studied the problem of estimation of valvular regurgitation by dye dilution in 15 dogs, where the technique was applied before and after the creation of mitral regurgitation. The range of regurgitant flow was 20 to 38 per cent of the cardiac output. With a control determination even small amounts of regurgitation could be detected but not quantified. Without a control dilution curve (with no leak introduced), no calculation applied to the curve would separate the states without, from those with, a leak. The authors concluded that the reasons for this wide overlap are variations in volume, mixing, and washout, which cannot be assessed at present.

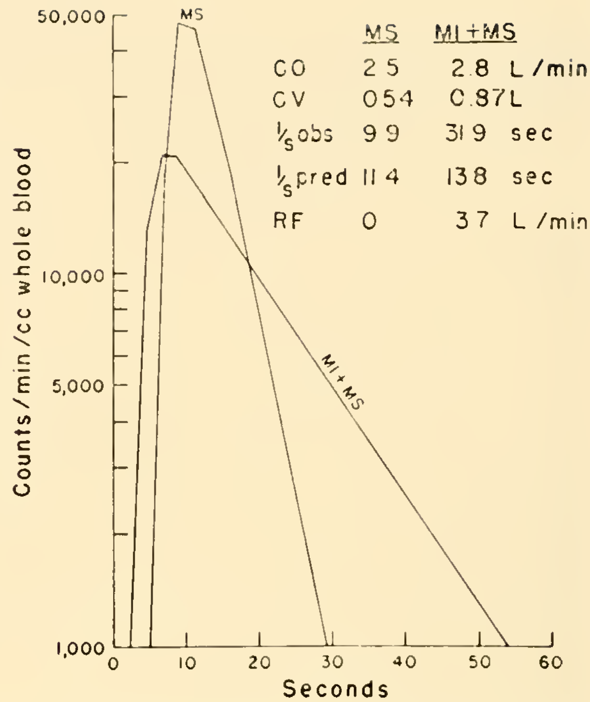

FIG. 1. Indicator dilution curves obtained by injecting I^{131}-tagged human serum albumin into left atrium in a case of pure mitral stenosis (*MS*) and combined mitral insufficiency and stenosis (*MI* + *MS*). [From Novack & Schlant (154).]

The deformation of the peripheral indicator dilution curve in mitral insufficiency has a complex mechanism. It is a consequence not only of the size of the altered left atrial and ventricular mixing volumes produced by the backflow, but also of changes in pulmonary blood volume and total blood flow. Model experiments and studies in dogs with acutely induced mitral insufficiency have demonstrated the inaccuracy of the indirect indicator dilution method for the detection of regurgitation as long as the blood flow and volume are unaltered. Hoffman & Rowe (104) especially have studied the behavior of indicator dilution curves in circulation models and have stressed the importance of chamber volume and blood flow. The most complete mathematical analysis based on logical statistical movement of indicator in a model system has recently been developed by Newman and his group (62, 63, 123, 124, 145). This analysis indicates that the shape of model indicator dilution curves is completely dependent on blood flow and the mixing volumes of ventricle and atrium. The results of these analyses compare well with earlier con-

clusions from studies in animals and man. The terminal slope of the peripheral dilution curve obtained following prepulmonary injection of indicator seems mainly determined by pulmonary volume. Valvular insufficiency does not decrease this slope until one of the downstream cardiac chamber mixing volumes approaches the pulmonary volume or until cardiac output falls. Several modifications of this method have been suggested by Dexter, Wood, Shillingford, and Lange, among others, which consist, for example, in the change of the injection site to the pulmonary artery or the left heart chambers, and the use of other constants for calculation.

In the experience of most investigators, random variability has been so great that the alteration in curves resulting from mild regurgitation could not be detected, and the variations in the case of severe regurgitation have been so wide as to make the method useless.

Levison & Sherman (137), at the Lincoln Laboratory of the Massachusetts Institute of Technology, have discussed the problem of using indicator dilution curves for estimation of regurgitation on a mathematical basis. They state that the assumption of complete and instantaneous mixing of the indicator in the cardiac chambers (upon which the usefulness of all the dilution techniques for regurgitation depend to some degree) is the one most likely to be violated. They also consider that the importance of the mixing problem requires further experimental study before any of the suggested methods should be used. Although this method cannot be used for any exact estimation of valvular regurgitation it has had some clinical application, with a fair predicting value in 90 to 95 per cent of the curves (33–36, 49, 207).

Methods have also been developed in order to record dilution curves simultaneously from the left atrium and systemic arterial and venous circulation, following injections of indicator into the left ventricle, left atrium, aorta, and various sites in the venous circulation. These methods have been used in the study of mitral or tricuspid regurgitation. After injection of an indicator into the left ventricle in the presence of an incompetent mitral valve, movement of the resulting mixture of blood may be either backward and into the left atrium or forward into the aorta. If an indicator dilution curve is recorded from the left atrium after injection of the indicator into the left ventricle, the early appearance of dye in the atrium indicates that regurgitation through the mitral valve has occurred. The failure to detect the early appearance of the indicator suggests that the mitral valve is competent. Comparison of the area of the rapidly appearing portion of such a left atrial dilution curve with the areas of curves recorded from the left ventricle or the pulmonary artery has been suggested as an exact means of estimating the quantity of blood regurgitated through the mitral valve. A necessary prerequisite for this is complete mixing of indicator and blood in the left heart. Studies in dogs and patients with mitral valve disease have demonstrated, however, that this method failed to discriminate between stenosis and regurgitation in a reliable manner, and thus cannot be used for the calculation of regurgitant flow (141, 142). Incomplete mixing, both in the ventricle where the indicator is injected and in the atrium where it is collected, may completely invalidate this method. Levison & Sherman (137), who recently treated this problem mathematically, stated that the importance of the mixing problem requires further experimental study.

Braunwald *et al.* (28) and Warner & Toronto (194), among others, have also made use of indicator dilution curves to estimate the regurgitant back flow in aortic incompetence, with the indicator injected distally and collected proximally in the aorta (28, 94, 194). Too few studies have been made with this method to assess its value. The lack of any figures for backflow as a comparison to what is obtained with the dilution methods also precludes any judgment as to its validity.

It seems safe to conclude that there is at present no method for employing indicator dilution curves in order to arrive at an exact evaluation of the degree of valvular regurgitation, although several applications in the hands of critical investigators may have limited clinical value.

ATRIAL PRESSURE PULSE

Left Atrium

Studies in laboratory animals and in man have shown similar findings (fig. 2). The atrial contraction causes a small pressure rise (the *a* wave) followed by a fall. Ventricular contraction causes the mitral valve to close. The positive *c* wave in the left atrium begins at this time. This wave is a function of the relative pressures within the atrium and ventricle with the onset of ventricular systole. If at the start of ventricular contraction the ventricular pressure is less than

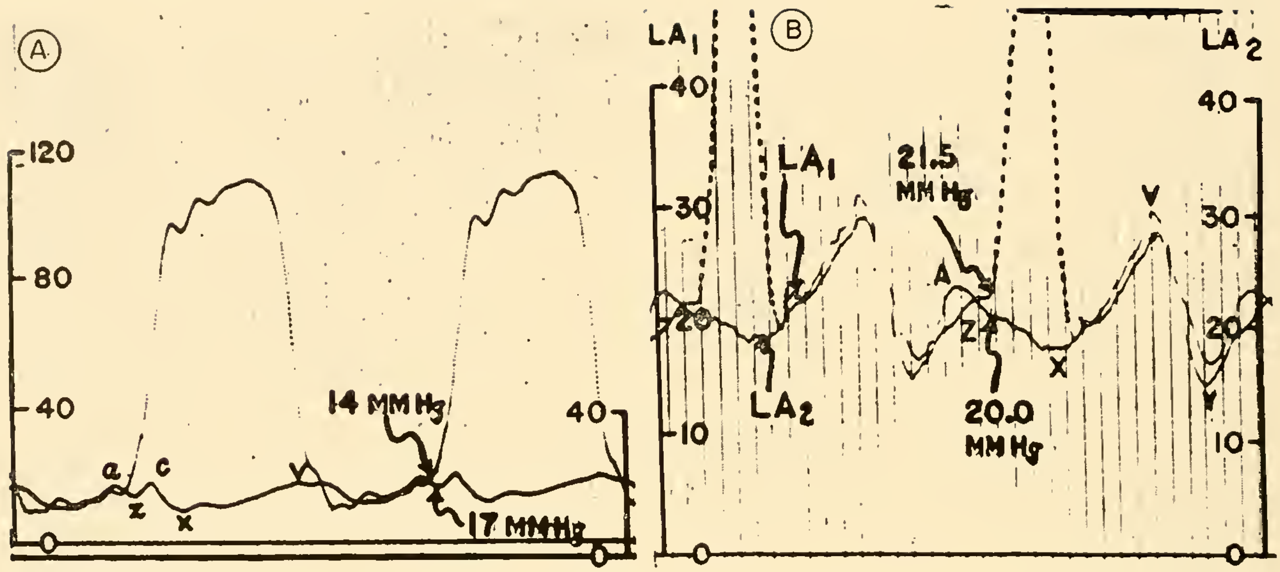

FIG. 2. Left atrial and ventricular pressure pulses recorded through double lumen catheters in normal subjects. Ordinate values in mm Hg. For labeled features, see text. [From Ankeney *et al.* (5).]

the atrial pressure, a prominent *c* wave appears. If, however, at this moment the ventricular pressure is higher than the atrial, no *c* wave is seen in the atrial curve (5, 157, 184).

During the ventricular contraction the pressure in the atrium falls (the negative *x* wave) and rises again to the *v* wave, the peak of which corresponds to the end of ventricular systole. When the ventricle relaxes and the mitral valve again opens, the period of rapid filling starts. This period, i.e., the diastolic inflow period, is marked by a continuous decline in the atrial curve, the *y* descent. Diastasis, or the period of slowed ventricular filling, starts when the atrial pressure begins to rise during diastole. The onset of the *a* wave produced by the next atrial contraction marks the end of diastasis. The dynamic interval of atrial systole lasts until the peak of the atrial contraction wave, whereas the inflow phase, which follows, ends at the onset of ventricular isometric contraction and completes the cardiac cycle. This point on the atrial curve has also been referred to as the *z* point (157).

PULMONARY ARTERIAL WEDGE PRESSURE. Much of the experience gained regarding the pulmonary hemodynamics in heart disease in man has been obtained using the pulmonary arterial wedge pressure as an index of left atrial pressure (7, 46, 48, 50, 51, 56, 58, 59, 78, 82, 85–87, 90, 108, 134, 136, 160, 184, 189, 191, 199, 206, 208, 214, 215). Even now, when it is possible to register directly the left atrial pressure in man, many authors still use the pulmonary arterial wedge pressure as an index of changes in the left atrial pressure, because the procedure of left atrial puncture is not without danger and has to be done under circumstances that more or less preclude any hemodynamic studies. It thus seems appropriate to discuss briefly the validity of the pulmonary arterial wedge pressure.

Dexter *et al.* (47), in 1946, observed in man that fully saturated blood was obtained through a heart catheter introduced so far into one of the branches of the pulmonary artery that its tip obstructed the lumen completely. Some years later the same group published pressure curves obtained through such an impacted catheter in animals, followed by similar studies conducted in man (102). The pressure pulses recorded showed no oscillations due to the insensitivity of the manometers used ("pulmonary capillary" pressures). Almost simultaneously, and independent of the Boston group, Lagerlöf & Werkö (126) published curves obtained in a similar manner in normal man and in patients with various heart diseases. They used the Tybjaerg-Hansen electrical capacitance manometer and demonstrated the occurrence of a venous pulse in most tracings. They also defined the tracing typical for a series of heart disorders, for example mitral stenosis and mitral incompetence

("pulmonary capillary venous" pressure). It has since been agreed to call the tracing, obtained in this way, pulmonary arterial wedge pressure.

In dog experiments the pulmonary arterial wedge pressure has been recorded simultaneously with the pressure in a pulmonary vein or the left atrium, reached either by arterial catheterization or by puncture at thoracotomy (3, 4, 51). In these experiments the two pressures have usually been found to be reasonably in accord. Following such experimental changes as rapid intravenous infusions, positive-pressure respiration, severe anoxia, constriction or embolization of the pulmonary artery, induced mitral stenosis or incompetence, and artificial septal defect, the wedge pressure has also been in close accord with the changes in pressure in the left atrium, but it has usually remained uninfluenced by changes in the pulmonary arterial pressure. Horvath & MacCanon (105) observed no pulsations in the wedge pressure when the tip of the catheter was situated near the surface of the lung, and suspected that the intrapleural pressure was dominating the measurements in such cases. Ankeney (3, 4) could in no case find convincing accord between the shape of the wedge pressure curve and that of the left atrial curve. On this basis—and from the (wrong) assumption that the higher pressure in the pulmonary artery than in the left atrium should prevent retrograde transmission of the atrial pulse wave—this author maintained that all possible pulsations in the wedge curve must be transmitted from the pulmonary artery, and that only curves without such pulsations could be considered a definite indication of the pulmonary capillary pressure. Werkö *et al.* (201) in 1953 reported some investigations in two patients with pulmonary hypertension, showing that the pulmonary artery wedge pressure remained uninfluenced by obstruction of the pulmonary artery proximal to the tip of the catheter, whereas positive-pressure respiration in another patient diminished or suspended the pulsations in the wedge pressure curve.

In patients with interatrial septal defect (or displaced pulmonary veins) direct catheterization affords an opportunity for recording the pressure in the left atrium or in a pulmonary vein. Comparisons between such measurements and the wedge pressure in single cases or in small series of up to six patients have been published (200). In these measurements, performed at minimal time intervals with few exceptions, the mean pressure was almost always in accord within limits of a few mm Hg; and in most cases with a slight positive difference between the wedge pressure and the left atrial pressure. Distinct accord in the shapes of the curves, with a delay slightly under 0.1 sec as compared to the left atrium, was found in most instances.

Allison & Linden (1), who punctured the left atrium from the right main bronchus and registered wedge and left atrial pressure simultaneously, state that the two curves are identical only under certain circumstances; they could, however, give an example in which the wedge pressure curve reproduced all main features of the left atrial pressure curve with a delay of about 0.09 sec. Epps & Adler (66) traced the two curves in immediate continuation, connecting by means of a three-way cock the same manometer with both the wedged catheter and the left atrial needle. In seven patients with mitral disease, in both sinus rhythm and auricular fibrillation, and at both high and low values of pressure and pulmonary resistance, the authors always found a close accord in the shape of the wedge and the left atrial pressure curves. No difference could be seen in the time relation to the electrocardiogram in these examples. Björk and coworkers (21) punctured the left atrium from the back, and in seven cases generally found good accord with the shape of the wedge pressure curve, which was delayed for about 0.10 sec; the mean pressure, however, showed differences from −1.5 to +10.9 mm Hg. This comparatively great variation could be partly explained by hydrostatic differences, as the measurements were performed with the patients in a lateral recumbent position. In a subsequent study complete parallelism was found between the variations in pressure levels and shapes of the two curves during Valsalva's experiment in nine patients with mitral disease. Using the same technique, Werkö, *et al.* (200) also found identity between the two pressure curves, except for a time difference of about 0.08 sec, in one patient with mitral disease.

At thoracotomy, too, the wedge pressure has been recorded simultaneously with the left atrial pressure. Connolly *et al.* (37) examined patients with mitral disease and found good accord between the two pressure curves, with regard to both level and configuration. In ten patients with mitral or pulmonary disease, Wilson *et al.* (205) also found fairly good accord between the pressure levels in the left atrium and the wedge curve (the maximal difference on either side being from 5 to 6 mm Hg), but in no case did they find distinct pulsations.

Much discussion has thus been conducted both in clinical and physiological literature as to whether the tracing obtained in this manner really reflects the

left atrial pressure. Authors, arguing that this is an unphysiological measurement, have usually founded their conclusions on dog experiments, where it may be difficult to get a true wedge tracing, or on unsuccessful clinical studies. Careful studies have, on the other hand, definitely shown that the true pulmonary arterial wedge pressure tracing has all the characteristics of the left atrial tracing, only slightly delayed, with a mean pressure that closely follows the left atrial mean pressure. It has also been demonstrated, by occluding the pulmonary artery with a balloon, that the pressure waves registered from the wedge position are not merely a distorted pulmonary arterial pulse. In this connection it is of interest that MacCallum & McClure (144), in 1906, demonstrated that the increased V wave of mitral incompetence could traverse the pulmonary vascular bed in the retrograde direction. There is a possibility that in some cases the tracing obtained through a wedged pulmonary arterial catheter is more representative of the over-all events in the left atrium during the cardiac cycle than the tracing obtained through a needle or thin catheter placed within the atrium and subject to direct influences giving rise to errors (i.e., jet effect of mitral regurgitation). It should be stressed, however, that it may be impossible to obtain a true wedge pressure tracing in a certain number of cases (from 10 to 30%). It is furthermore impossible to obtain more information from the wedge pressure tracing than from the left atrial record, and its use for diagnostic purposes is thus limited.

LEFT ATRIAL PRESSURE IN MITRAL VALVE DISEASE. In mitral valvular disease the normal train of events in the left atrial pulse is changed more or less markedly due to the extent of the valvular alteration, the time the valvular disease has lasted, and the presence or absence of other factors of importance for the atrial or ventricular performance [the prevailing heart rhythm and rate, the state of the myocardium, hypervolemia, etc. (80, 98)].

Mitral stenosis. In early mitral stenosis the atrial contraction produces a giant *a* wave, with a slight elevation of the left atrial mean pressure, otherwise the curve is normal. In cases more advanced, but still in sinus rhythm, the a-c complexes and *v* waves are of similar amplitude, the mean pressure is elevated, the pulse pressure is narrow, the *y* descent is slow, and diastasis is absent. In some of these cases the main feature is the prominent *c* wave. When atrial fibrillation supervenes, the picture is complicated and more difficult to analyze. Besides the absence of the *a* wave the striking changes from normal are the prominent positive *c* wave and the absent negative *x* wave. In the absence of atrial contraction, and thus relaxation of this chamber, no *x* wave can be seen. Immediately following the *c* wave there is a gradual rise in pressure forming a definite *v* wave. This type of tracing is apparently characteristic of either right or left atrial curves in the presence of atrial fibrillation and may not have anything to do with valvular stenosis per se (5, 165).

Mitral insufficiency. The findings described by Wiggers & Feil (204) during the acute phase of the production of marked mitral regurgitation are not always found in long-standing mitral insufficiency, probably due to secondary changes that have occurred, modifying the pressure-pulse response. After the establishment of mitral incompetence they found that the left atrial pressure was elevated only slightly during the isometric phase and that it fell quite normally during the latter portion of this phase. During systolic ejection the atrial pressure rose rapidly, producing a greatly elevated plateau. This increase in atrial pressure did not end with the onset of diastole, but continued for about 0.08 sec into diastole, i.e., throughout the protodiastolic and isometric relaxation phases.

In clinical mitral insufficiency in man the left atrial pressure pulse may undergo all degrees of changes, from virtually none to a tracing similar to the one recorded from the left ventricle. In the former case with slight regurgitation the most conspicuous finding is increase in amplitude of the *v* waves, that rises far above the a - c complexes. The *y* descent is rapid and brief, and diastasis is evident. In the latter case there is an early rise in left atrial pressure simultaneous to the ventricular systole, absence of a spiked *c* wave, and no pressure rise that appears to be similar to a *v* wave (fig. 3).

The changes in contour of left atrial pressure pulse curve also incorporate disappearance of the down slope following the *c* wave with a steep rise to the *v* peak. This rise begins at the *c* wave and is therefore initiated early in systole. The descending limb of the *v* wave (the *y* descent) drops sharply early in diastole (in the absence of concomitant stenosis). During the latter part of diastole, to the *a* wave in normal sinus rhythm or to the end-diastole in atrial fibrillation, there is sometimes a slight gradual increase in pressure. The degree of incompetence of the mitral valve is the factor of greatest importance for the difference between the ventricular type and the enlarged *v* wave type of atrial curve. The mean

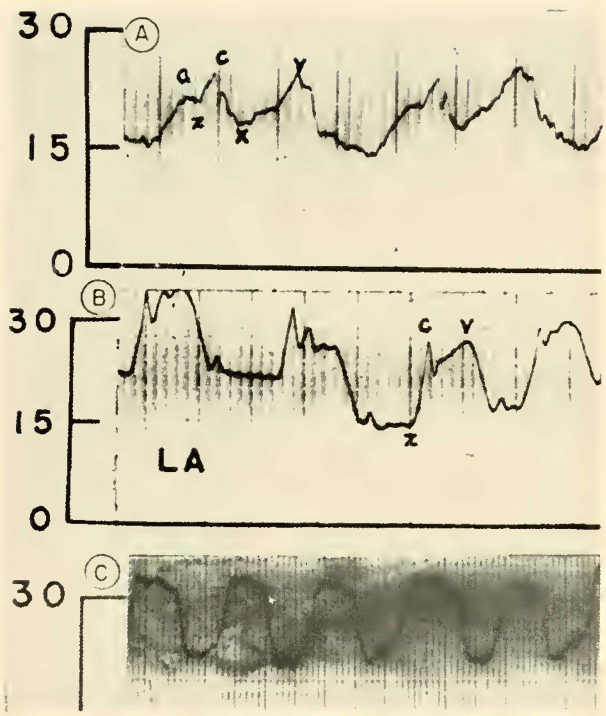

FIG. 3. Left atrial pressure pulses: *A*: mitral stenosis with normal sinus rhythm and no regurgitation detected by palpation. *B*: mitral stenosis with atrial fibrillation and no palpable regurgitation, and *C*: mitral stenosis with atrial fibrillation and a large regurgitation by palpation. [From Ankeney *et al.* (5).]

pressure level in the atrium is higher in the former type. It is conceivable that the larger the opening, the more ventricular in character will the atrial pulse be and the less will the pressure drop across the valve be. The smaller the opening in the valve, the less will the atrial cyclic variations deviate from the normal (5, 165, 167).

Davila (43), in a series of cases studied during operation, did not see any examples of the ventricular type described above. In most of his cases of mitral incompetence, the change in left atrial pressure curve that was most conspicuous was a sharp rise in the peaks of the *a* and *v* waves, particularly the latter; in which case the peak was reached late in systole or even in protodiastole. There was also an increase of mean pressure, particularly the systolic mean pressure. The mean diastolic and end-diastolic pressure levels were usually close to the respective left ventricular pressures.

In most cases of mitral incompetence these waves in the left atrial pressure pulse are transmitted backward through the pulmonary vascular bed and may be identified in the pulmonary arterial wedge

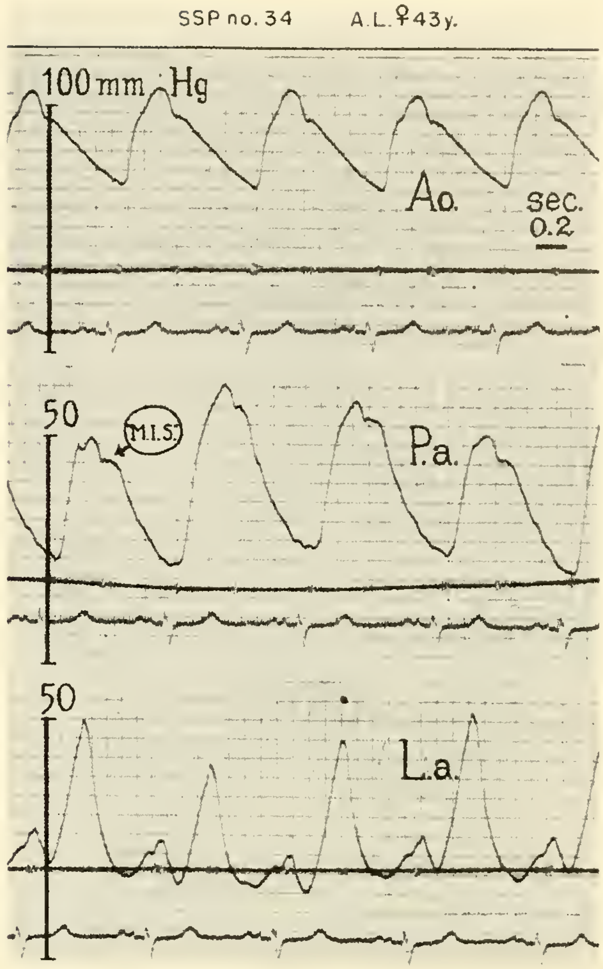

FIG. 4. Suprasternal pressure curves from the aortic arch, pulmonary artery, and left atrium in a case of predominant mitral regurgitation. Note the small head of the aortic curve, the "mitral insufficiency shoulder" (*MIS*) on the pulmonary artery curve, and the peaked second sound wave in the left atrial curve. [From Radner (167).]

pressure tracing, slightly delayed. In marked regurgitation the *v* wave may reach pressures higher than or equally as high as the systolic pressure in the pulmonary artery. This high regurgitant wave may be identified in the pulmonary artery tracing (fig. 4), as pointed out by Radner (167) and later by Levinson *et al.* (135). These latter authors point out that a prerequisite for the retrograde transmission of the *v* wave is a low or normal pulmonary vascular resistance.

MacCallum & McClure (144), who in 1906 produced mitral insufficiency in dogs, also showed that the regurgitant wave of mitral insufficiency was retrogradely transmitted from the left atrium through the pulmonary capillary bed, finally arriving in the

pulmonary artery. When the regurgitation is severe and long standing and has produced increased pulmonary vascular resistance, this retrograde transmission is rendered impossible or the *v* wave becomes so damped out that it cannot be identified in the pulmonary arterial wedge tracing.

Differentiation between mitral stenosis and insufficiency. The great interest in physiological methods that has been demonstrated in clinical work has been due partly to the hope that the use of these methods in the study of patients would aid in the differentiation between various disorders, a hope that has only partly been fulfilled. The expectation that the use of dilution curves or pressure recordings for the differentiation and quantitation of regurgitation in the atrioventricular valves has not led to any clear-cut result, although much work has been done to modify the original techniques. Several ways have been suggested to evaluate the left atrial or pulmonary arterial wedge tracing in these cases, but none has been completely satisfactory.

Allison & Linden (1) related the ratio of the pressure difference between the peak of the *v* wave and the *z* point to the peak *v* wave pressure to differentiate between regurgitation and stenosis, and reported a correct diagnosis in 59 of 61 patients. Owen & Wood (158), studying the pulmonary wedge pressure, utilized the rate of descent of the *v* wave to the height of the preceding *v* wave, and reported excellent discrimination between stenosis and incompetence. Connolly & Wood (38) were unable to confirm this, but these authors did find a close correlation between the average peak *v* wave pressure and the degree of regurgitation, as compared to the findings in patients with mitral stenosis for equivalent mean pressures. Neustadt & Shaffer (155) studied 54 left atrial pressure pulse curves in 43 patients with mitral valvular disease. All patients with mitral stenosis had an end-diastolic gradient across the mitral valve. Fifty per cent of the patients who had pure mitral insufficiency also exhibited a similar gradient. Numerous ways of analyzing the pulse contour or pressure level of the left atrial pulse gave a poor separation between those with and those without mitral regurgitation. The most useful feature of the left atrial pulse was the rate of *y* descent in its initial 0.1 sec related to the pressure at the *v* point, but even this did not always significantly characterize the patients with mitral incompetence.

In a comparison of these different methods of judging the degree of mitral regurgitation, where also the methods of Kent *et al.* (114), who used the difference of *c* wave and *v* wave pressures, and those of McMichael & Shillingford (150), using the difference between *c* wave and *x* wave pressures were incorporated, Marshall *et al.* (142) found that no simple method could be used for discrimination between mitral incompetence and mitral stenosis. However, a significant correlation could be demonstrated between many different parameters of the left atrial pulse and the degree of mitral regurgitation. These authors suggested that multiple-variable analysis, using various properly weighted combinations of these parameters, might improve the discrimination obtained; a hope that thus far has not been fulfilled.

Braunwald *et al.* (30) studied the left atrial pressure pulse in dogs before and during acute mitral incompetence at rest and during elevation of the peripheral resistance by infusion of norepinephrine. In the absence of mitral regurgitation, striking elevations of aortic pressure raised the v point of the left atrial tracing only slightly. In dogs with slight mitral incompetence (little or no elevation of the v points) the left atrial v point was strikingly elevated when aortic pressure was raised. These authors then studied 7 patients without mitral insufficiency and 13 with, and found a much more marked increase of left atrial pressure (mean and *v* point) in those with mitral incompetence as compared to those without (pure mitral stenosis with elevated left atrial pressure).

Studies of atrial volume pulsations have also been used in order to differentiate between stenosis and incompetence with varying degrees of success. The simultaneous recording of the pressures in the left atrium and ventricle has gained increasing importance after the introduction of left heart puncture, either through the left bronchus or from the back (1, 16, 17). The curves obtained during these circumstances have, however, usually been difficult to interpret, and the value of this method for routine clinical work or for exact hemodynamic studies has been disappointing. Moscovitz *et al.* (152) recorded left atrial and ventricular pressures simultaneously during chest surgery. In six control cases simultaneous recording of the pressure pulse on the left side of the heart was obtained. Virtually no pressure gradient between the left atrium and the left ventricle was found throughout the diastolic period. This was true also during the period of greatest mitral flow, immediately after the opening of the mitral valve.

In seven cases of mitral stenosis similar tracings were obtained before and after surgical opening of the stenosed valve. The mitral valve filling pressure gradient was between 5 and 20 mm Hg before sur-

gery. The diastolic pressure of the left ventricle ranged from 3 to 12 mm Hg (mean diastolic pressures). These figures were obtained with open chest and under anesthesia. The cardiac output was not determined but was presumably low.

Right Atrium

The right atrial pressure pulse has the same general characteristics as the left, with a generally lower mean pressure and perhaps less amplitude in the different waves. The right atrial pressure pulse changes in the same fashion as described for the left when stenosis or insufficiency of the atrioventricular valve occurs. It may be of importance to stress the occurrence of a giant *a* wave in cases with marked right ventricular hypertrophy.

McCord *et al.* (147) studied 23 patients with right ventricular hypertrophy due to pulmonary stenosis or pulmonary hypertension. They found an *a* wave of increased amplitude in 20 cases and propose that this giant *a* wave represents the characteristic response of the right atrium in the presence of severe right ventricular hypertrophy. Grishman *et al.* (93) likewise found a presystolic pulsation of the liver in the absence of tricuspid disease in cases with right ventricular hypertrophy.

A giant *a* wave (up to 20 mm Hg) in the absence of elevated mean pressure cannot thus be taken as an indication of tricuspid stenosis. For this diagnosis simultaneously obtained pressure curves from the right ventricle and atrium are necessary and should demonstrate a diastolic pressure gradient.

TRICUSPID STENOSIS. Ferrer *et al.* (71) describe the findings in two patients with tricuspid stenosis, one of them was also studied at autopsy. One of the cases had a low cardiac output and in the other the output was in the lower range of normal. The right atrial pressure curve showed: *a*) Very high peaks of atrial systole, ranging from 9 to 12 mm Hg. *b*) A marked fall in pressure during the ventricular contraction. *c*) The opening of the tricuspid valve, which should be followed by the rapid filling of the right ventricle, was not attended by any marked fall in pressure. The marked fall in pressure during ventricular contraction indicated the absence of any regurgitation, and the absence of pressure drop when the tricuspid valves opened showed that the rate of flow in diastole was reduced due to stenosis.

TRICUSPID INCOMPETENCE. Bloomfield *et al.* (23) described the right atrial pressure curves in eight cases of tricuspid incompetence and showed the normal systolic dip (the *x* descent) to be replaced by a positive wave that had the form of a plateau or showed an upward convexity; the pressure level was higher than in the intervening diastolic interval and was sustained until the end of isometric relaxation. Similar observations were made by Lagerlöf & Werkö (125) and by McCord & Blount (146). The latter authors also demonstrated that exercise or deep inspiration increased the systolic wave in the atrial tracing.

Clinical and physiological signs of tricuspid incompetence may occur in the absence of anatomical changes. Lottenbach & Shillingford (139) studied, at necropsy, 10 patients with heart disease of various etiology and accompanied by right heart failure, and 15 patients without evidence of heart disease, and concluded that functional tricuspid incompetence was present in all cases with a right atrial pressure during life of 8 mm of mercury or more.

From these and other findings it is evident that tricuspid incompetence of a functional nature is common and develops in the majority of patients as part of the progressive downhill course of cardiac disease.

ATRIAL VOLUME CHANGES

Attempts have been made to estimate the volume changes of the left atrium in man during the cardiac cycle, using two different methods: *1*) electrokymography (2, 74, 172) and *2*) serial angiocardiography with frequent exposures (91, 143, 187, 193, 216).

Electrokymography

This method gives only an estimate of the movements of the borders of the cardiac silhouette or records the intensity of the shadow caused by the moving heart (densitography). Most of the works published on the pulsations of the left atrium in mitral valvular disease have been inexact and impossible to reproduce. Only infrequently has it thus been possible to use the electrokymographic technique to study dynamic changes during the cardiac cycle. It is also important to stress that only qualitative changes can be recorded by this method. Thus, Andersson (2), after careful study of 122 cases of mitral stenosis, states that in mitral stenosis the electrokymographic tracing of the left appendage shows *a*) increased relative amplitude of the left auricular con-

traction descent; *b*) increased duration of the left auricular contraction descent; *c*) decreased fall of the curve during the rapid filling phase (less than the auricular contraction descent); *d*) steeper rise in the curve during the reduced ejection phase.

Even when objectively measurable parts of the curve (the duration of the auricular contraction descent) did not exhibit clearly pathologic values, the curve as a whole had a characteristic appearance that was encountered only in mitral stenosis.

In mitral incompetence characteristic changes were recorded in the electrokymographic curves from the left auricle. These changes consisted of an earlier steeper rise than ordinary during the ejection phase. In addition, the curves in pure incompetence showed a notably great fall during the rapid filling phase. These curves agreed fully with the pressure and volume curves obtained in experimentally induced mitral incompetence by Wiggers & Feil (204). Fleischner *et al.* (74) studied the atrial electrokymogram in 5 normal subjects and in 15 patients with rheumatic mitral valvular disease. They also found that only with the utmost careful evaluation of the tracings was it possible to diagnose stenosis and judge the degree of regurgitation. The differentiation between stenosis and incompetence was almost complete in patients with normal sinus rhythm, whereas in patients with atrial fibrillation tracings sometimes were obtained suggesting mitral incompetence where surgical exploration did not reveal other lesions than stenosis.

In studies of the normal right atrial electrokymogram Rudhe (172) found a good correlation between the pressure event in the atrium and the movement of the border of the right atrial shadow. Of special interest was the delay of movement of the wall in comparison to the rise of pressure during atrial systole, on the average 0.04 sec (range 0.02 to 0.06 sec, 13 cases). A similar delay was registered between the c wave in the pressure curve and the corresponding notch in the volume curve. Rudhe thought it probable that the initial displacement of the blood during atrial contraction takes place under acceleration, owing to the inertia of the blood mass. This implies that emptying is inappreciable in the earliest part of atrial systole. A further implication of the phase difference between the atrial pressure and the volume increase in the ventricle is that the maximum blood displacement is reached after the maximum rise in atrial pressure. This is also evident from experimental work by Wiggers.

Angiocardiography

Arvidsson (7) studied the changes of left atrial volume calculated from serially exposed biplane films during angiocardiography. He found in mitral stenosis that the maximum volume of the left atrium was between 75 and 265 ml, averaging 145 ml (18 cases of mitral stenosis in sinus rhythm). The volume variations during the cardiac cycle lay in most cases between 20 and 50 ml, the average being 35 ml. In 17 cases with sinus rhythm the changes in left atrial volume during the cardiac cycle were plotted. All the curves had approximately the same appearance in these cases. The maximum volume was recorded at the end of systole. During early diastole there was a fairly small decrease in volume. Before the atrial contraction there occurred either a plateau on the curve or, in some cases, a volume increase. A conspicuous decrease in volume took place during atrial systole, and this decrease continued in most cases beyond the QRS complex in the electrocardiogram.

In mitral stenosis with atrial fibrillation the maximum atrial volume varied from 150 to 400 ml, with the average at 230 ml. The volume variations in this group did not exceed 20 ml, the average being 16 ml. It was not possible to construct a left atrial volume curve but it was possible to register how the ventricular rate influenced the filling of the left ventricle. When ventricular contractions occurred in close succession, the atrium did not have time to empty, and this was reflected in an increased volume. When the intervals between ventricular systoles were longer, more effective filling of the ventricle was attained; this was reflected in an appreciable decrease in the volume of the atrium. In predominant mitral insufficiency with sinus rhythm the maximum volume of the atrium was between 120 and 200 ml, the average being 155 ml. The changes in maximum volume varied from 70 to 150 ml, with the average at 80 ml.

A left atrial volume curve could be constructed for eight cases. The volume curve was characterized by a rapid increase in volume during systole, which began before or in connection with the QRS complex. The maximum volume occurred near the close of systole. In early diastole there was a rapid volume decrease which diminished during diastasis, and in a few cases a volume increase occurred immediately before atrial systole. The decrease in volume during atrial systole was relatively small. In predominant mitral insufficiency with fibrillation the maximum volume of the atrium varied from 610 to 980 ml, with the average at 770 ml; and the volume variations from 110 to 140

ml, with the average at 125 ml. The left ventricle was, in the cases with mitral stenosis, of normal or small size and emptied almost completely at maximum systole. The thickness of the left ventricular wall lay between 7 and 10 mm, with the average at 8 mm. In mitral incompetence in sinus rhythm the left ventricular volume was increased in diastole, and the systolic residual blood was also increased. The left ventricular wall thickness lay between 8 and 13 mm, averaging 10 mm. When atrial fibrillation had occurred, the left ventricle had a greatly increased diastolic volume and residual blood volume. The left ventricular wall was between 10 and 15 mm thick.

Grant *et al.* (91) studied volume changes of the left atrium by angiocardiography and related them to pressures and flow. Increase in left atrial volume beyond 500 ml tended to be associated with mitral insufficiency. In six patients the left atrial volume exceeded 1 liter. Soloff *et al.* (187) used a similar technique but made no attempt to calculate the left atrial volume more accurately. They found the left atrial volume in patients with mitral stenosis to be 2 to 12 times the normal (estimated in four patients). The increase in volume was not related to age or duration of the rheumatic state. There was no constant relationship among various parts of intracardiac circulation time, left atrial size, and degree of mitral stenosis, as reported by the surgeon.

LEFT HEART LESIONS

Aortic Stenosis

The acute hemodynamic consequences of aortic stenosis have been studied in isolated heart preparations or in more or less intact, open-chest animals. Considerable difficulties hamper the reproduction of the human lesion, consisting of stenosis in the valve opening itself or in subaortic stenosis—where the resistance to flow is localized below the valve. In both these lesions the flow to the coronary ostia is reduced. In studies in circulatory models, Porjé *et al.* (162, 163) actually have demonstrated the low or even negative lateral pressures existing in the sinus of Valsalva during the ejection of blood through a stenosed aortic orifice. In contrast, most animal experiments have had to rely upon stenosis induced above the sinus of Valsalva, where the stenosis is caused by constriction of the aorta. This may give valid results for the study of acute lesions or for the study of the myocardial response to acute overload, but may not give exact information about the dynamics of the human lesion with its slowly developed stenosis, where the myocardium reacts with hypertrophy concomitant with decreased coronary flow. Katz and co-workers (110) in 1927 studied the cardiodynamic consequences of acute experimental stenosis of the aorta, which was produced with a ligature placed about 1 cm above the aortic valve (the coronary arteries thus had adequate or even higher systolic filling pressure in contrast to human aortic stenosis).

The contour of the left ventricular pressure curve was altered, with increased height and more peaked summit. The change in the ventricular pressure curve was partly the result of the constriction itself, which decreases the conversion of the potential mechanical energy to kinetic energy of flow, and partly the result of the increase in the diastolic stretch of the ventricle. The normal parallelism in the fundamental contour of the aortic and left ventricular curves during the ejection period disappeared when stenosis was produced. The amplitude of the curves, as well as the gradient of ascent, changed in opposite directions, and the peaks no longer coincided in time. The aortic pressure pulse changed in the following manner: the pulse amplitude decreased, the general pressure level was lowered, the ejection period was prolonged, the gradient of ascent was diminished, the curve was superimposed by systolic and early diastolic vibrations, and a sharp vibration occurred low down on the ascent of the curve. The authors suggested that this vibration was created by the suction action of the suddenly produced swift axial stream beyond the constriction.

Moscovitz & Wilder (153), who studied the arterial and ventricular pressure pulses, produced aortic stenosis in dogs by constricting the aorta at a level just above the valve cusps. They also attempted to evaluate the influence of combinations of stenosis and incompetence on these pressures.

The effect of superimposing stenosis on the normal and insufficient aortic pulses was in both instances to narrow the pulse pressure, delay the systolic peak, and produce a prominent anacrotic notch in a lowered position on the ascending limb. The contour characteristic of aortic insufficiency was dominated and masked by the superimposed stenosis, although the maintenance of a low diastolic pressure indicated that insufficiency was present.

In aortic stenosis the anacrotic notch retained its low position on the ascending limb, although its characteristics became less clear as the central pulse moved peripherally. When aortic stenosis was pro-

duced alone or in combination with aortic insufficiency, the anacrotic notch on the aortic curve was separated from a synchronous vibration on the ventricular curve by a pressure gradient.

The changes of left ventricular contraction depend on the degree of aortic narrowing. In mild degrees of stenosis the ventricular pressure curves resemble those produced by moderate augmentation of aortic resistance; initial tension and the isometric pressure gradient remain unaltered, but the pressure summit is higher and displaced to a later moment of systole. Isometric contraction is prolonged slightly, but the total duration of systole is not affected. The extensive experimental and clinical experience regarding the pressure pulses in aortic stenosis can be appreciated from the following papers: (22, 42, 68, 69, 110, 153, 162, 164, 209, 213).

As soon as the degree of stenosis becomes dynamically significant the ventricular pressure curves are more peaked. The pressure summit is reached earlier, not later, in systole. When ventricular ejection is seriously impeded, the ventricles approach an isometric type of contraction in which the increased residual volume and marked elevation of initial tension contribute to the production of high systolic ventricular pressure. It is important to point out that these experimental findings may differ considerably from what is found in clinical aortic stenosis, where the ventricular response is characterized by the gradual narrowing of the orifice with marked myocardial hypertrophy and by the relative degree of coronary insufficiency due to unfavorable pressure circumstances in the aorta close to the coronary artery ostia.

The aortic pressure curve, after the initial period of rapid ventricular ejection, shows a diminished though prolonged gradient of ascent, because of the impeded blood flow through the stenosis. The central arterial pressure curve vibrations correspond to the aortic systolic thrill and murmur. All of these indicate the obstruction to, and turbulence of, systolic blood flow at the aortic orifice. The arterial systolic and pulse pressure are typically decreased, and the diastolic pressure normal or slightly elevated. When the pulse pressure is narrow it may suggest severe aortic stenosis. Unfortunately, as many authors have emphasized, it is often normal even when aortic stenosis is severe. The radial pulse is usually of the flat, plateau variety and delayed, "pulsus parvus et tardus." An anacrotic wave is present in the peripheral arterial pulse tracing. The anacrotic notch is the lower in position, the greater the stenosis and the inpedance of the systolic discharge. However, cases are reported with severe aortic stenosis, where the carotid pulse was normal in every respect.

The left atrial, pulmonary venous, and pulmonary arterial wedge pressures may be typically altered in aortic stenosis, presumably as a consequence of the myocardial hypertrophy, impeding the inflow to the left ventricle. Gorlin *et al.* (88, 89) have described an increase of the amplitude of the *a* wave of the left atrial pressure pulse. As a consequence, the presystolic left ventricular tension is elevated. The atrial pressure pulse may then be similar to what is found in slight mitral stenosis in conformity with the findings in the right side of the heart with the giant *a* wave in pulmonary stenosis, simulating slight tricuspid narrowing. The only way definitely to rule out valvular changes in the atrioventricular valves, in the presence of severe semilunar valve stenosis with ventricular hypertrophy influencing the atrial pressure tracing, is through simultaneous pressure tracing from the atrium and the ventricle, with determination of the pressure gradients throughout the cardiac cycle.

Several studies have been published (81, 88, 89, 151, 174) regarding cardiac output, intracardiac and vascular pressures in patients with aortic stenosis, studied at rest. Cardiac output ranged from about 2 to 7.0 liters per min per m^2 BSA, with systolic ventricular pressures up to almost 300 mm Hg, and the pressure gradient over the aortic valve up to 180 mm Hg. The calculated aortic valve area has varied from 0.3 to 1.4 cm^2. In cases with left ventricular failure the cardiac output was lower and the pulmonary artery wedge or left atrial pressure markedly elevated, as compared to those not in failure.

In animal experiments the stroke and minute output of the heart decrease as soon as the orifice is narrowed by about 60 per cent. In contrast, the cardiac output in human aortic stenosis is maintained within normal limits until left ventricular failure supervenes—then the cardiac output decreases markedly together with an increase of the left atrial and pulmonary vascular pressures usually giving rise to pulmonary edema. Left ventricular hypertrophy, which presumably develops slowly, thus enables the heart to keep up a normal stroke volume even in the face of pronounced stenosis. This seems to constitute one of the most important differences between aortic and mitral stenosis—the atrial myocardium cannot compensate for the narrowing of the orifice as effectively as the ventricular myocardium. The maintenance of an adequate blood flow even later in the course of aortic valvular disease, in contrast to mitral disease

is also demonstrated by the behavior of the peripheral and renal blood flow (106, 107).

Sancetta & Kleinerman (174) studied the cardiac output at rest and in exercise in nine patients with aortic stenosis, seven of them in chronic left ventricular failure, indicated by increased pulmonary vascular pressures. The cardiac index was 1.98 and 4.04 liters per min per m^2 BSA in those not in failure, and ranged from 1.58 to 2.35 liters per min per m^2 in those in failure (wedge pressure 12 to 20 mm Hg) at rest. On slight exercise (increase in oxygen consumption 45 to 110%) the cardiac output increased from 0 to 43 per cent, less in those in failure. The brachial arterial pressure ranged from 87/48 to 135/57 (one patient had arterial hypertension 187/115) and showed insignificant changes on exercise. Others have reported similar findings (81, 88, 89).

Pulsus alternans—varying systolic pressure from beat to beat—has been taken as an indication of myocardial failure.

Cooper *et al.* (39) studied 50 patients with aortic stenosis (28 acquired, 22 congenital) by means of left heart catheterization. Persistent left ventricular pulsus alternans was observed in 15 patients with acquired stenosis. Those patients more frequently had congestive heart failure, angina pectoris, and cardiomegaly, and their left ventricular systolic pressures and left ventricular-aortic pressure gradients were significantly higher. The hemodynamic parameter (the blood flow was not determined) that afforded the best separation of those patients with acquired aortic stenosis and persistent pulsus alternans from those without alternans, was the product of the left ventricular systolic pressure and the heart rate. This product closely correlated with the tension-time index, which has been suggested to reflect myocardial oxygen requirement. The authors suggest that a disparity between the oxygen requirement of the heart and the oxygen available to it can so alter myocardial contractility as to result in alternation in the strength of the ventricular contraction.

Ferrer *et al.* (72), who studied the hemodynamics of 21 patients with pulsus alternans in the pulmonary and/or systemic circulation, observed alternation in only 4 patients with mitral valvular disease and 1 with aortic. The authors found no consistent relationship between the appearance or disappearance of pulsus alternans and several other factors in these patients, and particularly not with variations in stroke volume and vascular pressures. There was no alternating end-diastolic pressure, which one would expect if the Starling law applies in these conditions.

Aortic Incompetence

The immediate effect of an acute aortic leak is a reduction in the net stroke volume, a decrease of the aortic pulse pressure, and an increase in the diastolic ventricular volume. The myocardium usually responds at once to the greater initial length and tension with a more vigorous contraction. The total stroke volume thus immediately increases considerably. Of the blood ejected into the aorta, part reaches the descending aorta, whereas part is regurgitated back into the ventricle because of the larger pressure gradient existing between the ventricular cavity and the root of the aorta. This pressure gradient during diastole is governed by the size of the leak and the peripheral resistance, which thus also determines the amount regurgitated. In the past it was believed that most of the regurgitation occurred after the mitral valve opened and the ventricular cavity was filled from the left atrium. As a consequence, it was considered that the competition between the forward and backward flowing blood prevented any marked regurgitation. In addition to the size of the leak, the regurgitated amount is governed by the diastolic time—the longer this is, the more time for equilibration of pressure between aorta and the ventricular cavity.

These considerations were put to an experimental test by Wiggers & Maltby (203), who produced acute aortic regurgitation in dogs. They found a typical change of the left ventricular pressure curve with an increased end-diastolic tension, greater steepness, larger amplitude, and higher systolic pressure during the earlier systolic part of the curve, and a steep decline late in systole, i.e., a true "systolic collapse." This was thought to be due mostly to the lower arterial resistance against which ejection began when aortic incompetence was created. The increased total systolic discharge, occurring as a result of the increased initial tension, also played a part and was responsible for the increase in the height of systolic pressure. With these changes in pressures, most of the systolic discharge occurred earlier in systole than it did before the leak was created, causing the rapid systolic collapse.

Wiggers and Maltby also found that the greater part of the decrease of pressure sometimes occurred during isometric relaxation. In all but maximum size leaks, this early diastolic decline of aortic pressure occurred in two stages clearly separated by a halt and change of pressure gradient. A considerable portion of the backflow, increasing with the size of the leak,

flowed back before the mitral valve opened. There was thus really no competition for space in the left ventricle between the regurgitated volume and the inflow from the left atrium. The size of the leak was the chief factor determining the decline of pressure during isometric relaxation, and hence the degree of regurgitation. Changes in heart rate, on the other hand, did not seem to alter those factors.

It was also demonstrated that increasing the peripheral resistance definitely increased the actual volume of regurgitation. This followed the increase in pressure gradient aorta to ventricular cavity during diastole caused by the increased resistance. As long as the myocardium was able to respond normally, this increased the end-diastolic tension and thus the systolic discharge. The final result was that the percentage of regurgitation remained unaltered. The increased load imposed on the myocardium, when an acute aortic leak was created, was reflected by increased coronary blood flow and myocardial oxygen consumption (195, 196).

Moscovitz & Wilder (153) studied the pressure pulses in tracings obtained by direct puncture of the left atrium and ventricle, and of the aortic arch, descending aorta and femoral artery in dogs, with experimentally produced aortic lesions. Aortic insufficiency was created by partial evulsion of one aortic cusp. They found that the characteristics of the aortic pressure pulse in aortic insufficiency was a steep rise to an early peak due to the high velocity of the ejected blood, a steep fall in pressure with a lowered or absent dicrotic incisure, and a widened pulse pressure. At times a double-peaked or bisferious summit was present.

The isometric contraction phase of the ventricular pulse was shortened because of the lowered aortic diastolic pressure. During ejection the ventricular pressure rose in a fashion parallel to that of the aortic curve, with no detectable systolic gradient between the two. The slope of left ventricular pressure decline was unaffected unless the aortic leak was of great magnitude.

The anacrotic notch was a synchronous and superimposable event in the aortic and ventricular pulses in the normal dog and in aortic insufficiency.

As the normal central pulse was transformed into the peripheral, the anacrotic shoulder rose to become a primary peak. The systolic pressure increased, the mean and diastolic pressures decreased, and the curve was smoother as the pulse traveled towards the periphery. This was found in normal and in aortic valvular disease.

Welch *et al.* (197) studied the effects of quantitatively varied experimental aortic regurgitation in a specially constructed dog heart preparation. As aortic regurgitant flow was increased, effective systemic flow decreased substantially. This was always accompanied by a widening of pulse pressure and a lower diastolic pressure. Calculated total peripheral resistance rose as did the left ventricular end-diastolic pressure, whereas mean left atrial pressure exhibited only a slight elevation. The left ventricular function curve (15, 175) was always markedly depressed in the presence of aortic regurgitation. These findings were in contrast to what was found when mitral regurgitation was created (29). It should be pointed out that in these studies the heart rate was kept constant, thereby preventing the modifying effect of changes in diastolic time.

When mitral leaks were produced in the presence of aortic regurgitation, the left ventricular end-diastolic pressure fell, causing a further diminution in both total and effective stroke volume beyond that which had been produced by the aortic regurgitation alone (fig. 5).

From these studies it was concluded that a competent mitral valve acts in two ways to protect the circulation in the presence of aortic regurgitation. First, it limits the elevation of left atrial and pulmonary capillary pressures; second, it makes possible the high left ventricular end-diastolic pressure, as a result of which a more forceful ventricular contraction occurs.

The few clinical studies that have been made in patients with aortic regurgitation tend to confirm these findings. The common clinical observation that, once left ventricular failure has occurred in patients with aortic incompetence, the downhill course is rapid may be explained as an effect of ventricular dilatation with relative mitral incompetence. Thus, two debilitating influences occur at the same time—myocardial failure and mitral incompetence.

Regan *et al.* (168) studied the influence of an infusion of norepinephrine on eight patients with substantial aortic regurgitation (estimated to be about 61 per cent of aortic outflow). Norepinephrine markedly increased total peripheral resistance and pulmonary wedge pressure (from 8 to 29 mm Hg) concomitant with a decrease in regurgitation—probably due to diminished diastolic pressure gradient from the aorta to the left ventricle. In contrast to the normals studied as controls, the heart rate did not decrease and the pulmonary vascular resistance did not increase. Whereas the small increment of left

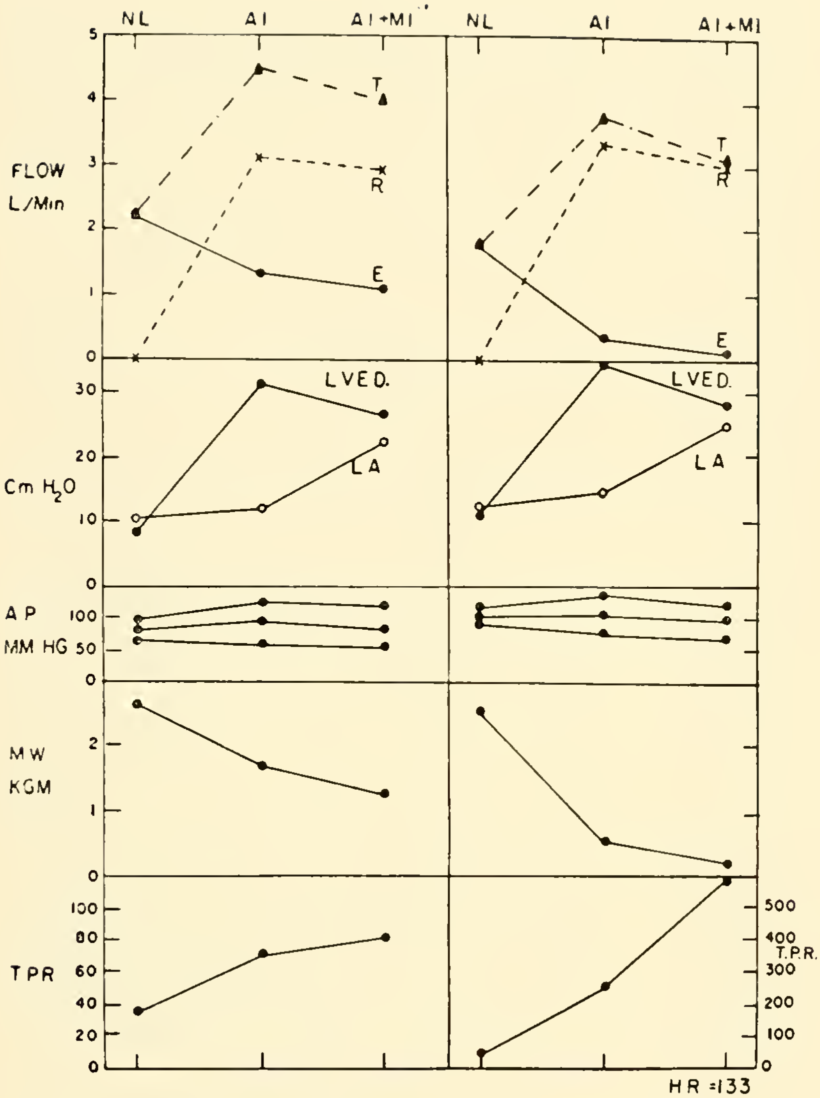

FIG. 5. Hemodynamic effects of superimposing mitral regurgitation on aortic regurgitation. *NL*, no lesion; *AI*, aortic regurgitation; *AI* + *MI*, after mitral regurgitation was superimposed; *T*, sum of effective and aortic regurgitant flows. *R*, aortic regurgitant flow; *E*, effective flow in liters/min; *LVED*, left ventricular end-diastolic pressure; *LA*, mean left atrial pressure; *AP*, aortic pressure; *MW*, effective minute work in kilogram meters; *TPR*, calculated total peripheral resistance; *HR*, constant heart rate 133/min. Dog weight, 25.0 kg. [From Welch *et al.* (197).]

ventricular filling pressure was associated with a sizable stroke work increase in the normal, no change was found in aortic regurgitation despite markedly elevated filling pressures. Regan and associates suggest that the twofold load on the left ventricular myocardium, with both increased aortic pressure, against which the contraction has to occur, and increased venous inflow in the presence of latent myocardial failure caused the ventricular failure to be manifested. This development could be prevented when the venous inflow was restricted by leg tourniquets.

The findings of Sancetta & Kleinerman (174), who studied patients with aortic valvular lesions at rest and during light exercise, agree with this conclusion. In those patients who had not been in failure and who had normal pulmonary pressures at rest, the increased venous inflow during exercise (if it was not combined with increased resistance to left ventricular outflow) did not give rise to any hemodynamic signs of ventricular failure. This was in contrast to those patients who had elevated pulmonary pressure at rest, and whose left ventricular myocardium already was consequently under strain. These latter patients had further increase in left ventricular filling pressure with inadequate total blood flow even in mild exercise.

Similar findings have been reported by Gorlin and co-workers (88, 89), who studied five patients with aortic incompetence and found the left atrial pressure elevated at rest in one and normal in four; and effective cardiac output normal in four and low in one. On exercise, the left atrial pressure increased in all.

In circulatory models or acute animal experiments even a slight diastolic regurgitation into the left ventricle reduces its effective output. In man, however, both effective stroke output and cardiac output may be maintained within normal limits. Even with more pronounced leaks and a decrease in stroke output the cardiac output may be kept normal through an increase in heart rate which serves to decrease the diastolic time during the cardiac cycle. Tachycardia is, therefore, beneficial in clinical cases of aortic regurgitation. The regurgitation of blood from the aorta in early diastole in aortic insufficiency may actually constitute 35 to 60 per cent of the stroke volume. In man no reliable method of determining the regurgitated amount exists, although attempts have been made to estimate total and effective stroke output through a combination of different methods, leading to estimates of from 15 to 50 per cent regurgitated portion of total stroke volume. In another estimate made by Braunwald *et al.* (28), using a dye dilution method with the injection of dye in the aorta, the regurgitant volume was estimated to vary between 27 and 73 per cent of the cardiac output corresponding to total aortic regurgitant flows ranging from 1.8 to 5.6 liters per min.

Both animal and human studies thus indicate that a normal effective cardiac output can be maintained through the increase of end-diastolic tension, occurring as a result of the increased ventricular filling from the aorta. The regurgitated volume may be equal to, or larger than, the net output. Most of it is regurgitated early and before any filling of the ventricle from the left atrium occurs. The size of the regurgitated volume is to a great extent determined by the actual area of the aortic orifice, and only to a small extent by the heart rate or peripheral resistance, as long as the myocardium responds normally. When the myocardium starts failing, the mitral ring dilates with the ventricle. With mitral incompetence added to the left ventricular failure the left atrial and pulmonary venous pressure increase rapidly, causing pulmonary edema or chronic pulmonary congestion. Once this train of events has started there is little chance for the left ventricular myocardium to regain its ability to contract normally. This explains the common clinical experience of the rapidly fatal course of aortic incompetence once signs of failure have appeared.

Mitral Stenosis

The study of experimental mitral stenosis has been especially difficult, since the production of this lesion in the laboratory animal has frequently been accompanied by secondary changes. These have usually been caused by artifacts in the form of inadvertent alterations in coronary circulation, the simultaneous production of aortic stenosis, or even constriction of the great veins. Such mishaps have certainly caused much of the disagreement between the results achieved by the earlier workers in this field.

Katz & Spiegel (111) were aware of these difficulties when they produced mitral stenosis in dogs, using ligatures placed around the mitral orifice and tightened. They studied the acute effects of producing stenosis on the pressure pulses in the left atrium, left ventricle, aorta, pulmonary artery, and right ventricle; but they did not measure blood flow.

The general pressure level of the left atrium was raised with a marked increase in magnitude of the left atrial contraction when stenosis was produced. The initial end-diastolic pressure of the left ventricle showed variable changes (perhaps due to artifacts), whereas the maximum left ventricular pressure decreased. The systolic, diastolic, and pulse pressure in the aorta fell. The heart rate usually, but not always, slowed. This caused a marked abbreviation of the ejection and total systolic time in both ventricles. The right ventricular response to the production of mitral stenosis was variable, the pressures sometimes fell, sometimes rose, or remained unchanged. These varying results were thought to be due only partly to stenosis, causing impediment of flow to the left ventricle and damming back of fluid in the pulmonary circuit. In part, they depended on the decrease in coronary flow resulting from the fall in the arterial blood pressure.

In two fairly recent publications on the effect of experimentally created mitral stenosis in dogs the results are also partly conflicting. Even though it was possible in both studies to keep the dogs alive for a considerable time with the mitral lesion, the results differed markedly in regard to the effect on the pulmonary arterial pressure and the right heart.

One of the groups making the study found that the elevation of the pulmonary venous pressure was associated with a decrease in the pressure gradient from the pulmonary artery to the pulmonary veins, with no change in cardiac output, and thus a decrease in pulmonary vascular resistance. These findings were similar to those found in isolated lungs when the venous pressure was passively elevated (25, 95). The other group found that the experimental mitral stenosis always resulted in right ventricular hypertension, similar to that found in patients with mitral stenosis (132). The pulmonary arterial pressure

exceeded the left atrial pressure by a wide margin during most of systole. During diastole, however, this margin was usually small, except at the time of the height of the *v* wave. This indicates that the pulmonary vascular resistance in these dogs also was fairly low.

It is of importance to consider that, in the experimental animal, compensatory mechanisms, come into play soon after the heart lesion develops, tending to restore the condition to normal. Most notable among these compensatory mechanisms are the increase in the pressure head of the left atrial activity, a prolongation of the time for diastolic filling, and an augmentation of the sucking action of the left ventricle, as evidenced by the steeper rise of the diastolic portion of its pressure curve. The extent of the created stenosis and the modifying effect of such compensatory mechanisms may explain the different results in the animal studies.

The infrequent occurrence in dogs of terminal right heart failure after the creation of mitral stenosis may be due to the small increase in the load on the right ventricle that is the consequence of most experimentally produced mitral lesions. This is in contrast to the long standing and marked elevation of pulmonary arterial pressure and right ventricular load that accompanies the human disease.

The extensive experience gained from right heart catheterization studies in several laboratories around the world has given a rather complete picture of the altered circulation in patients with mitral stenosis or incompetence of varying degrees (9, 13, 23, 24, 40, 48, 50, 53, 58, 59, 70, 85–87, 90, 91, 136, 138, 140, 142, 177, 180, 192, 199, 208, 214, 215). Left heart catheterization has added comparatively little to the knowledge of the circulation in mitral stenosis (16, 17, 20, 26, 42, 152). Some of this information has, however, been of extreme importance, as, for example, the height of the left ventricular diastolic pressure.

The constant and central finding in patients with mitral stenosis in any degree is the increase of the blood pressure in the left atrium and consequently also in the pulmonary veins, the pulmonary artery, and in the right ventricle during systole. In patients with early or slight mitral lesions the pressures may be normal at rest, only to increase on exercise with loads that do not raise the pulmonary pressure in normal individuals. With the gradual narrowing of the mitral orifice, the left atrial pressure and pulmonary arterial wedge pressure increase, up to a limit of about 40 mm Hg. The pulmonary arterial pressure increases in a similar fashion. The gradient from pulmonary artery to pulmonary vein, which is low in normal individuals, is also low in patients with mitral stenosis as long as the pressure in the pulmonary veins is relatively low—below 15 to 20 mm Hg. With the gradual narrowing of the mitral orifice and the increasing of the left atrial pressure, the pulmonary gradient increases, leading to marked pulmonary arterial hypertension and pulmonary arterial pressures that may exceed those in the systemic arteries.

A rise in pressure in the left atrium is an obvious condition for maintaining normal diastolic filling of the left ventricle through a narrowed mitral ostium. This causes a corresponding rise in pressure in the venous and capillary parts of the pulmonary circuit, with a risk of development of pulmonary edema when the pulmonary venous blood pressure approaches the oncotic pressure of the blood. This critical value is reached when the mitral orifice has decreased to less than one-fourth of its normal width. The exact height of the pressure is, however, a function not only of mitral valve opening, but also of the cardiac output—more specifically the diastolic flow—and thus also of the heart rate.

Contrary to what has been found in dogs or in isolated lung segments, the pulmonary vascular resistance, and consequently the pulmonary arterial pressure in mitral stenosis in man, is elevated when the disease is advanced and of long duration. Since changes of comparable magnitude were not observed in dogs over the periods of study by Hannon *et al.* (95), it may be concluded that the rise of pulmonary vascular resistance in man is not a passive hydrodynamic phenomenon but rather results from slow, chronic changes in the blood vessels that alter their elastic and/or muscular properties. Some active contraction of the hypertrophied small pulmonary arterial branches may also add to this raised resistance (103).

The cardiac output has been found to vary considerably at rest, depending on the degree of mitral stenosis. In patients with stenosis of minimal or moderate degree, it usually is within normal limits; in those with more advanced stenosis, the output has been reduced at rest. In patients with frank congestive failure this reduction has been still more pronounced, although the difference usually is small. During exercise, it has been found that the ability to increase the output is relatively unimpaired in most patients with minimal lesions. With increasing stenosis the ability to increase the cardiac output becomes less and less. In some patients, usually those in right heart failure and with added tricuspid regurgitation, the cardiac output is fixed and may actually fall during exercise (188).

The increase in cardiac output during physical effort occurs concomitantly with an increase in left atrial pressure, and presumably in the gradient over the stenosed valve. For more marked increases in output the pressure in the pulmonary veins and capillaries reaches heights which are close to the oncotic pressure of the blood, and favors the transudation of fluid and the appearance of pulmonary edema. When higher values of pulmonary venous pressure are reached, the pulmonary arterial pressure usually increases out of proportion to the increase in venous pressure.

In some patients with a tight mitral stenosis the left atrial pressure has been found to be comparatively low, concomitant with a low cardiac output. This has usually been the case in patients with excessive pulmonary arterial hypertension, right heart failure, or both, or in the presence of atrial fibrillation.

Studies repeated in the same patients after the stenosed valve has been opened (valvulotomy or commissurotomy) have shown decreased pulmonary vascular pressures and increased cardiac output, both at rest and during exercise. There are, however, a certain number of cases where clinical improvement has occurred with only a slight decrease of pulmonary pressures and unchanged or even decreased cardiac output.

Attempts have been made to influence the cardiac output in patients with mitral stenosis with the use of ganglionic blocking agents, other drugs like digitalis glucosides, or the rapid infusion of various fluids. Generally the output has been increased when digitalis was given only if congestive heart failure was the reason for the low output (70). When a rapid infusion of dextran was given to patients with mitral stenosis, augmenting the blood volume, the cardiac output rose less than in a comparable study of healthy individuals (177). When hexamethonium was given to block sympathetic impulses, the pressures in the pulmonary circuit fell considerably without change in cardiac output (214).

These studies thus seem to indicate that neither mechanical factors (increase in filling pressure with augmented blood volume) nor nervous (sympathetic) block alone are responsible for the low cardiac output seen in some patients with mitral stenosis.

It has been suggested that high pulmonary arterial pressure per se is a factor tending to keep the output low and fixed. A close examination of the literature reveals, however, that only a few cases with such an excessively high pulmonary arterial pressure have been adequately studied during rest and exercise. Only when such pressure was associated with signs of right ventricular failure was the output low and fixed. The presence of right heart failure with or without tricuspid incompetence was, on the other hand, more frequently the most obvious finding in the patients with low and fixed output—usually with a moderate rather than an excessive elevation in pulmonary arterial pressure.

The balance between the maintenance of an adequate blood supply to the periphery and avoidance of pulmonary edema is precarious in pronounced mitral stenosis. The range in variations of pressure and flow under these circumstances must necessarily be limited. It is rather remarkable to what extent many patients can carry on a useful life with marked mitral stenosis. An adequate regulation of total cardiac output, heart rate, diastolic filling time and pulmonary lymph flow, as well as the fact that most activities are carried out in the upright position, with the pulmonary blood volume thus relatively small, seems to be of greatest importance. The supposed protective nature of the pulmonary arterial hypertension does not seem to be of any great importance in this connection.

Mitral Incompetence

Incompetence has always been easier to produce experimentally than stenosis (181). Thus, experimental studies of mitral incompetence were started much earlier and provided better information than those on mitral stenosis. It was found early that incompetence of the mitral valve gave rise to a systolic pulsatile expansion of the left atrium together with a rise of its pressure. It was also suggested early that this pressure rise increased the filling of the left ventricle, with restoration of the forward cardiac output, and was transferred to the pulmonary circulation, leading eventually to pulmonary hypertension (178).

Acute mitral incompetence was produced in dogs by MacCallum & McClure (144). They found an acute decrease of the systemic blood pressure, with marked fluctuations of the left atrial pressure. The pulmonary arterial and systemic venous pressures remained unchanged in these short-term experiments, except for some change in the pulmonary arterial pulse contour, probably due to the backward transmission of the regurgitant pressure wave.

The hydrodynamic factors affecting the degree of mitral regurgitation was studied, by Rodbard & Williams (170), in specially constructed models. They concluded that forward flow into the aorta was en-

hanced by increases in atrial pressure, ventricular filling, viscosity of the blood, celerity of ventricular contraction, and by lateral pressure effects on the regurgitant orifice. The tendency to mitral regurgitation was, on the other hand, increased by a rise in systemic arterial pressure, enlargement of the regurgitant orifice, or reduced celerity of ventricular contraction.

Rodbard and Williams also discussed the influence of the relative positions of the aortic and mitral orifices to each other. The proximity of the aortic orifice to the mitral opening was found to reduce the tendency to reflux, because of competition of the two valve areas for streamlines of flow.

Wiggers & Feil (204) produced acute mitral incompetence in dogs and studied the influence of the lesion on atrial, ventricular, and aortic pressure pulses, as well as on atrial and ventricular volumes. Immediately after the induction of the lesion, the volume of blood was reduced in the aorta and increased in the left atrium. There was thus an increase in initial pressure of the left ventricle, confirming Straub's earlier observations that there was a definite retention of blood in the left ventricle that increased its diastolic volume. The tidal volume during mitral insufficiency represents the amount of the systolic discharge into the aorta and the volume regurgitated into the left atrium. Experiments conducted by Wiggers and Feil indicated that within a few beats after the production of a leak the systolic discharge was restored approximately to normal, due to the increased ejected volume.

This compensation may be explained by the following: The higher left atrial pressure and greater diastolic inflow supply a larger volume for systolic ejection. The mechanism whereby the left ventricle can expel this larger volume is the increased initial tension within the ventricle. By increasing the velocity of pressure developed, as well as the force of its stroke, the larger inflow is actually expelled from the ventricle during systole. Should this mechanism fail, systolic residues would progressively accumulate, rapidly and fatally dilating the ventricles. The amount of regurgitation in these experiments was not measured, and the conclusions may not be valid except for acute and moderate size leaks.

The compensation in forward blood flow does not include the restoration of aortic and left atrial pressures to normal, for once the arteriovenous balance has been upset the arterial system contains less blood and the left atrium more. In the acute experiments by Wiggers & Feil (204) no peripheral compensatory mechanisms came into play, which may explain why they did not find any back pressure effects in the pulmonary artery or on the right heart; nor did they find complete restoration of aortic pressure to normal.

The chief backflow occurred during systolic ejection and during a short interval (0.08 to 0.09 sec) into diastole. Little regurgitation occurred during the early phase of the systolic isometric tension increase.

When arterial resistance was increased in the systemic circuit the regurgitant volume at once increased markedly, thereby raising the left atrial pressure and causing a damming back of blood into the pulmonary artery and right heart [see also (61)].

In the anesthetized open-chest dog, Braunwald *et al.* (29) studied the effect of varying amounts of mitral regurgitation, using a specially designed preparation which permitted accurate measurement of the regurgitant flow. This regurgitant flow occurred through a separate connection between the ventricle and atrium.

Mitral regurgitant flows, from nothing to three times resting cardiac output, were tolerated with slight alterations of effective cardiac output, aortic, left atrial, and left ventricular pressures. There was little depression of the effective left ventricular function curves with regurgitant flows of approximately 2 liters per min. Any given increase in regurgitant flow required substantially smaller increments in ventricular filling pressure than similar increases in effective cardiac output. With any given regurgitant orifice, regurgitant flow was a function of aortic pressure.

When left atrial pressures were initially elevated by producing high effective left ventricular work levels and mitral regurgitation then progressively increased, substantial increments in mean left atrial and left ventricular filling pressures were produced. The extent of this rise, resulting from any given degree of mitral regurgitation, was a function of the mean left atrial pressure prior to the induction of regurgitation. The importance of the relationship between myocardial contractility and the hemodynamic effects of any given mitral regurgitant lesion was stressed (fig. 6).

The experimental design did not allow the regurgitant flow to go through the mitral valve. The competition between mitral and aortic orifices, discussed by Rodbard and Williams, therefore did not come into play and the results may not be strictly comparable to those found in the intact circulation.

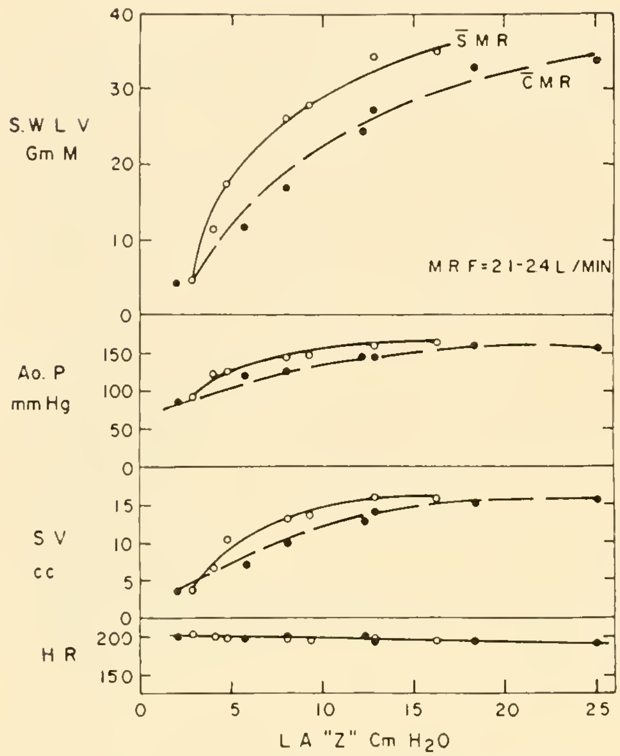

FIG. 6. Effect on left ventricular curve of mitral regurgitant flow (*MRF*). *s̄M.R.*, without; *c̄M.R.*, with mitral regurgitation; *SWLV*, left ventricular stroke work in gram meters; *Ao.P.*, mean aortic pressure; *SV*, stroke volume; *HR*, heart rate/min; *LA "Z"*, left atrial Z point pressure. Dog weight, 25.4 kg. [From Braunwald *et al.* (29).]

Braunwald *et al.* (27) in three experiments on dogs, induced mitral regurgitant flows of 2 to 4 liter per min while forward cardiac output was held constant. This did not influence the duration of ventricular ejection into the aorta. In contrast, in three other dogs of similar weight, aortic regurgitant flows of 2.2 to 3.5 liters per min were accompanied by substantial increases in the duration of systolic ejection, comparable to those observed when total ventricular stroke volume was increased by similar amounts in the absence of regurgitation.

STUDIES IN MAN. From clinical and patho-anatomical observations Edwards & Burchell (54) point out two striking phenomena occurring in mitral incompetence in man. First, mitral insufficiency may be present for years and may be well tolerated up to a certain point. Beyond that point clinical evidence for gross mitral incompetence may become apparent and the disease may continue in a severe, unrelenting, and possibly fulminating manner. Second, in some patients with dilated left ventricles, signs of mitral incompetence may be demonstrated during life; but at necropsy no anatomic basis for the incompetence may be demonstrated either in the nature of the chordae or leaflets.

These observations may serve to explain many of the different results obtained by different researchers, since it has not been possible, in the intact individual, to separate the myocardial factor from the valvular damage—at least no attempt has been made to analyze these factors in clinical cases. This should be possible now with the aid of the angiocardiographic technique.

McDonald *et al.* (149) studied patients with severe symptoms due to mitral valve disease and separated a larger group with stenosis, as the prominent feature, from a small group with incompetence based on the findings at surgical correction. The size of the mitral orifice was calculated by the Gorlin formula. The statement that a severe degree of mitral stenosis and of incompetence cannot coexist seems self-evident. McDonald and his group found in cases with dominant incompetence and without significant stenosis that the left ventricular diastolic pressure surprisingly was seldom raised in the presence of marked elevation of left atrial mean pressure. The elevation of left atrial mean pressure found was, on the other hand, greater than could be caused by a regurgitant jet. Thus a considerable increase of left atrial mean pressure appears to be necessary for sufficient diastolic blood flow through the mitral valve to maintain the large total left ventricular output (composed of a huge regurgitant flow and a reduced aortic flow). This mechanism was, more often than left ventricular failure, the cause of elevated pulmonary pressure in this series of patients with mitral incompetence.

Davila (43), who studied 58 patients with mitral incompetence during operation, also found a small atrioventricular pressure gradient during diastole in some of the cases with pure and pronounced mitral regurgitation. He also emphasized the ventricular-atrial systolic gradient that occurs across the leaking valve (fig. 7) and at least partly determined the amount of regurgitation. This gradient increases after surgical correction of the lesion, due either to a decrease in atrial pressure or to an increase in left ventricular and aortic systolic pressures. In Davila's series the atrial pressure decreased in most cases.

Davila also attempted to analyze the dynamics of the left ventricle. The total ejection time of the left ventricle in the aorta shortened slightly with less than normal difference in pressure between the left ventricle and the aorta during the rapid ejection

phase. This should be compared to the findings of Braunwald, Sarnoff and Stainsby who, in isolated dog hearts, did not find any shortening of the ejection time in mitral incompetence, if the forward cardiac output was held constant.

The elevation of left atrial pressure is transmitted backward and, as in mitral stenosis or other conditions with chronic elevation of the pulmonary venous pressure, the pulmonary artery pressure increases. Usually the increase of pulmonary vascular resistance is small, especially in early cases or cases with only a minor degree of regurgitation. In long standing lesions of marked degree the pulmonary vascular resistance may increase considerably, leading to right ventricular hypertension, right ventricular hypertrophy and, ultimately, right-sided congestive failure.

The cardiac output may be normal in cases with mitral incompetence. As long as the regurgitated amount is fairly small, the load on the myocardium is negligible and no difficulty seems to exist in keeping a normal forward output both at rest and during exercise. Only in cases with marked regurgitation, where the element of myocardial strain and failure has been added, does the cardiac output decrease below normal values (and below the needs of the body). An immediate increase in forward cardiac output usually follows the successful surgical correction of mitral regurgitation.

In the light of dog experiments by Braunwald *et al.* (29), the train of events in clinical mitral incompetence may be explained as follows: Large regurgitant flows may exist without striking elevations of left ventricular end-diastolic pressure or left atrial mean pressure if the myocardial contractility is unimpaired. However, ventricular function may be compromised by processes such as rheumatic carditis, by altered structure of contractile proteins accompanying an increased myocardial burden, or by the existence of arterial hypertension or aortic valve disease [see (115)]. (To this, acute or chronic hypervolemia may be added.) In these circumstances adequate forward cardiac output can be maintained only by elevation of ventricular end-diastolic pressure. The large regurgitant flow then results in further elevation of left atrial mean pressure; this in turn may be responsible for the development of increased pulmonary vascular resistance and anatomic changes in the pulmonary vascular bed. Right ventricular hypertrophy and ultimately failure then occurs as a consequence of the increased pressure load against which the ventricle has to work.

Because the presence or absence of myocardial

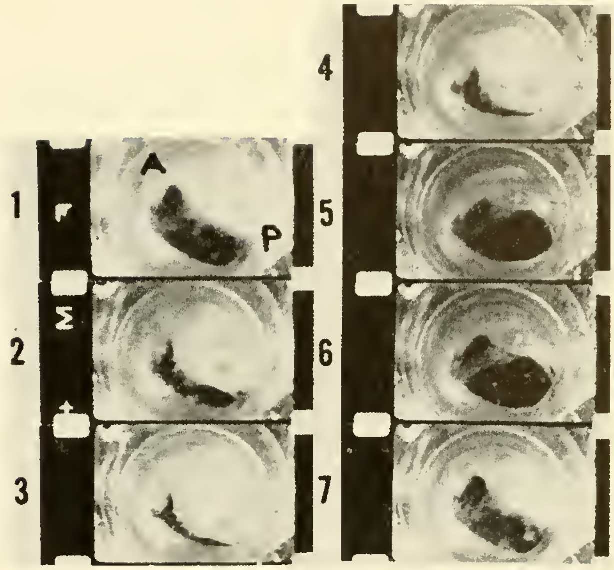

FIG. 7. Moving picture record of an incompetent mitral valve made on the pulse duplicator. Frames numbered 1, 2, and 3 are during ventricular systole. The cycle actually lasts through 14 frames, but for illustrative purposes alternate frames have been deleted. Note that the valve orifice is larger early in systole (frame 1) . . . . the valve does not "snap" to a closed position, rather it "floats" toward that position. This serves to illustrate the variation of valvular regurgitant orifice resistance. [From Davila (43).]

damage leads to important difference in clinical reaction to the cardiac lesions of mitral incompetence, several clinicians maintain that clinical symptoms of mitral incompetence do not appear until left ventricular failure has started. The findings in the acute experiments of Braunwald and associates strongly emphasize this possibility, at least that clinical symptoms do not appear until something else is added to the regurgitation, be this increased peripheral resistance, hypervolemia, or myocardial failure.

RIGHT HEART LESIONS

Valvular lesions of the right heart are less common than those of the left, and have consequently attracted less interest. The easy access to the great veins, the right atrium, and the different ostia of the right heart has, however, permitted a rapid increase in knowledge during the last decade, especially about the right-sided lesions occurring in clinical work. Experimental procedures have also been designed in increasing numbers for the creation and study of right heart lesions in animals.

The right-sided lesions of the semilunar valves are basically not much different from the corresponding left-sided lesions, except for the fact that the right ventricle has a weaker myocardium to start with, corresponding to the lower pressure in the pulmonary artery as compared to the pressure in the aorta. The right ventricular myocardium has, however, the same ability for hypertrophy as the left. Many of the right-sided lesions observed usually do not develop until the pressure in the pulmonary circuit has been elevated to a considerable degree. This is mostly due to the occurrence of valvular lesions of the left heart and is part of the natural history of rheumatic heart disease. The lesion then develops in a situation where the right ventricular myocardium is more like the left, due to the existing hypertrophy.

Some difference seems to exist between right and left hearts as the consequence of lesions in the atrioventricular valve apparatus. Much of the difference in dynamic behavior of the right and the left atria, respectively, is due to differences in the venous pool behind them. The much larger venous pool behind the right atrium permits more flexibility than the smaller venous pool behind the left atrium, where fairly small pressure rises can have great consequences on the pulmonary circulation and pulmonary function. Fatal pulmonary edema may thus be caused by the regulatory mechanism aiming at adequate peripheral blood flow, and may occur before the myocardium has failed completely.

Some of the studies reported during recent years have been concerned with the production of congestive heart failure in animals. Interference with the pulmonary and/or tricuspid valves seems to be the easiest and perhaps the only feasible way to create chronic congestive failure in dogs similar to the state observed in man.

Pulmonary Incompetence

Pulmonic regurgitation has been produced in dogs by complete or partial pulmonary valvectomy (60, 118). No change in pulmonary arterial pulse pressure was seen when less than one valvular cusp was removed; frequently no change was observed after removal of an aortic cusp. Widening of the pulmonary arterial pulse pressure could be produced by removal of more than one cusp, or by inducing pulmonary hypertension after removal of only one cusp.

Pulmonary hypertension was instituted by mechanical constriction of the pulmonary vascular bed or by hypoxia. In these dogs the systolic pulmonary artery pressure was 51 to 76 mm Hg in the preoperative and 59 to 92 mm Hg in the postoperative period. No evidence of right ventricular failure was noted up to 6 months after the operation. [Several of these dogs remained in good clinical condition for some years after complete valvulectomy.—Ed.]

Of a total of nine animals in which the cardiac output was determined, six showed evidence of a diminished cardiac output postoperatively. The diminution was small, and the authors are hesitant to conclude that partial pulmonary valvectomy produces permanent lowering of the cardiac output.

Kay & Thomas (112) also produced pulmonary insufficiency in dogs with a similar technique and observed more marked hemodynamic changes. One dog died in congestive failure and all 15 dogs exhibited signs of right ventricular dilatation. Ten of the dogs had systolic pressures in the right ventricle of 50 mm Hg or more, and in three, the systolic pressure was above 90 mm Hg. The diastolic pressure in the pulmonary artery was low. There seemed to be some systolic gradient over the incompetent valve. Although no determination of blood flow was made, this seems to indicate a large stroke volume with marked regurgitation, in contrast to the milder regurgitation of the dogs of Fowler *et al.* (79).

Barger and collaborators (11), during studies aimed at the creation of right heart failure, could not demonstrate any signs of heart failure or increase in right atrial pressure, even during strenuous exercise in dogs in which pulmonary insufficiency had been created through avulsion of the valve leaflets or through widening of the pulmonary ring.

Pulmonary regurgitation is a lesion that can be recorded rather frequently following long-standing pulmonary hypertension with or without valvular lesions in the left heart. It is rare as a single occurrence although some studies of such cases have been reported in the literature (133, 156). These reports indicate that in youth an isolated, although dynamically significant, pulmonic valvular regurgitation is well tolerated. As long as the blood pressure in the pulmonary artery is within normal limits or only slightly elevated, the amount of regurgitation and thus load on the right ventricle seem to be small. This finding is in good agreement with most of the experimental studies cited above.

Pulmonary Stenosis

Fineberg & Wiggers (73) studied the right ventricular and aortic pressures during progressive circular

compression of the pulmonary artery. The increases in initial tension and systolic summits, and the over-all change in ventricular contour were similar to changes observed in the left ventricle in acute experimental aortic stenosis. The aortic pressure started to decline when about 50 per cent of the pulmonary arterial lumen was still patent, and the pressure fall was marked as the constriction was increased.

Right-sided failure in dogs was produced by controlled progressive stenosis of the pulmonary artery (44, 45). Failure occurred only when the diameter of the artery was diminished to less than one-third of its original size. The cardiac output decreased, with marked increases in right ventricular systolic and atrial mean pressures and a marked increase in heart rate. The mean femoral arterial pressure usually decreased. It is impossible to decide to what extent the changes registered were due to the pulmonary stenosis and to what extent to failure of the heart.

Barger and collaborators (11) also produced pulmonary stenosis in dogs. When the pulmonary stenosis was less than 50 per cent of the diameter, a slight rise of right atrial pressure occurred with a further rise in pressure during strenuous exercise. The work capacity of these dogs was normal, and right heart failure did not develop. Superimposed pulmonary insufficiency produced only minor changes. Similar experiences have been reported by others (113).

Clinical studies of pulmonary stenosis started with the introduction of the cardiac catheter (41, 52, 92). Since then it has been demonstrated that pulmonary stenosis is one of the common congenital lesions, and is often symptom free.

Normally, there should be no systolic pressure gradient between the right ventricle and the pulmonary artery. Under the conditions of study, often with augmented blood flow due either to anxiety or to a concomitant congenital shunt, pressure gradients of around 10 mm Hg have been registered in the absence of anatomic stenosis. This is explained by the pressure loss to velocity and the sucking effect by the blood stream on the end hole of the catheter used.

Several groups have classified patients with systolic pressure gradients of less than 50 mm Hg as having mild stenosis; with a gradient of 50 to 100 mm Hg as having moderate stenosis; and only when the gradient is above 100 mm Hg as having severe stenosis (172). Only in cases with severe stenosis is the blood flow decreased.

During ejection, the blood is forced through the stenosed valve in a jet, which can be demonstrated by the use of angiocardiography. This jet has a high velocity at the orifice, but it slows down as it spreads in the pulmonary artery and starts forming turbulent eddies in the relatively stationary blood mass there. The kinetic energy of the jet is converted into potential energy which is measured as increased lateral pressure. The turbulent eddies, which can be demonstrated both by angiocardiography and in model experiments, are most evident a few centimeters from the orifice. The jet is most rapid in and just beyond the orifice and gives rise to negative pressure laterally. This has been demonstrated in model experiments.

In pulmonary valvular stenosis, emptying of the right ventricle is modified by the increased resistance in the pulmonary orifice. The pressure rise during the ventricular contraction occurs more or less continuously towards a peak, which is succeeded by a pressure fall with the same continuous course. The more severe the stenosis, the closer toward the end of systole is the peak found.

The right atrial pressure curve may be modified in severe pulmonary stenosis with right ventricular hypertrophy (147): The curve is dominated by a high peaked *a* wave which is transmitted to the jugular venous pulse as well as to the liver (93). As early as 1913 Lanberg and Pezzi pointed out the presence of this abnormal wave in the venous pulse, and interpreted it as a result of increased filling resistance in the ventricle. It is of importance that this increased *a* wave cannot be taken as a sign of tricuspid stenosis, which can be ascertained only through simultaneous or successive pressure tracings from the atrium and ventricle.

In pulmonary stenosis the pulmonary blood flow and content is reduced, whether the narrowing affects the subvalvular outflow tract (infundibular stenosis), the pulmonary valve itself, or the pulmonary artery. At rest, oxygenation is usually sufficient; but if the stenosis is severe, exertion may cause cyanosis due to inadequate pulmonary flow. The reported occurrence of chronic cyanosis in pure pulmonary stenosis has been discussed by Selzer & Carnes (179). They did not find any decrease in arterial oxygen saturation and consider the occurrence of peripheral cyanosis in pulmonary stenosis to be comparable to that found in mitral stenosis or other advanced heart lesions, where the slow peripheral circulation, perhaps in combination with local capillary damage, is responsible for the cyanotic skin changes.

The pressures in the pulmonary veins and the pulmonary artery are low, with normal pulmonary vascular resistance. The right ventricular systolic pressure is elevated; and when hypertrophy, dilatation

and/or failure have occurred, the diastolic pressure is elevated also. The right atrial systolic pressure and, in advanced cases, the atrial mean pressure also, are increased.

The production of pulmonary stenosis in the experimental animal may thus lead to right ventricular hypertrophy and ultimately failure, when the stenosis is marked enough—in contrast to pulmonary regurgitation which seems to be of minor importance even when the regurgitation is completely free. This is in good conformance with the findings of Greene *et al.* (92), who found that half of their reported patients with pure pulmonary stenosis died in right heart failure.

Tricuspid Valvular Deformities

Barger and his associates (11, 12) created tricuspid incompetence in dogs by tricuspid avulsion. Resting mean right atrial pressure increased 75 to 130 mm of water. With exercise the right atrial pressure increased further. Despite the elevation of the mean atrial pressure none of the dogs had any gross reduction in work tolerance.

The changes in the right atrial pressure pulse varied with the extent of insufficiency of the tricuspid valve. In mild insufficiency atrial pressure was elevated only during ventricular systole. In complete avulsion of the tricuspid leaflets right atrial pressure was nearly identical with right ventricular pressure.

When pulmonary stenosis also was produced in these dogs the atrial pressure rose further, work tolerance decreased, and right heart failure developed, characterized by markedly dilated right ventricle, elevated atrial pressure and distended veins, dyspnea on exertion, decreased work tolerance, hepatomegaly, ascites, tachycardia at rest, and a relatively fixed heart rate even during exercise.

Yu *et al.* (212) reported hemodynamic studies in five patients with tricuspid stenosis and concomitant rheumatic mitral stenosis. The authors point out the presence of a diastolic gradient between the right atrium and ventricle, most pronounced during early diastole. This gradient was accentuated by exercise and was not dependent upon the presence or absence of sinus rhythm. It is of interest that the end-diastolic pressure of the right ventricle was elevated in three of the cases (artifact?). Resting cardiac index and stroke index were subnormal in four patients with decreased stroke output during exercise.

McCord and collaborators (146, 148) reported hemodynamic studies in three patients with tricuspid stenosis of rheumatic origin and associated with mitral stenosis as well. The cardiac index was low, with only a small rise on exercise, moderately elevated pressures in the pulmonary artery, and markedly elevated right atrial pressure. The authors stress the inadequacy of analyzing only the right atrial pressure pulse for the diagnosis of tricuspid stenosis, since typical changes with increased *a* waves may occur in right ventricular hypertrophy: During exercise, with its increased blood transport, the abnormalities of the pulse may increase and be easier to evaluate. For exact assessment of the degree of stenosis, both atrial and ventricular pressures must be registered.

The importance of demonstrating a pressure gradient across the valve for the diagnosis of tricuspid stenosis must thus be stressed, since right ventricular hypertrophy alone may modify the right atrial pressure curve in a way similar to true stenosis.

In a study in patients with heart disease of varying etiology Korner & Shillingford (122) demonstrated that the effective cardiac output in patients with tricuspid incompetence did not increase on exercise in a normal fashion. They conclude that the regurgitant flow through the tricuspid valve is important in maintaining a low, fixed cardiac output in some cases of congestive cardiac failure. This may have a special significance, since right ventricular dilatation in myocardial failure in itself may cause a functional tricuspid incompetence (139, 150).

The factor of tricuspid incompetence must also be taken into consideration when discussing the role of pulmonary hypertension in keeping the cardiac output fixed in mitral stenosis, as most cases with such a low and fixed output have signs of tricuspid incompetence, whether the pulmonary arterial blood pressure is markedly elevated or not.

PULMONARY BLOOD VESSELS AND PULMONARY VASCULAR RESISTANCE

The fact that the most conspicuous symptoms in patients with mitral stenosis and advanced chronic left ventricular failure originate in the pulmonary circuit has focused attention on the pulmonary vascular bed. Several groups have demonstrated the occurrence of various degrees of increased vascular resistance in the pulmonary circulation. This increased resistance has been thought to be due to anatomical changes in the distal arterial branches ("arterioles"), to increased tone of these vessels, or to a combination of both (6, 32, 55, 64, 65, 77, 78, 82, 97, 103, 139).

The patho-anatomical changes observed can be graded from mild to severe, and seem to be correlated with the extent of impediment to the circulation in the left heart. Mild changes consist of dilatation of the capillaries to the extent that their width can accomodate five or six red blood cells. The number of capillaries seems to have increased and there is herniation of the capillaries into the alveolar spaces with slight thickening of the capillary basement membrane. Severe lesions are characterized by a further increase in interstitial connective tissue and further thickening of the capillary basement membrane. Interstitial collagen may separate the capillaries from the alveolar space. The capillary endothelium may change to a cuboidal form. The capillary lumen appears to be narrow within these thickened walls and may be difficult to discern. Intimal thickening of arteries and hyperplastic arteriolosclerosis tend to become increasingly marked with a greater degree of change in the alveolar walls. These changes are not uniform through the whole vascular bed in any given lung and tend to be more marked in the basal parts. In advanced cases the main pulmonary artery becomes more or less dilated with a thickened wall, which may show advanced sclerosis.

In several cases of mitral insufficiency pathological changes of the pulmonary vascular bed have been described that are essentially identical with those found earlier in mitral stenosis. Ross *et al.* (173) thus described medial hypertrophy sclerosis and intimal thickening of the pulmonary vessels in 4 of 23 patients with mitral incompetence where lung biopsies or post-mortem lung sections were available for microscopic study. Similarly, Becker *et al.* (14) and Smith and collaborators (186) described advanced changes of the pulmonary blood vessels in patients, with aortic stenosis or systemic hypertension, dying after long-standing chronic left ventricular failure. The most pronounced change here also was media hypertrophy.

The great resistance to flow through the small pulmonary arterial vessels found in mitral stenosis and other advanced left heart lesions is thus associated with medial hypertrophy of the small arteries. The specific mechanism by which this arterial response is brought about is not known [see (131)]. Most probably it is related to the increased pulmonary venous pressure resulting from the failing ventricle or the mitral block. The mechanism would then be identical in mitral stenosis, mitral incompetence, and left ventricular failure. Rheumatic vasculitis or other rheumatic changes in the lungs would not then have to be postulated.

Increase in left atrial pressure in isolated dog lungs or lung segments causes a decrease of pulmonary vascular resistance, presumably through the distention of the vascular bed (25). The same observation has been made in intact animals when mitral stenosis was acutely created (95). Common to these observations is the acute and short-lasting nature of the pressure elevations. In man, when the narrowing of the mitral valve occurs over a time space of several years or even decades, the elevation of the left atrial pressure is almost always followed by an increased vascular resistance. In some patients with marked and long-standing mitral stenosis the pulmonary arterial pressure may be so high as to exceed even the systemic arterial pressure. In these cases the pulmonary vascular resistance is markedly elevated, and the left atrial pressure is usually not excessively high and may even be lower than in other similar cases with lower resistance. To what extent this is due to the anatomical changes described above with chronic edema and fibrosis, or to active vascular constriction, is still unknown. It has been suggested that this increase in resistance serves the purpose of protecting the pulmonary capillaries from a high intravascular pressure which otherwise would cause fatal pulmonary edema ("protective pulmonary hypertension") (208). The increased pulmonary venous pressure would presumably govern the extent of vasoconstriction via some hypothetic pressure receptor in the venous bed or left atrium. Such an active increase in vascular tone could then give rise to the medial hypertrophy and other patho-anatomical changes that, according to this view, would be secondary to the functional protective hypertension.

Reports have been published comparing the findings from lung biopsies with the preoperatively determined pulmonary arteriolar resistance and showing a lack of correlation between the calculated resistance and the extent of vascular changes in the lung biopsies (32, 55, 82). From this it has been concluded that vasoconstriction within the lung is an important factor in producing pulmonary hypertension in mitral stenosis. As the lung biopsy usually was taken from the anterior border of the left upper lobe, a part of the lung that cannot be thought to be representative for the whole vascular bed, this conclusion does not seem to be justified.

Studies on the effect of a constant infusion of acetylcholine in the pulmonary artery of patients with mitral stenosis and pulmonary hypertension demon-

strated a lowering of pulmonary artery pressure and pulmonary vascular resistance, both at rest and during exercise (191). This did not cause any pulmonary edema or breathing difficulties, although both the heart rate and cardiac output usually increased. The "protection" afforded by the high resistance thus did not seem to be needed. The infusion of acetylcholine also caused a decrease in arterial oxygen saturation, indicating changes in the ventilation perfusion ratio of the lungs. Thus the increased resistance may be secondary to anoxic changes in the ventilation to perfusion ratio, rather than to the increased left atrial pressure per se (67, 159, 202). The rapid decrease of the pulmonary vascular resistance seen in some patients after the mitral block has been removed by commissurotomy also speaks in favor of its functional nature.

The anatomical lesions found in the lungs of patients with long-standing left heart disease may in itself, cause both increased resistance and rapid changes in resistance during different conditions of flow. As suggested by Folkow, even minor thickening of the inner layer of the vessel walls of the arteries of the systemic circulation causes a marked narrowing of the lumen and thereby increased resistance (75, 76). A similar mechanism operating in the pulmonary vascular bed could well explain the observed figures for pressures and flows in pulmonary hypertension in mitral stenosis. Also the rapid increase in resistance seen during exercise studies when heart rate and cardiac output (and presumably the pulmonary blood volume) increase, could be due to purely anatomical alterations.

Taking all facts into consideration, it may be concluded that the increased pulmonary vascular resistance seen in patients with left-sided heart disease is due partly to functional vasoconstriction within the lung, and partly to patho-anatomical changes of the small arterial branches. The extent to which one or the other mechanism is responsible for the changes in any given case may vary considerably.

Some studies of the pulmonary blood volume have been made using several indicator dilution techniques (24, 119, 127, 128). They have usually shown an absence of increased pulmonary blood volume in patients with mitral stenosis. The uncertain technique, combined with difficulties in obtaining comparable figures in normal individuals or patients with other heart lesions, invalidates any conclusions from most of the results published. It seems obvious furthermore that a "normal" figure for the amount of blood in the chest of a patient with marked perivascular pulmonary fibrosis, interstitial edema, and enlarged heart in itself may signify engorgement of the pulmonary vessels.

No studies regarding the lymph flow in pulmonary congestion have been reported. It is, however, a frequent finding, during surgery for mitral stenosis, that the pulmonary lymph vessels are markedly dilated and may have a diameter of 1 cm or more. This indicates the importance of good lymph drainage to maintain the lungs edema-free in conditions with elevated left atrial pressure.

In the discussion of the importance of increased pulmonary vascular resistance for the development of the progressive clinical picture in mitral stenosis, it is often stated that the cardiac output can no longer be increased when the pulmonary arterial pressure increases to systemic loads. There are, in reality, only a few such cases reported in the literature where the high arterial pressure existed in the absence of other hemodynamic abnormalities. In almost all cases signs of right ventricular failure were also present, with or without tricuspid incompetence. A similar inability to increase the cardiac output on exercise has also been found in patients with secondary myocardial changes, with much less pulmonary hypertension, or even almost normal pulmonary pressure. The primary importance of the high pulmonary arterial pressure for the regulation of the cardiac output in patients with mitral stenosis thus seems to have been exaggerated.

REGIONAL AND PERIPHERAL BLOOD FLOW

Regional blood flow has been studied only to a limited extent in various valvular heart disorders. Most interest has been directed to the renal blood flow in view of the possible connections between changes in renal hemodynamics and the development of the syndrome of congestive heart failure (10–12, 109, 199). When it was demonstrated, in 1946, that markedly decreased renal blood flow and glomerular filtration rate occurred in patients with chronic congestive failure, this gave rise to a large series of studies on the behavior of the kidney in patients with heart disease. It was soon found that similar renal changes could be demonstrated in some patients with valvular heart disease long before any signs of congestive failure had appeared. In a large series of patients with mitral stenosis, where the renal dynamics were studied simultaneously with the pulmonary circulation (199), it was found that the resting values for renal blood flow were close to normal in those patients who had

normal or almost normal pulmonary and systemic hemodynamics (and who usually were free of symptoms except during strenuous exercise). In patients with more marked alteration of pulmonary hemodynamics and already with symptoms during slight activity, the renal blood flow was lower but the glomerular filtration rate was still within normal limits. In still more disabled patients—i.e., with more tight mitral stenosis—these functions were also more depressed, with a decrease of glomerular filtration rate as well. In a fairly small group with clinically overt symptoms of right heart failure the findings were qualitatively the same, although those in failure had lower total blood flow, higher pulmonary arterial pressure, higher pulmonary vascular resistance, elevated renal venous (or right atrial) pressure, and slightly lower renal blood flow. Studies conducted during exercise showed that these patients reacted with more pronounced decrease in renal blood flow during a slight exercise test than normal individuals, with a concomitant decrease in sodium excretion.

It was also found that the alterations in renal blood flow and renal function had no patho-anatomical basis but seemed to be due to some regulatory mechanism. Hydralazine, fever, pregnancy, or the infusion of 3 per cent glucose in water thus increased the renal blood flow to or toward normal figures. The possible pathway for this regulatory mechanism could not be defined. There was no good correlation between the renal changes, on the one hand, and cardiac output, arteriovenous oxygen difference, pulmonary wedge, or pulmonary arterial pressure, on the other. The stroke output seemed to be fairly well correlated with the renal findings.

Similar results were obtained by Barger and associates (10–12) who studied the influence of graded destruction of the right heart valves on the renal function in the dog. They demonstrated that the renal response to exercise was altered earlier than general hemodynamic changes could be found. In further studies they showed that creation of minimal heart lesions (pulmonary insufficiency) changed the renal response to aldosterone or norepinephrine from the normal toward what was found in the dog with congestive failure.

The renal changes seemed to be more marked with mitral valvular disease than with aortic or congenital heart disease, which is of interest in view of what was found by Huckabee (106) regarding the anaerobic capacity of the heart in these valvular lesions.

Donald and his group studied the behavior of the blood flow in several regions, notably splanchnic, muscular, and cerebral flow in patients with mitral stenosis. They found that the blood flow to the exercising muscles (50) was about 8 per cent of that found in normal subjects with a normal cardiac output response to effort. As the cardiac output in the patients with mitral stenosis was low and fixed, the increase in blood flow to the exercising muscles was achieved by a considerable reduction of blood flow to the whole skin, to muscles not involved in the exercise, to the splanchnic area, and the kidneys. Only the cerebral flow was exempt and continued at the resting level, whereas the coronary flow was presumed to be sufficient, since the patients did not complain of any anginal symptoms. Donald suggests that both humoral and neural mechanisms were responsible for the integrated circulatory response in patients with cardiac disease during mild exercise.

Huckabee & Judson (107) have developed a method to evaluate the anaerobic metabolic rate in man, in order to study the adequacy of peripheral flow. By determining total body water, arterial and venous oxygen concentration, oxygen consumption, cardiac output, and the levels of blood pyruvate and lactate, they were able to calculate the "excess" lactate production, which is defined as the amount of lactate produced above that secondary to nonhypoxic causes. This serves as an estimate of the energy derived from the anaerobic lactate dehydrogenase system. In normal subjects 5 per cent of the energy required during mild exercise was supplied through anaerobic metabolism, whereas in patients in heart failure 20 to 50 per cent of the energy needed for mild exercise was supplied by anaerobic metabolism [see also (176)].

Huckabee (106) also studied several patients not in failure. These consisted of 11 patients with mitral valvular disease (7 patients with mitral incompetence and 2 with both stenosis and regurgitation), 6 patients with aortic valvular deformity (2 stenosis and 4 regurgitation, or both stenosis and regurgitation), 2 with tricuspid regurgitation and two with pulmonic valvular stenosis. All cases were studied at rest and during exercise, and the excess lactate concentration and anaerobic metabolic rate were calculated to judge the efficiency of cardiac performance. Although all patients considered themselves to be completely well and were engaged in full-time work, Huckabee demonstrated a definite abnormality of cardiac output response in patients with atrioventricular valve deformity, whereas those with semilunar valve deformity showed a normal response to exercise. Huckabee thought that the decreased response to slight physical activity in the patients with mitral or tricuspid disease

was due to an inadequate compensation from the pulmonary or systemic venous bed, which cannot increase the pressure filling the ventricle as easily as the ventricular muscle can increase its force and empty the ventricles in the presence of slight aortic or pulmonary disease. These findings agree well with the observation that patients with even slight mitral stenosis have a lower renal blood flow and react more to the stress of exercise than do patients with slight aortic disease or normals. They also provide a physiological background to the well-known clinical experience that a patient with aortic valvular disease may have a long active life without symptoms until signs of myocardial failure appear, after which the congestive failure rapidly develops and leads to a fatal termination within a few months. This pattern is quite different from the course in mitral disease where signs of failure develop slowly and congestive heart failure may be present for many years before death.

REFERENCES

1. ALLISON, P. R. AND R. J. LINDEN. The bronchoscopic measurement of left auricular pressure. *Circulation* 7: 699, 1953.
2. ANDERSSON, T. Electrokymographic examinations in mitral valve disease. *Acta Radiol.* Suppl. 106, 1953.
3. ANKENEY, J. L. Further experimental evidence that pulmonary capillary pressures do not reflect cyclic changes in left atrial pressure. *Circulation Res.* 1: 58, 1953.
4. ANKENEY, J. L. Interrelations of pulmonary arterial, "capillary" and left atrial pressures under experimental conditions. *Am. J. Physiol.* 169: 40, 1952.
5. ANKENEY, J. L., A. P. FISHMAN, AND H. W. FRITTS, JR. An analysis of normal and abnormal left atrial pressure pulse in man. *Circulation Res.* 4: 95, 1956.
6. ARAUJO, J. AND D. S. LUKAS. Interrelationships among pulmonary "capillary" pressure, blood flow and valve size in mitral stenosis. The limited regulatory effects of the pulmonary vascular resistance. *J. Clin. Invest.* 31: 1082, 1952.
7. ARVIDSSON, H. Angiocardiographic observations in mitral disease. *Acta radiol.* Suppl. 158, 1958.
8. BAJEC, D. F., N. C. BIRKHEAD, S. A. CARTER, AND E. H. WOOD. Localization and estimation of severity of regurgitant flow at the pulmonary and tricuspid valves. *Proc. Staff. Meet. Mayo Clin.* 33: 459, 1958.
9. BALL, J. D., H. KOPELMAN, AND A. C. WITHAM. Circulatory changes in mitral stenosis at rest and on exercise. *Brit. Heart J.* 14: 363, 1952.
10. BARGER, A. C., F. P. MULDOWNEY, AND M. R. LIEBOWITZ. Role of the kidney in the pathogenesis of congestive heart failure. *Circulation* 20: 273, 1959.
11. BARGER, A. C., B. B. ROE, AND G. S. RICHARDSON. Relation of valvular lesions and of exercise to auricular pressure, work tolerance and to development of chronic, congestive failure in dogs. *Am. J. Physiol.* 169: 384, 1952.
12. BARGER, A. C., R. S. ROSS, AND H. L. PRICE. Reduced sodium excretion in dogs with mild valvular lesions of the heart and in dogs with congestive failure. *Am. J. Physiol.* 180: 249, 1955.
13. BAYLISS, R. I. S., N. J. ETHERRIDGE, AND A. L. HYMAN. Pulmonary hypertension in mitral stenosis. *Lancet* 259: 899, 1950.
14. BECKER, D. L., H. B. BURCHELL, AND J. E. EDWARDS. Pathology of the pulmonary vascular tree. II. The occurrence in mitral insufficiency of occlusive pulmonary vascular lesions. *Circulation* 3: 230, 1951.
15. BERGLUND, E. The function of the ventricles of the heart. Studies on the relation between diastolic filling and ventricular work in the anesthetized dog. *Acta Physiol. Scandinav.* Suppl. 119: 1, 1955.
16. BJÖRK, V. O. Direct pressure measurement in the left atrium, the left ventricle and the aorta. *Acta chir. Scandinav.*, 107: fasc. 5, 1954.
17. BJÖRK, V. O., W. S. BLAKEMORE, AND G. MALMSTRÖM. Left ventricular pressure measurement in man. A new method. *Am. Heart J.* 48: 197, 1954.
18. BJÖRK, V. O. AND H. LODIN. Left heart catheterization with selective left atrial and ventricular angiocardiography in the diagnosis of mitral and aortic valvular disease. *Progr. Cardiovasc. Dis.* 2: 116, 1959.
19. BJÖRK, V. O. AND G. MALMSTRÖM. Left heart catheterization. *Circulation Res.* 2: 424, 1954.
20. BJÖRK, V. O. AND G. MALSTRÖM. The diastolic pressure gradient between the left atrium and the left ventricle in cases of mitral stenosis. *Am. Heart J.* 58: 486, 1959.
21. BJÖRK, V. O., G. MALMSTRÖM, AND L. G. UGGLA. Left auricular pressure measurements in man. *Ann. Surg.* 138: 718, 1953.
22. BLAKEMORE, W. S., T. G. SCHNABEL, JR., P. T. KUO, H. L. CONN, JR., S. B. LANGFELD, D. F. HEIMAN, AND H. WOSKE. Diagnostic and physiologic measurements using left heart catheterization. *J. Thoracic Surg.* 34: 436, 1957.
23. BLOOMFIELD, R., H. LAUSON, A. COURNAND, E. S. BREED, AND D. W. RICHARDS. Recording of right heart pressures in normal subjects and in patients with chronic pulmonary disease and various type of cardio-circulatory diseases. *J. Clin. Invest.* 25: 639, 1946.
24. BORDEN, C. W., R. V. EBERT, R. H. WILSON, AND H. S. WELLS. Studies of the pulmonary circulation. II. The circulation time from the pulmonary artery to the femoral artery and the quantity of blood in the lungs in patients with mitral stenosis and in patients with left ventricular failure. *J. Clin. Invest.* 28: 1138, 1949.
25. BORST, H. G., M. MCGREGOR, J. L. WHITTENBERGER, AND E. BERGLUND. Influence of pulmonary arterial and left atrial pressures on pulmonary vascular resistance. *Circulation Res.* 4: 393, 1956.

26. Braunwald, E., H. L. Moscovitz, S. S. Amran, R. P. Ladder, S. O. Sapins, A. Himmelstein, M. M. Ravitch, and A. J. Gordon. The hemodynamics of the left side of the heart as studied by simultaneous left atrial, left ventricular, and aortic pressures; particular reference to mitral stenosis. *Circulation* 12: 69, 1955.
27. Braunwald, E., S. J. Sarnoff, and W. N. Stainsby. Determinants of duration and mean rate of ventricular ejection. *Circulation Res.* 6: 319, 1958.
28. Braunwald, E., H. L. Tannenbaum, and A. G. Morrow. A method for the detection and estimation of aortic regurgitant flow in man. *Circulation* 17: 505, 1958.
29. Braunwald, E., G. H. Welch, Jr., and S. J. Sarnoff. Hemodynamic effect of quantitatively varied experimental mitral regurgitation. *Circulation Res.* 5: 539, 1957.
30. Braunwald, E., G. H. Welch, Jr., and A. G. Morrow. The effects of acutely increased systemic resistance on the left atrial pressure pulse. A method for the clinical detection of mitral insufficiency. *J. Clin. Invest.* 37: 35, 1958.
31. Burger, H. C., A. G. W. van Brummelen, and F. J. Dannenburg. Theory and experiments on schematized models of stenosis. *Circulation Res.* 4: 425, 1956.
32. Clowes, G. H. A., D. B. Hackel, R. P. Mueller, and D. G. Gillespie. Relationship of pulmonary functional and pathological changes in mitral stenosis. *A. M. A. Arch. Surg.* 67: 244, 1953.
33. Conn, H. L., Jr., and D. F. Heiman. Studies on mixing volumes in the central circulation of man and dog. *Clin. Research Proc.* 4: 99, 1956.
34. Conn, H. L., Jr., D. F. Heiman, W. S. Blakemore, P. T. Kuo, and S. B. Langfeld. Radiopotassium dilution studies from the "left" circulation in patients with rheumatic valvular disease. *J. Clin. Invest.* 35: 697, 1956.
35. Conn, H. L., Jr., D. F. Heiman, W. S. Blakemore, P. T. Kuo, and S. B. Langfeld. "Left heart" radiopotassium dilution curves in patients with rheumatic mitral valvular disease. *Circulation* 15: 532, 1957.
36. Conn, H. L., Jr., D. F. Heiman, J. C. Wood, B. Jumbala, and W. S. Blakemore. Study of mitral regurgitant blood flow in subjects with normal and deformed mitral valves. *Clin. Research Proc.* 5: 166, 1957.
37. Connolly, D. C., R. G. Tompkins, R. Lev, J. W. Kirklin, and E. H. Wood. Pulmonary-artery wedge pressures in mitral valve disease; relationship to left atrial pressure. *Proc. Staff. Meet. Mayo Clin.* 28: 72, 1953.
38. Connolly, D. C. and E. H. Wood. Hemodynamic data during rest and exercise in patients with mitral valve disease in relation to the differentiation of stenosis and insufficiency from the pulmonary artery wedge pressure pulse. *J. Lab. & Clin. Med.* 49: 526, 1957.
39. Cooper, T., E. Braunwald, and A. G. Morrow. Pulsus alternans in aortic stenosis. *Circulation* 18: 64, 1958.
40. Cournand, A. Some aspects of the pulmonary circulation in normal man and in chronic cardiopulmonary diseases. *Circulation* 2: 641, 1950.
41. Cournand, A., and E. Ranges. Catheterization of right auricle in man. *Proc. Soc. Exper. Biol. & Med.* 46: 462, 1941.
42. Dahlbäck, O. and S. Radner. Suprasternal pressure curves in combined aortic and mitral valvular disease. *Acta chir. scandinav.* 109: fasc. 5, 1955.
43. Dávila, J. C. Hemodynamics of mitral insufficiency. Observations from clinical and experimental surgery. *Am. J. Cardiol.* 2: 135, 1958.
44. Davis, J. O., M. J. Goodkind, and W. C. Bale, Jr Functional changes during high output failure produced by daily hemorrhage in dogs with pulmonic stenosis. *Circulation Res.* 5: 388, 1957.
45. Davis, J. O., R. E. Hyatt, and D. S. Howell. Right-sided congestive heart failure in dogs produced by controlled progressive constriction of the pulmonary artery. *Circulation Res.* 3: 252, 1955.
46. Desbaillets, P., B. Baudraz, R. O. West, and J. L. Rivier. La morphologie de la courbe de pression "capillaire pulmonaire." *Cardiologia* 25: 164, 1954.
47. Dexter, L., C. S. Burwell, F. W. Haynes, and R. E. Seibel. Oxygen content of pulmonary "capillary" blood in unanesthetized human beings. *J. Clin. Invest.* 25: 913, 1946.
48. Dexter, L., J. W. Dow, F. W. Haynes, J. L. Whittenberger, B. G. Ferris, W. T. Goodale, and H. K. Hellems. Studies of the pulmonary circulation in man at rest. Normal variations and the interrelations between increased pulmonary blood flow, elevated pulmonary arterial pressure, and high pulmonary "capillary" pressure. *J. Clin. Invest.* 29: 602, 1950.
49. Dexter, L., P. Novack, R. C. Schlant, A. O. Phinney, Jr., and F. W. Haynes. Mitral insufficiency. *Tr. A. Am. Physicians* 70: 262, 1957.
50. Donald, K. W. Exercise and heart disease. *Brit. Med. J.* 1: 985, 1959.
51. Dow, J. W. and R. Gorlin. Pulmonary "capillary" pressure as an index of left atrial mean pressure in dogs. *Fed. Proc.* 9: 33, 1950.
52. Dow, J. W., H. D. Levine, M. Elkin, F. W. Haynes, H. K. Hellems, J. L. Whittenberger, B. G. Ferris, W. T. Goodale, W. P. Harvey, E. C. Eppinger, and L. Dexter. Studies of congenital heart disease. IV. Uncomplicated pulmonic stenosis. *Circulation* 1: 267, 1950.
53. Draper, A., R. Heimbecker, R. Daley, D. Carroll, G. Mudd, R. Wells, W. Falholt, E. C. Andrus, and R. J. Bing. Physiologic studies in mitral valvular disease. *Circulation* 3: 531, 1951.
54. Edwards, J. E., and H. B. Burchell. Pathologic anatomy of mitral insufficiency. *Proc. Staff. Meet. Mayo Clin.* 33: 497, 1958.
55. Edwards, J. E., R. G. Tompkins, R. T. Hood, J. W. Kirklin, and H. B. Burchell. Biopsy of the lung and cardiac catheterization studies in patients treated surgically for mitral stenosis. *J. Lab. & Clin. Med.* 40: 795, 1952.
56. Edwards, W. D. The effects of lung inflation and epinephrine on pulmonary vascular resistance. *Am. J. Physiol.* 167: 756, 1951.
57. Eich, R. H., I. Staib, and D. Emerson. An experimental evaluation of the indicator dilution technique for the measurements of mitral regurgitation. *J. Clin. Invest.* 38: 2035, 1959.
58. Eliasch, H. The pulmonary circulation at rest and on effort in mitral stenosis. *Scandinav. J. Clin. & Lab. Invest.* 4: Suppl. 4, 1952.
59. Ellis, L. B., R. A. Blomfield, G. K. Grehan, D. J. Greenberg, H. N. Hultgren, H. Krans, G. Maresh,

J. G. Mebane, P. H. Pfeiffer, L. A. Selverstone, and J. A. Taylor. Studies in mitral stenosis. *A. M. A. Arch. Int. Med.* 88: 515, 1951.
60. Ellison, R. G., W. J. Brown, Jr., E. E. Hague, and W. F. Hamilton. Physiologic observations in experimental pulmonary insufficiency. *J. Thoracic Surg.* 30: 633, 1955.
61. Elkin, M., M. C. Sosman, D. W. Harken, and L. Dexter. Systolic expansion of the left auricle in mitral regurgitation. *New England J. Med.* 246: 958, 1952.
62. Emanuel, R. W., W. W. Lacy, and E. V. Newman. An improved method for the calibration of continuously recorded dye dilution curves. *Circulation Res.* 5: 527, 1957.
63. Emanuel, R. W., W. W. Lacy, and E. V. Newman. Relative effects of heart chambers, lungs, and mitral insufficiency on the shape of indicator dilution curves. *Circulation Res.* 7: 141, 1959.
64. Engell, H. C. and V. Eskelund. Histological pulmonary changes present at the time of mitral valvulotomy. *Acta Chir. Scandinav.* 106: 272, 1953.
65. Enticknap, J. B. Lung biopsy in mitral stenosis. *J. Clin. Path.* 6: 84, 1953.
66. Epps, R. G. and R. Adler. Left atrial and pulmonary capillary venous pressure in mitral stenosis. *Brit. Heart J.* 15: 298, 1953.
67. Euler, U. S. von, and G. Liljestrand. Observations on the pulmonary arterial blood pressure in the cat. *Acta physiol. Scandinav.* 12: 301 1946.
68. Feil, H. S. and M. D. D. Gilder. Pulse in aortic disease as felt and graphically inscribed. *Heart* 8: 4, 1921.
69. Feil, H. S. and L. N. Katz. The transformation of the central into the peripheral pulse in patients with aortic stenosis. *Am. Heart J.* 2: 12, 1926.
70. Ferrer, M. I., R. J. Harvey, R. T. Cathcart, A. Cournand, and D. W. Richards. Hemodynamic studies in rheumatic heart disease. *Circulation* 6: 688, 1952.
71. Ferrer, M. I., R. M. Harvey, M. Kuschner, D. W. Richards, and A. Cournand. Hemodynamic studies in tricuspid stenosis of rheumatic origin. *Circulation Res.* 1: 49, 1950.
72. Ferrer, M. I., R. N. Harvey, A. Cournand, and D. W. Richards, Jr. Cardiocirculatory studies in pulsus alternans of the systemic and pulmonary circulation. *Circulation* 14: 163, 1956.
73. Fineberg, M. H. and C. J. Wiggers. Compensation and failure of the right ventricle. *Am. Heart J.* 11: 255, 1936.
74. Fleischner, F. G., W. H. Abelmann, and R. Buka. The value of the atrial electrokymogram in the diagnosis of mitral regurgitation. *Circulation* 10: 71, 1954.
75. Folkow, B. Structural, myogenic, humoral and nervous factors controlling peripheral resistance. In: *Hypotensive Drugs;* A Wellcome Foundation Symposium. London: Pergamon Press, 1956.
76. Folkow, B. and B. Öberg. The effect of functionally induced changes of wall/lumen ratio on the vasoconstrictor response to standard amounts of vasoactive agents. *Acta physiol. Scandinav.* 47: 131, 1959.
77. Fowler, N. O., R. N. Westcott, V. D. Hauenstein, R. C. Scott, and J. McGuire. Observation on autonomic participation in pulmonary arteriolar resistance in man. *J. Clin. Invest.* 29: 1387, 1950.
78. Fowler, N. O., R. N. Westcott, R. C. Scott, and J. McGuire. The effect of nor-epinephrine upon pulmonary arteriolar resistance in man. *J. Clin. Invest.* 30: 517, 1951.
79. Fowler, N. O., E. P. Mannix, and W. Noble. Some effects of partial pulmonary valvectomy. *Circulation Res.* 4: 8, 1956.
80. Friedman, B., W. M. Daily, and R. H. Wilson. Studies on mitral valve function. Effect of acute hypervolemia, premature beats and other arrhythmias. *Circulation Res.* 4: 33, 1956.
81. Goldberg, H., A. A. Bakst, and C. P. Bailey. The dynamics of aortic valvular disease. *Am. Heart J.* 47: 527, 1954.
82. Goodale, F. Jr., G. Sanchez, A. L. Friedlich, J. G. Scannell, and G. S. Myers. Correlation of pulmonary arteriolar resistance with pulmonary vascular changes in patients with mitral stenosis before and after valvulotomy. *New England J. Med.* 252: 979, 1955.
83. Gorlin, R. Calculation of orifice areas within the cardiovascular system. *Methods in Med. Research,* 7: 102, 1958.
84. Gorlin, R. and S. G. Gorlin. Hydraulic formula for calculation of the area of the stenotic mitral valve, other cardiac valves, and central circulatory shunts. I. *Am. Heart J.* 41: 1, 1951.
85. Gorlin, R., F. W. Haynes, W. T. Goodale, C. G. Sawyer, J. W. Dow, and L. Dexter. Studies of the circulatory dynamics in mitral stenosis. II. Altered dynamics at rest. *Am. Heart J.* 41: 30, 1957.
86. Gorlin, R., B. M. Lewis, F. W. Haynes, and L. Dexter. Studies of the circulatory dynamics at rest in mitral valvular regurgitation with and without stenosis. *Am. Heart J.* 43: 357, 1952.
87. Gorlin, R., B. M. Lewis, F. W. Haynes, R. J. Spiegel, and L. Dexter. Factors regulating pulmonary "capillary" pressure in mitral stenosis. IV. *Am. Heart J.* 41: 834, 1951.
88. Gorlin, R., M. B. Matthews, I. K. R. McMillan, R. Daley, and W. E. Medd. Physiological and clinical observations in aortic valvular disease. *Bull. New England Med. Centr.* 16: 13, 1954.
89. Gorlin, R., I. K. R. McMillan, W. E. Medd, M. B. Matthews, and R. Daley. Dynamics of the circulation in aortic valvular disease. *Am. J. Med.* 18: 855, 1955.
90. Gorlin, R., C. G. Sawyer, F. W. Haynes, W. T. Goodale, and L. Dexter. Studies of the circulatory dynamics in mitral stenosis. III. Effects of exercise on circulatory dynamics in mitral stenosis. *Am. Heart J.* 41: 192, 1951.
91. Grant, R. P., A. G. Morrow, and E. Sharpe. Hemodynamic and volumetric changes in mitral valve disease in man. *Circulation* 14: 944, 1956.
92. Greene, D. G., E. de F. Baldwin, J. Baldwin, A. Himmelstein, C. E. Roh, and A. Cournand. Pure congenital pulmonary stenosis and idiopathic congenital dilatation of the pulmonary artery. *Am. J. Med.* 6: 24, 1949.
93. Grishman, A., I. G. Kroop, M. Steinberg, and S. Dack. Presystolic pulsations of the liver in the absence of tricuspid disease. *Am. Heart J.* 40: 731, 1950.
94. Guidry, L. D., E. H. Wood, and H. B. Burchell. Application of a method for detecting and estimating severity of aortic regurgitation alone or in association

with mitral regurgitation. *Proc. Staff. Meet. Mayo Clin.* 33: 596, 1958.

95. Hannon, D. W., A. Ferrin, F. Haddy, J. L. Sprafka, and I. D. Baronofsky. Pulmonary artery changes in mitral stenosis. *Surg. Forum* 7: 240, 1957.
96. Hamilton, W. F., J. W. Moore, J. M. Kinsman, and R. Spurling. Studies on circulation. IV. Further analysis of the injection method, and of changes in hemodynamics under physiological and pathological conditions. *Am. J. Physiol.* 99: 534, 1932.
97. Hamilton, W. F., R. L. Riley, A. M. Attyak, A. Cournand, D. M. Fowell, A Himmelstein, R. P. Noble, J. W. Remington, D. W. Richards, N. C. Wheeler, and A. C. Witham. Comparison of the Fick and dye dilution methods of measuring the cardiac output in man. *Am. J. Physiol.* 153: 309, 1948.
98. Haring, O. M., C. K. Lui, and H. D. Trace. The left atrial pressure in experimental mitral valve lesions. *Circulation Res.* 4: 381, 1956.
99. Harken, D. E. Mitral regurgitation. A group of surgical problems. *Am. J. Cardiol.* 2: 263, 1958.
100. Hayden, D. T., W. Garrett, and P. Jordan. Evaluation of mitral insufficiency in dogs by electronic analog simulation of radioisotope data. *Circulation Res.* 6: 77, 1958.
101. Heiman, D. F., W. S. Blakemore, H L. Conn, Jr., B. Jumbala, and H. M. Woske. Direct estimation of mitral regurgitant blood flow from "left-heart" isotope dilution curves. *Clin. Research Proc.* 6: 20, 1958.
102. Hellems, H. K., F. W. Haynes, and L. Dexter. Pulmonary "capillary" pressure in man. *J. Appl. Physiol.* 2: 24, 1949.
103. Henry, E. W. The small pulmonary vessels in mitral stenosis. *Brit. Heart J.* 14: 406, 1952.
104. Hoffman, J. I. E. and C. G. Rowe. Some factors affecting indicator dilution curves in the presence and absence of valvular incompetence. *J. Clin. Invest.* 38: 138, 1959.
105. Horvath, S. M. and D. M. MacCanon. Variations in pulmonary vascular pressures. *J. Thoracic Surg.* 27: 204, 1954.
106. Huckabee, W. E. The role of anaerobic metabolism in the performance of mild muscular work. II. The effect of asymptomatic heart disease. *J. Clin. Invest.* 37: 1593, 1958.
107. Huckabee, W. E. and W. E. Judson. The role of anaerobic metabolism in the performance of mild muscular work. I. Relationship to oxygen consumption and cardiac output and the effect of congestive heart failure. *J. Clin. Invest.* 37: 1577, 1958.
108. Janowski, W. Sur la courbe de l'oreillette gauche du coeur, son explication et sa valeur diagnostique. *Rév. Méd.* 30: 211, 1910.
109. Judson, W. E., W. Hollander, J. D. Hatcher, and M. H. Halperin. The effects of exercise on cardiovascular and renal function in cardiac patients with and without heart failure. *J. Clin. Invest.* 34: 1546, 1955.
110. Katz, L. N., E. P. Ralli, and S. Cheer. The cardiodynamic changes in the aorta and left ventricle due to stenosis of aorta. *J. Clin. Invest.* 5: 205, 1928.
111. Katz, L. N. and M. L. Siegel. The cardiodynamic effects of acute experimental stenosis. *Am. Heart J.* 6: 672, 1931.
112. Kay, J. H. and V. Thomas. Experimental production of pulmonary insufficiency. *A.M.A. Arch. Surg.* 69: 646, 1954.
113. Kay, J. H. and V. Thomas. Experimental production of pulmonary stenosis. *A.M.A. Arch. Surg.* 69: 661, 1954.
114. Kent, E. M., W. B. Ford, D. L. Fisher, and T. B. Child. The estimation of the severity of mitral regurgitation. *Ann. Surg.* 141: 47, 1955.
115. Keys, A., H. L. Friedell, L. H. Garland, and M. F. Madrazo. The valvular efficiency in mitral and aortic insufficiency. *Am. J. Physiol.* 129: 397, 1940.
116. Keys, J. R., H. J. C. Swan, and E. H. Wood. Dye-dilution curves from systemic arteries and left atrium of patients with valvular heart disease. *Proc. Staff. Meet. Mayo Clin.* 31: 138, 1956.
117. Kinsman, J. M., J. W. Moore, and W. F. Hamilton. Studies on the circulation. I. Injection method: Physical and mathematical considerations. *Am. J. Physiol.* 89: 322, 1929.
118. Kohout, F. W. and L. N. Katz. Pulmonic valvular regurgitation. *Am. Heart J.* 49: 637, 1955.
119. Kopelman, H. and G. De J. Lee. The intrathoracic blood volume in mitral stenosis and left ventricular failure. *Clin. Sc.* 10: 383, 1951.
120. Korner, P. I. and J. P. Shillingford. The quantitative estimation of valvular incompetency by dye dilution curves. *Clin. Sc.* 14: 553, 1955.
121. Korner, P. I. and J. P. Shillingford. Further observations on the estimation of valvular incompetence from indicator-dilution curves. *Clin. Sc.* 15: 417, 1956.
122. Korner, P. I and J. P. Shillingford. Tricuspid incompetence and right ventricular output in congestive heart failure. *Brit. Heart J.* 19: 1, 1957.
123. Lacy, W. W., R. W. Emanuel, and E. J. Newman. Effect of the sampling system on the shape of indicator-dilution curves. *Circulation Res.* 5: 568, 1957.
124. Lacy, W. W., W. H. Goodson, W. G. Wheeler, and E. V. Newman. Theoretical and practical requirements for the valid measurements by indicator-dilution of regurgitant flow across incompetent valves. *Circulation Res.* 7: 454, 1959.
125. Lagerlöf, H. and L. Werkö. The auricular pressure pulse. *Cardiologia* 13: 241, 1948.
126. Lagerlöf, H. and L. Werkö. Studies on the circulation of blood in man. VI. The pulmonary capillary venous pressure pulse in man. *Scandinav. J. Clin. Lab. Invest.* 1: 147, 1949.
127. Lagerlöf, H., L. Werkö, H. Bucht, and A. Holmgren. Separate determination of the blood volume of the right and left heart and the lungs in man with the aid of the dye injection method. *Scandinav. J. Clin. & Lab. Invest.* 1: 114, 1949.
128. Lammerant, J. *Le Volume Sanguin des Poumons chez l'Homme.* Brussels, Arscia; 1957.
129. Lange, R. L. and H H Hecht. Quantitation of valvular regurgitation from multiple indicator-dilution curves. *Circulation* 18: 623, 1958.
130. Lange, R., C. Smith, and H. H. Hecht. Skewing of indicator-dilution curves in the arterial system. *Fed. Proc.* 18: 86, 1959.
131. Larrabee, W. F., R. L. Parker, and J. E. Edwards. Pathology of intrapulmonary arteries and arterioles in mitral stenosis. *Proc. Staff. Meet. Mayo Clin.* 24: 316, 1949.

132. Lasser, R. P. and L. Loewe. Cardiac and pulmonary artery pressure pulses in experimental mitral stenosis. *Am. Heart J.* 48: 801, 1954.
133. Lendrum, B. L. and A. B. Shaffer. Isolated congenital pulmonic valvular regurgitation. *Am. Heart J.* 57: 298, 1959.
134. Lenègre, J., L. Scebat, S. H. Besson, F. Benchemoul, and J. Damien. Étude de la pression capillaire pulmonaire dans différents types de cardiopathies. *Arch. mal. coeur.* 46: 1, 1953.
135. Levinson, D. C., M. Wilburne, J. P. Meehan, Jr., and H. Shubin. Evidence for retrograde transpulmonary propagation of the V (or regurgitant) wave in mitral insufficiency. *Am. J. Cardiol.* 2: 159, 1958.
136. Lewis, B. M., R. Gorlin, H. E. J. Houssay, F. W. Haynes, and L. Dexter. Clinical and physiological correlation in patients with mitral stenosis. *Am. Heart J.* 43: 2, 1952.
137. Levison, W. H. and H. Sherman. The measurements of mitral regurgitation by indicator-dilution techniques. Massachusetts Institute of Technology Report 20, 1959.
138. Likoff, W., G. D. Geckeler, and J. E. Gregory. Functional mitral stenosis produced by an intramitral tumour. *Am. Heart J.* 47: 619, 1954.
139. Lottenbach, C. and J. P. Shillingford. Functional tricuspid incompetence in relation to the venous pressure. *Brit. Heart J.* 19: 395, 1957.
140. Lukas, D. S. and C. T. Dotter. Modifications of the pulmonary circulation in mitral stenosis. *Am. J. Med.* 12: 639, 1952.
141. Marshall, H. W. and E. H. Wood. Hemodynamic considerations in mitral regurgitation. *Proc. Staff. Meet. Mayo Clin.* 33: 517, 1958.
142. Marshall, H. W., E. Woodward, Jr., and E. H. Wood. Hemodynamic methods for differentiation of mitral stenosis and regurgitation. *Am. J. Cardiol.* 2: 24, 1958.
143. McAfee, J. G., T. F. Hilbish, and K. R. Stewart. Angiocardiography in the preoperative diagnosis of mitral stenosis and insufficiency. *Radiology* 67: 321, 1956.
144. MacCallum, W. G. and R. D. McClure. On the mechanical effects of experimental mitral stenosis and insufficiency. *Bull. Johns Hopkins Hosp.* 17: 260, 1906.
145. McClure, J. A., W. W. Lacy, P. Latimer, and E. V. Newman. Indicator dilution in an atrioventricular system with competent or incompetent valves. *Circulation Res.* 7: 794, 1959.
146. McCord, M. C. and S. G. Blount, Jr. The hemodynamic pattern in tricuspid valve disease. *Am. Heart J.* 44: 671, 1952.
147. McCord, M. C., S. Komesu, and S. G. Blount, Jr. The characteristics of the right atrial pressure wave associated with right ventricular hypertrophy. *Am. Heart J.* 45: 706, 1953.
148. McCord, M. C., H. Swan, and S. G. Blount, Jr. Tricuspid stenosis. Clinical and physiologic evaluation. *Am. Heart J.* 48: 405, 1954.
149. McDonald, L., J. B. Dealy, Jr., M. Rabinowitz, and L. Dexter. Clinical, physiological and pathological findings in mitral stenosis and regurgitation. *Medicine* 36: 237, 1957.
150. McMichael, J. and J. P. Shillingford. The role of valvular incompetence in heart failure. *Brit. Med. J.* 1: 537, 1957.
151. Morrow, A. G., E. H. Sharp, and E. Braunwald. Congenital aortic stenosis. *Circulation* 18: 1091, 1958.
152. Moscovitz, H. L., A. J. Gordon, E. Braunwald, S. S. Amram, S. O. Sapin, R. P. Lasser, A. Himmelstein, and M. M. Ravitch. The use of simultaneous left heart pressure pulse measurements in evaluating the effects of mitral valve surgery. *Am. J. Med.* 18: 406, 1955.
153. Moscovitz, H. L. and R. J. Wilder. The pressure events of the cardiac cycle in the dog: aortic valve lesions. *Am. Heart J.* 54: 572, 1957.
154. Novack, P. and R. C. Schlant. Korner-Shillingford method for estimating regurgitant flow. *Methods in Med. Research* 7: 76, 1960.
155. Neustadt, J. E. and A. B. Shaffer. Diagnostic valve of the left atrial pressure pulse in mitral valvular disease. *Am. Heart J.* 58: 675, 1959.
156. Olesen, K. H. and J. Fabricius. Pulmonic valvular regurgitation during twenty-seven years after gonorrhoeal endocarditis. *Am. Heart J.* 52: 791, 1956.
157. Opdyke, D. F., J. Duomarco, W. H. Dillon, H. Schreiber, R. C. Little, and R. D. Seely. Studies of right and left atrial pressure pulses under normal and experimentally altered conditions. *Am. J. Physiol.* 154: 258, 1948.
158. Owen, S. G. and P. Wood. A new method of determining the degree or absence of mitral obstruction. *Brit. Heart J.* 17: 41, 1955.
159. Parker, F. and S. Weiss. The nature and significance of the structural changes in the lungs in mitral stenosis. *Am. J. Pathol.* 12: 573, 1936.
160. Pedersen, A. *The Venous Pressure in the Pulmonary Circulation.* (Translated from Danish by Axel Anderson.) Copenhagen: Afhandling, 1956. 286 p.
161. Pearce, M. L., W. P. McKeever, P. Dow, and E. V. Newman. The influence of injection site upon the form of dye dilution curves. *Circulation Res.* 1: 112, 1953.
162. Porjé, I. G., J. Philipsson, and P. Ödman. Acquired aortic stenosis. *Cardiologia* 31: 508, 1957.
163. Porjé, I. G. and B. Rudewald. Studies on a new theory of determinations of some fundamental hemodynamic data in a circulation model, in normal persons and in aortic valvular diseases. *Opuscula Medica* 2: 10, 1957.
164. Raber, G. and H. Goldberg. Left ventricular, central aortic and peripheral pressure pulses in aortic stenosis. *Am. J. Cardiol.* 1: 572, 1958.
165. Radner, S. Suprasternal puncture of the left atrium for flow studies. *Acta Med. Scandinav.* 148: 57, 1954.
166. Radner, S. Suprasternal puncture technique for left heart flow studies. *Acta chir. scandinav.* 108: fasc. 1, 1954.
167. Radner, S. Suprasternal pressure curves in mitral insufficiency *Acta med. scandinav.* 152, fasc. 1, 1955.
168. Regan, T. J., V. De Fazio, K. Binak, and H. K. Hellems. Norepinephrine induced pulmonary congestion in patients with aortic valve regurgitation. *J. Clin. Invest.* 38: 1564, 1959.
169. Richards, D. W. Jr., A. Cournand, R. C. Darling, W. H. Gillespie, and E. De F. Baldwin. Pressure of blood in the right auricle, in animals and in man: under normal conditions and in right heart failure. *Am. J. Physiol.* 136: 115, 1942.

170. RODBARD, S. AND F. WILLIAMS. The dynamics of mitral insufficiency. *Am. Heart J.* 48: 521, 1954.
171. RODRIGO, F. A. AND H. SNELLEN. Estimation of valve area and valvular resistance. *Am. Heart J.* 45: 1, 1953.
172. RUDHE, U. Electrokymography. *Acta Radiol.* Suppl. 134, 1956.
173. ROSS, J. R. JR., E. BRAUNWALD, AND A. G. MORROW. Clinical and hemodynamic studies in pure mitral insufficiency. *Am. J. Cardiol* 1: 11, 1958.
174. SANCETTA, S. M. AND J. KLEINERMAN. Effect of mild steady state exercise on total pulmonary resistance of normal subjects and those with isolated aortic valvular lesions. *Am. Heart J.* 53: 404, 1957.
175. SARNOFF, S. J. AND E. BERGLUND. Ventricular function. I. Starling's law of the heart studied by means of simultaneous right and left ventricular curves in the dog. *Circulation* 9: 706, 1954.
176. SARNOFF, S. J., E. BRAUNWALD, G. H. WELCH, R. B. CASE, W. N. STAINSBY, AND R. MARCUS. Hemodynamic determinations of oxygen consumption of the heart with special reference to the tension-time index. *Am. J. Physiol.* 192: 148, 1958.
177. SCHNABEL, T. G. JR., H. ELIASCH, B. THOMASSON, AND L. WERKÖ. The effect of experimentally induced hypervolemia of cardiac function in normal subjects and patients with mitral stenosis. *J. Clin. Invest.* 38: 117, 1959.
178. SCHWARZ, E. Zur Dynamik der Mitralinsuffizienz. *Wien klin. Wchnschr.* 18: 632, 1905.
179. SELZER, A. AND W. H CARNES. The role of pulmonary stenosis in the production of chronic cyanosis. *Am. Heart J.* 45: 382, 1953.
180. SELZER, A., F. M. WILLETT, D. J. MCCAUGHEY, AND T. V. FEICHTMEISTER. Use of cardiac catheterization in acquired heart disease. *New England J. Med.* 257: 66, 1957.
181. SHAW, M. M., W. E. ADAMS, R. A. RASMUSSON, L. S. HERDINA, AND H. G. ARONSON. Experimental production of insufficiency and stenosis of the heart valves in dogs. *J. Thoracic Surg.* 12: 322, 1943.
182. SHILLINGFORD, J. P. Simple method for estimating mitral regurgitation by dye dilution curves. *Brit. Heart J.* 20: 229, 1958.
183. SHILLINGFORD, J. P. AND M. ZOOB. Dye dilution curves in the clinical assessment of mitral valvular diseases. *Brit. Heart J.* 19: 589, 1959.
184. SICOT, J. R., F. JOLY, AND J. CARLOTTI. Courbes de pressions auriculaires. *Presse méd.* 31: 558, 1950.
185. SILBER, E. N., O. PREC, N. GROSSMANN, AND L. N. KATZ. Dynamics of isolated pulmonary stenosis. *Am. J. Med.* 10: 21, 1951.
186. SMITH, R. C., H. B. BURCHELL, AND J. E. EDWARDS. Pathology of the pulmonary vascular tree. IV. Structural changes in the pulmonary vessels in chronic left ventricular failure. *Circulation* 10: 801, 1954.
187. SOLOFF, L. A., J. ZATUCHNI, H. M. STAUFFER, AND E. W. KELLY. Angiocardiographic observations of intracardiac flow in the normal and in mitral stenosis. *Circulation* 13: 334, 1956.
188. SOULIÉ, P., Y. BOUVRAIN, AND J. DIMATTEO. Les tricuspidités et l'insuffisance tricuspidienne fonctionelle au cours du retrecissement mitral. *Bull. Soc. Méd. Hosp.* Paris 68: 332, 1952.
189. SOULIÉ, P., J. CARLOTTI, J. SICOT, AND F. JOLY. Les pressions capillaires pulmonaires chez l'homme. *Bull. Soc. Méd. Hosp.* Paris 67: 293, 1951.
190. STEWART, C. N. The pulmonary circulation time, the quantity of blood in the lungs and the output of the heart. *Am. J. Physiol.* 58: 20, 1921.
191. SÖDERHOLM, B. AND L. WERKÖ. Acetylcholine and the pulmonary circulation in mitral valvular disease. *Brit. Heart J.* 21: 1, 1959.
192. TAQUINI, A. C., R. J. DONALDSON, E. S. BALLINA, R. E. H. D'AITOLO, AND B. B. LOZADA. Physiologic studies in mitral stenosis. *Am. Heart J.* 45: 691, 1953.
193. URICCHIO, J. F., J. S. LEHMAN, W. LEMMON, R. BOYER, AND W. LIKOFF. Cardiac ventriculography in the selection of patients for mitral valve surgery. *Am. J. Cardiol.* 3: 22, 1959.
194. WARNER, H. R. AND A. F. TORONTO. Quantitation of backflow in patients with aortic insufficiency using an indicator technic. *Circulation Res.* 6: 29, 1958.
195. WÉGRIA, R., G. MUELHEIMS, J. R. GOLUB, R. JREISSATY, AND J. NAKANO. Effect of aortic insufficiency on arterial blood pressure, coronary blood flow and cardiac oxygen consumption. *J. Clin. Invest.* 37: 471, 1958.
196. WÉGRIA, R., G. MUELHEIMS, R. JREISSATY, AND J. NAKANO. Effect of acute mitral insufficiency of various degrees on mean arterial blood pressure, coronary blood flow, cardiac output and oxygen consumption. *Circulation Res.* 6: 301, 1958.
197. WELCH, G. H., JR., E. BRAUNWALD, AND S. J. SARNOFF. Hemodynamic effect of quantitatively varied experimental mitral regurgitation. *Circulation Res.* 5: 546, 1957.
198. WERKÖ, L., H. LAGERLÖF, H. BUCHT, B. WEHLE, AND A. HOLMGREN. Comparison of the Fick and Hamilton method in the determination of cardiac output in man. *Scandinav. J. Clin. & Lab. Invest.* 1: 109, 1949.
199. WERKÖ, L., E. VARNAUSKAS, H. ELIASCH, J. EK, H. BUCHT, B. THOMASSON, AND J. BERGSTRÖM. Studies on the renal circulation and renal function in mitral valvular disease. I. Effect of exercise. *Circulation* 9: 687, 1954.
200. WERKÖ, L., E. VARNAUSKAS, H. ELIASCH, H. LAGERLÖF, A. SENNING, AND B. THOMASSON. Further evidence that the pulmonary capillary venous pressure pulse in man reflects cyclic pressure changes in the left atrium. *Circulation Res.* 1: 337, 1953.
201. WERKÖ, L., E. VARNAUSKAS, H. ELIASCH, AND B. THOMASSON. The influence of the pulmonary arterial pressure on the pulmonary capillary venous pressure in man. *Circulation Res.* 1: 340, 1953.
202. WESTCOTT, R. N., N. O. FOWLER, R. C. SCOTT, V. D. HAUENSTEIN, AND J. MCGUIRE. Anoxia and human pulmonary vascular resistance. *J. Clin. Invest.* 30: 957, 1951.
203. WIGGERS, C. J. *Circulatory Dynamics.* New York: Grune & Stratton, 1952.
204. WIGGERS, C. J. AND H. FEIL. The cardiodynamics of mitral insufficiency. *Heart* 9: 149, 1922.
205. WILSON, R. H., W. T. MCKENNA, F. E. JOHNSON, N. K. JENSEN, W. F. MAZZITELLO, AND M. E. DEMPSEY. The significance of the pulmonary arterial wedge pressure. *J. Lab. & Clin. Med.* 42: 408, 1953.
206. WOLTER, H H., O. BAYER, F. LOOGEN, AND R. RIPPERT. Die sogenannte Pulmonalkapillar-druckkurve und ihre

Beziehung zur Druckkurve des rechten und linken Vornofs. *Cardiologia* 23: 319, 1953.

207. WOOD, E. H. AND E. WOODWARD, JR. A simple method for differentiating mitral regurgitation from mitral stenosis by means of indicator-dilution curves. *Proc. Staff. Meet. Mayo Clin.* 32: 536, 1957.
208. WOOD, P. An appreciation of mitral stenosis. *Brit. M. J.* 1: 1051, 1954.
209. WOOD, P. Aortic stenosis. *Am. J. Cardiol.* 1: 553, 1958.
210. WOODWARD, E., JR., H. B. BURCHELL, AND E. H. WOOD. Dilution curves associated with valvular regurgitation. *Proc. Staff. Meet. Mayo Clin.* 32: 518, 1957.
211. WOODWARD, E., JR., H. J. SWAN, AND E. H. WOOD. Evaluation of a method for detection of mitral regurgitation from indicator-dilution curves recorded from the left atrium. *Proc. Staff. Meet. Mayo Clin.* 32: 525, 1957.
212. YU, P. N., D. E. HARKEN, F. W. LOVEJOY, JR., R. E. NYE, JR., AND E. B. MAHONEY. Clinical and hemodynamic studies of tricuspid stenosis. *Circulation* 13: 680, 1956.
213. YU, P. N., F. W. LOVEJOY, JR., B. F. SCHREINER, R. H. LEAHY, C. A. STANFIELD, AND H. WALTHER. Direct left ventricular puncture in the evaluation of aortic and mitral stenosis. *Am. Heart J.* 55: 926, 1958.
214. YU, P. N., R. E. NYE, JR., F. W. LOVEJOY, JR., B. F. SCHREINER, AND B. J. B. YIM. Studies of pulmonary hypertension. IX. The effects of intravenous hexamethonium on pulmonary circulation in patients with mitral stenosis. *J. Clin. Invest.* 37: 194, 1958.
215. YU, P. N., J. H. SIMPSON, F. W. LOVEJOY, JR., H. A. JOOS, AND R. E. NYE, JR. Studies of pulmonary hypertension. IV. Pulmonary circulatory dynamics in patients with mitral stenosis at rest. *Am. Heart J.* 47: 330, 1954.
216. ZINSSER, H. F., JR. AND J. JOHNSON. Use of angiocardiography in selection of patients for mitral valve surgery. *Ann. Int. Med.* 39: 1200, 1953.

Technical aspects of the study of cardiovascular sound

VICTOR A. McKUSICK
SAMUEL A. TALBOT
GEORGE N. WEBB
EDWARD J. BATTERSBY

Department of Medicine, Johns Hopkins University School of Medicine, Baltimore, Maryland

CHAPTER CONTENTS

THE FIRST PHONOCARDIOGRAMS in anything approaching the modern sense were made by Einthoven and Geluk (1894) using Lippmann's capillary electrometer. Otto Frank of Munich (1904) devised the technique of direct phonocardiography, that is, recording of the precordial vibrations with optical amplification. The so-called Frank segment capsule was improved on and used by workers such as Wiggers, and Orias and Braun-Menéndez. The fragility of the capsule membranes and unsatisfactory frequency response characteristics led to the replacement of this technique by others. Einthoven (1907) applied the string galvanometer to phonocardiography. The tremendous range of intensities found in cardiovascular sound, far exceeding that of the electrocardiogram, led to frequent accidents with fracture or other damage of the string. The development of the vacuum tube for electronic amplification and of various galvanometers opened a new era of phonocardiography. The review of Rappaport & Sprague (14) in 1942 marked the end of earlier techniques in phonocardiography.

Concern with the frequency dimension of cardiovascular sound led to the use of microphones of differing frequency response and to multichannel recording with various filtration and amplification applied in each channel. A number of different systems have been suggested (e.g., Mannheimer, Leatham, Luisada, Maass, Bekkering, and others), each aiming to encompass the wide frequency-intensity range of cardiovascular sound and to permit analysis of faint components in the presence of intense ones. Satisfactory display of all frequencies in a single record was accomplished by spectral phonocardiography, an adaptation of the Bell Telephone Laboratories' method of sound spectrography. A development of the 1950's, spectral phonocardiography was a major departure from all previous phonocardiography which had been oscillographic in nature. Also a development of the 1950's was intracardiac phonocardiography, the recording of vibrations in the audible frequency range using miniature transducers introduced into the heart on the tip of catheters. The barium titanate catheter

microphone was an adaptation of transducers used in underwater detection of sound, in submarine warfare, for example. About 1951 Soulié's group in Paris, while working with a newly designed micromanometer of the inductance type for registration of intracardiac pressure, were impressed with its high-frequency response. Vibrations in the auditory range were recorded when frequencies below 20 cycles per sec were cut out.

Beginning with the carbon-granule microphone of Einthoven, phonocardiographers have used a variety of transducers. The crystal microphone was popular for many years. The capacitance, or condenser, microphone seems to have been first used in phonocardiography by Trendelenberg. Selection (1953) of a condenser microphone of improved design (Altec) for use in spectral phonocardiography has led to its wide use in phonocardiography generally (8).

THE NATURE OF THE PHENOMENON

Physiologic Considerations

Cardiovascular sounds tend to be divisible rather sharply into two major categories: *1*) transients, referred to as "heart sounds," and *2*) more prolonged noises, referred to as "murmurs," which may be partially or purely musical. (Musicality is a subjective quality which is said to be present when harmonic organization is demonstrated by the spectral phonocardiogram.)

The heart sounds are considered to be the expression of hydraulic pressure transients associated with abrupt deceleration, and in some instances perhaps acceleration, in blood flow. For example, the first and second heart sounds are mainly the result of valve closure and more specifically the result of abrupt deceleration of the local flow which is responsible for coaptation of the valve cusps.

Noisy murmurs are essentially the expression of turbulence of blood flow. The soft elements of the heart and vessel walls undoubtedly interplay, in a complex manner, with the hemodynamic phenomenon.[1]

In the generation of musical murmurs a specific structural member, such as a pathologically altered valve cusp, seems to be involved. The proper combination of hemodynamic factor and structural factor seems essential for the periodic generation of vortices[1] resulting in musical murmurs. Unusually great intensity is a feature of musical murmurs as a class.

Physical Considerations

The vibrations at the skin surface which are in the audible range of frequency are of essentially the same nature as the grosser precordial movements of lower frequency accompanying and resulting from cardiac action. It seems most accurate to view the generation of cardiovascular sound as a setting into vibration, a "shaking," if you will, of the blood and wall structures, and to consider the propagation of cardiovascular sound as the transmission of these vibrations to contiguous structures lying between the site of generation and the site of detection. Specifically, the analogy to sound in air or even water, with alternate zones of condensation and rarefaction, is probably not appropriate. Although a rather philosophical one, the question might be raised as to whether cardiovascular sound is really sound, at least up to the point that the vibrations we so designate are translated into sound at the skin surface. Is the phenomenon recorded in intracardiac phonocardiography "sound"?

The record from sonic catheters is dominated by pressure fluctuations in a rapidly flowing stream containing obstructions. This flow is neither laminar nor turbulent, but vortical, i.e., filled with small waves and moving eddies, which excite a stationary pressure transducer in passing. In addition to these dynamical flow transients (of amplitude 1 to 10 mm Hg = 10^4 to 10^5 dynes/cm^2), there should indeed be true sound-pressure waves as well, at a much lower amplitude (.001 to .01 mm Hg = 10 to 10^2 dynes/cm^2) generated by interaction of vortices with the walls. However, these sound waves are all below the threshold (1 mm Hg) of existing sonic catheters.

Another factor which distinguishes between cardiovascular sound and what sonic catheters record is the great variation of the observed pressure pattern with position; it changes rapidly within centimeters, both across the lumen and up and down stream. Sound does not behave this way, but travels as a compressional wave largely unaffected by flow or, at these frequencies, by turbulence. Thus within the right ventricle, the catheter records predominantly the tricuspid valve "sound" rather than the pulmonic, showing that one senses here the fluid motion rather than transmitted sound. An analogy would be to put

[1] Bruns (3) suggests that vortex or wake formation rather than turbulence is the mechanism of all murmurs. In this view musical murmurs owe their harmonic organization to the regular, periodic shedding of vortices in contrast to the unorganized vortication in the generation of noisy murmurs.

a pressure transducer between a drumstick and a drum head. It would sense the forces which create the sound, but would not record the sound generated.

So one can hardly say that the sonic catheter senses cardiac sounds at their origin; but rather a complex of hydrodynamic flow pressures associated in various ways with their generation. This is not to minimize the importance of such observations in describing anomalies, but rather to avoid the irrational attempt to find correspondences of form between "sound" patterns recorded externally and internally. Because these vortical patterns are highly nonlinear, and spatially complex, any sound waves arising from their vicinity would have to be evoked rather than driven by them, much as with the blow on a drum.

The dynamic range of cardiovascular sound is considerable. In the case of the normal heart the range is as much as 80 db between the intense components at 10 cps and the extremely faint components with intensities of the order of the threshold sensitivity at the level of 1000 cps. In pathologic situations the range may be considerably greater.

The decibel (db) is a unit used to express power ratios such that

$$db = 10 \log_{10} \frac{P_1}{P_2}$$

A positive sign or no sign preceding the db value indicates P_1 is greater than P_2. The usefulness of db measurements comes from the ease with which large ratios can be expressed. Thus, 40 db represents a power ratio of 10,000. In electrical circuits the power is proportional to the square of the voltage or the current, and in acoustical measurements the intensity of sound is proportional to the square of pressure. Because of this second power relationship

$$db = 20 \log \frac{V_1}{V_2} \quad \text{or} \quad db = 20 \log \frac{P_1}{P_2}$$

Care must be exercised both in using db and interpreting how others have used it (1). Although originally it was applied only to constant impedance circuits the usage has been extended to ratio measurements of all kinds. However, the 10 log factor is retained for all power measurements and 20 log factor for units such as voltage, current, or pressure. For instance, a voltage amplifier may have a stated gain of 40 db. That is a voltage gain of 100. The power gain may not be stated or may not be of interest and, in fact, will probably not be 40 db.

Since the db unit is a ratio, it cannot be used to indicate an absolute value. However, in practice, there are several situations in which a reference level is assumed so that the db unit is in effect used to indicate an absolute value. For instance, a high impedance microphone (6) may have a stated sensitivity of −60 db. This means that its voltage output is −60 db or 1/1000 relative to one volt per dyne per square centimeter of incident pressure. The reference level of 1 volt per dyne per square centimeter may or may not be stated.

Similarly, sound pressure levels are often expressed in db with an implied reference level of 0.0002 dynes per cm^2, the accepted threshold of hearing at 1000 cycles per sec.

Low impedance microphones (1) may have a listed sensitivity expressed in dbm (output power) re 10 dynes per cm^2 (input pressure). In this case the power is referred to 1 milliwatt, hence dbm (decibel-milliwatt). To find the output voltage, the impedance must be stated also. Transformers are often rated in dbm.

It can be seen that the use of the db unit is widespread and can be useful. However, care must be exercised in stating the reference for the ratio measurement. Before making a plot in db, one should consider whether or not a plot in absolute units would be more helpful to the reader even though it may seem less sophisticated.

Due to the intensity relation shown in figure 3, the frequency range of displayed cardiovascular sound from the normal heart rarely extends higher than 1000 cps. In pathologic conditions resulting in much accentuated heart sounds and very loud murmurs the peak frequency range may exceed 1000 cps and even reach 2000 cps. Although only a small proportion of the total energy is distributed at frequencies above 1000 cps, one should not conclude it is without physiologic or clinical importance.

Analysis of results, such as those of Mannheimer, indicate that cardiovascular sound has a natural decrement of about 12 db per octave or 40 db per decade. [This is the physiologic decrement referred to by Zalter *et al.* (19). It means, in the opinion of the writers, that an additional physical decrement referred to by Zalter *et al.* is not operative in the recording of cardiovascular sound.] Considering the total spectrum of precordial vibration in a unified manner, a decrement of 40 db per decade represents a dynamic range of 120 db in the band from 1 to 1000 cps, and 80 db in the band from 10 to 1000 cps.

TRANSDUCERS

The ideal microphone should have a voltage output that is a faithful and undistorted image of the pressure variations at the input. The response should be independent of frequency in the pertinent range. The signal-to-noise ratio should be favorable. Noise is created by thermal agitation of molecules in the resistive components of the microphone or of air molecules against the diaphragm. Self-noise of a microphone may be of the order of 20 db, a not inconsiderable factor.

Microphones used in phonocardiography operate either *a*) indirectly, with a closed air chamber between the skin surface and the diaphragm of the microphone, and the conversion of the displacement at the skin surface into a pressure which acts on the diaphragm; or *b*) directly, with the application of an element of microphone, such as a button or bar, directly to the skin surface. In the Groom microphone the skin functions as one plate of a capacitance transducer.

In the indirect method, the shape, volume, and size of the air chamber are important because cavity resonance can distort the response at the frequency of natural resonance of the cavity. If the volume of a cylindrical cavity is kept large enough (around 10 cm^3) with a diameter-height ratio of 3:1 the response characteristics remain linear up to the resonance point well above 1000 cps.

Transducers in phonocardiography can be further classified as *a*) *displacement* and *b*) *dynamic*. Both the crystal and the capacitor microphone transduce displacement into emf, since the static pressure developed in the closed chamber is a function of the displacement of the skin which it overlies. The emf generated in the dynamic microphone (e.g., the "moving coil" microphone and the piston-phone) is proportional to the velocity of the moving element; that is, the derivative of displacement is sensed by the dynamic microphone. The response of the dynamic microphone increases with frequency. This characteristic can be advantageous in phonocardiography, since part of the equalization, or low-frequency attenuation, is accomplished at the transducer level. [A dynamic microphone has been used with the Sanborn Twin-Beam and Stethocardiette phonocardiograph, and the Elema phonocardiograph (20), as well as others.]

Microphones can be classed according to the physical principle underlying their function as transducers. For its transducer properties the *capacitor microphone* depends on variations in the capacitance of a condenser, one plate of which is free to move with the sound vibrations. An example is the Groom microphone in which the skin surface is itself the movable plate of the condenser element. A second example is the Altec microphone. Advantages of the Groom microphone are *1*) reduced influence of ambient noise, *2*) minimal loading of the precordium, and *3*) high sensitivity with favorable signal-to-noise ratio. Disadvantages are *1*) relatively large size which makes for difficulties of placement in some areas of the chest, *2*) lack of the possibility of acoustic filtration, and *3*) difficulties in calibration. Advantages of the Altec[2] microphone (e.g., 21 BR 150)—in which inert components such as glass, gold, stainless steel, and Mycalex are used—are temperature stability, permitting, for example, sterilization with the hot air oven, and stability to mechanical shocks. Acoustic filtration of low-frequency components can be used; it can be calibrated; it withstands high pressures with minimal distortion. Most important is its "flat" frequency response (amplitude proportional to pressure) in the pertinent range and its reasonable size and weight minimizing loading of the precordium. High humidity has ill effects and caution must be exercised when it is used in the presence of explosive anesthetics.

Examples of piezoelectric transducers are the crystal (Rochelle salts, sodium potassium tartrate) microphone and the ceramic (barium titanate) microphone. The latter is the type employed in intracardiac phonocardiography. Disadvantages of these transducers are vulnerability to mechanical and thermal injury and to the ill effects of humidity. An advantage is low cost. Ethylene oxide can be used, rather than heat, in the sterilization of some intracardiac catheters.

The electrodynamic, or moving-coil, microphone consists of a permanent magnet and a coil mounted on a diaphragm that moves with the vibrations under study. Disadvantages are the relatively large size and weight, and a tendency to pick up hum. The "variable-reluctance" microphone (13) can also be termed generically an electrodynamic microphone.

The piston-phone is useful mainly in the calibration of other microphones and in other situations requiring sound generation.

Microphones for use in phonocardiography are calibrated in terms of a constant pressure applied in a uniform manner to the diaphragm of the microphone. The sensitivity is customarily expressed in terms of output below 1 volt per microbar of pressure applied

[2] Altec-Lansing Corp., Beverly Hills, Calif.

at the diaphragm. For example, if the output level of a microphone is −45 db, the voltage generated is 45 db below the reference level of 1 volt per dyne per cm². The smaller the absolute value (in db) of the output expression the more sensitive is the microphone.

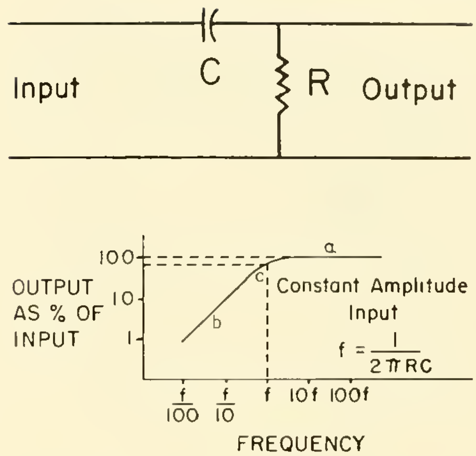

FIG. 1. *Upper:* circuit for low-frequency attenuation. *Lower:* output of circuit of type shown above. [Courtesy of Williams & Wilkins (12).]

FILTRATION, INCLUDING AMPLIFICATION AND LOW-FREQUENCY ATTENUATION (EQUALIZATION)

Overloading from the intense precordial vibrations of low frequency must be avoided in phonocardiography. For example, in early phonocardiography so-called "low-frequency attenuation" was achieved by acoustic filtration; an air leak eliminated gross low-frequency components of the precordial vibration. In more recent work electronic filtration has been used for the same purpose.

In optical registration the amplitude which can be encompassed is of the order of 50:1 (34 db). (In this estimate it is assumed that 1 inch is allowed for maximal deflection and that .02 inch is just distinguishable.) Because of the logarithmic compression characteristic of the function of the ear, in accordance with the Weber-Fechner law, sounds with an intensity range of 1,000,000:1 (120 db) can be detected. The intensity of cardiovascular sound decreases roughly with the second power of the frequency, or about 12 db per octave. Obviously a weak high-frequency signal requires much greater amplification for visual registration than does an intense low-frequency signal.

A single oscillogram cannot adequately represent the entire frequency intensity range of cardiovascular sound, and various techniques of differential filtration or amplification are necessary. Filters used in phonocardiography can be classed as *a*) low-cut, high-pass; *b*) high-cut, low-pass; and *c*) band-pass. The general definition of each is evident from its designation. The first and third are the types used in phonocardiography. The band-pass filter essentially combines a high-pass and a low-pass filter in series. Figure 1 presents (upper) a schematic view of the circuit for low-frequency attenuation (equalization; high-pass filtration). In the low-pass filter the positions of the resistor and capacitor are interchanged. In the lower section the output characteristics of the circuit above are schematized. Figure 2 presents the characteristics of two systems which have used multiple high-pass filters. More detailed descriptions of the characteristics of these and other systems are available elsewhere (20).

Experience with spectral phonocardiography suggests, and the work of Bekkering and his colleagues (personal communication) appears to establish, that five oscillographic channels, each with different frequency filtration and amplification, and each separated from the next by one octave, can adequately portray cardiovascular sound.

A schematic representation of a multichannel, multifilter system for oscillographic phonocardiography is presented in figure 3. The decrement in intensity of cardiovascular sound with frequency is represented by line *AB*. Band-pass filters may be unnecessary; high-pass filters as shown in figure 3 here may suffice, inasmuch as the natural decrement of cardiovascular sound takes care of the upper end of the frequency scale. The system indicated here can theoretically be calibrated and standardized if the amplification in each channel is so adjusted as to bring the registered amplitude to a uniform level, and if the amount of amplification necessary to accomplish this is recorded. An alternative to the use of different amplification in each channel as the findings in the individual patient may require is to apply a different and somewhat arbitrarily selected amplification in each channel, let us say 0, 12, 24, 48, and 60 db in the five schematized in figure 3, keeping said amplification the same in all patients studied.

Much of the information represented in a single spectral (SPCG) display can be derived from such a system as this. For example, improved representation of the shape of murmurs useful in diagnosis and in hemodynamic correlation, and of the splitting of heart sounds, tends to appear in the channels with higher

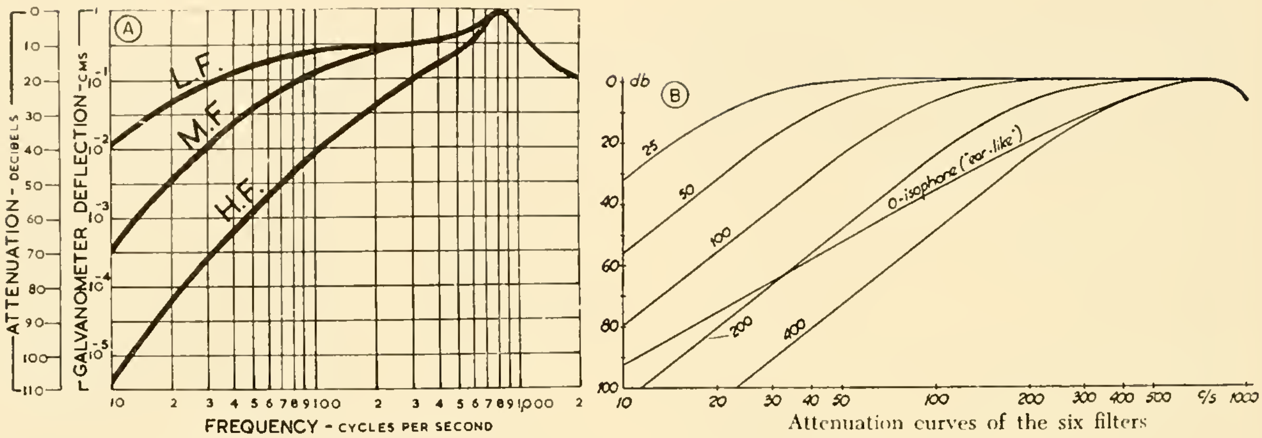

FIG. 2. A schematic representation of the frequency response characteristics of several phonocardiographic systems. *A:* Leatham's high-, mid- and low-frequency systems. *B:* Mannheimer's multiple filter system. These various systems are needed because the wide intensity range of cardiovascular sound, particularly the very intense low-frequency components and the relatively faint higher frequency components cannot be displayed simultaneously in a single oscillogram. A second motivation is the desire to obtain approximate information on the frequency composition of heart sounds and murmurs by the examination of oscillographic displays of various frequency bands. The system of Maass and Weber is similar to that of Mannheimer. Luisada's selective phonocardiography uses a filter which cuts off those components above as well as below a certain frequency band. [Courtesy of Williams & Wilkins (12).]

frequency response characteristics, precisely as one would predict from spectral phonocardiography. A single channel phonocardiograph can be used if necessary, since the five separately filtered displays can be made seriatim from magnetic tape or directly from the patient.

Two central questions regarding amplification and filtration for phonocardiography are, *1*) at what point should equalization (the pre-emphasis of higher frequency components to compensate for the 12 db decrement with frequency) be performed, and *2*) should low-cut, high-pass filters, or band-pass[3] filters be used.

Filter Systems in Spectral Phonocardiography

The filter system in the commercially available sound spectrograph (Kay "Vibralizer"), which was adapted for phonocardiography and has been used almost exclusively, is of the heterodyne type. The sounds to be analyzed are essentially passed through a filter mechanism, the tuning of which is changed progressively in coordination with the write-out of

[3] Luisada & Zalter (9) have used band-pass filters with a decrement of 24 db per octave at each end (Krohn-Hite Corp., Cambridge, Mass.). Satisfactory results should be achieved, for example, with the following five octave bands: 30–60, 60–120, 120–240, 240–480, and 480–960.

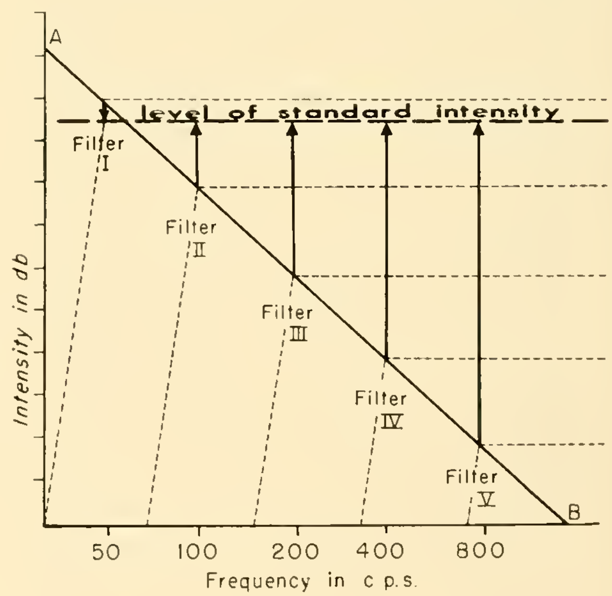

FIG. 3. An idealized multifilter system for phonocardiography. Line *AB* represents the natural intensity decrement of cardiovascular sound with frequency. Five high-pass, low-cut filters with the shoulder at successively higher frequencies are shown. Standardization of amplitude to a constant level is represented by the vertical arrows. The length of each arrow represents the amount of attenuation or amplification necessary to bring all signals to the standard level. The interrupted line represents, in the case of each filter, the pass characteristics of the filter.

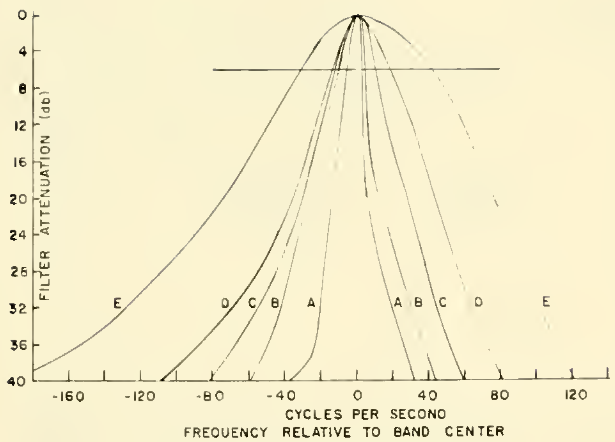

FIG. 4. The pass-band characteristics of five filter setups tested to determine empirically the optimum system for study of heart sounds. Defined in terms of width at 6 db attenuation (indicated by the horizontal line), these are $A = 9$ cps, $B = 16$ cps, $C = 23$ cps, $D = 34$ cps and $E = 71$ cps. [Courtesy of Williams & Wilkins (12).]

consecutively higher frequency bands. In fact, the vibrations being analyzed are *in toto* progressively altered in frequency and passed over a single constant filter. The process of "heterodyning" is performed at the approximate level of 15 kc. The filter setup of the heterodyne type can be understood by comparison to the tuning arrangement of the ordinary radio which uses the same principle. By turning the dial for "tuning in" stations one changes the tuning of the oscillator in the radio set. When the sum of the oscillator and the pertinent sound component is in perfect resonance with a particular frequency, the sounds at that frequency are picked up. Only a station operating in the same frequency band as that at which the set is operating will come through clearly.

In the original investigations of the applicability of sound spectrography to cardiovascular sound (1953) five filter systems (i.e., five heterodyne modifications, according to effective width of the band-pass) were tested. The band-pass characteristics of each filter system are shown in figure 4. The width of each band-pass at 6 db attenuation is approximately 9 (A), 16 (B), 23 (C), 34 (D) and 71 cps (E). It is evident from comparisons such as those shown in figure 5 that the recordings produced by the five different filter systems are quite different. The filter system with narrowest pass-band by definition gives finest frequency definition but is slower in onset and offset, giving excessive temporal lag, improper delineation of transients, and "after smudging." The filter system with the widest pass-band characteristic gives minimum time lag and minimal ringing, but also, of course, by definition gives least detail in the frequency dimension. It was concluded that filter C represented the best compromise for display of both the temporal and the tonal characteristics of cardiovascular sound.

The use of a single variable filter has the theoretical disadvantage that the Q, or characteristic with respect to ringing, varies with frequency. The temporal error increases at higher frequencies. It is doubtful that error significant to spectral phonocardiography is introduced, however.

A second major type of filter system which was explored was the phase filter, which has the advantage of providing a cleaner display of musical tones than does the heterodyne system. For example, the har-

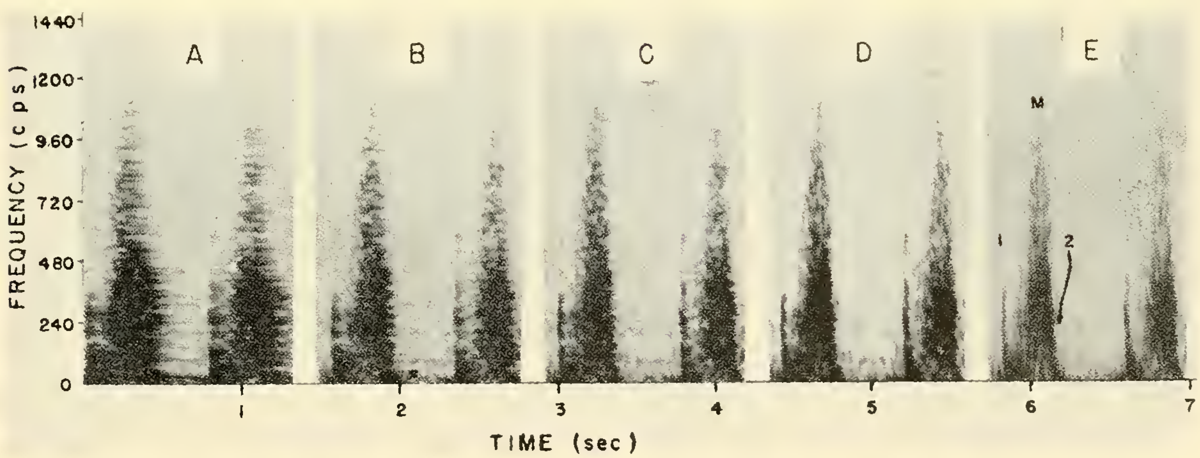

FIG. 5. Crescendo or late systolic murmur displayed by the five filter systems. Pass-band C is considered the best compromise for routine use in the study of cardiovascular sound. [Courtesy of Williams & Wilkins (12).]

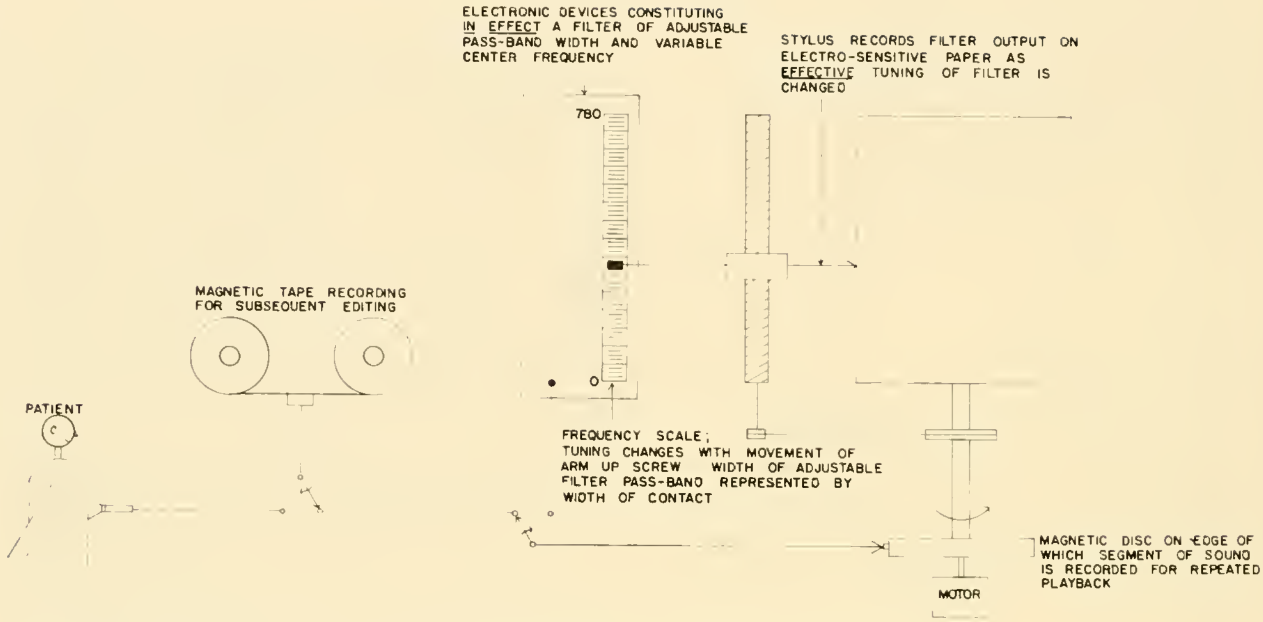

FIG. 6. Schematic representation of the sound spectrograph used in making most of the spectral phonocardiograms presented in this chapter. The intermediate step of tape recording and the seriatim rather than simultaneous frequency analysis are shown. [Courtesy of Williams & Wilkins (12).]

monics of musical murmurs are displayed as narrower bands, more nearly approaching what must be their true state, than in the records made by the usual method. However, no particular value of this more precise definition is evident, and the transients and noisy murmurs which constitute the great bulk of cardiovascular sound are unsatisfactorily displayed. Hence, the phase filter has nothing to recommend it for routine use.

The general principle and mechanical design of the spectral phonocardiograph is shown in figure 6. As now practiced, the sounds first recorded on magnetic tape are audited and sections selected for analysis. One such section is played over onto the magnetizable margin of a disk mounted on the same axis as the kymograph drum on which the records are made. As explained above, the analyzer is in essence a single pass-band filter, the tuning of which is changed progressively as the segment of sound is played back repetitively through it. For example, during the first rotation of the magnetic disk and the coaxial drum, the information in the 15 to 20 cps band might be inscribed on the record, with the second rotation the information in the 20 to 25 cps band, and so on from bottom to top of the record until the entirety of the frequency scale desired has been scanned. There is, of course, much overlap of the individual frequency bands. In making an analysis from 0 to 750 cps the sound must be passed through the equivalent of as many as 425 individual filters, each with its pass-band overlapping others but with its center frequency about 1.8 cps removed from the center frequency of the filters next above and below it.

A frequency scale from 0 to 720 cps encompasses most of the information in cardiovascular sound, as recorded at the chest surface.

THE DISPLAY

Oscillography

Display of the oscillogram is accomplished by means of a cathode-ray tube or a galvanometer.[4] The cathode-ray oscillograph has the advantage of total lack of inertia so that its frequency response is unlimited. In phonocardiography, necessitating photography of a fluorescent screen, difficulties arise as a result of limitations on the brightness of the spot where vibrations of high frequency are to be recorded. The faster the spot moves the fainter becomes the trace. Several methods exist for circumventing this

[4] Yet a third method for display of the oscillogram is the jet-ink writer (Mingograph) devised by Elmqvist and produced by the Elema Co., Stockholm. The pressure of the ink jet is modulated as a function of the amplitude of the vibrations being recorded. The system has little inertia and consequently an advantageously high-frequency response.

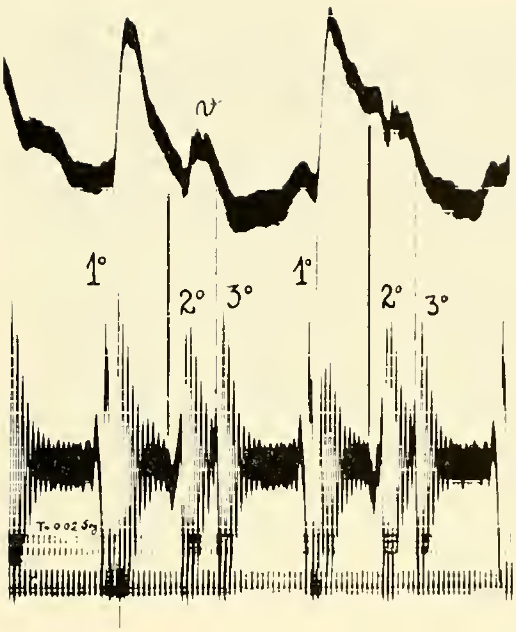

FIG. 7. In this oscillogram the instrumental frequency dominates the picture. Since it is almost purely the natural frequency of the recording membrane which is activated by the sound vibrations, the recording suggests transient pure tones. (From Orias and Braun-Menèndez, *Heart Sounds in Normal and Pathological Conditions*, 1939.)

difficulty but these are not entirely satisfactory solutions. The use of an electronic switch to provide multiple recordings from a single electron beam[5] further detracts from the resolution at higher frequencies. For these reasons, the opinion has been expressed (19) that "the moving-coil galvanometer (or its modifications) is today, pending the development of a compact multiple-gun cathode-ray tube, more suitable for phonocardiographic practice than any other recording device."

The moving-coil, or D'Arsonval, galvanometer has a moving element consisting of a coil or loop of fine wire suspended in a strong magnetic field. Current is conducted to the coil, causing it to turn in the magnetic field. A mirror or writing arm is mounted on the coil for recording either photographically or by direct writing.

Some (8) have considered it necessary to use galvanometers of different frequency characteristics for recording information from different areas of the frequency spectrum. In the opinion of the writers, such a practice introduces further complications in calibration. A 2-kc galvanometer can, and we think should, be used for recordings at all frequency levels, thus eliminating one variable in the interpretation of findings in different channels.

Flexibility in manipulation of the time scale is a valuable feature of oscillographic recording. "Stretching out" the sounds is often desirable. Clearly a greater paper speed is required for routine phonocardiography than for routine electrocardiography. Whereas 25 mm per sec has been satisfactory for the latter, a paper speed of 50 mm per sec is more useful in phonocardiography.

Figures 7, 8, 9 are examples of oscillographic recordings.

The write-out of the *spectral phonocardiogram* can be made in several ways: *1*) The output of the filter can be used to activate an electric spark which marks electrosensitive paper. Electrosensitive paper has a rather poor intensity depth. (In the spectral phonocardiogram time is represented by the horizontal axis, and frequency scale by the vertical axis and the loudness, amplitude, or intensity of a component at a given frequency and time is indicated by the intensity of the mark on the record.) Only about 10 to 20 db, or at the most 30 db, from faintest to loudest can be displayed using such a method. However, this intensity span seems to be adequate for most purposes, probably inasmuch as the sounds are "spread out" in the frequency dimension. (Empirically, 6 db initial equalization seems to give satisfactory results. More or less is less satisfactory.) *2*) Or, the output can modulate a tiny light which is made to play on photographic paper (fig. 10). The photographic record provides improved intensity resolution but again it is not certain that this refinement is necessary in most applications. *3*) Finally, the output can be put into a cathode-ray oscilloscope with a long-persistence face and the image photographed. The last method has the advantage of flexibility in manipulation of the time scale without influencing the frequency scale.

One of the open questions in the final design of a spectral phonocardiograph is the best method for repetitively playing back the recorded information for the seriatim frequency analysis. The magnetic drum has the limitation of fixed playing time and difficulties with "wow" and "flutter" (artifactual variations in frequency in the final display due to lack of uniform speed of rotation of the disk). Alternatives to the disk include the use of tape loops with either moving head or moving loop.

Display of the frequency spectrum is responsible for the three advantages of spectral phonocardiography:

[5] As in the recorders of Electronics for Medicine, Inc., White Plains, N. Y.

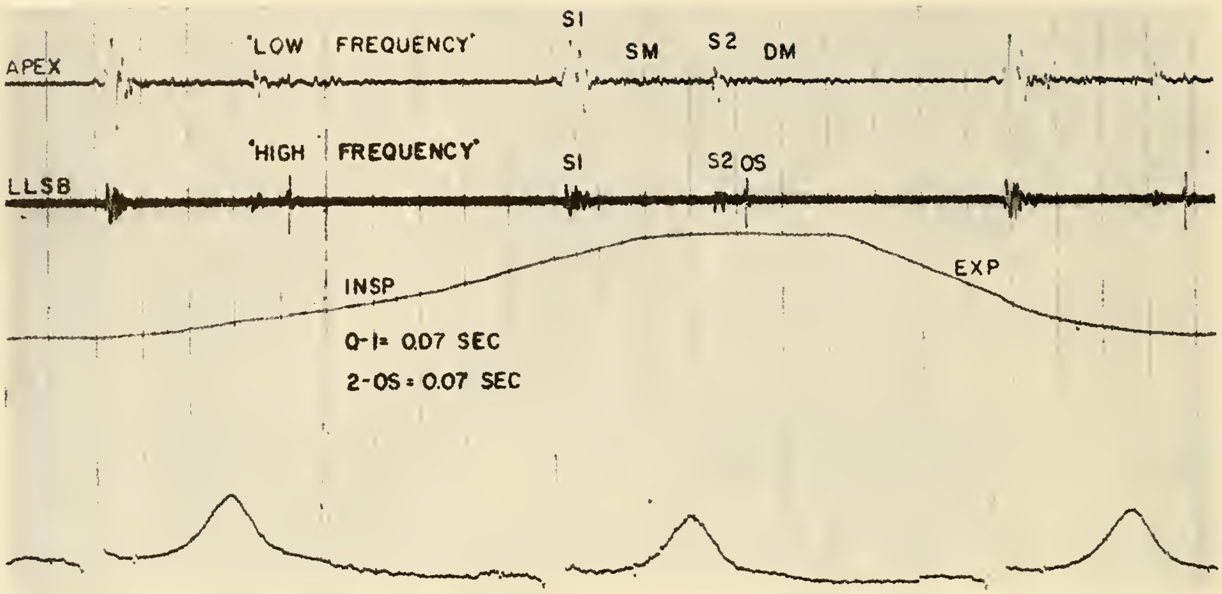

FIG. 8. A modern oscillographic phonocardiogram revealing more faithful representation of the sound vibrations. The patient has mitral stenosis. The low-frequency recording at the apex reveals a loud first sound (*S*1) and a diastolic murmur (*DM*). The recording from the LLSB with high-frequency emphasis shows an opening snap (*OS*). The second sound becomes split at the height of inspiration.

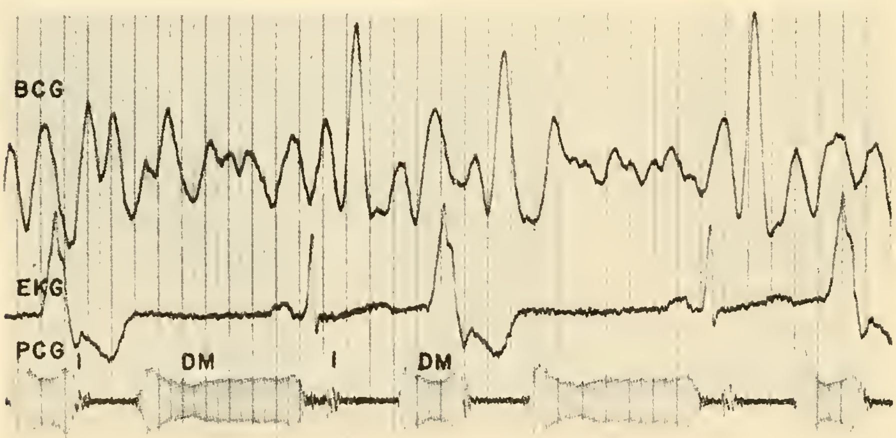

FIG. 9. Oscillographic recording of musical murmur. The patient had a retroverted aortic cusp due to syphilis. Ballistocardiogram and electrocardiogram are also shown. The regular vibrations of the diastolic murmur indicate its musical quality. Only the fundamental is demonstrated. Overtone harmonics cannot be identified.

1) Quality, or timbre, is represented objectively and given physical definition in terms of frequency, time, and intensity. *2*) Resolution in the dimension of time is improved. For example, two elements of the second heart sound, which are indistinguishable in the oscillogram and at some levels of frequency in the spectrogram, may be distinguished at other levels of frequency in the spectrogram. *3*) A more accurate display of the wide dynamic (i.e., intensity) range of cardiovascular sound is attained. For example, a very loud systolic murmur of aortic stenosis and a very faint diastolic murmur of aortic regurgitation can be displayed at nearly their true relative intensity proportions in a single spectral phonocardiogram.

Rushmer and colleagues (15) have developed a method for producing what they call "sonvelograms." In essence, these are the intensity envelope of the sound. The method involves, first, half-wave rectification of the oscillographic phonocardiogram, and, second, electrical integration. The resulting curves can be used for timing purposes, and possibly the shape of murmurs will have some useful hemodynamic correlations.

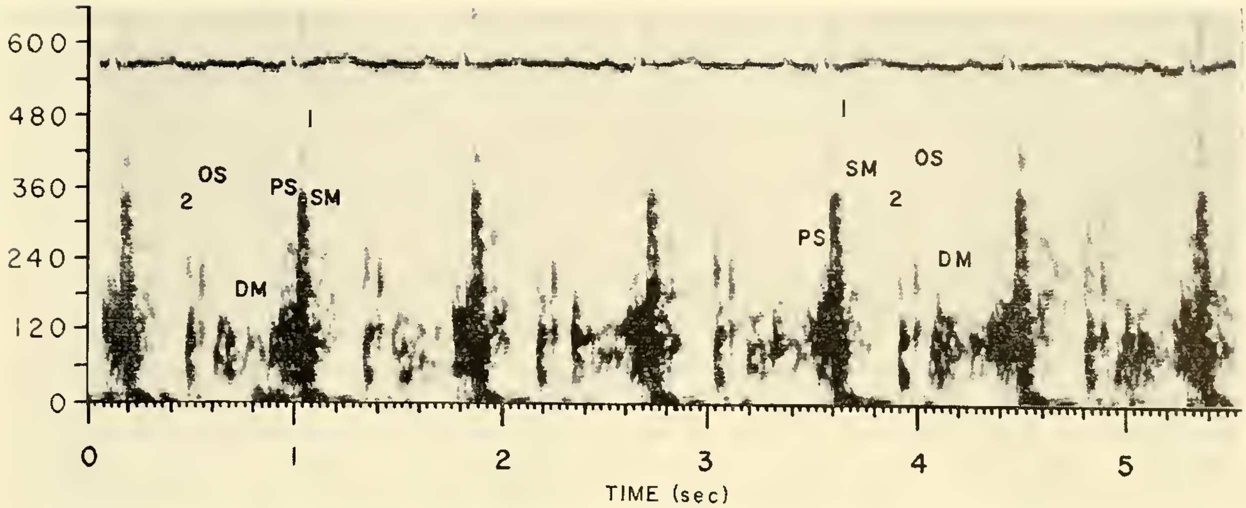

FIG. 10. Spectral phonocardiogram, apex, in patient with classical mitral stenosis. The loud ringing first heart sound (*1*), mitral opening snap (*OS*), mid-diastolic murmur (*DM*), and crescendo presystolic murmur (*PS*) are well demonstrated.

PHYSIOLOGIC DATA FOR CORRELATION

The electrocardiogram is a minimal requirement for physiologic correlative data in phonocardiography. As an additional timing device, the arterial pulse, usually the carotid pulse, has had favor because it provides an indication of the time of closure of the aortic valve. The jugular venous pulse, sponsored by earlier workers as a useful indicator of diastolic events such as opening of the tricuspid valve, has fallen into disfavor with appreciation of the considerable and not easily quantifiable delay between cardiac events and their reflection in the venous pulse. Respirations represent, next to the electrocardiogram, perhaps the most useful phenomenon for correlative purposes because of the potent influence of respiration in splitting of the second heart sound and on some murmurs, such as those of tricuspid valve disease. In patients it is possible to follow respirations visually and mark them appropriately in the recording. Devices which automatically pick up respiration, such as a strap around the chest or a detector of air movement at the mouth or nose, incur practical difficulties particularly in ill patients, and may be limited in the faithfulness with which they follow the respiratory phase. Intracardiac pressure recordings are, of course, useful for correlative purpose.[6] In general, the type of correlative recordings made in phonocardiography are dictated by the nature of the study, i.e., the questions to which answers are sought. Transducers for use in recording various pressure pulses are discussed elsewhere.

Techniques for recording low-frequency physiologic data on magnetic tape (using frequency modulation) along with cardiovascular sound have increased the flexibility of methods for studying cardiovascular sound. The recording of electrocardiogram, respiratory mark, or pressure pulse can be demodulated for oscillographic display. If they are to be used in conjunction with the spectral phonocardiogram demodulation is not required, since the write-out is in terms of frequency and the correlative physiologic trace is inscribed directly on the spectral record. If the sound recordings are to be used for teaching purposes, separate tape channels can be used for the correlative recordings, or the correlative recordings applied at a higher frequency level, e.g., 3.0 kc, can be filtered off.

SOME PRACTICAL ASPECTS OF RECORDING, WITH A DISCUSSION OF ARTIFACTS

As in the other parts of this discussion, the comments made here concern mainly recording in man but are pertinent also to work in animals.

[6] Eldridge & Hultgren (4) point out the production of spurious heart sounds by cardiac catheters, especially when the tip is located at or near a valve orifice. Such artifacts must be guarded against when doing correlative studies involving intracardiac catheterization (and must also be kept in mind in intracardiac phonocardiography).

Ambient noise in the recording area must, of course, be kept at a minimum. A soundproof room may be necessary or desirable; but before such an expensive investment is made, the investigator should convince himself that the signal-to-noise ratio of his recording equipment is sufficiently favorable that ambient noise, not electronic noise, is the factor limiting clean recording. An advantage of heart sound recording—over the recording of music, for example, in free air— is the considerable attenuation (as much as 20 db) provided merely by the coupling of the microphone to the chest. More often than one might think, a quiet room with attention to avoiding unusual noise suffices.

The subject should be relaxed, comfortable, and warm to prevent muscle noise. The application of the microphone to the chest can be accomplished by a rubber strap surrounding the chest, by local mooring (with tape or suction cup), or by hand. The strap has the possible disadvantage of variations in pressure on the microphone with varying phase of respiration. The pressure with which the microphone is applied influences the vibrations of the portion of skin underlying the microphone and therefore the sounds which are recorded. Greater pressure preferentially attenuates lower frequencies. Hair on the chest may require shaving or plastering down.

Standard loci for recording from the surface of the chest in man are *1*) aortic area (second intercostal space at the right sternal margin); *2*) pulmonary area (second intercostal space at the left sternal margin); *3*) LLSB (left lower sternal border; fourth intercostal space at the left sternal border); *4*) apex (in the area of the apex beat, on the left border of cardiac dullness in the fifth intercostal space, or the midclavicular line in the fifth interspace). Recordings are made in other areas in which auscultation reveals sounds of interest.

The value of simultaneous multilocus recording, i.e., parallel recording from at least two precordial locations, has been demonstrated particularly by Leatham. The precordial topography of the several components of the heart sounds and the effects of respiration lend themselves well to study by this method. Especially when studying respiratory effects it is much easier to be certain of results if the changes are observed in the same cardiac cycles in two or more areas.

STORAGE OF CARDIOVASCULAR SOUND AND CORRELATED INFORMATION

Storage of cardiovascular sound and other physiologic data on magnetic tape has increased considerably the flexibility of methods of study. Data can be preserved for future reference and comparisons, for analysis by newly devised techniques, and for teaching purposes. Minimal low-frequency attenuation of cardiovascular sound consistent with placement on tape without overloading is recommended. A tape speed of 7½ inches per sec has been found satisfactory in our laboratory.

As an alternative to direct tape recording of the heart sounds, one may consider recording with the use of an FM system. Direct magnetization of the tape by the method normally used for tape recording of voice and music seems adequate; however, there has been no systematic investigation of whether FM recording of the heart sounds might be superior in some applications. At a given tape speed there is, with direct recording, a limit below which distortions on playback become excessive because the recorded wavelengths exceed the length of tape covered by the playback head. With the low-frequency elements of cardiovascular sound such distortion might be serious. Nonuniformity of magnetic material on the tape adds to the distortion. In the FM method a carrier signal saturates the magnetic material, thus minimizing the effects of nonuniformity of tape. Since the physiologic information is, in the FM system, contained in the frequency level of the carrier signal, its faithful reproduction is dependent on uniformity of tape speed. In direct recording, uniformity of tape speed is a factor of secondary importance, just as uniformity of the magnetizable material on the tape is a second-order factor in frequency modulation. Direct recording probably provides the most favorable signal-to-noise ratio for the investigation of cardiovascular sound.

The FM method is used for recording the electrocardiogram, respiratory phase, pressure pulses, and other low-frequency physiologic phenomena discussed earlier. Details of such recording are presented in Chapter 22. The electronic details of frequency modulation and demodulation of low-frequency physiologic data are beyond the scope of this discussion.

SPECIAL TECHNIQUES

Direct phonocardiography is a term now used to indicate the making of recordings directly from the surface of the heart or great vessels (11). (Historically, the same term was used for the method devised by Frank.) The technique has difficulties because the surface underlying the microphone is almost always moving, possibly introducing vibrations without physiologic

significance, and because the weight of the microphone has a "loading" effect. Some (2) have used a suction cup to hold the microphone to the surface from which recording was to be done.

Intracardiac phonocardiography had its crude beginnings with the intracardiac pressure recordings of MacLeod & Cohn (10), who found high-frequency vibrations synchronous to the heart sounds superimposed on the pressure trace. Recording of the rapid pressure transients within the heart has been performed by means of a barium titanate[7] (17) or miniature electromagnetic[7] (7, 16) transducer on the tip of a catheter, by a condenser microphone with one pole at the tip of the catheter and the other the body itself (18), or a transducer located on the external end of the catheter and communication with the interior via the blood filling the catheter. If one uses an internal transducer, a double lumen catheter permits one to combine intracardiac phonocardiography with pressure recording, sampling of blood, and administration of indicator dilution agents.

Information obtained with the transducer at the external end of a catheter must be interpreted with exceeding caution. Intracardiac transducers of the barium titanate type are disturbingly sensitive to bending of the catheter (4), to impacts at a distance from the tip, and even to minor temperature changes. On the other hand, they are relatively insensitive to localized pressure changes at the tip.

The analysis of heart sounds by *digital computer* techniques appears to have promise. For example, in determining the "normal" spectral phonocardiogram, difficulties result from the wealth of information contained in the recording. A possible solution for this "embarrassment of riches" is the translation of the information into the digital language of the computer and the use of machine methods for determining the biological variability of the normal.

Other special techniques such as esophageal phonocardiography, fetal phonocardiography, and others require no special consideration here.

CALIBRATION OF INTENSITY

Intensity calibration in phonocardiography presents many problems. There are variables in the sound-transmitting properties of the chest among subjects and in the same subject under different circumstances. There can be variability in the performance of the microphone which is often difficult to calibrate in the first place. As mentioned earlier, even the pressure with which the microphone is applied to the skin surface introduces variability. As pointed out, in the analyses of Rappaport & Sprague (14), the influence of different chest pieces, with and without diaphragm, is considerable. The electronic amplification requires calibration. Changes in intensity must be considered in relation to frequency. Sounds of quite different frequency composition may be of identical over-all intensity.

The use of calibrating signal in the form of a vibration generator strapped elsewhere on the chest or even placed in the esophagus has insufficient comparability to the real situation to be reliable. Others have calibrated from the microphone by imposing a calibrating signal just proximal to the microphone.

The idealized system (for oscillographic phonocardiography), shown in figure 3, permits semiquantitative calibration, as was indicated previously. We shall probably have to be satisfied with rather qualitative and, at the best, semiquantitative statements about intensity. The use of a roughly calibrated gray scale with spectral phonocardiograms is a beginning. For clinical use, precise quantitation is probably not very important.

Careful specification of the characteristics of the phonocardiographic system used in any study is essential and should be clearly stated in reports. [Recommendations for methods in indicating the frequency characteristics of systems have been made (5).] However, it can be seriously questioned whether the time is ripe for standardization of technique. Admittedly, it will be a convenience if many laboratories can use a few well-specified systems and in their reports merely refer to the published characteristics of the particular system used. For example, much phonocardiography in this country has been with the Sanborn Twin-Beam (and its predecessor the Sanborn Stethocardiette), the characteristics of which were rather completely determined by Rappaport.

In summary, a five-filter system for oscillographic phonocardiography, such as that schematized in figure 3, can provide most of the information incorporated in the spectral phonocardiogram. It is a less elegant approach than the spectral phonocardiogram which provides the full picture in a single display, together with a wealth of detail which is necessary for a precise visual impression of timbre.

[7] The barium titanate microphone and preamplifier used by Lewis and his colleagues (17) are available from the American Electronics Laboratories, Inc., Philadelphia, Pa. The Allard-Laurens micromanometer system used by Soulié and his colleagues (16) is available from Telco Inc., Gentilly, Seine, France.

Musicality, for example, is represented adequately only by the spectral phonocardiogram. The oscillographic method has the advantage of direct applicability to instruments used in other physiologic recording and by the same token easier direct correlation with recordings of other physiologic variables.

Direct correlation with auscultatory findings is easier for spectral phonocardiography than for oscillographic phonocardiography. Functionally, the spectral phonocardiograph resembles the ear rather closely and the visual image in the spectral phonocardiogram seems to be rather similar to the auditory impression derived with the stethoscope. For example, we find that physicians untrained in oscillographic phonocardiography learn very quickly, or even recognize at sight, what is being represented in the spectral phonocardiogram. Persons trained in oscillographic phonocardiography often have more difficulties because of the change in the ordinate from intensity to frequency.

REFERENCES[8]

1. Beranek, L. L. *Acoustic Measurements.* New York: Wiley & Sons, 1950, pp. 18, 19.
2. Bertrand, C. A., I. G. Milne, and R. Hornick. A study of heart sounds and murmurs by direct heart recordings. *Circulation* 13: 49, 1956.
3. Bruns, D. L. A general theory of the causes of murmurs in the cardiovascular system. *Am. J. Med.* 27: 360, 1959.
4. Eldridge, F. L., and H. N. Hultgren. Production of heart sounds by the cardiac catheter. *Circulation* 19: 557, 1959.
5. Kleyn, J. B., K. Holldack, and A. A. Luisada. Further international efforts for standardization of phonocardiography. *Am. J. Cardiol.* 4: 675, 1959.
6. Landford-Smith, F. *Radiotron Designer's Handbook.* Sidney, Australia: Wireless Press, 1952, p. 808.
7. Laurens, P., F. Bouchard, E. Brial, C. Cornu, P. Baculard, and P. Soulié. Bruit et pressions cardiovasculaires enregistrés in situ à l'aide d'un micromanomètre. *Arch. mal. coeur* 52: 121, 1959.
8. Luisada, A. A., and R. Zalter. Phonocardiography. III. Design of the ideal phonocardiograph. *Am. J. Cardiol.* 4: 24, 1959.
9. Luisada, A. A., and R. Zalter. A new standardized and calibrated system. *IRE Trans. on Med. Electronics* ME-7: 15, 1960.
10. MacLeod, A. G., and A. E. Cohn. A new piezo-electric manometer to record intracardiac pressure. *Am. Heart J.* 21: 343, 1941.
11. Magri, G., E. Jona, D. Messina, and A. Actis-Dato. Direct recording of heart sounds and murmurs from the epicardial surface of the exposed human heart. *Am. Heart J.* 57: 449, 1959.
12. McKusick, V. A. *Cardiovascular Sound in Health and Disease.* Baltimore: Williams & Wilkins, 1958.
13. Moyer, D. F., and G. D. Talbott. Instrumentation for the diagnosis of coronary-artery disease. *Trans. Am. Inst. Elec. Engrs.* 79: 60, 1960.
14. Rappaport, M. B., and H. B. Sprague. The graphic registration of the normal heart sounds. A graphic analysis of the normal heart sounds. *Am. Heart J.* 23: 591, 1942.
15. Rushmer, R. F., T. A. Tidwell, and R. M. Ellis. Sonvelographic recording of murmurs during acute myocarditis. *Am. Heart J.* 48: 835, 1954.
16. Soulié, P., P. Laurens, F. Bouchard, C. Cornu, and E. Brial. Enrégistrement des pressions et des bruits intracardiaques à l'aide d'un micromanomètre. *Bull. mém. soc. méd. hôp. Paris* 73: 713, 1957.
17. Wallace, J. D., J. R. Brown, Jr., D. H. Lewis, G. W. Deitz, and A. Ertugrul. Intracardiac acoustics. *J. Acoust. Soc. Am.* 31: 712, 1959.
18. Yamakawa, K., Y. Shionoya, R. Nagai, K. Kitamura, T. Yamamoto, and S. Ohta. Intracardiac phonocardiography. *Am. Heart J.* 47: 424, 1954.
19. Zalter, R., H. Hodara, and A. A. Luisada. Phonocardiography. I. General principles and problems of standardization. *Am. J. Cardiol.* 4: 3, 1959.
20. Zalter, R., and A. A. Luisada. Phonocardiography. II. Appraisal and critical analysis of existing systems. *Am. J. Cardiol.* 4: 16, 1959.

[8] Whenever references are not specifically indicated, direction to the pertinent literature (before 1958) is provided in the monograph in ref. 12.

Phonocardiography

DAVID H. LEWIS[1] | *Philadelphia General Hospital and Graduate School of Medicine*
University of Pennsylvania, Philadelphia, Pennsylvania

CHAPTER CONTENTS

[1] Established investigator, American Heart Association. Supported by a grant-in-aid from the American Heart Association, by a research grant (H-2559) from the National Institutes of Health, and by a contract (Nonr 2744-00) from the Office of Naval Research, Department of the Navy.

HISTORICALLY, cardiac acoustics may be said to begin with Harvey (40), and phonocardiography, the graphic representation of cardiac acoustics, with Einthoven (29). Both of these complementary types of information have traditionally been more the province of the clinician than of the physiologist. Although no one would suggest that the pendulum has swung the other way, there appears definitely to be a rise in interest in the physiological aspects of cardiac acoustics and phonocardiography. This shift in emphasis seems to stem from a change in the bases of our knowledge. Until recently, questions raised by cardiac acoustics at the bedside could be answered only by the gross anatomy seen at the autopsy table. With the advent of cardiac catheterization and its related techniques, interest has begun to move away from purely anatomical concepts to thinking in functional terms. The growth of this new body of knowledge, mainly in the field of human cardiovascular physiology, has been rapid and, as of this date, incomplete. The purpose of this communication is to survey what is currently known concerning the physical and physiological bases of heart sounds and murmurs, and to indicate what gaps exist in this information. Since the author's experience has been almost wholly in the field of human cardiac acoustics, the material to be presented will be drawn from this species. However, no attempt will be made here to catalogue the sounds and murmurs in the various types of human cardiac lesions. For those interested, reference should be made to one of the several recent monographs in the field (17, 41, 57, 68, 76, 81) or the two recent symposia (69, 70). Those lesions that seem pertinent will be discussed as they serve to illustrate physiological principles.

Since the following presentation divides itself

sharply into heart sounds and heart murmurs, it would seem wise, at the outset, to define our terms. To the uninitiated and to the musically inclined everything seems really to be noise and, indeed, it is. The division into sounds and murmurs, however, not only is useful clinically and physiologically, but also has some basis in fact, in that it appears that they are caused by different mechanisms, as will be discussed below.

PHYSICAL BASIS FOR THE PRODUCTION OF HEART SOUNDS

The physical factors responsible for the genesis of heart sounds have always been and continue to be an intriguing question for both physiologists and clinicians. It must be admitted that despite the great interest displayed in this subject and the wealth of available published material, there is no explanation universally agreed upon. Many conclusions about cause and effect in heart sound production have been based upon a consideration of those events of the cardiac cycle that occur at the time of the particular acoustic event under scrutiny. Although such evidence is necessary to prove cause and effect, it is, however, not sufficient. A great deal of dispute has arisen perhaps from a desire on the part of many investigators to pinpoint one single responsible factor to the exclusion of all others. The ingenious experiments of Dock (24–26) have pointed toward the valves as the major vibratory structures responsible for the production of vibrational energy sufficiently great to be audible. Rushmer (86) has rightly pointed out that, "Since the chambers of the heart are filled with blood, none of these structures can vibrate independently without producing movements of the blood. Similarly, vibrations in the blood must be transmitted to the surrounding structures. If the sounds can be picked up from the external surface of the body, all structures between the heart and thoracic wall must be vibrating."

Whereas no unified thesis for all heart sounds appears wholly justifiable at this time, it seems likely that the genesis of sounds is related to the acceleration and deceleration of the blood at specific loci within the cardiovascular system, and that associated with such velocity changes vibrations of blood and heart structures are set up. As will be discussed below, each sound is created by specific velocity changes and system vibrations based on the particular physiological circumstances at that time in the cardiac cycle.

PHYSICAL BASIS FOR THE PRODUCTION OF MURMURS

There is general agreement that the source of murmur formation is the development of nonlaminar blood flow. With laminar flow, the fluid particles flow unidirectionally downstream and all the energy is in a direction parallel to the long axis of the vessel. Indeed, the layer that adjoins the wall of the tube does not flow. Consequently, there is no source for the development of vibrations of either the fluid or the vessel in which it flows. With the development of nonlaminar flow, some of the particles move in directions other than parallel to the long axis of the tube. These particles flowing, for example, at right angles to the long axis of the tube (i.e., toward the wall), even flowing directly upstream temporarily, or in any direction, have the potential of setting up vibrations of the fluid and of the vessel in which they are contained. When such vibrations are in the audible frequency range of the human ear they may be perceived as sound.

For many years, physiologists have assumed that the type of nonlaminar flow responsible for murmur genesis was turbulence. Turbulence, for this purpose, may be described as a random distribution of those energies not directed downstream parallel to the long axis of the tube. The flow of the stray particles is "irregularly irregular"; they show no pattern to their "irregularity." This concept has recently been challenged by Bruns (15). He found, in model experiments, that there was insufficient energy produced by these "irregularly irregular" stray particles to produce audible noise. However, the development of nonlaminar flow with what might be called a "regular irregularity" (e.g., vortex formation) could yield sufficient energy to produce vibrations of the fluid and of the vessel wall to create audible noise. One other important source of nonlaminar flow was considered and discarded by Bruns, namely, cavitation. Here he suggested that whereas cavitation would yield sufficient energy to cause audible noise, the hemodynamic circumstances seen in vivo were insufficient to produce cavitation.

At the present time, one might take the following position regarding the physical factors responsible for the genesis of murmurs. Any circumstance that changes the pattern of flow from laminar to nonlaminar has the potential for producing noise (i.e., murmur). Nonlaminar flow is produced under conditions where there is a disparity between the flow rate and the tube (or vessel or chamber) size. Circumstances that increase the flow rate (e.g., exercise, anemia, shunts) or decrease the tube size (e.g., stenosis) or,

decrease the fluid viscosity have the capacity to produce nonlaminar flow, which, in turn, has the potential for producing noise. Whereas it appears that we must abandon turbulence for vortex formation as the type of nonlaminar flow responsible for murmurs, perhaps more experimentation, especially in vivo studies, ought to be carried out to confirm this opinion. Furthermore, although the switch-over from thinking "turbulence" to thinking "vortex formation" is desirable for the sake of accuracy and for what additional data will follow from this, it may well be that, in vivo, circumstances which produce vortex formation simultaneously produce turbulence, as defined here.

PHYSICAL BASIS FOR THE TRANSMISSION OF SOUNDS AND MURMURS

The information on the transmission of heart sounds and murmurs is at present sketchy. It is only with the development of techniques for recording the various acoustic events from their site of origin that any systematic study of this subject has been begun. It must be kept in mind that we are not here using the word transmission in the same sense as used by the clinician. Clinically, the word transmission has been used to signify those areas on the chest other than the area of maximum intensity over which a particular event is heard. For example, one would say that the murmur of mitral insufficiency is heard loudest at the apical region on the chest and is transmitted to the left axilla. Such usage of the word transmission is not in keeping with our present understanding and should be abandoned. Indeed, the murmur of mitral insufficiency is transmitted from its site of origin within the heart to both the apical region of the chest and to the left axilla.

It has been known for a long time that there are areas on the chest wall to which the various acoustic events are preferentially transmitted. For example, all books on human cardiac acoustics show a diagram indicating where the four valves are located within the thorax, and, in addition, the areas on the thorax to which events occurring at these valves are usually preferentially transmitted. Thus, the aortic valve area is at the upper right sternal border. The mitral valve area is in the region of the apical impulse. The pulmonic valve area is at the upper left sternal border, and the tricuspid valve area is variously described at the lower sternal border, right or left, or at the xiphoid. Other sources of acoustics have their own preferential areas.

The factors responsible for this preferential transmission to the chest wall are not completely understood. First and foremost among the apparent causes are the size and position of the heart in the thorax. One can assign so-called valve areas on the thorax because in most patients the heart is in about the same place in the thorax. However, important exceptions occur so that this point must be kept in mind. For example, in mirror image dextrocardia, since the position of the heart is a mirror image of the normal, it is logical to expect that the chest wall areas are also a mirror image of the normal, and such is the case. Of importance too is the direction of blood flow. This appears to be of greater importance for the transmission of murmurs than for heart sounds, but the extent to which each type of acoustic event depends upon blood flow for its transmission remains to be settled. Studies of murmurs from within the heart by a number of groups demonstrate clearly that murmurs are, in the main, transmitted in the bloodstream from their point of origin downstream and not upstream. Thus, for example, the murmur of aortic stenosis created at the aortic valve during systole when the blood is flowing away from the heart is transmitted not only to the aortic area on the chest but also to the neck. On the other hand, the murmur of aortic insufficiency, created at the aortic valve during diastole when blood is flowing abnormally back into the left ventricle, is transmitted not only to the aortic area, but often more loudly to the left sternal border and to the apical region.

There are other factors known which determine the transmission of sounds to the chest. These affect, by and large, the over-all intensity and perhaps the frequency that reaches the chest wall and would appear to alter the distribution of noise on the thorax only as they affect the above considered factors of heart size, position, and direction of blood flow. The presence of fluid in or fibrous thickening of the pericardium may reduce the intensity of sound that reaches the chest wall. It has generally been assumed that this is due to interference with sound transmission, but interference with sound production has not been ruled out. On two occasions we have had the opportunity of studying the intracardiac sounds in patients with pericardial thickening. In neither did it appear that the sound intensity within the heart was diminished. However, the sound intensity on the thorax in both cases was not remarkably reduced and this point remains unsettled in our minds.

The position and degree of aeration of the lungs also seem to play a role in sound transmission. It has

been known for a long time that patients with pulmonary emphysema in which situation there is more air-breathing tissue, a poor sound conductor, between the heart and the chest wall than in the normal, have decreased intensity of heart sounds. The few cases of emphysema that we have studied with the intracardiac phonocardiogram would seem to bear out this contention, but more examples are needed.

Although the above information is interesting and there are now techniques for comparing sound intensity and frequency within the heart with that on the chest wall, many questions remain unanswered. Exact data on the energy decrement are lacking. The form in which the vibrations are transmitted by the thoracic tissues is not known, and the nature of the acoustic coupling between the various tissues remains to be discerned.

PHYSIOLOGICAL BASIS OF ACOUSTICS

Relationship of Heart Sounds to Events of the Cardiac Cycle

Since the acoustic events are determined by the mechanical activity of the cardiac structures, any attempt at understanding acoustics must be based on a firm understanding of the events of the cardiac cycle.

Consider first the relationship between the acoustic events and the intravascular pressures as displayed on one side of the heart. Figure 1 shows the heart sounds and the intravascular pressures from the great vessel, ventricle, and atrium. The data apply to either the right heart or the left heart. The following features of the intravascular pressures are important to our discussion and should be noted. With the onset of mechanical activity of the ventricle, the ventricular pressure rises rapidly to a peak (or more often a plateau). As it rises it becomes first greater than the atrial pressure and then a short, but nonetheless appreciable time later becomes greater than the pressure in the great vessel. The rise of ventricular pressure above atrial pressure is associated with closure of the atrioventricular valve (mitral or tricuspid), and the rise of ventricular pressure above great vessel pressure is associated with opening of the semilunar valve (aortic or pulmonic). The motion of these two valves is not synchronous. There is a definite time interval between them. This interval, during which the ventricular pressure is rising with no change in ventricular volume, since both inlet and outlet valves are closed, is called the period of isometric (or more properly, isovolumetric) contraction. With the cessation of ventricular mechanical activity ventricular pressure drops first below great vessel pressure and this is associated with closure of the semilunar valve. Shortly thereafter the ventricular pressure falls below atrial pressure, at which time the atrioventricular valve opens. Again, note that these two events do not occur simultaneously. There is, therefore, a period of isovolumetric relaxation, during which ventricular pressure is falling and both valves are closed. The significance of these two isovolumetric periods to the acoustic events will be made more apparent below.

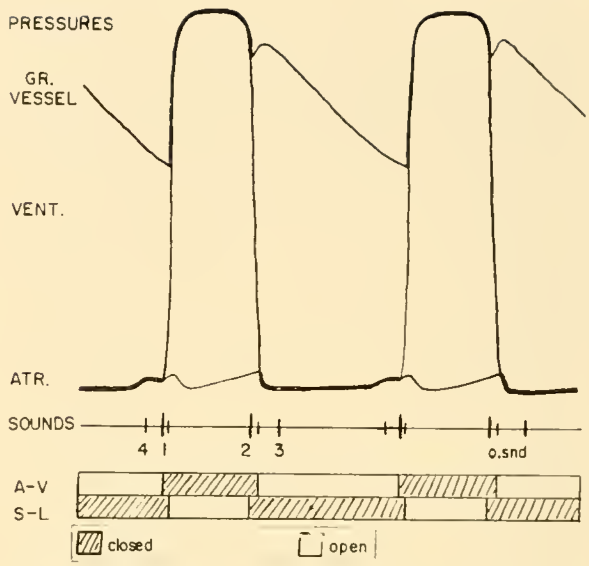

FIG. 1. Relationship of intravascular pressures to heart sounds. Simultaneous pressures from great vessel, ventricle, and atrium from one side of the heart. Normal heart sounds also from one side of the heart: fourth (4), two components of first sound (1), occurring with closure of the atrioventricular valve and opening of the semilunar valve, second sound (2), opening sound of the atrioventricular valve (o. snd) (put in for the sake of completeness), and third sound (3). Action of valves: atrioventricular valve (A-V) and semilunar valve (S-L). The hatched area indicates the interval during which the valve is closed, and the clear area the interval during which the valve is open. The valve motion is almost but not quite reciprocal. There are two intervals, one at the onset and one at the end of mechanical activity of the ventricle during which both valves are closed.

With the rise of ventricular pressure above great vessel pressure note that the direction of the great vessel pressure curve changes abruptly and becomes virtually identical with that in the ventricle, and that when ventricular pressure falls below great vessel pressure the two go apart from one another. During the time that the semilunar valve is open, therefore, these two pressures are similar, and when the semilunar

valve is closed they are dissimilar. In the same way, note that comparison of the atrial and ventricular pressures reveals that they, too, are similar during the period of time that the atrioventricular valve is open, and are dissimilar when it is closed. This consideration of similarity and dissimilarity will become important when the subject of valvular pathology is discussed. For, here, pressures that were similar become dissimilar and vice versa, and the degree of change is related to the severity of the valvular lesion, which, in turn, is related to the acoustic manifestations produced.

It should be further noted that there are three positive (upward) deflections in the atrial tracing and two negative (downward) deflections. With the onset of mechanical activity of the atrium (mechanical systole) there is a rise in the atrial pressure. This is the first positive wave, the *a* wave, and it carries with it the ventricular pressure curve. Early in mechanical ventricular systole there is the second positive wave, the *c* wave, currently ascribed to transmission of ventricular pressure through the closed atrioventricular valve which at this point is said to be bulging back into the atrium. This is followed by the first negative wave, the *x* descent ascribed to the movement of the atrioventricular ring away from the atrial cavity which makes for a potential enlargement of the atrial cavity. This explanation, it should be noted, has been challenged by Wood (107, p. 48). This is followed by the gradual rise of atrial pressure as the atrium fills up to the third positive wave, the *v* wave. At the time of the opening of the atrioventricular valve the atrial pressure falls along with the ventricular pressure and produces the second negative wave, the *y* descent. The importance of these waves to acoustics will be considered in more detail when the subject of valvular pathology is discussed. They also are of importance in understanding the nature of the waves of the jugular venous pulse.

With this abbreviated background of the nature of the intravascular pressure phenomena, consider now the factors that would be responsible for acceleration and deceleration of blood at specific loci within the cardiovascular system, and thereby result in vibrations of blood and heart structures. Reference has already been made to the consideration of valves as the major vibratory structures. A moment's reflection will recall that many factors play a role in the manner in which the valves move. For example, the closure of the atrioventricular valve depends certainly on the nature of the valve structure, on the chordae tendineae, and on the papillary muscles. It surely is dependent on the time course of mechanical ventricular activity, on the state of the ventricle in the preceding diastole, and on the contribution of atrial contraction to ventricular filling, and, undoubtedly, on other factors too. The mere fact that all of these events contribute to the manner of closure of the atrioventricular valve suggests that perhaps some type of analysis of this heart sound has the potential of yielding valuable physiological information on these various factors. We may never learn how to extract these data from the first sound, or similar information from other acoustic events, but to attempt to pinpoint cause and effect, when the information is obviously so scanty, in this author's opinion is not helpful at present.

FIRST HEART SOUND. Whereas it is true, therefore, that no single structure can be considered to be vibrating independently, it appears from our data and from those of others that the first heart sound complex occurs at the time of valve motion, during the period of ventricular contraction. There is a component which coincides with the closure of the atrioventricular valve, and a second component associated with the opening of the semilunar valve. These appear to be the major components visible on a phonocardiogram and represent the acoustic events that may be audible, though not necessarily separable into two distinct events. The relationship of the sound components to valve motion becomes clearer when circumstances, such as disease, alter the time at which the various mechanical and acoustic events occur. For example, in the normal, the beginning of mechanical activity of the ventricle, the rise of ventricular pressure above atrial pressure, and the closure of the atrioventricular valve are very closely related in time. When there is stenosis of the atrioventricular valve, there is a readily measurable gradient of pressure between atrium and ventricle at the onset of mechanical activity of the ventricle. It is possible in this situation to see that the first component of the first sound complex occurs not with the onset of mechanical activity of the ventricle but rather with the rise of ventricular pressure above atrial pressure. Of further interest in this regard is the complementary observation that when the valve is prevented by disease from closing as in the case of atrioventricular regurgitation (or insufficiency), despite the fact that mechanical contraction is forceful, there may be no noticeable first component to the first sound complex. The value of such observations in disease is that they represent experiments of nature not wholly reproducible in the human physiology laboratory at this time, and permit a glimpse into the situation in which contraction of the myocardium

and valve motion are separable. We have attempted such a separation in normals, but with little success. It seemed possible that the technique of Reale *et al.* (82) developed for the purpose of measuring valve area in vivo could be applied to this problem. They suggested that the area of the tricuspid valve could be measured in man if a balloon on a catheter in the right ventricle was inflated and drawn back through the valve into the atrium. The size that could be just gotten back across the valve could then be used to calculate valve area by reproducing the experiment with the same volume in the balloon outside the body. We felt that recording sounds, both within the heart and on the thorax, when the balloon was in the valve orifice and preventing the valve from closing, but not interfering with myocardial contraction (in the first cycle), would allow for the separation of these two events and cast some further light on the first sound. A few tries at this revealed the technical difficulties involved and no conclusive results were obtained. However, furthei experimentation along this or similar lines might well reveal some interesting information.

SECOND HEART SOUND. The sole mechanical event that can be related to the second heart sound is the closure of the semilunar valve. Since both closing of the atrioventricular valve and opening of the semilunar valve are considered to play a part in the make-up of the first sound complex, there would appear to be no physiological reason to limit the second heart sound

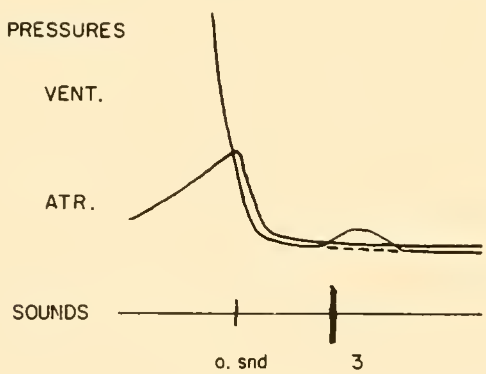

FIG. 2. Suggested mechanism of third sound indicating transient A-V valve closure. The pressures are of ventricle and atrium. Only that part of the cycle from shortly after the closure of the semilunar valve (not shown here) to mid-diastole is shown. The ventricular pressure falls below atrial pressure at which time the atrioventricular valve opens as indicated on the sound tracing as the time of the opening sound (o. snd). Early in diastole the ventricular pressure according to this suggested mechanism rebounds at which time the protodiastolic sound (3) occurs. The dotted line is the normal course of the ventricular pressure. [Adapted from the work of Warren *et al.* (102).]

to closure of the semilunar valve and not include the immediately following event of opening of the atrioventricular valve. However, traditionally, opening of the atrioventricular valve, if audible or even if only seen on a phonocardiogram, is not considered part of the second heart complex. It will not be considered so here. Again, in the case of the second sound, the evidence that acoustics is closely related to valve motion is strong. For example, the absence of the semilunar valve or its failure to close when disease is present is associated with absence of the second sound.

THIRD HEART SOUND. Although the relationship between valve motion and acoustics can be demonstrated for the "systolic" sounds (i.e., first and second sounds), the precise physical correlate for the "diastolic" sounds (i.e., third and fourth sounds) remains the subject of vigorous investigation. Both of these sounds occur at periods of rapid ventricular filling. The earlier third heart sound occurs during the initial rapid filling phase when the ventricle fills passively in relation to the atrioventricular gradient. The latter, fourth sound, occurs during the second phase of rapid filling, when, near the end of ventricular diastole, the ventricle receives additional blood by active atrial contraction.

For the third heart sound it has long been held that the vibrations heard are those set up by the motion of the mass of ventricular muscle (along with the blood) caused by the rapid inrush from the atrium (77, 104). The time of occurrence of the sound, at the end of the rapid filling phase (46–48) fits with the concept that the sound is associated with or caused by the "checking" of ventricular motion, as it reaches the limit of free distensibility.

In recent years, this mechanism has been challenged. It has been shown that at the end of the rapid filling phase, ventricular pressure may transiently rise above atrial pressure, thus setting the stage for transient closure of the atrioventricular valve (27, 101, 102) (see fig. 2). From this observation it has been suggested that, like the first and second sounds, the third sound is the product of valve closure. At the present time, it does not appear that all investigators agree as to what part valve motion and/or ventricular "checking" play in the causation of the vibrations that produce a sound in early diastole, both in the normal and in disease. In our own studies we have observed a sound in early diastole when it would appear that ventricular pressure did not rise above atrial pressure, but we have also seen situations in which there was a marked rebound of ventricular pressure early in diastole certainly great enough to carry it above atrial pressure

and associated with a sound. What does seem pertinent is that further study with an approach more direct than correlation of acoustics with intravascular pressure is needed to identify the precise physiological events that occur at the time of the production of the third heart sound.

FOURTH HEART SOUND. As noted above, this sound occurring in presystole comes as a result of atrial mechanical activity. Its relationship to atrial mechanical activity is clear, for as the relationship between atrial and ventricular mechanical activity changes, so does the relationship between the fourth heart sound and those produced by mechanical activity of the ventricle. Changes in the length of the P-R interval are associated with like changes in the interval between the fourth and first heart sounds, and when the atrium no longer contracts, as in atrial fibrillation, the fourth sound disappears. For this sound, perhaps above all, the precise physical correlate responsible for its genesis remains to be established. It has only been with studies of sounds from within the heart that the true frequency of occurrence of this acoustic event has been appreciated (58). Whereas it is a rare event in chest phonocardiograms, it is the rule rather than the exception in intracardiac phonocardiograms. It may well be that this sound, like the third sound, is related to either motion of the atrioventricular valve (or some other valvular motion) or primarily to vibration of the wall of the ventricle. We have not seen, in our pressure recording, any concrete evidence that at this time ventricular pressure rises above atrial pressure. For this event, therefore, one might well be justified in saying that transient closure of the atrioventricular valve does not occur. Furthermore, vibrations originating in the ventricle cannot always be responsible either. We have made observations of the fourth sound from within the right atrium in a patient with a complete heart block. When atrial contraction occurred during ventricular systole, the fourth sound was still present, despite the fact that there could be no flow into the ventricle at this time. It may well be that this sound arises out of the vibrations set up by the muscular contraction of the atrium, and, although not independent of vibrations of blood, may be independent of translation of blood with or without valve motion. The problem is further complicated by the suggestion that there may well be two sets of vibrations rather than one. Some of our recordings have suggested the presence of secondary vibrations of greatest intensity in the ventricular inflow tract (we have studied this only in the right ventricle) following the vibrations described above, and at a time when one might expect inflow of blood into the ventricle. The fate of these in the presence of complete heart block is not known to us.

In summary then, when one considers the relationship between the acoustic events and the intravascular pressures as displayed on one side of the heart, there are six separate events at which normal heart sounds may occur: the two components of the first heart sound complex associated with atrioventricular valve closure followed closely by semilunar valve opening, the second sound associated with semilunar valve closure, which is closely followed by atrioventricular valve opening, followed, in turn, by the third sound of early rapid filling, and finally, by the fourth sound at the time of late rapid filling.

Consider now the actual circumstance, namely, that there are two sides to every heart, and consequently twelve separate acoustic events with each cycle. It is necessary now to determine, from the order of the mechanical events of the two circuits, the order of the twelve acoustic events. For this purpose it may be more meaningful to begin with the true beginning of the cycle, the depolarization of the sinoatrial node. Electrical activity spreads from here to the right atrium and by direct continuity to the left atrium, and, as expected, therefore, the mechanical activity begins first in the right atrium. From this view of the cycle the first acoustic event is the fourth heart sound from the right atrium, followed by the fourth heart sound from the left atrium. Figure 3, adapted for this presen-

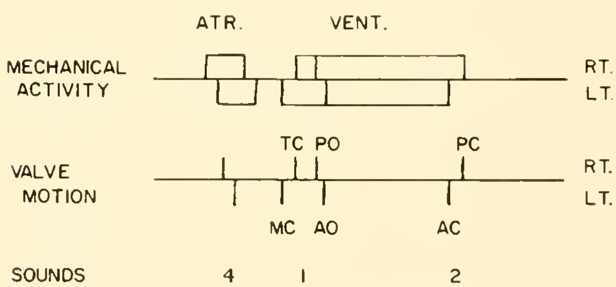

FIG. 3. Relationship of order of mechanical activity to valve motion and sounds. The order and duration of mechanical activity is shown for each chamber. Right heart events are above the line, left heart events below. In addition the duration of isometric contraction for each ventricle is shown. Valve motion is depicted showing the order of events: mitral closure (*MC*), tricuspid closure (*TC*), pulmonic opening (*PO*), aortic opening (*AO*), aortic closure (*AC*), and pulmonic closure (*PC*). At the bottom are shown the sounds: the two atrial sounds, the four components of the first sound, and the two components of the second sound. [Adapted from the work of Braunwald *et al.* (10).]

tation from the work of Braunwald *et al.* (10), shows the order of mechanical activity of the four chambers.

Whereas the electrical activity and mechanical activity of the atria begin first on the right side, the electrical and mechanical activity of the ventricles begin first on the left. Since the initial depolarization is on the left side of the interventricular septum (72, 89), considered to be part of the left ventricle, it is not unreasonable, therefore, that mechanical activity begins first on the left. However, whereas the onset of mechanical activity occurs first on the left side, ejection begins first on the right side. With these two pieces of information it is possible to construct the order of events of valve motion at the onset of systole and from the order of the acoustic events of the first sound complex. As stated, the first event is the onset of left ventricular contraction, followed by the onset of right ventricular contraction, then right ventricular ejection begins, followed, finally, by the onset of left ventricular ejection. From this, the order of valve motion, and the four apparent components of the first heart sound complex would be: closure of the mitral valve (MC), closure of the tricuspid valve (TC), opening of the pulmonic valve (PO), and the opening of the aortic valve (AO) (64, 67). What relationship these four separate events bear to the make-up of the first sound complex, as seen in the usual chest phonocardiogram, remains to be determined. Classically, four sets of vibrations have been described for the first heart sound complex as seen in the chest phonocardiogram (77) and it might seem at first that a ready explanation is available, since there are four distinct valve motions. This, however, has not been the classical explanation. Moreover, although there may be several sets of small vibrations, the major ones most often appear to be only two in number. Our thought in this matter has been that most often the first loud vibration can be associated with closure of the mitral valve. In the normal there appears to be difficulty in assigning any given vibration to closure of the tricuspid valve. Since the acoustic events from the left side of the heart are louder than those from the right side, it may be that valve motion of this side predominates in the acoustic representation of the first sound. Again, it is difficult to say what part opening of the pulmonic valve plays in this. The physiological value of such a precise mechanical-acoustical correlation resides in the fact that proper identification of valve motion at the time of ventricular contraction provides a relatively simple way of quantitating the duration of isometric contraction.

Figure 3 also shows that the cessation of ventricular mechanical activity occurs first on the left side. Consequently, it is to be expected that closure of the aortic valve (AC) precedes closure of the pulmonic valve (PC). From this asynchronous occurrence of semilunar valve closure it would be expected that there would be two components to the second sound, and such is the case. The importance of this observation rests in the physiological correlates possible. First, the presence of two components to the second sound identifies the presence of two semilunar valves. Second, proper identification of the source of each component allows for certain deductions about the state of affairs on that side of the heart. Third, since conclusions made from point two depend on the source of the acoustic event and not on the site on the chest wall to which the event is transmitted, they are more rigorous. Furthermore, consideration of this point leads to the conclusion that terminology based solely on the site on the chest to which the acoustic event is transmitted is not in keeping with the breadth of current knowledge and deprives one of potentially valuable information. It has, therefore, been suggested that the terminology regarding the second sound be altered to refer not to location on the chest but to site of origin within the heart (50).

The information regarding the order of events of atrioventricular valve opening is small but it would appear that the opening of the tricuspid valve precedes the opening of the mitral valve (67). This point will be dealt with in more detail when the correlation between the acoustic events and the jugular venous pulse is discussed. It must also be stated that only a small amount of information regarding the order of events with respect to the early diastolic sound in the normal is available. Simultaneous observations from within each ventricle by Luisada and associates (64) indicate that the third sound from the right ventricle precedes that from the left. Our studies suggest that the third sound is not commonly observed within the cavity of the right ventricle.

In summary then, comparison of the order of events of all 12 of the theoretically possible normal sounds indicates that starting with the depolarization of the sinoatrial node there occurs: *1*) the right atrial component of the fourth heart sound, *2*) the left atrial component of the fourth heart sound, *3*) the mitral valve closure component of the first heart sound, *4*) the tricuspid valve closure component of the first heart sound, *5*) the pulmonic valve opening component of the first heart sound, *6*) the aortic valve opening component of the first heart sound, *7*) the aortic valve closure component of the second heart sound, *8*) the

pulmonic valve closure component of the second heart sound, *9*) the opening of the tricuspid valve, *10*) the opening of the mitral valve, *11*) the right ventricular third heart sound, and finally *12*) the left ventricular third heart sound. This order must be considered tentative and in need of further documentation.

Relationship Between Acoustic Events and Other Physiological Parameters

Although it is clear that the closest physiological parameter, that is readily measurable at the present time, is the intravascular pressure, it is not always practicable nor desirable to carry out such a comparison. In such circumstances other phenomena may be used to substitute for certain of the wished-for mechanical correlates. Rather than obtaining the correlate from within the heart, phenomena seen "on the surface" of the body are used, in much the same way that the heart sounds "on the surface" of the body are used in lieu of information from the source.

ELECTROCARDIOGRAM. This parameter is certainly the most venerable and although it has clear-cut benefits, its limitations must be recognized. First in its favor is the ease with which technically satisfactory recordings can be obtained. Second, it is the least liable of all the "surface" phenomena to deceive one in differentiating systole from diastole. However, since precise electrico-acoustical correlation has not yet been established and since this may well vary under differing circumstances, the differentiation of systole from diastole, by this method, is less exact than when mechanico-acoustical correlation is used. That is to say, that although the electrocardiogram can be used to establish the onset, duration, and end of both electrical systole and diastole, it can only approximate these findings for mechanical systole and diastole. Its greatest value appears to lie in its ability to place sets of acoustic vibrations into certain classes of events and ruling out their placement in other sets. The basis upon which this can be done is the well-known fact that electrical events always precede mechanical events of the same order. So that, for example, a set of vibrations postulated to represent the fourth heart sound must succeed the P wave of the electrocardiogram. If they precede this electrical event the suggested identification is then known to be false. Similarly, the first sound must follow the onset of the QRS complex. Having established that the vibrations follow their electrical counterpart, there are rough guides as to the minimum and maximum allowable intervals, but, as stated previously, precise quantitation has not been established, and indeed may be physiologically impossible. What physiological knowledge is to be gained from the elucidation of this parameter remains to be established. There is clearly no consistent relationship between the second sound and the T wave of the electrocardiogram, though a possible relationship with the U wave exists, which deserves further investigation. The electrico-acoustical relationships for the atrioventricular valve openings and third sounds are not known.

JUGULAR VENOUS PULSE. Since, in the human, there are no valves between the right atrium and the jugular vein, pressure phenomena in the former are well reflected in the latter. The jugular venous pulse can therefore be used as a "surface" phenomenon reflecting the mechanical events within the right atrium, i.e., from the "source." A number of workers have studied the time delay between right atrium and jugular vein, and reached different conclusions (28, 38, 46, 49, 107, p. 164). The problem appears to lie in the different techniques used, and any laboratory attempting correlation between acoustic events and jugular venous pulse should certainly establish its own figures. The recording obtained from the neck resembles the source not only in time-course of events but also in the shape and magnitude. In this way information can be obtained about the three positive and two negative deflections. Concerning the deflections, one technical problem presents itself. This is the extent to which the pulsations of the carotid artery may interfere with bona fide venous pulsations. Depending upon the technique and the presence of abnormally increased systolic expansion of the artery, the *c* wave may represent in part or in full a carotid artery event. For this reason few workers have confidence in their conclusions regarding this particular wave in the venous pulse. A rigorous solution to this problem, however, has not been carried out. It must be remembered that the data reflect only right atrial events which can safely be correlated, if desired, with right ventricular events. The jugular pulse does not and cannot reflect the time-course, magnitude, or the shape of the deflections in the left atrium, and therefore cannot safely be correlated with left ventricular events. It is only in the special circumstance, in which a defect in the atrial septum of size sufficient to render the two atria into one hemodynamic chamber, that the jugular pulse wave would bear any relation to left atrial activity.

Since there is a reliable correlation between right

atrial hemodynamics and the jugular venous pulse, acoustico-mechanical correlates can be made which can be used to reflect hemodynamics. For example, the pulmonic component of the second sound denotes the beginning of the phase of isometric relaxation of the right ventricle. The beginning of the *y* descent of the jugular venous pulse, indicating the opening of the tricuspid valve, denotes the end of this phase. Therefore, the interval between these two events is a measure of the duration of right ventricular isometric relaxation. Abnormal increases in this interval have been used to indicate pulmonary hypertension (39). Disease of the tricuspid valve, both stenosis and insufficiency, if it reflects itself in changes in right atrial hemodynamics, can be detected in the jugular pulse. Similarly, decrease in right ventricular distensibility with increased force of right atrial contraction, as seen, for example, in severe pulmonic stenosis, primary pulmonary hypertension, and others, will be reflected in an increased amplitude of the *a* wave.

A thoroughgoing study of the jugular venous pulse and its relationship to the acoustic events of the heart has been published by Altmann (1) and should be consulted by those interested.

CAROTID ARTERY PULSE. This surface phenomenon reflects directly the time-course, amplitude, and shape of the pulse of the carotid artery, and, indirectly, of the aorta. Here the time delay is agreed upon to be appreciable, should be measured by those who are using this parameter to correlate with acoustics, and must always be taken into account when used. Again, no thoroughgoing analysis of the relationship between aortic and carotid pulse times has been undertaken for the variety of disease states. It is known that the dicrotic notch of the wave occurs simultaneously with aortic valve closure and traditionally all measurements of time delay are made from this feature. Here again the implication is made that over this short distance of arterial tree all phases of the wave travel with virtually the same velocity, an assumption which needs to be investigated. This has greatest bearing, perhaps, on the attempts to define the duration of left ventricular isometric contraction as the interval from mitral valve closure (the first loud part of the first heart sound) to the beginning of the upstroke of the carotid pulse corrected by moving the whole curve forward until the dicrotic notch coincides with the aortic valve closure sound.

The unfortunate feature of the problem of the time delay of the pulse reaching the carotid artery is that it tends to complicate the usefulness of this phenomenon in identification of the components of the second sound. Using a mean figure for time delay one can often be satisfied as to which component is which. However, this is not always the case. Since there is no synchrony of aortic valve closure with the dicrotic notch (as recorded) it can be seen that should any part of the second sound coincide with this event, it is thereby ruled out as aortic valve closure, as is any event that follows the dicrotic notch. These points are often useful.

Disease of the aortic valve, both stenosis and insufficiency, if it alters central aortic dynamics, will be reflected in the carotid artery pulse contour. Since, oftentimes, the degree of valvular involvement is reflected in the change in central aortic pulse contour, one may be permitted to see the same correlation with the carotid pulse (22).

Pulse tracings of arteries more distally situated (i.e., brachial, radial, femoral) may be recorded. They have a value in assessing certain aspects of the arterial circulation, but the uncertainties of transmission time make them unreliable as correlates of the acoustic events of the heart.

LOW FREQUENCY RECORDINGS FROM THE THORAX. In much the same way that vibrations in the audible frequency range are transmitted to the chest wall, vibrations of lower than audible frequency are also transmitted. These are due apparently to changes in the size, shape, and position of the heart and great vessels during the cardiac cycle. The most commonly used are those caused by the impingement of a cardiac or vascular structure against the anterior and left lateral thoracic wall. These include, in the main, the two ventricles, the pulmonary artery, and at times the aorta. They are not direct mechanical correlates in the sense that intravascular pressures or pulses, or their surface representations are, but they do serve as correlates, since they reflect certain definite events. To say that they represent well-defined events would perhaps be overstating the case, since here too a rigorous appraisal of the detailed etiology of these vibrations in various disease states is not available.

The most frequently used in empirical clinical correlations are those due to ventricular activity. Since either ventricle may be the responsible agent it must be remembered that before acoustic correlation can be carried out the responsible ventricle must be identified. It has been suggested that this can be done with the precordial electrocardiogram (37). Rivero Carvallo's

warnings about the "false apex impulse" in right ventricular enlargement are well worth remembering in this regard (85).

The feature of the so-called apex cardiogram most commonly utilized in diagnosis is the nature of the outward (toward the thorax) movement of the ventricle during diastole. During this period the recording, as traditionally obtained, shows a continuous rise from the onset of ventricular filling to the end of the phase of rapid filling when the outward movement either ceases or is impeded. It is at this latter point that the third sound and/or the protodiastolic gallop sound occur. It is also the point at which the diastolic sound of constrictive pericarditis occurs. The opening snap of the atrioventricular valve coming before the end of rapid filling precedes this point. Since it heralds the opening of the atrioventricular valve and the onset of ventricular filling it occurs at the bottom (o point) of the recording which denotes the beginning of the early filling phase.

The feature of the vibrations recorded over the great vessels (e.g., pulmonary artery cardiogram) most frequently used is the recording of semilunar valve closure. In this respect, the tracing is a counterpart of the tactile sensation called the diastolic shock felt, at times, over the thorax in the region of the pulmonary artery in certain disease states. Other mechanico-acoustical correlates have been studied. These include the ballistocardiogram (65) and the electrokymogram (66). These will not be discussed here.

Effect of Respiration on Heart Sounds

The major effect of respiration on heart sounds has been noted on the second sound. Whereas there are certainly changes in intensity of the other sounds with respiration (as will be discussed below briefly), and there may well be changes in their appearance time, the greatest study thus far has centered around semilunar valve closure. The effect of respiration on the appearance time of the components of semilunar valve closure is now well known, but at present the precise mechanism of this effect in humans can only be surmised. This is due mainly to the lack of methods for precise measurements of stroke output, beat by beat.

Consider first the train of events that might be expected to occur on the right side of the heart following inspiration. Inspiration lowers intrathoracic pressure. Since the vessels returning blood to the right heart connect with vessels that lie outside the thorax, and since they are exposed to atmospheric pressure, the gradient of pressure between extrathoracic and intrathoracic vessels increases. This is somewhat greater when one considers the return from the intra-abdominal vessels, since inspiration tends to increase intra-abdominal pressure. The result is that inspiration increases venous return to the right heart. The response of the right ventricle to this increase in venous return is an increase in stroke output (Starling). As the stroke volume increases, and thereby the right ventricular work, the duration of mechanical systole increases. The increase in the duration of mechanical systole results in a delay in the appearance time of the pulmonic component of the second sound. Consider now the effect of inspiration on the left ventricle. Here again one must start with the lowering of intrathoracic pressure. However, in this case the venous supply to this ventricle lies wholly within the thorax. One must consider the effect of inspiration on the vascular volume of the lung to find the answer to the effect of inspiration on return to the left ventricle. This information is far from complete, but some studies in the past by a number of workers have suggested that with inspiration the volume of blood in the pulmonary capillary bed decreases (7, 80, 98), that blood is, perhaps, squeezed out of these vessels. Such an effect would be expected to result in an increase in return to the left ventricle. As will be seen below, this is not in keeping with the effect of inspiration giving an earlier time of aortic valve closure. This observation fits better with inspiration resulting in a decrease in return to the left heart. A way out of this seeming paradox has been provided by Howell *et al.* (42), who suggest that the effect of inspiration on the pulmonary vessels depends in large part on the particular segment involved. Since the capillaries run in the alveolar septa, it is reasonable to suppose that they may be squeezed during alveolar expansion and thereby contain less blood. However, the arteries and veins which lie in the interstices of the lung will tend to be pulled open as the lung expands and their vascular volume thereby increased. One needs only to suggest that the volume of these vessels is greater than that of the capillaries, and overbalances them, to arrive at the hoped-for conclusion that inspiration increases the vascular volume of the lung. Verification of this hypothesis is much needed. If we use this supposition for the moment, then, since there is a greater potential room for blood in the lung, inspiration would be expected to reduce venous return to the left heart. From this it follows that stroke volume and thereby stroke work and thereby the duration of mechanical

systole are all reduced. This would result in an earlier appearance time of aortic valve closure and the aortic component of the second sound.

From the acoustic standpoint the effect of inspiration is to cause the aortic component of the second sound to come earlier and the pulmonic component to come later (9). Since normally aortic closure precedes pulmonic closure, inspiration has the effect of increasing the gap between these two events, and can, thereby, produce splitting of the second sound. Components that could not be distinguished as separate events may now be so recognized. Components that could be recognized may now be heard to be further separated. The importance of this observation is severalfold. First, by separating the components in time two events may be observed and, as discussed above, certify that there are two semilunar valves. Second, the increase in splitting further certifies that respiration is affecting semilunar valve closure, which is the normal circumstance. Third, the increase in splitting means that aortic closure precedes pulmonic closure, which again is the normal phenomenon. All three points provide valuable acoustic information, since any deviation from this may well be associated with some abnormality. Points one and two need no further elaboration, but point three deserves some clarification, as to why an increased degree of splitting with inspiration identifies the order of the components. Consider the various possible orders of events of semilunar valve closure. First, aortic closure precedes pulmonic valve closure, even though they cannot be heard as two separate events. Inspiration will increase the splitting by the mechanism noted above. Second, both events truly occur simultaneously. Here, again, inspiration will increase the splitting and again, although not separate before inspiration as they become separated with inspiration, aortic closure comes first. Third, and finally, pulmonic closure may precede aortic closure. In this case, as in the other cases, inspiration can only cause pulmonic closure to be delayed, if it affects its time of appearance. It cannot make it come earlier. Similarly, inspiration can only cause aortic closure to come earlier, if it affects its appearance time. It cannot delay it. Therefore, with inspiration the two components approach each other and the splitting decreases or disappears if the events become synchronous. In this circumstance therefore, when pulmonic closure precedes aortic closure, inspiration decreases rather than increases the degree of splitting. There is the theoretical possibility, still unexplored, that with pulmonic closure preceding aortic closure, inspiration may not only cause the splitting to decrease, then disappear, but then reappear again as, in effect, the two components cross each other, and perhaps go on to an even greater degree of splitting than before inspiration. Such an observation would be detrimental to the thesis that respiration can be used to identify the components of the second sound. The fact that this example just cited does not seem to occur suggests that although respiration can alter the duration of mechanical systole it cannot alter it to such a magnitude as to cause that great a shift in the components of the second sound. Since the theoretical possibility discussed does not occur, it means that changes in the splitting of the second sound with respiration can be used to identify the components of the second sound.

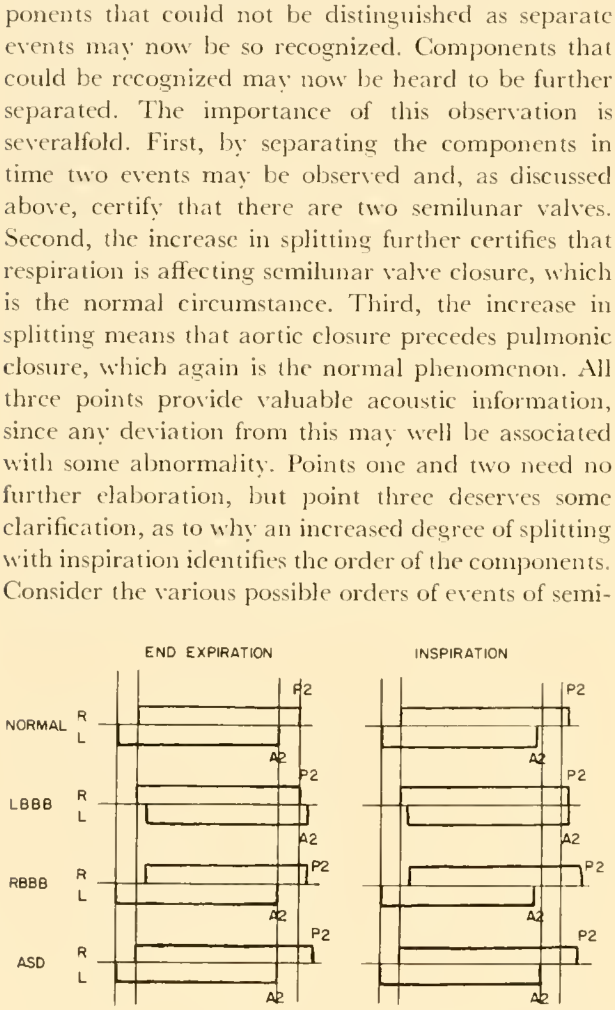

FIG. 4. Effect of respiration on mechanical activity and second sound. The presentation is similar to that shown in fig. 3. Atrial events are not shown, nor is the duration of isometric contraction. The vertical lines indicate the onset and end of mechanical activity of each ventricle as it is for the normal at the end of expiration. The onset of mechanical activity for left bundle branch block (*LBBB*), right bundle branch block (*RBBB*), and atrial septal defect (*ASD*), as depicted here, are subject to revision as the matter is currently in dispute. However, there is general agreement as to the effect on the components of the second sound, aortic closure (*A2*) and pulmonic closure (*P2*). See text for detailed description.

In summary, an increase in the degree of splitting with inspiration means that aortic closure precedes pulmonic closure (at least during inspiration), a normal finding. A decrease in the degree of splitting, or disappearance with inspiration, means that pulmonic closure precedes aortic closure, an abnormal finding, and one that requires investigation. The circumstance in which pulmonic closure precedes aortic closure has been termed paradoxical splitting of the second sound (36). This is an unfortunate term in that it does not convey precisely what has occurred. Furthermore, it may convey the erroneous impression that there is also some difference in the respiratory response, which is not the case. Indeed there is no

paradox. A more satisfactory term would be reversed splitting of the second sound with a normal respiratory response. The circumstances that produce this will be discussed below. It should be obvious that expiration, which increases intrathoracic pressure, induces a train of events in each side of the heart opposite to that described for inspiration. The effect of respiration on the appearance time of the second sound in the normal and in three other situations, discussed more fully below, is depicted in figure 4.

In addition to changing the appearance time of the second sound, respiration also may alter intensity. Inspiration by increasing the flow through the right heart has the tendency to increase the intensity of the sound. The second sound shows this definitely, the first not so well. It also increases the intensity of the diastolic sounds originating in the right heart and can be used as a means of identifying their site of origin. Chest phonocardiograms show it for the fourth sound, and for the presystolic gallop sound, sometimes quite well but at other times less well. On the other hand, intracardiac recordings of these two presystolic sounds usually show quite marked respiratory variations.

Effect of Alterations in Electrical Activity on Heart Sounds

Since the nature of the initiating electrical signal determines in large part the succeeding mechanical phase, it is not unexpected that alterations in the rate, rhythm, and order of depolarization of the various parts of the heart should manifest themselves in alterations in cardiac acoustics. Analysis of the change in acoustics induced by a change in the electrical activity can be used to evaluate more fully cardiac dynamics. It can also be used, as Levine & Harvey (57) have very properly stressed, as an aid in the diagnosis of the type of arrhythmia present. This discussion will be limited to two types of altered electrical response, heart block and bundle branch block, since here some detailed information is available concerning the physiological correlate between electrical impulse and acoustic response. A catalogue of the various acoustic manifestations of the different types of supraventricular and ventricular arrhythmias will not be given. Those interested in this phase of the subject should refer to the excellent discussion by Levine and Harvey.

HEART BLOCK. This term is used to signify impairment in the transmission of the electrical impulse from the atria to the ventricles. Traditionally, three degrees are recognized: delay in transmission (first degree), partial impairment with loss of the normal one-to-one relationship between atrial stimulus and ventricular response (second degree), and complete failure of transmission in which a region below the block assumes responsibility for the ventricles with the result that two independent pacemakers exist (third degree). Since the electrical abnormality involves an alteration in the relationship of atrial activity to ventricular activity, it is here that the characteristic alterations in acoustics occur. There are changes in the late rapid filling phase of the ventricle and, since this affects the atrioventricular valves, it produces changes in the first heart sound as well as in the fourth heart sound. Little *et al.* (61, 62) and Boyer (8) have investigated in detail the mechanism of alteration in acoustics with changes in the time-course of atrial-ventricular activity. Several clinical studies have also been reported (4, 87, 93). The essential feature in the alterations produced in the first heart sound is the position in which the atrioventricular valves are left at the onset of ventricular mechanical activity. With atrial contraction immediately preceding ventricular contraction, that is, in situations where the P-R interval is shorter than normal, the atrioventricular valves are left with their greatest aperture at the time of ventricular contraction. In effect they have been driven down into the ventricular cavity and have not had time to float back toward a more closed position. The consequently great distance that the valve leaflets have to travel to close is associated with a loud first heart sound. As the P-R interval lengthens to normal values and beyond that to those seen with a minimal degree of heart block, the atrioventricular valves have time to float back toward a more closed position due, most likely, to the pressure of blood behind the valve leaflets. With a shorter distance for the leaflets to travel there is a decrease in the intensity of the first heart sound. Still further lengthening of the P-R interval allows the leaflets to move again toward a more open position and consequently increases the intensity of the first heart sound. There is no doubt that the variations in the range of movement of the atrioventricular valve leaflets play an important part in the observed variations in first heart sound intensity with changes in the P-R interval. Although this feature alone can explain the phenomenon observed, the effect of the altered ventricular filling on the time-course of ventricular contraction and its effect, in turn, on the time-course of valve motion deserves further study. Clinically, in cases of first degree heart

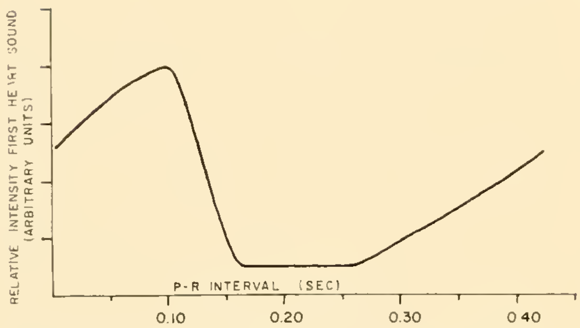

FIG. 5. Relationship of intensity of first heart sound to P-R interval. The effect of variations in the P-R interval on the relative intensity of the first heart sound is shown. This information is from a dog with surgically produced complete heart block. The curve has been drawn from the data of Boyer (8). Similar curves obtained in children with complete heart block have been published by Shearn *et al.* (93).

block, with a constant and minimally or moderately lengthened P-R interval, there is a selective decrease in the intensity of the first heart sound. In cases of third degree heart block or complete heart block the full range of alterations in first heart sound intensity is seen. Here the intensity for any given cycle is dependent upon the coincidental relationship between the atrial and ventricular activity. Though no atrial impulses reach the ventricle there is still for each cycle a P-R interval. Figure 5 taken from the work of Boyer (8) shows the relationship between P-R interval and intensity of the first heart sound.

In situations in which the atrial sound reaches intensities sufficient to be audible on the chest wall a further feature of the acoustics in heart block is observed. With P-R intervals of sufficient length to allow atrial contraction to be over before ventricular contraction begins, the atrial sound is heard as a separate entity, as described above for the normal. This applies also for a lengthened P-R interval and for those cycles in complete heart block where atrial activity is far removed from ventricular activity. For those cycles with short P-R intervals the two sounds may become fused. There is, then, this further factor which lends itself to increasing the intensity of the first heart sound.

BUNDLE BRANCH BLOCK. This term is used to signify impairment in transmission of the electrical impulse through the specialized conducting tissue of the ventricle, in particular, the right or left bundle of His. Other types of impaired ventricular conduction including intraventricular conduction delay, arborization block, and peri-infarction block will not be considered here. In the common types of right and left bundle branch block the feature of importance from the acoustic standpoint is the delay in the impulse reaching the involved ventricle, with the consequent delay in onset and cessation of mechanical activity. This classical interpretation of the dynamics of bundle branch block has recently been challenged in part by Braunwald & Morrow (11). On the basis of simultaneous right and left ventricular pressure measurements in patients with bundle branch block they have concluded that there is the expected delay in some patients with right bundle branch block but interestingly not in the cases with left bundle branch block. Our own attempts to restudy this problem have revealed to us the oftentimes great difficulty we have in deciding on a pressure curve exactly where ventricular contraction begins. It appears to us that the problem is deserving of further investigation before one can confidently cast out the traditional thesis. Since, as mentioned, the change from the normal involves a delay in the onset and the cessation of ventricular activity (classical explanation) it follows that one would expect changes in the time-course of the acoustic events, which indeed do occur. Due perhaps to the current inability to identify the components of the first sound there is often question as to the acoustic representation in the supposed delay in the onset of ventricular activity. However, the ability to identify clearly the components of the second sound make it much easier to note changes in the termination of ventricular activity. In right bundle branch block the greater than normal delay of right-sided events causes the pulmonic component of the second sound to occur even later after the aortic component than in the normal (fig. 4). However, if the etiology of the alteration is purely an electrical phenomenon and not a mechanical one, then the response of the ventricles to respiration should be normal. Therefore, with inspiration there is still further delay in the pulmonic component with a greater degree of splitting. In right bundle branch block, then, the order of events of the second sound is normal and the respiratory response is normal, but the degree of splitting is greater than normal throughout the respiratory cycle. On the other hand, in left bundle branch block, the classical explanation holds that there is definite change in the order of events. Here, the impulse activates the right ventricle first and left ventricular activity follows rather than precedes right ventricular activity. In this circumstance, the pulmonic component of the second sound precedes the aortic component. Since the response to respiration is presumably normal, inspiration

delays the appearance of the pulmonic component and makes the aortic component appear earlier. Consequently, with inspiration there is a loss of the splitting (fig. 4). This phenomenon, as mentioned above, has been called paradoxical splitting of the second sound. It seems preferable to state that there is reversed splitting of the second sound with a normal respiratory response.

There is a paradox here, however, if subsequent investigations confirm the suggestion that in left bundle branch block, and in some cases of right bundle branch block, ventricular activity is not different from that in the normal. It becomes then a problem to explain the obvious delay in the second sound component. A possible explanation, capable of investigation and proof, or denial, resides in the clinical experience that whereas right bundle branch block may or may not be associated with myocardial disease, it is decidedly unusual to have left bundle branch block without disease of the left ventricle. One might then suggest, as Braunwald and Morrow have, that the problem is not purely an electrical phenomenon, but also a mechanical one, in which the abnormality is the duration of mechanical systole. For, if the onset of ventricular activity of the involved ventricle is not delayed, but the duration of mechanical systole is prolonged, then there will be delay in relaxation and in the appearance of the second sound component. The question is deserving of further investigation, since such an explanation offers the possibility of differentiating bundle branch block associated with myocardial disease from that not associated with myocardial disease.

Effect of Disease States on Heart Sounds

In addition to the production of abnormal heart sounds and murmurs, to be described below, various disease states will alter the normal heart sounds. Again, no attempt will be made to provide a complete listing of these, but rather to cite the ways in which disease alters cardiac dynamics and thereby the accompanying acoustic representation.

The most clear-cut correlation between dynamics and acoustics is seen when disease involves the heart valves. Furthermore, since the acoustic representation of valve action is best seen with valve closure, the direct effect of disease of the atrioventricular valve is seen in alterations in the first heart sound. Similarly, the direct effect of disease of the semilunar valve is seen best in alterations in the second sound, but these are not the only changes seen. Alterations in the other sounds may be difficult to verify. They can be secondary changes, due not primarily to the valve lesion but to the alterations in the circulation or compensations for the abnormal load placed on it by the primary lesion. For example, hemodynamically significant lesions of the mitral valve change the first heart sound by a direct action on the cardiac events at the time of the onset of ventricular activity. Oftentimes there are changes in the second sound, particularly the pulmonic component, due to the secondary circulatory alterations, such as pulmonary hypertension.

With stenosis of the atrioventricular valve, especially that produced by rheumatic fever, there is an increase in the intensity of the component of the first sound associated with valve closure, a change in the quality, best described as a snapping quality, and a delay in the appearance of the sound. Two factors seem to be important in the genesis of this change. First is the alteration in dynamics at the time of valve closure. In the normal, the resistance to flow offered by the valve is so low that with present recording techniques little or no difference between atrial and ventricular pressures can be noted during the filling phases of ventricular diastole. Since the pressures are virtually identical the increase in ventricular pressure at the onset of ventricular systole carries ventricular pressure quickly above atrial pressure. In this circumstance there is said to be partial (or even perhaps complete) flotation of the valve leaflets towards a closed position, with valve closure (and/or valve closure sound) soon after the onset of mechanical ventricular activity. In the presence of stenosis, the resistance to flow offered by the valve is increased and a recognizable difference between atrial and ventricular pressures is observed. Consequently, at the onset of ventricular activity, ventricular pressure must rise to a higher level than in the normal to exceed atrial pressure. The result is that the interval between the onset of ventricular activity and the sound associated with valve closure is increased. In addition to this, inspection of the ventricular pressure curve indicates that at this later time the rate of rise of the pressure is greater, suggesting a more rapid rate of valve motion which might well contribute to the increased intensity. It has been suggested that the change in the quality of the sound to a snapping one is related to the second important factor, that of the change in the valve structure as a result of the rheumatic inflammation and subsequent scarring.

With insufficiency of the atrioventricular valve, the resultant of rheumatic fever, the pathology involves a retraction and binding down of the valve leaflets so

that with the severest lesion there is no valve closure. In such circumstances, despite the very forceful ventricular contraction, the evidence is that there is no first heart sound component produced. With lesser degrees than this the sound component is less than normal in amplitude but still present. The strict dependence of the acoustic manifestations upon dynamics can be seen in the cases of mitral valve insufficiency produced by mitral commissurotomy. We have observed an occasional patient with mitral stenosis in whom mitral commissurotomy unfortunately, either by splitting of a valve leaflet or by cutting a chorda tendinea, was followed by mitral insufficiency. In such a circumstance the regurgitation is not produced by failure of the valve to close, but rather by a failure of the valve to hold closed during ventricular systole. These patients retained their loud sound. Similarly, patients with a congenitally cleft mitral valve have had a loud first heart sound. In such a circumstance the valve that is present closes normally but part of the valve is missing. Such observations strengthen the belief that the closure of the atrioventricular valve is the integral feature leading to the acoustic event.

With stenosis of the semilunar valve there are two main changes in the component of the second sound due to closure of the involved valve, a delay in appearance time and a diminution in intensity. It has also been suggested that under certain circumstances there are significant changes in quality (71). In this situation, as with atrioventricular valve, the significant hemodynamic alteration is the increase in resistance to flow across the stenotic valve. There is compensation on the part of the ventricle, such that flow is maintained by increasing the energy expended with each contraction. By increasing stroke work, that is, raising a normal stroke volume to a higher pressure level, the resistance can be overcome and a reasonably normal flow maintained. This is, of course, dependent upon the ability of the ventricle to meet the increased load and upon the severity of the stenosis. From the acoustic standpoint the important hemodynamic correlate is that as stroke work increases the duration of mechanical systole increases. It is this increase that is responsible for the delay in the time of appearance of the second sound. It has been pointed out that for situations where ventricular compensation is adequate there appears to be a generally linear relationship between the severity of the stenosis and the degree of the splitting of the second sound (55). The phenomenon of increased splitting of the second sound here is due to the fact that, except in unusual circumstances, only one semilunar valve is involved, so that the duration of mechanical systole and the appearance time of the second sound on the uninvolved side can be presumed to be normal. The decrease in the intensity of the sound is due apparently to the valvular pathology and the fact that there is impaired motion of the leaflets.

With insufficiency of the semilunar valve there are variable alterations in the second sound component depending upon the mechanism of production of the regurgitation. In some situations the valve leaflets are normal or only slightly damaged. Here insufficiency may be due to dilatation of the valve ring making it impossible for the cusps to meet all along their line of closure. If the circulatory dynamics are normal there will be little or no change in the second sound. If the insufficiency is hemodynamically significant, calling forth an increased ventricular stroke output with a low diastolic pressure, then the second sound may well be increased in intensity. On the other hand if the pathology involves primarily the valve leaflets themselves, so that they cannot meet at all, then there will be disappearance of the second sound.

Alterations in the third and fourth heart sounds in the presence of heart disease will be discussed below in the section on gallop sounds.

For a discussion of the nature of the alterations in the normal heart sounds produced by various other diseases, reference should be made to the monographs on acoustics noted earlier.

Abnormal Heart Sounds

In addition to the alterations in the nature of the normal sounds, disease states may also be associated with the production of abnormal sounds. Some of these appear to be new phenomena, that is, they have no counterpart in the normal. Others perhaps represent normally occurring events with merely changes in intensity and/or quality. This point deserves further investigation. The so-called abnormal sounds, like the normal acoustic events, are dependent for their genesis upon certain hemodynamic events. Here again the correlate is with a dynamic event and not necessarily with a specific disease process.

GALLOP SOUND. The most celebrated of all the abnormal sounds is the gallop sound, so called because it converts the normal double rhythm of each cycle into a triple rhythm and is thereby reminiscent of the sounds made by a galloping horse. Two types of gallop rhythm are recognized. One is the proto-

diastolic gallop, in which the gallop sound occurs in early diastole at the end of the phase of early rapid ventricular filling. The other is the presystolic gallop which occurs late in diastole during the phase of late rapid ventricular filling. The question as to whether or not these sounds represent new phenomena cannot be answered at the present time, since they appear to occur at the same time that one expects the normal third and fourth sounds to occur. There also seem to be no rigorous criteria which, at least on a hemodynamic basis, will allow one to differentiate between the normal and the abnormal sound. In view of the fact that this differentiation can be of great clinical importance it is suggested that the problem is deserving of solution. Furthermore, the traditional explanation for the production of gallop sounds has been challenged, and there is no certain evidence at present as to which explanation is the more likely. It is not clear either whether under differing circumstances there may be different mechanisms. This dichotomy has been discussed above in the section on the normal diastolic sounds. Briefly, to recapitulate, the traditional view holds that the sound, either gallop sound, is due to the sudden "checking" of the outward movement of the ventricular wall, whereas the newer viewpoint suggests that the filling of the ventricle causes a sufficient rise in ventricular pressure to close the atrioventricular valve, transiently. From simultaneous recordings of atrial and ventricular pressure tracings in patients with gallop sounds we have seen cases where it would appear that ventricular pressure does rise above atrial pressure at the time of the sound, indicating that atrioventricular valve closure may occur. However, recordings in other patients have not shown this. It may well be that in intact man the manner in which intravascular pressures now have to be taken cannot yield recordings with the fidelity needed to answer the question. Whether or not transient atrioventricular valve closure occurs may be better answered with high speed cineangiography. One observation on the question of valve motion appears pertinent. We have seen an occasional patient with severe mitral insufficiency due to rheumatic fever in whom there appears to be no mitral closure sound. This is in keeping, as described above, with the nature of the pathology which causes a binding down of the leaflets and the hemodynamic-acoustic correlate which relates this sound to the events associated with closure of the mitral valve. If this reasoning is correct, then the additional presence of a gallop sound, identified by recordings from within the heart as coming from that ventricle, could not be explained on the basis of transient atrioventricular valve closure.

In human clinical situations the presence of a gallop sound correlates best with the presence of ventricular failure. Identification of the ventricle of origin can be carried out by resorting to the effect of respiration on sound intensity. The mode of action is the same as that for the normal diastolic sounds, namely, that inspiration can be expected to increase the intensity of a gallop sound from the right ventricle and decrease the intensity of a left ventricular gallop The presystolic gallop, related as it is to mechanical activity of the atrium, disappears, as expected, in the presence of atrial fibrillation. Finally, at sufficiently rapid rates to cause early and late diastolic filling to occur simultaneously, the two gallop sounds may occur simultaneously. The term summation gallop has been applied to this situation.

DIASTOLIC KNOCK. Closely related hemodynamically to the protodiastolic gallop sound of ventricular failure is the diastolic knock or diastolic sound of constrictive pericarditis. The term is applied to the sound that occurs at the end of the phase of early rapid ventricular filling in this disease, and with the start of the rapid early diastolic pressure rise in the ventricle (74). At times the forcefulness of the outward thrust is sufficient to be palpable, as it may be also with a gallop, and even forceful enough to warrant the term, diastolic heartbeat (105). The phenomenon of the sound and its tactile counterpart seem to arise out of the change in the nature of ventricular filling imposed by the pathological process. In the normal, the inrush of blood into the ventricle at the onset of diastole is met by a distensible ventricular wall which gives way so that volume increases with little or no increase in pressure. In constrictive pericarditis, presumably because of restriction by the diseased pericardium, the ventricle is not allowed to yield and diastolic pressure rises rapidly to plateau with, it is thought, early cessation of ventricular filling. This abrupt transient as blood is suddenly checked on its way into the ventricle appears responsible for the sound and the "diastolic heartbeat." This explanation is, perhaps, somewhat at variance with the observations of Mounsey (74) on the right ventricular pressure. However, it would seem wise to record right and left ventricular pressures before any final conclusion is reached. One of the questions that deserves an answer is the true role that the diseased pericardium plays in the alteration of the hemodynamics and, consequently, the acoustics. Hemodynamic studies made before and

after pericardiectomy support, in part, the explanation offered, but the problem is complicated by the frequent accompaniment of underlying myocardial disease. When a precise identification of the part played by each process (pericardial and myocardial) is available, differences in the acoustic manifestations may be used to identify the relative role played by each process.

OPENING SNAP OF ATRIOVENTRICULAR VALVE. As mentioned in the analysis of the normal sounds, the opening of the atrioventricular valve is rarely if ever accompanied by an audible sound. On occasion it has been reported that such an event has been seen in the chest phonocardiogram. In states in which there is a marked increase in flow across the valve, and most especially with disease of the atrioventricular valve, an audible acoustic event may be present. In the former situation the event, not associated with valvular pathology, represents an opening sound. For example, in patients with atrial septal defect with a large left-to-right shunt the greatly increased flow across the tricuspid valve may be associated with a sound occurring at the time of the opening of that valve (53). The abnormal sound, usually called a snap because of its quality, occurs in the presence of stenosis of the atrioventricular valve. In order to understand this phenomenon more fully it is necessary to consider first the dynamics of the atrioventricular valve in the normal and in the presence of stenosis (2, 14). Since in most human clinical situations the event is a direct consequence of mitral valve pathology, the following discussion will concern itself with this valve.

The human mitral valve consists of two leaflets, a larger anterior or septal leaflet and a smaller posterior or mural leaflet. The line of approximation viewed from the left atrium is not a straight line but a crescent with the concavity directed anteriorly. The point at which the line of approximation meets the valve ring is the commissure and one is located anteriorly and laterally, the other posteriorly and medially. Beneath these commissures on the ventricular side are located the respective papillary muscles which connect to the leaflets, mainly at the commissures, by the chordae tendineae. A frequent natural misconception is to regard the anterior papillary muscles as connecting to the anterior leaflet and the posterior papillary muscle to the posterior leaflet. In actual fact the major attachments of the anterior papillary muscle go to each leaflet primarily at the anterolateral commissure, and those of the posterior papillary muscle to the posteromedial commissure. Since the papillary muscles depolarize first and repolarize last it may be considered that their function, during systole, is to guard the commissures. This is, in effect, an extension of a concept of papillary muscle function originally proposed by Lepeschkin (56). During diastole the papillary muscles are relaxed and allow the leaflets to move freely down into the ventricle under the force of atrial flow. When the commissure is viewed from the side it can be seen that the major attachments of the chordae form a *V* or a *Y* from the papillary muscle to the leaflet. With rheumatic inflammation there is, because of the involvement of the chordae tendineae as well as the leaflets, a filling in of the *V* or the *Y* and a fusion of the chordae which is thereby associated with a fusion of the line of approximation of the leaflets at the commissures. There results a stenosis of the orifice in which the leaflets proper are unaffected, but they are now held not only at the valve ring but also at the commissures and, for a variable distance, in toward the center of the line of approximation. In this circumstance, when ventricular pressure falls below atrial pressure, the bodies of the leaflets proper are free to move toward the ventricle, but this movement is soon checked by the fusion at the commissures. It is this checking of the downward movement of the leaflet, much like a sail filling with wind, that appears to be responsible for the opening snap of the valve. The most direct evidence for this explanation comes from the observations of Sellors (91) at the time of operation. With a finger in the ventricle and a stethoscope on the heart he was able to note obliteration of the opening snap when he prevented the leaflets from bellying downward. Since the presence of the opening snap depends not only on the presence of stenosis but also on the mobility of the leaflet, it is not surprising that when the pathology extends into the leaflet proper and renders it immobile an opening snap is not observed.

The presence of an opening snap, denoting as it does the time of opening of the atrioventricular valve, allows for a measurement of the duration of isometric relaxation of the ventricle by acoustic means. This time interval is that from the closing of the semilunar valve, at which time the second sound component occurs, to the opening of the atrioventricular valve, at which time the opening snap occurs. It must be remembered that so far as the second sound is concerned this must refer to the component of the sound due to closure of the semilunar valve on that side of the heart from which the opening snap occurs. The

duration of this interval has been used clinically to assess the severity of the stenosis of the atrioventricular valve. It has been reasoned that as the stenosis becomes more severe the atrial pressure rises and this causes an earlier appearance of the opening snap. Whereas there is generally good agreement between the severity of the mitral stenosis and the shortening of the A2-OS interval (aortic closure to opening snap) (79) there are a number of other factors which contribute to the duration of this interval. These must be accounted for before any widely applicable formula can be suggested. Such parameters as the presence of abnormalities of the semilunar valve, the pressure at which that valve closes, the rate of decline of ventricular pressure, and the presence of coexisting mitral insufficiency must play a part. In our limited experience, the use of this interval in noting the degree of mitral stenosis in absolute terms has been more meaningful when comparison is limited to an individual subject, as, for example, comparing values obtained postoperatively with those noted preoperatively. That there is good agreement between the level of atrial pressure and the appearance time of the opening snap in one subject can also be seen in records obtained from patients with atrial fibrillation. Here, with variations in the cycle length there are inverse variations in ventricular filling. A short diastole, which will not allow for as complete emptying of the atrium into the ventricle as a long diastole, leaves atrial pressure higher at the end of the next ventricular systole and consequently causes an earlier appearance of the opening snap. In certain clinical situations, wide splitting of the second sound as well as a protodiastolic gallop sound may resemble an opening snap, and precise identification may be important. For example, whereas an opening snap is often part of the picture of severe mitral stenosis, a protodiastolic gallop from the left ventricle would not be expected to occur. This is based on the fact that a significant grade of obstruction to ventricular inflow removes the possibility for rapid inflow, a prerequisite for the early gallop sound. Differentiation between these two acoustic events has been alluded to above in the relationship between the gallop sound and the outward movement of the ventricle as seen in the low frequency recordings of the chest wall (apex cardiogram). The gallop sound occurs at the end of the outward movement and the opening snap at the beginning.

Differentiation of an opening snap from the second component of the second sound, usually pulmonic, can be carried out by resorting to fluctuations in duration of mechanical systole of the ventricle and left atrial pressure with changes in flow. With increases in flow, as with exercise, the apparent prolongation of right ventricular systole over that of the left is associated with a wider degree of splitting of the second sound. On the other hand, as noted above, increase in flow cannot be handled well by the stenotic mitral orifice, and as left atrial pressure rises the opening snap occurs earlier. Since the two events move in opposite directions with changes in flow (either increase or decrease) precise identification becomes possible.

SYSTOLIC CLICKS, SYSTOLIC GALLOPS, AND EJECTION SOUNDS. There are a number of abnormal sounds that occur during systole and these have received various names. The current nomenclature is often confusing, probably due in part to imprecise information regarding the detailed nature of these events.

First, the term systolic gallop has been used to refer to certain sounds occurring in systole which render a triple rhythm. From the definition of a gallop sound given above, which relates the acoustic event to the rapid phases of ventricular filling, the words "systolic gallop" would seem to be mutually contradictory. Furthermore, since such a use of the word gallop may have the tendency to confuse, it would seem best until more information is gathered to withhold this term from general use as Minhas & Gasul (73) have suggested.

Second, the term ejection sound has been used to refer to the acoustic event which occurs during the early rapid phase of ventricular ejection. It has been suggested that the sound arises from either great vessel (aorta or pulmonary artery) in situations in which there is dilatation of the vessel and/or hypertension in it. It has been said that it is due to a sudden distention of the vessel imparted by the nature of the force of ventricular ejection. For example, in mild degrees of valvular pulmonic stenosis in which there is some dilatation of the vessel immediately beyond the valve (poststenotic dilatation) and in which ventricular ejection is not impaired, an early systolic ejection sound can be observed (54). With more severe degrees of stenosis while there is still vessel dilatation, the impairment of ventricular ejection (not in total stroke volume but presumably in the rate of ejection) may not produce an ejection sound (20, 23, 55, 108). The exact hemodynamic correlate of the ejection sound and its genesis deserve further investigation. There is some question as to whether the event represents an exaggeration of the normally oc-

curring semilunar valve opening sound or whether it occurs after this event and represents an additional sound. Our experience is in agreement with the latter suggestion.

The systolic ejection sound may be mistaken for the second component of a split first heart sound. More often it is the other way around. Whereas there do appear to be circumstances in which a true splitting of the first heart sound does occur, much more frequently when two separate acoustic events are heard in close approximation, it is the addition of an ejection sound which causes the doubling. At the present time there appear to be no completely satisfactory acoustic criteria for deciding the precise site of origin of an ejection sound and recourse must be had to the accompanying clinical picture. However, several differentiating features have been described (52, 54, 73). Ejection sounds that arise from the pulmonary artery are said to be quite sharp in quality and of maximal intensity at the pulmonary area on the thorax, and to become louder in expiration. One might expect intensification with inspiration as is noted with other right heart sounds. It is possible that if the audibility of the sound is due to closer approximation of the dilated pulmonary artery to the chest, changes in intensity with respiration are due to alterations in the amount of interposed lung. This is merely a conjecture. The mechanism of the respiratory variation deserves further investigation. In contradistinction to right-sided ejection sounds, those that arise in the aorta are said to be less sharp in quality, audible at both the aortic and mitral areas on the thorax, and less augmented by expiration.

Third, the term systolic click, which has been applied to a number of systolic acoustic events, refers to the sharp clicking sound heard often in midsystole or late systole, though it may occur at any time in systole. Systolic clicks may be single or multiple and, when multiple, may be mistaken for a systolic murmur. There is no certain explanation as to their site of origin. The current opinion of interested observers suggests that they are most likely extracardiac in origin, coming possibly either from the pericardium or from the pleuropericardial junction. The fact that these events occur at varying times in systole, either spontaneously or with respiration, lends credence to the suggestion that they are not related to or produced by an intracardiac hemodynamic event. These acoustic phenomena in themselves appear to carry no clinical significance, though they have often been heard following episodes of pericarditis or in the presence of extensive pleural involvement from tuberculosis (68). Their clinical importance lies mainly in the fact that they may be mistaken for other less benign events.

It is suggested that the term systolic click be reserved for this type of acoustic event, and that the term ejection sound be used to refer to the early sound described above. The term ejection click or early systolic click, although descriptive of the event, may lead to a confusion of terms.

PERICARDIAL FRICTION RUB. In situations in which the normal lubricating function of the apposed layers of pericardium is lost, the movement of the heart within these diseased membranes may cause them to produce audible acoustic events. In most circumstances the sounds produced have a to-and-fro quality with one component during ventricular systole and the other in diastole, more commonly presystole but at times protodiastole. Occasionally all three components are audible. The sounds are usually described as leathery or scratchy and traditionally are said to sound as though they are close to the ear. Due undoubtedly to the nature of the pathology, which always is transient and often varying in degree, there are characteristically marked changes in the intensity and location of the sounds and often of the presence or absence of the several components with time. Localization on the chest for the same reason is also variable. The most frequent clinical problem is that of certain differentiation between these pericardial sounds and murmurs of intracardiac origin. The problem if not solved by one observation may often be resolved by serial observations.

Murmurs

In the discussion on the physical basis of murmur production it was pointed out that these acoustic events arise out of disturbances in the pattern of blood flow. The location within the circulation at which the disturbance arises and its time-course in the cardiac cycle are dependent upon both the anatomical structure involved and the physiological circumstances at the time of its production. Certain anatomical lesions cause changes in the pattern of blood flow at the lesion and at specific times in the cardiac cycle, and thereby produce characteristic acoustic information. In this circumstance, the relationship between the lesion and the murmur is close, and the murmur may be virtually diagnostic or even pathognomonic. When the hemodynamic consequences of any given lesion are atypical or when two

lesions produce similar hemodynamic changes, the murmur becomes less characteristic.

When a lesion produces a change in hemodynamics or in flow pattern at a distance from the lesion, murmurs, if produced, are characteristic not necessarily of the lesion but rather of the flow pattern changes at the site where these occur. Finally, both types of murmurs may be produced by a lesion, one due to the change in flow pattern at the lesion and one at a distance. This information is essential to understand the current problems in devising a satisfactory classification of murmurs. The traditional classification of differentiating between so-called organic and functional murmurs is less than ideal. In the sense that all murmurs are produced by changes in blood flow, they can be said to be "functional." Furthermore, changes in blood flow at a distance from a lesion are often indistinguishable from changes produced by physiological alterations in the circulation (i.e., not associated with heart disease or any given lesion), and from this will often come indisguishable murmurs. For example, an increased cardiac output, such as seen in anemia, will increase flow in the pulmonary artery and may produce a murmur which is indistinguishable from the murmur produced by increased pulmonary artery flow secondary to the left-to-right shunt of an atrial septal defect. The problem is further complicated by the attempts to classify separately changes in the flow pattern produced at a valve area by increases in flow across a normal orifice, from those produced by normal or reduced flow across a reduced valve area. Additionally, problems arise in classification and differentiation of murmurs at valve areas caused by regurgitation due to structural changes in the leaflets from those produced by dilatation of the valve ring. There appears to be no ready answer to the problem of classification. At present, one way of handling it is first to recognize certain murmurs which bear a close enough relationship to the anatomical lesion that they may be called organic. The murmur is caused by flow through the lesion itself. Second, there is a group of murmurs clearly unassociated with clinically significant cardiac lesions and they may be called functional or unassociated with heart disease. And third, there is a group of murmurs which may or may not be associated with cardiac lesions, and the differentiation is made by reference to other information. Until such time as a more precise identification of all of the factors involved in murmur production and transmission are known, any classification will remain inadequate.

MURMURS OF VALVULAR ORIGIN. Disorders in valve function, both stenosis and insufficiency, have the capacity of producing changes in blood flow that yield murmurs. Since there are four valves and since each valve can be diseased in two ways, there are eight possible murmurs of valvular origin. To identify precisely the site of origin of the murmur, criteria are needed to separate these eight possibilities. The first important criterion is the phase of the cardiac cycle in which the murmur occurs. The eight can in this way be divided into two groups of four murmurs each. The systolic murmurs are those of mitral insufficiency, tricuspid insufficiency, aortic stenosis, and pulmonic stenosis. The diastolic murmurs are those of mitral stenosis, tricuspid stenosis, aortic insufficiency, and pulmonic insufficiency. In the case of valvular stenosis the flow pattern is altered by the obstruction to forward flow. Since the forward flow across the semilunar valves occurs in systole, these murmurs are systolic, and since forward flow across the atrioventricular valves occurs in diastole, these are diastolic murmurs. In the case of valvular insufficiency the valve allows blood to flow backward into the next most proximal chamber during the period of time when the valve is normally closed. Since the semilunar valves are normally closed in diastole, insufficiency produces a diastolic murmur, and since the atrioventricular valves are normally closed in systole, here insufficiency produces a systolic murmur.

Consider first the systolic murmurs. Traditionally, the most important acoustic criterion for identification has been the area on the thorax to which the murmur shows preferential transmission. In most cases this criterion holds true due undoubtedly to the fact that from patient to patient not only is the heart in about the same place in the thorax but the nature of transmission is probably nearly the same. However, exceptions do occur and, in order to validate the first criterion and provide rigorous support for identification, recourse must be had to the physiological basis of murmur production. In order to understand these criteria, basic information must be at hand on the nature of the hemodynamic changes produced by the various valvular lesions.

In the presence of stenosis of the semilunar valve the relationship between the ventricular pressure and the pressure in the great vessel is changed. In the normal, these two pressures are virtually identical during systole, but because of the obstruction to flow imposed by the diseased valve there is a loss of energy across the valve. This manifests itself as a difference in the pressures, and the amount of this difference

(for any given flow value) is an index of the severity of the obstruction. The usual type of compensation for this lesion is an increase in the amplitude of the ventricular pressure, often with alterations in the rate of rise and decline. The level of the great vessel pressure may be unchanged (or lower) but the shape of the pressure curve is greatly altered. It rises much more slowly than in the normal, and reaches its peak later. The gradient of pressure increases from the time of valve opening to a point near the middle of systole and then declines so that there is little or no gradient just before valve closure. If one makes a first approximation assumption that the intensity of the murmur is related to the pressure gradient, then the time-course of the acoustics can be deduced. There will be no murmur from the time of the atrioventricular valve closure component of the first heart sound until the end of isometric contraction. This will be followed by the onset of the murmur with an increase in intensity to mid-systole, followed by a decline in intensity with disappearance shortly before the second sound component. The form of the murmur is crescendo-decrescendo, and its envelope is diamond-shaped. The three characteristics which define this murmur are: *1*) it begins not with the first sound but shortly thereafter, *2*) it is crescendo-decrescendo (diamond-shaped), and *3*) it ends before the second sound. The last point needs some clarification, since, when the whole of cardiac acoustics (both sides of the heart) is considered, the murmur may not appear in this fashion. Assuming that only one semilunar valve is stenosed, then the change in dynamics will occur and the murmur will arise from only one side of the heart. The other is unaffected. On the unaffected side the duration of systole and the time of appearance and intensity of the second sound component are normal. On the affected side, systole is prolonged and the intensity of the second sound component, as discussed previously, is reduced. In such a situation, although the murmur ends before its own second sound component, it may not end before the other. It has also been stated that as the severity of the stenosis increases the point of maximum intensity of the murmur (peak of the diamond) occurs later in systole. This appears not to be in agreement with the statement presented here that the maximum intensity occurs at or near midsystole. This seeming discrepancy is resolved by the fact that, in the former statement, the end of systole is being taken as the time of occurrence of the second sound component on the unaffected side, whereas the latter statement considers only the affected side. Therefore, both considerations are true.

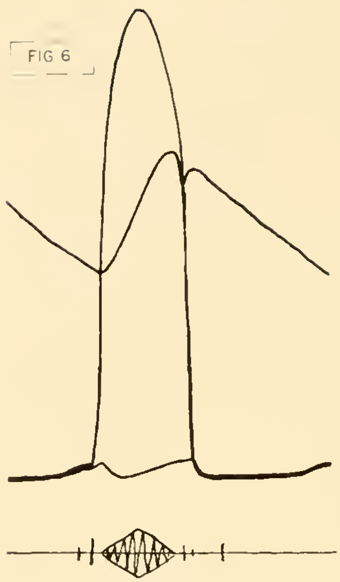

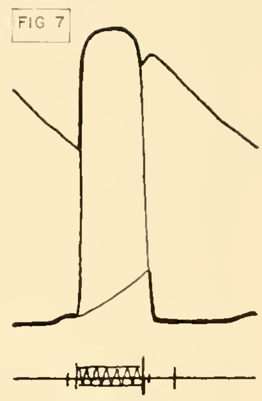

FIG. 6. Ejection-type systolic murmur due to semilunar stenosis. The pressure curves are of great vessel, ventricle, and atrium, for a subject with semilunar valvular stenosis. Below is shown the ejection-type systolic murmur. The various sounds have also been added. Compare with fig. 1 (normal) and fig. 7 (atrioventricular insufficiency).

FIG. 7. Regurgitant-type systolic murmur due to atrioventricular insufficiency. Similar to fig. 6, but for a subject with atrioventricular valvular insufficiency. Below are shown the regurgitant-type systolic murmur, and the sounds. Compare with fig. 1 (normal) and fig. 6 (semilunar stenosis).

This type of systolic murmur, the internal characteristics of which identify it, regardless of location on the thorax, as a murmur originating at the semilunar valve, has been named by Leatham (51), who first called attention to it, an ejection murmur (fig. 6). It should be remembered that whereas murmurs due to semilunar stenosis are ejection murmurs, not all ejection murmurs are due to pathological obstruction to flow. Regardless of etiology, systolic murmurs that originate at the semilunar valve are ejection in type. For the diagnosis of stenosis, as the term is used here, one might expect not only the murmur but also increase in the duration of mechanical systole with delay and diminution of the second sound component. Unfortunately, to complicate matters still further, these criteria may not always be present (83). In addition to these criteria we have felt, as others have, that an additional distinguishing feature between so-called "functional" ejection murmurs and "organic" ejection murmurs is that the organic murmurs have higher frequency components (60).

Consider next systolic murmurs that arise out of insufficiency of the atrioventricular valves. In this circumstance there is regurgitation of blood from the ventricle back into the atrium during ventricular systole. The atrial pressure, which normally declines early in systole and rises gradually in late systole up to the point of opening of the atrioventricular valve, shows instead a progressive rise up to the peak of the *v* wave. This contour is variable, however, and in certain cases atrial pressure may rise sharply early in systole mimicking the ventricular pressure. This has been called ventricularization of the atrial pressure curve. The level and contour of the atrial pressure bear no strict relationship to the severity of the regurgitation, due undoubtedly to the fact that other parameters such as atrial volume and distensibility play an unquantifiable role. In any case, there is a gradient of pressure from ventricle to atrium all the time between the upward and downward crossings of the pressure curves. From the acoustic standpoint, then, the murmur can begin immediately with the atrioventricular closure component of the first sound (if it is present) and can continue to the time of opening of the atrioventricular valve which occurs later than the second sound component. The time-course of the murmur between these two points varies. In the case of the ejection murmur a first approximation attempt has been made to correlate murmur intensity with pressure gradient and found not to be unreasonable (35). Such a correlation appears to be not as good for atrioventricular regurgitation. It is possible that this difference between the two types of murmurs is due to a better correlation between pressure gradient and flow in the former case than in the latter. Such an explanation implies a relatively constant resistance during systole on the part of the semilunar valve with stenosis and a varying resistance on the part of the atrioventricular valve with regurgitation. It is hoped that techniques will become available to investigate this question more thoroughly. With well-developed cases of atrioventricular valve insufficiency the most common finding is a murmur that shows little or no variation in intensity from the beginning to the end. Other cases show increasing intensity from onset to end. Still others show maximum intensity early with declining intensity with time, and in some cases there appear to be fluctuations in murmur intensity throughout its course. A detailed correlation between murmur contour and the exact nature of any given lesion awaits further investigation. In any event, regardless of the type of envelope, that of crescendo-decrescendo is not seen. This murmur therefore has three attributes, which are: *1)* it begins with the first sound, *2)* it is not crescendo-decrescendo but is usually unchanged in intensity throughout systole, and *3)* it continues up into and perhaps beyond the second sound component. This type of murmur, which is different in all three characteristics from the ejection type, Leatham has called the regurgitant type (fig. 7). Again, because of the physiological circumstances surrounding its origin, this valvular murmur, regardless of location on the thorax, comes from an atrioventricular valve.

For systolic murmurs of valvular origin, those from the semilunar valve can be recognized by the fact that they are of the ejection type, whereas murmurs from the atrioventricular valve are of the regurgitant type. Such a division, although it undoubtedly has exceptions (92), is well based on hemodynamics and represents a notable contribution. One problem for the future is a more precise correlation between the variations within each type and the specific hemodynamic and anatomical variations of the pathology.

In the same way that the hemodynamic events control the nature of the production of systolic murmurs, just so do they control diastolic murmurs. Consider first diastolic murmurs that arise out of insufficiency of the semilunar valve. Here again the relationship between ventricular and great vessel pressure is altered. In the well-established case there is a more rapid decline of the great vessel pressure in diastole with a lower end-diastolic level. The ventricular pressure in diastole is either unaltered or shows a gradually increasing level up to end-diastolic pressure. Indeed, in the severe case these two pressures may be virtually identical at the start of ventricular systole. There is therefore a gradient of pressure from the time that the ventricular pressure falls below great vessel pressure to the end of the next phase of isometric contraction, and this gradient shows a steady decline throughout the course of diastole. From the point of view of the acoustics, then, the murmur will begin with the closure of the semilunar valve, the second sound component if it occurs, and then show a gradually decreasing intensity (decrescendo). Note that as in atrioventricular insufficiency a strict correlation between murmur and pressure gradient is not present, and no final answer can be expected until the time-course of regurgitant flow is measured. It is due to this and other factors that an assessment of the severity of semilunar insufficiency on the basis of the murmur may be hazardous. The other important characteristics of semilunar insufficiency murmurs is that they are almost all uniformly high-pitched in

quality, and oftentimes this factor, regardless of time-course or nature of the murmur envelope, points to the site of origin. This feature is due apparently to the nature of the principal vibrating structure. One highly characteristic murmur which is related to a specific valvular deformity deserves mention. When one or more cusps of a semilunar valve become everted (bent back toward the ventricle), the vibrations develop a predominance of a single frequency, which lends a musical quality to the murmur (5, 34). This happens most frequently to the right anterior cusp of the aortic valve. Tears in the free margin of a cusp or perforations of a cusp seem to present more often with sets of dominant vibrations, and the murmur thus created is often harsh and not so musical.

Consider finally murmurs that arise from the atrioventricular valve as a result of stenosis. In this circumstance there is an alteration in the relationship between the atrial and ventricular pressure in diastole. In many cases the contour of the ventricular pressure is unchanged, and the main alteration is in the atrial pressure curve. At the time of the opening of the atrioventricular valve, at the end of the period of isometric relaxation, the atrial pressure falls, but not to the level of the ventricular pressure. The difference between the two pressures for any given flow rate is an index of the severity of the stenosis. There is a continuous decline in atrial pressure until the onset of mechanical activity of the atrium, at which time there is a secondary rise in atrial pressure and a consequent increase in pressure gradient. From the standpoint of the acoustics the murmur can be expected to begin at the time of the atrioventricular valve opening. This is in contradistinction to semilunar valve diastolic murmurs which begin with the second sound component. As the gradient of pressure falls there is a decline in the intensity of the murmur, and with the increase in gradient due to atrial activity there is a secondary increase in murmur intensity. Like semilunar valve stenosis the correlation between pressure gradient and murmur is reasonable. From this point several features may be noted. First, in the mildest degrees of stenosis the atrial pressure quickly declines to ventricular pressure only to rise above it again late in diastole. In this circumstance the early diastolic component of the murmur, irrespective of intensity, is of short duration, and there is a silent gap between it and the presystolic component. As the severity of the stenosis increases, the atrial pressure declines more slowly. This results in a longer diastolic component with less of a gap between it and the presystolic phase. Finally, when the severity of the lesion is sufficient to prevent atrial pressure from reaching ventricular pressure before it rises due to atrial activity, the gap between the two components disappears (fig. 8). In this way one can see, as Wood (106) has pointed out, that the duration of the diastolic component of the murmur (without considering the presystolic component) is directly related to the severity of the lesion. We have made this correlation enough times now in our own cases to attest to its validity and its importance. This same phenomenon, since it does not depend on the atrial component, applies and can be used when there is atrial fibrillation.

In atrial fibrillation without an atrial contraction there is no late increase in the gradient of pressure. It continues to decline to the end of diastole, and consequently there is no secondary increase in murmur intensity. It must be remembered that the change in the murmur with atrial fibrillation is primarily the loss of the presystolic accentuation. It need not be the loss of presystolic murmur. The question as to whether or not there is an audible murmur just before systole depends on the severity of the stenosis, as described above. Indeed the alteration in the murmur with atrial fibrillation is only a particular example of a more general rule that the nature of the presystolic phase of the murmur depends on the nature of the atrial activity. When atrial activity immediately precedes ventricular activity, as with a short P-R interval, the atrial pressure rises just before ventricular systole and is high when mechanical activity of the ventricle begins. In this circumstance the presystolic phase of the murmur is short and is increasing in intensity when it is cut off by the atrioventricular valve closure sound. As the P-R interval lengthens to normal values and beyond, there is time for atrial pressure to peak and begin to decline. In this circumstance, the presystolic phase of the murmur is longer and the peak intensity may occur enough before the onset of the first sound to show a decline in murmur intensity (fig. 9). In each case the murmur appears to be due to the nature of atrial mechanical activity and its effect on pressure gradient and, obviously, flow into the ventricle. It is because atrial systole is most commonly presystolic in time that this murmur is most commonly presystolic. However, since the murmur is dependent upon atrial systole and not upon its relationship to ventricular systole, the term presystolic used for all of the variations seen may cause confusion. The term atriosystolic, as used by Wood (107) and McKusick (68) conveys more precisely the

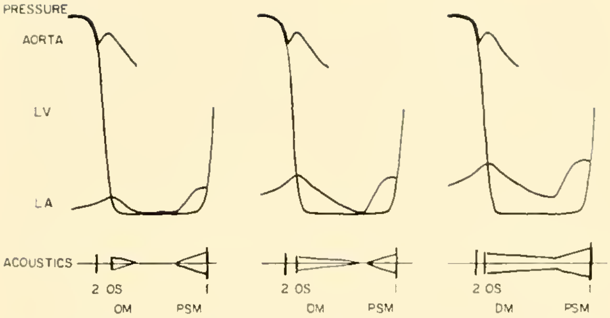

FIG. 8. Mitral stenosis: correlation of pressures and acoustics. The relationship between the left heart pressures and the acoustic manifestations of mitral stenosis are shown. The three sets of curves represent from left to right increasing degrees of stenosis. The pressures are shown from just before the time of the second sound near the end of systole to just after the time of the first heart sound at the beginning of systole. In each case there is normal sinus rhythm. As the severity of the lesion increases the level of atrial pressure, at the time of the opening of the atrioventricular valve, rises with a resultant progressive shortening of the interval from second sound component to opening snap (2-*OS*). Also as the severity of the lesion increases the duration of the diastolic gradient increases with a resultant lengthening of the duration of the diastolic murmur. Finally, as the severity of the lesion increases, the level of atrial pressure at the time it is exceeded by the ventricular pressure rises with a resultant delay in the appearance of the first heart sound component.

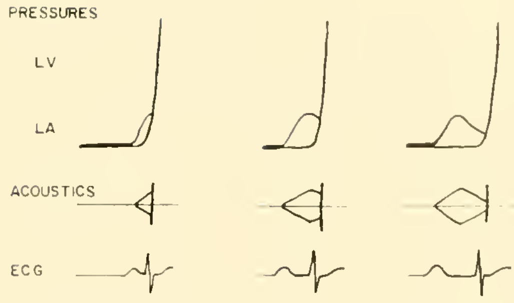

FIG. 9. Effect of P-R interval on presystolic murmur. The pressures are of left ventricle and left atrium in a subject with mitral stenosis. The part of the cycle shown is from near the end of diastole to shortly after the beginning of systole. The part of the acoustic cycle shown is the envelope of the presystolic murmur and the first sound. At the bottom is the electrocardiogram (ECG) showing from left to right an increasing P-R interval

nature of the event. There is no basis for the suggestion that since ventricular pressure is rising during the time of the murmur, it is due to flow from the ventricle back into the atrium (75, 97).

From these considerations and from those on the effect of stenosis on the heart sounds, a complete picture of the acoustics in atrioventricular valve stenosis can be drawn up. (Similar interesting examples could be cited for the other valvular lesions.) If one begins with the point at which the ventricular pressure falls below pressure in the great vessel, there is first a normal second sound component from the side of the lesion. Following this is a short interval until the end of isometric relaxation, when the ventricular pressure falls below atrial pressure. There is then the opening snap of the atrioventricular valve, the distance of which, from the second sound component, is roughly inversely proportional to the severity of the lesion. The opening snap ushers in the murmur, which because of the nature of the valve structure is low pitched. The murmur is decrescendo in nature, its duration varying directly with the severity of the lesion. With the onset of atrial mechanical activity, late in diastole, the murmur becomes crescendo ending in a late appearing, snapping first sound, the degree of lateness varying directly with the severity of the lesion. Furthermore, having now considered in detail the relationship between atrial activity and ventricular activity and the effect of exact juxtaposition of these events on the level at which atrial pressure is left at the onset of ventricular contraction, one can see that the lateness of the first sound depends upon this as well as upon the severity of the lesion. This may well account for the poorer correlation between severity and prolongation of the Q-M1 interval than between severity and the A2-OS interval (44, 45, 103).

On the basis not only of pitch but also of time-course of events a differentiation can be made between diastolic murmurs that originate at the semilunar valve and those that originate at the atrioventricular valve. This discussion can be concluded with a consideration of two interesting "functional" diastolic murmurs that occur in the presence of "organic" diastolic murmurs.

First, consider the patient known to have an "organic" mitral stenosis with its attendant atrioventricular diastolic murmurs. There may be associated with this a short semilunar diastolic murmur due to one of two reasons. The murmur may be due to aortic valve insufficiency, which is also usually due to rheumatic valvulitis. On the other hand the murmur may be due to pulmonic valve insufficiency. This can arise out of the train of events that start with atrial pressure causing an increase in pulmonary artery pressure which may further rise as pulmonary vascular resistance increases. Finally, the rise in pulmonary artery pressure may then cause dilatation not only of the pulmonary artery but also of the

pulmonic valve ring yielding valvular insufficiency. This causes a semilunar diastolic murmur, the so-called Graham Steell murmur (96). Although it is clear that theoretical acoustic criteria can be set up to differentiate these two, in actual practice the associated nonacoustic phenomena must be used. In the presence of clear-cut hemodynamic evidence for aortic insufficiency one need not invoke the Graham Steell murmur. The difficulty ensues when there is no definite hemodynamic evidence for aortic insufficiency. One must also look for circumstances that would produce dilatation of the pulmonic valve ring, namely, the degree of pulmonary hypertension must be severe to expect this to occur. Lacking this evidence, it is much more likely that the murmur is due to aortic valvulitis. Indeed, thus far in our small series, despite the clinical suggestion of Graham Steell murmur, we have not been able to localize the murmur to the right heart, but rather have heard it in the left heart. Our findings, in this respect, are in agreement with the conclusions reached by Brest *et al.* (13) from their operative series.

Conversely, consider the patient with known "organic" aortic insufficiency with its attendant semilunar diastolic murmur. There may be associated with this a mitral diastolic murmur due to either of two reasons. It may be due to "organic" mitral stenosis. On the other hand it may be due to "functional" mitral stenosis, the so-called Austin Flint murmur (32). This murmur is not the semilunar diastolic murmur heard on that part of the thorax where one usually hears murmurs originating at the mitral valve. The Austin Flint murmur is truly a mitral murmur and, as such, has the characteristics of an "organic" murmur. Again there appear to be no rigorous acoustic criteria which will confidently separate these two types, and recourse must be had to the accompanying hemodynamic circumstances. In order to understand the mechanism of production of the Austin Flint murmur and any possible means of providing accurate diagnosis, one must reconsider the function of the mitral valve. The anterior or septal leaflet of the mitral valve moves between the inflow and outflow tracts of the left ventricle. In systole this leaflet moves into the inflow tract and shuts off the entrance from the atrium. In diastole the leaflet moves downward (into the ventricle) and anteriorly toward the septum into the outflow tract. In normal diastole the leaflet is free to move into the outflow tract as the ventricle fills only through the inflow tract. However, in the presence of aortic insufficiency the ventricle fills from both the inflow tract and the outflow tract with the result that the leaflet is caught between two streams. If the regurgitant flow from the aorta is large and forceful enough it will cause the leaflet to impinge in part on the inflow tract. And just as a stenosed valve reduces the inflow orifice and produces a mitral diastolic murmur, so will the normal leaflet held in the stream. The result is a mitral diastolic murmur. If this explanation of the mechanism is a valid one then one associated hemodynamic factor can be deduced. One cannot expect the leaflet to be held in the inflow stream if the amount of regurgitation is small. Therefore, one cannot expect an Austin Flint murmur with minor degrees of aortic insufficiency. The other important factor involves the sounds. If the opening snap is produced as was previously described, then one would not expect this in the presence of a "functional" mitral stenosis, nor would one expect delay in the appearance or a snapping quality to the mitral component of the first heart sound.

MURMURS OF NONVALVULAR ORIGIN. When an abnormal communication, either congenital or acquired, exists between two cardiac chambers or vessels, there exists the possibility of flow through this defect with the resultant production of a murmur. This type of approach to the problem is essential, since the mere presence of an anatomical lesion does not assure that a murmur will be generated. There must be flow through it. It is also important to remember that even with flow through an abnormal communication a murmur, if produced, must reach a certain intensity to be detected on the thorax.

Consider first communications at the three levels, namely, at the level of the great vessels, at the level of the ventricles, and at the level of the atria. Communications at the level of the great vessels (aorta to pulmonary artery) may be congenital, as in patent ductus arteriosus, aortic septal defect (aortico-pulmonary window), and ruptured sinus of Valsalva aneurysm into the pulmonary artery. They may also be acquired as in the Blalock (6) or Potts (78) type of anatomosis designed to increase pulmonary blood flow. In the normal, the pressure in the aorta fluctuates between approximately 80 and 120 mm Hg, whereas in the pulmonary artery the pressures vary in the cycle between approximately 10 and 30 mm Hg. If an existing communication does not significantly disturb this relationship, then, since the pressure in the aorta exceeds the pressure in the pulmo-

nary artery throughout the cycle, one can expect flow throughout the cycle and a murmur throughout the cycle. In this circumstance, then, one expects and does find a continuous murmur, or a so-called machinery murmur. Furthermore, the gradient of pressure increases during systole and decreases during diastole which yields the expected effect on murmur intensity.

When the normal relationship between the two pressures is disturbed for any reason, then there may be a change in the time-course of flow and consequently of the murmur. Here again the pressure gradient yields a first approximation as an acoustic correlate, the prime correlate remaining the flow. With a lessening of the pressure gradient, due most often clinically to increased pulmonary vascular resistance, a number of hemodynamic situations are possible. Perhaps the most common situation is the retention of a systolic gradient with the loss of the diastolic gradient. Here, as might be expected, the diastolic component of the murmur is lost. The reverse, retention of the diastolic gradient alone, is much less common. When the two pressures become identical and there is little or no flow, the murmur disappears. For completeness it should be pointed out that identity of the pressure carries with it three possible hemodynamic situations: a left-to-right shunt, no shunt, or a right-to-left shunt. It is only in the second case that there is no potential for murmur production. In the first case there is the potential for the production of a murmur originating in the pulmonary artery. In the third case there is the potential for murmur production, but here it would be directed into the aorta. This might well be localized by recording at the site of murmur production but would be expected to be difficult from recordings taken on the thorax. With pressure in the pulmonary artery in excess of that in the aorta, one would have to expect that a murmur, if present, would be produced in the aorta. This is an unusual circumstance but has been observed (18). It should be remembered that the above discussion of murmur production and localization deals only with murmurs produced by the flow through the lesion itself and is not meant to include other murmurs that may be present as a result of the altered hemodynamics.

One final consideration that applies particularly to patent ductus arteriosus should be noted. For this lesion there are two circumstances in which the murmur may appear with only the systolic component. The first, as discussed, is due to a rise in pulmonary artery pressure, due most often to an increased pulmonary vascular resistance, such that the diastolic pressure gradient and flow are abolished. The second is due to closure of the ductus during diastole. This may occur when the communication is small and the movement of the heart or the ductus itself twists off the passageway. Here the two pressures (aorta and pulmonary artery) are widely different and, although a gradient is present, a communication is not. Differentiation between these two similar acoustic events can be based on the very dissimilar accompanying hemodynamic and therefore clinical presentation.

A defect in the ventricular septum may arise out of a congenital cardiac malformation or be acquired following myocardial infarction (88) or trauma. In the normal, the left ventricular pressure is between 0 and 10 mm Hg in diastole and rises to approximately 120 mm Hg in systole, whereas the right ventricular diastolic pressure is between 0 and 5 mm Hg and the systolic pressure rises to 30 mm Hg. At the onset of systole left ventricular pressure rises before right ventricular pressure, and begins to fall first at the end. The result is that from the time of the initial valve component of the first sound until at least the aortic valve component of the second sound, left ventricular pressure exceeds right ventricular pressure. In fact a gradient may exist throughout the cycle, since the diastolic pressure in the left ventricle may be higher than that in the right, but more information is needed on this point. From the acoustic standpoint, the above circumstance would be expected to produce a systolic murmur that begins with the first sound and goes at least up to and perhaps beyond the aortic component of the second sound. Furthermore, since the ventricular pressures rise rapidly to peak value there is little variation of the gradient throughout systole. The result is that the murmur shows little variation in intensity throughout systole. Such a murmur meets all three criteria for a regurgitant type of systolic murmur and may be classified as such.

The usual type of deviation of the dynamics from the normal is an increased right ventricular systolic pressure. So long as the normal order of events is preserved, there will remain a gradient of pressure from left ventricle to right ventricle that begins with mitral closure and persists up to aortic closure, for all right ventricular pressures below left. Therefore, so long as right ventricular systolic pressure does not equal left ventricular systolic pressure, the circumstances will be present for the potential production of a regurgitant type of systolic murmur. We

have seen this in two cases in which the right ventricular systolic pressure was artificially raised by partially occluding the pulmonary tree. The form of the murmur remained the same, though there was diminution in intensity with eventual disappearance when the two systolic pressures became equal. In the usual clinical circumstance, intensity is dependent upon an additional factor, namely, defect size. Ordinarily, an increased level of right ventricular systolic pressure is found in the congenital type of lesion in patients with large defects.

With identity of systolic pressures as found clinically there may be a left-to-right shunt, no shunt, or a right-to-left shunt. Here, as in great vessel defects, the exact hemodynamic circumstance determines the intracardiac location of murmur production or the absence of a murmur.

A number of interesting problems remain concerning the murmur produced by a ventricular septal defect. One has already been alluded to, namely, the exact relationship between pressures and the question of flow through the shunt in diastole. For example, despite the fact that presumably left ventricular diastolic pressure is greater than right we have not observed a diastolic component to this murmur even when listening just at the defect within the heart. Clearly, more detailed studies of dynamics, shunt flows, and position of the leaflets of the atrioventricular valves is needed to tell whether there is a communication in diastole and, if so, the nature of any possible flow. In addition, studies are needed on the differences, if any, between defects of the membranous and muscular portions of the septum. It has been suggested that contraction of the septum during systole changes the size of the latter type of defect and thereby alters the acoustics. This highly likely phenomenon deserves more careful investigation. We have also seen, particularly in cases with elevated right heart pressures, minor deviations in murmur form, such as a short silent period after the first heart sound. The precise meaning of such observations and their value remain to be investigated.

Defects in the atrial septum present an extremely fascinating situation acoustically. To understand this, an understanding of the altered hemodynamics produced by this lesion is necessary. In the usual clinical situation such a defect produces a left-to-right shunt. This is due not only to the greater distensibility of the right atrium than of the left but also to the greater diastolic distensibility of the right ventricle than of the left. The result is an increase in inflow into the right ventricle in diastole with a necessary increase in stroke output in systole. This increased volume of blood then flows through the lungs to be returned to the left atrium and made available for reshunting through the lesser circulation. The amount of blood that passes through the mitral valve and is thereby available for left ventricular ejection and circulation through the body is either normal or reduced. The time-course of flow through the defect itself appears to be throughout the cycle with the major shunt in ventricular diastole, though the details of this and the time at which the small right-to-left shunt occurs remains to be elucidated completely. Recordings from the site of the lesion indicates that many patients have a murmur in ventricular diastole (31, 59, 63). It appears, however, that the intensity of this murmur rarely if ever is sufficient to allow it to be heard on the thorax. There is, though, an increased flow across both the tricuspid valve (in diastole) and the pulmonic valve (in systole). Both of these have the potential for producing murmurs because often the flow is torrential. It is most usual in patients with atrial septal defect to hear a systolic murmur. Since this murmur is ejection in type it appears to be of semilunar valve in origin. Comparison of this murmur on the thorax with recordings from within the heart reveals the virtual identity with the murmur that can be localized to the pulmonary artery. In like manner, the increased flow across the tricuspid valve may, if the flow is great enough, produce a diastolic murmur that has the characteristics of a murmur originating from an atrioventricular valve. It must be remembered that neither one of these murmurs is produced by the flow through the defect itself but rather by the increased flow through the right heart. When one compares the acoustic events that arise out of shunts at the three levels an interesting point arises. In the usual circumstance, the murmurs from great vessel communications and from ventricular septal defects arise out of flow through the lesion itself. It is in this way that they, as well as the murmurs from organic valvular lesions, come to have certain recognizable characteristics. However, for atrial septal defect the murmurs that reach sufficient intensity to be heard on the thorax come not from flow through the defect but from increased flow across usually normal valves. It is for this reason that these murmurs are not necessarily characteristic of the lesion and a precise correlation must depend upon associated hemodynamic and acoustic data.

Occasionally, communications may exist between

the greater and lesser circulations not at comparable levels, as described above, but from one level to another. For example, the aorta, through a ruptured sinus of Valsalva aneurysm, may communicate with either the right ventricle or the right atrium (30). The form of the acoustic events is determined by the pressure gradient and consequent flow that ensues. If the normal pressure values are retained, the aortic pressure in both lesions is always greater than the pressure of the chamber into which the shunt empties, with the result that continuous murmurs are present. It would be virtually impossible for any other situation to obtain with a communication into the right atrium, whereas for a shunt into the ventricle there may be identity of the pressures in systole. In this case the gradient would be present only in diastole, and if flow were present only in diastole then the murmur would be present only in diastole. An interesting situation that resembles this, but has peculiarities of its own, is the communication between a coronary artery and the various levels of the lesser circulation. The best described of these (33) is the circumstance in which the shunt enters the right ventricle. Here the pressure gradient would suggest a continuous murmur, which is the observed phenomenon. However, in order to understand the acoustic phenomenon in its entirety recourse must be had to the time-course of coronary flow, which one expects to be the prime correlate of murmur production. Due to the nature of coronary flow, which is greater in diastole than in systole, the murmur has a diastolic accentuation, which gives it an unique and virtually diagnostic form. Gasul *et al.* have suggested that flow in systole is reduced due to reduction in the size of the fistula during systole, and have called upon diastolic suction of the ventricle to explain the nature of the flow in diastole. A true understanding of the acoustic phenomena awaits a more detailed description of the time-course of flow through the shunt. Such information would be of value in explaining the absence of diastolic accentuation of the murmur when the shunt from the coronary artery enters either atrium or pulmonary artery.

At the next level down, there are cases in which the left ventricle communicates with the right atrium. This may occur directly through the portion of the membranous septum above the implantation of the septal leaflet of the tricuspid valve or just below this point and the entrance into the right atrium obtained through a defect in the tricuspid valve. In this situation the pressures will be different during systole from the onset of left ventricular activity until at least the left ventricular pressure reaches its diastolic level. Since during diastole right atrial pressure is identical with right ventricular pressure, an analogy with ventricular septal defect may be drawn. From this one would expect that the acoustic representation of such a lesion would mimic a ventricular septal defect entering the right ventricle, and such is the case. Again, where the acoustic manifestations of two lesions have reason to be identical, differentiation must be made by associated phenomena.

The presence of an arteriovenous fistula in the thorax (or for that matter anywhere) is yet another source of acoustic phenomena. A fistula between the pulmonary artery and pulmonary vein is associated with flow through the lesion throughout the cardiac cycle, since there is usually a pressure gradient throughout the cycle, except perhaps at the end of diastole. This fact, coupled with the fact that the gradient is greater in systole than in diastole, suggests the production of a continuous murmur with accentuation in systole. Similarly, a systemic arteriovenous fistula, as for example, between the subclavian artery and vein, yields a pressure gradient throughout the cycle, greater in systole, and therefore, too, a continuous murmur with systolic accentuation. It is to be noted that in form, these murmurs resemble those that arise out of communications between the aorta and pulmonary artery.

Normal arteriovenous communications may produce continuous murmurs in the same way that abnormal arteriovenous connections do. This situation arises when there is increased flow through channels that normally carry small flow loads. Such a circumstance may occur normally when specific physiological demands call for increased flow. For example, during lactation the markedly increased mammary blood flow may produce a continuous murmur (43, 90). Also when there is arterial obstruction, the development of collaterals, if great enough, may increase the flow through these vessels enough to produce murmurs. For example, coarctation of the aorta, which impedes flow at the aortic isthmus, calls forth the development of collateral circulation which supplies the lower part of the body. The increased flow through the vessels around the shoulder girdle and intercostal vessels may produce murmurs, as well as the murmur produced by flow through the stenosed isthmus itself. For this lesion Spencer *et al.* (95) have shown that the murmur produced by the collateral channels is systolic in

time, whereas that produced by the coarctation itself depends upon the severity of the obstruction.

Effect of Respiration on Murmurs

Consider first the effect of inspiration on the right heart. In the discussion on heart sounds a train of events was pictured that began with the decrease in intrathoracic pressure and led to an increase in the flow into and the stroke volume from the right ventricle. There is also an increase in the flow into the pulmonary vascular bed. If one returns to the suggestion that the prime correlate of murmur intensity (and presence) is the volume (and time-course) of the flow, then it follows from this that murmurs originating in and exclusively limited to the right heart would be expected to increase in intensity with inspiration. Thus, the increased inflow into the right heart increases the intensity of the murmur of tricuspid stenosis. The increase in right ventricular stroke volume increases the intensity of the murmur of tricuspid insufficiency [pointed out some time ago by Rivero Carvallo (84)] and of murmurs created at the pulmonic valve. The increase in flow into the pulmonary tree will increase the intensity of the murmur of pulmonary arteriovenous fistula. Our own experience with this phenomenon indicates a number of additional features. We have had the greatest experience with the murmur of tricuspid insufficiency and will use this as an example. First, there is not always an exact correlation between what is heard inside the heart at the site of murmur production and what is heard on the thorax. Intensity may clearly increase at the site of production, and yet it may be difficult from recordings on the thorax to decide that this has occurred. Second, the change with inspiration may manifest itself more clearly by a change in quality than by a change in intensity. This can best be described by noting that the murmur assumes a harsher quality.

In considering the effect of inspiration on the left heart it will be remembered that the train of events from the initial effect of the lowering of intrathoracic pressure proceeded via the increased vascular volume of the lung to a decreased left ventricular filling and stroke volume, and a decrease in aortic flow. As a result, murmurs that originate in the left side of the circulation and are limited thereto can be expected to decrease in intensity with inspiration. Therefore, the reduced ventricular inflow decreases the intensity of the murmur of mitral stenosis. The reduced stroke output decreases the intensity of the murmur of mitral insufficiency and of murmurs from the aortic valve. One can expect also a decrease in intensity of murmurs dependent upon aortic flow for their generation.

Conversely, one may consider that the effect of expiration will be to decrease the intensity of murmurs from the right side and increase the intensity of those from the left side.

Additional information on the site of murmur production can be obtained by utilizing the Valsalva maneuver (109). When the forced expiratory phase is maintained for a sufficiently long time, the reduced inflow into the right heart causes not only a reduced right output but as a consequence a decreased left heart output. In this situation murmurs originating in either side of the heart will decrease in intensity. From this new equilibrium point one can then observe the time-course of the return of murmur intensity to the control level following the cessation of the forced expiration. There is first an increase in right heart output followed later by an increase in left heart output. Thus the time interval for the right heart murmurs to return will be shorter than those from the left heart.

The same appreciation of the effects of normal respiration can be used to deduce the effects of both inspiration and expiration on the intensity of murmurs arising out of abnormal communications. Consider first communications at corresponding levels where the shunt is left-to-right. For these lesions inspiration, which raises right heart pressure and flow and lowers left heart pressure and flow, can be expected to produce a decreased gradient across the defect, a decreased shunting, and consequently a decrease in murmur intensity. The situation in shunts at the level of the great vessels and ventricle appears clear-cut. The situation in shunts at the atrial level is complicated by the fact that the right ventricular inflow depends upon systemic venous return, which would appear to be increasing, and upon flow through the defect. This latter might decrease due to the decrease in return to the left atrium, though it is fair to say that more knowledge on this point is required. Depending therefore on the relative effects upon systemic inflow, pulmonary venous return, and flow through the shunt, the right heart inflow may increase, decrease, or remain the same. Efforts to analyze the resultant effects is complicated by this lack of precise knowledge. In many cases, as discussed above on the section on heart sounds, it appears that the duration of mechanical systole of the right ventricle remains unchanged. This may be due to a balanced alteration

in the volume of right heart filling from the two sources. If this is the case, then murmur intensity of the audible murmurs on the thorax would be expected not to change. There is, however, an alternate explanation for the relatively unvarying systolic duration. In the normal, it appears that stroke volume can be increased by an increased systemic venous return with consequent lengthening of systole. With atrial septal defect the stroke volume is greater than normal. In this circumstance the same volume of increased venous return results in a smaller percentage increment in stroke volume which may not appreciably affect the duration of mechanical systole. In this circumstance, whereas the duration of systole is invariant the right heart inflow and outflow are increased and one would expect an increase in murmur intensity. Our own experience indicates that there may be either no change in murmur intensity or an increase with inspiration, but the exact hemodynamic circumstances in which each obtains is not clear. Further investigation is warranted.

When murmurs arise out of communications where the shunt is right-to-left, the alterations in pressure and flow produced by inspiration, if it has any effect at all, can be expected to cause an increase in the intensity of the murmur. Also one would not expect the problem of the balance of effects with regard to atrial septal defects.

When the Valsalva maneuver is employed in the manner described above, changes in the intensity of shunt murmurs will also be noted. Following release of the forced expiration there is an appreciable delay in the return of left heart flow so that for left-to-right shunts there is a delay in the return of murmur intensity. For murmurs due to right-to-left shunts one expects an immediate return of murmur intensity.

Effect of Pharmacological Agents on Murmurs

Since murmur intensity is based on flow one can employ, in addition to respiration, certain pharmacological agents to change temporarily the flow and thereby elucidate valuable information.

This discussion will be concerned primarily with the hemodynamic principles involved, and no discussion of the specific agents or means of administration will be attempted. Reference should be made to original publications (3, 19, 21, 94, 99, 100).

Consider first the effect of changing arteriolar resistance to flow on systolic murmurs of valvular origin. If the murmur originates at the semilunar valve, decreasing vascular resistance will cause a faster runoff of blood and tend to decrease the great vessel pressure. This will result in an increased gradient of pressure and if the ventricle is able to meet the demand, an increased volume ejected. In this circumstance one would expect an increased intensity of the murmur. On the other hand if resistance is increased, there will be a tendency for the gradient and flow to be reduced transiently with a decrease in murmur intensity. If the murmur originates at the atrioventricular valve then one can expect changing arteriolar resistance to produce just the opposite effect. It should be remembered here, in the case of atrioventricular valve insufficiency, that the ventricle is ejecting blood both forward into the great vessel and backward into the atrium. The percentage of the total amount moved that goes in each direction is a function of the resistance to flow in that direction. Therefore, when the resistance to flow forward in the direction of the great vessel is increased, the relative backflow into the atrium is increased, with a consequent increase in murmur intensity. Conversely, a decrease in forward resistance increases the flow in this direction and, by decreasing the relative backward flow, decreases murmur intensity. This phenomenon put forward first with respect to the effects on pressure (12), but equally effective on murmur production, has been found of value in the recognition and assessment of mitral insufficiency.

A very similar situation exists with diastolic murmurs arising out of insufficiency of the semilunar valve. Here the great vessel flow divides itself between forward flow into the smaller vessels and back flow into the ventricle on the basis of the relative resistance offered to each pathway. If the small vessel resistance is increased then the relative backward flow will increase with a consequent increase in murmur intensity. A decrease in vascular resistance will increase the relative forward flow and decrease murmur intensity. Since forward flow across the atrioventricular valve in atrioventricular stenosis is determined by the gradient of pressure across the valve, changes in vascular resistance affecting great vessel flow and ventricular performance will not directly affect this murmur. Alterations produced can be variable depending in large part on the nature of the ventricular response; in particular, the effect on the ventricular diastolic pressure.

In all of the above considerations attention must be directed not only at the primary effect of changes in vascular resistance but also at secondary or compensatory effects. In some situations these will affect murmur intensity in the same direction as the primary

effect, but in others there will be an opposite effect which may tend to cancel out or even overbalance the primary effect. For example, in the effect of the decrease in vascular resistance on murmurs produced at the semilunar valve, the primary effect of lowering on-going resistance and great vessel pressure tended to increase the systolic murmur and decrease the diastolic murmur. The compensatory phenomenon of an increased stroke output acts in the same direction for the systolic murmur and, if anything, tends to accentuate its increase. However, so far as the diastolic murmur is concerned an increased stroke output makes more blood available for regurgitation, and this tends to act in the opposite direction on murmur intensity.

When the action of pharmacological agents is considered in reference to shunt murmurs, the important consideration is the effect of the agent on the balance between systemic and pulmonary vascular resistance. The direction and magnitude of the shunt depends on systemic vascular resistance, pulmonary vascular resistance, and the resistance imposed by the communication itself. Since this last is constant in this situation any alteration in the vascular resistance of either bed will result in a change in shunt flow. From this consideration one can reasonably predict the effects. For left-to-right shunts an increase in systemic resistance and/or a decrease in pulmonary resistance will increase the shunt flow and the murmur. Conversely, a decrease in systemic resistance and/or an increase in pulmonary resistance will decrease murmur intensity. For example, mephentermine, which increases primarily the systemic resistance, increases the intensity of the murmur of patent ductus arteriosus. Such an effect is of greatest clinical assistance when a part of the murmur is inaudible on the thorax. Here the increase in intensity produced may raise this inaudible segment to the level of audibility thus converting it from an "atypical" murmur to a "typical" murmur. We have discussed above the observation that partial balloon occlusion of the pulmonary artery could be made to abolish the murmur of ventricular septal defect. Alterations in vascular resistances in the presence of right-to-left shunts have been carried out mainly to demonstrate the effect upon arterial oxygen saturation (16). The effect on the acoustic events has been less well studied. However, the observations on left-to-right shunts suggest that one might be able to predict the effect on the murmurs due to these shunts. This deserves careful analysis, since often such murmurs as are present may be due to relative changes in flow through normal channels rather than flow through the shunt itself.

Occasionally, agents employed primarily to change vascular resistance will produce side effects that may be used to obtain information on the acoustic events. For example, certain agents at times will produce premature ventricular contractions. These may also occur spontaneously. Although numbers of these can be considered troublesome, an occasional one can be helpful. Consider the effect of a premature ventricular contraction on the intravascular pressures. Due mainly to the smaller diastolic volume, but perhaps to other factors as well, the systolic pressure produced by the premature ventricular contraction is less than normal. The great vessel pressure will also be less, since the energy supplied by the ventricle is less. The atrial pressure during the premature systole will rise, since at the beginning of the premature contraction the atrium was left with a more than normal volume of blood. Consider now the effect that this would have on systolic murmurs of valvular origin. The premature contraction would decrease the gradient of pressure across the semilunar valve, and since ventricular pressure is lower and atrial pressure is higher, the systolic gradient across the atrioventricular valve would also be decreased. Both would result in a decrease in murmur intensity. However, since the ventricular pressure must rise to a reasonably high level to open the semilunar valve, the effect on the gradient across the semilunar valve would be expected to be much greater than that across the atrioventricular valve (fig. 10). The result is that, whereas the intensity of both murmurs will move in the direction of a decrease, the decrease is much greater for the semilunar murmur than for the atrioventricular murmur. So that on auscultation premature ventricular contractions can be expected to produce quite easily recognizable changes in the intensity of semilunar ejection type systolic murmurs, and less readily recognizable changes in atrioventricular regurgitant type systolic murmurs.

Premature ventricular contractions can also be used to help identify the site of origin of heart sounds. This has been discussed by Hartman (37) and deserves further application. The basis for the application to sound identification resides in the fact that if the ventricle from which the premature contraction originates can be identified (e.g., from the electrocardiogram), then advantage can be taken of the fact that the opposite ventricle will be delayed in the onset of its mechanical activity. By combining sound re-

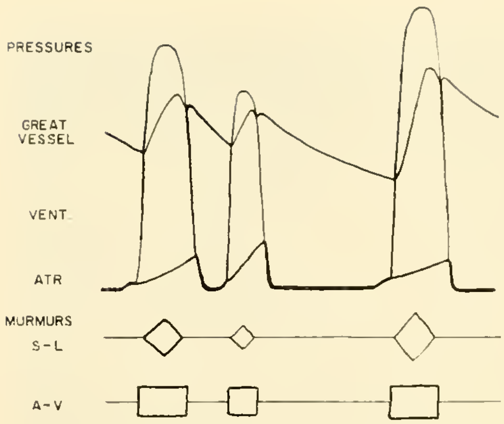

FIG. 10. Effect of premature ventricular contraction on systolic murmurs of valvular origin. The pressures are from the great vessel, ventricle, and atrium of a subject with both semilunar valvular stenosis and atrioventricular valvular insufficiency. The acoustics below show only the envelopes of the respective murmurs from the semilunar valve (S-L) and from the atrioventricular valve (A-V). The first beat is normal, followed by a premature ventricular contraction, and the last a normal beat after a compensatory pause. Note the relatively greater effect of the premature contraction on the systolic pressure gradient across the semilunar valve and its murmur than on the systolic pressure gradient across the atrioventricular valve and its murmur.

cordings with other parameters on the surface, as discussed above, the timing of various events can be implemented.

Method of Identification of Site of Origin of a Murmur

With the physiological basis for murmur production described, one can now set down certain methods of approach and criteria that will allow for identification of the site of murmur production. Where the physiological circumstances surrounding murmur production are unique, a characteristic or pathognomonic murmur may result which leads immediately to identification. However, more often similar physiological circumstances coexist for more than one lesion and the best that can be done on purely acoustic grounds is a differential diagnosis. Again, this discussion will be limited to physiological principles and no attempt will be made to catalogue in detail all lesions and their variations.

The first step, as mentioned previously, is to identify the phase of the cardiac cycle in which the murmur occurs. When a murmur or combination of murmurs occurs in both systole and diastole, a distinction should be made as to whether the murmur has a systolic and a diastolic component, or whether it is truly a continuous murmur. Next, one should determine the region on the thorax over which the murmur is heard. Although this criterion is not without exceptions, in the vast majority of cases there is good uniformity with expected localization. The next step should be the determination of the internal characteristics of the murmur, this is, the form. This may not always be readily discernible by auscultation, and, if important, should be determined by phonocardiography. For systolic murmurs, this allows separation of murmurs from the semilunar valve from those originating at the atrioventricular valve. The former group yield ejection-type murmurs and the latter group yield regurgitant-type murmurs. To this latter group must be added the murmur of ventricular septal defect. The next step should be to note the effect of respiration, including the Valsalva maneuver if necessary, on the intensity of the murmur. This allows for a separation into two different groups; one that originates and is limited to the right heart (increase with inspiration) and the other that originates in the left heart or from left-to-right shunts (decrease with inspiration).

Therefore for systolic murmurs of valvular origin, a murmur may be pinpointed to the tricuspid valve if it is regurgitant in type and increases on inspiration. Murmurs from the pulmonic valve also increase with inspiration but are ejection in type. A murmur is identified as coming from the mitral valve if it is regurgitant in type and either decreases on inspiration or increases on expiration. This same response to respiration occurs if the murmur originates at the aortic valve but it is ejection in type rather than regurgitant (table 1).

It should be noted that the murmur of ventricular

TABLE 1. *Systolic Murmurs of Valvular Origin, Criteria for Identification of Site of Origin (Other Than Localization on Thorax)*

	Internal Characteristics	Effect of Inspiration*
Mitral insufficiency (MI)†	R	D
Tricuspid insufficiency (TI)	R	I
Aortic stenosis (AS)	E	D
Pulmonic stenosis (PS)	E	I

E = ejection type; R = regurgitant type; I = increased intensity; D = decreased intensity. * The effect of expiration is just the opposite. † The murmur of ventricular septal defect with left-to-right shunt (VSD, L-R) has the same characteristics.

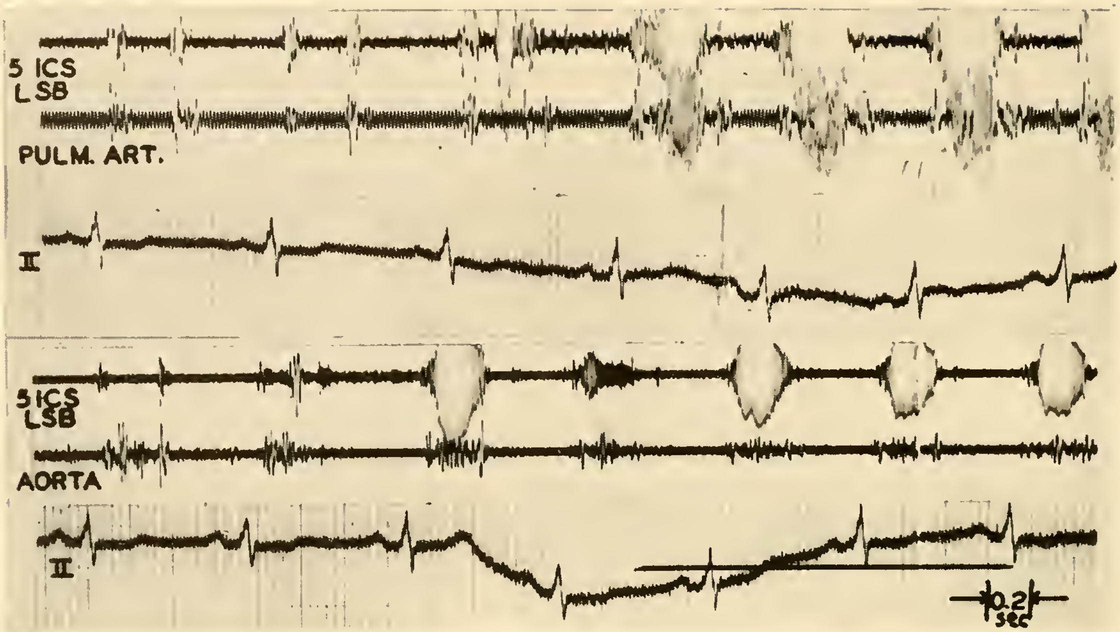

FIG. 11. Intracardiac phonocardiogram, illustrating one aspect of acoustic localization with this technique. The recordings were taken from a 59-year-old male with tricuspid insufficiency secondary to right heart failure. The upper recording shows from the top down: chest phonocardiogram from the fifth intercostal space at the left sternal border (5ics *LSB*); next, the intracardiac phonocardiogram from the main pulmonary artery; and below this, lead II of the electrocardiogram. The lower recording is the same with the exception that the intracardiac phonocardiogram is recorded from the ascending aorta just above the aortic valve. In each recording the beginning was taken near the end of the phase of expiration, and inspiration begins about in the middle of the record. Note that in each recording the tracing taken from the chest shows the increase in the intensity of the murmur with inspiration. In the intracardiac recordings this is well shown in the pulmonary artery but not in the aorta, pointing toward localization of the murmur to the right heart. The demonstration of an increase in the intensity of this murmur with inspiration confirms the thesis of Rivero Carvallo (84) that the change in intensity of the murmur on the chest is due to a change in dynamics. It cannot be considered as being due to a change in the position of the heart or in its relation to the chest wall. In addition, note that both components of the second sound are present in the pulmonary artery tracing, whereas only the aortic valve closure component is seen in the tracing taken in the aorta.

septal defect is regurgitant in type and decreases on inspiration. These two criteria are those of the murmur of mitral insufficiency. It must be remembered, therefore, that on these two acoustic criteria alone one cannot confidently make the differential diagnosis between mitral insufficiency and ventricular septal defect.

For diastolic murmurs of valvular origin, the major differentiating feature besides the frequency characteristics is again the form of the murmur. Murmurs from the semilunar valve begin with the second sound component and are decrescendo in character. Murmurs from the atrioventricular valve begin shortly after the second sound component with the opening of the atrioventricular valve. They are decrescendo in character with presystolic accentuation, the latter occurring in the presence of atrial contractions. For the group that originate at the atrioventricular valve a murmur that increases in intensity with inspiration identifies the site of origin as the tricuspid valve. A decrease with inspiration or an increase with expiration identifies the murmur as mitral in origin. The effect of normal respiration on semilunar diastolic murmurs, although theoretically following the pattern established, is less well brought out than the others, and care must be used in reaching conclusions. Of help here should be a properly performed Valsalva maneuver or the proper pharmacological agent.

For continuous murmurs which arise at abnormal communications of one sort or another, respiration can be used to provide a partial differentiation. An increase in intensity with inspiration identifies the

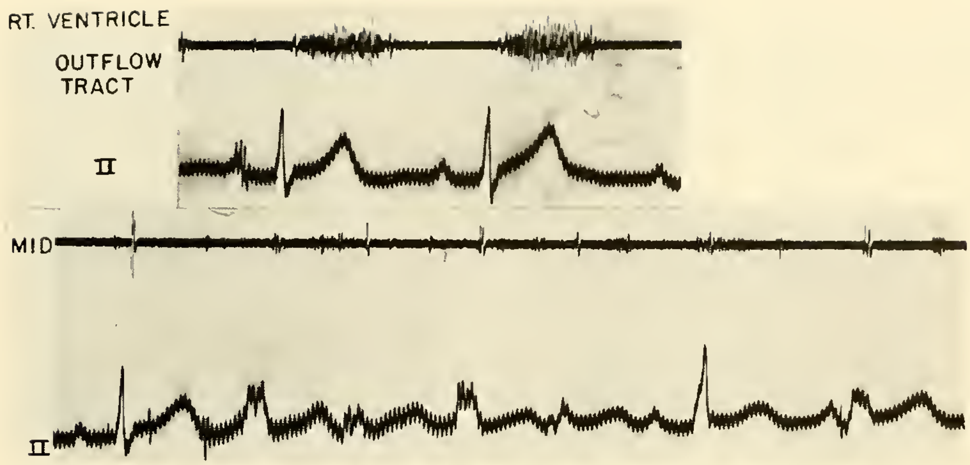

FIG. 12. Intracardiac phonocardiogram, illustrating another aspect of acoustic localization. These recordings were taken from a 7-year-old boy with a ventricular septal defect with a left-to-right shunt. The upper recording shows the intracardiac phonocardiogram taken from the outflow tract of the right ventricle and shows a loud regurgitant-type systolic murmur. The lower recording taken from the midportion of the right ventricle (note the premature ventricular contractions) shows little or none of the murmur heard in the outflow tract.

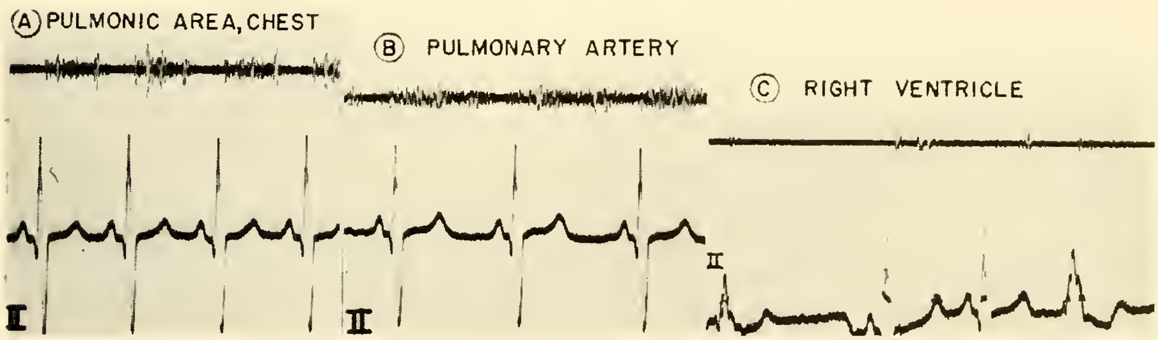

FIG. 13. Intracardiac phonocardiogram, illustrating the use of this technique in investigating the transmission of acoustic events to the chest wall. These recordings were taken from a 3-month-old boy with a patent ductus arteriosus with a left-to-right shunt and with pulmonary hypertension. The pulmonary artery pressure was equal to the pressure in the aorta. The *A* recording shows the phonocardiogram at the time of cardiac catheterization recorded at the pulmonic area on the chest (upper left sternal border). Note that here there is a systolic murmur, a loud second sound, but no diastolic murmur. In contradistinction to this, the recording taken from within the pulmonary artery (record *B*) shows both systolic and diastolic components, in reality a continuous murmur. The recording *C* from within the right ventricle shows no murmur.

communication as being in the lesser circulation. A decrease with inspiration or an increase with expiration identifies the murmur as either wholly originating on the systemic side or from a left-to-right shunt.

INTRACARDIAC PHONOCARDIOGRAPHY

In the investigation of the physiological correlates of cardiac acoustics one powerful tool that has recently been introduced is the intracardiac phonocardiogram. This method utilizes the technique of cardiac catheterization to record the events from within the heart and circulation. The proper application of all of the various types of catheterization, i.e., sites of entry of the catheter, allows for introduction of the transducer into all chambers of the heart and virtually all major vessels. Various transducers have been applied, all with the aim of recording the vibrations in the audible frequency range.

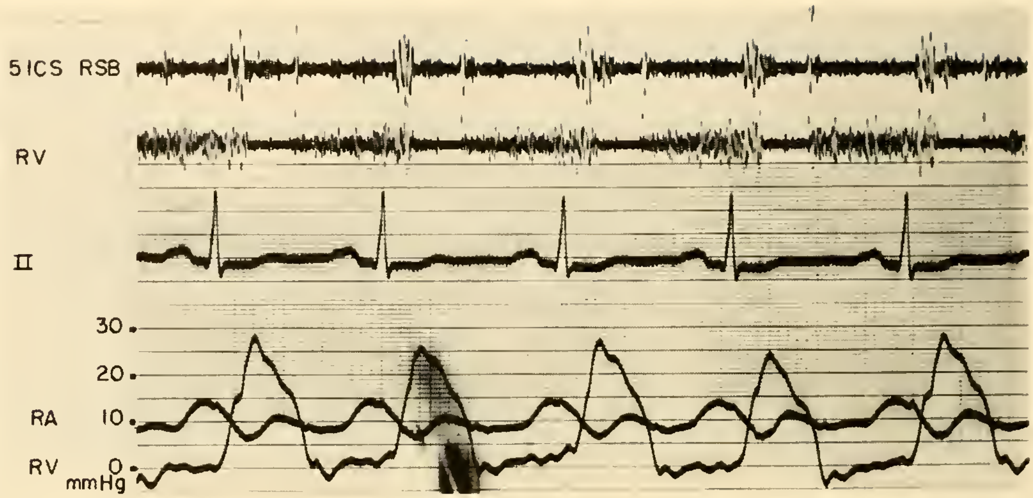

FIG. 14. Intracardiac phonocardiogram, illustrating the use of this technique in the correlation of acoustic events with hemodynamics. These recordings were taken from a 30-year-old female with rheumatic heart disease with both mitral stenosis and tricuspid stenosis. The recording shows from above downward: the chest phonocardiogram from the fifth intercostal space at the right sternal border (5ics RSB) (where the tricuspid murmur could be heard best), the intracardiac phonocardiogram from the inflow tract of the right ventricle (RV), lead II of the electrocardiogram, right atrial pressure (RA), and right ventricular pressure (RV). The pressures were recorded from the same base line with identical calibrations. Note that at the point at which ventricular pressure falls below atrial pressure a murmur begins in the right ventricle which continues up to the time at which right ventricular pressure rises above right atrial pressure. With an increase in the gradient of pressure across the valve late in diastole with atrial contraction there is an increase in the intensity of the murmur. Not shown here is the mitral diastolic murmur from within the cavity of the left ventricle which had a different configuration than this murmur originating at the tricuspid valve.

The technique of intracardiac phonocardiography has certain advantages as well as certain disadvantages. Its great value lies in its ability to record the events from close to their site of origin. This not only provides a means of direct comparison with other events of the cardiac cycle but also provides a means for studying transmission through the thoracic tissues to the chest wall. In addition, intracardiac phonocardiography has proved of great value in that it has the ability to localize sharply the production of sounds and murmurs. This feature, which, perhaps, could not have been predicted prior to the actual observations, appears to be due to the damping characteristics of the structures involved, including the blood. The details of this parameter are as yet incompletely understood. From the records obtained it is clear that the intracardiac transmission of the various events differs. For example, it is not unusual to record aortic valve closure with the transducer located in the outflow tract of the right ventricle. It is decidedly unusual to record an aortic diastolic murmur here. In general, there appears to be wider transmission within the heart and circulation of sounds than of murmurs. Indeed the localization of murmurs may be quite precise. For example, in ventricular septal defect with a left-to-right shunt, cases have been seen in which the murmur was well recorded in only part of the right ventricle, and not in another part. This fascinating feature not only provides a powerful physiological tool for delineating flow patterns secondary to intracardiac lesions, but also has added a new cardiovascular diagnostic tool. In situations in which murmur localization can provide the clue to the site of the lesion, intracardiac phonocardiography appears to provide information unequaled by any other method. Figures 11 through 15 illustrate some of the types of information that can be obtained with intracardiac phonocardiography.

Certain problems also arise. The technique requires cardiac catheterization and although, in our hands, it does not add to the risks, it does not reduce them either. The problem of artifacts produced by the catheter is a real one. That such artifacts can be produced by any cardiac catheter and be of sufficient intensity to be audible on the chest wall has been very clearly pointed out by Eldridge & Hultgren

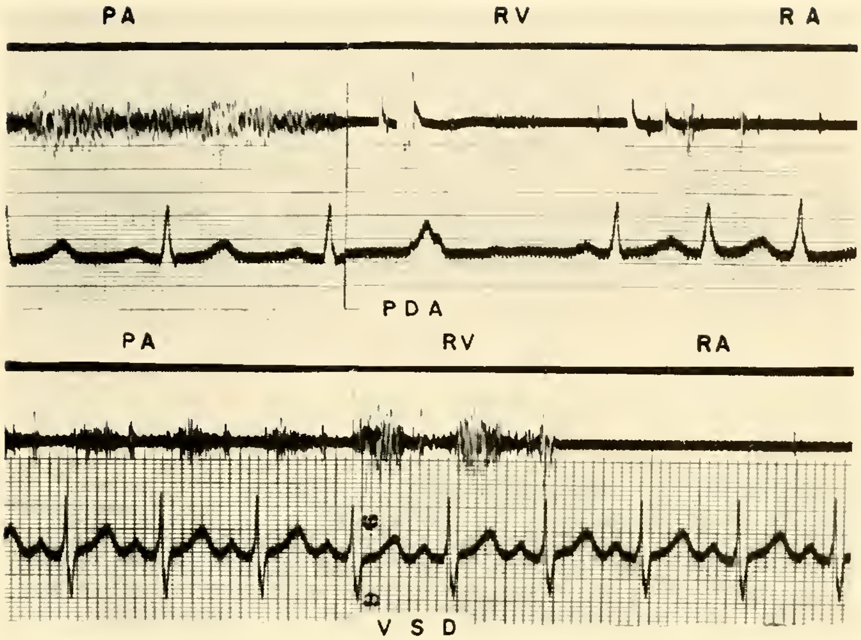

FIG. 15. Intracardiac phonocardiogram, illustrating the use of this technique in the diagnosis of congenital heart disease by sharp intracardiac localization of murmur production. Each recording was taken as the phonocatheter was pulled back from the pulmonary artery into the right ventricle and then into the right atrium. The upper tracing was taken from a child with a patent ductus arteriosus with a left-to-right shunt. There is a continuous murmur in the pulmonary artery and no significant murmur in either the right ventricle or right atrium. The lower tracing was taken from another child with a ventricular septal defect with a left-to-right shunt. There is a systolic murmur in the pulmonary artery, which is much louder and harsher in the right ventricle, and again no murmur in the right atrium.

(29a). The fact that none may be heard on the chest wall clearly does not mean that they are not present, since, as has been previously stated, events may be recorded within the heart that do not reach the chest wall. Certain artifacts can be easily recognized. The flinging of the catheter against the inner wall of the heart or great vessels by cardiac action results in sharp clicking transients that can usually be abolished by changing the position of the transducer. Other possible artifacts are less easily ruled out. The likelihood that the mere presence of the transducer in a flow stream would change the pattern of flow and thereby cause the production of a murmur has been considered since the introduction of the technique. No rigorous evaluation of this has been carried out, so that no completely satisfactory answer is available. However, certain observations in humans shed some light on this problem. There are many areas in the cardiovascular system in which no murmur is heard. For example, although there is almost always a systolic murmur in the pulmonary artery, most often there is no murmur in the outflow tract of the right ventricle. During systole the volume rate of flow and probably the linear velocity of flow are similar in these two closely adjacent areas, which suggests that the murmur is not produced by the catheter but has something to do with the vascular system itself. The additional observation that the form of the murmur at the pulmonic area on the chest is unchanged by the presence of the catheter in the pulmonary artery, and that the form of the murmur within the pulmonary artery is the same as that on the chest, are in agreement with this conclusion, but, again, are not proof of it. Care must be taken to see that the location of the catheter does not interfere with valvular function and thereby produce a murmur. For example, when the transducer is passed in a retrograde direction against the aortic valve, it appears that valve closure can be impaired with the consequent production of an artifactual aortic diastolic murmur. However, when the catheter is passed through the valve down into the ventricle, disturbance of valve function does not seem to be produced. For, in this case, withdrawal of the catheter from the ventricle up into the aorta is not associated with a diastolic murmur.

As more and more interested workers apply the technique of intracardiac phonocardiography to the study of cardiac acoustics, an evaluation of its role in physiological investigations becomes clearer. There is no doubt that it offers, at the present time, the best single approach to the study of the problems of sound and murmur transmission. Regarding the usefulness of the technique in unraveling problems connected with the genesis of sounds and murmurs, it offers recordings which do not suffer from possible loss in transmission, and which provide for a varying degree of localization, depending upon the event under investigation. However, concerning answers to questions about the factors responsible for the various events, the problem here resides more with the ability of the investigator to devise unequivocal

experiments than it does with the ability of the investigator to record from the site of origin of the events.

CURRENT PROBLEMS IN CARDIOVASCULAR ACOUSTICS

Throughout the length of this discussion, attention has been directed toward a number of unsolved problems in acoustics. At both the physical level and the physiological level much remains to be done. The central feature at the present time appears to be the problem of providing a more fundamental and broader base of experience in the correlation between hemodynamics and acoustics. In many situations the hemodynamic factors seem to be well understood and predictable correlations obtain. In a great number of other situations, however, such is not the case. This is due in part to imperfections in our knowledge regarding genesis and transmission of both sounds and murmurs. In part it is due to lack of precise knowledge of hemodynamics, especially here the inability to measure the volume and time-course of flow at various critical locations. When these gaps are closed then the physiologist and the interested clinician will be able to answer what is perhaps the most important current question in acoustics: To what extent can the acoustic phenomena reveal the details of the hemodynamic events both in normal condition and in disease? A thoroughgoing appraisal of this promises to yield rich dividends.

REFERENCES

1. ALTMANN, R. *Der Venenpuls*. Munich. Urban & Schwarzenberg, 1956.
2. BAILEY, C. P., T. HIROSE, AND D. P. MORSE. Mitral stenosis—New concept of correction by rehinging of the septal leaflet. *Am. J. Cardiol.* 1: 81, 1958.
3. BARLOW, J. AND J. SHILLINGFORD. The use of amyl nitrite in differentiating mitral and aortic systolic murmurs. *Brit. Heart J.* 20: 162, 1958.
4. BEARD, O. W. AND G. M. DECHERD, JR. Variations in the first heart sound in complete A-V block. *Am. Heart J.* 34: 809, 1947.
5. BELLET, S., B. GOULEY, C. F. NICHOLS, AND T. M. McMILLAN. Loud, musical, diastolic murmurs of aortic insufficiency. *Am. Heart J.* 18: 483, 1939.
6. BLALOCK, A. AND H. B. TAUSSIG. The surgical treatment of malformations of the heart in which there is pulmonary stenosis or pulmonary atresia. *J.A.M.A.* 128: 189, 1945.
7. BOWDITCH, H. P. and G. M. GARLAND. The effect of respiratory movements on the pulmonary circulation. *J. Physiol.* 2: 91, 1879.
8. BOYER, S. H. Quoted by V. A. McKusick (68).
9. BOYER, S. H. AND A. W. CHISHOLM. Physiologic splitting of the second heart sound. *Circulation* 18: 1010, 1958.
10. BRAUNWALD, E., A. P. FISHMAN, AND A. COURNAND. Time relationship of dynamic events in the cardiac chambers, pulmonary artery and aorta in man. *Circulation Res.* 4: 100, 1956.
11. BRAUNWALD, E. AND A. G. MORROW. Sequence of ventricular contraction in human bundle branch block. A study based on simultaneous catheterization of both ventricles. *Am. J. Med.* 23: 205, 1957.
12. BRAUNWALD, E., G. H. WELCH, JR., AND A. G. MORROW. The effects of acutely increased systemic resistance on the left atrial pressure pulse: a method for the clinical detection of mitral insufficiency. *J. Clin Invest.* 37: 35, 1958.
13. BREST, A. N., V. UDHOJI, AND W. LIKOFF. A re-evaluation of the Graham Steell murmur. *New England J. Med.* 263: 1229, 1960.
14. BROCK, R. C. The surgical and pathological anatomy of the mitral valve. *Brit. Heart J.* 14: 489, 1952.
15. BRUNS, D. L. A general theory of the causes of murmurs in the cardiovascular system. *Am. J. Med.* 27: 360, 1959.
16. BURCHELL, H. B., H. J. C. SWAN, AND E. H. WOOD. Demonstration of differential effects on pulmonary and systemic arterial pressure by variation in oxygen content of inspired air in patients with patent ductus arteriosus and pulmonary hypertension. *Circulation* 8: 681, 1953.
17. BUTTERWORTH, J. S., M. R. CHASSIN, R. McGRATH, AND E. H. REPPERT. *Cardiac Auscultation*, 2nd ed. New York: Grune & Stratton, 1960.
18. CHÁVEZ, I., E. CABRERA, AND R. LIMÓN. La persistencia del conducto arterial complicada de hipertensión pulmonar. *Arch. Inst. cardiol. Mexico* 23: 131, 1953.
19. CREVASSE, L. The use of a vasopressor agent as a diagnostic aid in auscultation. *Am. Heart J.* 58: 821, 1959.
20. CREVASSE, L. AND R. B. LOGUE. Valvular pulmonic stenosis: Auscultatory and phonocardiographic characteristics. *Am. Heart J.* 56: 898, 1958.
21. CREVASSE, L. AND R. B. LOGUE. Atypical patent ductus arteriosus: the use of a vasopressor agent as a diagnostic aid. *Circulation* 19: 332, 1959.
22. DAOUD, G., E. H. REPPERT, AND J. S. BUTTERWORTH. Basal systolic murmurs and the carotid pulse curve in the diagnosis of calcareous aortic stenosis. *Ann. Int. Med.* 50: 323, 1959.
23. DIMOND, E. G. AND A. BENCHIMOL. Phonocardiography in pulmonary stenosis: Special correlation between hemodynamics and phonocardiographic findings. *Ann. Int. Med.* 52: 145, 1960.
24. DOCK, W. Mode of production of the first heart sound. *A.M.A. Arch. Int. Med.* 51: 737, 1933.
25. DOCK, W. Further evidence for the purely valvular

origin of the first and third heart sounds. *Am. Heart J.* 30: 332, 1945.
26. Dock, W. The forces needed to evoke sounds from cardiac tissues, and the attenuation of heart sounds. *Circulation* 19: 376, 1959.
27. Dock, W., F. Grandell, and F. Taubman. The physiologic third heart sound: Its mechanism and relation to protodiastolic gallop. *Am. Heart J.* 50: 449, 1955.
28. Edelman, E. E., Jr., K. Willis, R. P. Walker, L. Christianson, and J. R. Pierce. Relationship of the physiologic third heart sound to the jugular-venous pulse. *Am. J. Med.* 17: 15, 1954.
29. Einthoven, W. Die Registrirung der menschlichen Herztone mittels des Saitengalvanometers. *Arch. ges. Physiol.* 117: 461, 1907.
29a. Eldridge, F. L. and H. N. Hultgren. Production of heart sounds by the cardiac catheter. *Circulation* 19: 557, 1959.
30. Feldman, L., J. Friedlander, R. Dillon, and R. Wallyn. Aneurysm of right sinus of Valsalva with rupture into right atrium and into right ventricle. *Am. Heart J.* 51: 314, 1956.
31. Feruglio, G. A. and A. Sreenivasan. Intracardiac phonocardiogram in thirty cases of atrial septal defect. *Circulation* 20: 1087, 1959.
32. Flint, A. On cardiac murmurs. *Am. J. M. Sc.* 44: 29, 1862.
33. Gasul, B. M., R. A. Arcilla, E. H. Fell, J. Lynfield, J. P. Bicoff, and L. L. Luan. Congenital coronary arteriovenous fistula. *Pediatrics* 25: 531, 1960.
34. Gelfand, D. and S. Bellet. The musical murmur of aortic insufficiency: clinical manifestations; based on a study of 18 cases. *Am. J. Sc.* 221: 644, 1951.
35. Gordon, A. J., L. Steinfeld, M. Dunst, and P. A. Kirschner. Correlation of heart sounds and murmurs with pressure during left heart catheterization. *Circulation* 18: 979, 1958.
36. Gray, I. R. Paradoxical splitting of the second heart sound. *Brit. Heart J.* 18: 21, 1956.
37. Hartman, H. *Exhibit, 3rd World Congress of Cardiology*, Brussels, 1958. Quoted by H. Hartman (38).
38. Hartman, H. The jugular venous tracing. *Am. Heart J.* 59: 698, 1960.
39. Hartman, H. and H. A. Snellen. Die klinische Bedeutung des Venepulses. *Arztl. Forsch.* 13: 404, 1959.
40. Harvey, W. *Exercitatio Anatomica de Motu Cordis et Sanguinis in Animalibus.* Translated by C. D. Leake. Springfield, Ill.: Thomas, 1928.
41. Holldack, K. and D. Wolf. *Atlas und Kurzgefasstes Lehrbuch der Phonokardiographie*, 2nd ed. Stuttgart: Thieme, 1958.
42. Howell, J. B. L., S. Permutt, and D. F. Proctor. Effect of lung inflation upon the pulmonary vascular bed of excised dog lungs. *Fed. Proc.* 17: 74, 1958.
43. Hurst, J. W., T. Staton, and D. Hubbard. Precordial murmurs during pregnancy and lactation. *New England J. Med.* 259: 515, 1958.
44. Julian, D. and L. G. Davies. Heart sounds and intracardiac pressures in mitral stenosis. *Brit. Heart J.* 19: 486, 1957.
45. Kelly, J. J., Jr. Diagnostic value of phonocardiography in mitral stenosis. *Am. J. Med.* 19: 862, 1955.
46. Kuo, P. T. The gallop sounds. Studies of the mechanism of production. *Circulation* 16: 276, 1957.
47. Kuo, P. T., E. A. Hildreth, and C. F. Kay. The mechanism of gallop sounds, studied with the aid of the electrokymography. *Ann. Int. Med.* 35: 1306, 1951.
48. Kuo, P. T., T. G. Schnabel, Jr., W. S. Blakemore, and A. F. Whereat. Diastolic gallop sounds, the mechanism of production. *J. Clin. Invest.* 36: 1035, 1957.
49. Lagerlof, H. and L. Werkö. Studies on the circulation in man. III. The auricular pressure pulse. *Cardiologia* 13: 241, 1948.
50. Leatham, A. Phonocardiography. *Brit. M. Bull.* 8: 333, 1952.
51. Leatham, A. A classification of systolic murmurs. *Brit. Heart J.* 17: 574, 1955.
52. Leatham, A. Auscultation of the heart. *Pediat. Clin. North America* 5: 839, 1958.
53. Leatham, A. and I. Gray. Auscultatory and phonocardiographic signs of atrial septal defect. *Brit. Heart J.* 18: 193, 1956.
54. Leatham, A. and L. Vogelpoel. The early systolic sound in dilatation of the pulmonary artery. *Brit. Heart J.* 16: 21, 1954.
55. Leatham, A. and D. Weitzman. Auscultatory and phonocardiographic signs of pulmonary stenosis. *Brit. Heart J.* 19: 303, 1957.
56. Lepeschkin, E. Zur electrophysiologischen Erklarung des normalen und pathologischen Electrokardiogramms. *Klin. Wchnschr.* 18: 1509, 1939
57. Levine, S. A. and W. P. Harvey. *Clinical Auscultation of the Heart*, 2nd ed. Philadelphia: Saunders, 1959.
58. Lewis, D. H., G. W. Deitz, J. D. Wallace, and J. R. Brown, Jr. Intracardiac phonocardiography in man. *Circulation* 16: 764, 1957.
59. Lewis, D. H., A. Ertugrul, G. W. Deitz, J. D. Wallace, J. R. Brown, Jr., and A. N. Moghadam. Intracardiac phonocardiography in the diagnosis of congenital heart disease. *Pediatrics* 23: 837, 1959.
60. Lewis, D. H., A. N. Moghadam, G. W. Deitz, J. D. Wallace, J. R. Brown, Jr., and S. A. Khalil. The Present Status of Intracardiac Phonocardiography. In: *Congenital Heart Disease*, edited by Bass, A. D. and G. K. Moe. Washington, D. C.: Am. Assoc. Adv. Sc. 1960, p. 269.
61. Little, R. C. Effect of atrial systole on ventricular pressure and closure of the A-V valves. *Am. J. Physiol.* 166: 289, 1951.
62. Little, R. C. and J. G. Hilton. Effect of ectopic ventricular contractions on the first heart sound. *Fed. Proc.* 12: 89, 1953.
63. Liu, C. K. and A. Jacono. Phonocardiography in atrial septal defect. External and intracardiac phonocardiograms. *Am. J. Cardiol.* 2: 714, 1958.
64. Luisada, A. A., M. M. Alimurung, and L. Lewis. Mechanisms of production of the first heart sound. *Am. Physiol.* 168: 226, 1952.
65. Luisada, A. A. and S. Contro. On the time relationship of the waves of the ballistocardiogram. *Acta Cardiol.* 6: 847, 1951.
66. Luisada, A. A., F. G. Fleischner, and M. B. Rappaport. Fluorocardiography (electrokymography). II. Observations on normal subjects. *Am. Heart J.* 35: 348, 1948.

67. Luisada, A. A., C. K. Liu, C. Aravanis, M. Testelli, and J. Morris. On the mechanism of production of the heart sounds. *Am. Heart J.* 55: 383, 1958.
68. McKusick, V. A. *Cardiovascular Sound in Health and Disease.* Baltimore: Williams & Wilkins, 1958.
69. Symposium on cardiovascular sound, edited by V. A. McKusick. *Circulation* 16: 270, 414, 1957.
70. Second symposium on cardiovascular sound, edited by V. A. McKusick. *Circulation* 18: 946, 1958.
71. McKusick, V. A., O. N. Massengale, Jr., M. Wigod, and G. N. Webb. Spectral phonocardiographic studies in congenital heart disease. *Brit. Heart J.* 18: 403, 1956.
72. Medrano, G. A., A. Bisteni, R. W. Brancato, F. Pileggi, and D. Sodi-Pallares. The activation of the interventricular septum in the dog's heart under normal conditions and in bundle-branch block. *Ann. New York Acad. Sci.* 65: 804, 1957.
73. Minhas, K. and B. M. Gasul. Systolic clicks: A clinical, phonocardiographic, and hemodynamic evaluation. *Am. Heart J.* 57: 49, 1959.
74. Mounsey, P. The early diastolic sound of constrictive pericarditis. *Brit. Heart J.* 17: 143, 1955.
75. Nichols, H. T., W. Likoff, H. Goldberg, and M. Fuchs. The genesis of the "presystolic" murmur in mitral stenosis. *Am. Heart J.* 52: 379, 1956.
76. Ongley, P. A., H. B. Sprague, M. B. Rappaport, and A. S. Nadas. *Heart Sounds and Murmurs.* New York: Grune & Stratton, 1960.
77. Orias, O. and E. Braun-Menéndez. *The Heart-Sounds in Normal and Pathological Conditions.* London: Oxford Univ. Press, 1939.
78. Potts, W. J., S. Smith, and S. Gibson. Anastomosis of the aorta to a pulmonary artery. Certain types in congenital heart disease. *J.A.M.A.* 132: 627, 1946.
79. Proctor, M. H., R. P. Walker, E. W. Hancock, and W. H. Abelmann. The phonocardiogram in mitral valvular disease. A correlation of Q-1 and 2-OS intervals with findings at catheterization of the left side of the heart and at mitral valvuloplasty. *Am. J. Med.* 24: 861, 1958.
80. Quincke, H. and E. Pfeiffer. Uber den blutstrom in den lungen. *Arch. Anat. Physiol. Wiss. Med.* 39: 90, 1871.
81. Ravin, A. *Auscultation of the Heart.* Chicago: Yearbook, 1958.
82. Reale, A., H. Goldberg, W. Likoff, and C. Denton. Rheumatic tricuspid stenosis. A clinical and physiologic study with a suggested method of diagnosis. *Am. J. Med.* 21: 47, 1956.
83. Reinhold, J., U. Rudhe, and R. E. Bonham-Carter. The heart sounds and the arterial pulse in congenital aortic stenosis. *Brit. Heart J.* 17: 327, 1955.
84. Rivero Carvallo, J. M. Signo para el diagnóstico de las insuficiencias tricuspideas. *Arch. Inst. cardiol. Mexico* 16: 531, 1946.
85. Rivero Carvallo, J. M and A. Garza de los Santos. Real and apparent apical impulses in tricuspid lesions. *Am. J. Cardiol.* 4: 367, 1959.
86. Rushmer, R. F. *Cardiac Diagnosis. A Physiologic Approach.* Philadelphia. Saunders, 1955, p. 218.
87. Rytand, D. A. An analysis of the variable amplitude of the first heart sound in complete heart block. *Stanford M. Bull.* 6: 187, 1948.
88. Sanders, R. J., W. H. Kern, and S. G. Blount, Jr. Perforation of the interventricular septum complicating myocardial infarction. *Am. Heart J.* 51: 736, 1956.
89. Scher, A. M. and A. C. Young. Ventricular depolarization and the genesis of QRS. *Ann. New York Acad. Sci.* 65: 768, 1957.
90. Scott, J. T. and E. A. Murphy. Mammary souffle of pregnancy. *Circulation* 18: 1038, 1958.
91. Sellors, T. H. 3rd World Congress of Cardiology, Brussels, 1958. Abstracts of Round Table Conferences, p. 161.
92. Shapiro, H. A. and D. R. Weiss. Mitral insufficiency due to ruptured chordae tendineae simulating aortic stenosis. *New England J. Med.* 261: 272, 1959.
93. Shearn, M. A., E. Tarr, and D. A. Rytand. The significance of changes in amplitude of the first heart sound in children with A-V block. *Circulation* 7: 839, 1953.
94. Soloff, L. A., F. Cortes, W. L. Winters, Jr., and J. Zatuchni. The pansystolic regurgitant murmur: a simple method of identifying its anatomic source. *Am. J. M. Sc.* 237: 744, 1959.
95. Spencer, M. P., F. R. Johnston, and J. H. Meredith. The origin and interpretation of murmurs in coarctation of the aorta. *Am. Heart J.* 56: 722, 1958.
96. Steell, G. The murmur of high pressure in the pulmonary artery. *Med. Chronicle* 9: 182, 1888.
97. Van der Spuy, J. C. The Functional and Clinical Anatomy of the Mitral Valve. *Brit. Heart J.* 20: 471, 1958.
98. Visscher, M. B. The capacity changes in the pulmonary vascular bed with the respiratory cycle. *Fed. Proc.* 7: 128, 1948.
99. Vogelpoel, L., M. Nellen, A. Swanepoel, and V. Schrire. The use of amyl nitrite in the diagnosis of systolic murmurs. *Lancet* 2: 810, 1959.
100. Vogelpoel, L., V. Schrire, M. Nellen, and A. Swanepoel. The use of amyl nitrite in the differentiation of Fallot's tetralogy and pulmonary stenosis with intact ventricular septum. *Am. Heart J.* 57: 803, 1959.
101. Warren, J. V. Gallop rhythm. *Circulation* 15: 321, 1957.
102. Warren, J. V., J. J. Leonard, and A. M. Weissler. Gallop rhythm. *Ann. Int. Med.* 48: 580, 1958.
103. Wells, B. The assessment of mitral stenosis by phonocardiography. *Brit. Heart J.* 16: 261, 1954.
104. Wolferth, C. C. and A. Margolies. Gallop rhythm and the physiological third heart sound. Characteristics of sounds, classifications, comparative incidence of various types, and differential diagnosis. *Am. Heart J.* 8: 441, 1933.
105. Wood, F. C., J. Johnson, T. G. Schnabel, Jr., P. T. Kuo, and H. F. Zinsser. The diastolic heart beat. *Tr. A. Am. Physicians* 64: 95, 1951.
106. Wood, P. An appreciation of mitral stenosis. *Brit. M. J.* 1: 1051, 1113, 1954.
107. Wood, P. *Diseases of the Heart and Circulation*, 2nd ed. Philadelphia: Lippincott, 1956.
108. Wood, P., L. McDonald, and R. Emanuel. The clinical picture correlated with physiological observations in the diagnosis of congenital heart disease. *Pediat. Clin. North America* 5: 981, 1958.
109. Zinsser, H. F., Jr., and C. F. Kay. The straining procedure as an aid in the anatomic localization of cardiovascular murmurs and sounds. *Circulation* 1: 523, 1950.

INDEX

Index